A Report to

The National Science Foundation

for

Satellite Derived Earth and Atmospheric Energy Balance Components

During

The Summer MONEX

Grant #ATM-8205-386
#ATM-8342-619

University of Wisconsin Account #144-SØ39

for the period of

1 June 1982 - 30 November 1984

submitted by

Anthony J. Schreiner

Space Science and Engineering Center
at the University of Wisconsin-Madison
1225 West Dayton Street
Madison, Wisconsin 53706
(608) 263-5862

November 1984

ABSTRACT

For the 1979 summer MONEX, satellite data (both TIROS-N and GOES-I) are used to describe the atmospheric energy balance components for the onset period, 11-20 June. Top of the atmosphere and tropospheric radiational components, and moist static energy components for the Arabian Sea and its littoral are calculated. Top of the atmosphere longwave, shortwave, net radiation, and albedo calculations are generated from calibrated GOES-I imagery for the southern Indian Ocean, 0° to 30S and 40E to 80E. Tropospheric radiational components are calculated using the Chou-Arking algorithms with relative cloudiness (GOES-I) and temperature and relative humidity (TIROS-N) serving as input. In addition, moist static energy component calculations are based on vertical temperature and moisture profiles (TIROS-N) and cloud-drift winds (GOES-I). Relative cloud cover is a primary factor in affecting the radiative balance of the earth-atmosphere system. The divergence of moist static energy at low levels was found to 10^3 larger than either the advective or local rate of change component. Temporal and spatial analyses were generated for the onset period, and the data are available to users on computer compatible tape in grid format.

TABLE OF CONTENTS

I. INTRODUCTION

During the Summer Monsoon Experiment (SMONEX), a sub-program of the First GARP Global Experiment (FGGE), multispectral scanning radiometer (MSR) and radiation flux measuring instruments were flown on the NASA CV-990 aircraft over India, Saudi Arabia, and the Arabian Sea. In addition, dropsondes were deployed from aircraft. The MSR, radiation flux, and dropsonde measurements provided the ground truth needed for precise interpretations of satellite radiance observations in terms of surface temperature fields, vertical temperature profiles, and regional radiation budgets.

The research work included in this report was carried out in two stages. During the first stage (under NSF grant #ATM-801-4892) of the effort attention was focused on careful and detailed calibration of GOES-I measurements of reflected shortwave and emitted window infrared radiances using in situ aircraft MSR measurements and TIROS-N longwave flux (Virji, 1982). The derived calibration relationships were used to estimate the spatial and temporal distribution of the radiation balance of the earth-atmosphere system over the Arabian Sea and its littoral during the onset phase of the 1979 summer monsoon (11-20 June 1979). The results of this analysis were presented in a paper (Smith, et al., 1981) at the Tallahassee FGGE/MONEX conference. Based upon the results, a second stage of the research effort was begun on 1 June 1982 (under NSF grants #ATM-8205-386 and #ATM 8342-619). This document summarizes the effort during the second stage of the analyses.

The research effort focused on (i) a full documentation of the high resolution earth-atmosphere (E-A) radiation balance components (Virji et al., 1982; Appendix A), and (ii) estimation of tropospheric and surface

energy balance components (both radiative and thermodynamic) for the Arabian Sea and surrounding region for the onset period. The evolution of tropospheric radiative and moist static energy balance components is emphasized in this report. Manuscripts of papers for publication in refereed journals (in draft form) are included in the appendices.

A detailed analysis for the onset phase of 1979 summer monsoon over the Arabian Sea region has been completed. The study could not be extended to the established and break phases of the monsoon as continuous satellite (GOES-I) data in the infrared channel was unavailable after 21 June 1979 due to satellite sensor malfunction. No analysis over the Tibetan Plateau region was attempted either because of problems related to limb darkening effects at the periphery of the GOES-I visible image. Instead, the spatial domain of the analysis for the onset phase was extended over the Southern Indian Ocean to 30° S latitude and 40°E and 80°E longitude. For this region, the earth-atmosphere (E-A) radiation balance components were derived in a similar manner as for the Arabian Sea region analysis contained in the Atlas (Virji et al., 1982; Appendix A).

The balance of this report discusses the main results of the completed analyses for the onset phase over the Arabian Sea region (Section II.A). The results of the E-A radiation balance analyses for the southern hemisphere are discussed in Section II.B.

II. SUMMARY OF WORK COMPLETED

A. ARABIAN SEA AND ITS LITTORAL

1. Earth-Atmosphere Radiation Budget Analysis

The published Atlas (Virji et al., 1982) based on this analysis is included in Appendix A. A detailed description of the analyses can be

found therein. Briefly, what is included are hourly analyses of longwave flux, albedo, absorbed solar, and net radiation derived from calibrated visible and infrared GOES-I satellite imagery on a 2° x 2° latitude-longitude grid for the period 11-20 June 1979 for the Arabian Sea and its littoral. In addition, daily averaged analyses for the variables mentioned above are available for the ten day period. Diurnal variation of the E-A radiation balance components during the 1979 monsoon onset phase can be obtained from virtually any location within the analysis grid. Mean diurnal variations in the radiation balance components for the onset period at five selected locations are included in the atlas. There may be some inherent navigation and line offset problems between visible and infrared images from the GOES-I satellite. This offset over the ten day period averaged less than 2 pixels/day. Hence, the offset error is minimal compared to the large-scale (8 km resolution and 2° x 2° grid spacing) analysis performed.

A total of 250 copies were printed of which 120 were disseminated to both domestic and international MONEX researchers. This data is also available on computer compatible tapes to researchers at a nominal charge, mainly for the cost of the magnetic tape.

2. Tropospheric Energy Balance Analysis

Table 1 shows a schematic of equations and data used. Part 1 of Table 1, the E-A radiation budget analysis, provided good estimates of the top boundary conditions. The next step was to calculate tropospheric heating. As indicated in Table 1, vertical profiles of temperature and humidity for local noon conditions were derived from the TIROS-N sounder data using the iterative retrieval algorithms with a statistical first

guess (Smith, 1983). Cloud drift winds at 1000 GMT (Young et al., 1980) and relative cloud cover (Virji and Herman, 1984; Appendix B) were used together with the retrieved temperature and humidity profiles to compute both the tropospheric radiative heating and the moist static energy balance. The terms described in this section will be discussed under two major groups:

(a) Tropospheric radiative heating analyses

$$(F_{SW},\ F_{LW})$$

(b) Moist static energy balance analyses

$$\int_p \left(\frac{\partial Q}{\partial t}\frac{dp}{g}\right)\ ,\ \int\left(\nabla \cdot \vec{V}Q\right)\frac{dp}{g}$$

The terms not discussed are the vertical advection of moist static energy $[\int(\partial\omega/\partial p)\ Q\ (dp/g)]$, latent heat, and sensible heat release as they were not directly calculated from our data.

a. Tropospheric radiative heating

The three state parameters which affect the radiation balance within the atmosphere are temperature, humidity, and cloudiness. While cloudiness can change extensively in the summer monsoon region of the Arabian Sea, temperature and relative humidity profiles undergo relatively less fluctuation from one day to another. Therefore, knowledge of the relative cloudiness is crucial in defining the shortwave flux (F_{SW}) and longwave flux (L_{LW}) within the atmosphere, as will be discussed later.

A detailed explanation of the derivation of cloudiness during the onset phase is given in the Virji and Herman paper found in Appendix B. Briefly, the model used a bi-dimensional histogram based on infrared brightness temperature and reflectance (derived from visible digital

counts) to specify cloud types and their altitudes. It was assumed that a given cluster of brightness temperature and reflectance classes could be assigned common cloud height, amount, opacity, and thickness. For each 2°x 2° grid box a two dimensional histogram was constructed and from these histograms four cloud types were identified as: low (950-700 mb), middle (699-400 mb), high (399-100 mb) and cumulonimbus (950-100 mb). The analysis was done once per day around 1000 GMT over the Arabian Sea for the ten day onset period (11-20 June 1979). Relative cloudiness was not calculated for 13 June because the infrared sensor malfunctioned for an eleven hour period during the day. Some shortcomings inherent in this technique are (i) maximum cloudiness of 100% per grid box (no vertical cloud stacking), (ii) ignoring semi-transparent clouds (e.g., thin cirrus), and (iii) using the plane parallel model which ignored the fact clouds have different shapes. An example of relative cloud cover for 20 June is shown in Figure 1.

The relative cloudiness and the satellite (TIROS-N) derived temperature and humidity profiles were used as input to calculate shortwave and longwave cooling in the troposphere through the application of radiative transfer calculations as formulated by Chou and Arking (1980, 1981). Surface albedo (a necessary additional parameter) was obtained from a minimum albedo image derived from a sequence of GOES-I visible satellite images at local noon time for the center of the analysis area. Here, for a series of images (in this case, ten days worth) the lowest digital count at each pixel location was saved resulting in a picture with all the clouds removed (except for persistent clouds associated with orography and sea breeze, and contamination and sun glint) as seen in Figure 2.

The radiative transfer calculations were carried out for nine layers between 1 mb and the surface for the infrared portion of the spectrum. The shortwave calculations also consist of nine layers, but the output parameters saved were the incident shortwave at the top of the atmosphere (SFI), the amount absorbed at the top of the atmosphere (SFT), and the amount absorbed at the surface (SFS). All calculations were made once per day (near local noon, 0900 GMT) on a 2°x 2° grid covering the Arabian Sea and its littoral for the ten day period, 11-20 June 1979.

(1) Longwave cooling

The results discussed here, are the cooling rates at the top of the atmosphere (or in the uppermost layer), longwave cooling at the surface, and profiles of cooling rates for selected locations. Figures 3a and b show the outgoing longwave radiation in the uppermost layer as measured by the Chou-Arking algorithm (a) and the independent analysis contained in the GOES-I radiation Atlas (Appendix A) for 20 June 1000 GMT. The two independent analyses compared well not only in location of maxima and minima, but also the absolute values. This close agreement between the two independent calculations existed for all ten days.

A comparison between Figs. 3a and 1 shows the close correlation between relative cloudiness and outgoing long wave radiation at the uppermost layer. There was a close correlation between high clouds (Fig. 1c) and Cb's (Fig. 1d) and the major minima found in longwave flux analysis (Fig. 3a), whereas the mid (Fig. 1b) and especially the low level (Fig. 1a) analyses did not have a direct influence in the amount of outgoing longwave radiation for the uppermost layer in the atmosphere. This pattern was repeated throughout the ten day onset period.

Figs. 4a, 4b and 4c show outgoing, downward, and net longwave radiation respectively at the lowest level (1000 mb) for 20 June 1979. The relationship of relative cloudiness (Fig. 1) and outgoing longwave radiation (Fig. 4a) was not as straight forward as was depicted for the uppermost layer (Fig. 3a). Yet, an area of minimum values of upward-directed longwave radiation was seen along the west coast of India. This area was evident throughout the ten day onset period only changing in absolute value. Downward-directed longwave flux (Fig. 4b) for the lowest layer also showed a complicated relationship with relative cloudiness. Generally speaking, where total (total = low + mid + high + Cb) relative cloudiness was a minimum, downward flux was also minimum and vice versa. There was also a relative maximum of downward-directed longwave flux located over north central India which showed up for each of the ten days of the onset period changing only in absolute magnitude. The net longwave flux (Fig. 4c) showed a gain in longwave radiation for the lowest layer over western India. This feature persisted during the ten day analysis period. Generally, over the remainder of the analysis area, negative net longwave radiation was found except for a small area over the eastern portion of Saudi Arabia, and this only occurred during the time when a cyclone was located in that area.

Calculated profiles of infrared radiation cooling rates at selected grid locations at the end of onset phase for 20 June 1979 are shown in Fig. 5. Profile A is located off the west coast of India in an area of convection (14 N, 70E); profile B was located near the southern edge of the analysis area in relatively clear air (4N, 74E). For this day, a cyclone is located along the coast of Saudi Arabia and an intense convective system is just off the west coast of India (Profile A), while

Profile B is imbedded in an area of anticyclonic flow at low levels and confluence at upper levels south of the southern tip of India. Both figures display the upward directed (UF), downward directed (DF), and the net (UF-DF) longwave radiation vertical profiles, where a positive value indicates a net cooling and vice versa for a negative value for that level.

(2) Shortwave cooling/heating

Of the three output parameters for short wave radiational heating, the terms discussed here are shortwave absorbed at the top of the atmosphere (SFT) and shortwave absorbed at the surface (SFS). As with the infrared cooling, the Chou-Arking algorithm based SFT (Fig. 6a) was in good agreement with the independently calculated absorbed shortwave radiation (Fig. 6b) from the MONEX radiation Atlas (Appendix A). Although the absolute value comparison was not as good as for the longwave cooling, the major features (locations of absolute maxima and minima and the overall patterns) corresponded well.

Figs. 7a-e show the evolution of SFS for every other day of the ten day period. Over the Arabian Sea off the west coast of India absolute values of 500 w/m^2 occurred at the beginning of the period and decreased to values of 100 w/m^2 by 20 June. There was a net decrease of absorbed short wave at the surface as one progressed through the onset period over Saudi Arabia due to the tropical depression over Oman. Values of SFS were less over India than over Saudi Arabia for any given day.

Since values of longwave and shortwave radiation cooling/heating at the surface and top of the atmosphere were available, net radiative

heating at these two levels and by the troposphere could be estimated. These calculations are not presented here.

b. Moist static energy balance analysis

The moist static energy of the atmosphere (Q) is comprised of three components:

$$\underset{1}{gz} + \underset{2}{CpT} + \underset{3}{Lq}$$

Terms 1 and 2 are defined as the dry static energy (or potential energy plus enthalpy) and term 3 is latent energy.

The terms discussed in this section are the horizontal flux divergence

$$\int_p \nabla\cdot(\vec{V}Q)\left(\frac{dp}{g}\right)$$

and the local rate of change term

$$\int_p \left(\frac{\partial Q}{\partial t}\right)\left(\frac{dp}{g}\right) \quad .$$

The vertical advection term

$$\int_p \left(\frac{\partial \omega Q}{\partial P}\right)\frac{dp}{g}$$

was not calculated because we did not have good estimates of ω.

The flux divergence term can be broken down into two component parts:

$$\underset{1}{\int_p \nabla\cdot(\vec{V}Q)\,\frac{dp}{g}} = \underset{2}{\int_p (\nabla\cdot\vec{V})Q\,\frac{dp}{g}} + \underset{3}{\int_p (\nabla Q)\cdot\vec{V}\,\frac{dp}{g}}$$

an advective component (3) and a divergent component (2). Cloud drift winds derived from the GOES-I Indian Ocean satellite (Young et al., 1980) and temperature, dewpoint, and geopotential height from TIROS-N radiance information (Smith, 1983) were used to calculate these terms for a two

layer atmosphere. The lower layer was from surface to 500 mb and the upper layer from 499 to 10 mb. Each analysis was performed once per day (near local noon) on a 2°x 2° grid resolution for the period 11-20 June 1979.

Fig. 8 shows low level advection of moist static energy for every other day of the onset period. Over the ten day period, there was an overall increase in gradient especially over the western Arabian Sea and eastern Saudi Arabia. Along with this the positive maxima increased from a value of 125 w/m^2 to over 300 w/m^2 on 20 June, while the minima generally maintained the same magnitude throughout the onset period. Except for the period around 14 June, no real significant maxima (or minima) occurred over the southern portion of India and Sri Lanka. On 18 and 20 June an area of positive advection occurred which is closely associated with the onset vortex approaching the east coast of Saudi Arabia.

The most obvious difference between the low level advection and upper level advection of Q (Fig. 9) was the lack of definition of the upper level analyses. The low level component was 10 to 10^2 times larger than the upper level component.

The low level flux divergence of moist static energy is shown in Fig.10a-e. Generally, convergence dominated the central region of the Arabian Sea, while divergence although relatively weak occurred over the subcontinent of India for the ten day onset period of the 1979 Indian summer monsoon with the exception of 18 June. Except for 12 June, weak convergence was observed over Saudi Arabia probably associated with the heat low. The convergent/divergent patterns tended to align themselves in zonal bands for the first five days and in longitudinal bands for the

five final days. Divergence of Q at low levels was observed for the ten day period over the Horn of Africa maintaining a relatively constant value throughout the onset.

In contrast to low level, upper level divergence of Q (Fig. 11a-e) showed a divergence zone over the Arabian Sea, and the Indian sub-continent was under the influence of convergence, although at times was not well-defined and weak (e.g., 12 June). There was a rapid northward transition of the maximum band of divergence between 14 and 16 June. During the first four days of the onset, the maximum band was below the island of Socotra (13.0N 53.5E) and the orientation was from southwest to northeast. By 16 June the band moved north of Socotra and changed orientation from northwest to southeast. Upper level analyses displayed a consistent signature of divergence along the west coast of India for all days. In summation, the upper and lower divergence of Q analyses showed vertical cells with rising motion over the eastern Arabian Sea and descending motion over western India and Saudi Arabia.

Fig. 12a-e shows the low layer evolution of the local rate of change of moist static energy term for the ten day onset period. The patterns in these fields are complex. A consistent positive local rate of change along the northern fringes of the Arabian Sea occurs from 16 to 20 June in parallel with the intensification of the onset vortex.

As in advection, a comparison of low versus high local rate of change showed the low level parameter to 10 to 10^2 larger in absolute value than the upper level local rate of change. This term for upper layers is not discussed here. The total local rate of change (low + high) strongly relfects the pattern of the low level component during this onset period of the 1979 Indian monsoon.

One point which has been carried through this discussion of moist static energy budget analyses is the relative magnitude of low level versus upper level. In each of the three cases the magnitude of the low level analyses was 10 to 10^2 larger in absolute value than its upper level counterpart. The latent heat term (LQ) was the main contributor to this factor. A scale analysis of the various terms shows that the flux divergent component is on the order of 10^2 to 10^3 larger than advection component (Virji et al., 1982; Appendix C) in absolute value and of the same order of magnitude for the local rate of change of moist static energy for the ten day onset period. The moist static energy budget is dominated by the flux divergence of Q and the distribution of the low level moisture for the 1979 Indian monsoon.

B. SOUTHERN INDIAN OCEAN

For the southern Indian Ocean (area of coverage was approximately 0° to 30°S and 40°E to 80°E) calculations for the earth-atmosphere radiation balance components were generated for the ten day (11-20 June 1979) onset period. The same calibration equations, which were used in the Arabian Sea calculations (Virji et al., 1982; see Appendix A), were also used for the Southern Indian Ocean. This resulted in hourly as well as daily analyses of the same parameters (albedo, long wave flux, absorbed solar, and net radiation).

One difference between the Arabian Sea and southern Indian Ocean E-A analyses, was the lack of extreme values for the four parameters. This may be due to the fact that the southern hemisphere at this time was receiving less incoming solar radiation than the northern hemisphere. In

addition, there were few organized convective systems passing through the analysis area.

Figs. 13a-e and 14a-e show the evolution of the daily averaged fields of albedo and long wave flux respectively, for every other day of the onset period. From the albedo fields two convective systems located just north and south of the equator and either side of 67°E longitude were seen to move through the analysis area in an eastward direction. By 18 June the convective systems had exited the area. Of note was that the northern system tended to decay during its transit while the southern cluster was intensifying. This was also brought out in the long wave analyses (Fig. 14a-e). The northern fringes of a cold front passed through the analysis area during the Indian monsoon onset period. The first indications of this front were seen on the 14th of June (Fig. 14b), and its signature was seen to move eastward through the remainder of the period. Very little deep convection was associated with this front as is brought out by the long wave flux analyses showing a minimum of high, cold clouds. The cold front was also well-defined by the daily net radiation analysis for 18 June (Fig. 15).

In summary, the E-A radiation fields for the southern Indian Ocean lack the definition which was displayed in the Arabian Sea analyses. Yet significant weather systems were accounted for in this radiation budget analysis (e.g., the cold front passage).

III. CONCLUSIONS

For the ten days of the onset of the Indian monsoon, we have described the evolution of the relative cloudiness over the Arabian Sea and its littoral and found it to be an important parameter affecting the

radiative balance of the earth-atmosphere system. An inspection of the moist static energy balance components shows that the divergence component was shown to be a factor 10^3 larger in magnitude than either the advective component or the local rate of change term. In the low tropospheric layer (surface to 500 mb), the latent energy was found to play an important role in determining the moist static energy balance.

One goal of the grant was to provide satellite derived data sets and analyses which could be readily used by researchers in their investigations of the onset of the Indian monsoon. This to a large extent was successfully accomplished. The analyses described above are available in grid point format on magnetic tape or hard copy form in the Earth-Atmosphere Radiation Atlas (Appendix A). Throughout this effort, the different data sets (e.g., radiation parameters, moist static energy analyses and relative cloudiness) were kept compatible with each other so they could be readily combined for easy calculations and manipulations.

We have produced a temporally and spatially complete analysis of the radiative and thermodynamic heating of the troposphere during the onset period. Further, we have developed algorithms which use satellite information to determine cloud cover, and the regional energy balance for the unique region of the developing onset vortex. Finally, portions of this work are being written up for publication in refereed literature.

4/SEC/08

IV. LIST OF ILLUSTRATIONS

(d) Same as (a) except for 18 June 1979 1000 GMT
(e) Same as (a) except for 20 June 1979 1000 GMT

Fig. 11 (a) Upper level divergence of moist static energy in $(W/m^2)x10^{-4}$ for 12 June 1979 1000 GMT
(b) Same as (a) except for 14 June 1979 1000 GMT
(c) Same as (a) except for 16 June 1979 1000 GMT
(d) Same as (a) except for 18 June 1979 1000 GMT
(e) Same as (a) except for 20 June 1979 1000 GMT

Fig. 12 (a) Low level local rate of change of moist static energy in W/m^2 for 12 June 1979
(b) Same as (a) except for 14 June 1979 1000 GMT
(c) Same as (a) except for 16 June 1979 1000 GMT
(d) Same as (a) except for 18 June 1979 1000 GMT
(e) Same as (a) except for 20 June 1979 1000 GMT

Fig. 13 (a) Daily albedo (per cent)$x10^{-1}$ for 12 June 1979
(b) Daily albedo (per cent)$x10^{-1}$ for 14 June 1979
(c) Daily albedo (per cent)$x10^{-1}$ for 14 June 1979
(d) Daily albedo (per cent)$x10^{-1}$ for 14 June 1979
(e) Daily albedo (per cent)$x10^{-1}$ for 14 June 1979

Fig. 14 (a) Daily long wave radiation in W/m^2 for 12 June 1979
(b) Daily long wave radiation in W/m^2 for 14 June 1979
(c) Daily long wave radiation in W/m^2 for 16 June 1979
(d) Daily long wave radiation in W/m^2 for 18 June 1979
(e) Daily long wave radiation in W/m^2 for 20 June 1979

Fig. 15 Daily net radiation W/m^2 for 18 June 1979

Table 1

SATELLITE DERIVED EARTH AND ATMOSPHERE ENERGY BALANCE COMPONENTS DURING THE SUMMER MONEX

	DATA	PARAMETERS	RESOLUTION AND PERIOD
1. EARTH-ATMOSPHERE (TOP) RADIATION BUDGET $F_{N,top} = F_{A,top} - F_{L,top}$ (via Smith et al, 1981)	MSR calibrated GOES I.O. VISSR imagery at 8km resolution at hourly intervals	a) Outgoing Longwave flux ($F_{L,top}$) b) Absorbed Solar radiation ($F_{A,top}$) c) Net Radiation ($F_{N,top}$)	Onset of 1979 summer monsoon (10-20 June) over the Arabian Sea and its littoral.
2. HEATING IN THE ATMOSPHERE $\int \frac{\partial Q}{\partial t} \frac{dp}{g} + \int (\nabla \cdot \vec{V}Q) \frac{dp}{g} + \int \frac{\partial}{\partial p} \omega Q \frac{dp}{g} = F_{SW} \uparrow\uparrow + F_{LW} \uparrow\uparrow + LP - LE + Q_o$ $Q = CpT + gz + Lq$	TIROS-N sounder and GOES I.O. cloud winds ($\vec{V}$) at 2°x 2° spatial resolution, 1000 GMT (Young, et al, 1980) GOES I.O. VISSR derived relative cloud cover	a) T, T_d, Δz (via Smith & Woolf, 1981) b) $C_p T$, gz, Lq, and Q c) for 2 or 3 layer atmosphere: (i) $\int (\nabla \cdot \vec{V}) Q \frac{dp}{g}$ (ii) $\int (\nabla Q \cdot \vec{V}) \frac{dp}{g}$ d) F_{SW}, F_{LW} (via Chou-Arking, 1980, 1981)	Mandatory levels, 2°x 2° 1000 GMT, same period as above.
3. HEATING AT THE EARTH SURFACE $F_{N,sfc} = (F_{N,SW} + F_{N,LW})_{sfc}$ $F_{N,sfc} + LE_o + Q_o + S_o = \frac{\partial T}{\partial t}$	GOES I.O. VISSR image at 8 km resolution at hourly intervals and TIROS-N temperature humidity soundings and T_{skin}	a) Albedo b) $F_{N,SW}$ (via Chou-Arking, 1980, 1981) c) $F_{N,LW}$ (via TIROS-N T_{skin} and Chou-Arking (1981) d) $F_{N,sfc}$	2°x 2° 2°x 2°, hourly (0500 - 1200 GMT) 2°x 2°, 1000 GMT

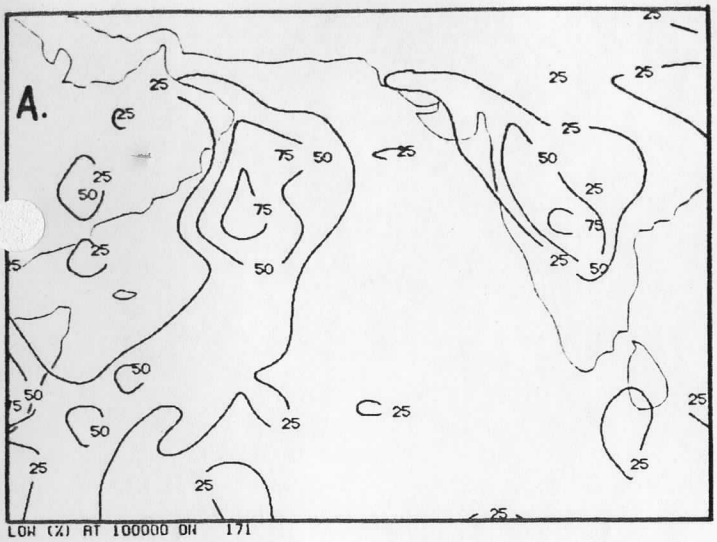
A.
LOW (%) AT 100000 ON 171

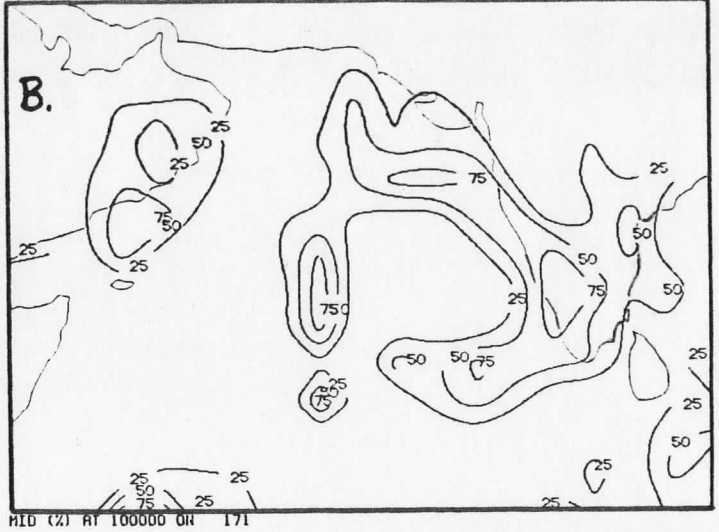
B.
MID (%) AT 100000 ON 171

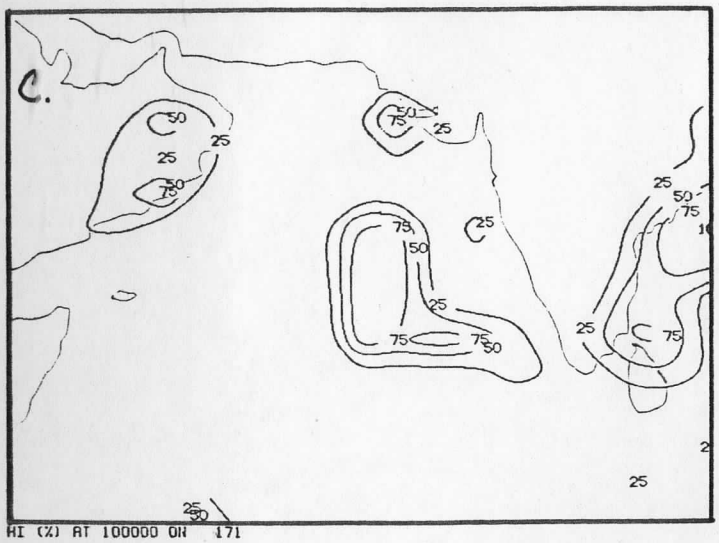
C.
HI (%) AT 100000 ON 171

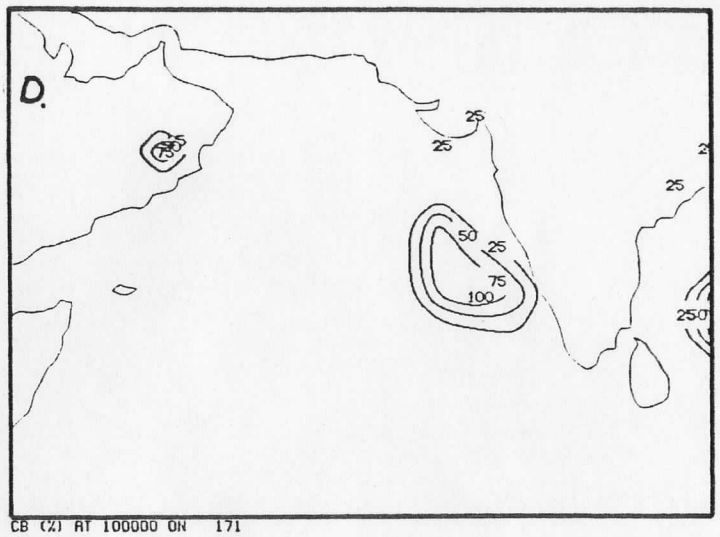
D.
CB (%) AT 100000 ON 171

Fig. 1

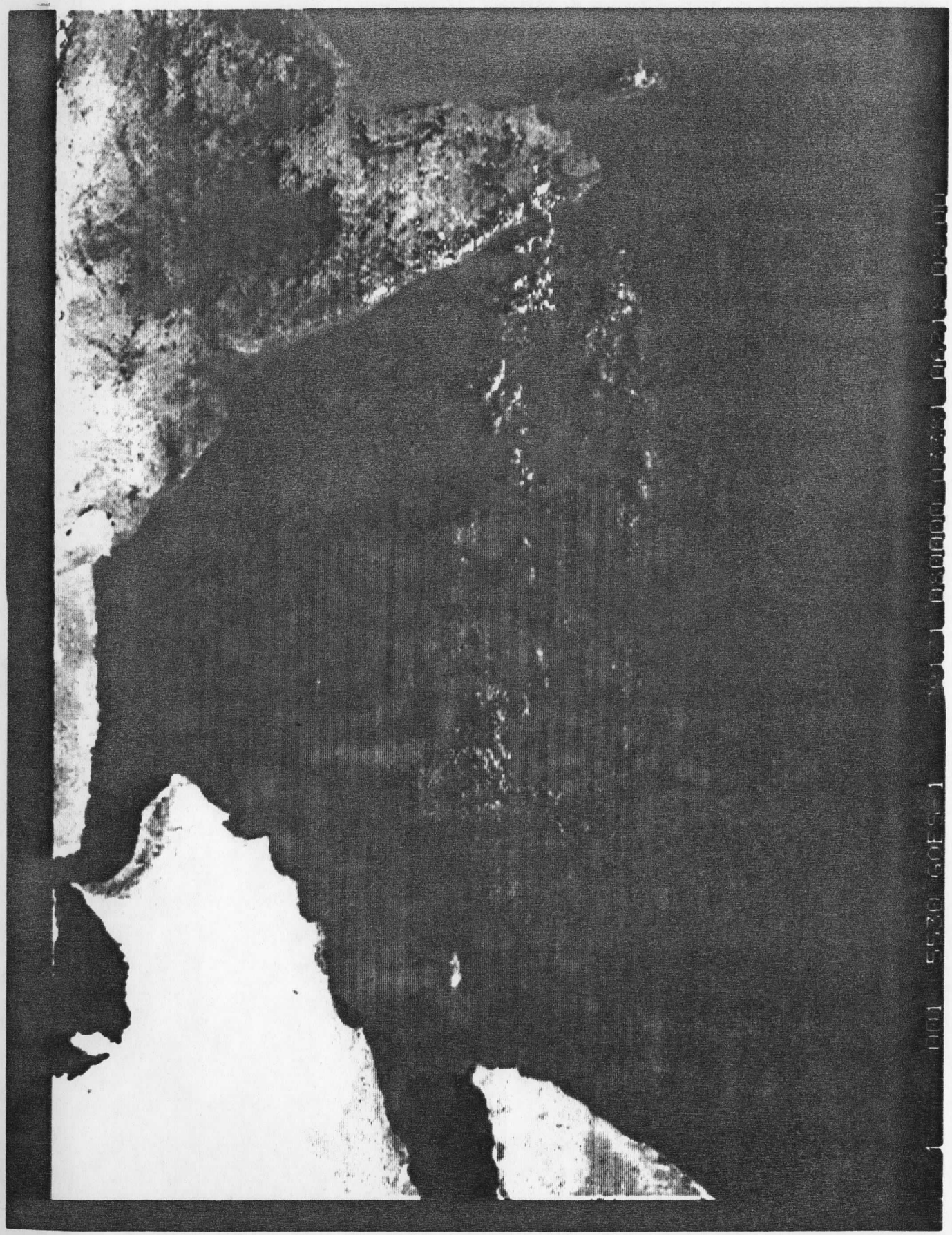

Fig. 2

A

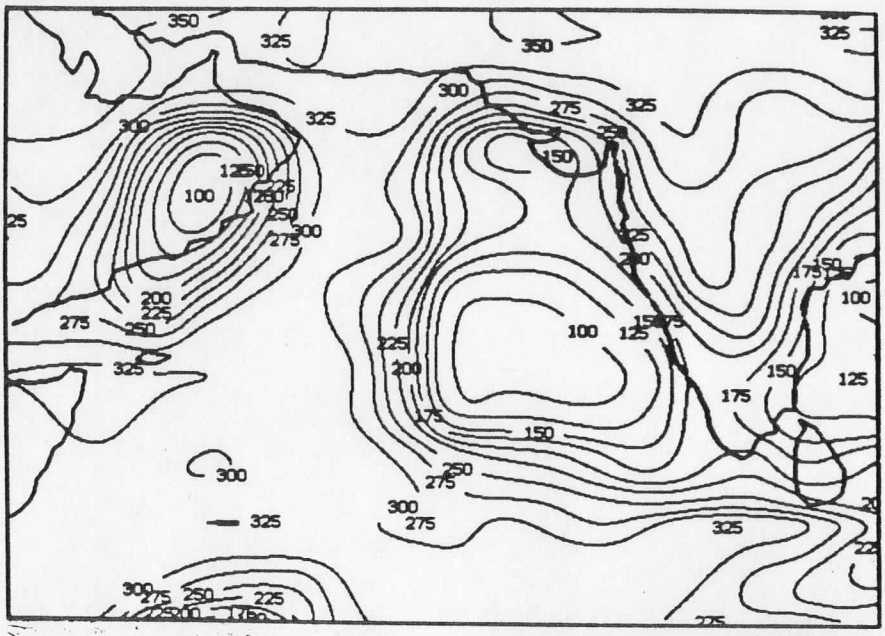
UF (W/m²)
1ΦΦΦ GMT 79171

B

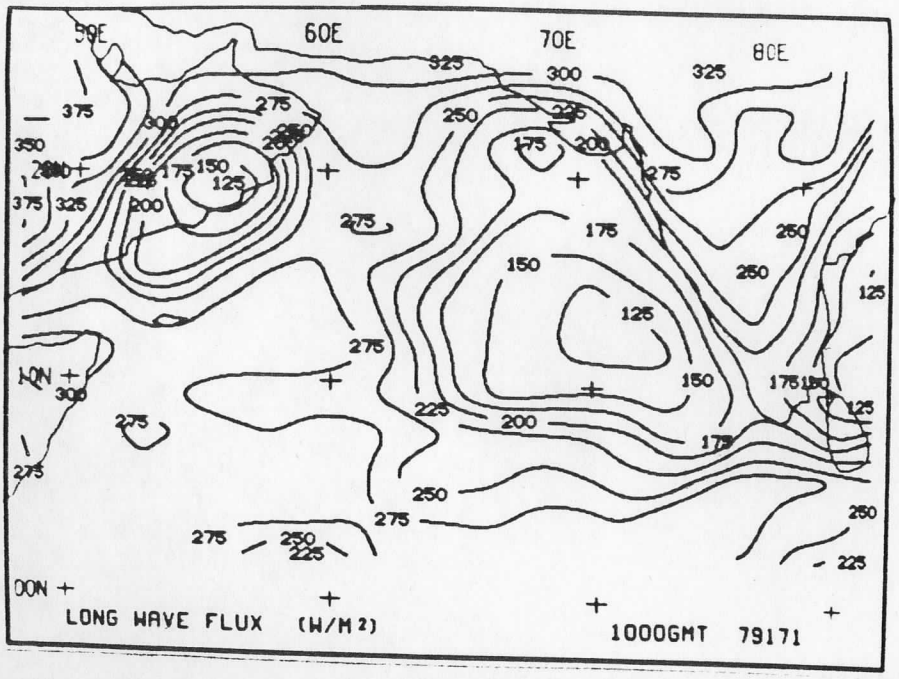
50E
60E
70E
80E
00N
LONG WAVE FLUX (W/M2)
1000GMT 79171

Fig. 3

A

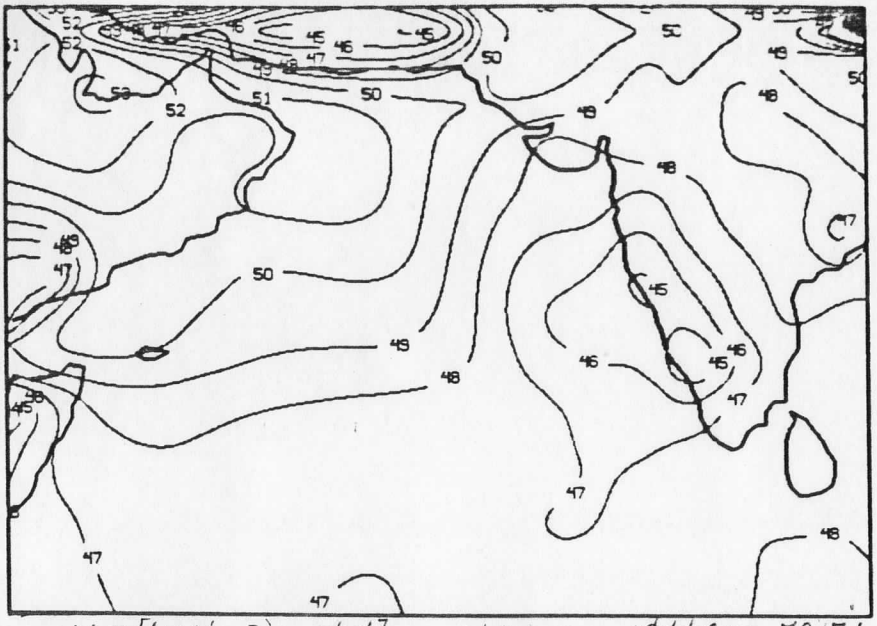

UF [(W/m²) x 1Φ⁻¹] 1ΦΦΦmb 1ΦΦΦGMT 79171

B

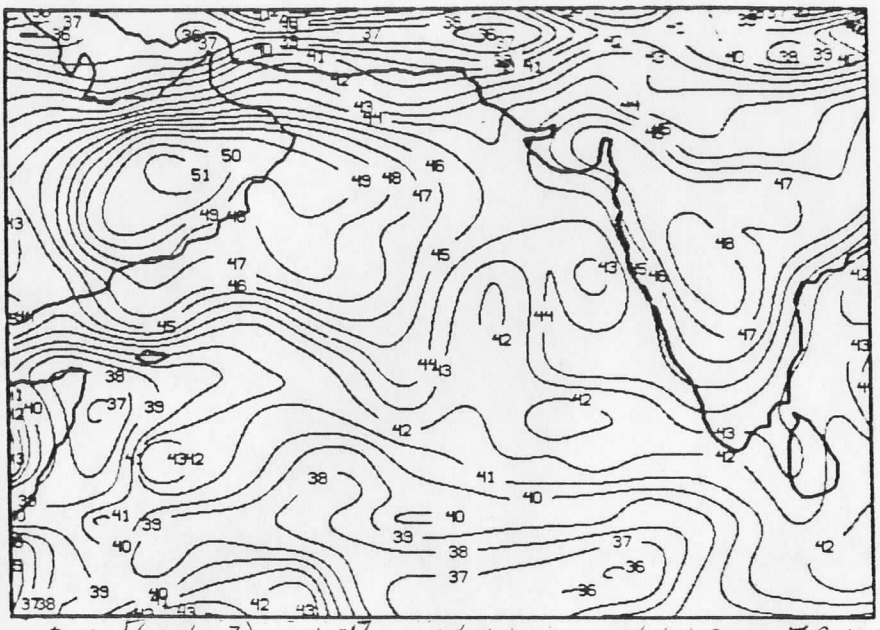

DF [(W/m²) x 1Φ⁻¹] 1ΦΦΦmb 1ΦΦΦGMT 79171

C

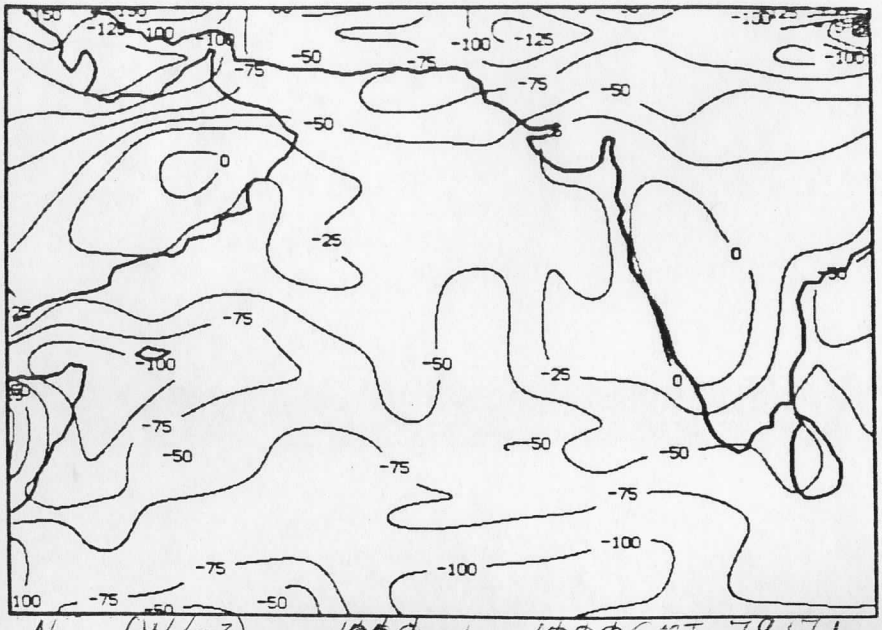

NET (W/m²) 1ΦΦΦmb 1ΦΦΦGMT 79171

Fig. 4

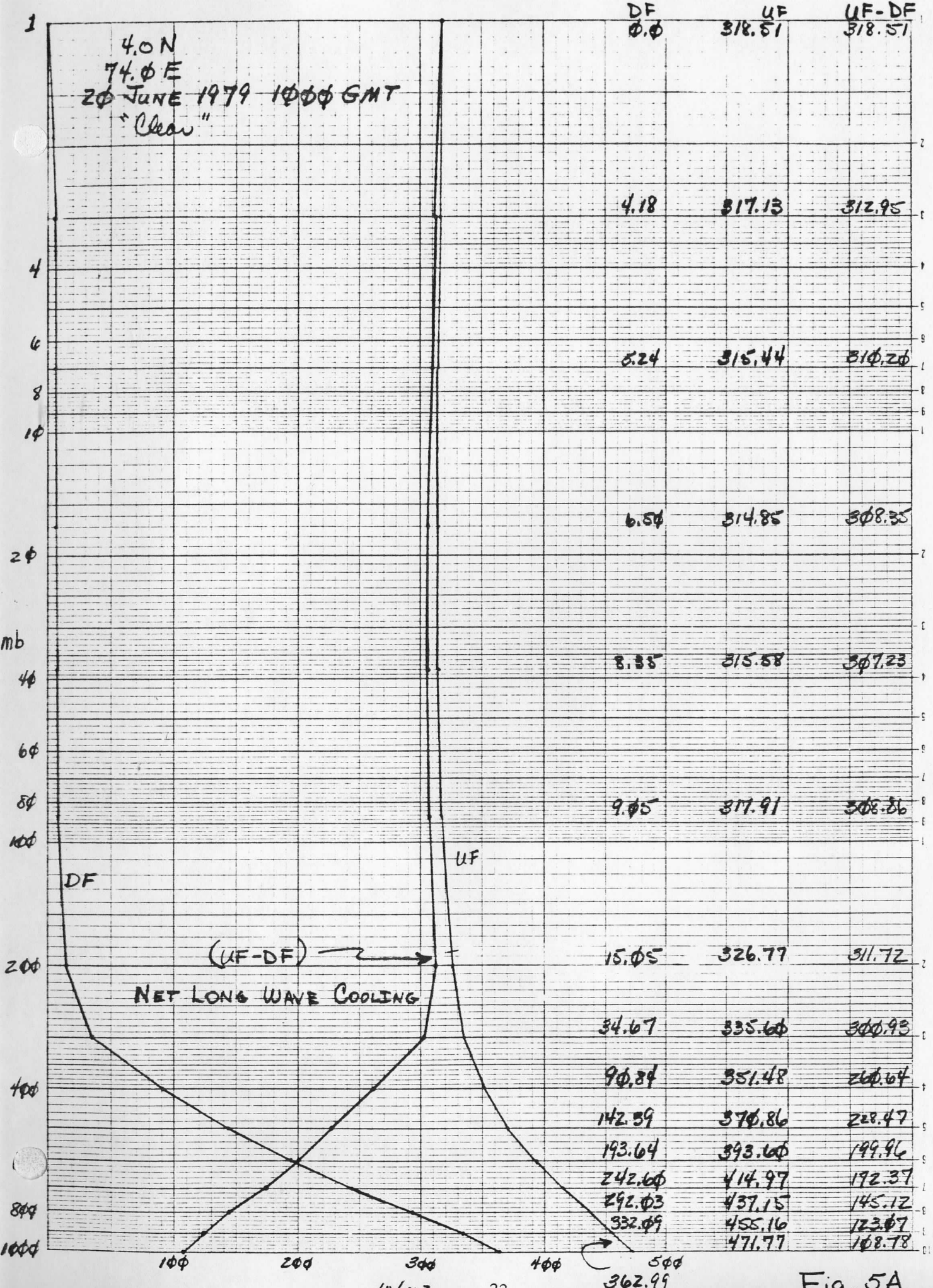

DF	UF	UF-DF
0.0	318.51	318.51
4.18	317.13	312.95
5.24	315.44	310.20
6.50	314.85	308.35
8.38	315.58	307.23
9.05	317.91	308.86
15.05	326.77	311.72
34.67	335.60	300.93
90.84	351.48	260.64
142.59	370.86	228.47
193.64	393.60	199.96
242.60	414.97	192.37
292.03	437.15	145.12
332.09	455.16	123.07
362.99	471.77	108.78

Fig. 5A

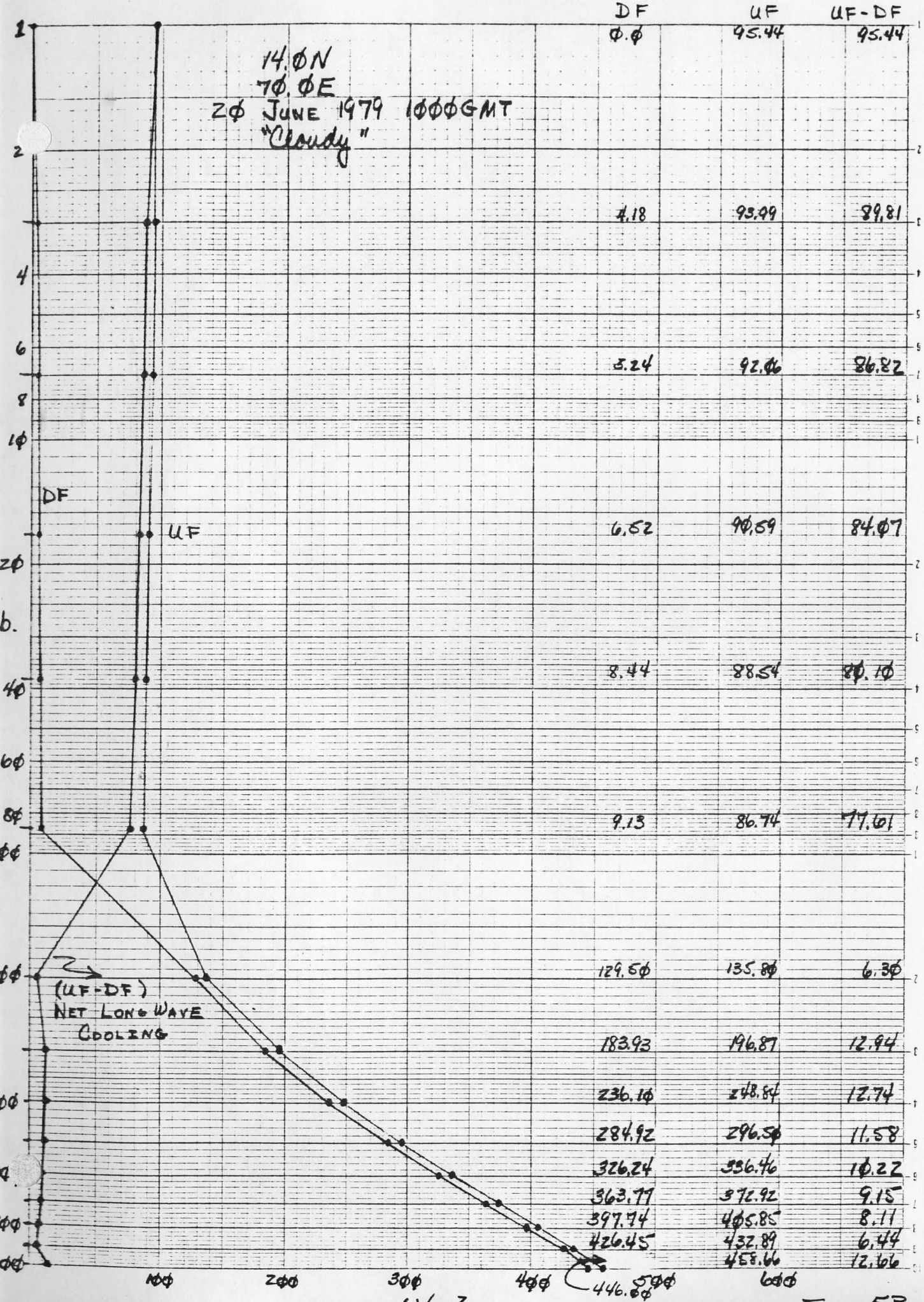

DF	UF	UF-DF
0.0	95.44	95.44
4.18	93.99	89.81
5.24	92.06	86.82
6.52	90.59	84.07
8.44	88.54	80.10
9.13	86.74	77.61
129.50	135.80	6.30
183.93	196.87	12.94
236.10	248.84	12.74
284.92	296.50	11.58
326.24	336.46	10.22
363.77	372.92	9.15
397.74	405.85	8.11
426.45	432.89	6.44
	458.66	12.66

Fig. 5B

A

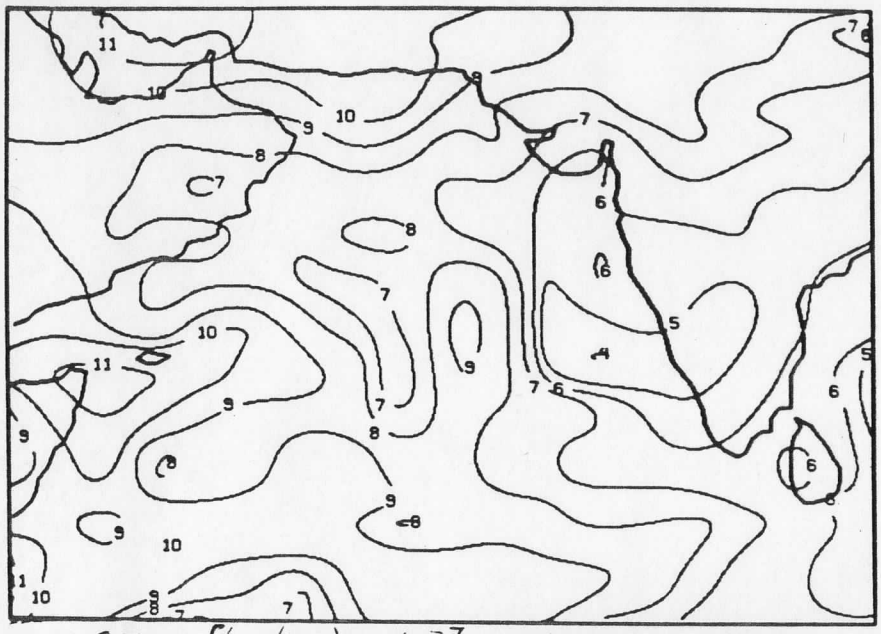

SFT [(W/m²) x 10⁻²] 1000GMT 79171

B

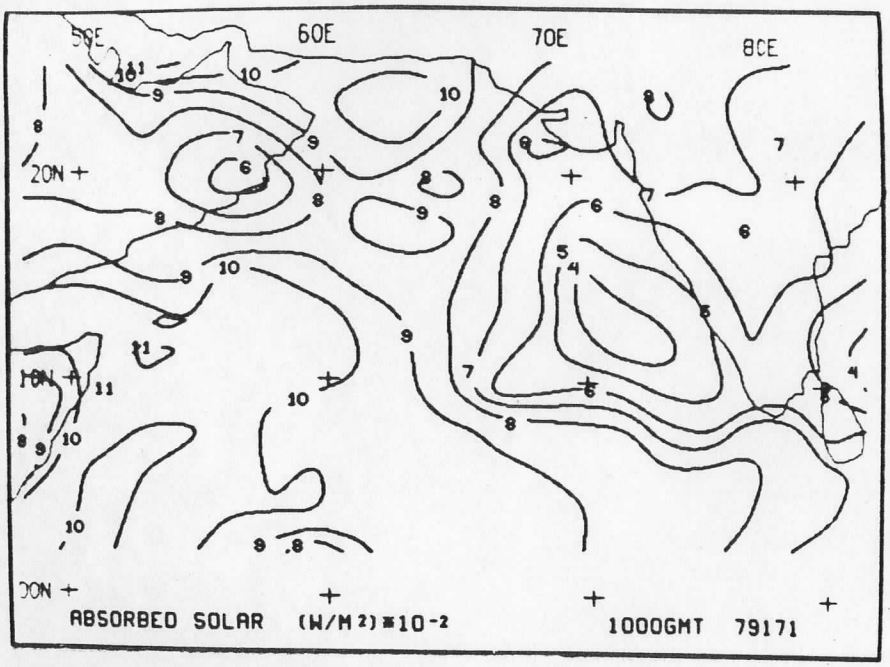

Fig. 6

A

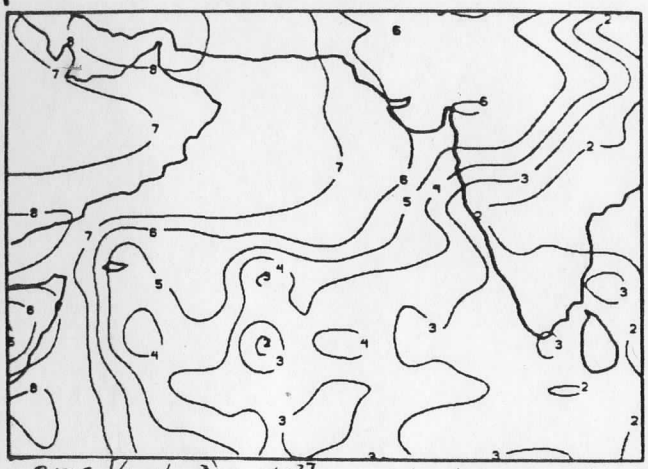

SFS [(W/m²) x 1Φ⁻²] 1ΦΦΦ GMT 79163

B

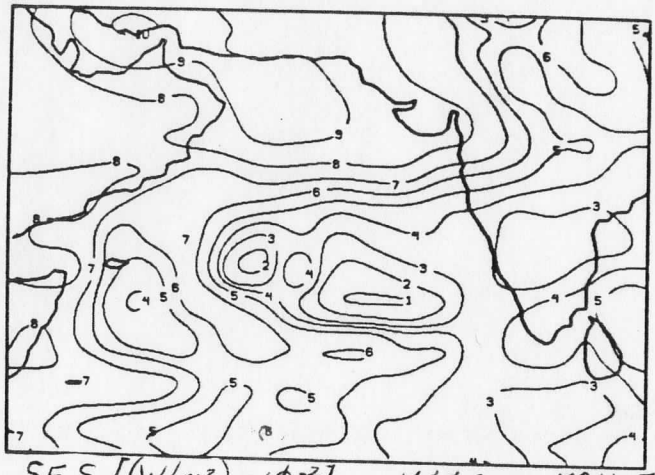

SFS [(W/m²) x 1Φ⁻²] 1ΦΦΦ GMT 79165

C

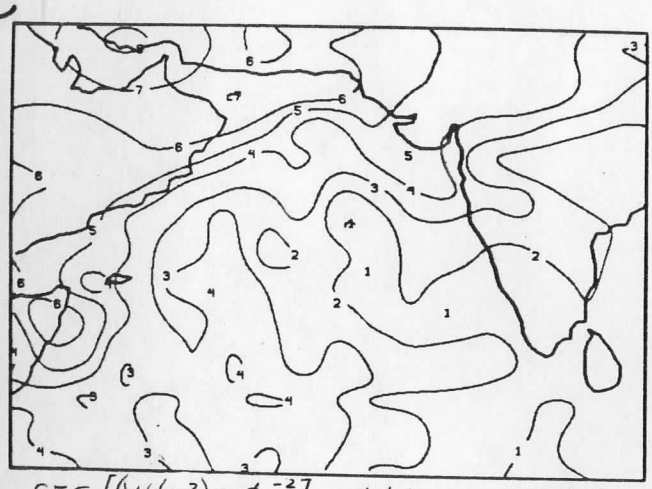

SFS [(W/m²) x 1Φ⁻²] 1ΦΦΦ GMT 79167

D

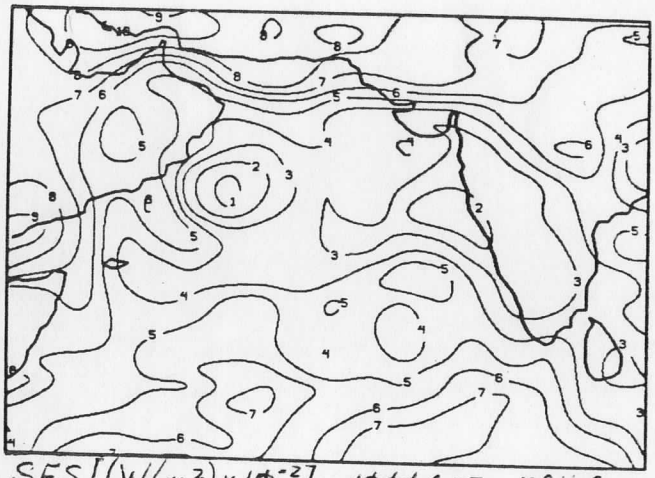

SFS [(W/m²) x 1Φ⁻²] 1ΦΦΦ GMT 79169

E

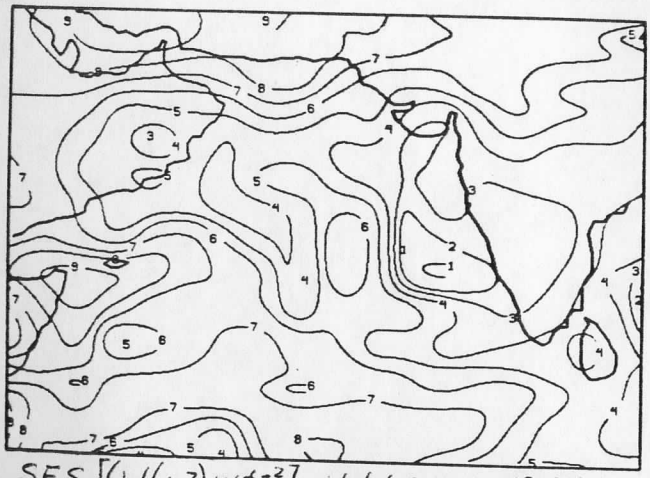

SFS [(W/m²) x 1Φ⁻²] 1ΦΦΦ GMT 79171

Fig. 7

A

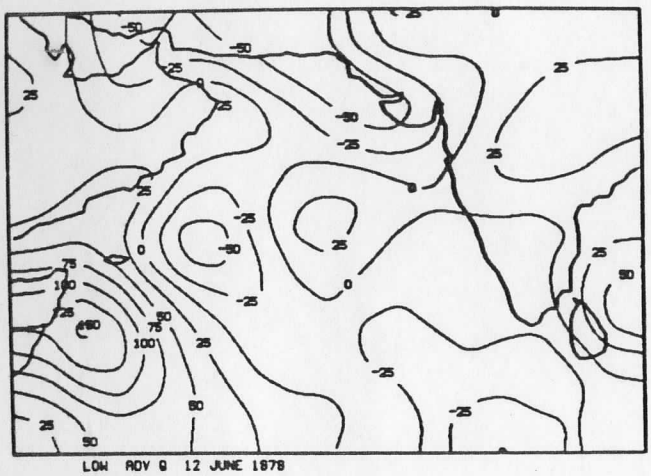
LOW ADV Q 12 JUNE 1878

B

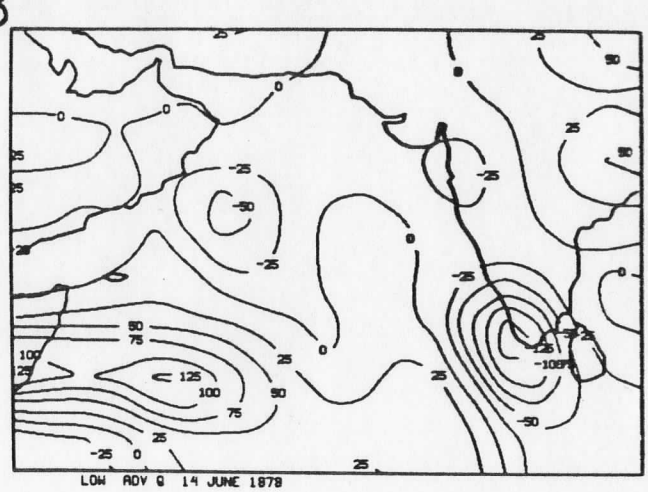
LOW ADV Q 14 JUNE 1878

C

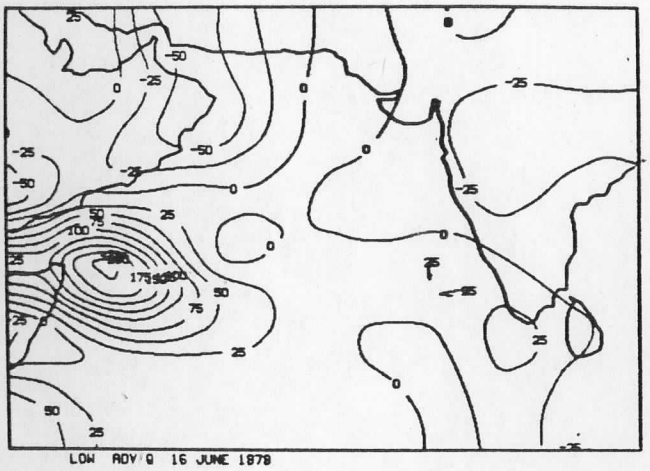
LOW ADV Q 16 JUNE 1878

D

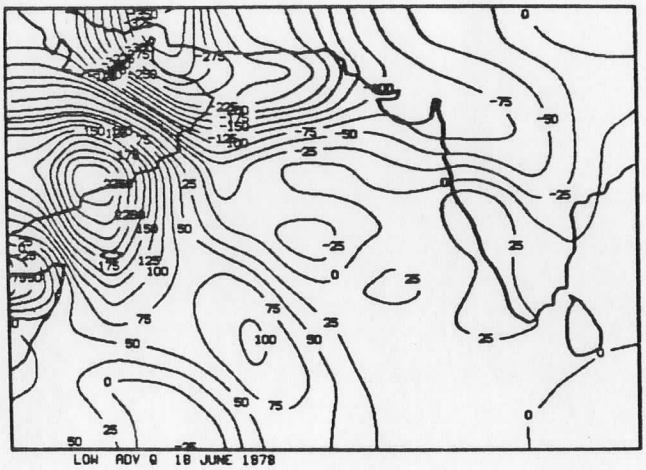
LOW ADV Q 18 JUNE 1878

E

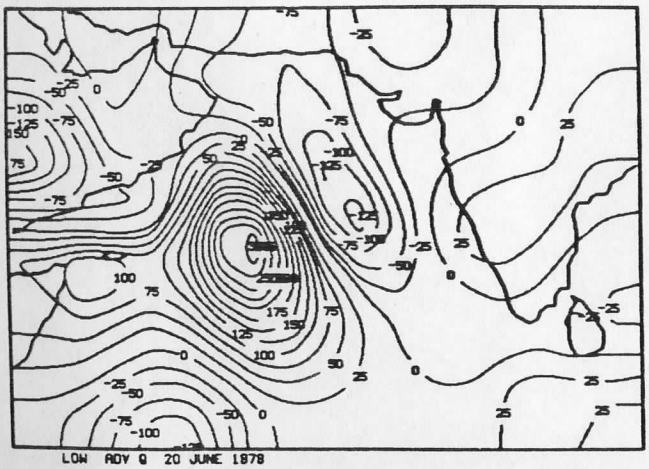
LOW ADV Q 20 JUNE 1878

Fig. 8

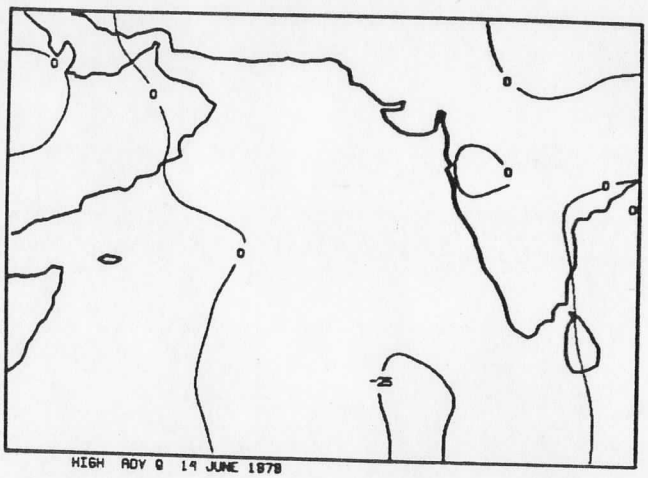

Fig 9

A

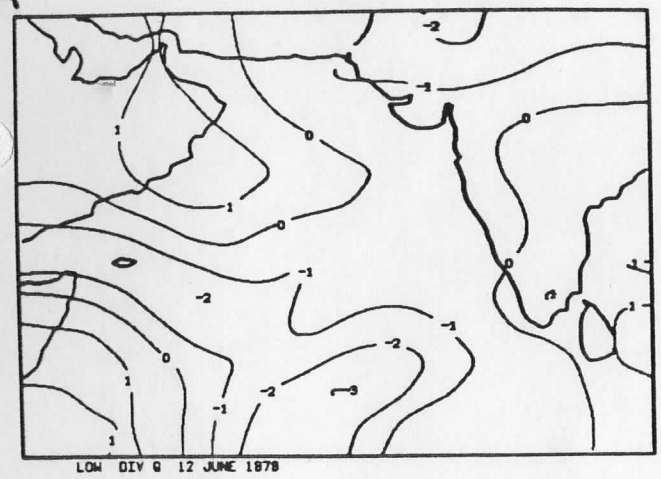
LOW DIV Q 12 JUNE 1878

B

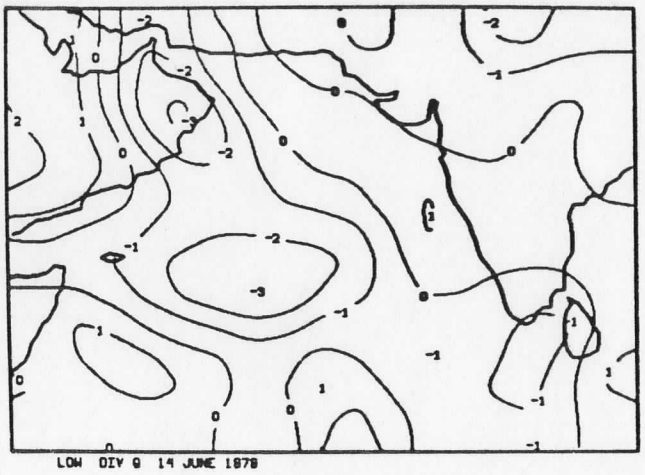
LOW DIV Q 14 JUNE 1878

C

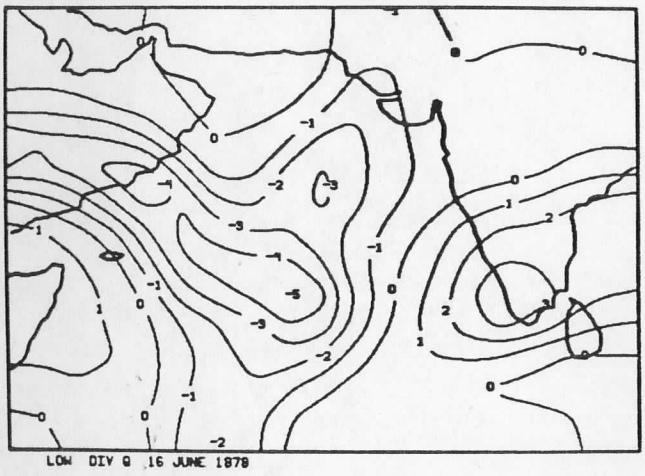
LOW DIV Q 16 JUNE 1878

D

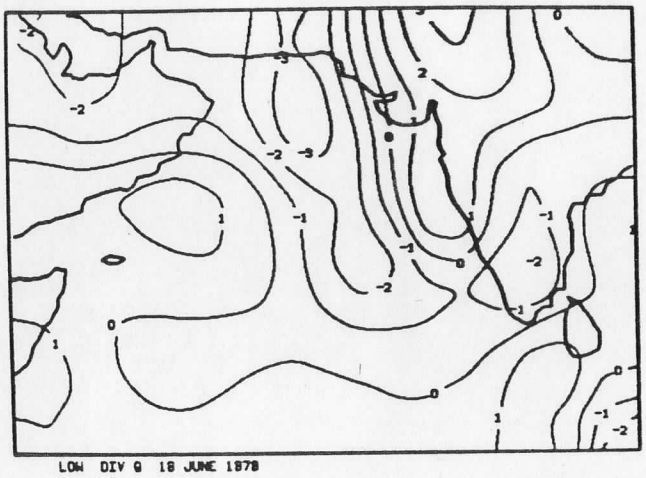
LOW DIV Q 18 JUNE 1878

E

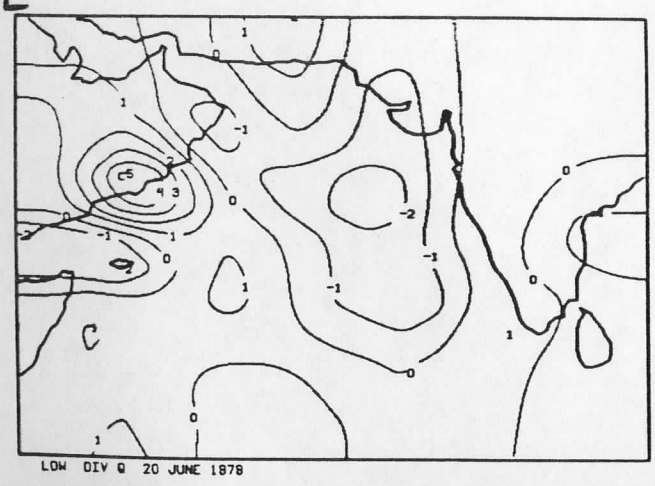
LOW DIV Q 20 JUNE 1878

Fig. 10

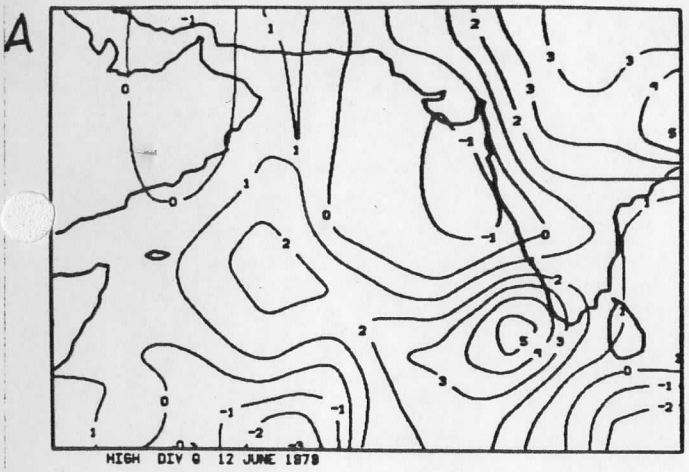
A
HIGH DIV Q 12 JUNE 1978

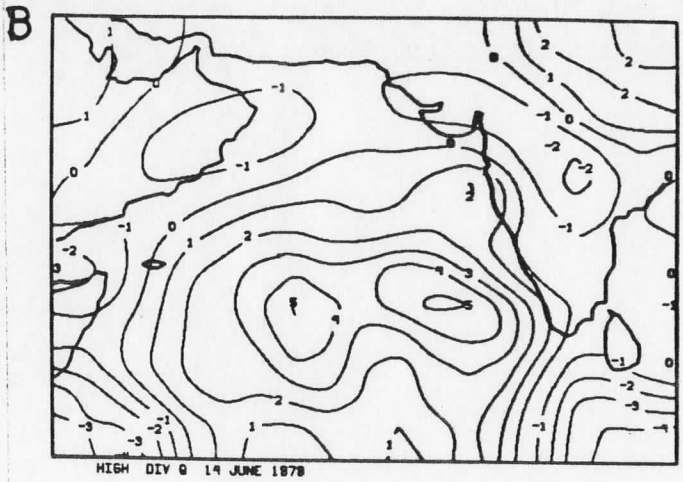
B
HIGH DIV Q 14 JUNE 1978

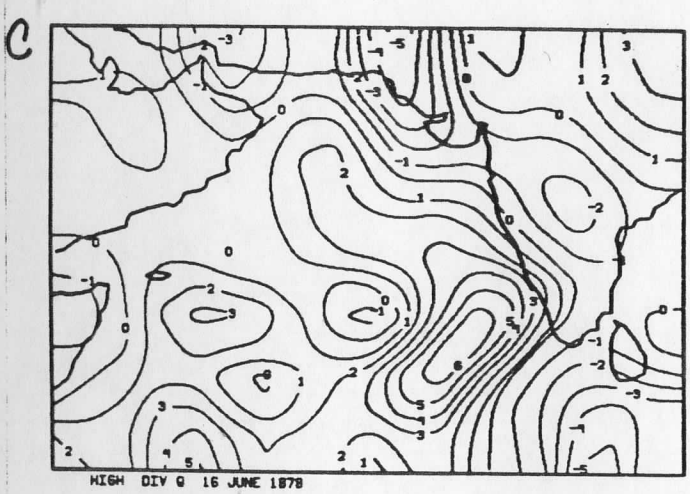
C
HIGH DIV Q 16 JUNE 1978

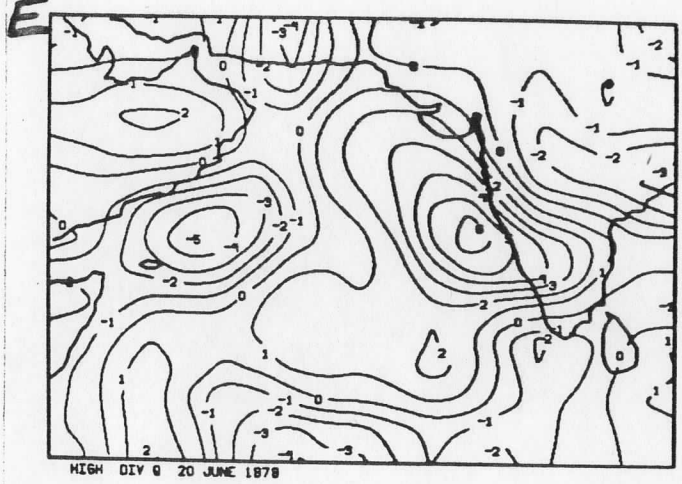
E
HIGH DIV Q 20 JUNE 1978

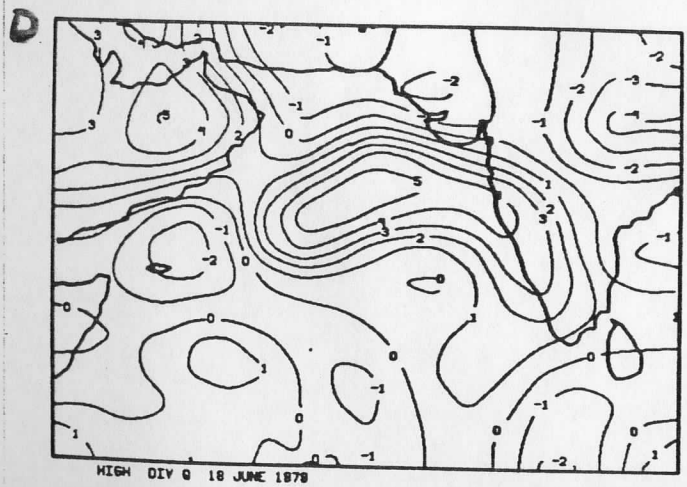
D
HIGH DIV Q 18 JUNE 1978

Fig. 11

A

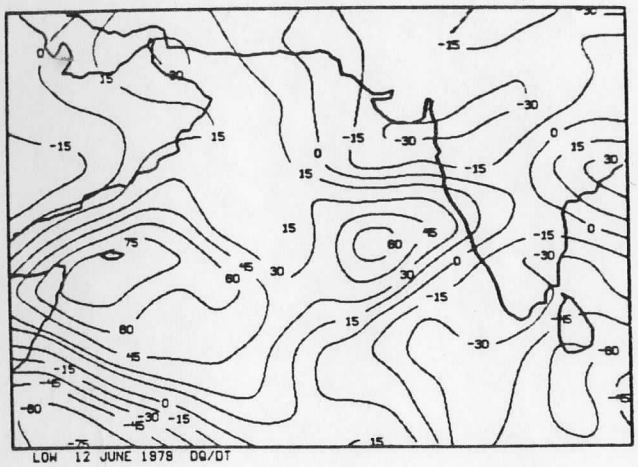
LOW 12 JUNE 1978 DQ/DT

B

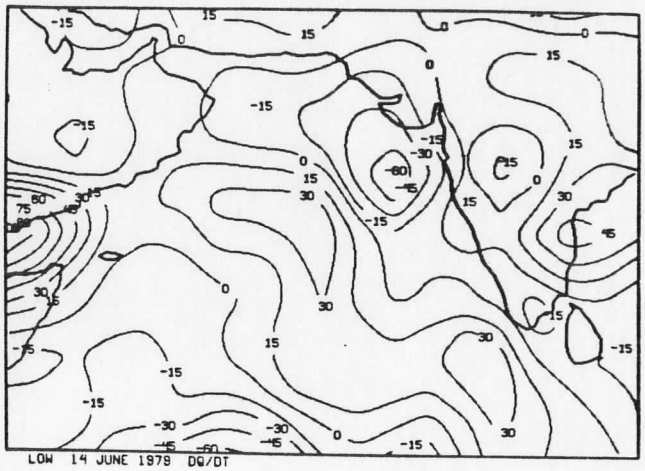
LOW 14 JUNE 1978 DQ/DT

C

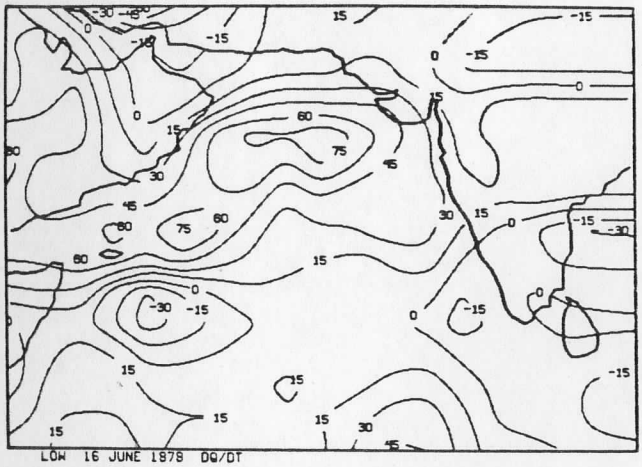
LOW 16 JUNE 1978 DQ/DT

D

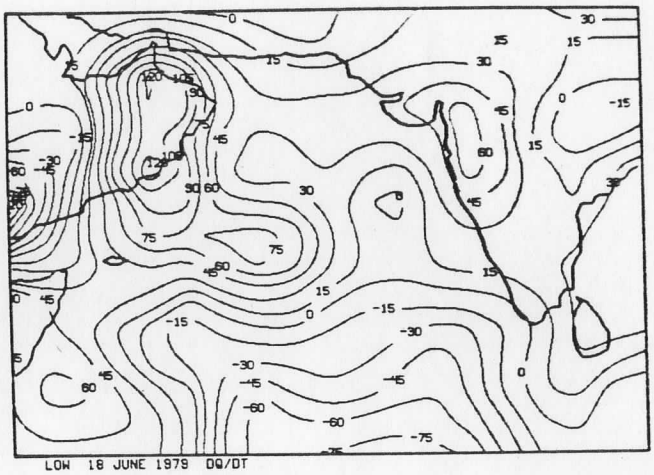
LOW 18 JUNE 1979 DQ/DT

E

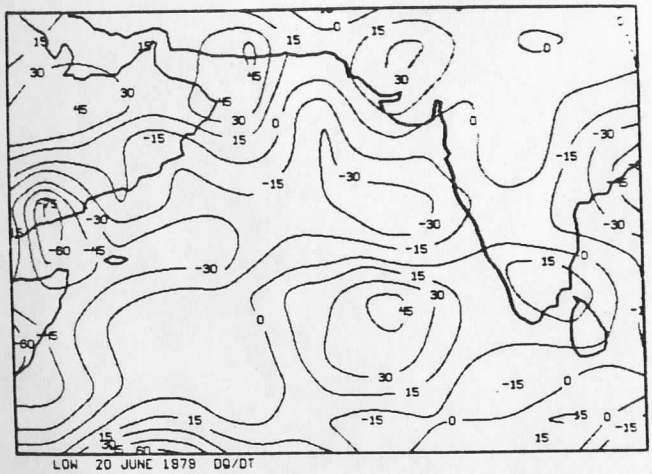
LOW 20 JUNE 1979 DQ/DT

Fig. 12

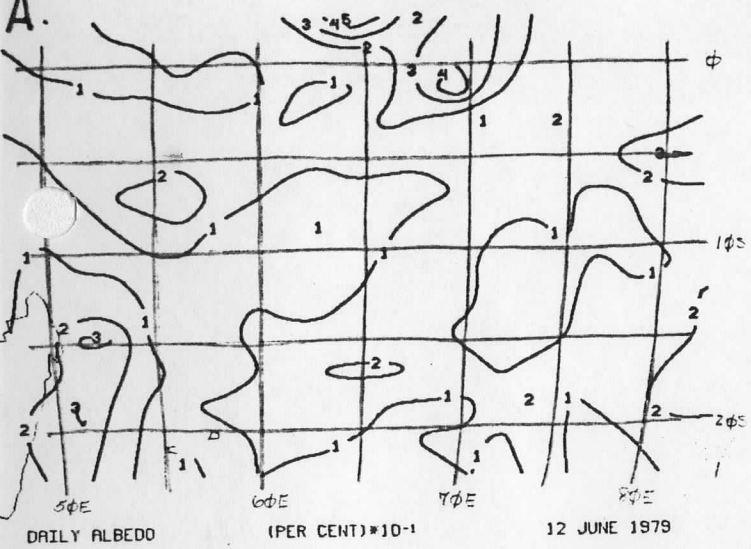
A.
DAILY ALBEDO
(PER CENT)*10⁻¹
12 JUNE 1979

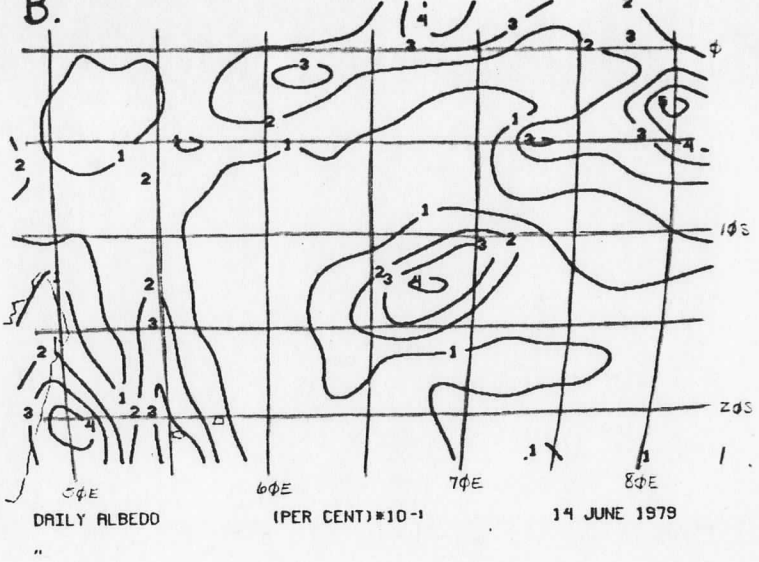
B.
DAILY ALBEDO
(PER CENT)*10⁻¹
14 JUNE 1979

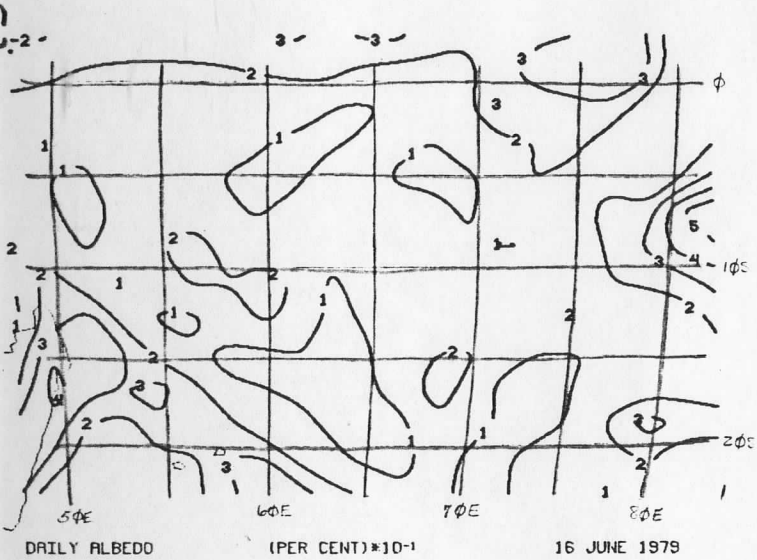
DAILY ALBEDO
(PER CENT)*10⁻¹
16 JUNE 1979

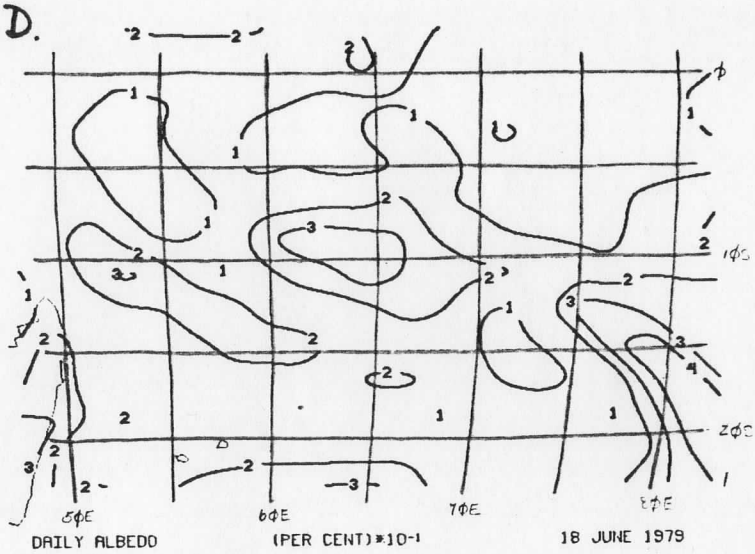
D.
DAILY ALBEDO
(PER CENT)*10⁻¹
18 JUNE 1979

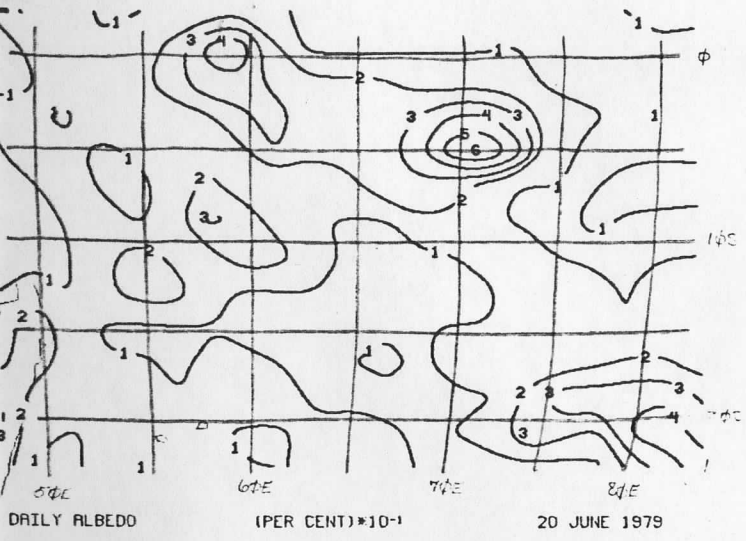
E.
DAILY ALBEDO
(PER CENT)*10⁻¹
20 JUNE 1979

Fig. 13

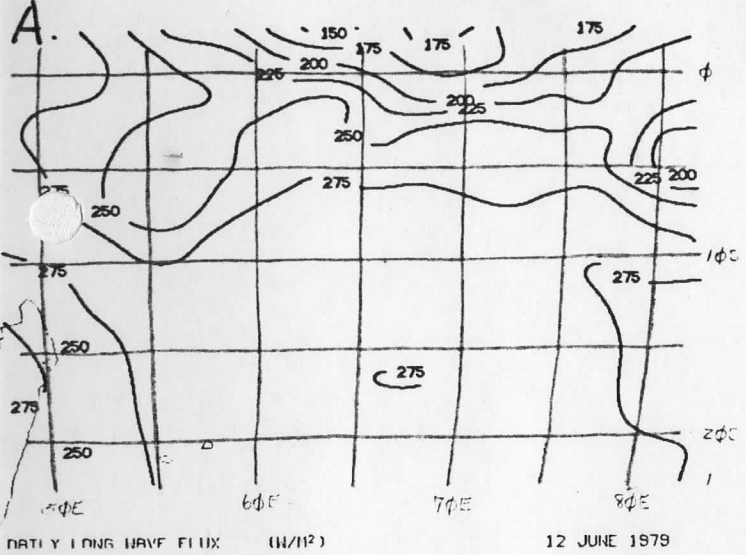
A.
DAILY LONG WAVE FLUX (W/M²)
12 JUNE 1979

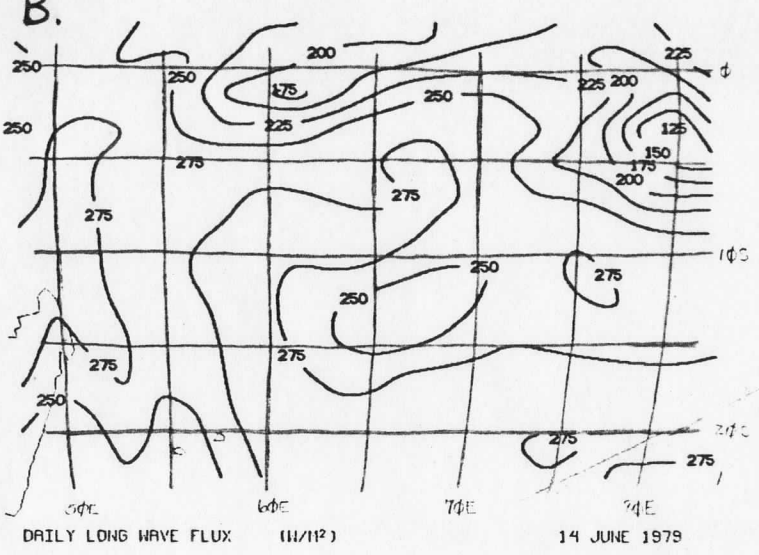
B.
DAILY LONG WAVE FLUX (W/M²)
14 JUNE 1979

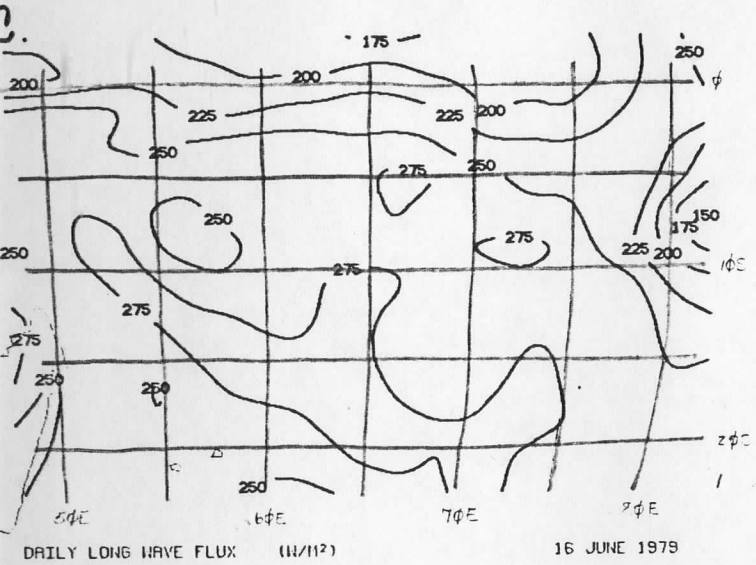
C.
DAILY LONG WAVE FLUX (W/M²)
16 JUNE 1979

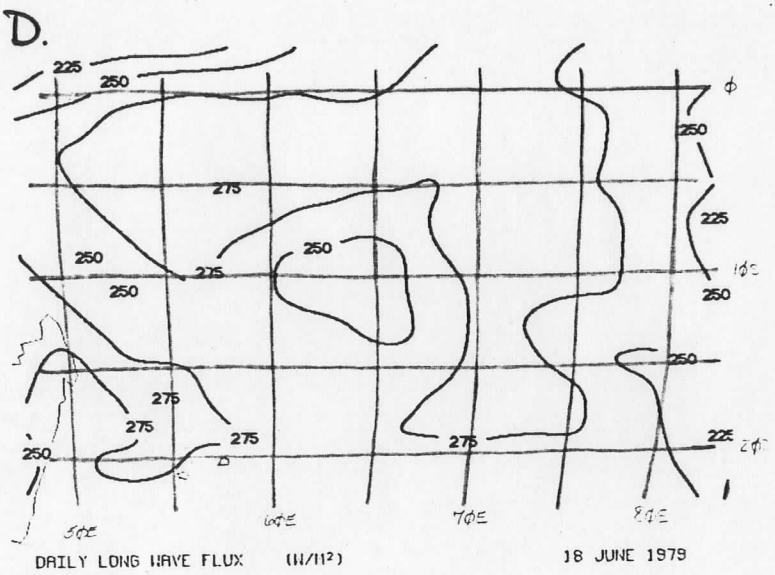
D.
DAILY LONG WAVE FLUX (W/M²)
18 JUNE 1979

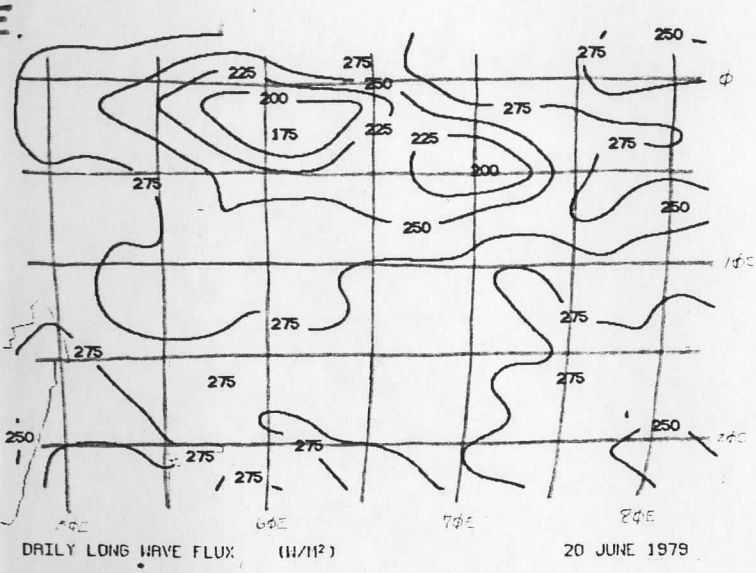
E.
DAILY LONG WAVE FLUX (W/M²)
20 JUNE 1979

Fig. 14

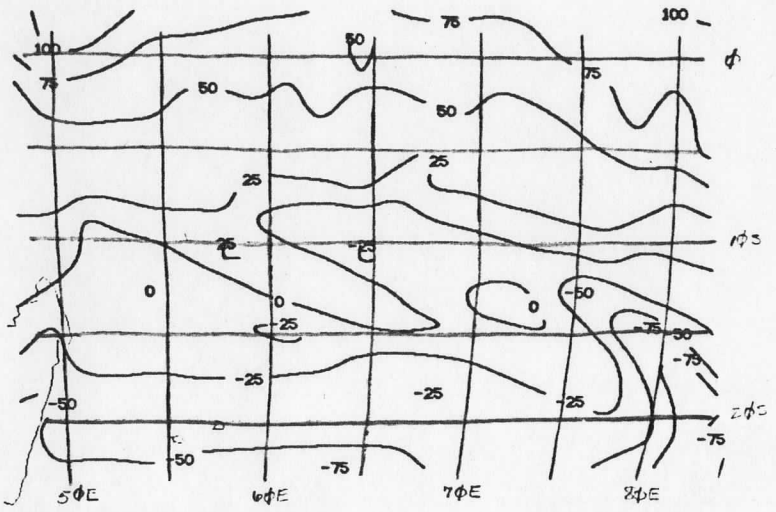

DAILY NET RADIATION (W/M²) 18 JUNE 1979

Fig. 15

V. REFERENCES

Chou, M-D, and A. Arking, 1980: Computation of Infrared Cooling Rates in the Water Vapor Bands. J. Atmos. Sci., 37, 855-867.

Chou, M-D, and A. Arking, 1981: An Efficient Method for Computing the Absorption of Solar Radiation by Water Vapor. J. Atmos. Sci., 38, 798-807.

Smith, W. L., L. D. Herman, A. Schreiner, H. B. Howell, and W. P. Menzel, 1981: Radiation Budget Characteristics of the onset of the summer monsoon. Proceedings of the internation conference on early results of FGGE and large-scale of its monsoon experiments, Tallahassee, FL, (ed. J.A. Young) pp. 6-16 through 6-26.

Smith, W. L., 1983: The Retrieval of Atmospheric Profiles from VAS Geostationary Radiance Observations. J. Atmos. Sci., 40, 2025-2035.

Virji, H., 1982: Analysis of Aircraft and Satellite Radiation During Summer MONEX. Final Report to NSF, University of Wisconsin, pp.30.

Virji, H., A. J. Schreiner, W. L. Smith, and L. D. Herman, 1982: Earth-Atmosphere Radiation Balance from Geostationary Satellite Data for the Summer Monsoon Onset Region. University of Wisconsin-Madison. National Science Foundation, p. 252.

Virji, H., W. L. Smith, A. J. Schreiner, L. Herman, W. P. Menzel, 1982: Satellite Derived Earth and Atmosphere Energy Balance Components During the Summer MONEX. Proceedings of the International Conference on the Scientific Results of the Monsoon Experiment, Deupasar, Bali, Indonesia, WMO, ICSU, pp.1-46 through 1-52.

Virji, H. and L. D. Herman, 1984: The Regional Cloud Distribution During the Onset Phase of the 1979 Summer Monsoon Based on GOES-I Imagery. J. Clim. and Atmos. Sci. (Submitted)

EARTH-ATMOSPHERE RADIATION BALANCE FROM GEOSTATIONARY SATELLITE DATA FOR THE SUMMER MONSOON ONSET REGION

SUMMER MONEX ONSET PERIOD: 11-20 June 1979

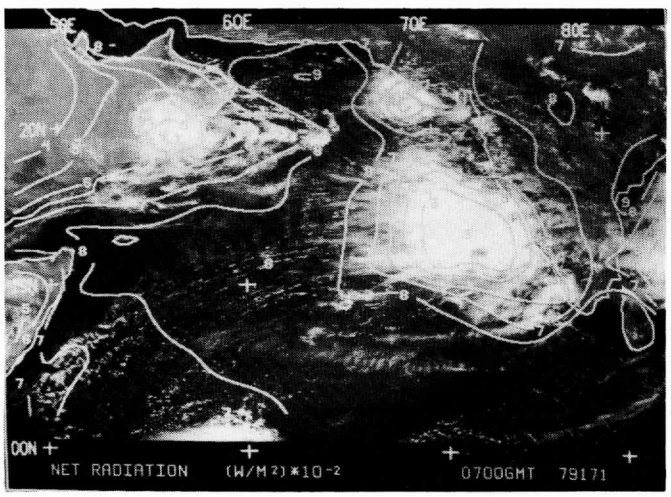

By

H. Virji

A. J. Schreiner

Space Science and Engineering Center

and

W. L. Smith

L. D. Herman

NOAA/NESS Development Laboratory

University of Wisconsin - Madison

December 1982

National Science Foundation, under grant ATM-8205386

Table of Contents

EARTH-ATMOSPHERE RADIATION BALANCE FROM GEOSTATIONARY SATELLITE DATA FOR THE SUMMER MONSOON ONSET REGION

1. Introduction

During the 1979 Summer Monsoon Experiment (MONEX) radiometers were flown aboard the NASA CV-990 aircraft to calibrate the narrow angle spectral-window scanning radiometer aboard the GOES-1 geosynchronous satellite stationed over the Indian Ocean. The purpose of the calibration was to enable accurate diagnoses of the detailed radiation budget characteristics throughout the life cycle of the summer monsoon circulation. GOES-1 measurements are ideal for this purpose because they possess both high spatial and high temporal resolution (1 km in the visible and 8 km in the infrared, half hourly sampling frequency). The interpretation of these data in terms of radiation budget parameters requires relationships for transforming the narrow spectral band narrow angle directional measurements of reflected and emitted radiation in the visible and infrared spectral window regions (0.5-0.9 μm and 11-12 μm, respectively) into broadband (0.2-4 μm and 4-100 μm) angularly integrated radiation fluxes of reflected solar and emitted terrestrial radiation. Such algorithms are presented in section 2. Estimates of the components of the earth-atmosphere radiation balance and top albedo obtained from application of these algorithms to the GOES-1 radiance data for the period 11-20 June 1979 form the basis of this atlas.

It is intended that this atlas be used as a reference for the evolution of the earth-atmosphere radiation balance during the onset phase of the summer monsoon. The atlas provides (a) hourly and daily averaged fields of the top radiation balance components and (b) mean diurnal variation characteristics of these parameters. GOES-1 VIS/IR imagery is also included in order to relate the evolution of the monsoon cloud cover to radiation balance. The flux data

has been interpolated, gridded and analyzed for easy inspection of the satellite derived radiation balance components. Computer tapes containing the complete data set are available from the Space Science and Engineering Center at the University of Wisconsin-Madison.

2. Algorithms

The NASA CV-990 aircraft flown during MONEX carried narrow band and broadband, narrow angle, directional radiometers (Smith et al., 1978) and broadband flux radiometers (Ackerman and Cox, 1980) to enable:

a) The calibration of the GOES-1 0.5-0.9 μm detector digital output in terms of the reflectance of solar radiance within this spectral band.

b) The specification of different relationships, dependent upon earth surface and cloud condition, between earth atmosphere reflectance observations in the GOES 0.5-0.9 μm region and the broadband reflectance observed over the 0.3-4 μm region.

c) The specification of a relationship between broadband directional reflectance measured at small local zenith angles and broadband angularly integrated albedo.

The relationships provided by (a)-(c) above are used to determine instantaneous or temporally averaged albedo and absorbed solar radiation from the GOES-1 visible channel data.

The GOES-1 infrared window (11-12.5 μm) observations are calibrated in terms of total outgoing longwave radiation flux using a relationship based on simultaneous GOES-1 and TIROS-N multi-spectral (HIRS) radiometer data. The TIROS-N multi-spectral water vapor, carbon dioxide, ozone, and window radiation emission measurements over the 3.7-16 μm region were transformed into total

terrestrial flux values spectrally and angularly integrated using a relationship based upon theoretical calculations. GOES-1 IR data was not calibrated using the aircraft pyrgeometer flux measurements directly because of the problem of registering the fields of view of the narrow angle satellite radiometer and the wide angle aircraft pyrgeometer and because of the significant contribution to the total outgoing longwave flux from the upper troposphere and stratosphere above the aircraft. Intercomparison of the TIROS-N longwave flux estimates with high altitude longwave flux observations by pyrgeometers aboard the CV-990, however, compared to within 5% over a wide range of homogeneous surface conditions (i.e., cloud-free desert, cloud-free ocean, and extended cloud).

The relationships between the GOES-1 radiometer data and shortwave and longwave fluxes were obtained using data from several CV-990 flights over a variety of surface and cloud conditions (e.g., desert, vegetation, ocean, and opaque and semi-transparent cloud). Table 1 summarizes the characteristics of these flights.

TABLE 1
CHARACTERISTICS OF CV-990 FLIGHTS USED FOR CALIBRATION ANALYSIS

Date	Flight	Origin	Objective
May 14	10	Dhahran	Saudi Arabia Land/Sea Heating Differential (Albedo of Desert and Ocean)
June 5	15	Bombay	Albedo Survey of North-Central India (Albedo of Vegetated Terrain)
June 12	18	Bombay	Land/Sea Heating Differential Along N-S Meridian (75E) (Albedo of Ocean and Terrain)
June 15	20	Bombay	Monsoon Flow Pattern (Albedo of Clouds)
June 18	22	Bombay	Monsoon Flow Pattern (Albedo of Clouds)

The selection of time and space coincident aircraft, GOES-1 and TIROS-N radiation observation values was accomplished using the Man-computer Interactive Data Access System (McIDAS) developed by the University of Wisconsin (Suomi and Menzel, 1980). The GOES-1 and TIROS-N images, coincident in space and nearly at the same time as CV-990 flights, were stored in sequence in McIDAS for processing with the aircraft information. The aircraft flight track was superimposed on the images at 10 minute time intervals using the McIDAS graphics capability. Nearly colocated aircraft and satellite data were then selected manually by placing a cursor on the TV image of the satellite data at the appropriate position along the aircraft flight track. The manual selection of the space and time coincident data insured that the viewing conditions were homogeneous with the area encompassing the fields of view of the aircraft and satellite borne radiometers.

Table 2 shows the linear regression equations and their standard errors of regression used to describe the relation between the various radiometric data. It is noted that only relations (1) and (4) depend directly on the GOES-1 data. Relations (2) are achieved from the multi-spectral radiometer (MSR) 0.3-4.0 μm and 0.5-0.9 μm (matched GOES-1 filter) directional radiances observed from the CV-990 and relation (3) is obtained from CV-990 MSR 0.3-4.0 μm directional radiance observed at small view angles and simultaneous 0.3-4.0 μm flux pyronometer observations. Relation (4) is obtained from nearly colocated GOES-1 and TIROS-N infrared radiance observations.

TABLE 2
RESULTS OF REGRESSION ANALYSIS USED TO DETERMINE GOES-1 ALBEDO AND LONGWAVE FLUX CALIBRATION RELATIONS

	Equation	N	RMS	CC	Condition
1:	$r_g=0.0000164C_g-0.00077$	116	0.052	0.98	All
2:	(a) $r_b=0.749r_g+0.01747$	65	0.003	0.99	Ocean
	(b) $r_b=0.736r_g+0.02385$	55	0.007	0.99	Thin Cloud
	(c) $r_b=0.600r_g+0.08849$	48	0.012	0.99	Thick Cloud
	(d) $r_b=0.840r_g+0.03116$	32	0.007	0.99	Vegetation
	(e) $r_b=0.781r_g+0.08399$	92	0.003	0.99	Desert
3:	$A=1.174r_b$	91	0.023	0.99	All
4:	$F=0.543\sigma T_g^4+44.538$	83	12 w/m^2	0.99	All

C_g ≡ the square* of the digital brightness (0-255) obtained from the GOES-1 visible channel detectors divided by the cosine of the solar zenith angle and earth-sun distance factor.
r_g ≡ reflectance for the GOES-1 spectral region (0.5-0.9μm) as measured from CV-990.
r_b ≡ broadband (0.3-4.0 μm) reflectance as measured from CV-990.
A^b ≡ broadband angularly integrated albedo as measured from CV-990.
F ≡ longwave radiation flux (w/m^2) as measured from TIROS-N.
T_g ≡ GOES-1 brightness temperature (°K).
σ ≡ Stefan-Boltzman constant (5.66×10^{-8} w/m^2-deg^{-4}).
N ≡ number of observations used to obtain linear fit.
RMS≡ root mean square deviation of data from linear fit.
CC ≡ correlation coefficient.
* The digital brightness count is generated from a function of the square root of the detector output (radiance).

The relationships (1)-(3) are applied to the GOES-1 visible channel data in a step-wise fashion to estimate the shortwave flux reflected to space from the area viewed. After equation (1) is applied to the linearized GOES-1 digital data (digital count squared divided by the cosine of the solar zenith angle and the earth sun distance factor), the appropriate relation between broadband and GOES-1 narrow band reflectance is chosen on the basis of: (a) land or ocean,

(b) the GOES-1 reflectance value (the result of equation (1)), and (c) the corresponding GOES-1 infrared brightness temperature value. The thresholds used to specify the appropriate relationship are given in Table 3.

TABLE 3
CRITERIA FOR SELECTING PROPER RELATION BETWEEN BROADBAND AND GOES-1 VISIBLE BAND REFLECTANCE

Equation	Condition	Reflectance/IR Brightness Temperature Condition	
		Land	Ocean
2(a)	Ocean		$r_g \leq 0.15$
2(b)	Thin Cloud	$0.28 < r_g \leq 0.50$, $T_g < 290$	$0.15 \leq r_g \leq 0.50$
2(c)	Thick Cloud	$r_g > 0.50$	$r_g > 0.50$
2(d)	Vegetation	$r_g \leq 0.28$, $T_g \geq 290$	
2(e)	Desert	$0.28 \leq r_g \leq 0.50$, $T_g \geq 290$	

The result of equation (2) is then used in (3) to obtain an estimate of the albedo, A. Subsequently the reflected solar flux is calculated using the relation

$$F_s = AI_o\mu_o d \qquad (5)$$

where I_o is constant, 1375 w/m^2 (Hickey et al., 1980), d is the earth-sun distance factor (square of the ratio of the solid angle subtended by the sun at the time of the observation and the annual mean value), and μ_o is the cosine of the solar zenith angle at the location of the viewed spot. The longwave flux, F_L, is then estimated using equation (4). Spatial averages of the 8 km resolution values over 250 x 250 km areas are then calculated. For each 250 km area (approximately 2° x 2°) the absorbed solar radiation flux

$$F_A = I_o\mu_o d - F_s \qquad (6)$$

and the net radiation flux,

$$F_N = F_A - F_L \tag{7}$$

are calculated. Daily average values are obtained from an integration of hourly results.

It is noted that for the region analyzed, the variability in the GOES infrared radiance observations due solely to view angle variations (i.e., limb darkening) is negligible and therefore not taken into account. Also, variations in the visible channel radiance due to the angular dependence of target reflectance is not taken into account because this variability is small compared to the reflectance variability within and among the 250 x 250 km sample regions due to cloudiness. For the Arabian Desert, which is generally devoid of cloudiness, the implicit diffuse scattering assumption is valid because of the sand surface.

3. Analyzed fields for the monsoon onset region

a. Hourly fields

All data from 26°N to Equator and 46°E to 84°E were analyzed on a 2° x 2° grid. No analysis was performed when hourly GOES-1 data was unavailable. Such instances are labelled as "NO DATA" in this atlas. The few cases when the satellite imagery was of questionable quality due to bad scan lines are labelled as "?." The times of unavailable and questionable satellite products are listed in Table 4. Out of a total of 240 time periods analyzed from 11-20 June 1979, the satellite products were missing or of questionable quality around 6% of the time.

TABLE 4
A Listing of Unavailable or Questionable
GOES-1 VIS/IR Data During the Onset Period

DATE 1979 June	HOUR (GMT)	STATUS OF GOES-1 DATA VIS	IR
11	00	N	N
	01-04		N
	14-15	N	N
13	06-15		Q
	16	N	N
15	13		Q
16	10	N	N
18	11	Q	Q
19	10	Q	Q

N: No data Q: Data quality questionable

The analyzed hourly radiative flux fields for the above period are shown in Plates 1-240. These fields depict the evolution of the earth-atmosphere radiation balance components during the formation of the onset vortex of 1979 summer monsoon. The well defined hourly variability in the structure of these fields describes the diurnal modulation of the flux parameters. For five selected locations, the average diurnal variation in the top radiation balance parameters during the onset phase is shown in Plates 251-252. These locations were selected as representative of the general conditions over the Saudi Arabian desert, the clear region in north central Arabian Sea, the Indian sub-continent, the equatorial trough region, and the low level jet region off the Somali coast.

b. Daily averaged fields

The hourly flux values were integrated and analyzed to obtain the daily averaged top radiation balance components. The mean top albedo represents an integration of seven consecutive hourly top albedo values per day, centered around the local noon hour at 12°N, 65°E. In contrast, the daily average flux values represent an integration over all hours of the day. For the few cases when the hourly data was unavailable or of questionable quality, the flux

values were interpolated from the nearest available hourly data before performing the integration into daily averages. As the GOES-1 infrared radiance data for the first 5 hours of 11 June 1979 were unavailable, the daily averaged flux values for this day may not be very reliable at individual grid locations.

The daily averaged fields of the radiation balance components for the monsoon onset phase are shown in Plates 241-250. A description of the evolution of the major features of the radiation balance components based upon these fields is given in Smith et al. (1981).

4. Acknowledgments

The material contained in this atlas is part of an ongoing cooperative research program between the scientists at the NOAA/NESDIS Development Laboratory and the Space Science and Engineering Center, University of Wisconsin-Madison. The diligent efforts of the scientists of the above groups are gratefully acknowledged. Tom Rust processed photographs of GOES imagery and analyses taken on the McIDAS facility and Gail Turluck typed the manuscript. This work is funded by the National Science Foundation (NSF) under grant ATM-8205386; we gratefully acknowledge the enthusiastic support of J. Fein and P. Stephens of NSF for this work.

5. References

Ackerman, S., and S. K. Cox, 1980: Colorado State University Radiation Instrumentation and Data Reduction Procedures for the CV-990 During Summer MONEX. Colorado State University, Atmospheric Science Paper No. 325, Fort Collins, Colorado.

Hickey, J. R., F. House, H. Jacobowitz, R. H. Maschoff, P. Pellegrino, L. L. Stowe, and T. H. Vonder Haar, 1980: Initial Solar Irradiance Determinations from Nimbus-7 Cavity Radiometer Measurements. Science, 208, 281-283.

Smith, W. L., D. Q. Wark, P. G. Abel, and S. K. Cox, 1978: The CV-990 Multi-spectral Scanning Radiometer (MSR) Measurement Program for the MONEX. Proposal to the National Science Foundation from the National Environmental Satellite Service (NOAA), Washington, D.C.

Smith, W. L., L. D. Herman, T. Schreiner, H. B. Howell, and P. Menzel, 1981: Radiation budget characteristics of the onset of the summer monsoon. Proceedings of the International Conference on Early Results of FGGE and Large Scale Aspects of its Monsoon Experiments, Tallahassee, Florida.

Suomi, V. E., and P. Menzel, 1980: The University of Wisconsin VAS Data Processing System. Report to NASA under Contract NAS5-21965 from the Space Science and Engineering Center, University of Wisconsin, Madison, Wisconsin.

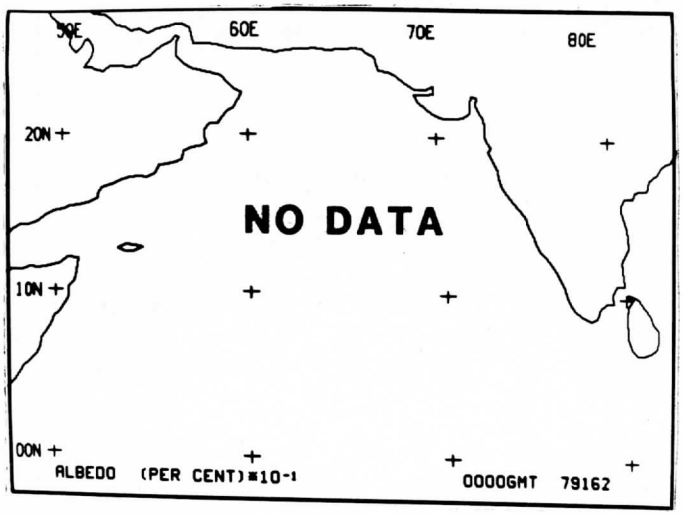
50E
60E
70E
80E
20N
10N
0ON
NO DATA
ALBEDO (PER CENT)*10-1
0000GMT 79162

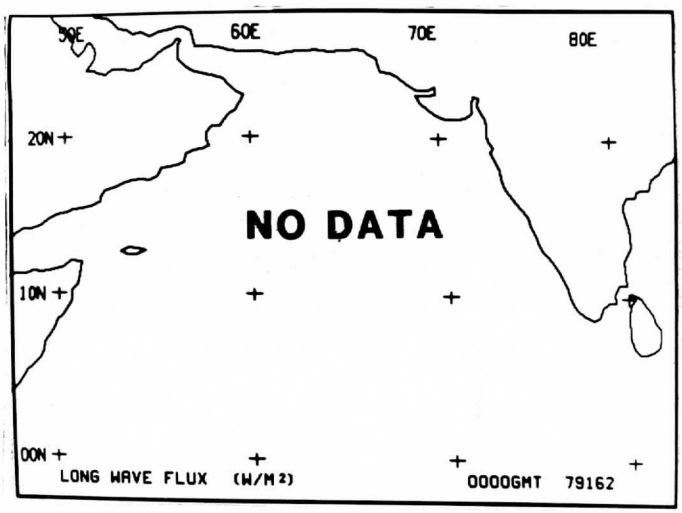
50E
60E
70E
80E
20N
10N
0ON
NO DATA
LONG WAVE FLUX (W/M2)
0000GMT 79162

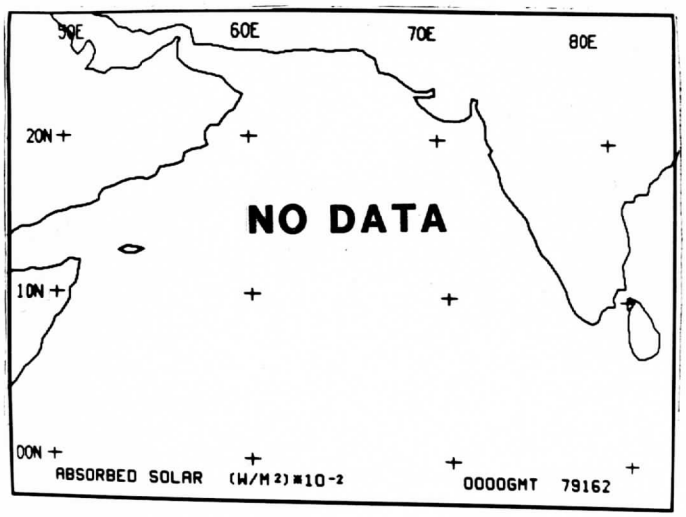
50E
60E
70E
80E
20N
10N
0ON
NO DATA
ABSORBED SOLAR (W/M2)*10-2
0000GMT 79162

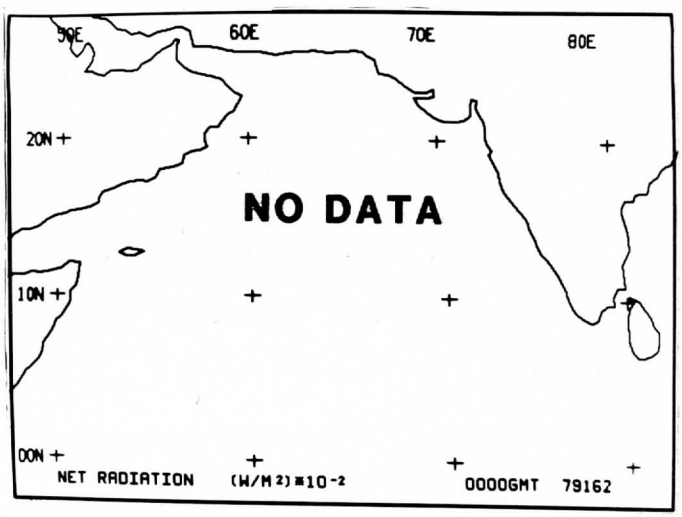
50E
60E
70E
80E
20N
10N
0ON
NO DATA
NET RADIATION (W/M2)*10-2
0000GMT 79162

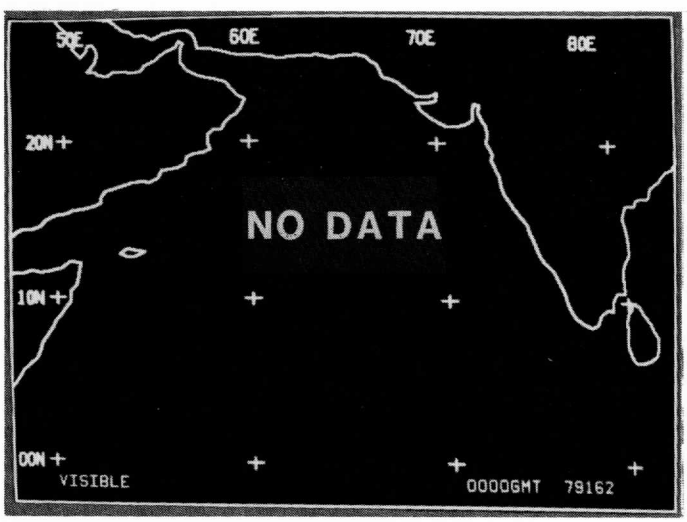
50E
60E
70E
80E
20N
10N
0ON
NO DATA
VISIBLE
0000GMT 79162

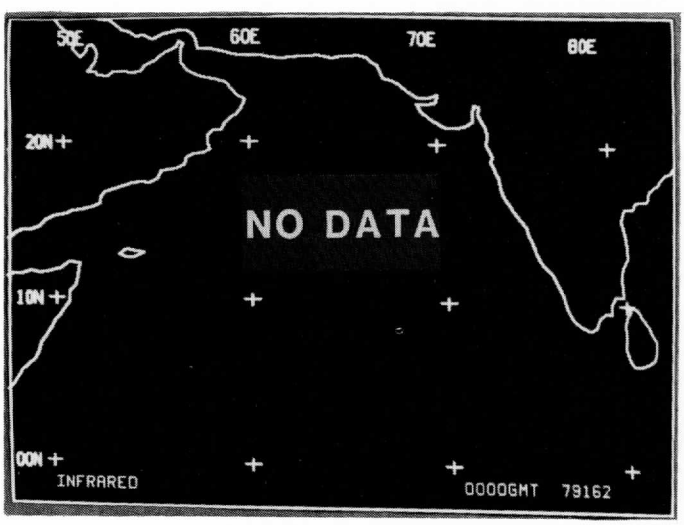
50E
60E
70E
80E
20N
10N
0ON
NO DATA
INFRARED
0000GMT 79162

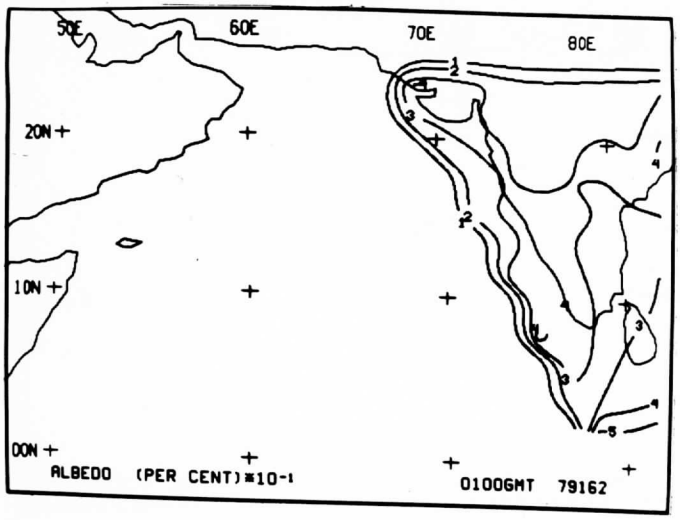
50E
60E
70E
80E
20N
10N
0ON
ALBEDO (PER CENT)×10-1
0100GMT 79162

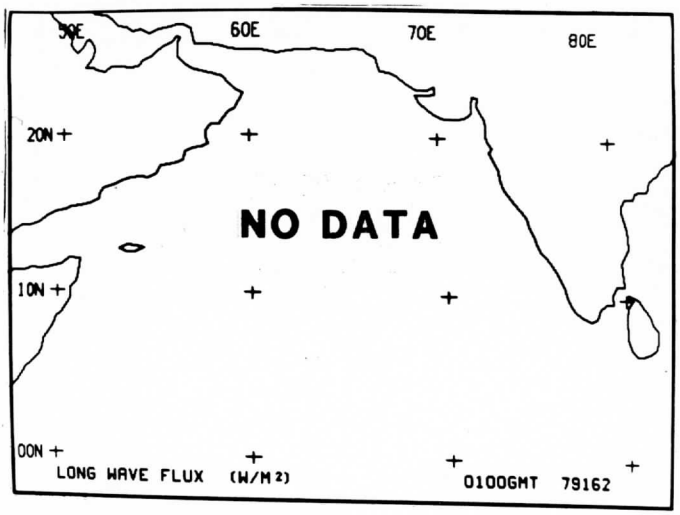
50E
60E
70E
80E
20N
10N
0ON
NO DATA
LONG WAVE FLUX (W/M2)
0100GMT 79162

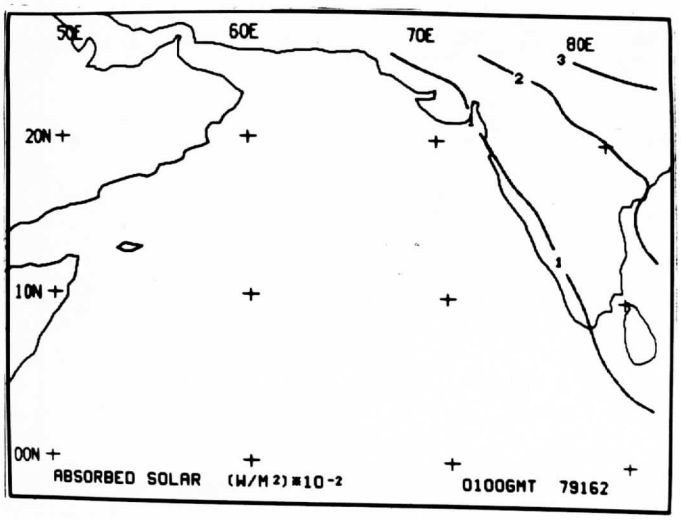
50E
60E
70E
80E
20N
10N
0ON
ABSORBED SOLAR (W/M2)×10-2
0100GMT 79162

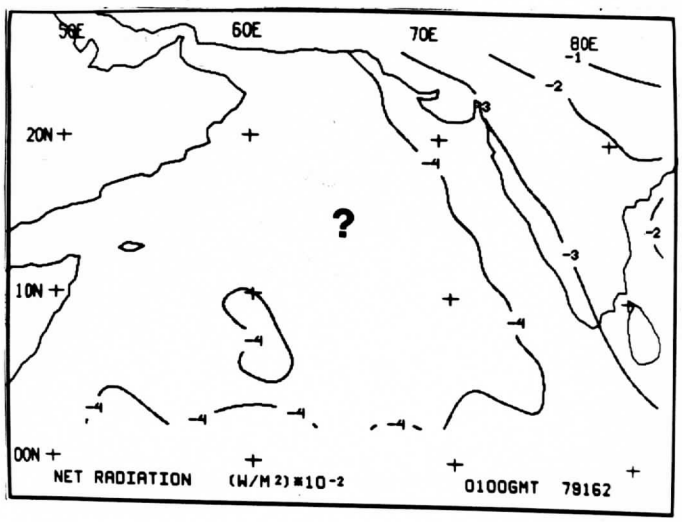
50E
60E
70E
80E
20N
10N
0ON
?
NET RADIATION (W/M2)×10-2
0100GMT 79162

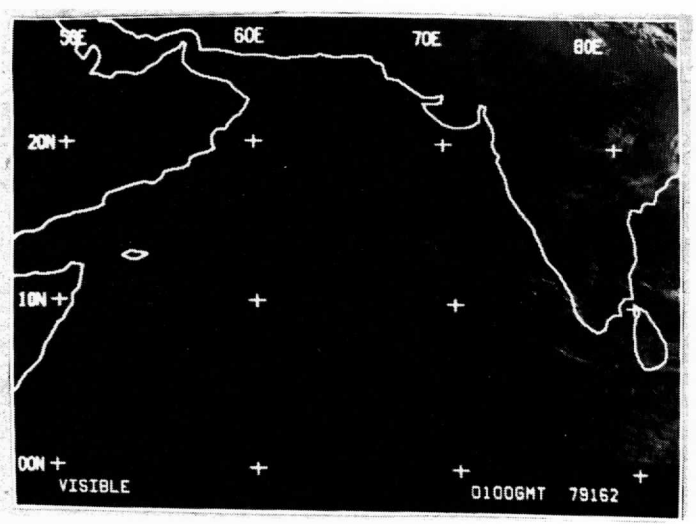
50E
60E
70E
80E
20N
10N
0ON
VISIBLE
0100GMT 79162

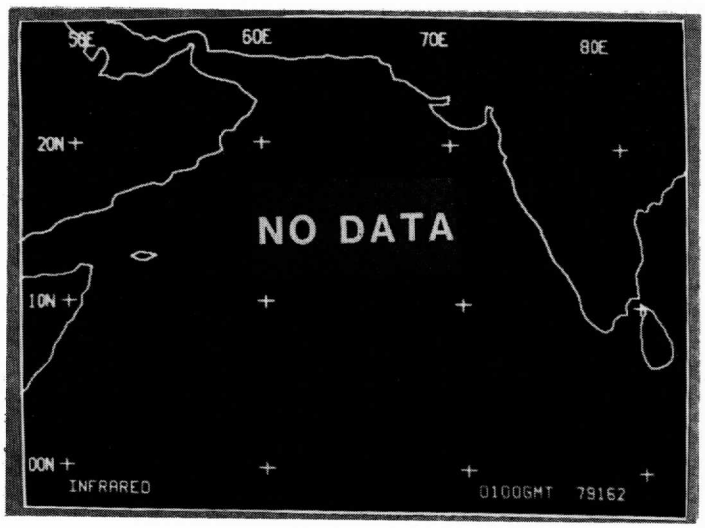
50E
60E
70E
80E
20N
10N
0ON
NO DATA
INFRARED
0100GMT 79162

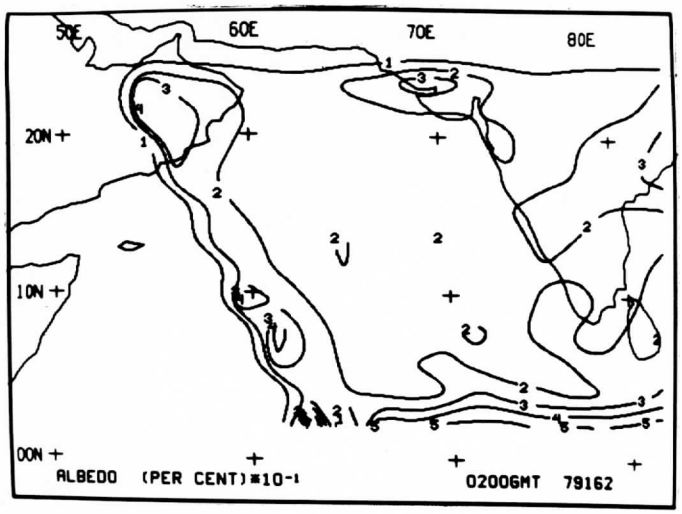
50E
60E
70E
80E
20N
10N
0ON
ALBEDO (PER CENT)*10-1
0200GMT 79162

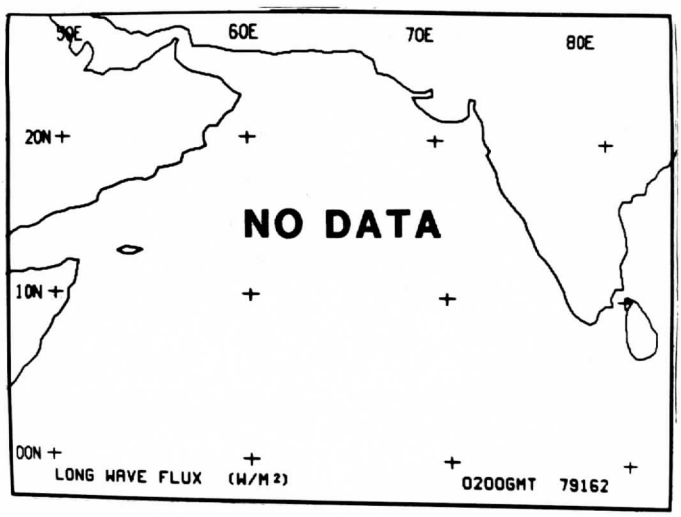
50E
60E
70E
80E
20N
10N
0ON
NO DATA
LONG WAVE FLUX (W/M2)
0200GMT 79162

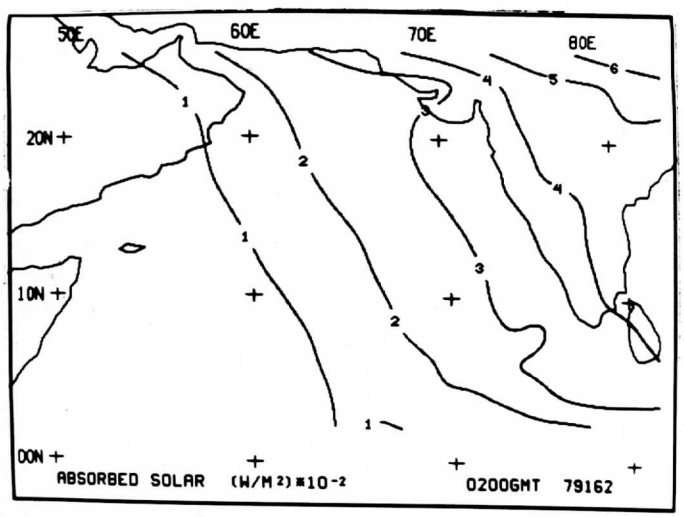
50E
60E
70E
80E
20N
10N
0ON
ABSORBED SOLAR (W/M2)*10-2
0200GMT 79162

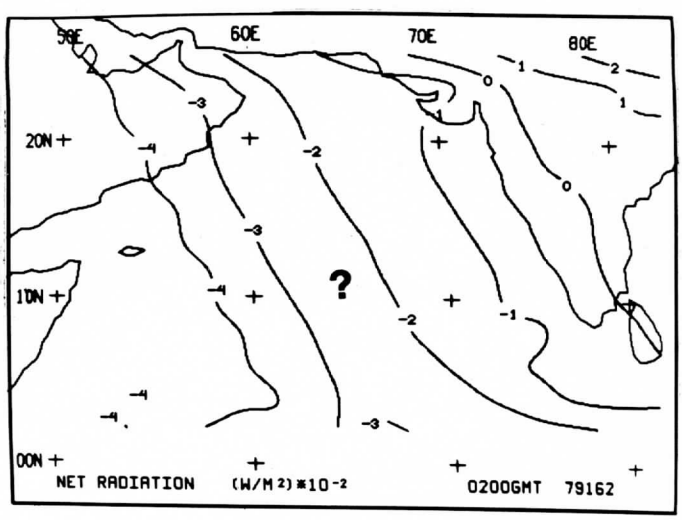
50E
60E
70E
80E
20N
10N
0ON
?
NET RADIATION (W/M2)*10-2
0200GMT 79162

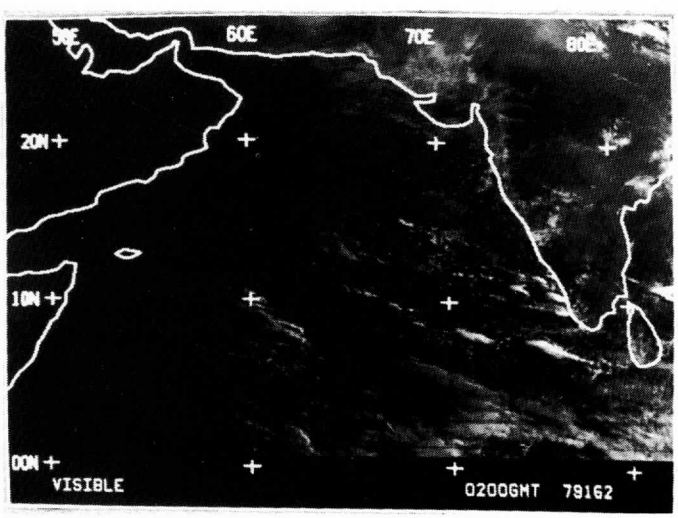
50E
60E
70E
80E
20N
10N
0ON
VISIBLE
0200GMT 79162

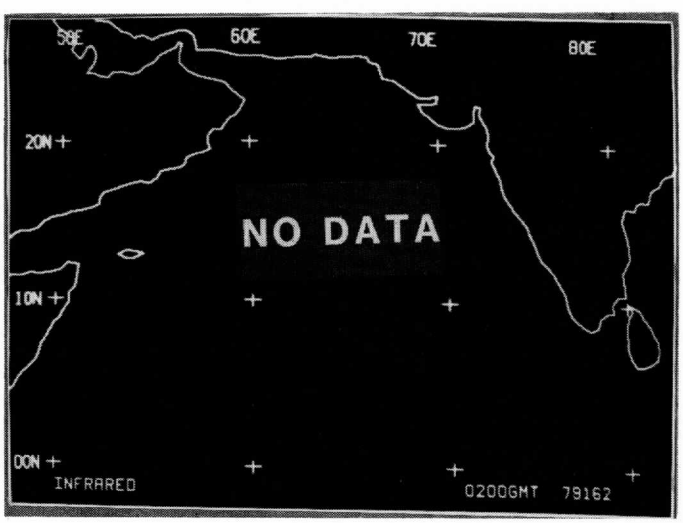
50E
60E
70E
80E
20N
10N
0ON
NO DATA
INFRARED
0200GMT 79162

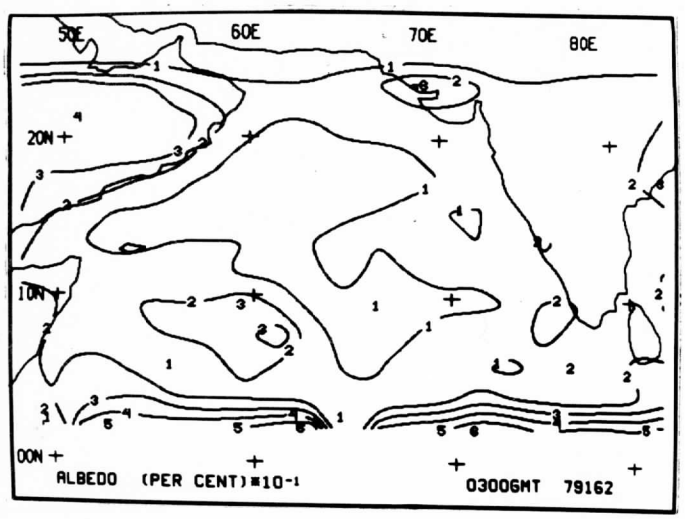
50E
60E
70E
80E
20N
10N
0ON
ALBEDO (PER CENT)*10-1
0300GMT 79162

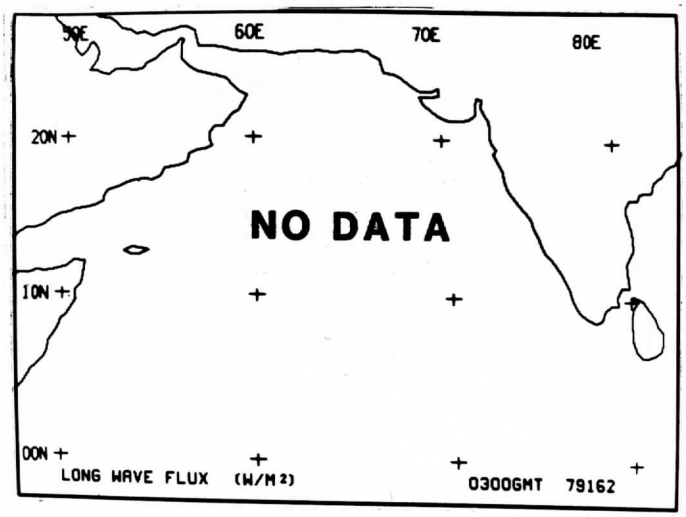
50E
60E
70E
80E
20N
10N
0ON
NO DATA
LONG WAVE FLUX (W/M2)
0300GMT 79162

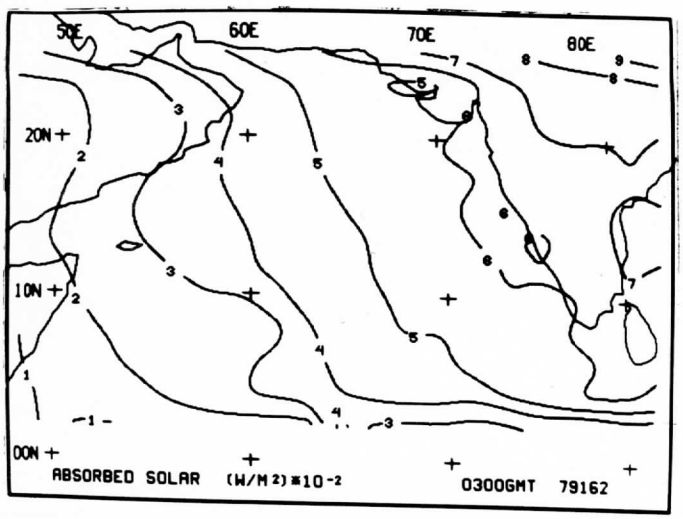
50E
60E
70E
80E
20N
10N
0ON
ABSORBED SOLAR (W/M2)*10-2
0300GMT 79162

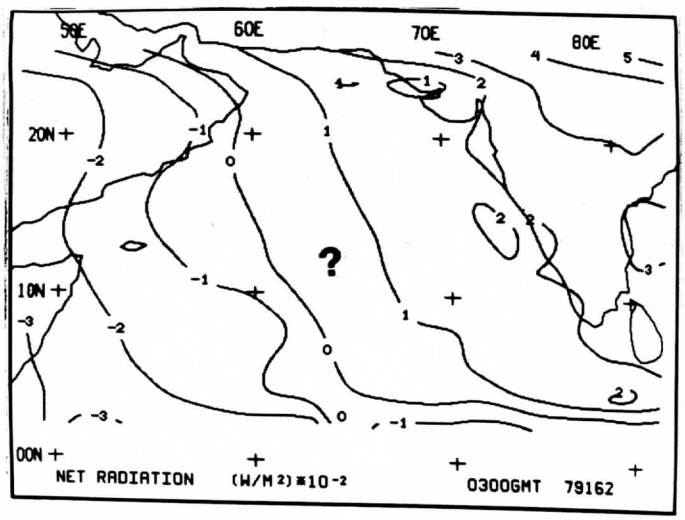
50E
60E
70E
80E
20N
10N
0ON
?
NET RADIATION (W/M2)*10-2
0300GMT 79162

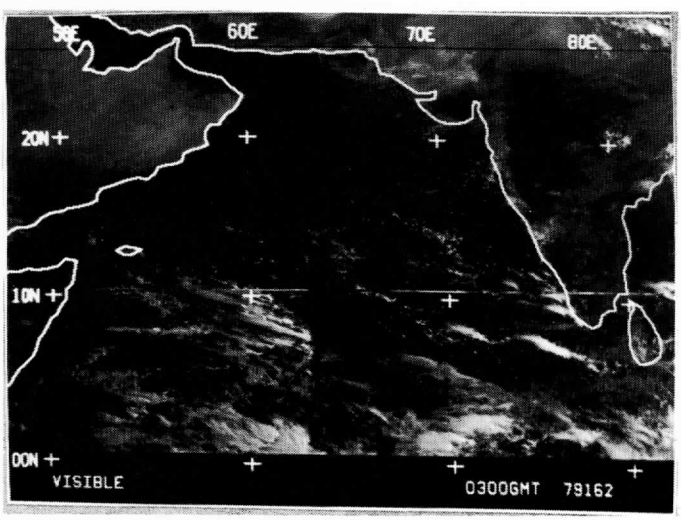
50E
60E
70E
80E
20N
10N
0ON
VISIBLE
0300GMT 79162

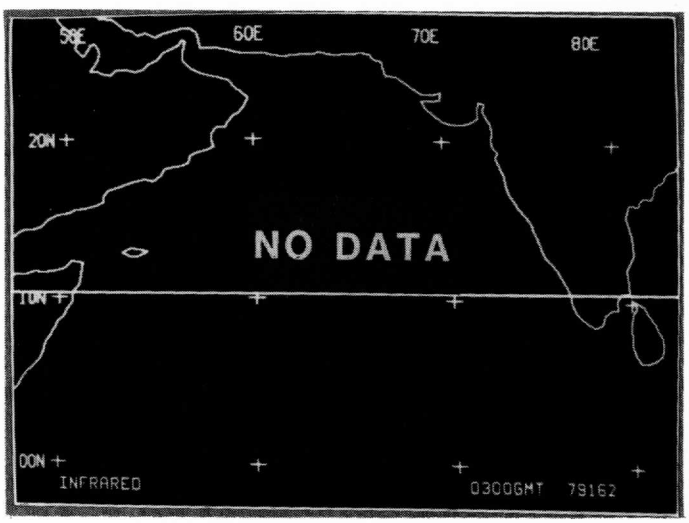
50E
60E
70E
80E
20N
10N
0ON
NO DATA
INFRARED
0300GMT 79162

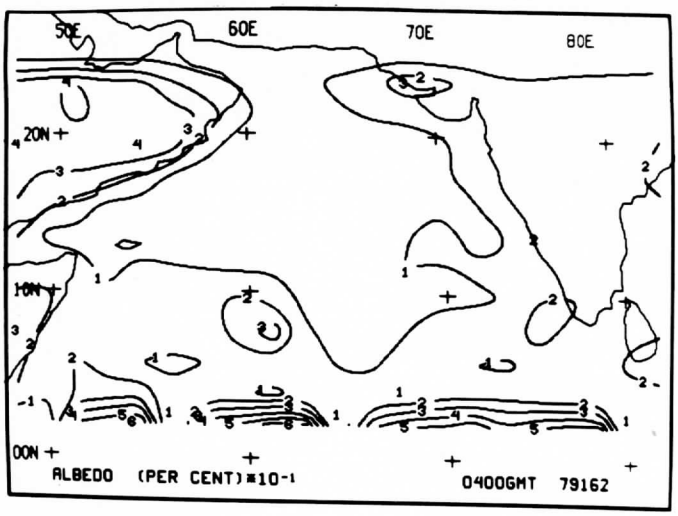
50E
60E
70E
80E
20N
10N
0ON
ALBEDO (PER CENT)*10-1
0400GMT 79162

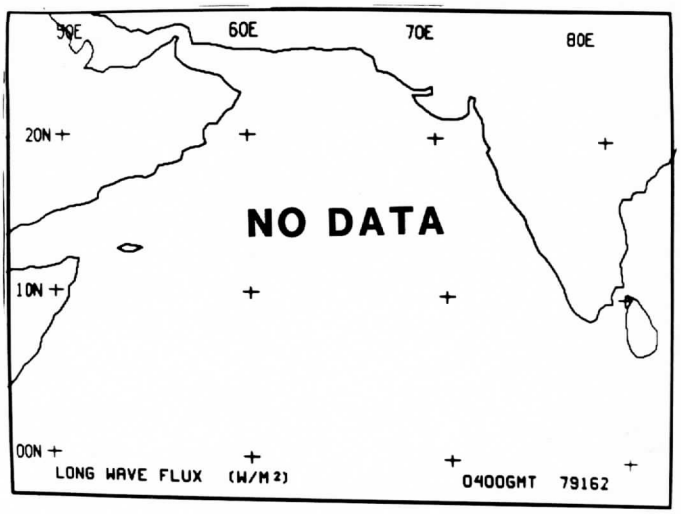
50E
60E
70E
80E
20N
NO DATA
10N
0ON
LONG WAVE FLUX (W/M2)
0400GMT 79162

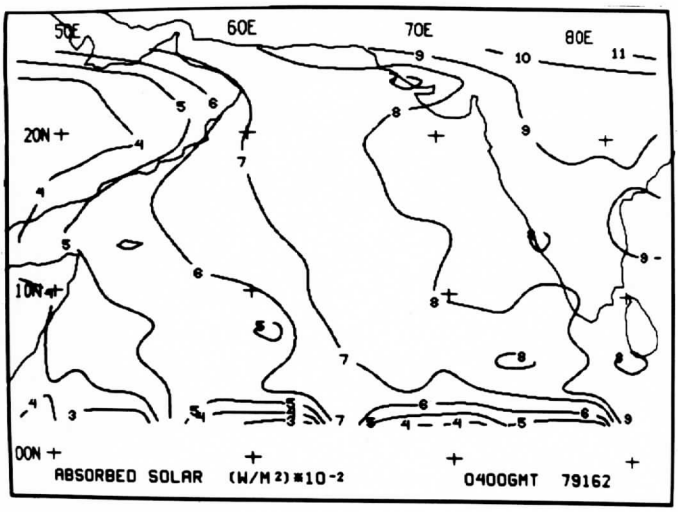
50E
60E
70E
80E
20N
10N
0ON
ABSORBED SOLAR (W/M2)*10-2
0400GMT 79162

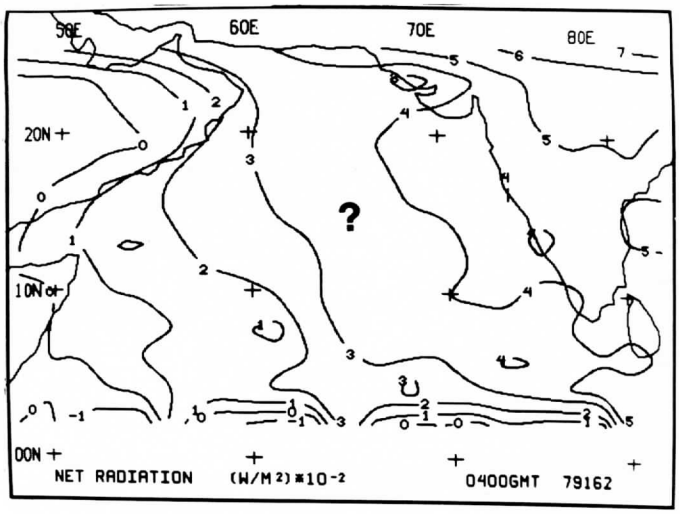
50E
60E
70E
80E
20N
?
10N
0ON
NET RADIATION (W/M2)*10-2
0400GMT 79162

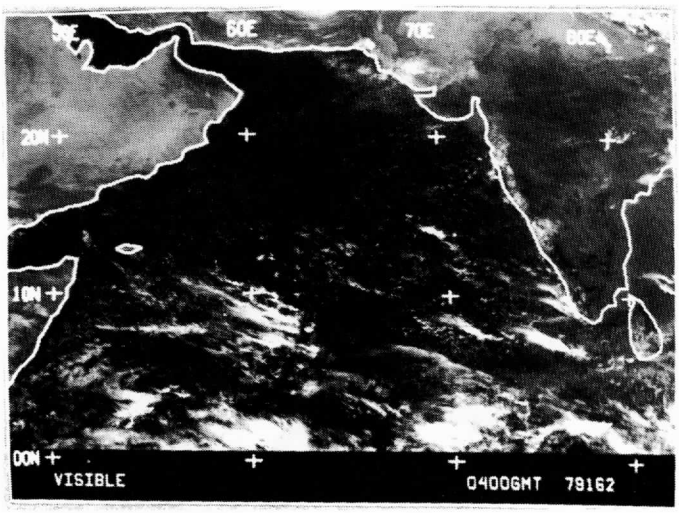
50E
60E
70E
80E
20N
10N
0ON
VISIBLE
0400GMT 79162

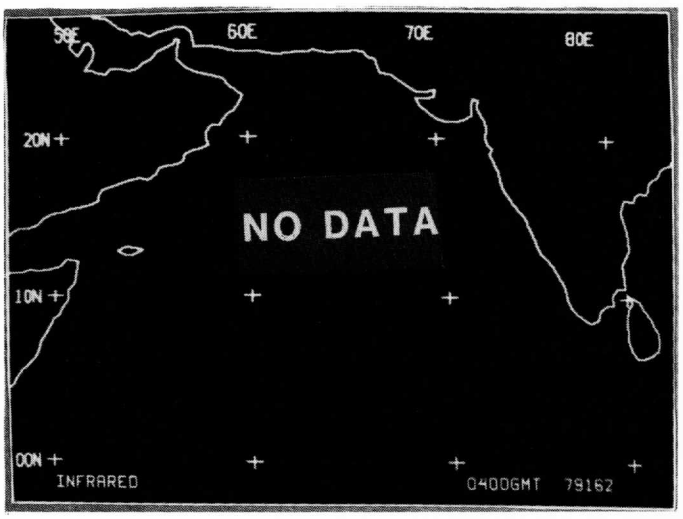
50E
60E
70E
80E
20N
NO DATA
10N
0ON
INFRARED
0400GMT 79162

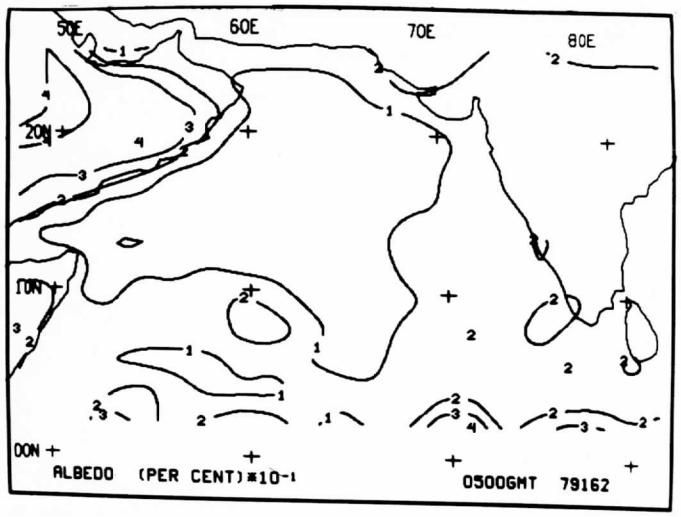
50E
60E
70E
80E
20N
10N
0ON
ALBEDO (PER CENT)*10-1
0500GMT 79162

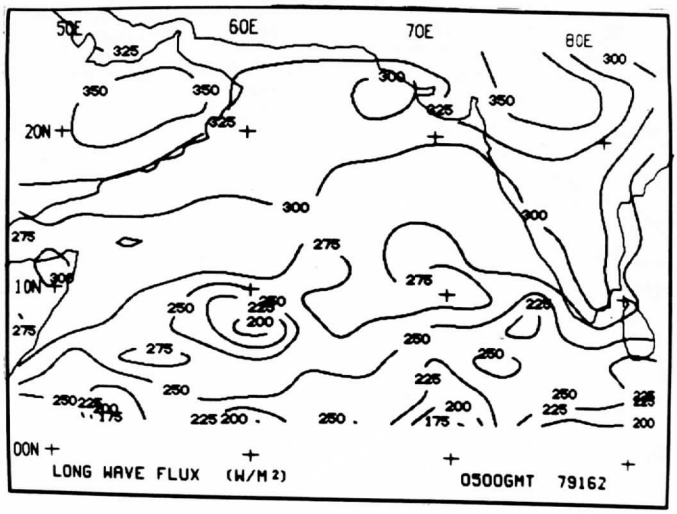
50E
60E
70E
80E
20N
10N
0ON
LONG WAVE FLUX (W/M2)
0500GMT 79162

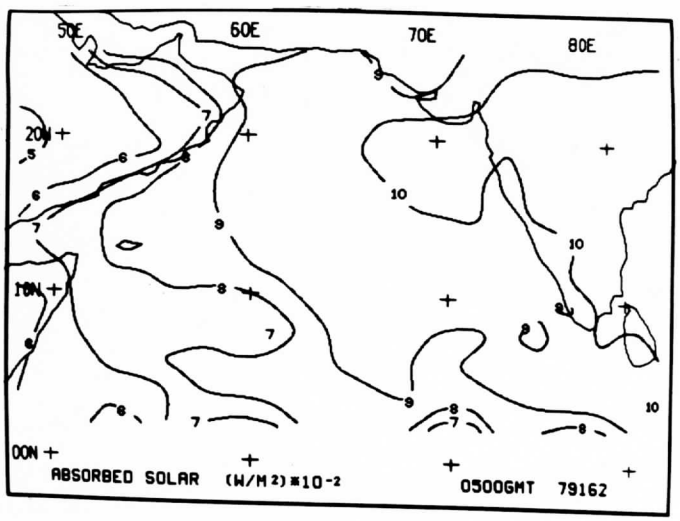
50E
60E
70E
80E
20N
10N
0ON
ABSORBED SOLAR (W/M2)*10-2
0500GMT 79162

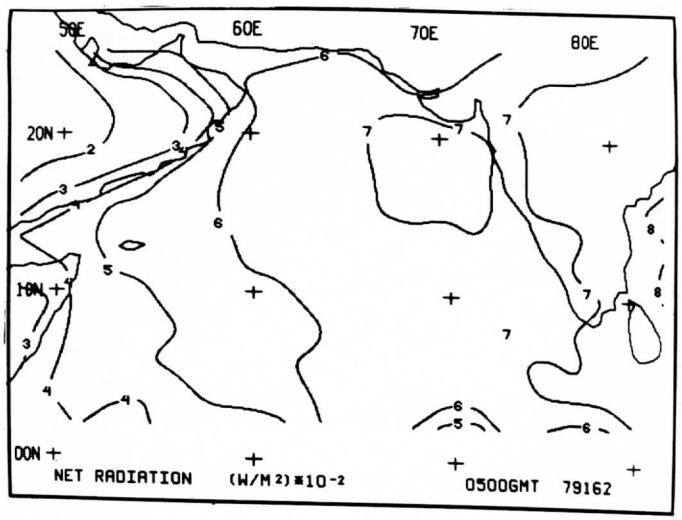
50E
60E
70E
80E
20N
10N
0ON
NET RADIATION (W/M2)*10-2
0500GMT 79162

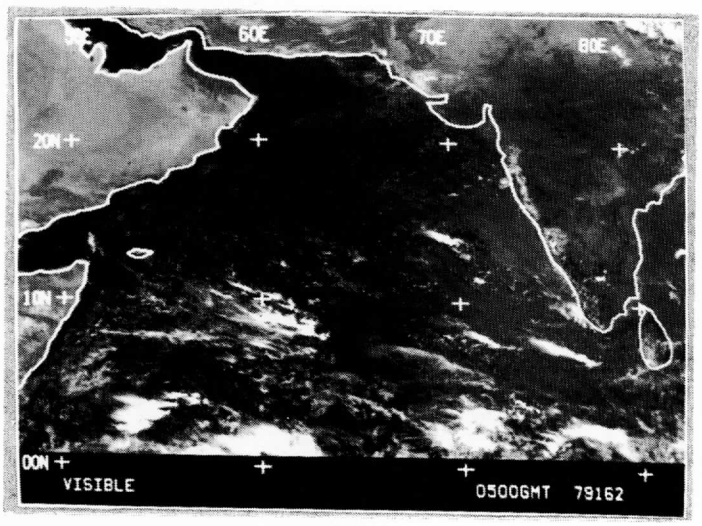
50E
60E
70E
80E
20N
10N
0ON
VISIBLE
0500GMT 79162

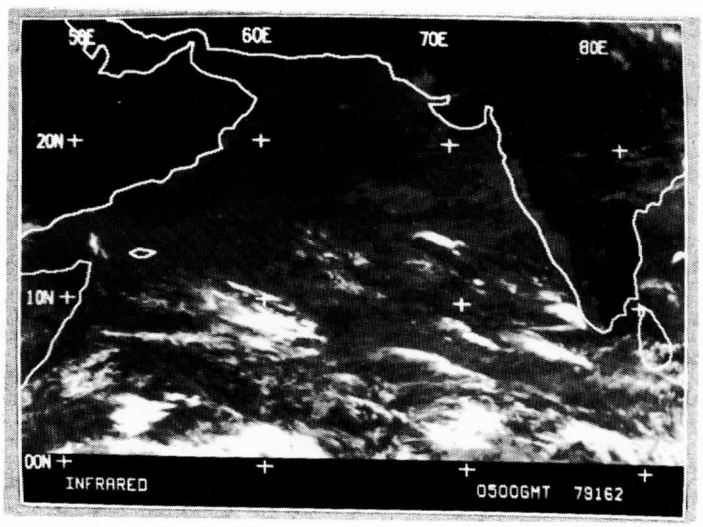
50E
60E
70E
80E
20N
10N
0ON
INFRARED
0500GMT 79162

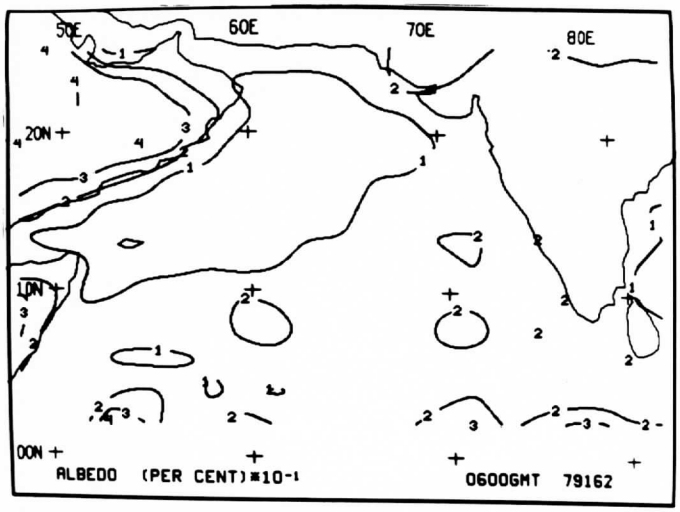
50E
60E
70E
80E
20N
10N
0ON
ALBEDO (PER CENT)*10-1
0600GMT 79162

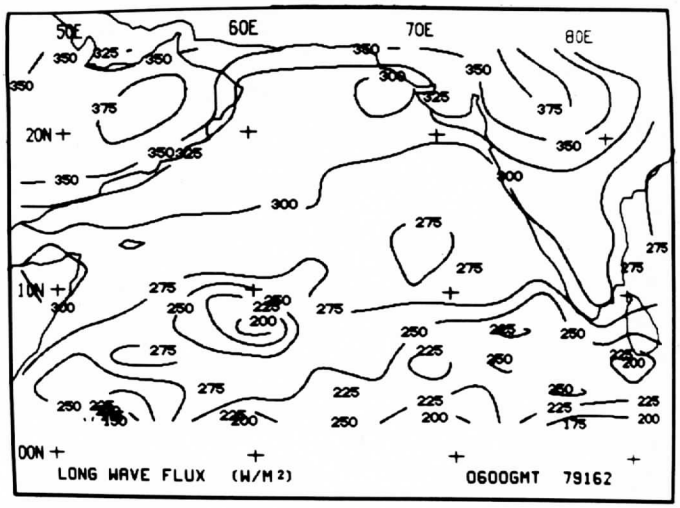
50E
60E
70E
80E
20N
10N
0ON
LONG WAVE FLUX (W/M2)
0600GMT 79162

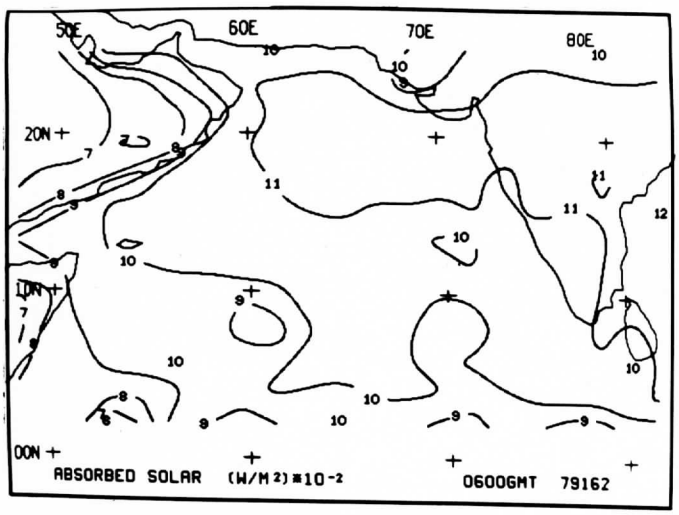
50E
60E
70E
80E
20N
10N
0ON
ABSORBED SOLAR (W/M2)*10-2
0600GMT 79162

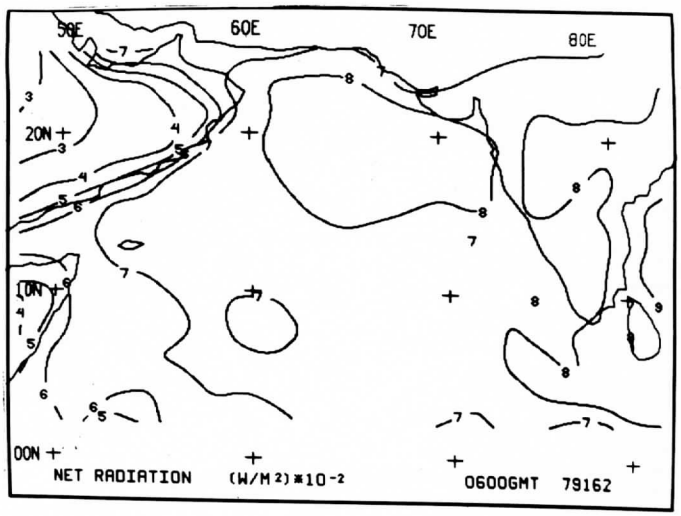
50E
60E
70E
80E
20N
10N
0ON
NET RADIATION (W/M2)*10-2
0600GMT 79162

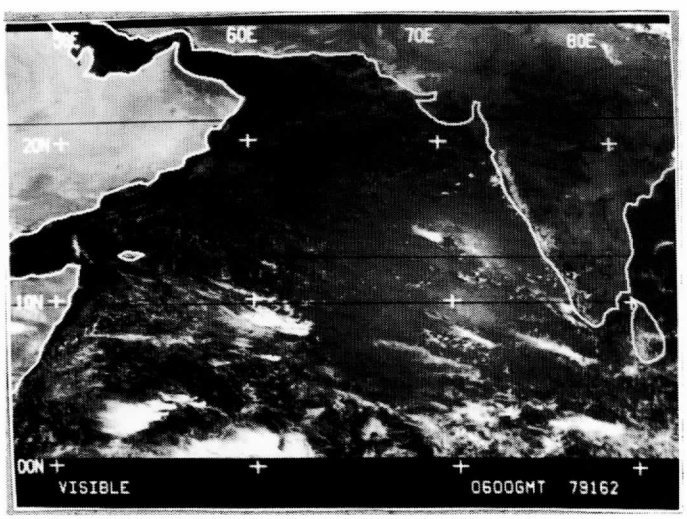
60E
70E
80E
20N
10N
0ON
VISIBLE
0600GMT 79162

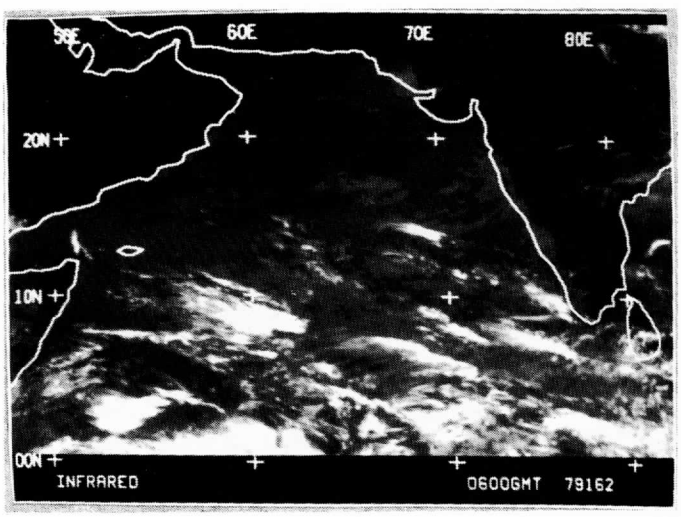
50E
60E
70E
80E
20N
10N
0ON
INFRARED
0600GMT 79162

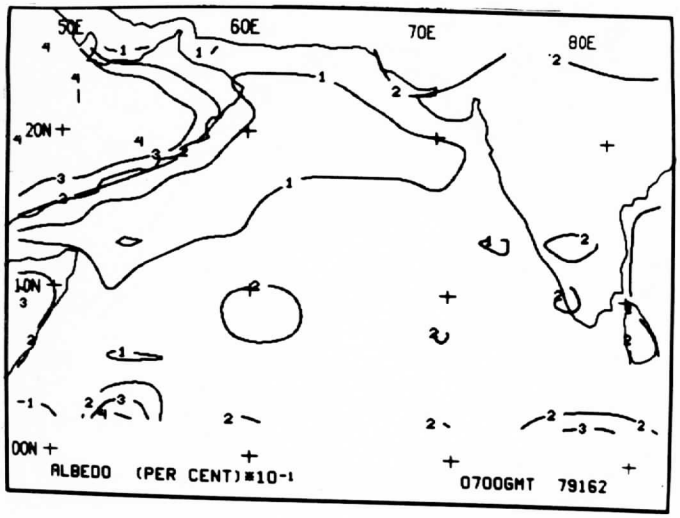
50E
60E
70E
80E
20N
10N
0ON
ALBEDO (PER CENT)*10-1
0700GMT 79162

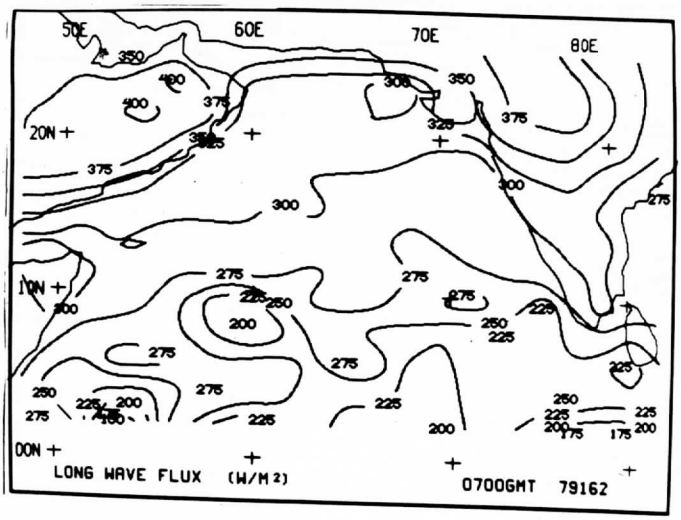
50E
60E
70E
80E
20N
10N
0ON
LONG WAVE FLUX (W/M2)
0700GMT 79162

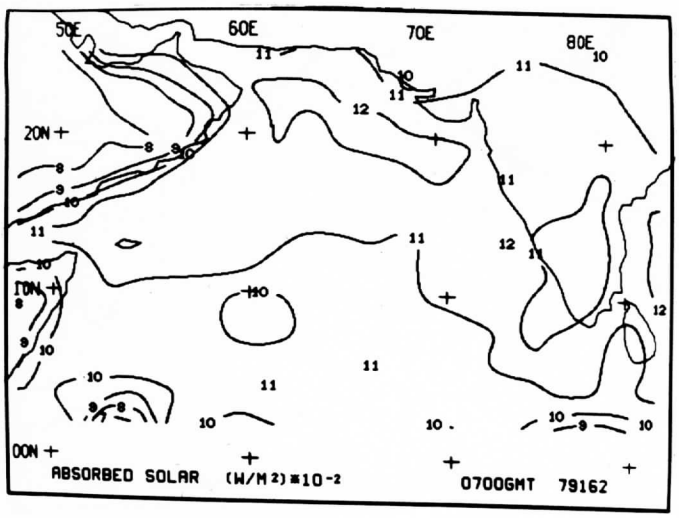
50E
60E
70E
80E
20N
10N
0ON
ABSORBED SOLAR (W/M2)*10-2
0700GMT 79162

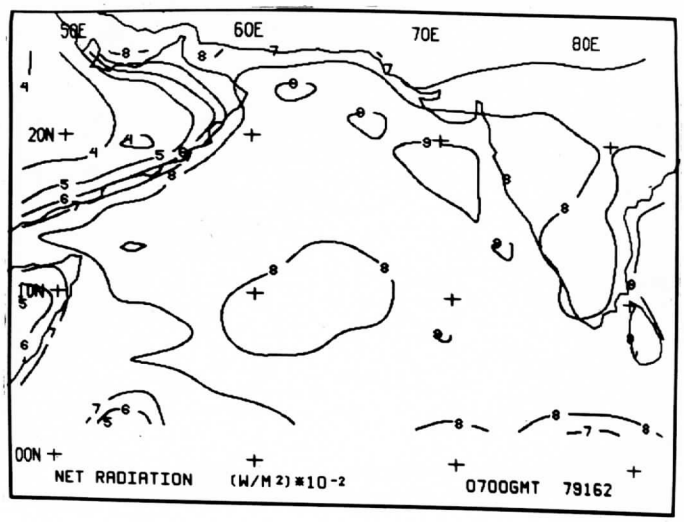
50E
60E
70E
80E
20N
10N
0ON
NET RADIATION (W/M2)*10-2
0700GMT 79162

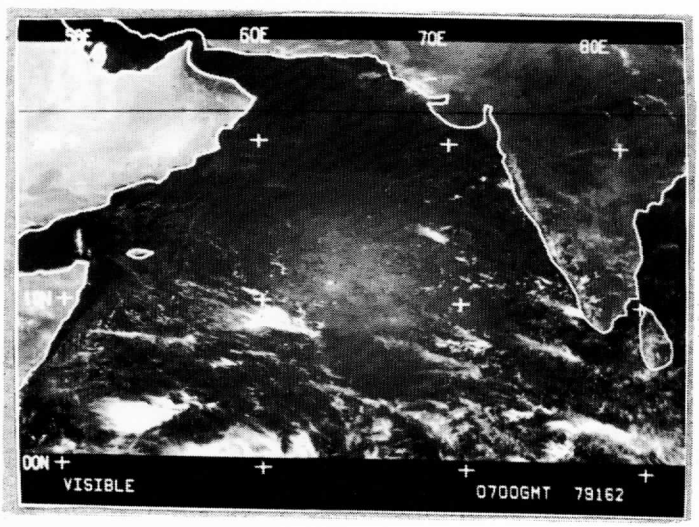
50E
60E
70E
80E
10N
0ON
VISIBLE
0700GMT 79162

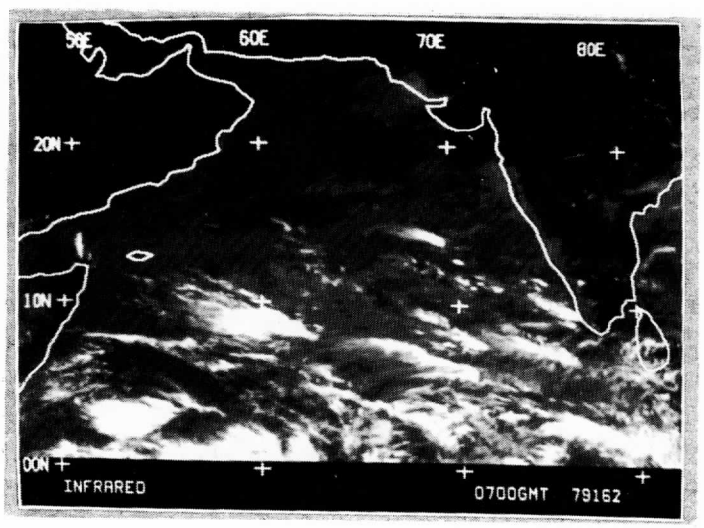
50E
60E
70E
80E
20N
10N
0ON
INFRARED
0700GMT 79162

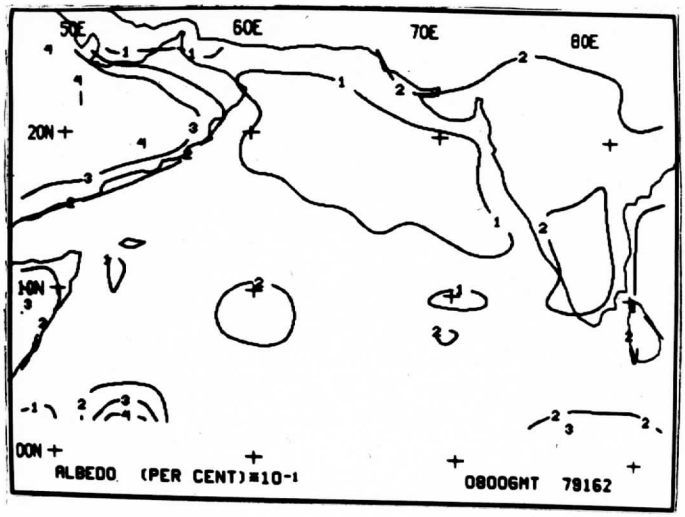
50E
60E
70E
80E
20N
10N
0ON
ALBEDO (PER CENT)×10-1
0800GMT 79162

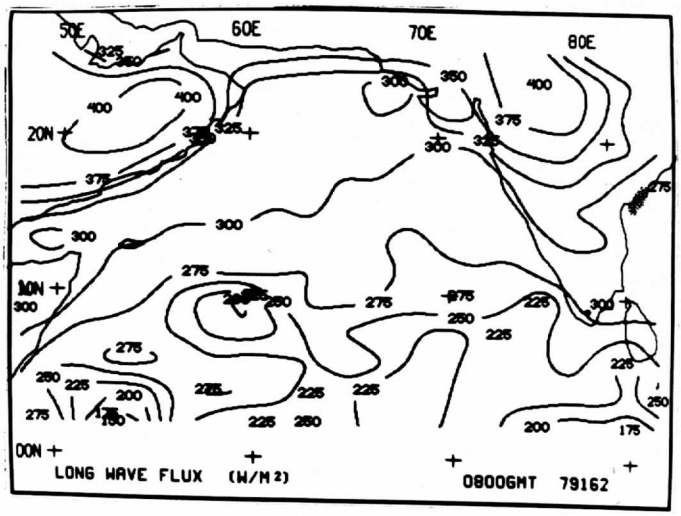
50E
60E
70E
80E
20N
10N
0ON
LONG WAVE FLUX (W/M2)
0800GMT 79162

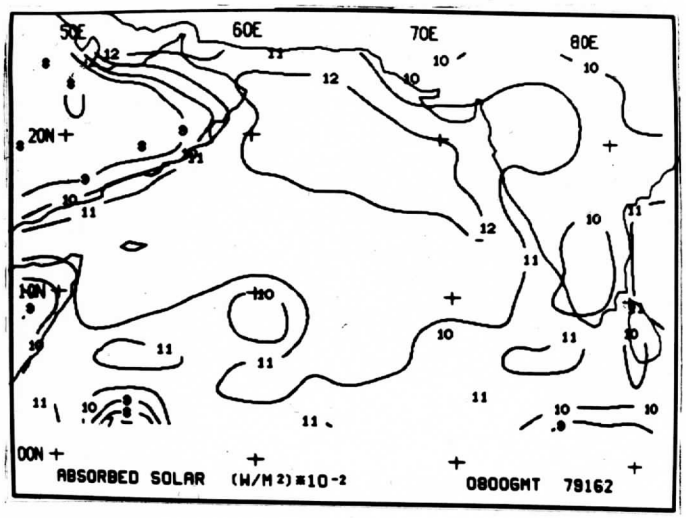
50E
60E
70E
80E
20N
10N
0ON
ABSORBED SOLAR (W/M2)×10-2
0800GMT 79162

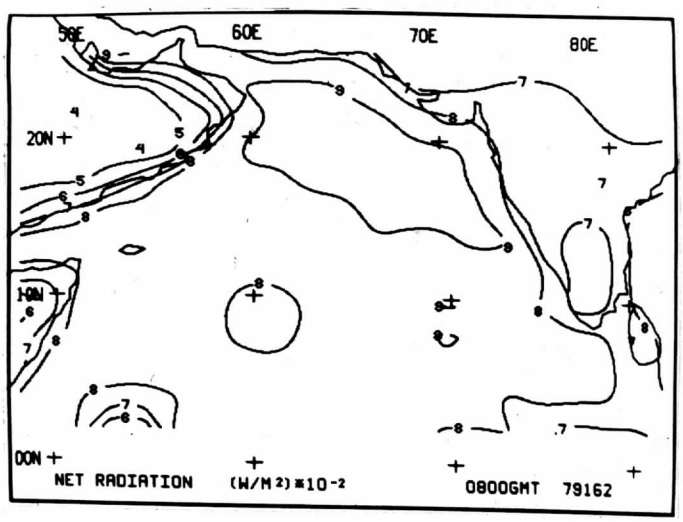
50E
60E
70E
80E
20N
10N
0ON
NET RADIATION (W/M2)×10-2
0800GMT 79162

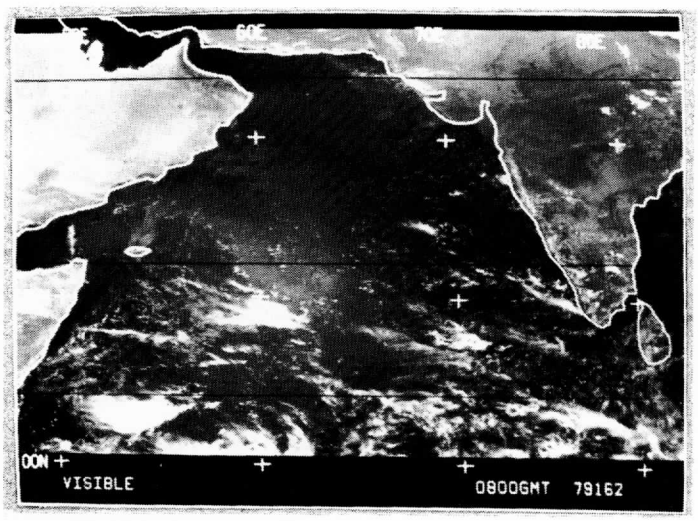
60E
70E
80E
0ON
VISIBLE
0800GMT 79162

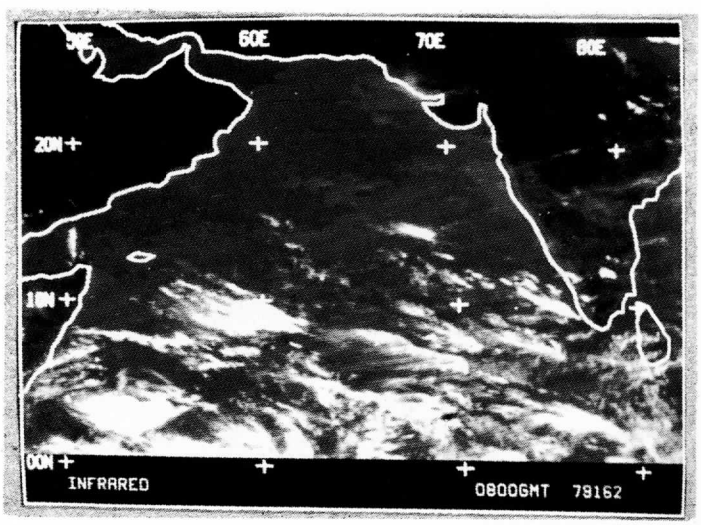
60E
70E
80E
20N
10N
0ON
INFRARED
0800GMT 79162

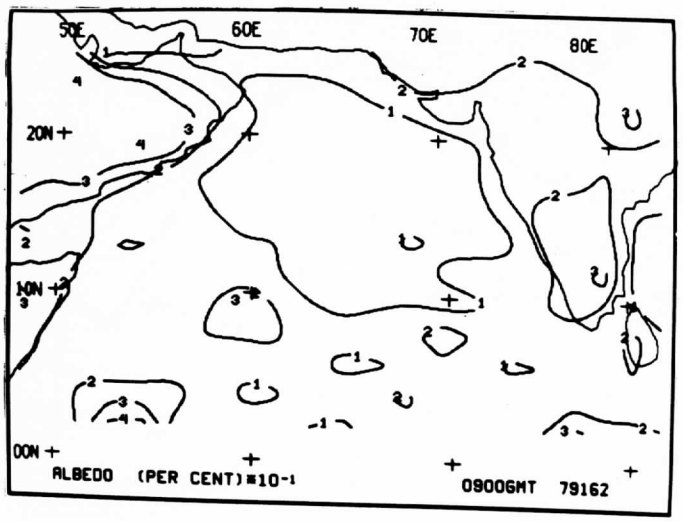
50E
60E
70E
80E
20N
10N
0ON
ALBEDO (PER CENT)*10-1
0900GMT 79162

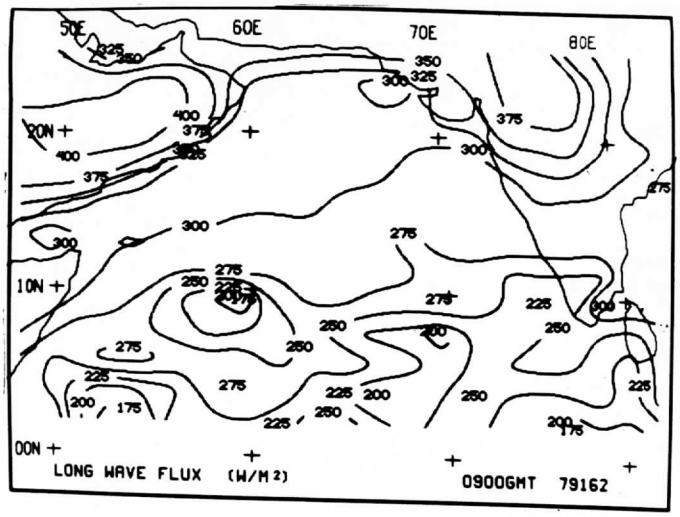
50E
60E
70E
80E
20N
10N
0ON
LONG WAVE FLUX (W/M2)
0900GMT 79162

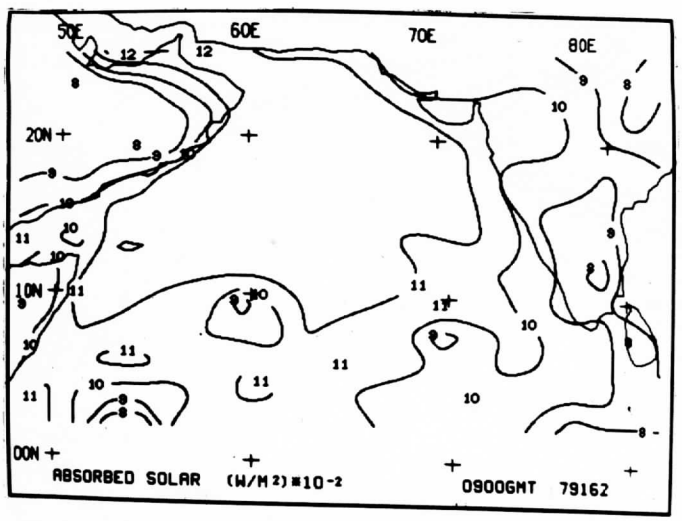
50E
60E
70E
80E
20N
10N
0ON
ABSORBED SOLAR (W/M2)*10-2
0900GMT 79162

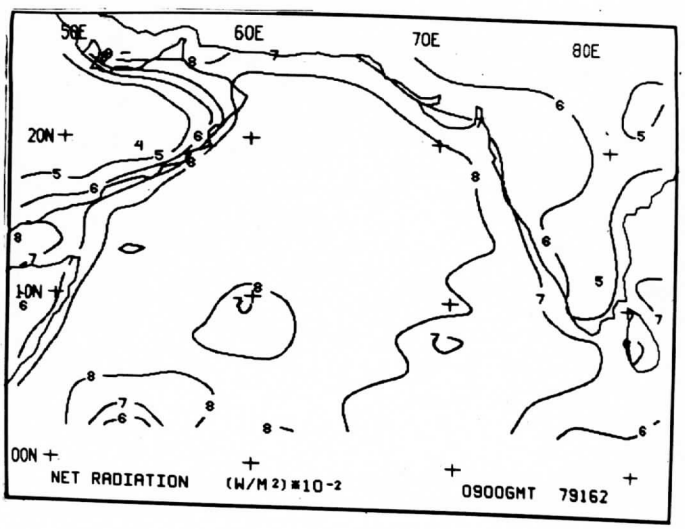
50E
60E
70E
80E
20N
10N
0ON
NET RADIATION (W/M2)*10-2
0900GMT 79162

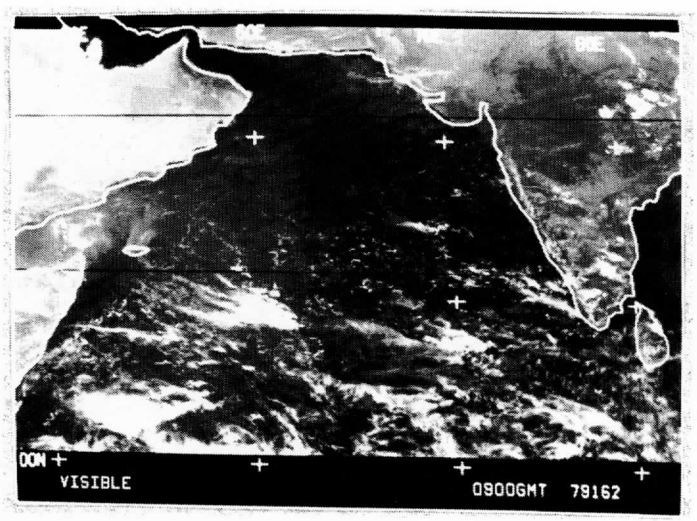
0ON
VISIBLE
0900GMT 79162

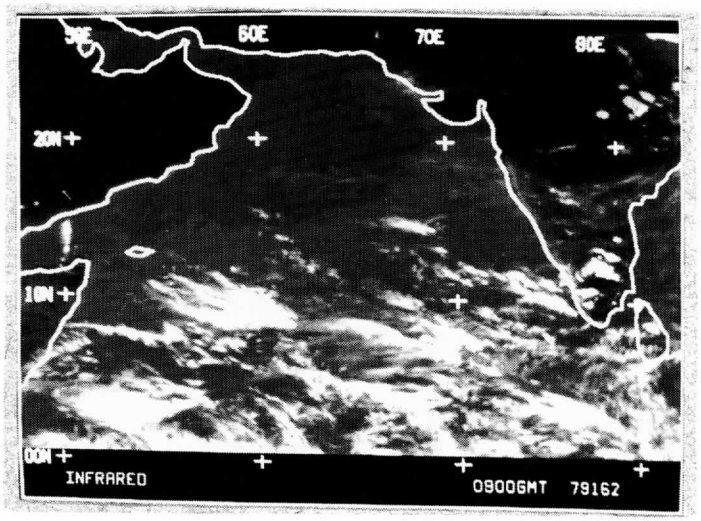
60E
70E
80E
20N
10N
0ON
INFRARED
0900GMT 79162

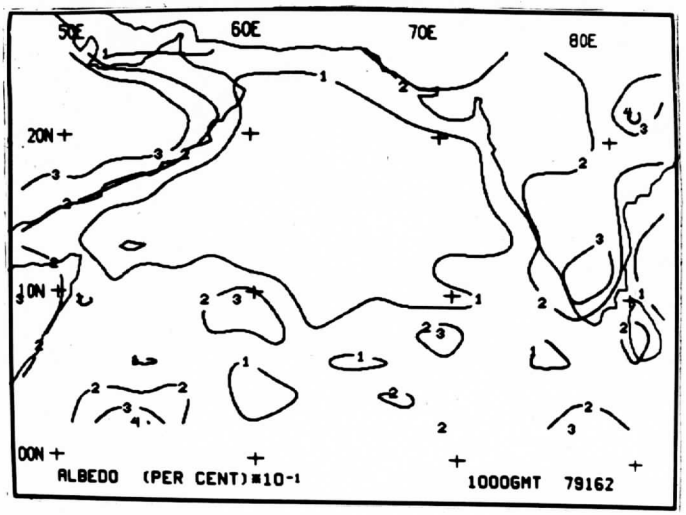
50E
60E
70E
80E
20N
10N
0ON
ALBEDO (PER CENT)*10-1
1000GMT 79162

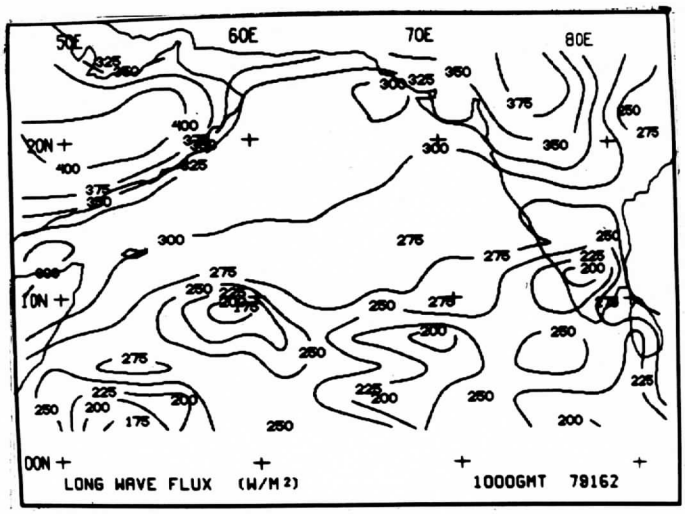
50E
60E
70E
80E
20N
10N
0ON
LONG WAVE FLUX (W/M2)
1000GMT 79162

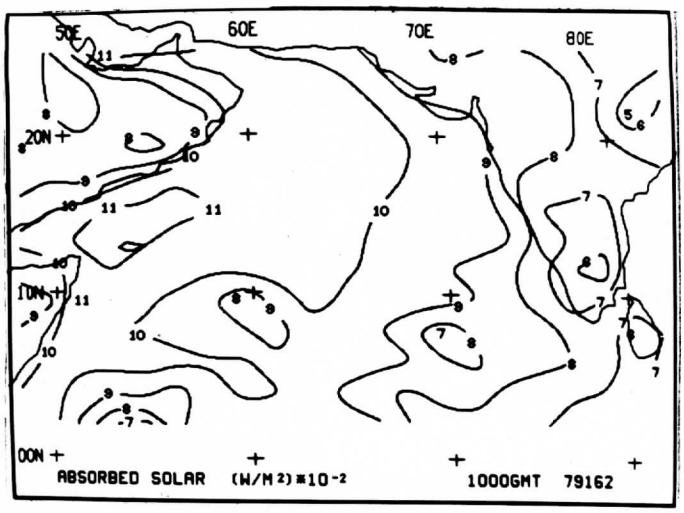
50E
60E
70E
80E
20N
10N
0ON
ABSORBED SOLAR (W/M2)*10-2
1000GMT 79162

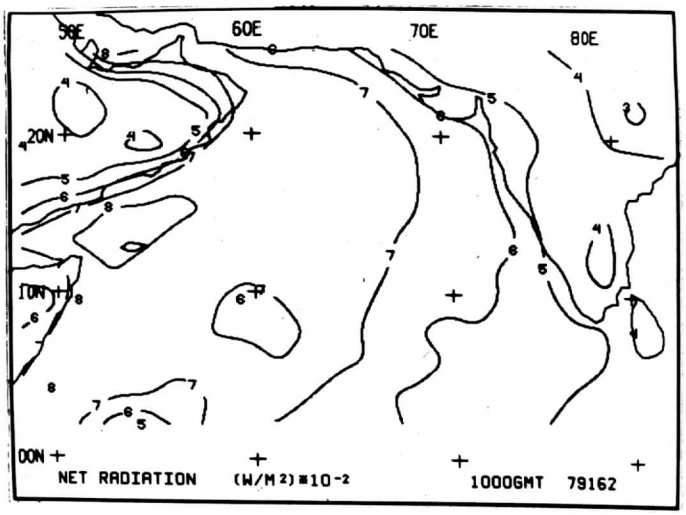
50E
60E
70E
80E
20N
10N
0ON
NET RADIATION (W/M2)*10-2
1000GMT 79162

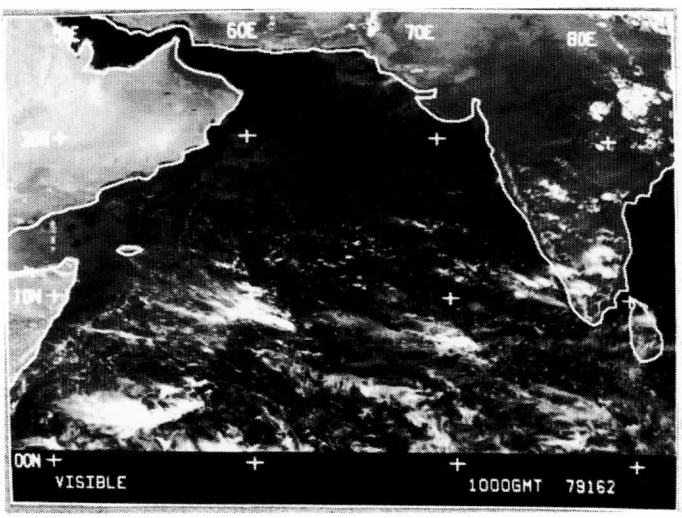
60E
70E
80E
10N
0ON
VISIBLE
1000GMT 79162

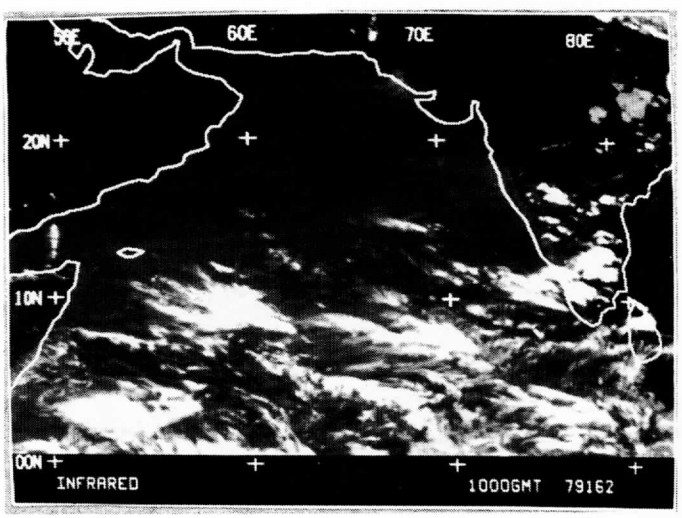
50E
60E
70E
80E
20N
10N
0ON
INFRARED
1000GMT 79162

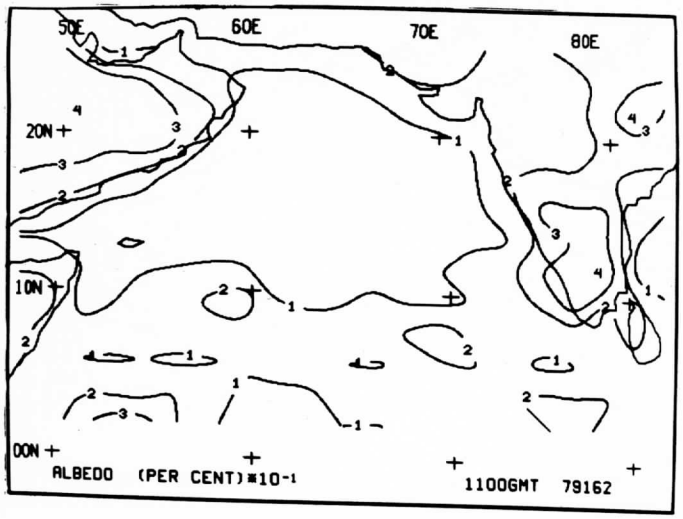
50E
60E
70E
80E
20N
10N
0ON
ALBEDO (PER CENT)*10-1
1100GMT 79162

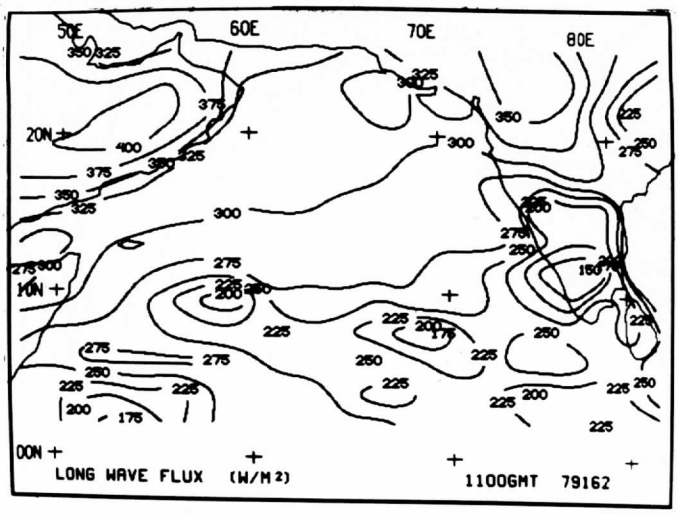
50E
60E
70E
80E
20N
10N
0ON
LONG WAVE FLUX (W/M2)
1100GMT 79162

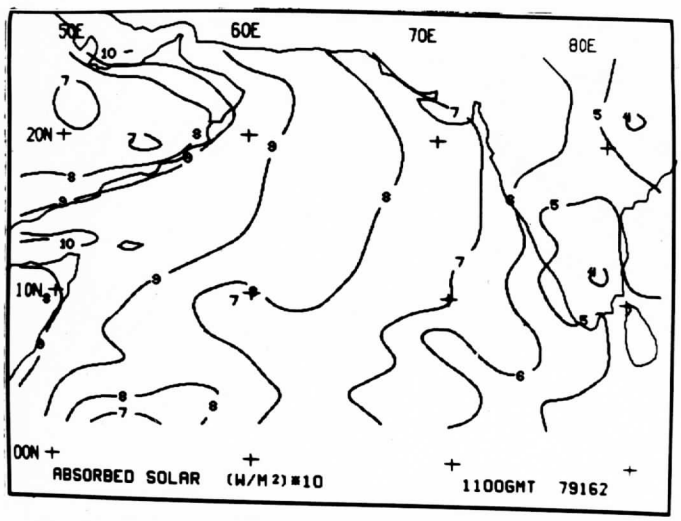
50E
60E
70E
80E
20N
10N
0ON
ABSORBED SOLAR (W/M2)*10
1100GMT 79162

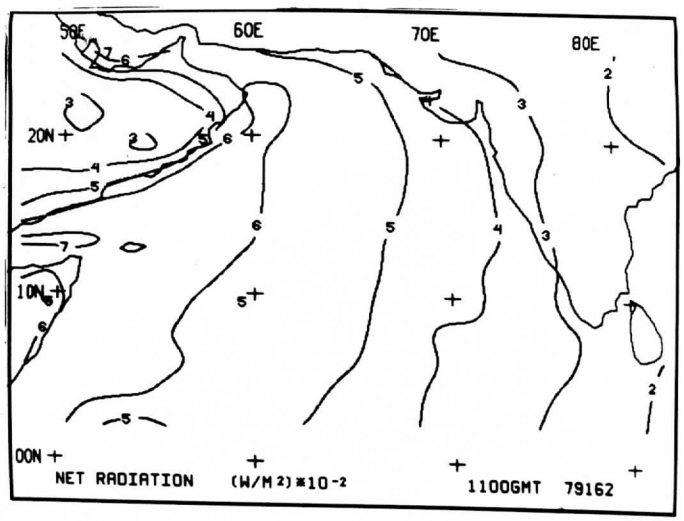
50E
60E
70E
80E
20N
10N
0ON
NET RADIATION (W/M2)*10-2
1100GMT 79162

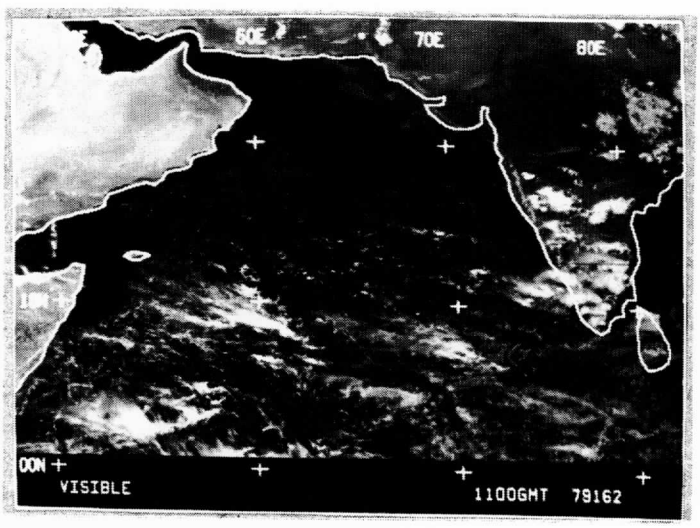
60E
70E
80E
0ON
VISIBLE
1100GMT 79162

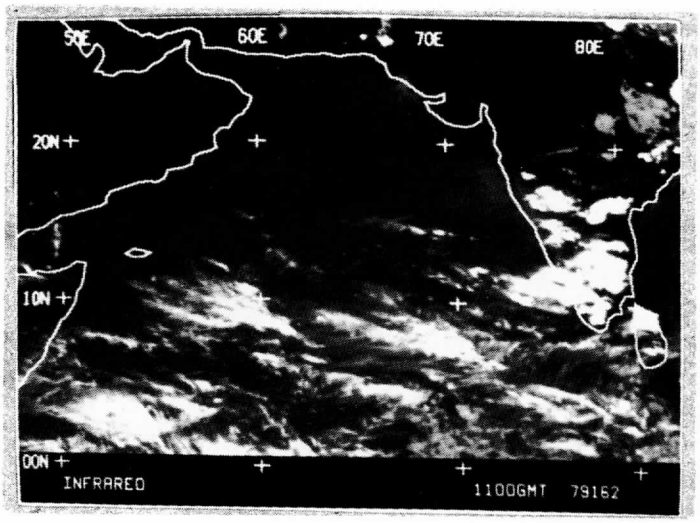
50E
60E
70E
80E
20N
10N
0ON
INFRARED
1100GMT 79162

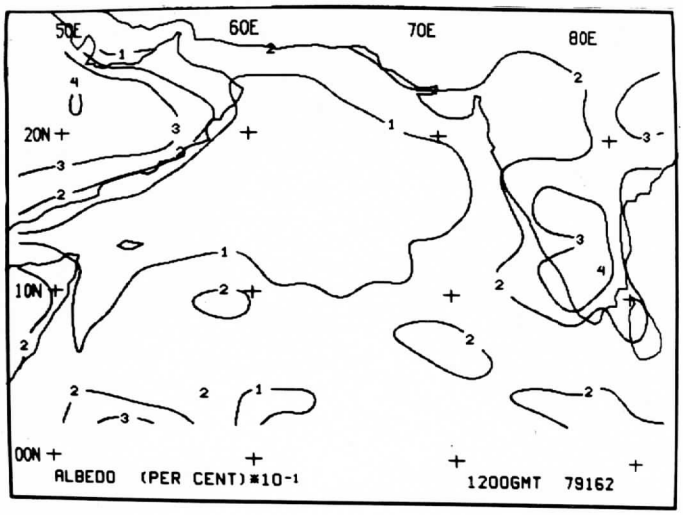
50E
60E
70E
80E
20N
10N
0ON
ALBEDO (PER CENT)*10-1
1200GMT 79162

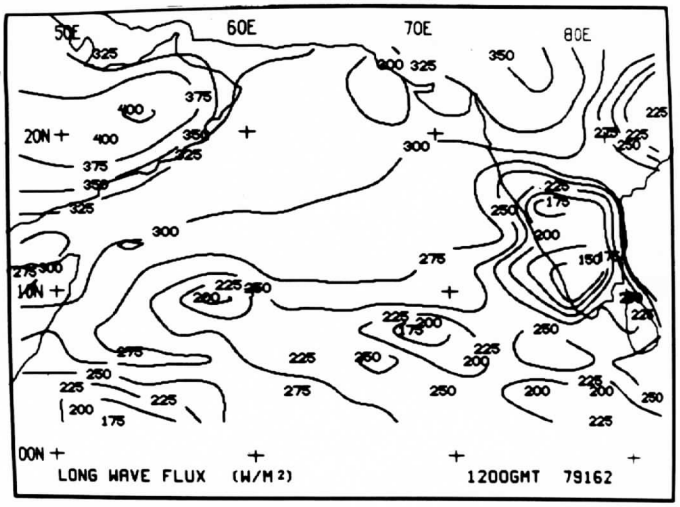
50E
60E
70E
80E
20N
10N
0ON
LONG WAVE FLUX (W/M2)
1200GMT 79162

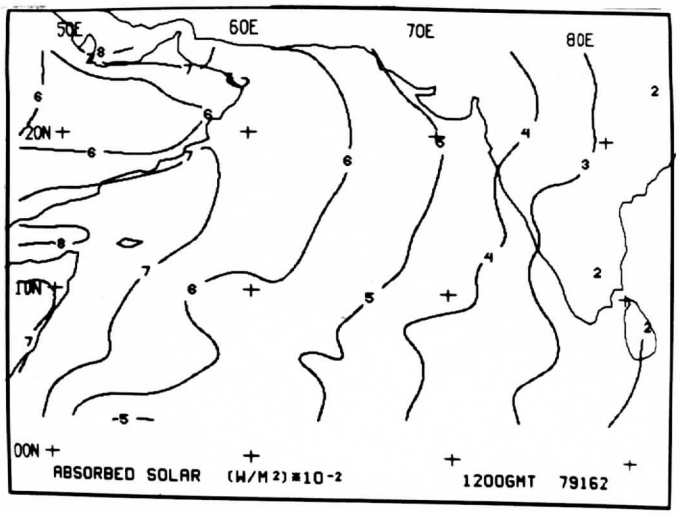
50E
60E
70E
80E
20N
10N
0ON
ABSORBED SOLAR (W/M2)*10-2
1200GMT 79162

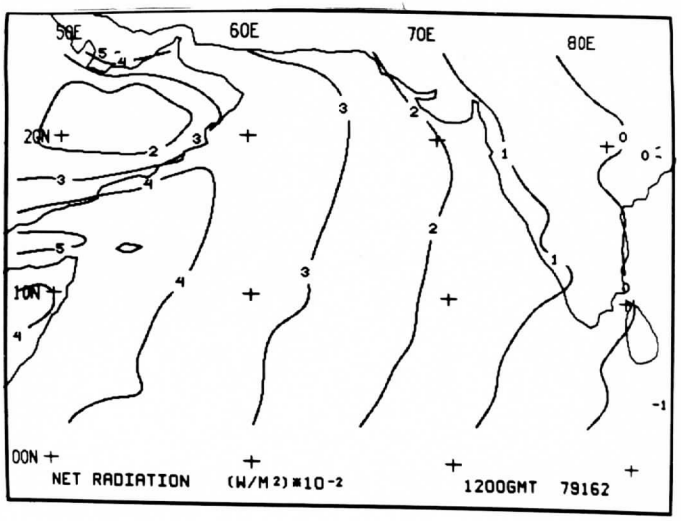
50E
60E
70E
80E
20N
10N
0ON
NET RADIATION (W/M2)*10-2
1200GMT 79162

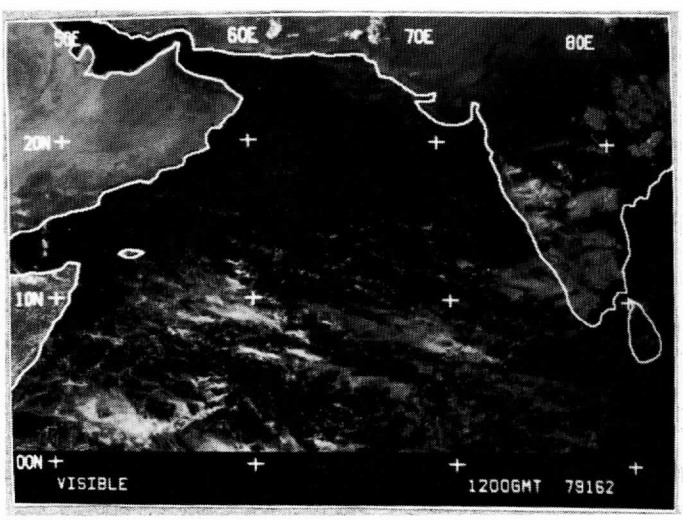
50E
60E
70E
80E
20N
10N
0ON
VISIBLE
1200GMT 79162

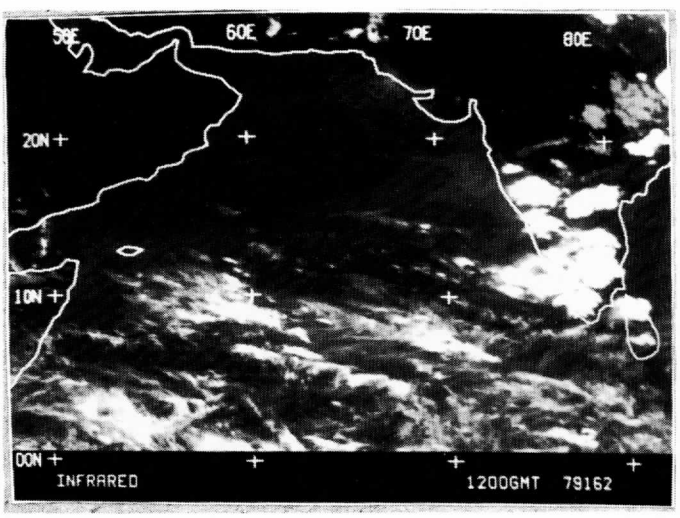
50E
60E
70E
80E
20N
10N
0ON
INFRARED
1200GMT 79162

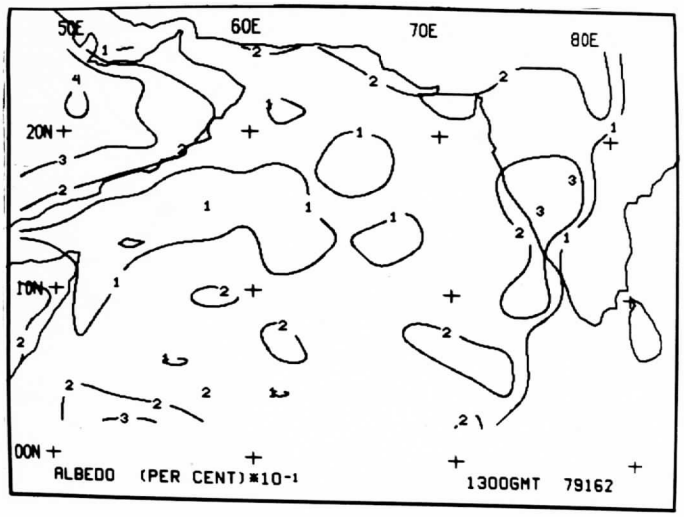
50E
60E
70E
80E
20N
10N
0ON
ALBEDO (PER CENT)*10-1
1300GMT 79162

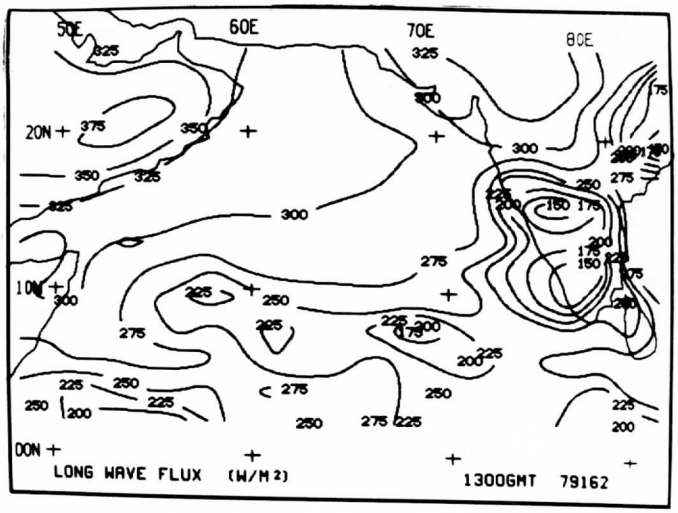
50E
60E
70E
80E
20N
10N
0ON
LONG WAVE FLUX (W/M2)
1300GMT 79162

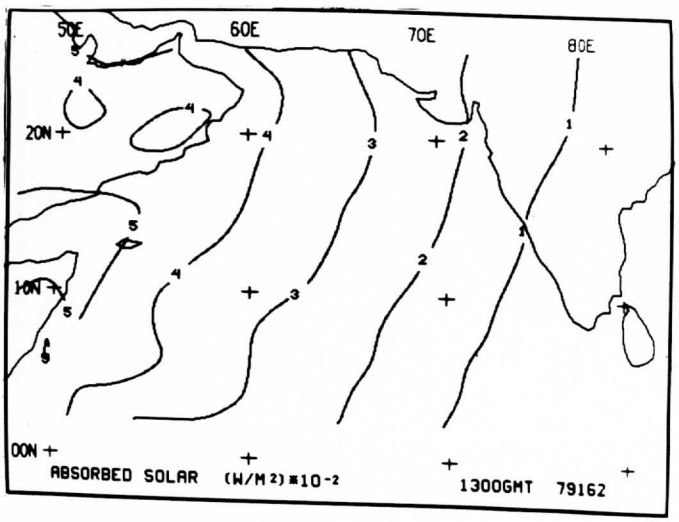
50E
60E
70E
80E
20N
10N
0ON
ABSORBED SOLAR (W/M2)*10-2
1300GMT 79162

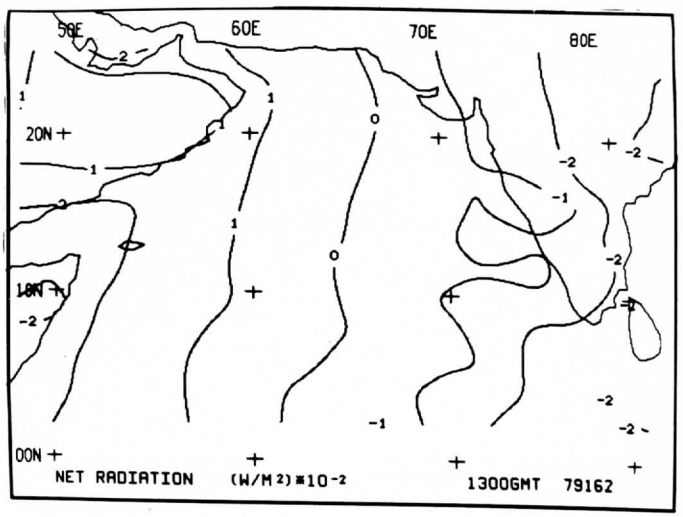
50E
60E
70E
80E
20N
10N
0ON
NET RADIATION (W/M2)*10-2
1300GMT 79162

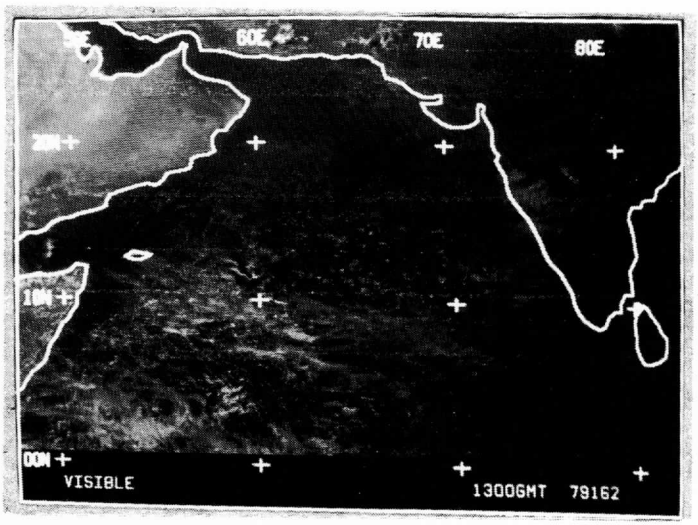
50E
60E
70E
80E
20N
10N
0ON
VISIBLE
1300GMT 79162

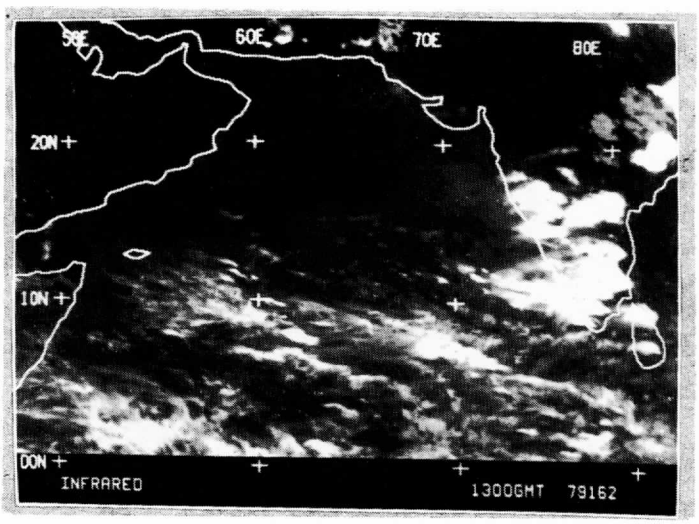
50E
60E
70E
80E
20N
10N
0ON
INFRARED
1300GMT 79162

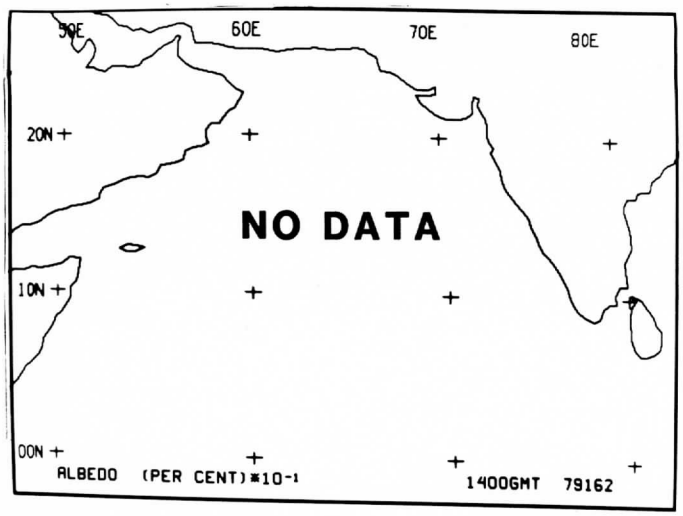
50E
60E
70E
80E
20N
10N
00N
NO DATA
ALBEDO (PER CENT)*10-1
1400GMT 79162

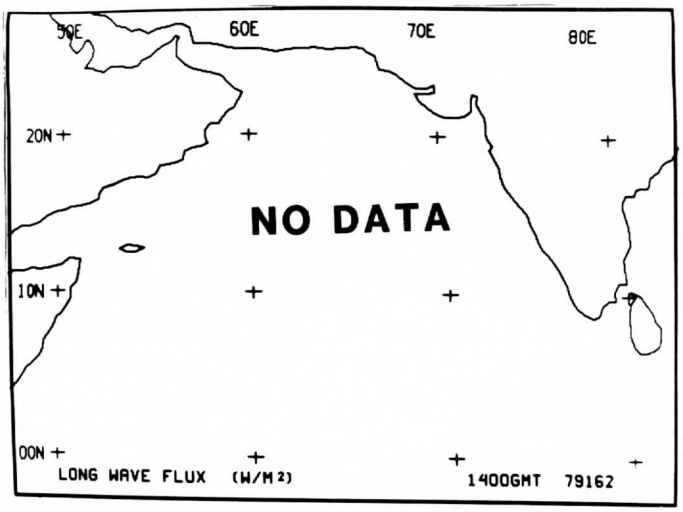
50E
60E
70E
80E
20N
10N
00N
NO DATA
LONG WAVE FLUX (W/M2)
1400GMT 79162

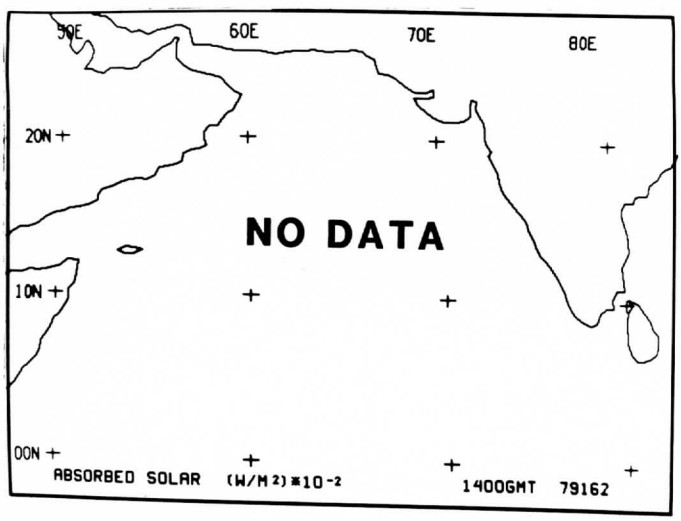
50E
60E
70E
80E
20N
10N
00N
NO DATA
ABSORBED SOLAR (W/M2)*10-2
1400GMT 79162

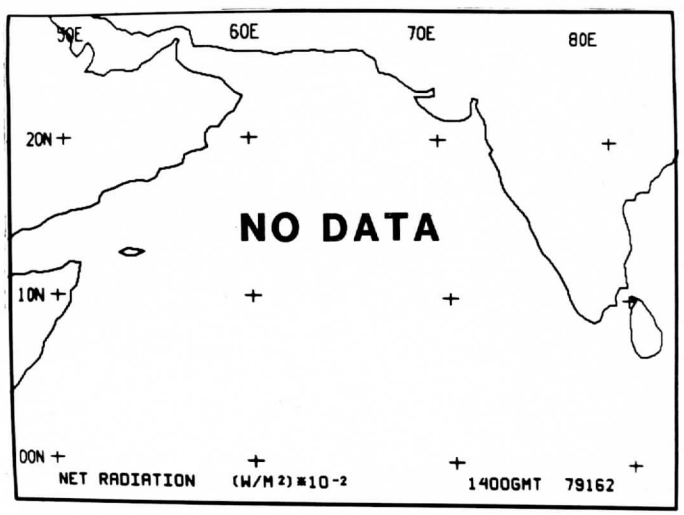
50E
60E
70E
80E
20N
10N
00N
NO DATA
NET RADIATION (W/M2)*10-2
1400GMT 79162

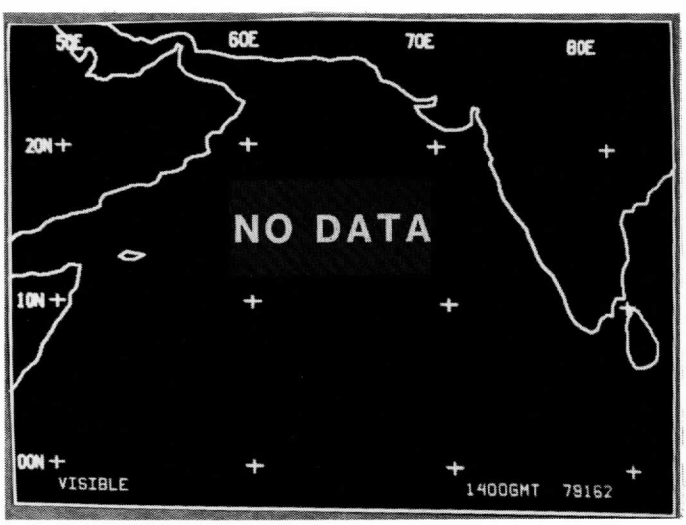
50E
60E
70E
80E
20N
10N
00N
NO DATA
VISIBLE
1400GMT 79162

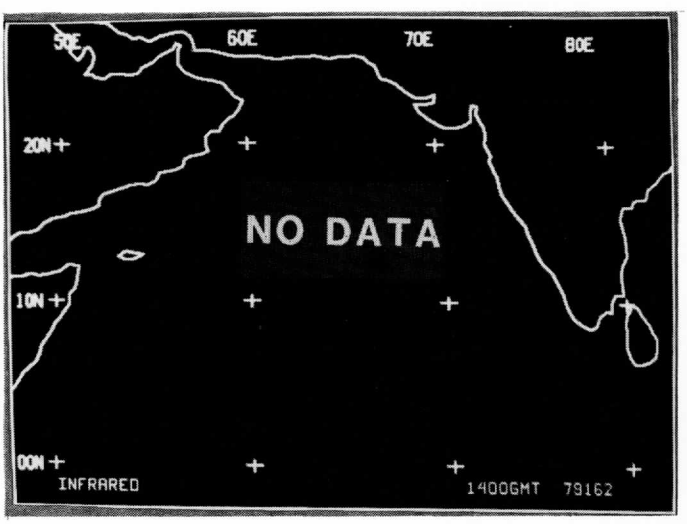
50E
60E
70E
80E
20N
10N
00N
NO DATA
INFRARED
1400GMT 79162

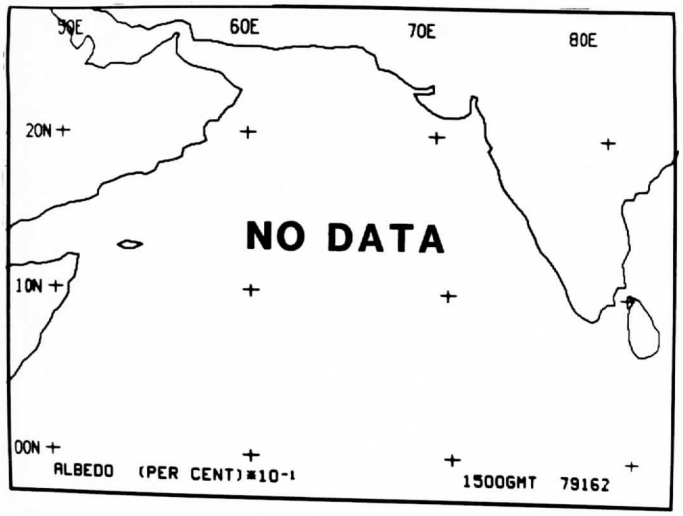
50E
60E
70E
80E
20N
10N
00N
NO DATA
ALBEDO (PER CENT)*10-1
1500GMT 79162

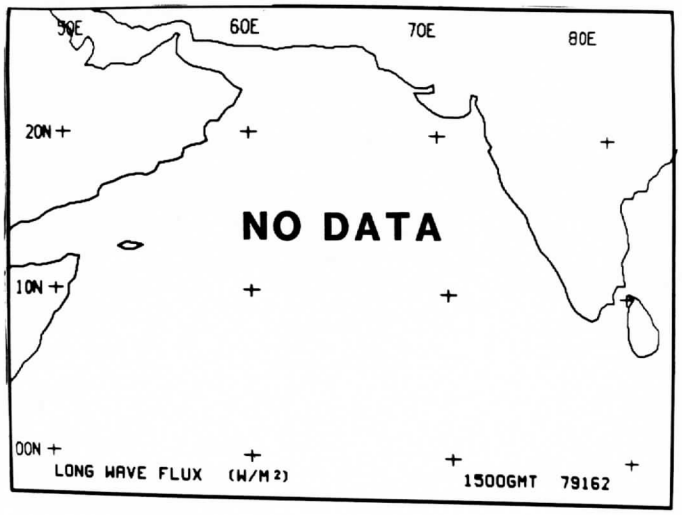
50E
60E
70E
80E
20N
10N
00N
NO DATA
LONG WAVE FLUX (W/M2)
1500GMT 79162

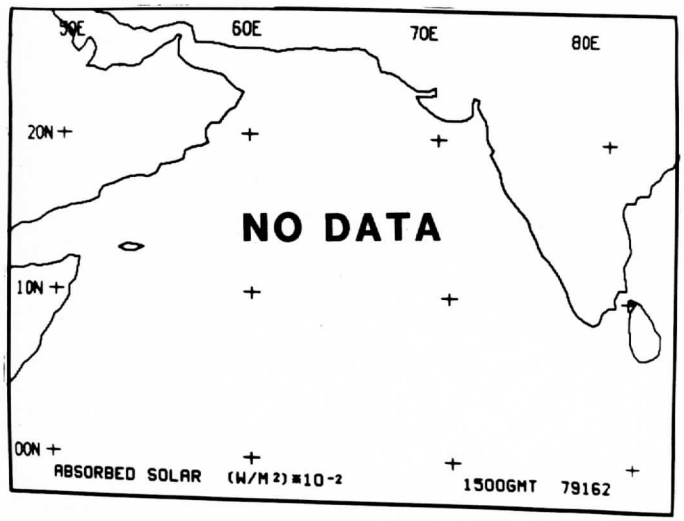
50E
60E
70E
80E
20N
10N
00N
NO DATA
ABSORBED SOLAR (W/M2)*10-2
1500GMT 79162

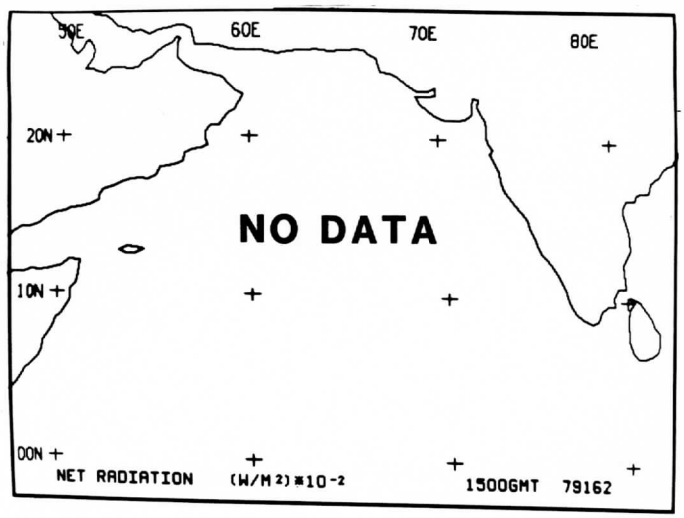
50E
60E
70E
80E
20N
10N
00N
NO DATA
NET RADIATION (W/M2)*10-2
1500GMT 79162

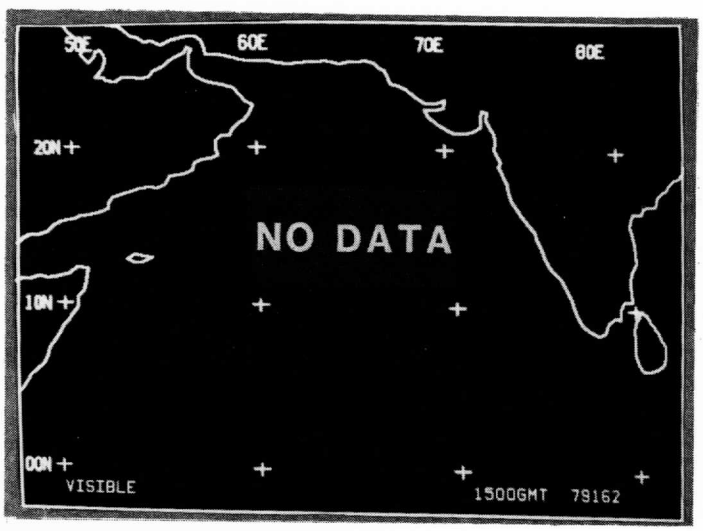
50E
60E
70E
80E
20N
10N
00N
NO DATA
VISIBLE
1500GMT 79162

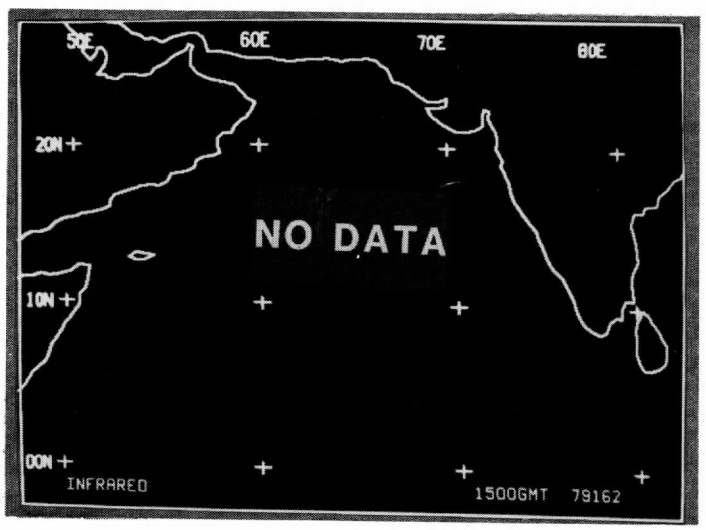
50E
60E
70E
80E
20N
10N
00N
NO DATA
INFRARED
1500GMT 79162

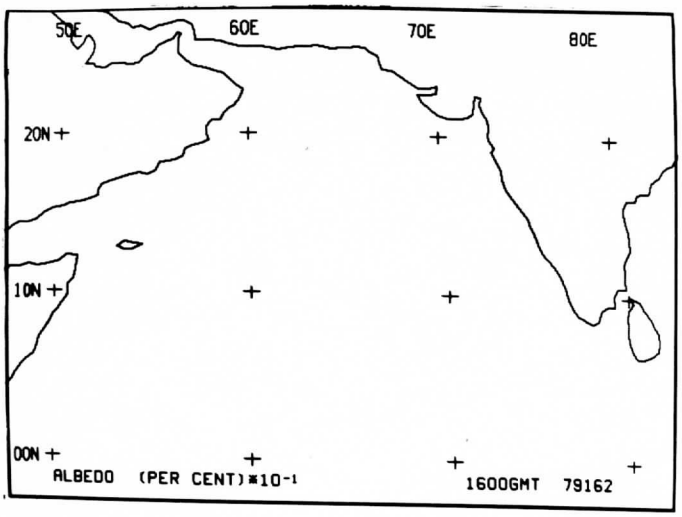
50E
60E
70E
80E
20N
10N
0ON
ALBEDO (PER CENT)*10-1
1600GMT 79162

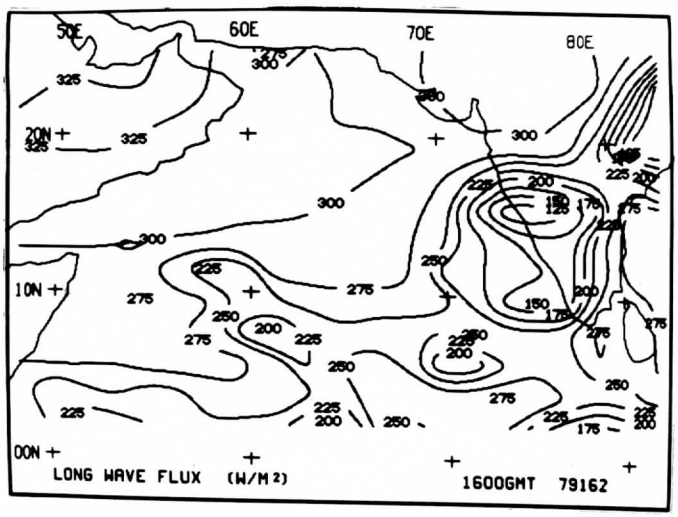
50E
60E
70E
80E
20N
10N
0ON
LONG WAVE FLUX (W/M2)
1600GMT 79162

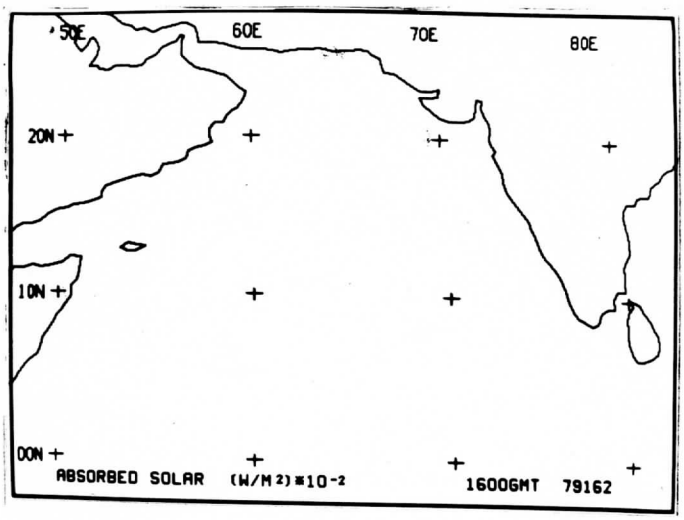
50E
60E
70E
80E
20N
10N
0ON
ABSORBED SOLAR (W/M2)*10-2
1600GMT 79162

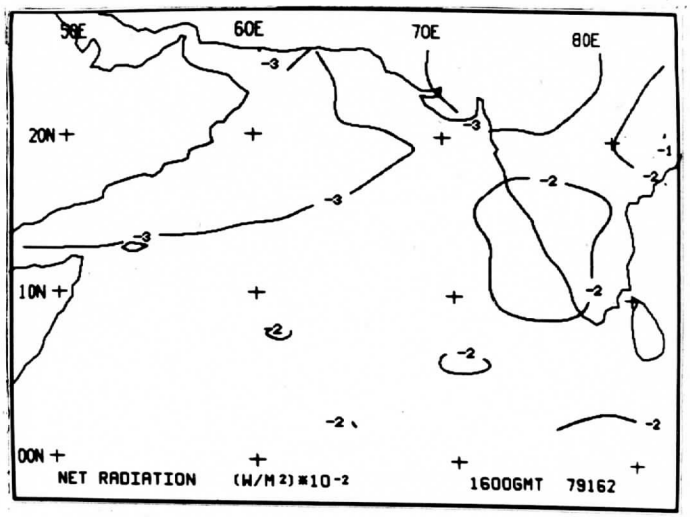
50E
60E
70E
80E
20N
10N
0ON
NET RADIATION (W/M2)*10-2
1600GMT 79162

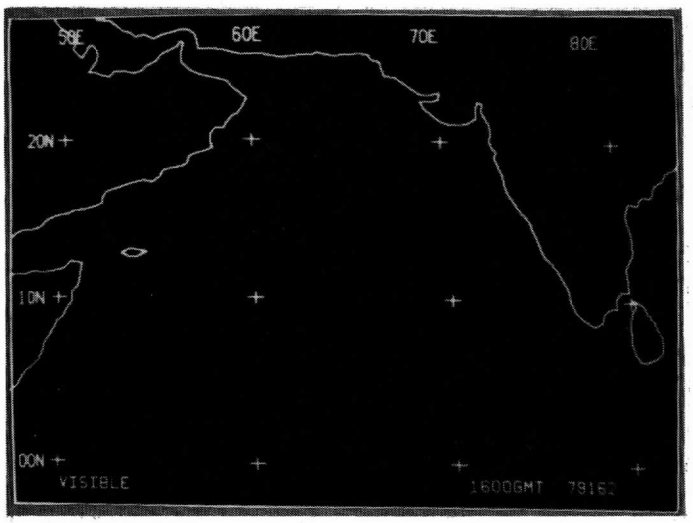
50E
60E
70E
80E
20N
10N
0ON
VISIBLE
1600GMT 79162

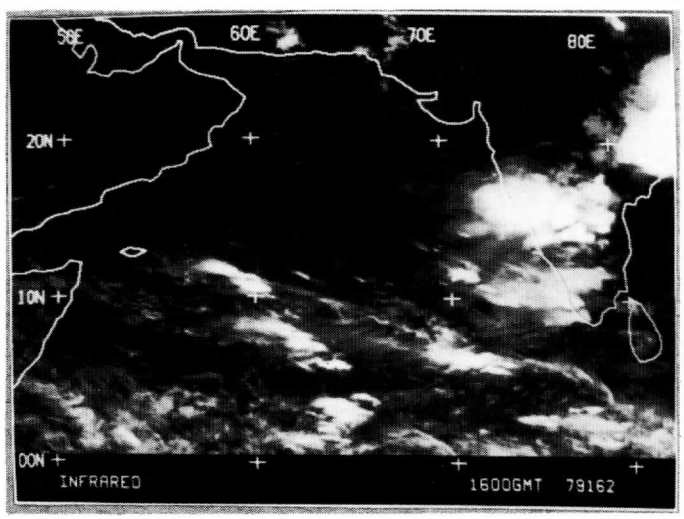
50E
60E
70E
80E
20N
10N
0ON
INFRARED
1600GMT 79162

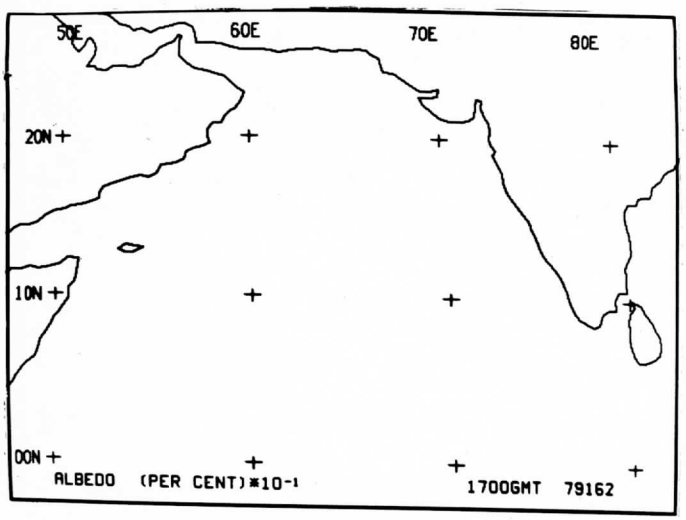
50E
60E
70E
80E
20N
10N
0ON
ALBEDO (PER CENT)*10-1
1700GMT 79162

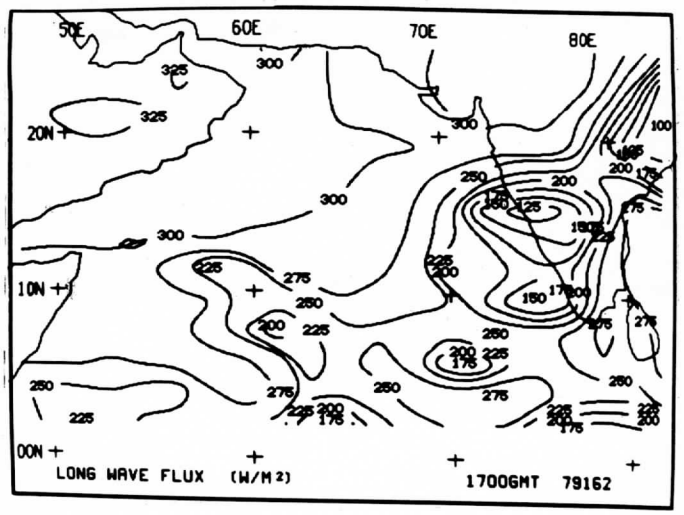
50E
60E
70E
80E
20N
10N
0ON
LONG WAVE FLUX (W/M2)
1700GMT 79162

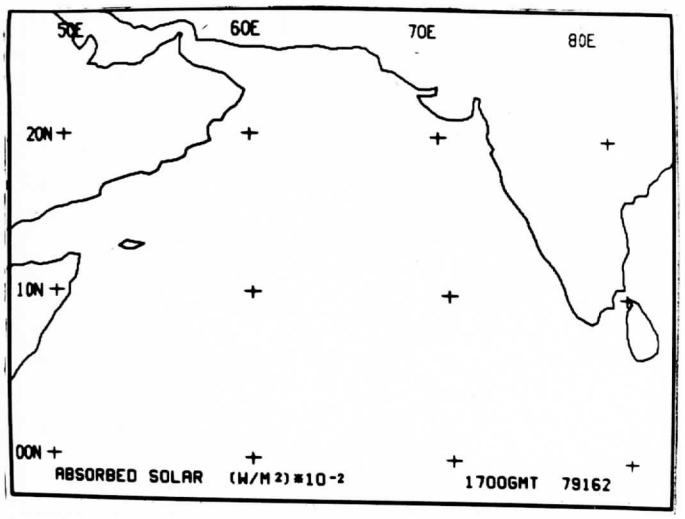
50E
60E
70E
80E
20N
10N
0ON
ABSORBED SOLAR (W/M2)*10-2
1700GMT 79162

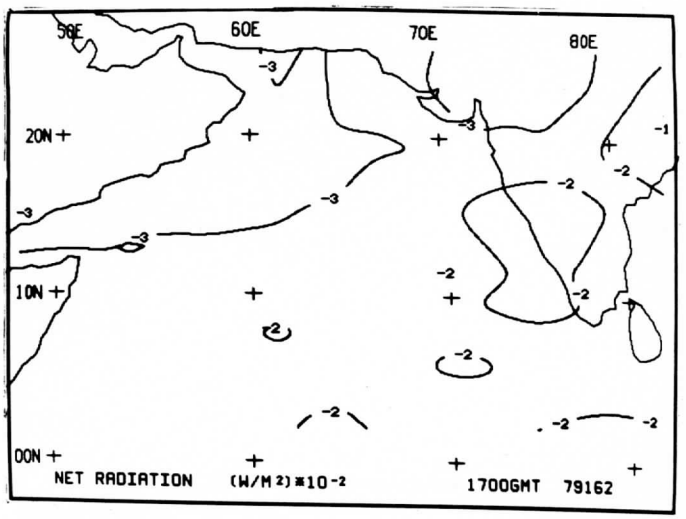
50E
60E
70E
80E
20N
10N
0ON
NET RADIATION (W/M2)*10-2
1700GMT 79162

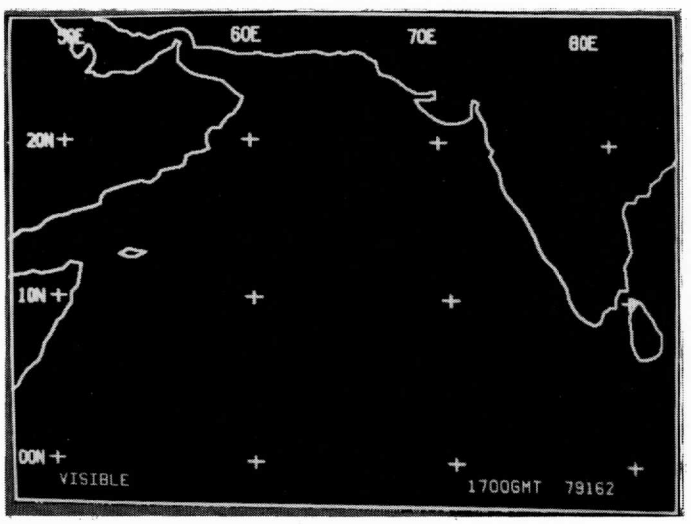
50E
60E
70E
80E
20N
10N
0ON
VISIBLE
1700GMT 79162

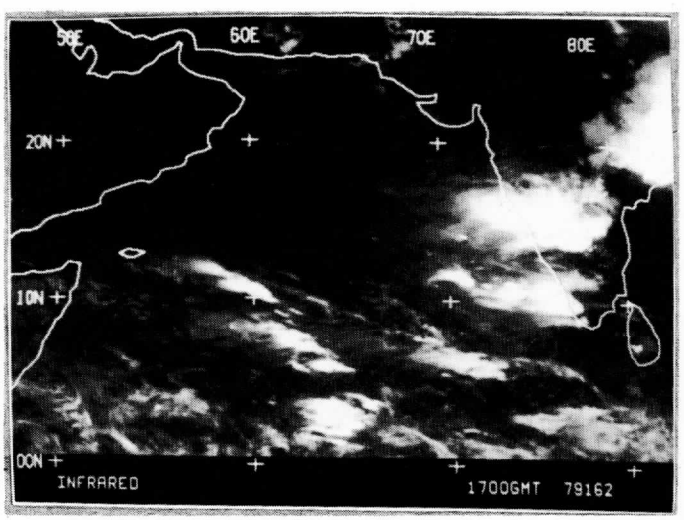
50E
60E
70E
80E
20N
10N
0ON
INFRARED
1700GMT 79162

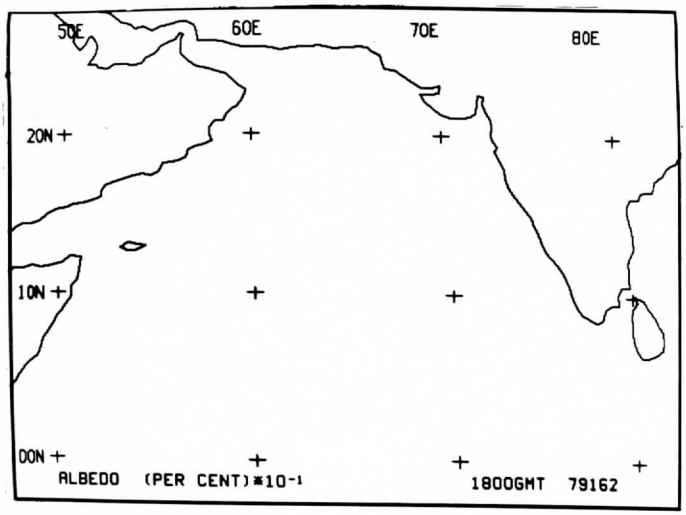
50E
60E
70E
80E
20N
10N
0ON
ALBEDO (PER CENT)*10-1
1800GMT 79162

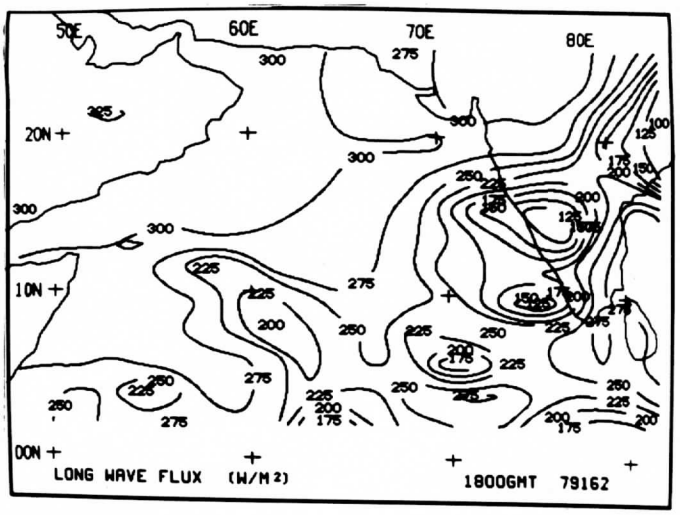
50E
60E
70E
80E
20N
10N
0ON
LONG WAVE FLUX (W/M2)
1800GMT 79162

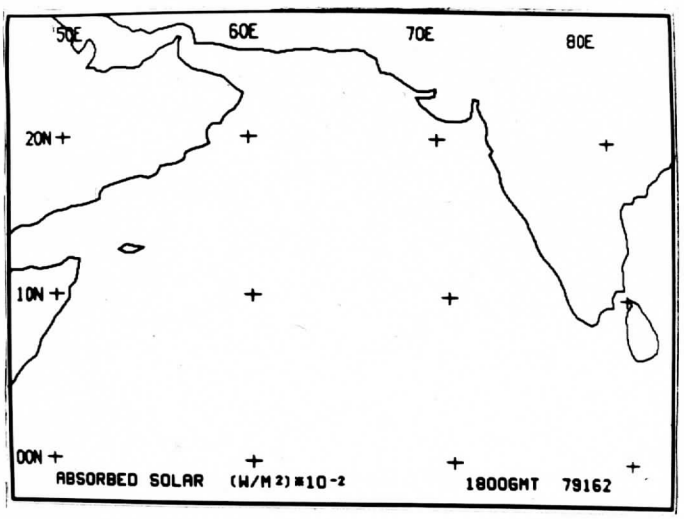
50E
60E
70E
80E
20N
10N
0ON
ABSORBED SOLAR (W/M2)*10-2
1800GMT 79162

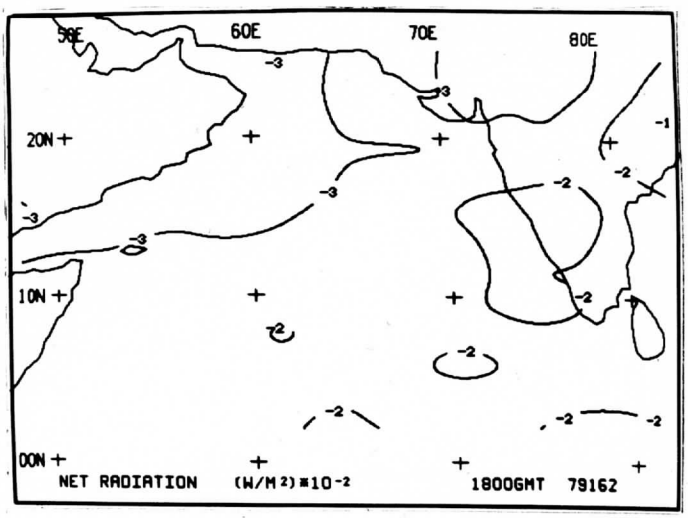
50E
60E
70E
80E
20N
10N
0ON
NET RADIATION (W/M2)*10-2
1800GMT 79162

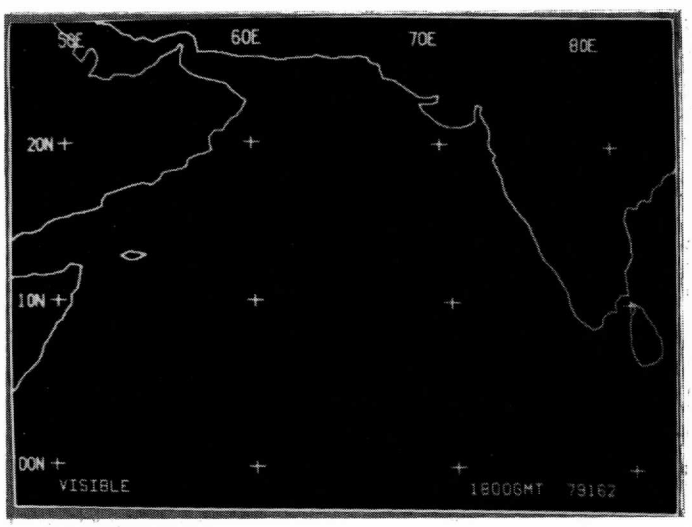
50E
60E
70E
80E
20N
10N
0ON
VISIBLE
1800GMT 79162

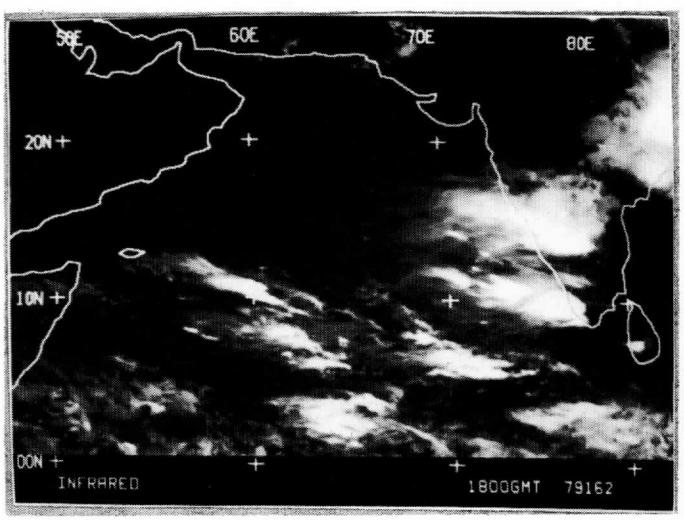
50E
60E
70E
80E
20N
10N
0ON
INFRARED
1800GMT 79162

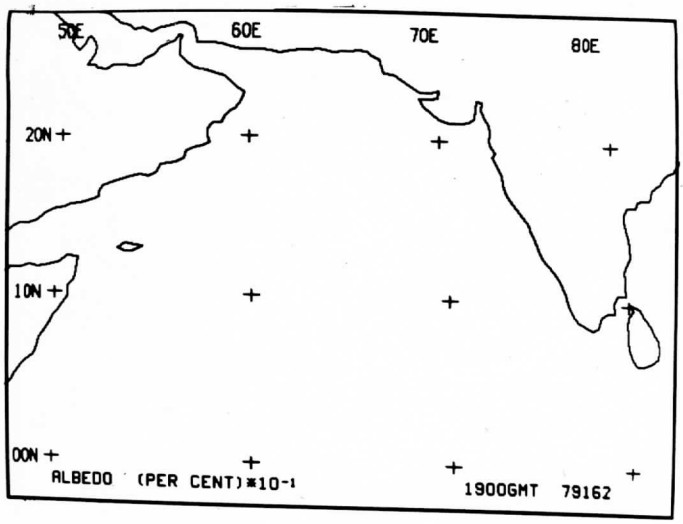
50E
60E
70E
80E
20N
10N
00N
ALBEDO (PER CENT)*10-1
1900GMT 79162

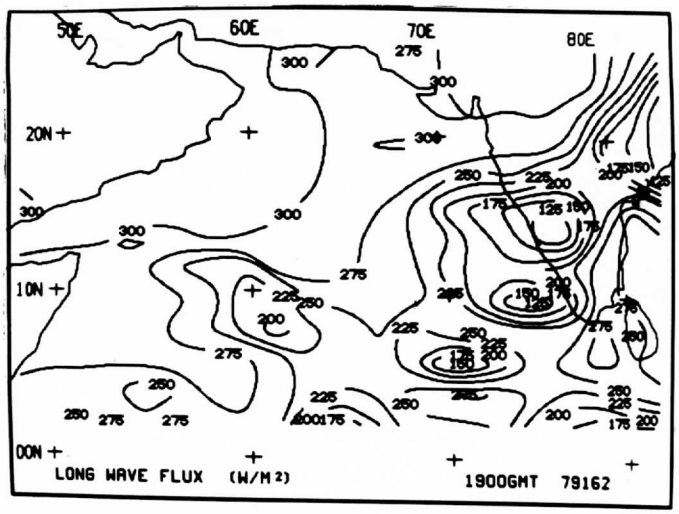
50E
60E
70E
80E
20N
10N
00N
LONG WAVE FLUX (W/M2)
1900GMT 79162

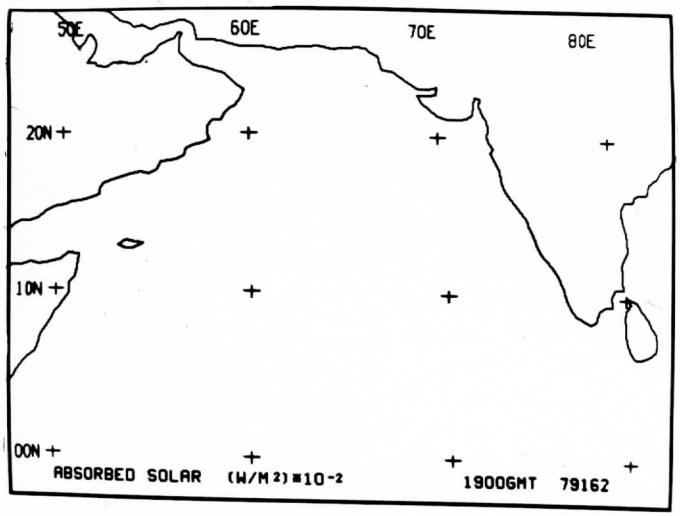
50E
60E
70E
80E
20N
10N
00N
ABSORBED SOLAR (W/M2)*10-2
1900GMT 79162

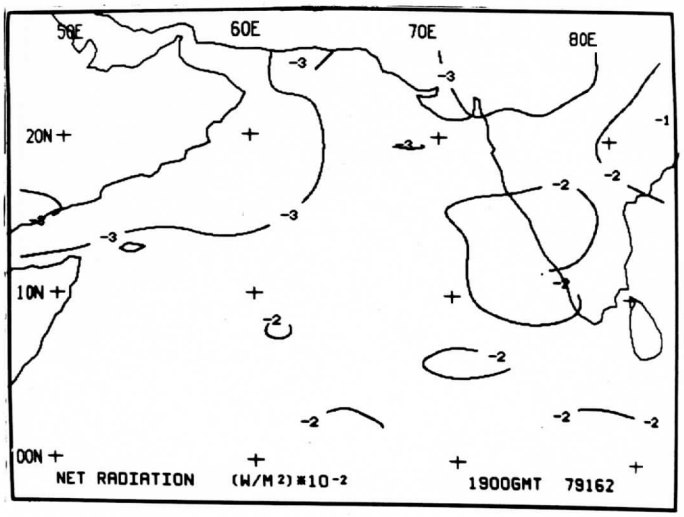
50E
60E
70E
80E
20N
10N
00N
NET RADIATION (W/M2)*10-2
1900GMT 79162

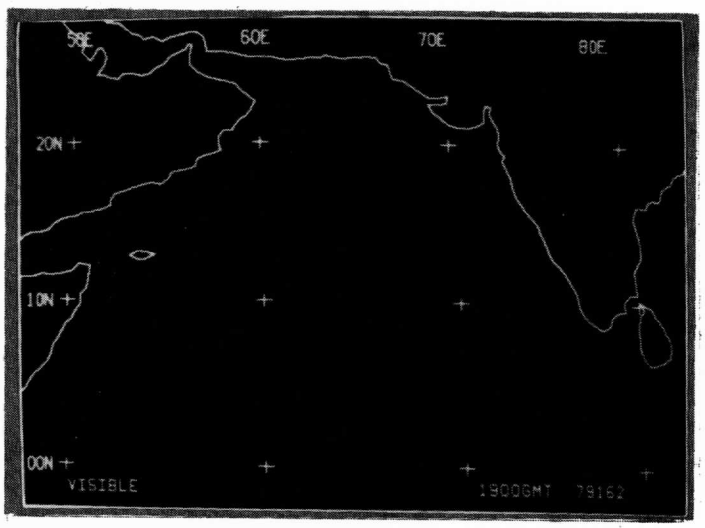
50E
60E
70E
80E
20N
10N
00N
VISIBLE
1900GMT 79162

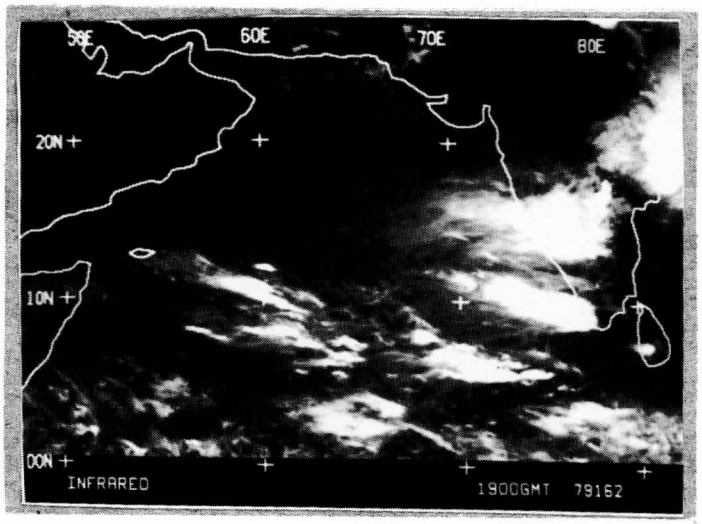
50E
60E
70E
80E
20N
10N
00N
INFRARED
1900GMT 79162

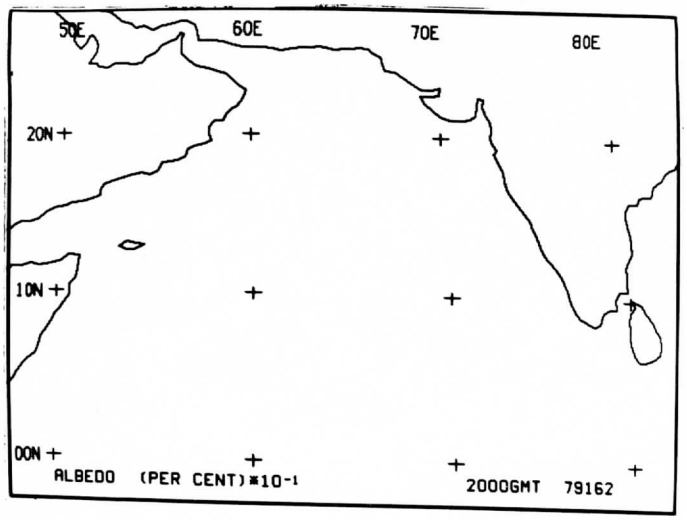
50E
60E
70E
80E
20N
10N
0ON
ALBEDO (PER CENT)*10-1
2000GMT 79162

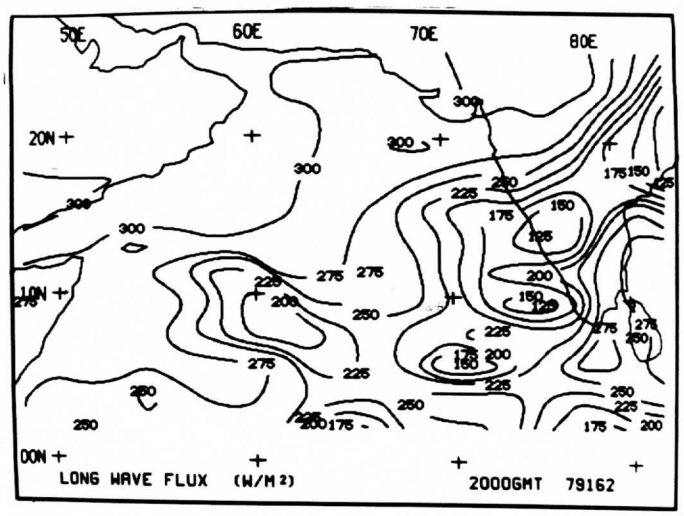
50E
60E
70E
80E
20N
10N
0ON
LONG WAVE FLUX (W/M2)
2000GMT 79162

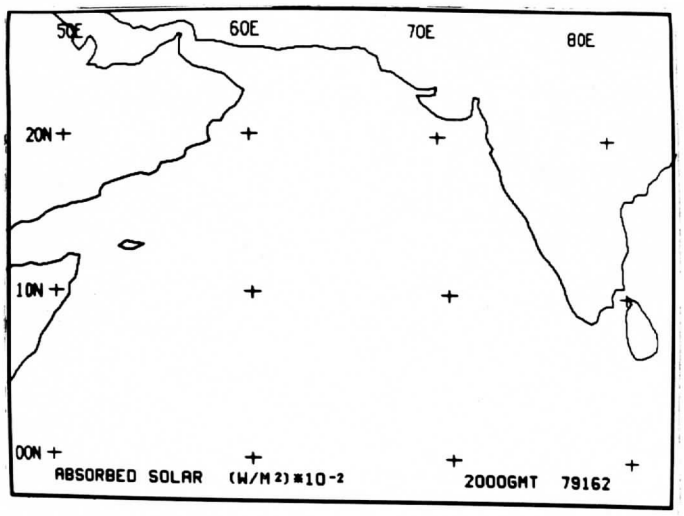
50E
60E
70E
80E
20N
10N
0ON
ABSORBED SOLAR (W/M2)*10-2
2000GMT 79162

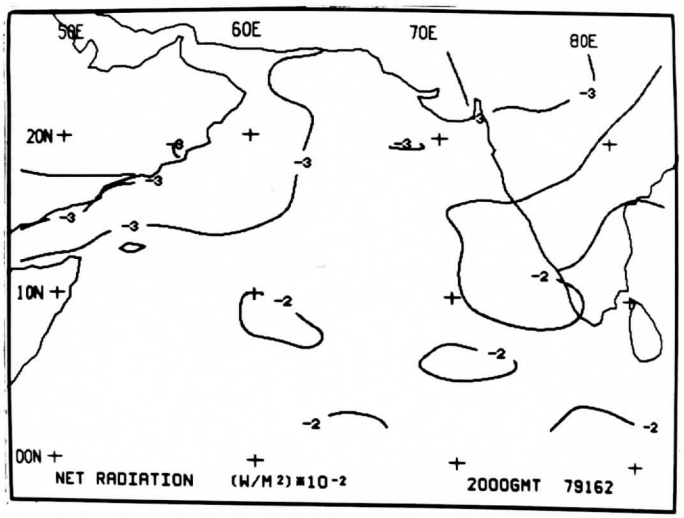
50E
60E
70E
80E
20N
10N
0ON
NET RADIATION (W/M2)*10-2
2000GMT 79162

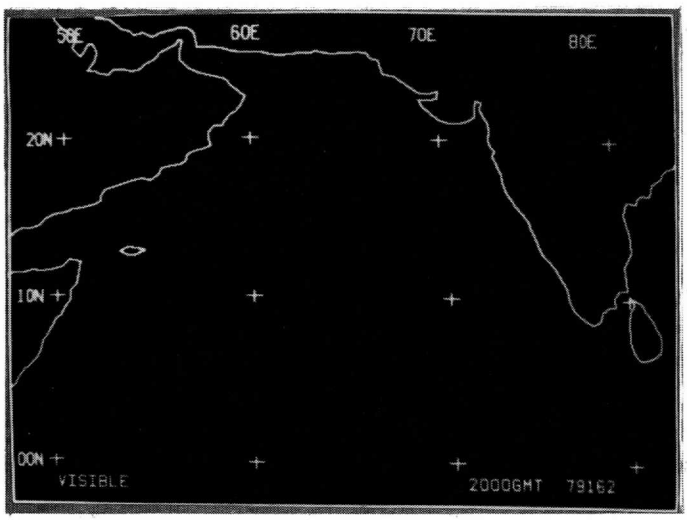
50E
60E
70E
80E
20N
10N
0ON
VISIBLE
2000GMT 79162

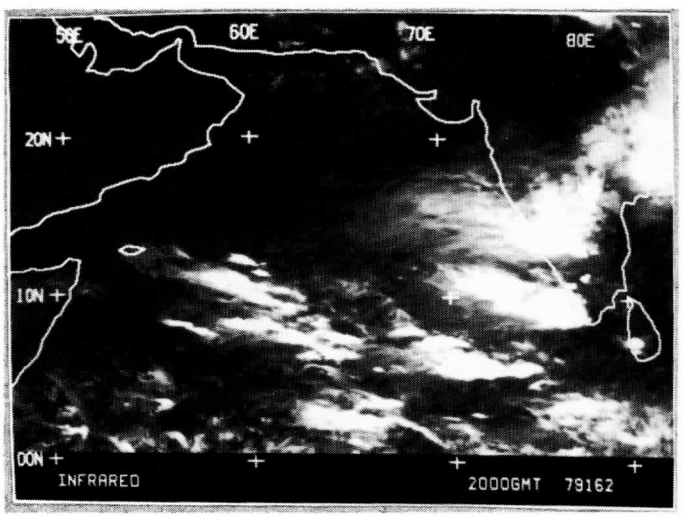
50E
60E
70E
80E
20N
10N
0ON
INFRARED
2000GMT 79162

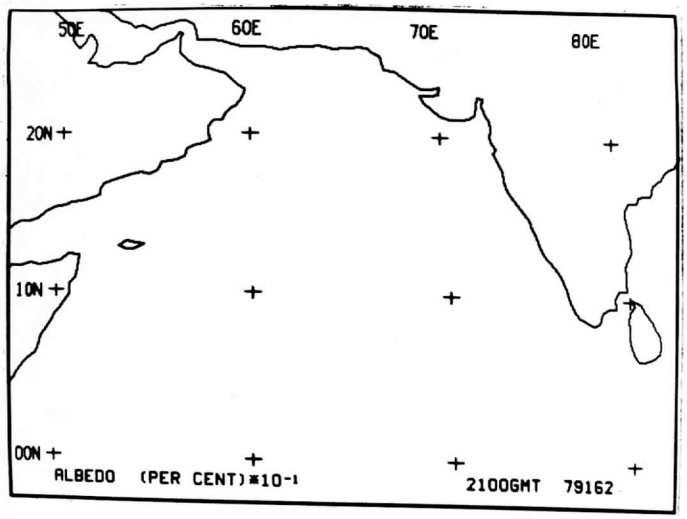
50E
60E
70E
80E
20N
10N
0ON
ALBEDO (PER CENT)*10-1
2100GMT 79162

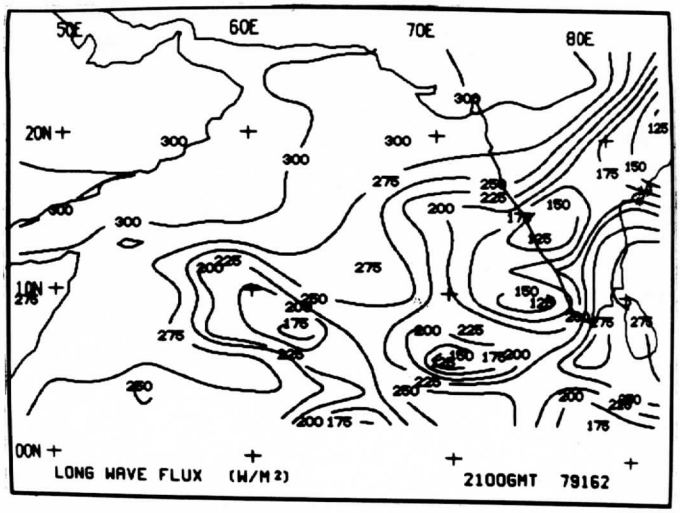
50E
60E
70E
80E
20N
10N
0ON
LONG WAVE FLUX (W/M2)
2100GMT 79162

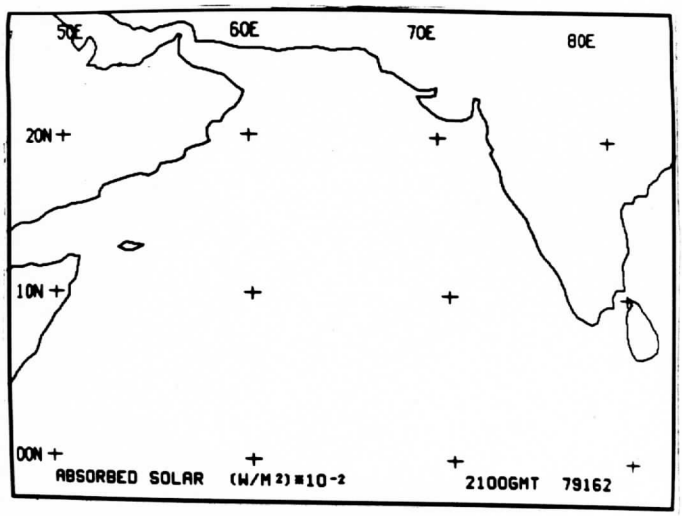
50E
60E
70E
80E
20N
10N
0ON
ABSORBED SOLAR (W/M2)*10-2
2100GMT 79162

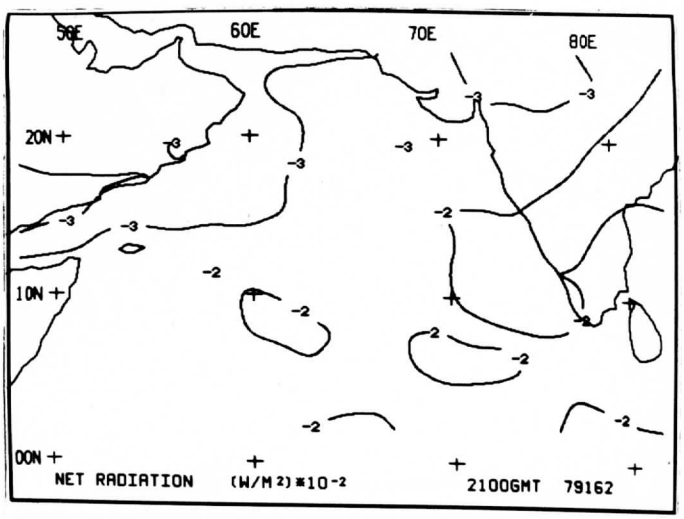
50E
60E
70E
80E
20N
10N
0ON
NET RADIATION (W/M2)*10-2
2100GMT 79162

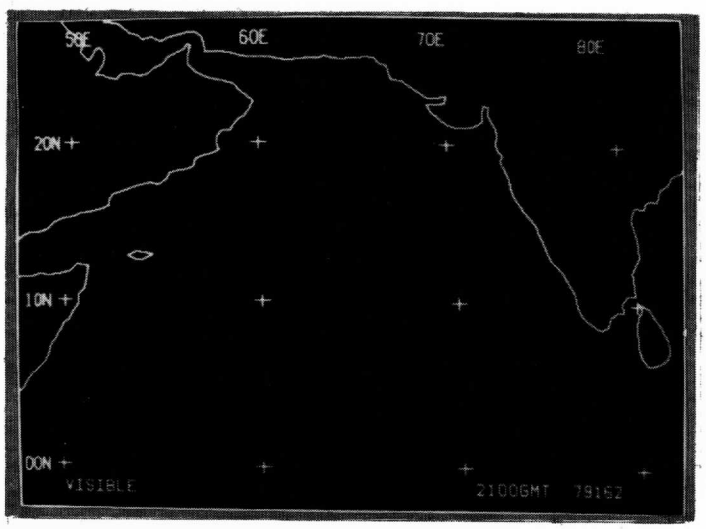
50E
60E
70E
80E
20N
10N
0ON
VISIBLE
2100GMT 79162

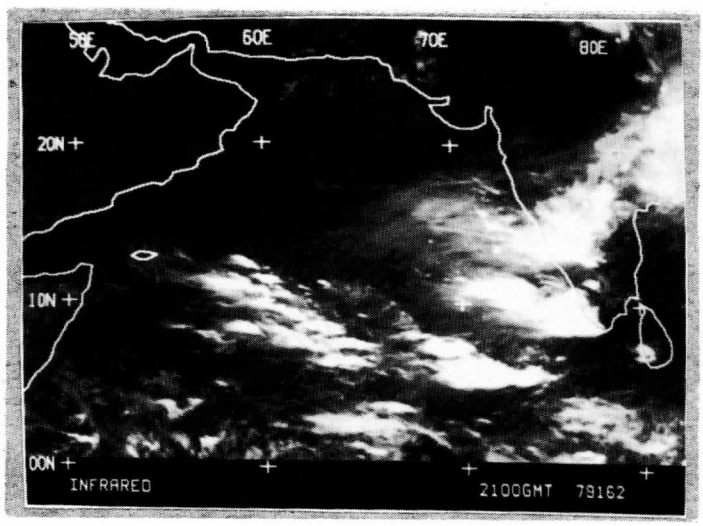
50E
60E
70E
80E
20N
10N
0ON
INFRARED
2100GMT 79162

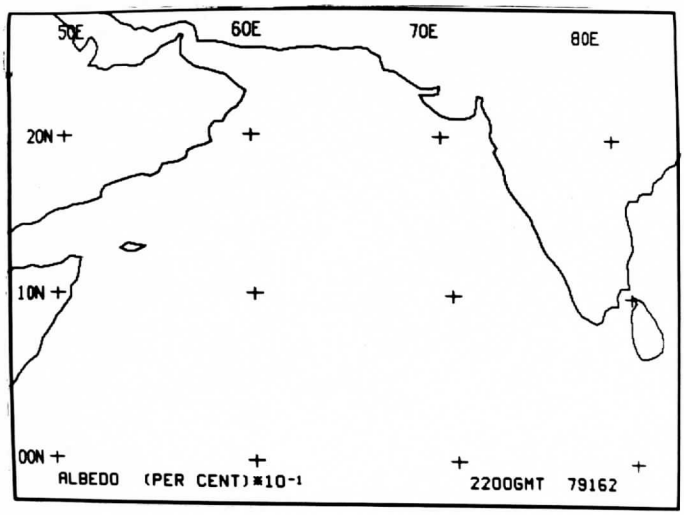
50E
60E
70E
80E
20N
10N
0ON
ALBEDO (PER CENT)*10-1
2200GMT 79162

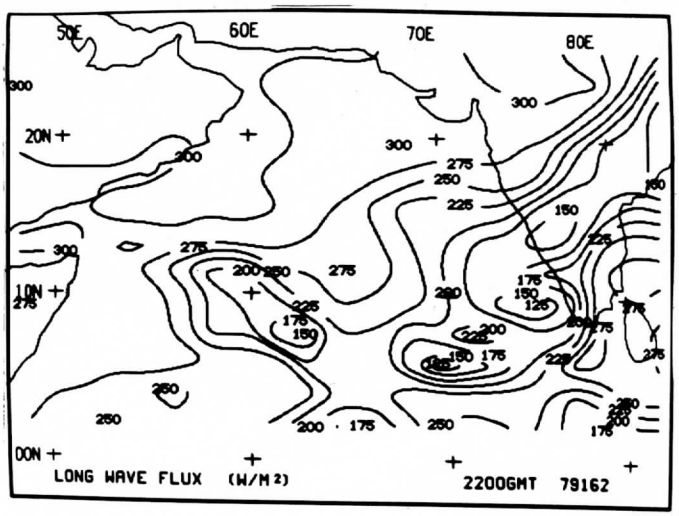
50E
60E
70E
80E
20N
10N
0ON
LONG WAVE FLUX (W/M2)
2200GMT 79162

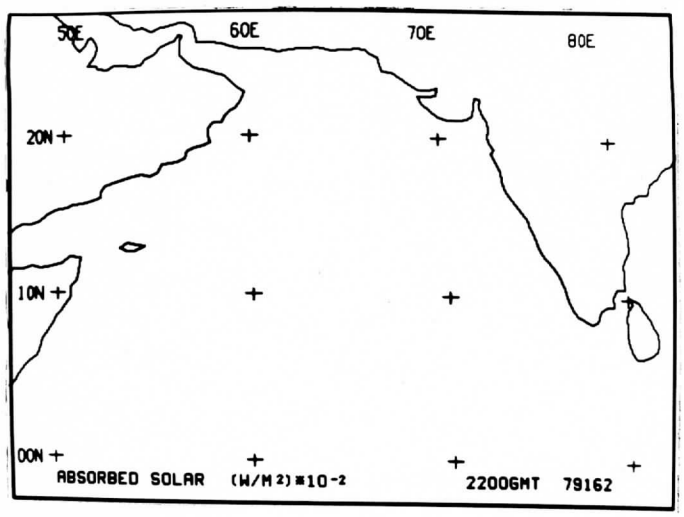
50E
60E
70E
80E
20N
10N
0ON
ABSORBED SOLAR (W/M2)*10-2
2200GMT 79162

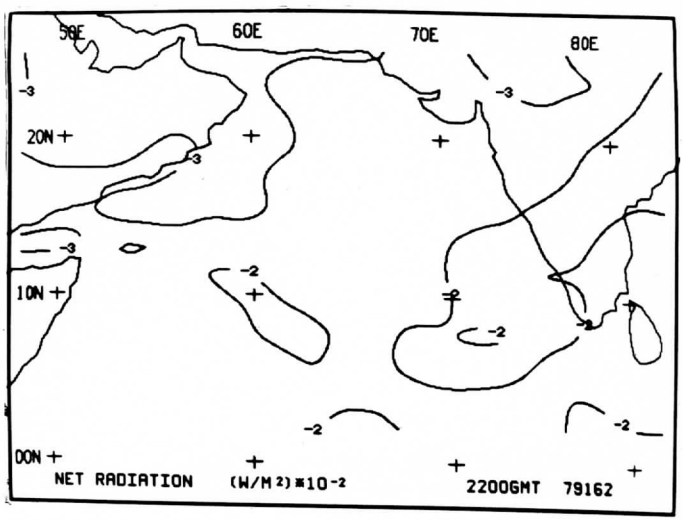
50E
60E
70E
80E
20N
10N
0ON
NET RADIATION (W/M2)*10-2
2200GMT 79162

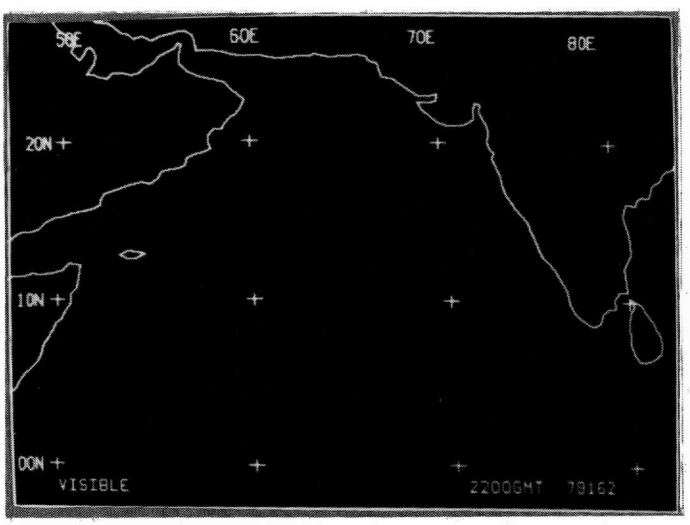
50E
60E
70E
80E
20N
10N
0ON
VISIBLE
2200GMT 79162

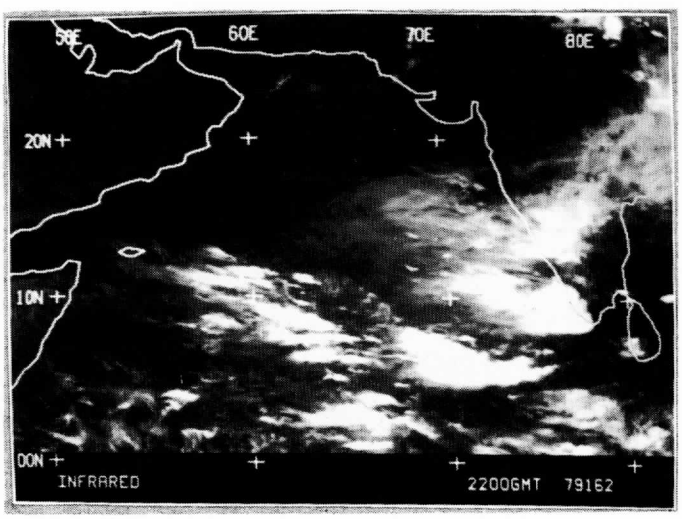
50E
60E
70E
80E
20N
10N
0ON
INFRARED
2200GMT 79162

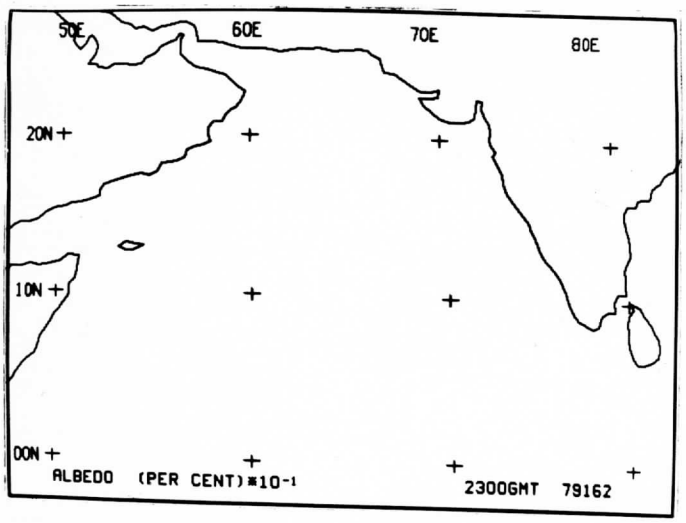
50E
60E
70E
80E
20N
10N
00N
ALBEDO (PER CENT)*10-1
2300GMT 79162

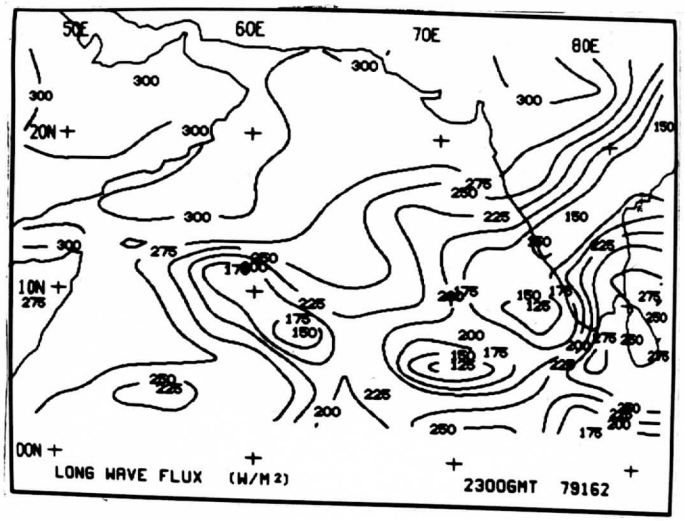
50E
60E
70E
80E
20N
10N
00N
LONG WAVE FLUX (W/M2)
2300GMT 79162

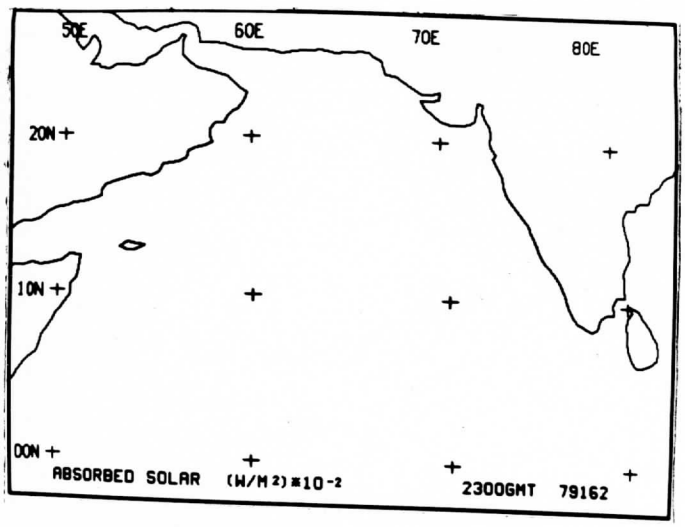
50E
60E
70E
80E
20N
10N
00N
ABSORBED SOLAR (W/M2)*10-2
2300GMT 79162

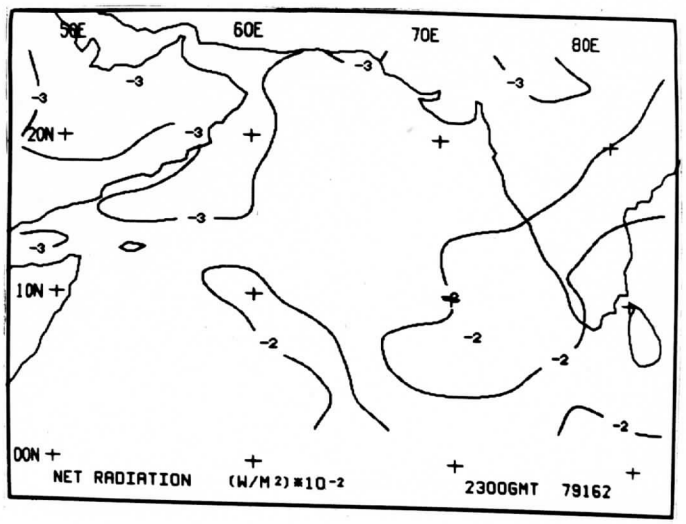
50E
60E
70E
80E
20N
10N
00N
NET RADIATION (W/M2)*10-2
2300GMT 79162

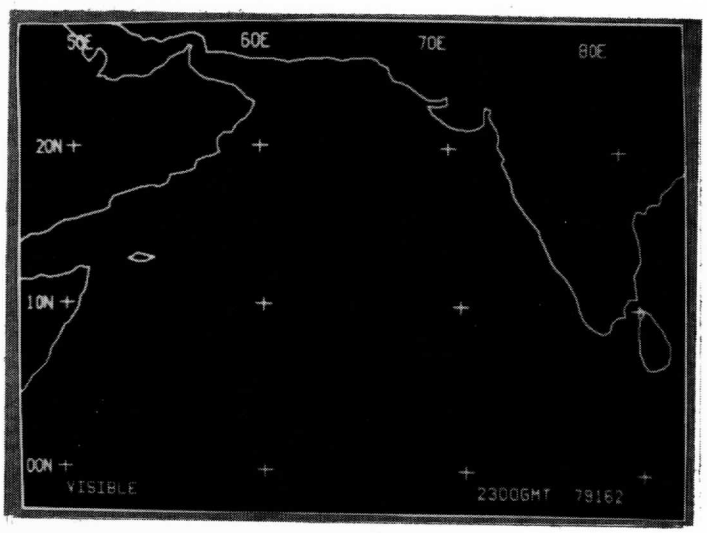
50E
60E
70E
80E
20N
10N
00N
VISIBLE
2300GMT 79162

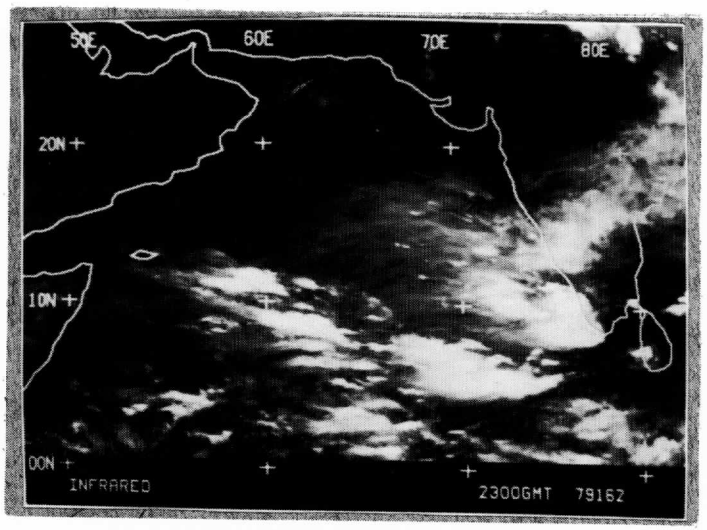
50E
60E
70E
80E
20N
10N
00N
INFRARED
2300GMT 79162

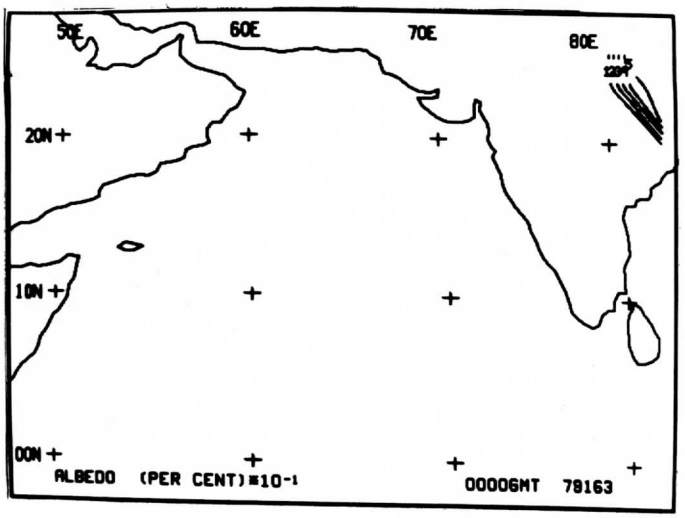
50E
60E
70E
80E
20N
10N
0ON
ALBEDO (PER CENT)*10-1
0000GMT 79163

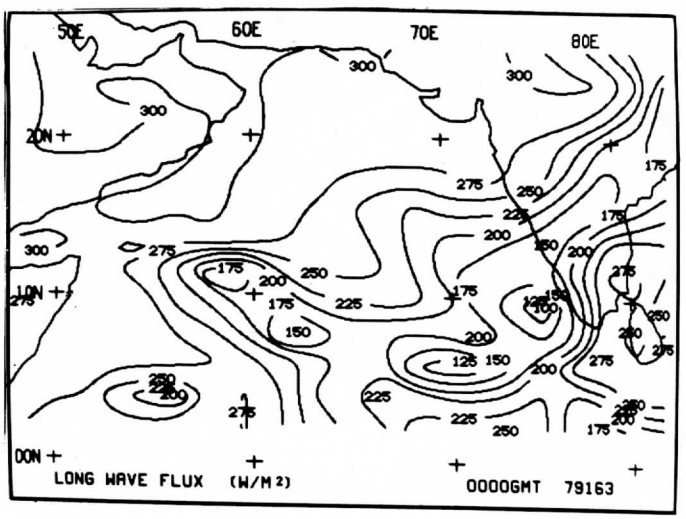
50E
60E
70E
80E
20N
10N
0ON
LONG WAVE FLUX (W/M2)
0000GMT 79163

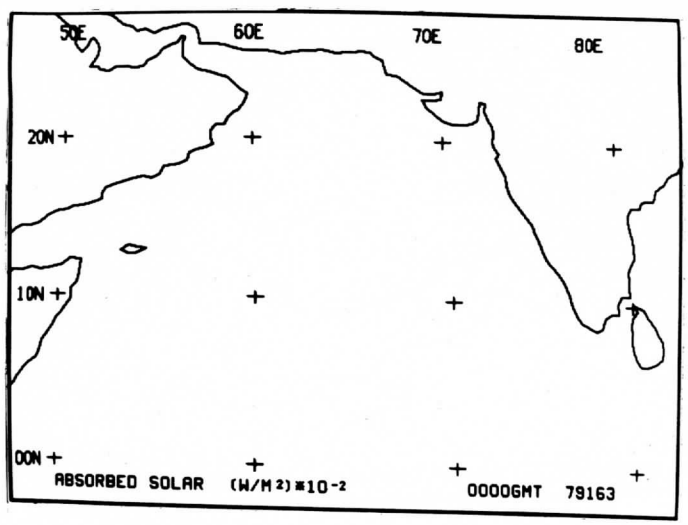
50E
60E
70E
80E
20N
10N
0ON
ABSORBED SOLAR (W/M2)*10-2
0000GMT 79163

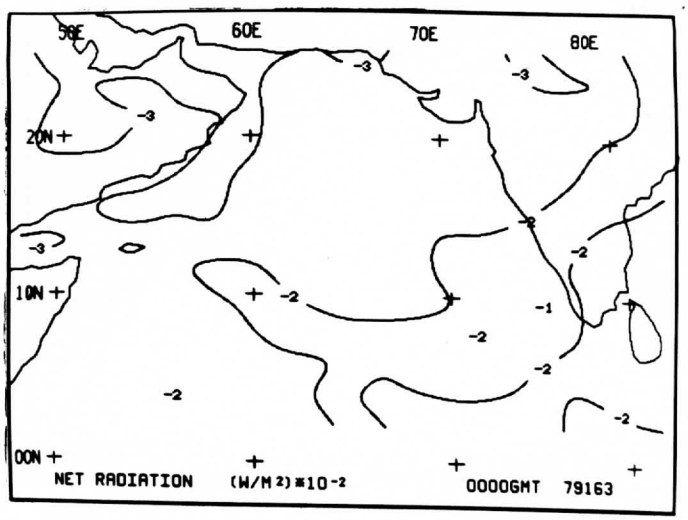
50E
60E
70E
80E
20N
10N
0ON
NET RADIATION (W/M2)*10-2
0000GMT 79163

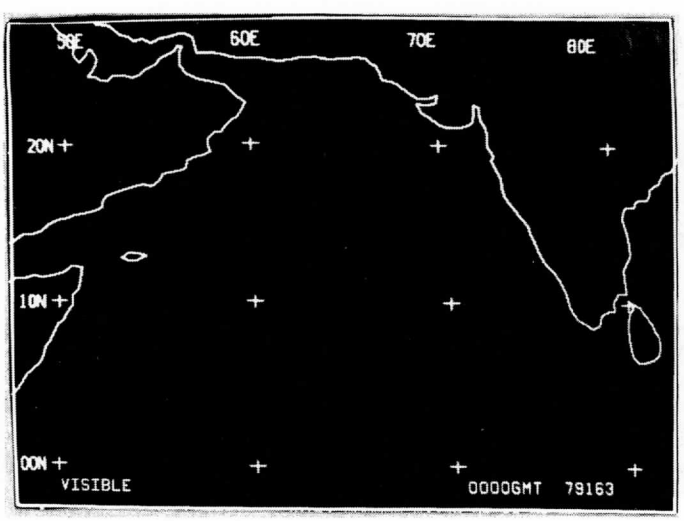
50E
60E
70E
80E
20N
10N
0ON
VISIBLE
0000GMT 79163

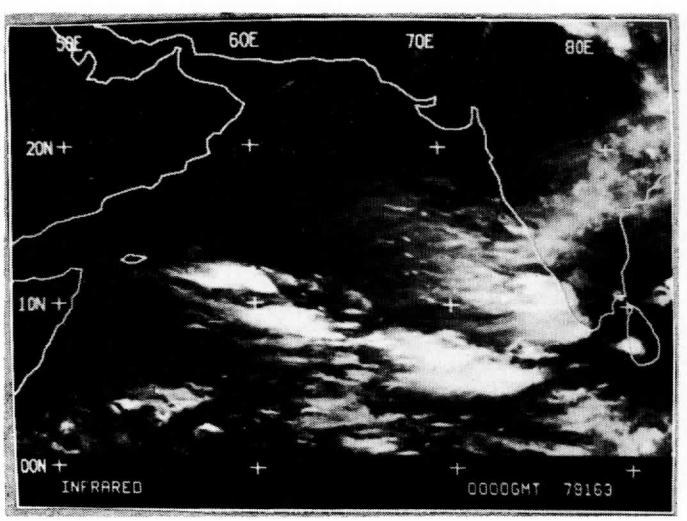
50E
60E
70E
80E
20N
10N
0ON
INFRARED
0000GMT 79163

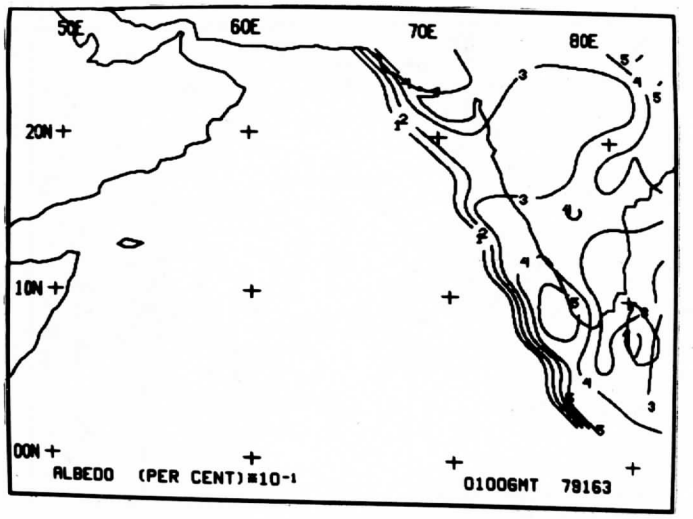
50E
60E
70E
80E
20N
10N
0ON
ALBEDO (PER CENT)*10-1
0100GMT 79163

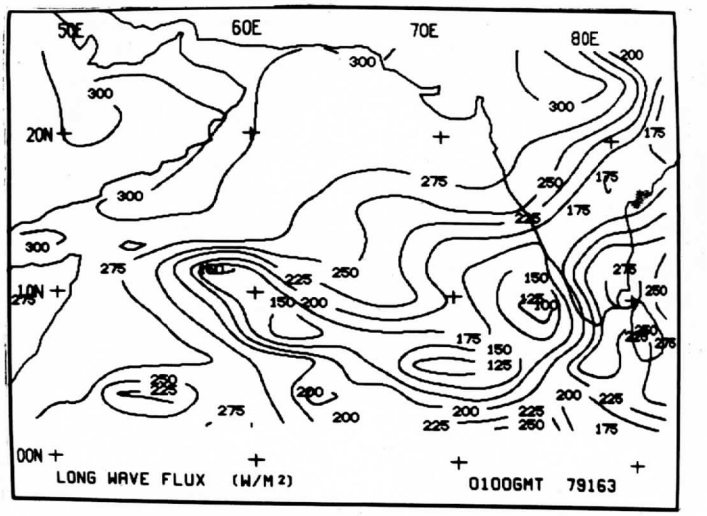
50E
60E
70E
80E
20N
10N
0ON
LONG WAVE FLUX (W/M2)
0100GMT 79163

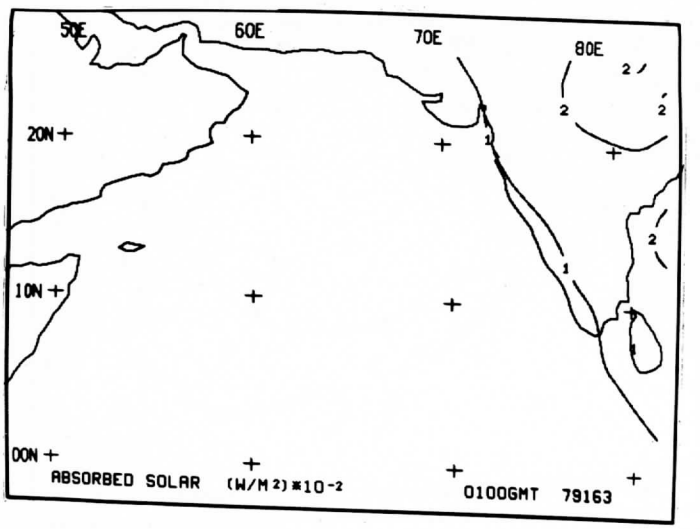
50E
60E
70E
80E
20N
10N
0ON
ABSORBED SOLAR (W/M2)*10-2
0100GMT 79163

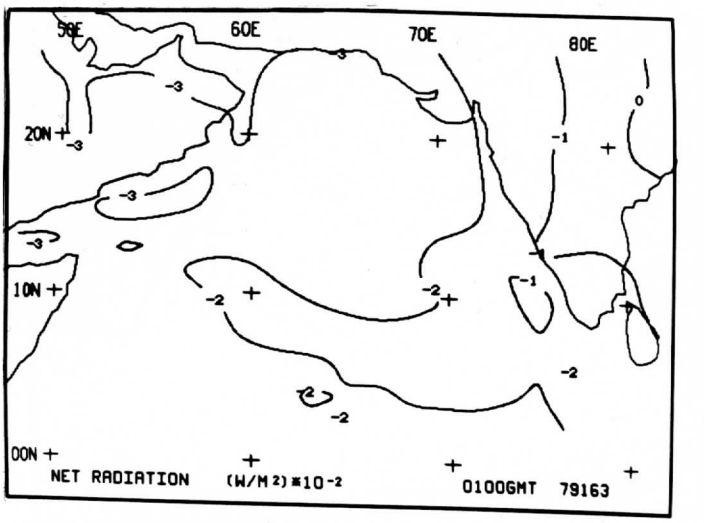
50E
60E
70E
80E
20N
10N
0ON
NET RADIATION (W/M2)*10-2
0100GMT 79163

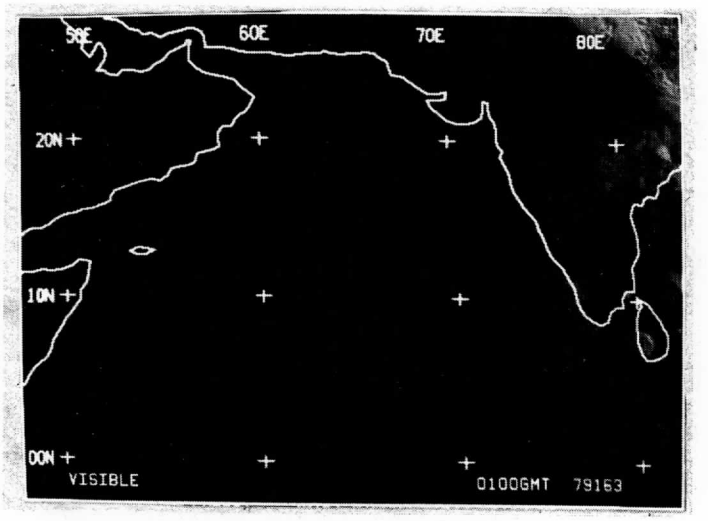
50E
60E
70E
80E
20N
10N
0ON
VISIBLE
0100GMT 79163

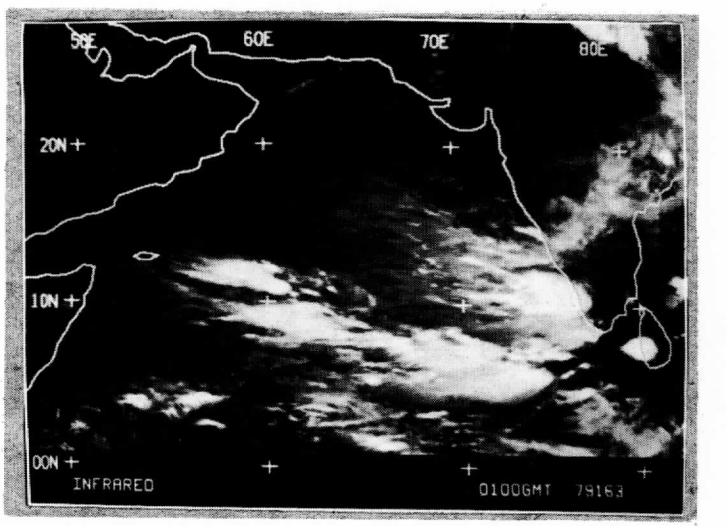
50E
60E
70E
80E
20N
10N
0ON
INFRARED
0100GMT 79163

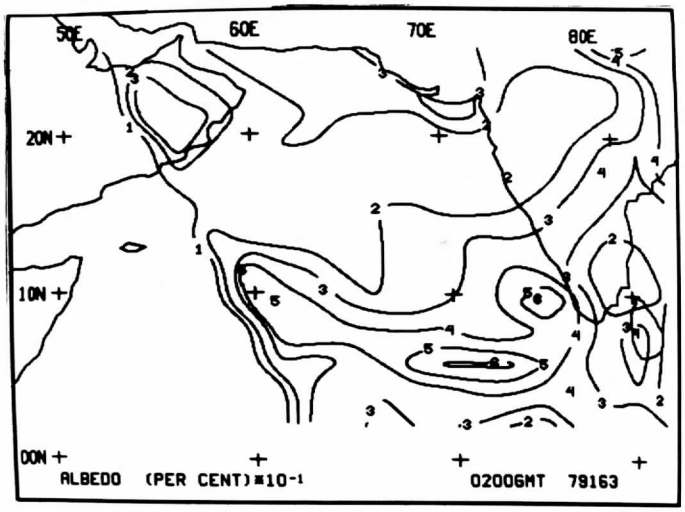
50E
60E
70E
80E
20N
10N
0ON
ALBEDO (PER CENT)*10-1
0200GMT 79163

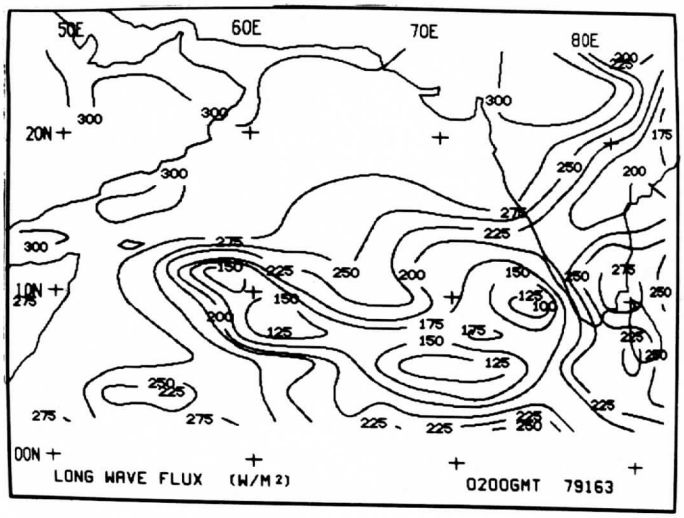
50E
60E
70E
80E
20N
10N
0ON
LONG WAVE FLUX (W/M2)
0200GMT 79163

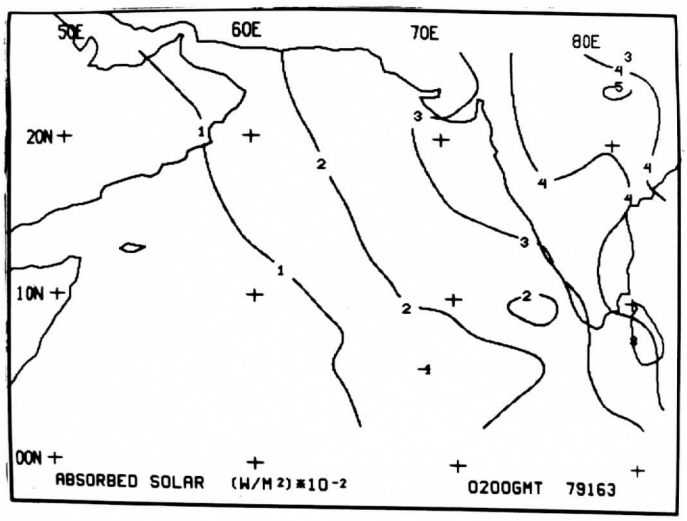
50E
60E
70E
80E
20N
10N
0ON
ABSORBED SOLAR (W/M2)*10-2
0200GMT 79163

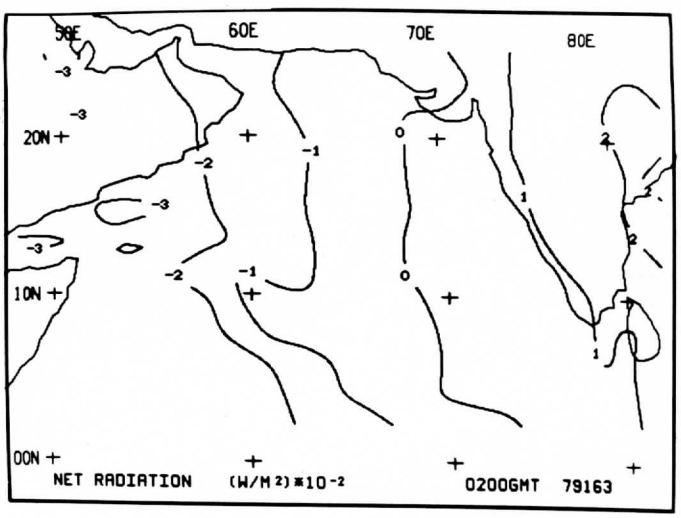
50E
60E
70E
80E
20N
10N
0ON
NET RADIATION (W/M2)*10-2
0200GMT 79163

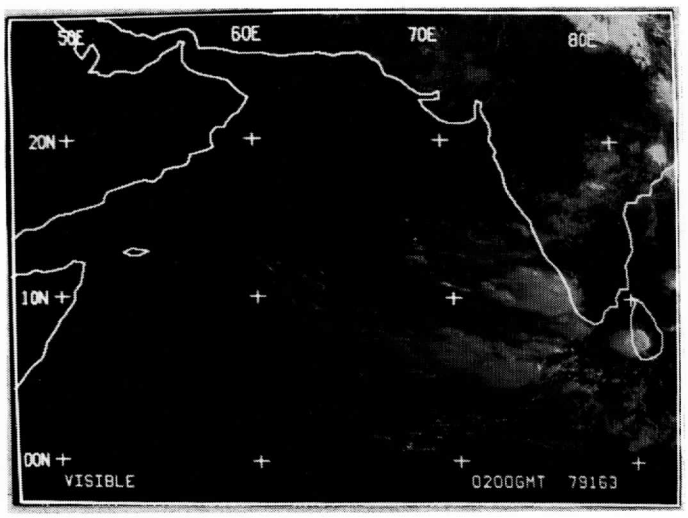
50E
60E
70E
80E
20N
10N
0ON
VISIBLE
0200GMT 79163

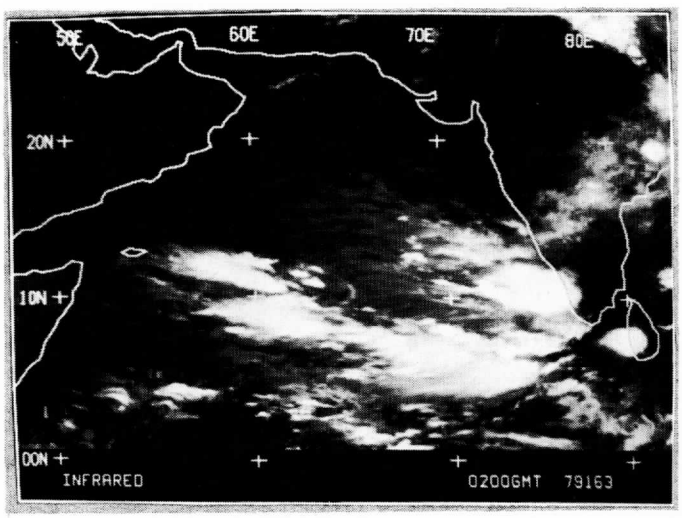
50E
60E
70E
80E
20N
10N
0ON
INFRARED
0200GMT 79163

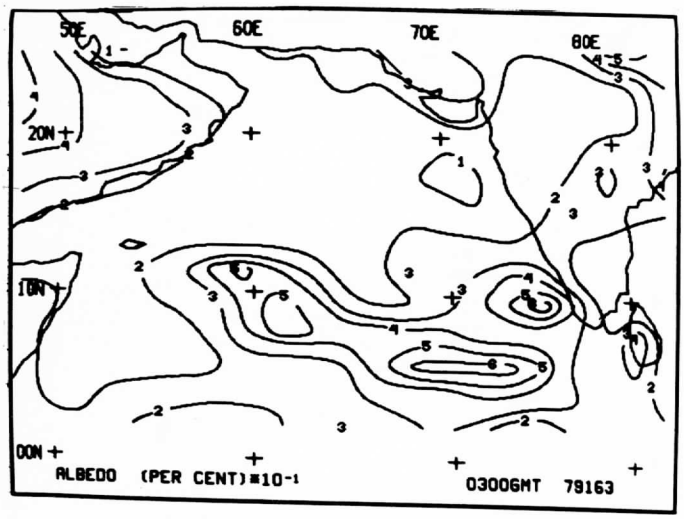
50E
60E
70E
80E
20N
10N
0ON
ALBEDO (PER CENT)*10-1
03006MT 79163

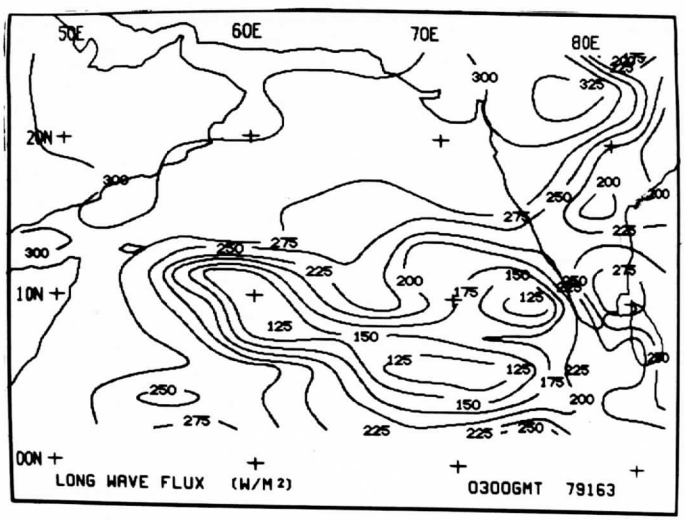
50E
60E
70E
80E
20N
10N
0ON
LONG WAVE FLUX (W/M2)
03006MT 79163

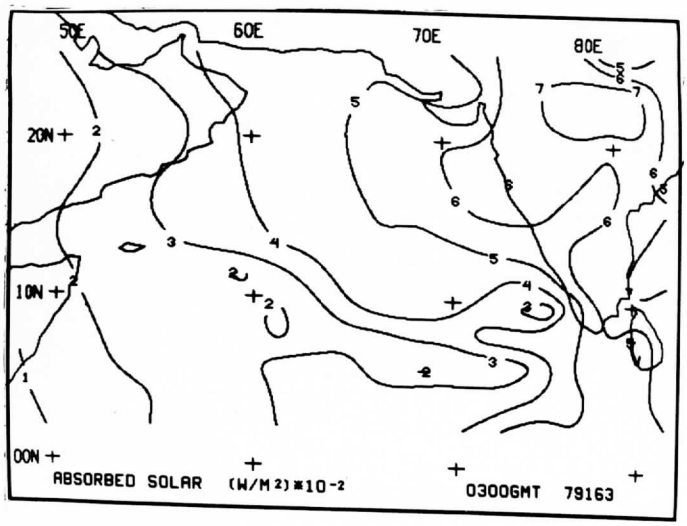
50E
60E
70E
80E
20N
10N
0ON
ABSORBED SOLAR (W/M2)*10-2
03006MT 79163

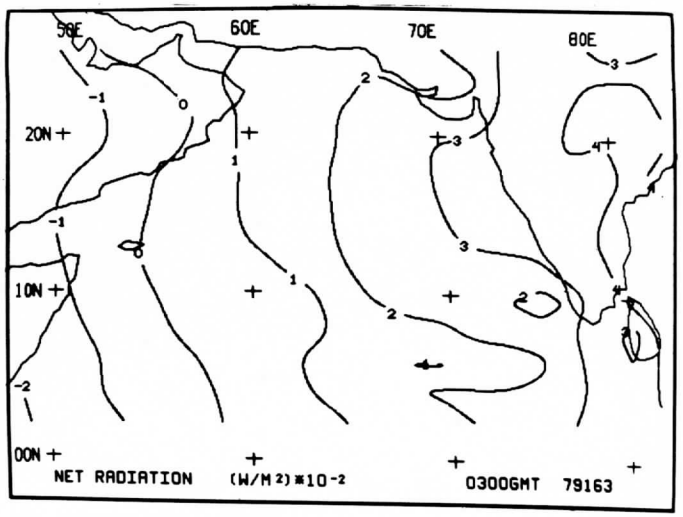
50E
60E
70E
80E
20N
10N
0ON
NET RADIATION (W/M2)*10-2
03006MT 79163

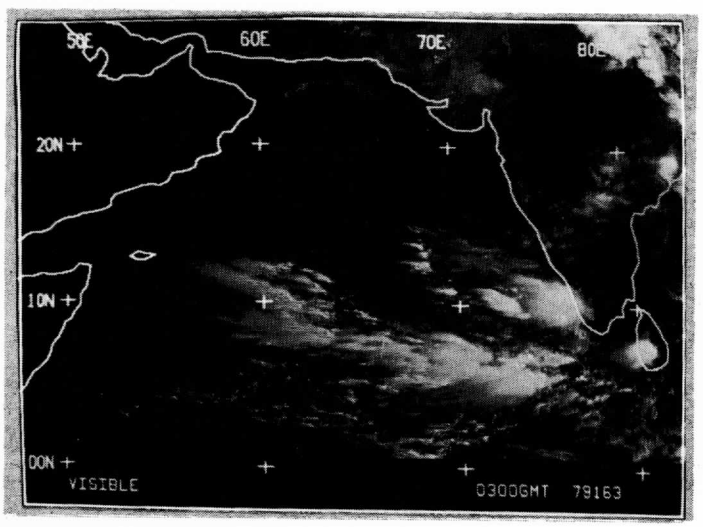
50E
60E
70E
80E
20N
10N
0ON
VISIBLE
03006MT 79163

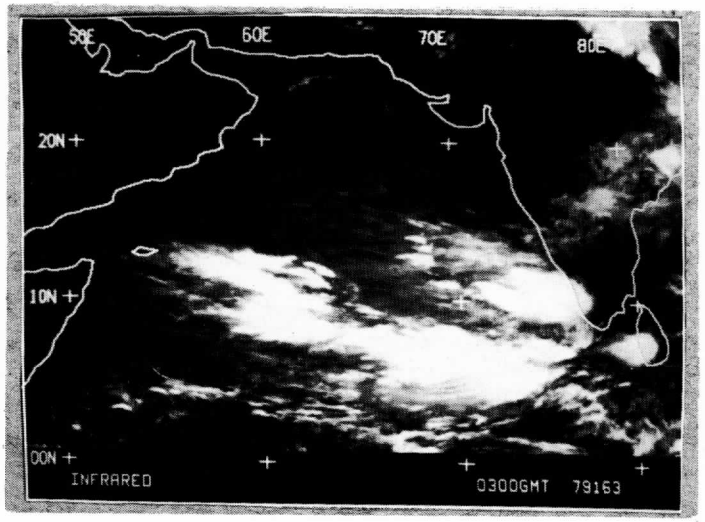
50E
60E
70E
80E
20N
10N
0ON
INFRARED
03006MT 79163

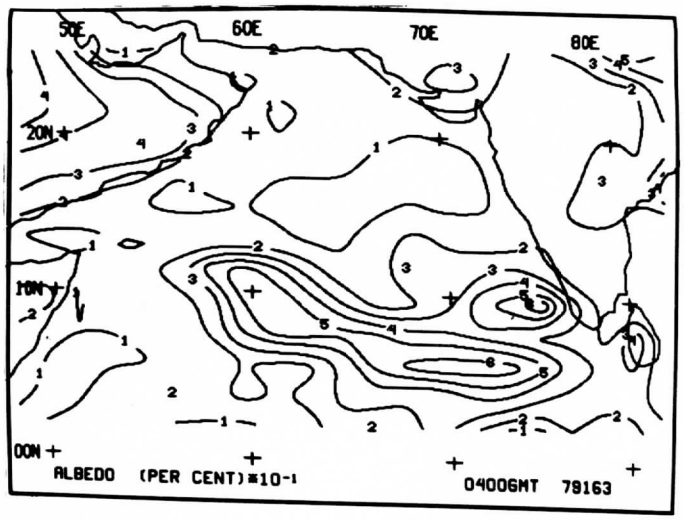
50E
60E
70E
80E
20N
10N
0ON
ALBEDO (PER CENT)×10-1
0400GMT 79163

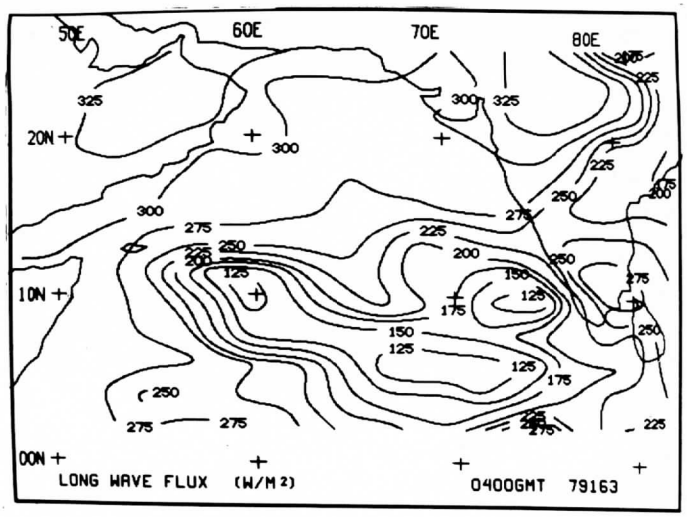
50E
60E
70E
80E
20N
10N
0ON
LONG WAVE FLUX (W/M2)
0400GMT 79163

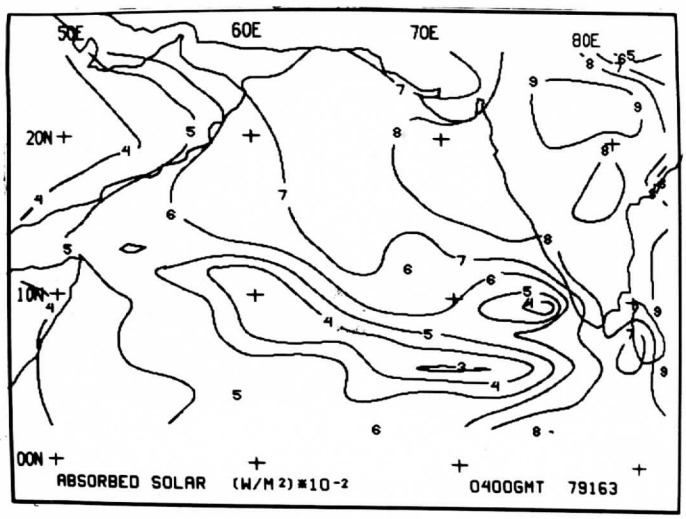
50E
60E
70E
80E
20N
10N
0ON
ABSORBED SOLAR (W/M2)×10-2
0400GMT 79163

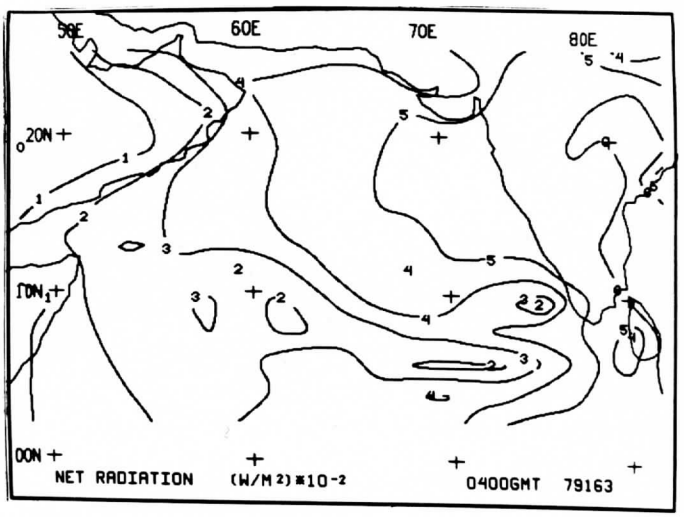
50E
60E
70E
80E
20N
10N
0ON
NET RADIATION (W/M2)×10-2
0400GMT 79163

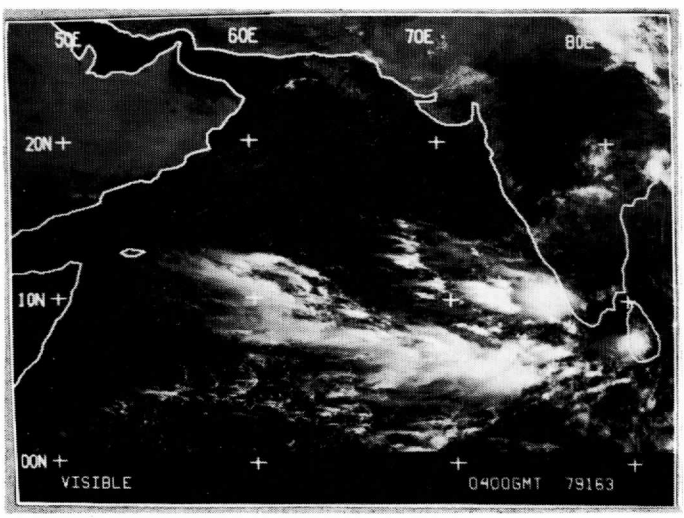
50E
60E
70E
20N
10N
0ON
VISIBLE
0400GMT 79163

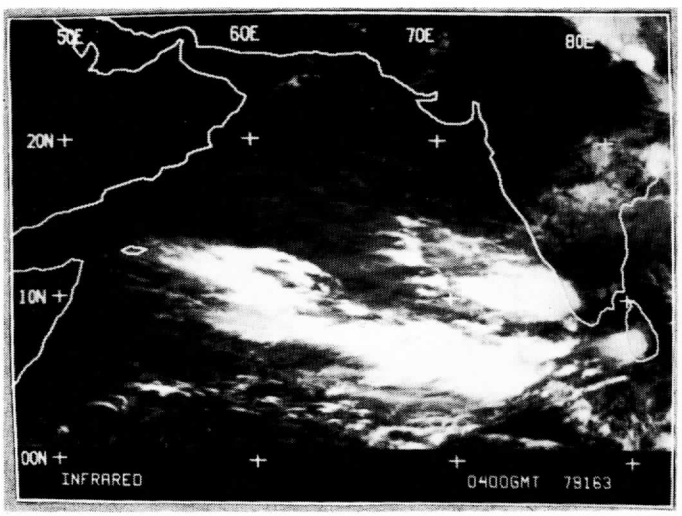
50E
60E
70E
20N
10N
0ON
INFRARED
0400GMT 79163

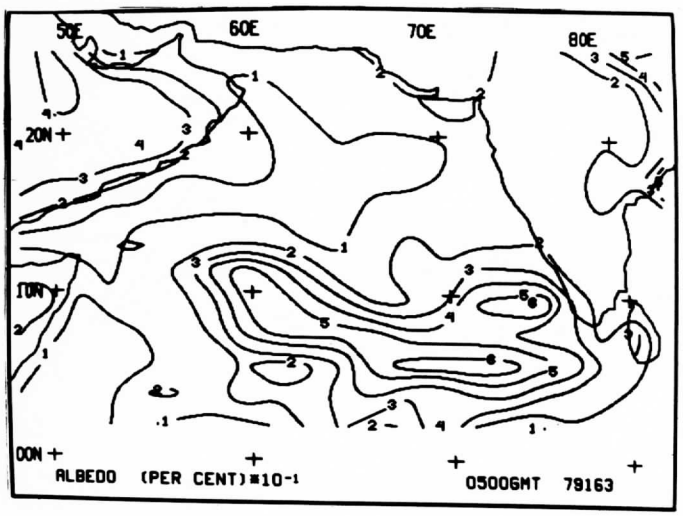
50E
60E
70E
80E
20N
10N
0ON
ALBEDO (PER CENT)*10-1
0500GMT 79163

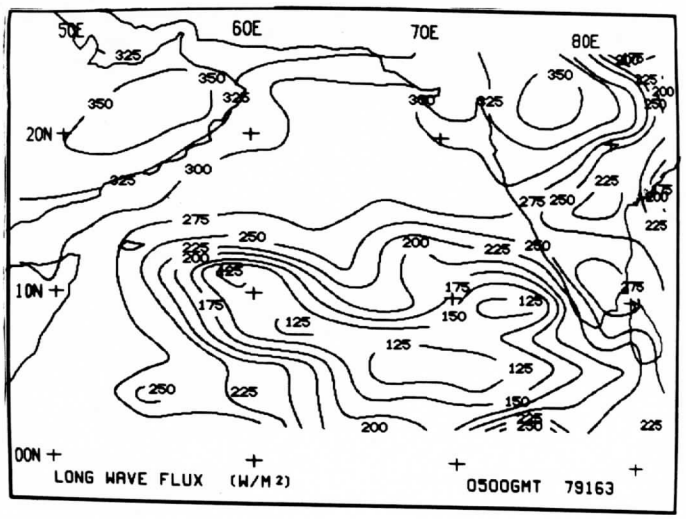
50E
60E
70E
80E
20N
10N
0ON
LONG WAVE FLUX (W/M2)
0500GMT 79163

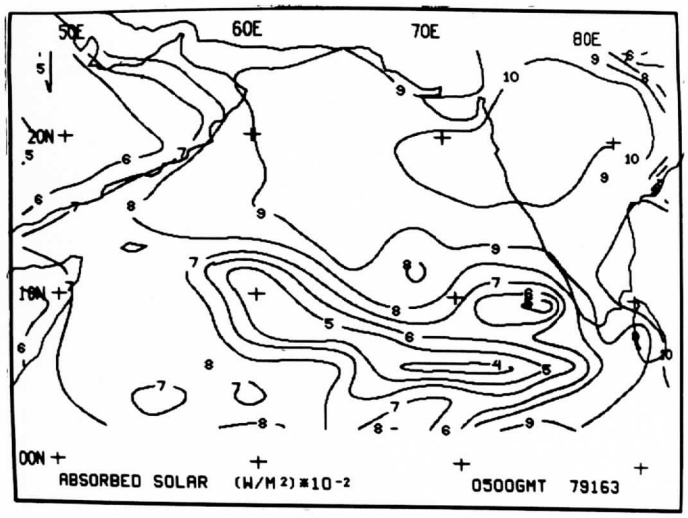
50E
60E
70E
80E
20N
10N
0ON
ABSORBED SOLAR (W/M2)*10-2
0500GMT 79163

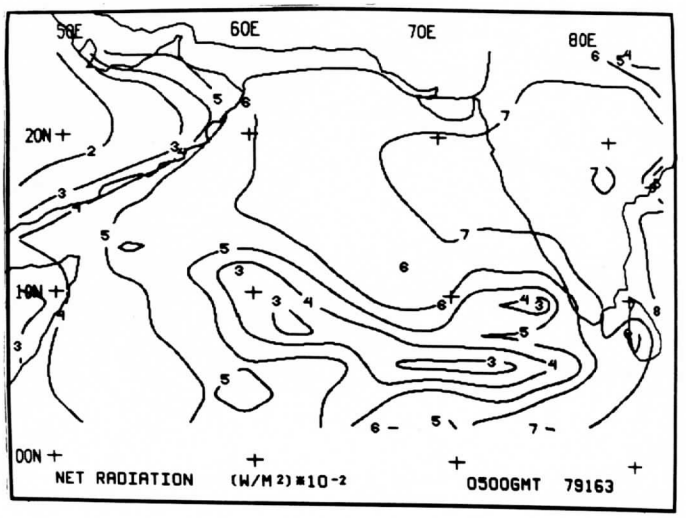
50E
60E
70E
80E
20N
10N
0ON
NET RADIATION (W/M2)*10-2
0500GMT 79163

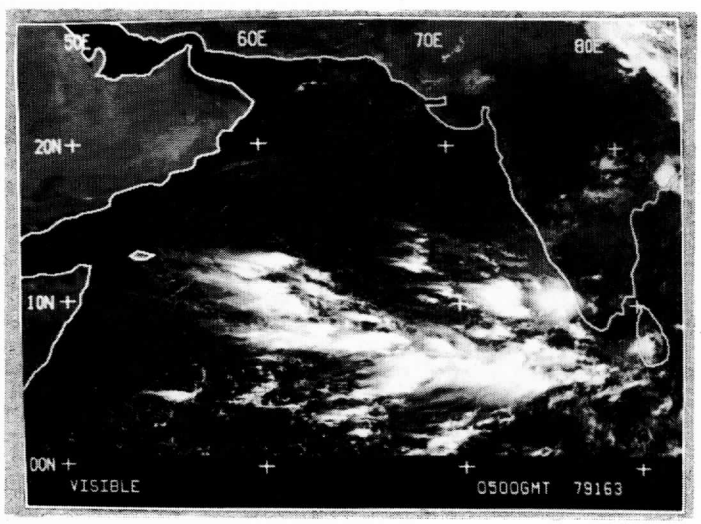
50E
60E
70E
80E
20N
10N
0ON
VISIBLE
0500GMT 79163

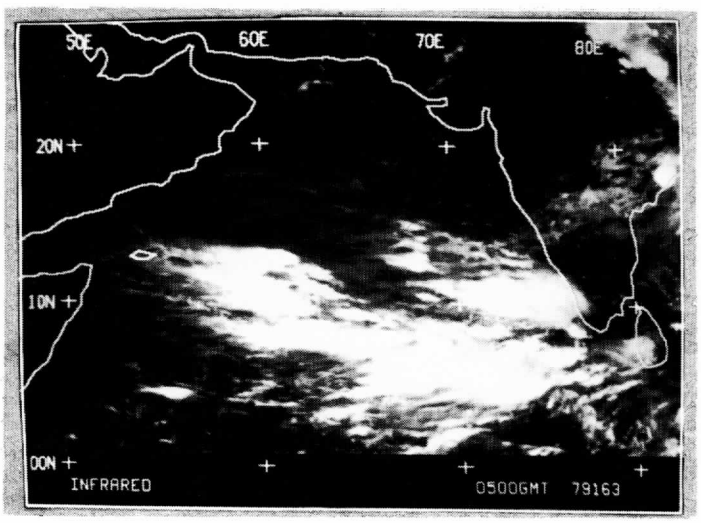
50E
60E
70E
80E
20N
10N
0ON
INFRARED
0500GMT 79163

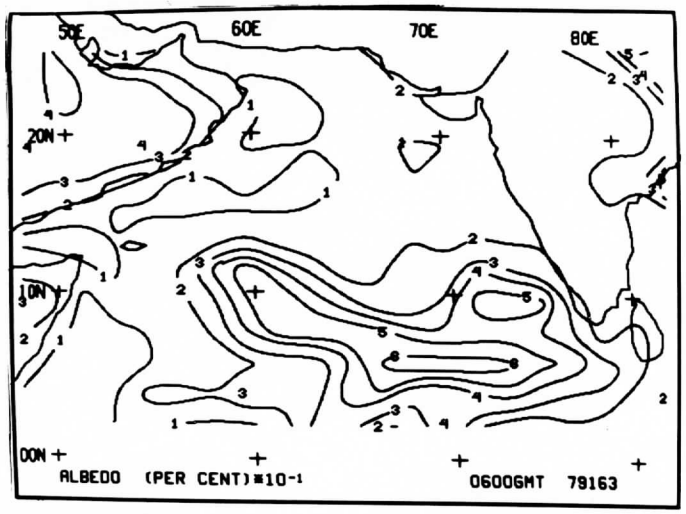
50E
60E
70E
80E
20N
10N
0ON
ALBEDO (PER CENT)*10-1
0600GMT 79163

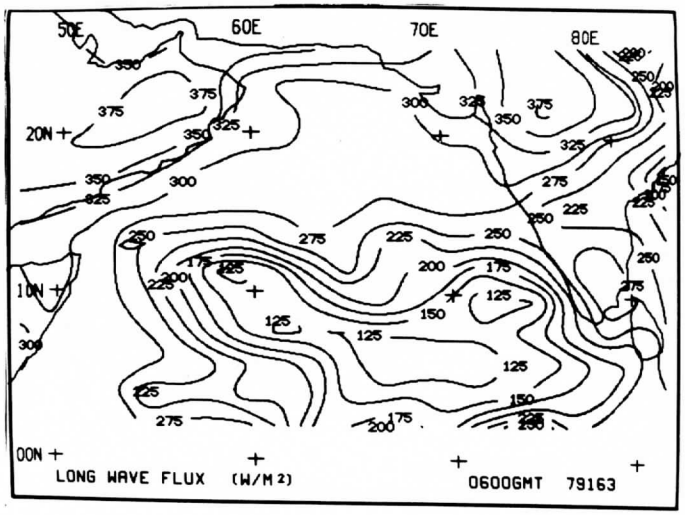
50E
60E
70E
80E
20N
10N
0ON
LONG WAVE FLUX (W/M2)
0600GMT 79163

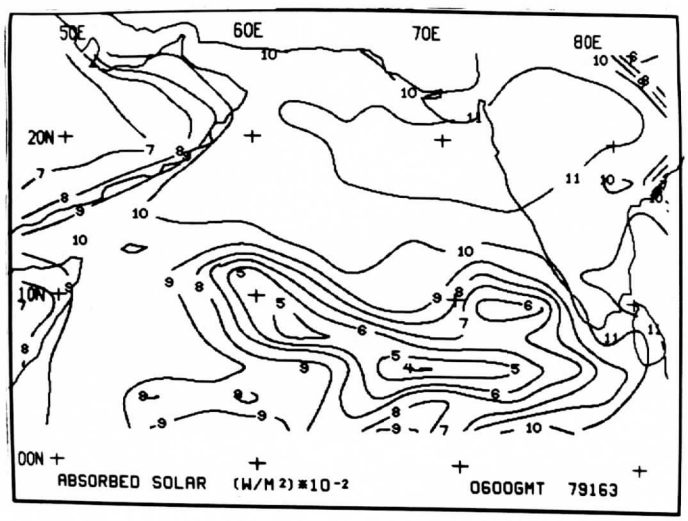
50E
60E
70E
80E
20N
10N
0ON
ABSORBED SOLAR (W/M2)*10-2
0600GMT 79163

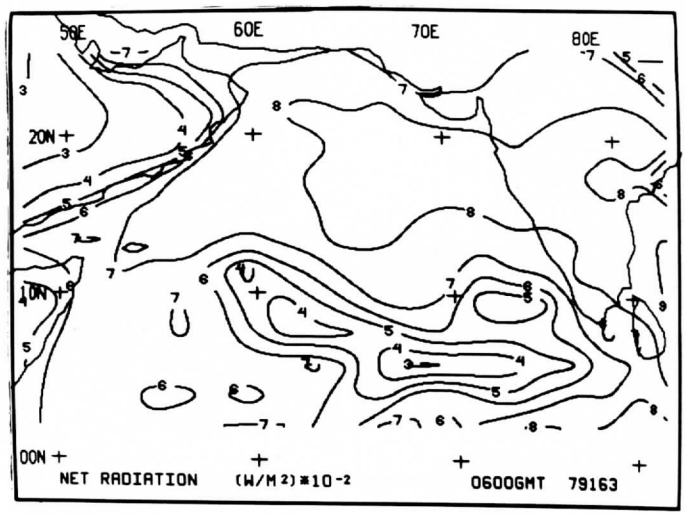
50E
60E
70E
80E
20N
10N
0ON
NET RADIATION (W/M2)*10-2
0600GMT 79163

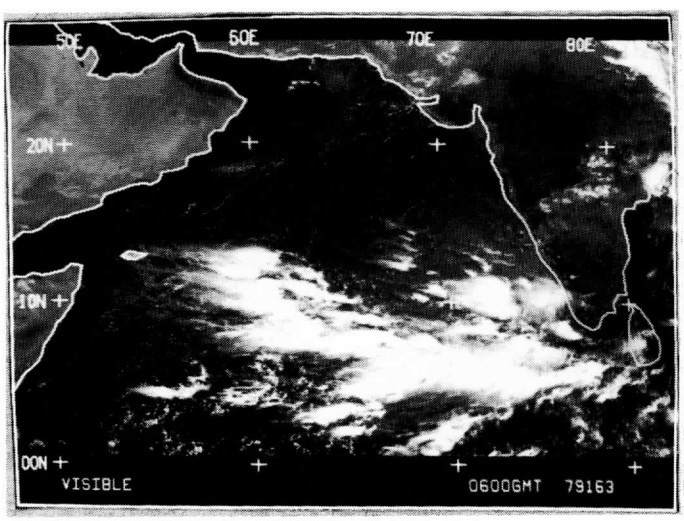
50E
60E
70E
80E
20N
10N
0ON
VISIBLE
0600GMT 79163

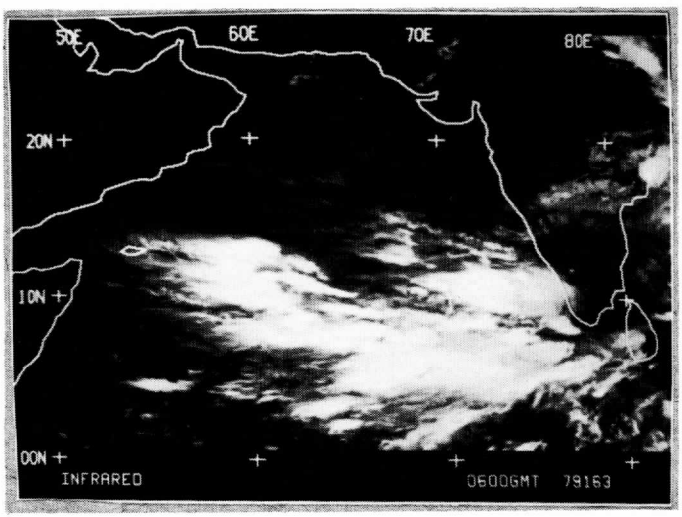
50E
60E
70E
80E
20N
10N
0ON
INFRARED
0600GMT 79163

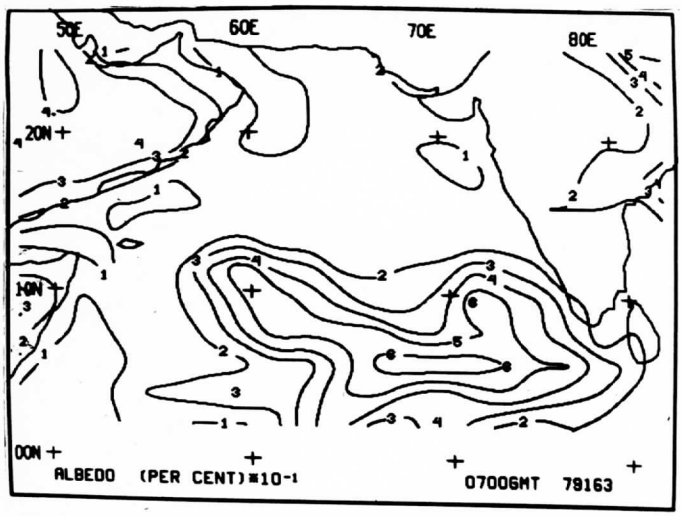
50E
60E
70E
80E
20N
10N
00N
ALBEDO (PER CENT)*10-1
0700GMT 79163

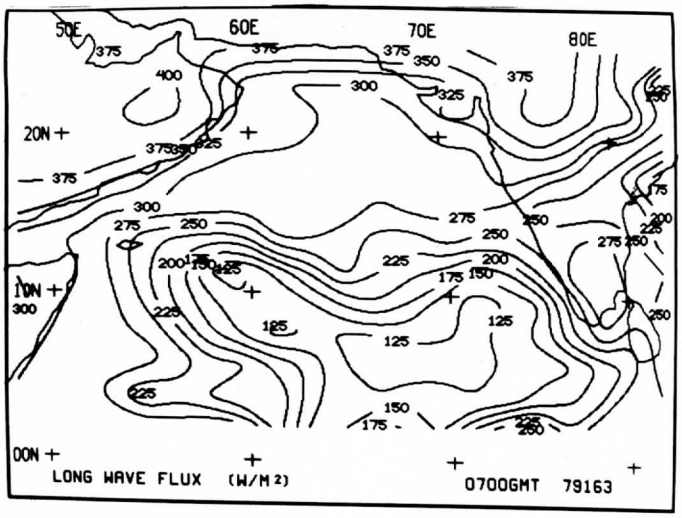
50E
60E
70E
80E
20N
10N
00N
LONG WAVE FLUX (W/M2)
0700GMT 79163

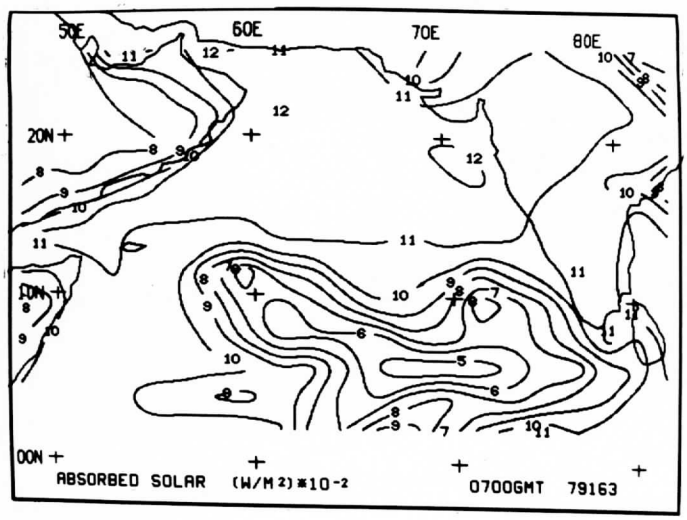
50E
60E
70E
80E
20N
10N
00N
ABSORBED SOLAR (W/M2)*10-2
0700GMT 79163

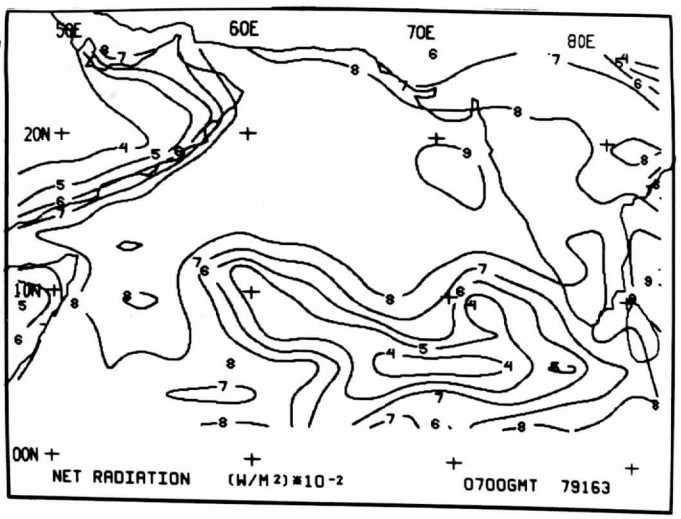
50E
60E
70E
80E
20N
10N
00N
NET RADIATION (W/M2)*10-2
0700GMT 79163

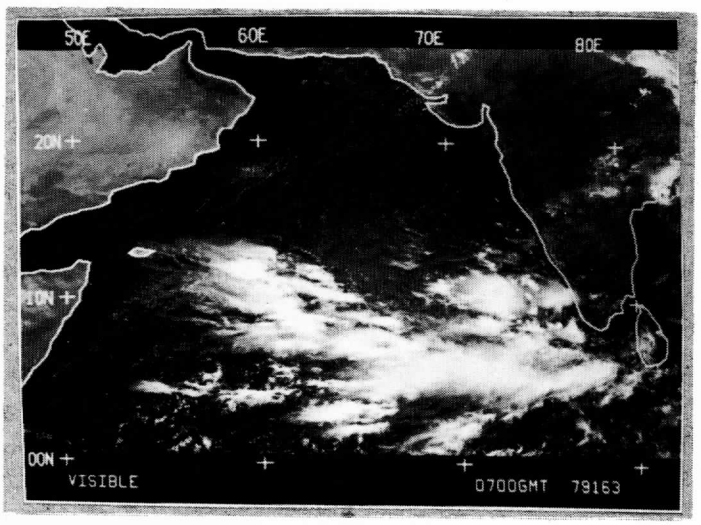
50E
60E
70E
80E
20N
10N
00N
VISIBLE
0700GMT 79163

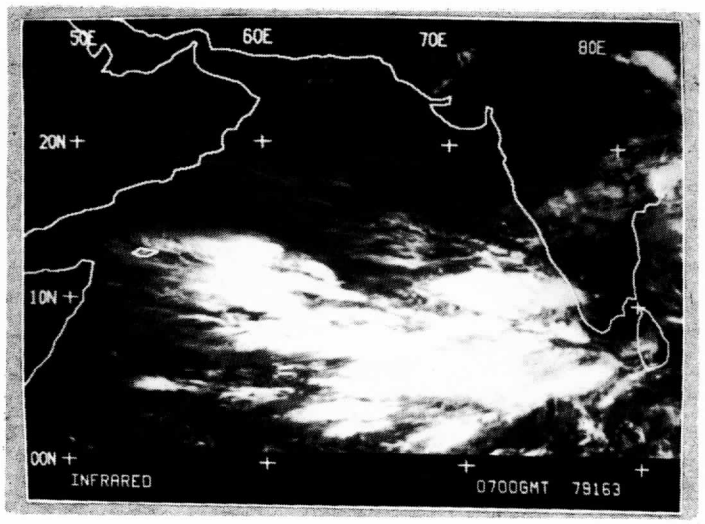
50E
60E
70E
80E
20N
10N
00N
INFRARED
0700GMT 79163

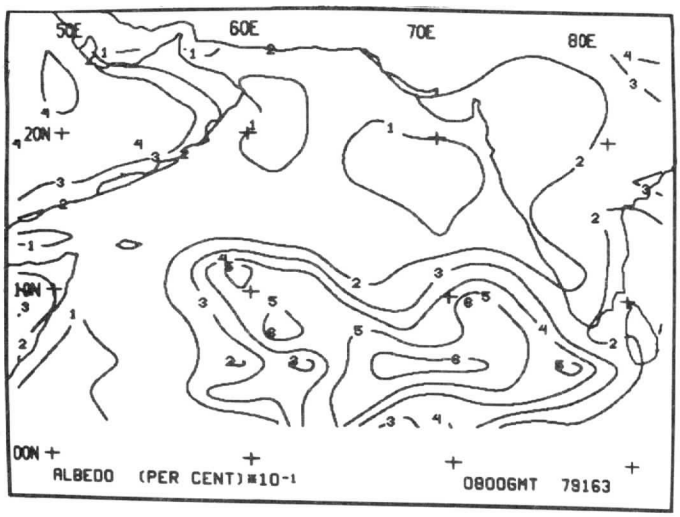
50E
60E
70E
80E
20N
10N
0ON
ALBEDO (PER CENT)*10-1
0800GMT 79163

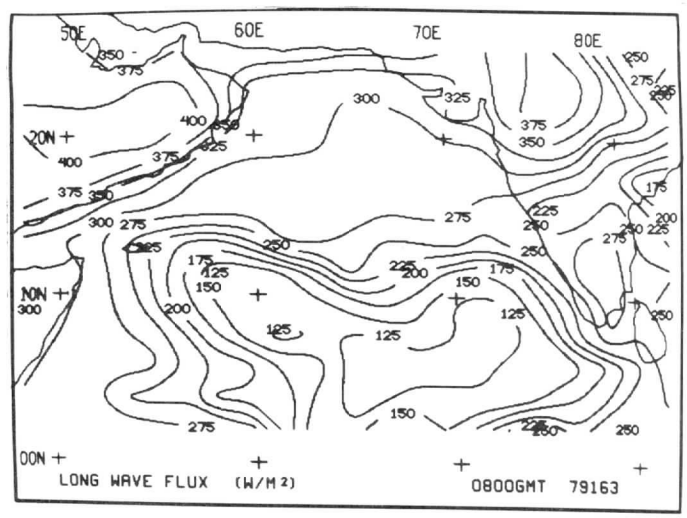
50E
60E
70E
80E
20N
10N
0ON
LONG WAVE FLUX (W/M2)
0800GMT 79163

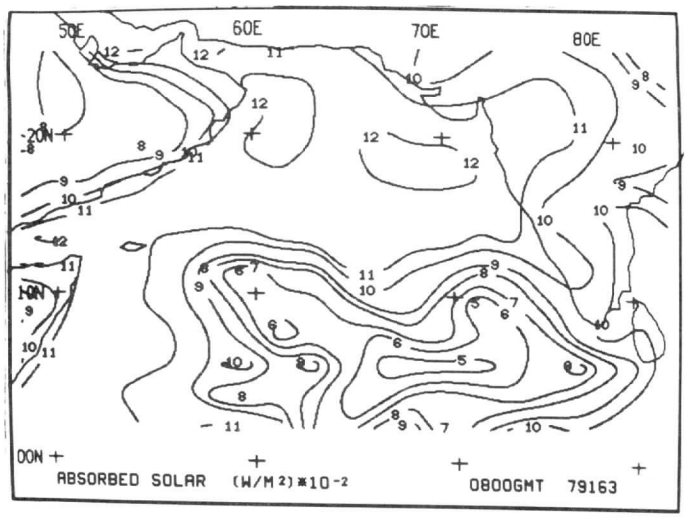
50E
60E
70E
80E
20N
10N
0ON
ABSORBED SOLAR (W/M2)*10-2
0800GMT 79163

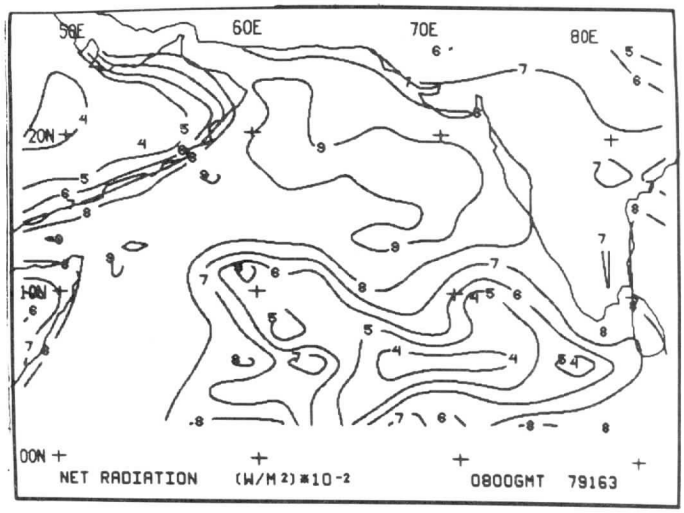
50E
60E
70E
80E
20N
10N
0ON
NET RADIATION (W/M2)*10-2
0800GMT 79163

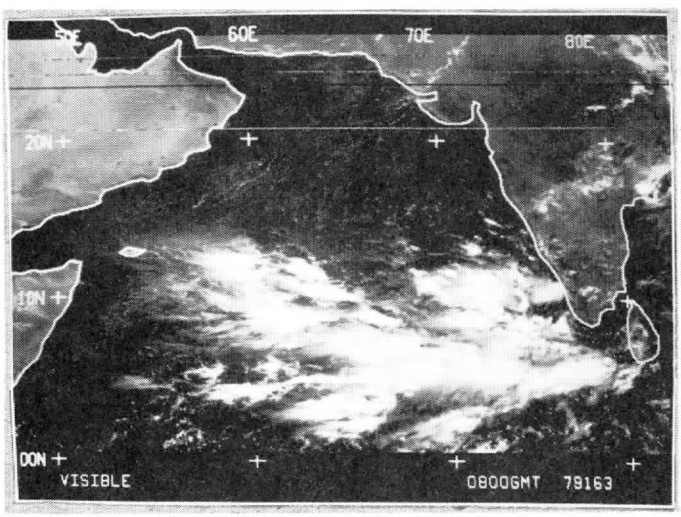
50E
60E
70E
80E
20N
10N
0ON
VISIBLE
0800GMT 79163

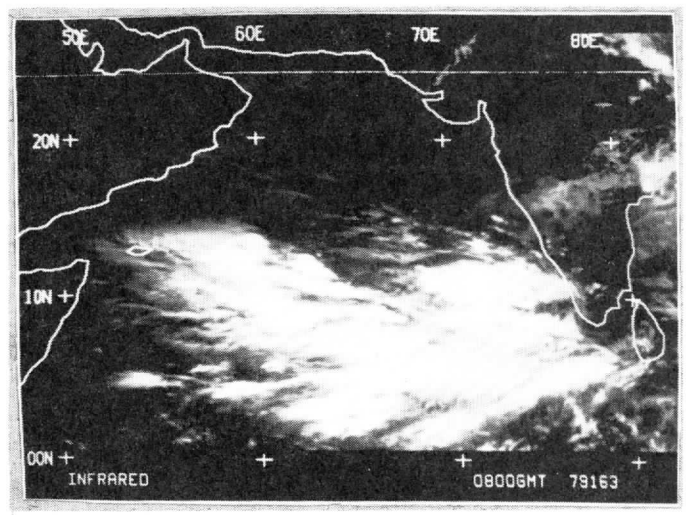
50E
60E
70E
80E
20N
10N
0ON
INFRARED
0800GMT 79163

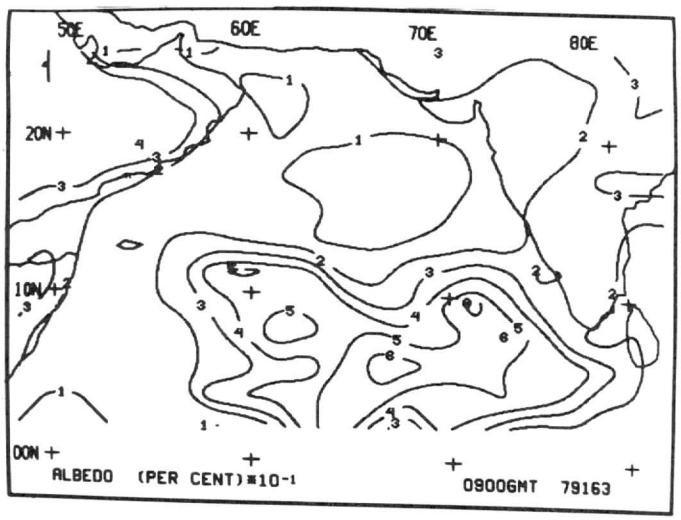
50E
60E
70E
80E
20N
10N
0ON
ALBEDO (PER CENT)*10-1
0900GMT 79163

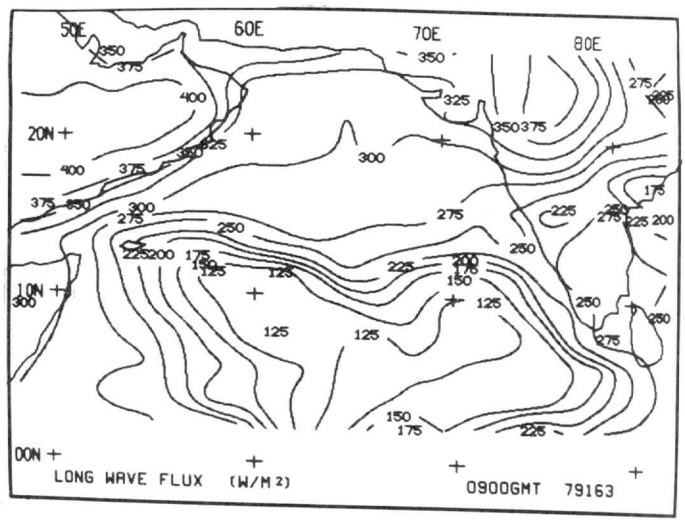
50E
60E
70E
80E
20N
10N
0ON
LONG WAVE FLUX (W/M2)
0900GMT 79163

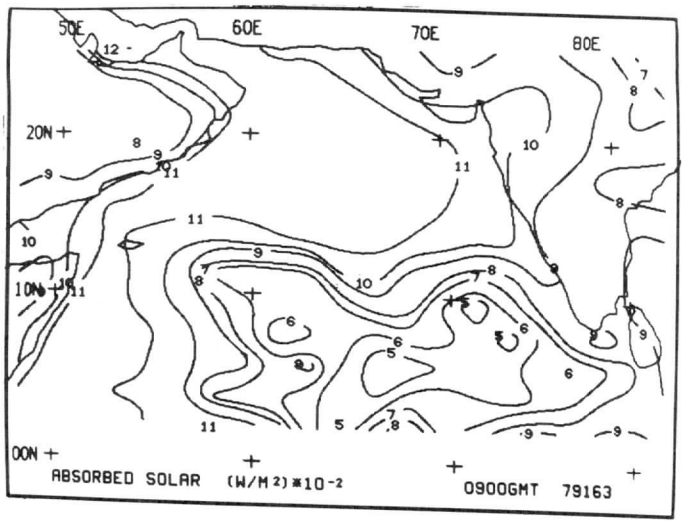
50E
60E
70E
80E
20N
10N
0ON
ABSORBED SOLAR (W/M2)*10-2
0900GMT 79163

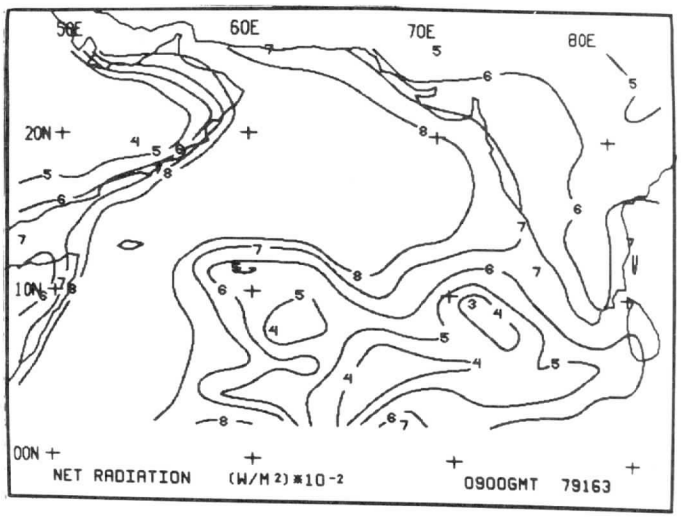
50E
60E
70E
80E
20N
10N
0ON
NET RADIATION (W/M2)*10-2
0900GMT 79163

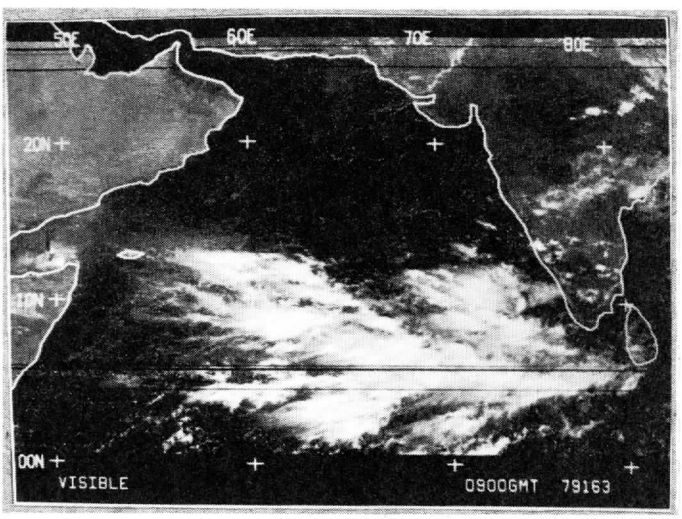
50E
60E
70E
80E
20N
10N
0ON
VISIBLE
0900GMT 79163

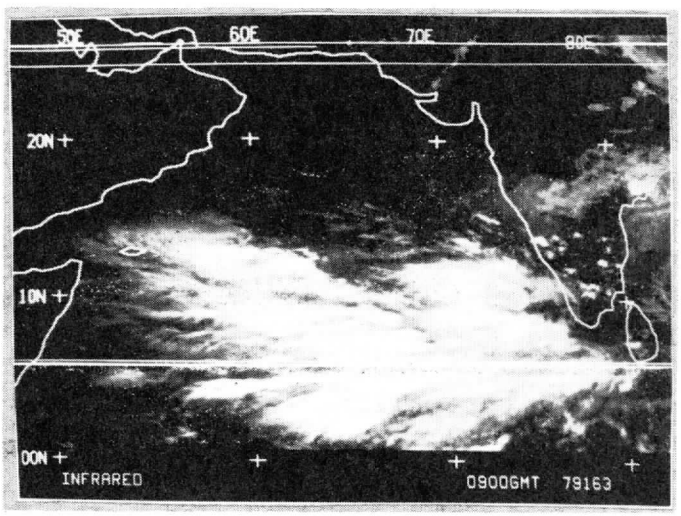
50E
60E
70E
80E
20N
10N
0ON
INFRARED
0900GMT 79163

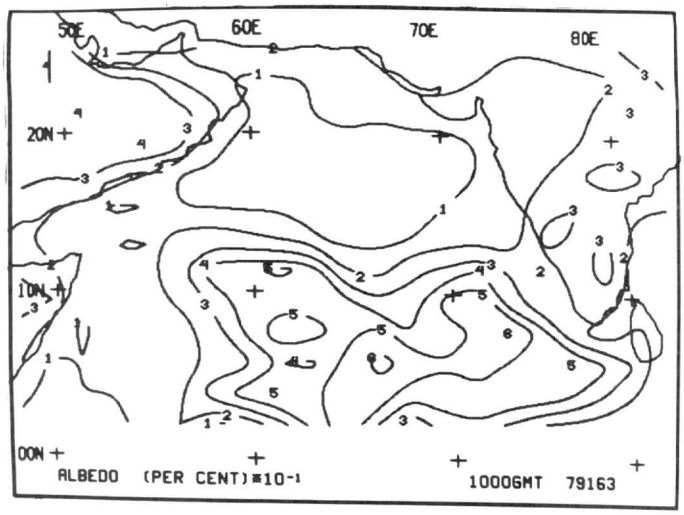
50E
60E
70E
80E
20N
10N
0ON
ALBEDO (PER CENT)*10-1
1000GMT 79163

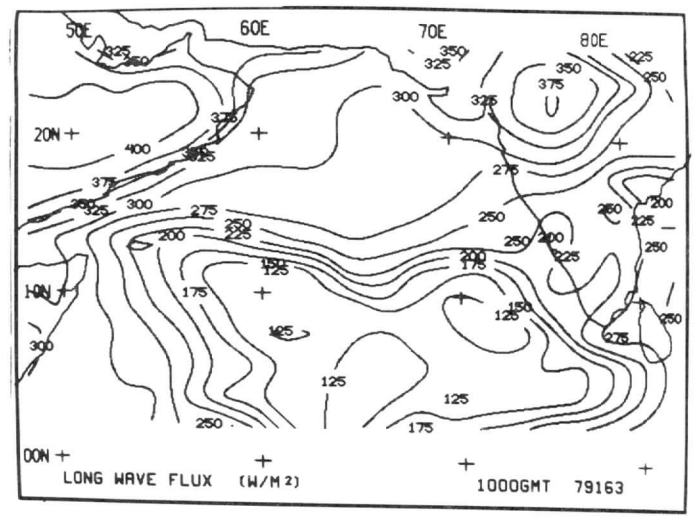
50E
60E
70E
80E
20N
10N
0ON
LONG WAVE FLUX (W/M2)
1000GMT 79163

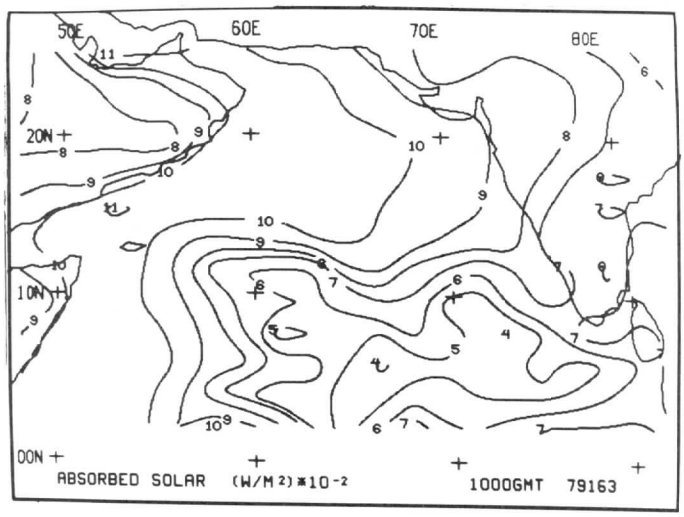
50E
60E
70E
80E
20N
10N
0ON
ABSORBED SOLAR (W/M2)*10-2
1000GMT 79163

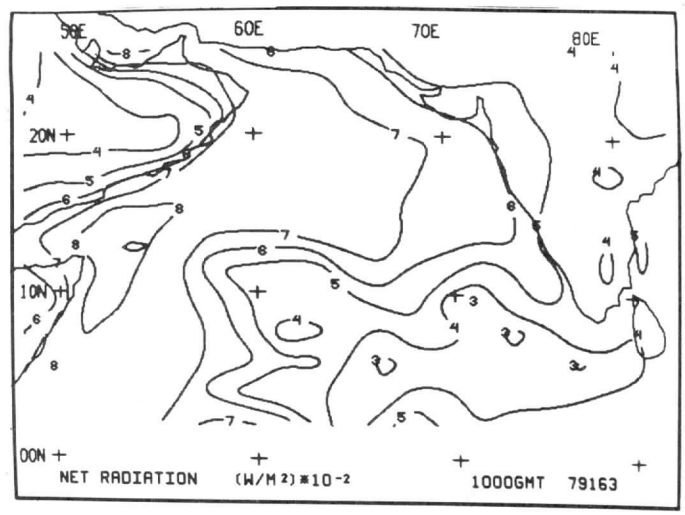
50E
60E
70E
80E
20N
10N
0ON
NET RADIATION (W/M2)*10-2
1000GMT 79163

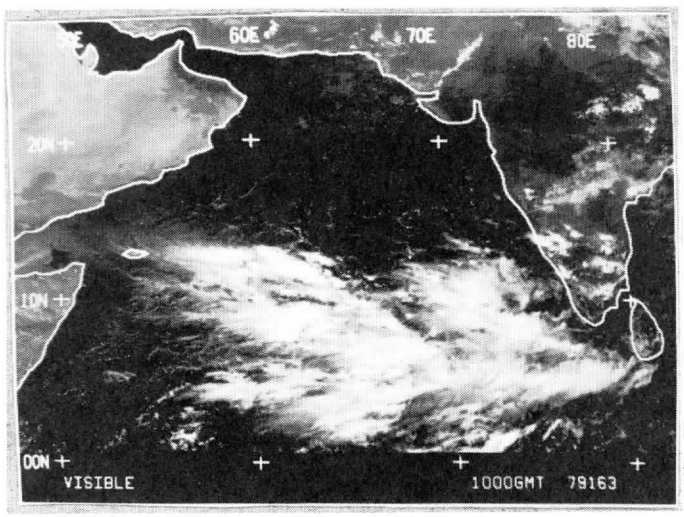
60E
70E
80E
20N
10N
0ON
VISIBLE
1000GMT 79163

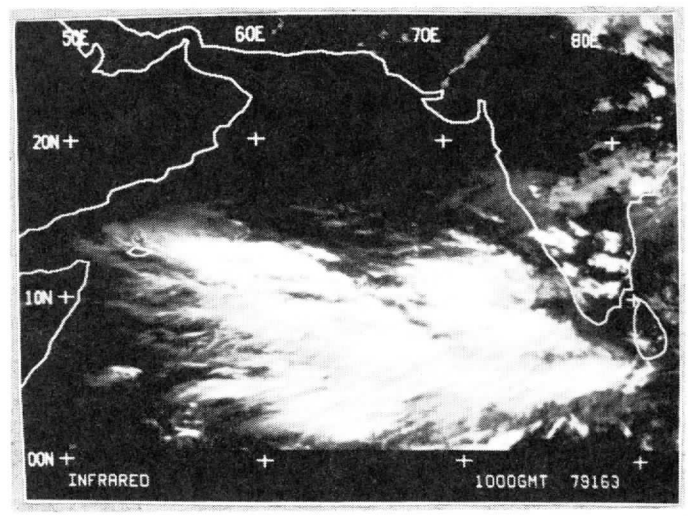
50E
60E
70E
80E
20N
10N
0ON
INFRARED
1000GMT 79163

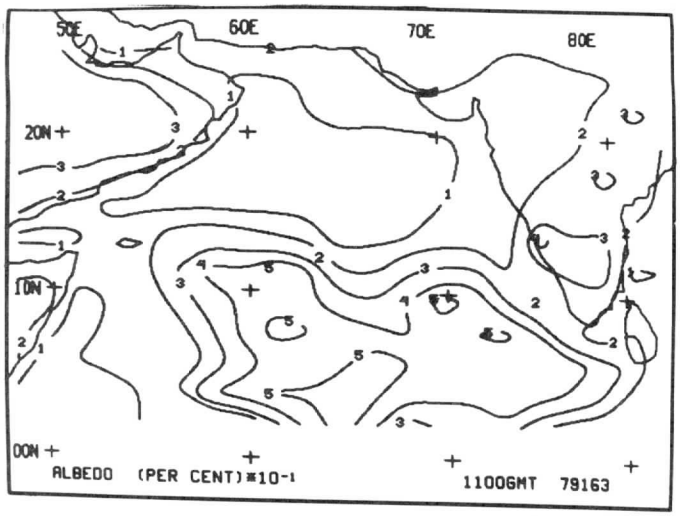
50E
60E
70E
80E
20N
10N
0ON
ALBEDO (PER CENT)*10-1
1100GMT 79163

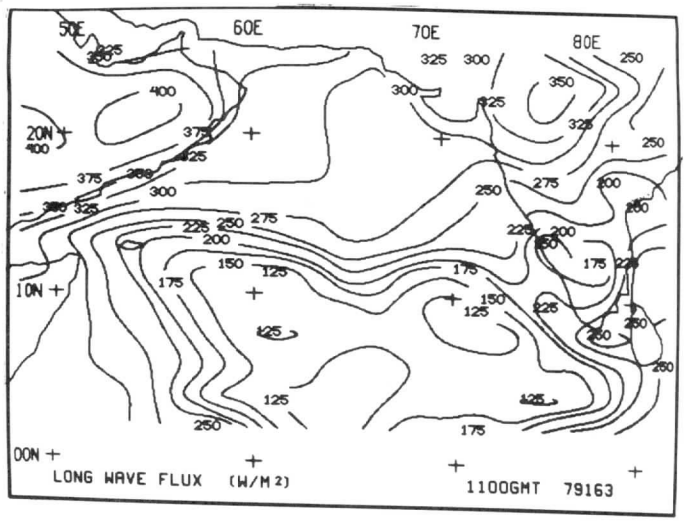
50E
60E
70E
80E
20N
10N
0ON
LONG WAVE FLUX (W/M2)
1100GMT 79163

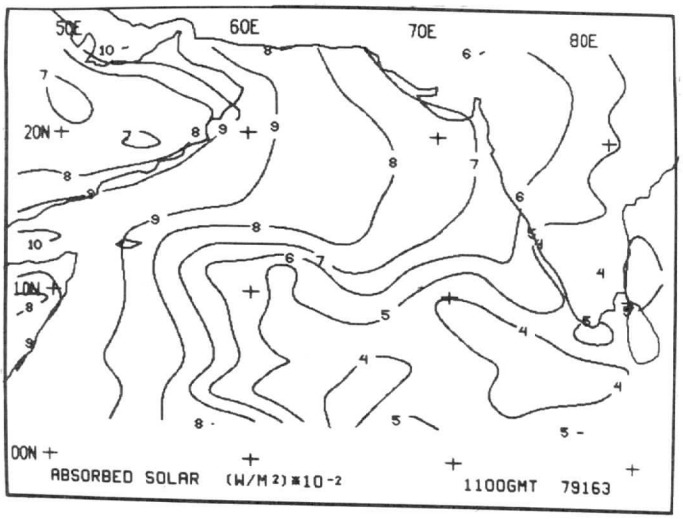
50E
60E
70E
80E
20N
10N
0ON
ABSORBED SOLAR (W/M2)*10-2
1100GMT 79163

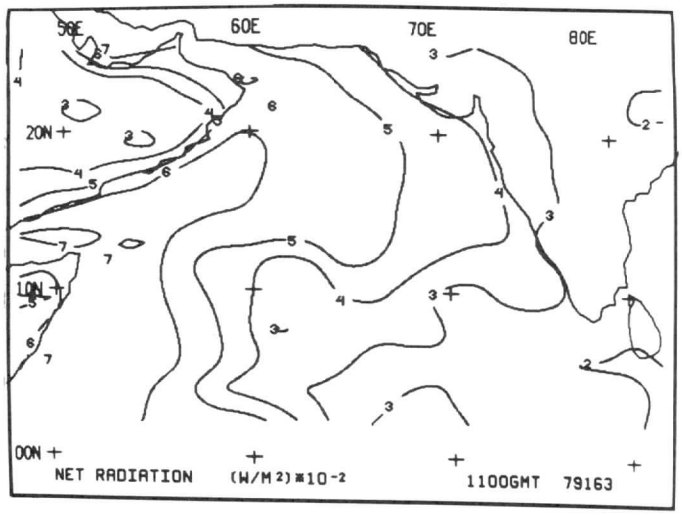
50E
60E
70E
80E
20N
10N
0ON
NET RADIATION (W/M2)*10-2
1100GMT 79163

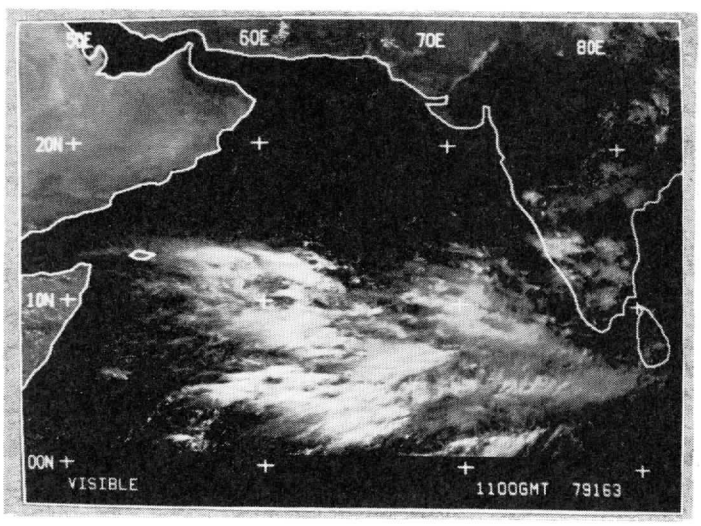
50E
60E
70E
80E
20N
10N
0ON
VISIBLE
1100GMT 79163

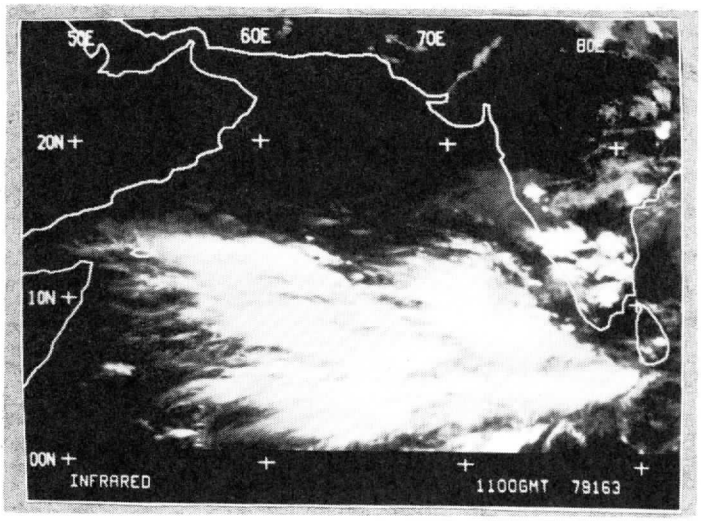
50E
60E
70E
80E
20N
10N
0ON
INFRARED
1100GMT 79163

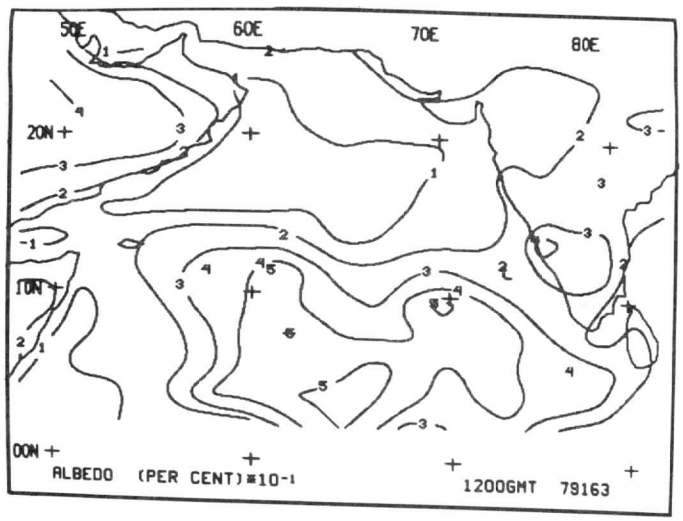
50E
60E
70E
80E
20N
10N
0ON
ALBEDO (PER CENT)*10-1
1200GMT 79163

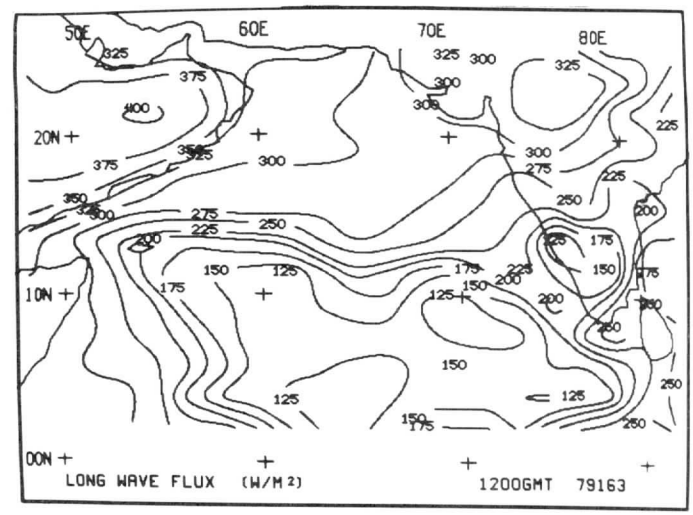
50E
60E
70E
80E
20N
10N
0ON
LONG WAVE FLUX (W/M2)
1200GMT 79163

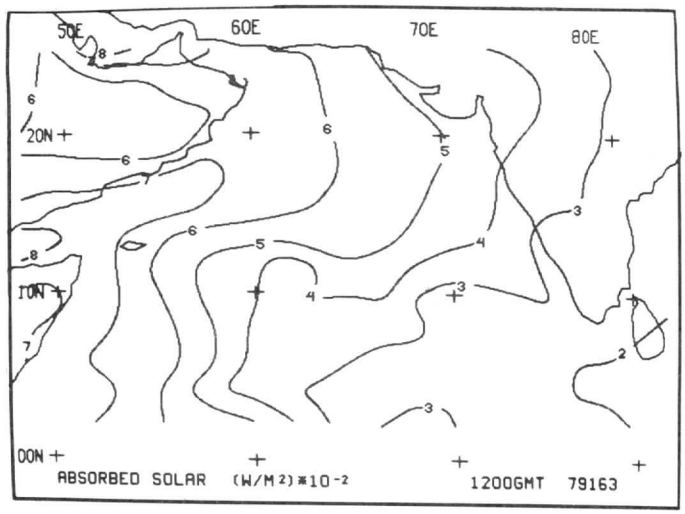
50E
60E
70E
80E
20N
10N
0ON
ABSORBED SOLAR (W/M2)*10-2
1200GMT 79163

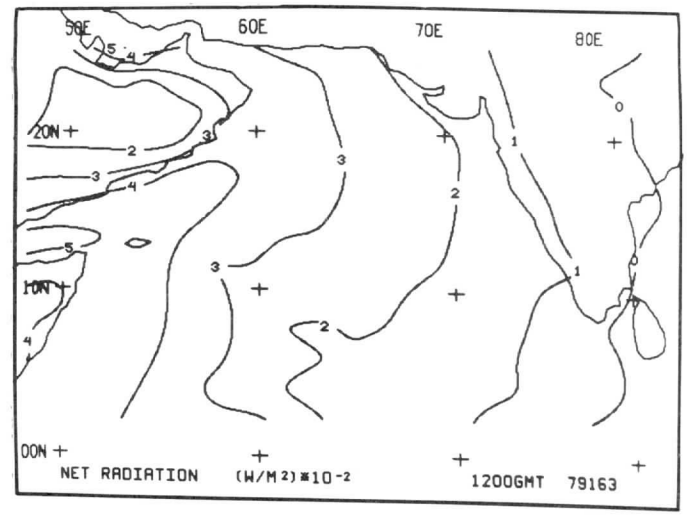
50E
60E
70E
80E
20N
10N
0ON
NET RADIATION (W/M2)*10-2
1200GMT 79163

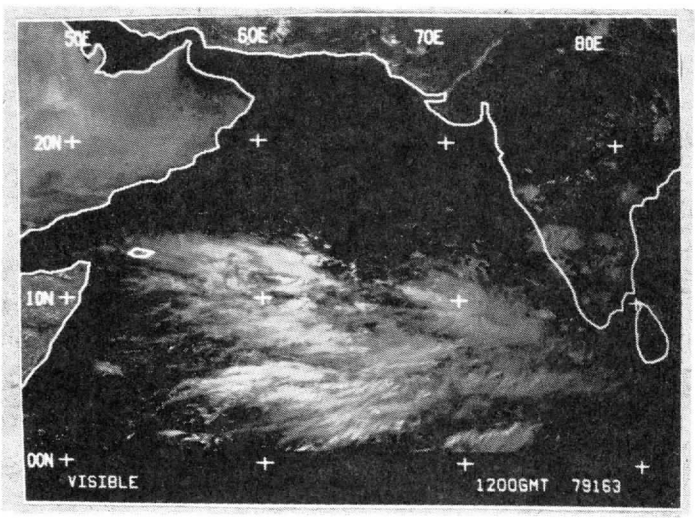
50E
60E
70E
80E
20N
10N
0ON
VISIBLE
1200GMT 79163

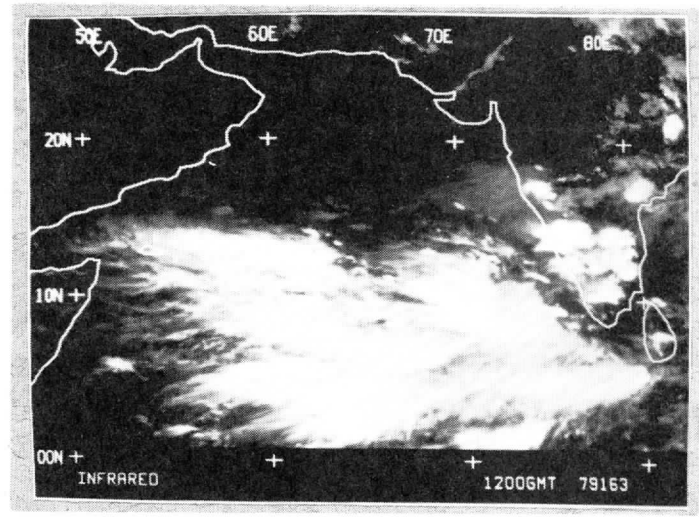
50E
60E
70E
80E
20N
10N
0ON
INFRARED
1200GMT 79163

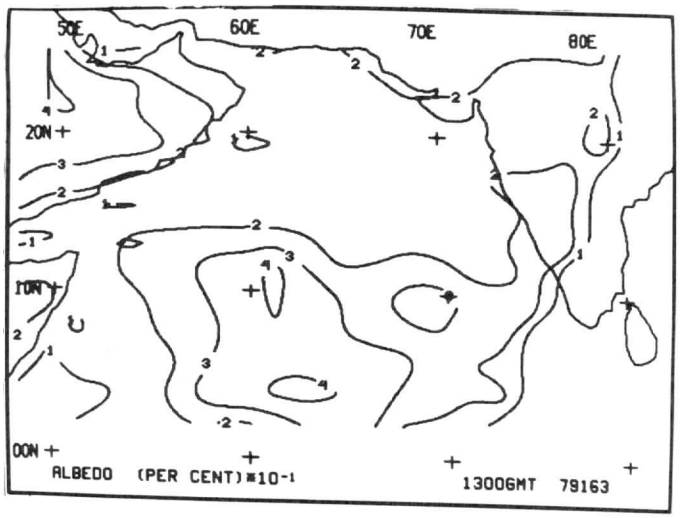
50E
60E
70E
80E
20N
10N
0ON
ALBEDO (PER CENT)*10-1
1300GMT 79163

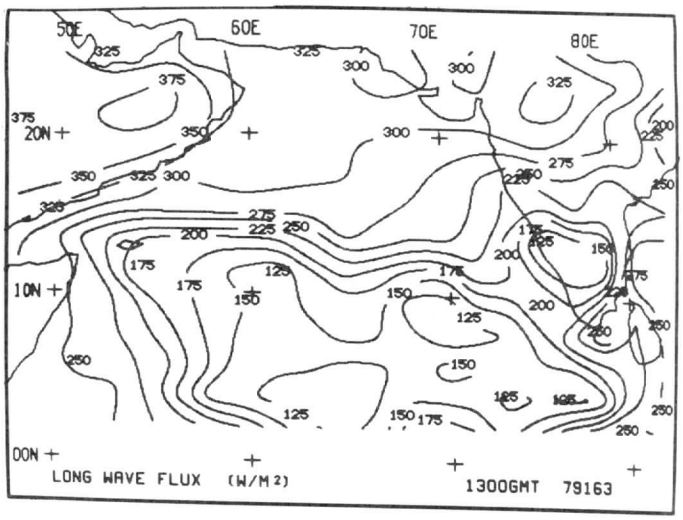
50E
60E
70E
80E
20N
10N
0ON
LONG WAVE FLUX (W/M2)
1300GMT 79163

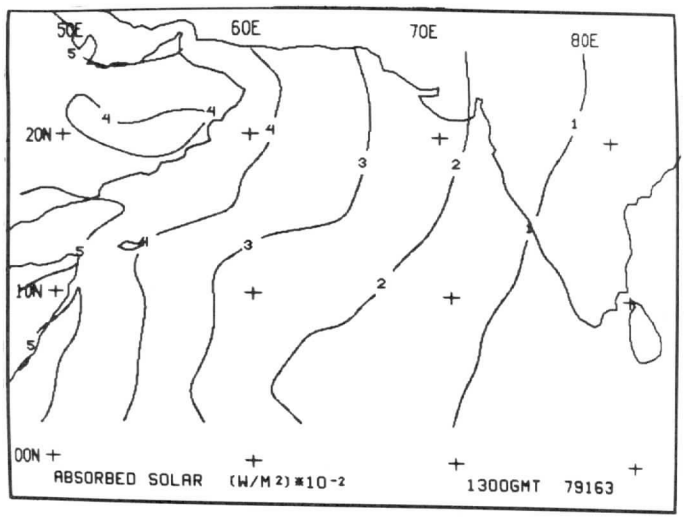
50E
60E
70E
80E
20N
10N
0ON
ABSORBED SOLAR (W/M2)*10-2
1300GMT 79163

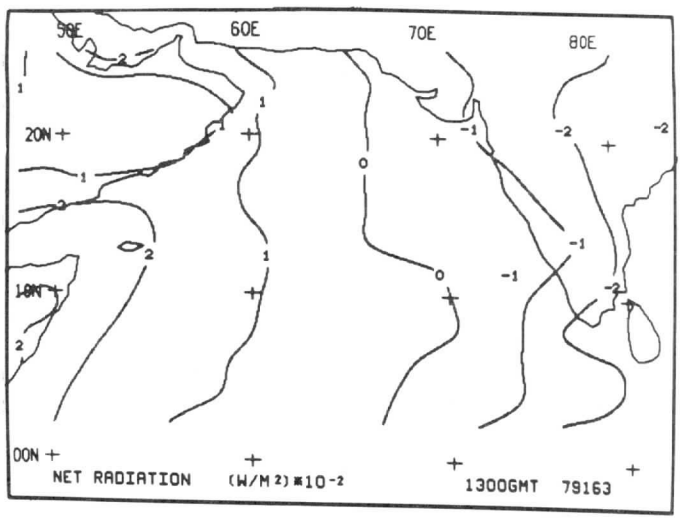
50E
60E
70E
80E
20N
10N
0ON
NET RADIATION (W/M2)*10-2
1300GMT 79163

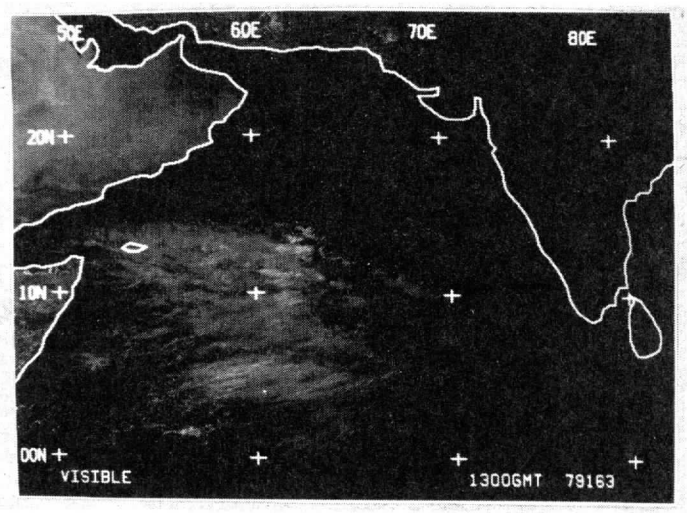
50E
60E
70E
80E
20N
10N
0ON
VISIBLE
1300GMT 79163

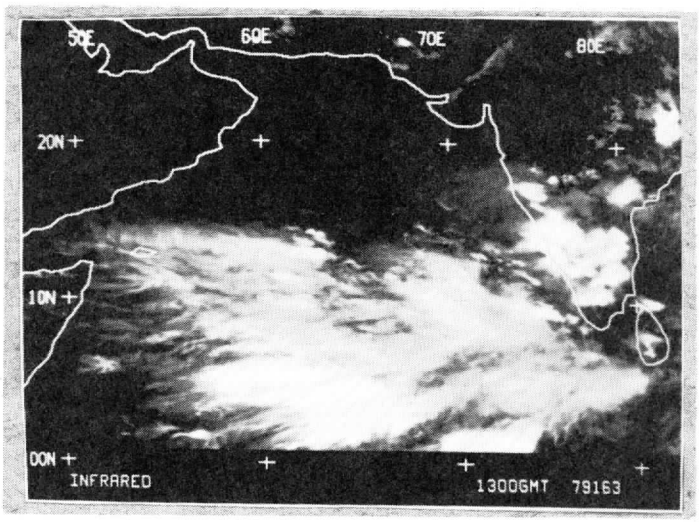
50E
60E
70E
80E
20N
10N
0ON
INFRARED
1300GMT 79163

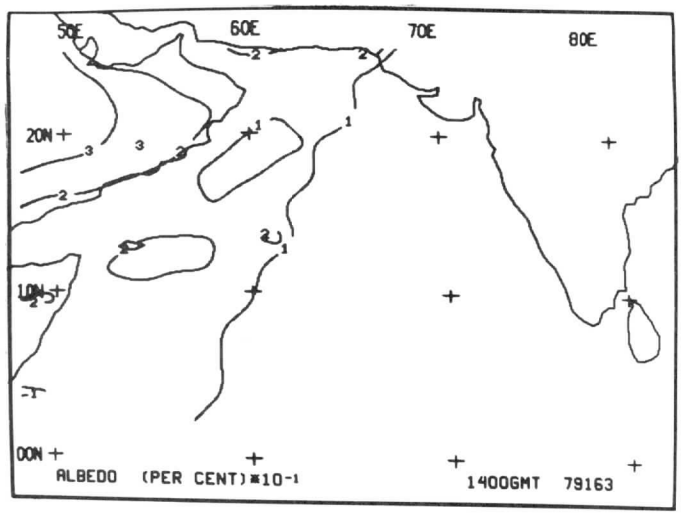
50E
60E
70E
80E
20N
10N
00N
ALBEDO (PER CENT)*10-1
1400GMT 79163

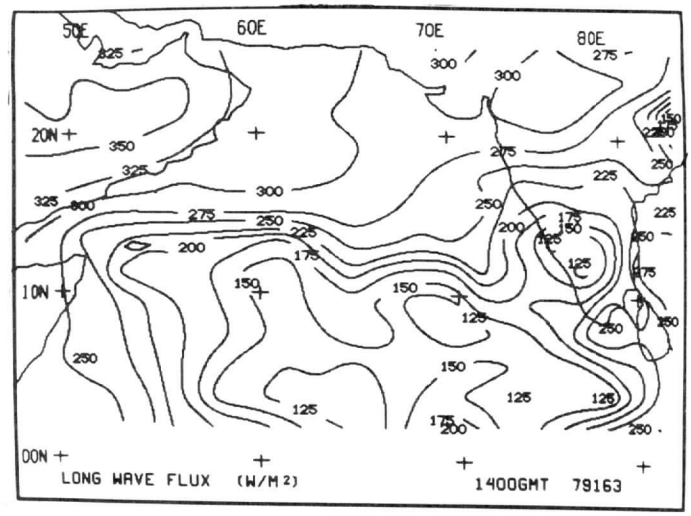
50E
60E
70E
80E
20N
10N
00N
LONG WAVE FLUX (W/M2)
1400GMT 79163

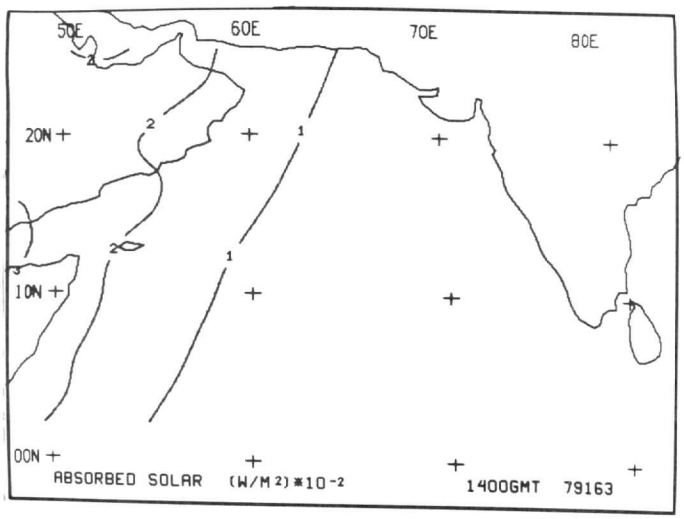
50E
60E
70E
80E
20N
10N
00N
ABSORBED SOLAR (W/M2)*10-2
1400GMT 79163

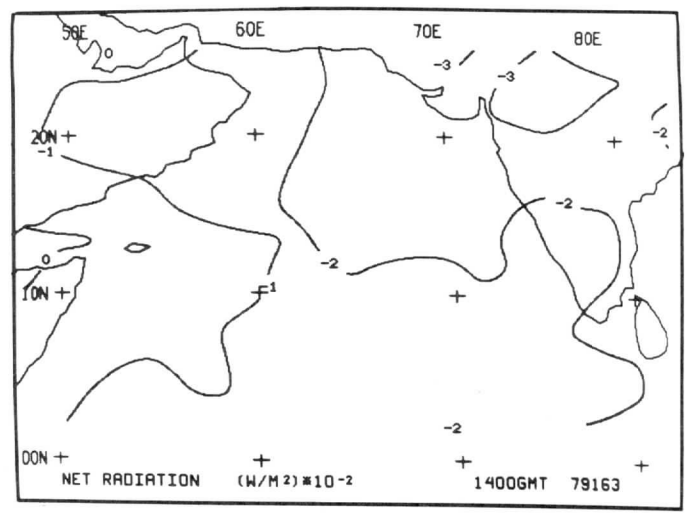
50E
60E
70E
80E
20N
10N
00N
NET RADIATION (W/M2)*10-2
1400GMT 79163

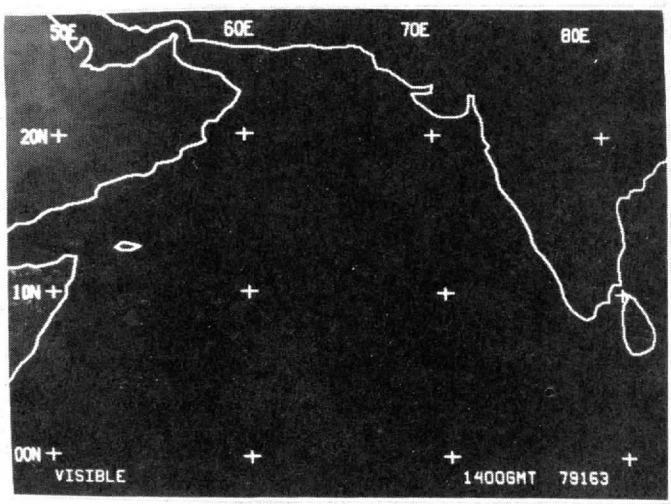
50E
60E
70E
80E
20N
10N
00N
VISIBLE
1400GMT 79163

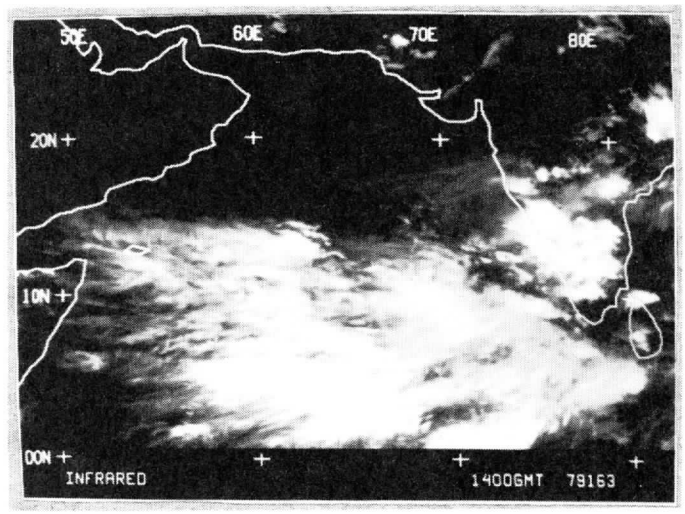
50E
60E
70E
80E
20N
10N
00N
INFRARED
1400GMT 79163

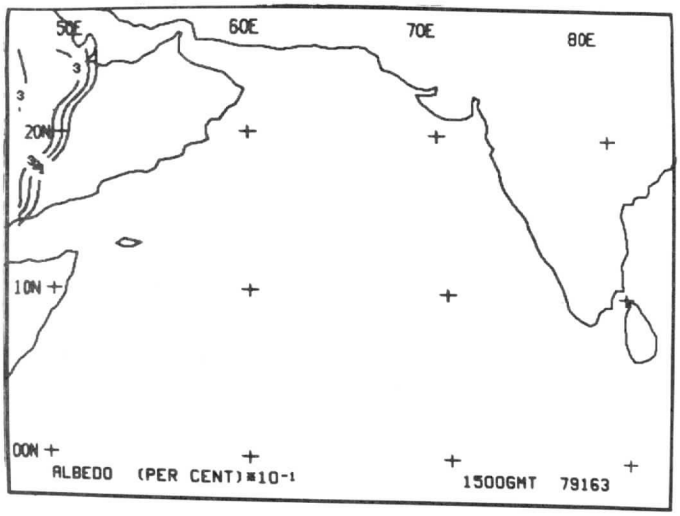
50E
60E
70E
80E
20N
10N
00N
ALBEDO (PER CENT)*10-1
1500GMT 79163

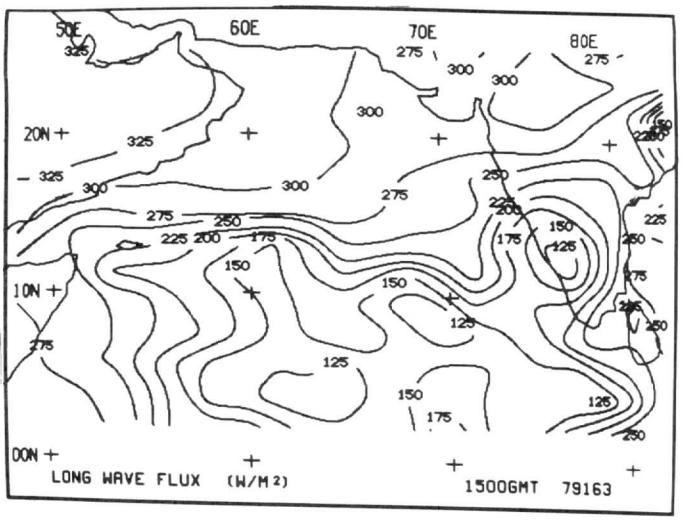
50E
60E
70E
80E
20N
10N
00N
LONG WAVE FLUX (W/M2)
1500GMT 79163

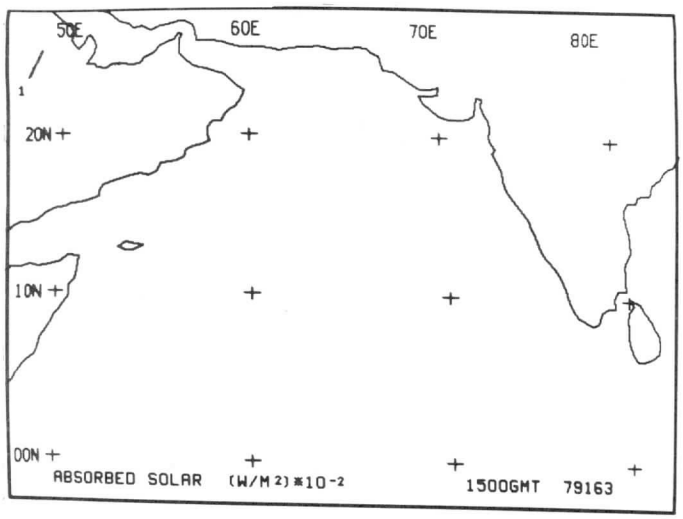
50E
60E
70E
80E
20N
10N
00N
ABSORBED SOLAR (W/M2)*10-2
1500GMT 79163

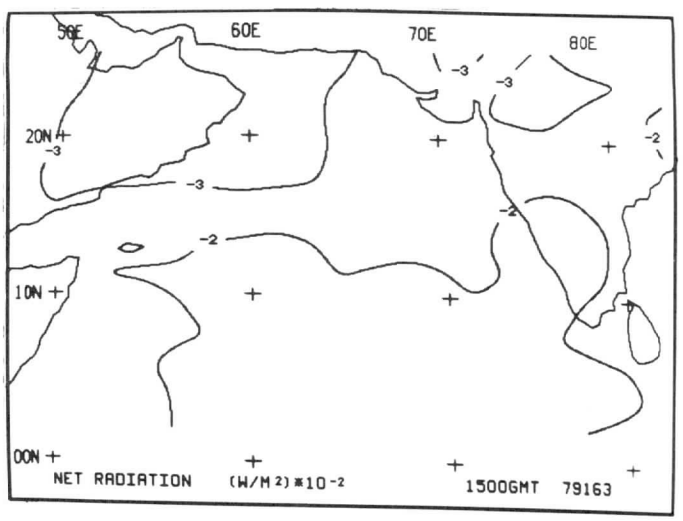
50E
60E
70E
80E
20N
10N
00N
NET RADIATION (W/M2)*10-2
1500GMT 79163

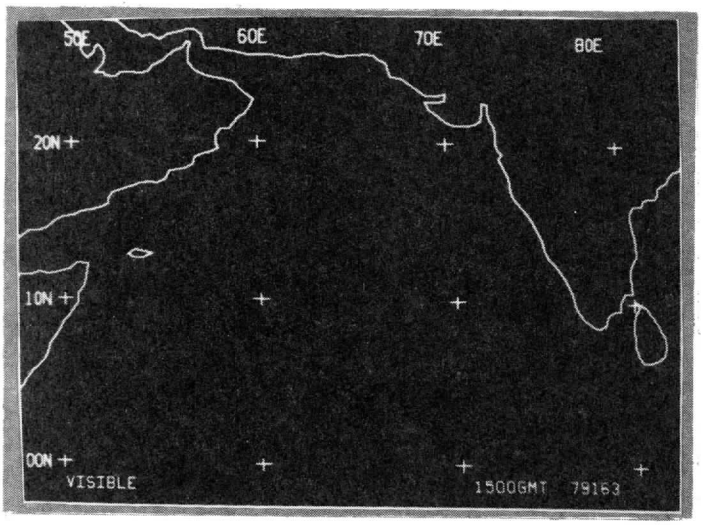
50E
60E
70E
80E
20N
10N
00N
VISIBLE
1500GMT 79163

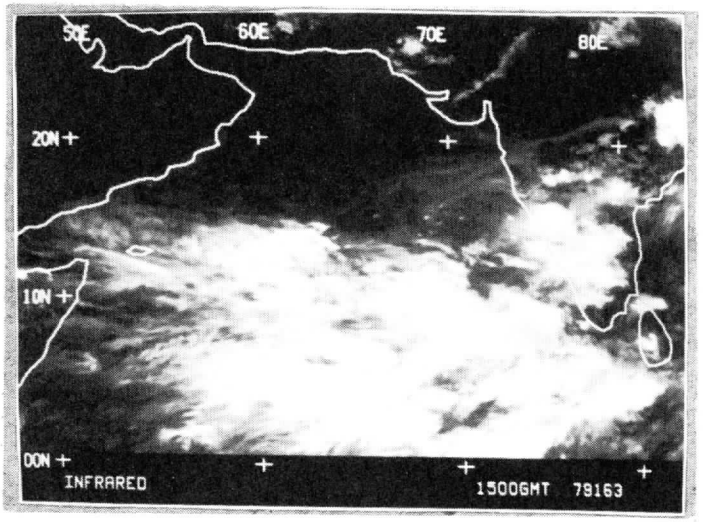
50E
60E
70E
80E
20N
10N
00N
INFRARED
1500GMT 79163

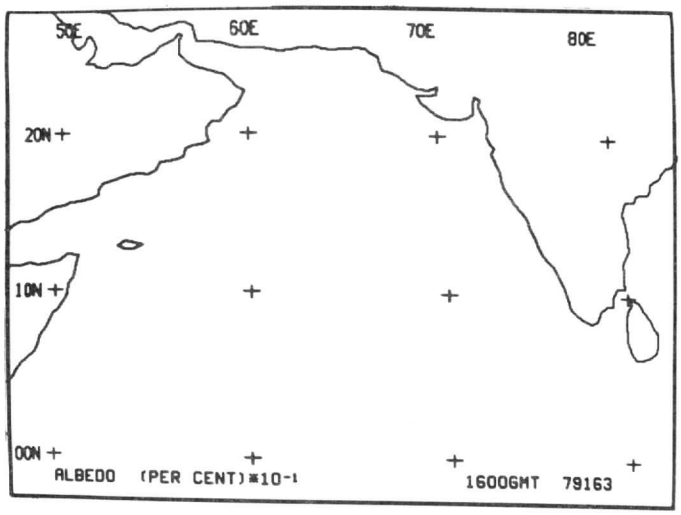
50E
60E
70E
80E
20N
10N
0ON
ALBEDO (PER CENT)*10-1
1600GMT 79163

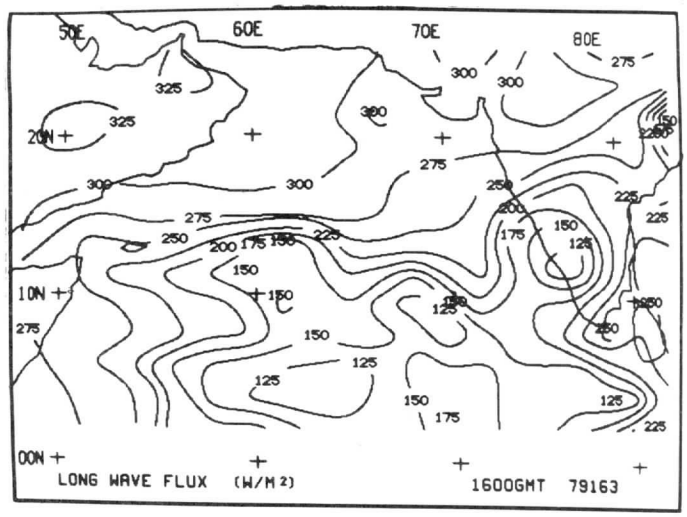
50E
60E
70E
80E
20N
10N
0ON
LONG WAVE FLUX (W/M2)
1600GMT 79163

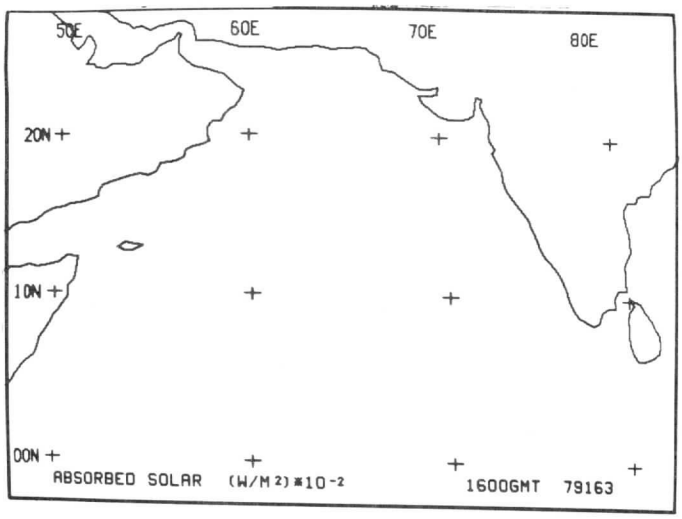
50E
60E
70E
80E
20N
10N
0ON
ABSORBED SOLAR (W/M2)*10-2
1600GMT 79163

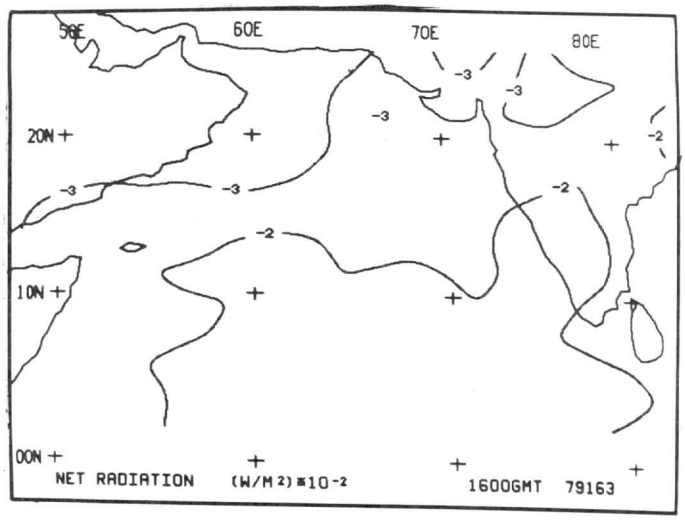
50E
60E
70E
80E
20N
10N
0ON
NET RADIATION (W/M2)*10-2
1600GMT 79163

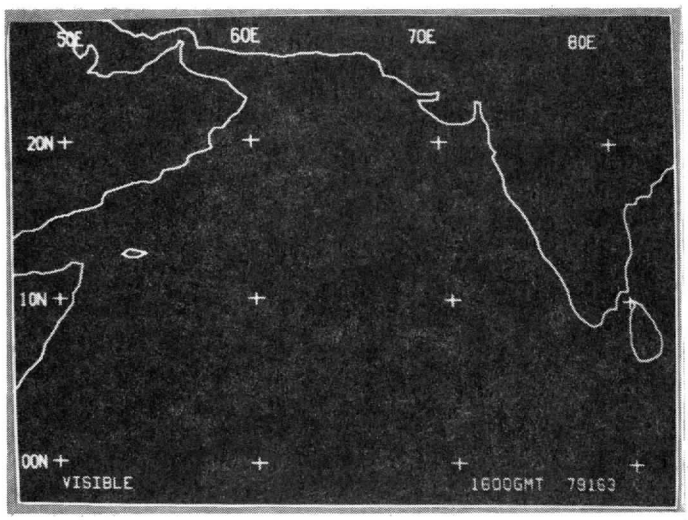
50E
60E
70E
80E
20N
10N
0ON
VISIBLE
1600GMT 79163

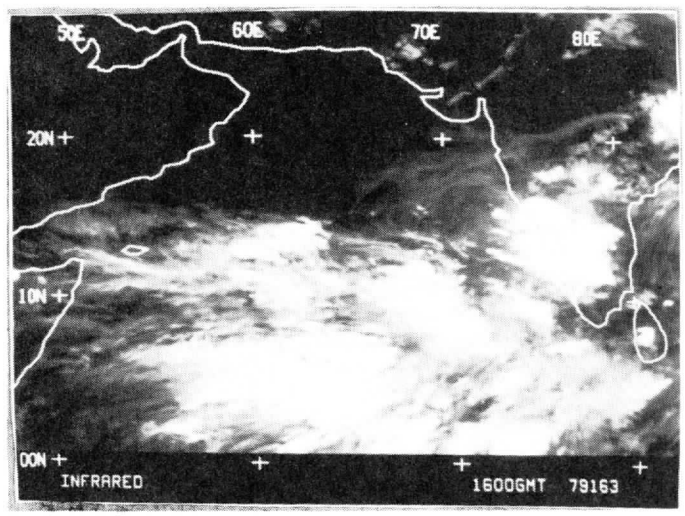
50E
60E
70E
80E
20N
10N
0ON
INFRARED
1600GMT 79163

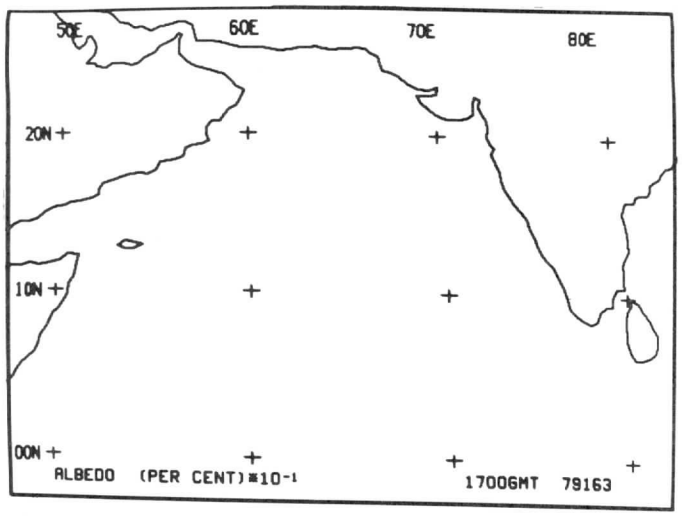
50E
60E
70E
80E
20N
10N
00N
ALBEDO (PER CENT)*10-1
1700GMT 79163

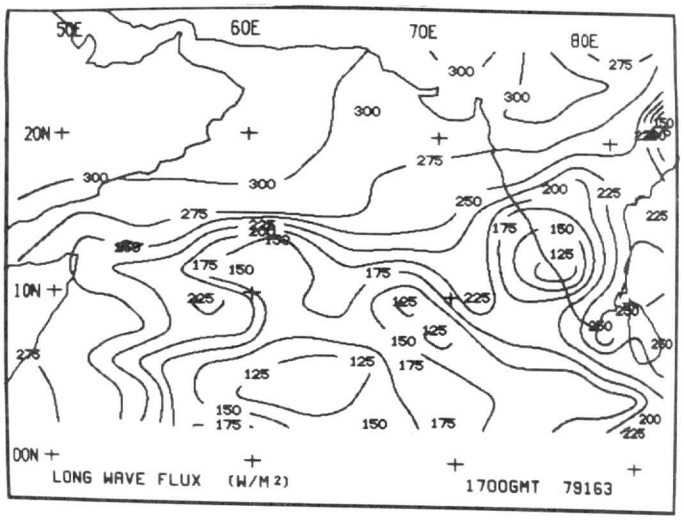
50E
60E
70E
80E
20N
10N
00N
LONG WAVE FLUX (W/M2)
1700GMT 79163

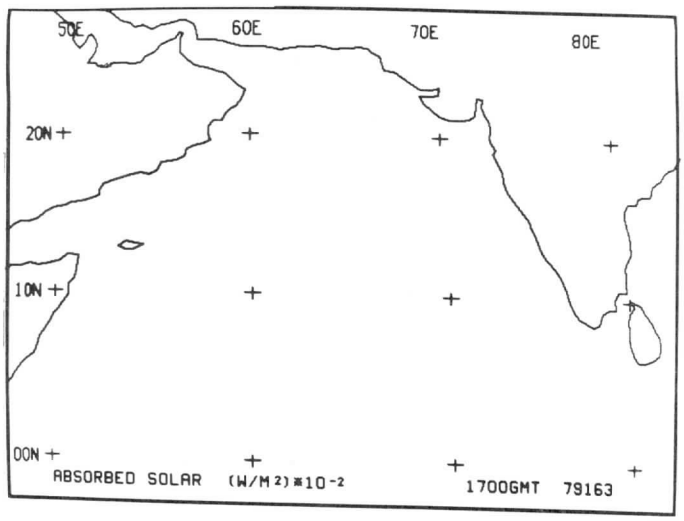
50E
60E
70E
80E
20N
10N
00N
ABSORBED SOLAR (W/M2)*10-2
1700GMT 79163

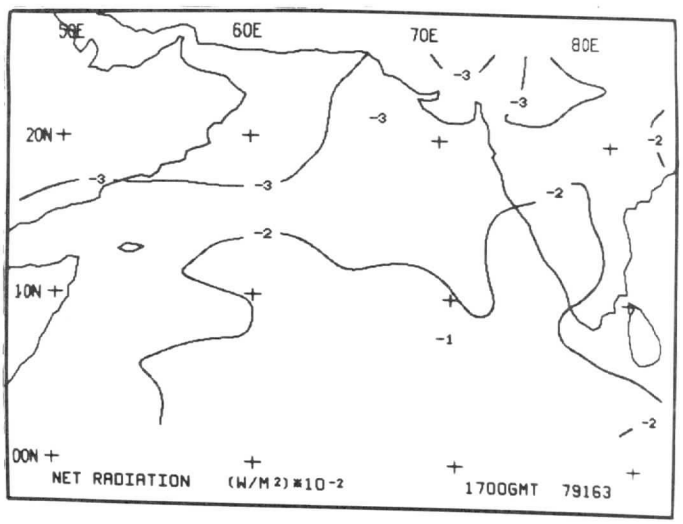
50E
60E
70E
80E
20N
10N
00N
NET RADIATION (W/M2)*10-2
1700GMT 79163

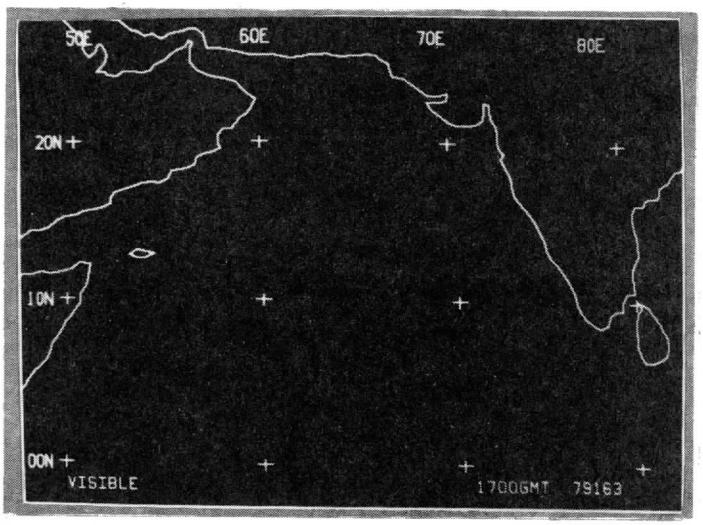
50E
60E
70E
80E
20N
10N
00N
VISIBLE
1700GMT 79163

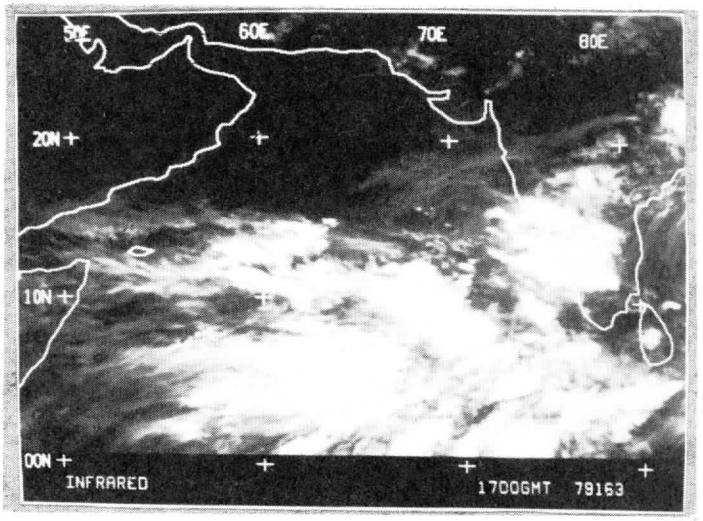
50E
60E
70E
80E
20N
10N
00N
INFRARED
1700GMT 79163

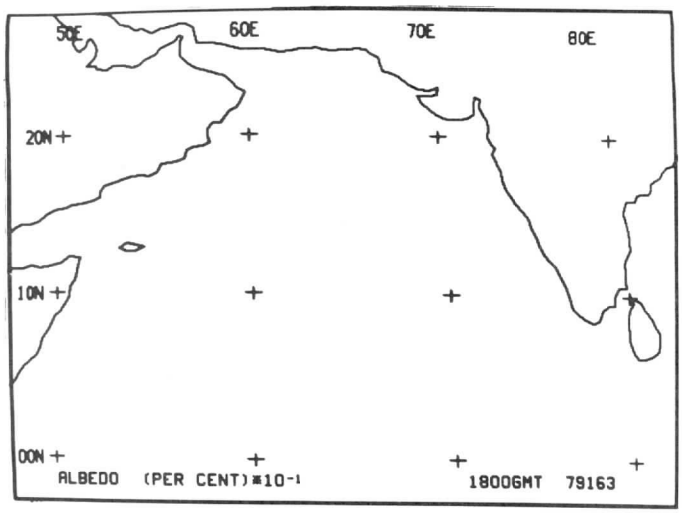
50E
60E
70E
80E
20N
10N
0ON
ALBEDO (PER CENT)*10-1
1800GMT 79163

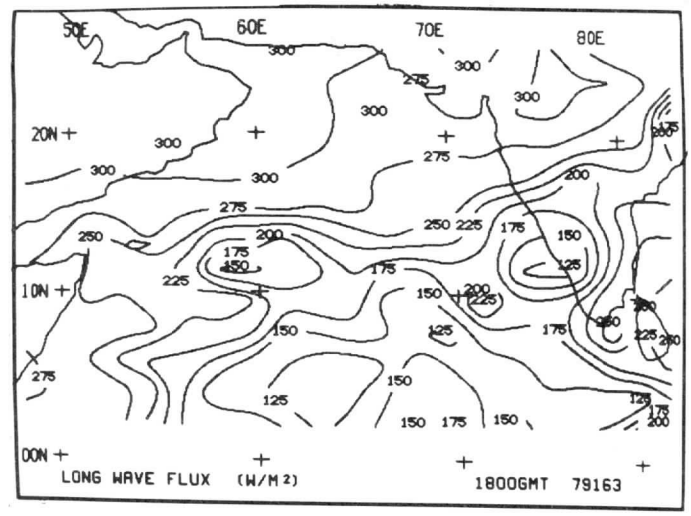
50E
60E
70E
80E
20N
10N
0ON
LONG WAVE FLUX (W/M2)
1800GMT 79163

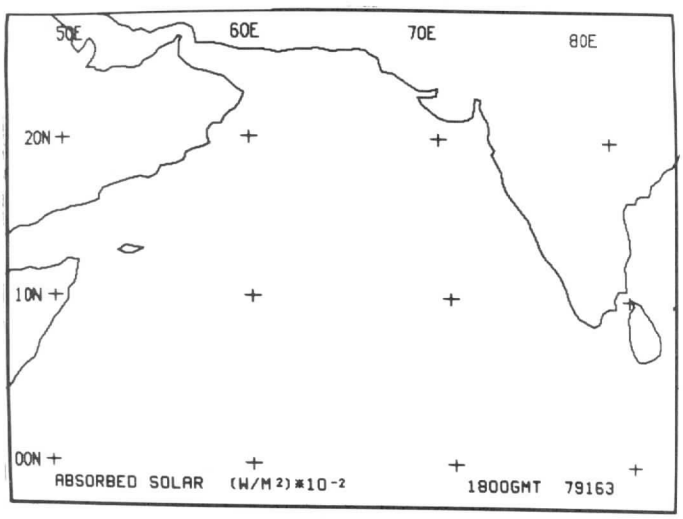
50E
60E
70E
80E
20N
10N
0ON
ABSORBED SOLAR (W/M2)*10-2
1800GMT 79163

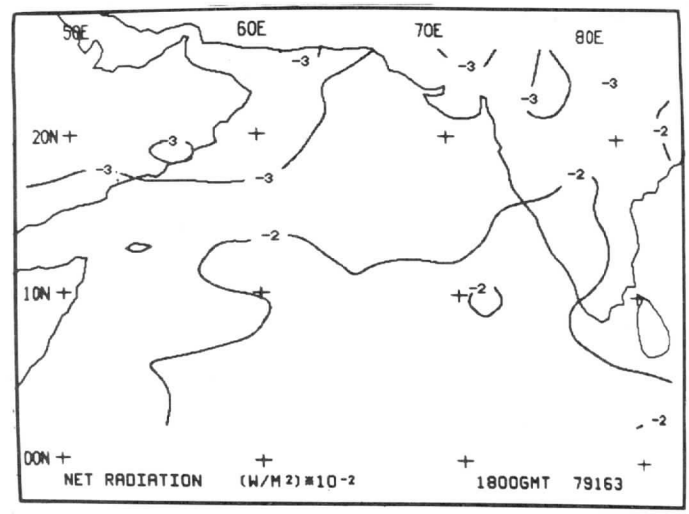
50E
60E
70E
80E
20N
10N
0ON
NET RADIATION (W/M2)*10-2
1800GMT 79163

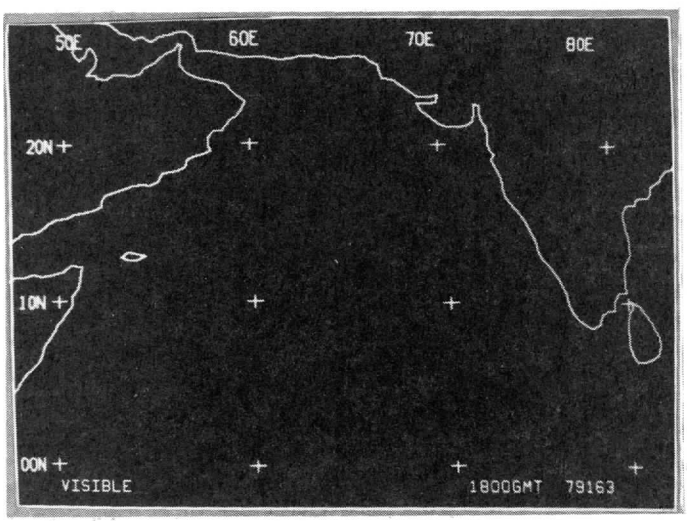
50E
60E
70E
80E
20N
10N
0ON
VISIBLE
1800GMT 79163

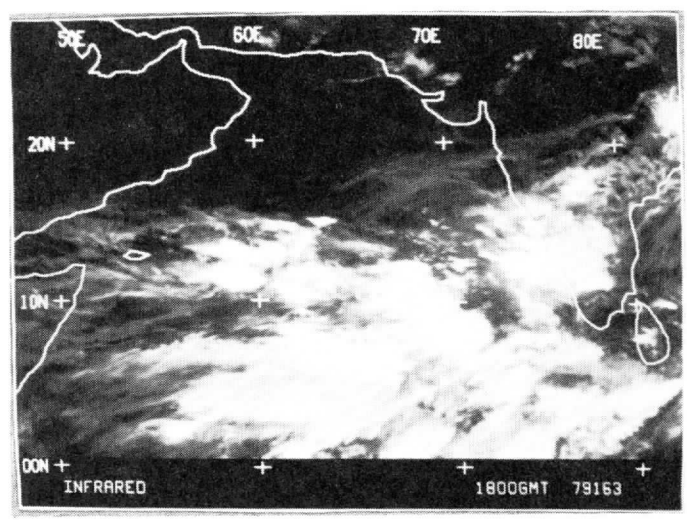
50E
60E
70E
80E
20N
10N
0ON
INFRARED
1800GMT 79163

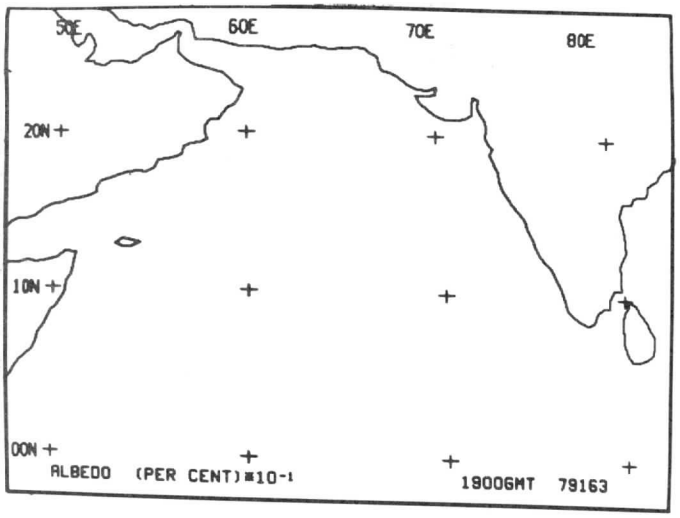
50E
60E
70E
80E
20N
10N
00N
ALBEDO (PER CENT)*10-1
1900GMT 79163

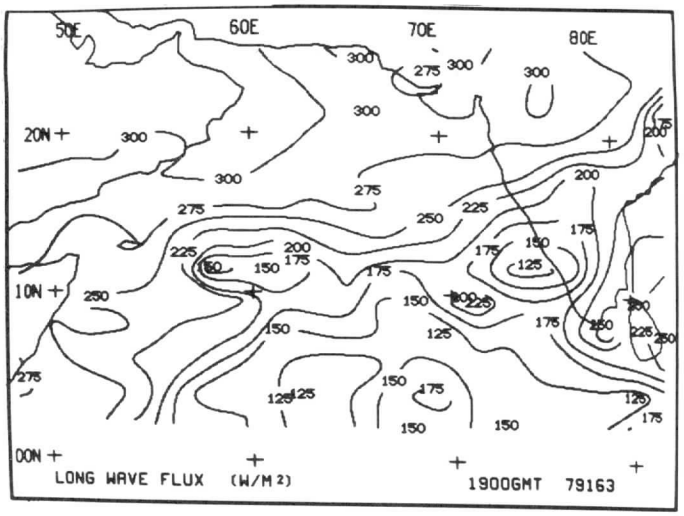
50E
60E
70E
80E
20N
10N
00N
LONG WAVE FLUX (W/M2)
1900GMT 79163

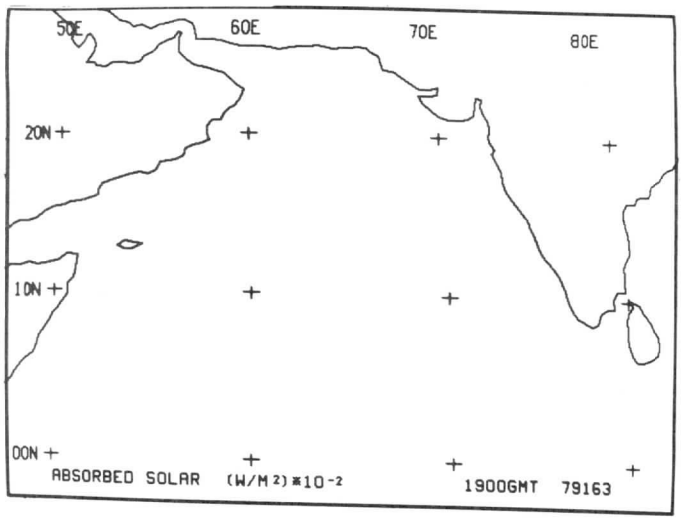
50E
60E
70E
80E
20N
10N
00N
ABSORBED SOLAR (W/M2)*10-2
1900GMT 79163

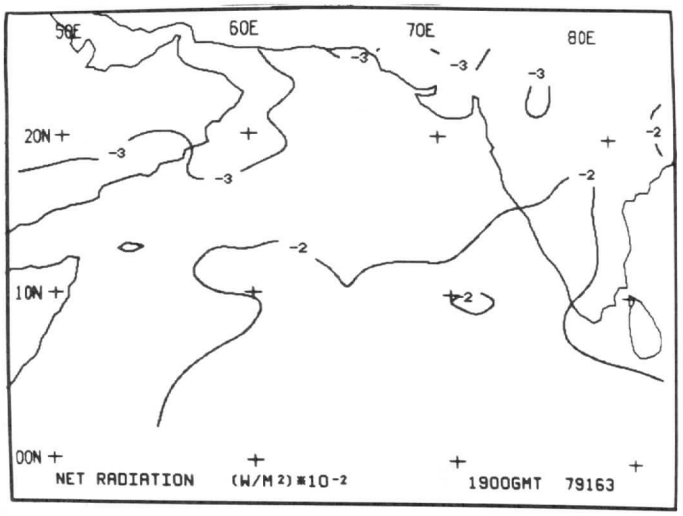
50E
60E
70E
80E
20N
10N
00N
NET RADIATION (W/M2)*10-2
1900GMT 79163

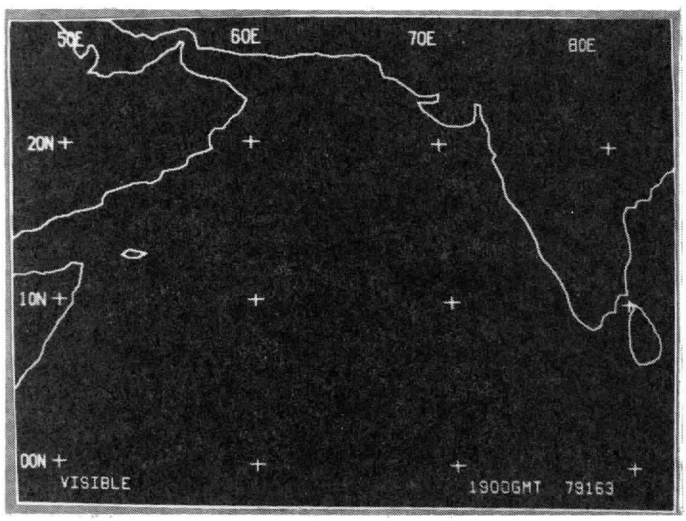
50E
60E
70E
80E
20N
10N
00N
VISIBLE
1900GMT 79163

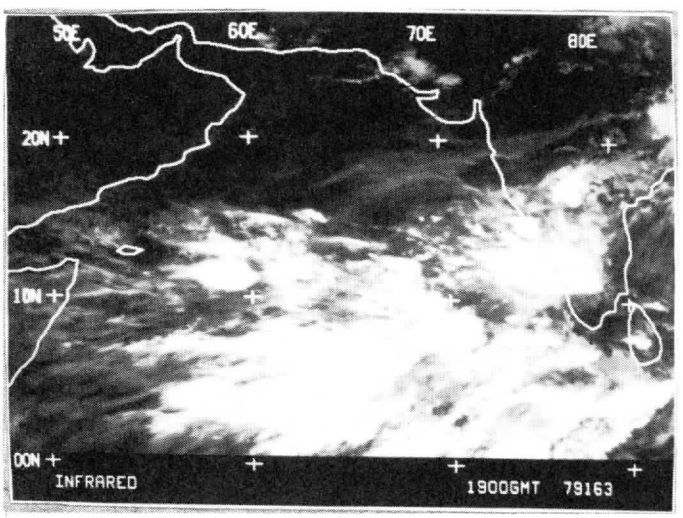
50E
60E
70E
80E
20N
10N
00N
INFRARED
1900GMT 79163

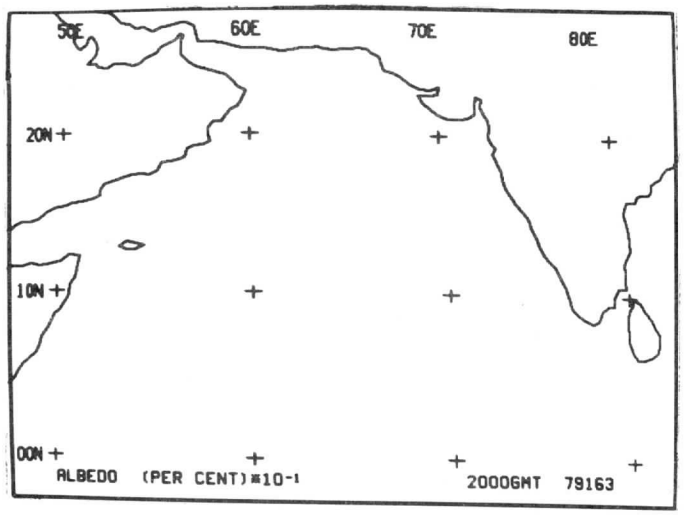
50E
60E
70E
80E
20N
10N
00N
ALBEDO (PER CENT)*10-1
2000GMT 79163

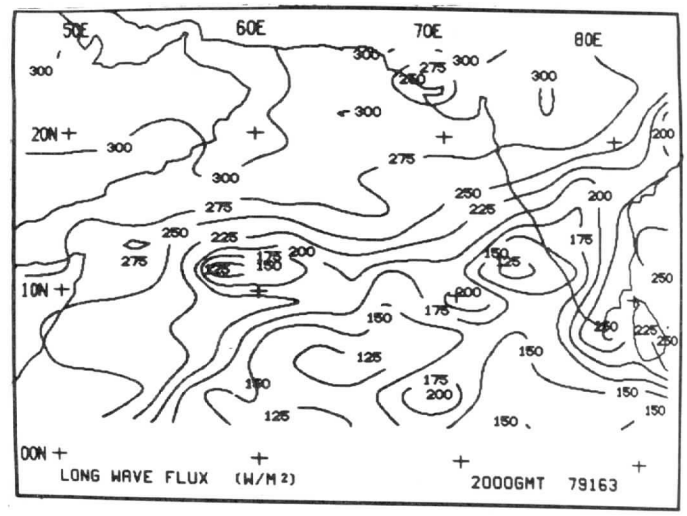
50E
60E
70E
80E
20N
10N
00N
LONG WAVE FLUX (W/M2)
2000GMT 79163

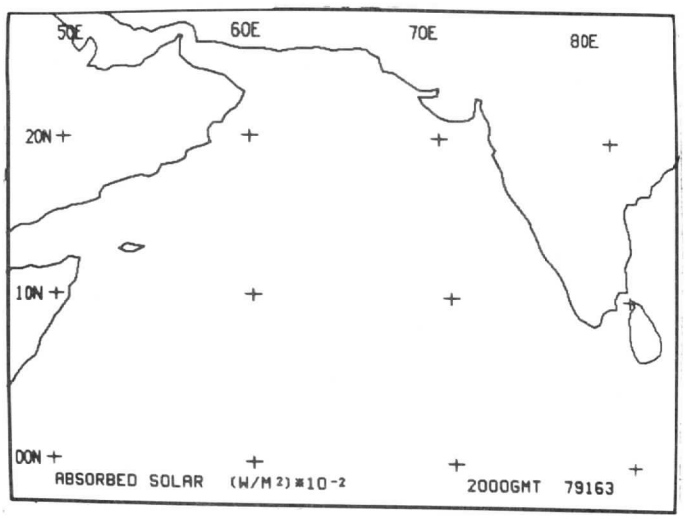
50E
60E
70E
80E
20N
10N
00N
ABSORBED SOLAR (W/M2)*10-2
2000GMT 79163

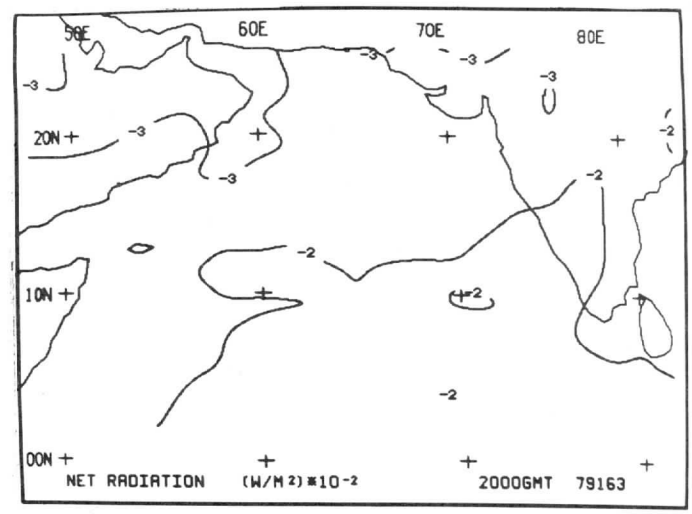
50E
60E
70E
80E
20N
10N
00N
NET RADIATION (W/M2)*10-2
2000GMT 79163

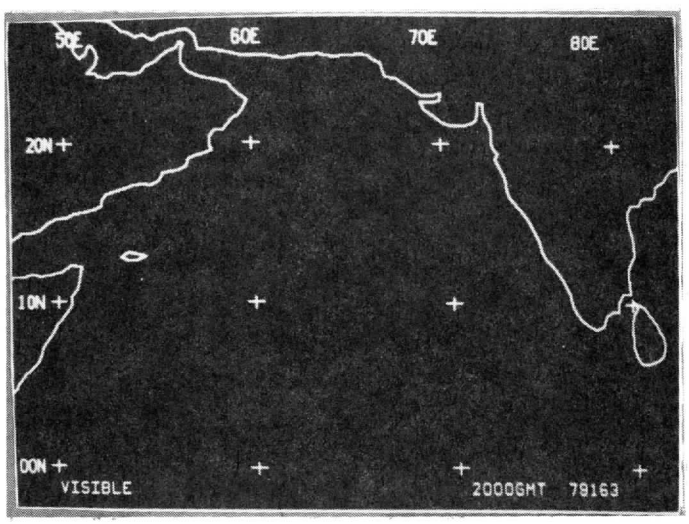
50E
60E
70E
80E
20N
10N
00N
VISIBLE
2000GMT 79163

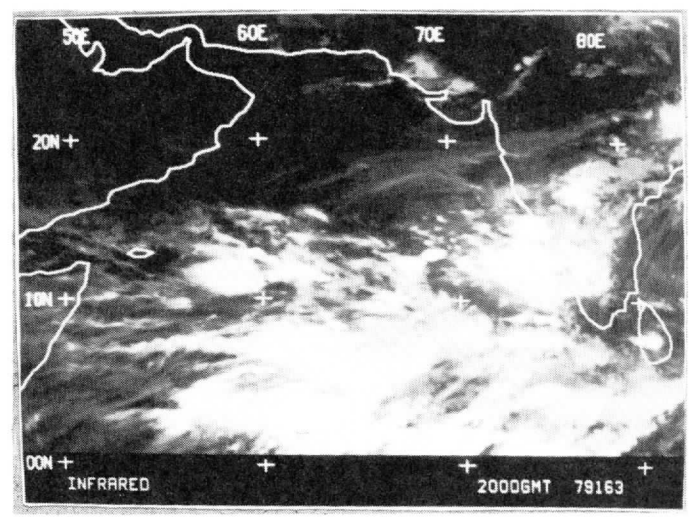
50E
60E
70E
80E
20N
10N
00N
INFRARED
2000GMT 79163

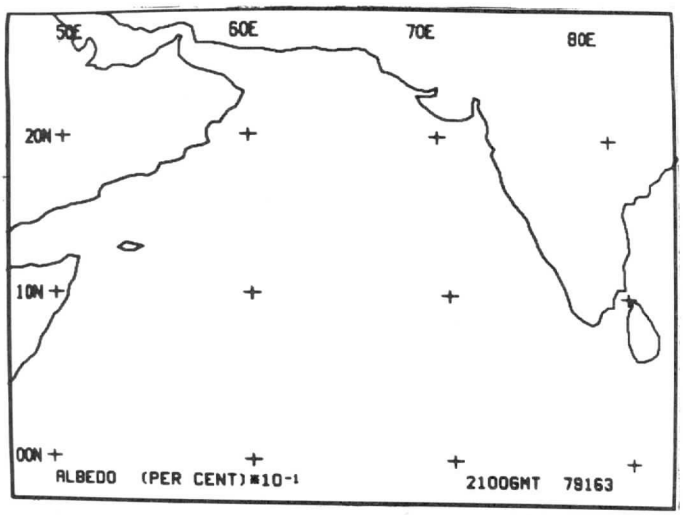
50E
60E
70E
80E
20N
10N
00N
ALBEDO (PER CENT)*10-1
2100GMT 79163

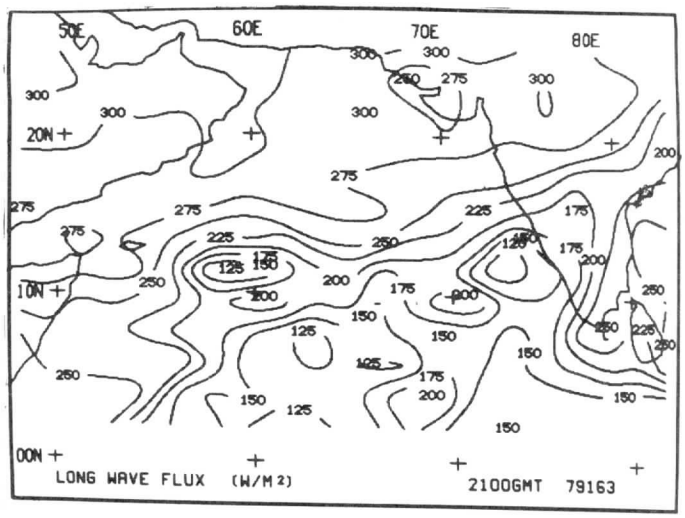
50E
60E
70E
80E
20N
10N
00N
LONG WAVE FLUX (W/M2)
2100GMT 79163

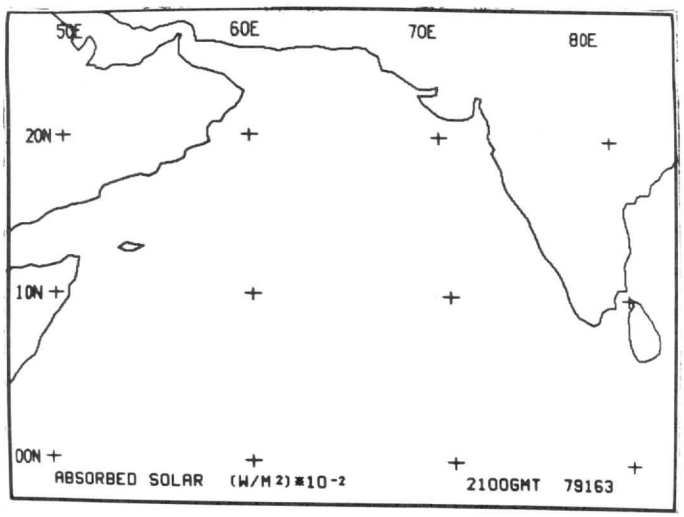
50E
60E
70E
80E
20N
10N
00N
ABSORBED SOLAR (W/M2)*10-2
2100GMT 79163

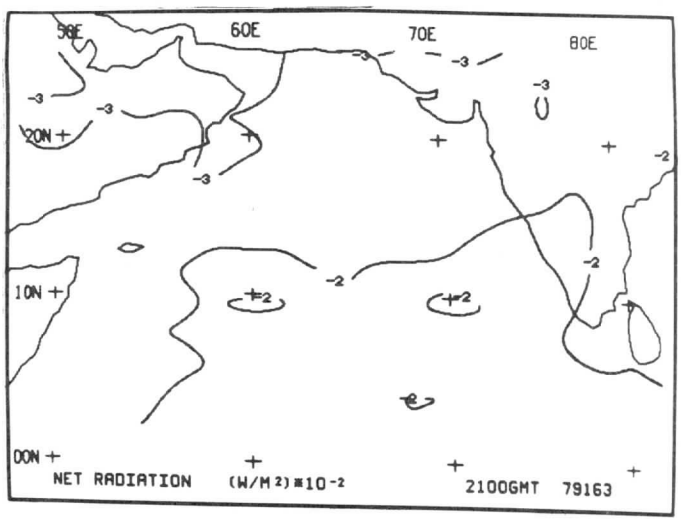
50E
60E
70E
80E
20N
10N
00N
NET RADIATION (W/M2)*10-2
2100GMT 79163

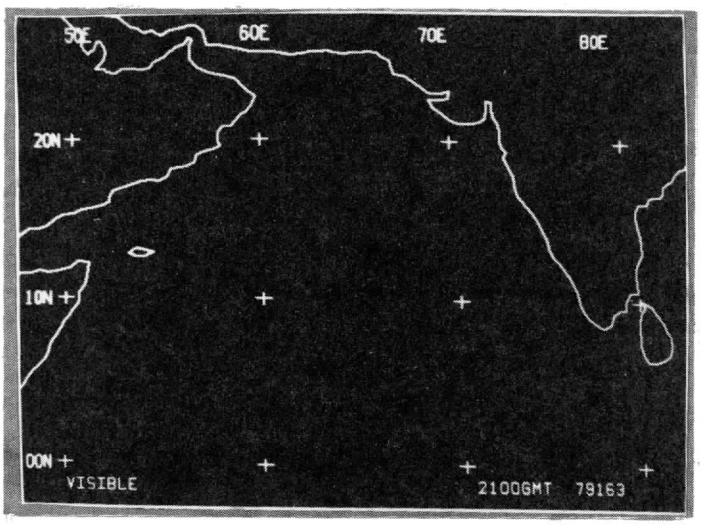
50E
60E
70E
80E
20N
10N
00N
VISIBLE
2100GMT 79163

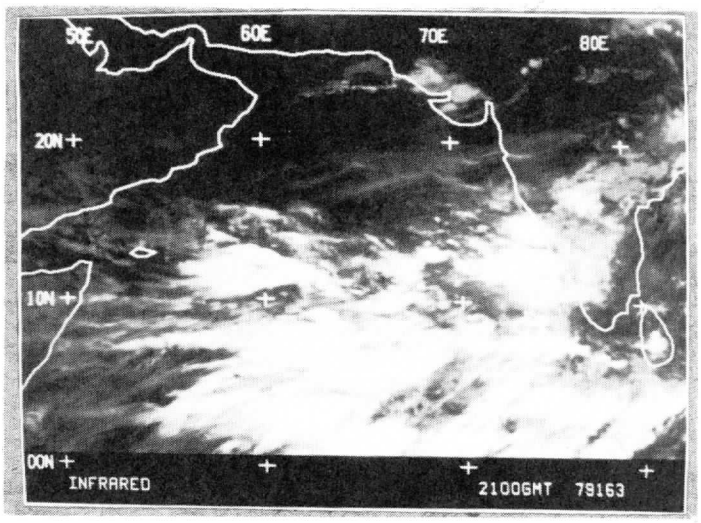
50E
60E
70E
80E
20N
10N
00N
INFRARED
2100GMT 79163

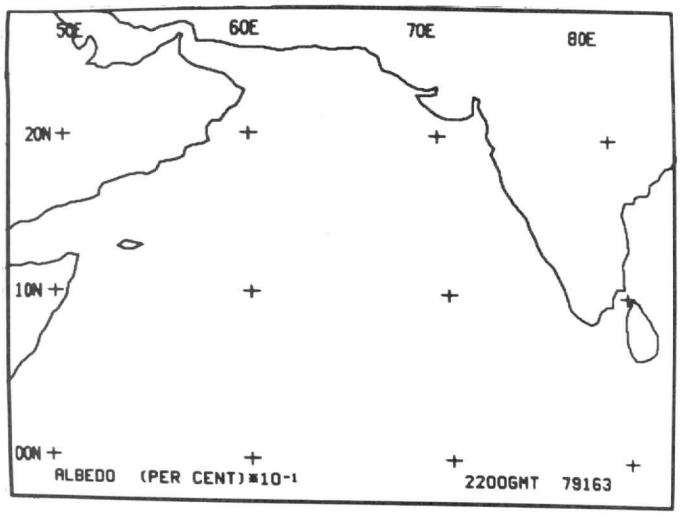
50E
60E
70E
80E
20N
10N
0ON
ALBEDO (PER CENT)*10-1
2200GMT 79163

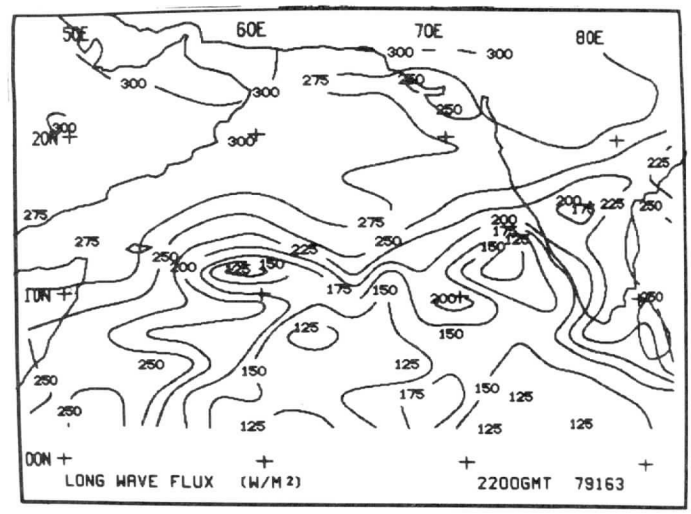
50E
60E
70E
80E
20N
10N
0ON
LONG WAVE FLUX (W/M2)
2200GMT 79163

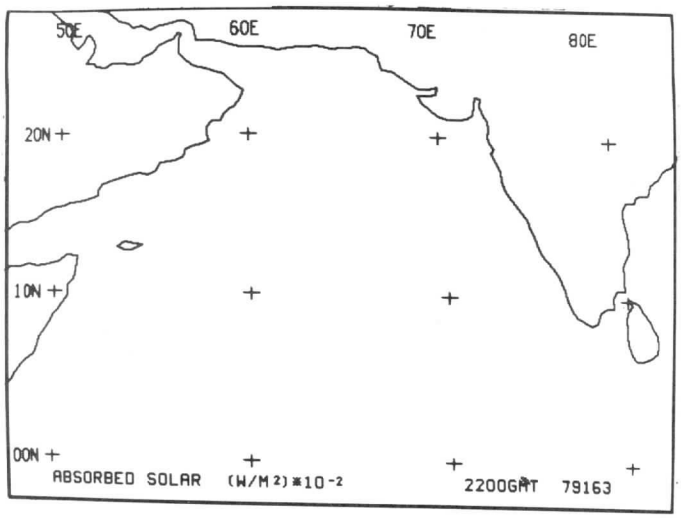
50E
60E
70E
80E
20N
10N
0ON
ABSORBED SOLAR (W/M2)*10-2
2200GMT 79163

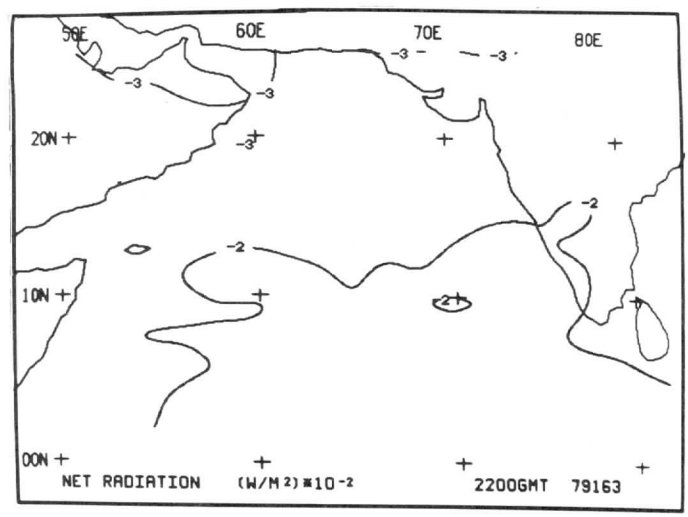
50E
60E
70E
80E
20N
10N
0ON
NET RADIATION (W/M2)*10-2
2200GMT 79163

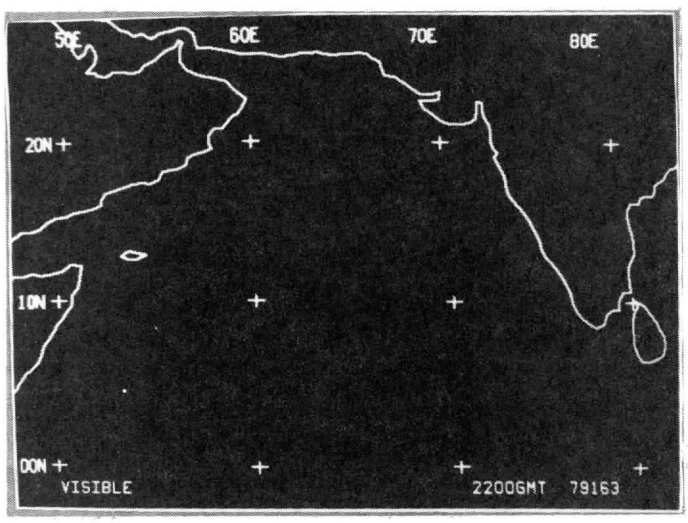
50E
60E
70E
80E
20N
10N
0ON
VISIBLE
2200GMT 79163

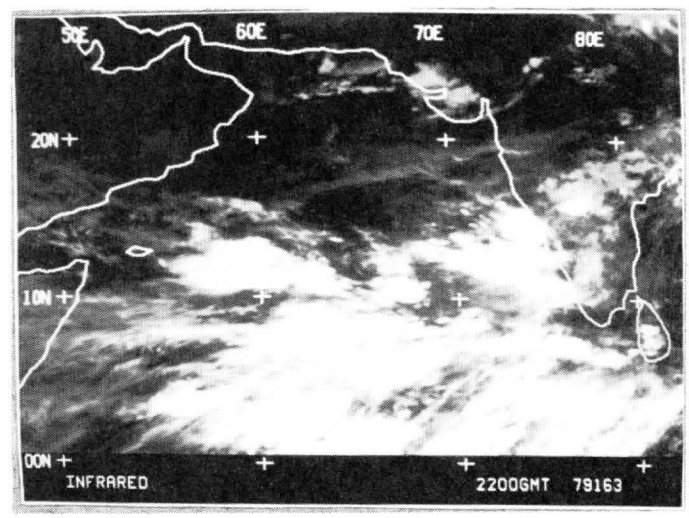
50E
60E
70E
80E
20N
10N
0ON
INFRARED
2200GMT 79163

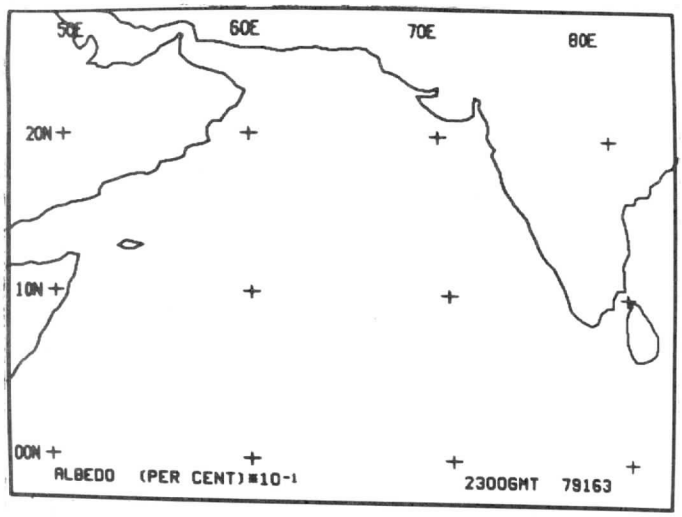
50E
60E
70E
80E
20N
10N
00N
ALBEDO (PER CENT)*10-1
2300GMT 79163

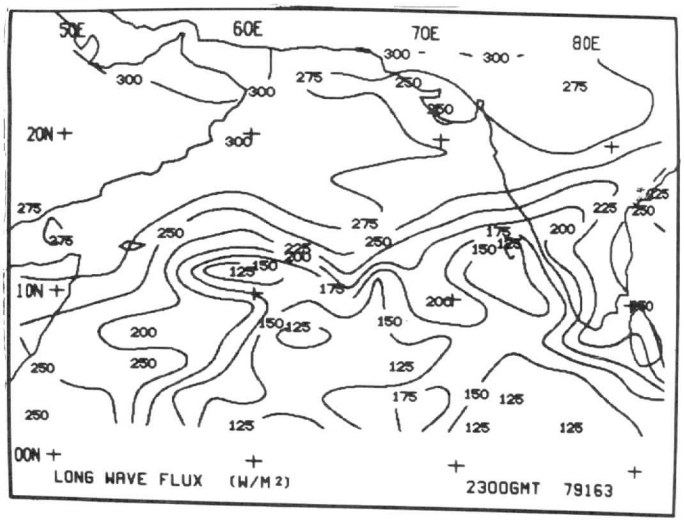
50E
60E
70E
80E
20N
10N
00N
LONG WAVE FLUX (W/M2)
2300GMT 79163

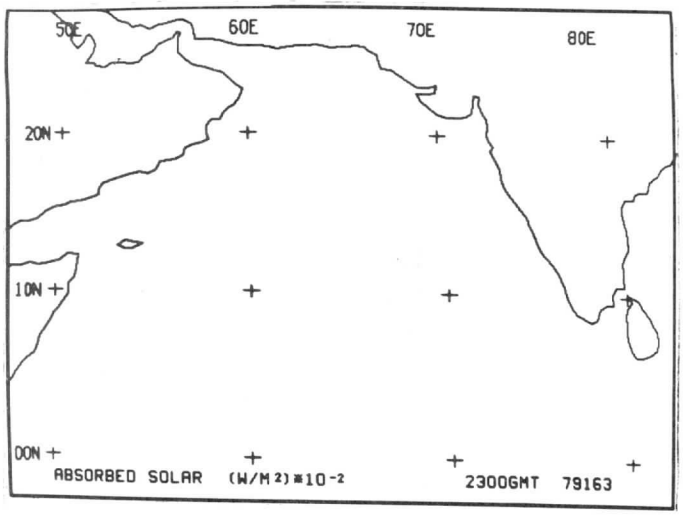
50E
60E
70E
80E
20N
10N
00N
ABSORBED SOLAR (W/M2)*10-2
2300GMT 79163

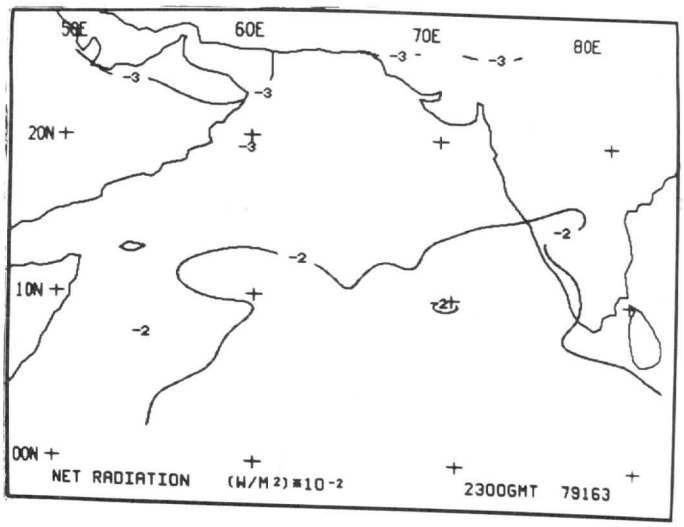
50E
60E
70E
80E
20N
10N
00N
NET RADIATION (W/M2)*10-2
2300GMT 79163

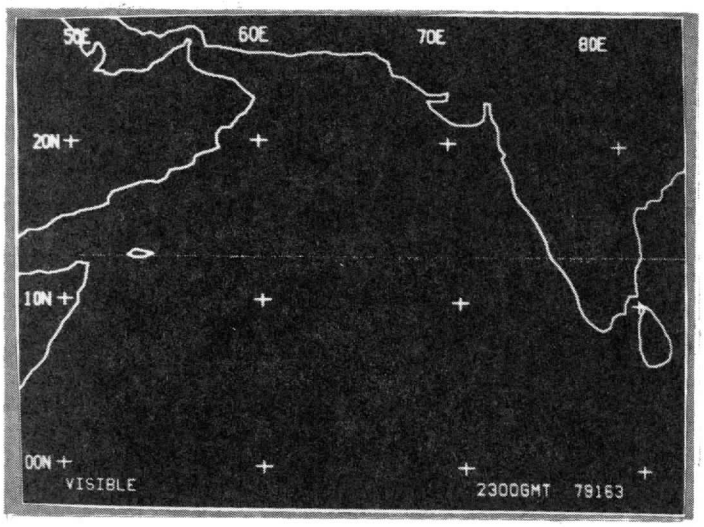
50E
60E
70E
80E
20N
10N
00N
VISIBLE
2300GMT 79163

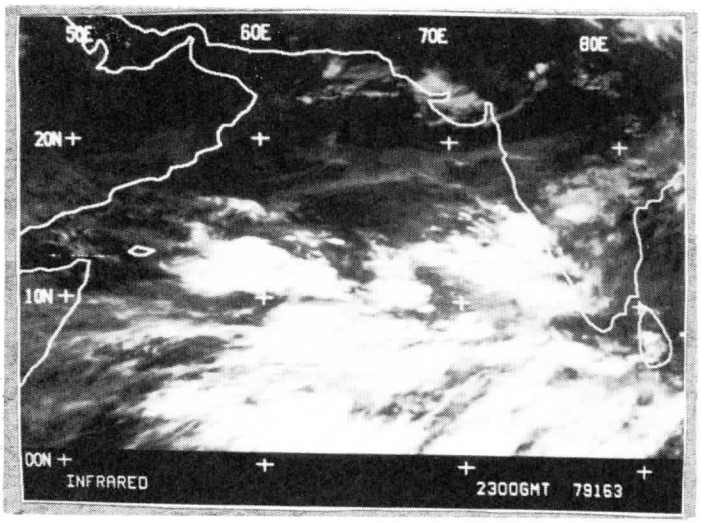
50E
60E
70E
80E
20N
10N
00N
INFRARED
2300GMT 79163

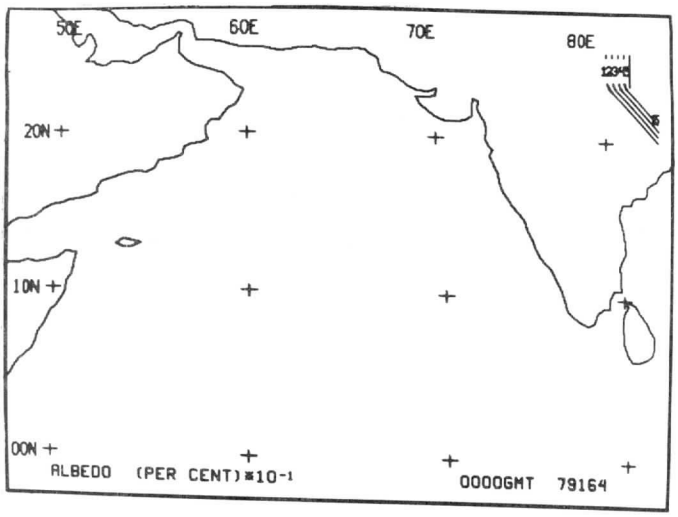
50E
60E
70E
80E
20N
10N
00N
ALBEDO (PER CENT)*10-1
0000GMT 79164

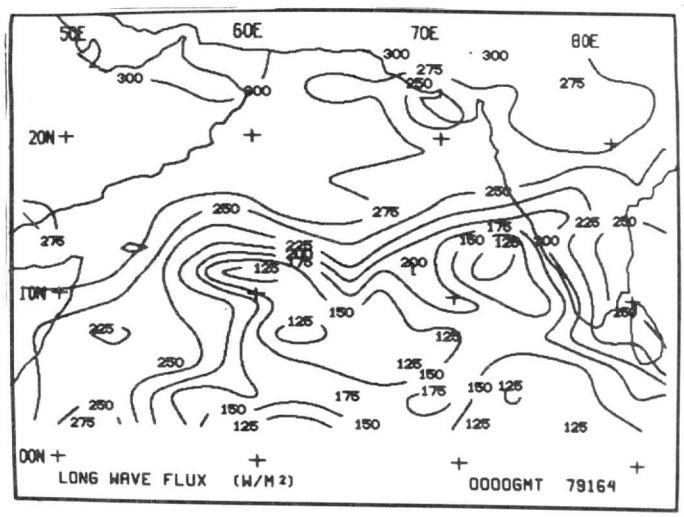
50E
60E
70E
80E
20N
10N
00N
LONG WAVE FLUX (W/M2)
0000GMT 79164

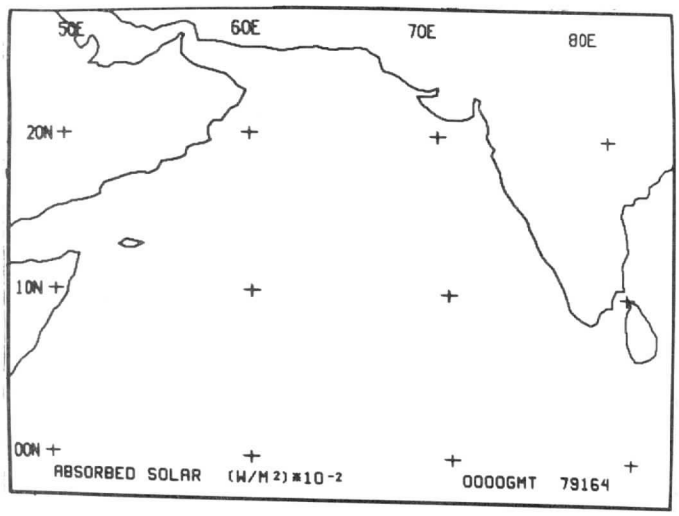
50E
60E
70E
80E
20N
10N
00N
ABSORBED SOLAR (W/M2)*10-2
0000GMT 79164

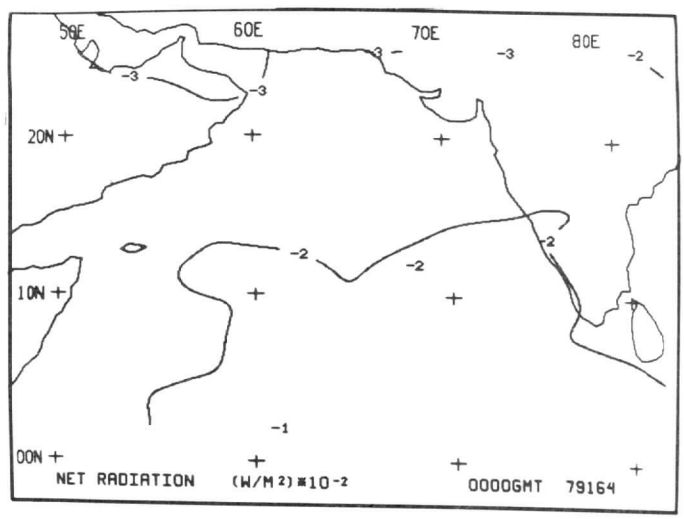
50E
60E
70E
80E
20N
10N
00N
NET RADIATION (W/M2)*10-2
0000GMT 79164

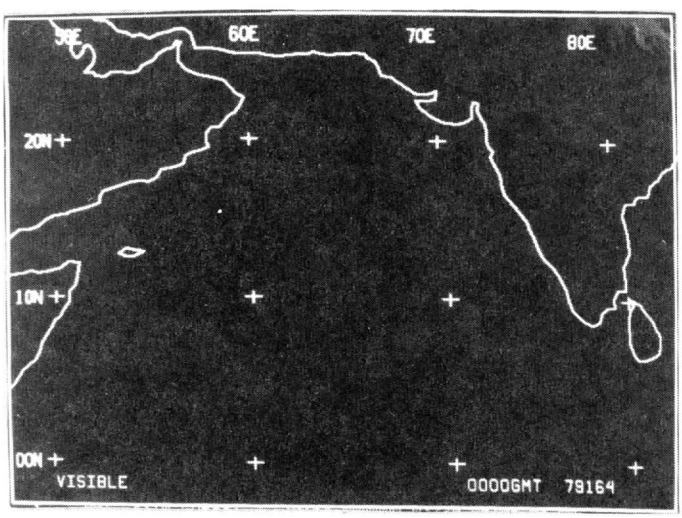
50E
60E
70E
80E
20N
10N
00N
VISIBLE
0000GMT 79164

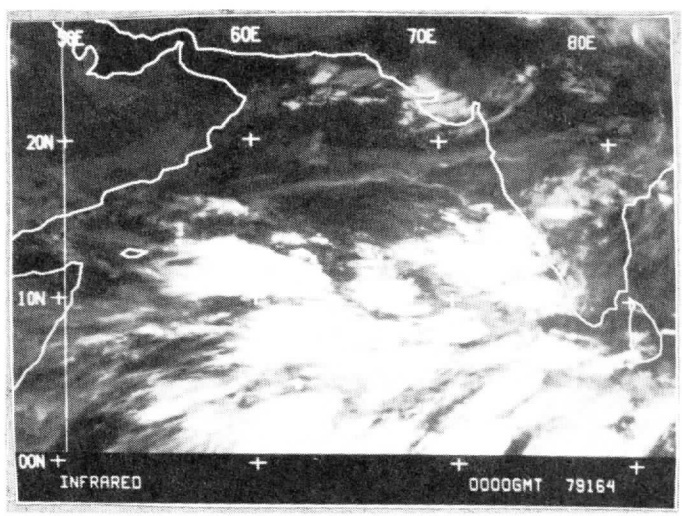
50E
60E
70E
80E
20N
10N
00N
INFRARED
0000GMT 79164

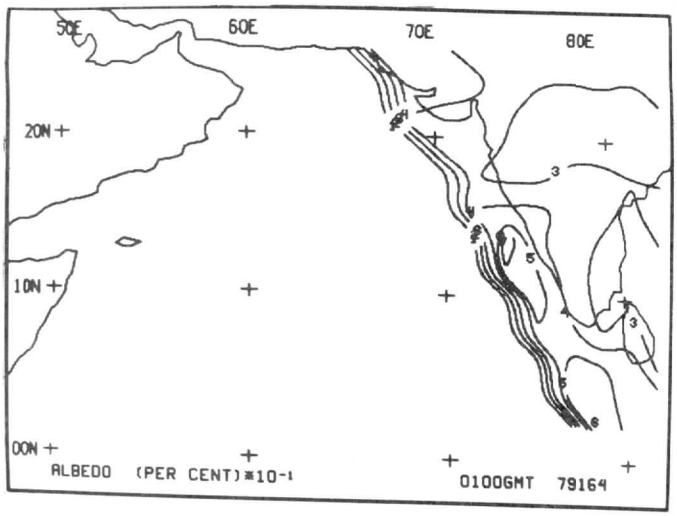
50E
60E
70E
80E
20N
10N
00N
ALBEDO (PER CENT)*10-1
0100GMT 79164

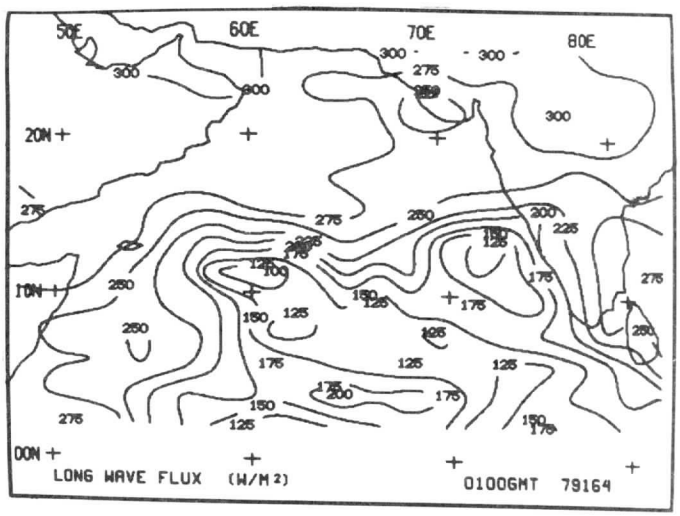
50E
60E
70E
80E
20N
10N
00N
LONG WAVE FLUX (W/M2)
0100GMT 79164

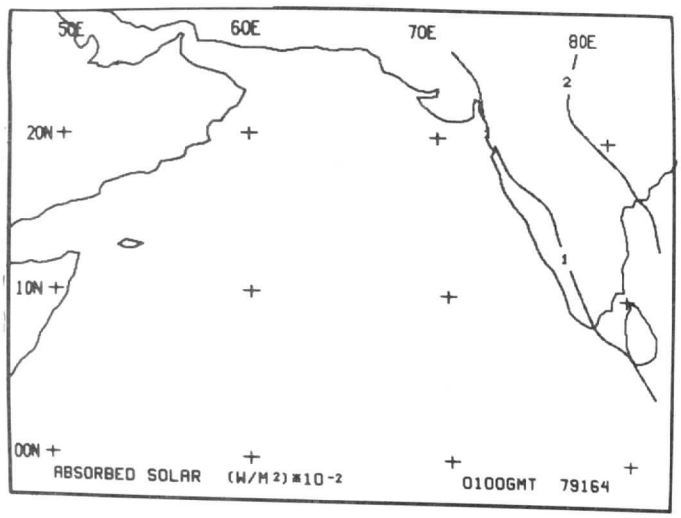
50E
60E
70E
80E
20N
10N
00N
ABSORBED SOLAR (W/M2)*10-2
0100GMT 79164

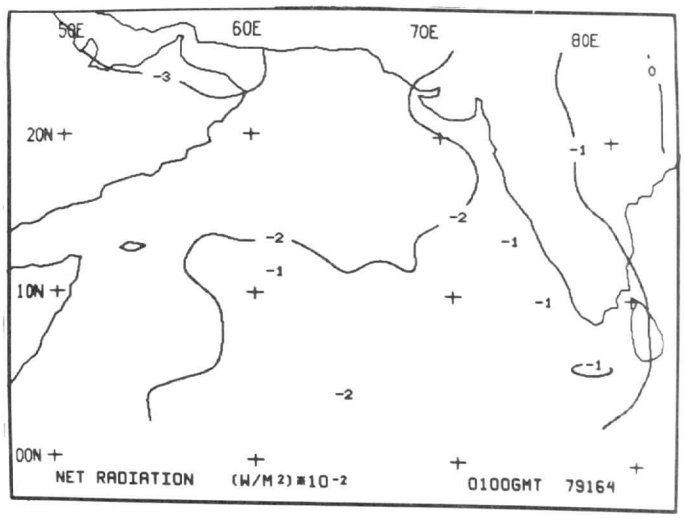
50E
60E
70E
80E
20N
10N
00N
NET RADIATION (W/M2)*10-2
0100GMT 79164

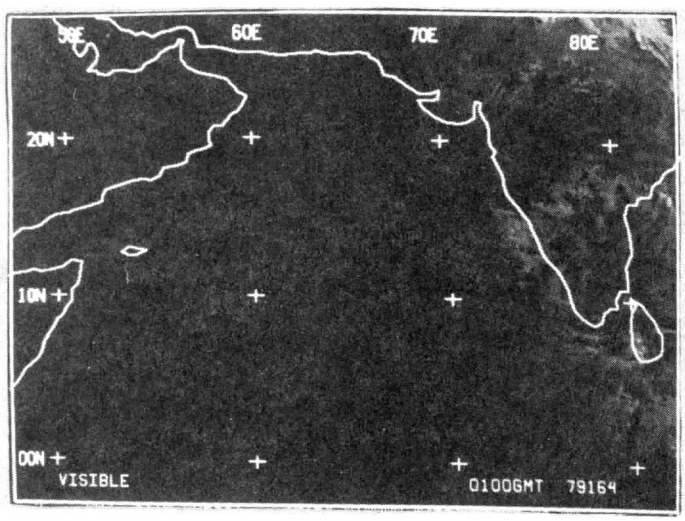
50E
60E
70E
80E
20N
10N
00N
VISIBLE
0100GMT 79164

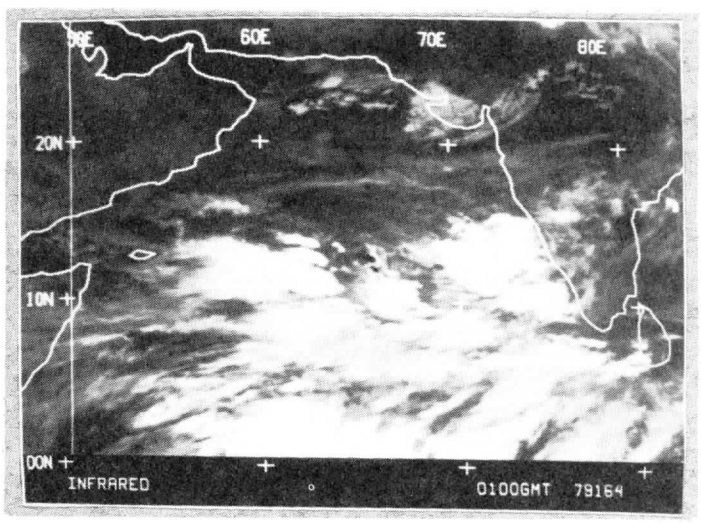
50E
60E
70E
80E
20N
10N
00N
INFRARED
0100GMT 79164

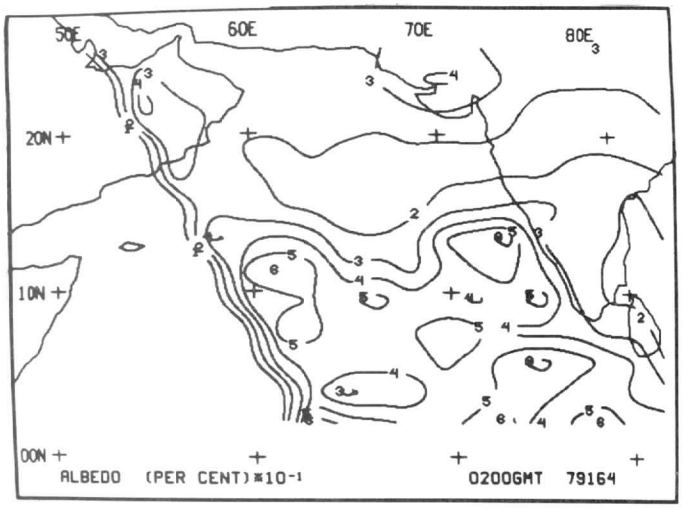
50E
60E
70E
80E
20N
10N
0ON
ALBEDO (PER CENT)*10-1
0200GMT 79164

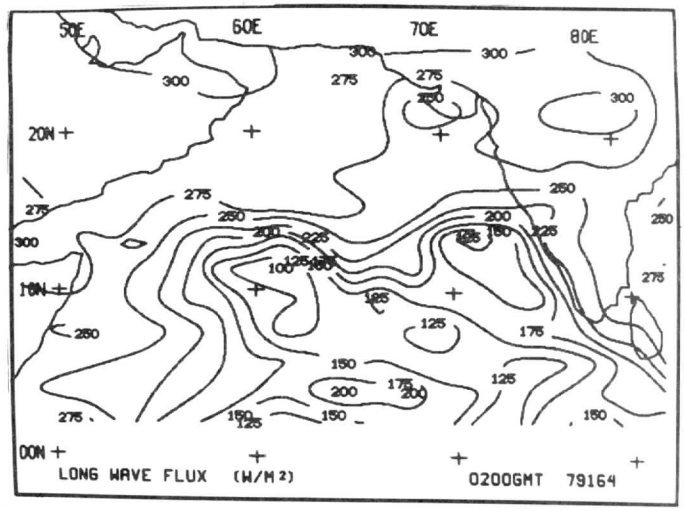
50E
60E
70E
80E
20N
10N
0ON
LONG WAVE FLUX (W/M2)
0200GMT 79164

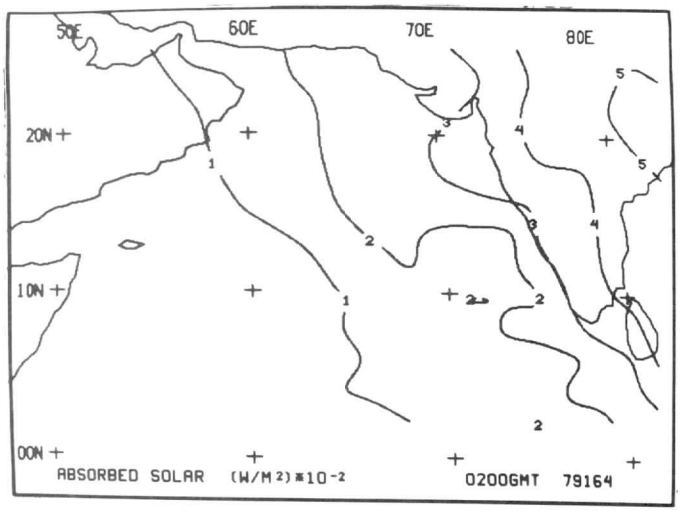
50E
60E
70E
80E
20N
10N
0ON
ABSORBED SOLAR (W/M2)*10-2
0200GMT 79164

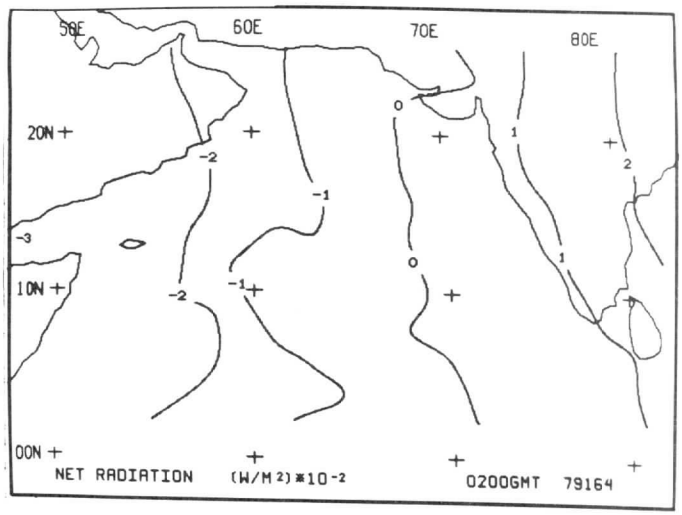
50E
60E
70E
80E
20N
10N
0ON
NET RADIATION (W/M2)*10-2
0200GMT 79164

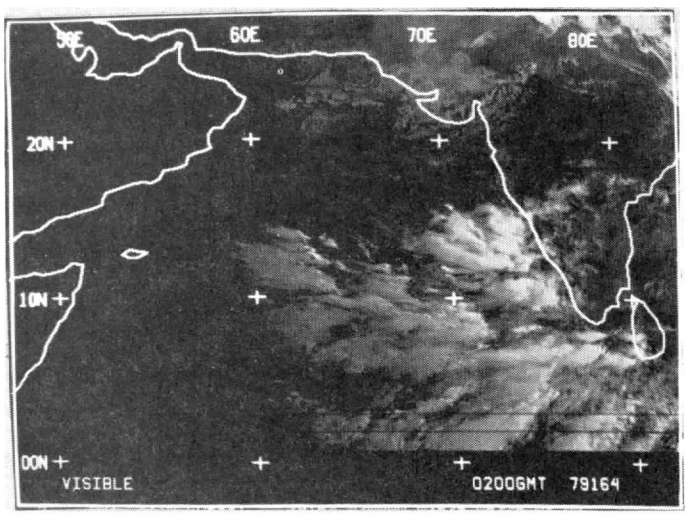
50E
60E
70E
80E
20N
10N
0ON
VISIBLE
0200GMT 79164

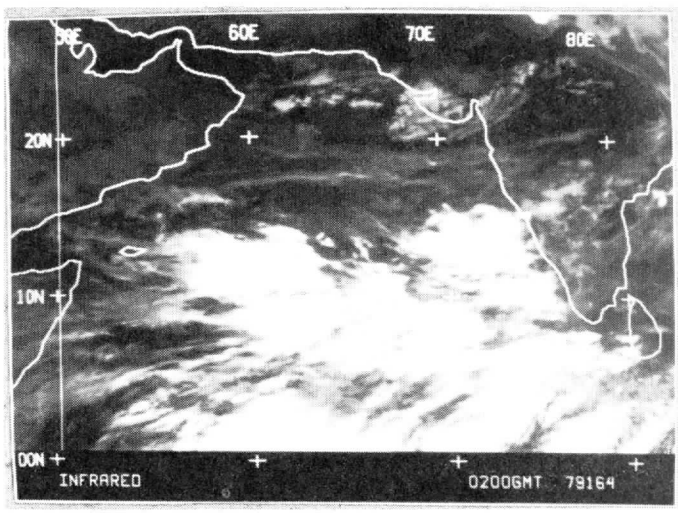
50E
60E
70E
80E
20N
10N
0ON
INFRARED
0200GMT 79164

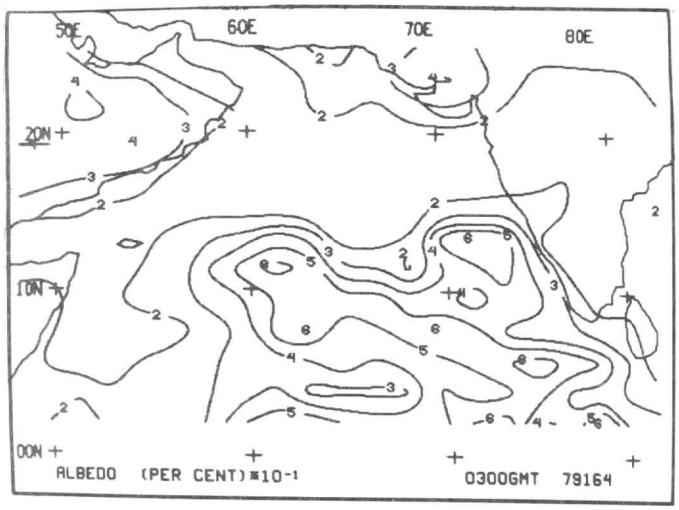
50E
60E
70E
80E
20N
10N
0ON
ALBEDO (PER CENT)*10-1
0300GMT 79164

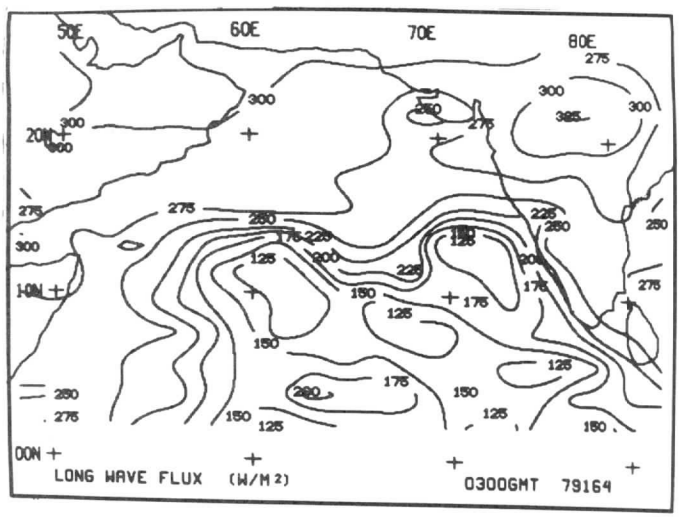
50E
60E
70E
80E
20N
10N
0ON
LONG WAVE FLUX (W/M2)
0300GMT 79164

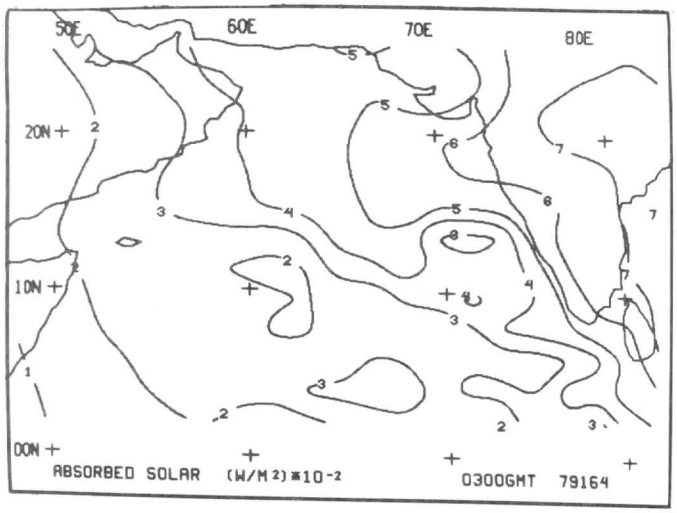
50E
60E
70E
80E
20N
10N
0ON
ABSORBED SOLAR (W/M2)*10-2
0300GMT 79164

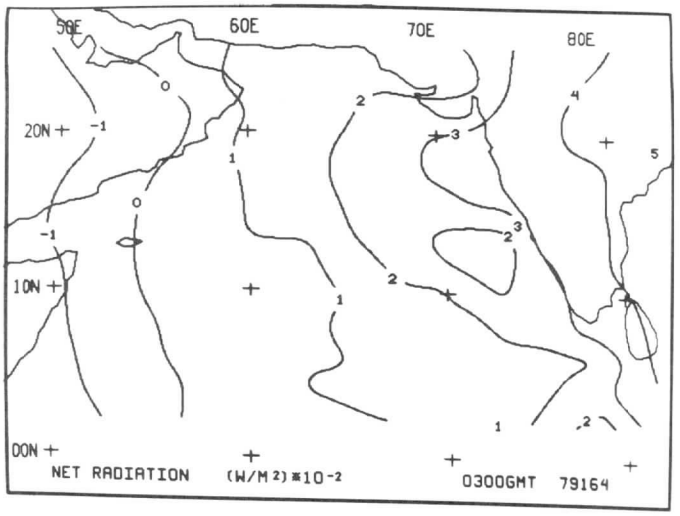
50E
60E
70E
80E
20N
10N
0ON
NET RADIATION (W/M2)*10-2
0300GMT 79164

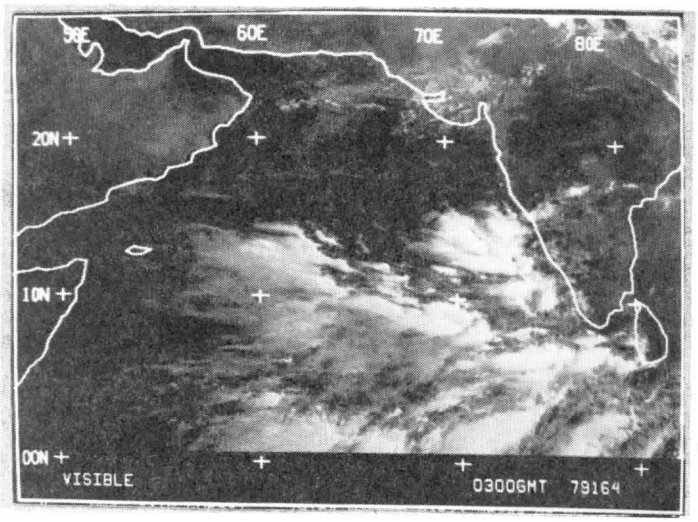
50E
60E
70E
80E
20N
10N
0ON
VISIBLE
0300GMT 79164

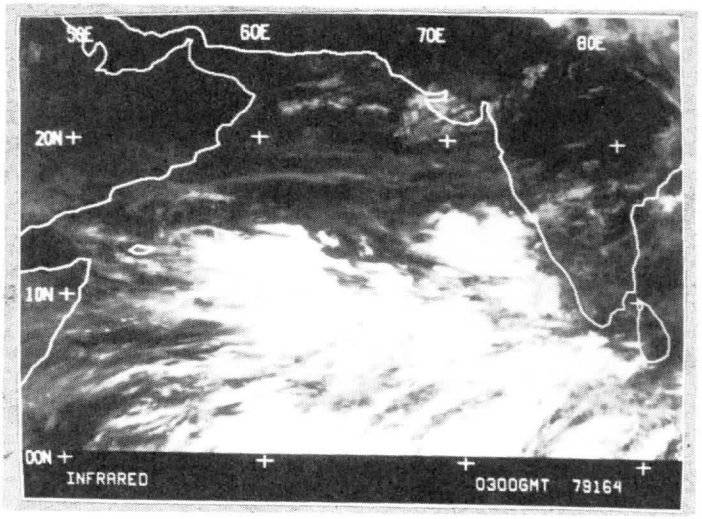
50E
60E
70E
80E
20N
10N
0ON
INFRARED
0300GMT 79164

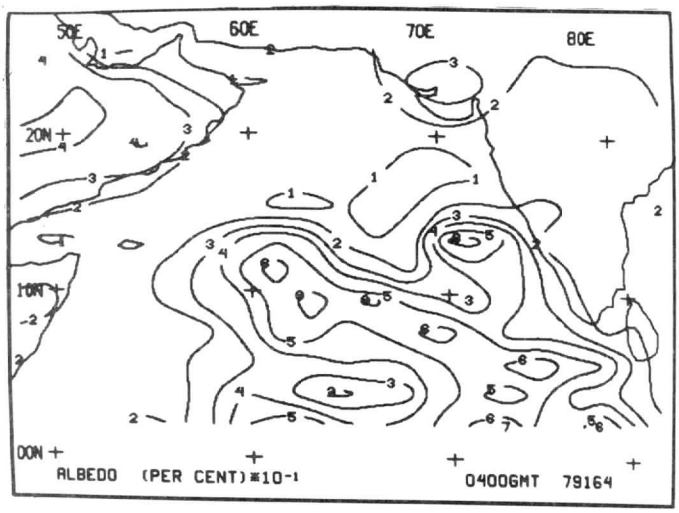
50E
60E
70E
80E
20N
10N
0ON
ALBEDO (PER CENT)*10-1
0400GMT 79164

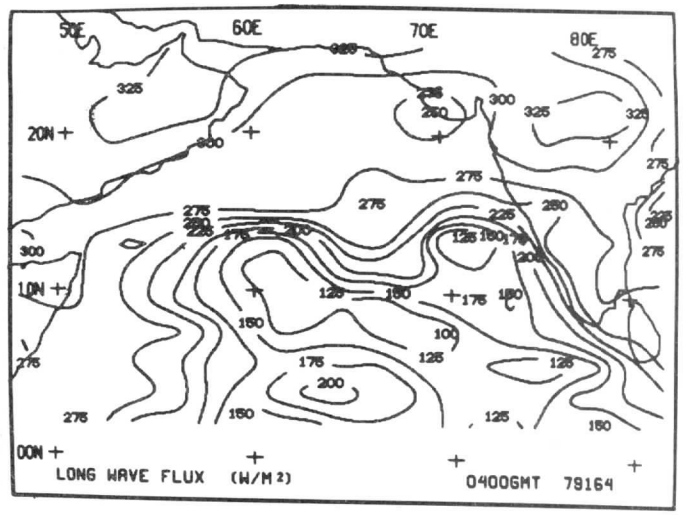
50E
60E
70E
80E
20N
10N
0ON
LONG WAVE FLUX (W/M2)
0400GMT 79164

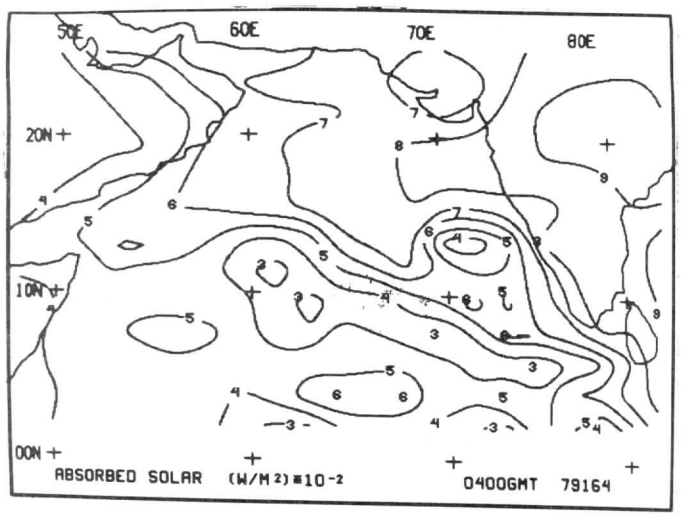
50E
60E
70E
80E
20N
10N
0ON
ABSORBED SOLAR (W/M2)*10-2
0400GMT 79164

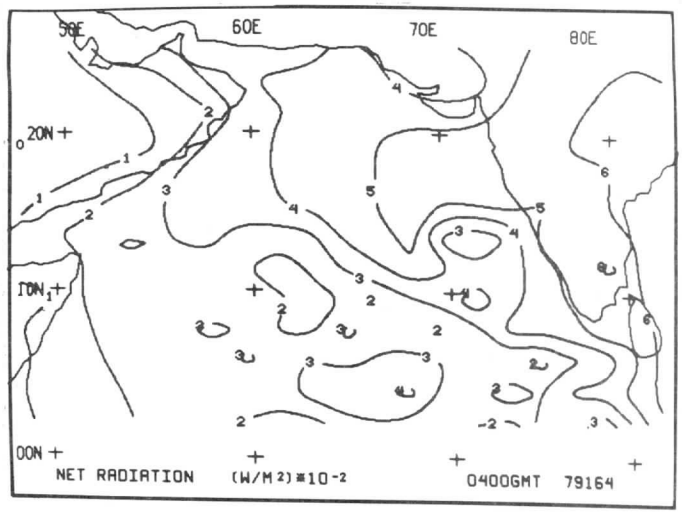
50E
60E
70E
80E
20N
10N
0ON
NET RADIATION (W/M2)*10-2
0400GMT 79164

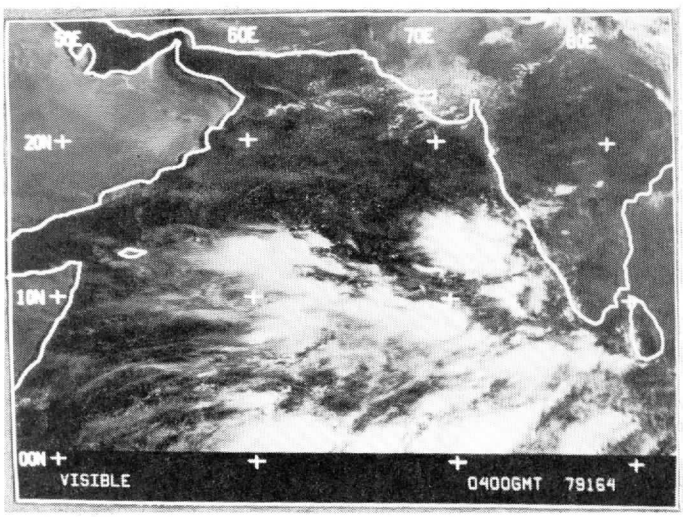
50E
60E
70E
80E
20N
10N
0ON
VISIBLE
0400GMT 79164

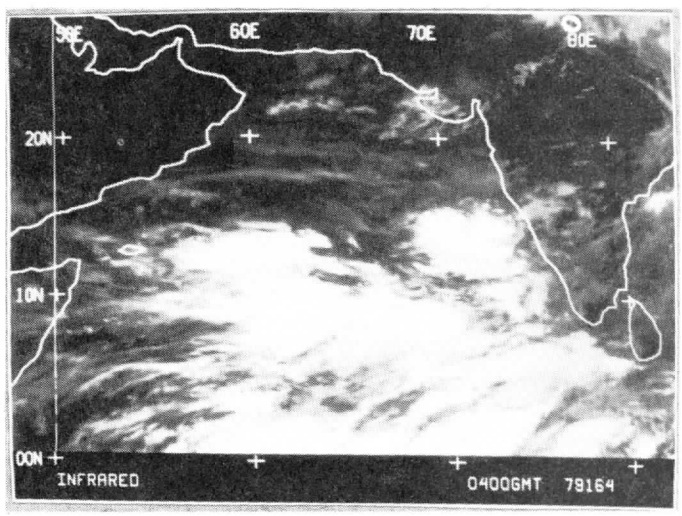
50E
60E
70E
80E
20N
10N
0ON
INFRARED
0400GMT 79164

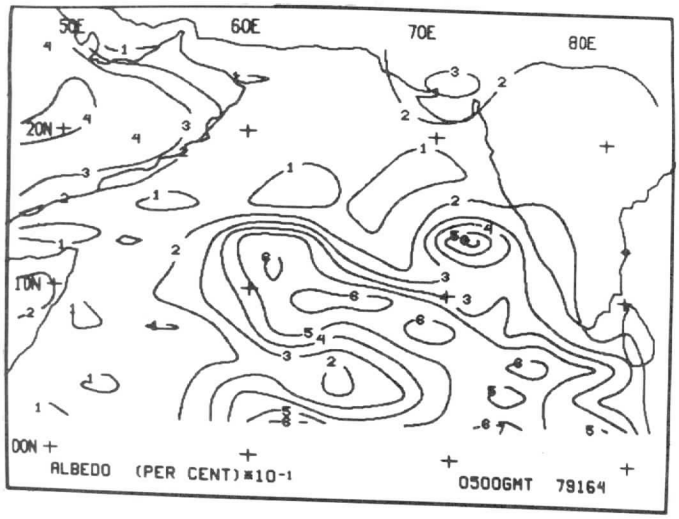
50E
60E
70E
80E
20N
10N
0ON
ALBEDO (PER CENT)*10-1
0500GMT 79164

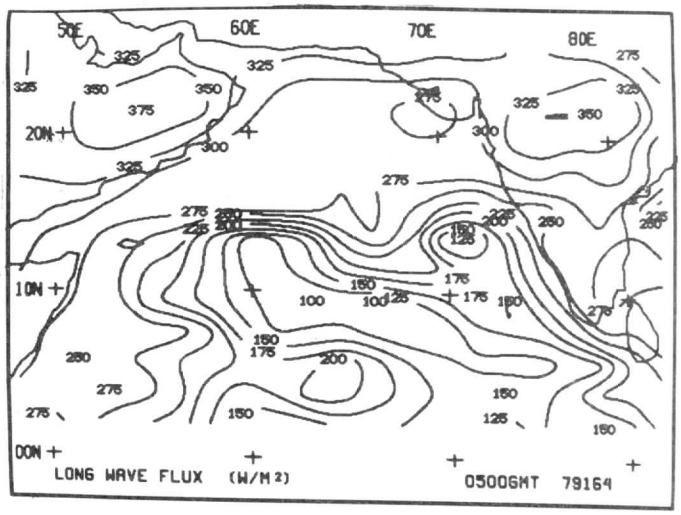
50E
60E
70E
80E
20N
10N
0ON
LONG WAVE FLUX (W/M2)
0500GMT 79164

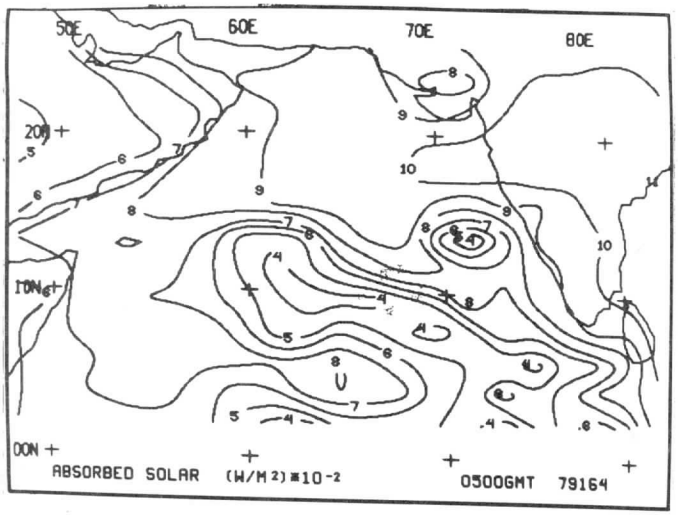
50E
60E
70E
80E
20N
10N
0ON
ABSORBED SOLAR (W/M2)*10-2
0500GMT 79164

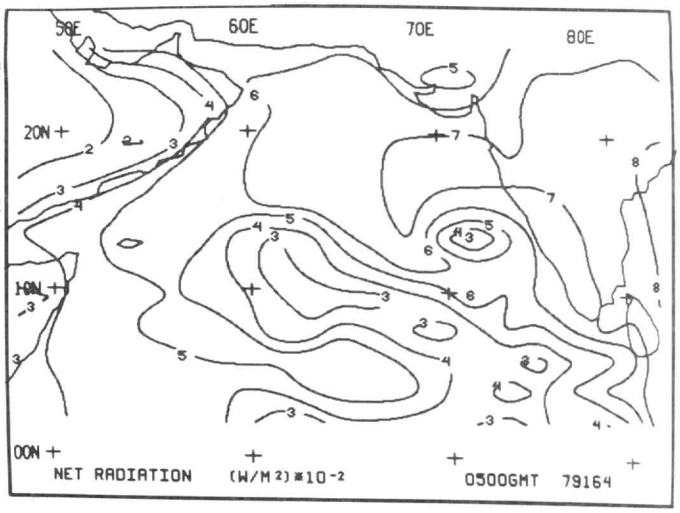
50E
60E
70E
80E
20N
10N
0ON
NET RADIATION (W/M2)*10-2
0500GMT 79164

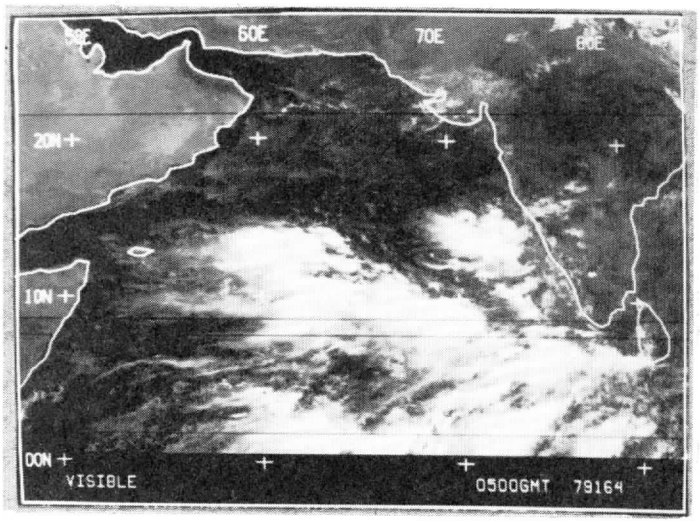
50E
60E
70E
80E
20N
10N
0ON
VISIBLE
0500GMT 79164

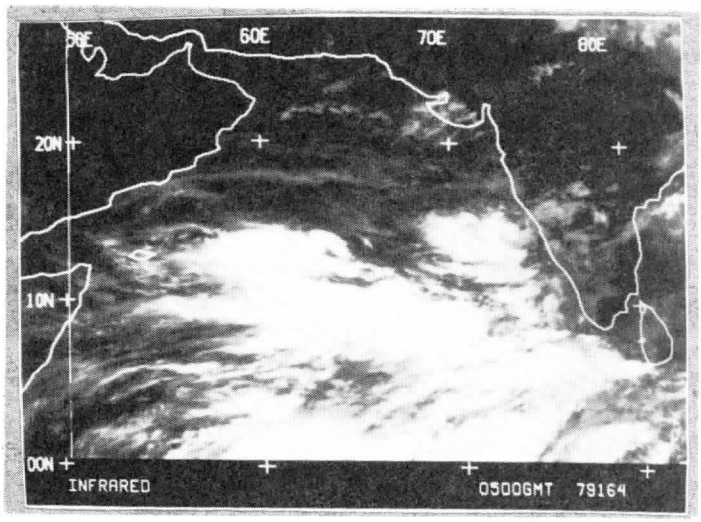
50E
60E
70E
80E
20N
10N
0ON
INFRARED
0500GMT 79164

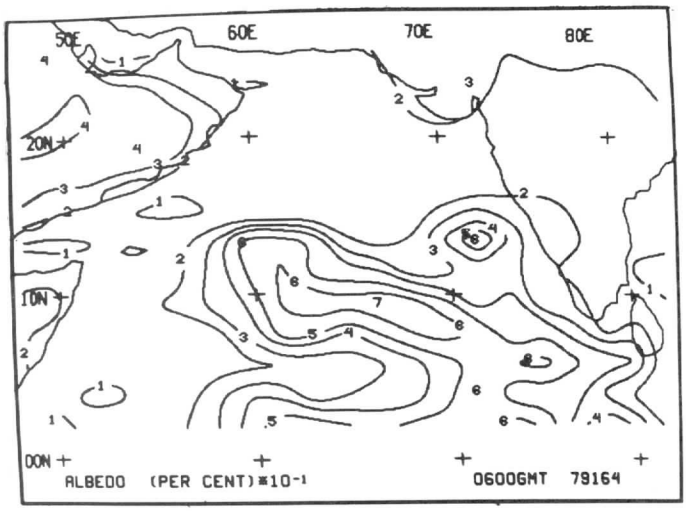
50E
60E
70E
80E
20N
10N
0ON
ALBEDO (PER CENT)*10-1
0600GMT 79164

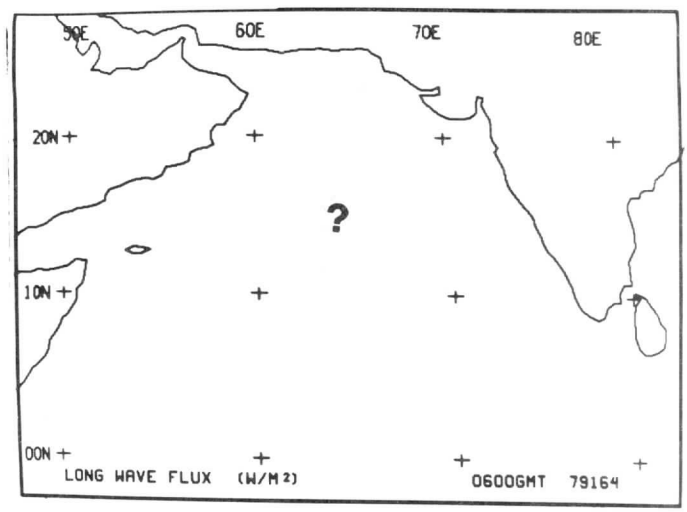
50E
60E
70E
80E
20N
10N
0ON
?
LONG WAVE FLUX (W/M2)
0600GMT 79164

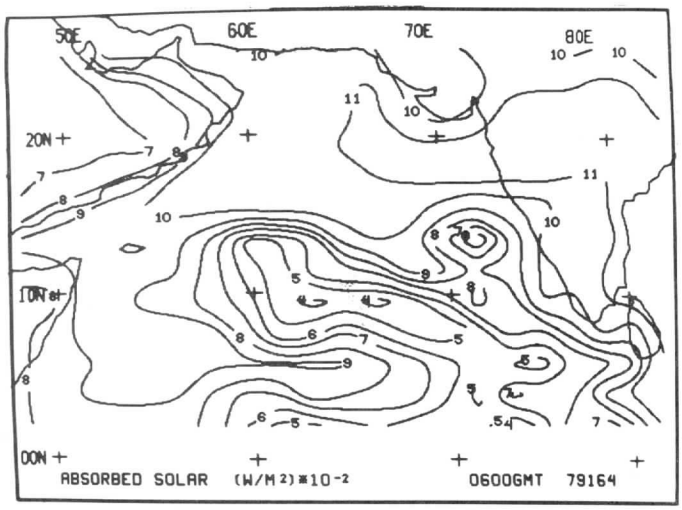
50E
60E
70E
80E
20N
10N
0ON
ABSORBED SOLAR (W/M2)*10-2
0600GMT 79164

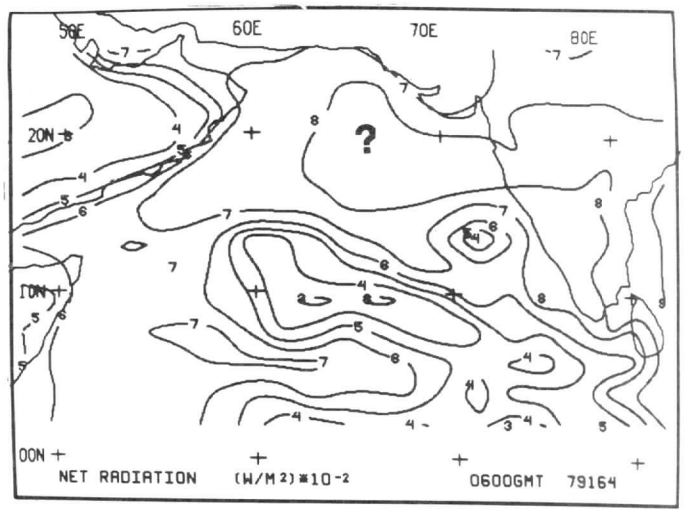
50E
60E
70E
80E
20N
10N
0ON
?
NET RADIATION (W/M2)*10-2
0600GMT 79164

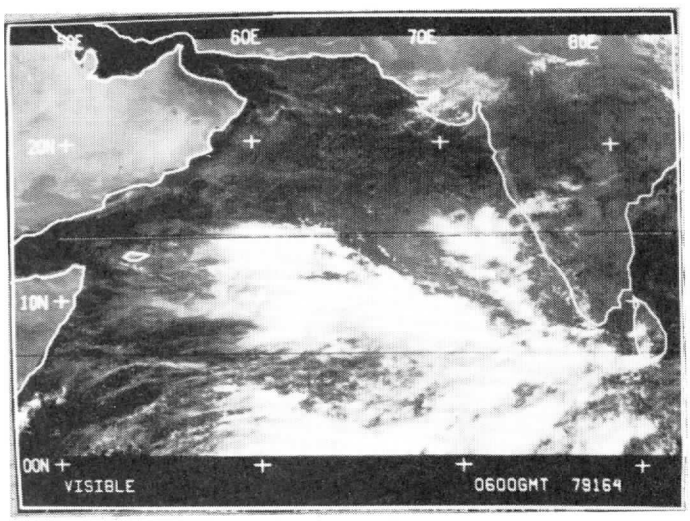
50E
60E
70E
80E
20N
10N
0ON
VISIBLE
0600GMT 79164

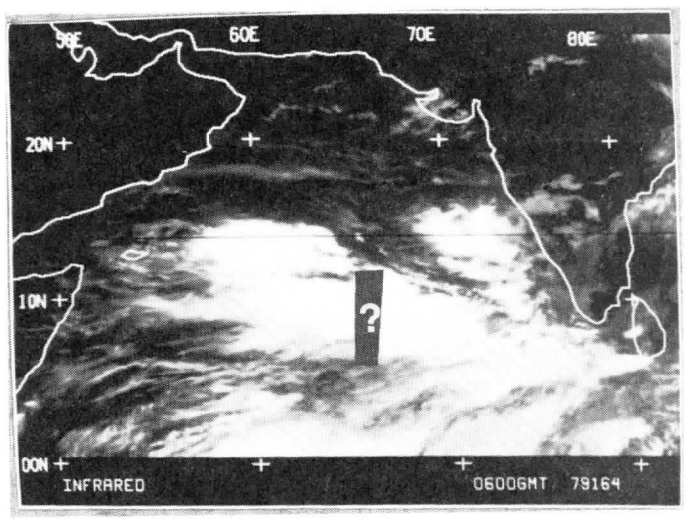
50E
60E
70E
80E
20N
10N
?
0ON
INFRARED
0600GMT 79164

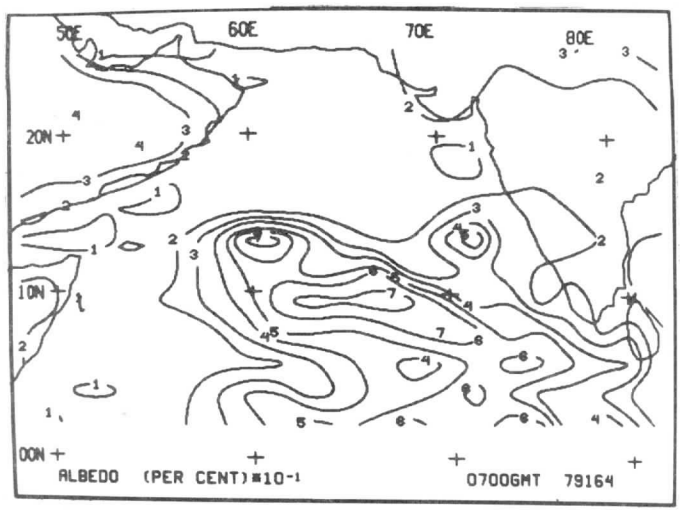
50E
60E
70E
80E
20N
10N
0ON
ALBEDO (PER CENT)*10-1
0700GMT 79164

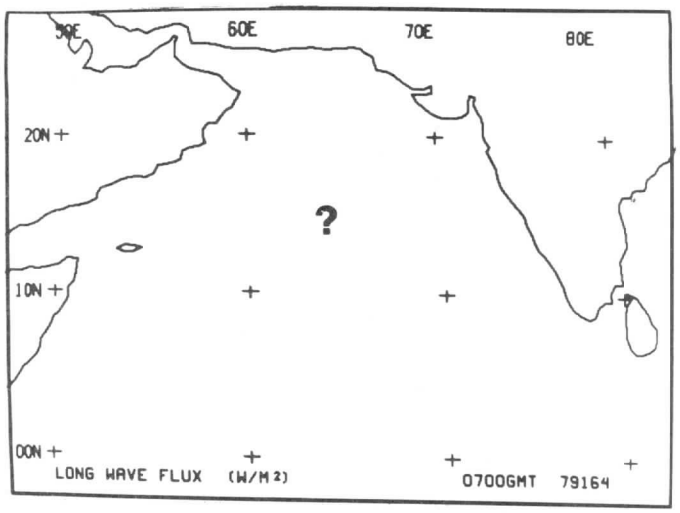
50E
60E
70E
80E
20N
10N
0ON
?
LONG WAVE FLUX (W/M2)
0700GMT 79164

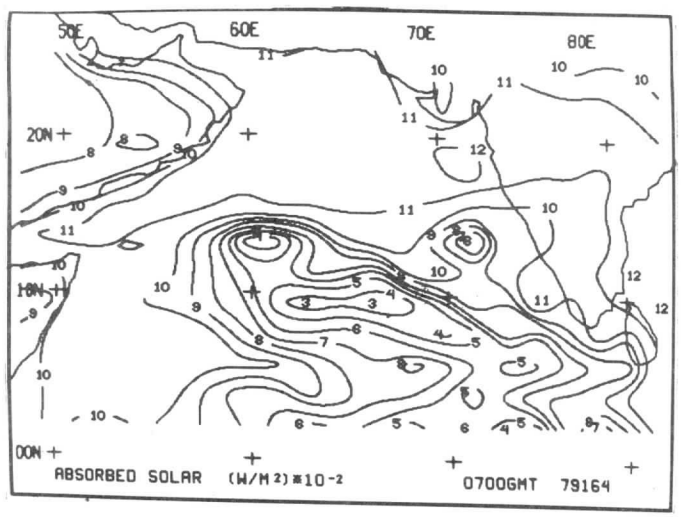
50E
60E
70E
80E
20N
10N
0ON
ABSORBED SOLAR (W/M2)*10-2
0700GMT 79164

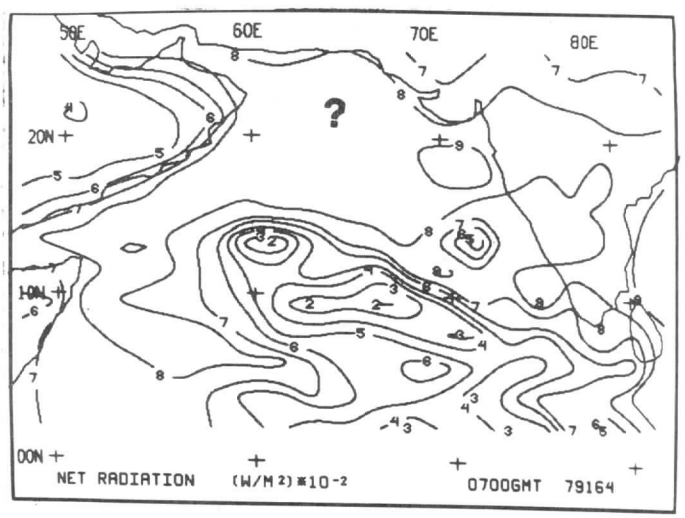
50E
60E
70E
80E
20N
10N
0ON
?
NET RADIATION (W/M2)*10-2
0700GMT 79164

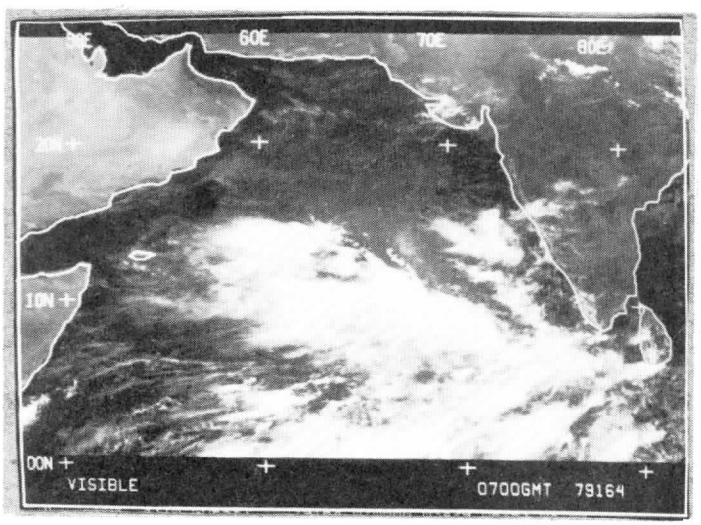
50E
60E
70E
80E
20N
10N
0ON
VISIBLE
0700GMT 79164

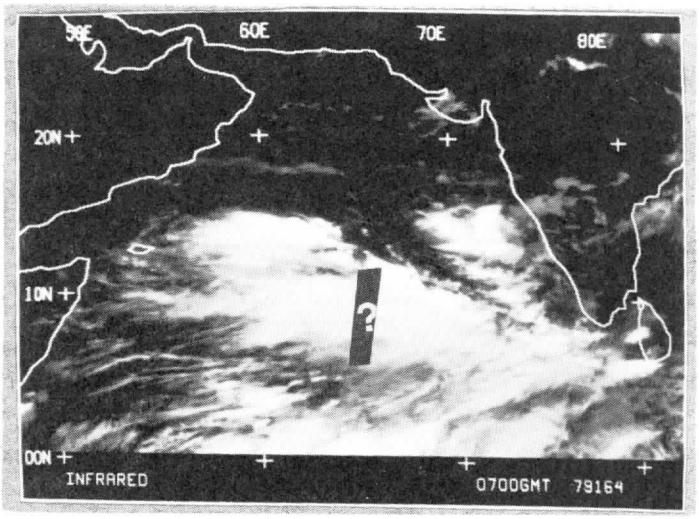
50E
60E
70E
80E
20N
10N
0ON
?
INFRARED
0700GMT 79164

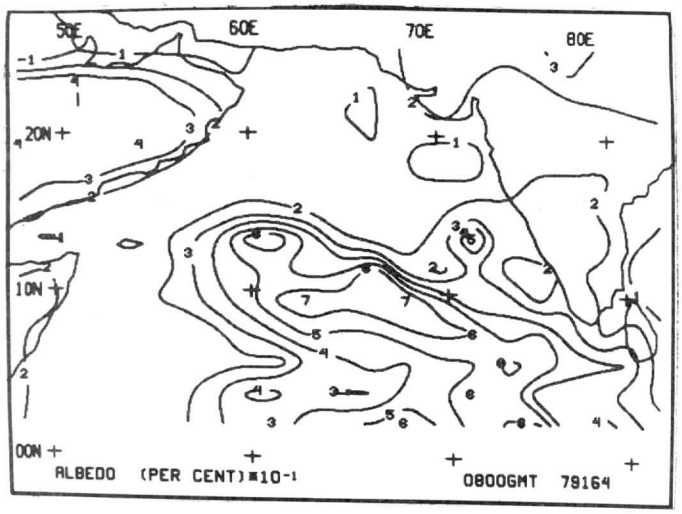
50E
60E
70E
80E
20N
10N
0ON
ALBEDO (PER CENT)×10-1
0800GMT 79164

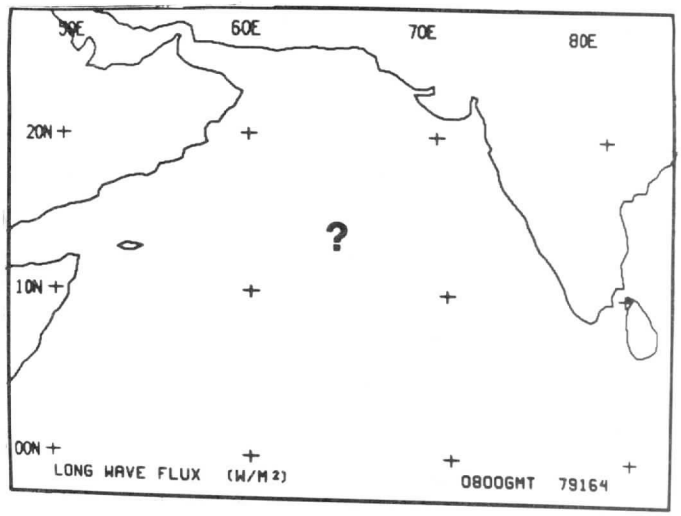
50E
60E
70E
80E
20N
10N
0ON
?
LONG WAVE FLUX (W/M2)
0800GMT 79164

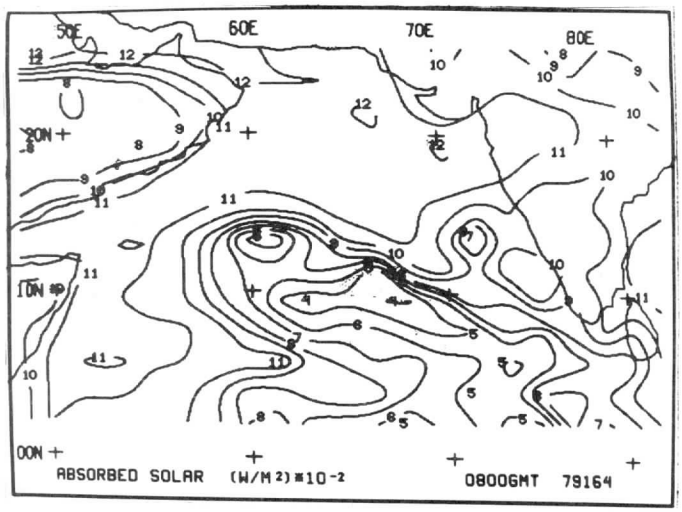
50E
60E
70E
80E
20N
10N
0ON
ABSORBED SOLAR (W/M2)×10-2
0800GMT 79164

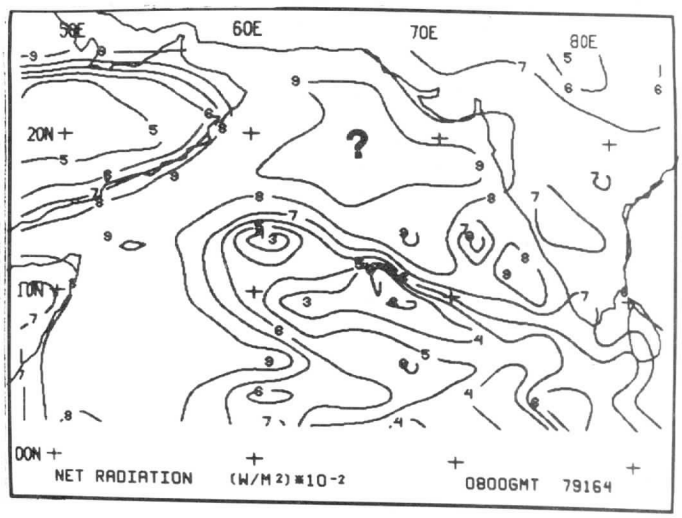
50E
60E
70E
80E
20N
10N
0ON
?
NET RADIATION (W/M2)×10-2
0800GMT 79164

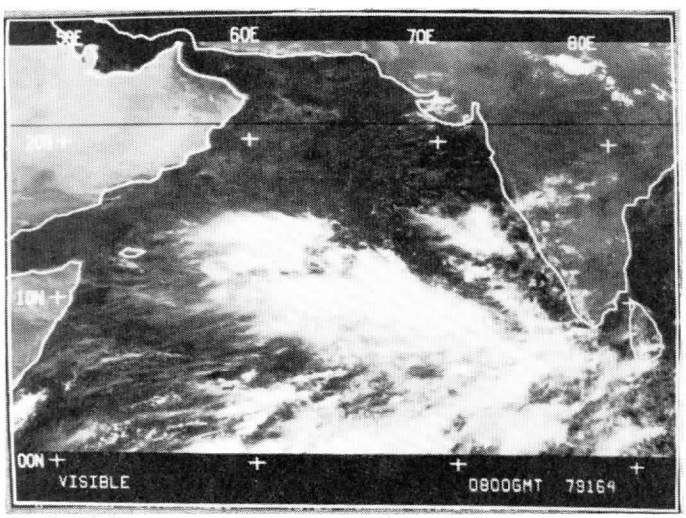
50E
60E
70E
80E
20N
10N
0ON
VISIBLE
0800GMT 79164

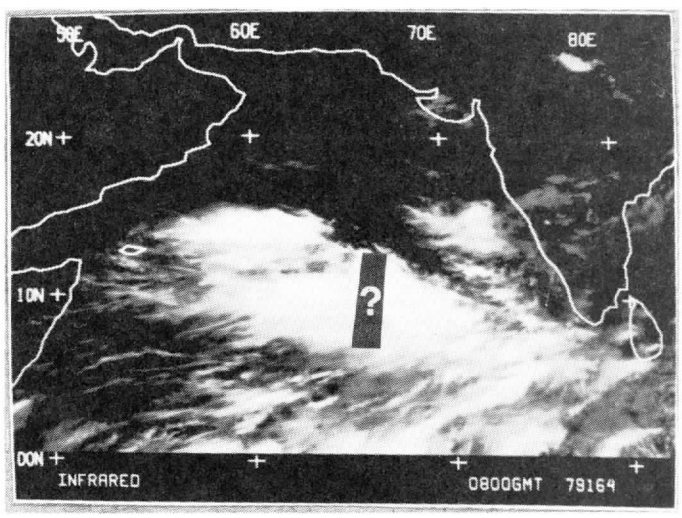
50E
60E
70E
80E
20N
10N
0ON
?
INFRARED
0800GMT 79164

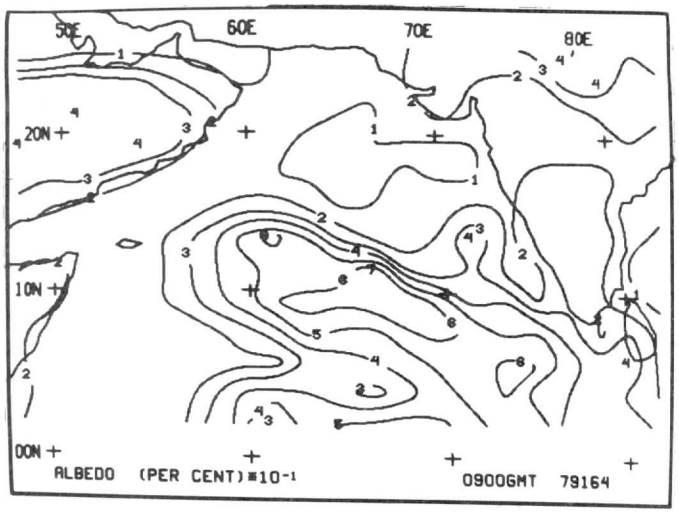
50E
60E
70E
80E
20N
10N
0ON
ALBEDO (PER CENT)*10-1
0900GMT 79164

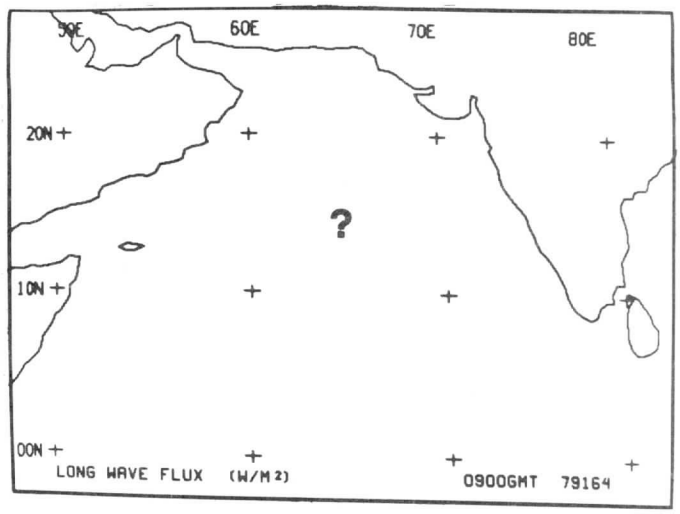
50E
60E
70E
80E
20N
10N
0ON
?
LONG WAVE FLUX (W/M2)
0900GMT 79164

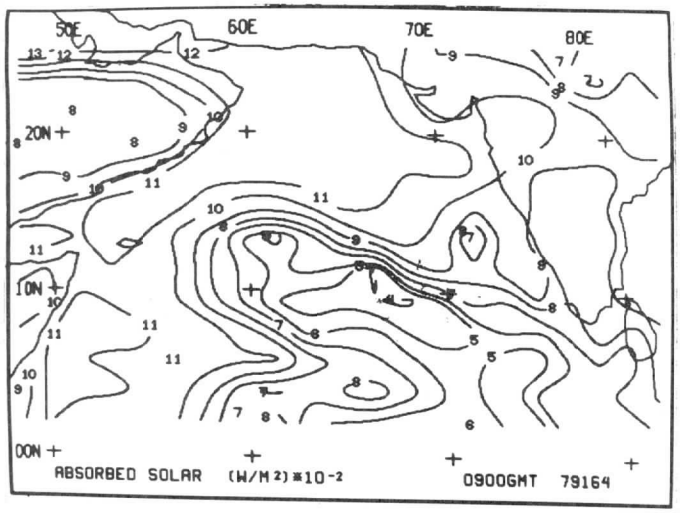
50E
60E
70E
80E
20N
10N
0ON
ABSORBED SOLAR (W/M2)*10-2
0900GMT 79164

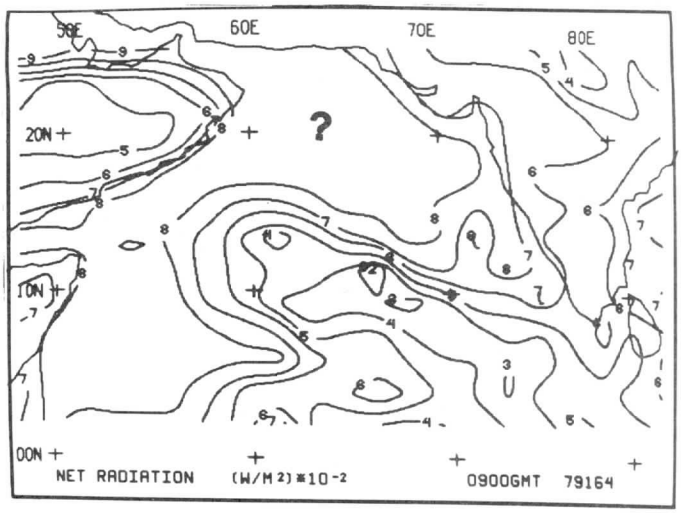
50E
60E
70E
80E
20N
10N
0ON
?
NET RADIATION (W/M2)*10-2
0900GMT 79164

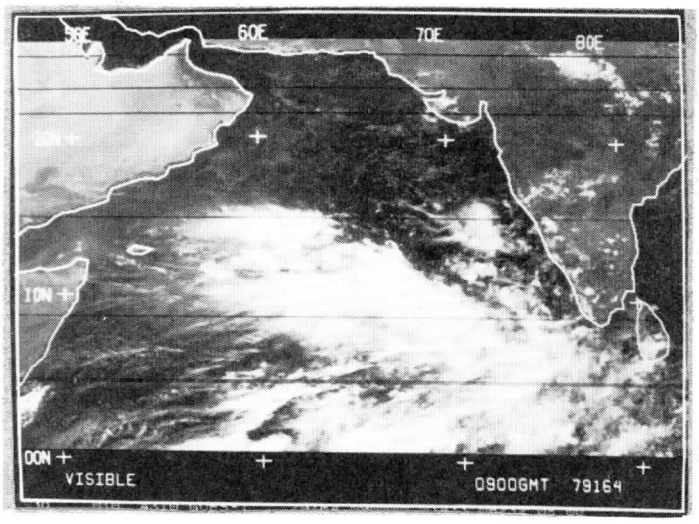
50E
60E
70E
80E
20N
10N
0ON
VISIBLE
0900GMT 79164

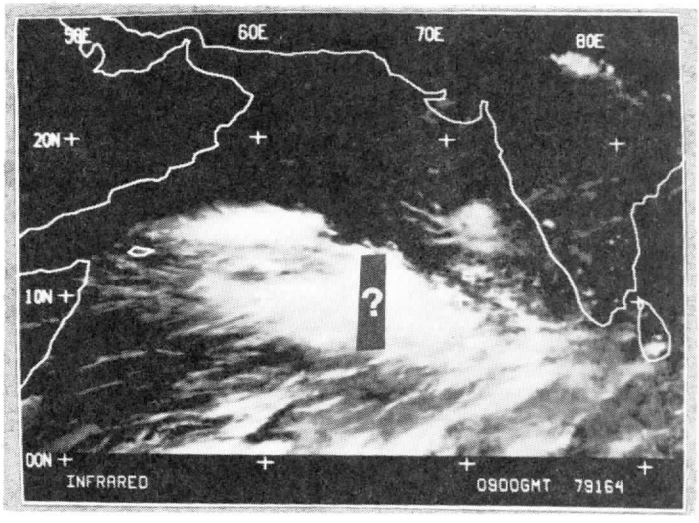
50E
60E
70E
80E
20N
10N
0ON
?
INFRARED
0900GMT 79164

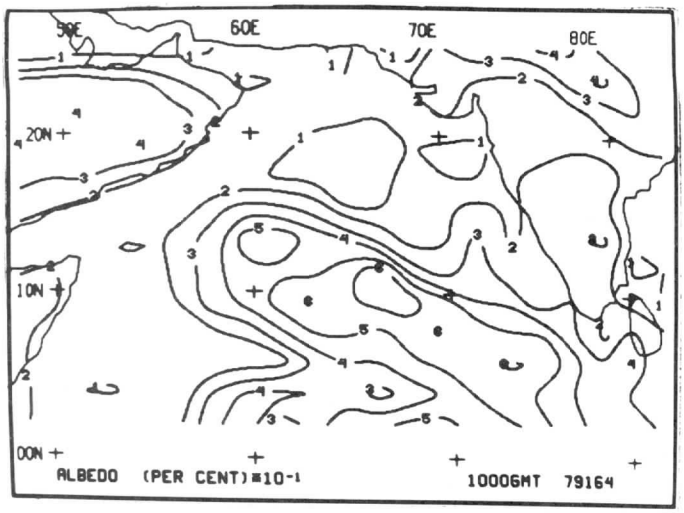
50E
60E
70E
80E
20N
10N
0ON
ALBEDO (PER CENT)×10-1
1000GMT 79164

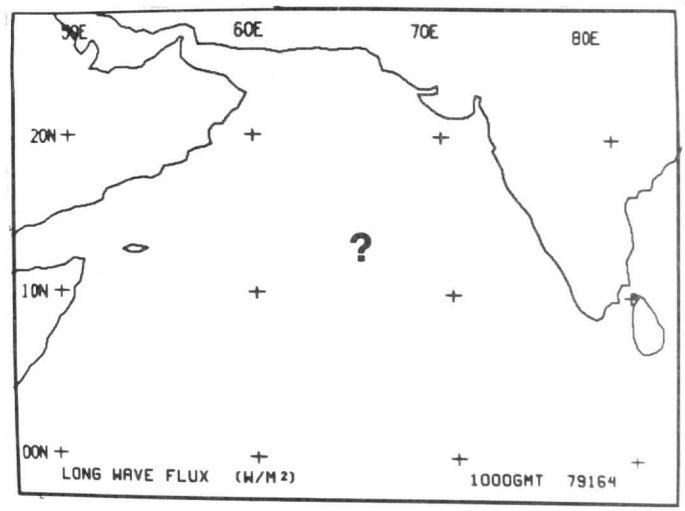
50E
60E
70E
80E
20N
10N
0ON
?
LONG WAVE FLUX (W/M2)
1000GMT 79164

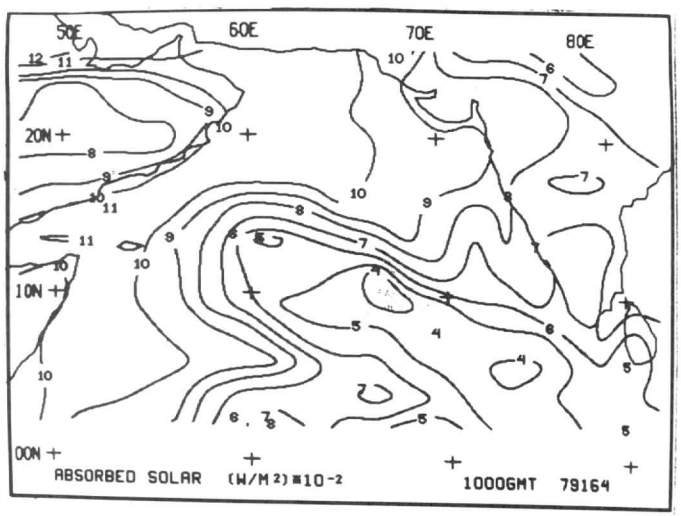
50E
60E
70E
80E
20N
10N
0ON
ABSORBED SOLAR (W/M2)×10-2
1000GMT 79164

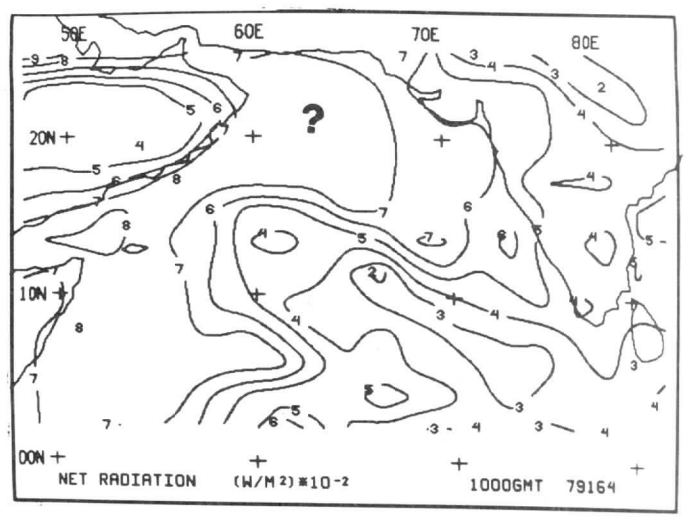
50E
60E
70E
80E
20N
10N
0ON
?
NET RADIATION (W/M2)×10-2
1000GMT 79164

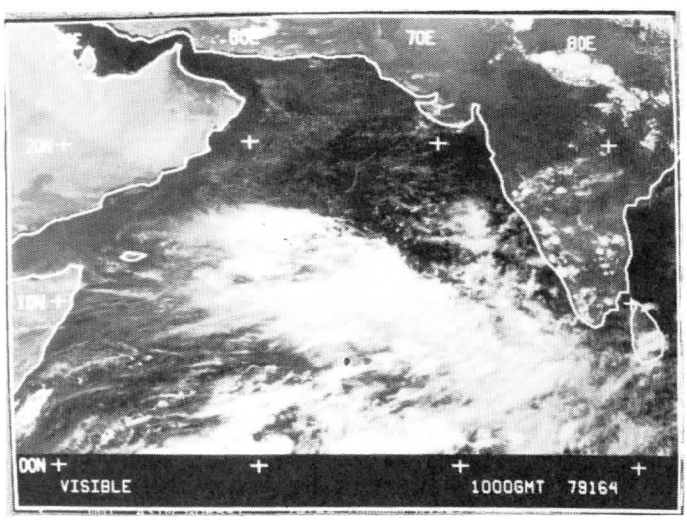
70E
80E
20N
10N
0ON
VISIBLE
1000GMT 79164

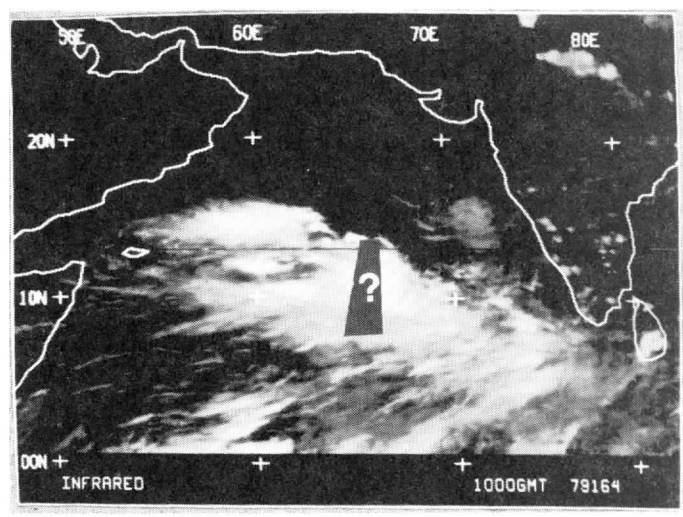
50E
60E
70E
80E
20N
10N
0ON
?
INFRARED
1000GMT 79164

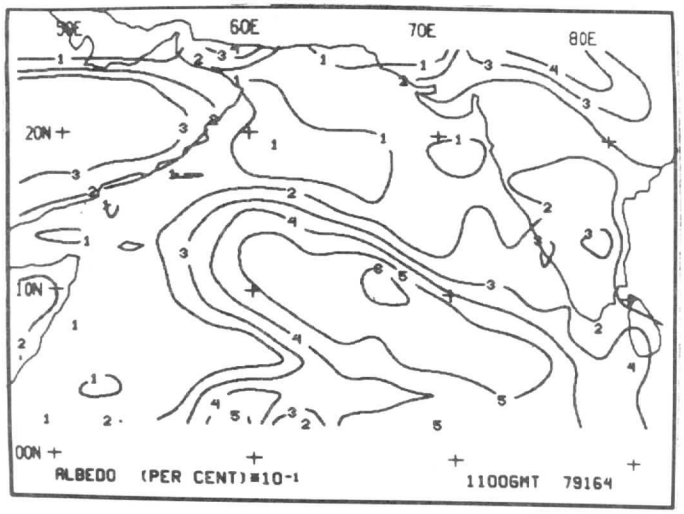
50E
60E
70E
80E
20N
10N
0ON
ALBEDO (PER CENT)*10-1
1100GMT 79164

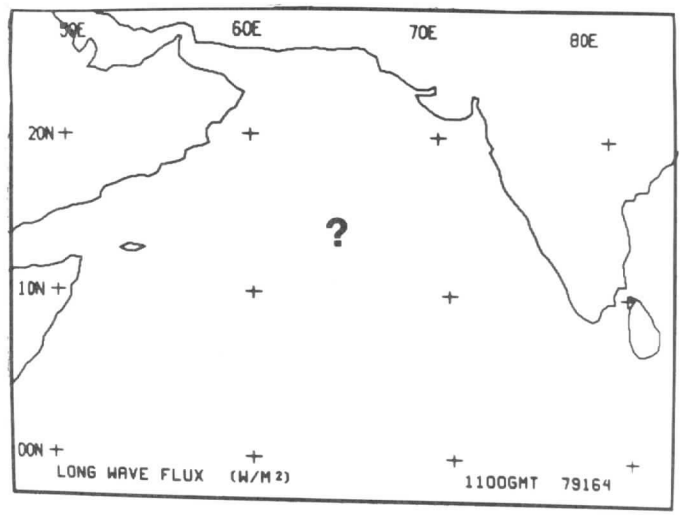
50E
60E
70E
80E
20N
10N
0ON
?
LONG WAVE FLUX (W/M2)
1100GMT 79164

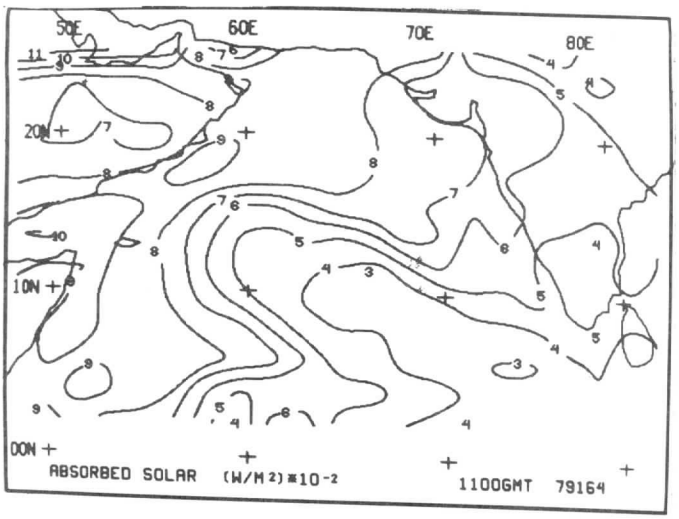
50E
60E
70E
80E
20N
10N
0ON
ABSORBED SOLAR (W/M2)*10-2
1100GMT 79164

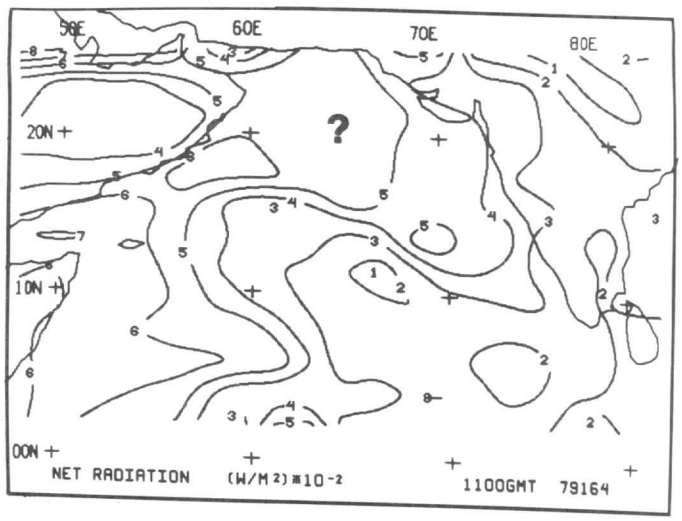
50E
60E
70E
80E
20N
10N
0ON
?
NET RADIATION (W/M2)*10-2
1100GMT 79164

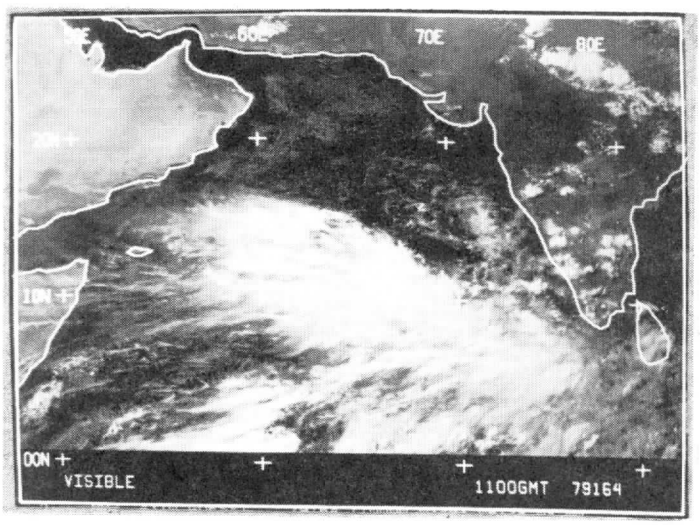
60E
70E
80E
10N
0ON
VISIBLE
1100GMT 79164

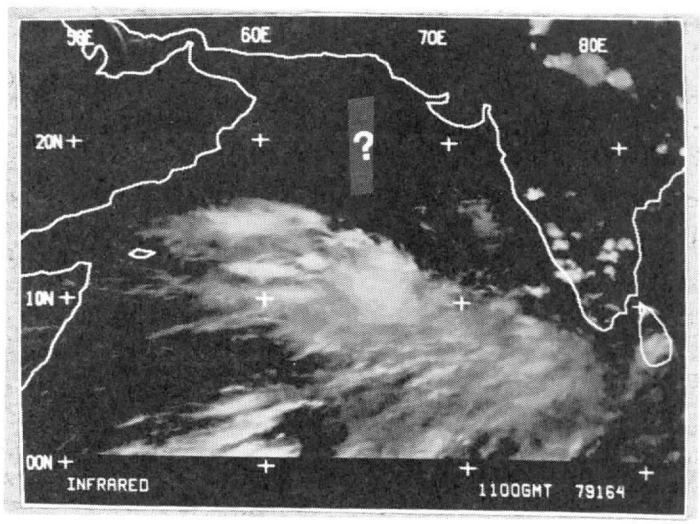
50E
60E
70E
80E
20N
10N
0ON
?
INFRARED
1100GMT 79164

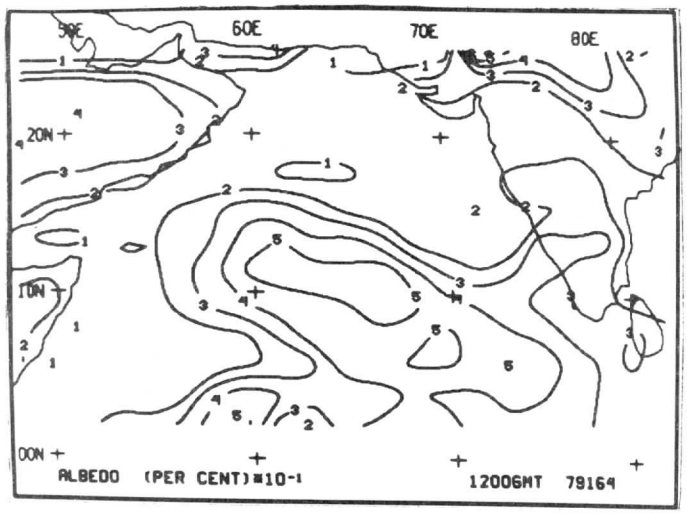
50E
60E
70E
80E
20N
10N
0ON
ALBEDO (PER CENT)*10-1
1200GMT 79164

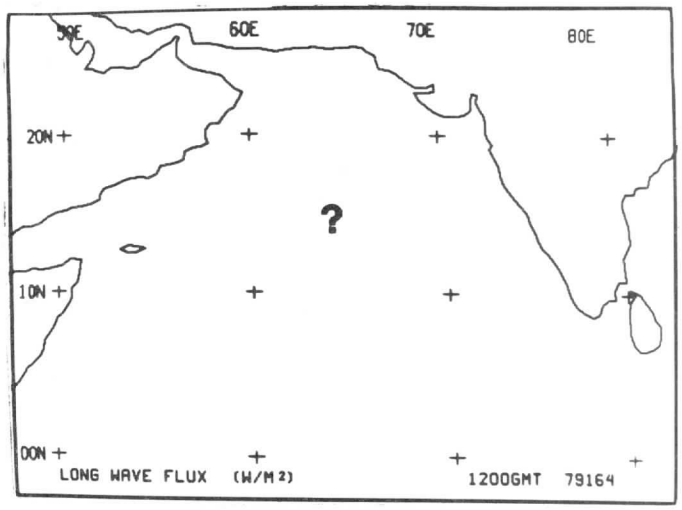
50E
60E
70E
80E
20N
10N
0ON
?
LONG WAVE FLUX (W/M2)
1200GMT 79164

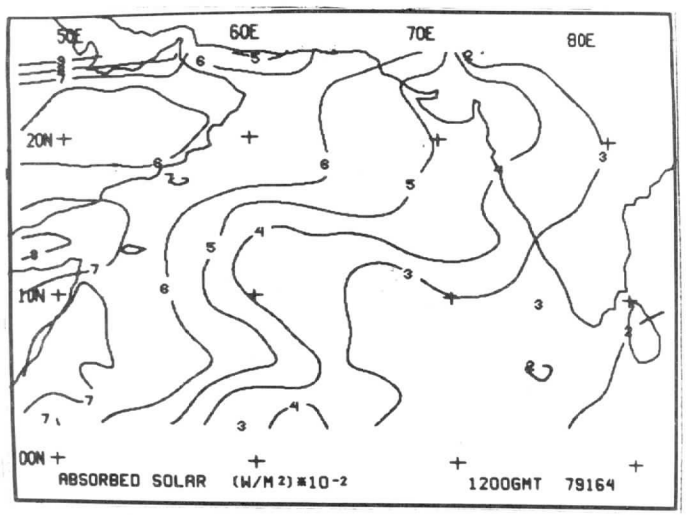
50E
60E
70E
80E
20N
10N
0ON
ABSORBED SOLAR (W/M2)*10-2
1200GMT 79164

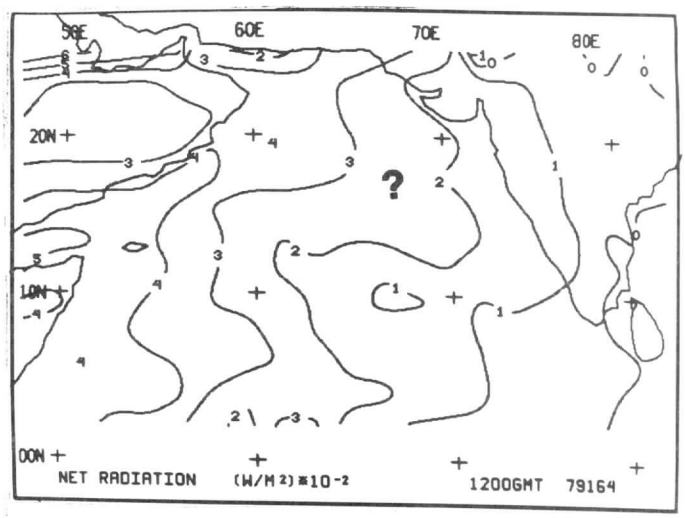
50E
60E
70E
80E
20N
10N
0ON
?
NET RADIATION (W/M2)*10-2
1200GMT 79164

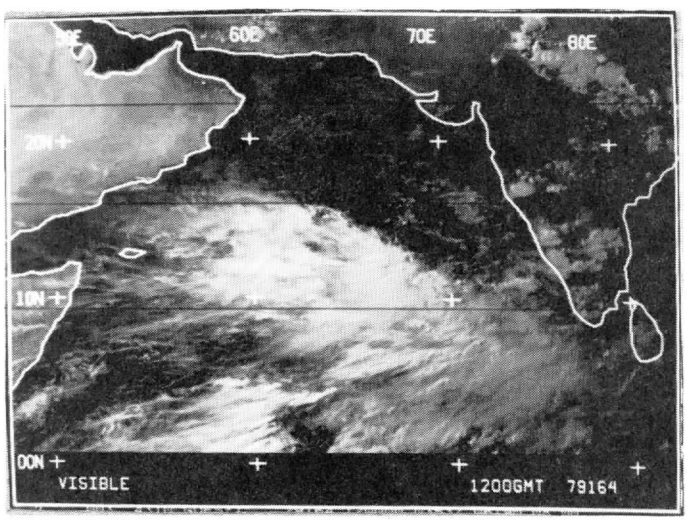
50E
60E
70E
80E
20N
10N
0ON
VISIBLE
1200GMT 79164

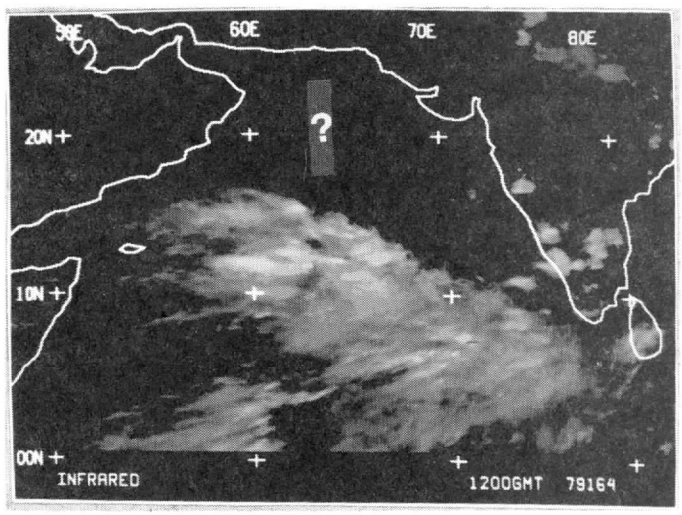
50E
60E
70E
80E
20N
10N
0ON
?
INFRARED
1200GMT 79164

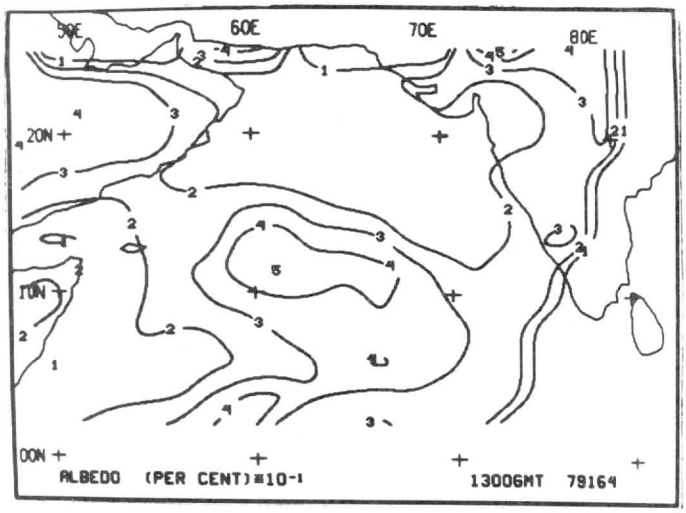
50E
60E
70E
80E
20N
10N
0ON
ALBEDO (PER CENT)*10-1
1300GMT 79164

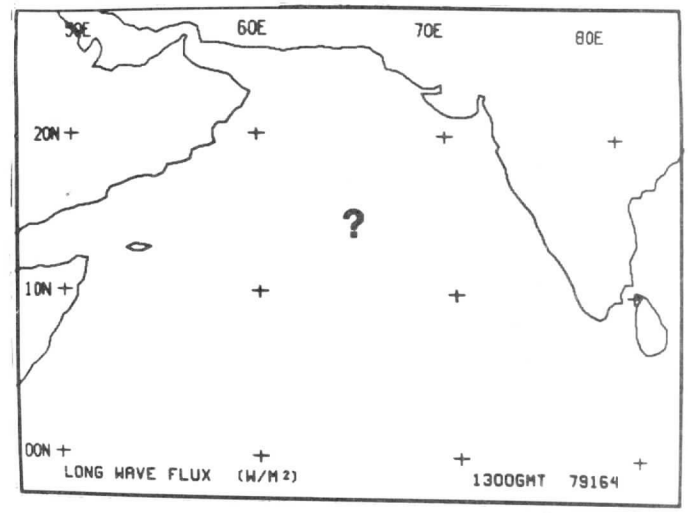
50E
60E
70E
80E
20N
10N
0ON
?
LONG WAVE FLUX (W/M2)
1300GMT 79164

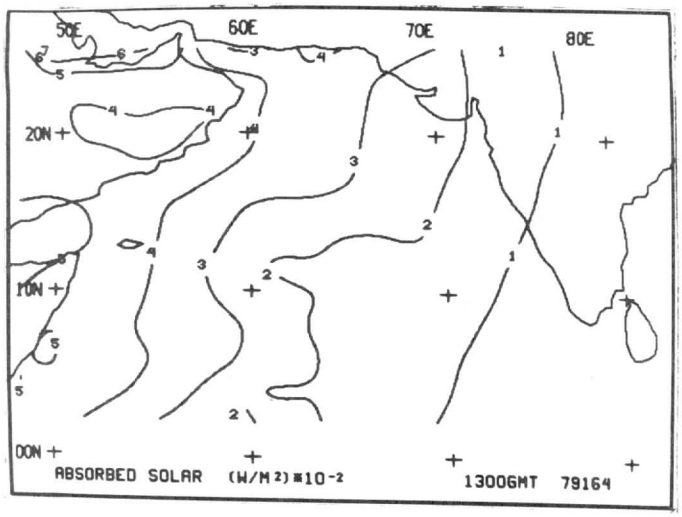
50E
60E
70E
80E
20N
10N
0ON
ABSORBED SOLAR (W/M2)*10-2
1300GMT 79164

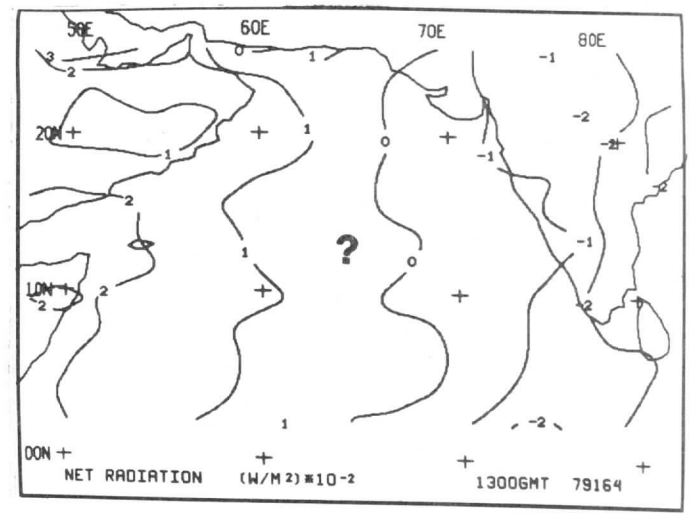
50E
60E
70E
80E
20N
10N
0ON
?
NET RADIATION (W/M2)*10-2
1300GMT 79164

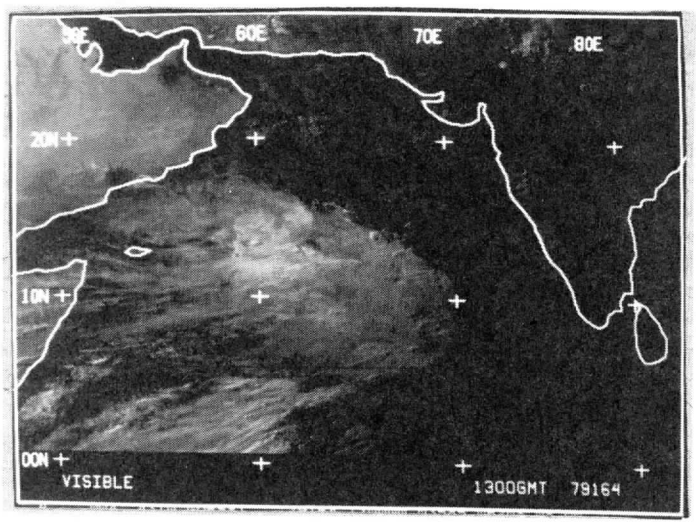
50E
60E
70E
80E
20N
10N
0ON
VISIBLE
1300GMT 79164

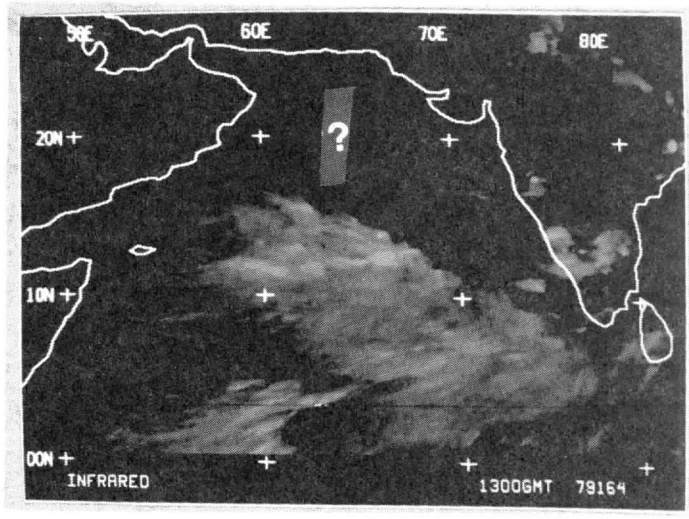
50E
60E
70E
80E
20N
10N
0ON
?
INFRARED
1300GMT 79164

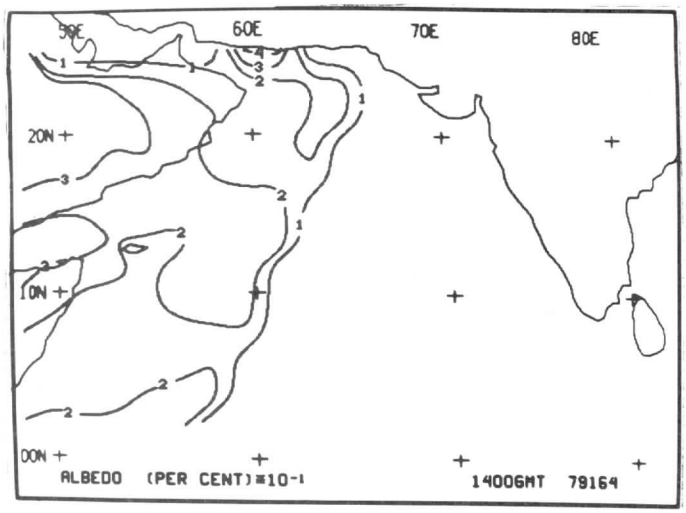
50E
60E
70E
80E
20N
10N
0ON
ALBEDO (PER CENT)*10-1
1400GMT 79164

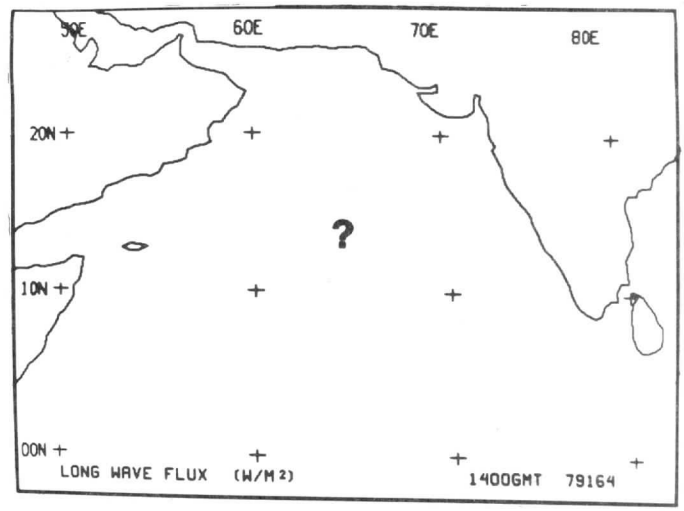
50E
60E
70E
80E
20N
10N
0ON
?
LONG WAVE FLUX (W/M2)
1400GMT 79164

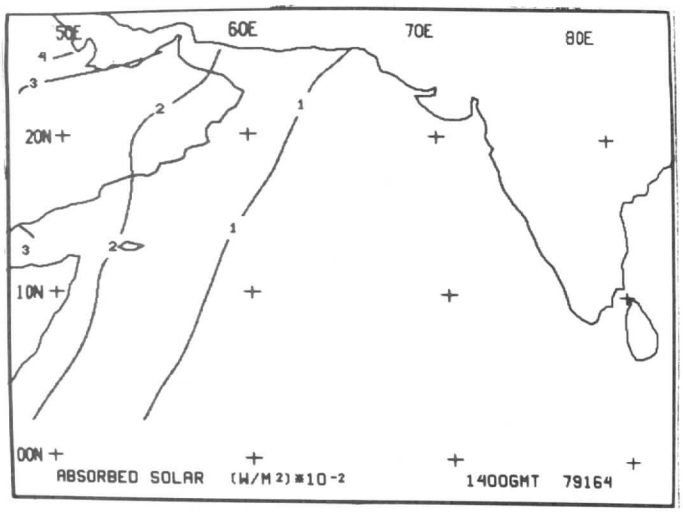
50E
60E
70E
80E
20N
10N
0ON
ABSORBED SOLAR (W/M2)*10-2
1400GMT 79164

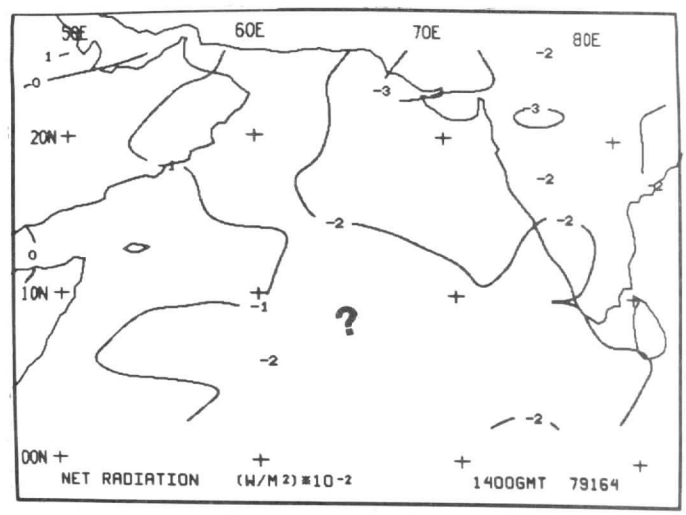
50E
60E
70E
80E
20N
10N
0ON
?
NET RADIATION (W/M2)*10-2
1400GMT 79164

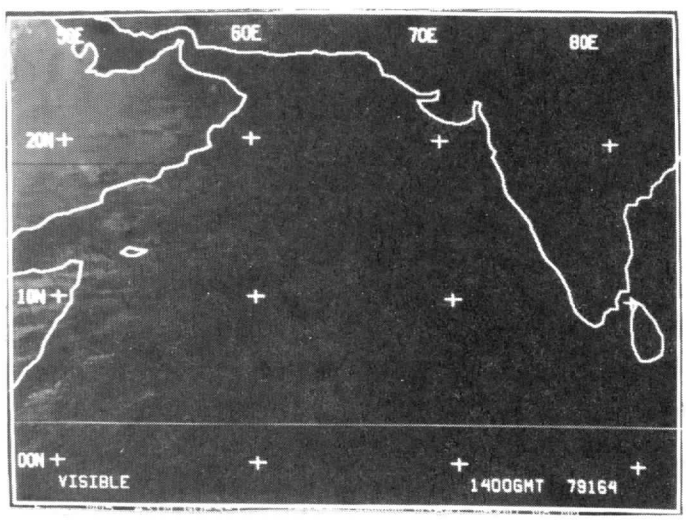
50E
60E
70E
80E
20N
10N
0ON
VISIBLE
1400GMT 79164

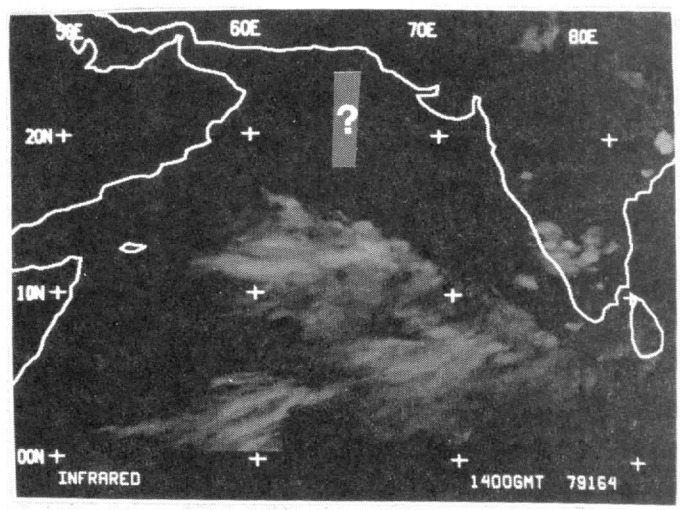
50E
60E
70E
80E
20N
10N
0ON
?
INFRARED
1400GMT 79164

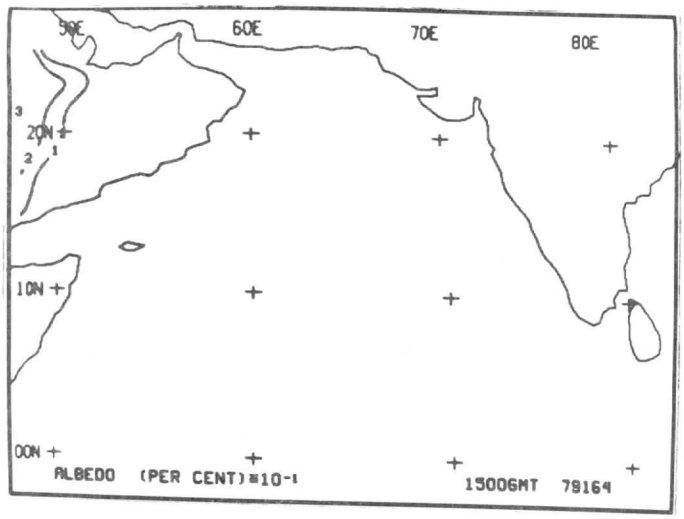
50E
60E
70E
80E
20N
10N
0ON
ALBEDO (PER CENT)=10-1
1500GMT 79164

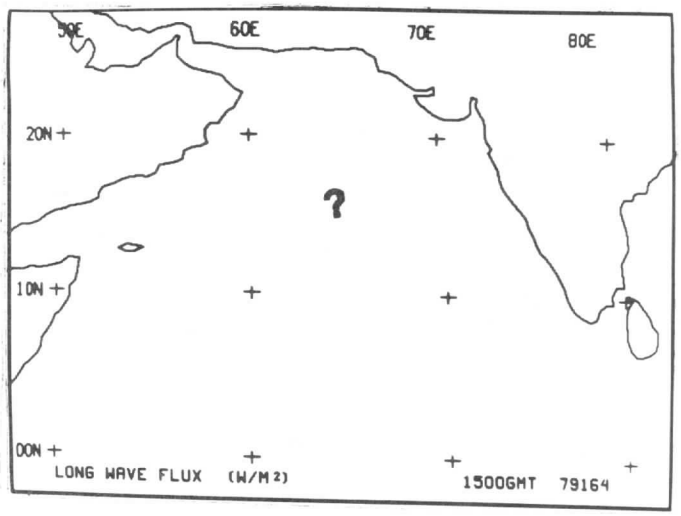
50E
60E
70E
80E
20N
10N
0ON
?
LONG WAVE FLUX (W/M2)
1500GMT 79164

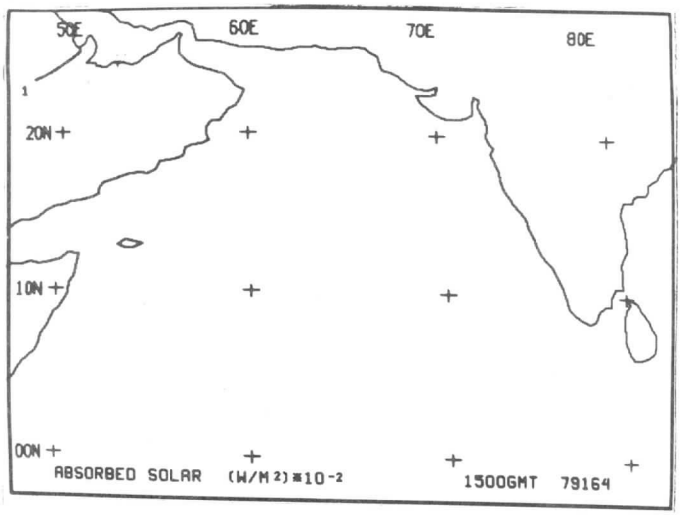
50E
60E
70E
80E
20N
10N
0ON
ABSORBED SOLAR (W/M2)=10-2
1500GMT 79164

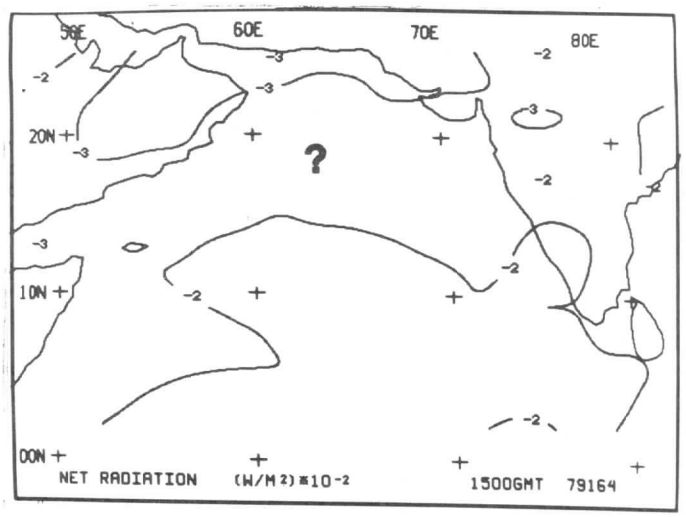
50E
60E
70E
80E
20N
10N
0ON
?
NET RADIATION (W/M2)=10-2
1500GMT 79164

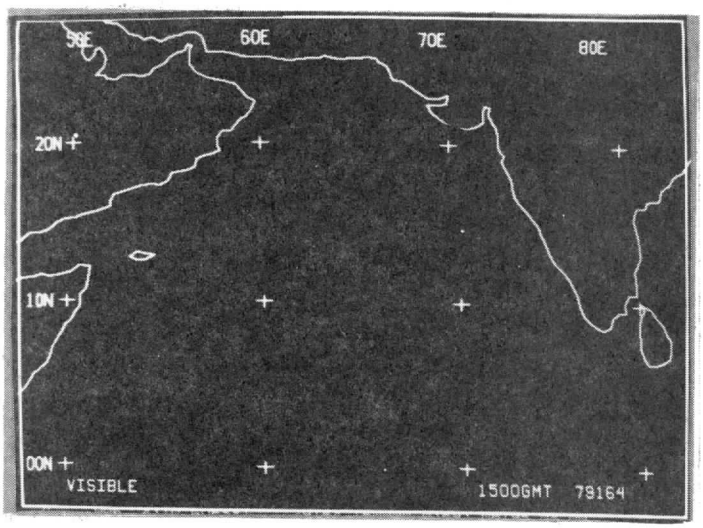
50E
60E
70E
80E
20N
10N
0ON
VISIBLE
1500GMT 79164

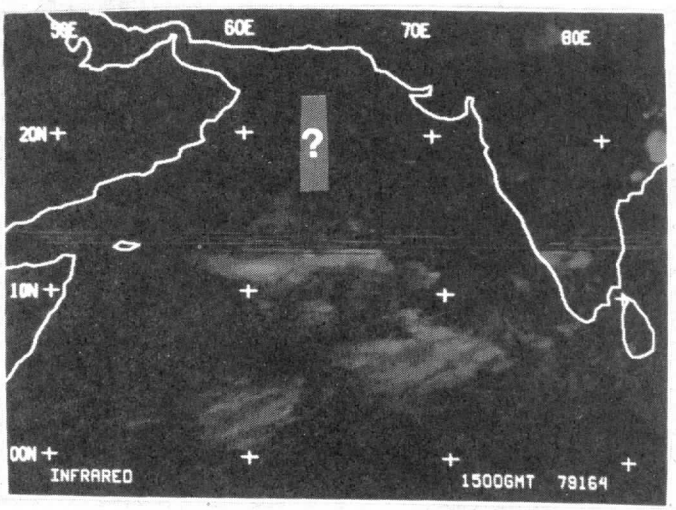
50E
60E
70E
80E
20N
10N
0ON
?
INFRARED
1500GMT 79164

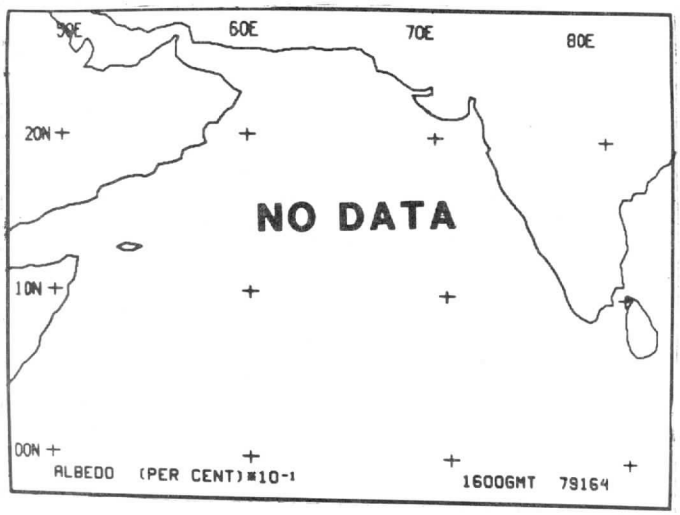
50E
60E
70E
80E
20N
10N
0ON
NO DATA
ALBEDO (PER CENT)*10-1
1600GMT 79164

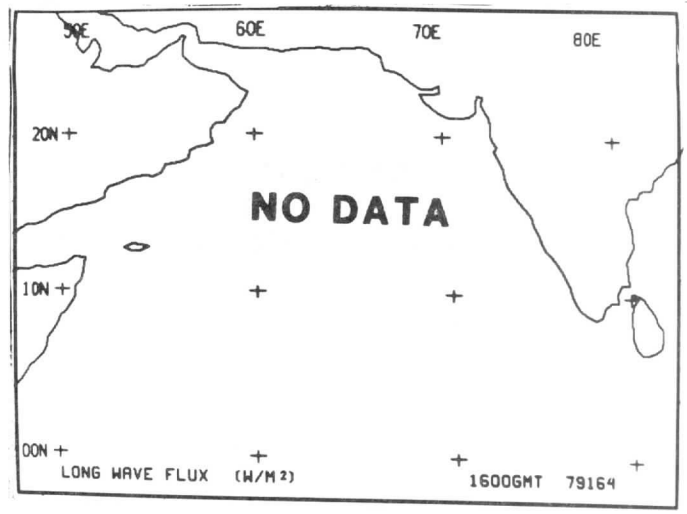
50E
60E
70E
80E
20N
10N
0ON
NO DATA
LONG WAVE FLUX (W/M2)
1600GMT 79164

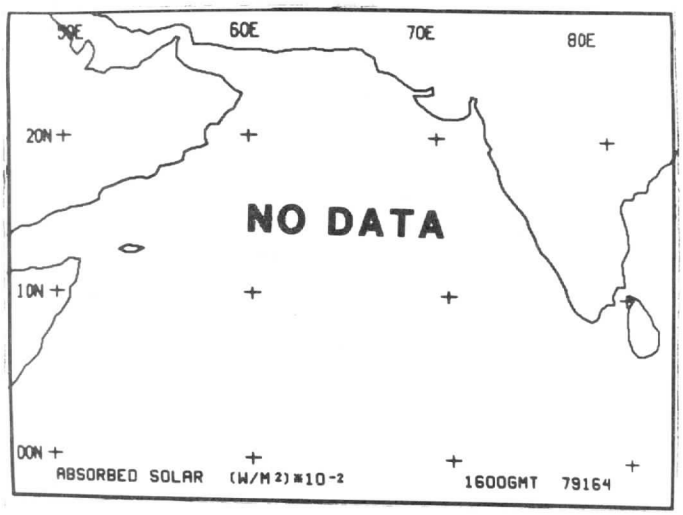
50E
60E
70E
80E
20N
10N
0ON
NO DATA
ABSORBED SOLAR (W/M2)*10-2
1600GMT 79164

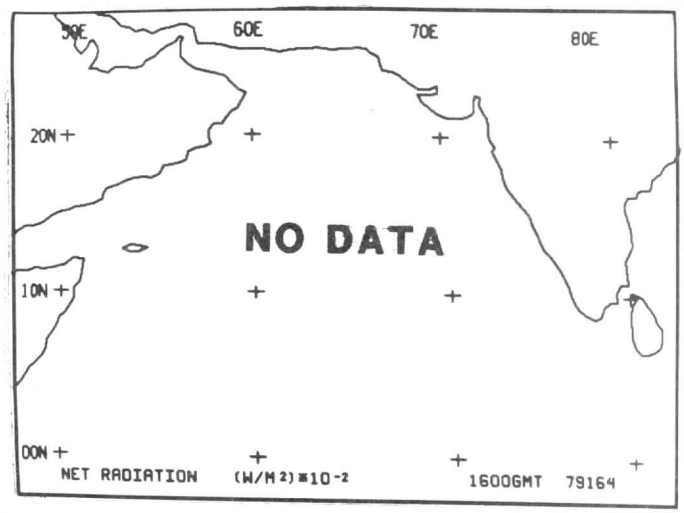
50E
60E
70E
80E
20N
10N
0ON
NO DATA
NET RADIATION (W/M2)*10-2
1600GMT 79164

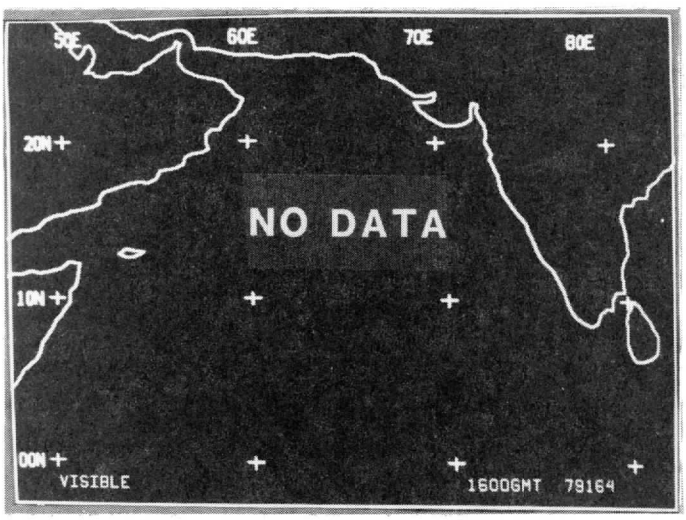
50E
60E
70E
80E
20N
10N
0ON
NO DATA
VISIBLE
1600GMT 79164

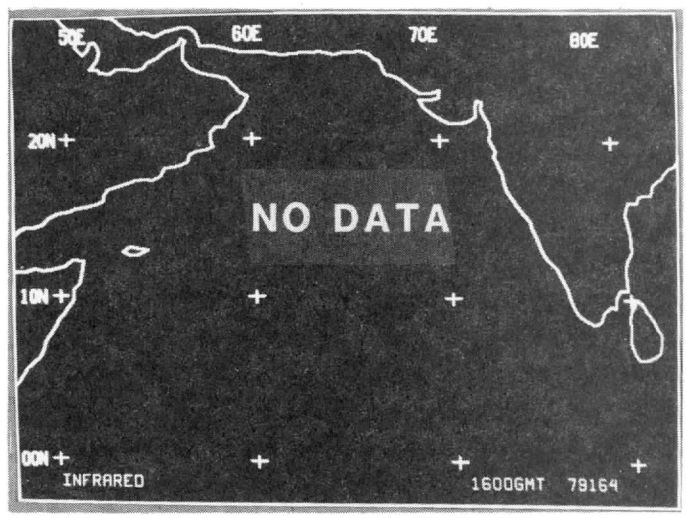
50E
60E
70E
80E
20N
10N
0ON
NO DATA
INFRARED
1600GMT 79164

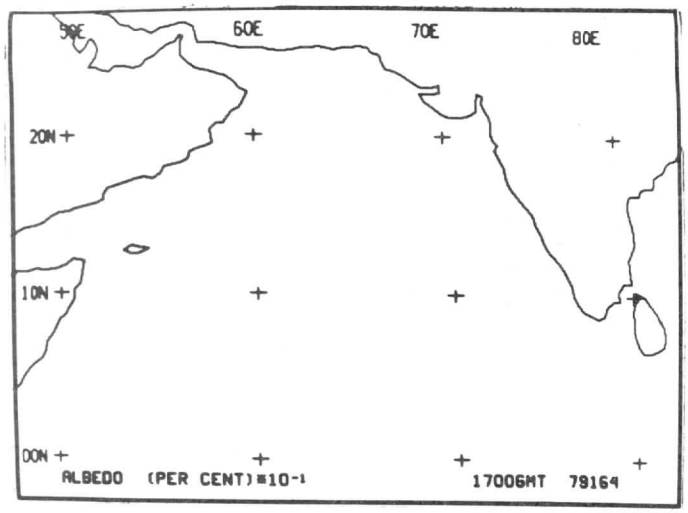
50E
60E
70E
80E
20N
10N
00N
ALBEDO (PER CENT)×10⁻¹
1700GMT 79164

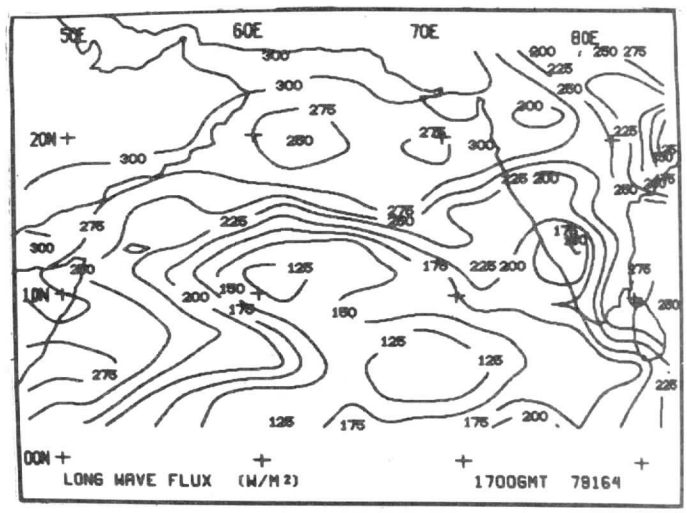
50E
60E
70E
80E
20N
10N
00N
LONG WAVE FLUX (W/M²)
1700GMT 79164

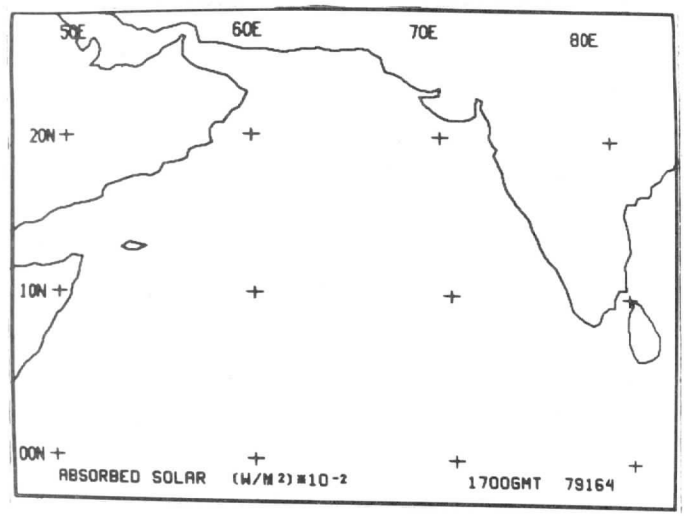
50E
60E
70E
80E
20N
10N
00N
ABSORBED SOLAR (W/M²)×10⁻²
1700GMT 79164

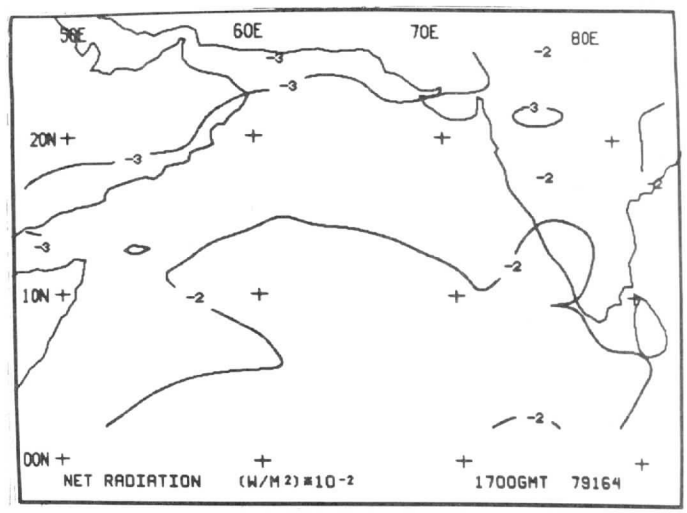
50E
60E
70E
80E
20N
10N
00N
NET RADIATION (W/M²)×10⁻²
1700GMT 79164

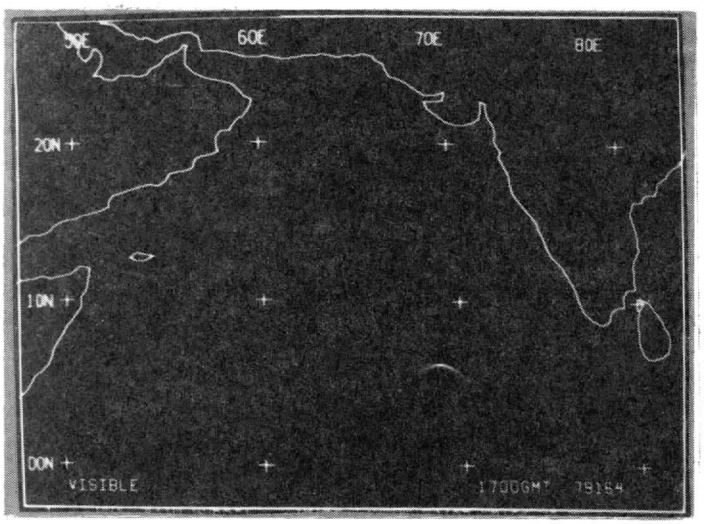
50E
60E
70E
80E
20N
10N
00N
VISIBLE
1700GMT 79164

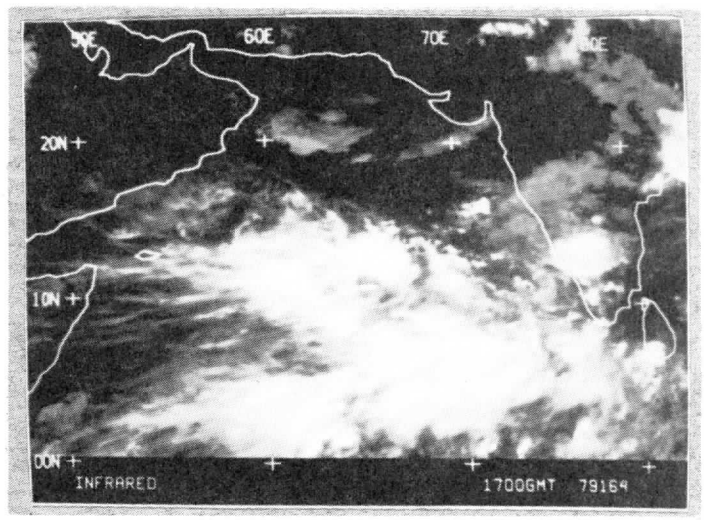
50E
60E
70E
20N
10N
00N
INFRARED
1700GMT 79164

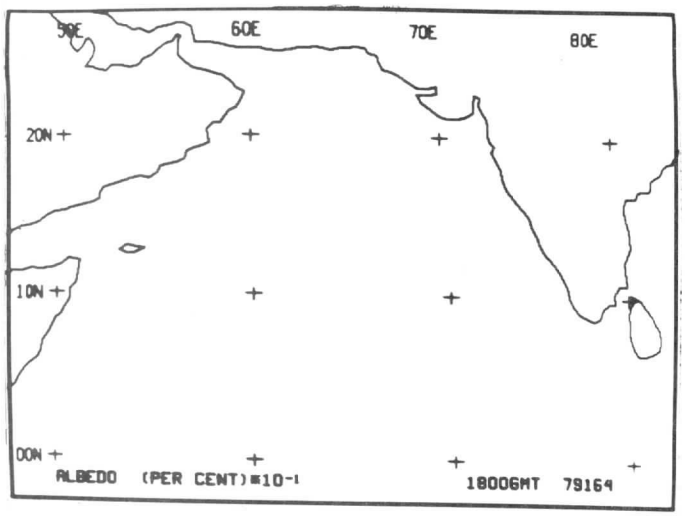
50E
60E
70E
80E
20N
10N
0ON
ALBEDO (PER CENT)*10-1
1800GMT 79164

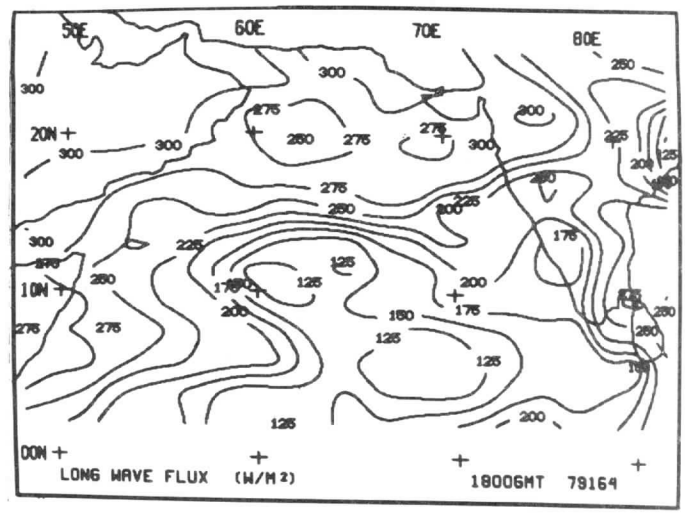
50E
60E
70E
80E
20N
10N
0ON
LONG WAVE FLUX (W/M2)
1800GMT 79164

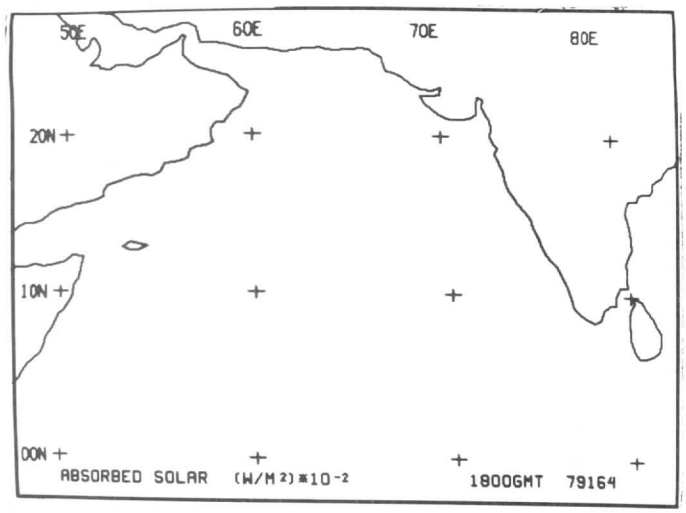
50E
60E
70E
80E
20N
10N
0ON
ABSORBED SOLAR (W/M2)*10-2
1800GMT 79164

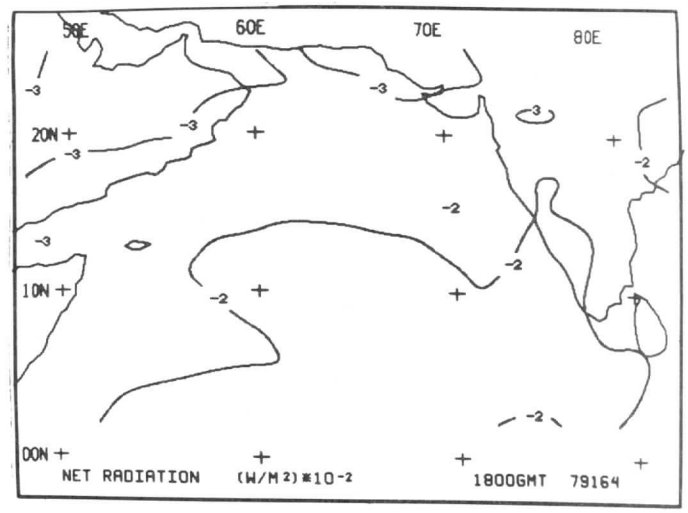
50E
60E
70E
80E
20N
10N
0ON
NET RADIATION (W/M2)*10-2
1800GMT 79164

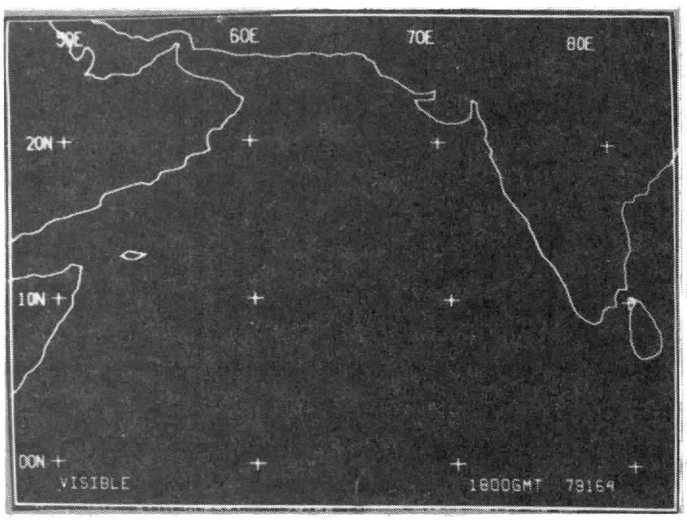
50E
60E
70E
80E
20N
10N
0ON
VISIBLE
1800GMT 79164

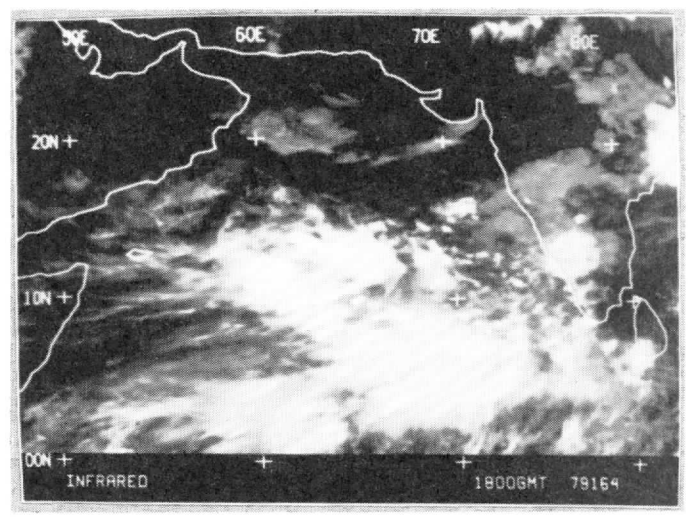
50E
60E
70E
80E
20N
10N
0ON
INFRARED
1800GMT 79164

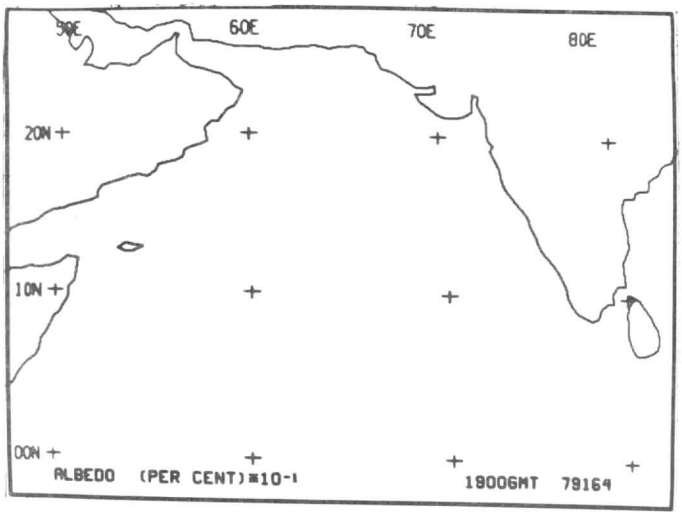
50E
60E
70E
80E
20N
10N
0ON
ALBEDO (PER CENT)*10-1
1900GMT 79164

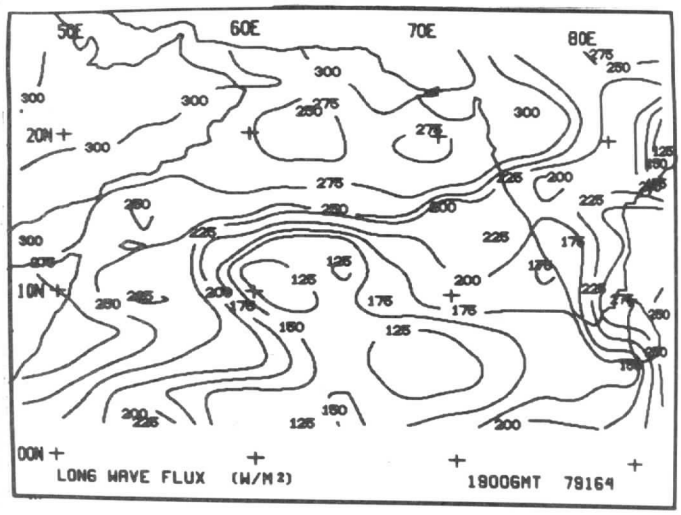
50E
60E
70E
80E
20N
10N
0ON
LONG WAVE FLUX (W/M2)
1900GMT 79164

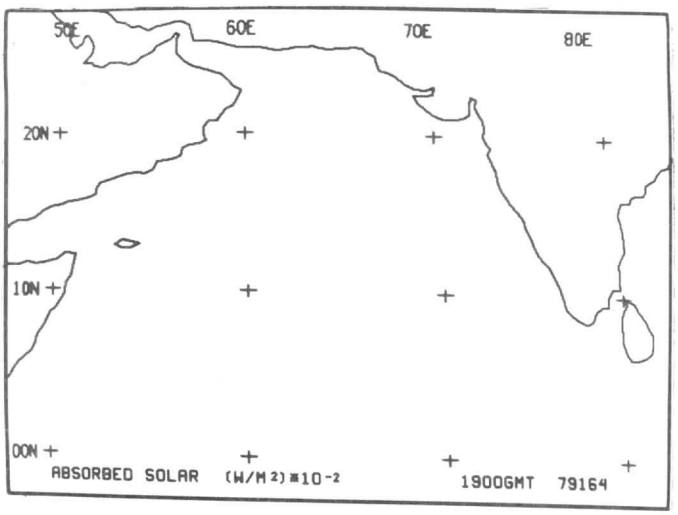
50E
60E
70E
80E
20N
10N
0ON
ABSORBED SOLAR (W/M2)*10-2
1900GMT 79164

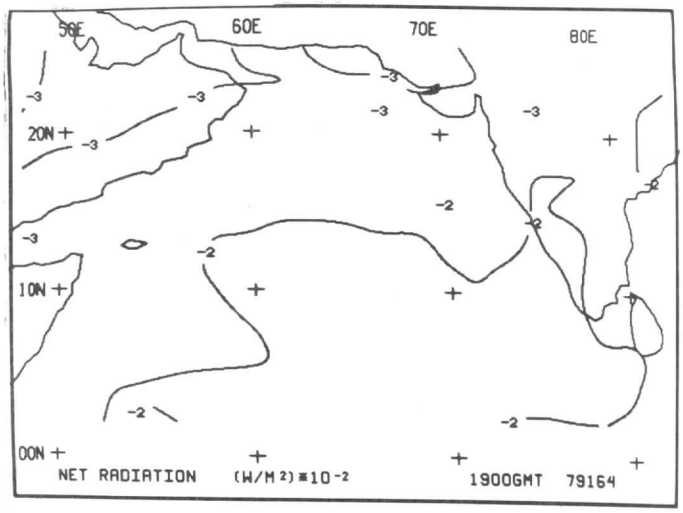
50E
60E
70E
80E
20N
10N
0ON
NET RADIATION (W/M2)*10-2
1900GMT 79164

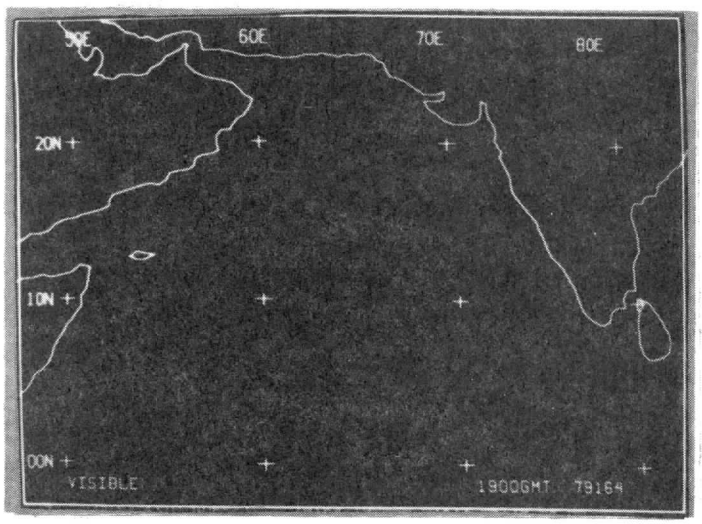
50E
60E
70E
80E
20N
10N
0ON
VISIBLE
1900GMT 79164

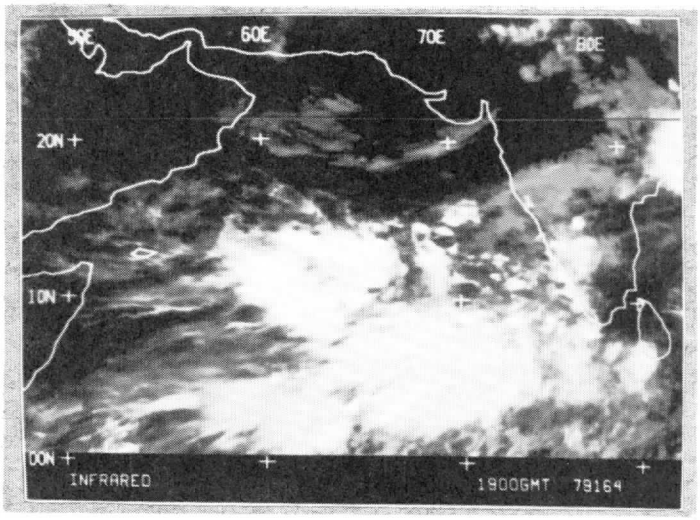
50E
60E
70E
80E
20N
10N
0ON
INFRARED
1900GMT 79164

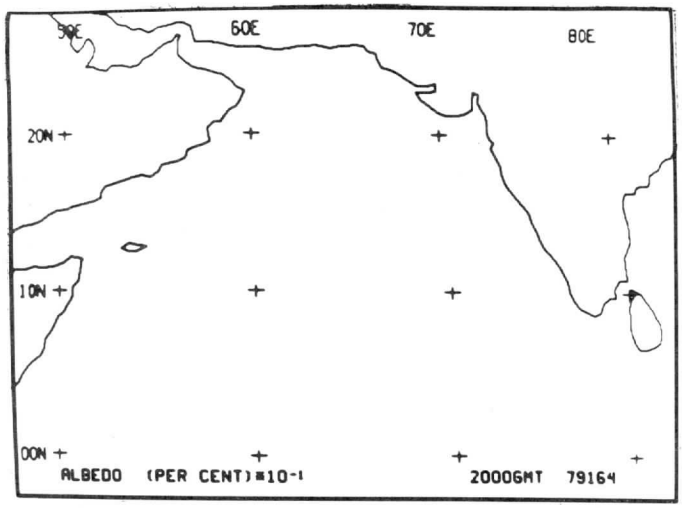
50E
60E
70E
80E
20N
10N
00N
ALBEDO (PER CENT)*10-1
2000GMT 79164

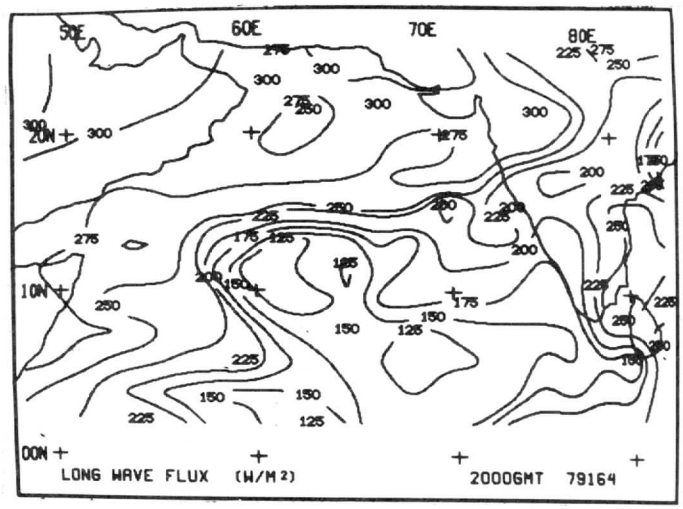
50E
60E
70E
80E
20N
10N
00N
LONG WAVE FLUX (W/M2)
2000GMT 79164

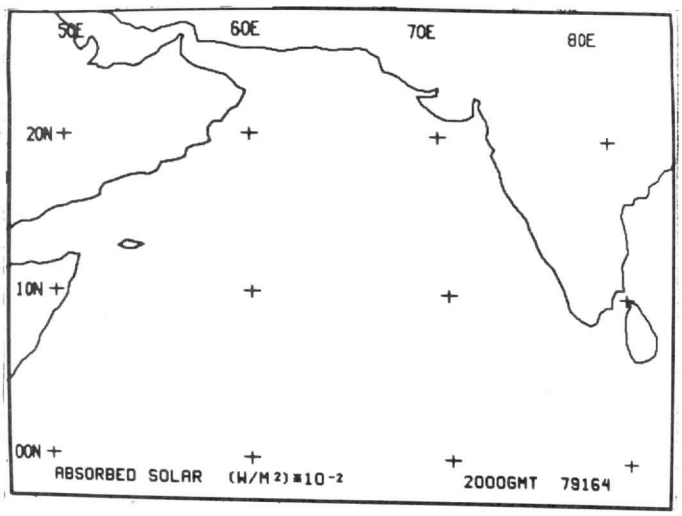
50E
60E
70E
80E
20N
10N
00N
ABSORBED SOLAR (W/M2)*10-2
2000GMT 79164

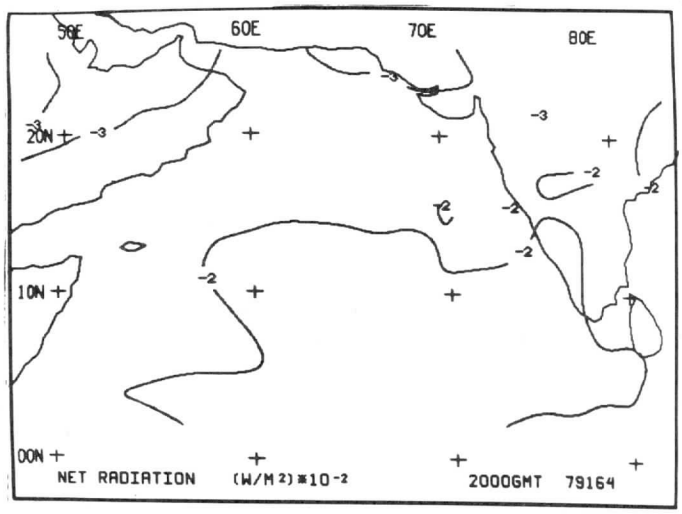
50E
60E
70E
80E
20N
10N
00N
NET RADIATION (W/M2)*10-2
2000GMT 79164

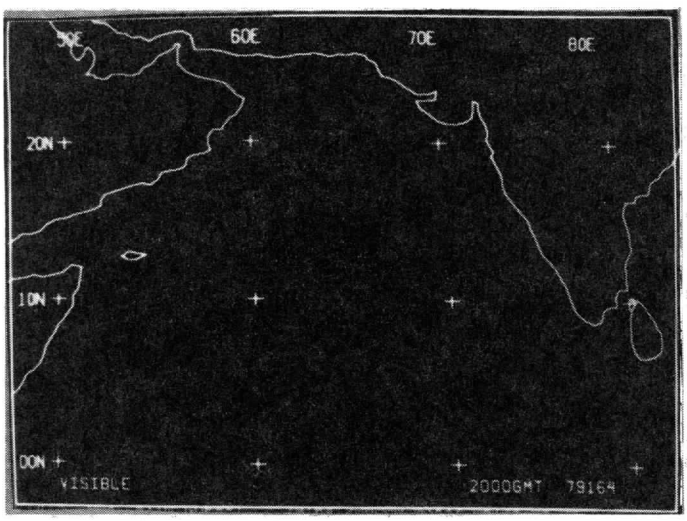
50E
60E
70E
80E
20N
10N
00N
VISIBLE
2000GMT 79164

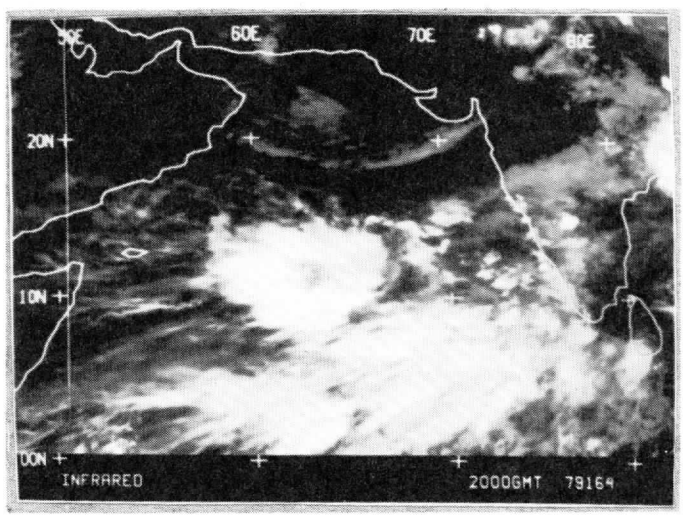
50E
60E
70E
80E
20N
10N
00N
INFRARED
2000GMT 79164

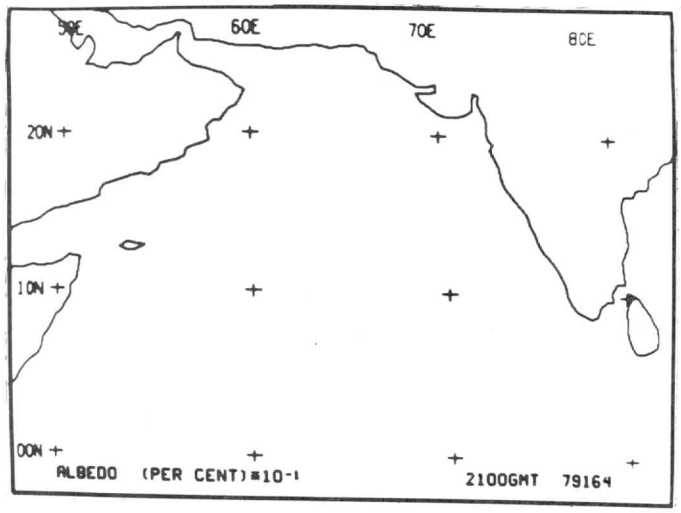
50E
60E
70E
80E
20N
10N
00N
ALBEDO (PER CENT)*10-1
2100GMT 79164

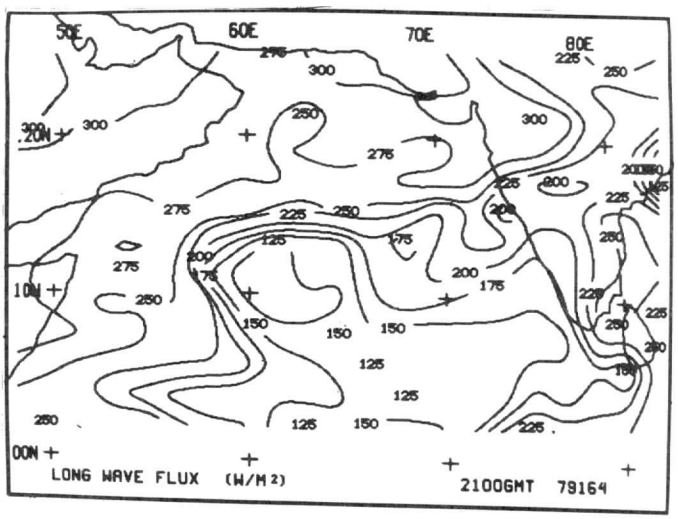
50E
60E
70E
80E
20N
10N
00N
LONG WAVE FLUX (W/M2)
2100GMT 79164

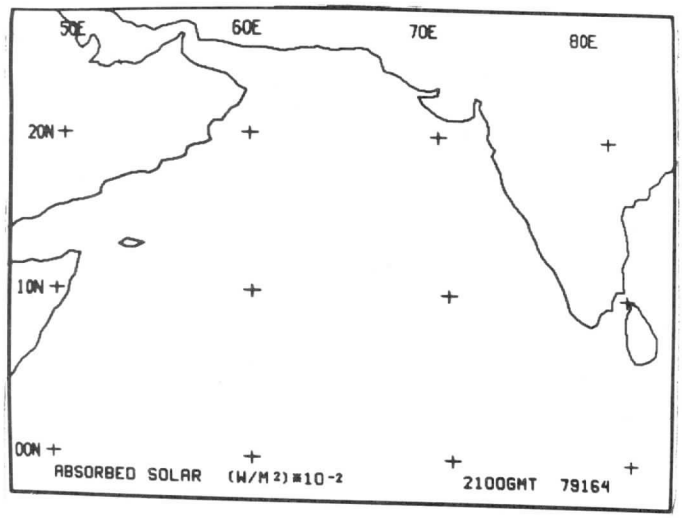
50E
60E
70E
80E
20N
10N
00N
ABSORBED SOLAR (W/M2)*10-2
2100GMT 79164

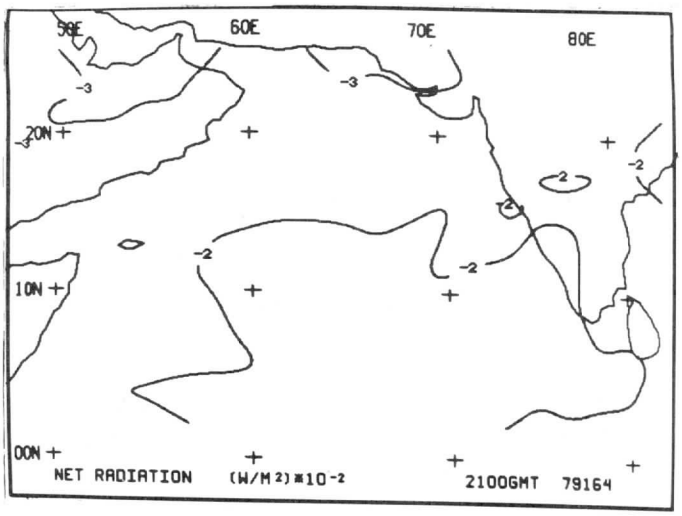
50E
60E
70E
80E
20N
10N
00N
NET RADIATION (W/M2)*10-2
2100GMT 79164

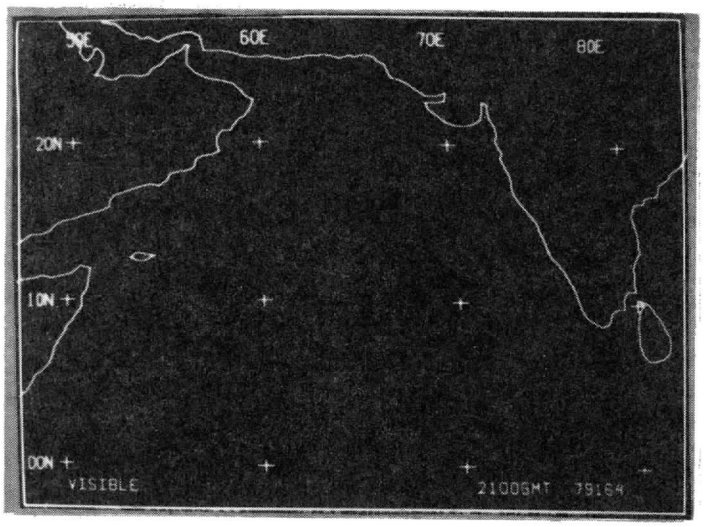
50E
60E
70E
80E
20N
10N
00N
VISIBLE
2100GMT 79164

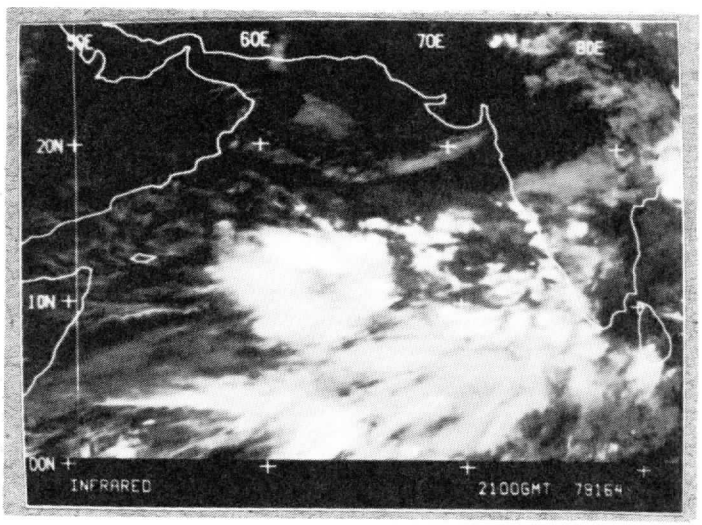
50E
60E
70E
80E
20N
10N
00N
INFRARED
2100GMT 79164

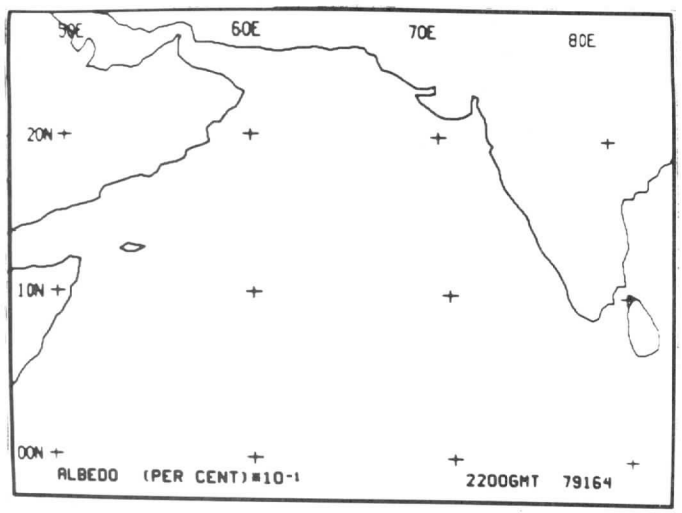
50E
60E
70E
80E
20N
10N
0ON
ALBEDO (PER CENT)*10-1
2200GMT 79164

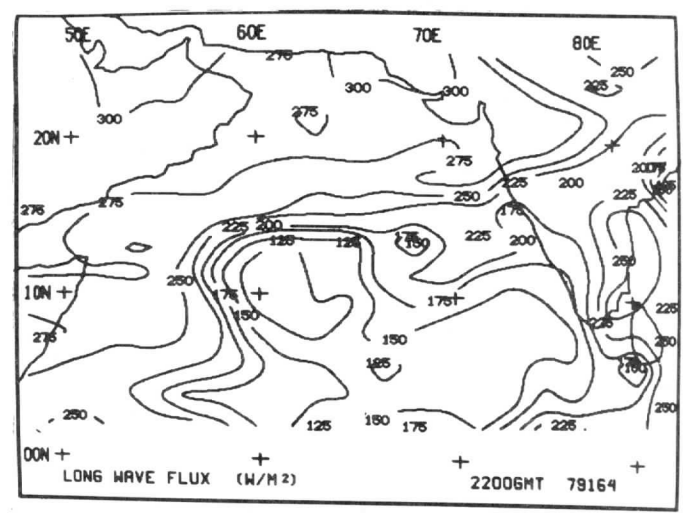
50E
60E
70E
80E
20N
10N
0ON
LONG WAVE FLUX (W/M2)
2200GMT 79164

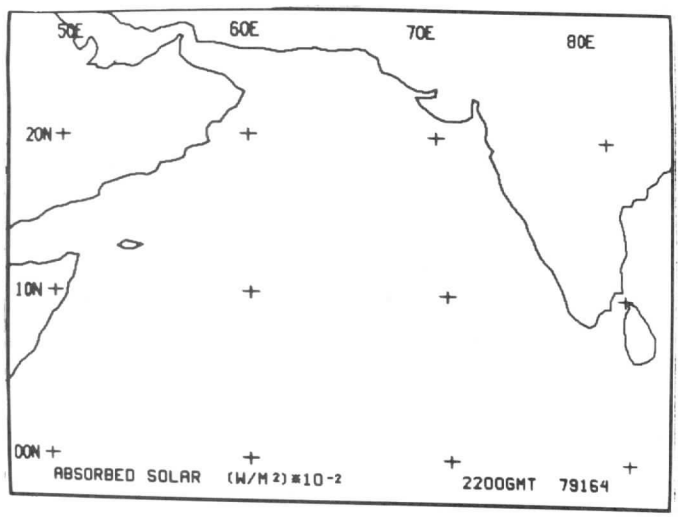
50E
60E
70E
80E
20N
10N
0ON
ABSORBED SOLAR (W/M2)*10-2
2200GMT 79164

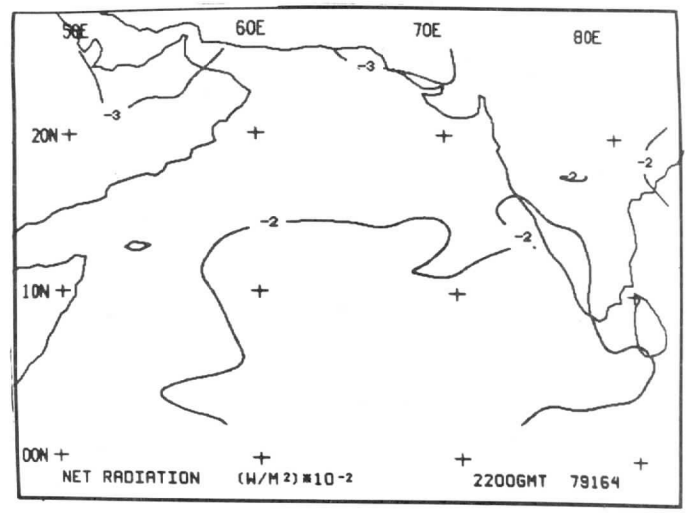
50E
60E
70E
80E
20N
10N
0ON
NET RADIATION (W/M2)*10-2
2200GMT 79164

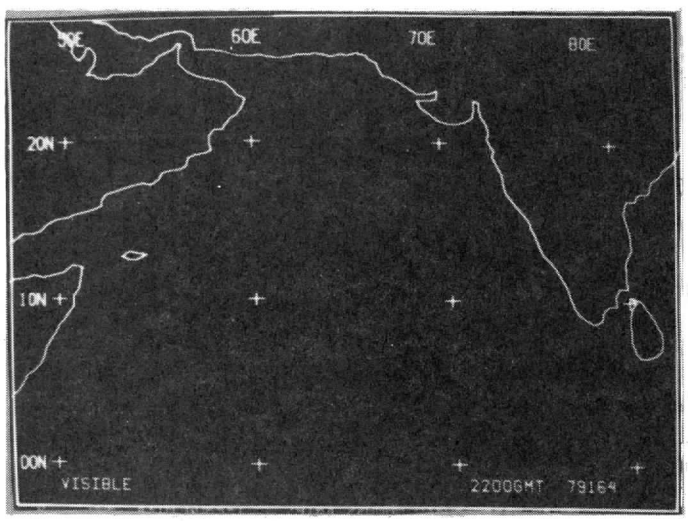
50E
60E
70E
80E
20N
10N
0ON
VISIBLE
2200GMT 79164

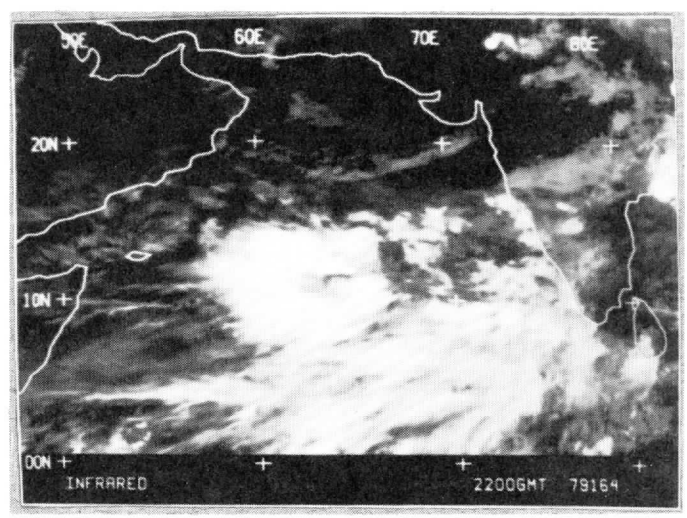
50E
60E
70E
80E
20N
10N
0ON
INFRARED
2200GMT 79164

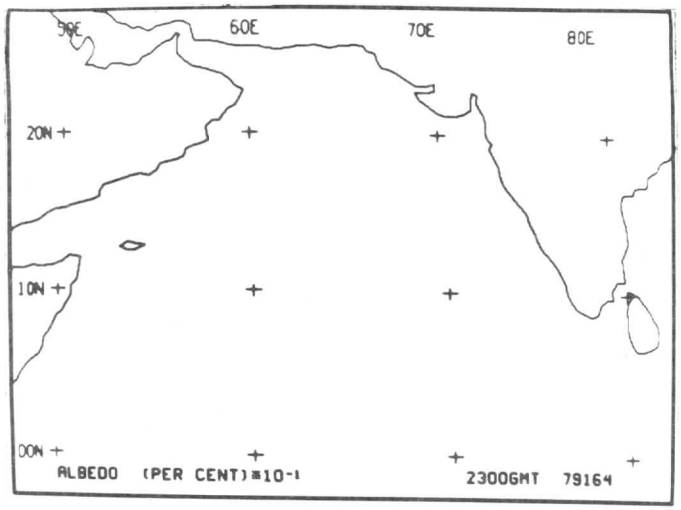
50E
60E
70E
80E
20N
10N
0ON
ALBEDO (PER CENT)×10-1
2300GMT 79164

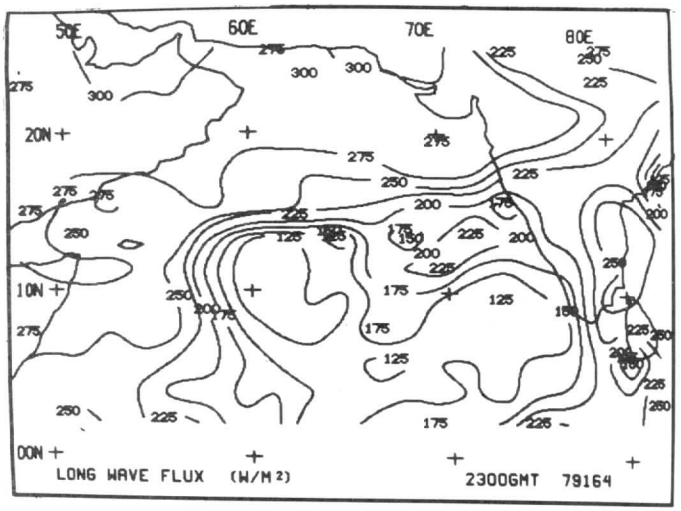
50E
60E
70E
80E
20N
10N
0ON
LONG WAVE FLUX (W/M2)
2300GMT 79164

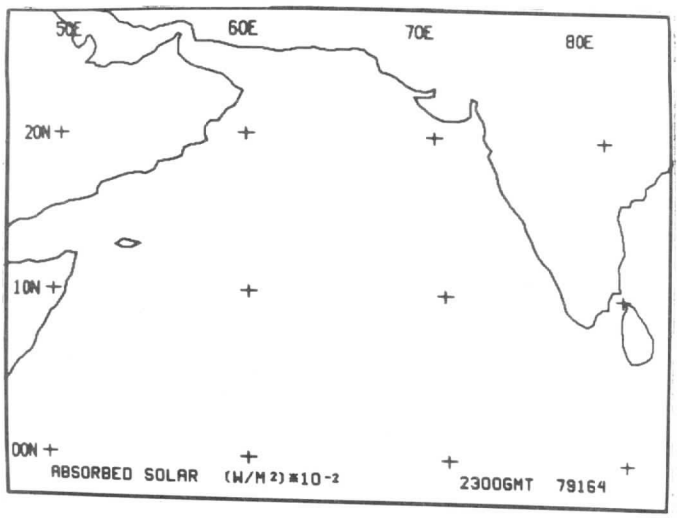
50E
60E
70E
80E
20N
10N
0ON
ABSORBED SOLAR (W/M2)×10-2
2300GMT 79164

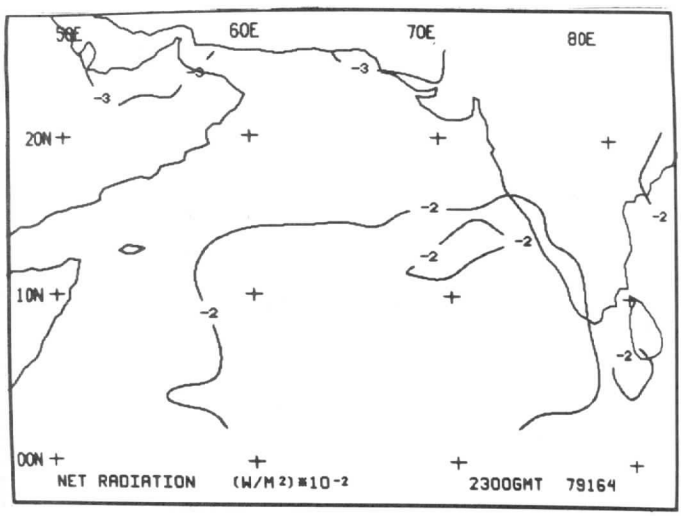
50E
60E
70E
80E
20N
10N
0ON
NET RADIATION (W/M2)×10-2
2300GMT 79164

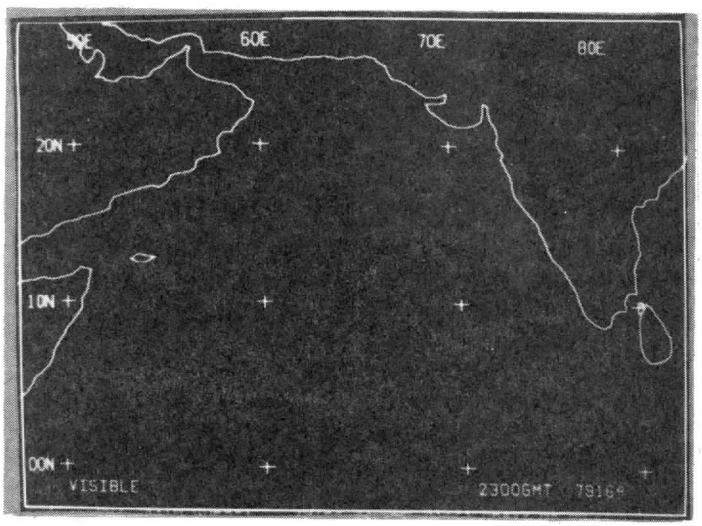
50E
60E
70E
80E
20N
10N
0ON
VISIBLE
2300GMT 79164

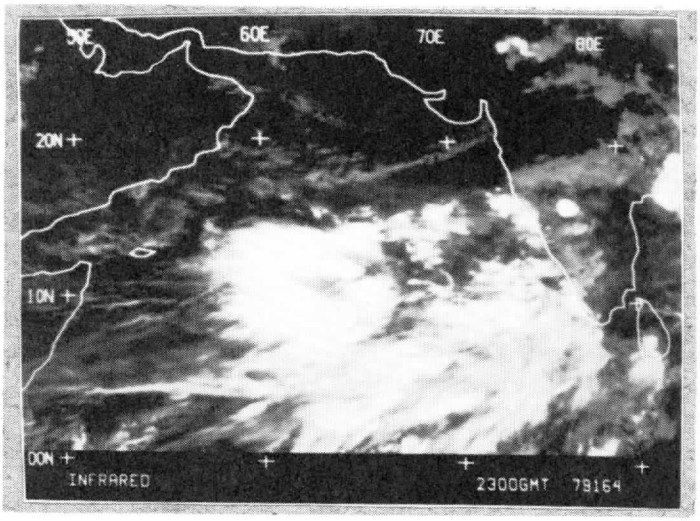
50E
60E
70E
80E
20N
10N
0ON
INFRARED
2300GMT 79164

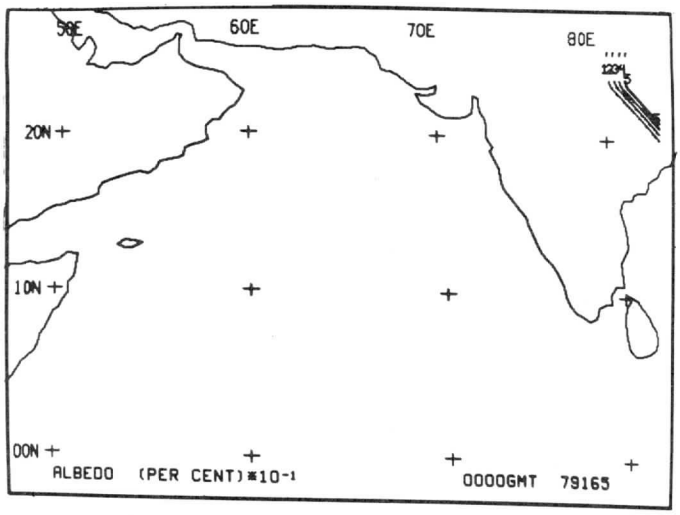
50E
60E
70E
80E
20N
10N
00N
ALBEDO (PER CENT)*10-1
0000GMT 79165

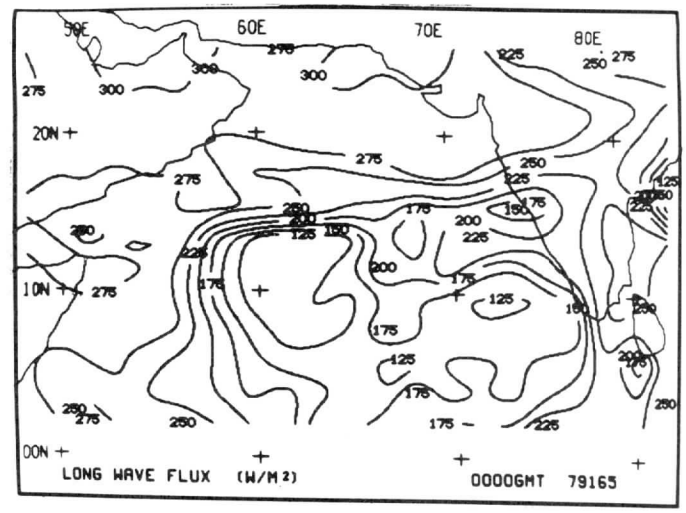
50E
60E
70E
80E
20N
10N
00N
LONG WAVE FLUX (W/M2)
0000GMT 79165

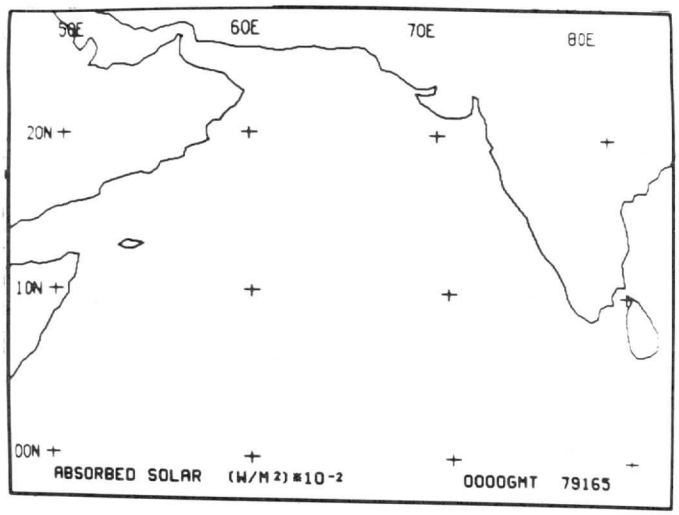
50E
60E
70E
80E
20N
10N
00N
ABSORBED SOLAR (W/M2)*10-2
0000GMT 79165

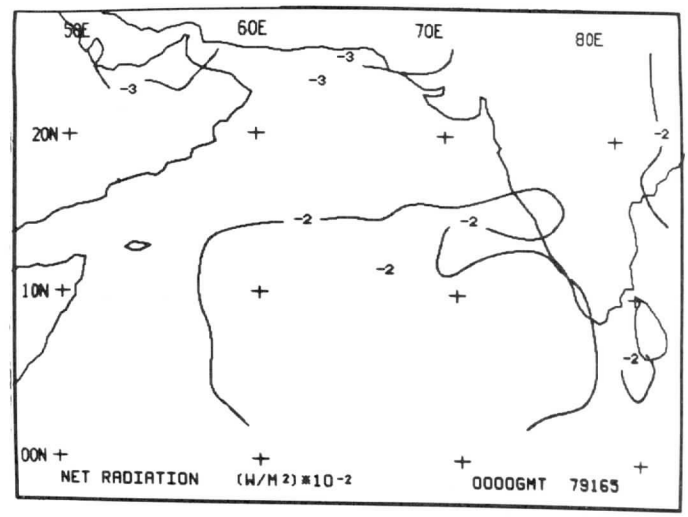
50E
60E
70E
80E
20N
10N
00N
NET RADIATION (W/M2)*10-2
0000GMT 79165

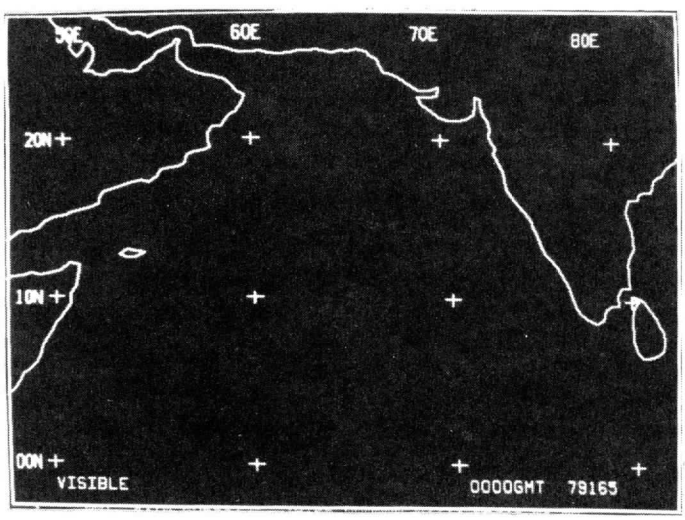
50E
60E
70E
80E
20N
10N
00N
VISIBLE
0000GMT 79165

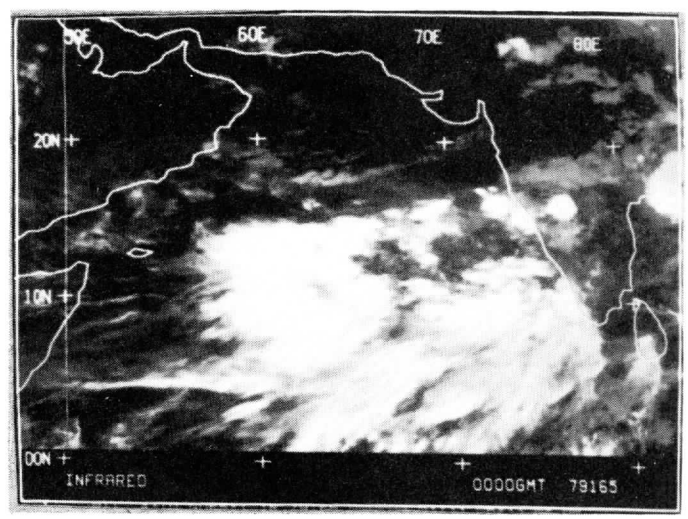
50E
60E
70E
80E
20N
10N
00N
INFRARED
0000GMT 79165

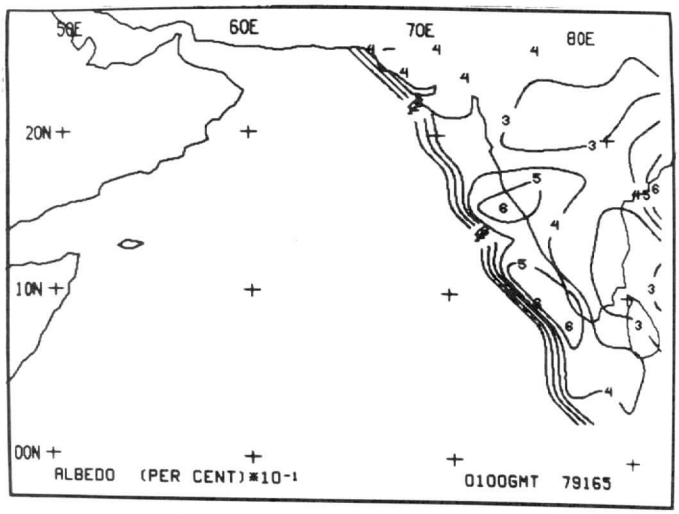
50E
60E
70E
80E
20N
10N
0ON
ALBEDO (PER CENT)*10-1
0100GMT 79165

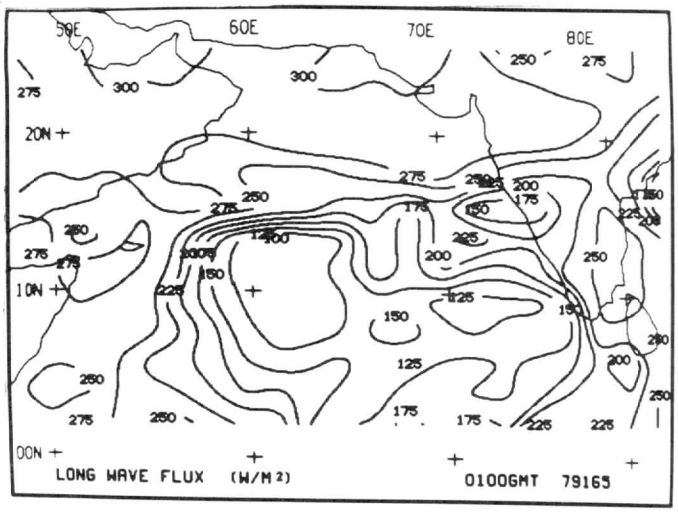
50E
60E
70E
80E
20N
10N
0ON
LONG WAVE FLUX (W/M2)
0100GMT 79165

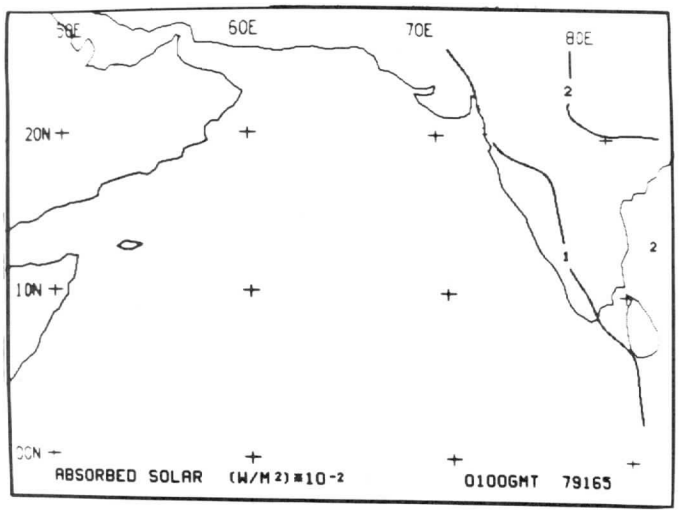
50E
60E
70E
80E
20N
10N
0ON
ABSORBED SOLAR (W/M2)*10-2
0100GMT 79165

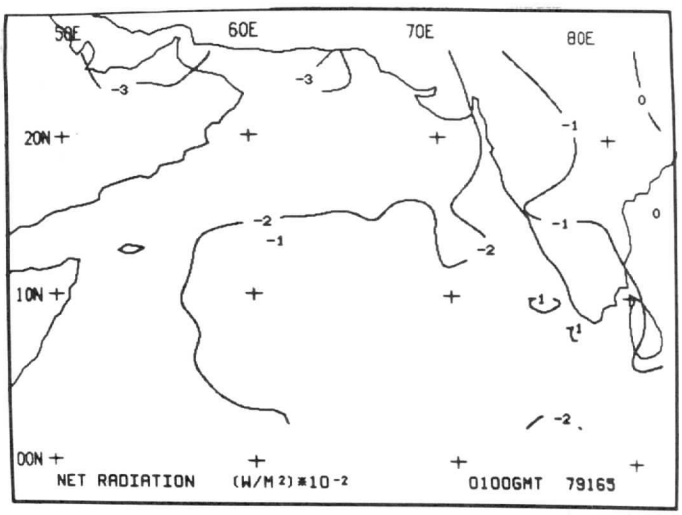
50E
60E
70E
80E
20N
10N
0ON
NET RADIATION (W/M2)*10-2
0100GMT 79165

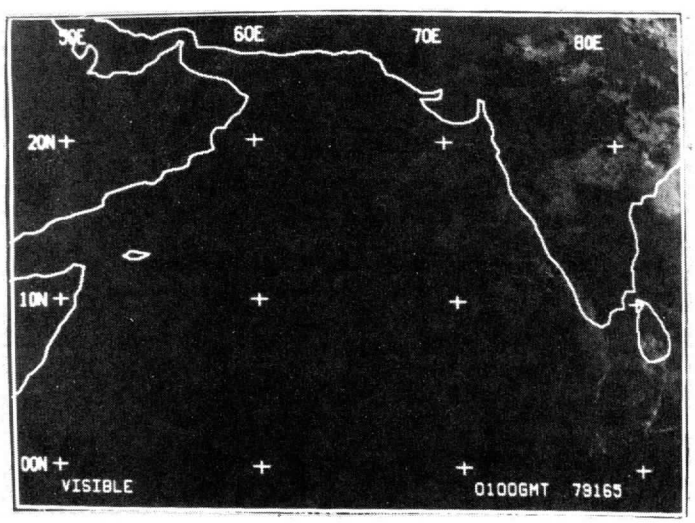
50E
60E
70E
80E
20N
10N
0ON
VISIBLE
0100GMT 79165

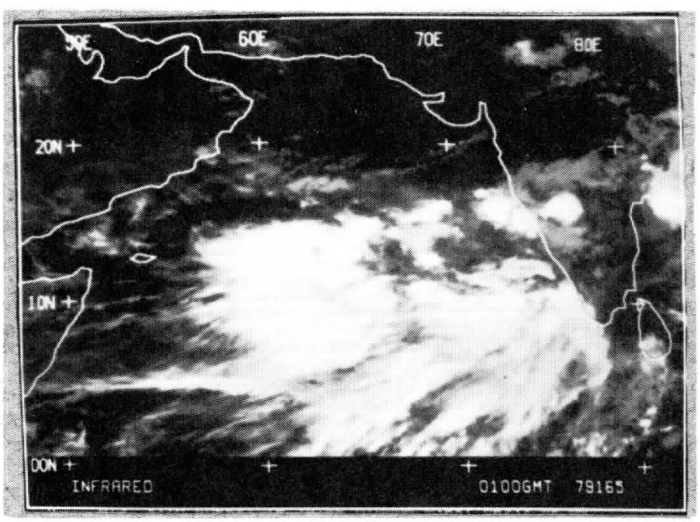
50E
60E
70E
80E
20N
10N
0ON
INFRARED
0100GMT 79165

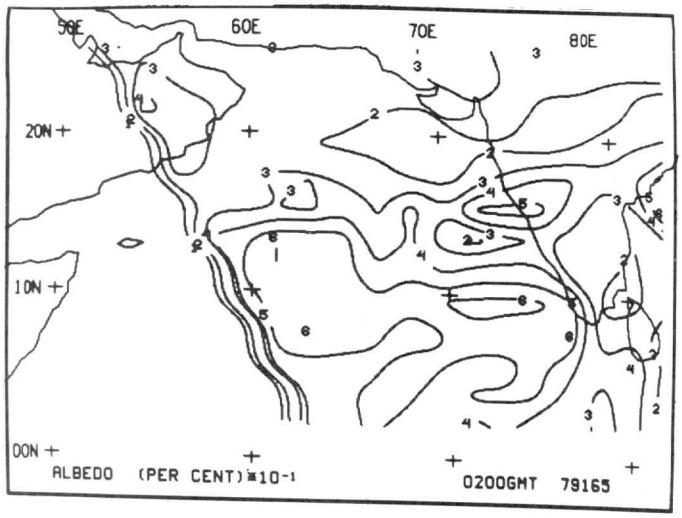
50E
60E
70E
80E
20N
10N
0ON
ALBEDO (PER CENT)*10-1
0200GMT 79165

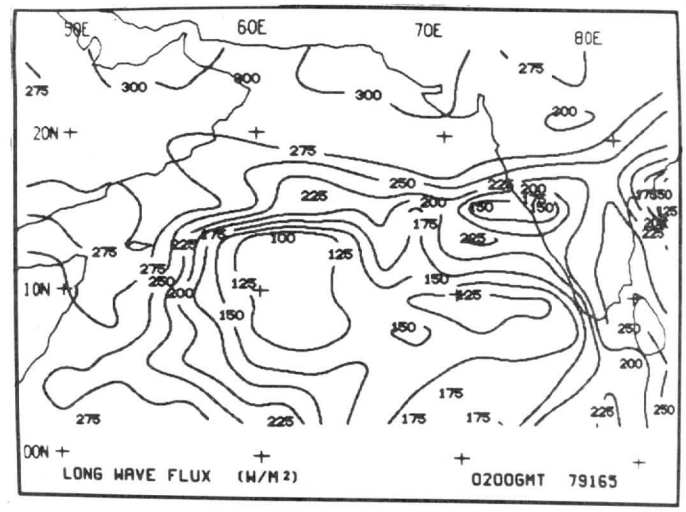
50E
60E
70E
80E
20N
10N
0ON
LONG WAVE FLUX (W/M2)
0200GMT 79165

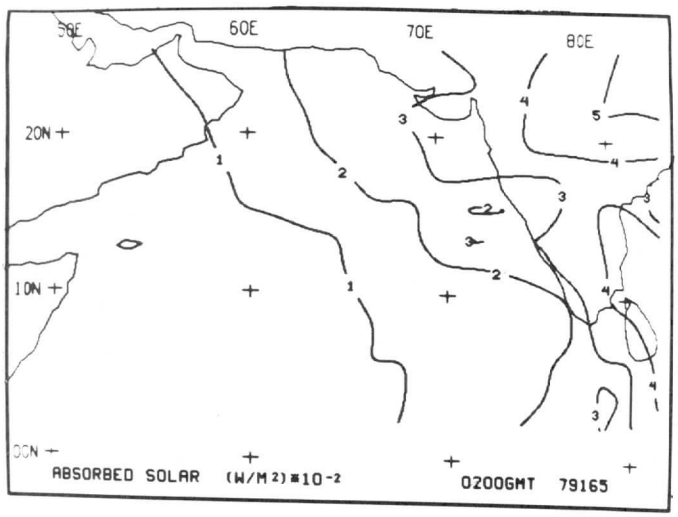
50E
60E
70E
80E
20N
10N
0ON
ABSORBED SOLAR (W/M2)*10-2
0200GMT 79165

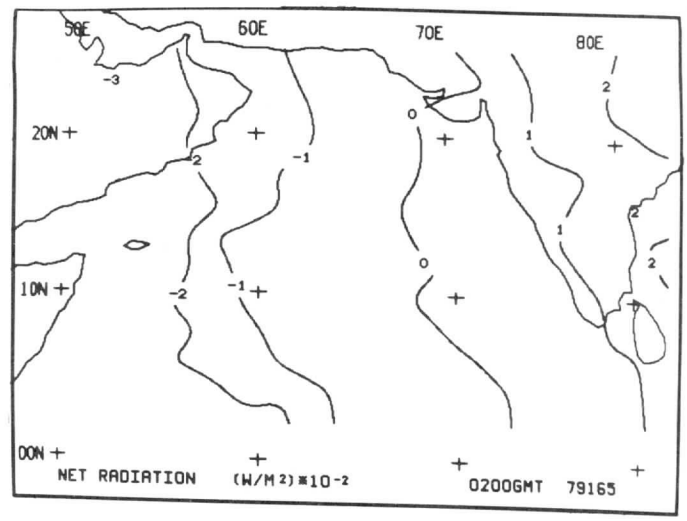
50E
60E
70E
80E
20N
10N
0ON
NET RADIATION (W/M2)*10-2
0200GMT 79165

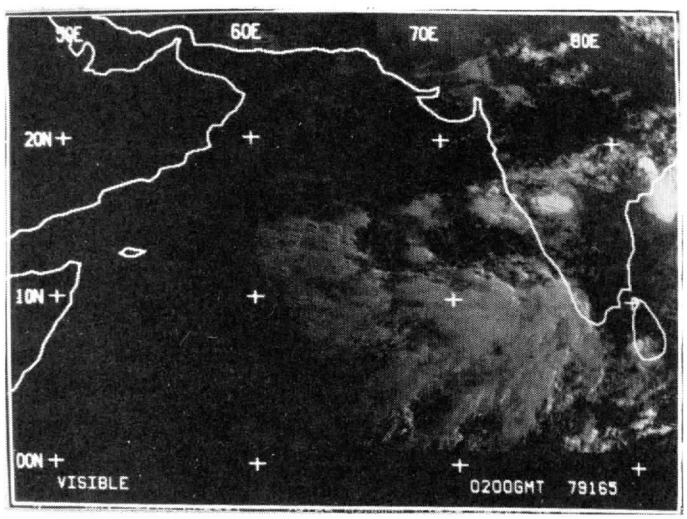
50E
60E
70E
80E
20N
10N
0ON
VISIBLE
0200GMT 79165

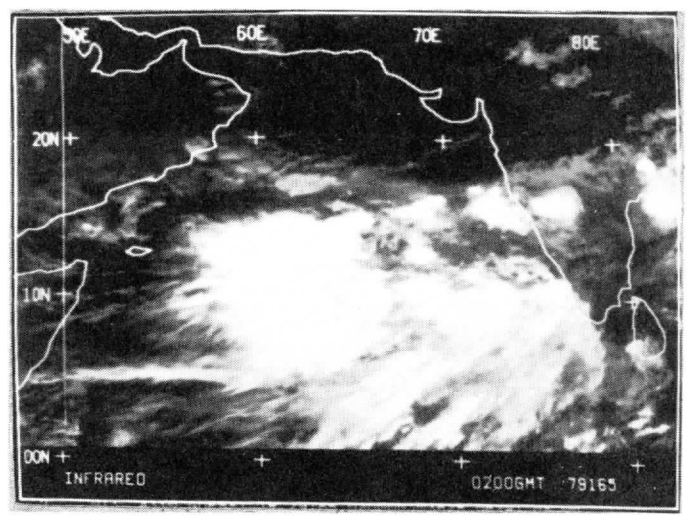
50E
60E
70E
80E
20N
10N
0ON
INFRARED
0200GMT 79165

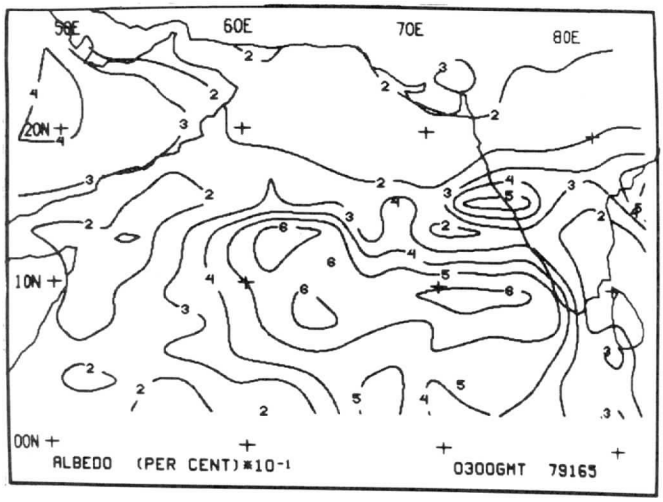
50E
60E
70E
80E
20N
10N
0ON
ALBEDO (PER CENT)*10-1
0300GMT 79165

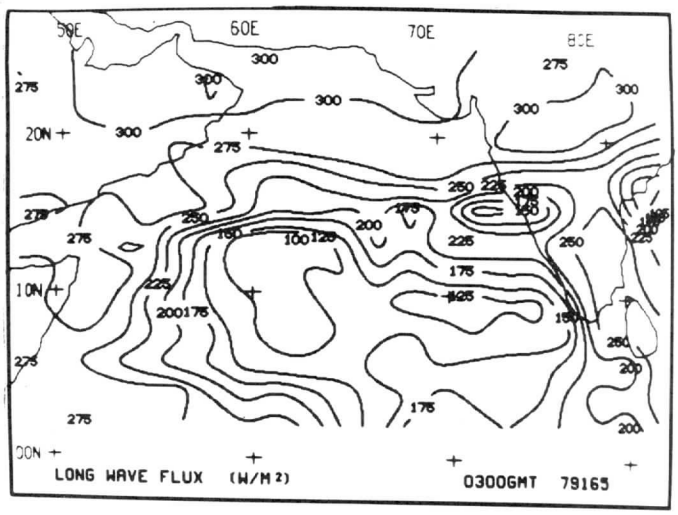
50E
60E
70E
80E
20N
10N
0ON
LONG WAVE FLUX (W/M2)
0300GMT 79165

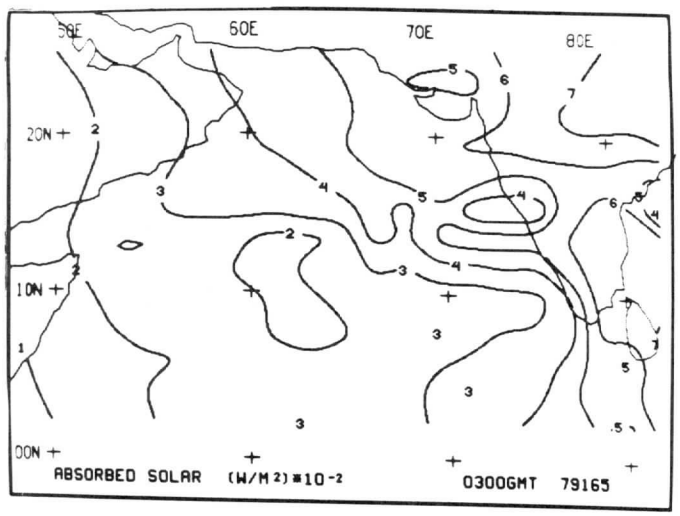
50E
60E
70E
80E
20N
10N
0ON
ABSORBED SOLAR (W/M2)*10-2
0300GMT 79165

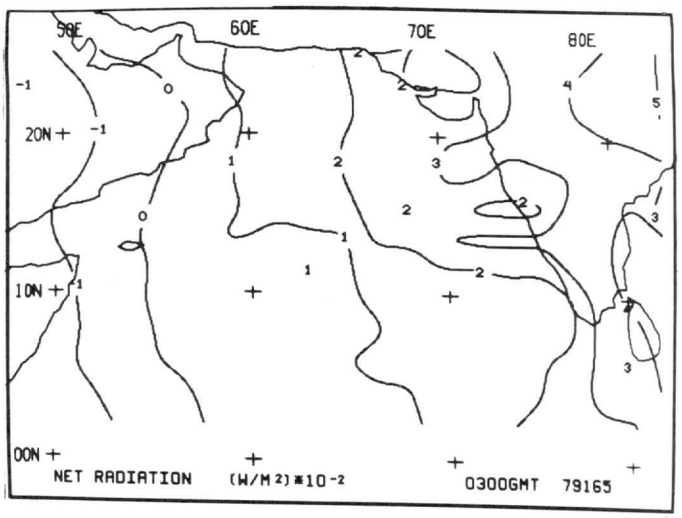
50E
60E
70E
80E
20N
10N
0ON
NET RADIATION (W/M2)*10-2
0300GMT 79165

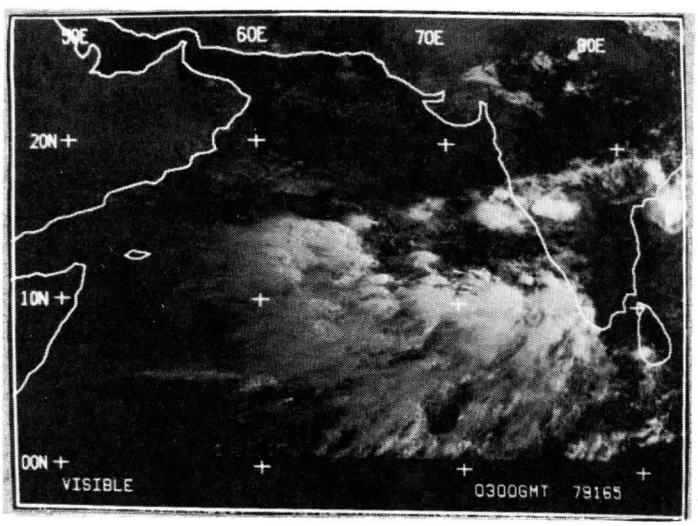
50E
60E
70E
80E
20N
10N
0ON
VISIBLE
0300GMT 79165

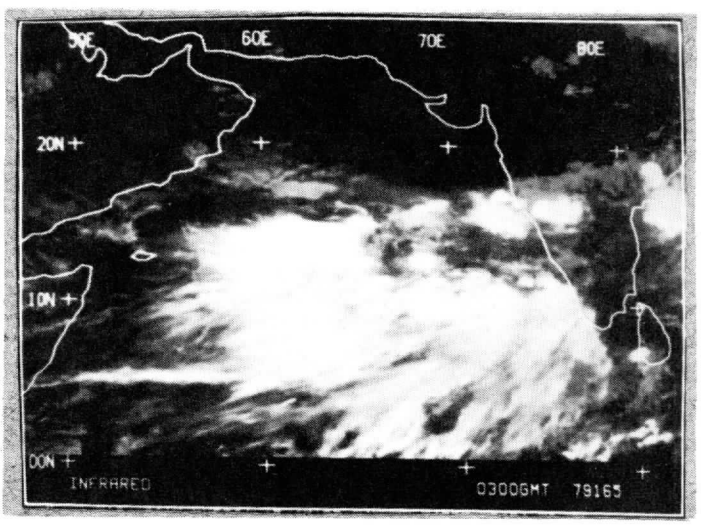
50E
60E
70E
80E
20N
10N
0ON
INFRARED
0300GMT 79165

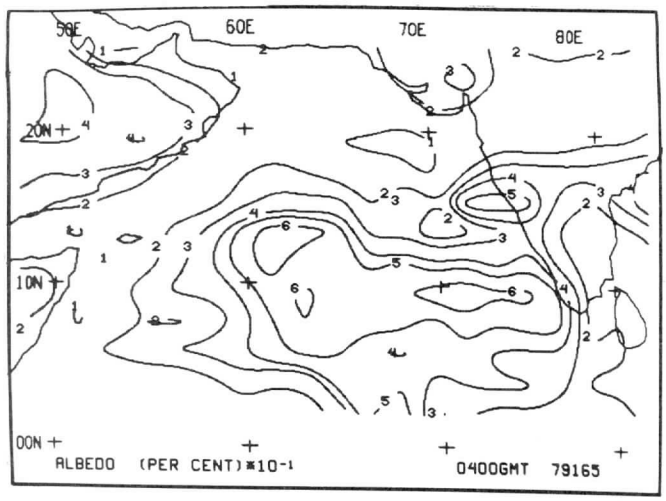
50E
60E
70E
80E
20N
10N
0ON
ALBEDO (PER CENT)*10-1
0400GMT 79165

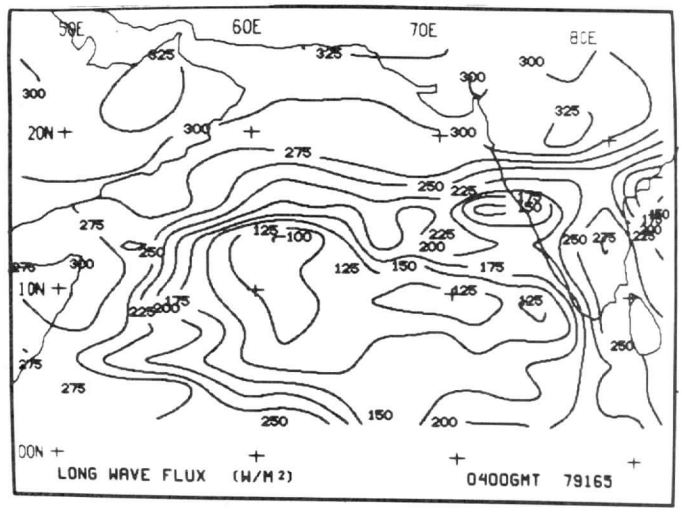
50E
60E
70E
80E
20N
10N
0ON
LONG WAVE FLUX (W/M2)
0400GMT 79165

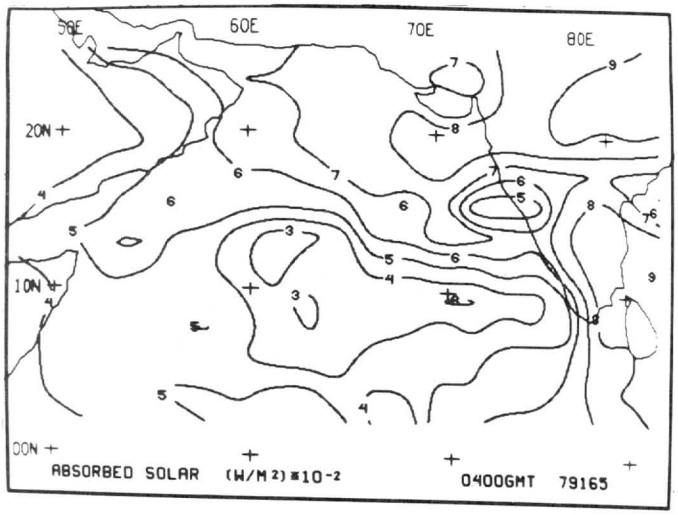
50E
60E
70E
80E
20N
10N
0ON
ABSORBED SOLAR (W/M2)*10-2
0400GMT 79165

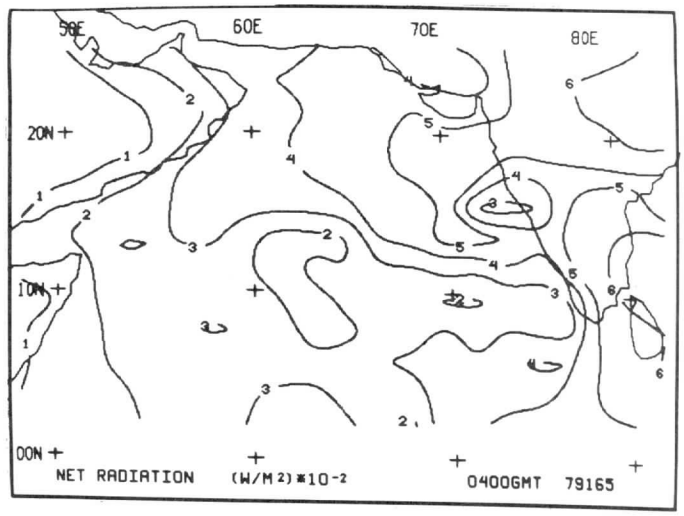
50E
60E
70E
80E
20N
10N
0ON
NET RADIATION (W/M2)*10-2
0400GMT 79165

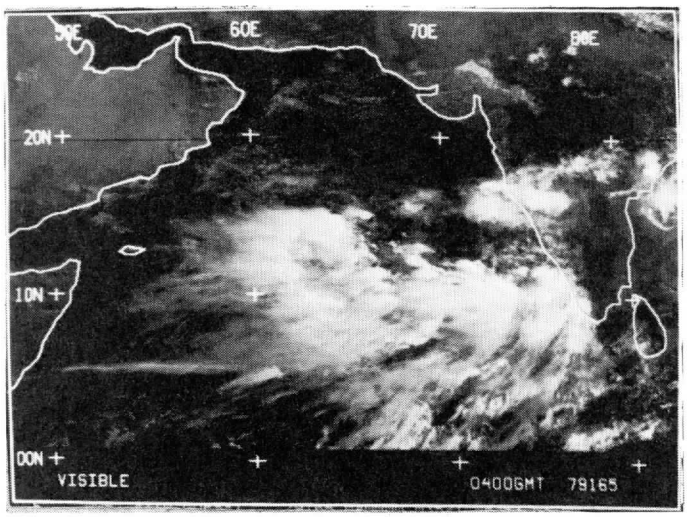
50E
60E
70E
80E
20N
10N
0ON
VISIBLE
0400GMT 79165

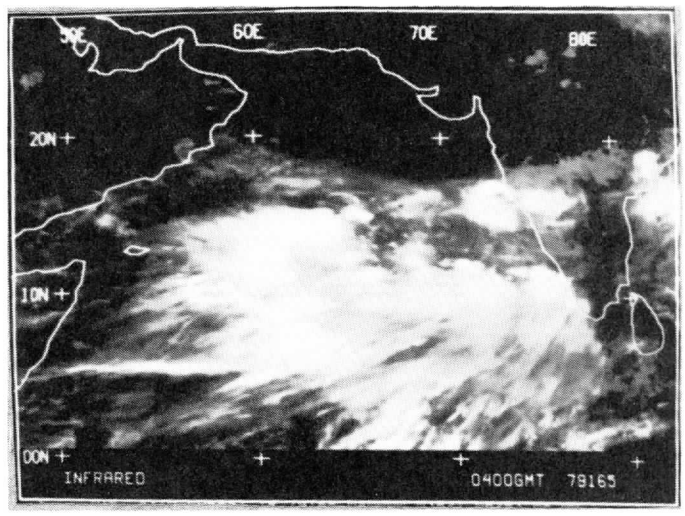
50E
60E
70E
80E
20N
10N
0ON
INFRARED
0400GMT 79165

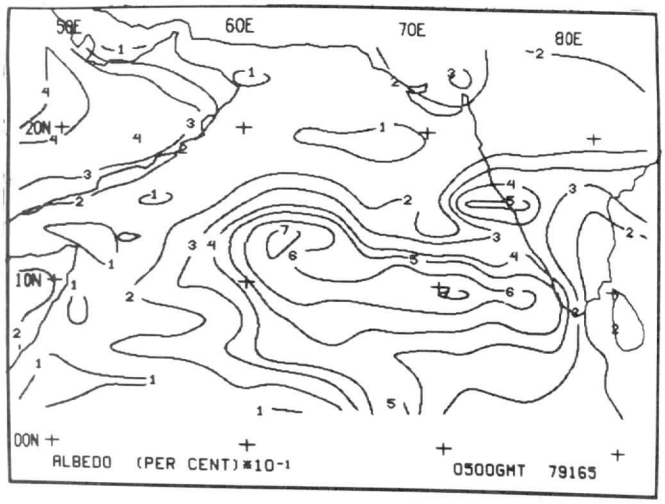
50E
60E
70E
80E
20N
10N
0ON
ALBEDO (PER CENT)*10-1
0500GMT 79165

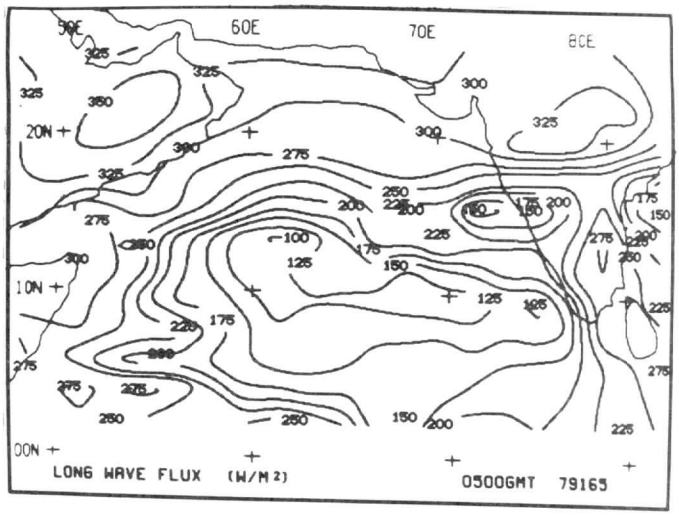
50E
60E
70E
80E
20N
10N
0ON
LONG WAVE FLUX (W/M2)
0500GMT 79165

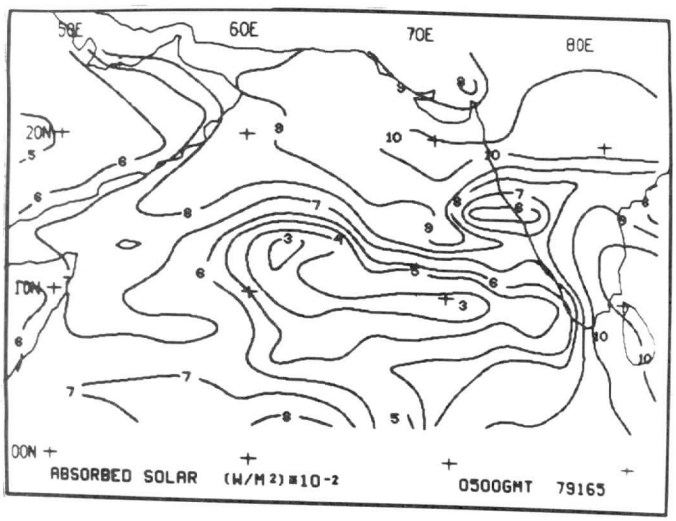
50E
60E
70E
80E
20N
10N
0ON
ABSORBED SOLAR (W/M2)*10-2
0500GMT 79165

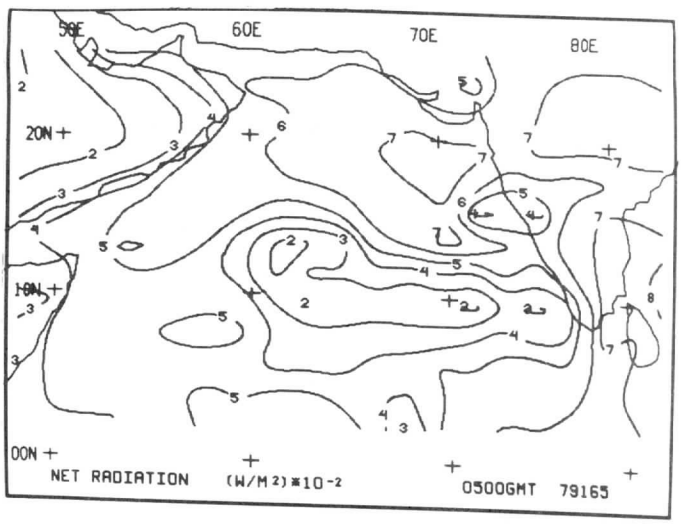
50E
60E
70E
80E
20N
10N
0ON
NET RADIATION (W/M2)*10-2
0500GMT 79165

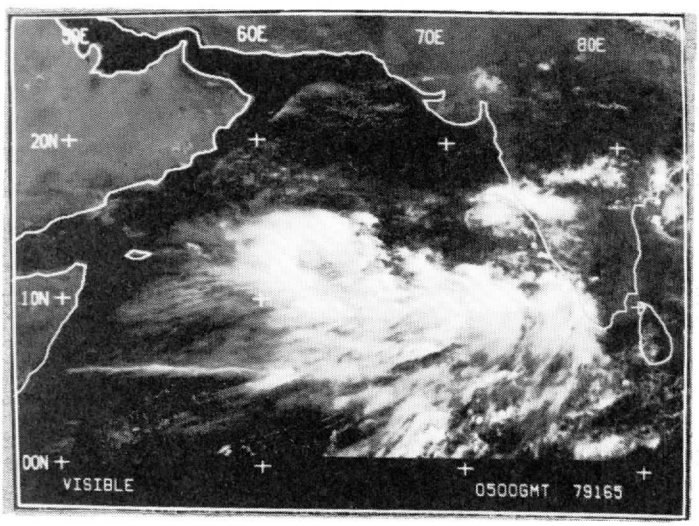
50E
60E
70E
80E
20N
10N
0ON
VISIBLE
0500GMT 79165

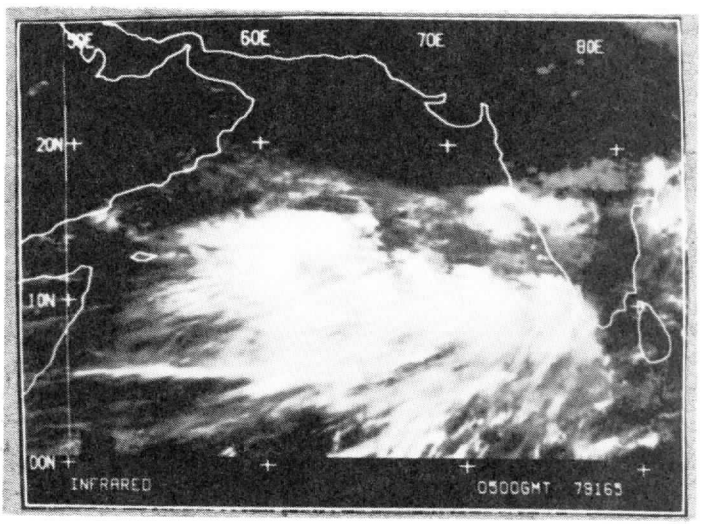
50E
60E
70E
80E
20N
10N
0ON
INFRARED
0500GMT 79165

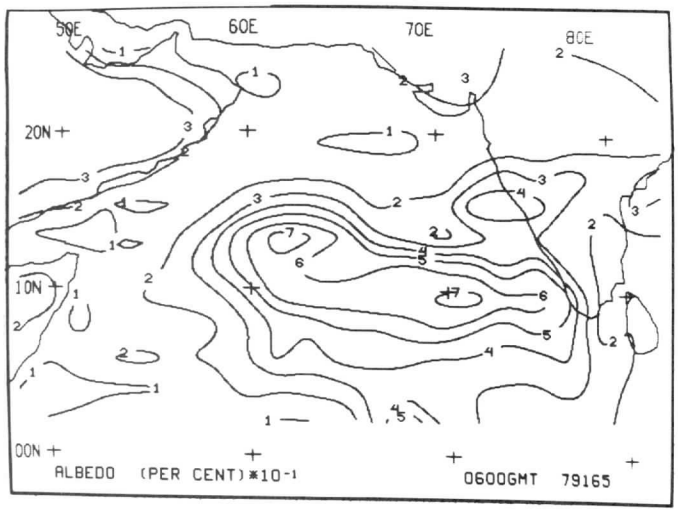
50E
60E
70E
80E
20N
10N
00N
ALBEDO (PER CENT)*10-1
0600GMT 79165

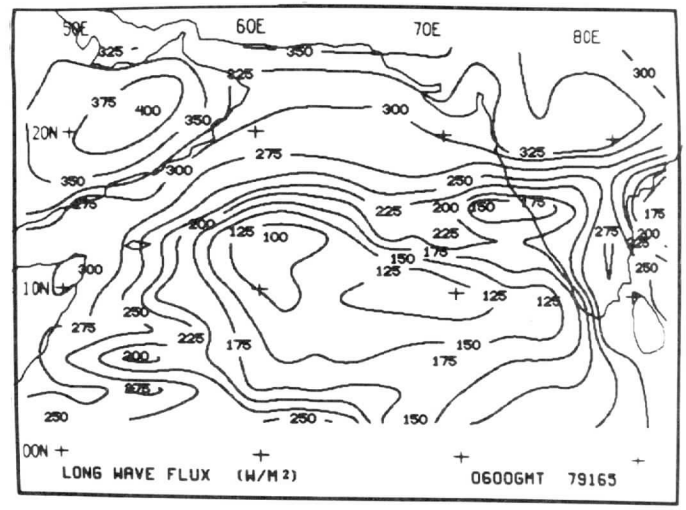
50E
60E
70E
80E
20N
10N
00N
LONG WAVE FLUX (W/M2)
0600GMT 79165

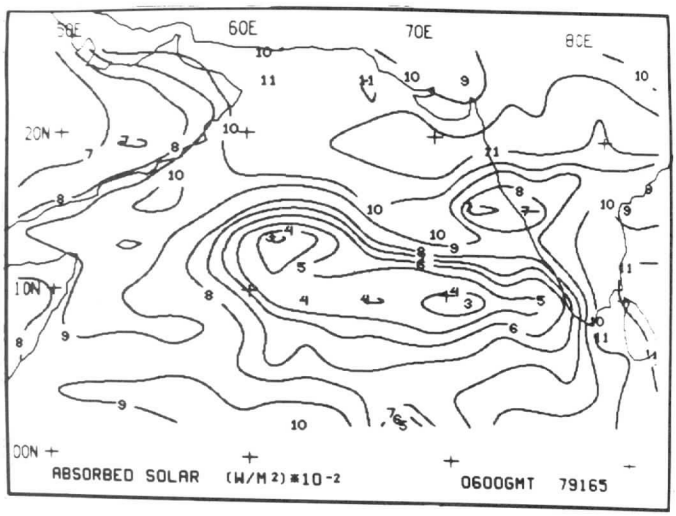
50E
60E
70E
80E
20N
10N
00N
ABSORBED SOLAR (W/M2)*10-2
0600GMT 79165

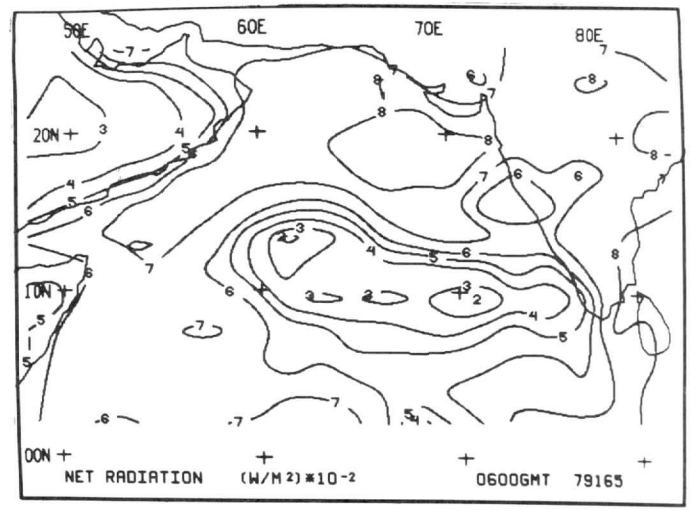
50E
60E
70E
80E
20N
10N
00N
NET RADIATION (W/M2)*10-2
0600GMT 79165

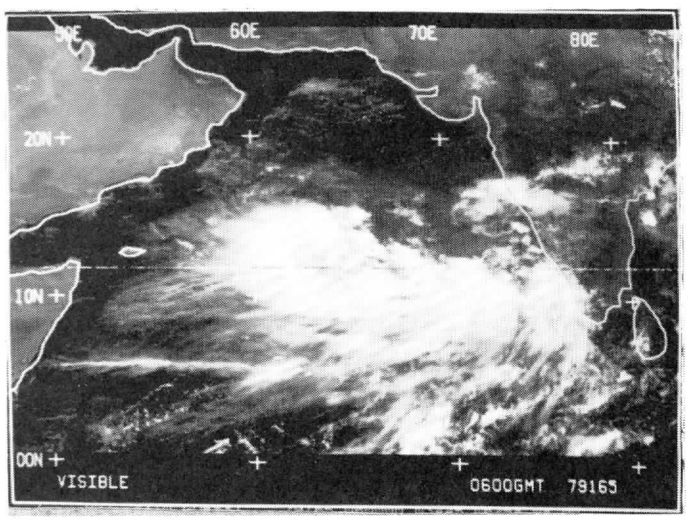
50E
60E
70E
80E
20N
10N
00N
VISIBLE
0600GMT 79165

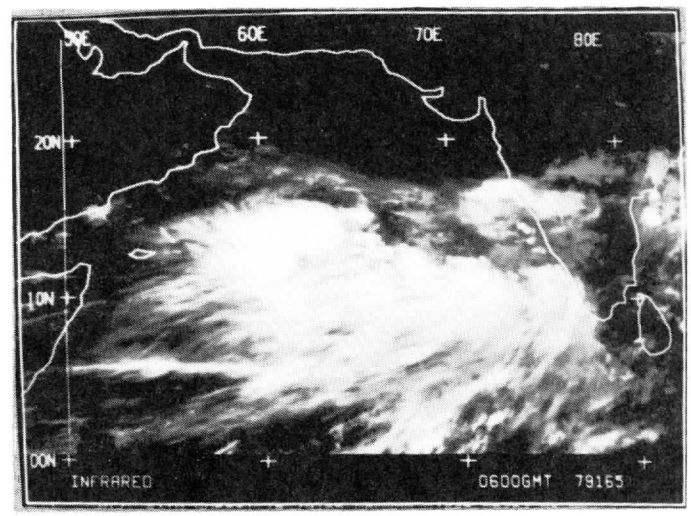
50E
60E
70E
80E
20N
10N
00N
INFRARED
0600GMT 79165

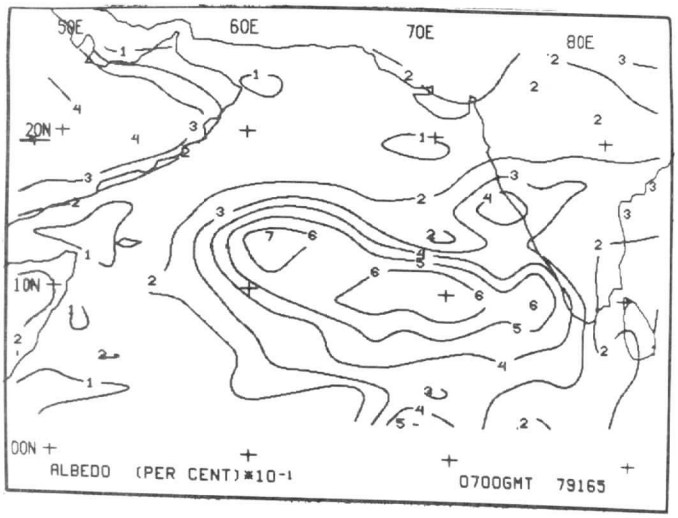
50E
60E
70E
80E
20N
10N
0ON
ALBEDO (PER CENT)*10-1
0700GMT 79165

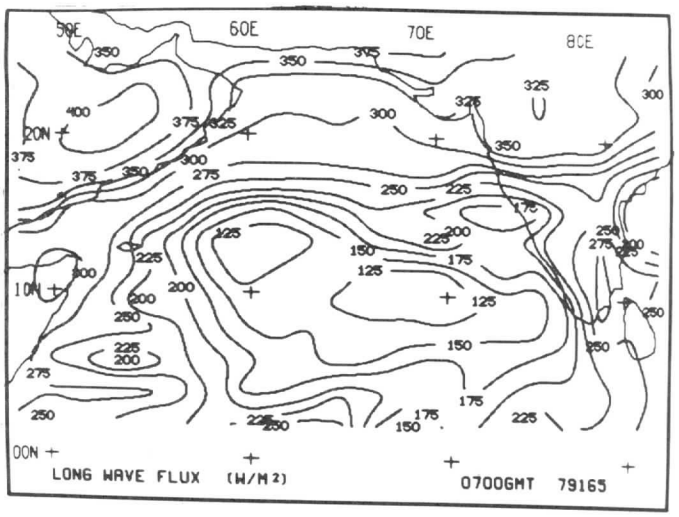
50E
60E
70E
80E
20N
10N
0ON
LONG WAVE FLUX (W/M2)
0700GMT 79165

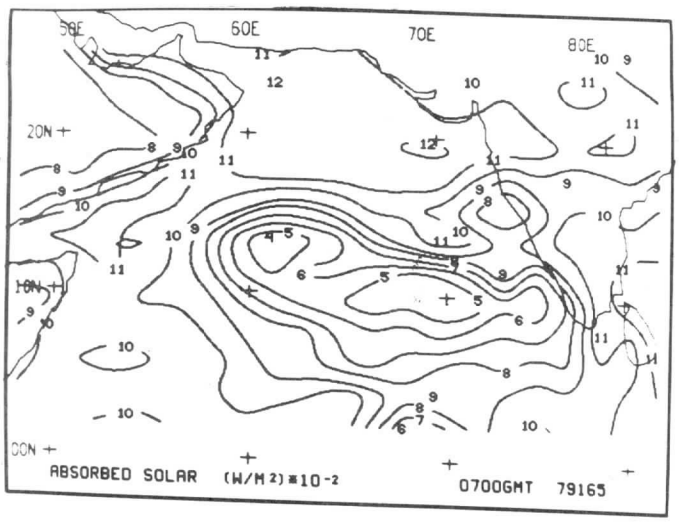
50E
60E
70E
80E
20N
10N
0ON
ABSORBED SOLAR (W/M2)*10-2
0700GMT 79165

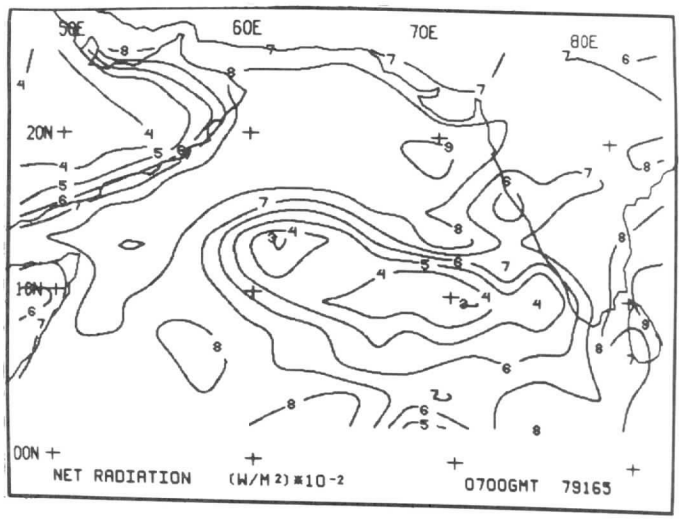
50E
60E
70E
80E
20N
10N
0ON
NET RADIATION (W/M2)*10-2
0700GMT 79165

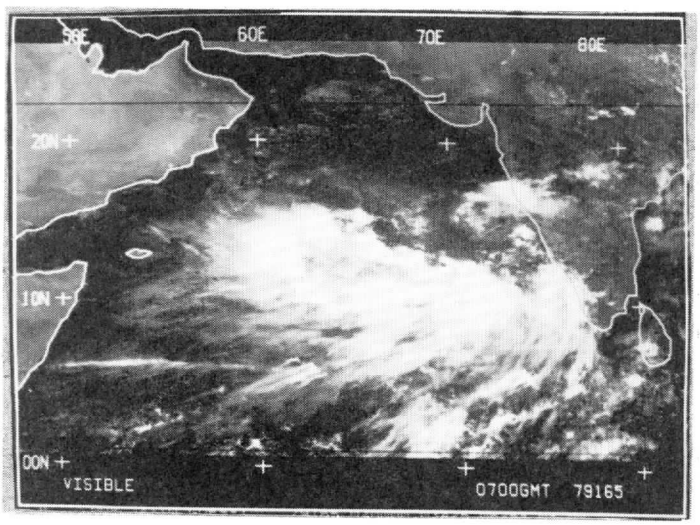
50E
60E
70E
80E
20N
10N
0ON
VISIBLE
0700GMT 79165

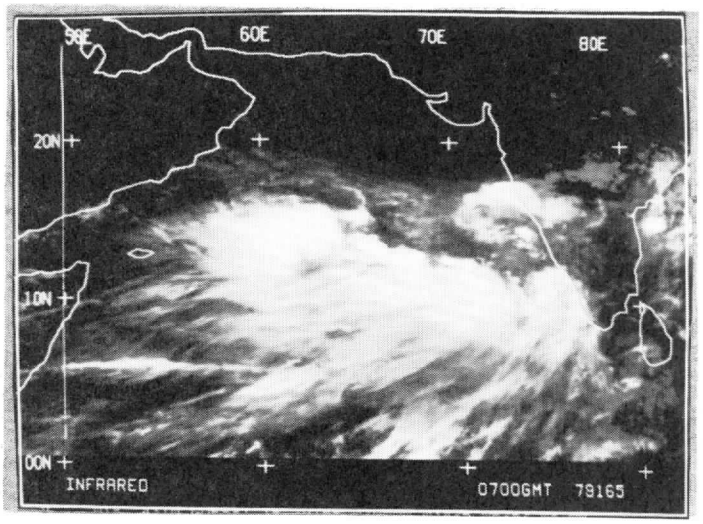
50E
60E
70E
80E
20N
10N
0ON
INFRARED
0700GMT 79165

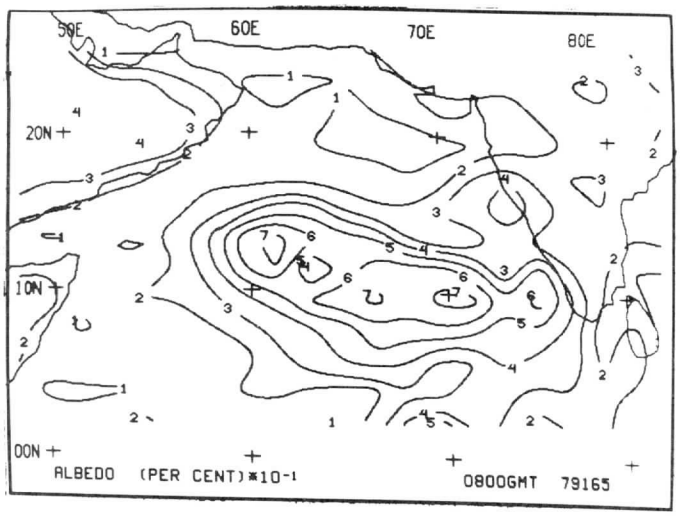
50E
60E
70E
80E
20N
10N
0ON
ALBEDO (PER CENT)*10-1
0800GMT 79165

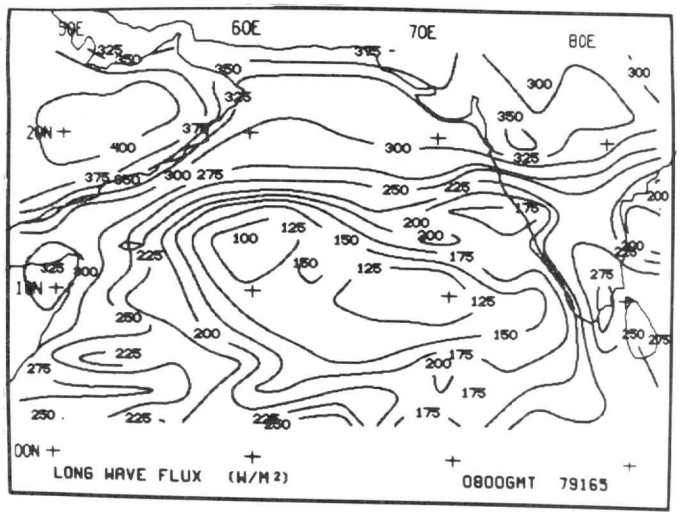
50E
60E
70E
80E
20N
10N
0ON
LONG WAVE FLUX (W/M2)
0800GMT 79165

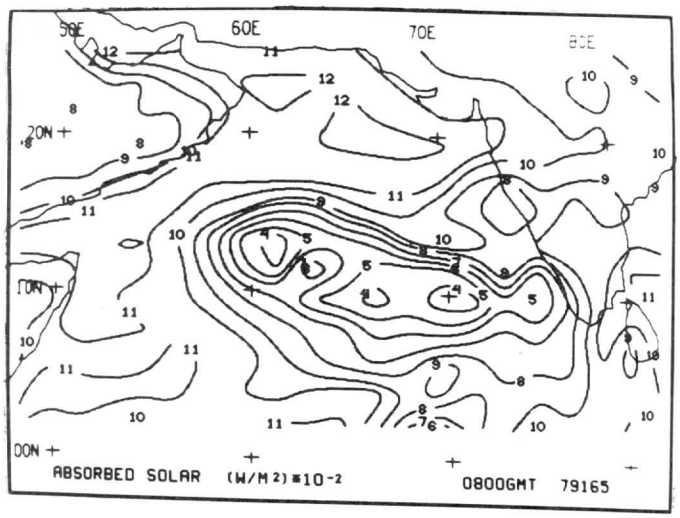
50E
60E
70E
80E
20N
10N
0ON
ABSORBED SOLAR (W/M2)*10-2
0800GMT 79165

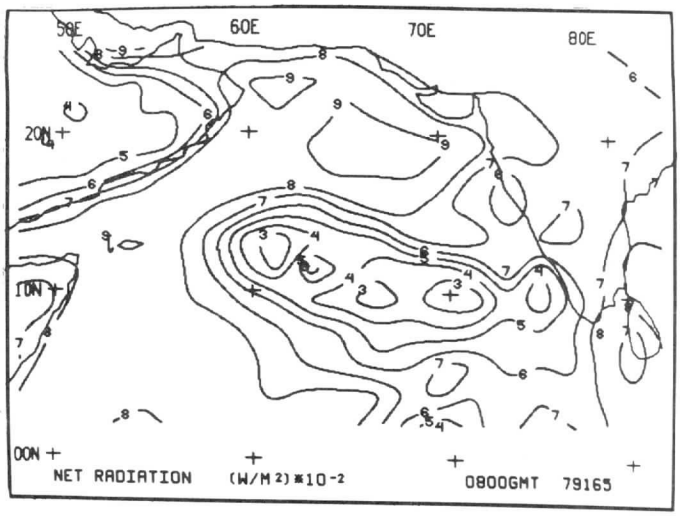
50E
60E
70E
80E
20N
10N
0ON
NET RADIATION (W/M2)*10-2
0800GMT 79165

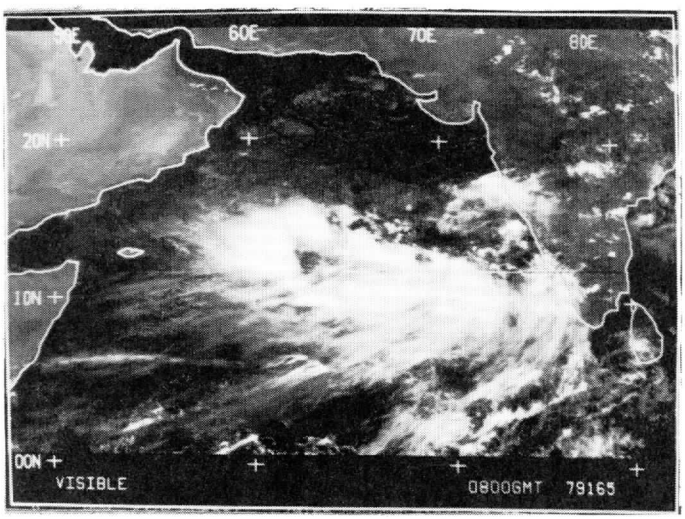
50E
60E
70E
80E
20N
10N
0ON
VISIBLE
0800GMT 79165

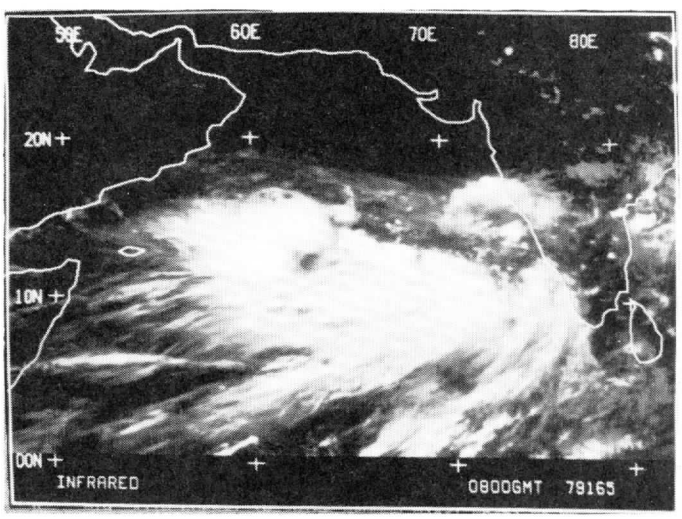
50E
60E
70E
80E
20N
10N
0ON
INFRARED
0800GMT 79165

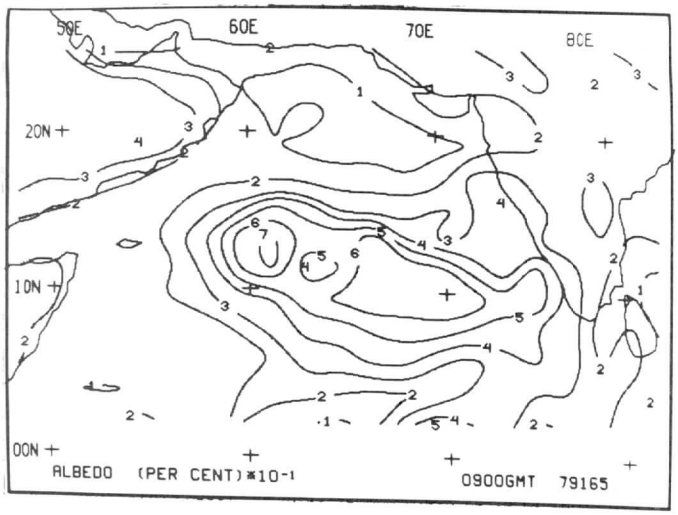
50E
60E
70E
80E
20N
10N
00N
ALBEDO (PER CENT)*10-1
0900GMT 79165

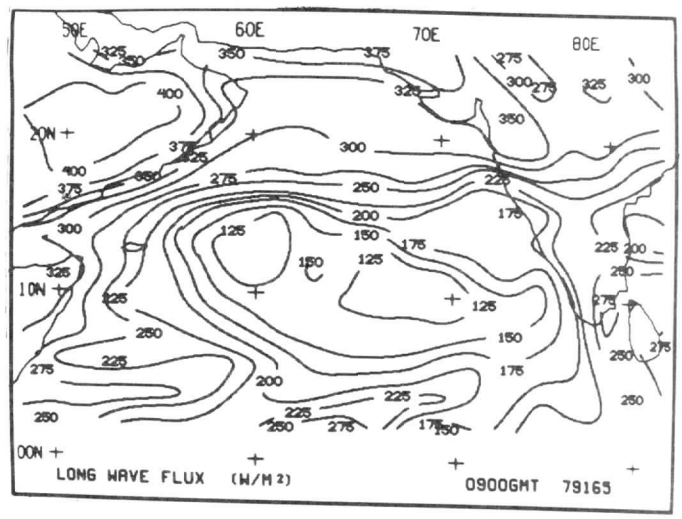
50E
60E
70E
80E
20N
10N
00N
LONG WAVE FLUX (W/M2)
0900GMT 79165

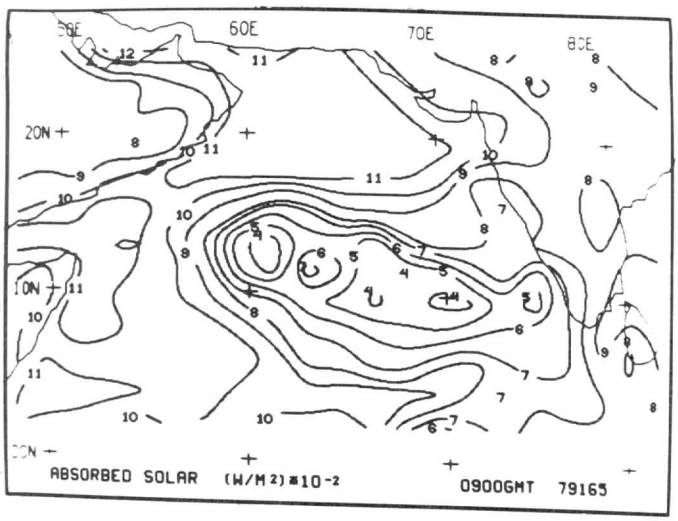
50E
60E
70E
80E
20N
10N
00N
ABSORBED SOLAR (W/M2)*10-2
0900GMT 79165

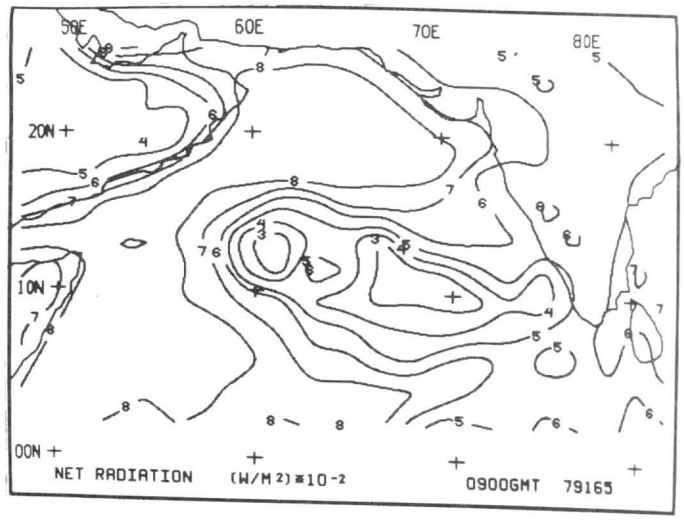
50E
60E
70E
80E
20N
10N
00N
NET RADIATION (W/M2)*10-2
0900GMT 79165

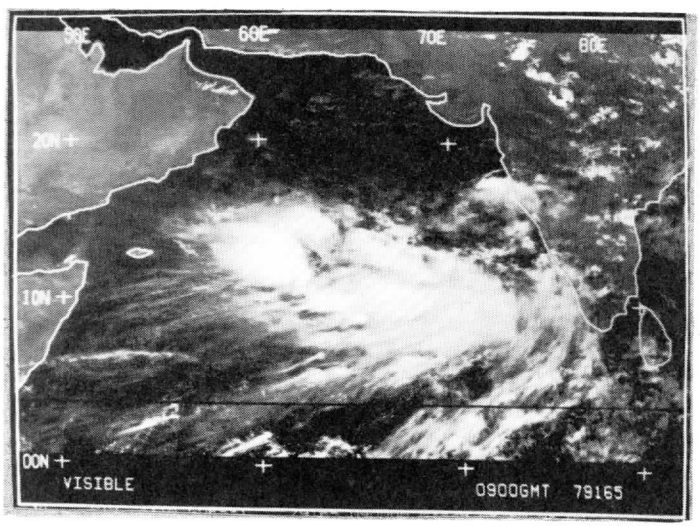
50E
60E
70E
80E
20N
10N
00N
VISIBLE
0900GMT 79165

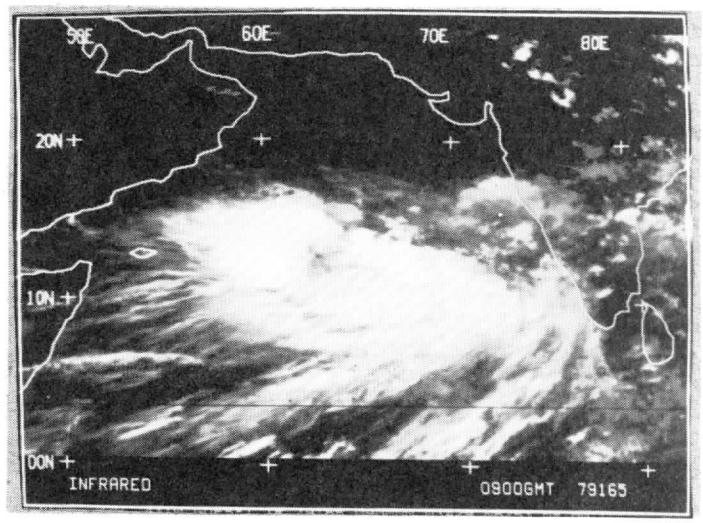
50E
60E
70E
80E
20N
10N
00N
INFRARED
0900GMT 79165

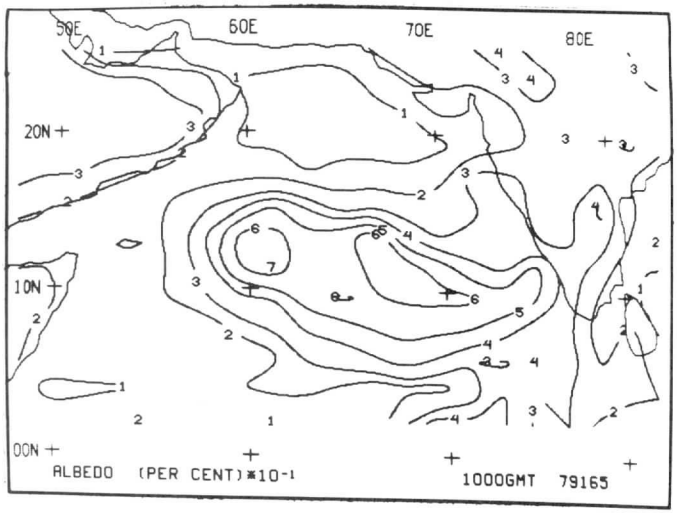
50E
60E
70E
80E
20N
10N
0ON
ALBEDO (PER CENT)*10-1
1000GMT 79165

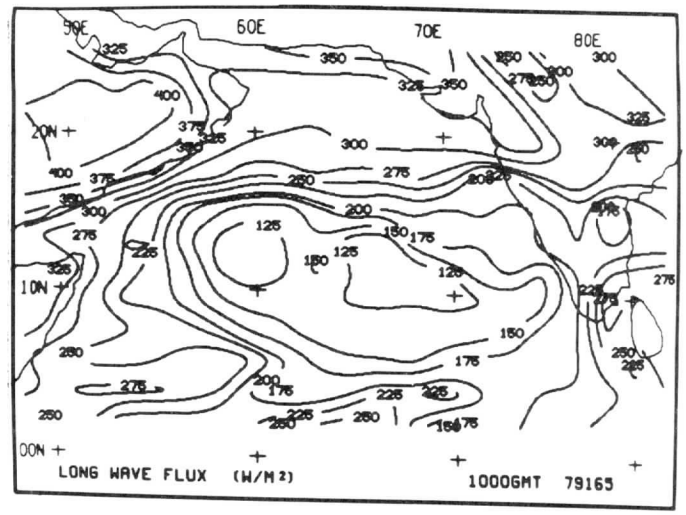
50E
60E
70E
80E
20N
10N
0ON
LONG WAVE FLUX (W/M2)
1000GMT 79165

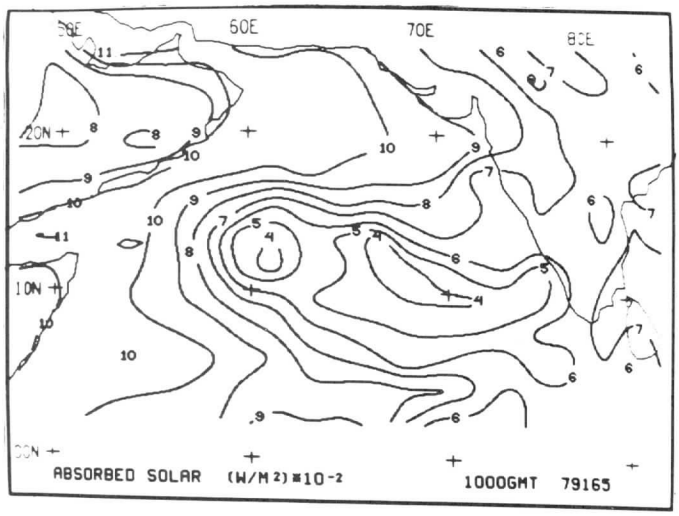
50E
60E
70E
80E
20N
10N
0ON
ABSORBED SOLAR (W/M2)*10-2
1000GMT 79165

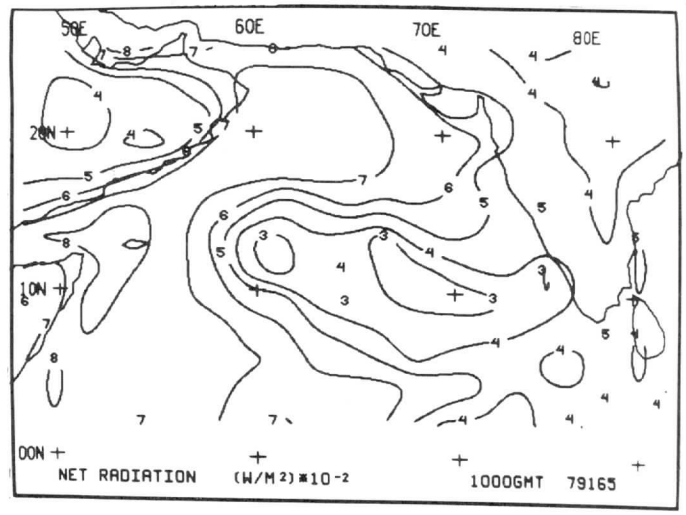
50E
60E
70E
80E
20N
10N
0ON
NET RADIATION (W/M2)*10-2
1000GMT 79165

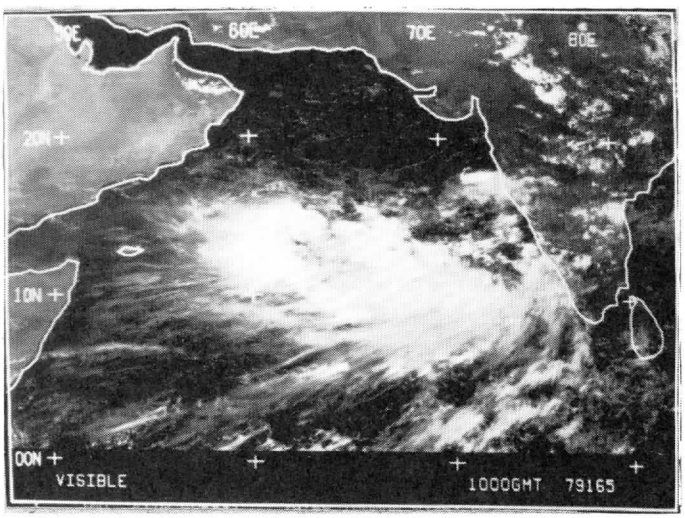
50E
60E
70E
80E
20N
10N
0ON
VISIBLE
1000GMT 79165

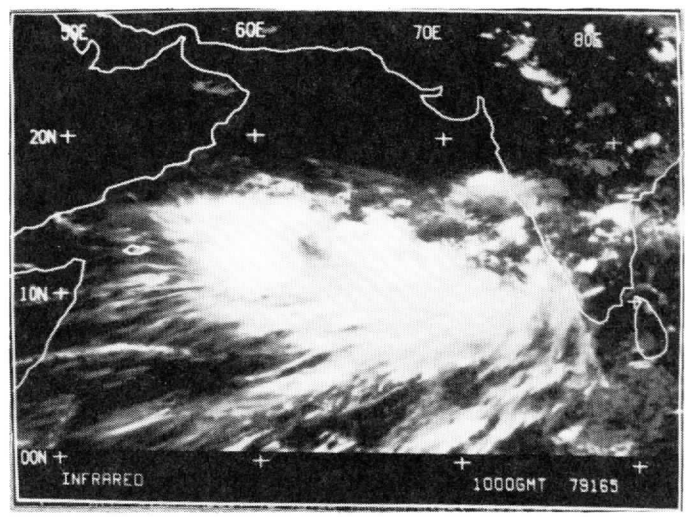
50E
60E
70E
80E
20N
10N
0ON
INFRARED
1000GMT 79165

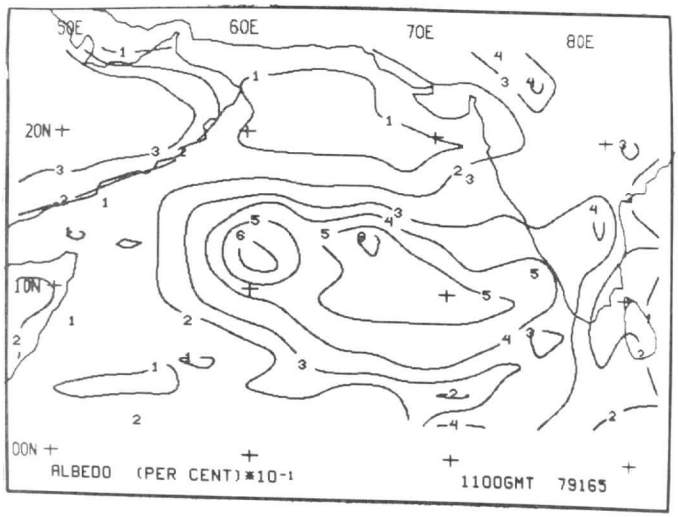
50E
60E
70E
80E
20N
10N
0ON
ALBEDO (PER CENT)*10-1
1100GMT 79165

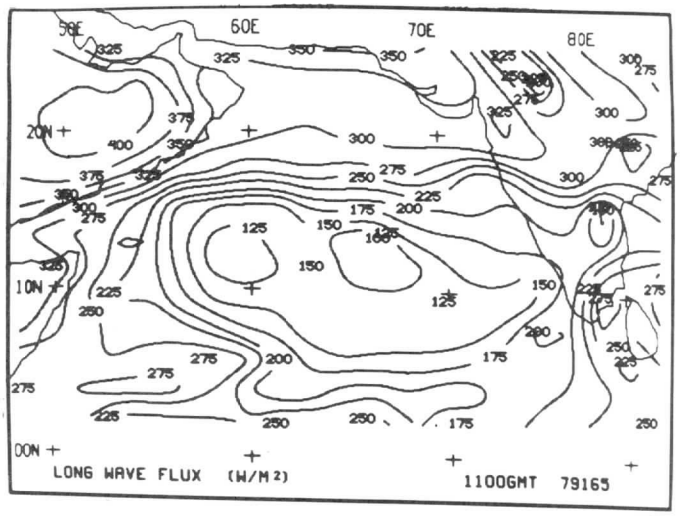
50E
60E
70E
80E
20N
10N
0ON
LONG WAVE FLUX (W/M2)
1100GMT 79165

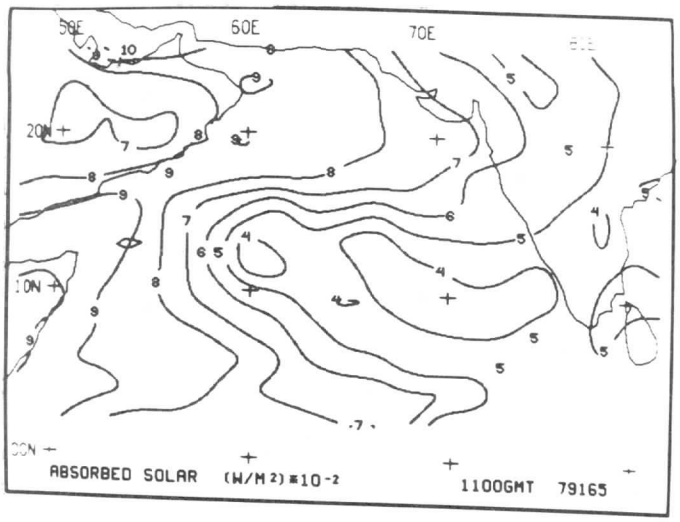
50E
60E
70E
20N
10N
0ON
ABSORBED SOLAR (W/M2)*10-2
1100GMT 79165

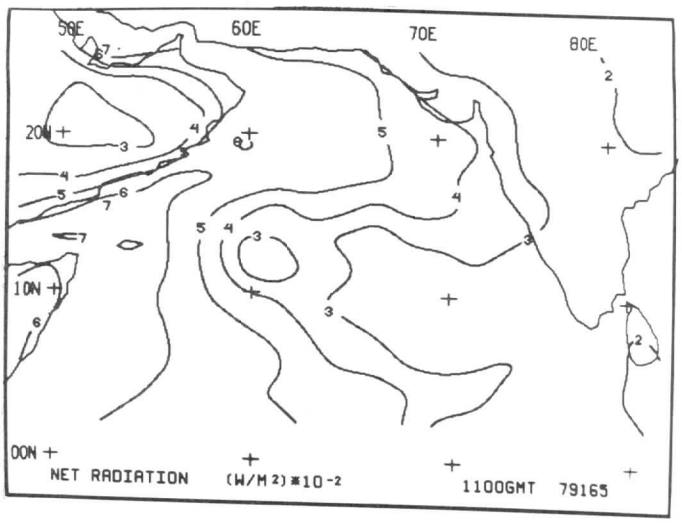
50E
60E
70E
80E
20N
10N
0ON
NET RADIATION (W/M2)*10-2
1100GMT 79165

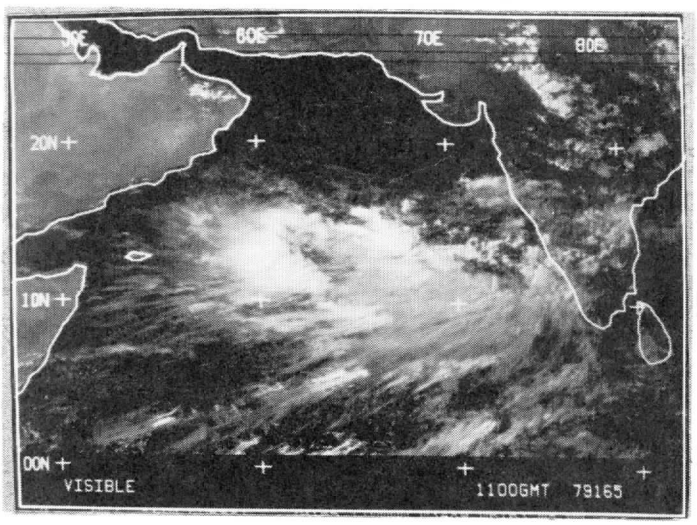
50E
60E
70E
80E
20N
10N
0ON
VISIBLE
1100GMT 79165

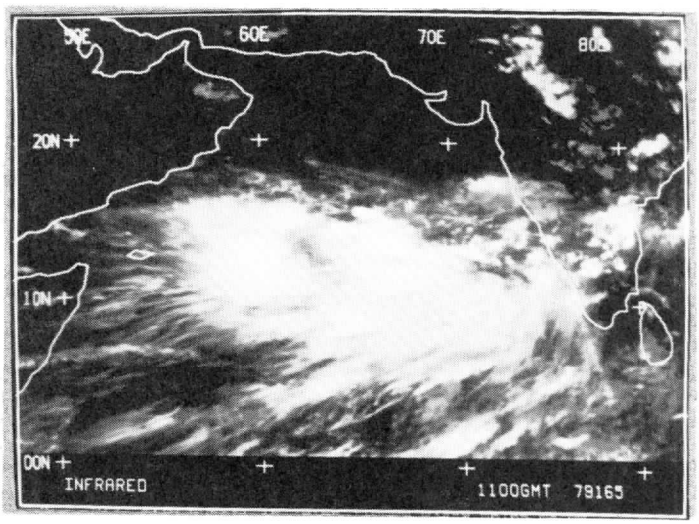
50E
60E
70E
80E
20N
10N
0ON
INFRARED
1100GMT 79165

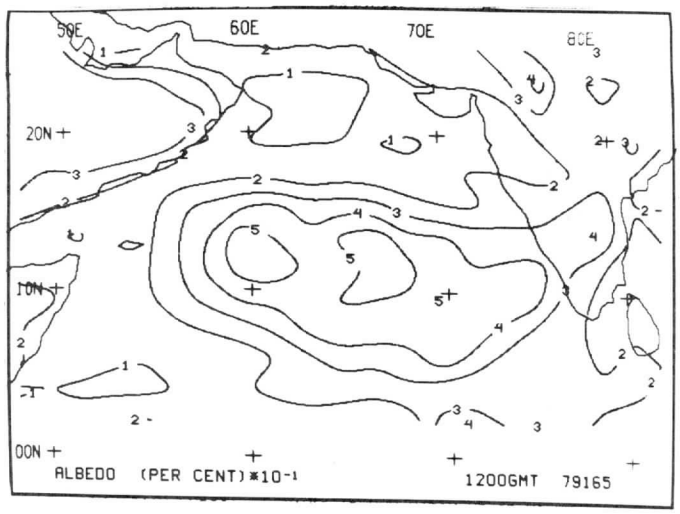
50E
60E
70E
80E
20N
10N
0ON
ALBEDO (PER CENT)*10-1
1200GMT 79165

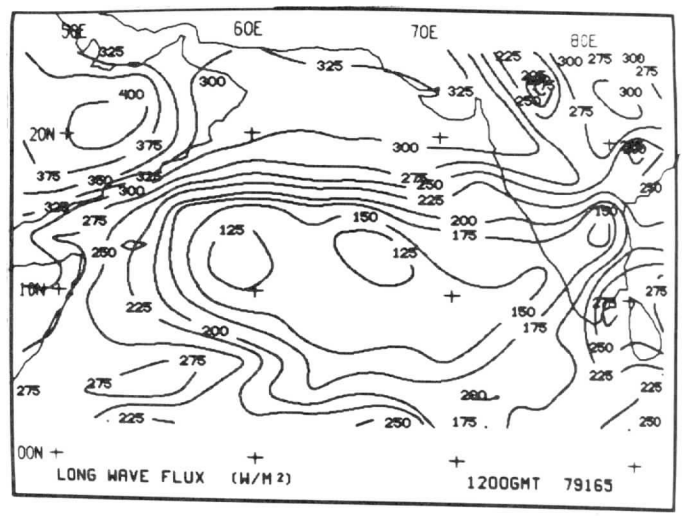
50E
60E
70E
80E
20N
10N
0ON
LONG WAVE FLUX (W/M2)
1200GMT 79165

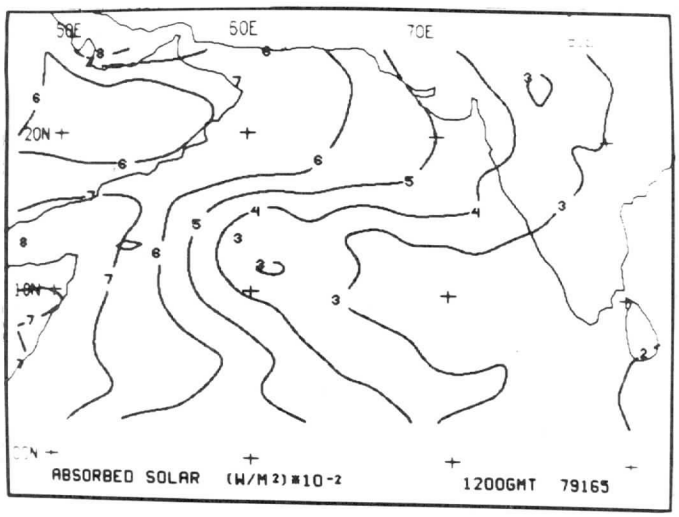
50E
60E
70E
20N
10N
ABSORBED SOLAR (W/M2)*10-2
1200GMT 79165

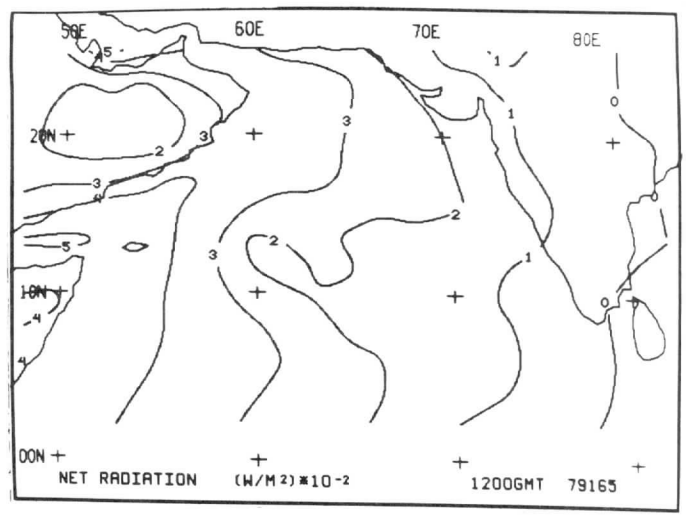
50E
60E
70E
80E
20N
10N
0ON
NET RADIATION (W/M2)*10-2
1200GMT 79165

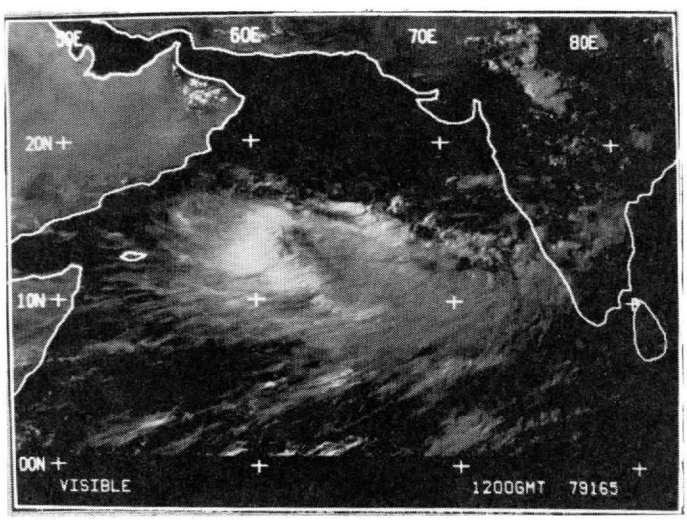
50E
60E
70E
80E
20N
10N
0ON
VISIBLE
1200GMT 79165

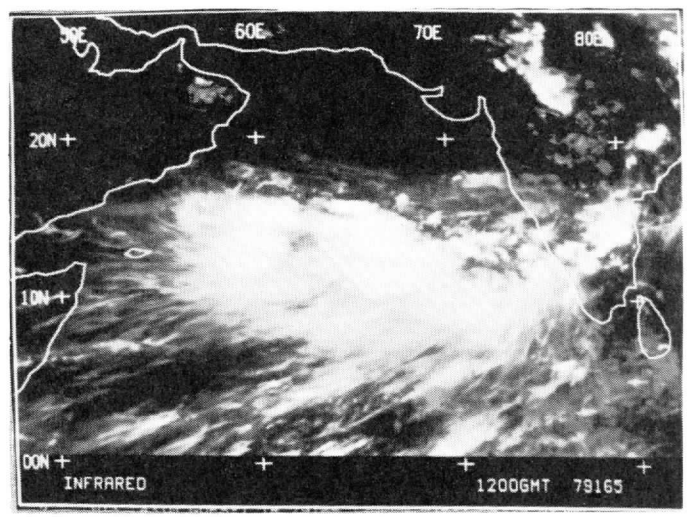
50E
60E
70E
80E
20N
10N
0ON
INFRARED
1200GMT 79165

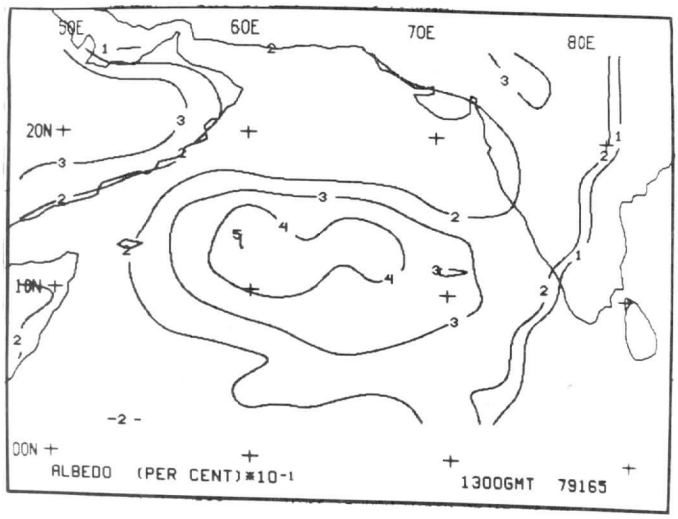
50E
60E
70E
80E
20N
10N
0ON
ALBEDO (PER CENT)*10-1
1300GMT 79165

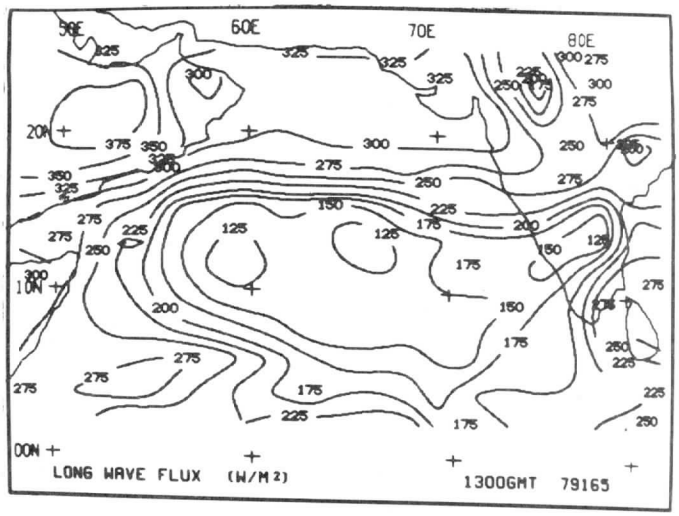
50E
60E
70E
80E
20N
10N
0ON
LONG WAVE FLUX (W/M2)
1300GMT 79165

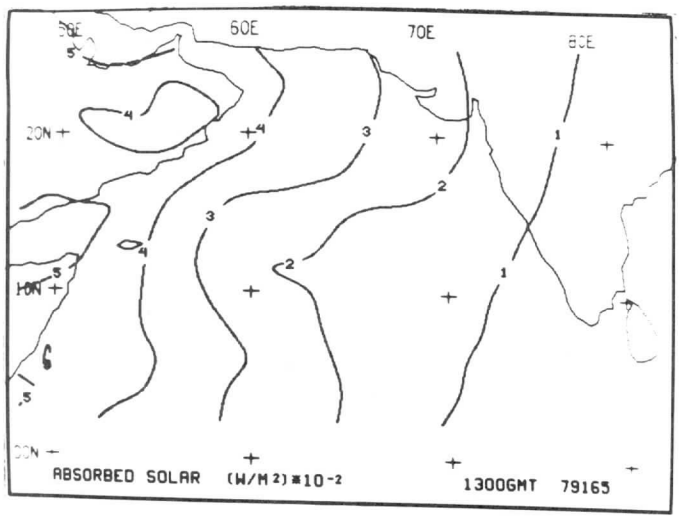
50E
60E
70E
80E
20N
10N
0ON
ABSORBED SOLAR (W/M2)*10-2
1300GMT 79165

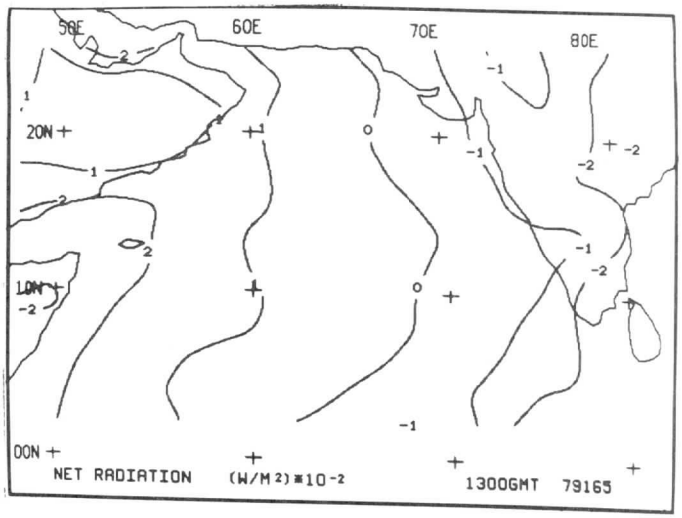
50E
60E
70E
80E
20N
10N
0ON
NET RADIATION (W/M2)*10-2
1300GMT 79165

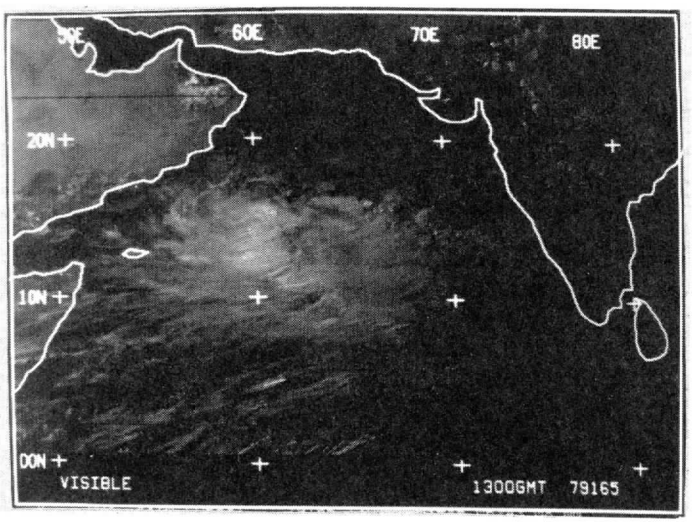
50E
60E
70E
80E
20N
10N
0ON
VISIBLE
1300GMT 79165

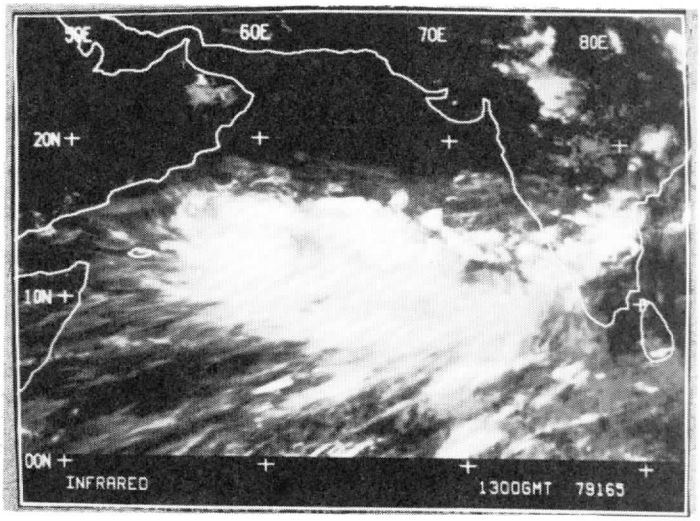
50E
60E
70E
80E
20N
10N
0ON
INFRARED
1300GMT 79165

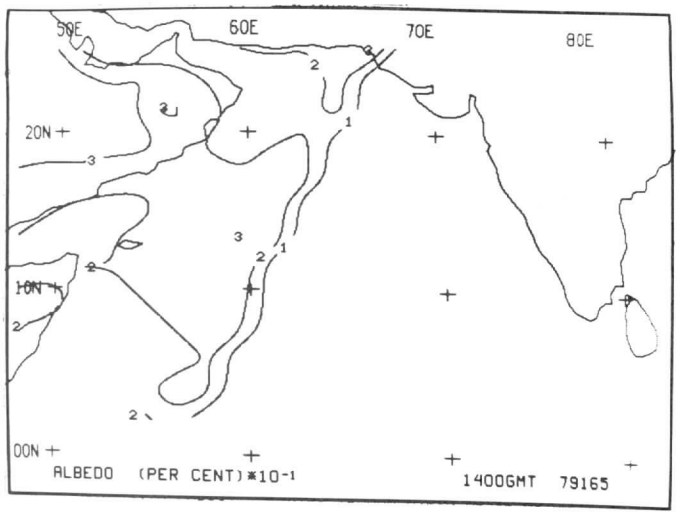
50E
60E
70E
80E
20N
10N
0ON
ALBEDO (PER CENT)*10-1
1400GMT 79165

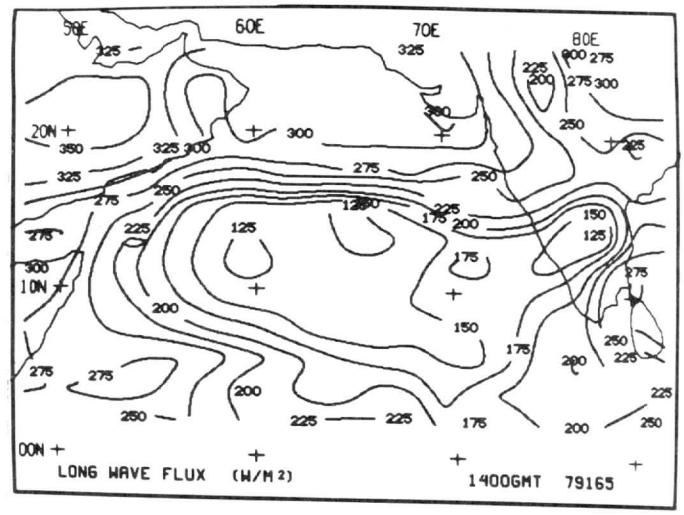
50E
60E
70E
80E
20N
10N
0ON
LONG WAVE FLUX (W/M2)
1400GMT 79165

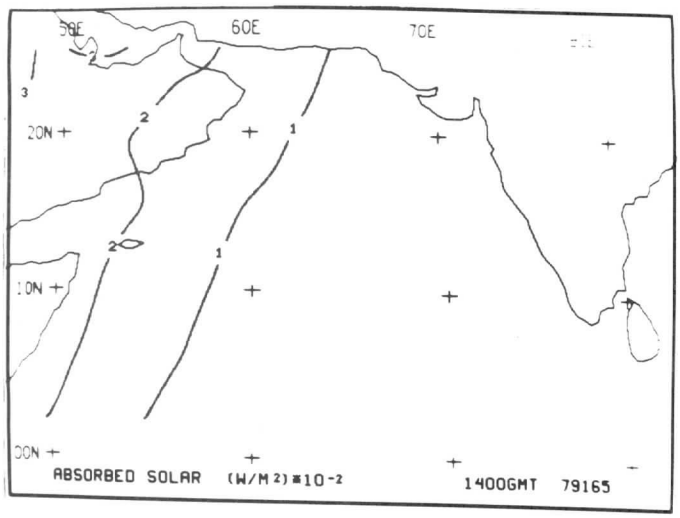
50E
60E
70E
20N
10N
0ON
ABSORBED SOLAR (W/M2)*10-2
1400GMT 79165

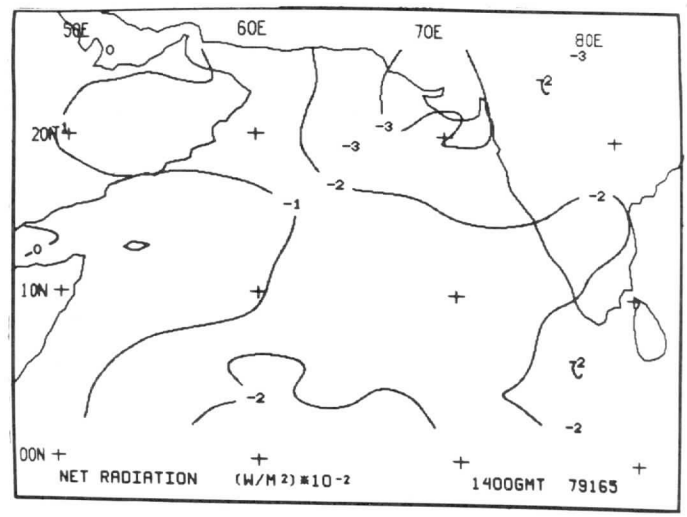
50E
60E
70E
80E
20N
10N
0ON
NET RADIATION (W/M2)*10-2
1400GMT 79165

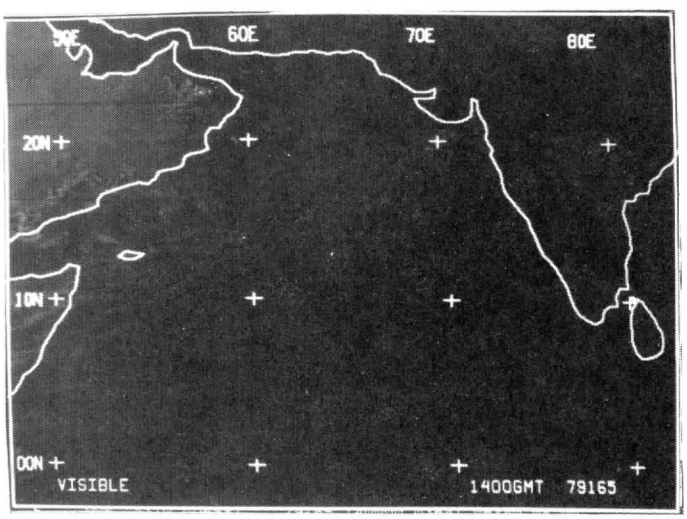
50E
60E
70E
80E
20N
10N
0ON
VISIBLE
1400GMT 79165

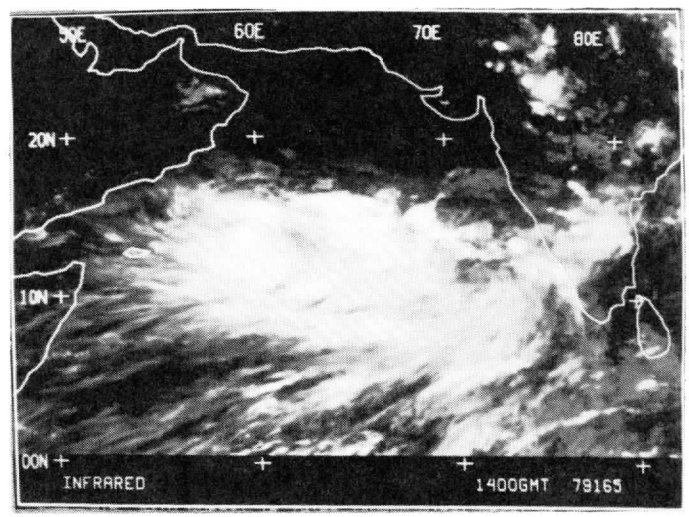
50E
60E
70E
80E
20N
10N
0ON
INFRARED
1400GMT 79165

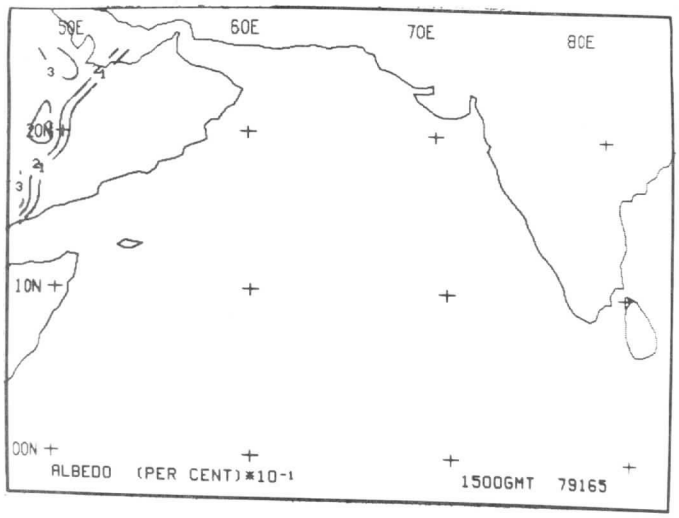
50E
60E
70E
80E
20N
10N
0ON
ALBEDO (PER CENT)*10-1
1500GMT 79165

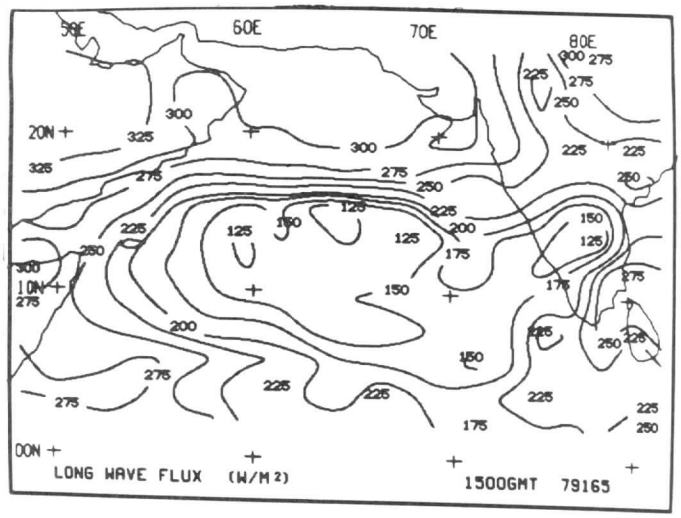
50E
60E
70E
80E
20N
10N
0ON
LONG WAVE FLUX (W/M2)
1500GMT 79165

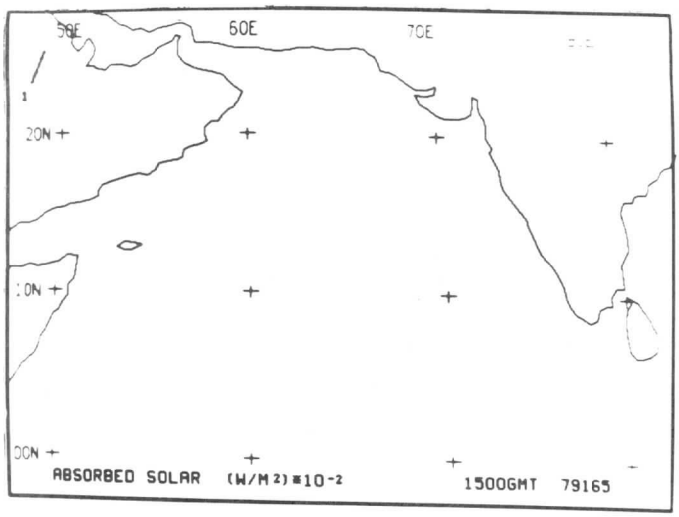
50E
60E
70E
20N
10N
0ON
ABSORBED SOLAR (W/M2)*10-2
1500GMT 79165

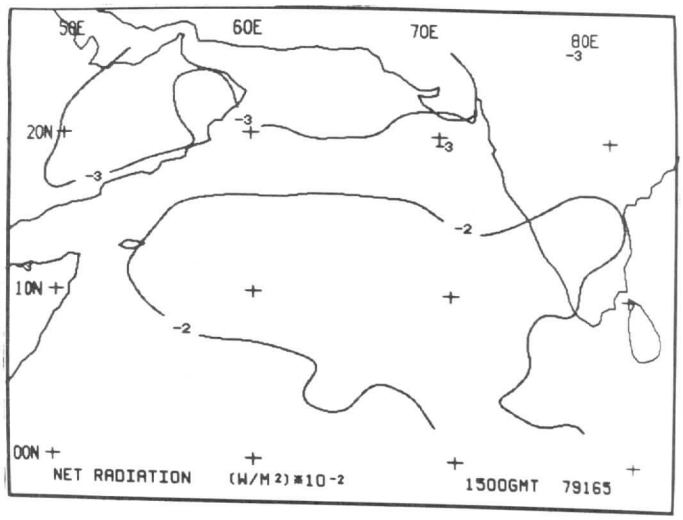
50E
60E
70E
80E
20N
10N
0ON
NET RADIATION (W/M2)*10-2
1500GMT 79165

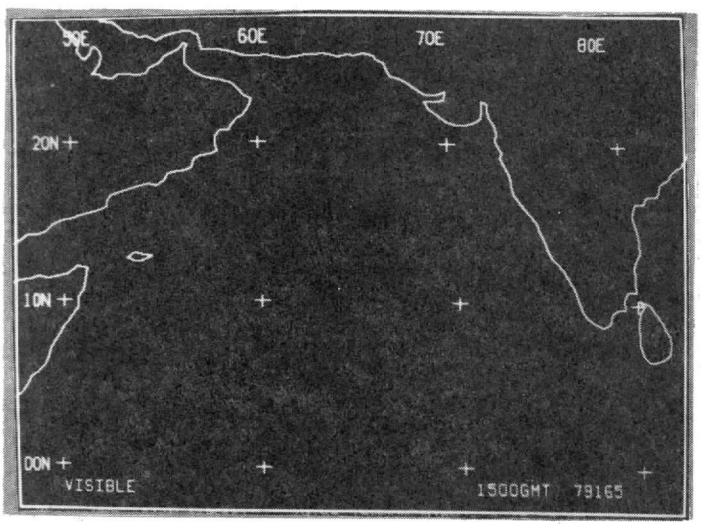
50E
60E
70E
80E
20N
10N
0ON
VISIBLE
1500GMT 79165

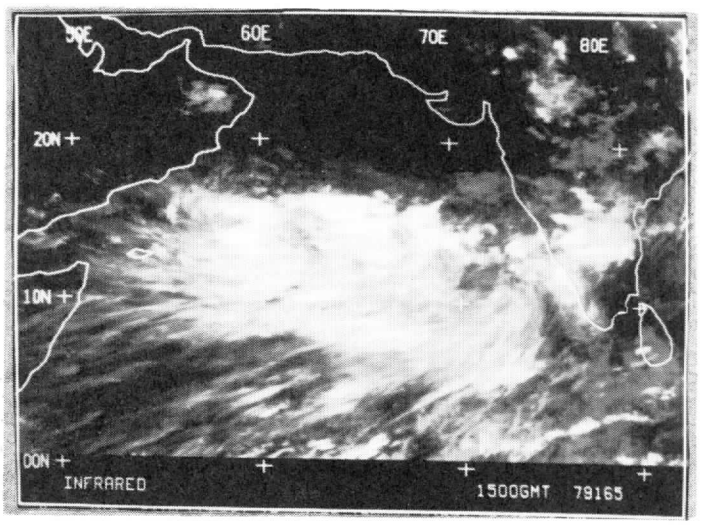
50E
60E
70E
80E
20N
10N
0ON
INFRARED
1500GMT 79165

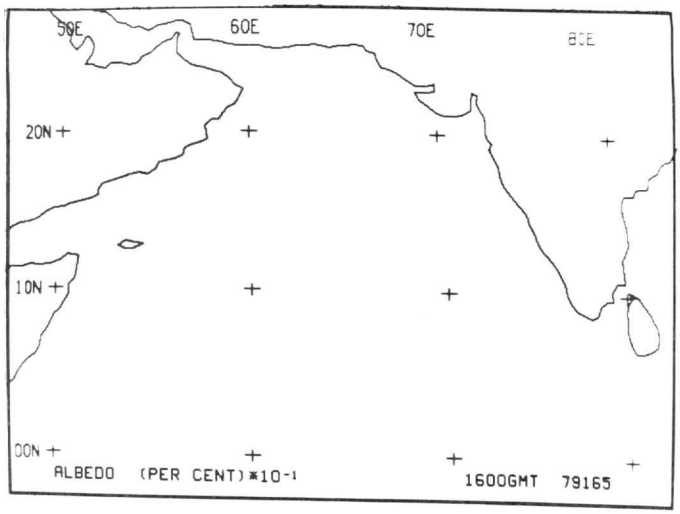
50E
60E
70E
80E
20N
10N
0ON
ALBEDO (PER CENT)*10-1
1600GMT 79165

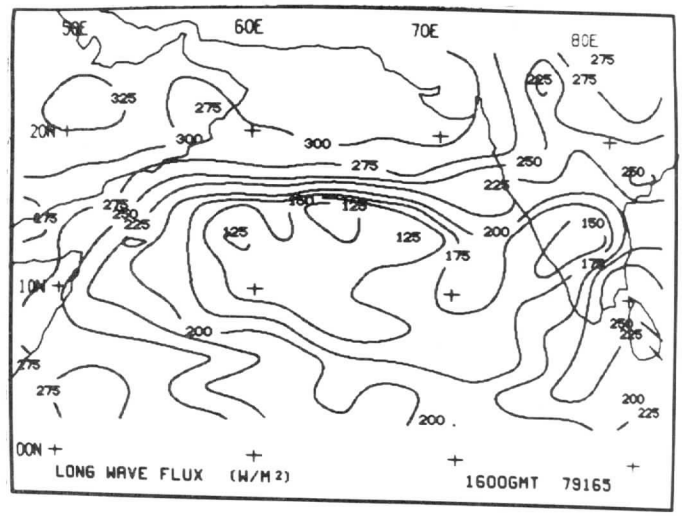
50E
60E
70E
80E
20N
10N
0ON
LONG WAVE FLUX (W/M2)
1600GMT 79165

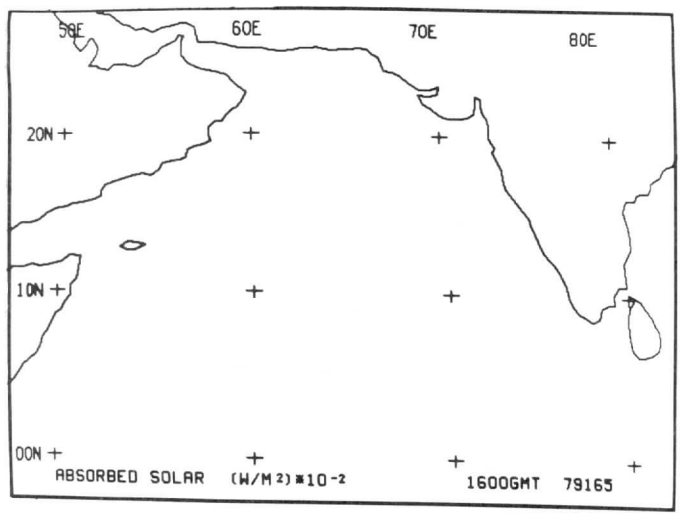
50E
60E
70E
80E
20N
10N
0ON
ABSORBED SOLAR (W/M2)*10-2
1600GMT 79165

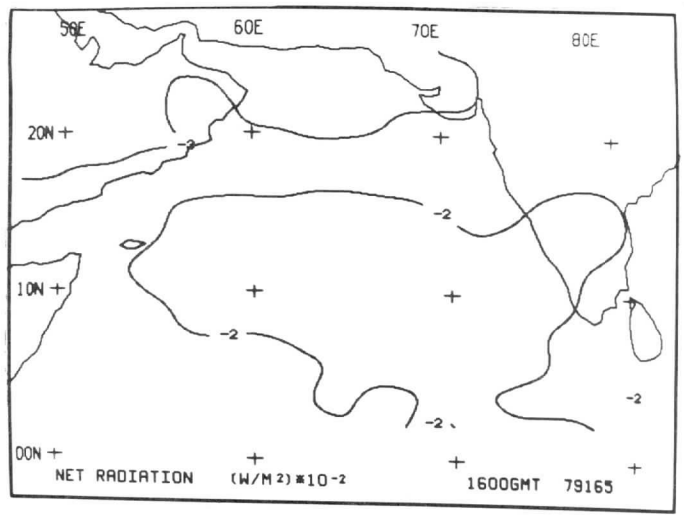
50E
60E
70E
80E
20N
10N
0ON
NET RADIATION (W/M2)*10-2
1600GMT 79165

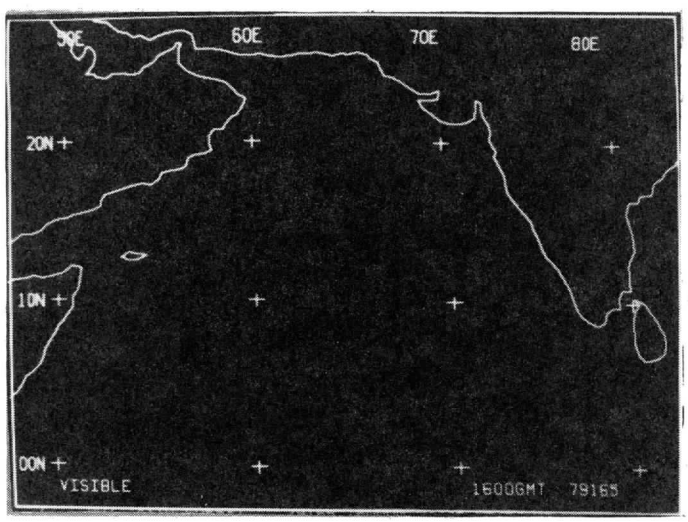
50E
60E
70E
80E
20N
10N
0ON
VISIBLE
1600GMT 79165

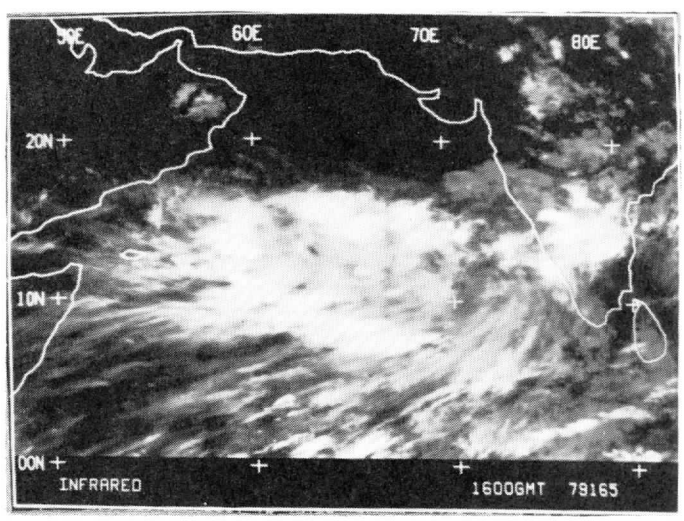
50E
60E
70E
80E
20N
10N
0ON
INFRARED
1600GMT 79165

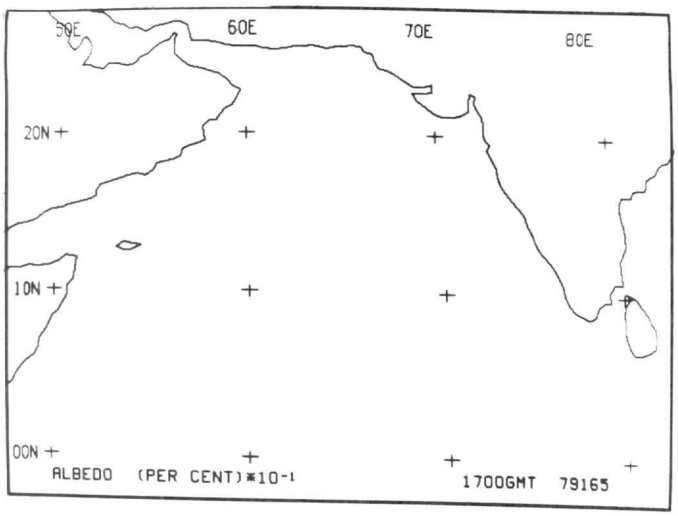
50E
60E
70E
80E
20N
10N
00N
ALBEDO (PER CENT)*10-1
1700GMT 79165

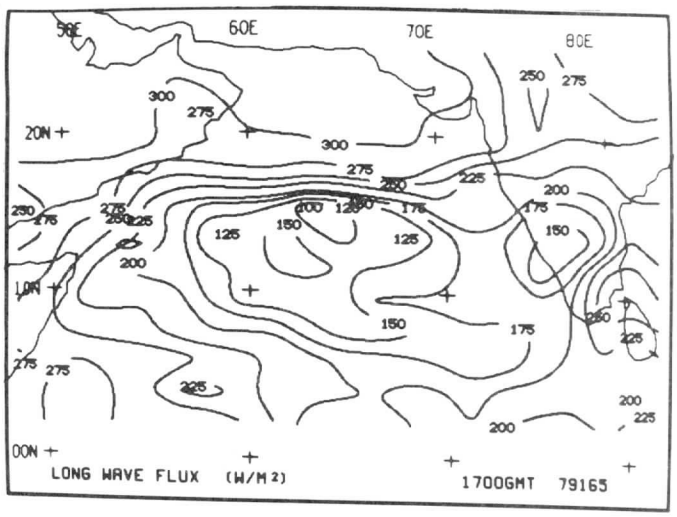
50E
60E
70E
80E
20N
10N
00N
LONG WAVE FLUX (W/M2)
1700GMT 79165

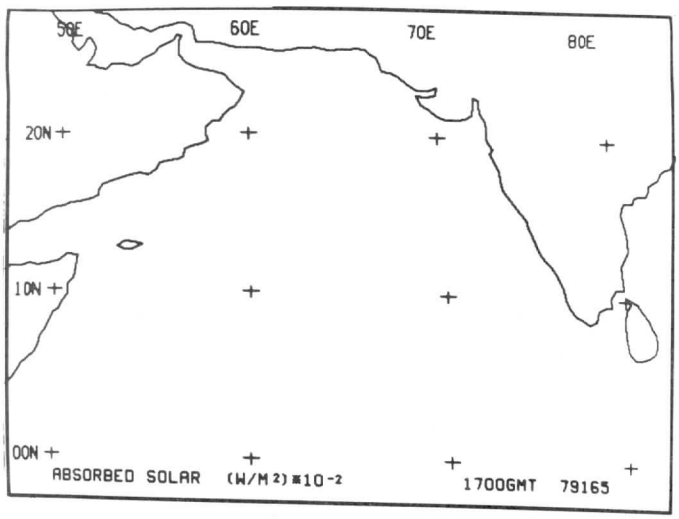
50E
60E
70E
80E
20N
10N
00N
ABSORBED SOLAR (W/M2)*10-2
1700GMT 79165

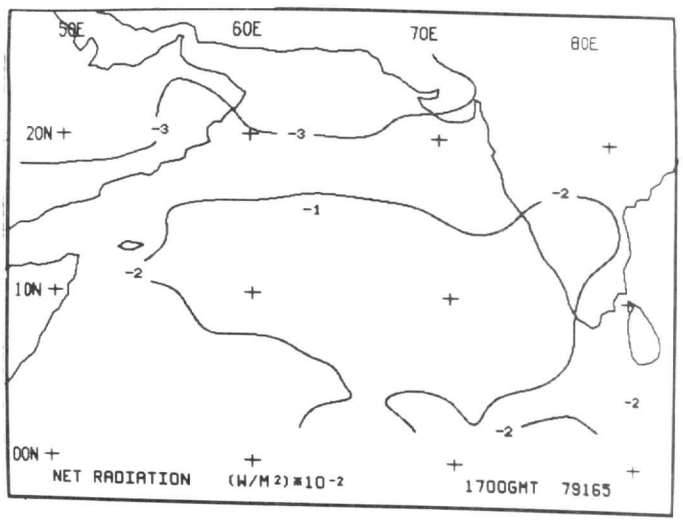
50E
60E
70E
80E
20N
10N
00N
NET RADIATION (W/M2)*10-2
1700GMT 79165

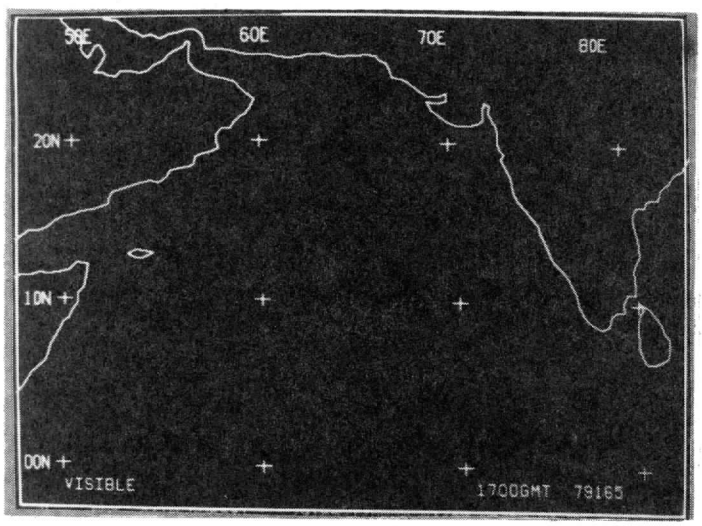
50E
60E
70E
80E
20N
10N
00N
VISIBLE
1700GMT 79165

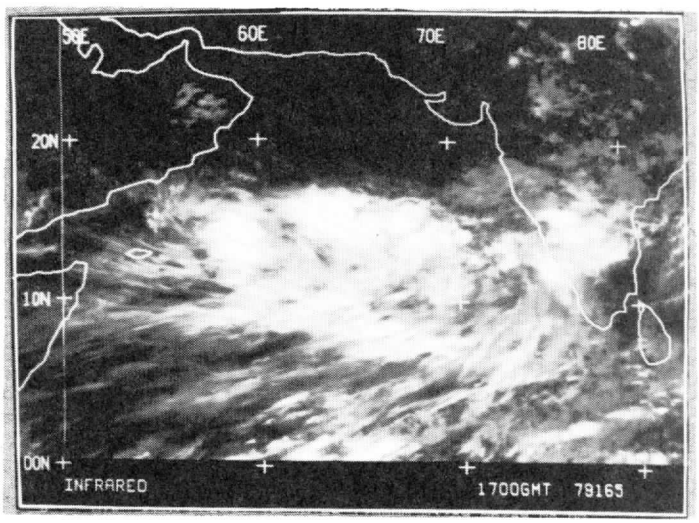
50E
60E
70E
80E
20N
10N
00N
INFRARED
1700GMT 79165

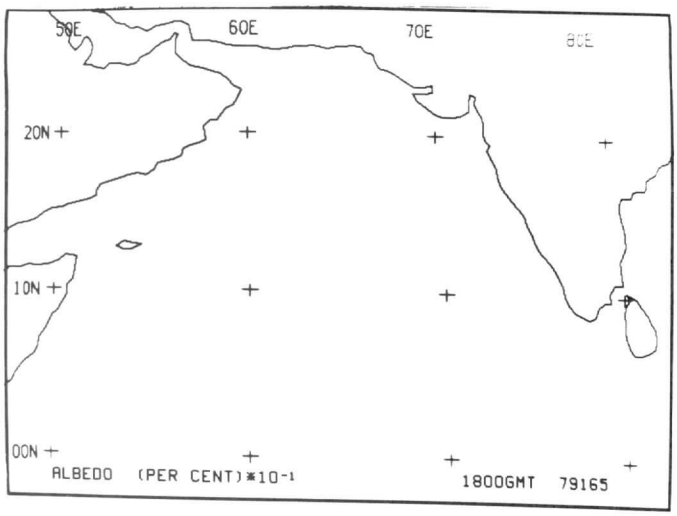
50E
60E
70E
80E
20N
10N
0ON
ALBEDO (PER CENT)*10-1
1800GMT 79165

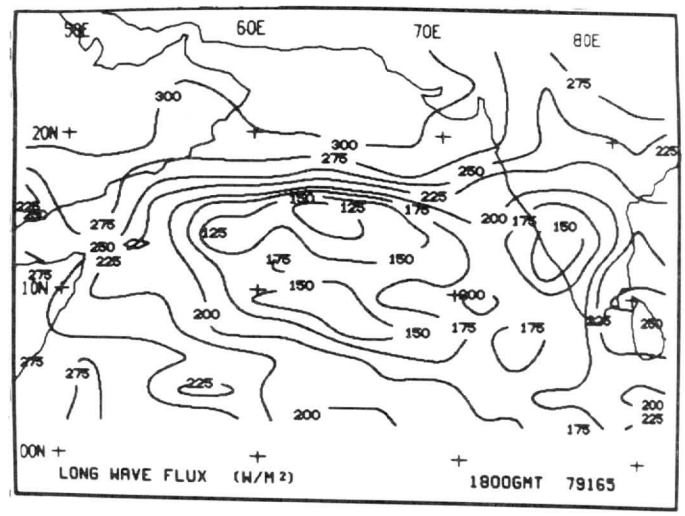
50E
60E
70E
80E
20N
10N
0ON
LONG WAVE FLUX (W/M2)
1800GMT 79165

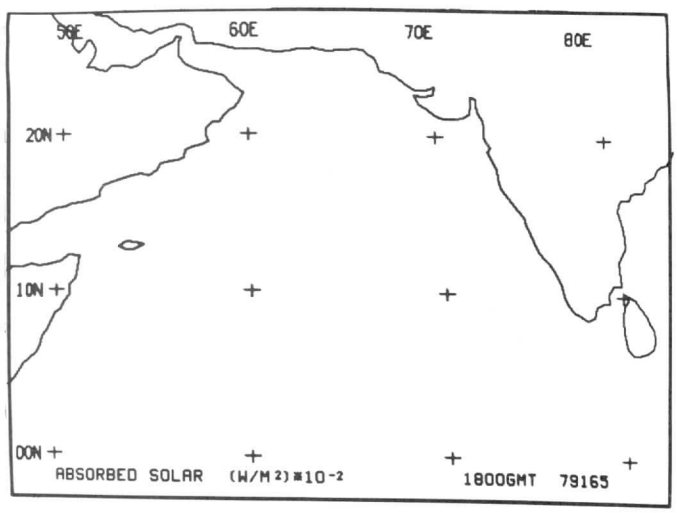
50E
60E
70E
80E
20N
10N
0ON
ABSORBED SOLAR (W/M2)*10-2
1800GMT 79165

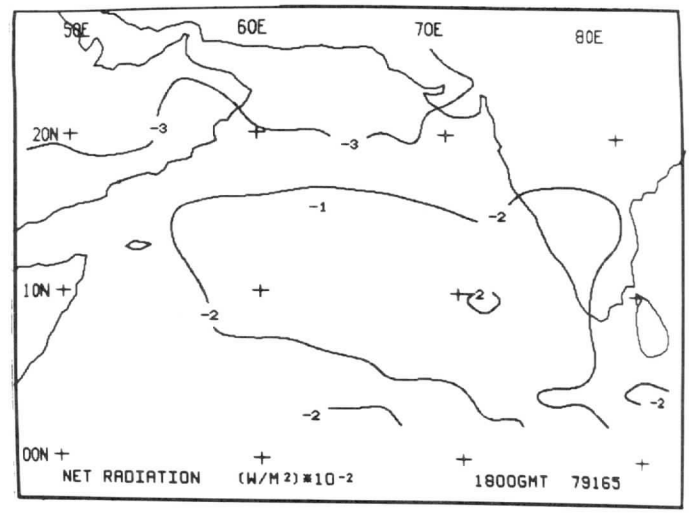
50E
60E
70E
80E
20N
10N
0ON
NET RADIATION (W/M2)*10-2
1800GMT 79165

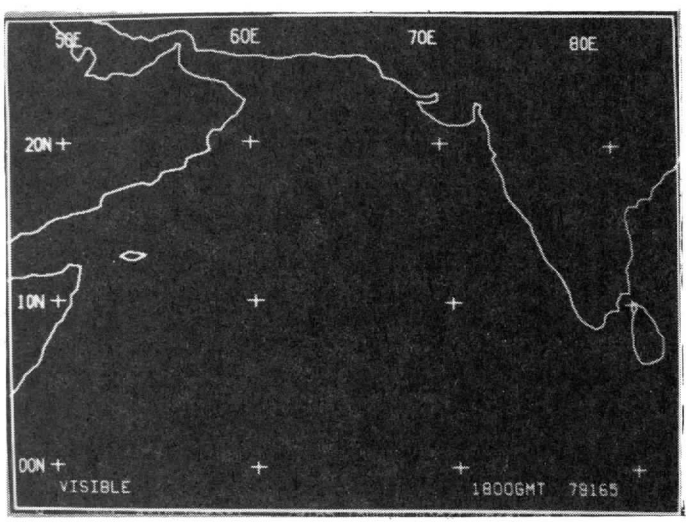
50E
60E
70E
80E
20N
10N
0ON
VISIBLE
1800GMT 79165

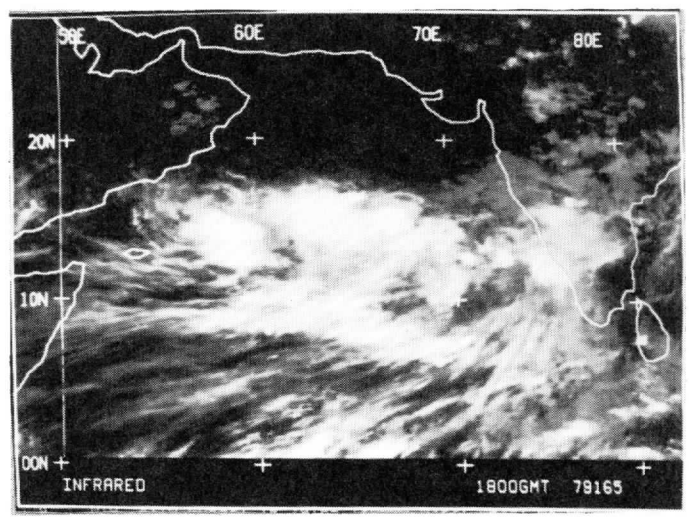
50E
60E
70E
80E
20N
10N
0ON
INFRARED
1800GMT 79165

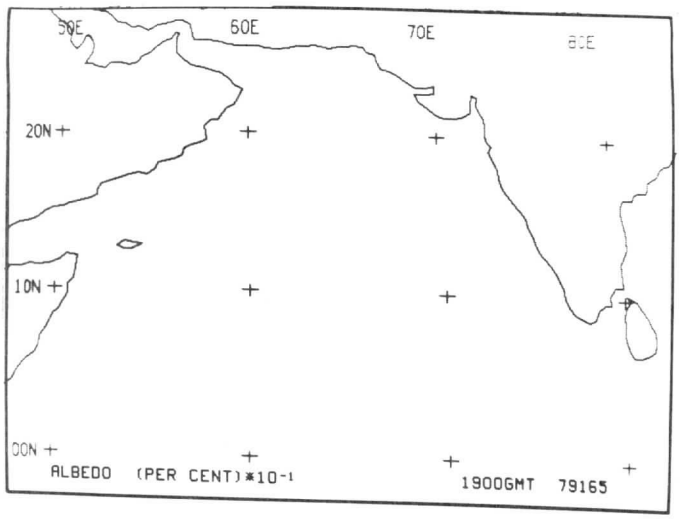
50E
60E
70E
80E
20N
10N
0ON
ALBEDO (PER CENT)*10-1
1900GMT 79165

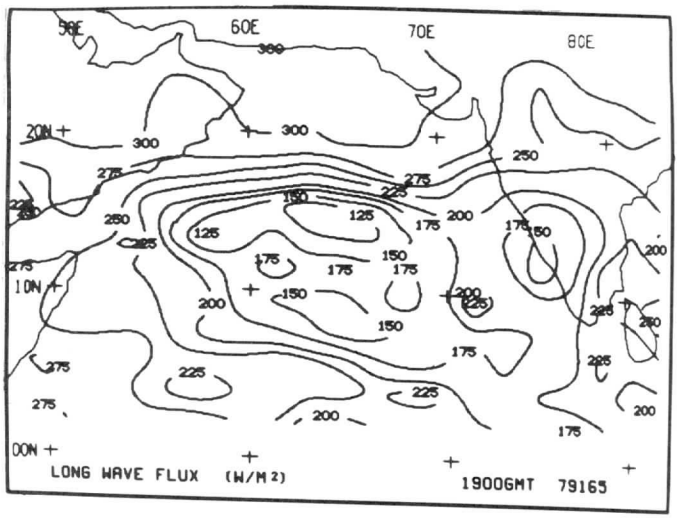
50E
60E
70E
80E
20N
10N
0ON
LONG WAVE FLUX (W/M2)
1900GMT 79165

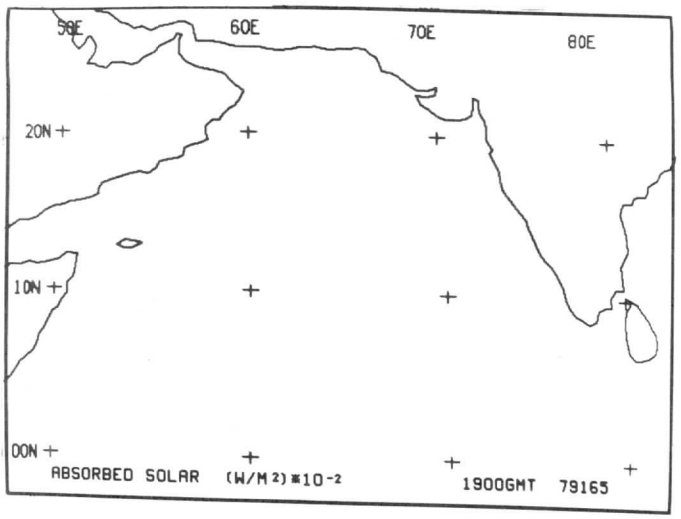
50E
60E
70E
80E
20N
10N
0ON
ABSORBED SOLAR (W/M2)*10-2
1900GMT 79165

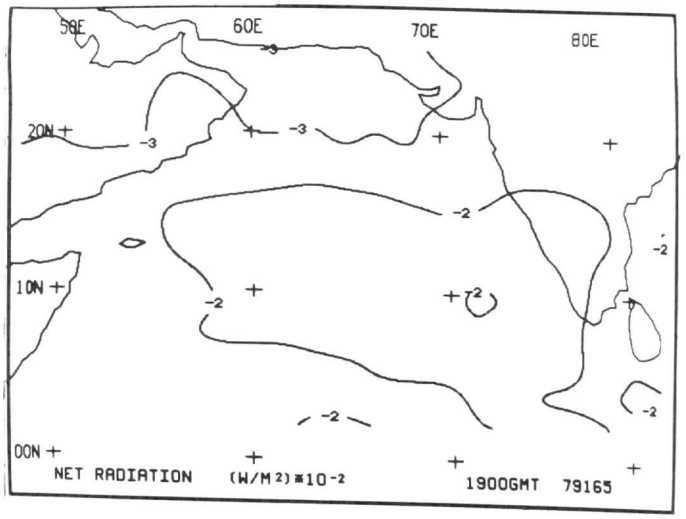
50E
60E
70E
80E
20N
10N
0ON
NET RADIATION (W/M2)*10-2
1900GMT 79165

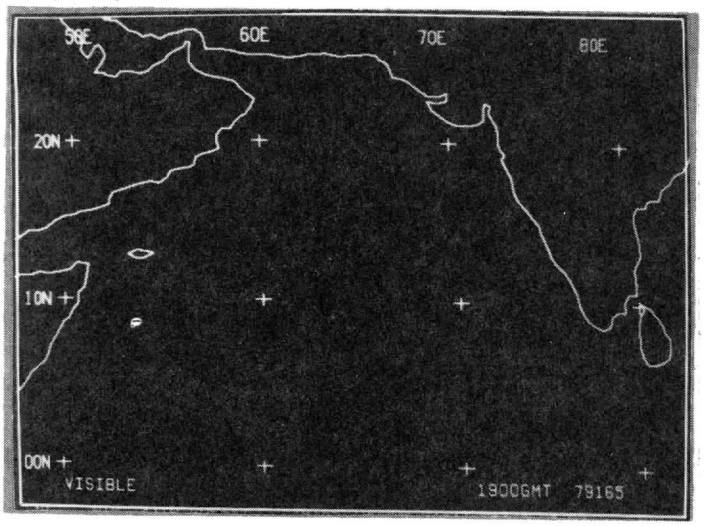
50E
60E
70E
80E
20N
10N
0ON
VISIBLE
1900GMT 79165

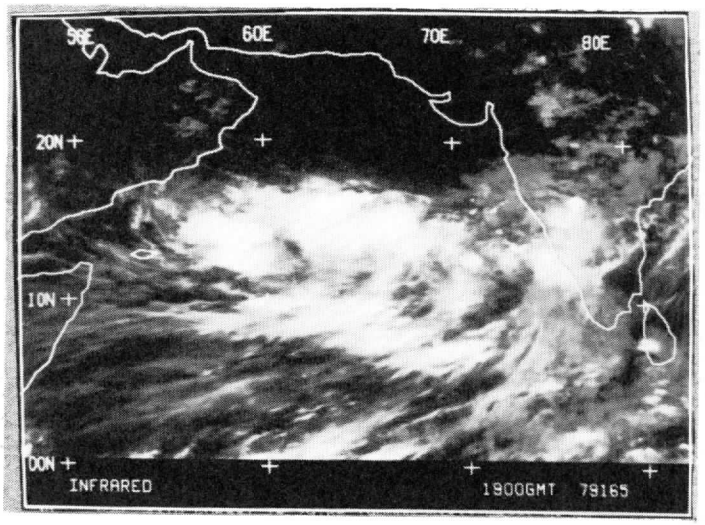
50E
60E
70E
80E
20N
10N
0ON
INFRARED
1900GMT 79165

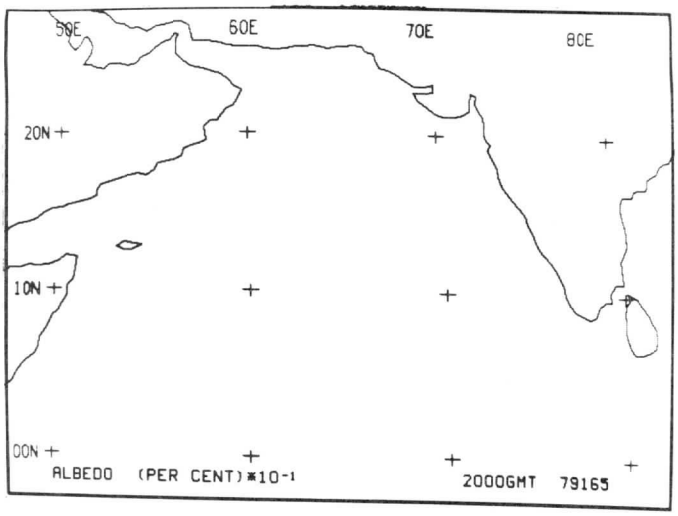
50E
60E
70E
80E
20N
10N
00N
ALBEDO (PER CENT)*10-1
2000GMT 79165

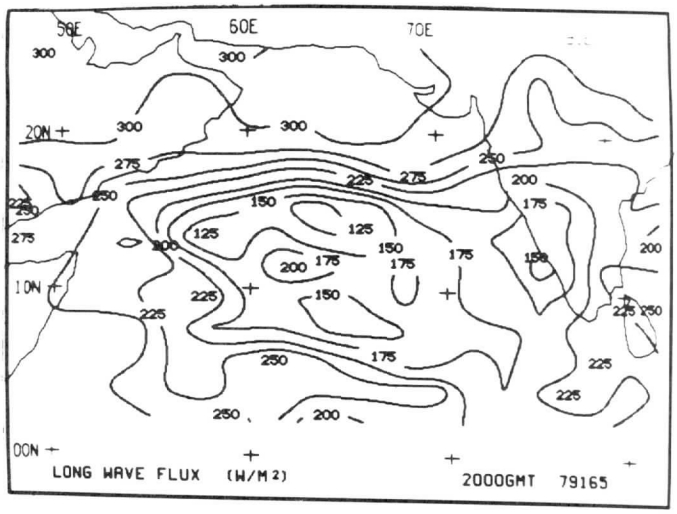
50E
60E
70E
20N
10N
00N
LONG WAVE FLUX (W/M2)
2000GMT 79165

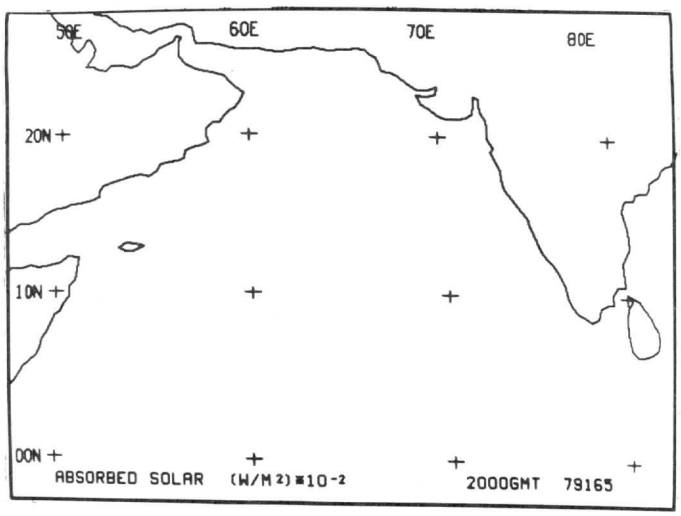
50E
60E
70E
80E
20N
10N
00N
ABSORBED SOLAR (W/M2)*10-2
2000GMT 79165

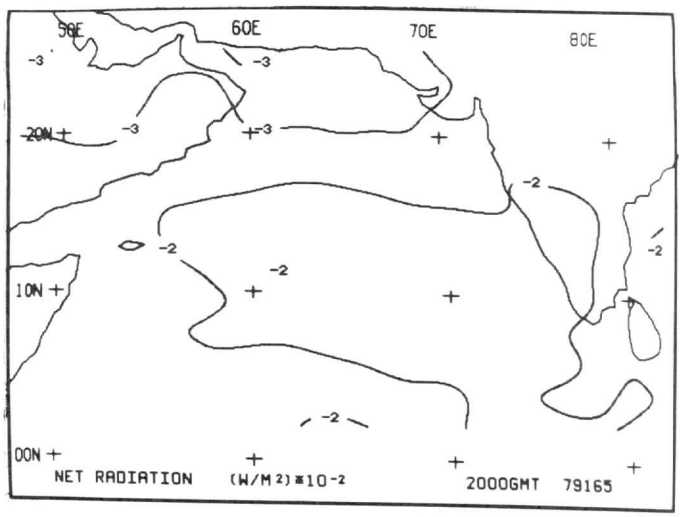
50E
60E
70E
80E
20N
10N
00N
NET RADIATION (W/M2)*10-2
2000GMT 79165

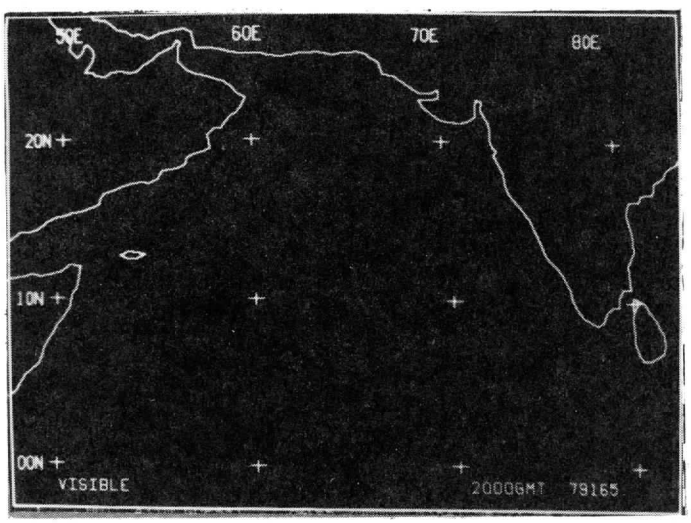
50E
60E
70E
80E
20N
10N
00N
VISIBLE
2000GMT 79165

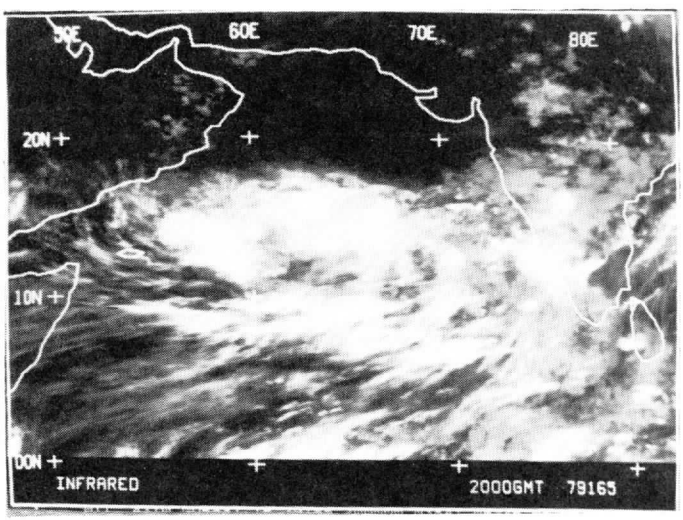
50E
60E
70E
80E
20N
10N
00N
INFRARED
2000GMT 79165

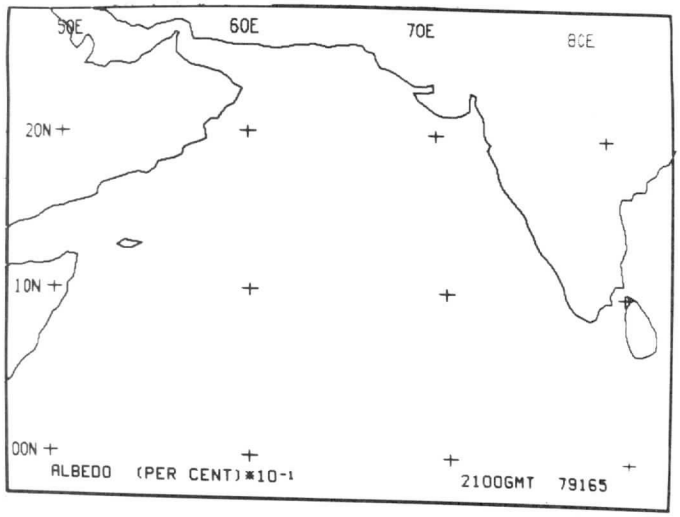
50E
60E
70E
80E
20N
10N
0ON
ALBEDO (PER CENT)*10-1
2100GMT 79165

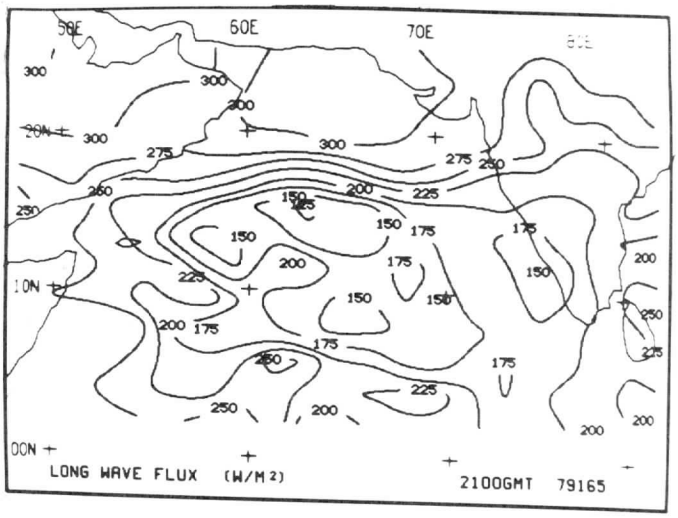
50E
60E
70E
80E
20N
10N
0ON
LONG WAVE FLUX (W/M2)
2100GMT 79165

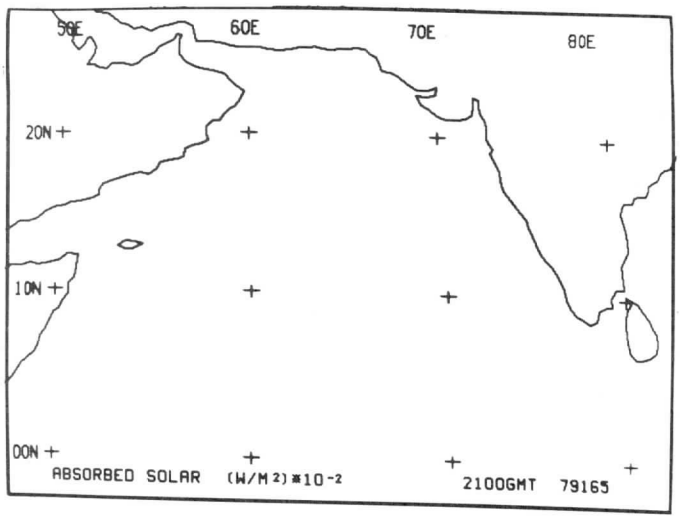
50E
60E
70E
80E
20N
10N
0ON
ABSORBED SOLAR (W/M2)*10-2
2100GMT 79165

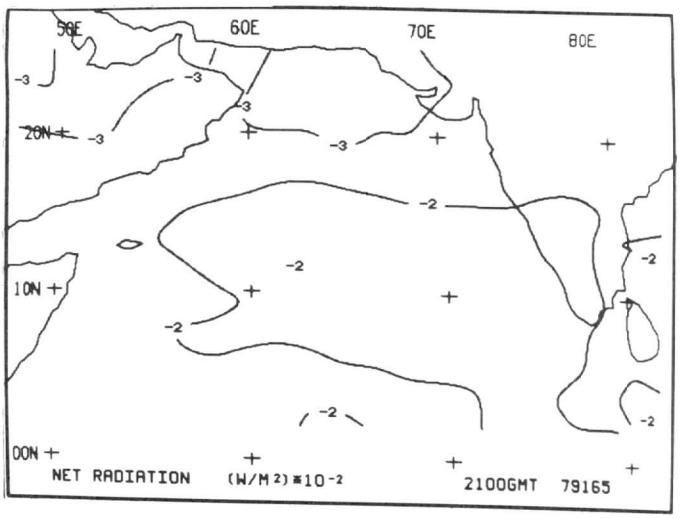
50E
60E
70E
80E
20N
10N
0ON
NET RADIATION (W/M2)*10-2
2100GMT 79165

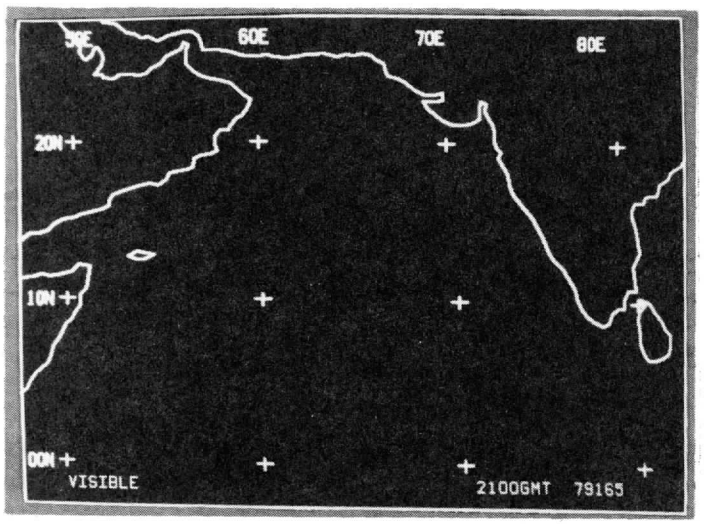
50E
60E
70E
80E
20N
10N
0ON
VISIBLE
2100GMT 79165

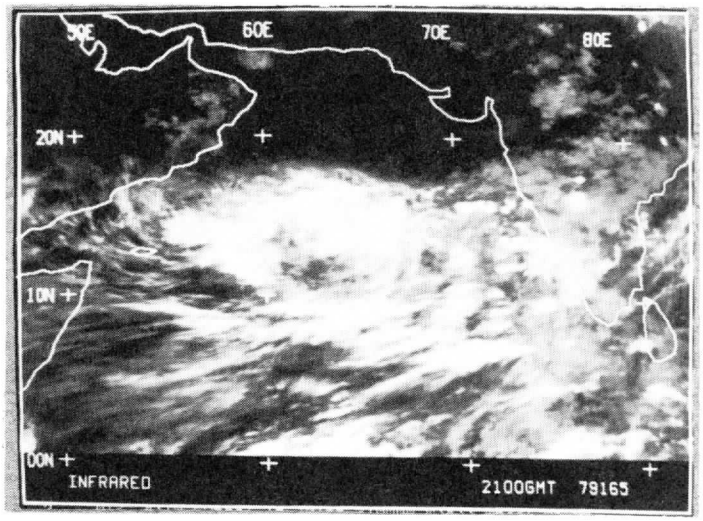
50E
60E
70E
80E
20N
10N
0ON
INFRARED
2100GMT 79165

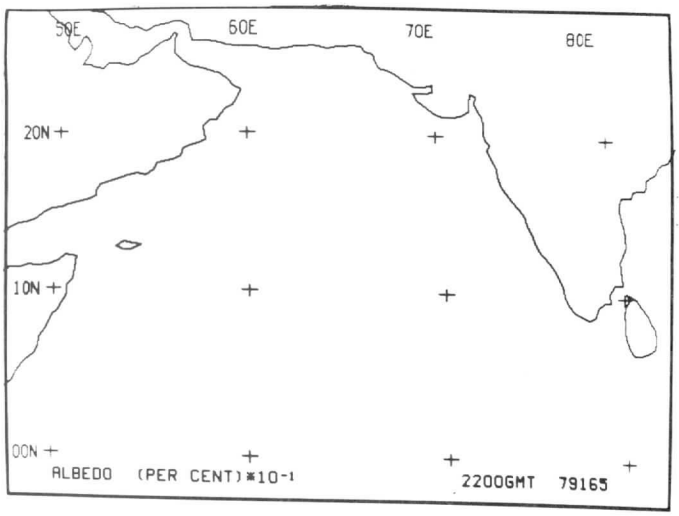
50E
60E
70E
80E
20N
10N
0ON
ALBEDO (PER CENT)*10-1
2200GMT 79165

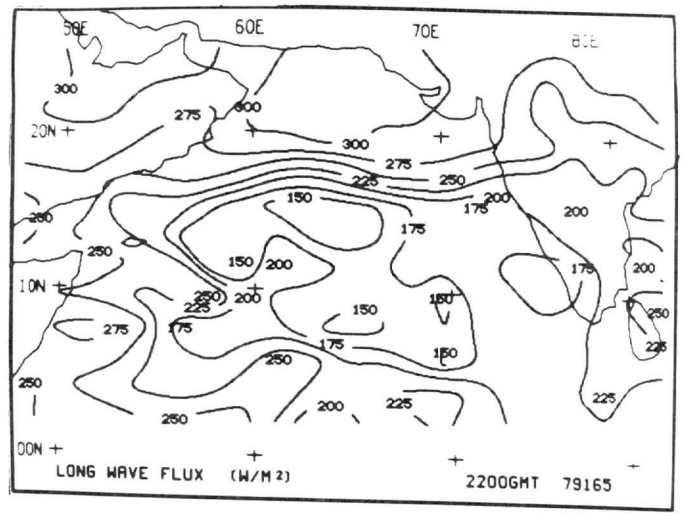
50E
60E
70E
80E
20N
10N
0ON
LONG WAVE FLUX (W/M2)
2200GMT 79165

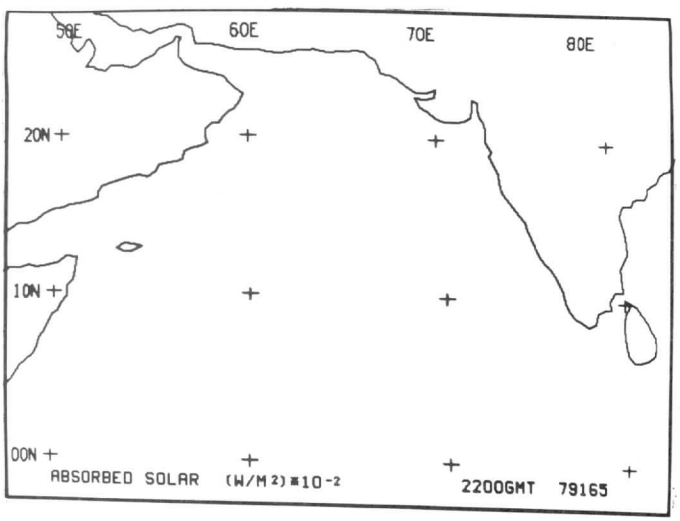
50E
60E
70E
80E
20N
10N
0ON
ABSORBED SOLAR (W/M2)*10-2
2200GMT 79165

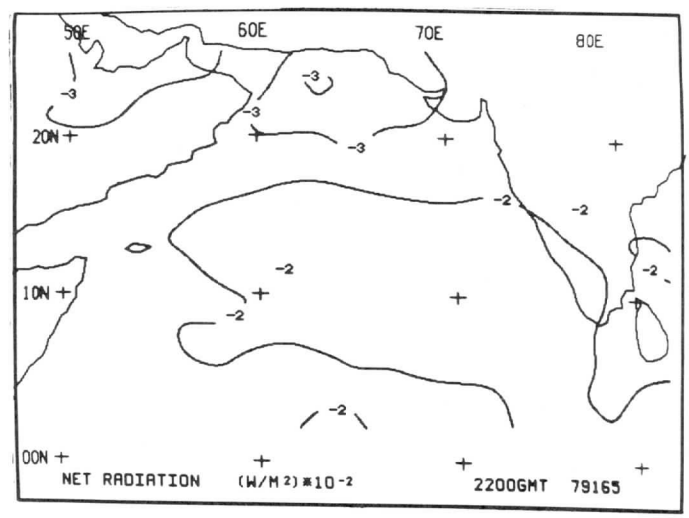
50E
60E
70E
80E
20N
10N
0ON
NET RADIATION (W/M2)*10-2
2200GMT 79165

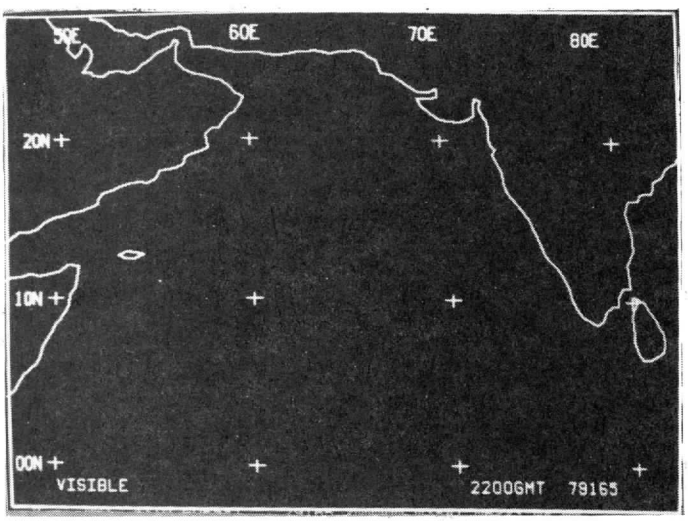
50E
60E
70E
80E
20N
10N
0ON
VISIBLE
2200GMT 79165

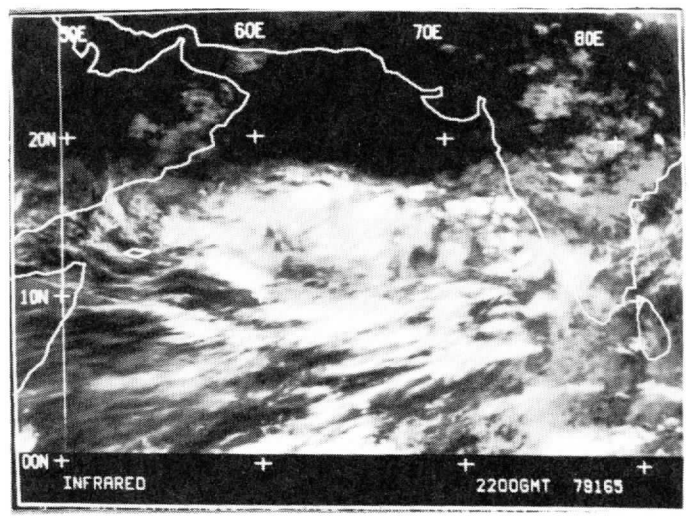
50E
60E
70E
80E
20N
10N
0ON
INFRARED
2200GMT 79165

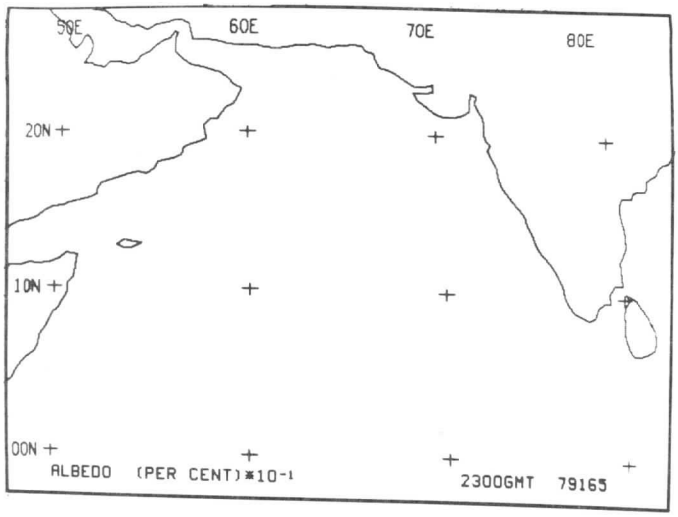
50E
60E
70E
80E
20N
10N
0ON
ALBEDO (PER CENT)*10-1
2300GMT 79165

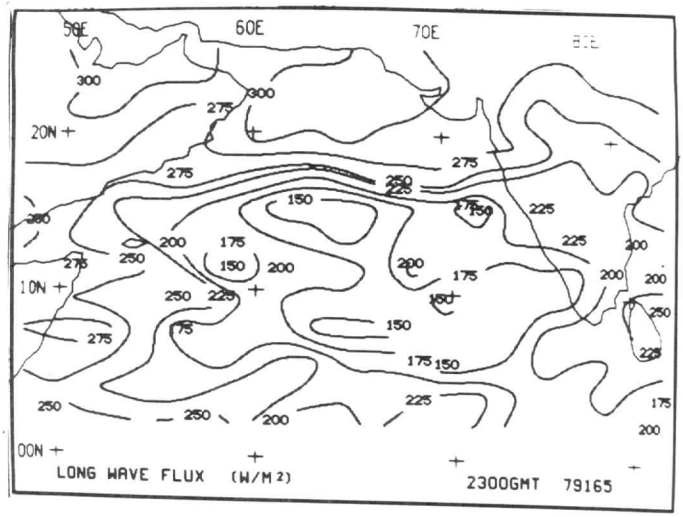
50E
60E
70E
80E
20N
10N
0ON
LONG WAVE FLUX (W/M2)
2300GMT 79165

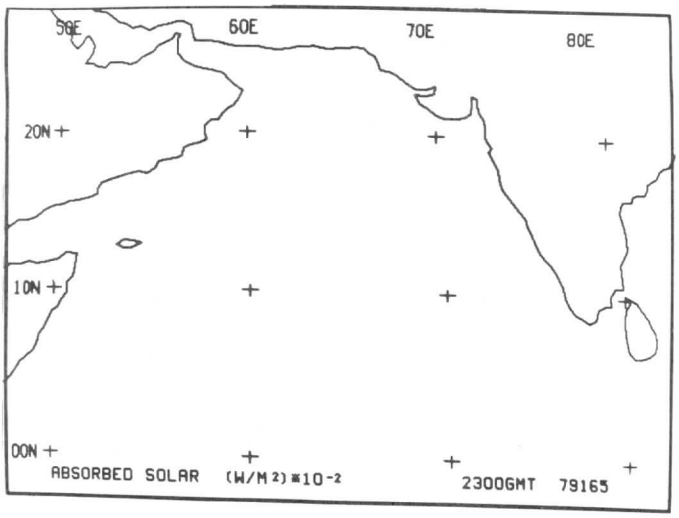
50E
60E
70E
80E
20N
10N
0ON
ABSORBED SOLAR (W/M2)*10-2
2300GMT 79165

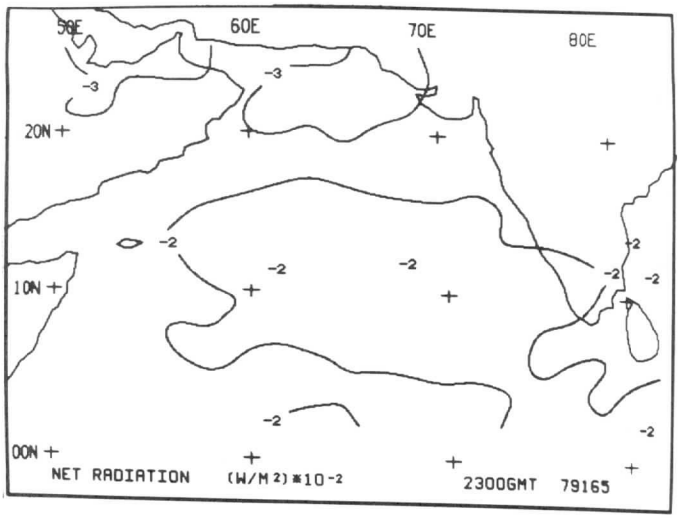
50E
60E
70E
80E
20N
10N
0ON
NET RADIATION (W/M2)*10-2
2300GMT 79165

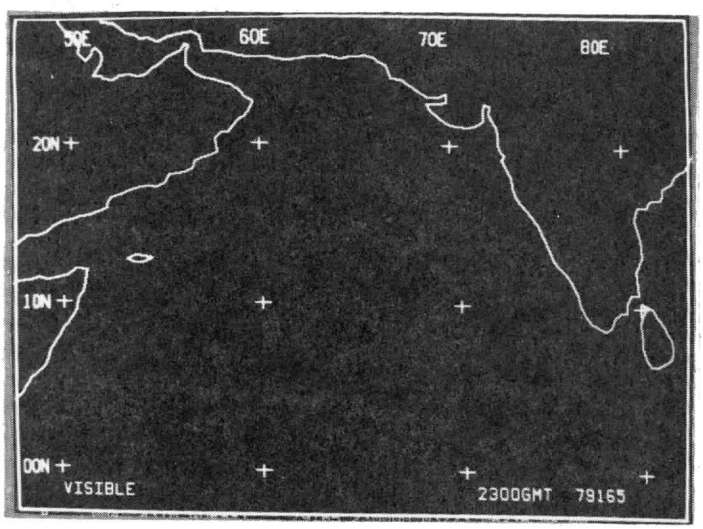
50E
60E
70E
80E
20N
10N
0ON
VISIBLE
2300GMT 79165

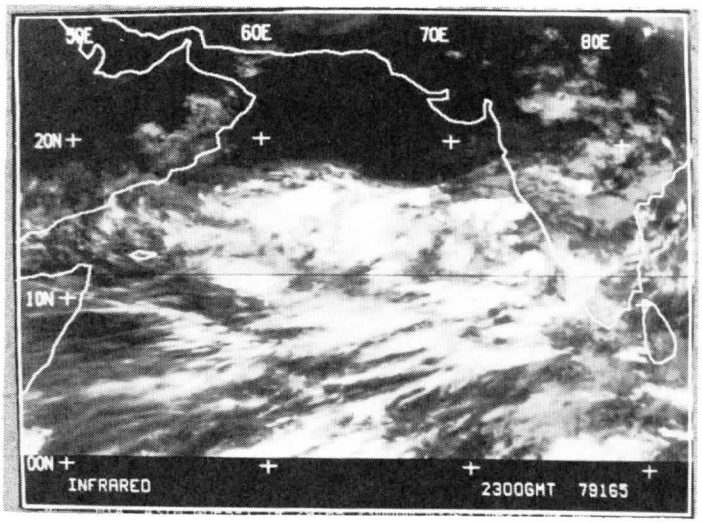
50E
60E
70E
80E
20N
10N
0ON
INFRARED
2300GMT 79165

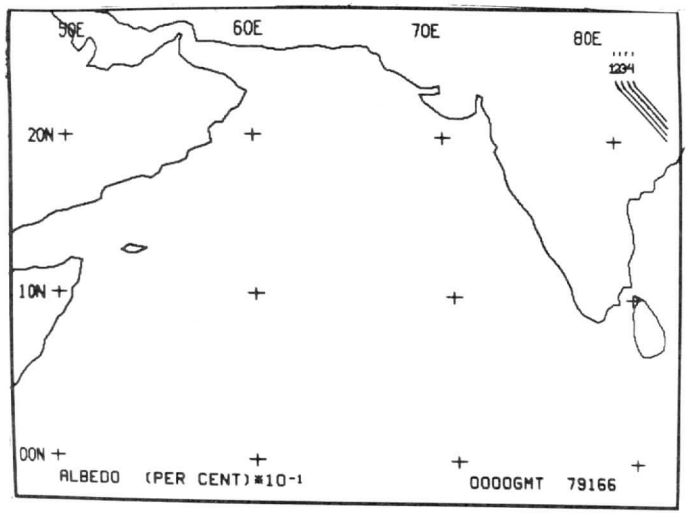
50E
60E
70E
80E
20N
10N
00N
ALBEDO (PER CENT)*10-1
0000GMT 79166

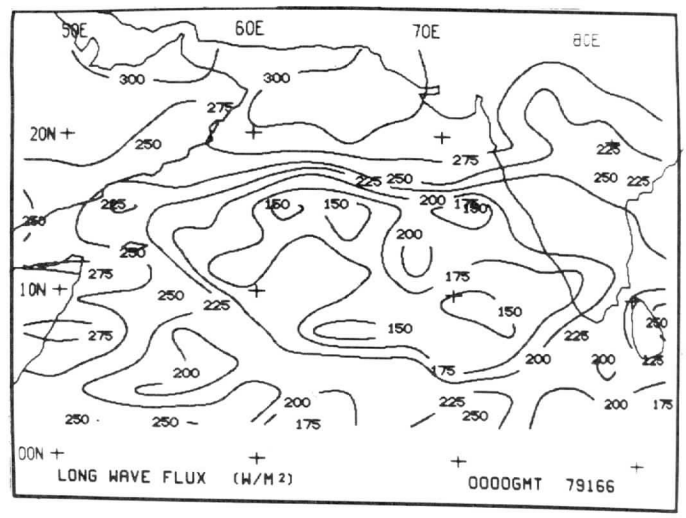
50E
60E
70E
80E
20N
10N
00N
LONG WAVE FLUX (W/M2)
0000GMT 79166

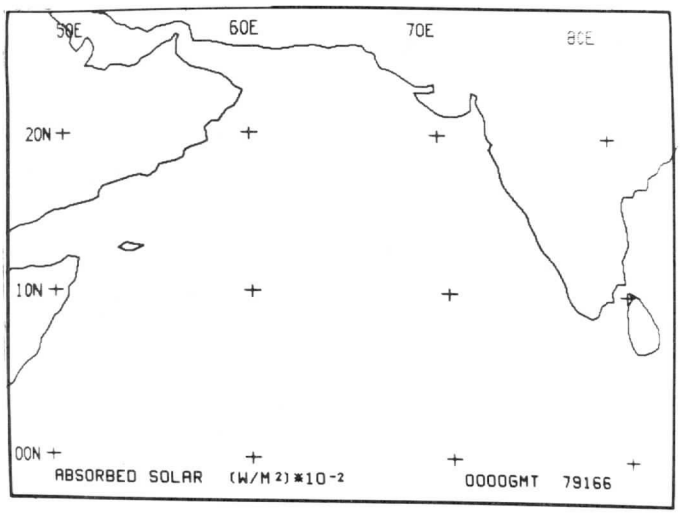
50E
60E
70E
80E
20N
10N
00N
ABSORBED SOLAR (W/M2)*10-2
0000GMT 79166

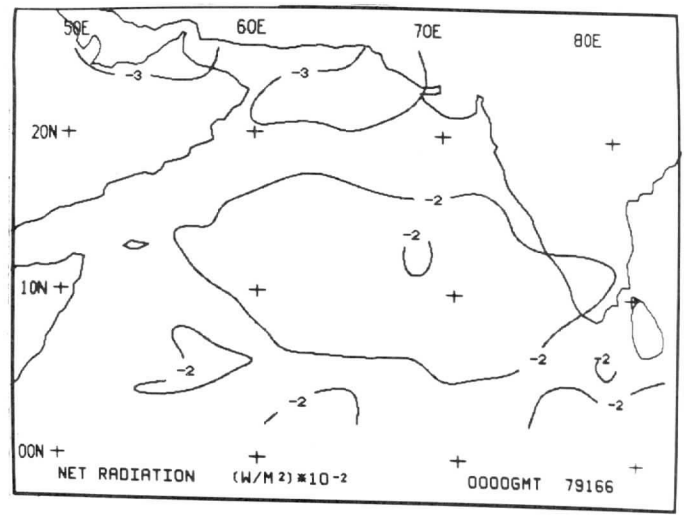
50E
60E
70E
80E
20N
10N
00N
NET RADIATION (W/M2)*10-2
0000GMT 79166

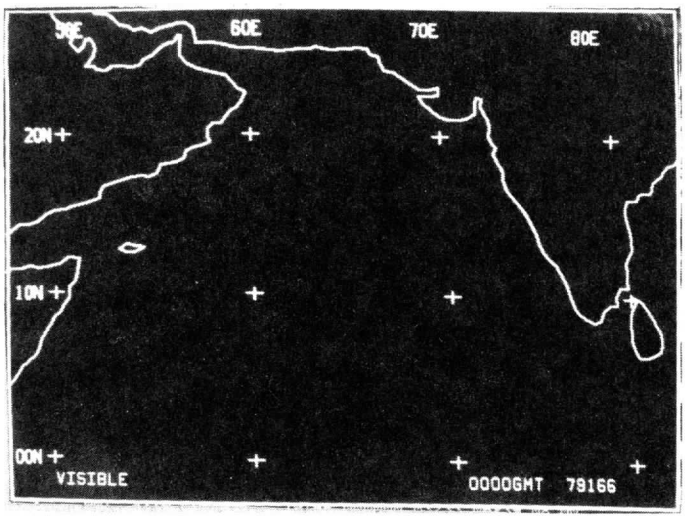
50E
60E
70E
80E
20N
10N
00N
VISIBLE
0000GMT 79166

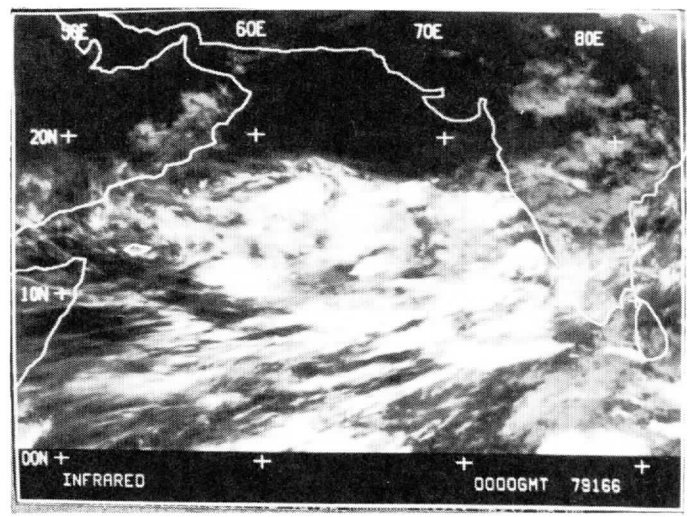
50E
60E
70E
80E
20N
10N
00N
INFRARED
0000GMT 79166

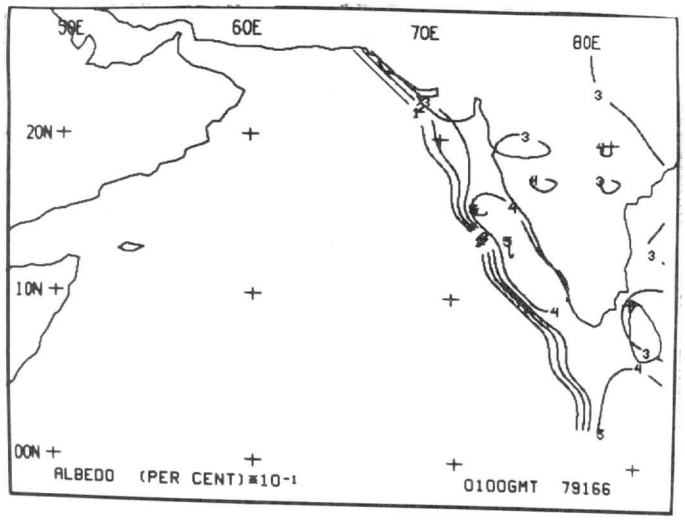
50E
60E
70E
80E
20N
10N
0ON
ALBEDO (PER CENT)*10-1
0100GMT 79166

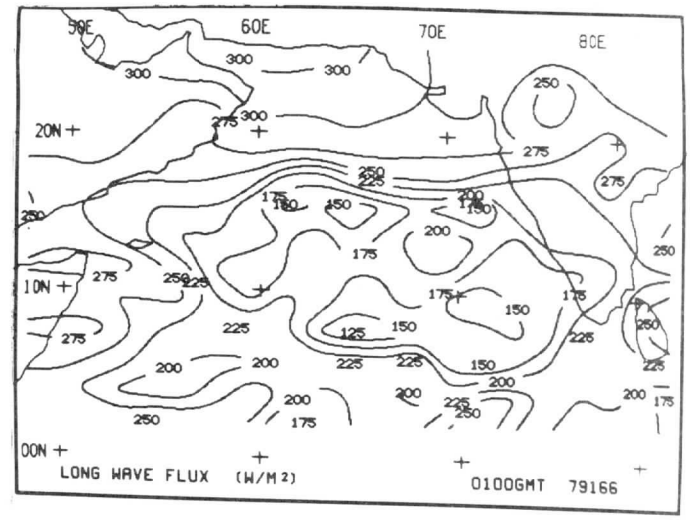
50E
60E
70E
80E
20N
10N
0ON
LONG WAVE FLUX (W/M2)
0100GMT 79166

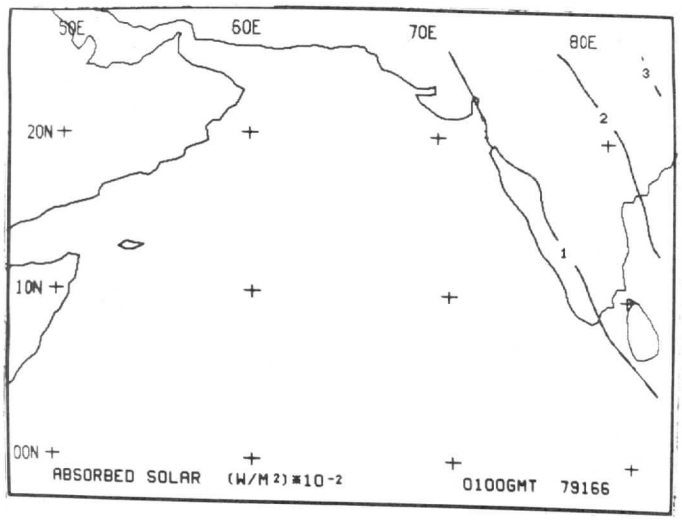
50E
60E
70E
80E
20N
10N
0ON
ABSORBED SOLAR (W/M2)*10-2
0100GMT 79166

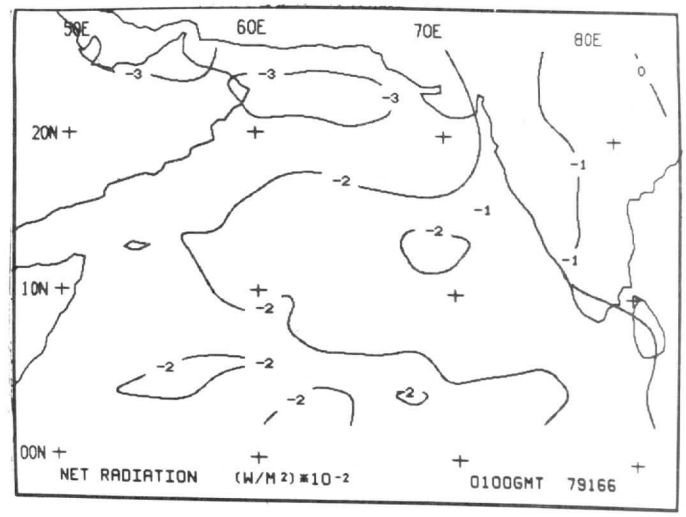
50E
60E
70E
80E
20N
10N
0ON
NET RADIATION (W/M2)*10-2
0100GMT 79166

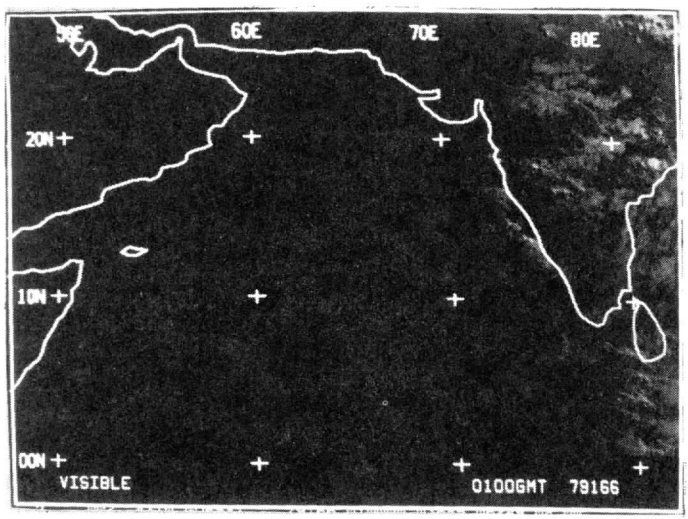
50E
60E
70E
80E
20N
10N
0ON
VISIBLE
0100GMT 79166

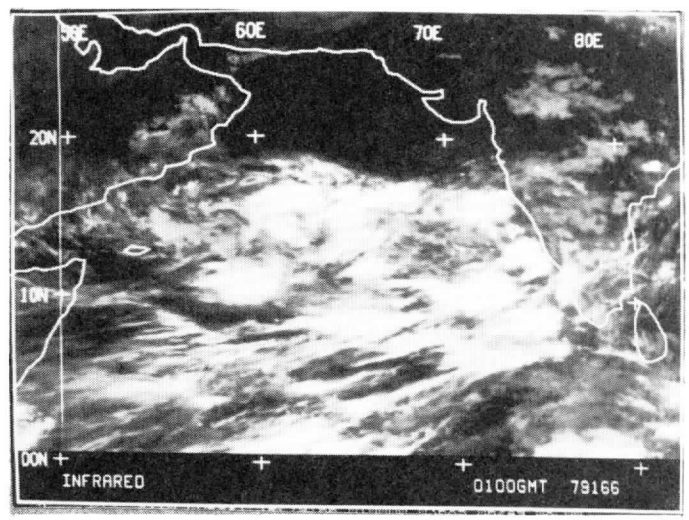
50E
60E
70E
80E
20N
10N
0ON
INFRARED
0100GMT 79166

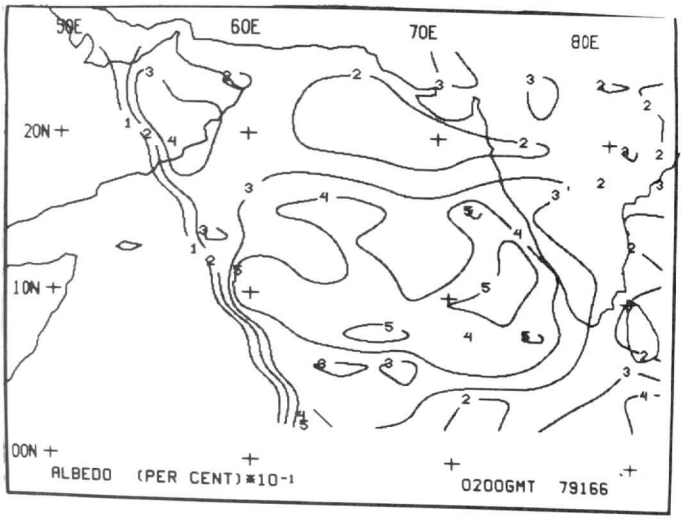
50E
60E
70E
80E
20N
10N
00N
ALBEDO (PER CENT)*10-1
0200GMT 79166

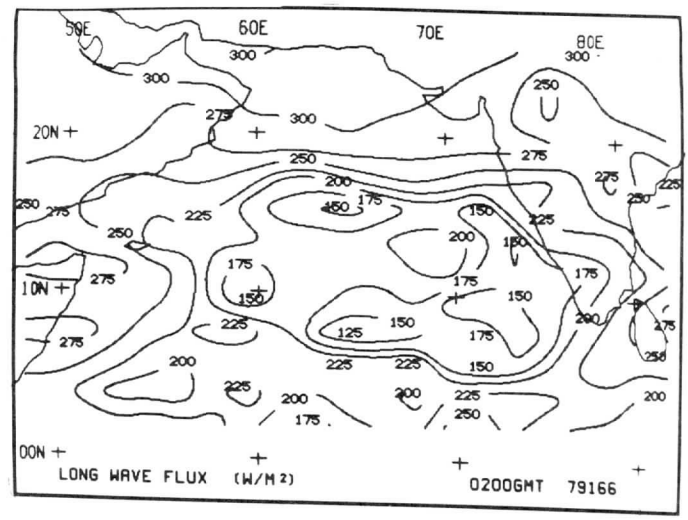
50E
60E
70E
80E
20N
10N
00N
LONG WAVE FLUX (W/M2)
0200GMT 79166

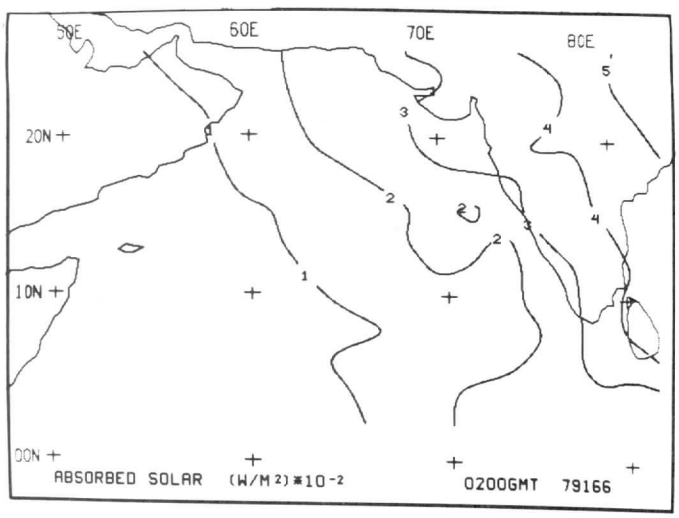
50E
60E
70E
80E
20N
10N
00N
ABSORBED SOLAR (W/M2)*10-2
0200GMT 79166

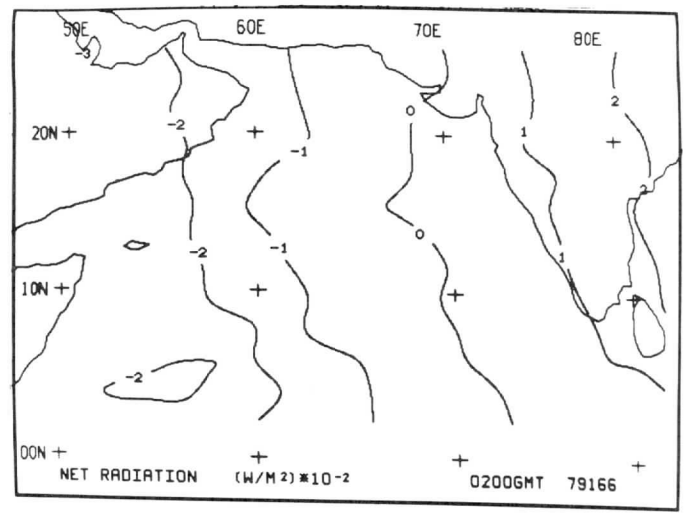
50E
60E
70E
80E
20N
10N
00N
NET RADIATION (W/M2)*10-2
0200GMT 79166

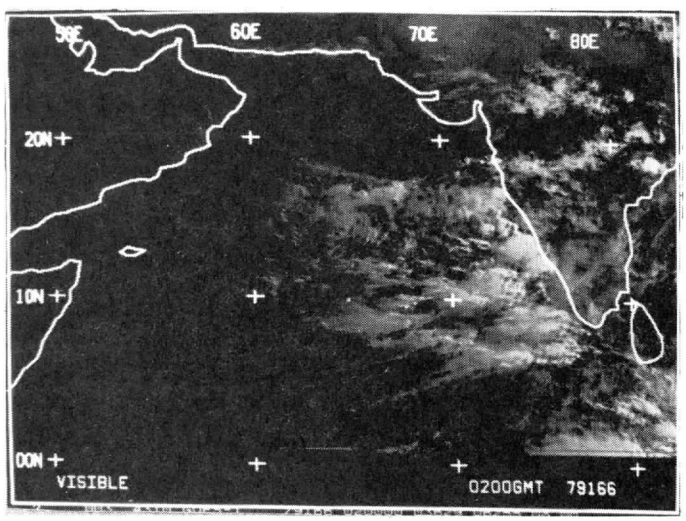
50E
60E
70E
80E
20N
10N
00N
VISIBLE
0200GMT 79166

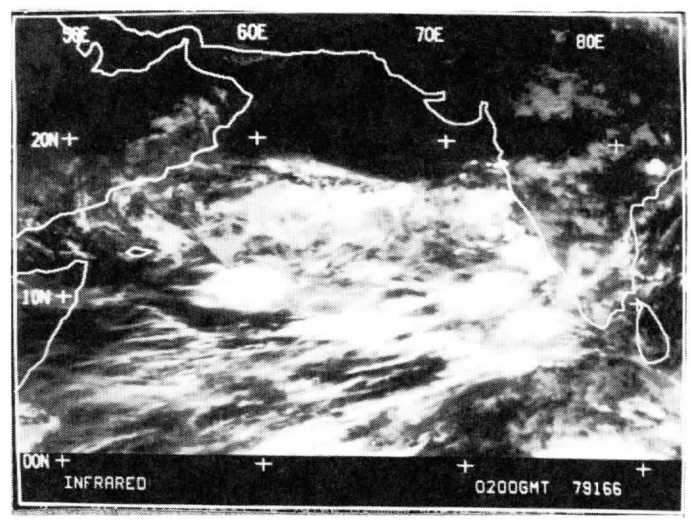
50E
60E
70E
80E
20N
10N
00N
INFRARED
0200GMT 79166

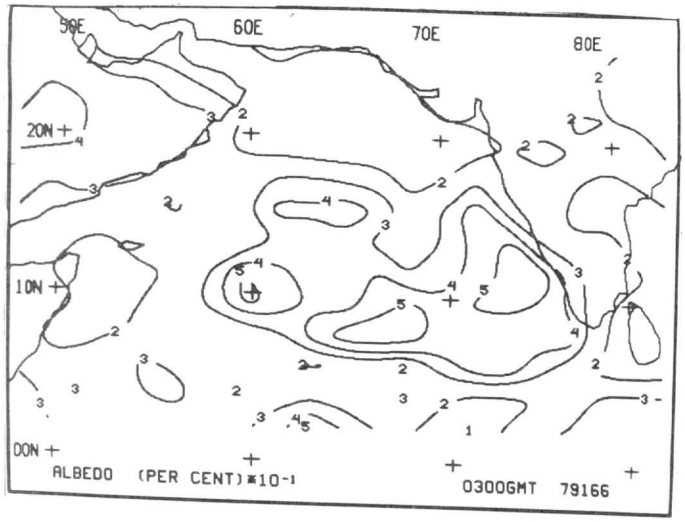
50E
60E
70E
80E
20N
10N
0ON
ALBEDO (PER CENT)*10-1
0300GMT 79166

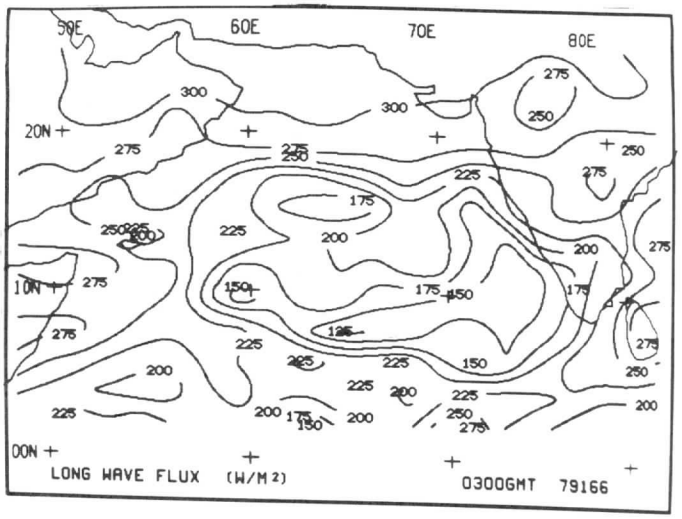
50E
60E
70E
80E
20N
10N
0ON
LONG WAVE FLUX (W/M2)
0300GMT 79166

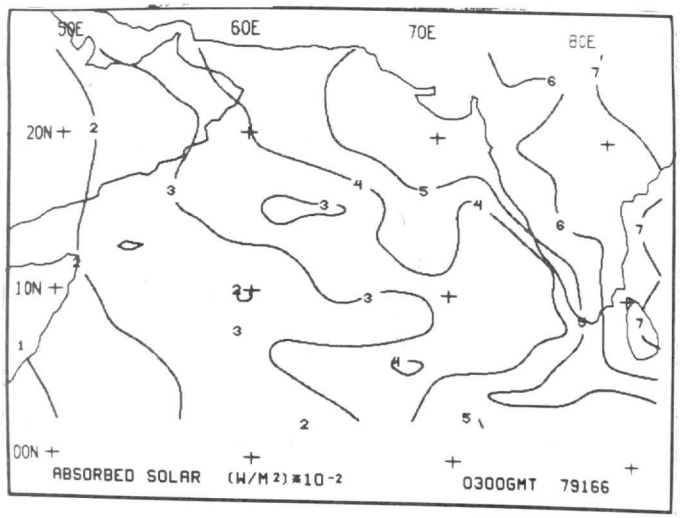
50E
60E
70E
80E
20N
10N
0ON
ABSORBED SOLAR (W/M2)*10-2
0300GMT 79166

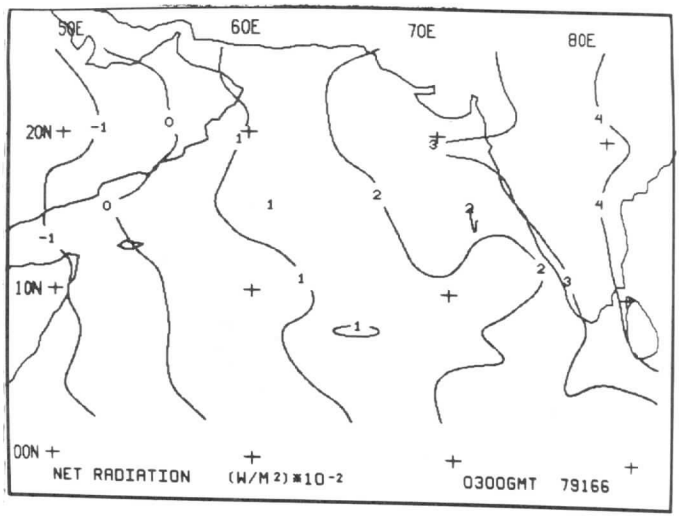
50E
60E
70E
80E
20N
10N
0ON
NET RADIATION (W/M2)*10-2
0300GMT 79166

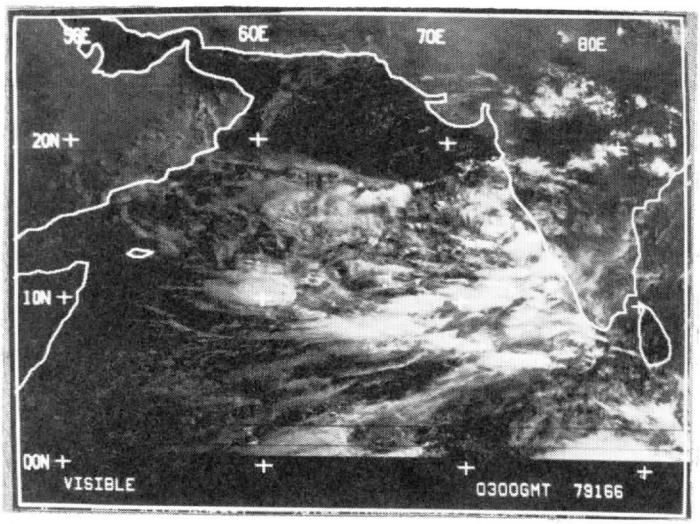
50E
60E
70E
80E
20N
10N
0ON
VISIBLE
0300GMT 79166

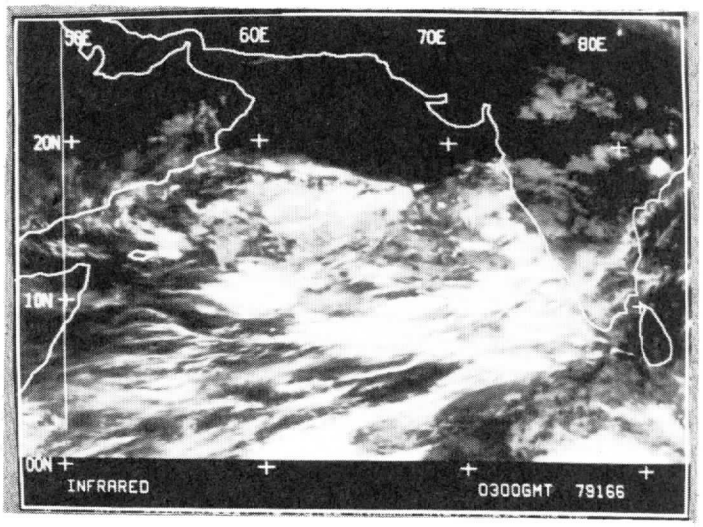
50E
60E
70E
80E
20N
10N
0ON
INFRARED
0300GMT 79166

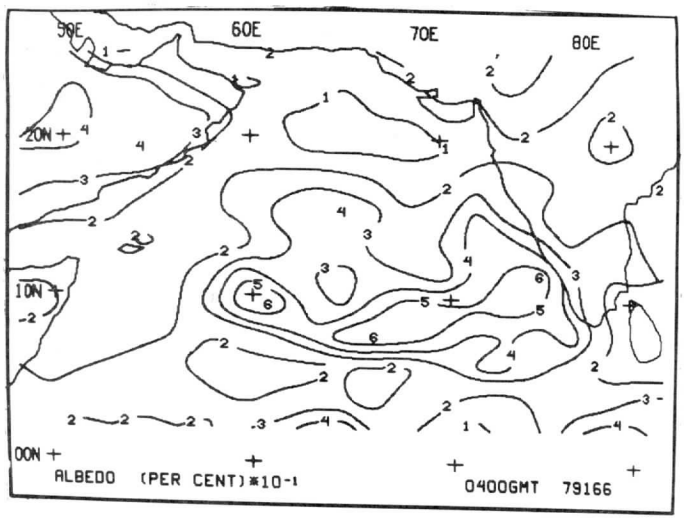
50E
60E
70E
80E
20N
10N
0ON
ALBEDO (PER CENT)*10-1
0400GMT 79166

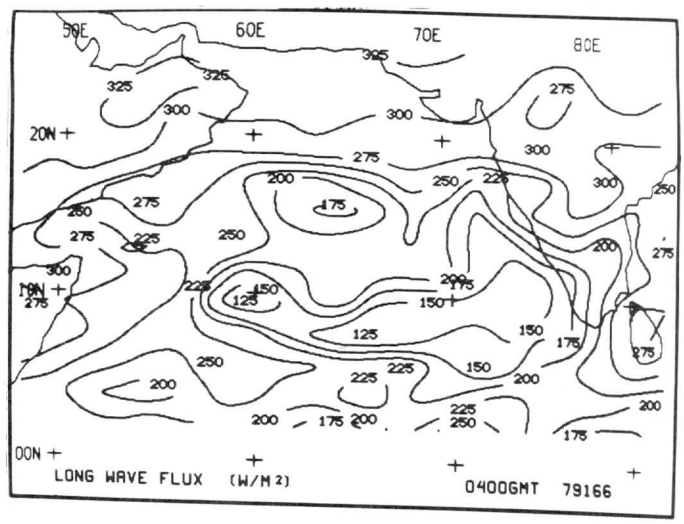
50E
60E
70E
80E
20N
10N
0ON
LONG WAVE FLUX (W/M2)
0400GMT 79166

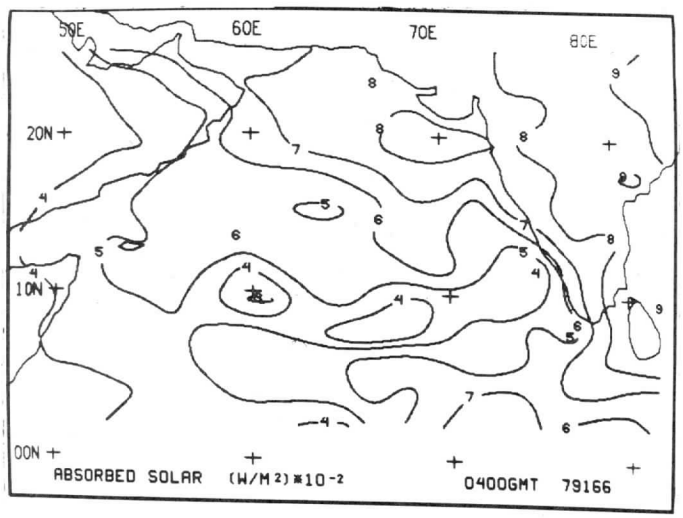
50E
60E
70E
80E
20N
10N
0ON
ABSORBED SOLAR (W/M2)*10-2
0400GMT 79166

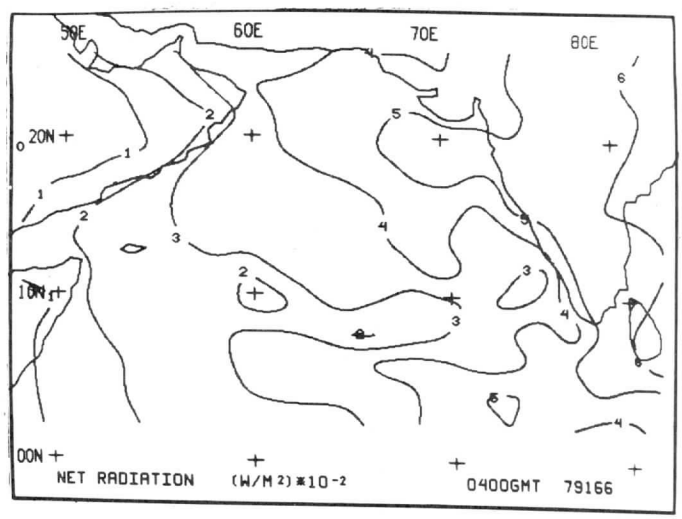
50E
60E
70E
80E
20N
10N
0ON
NET RADIATION (W/M2)*10-2
0400GMT 79166

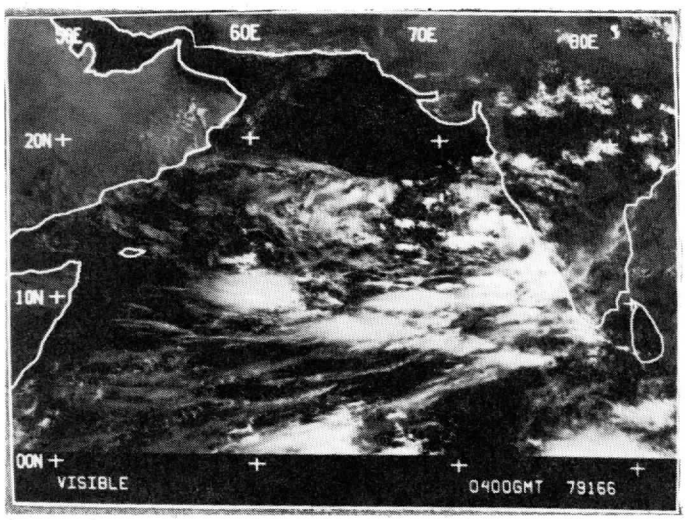
50E
60E
70E
80E
20N
10N
0ON
VISIBLE
0400GMT 79166

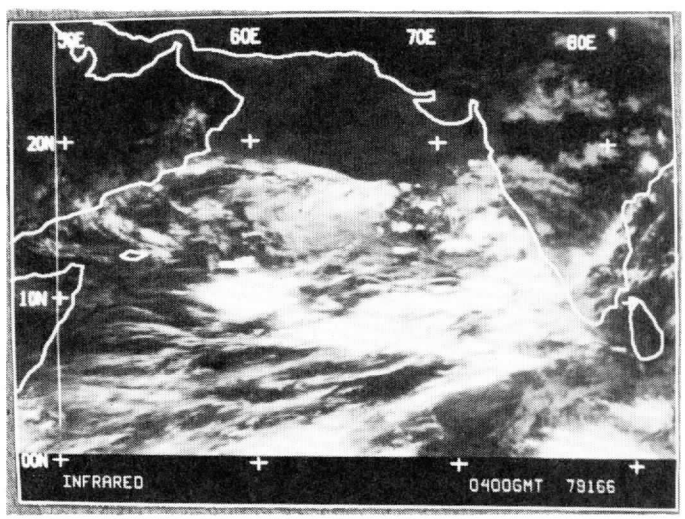
50E
60E
70E
80E
20N
10N
0ON
INFRARED
0400GMT 79166

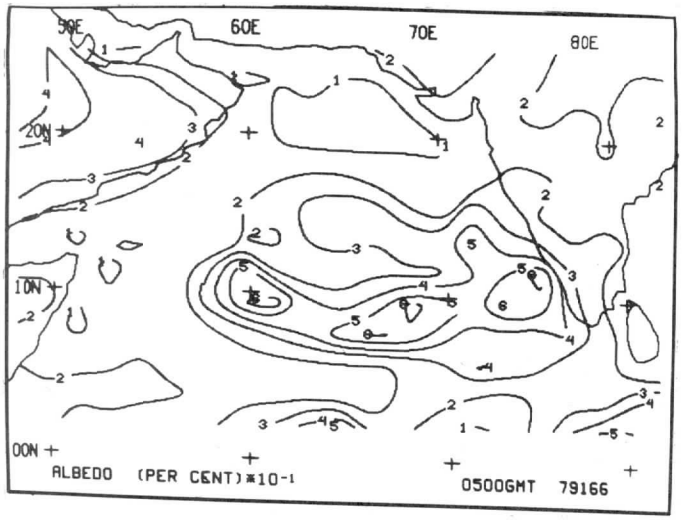
50E
60E
70E
80E
20N
10N
0ON
ALBEDO (PER CENT)*10-1
0500GMT 79166

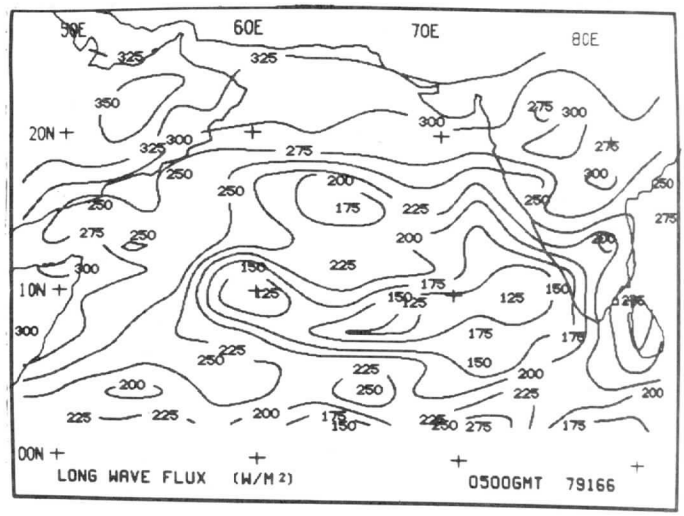
50E
60E
70E
80E
20N
10N
0ON
LONG WAVE FLUX (W/M2)
0500GMT 79166

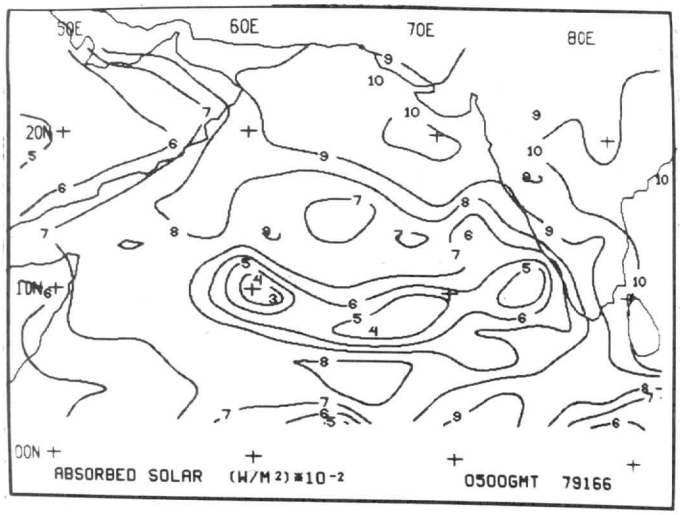
50E
60E
70E
80E
20N
10N
0ON
ABSORBED SOLAR (W/M2)*10-2
0500GMT 79166

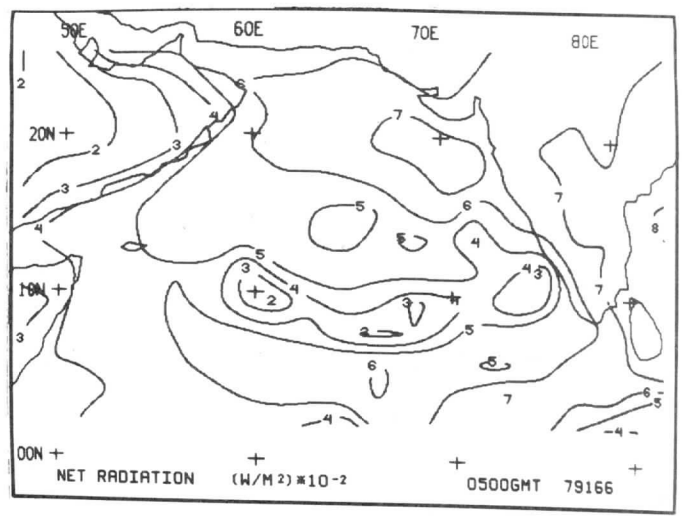
50E
60E
70E
80E
20N
10N
0ON
NET RADIATION (W/M2)*10-2
0500GMT 79166

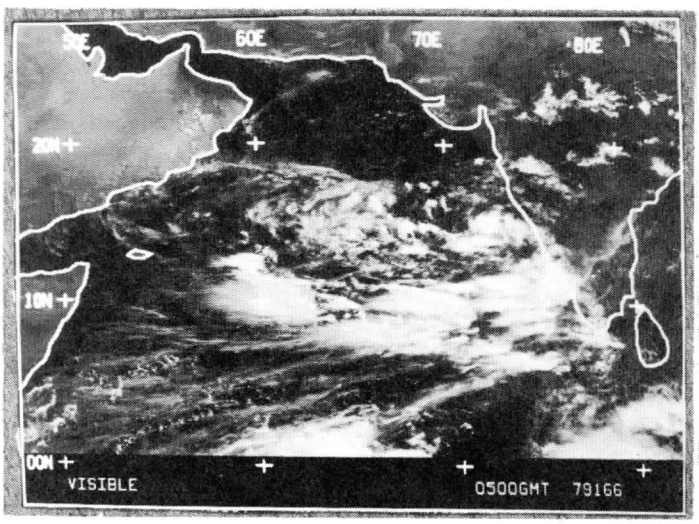
50E
60E
70E
80E
20N
10N
0ON
VISIBLE
0500GMT 79166

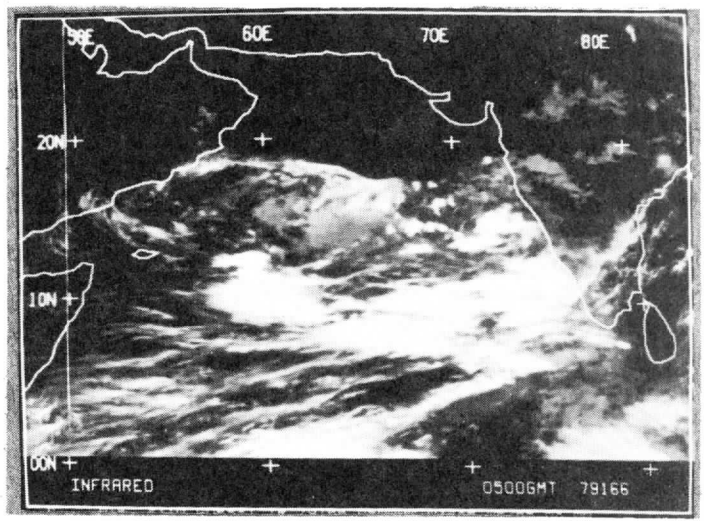
50E
60E
70E
80E
20N
10N
0ON
INFRARED
0500GMT 79166

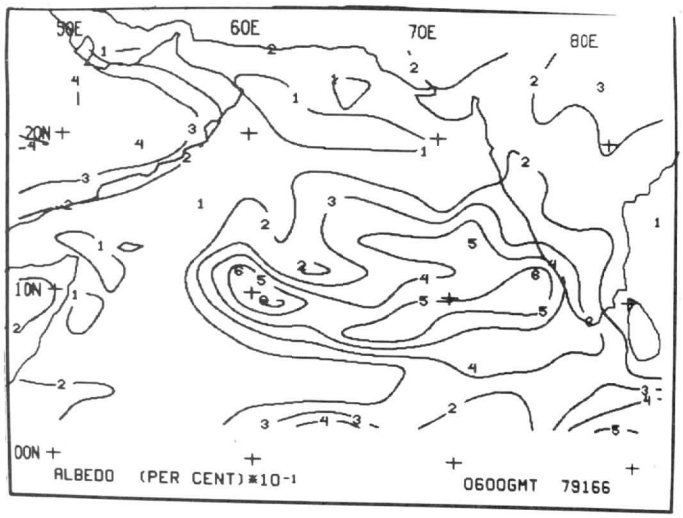
50E
60E
70E
80E
20N
10N
00N
ALBEDO (PER CENT)*10-1
0600GMT 79166

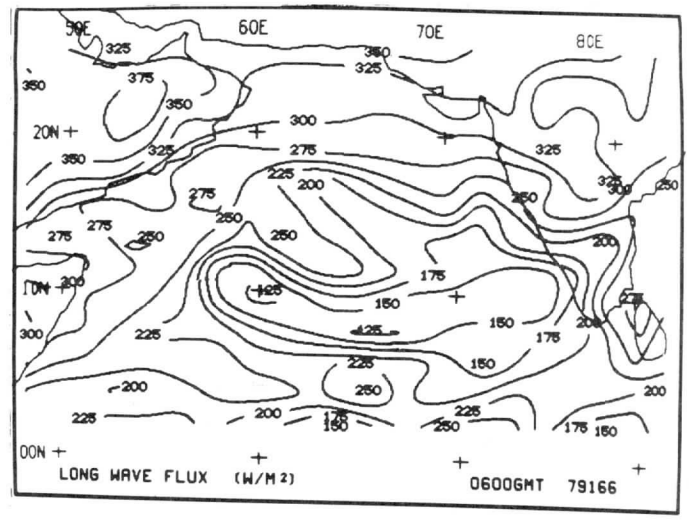
50E
60E
70E
80E
20N
10N
00N
LONG WAVE FLUX (W/M2)
0600GMT 79166

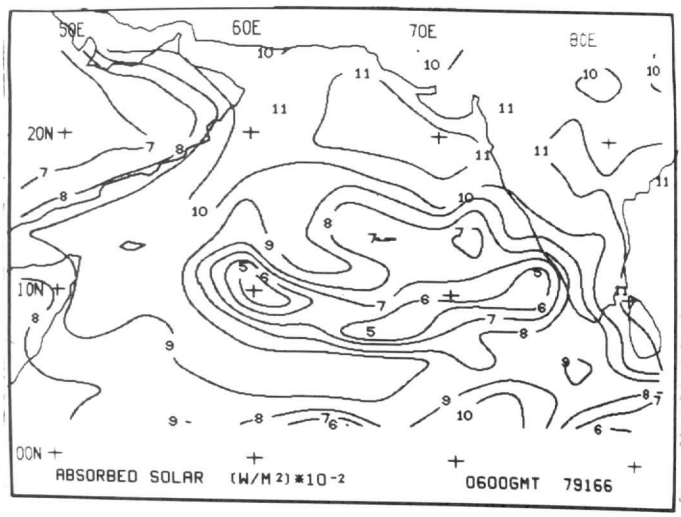
50E
60E
70E
80E
20N
10N
00N
ABSORBED SOLAR (W/M2)*10-2
0600GMT 79166

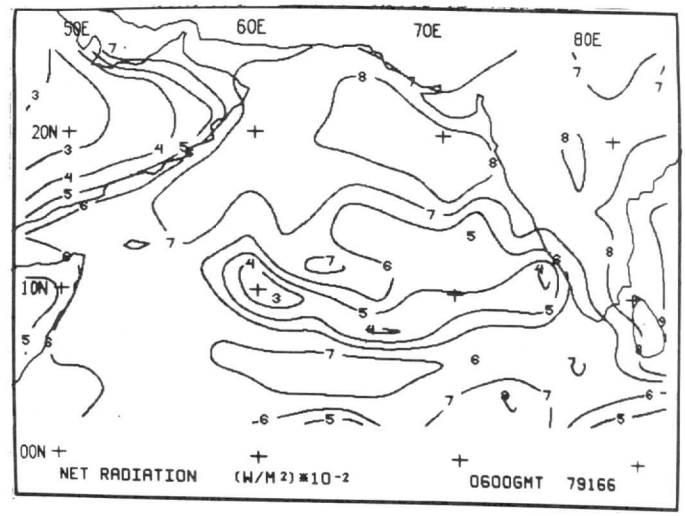
50E
60E
70E
80E
20N
10N
00N
NET RADIATION (W/M2)*10-2
0600GMT 79166

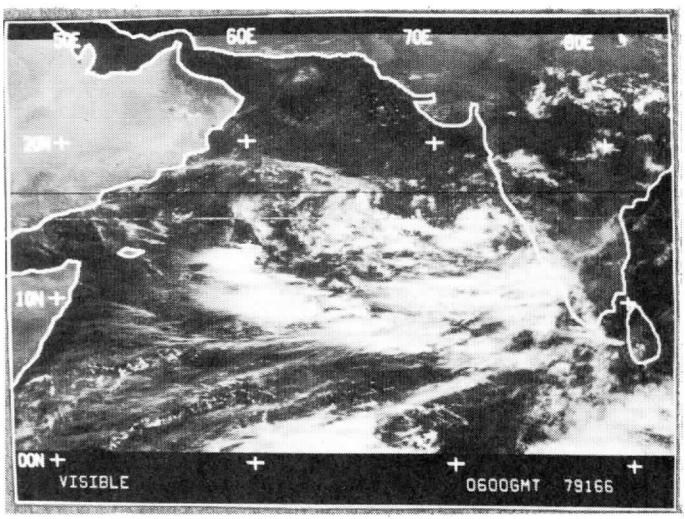
50E
60E
70E
80E
20N
10N
00N
VISIBLE
0600GMT 79166

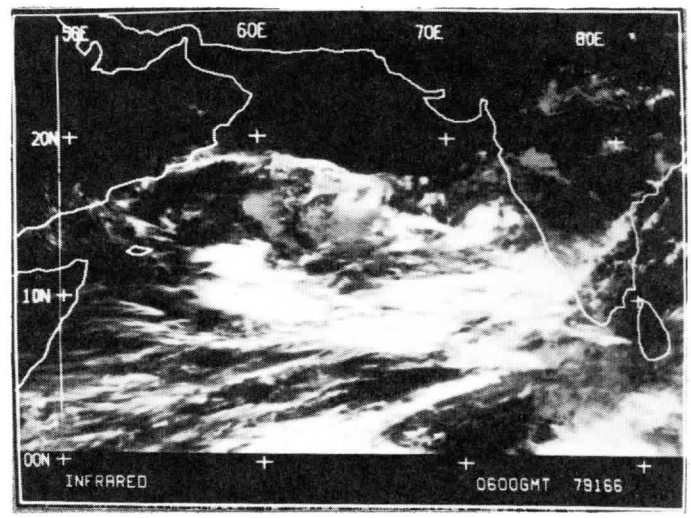
50E
60E
70E
80E
20N
10N
00N
INFRARED
0600GMT 79166

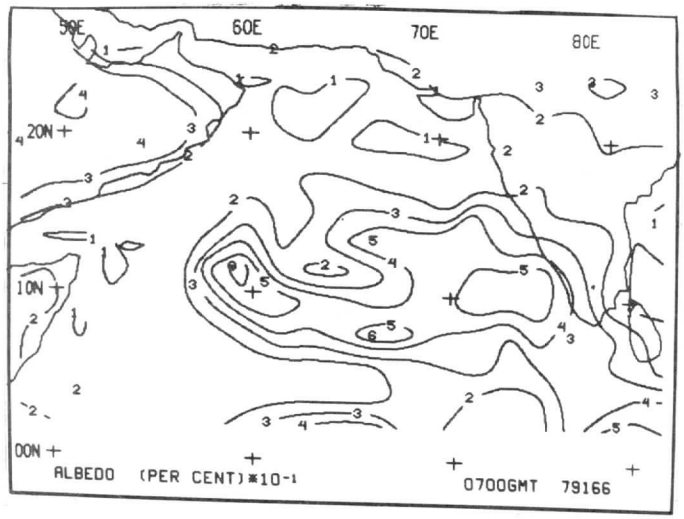
50E
60E
70E
80E
20N
10N
0ON
ALBEDO (PER CENT)*10-1
0700GMT 79166

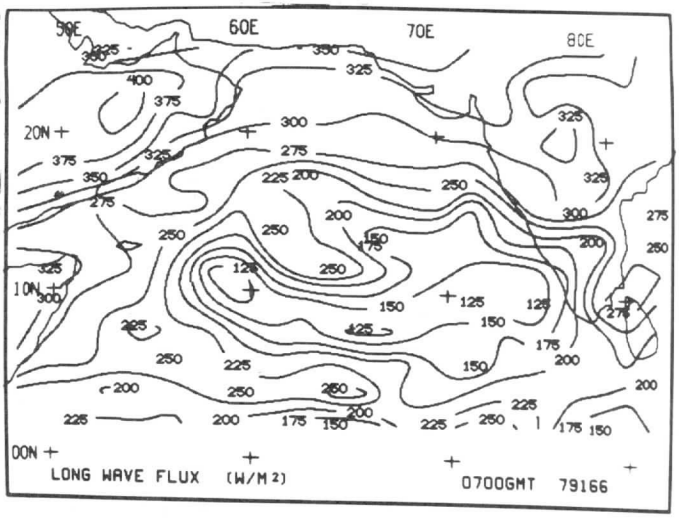
50E
60E
70E
80E
20N
10N
0ON
LONG WAVE FLUX (W/M2)
0700GMT 79166

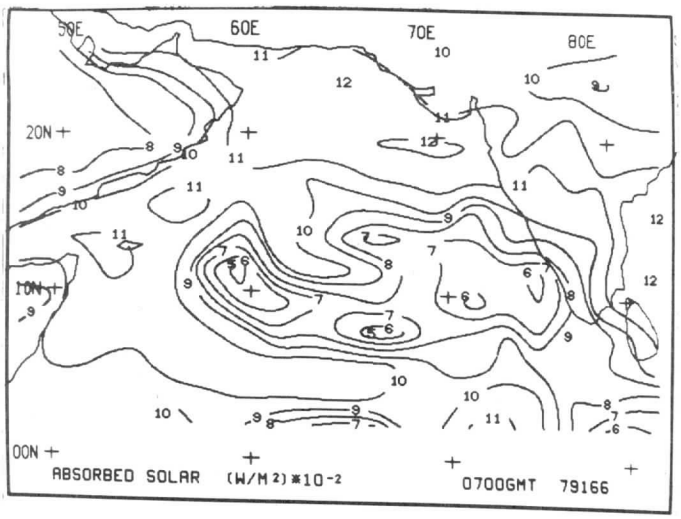
50E
60E
70E
80E
20N
10N
0ON
ABSORBED SOLAR (W/M2)*10-2
0700GMT 79166

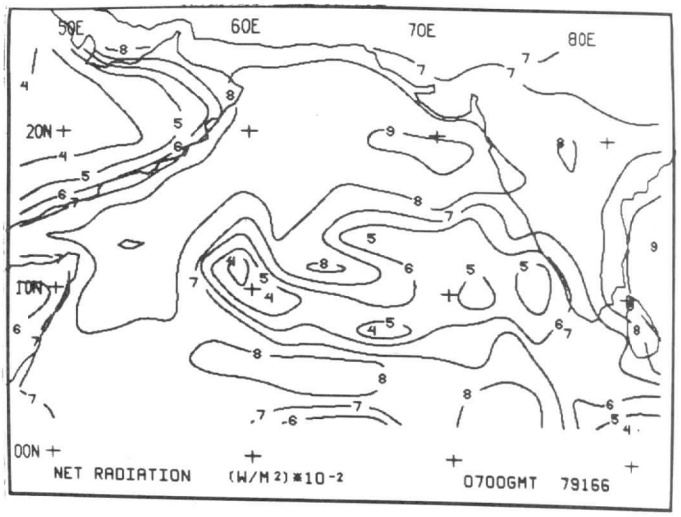
50E
60E
70E
80E
20N
10N
0ON
NET RADIATION (W/M2)*10-2
0700GMT 79166

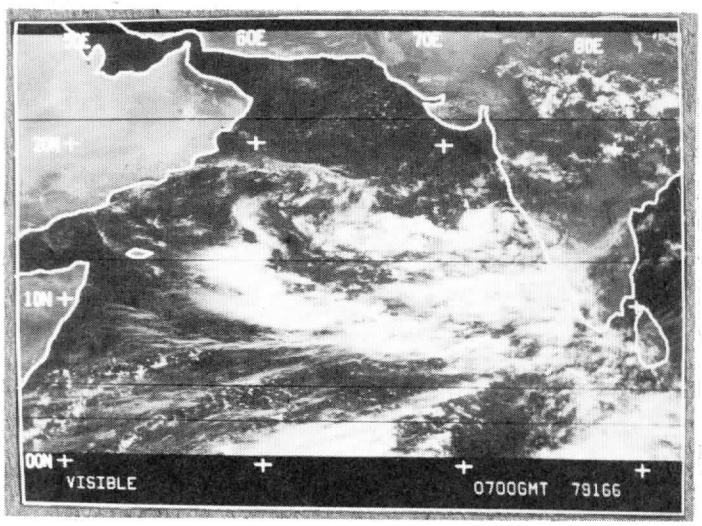
60E
70E
80E
20N
10N
0ON
VISIBLE
0700GMT 79166

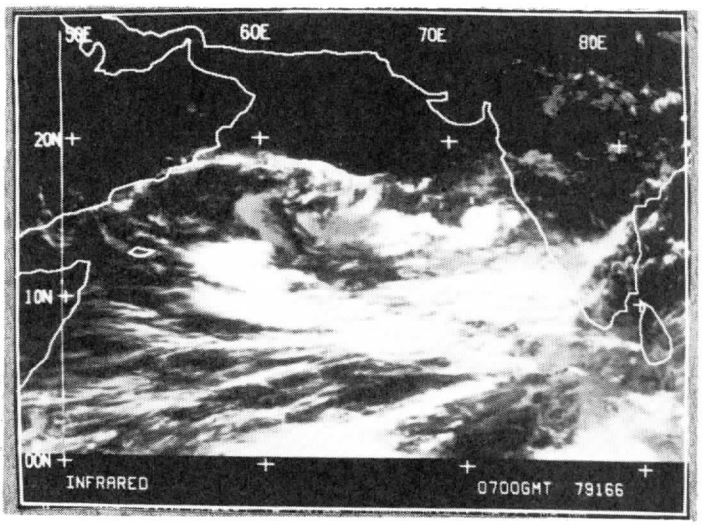
50E
60E
70E
80E
20N
10N
0ON
INFRARED
0700GMT 79166

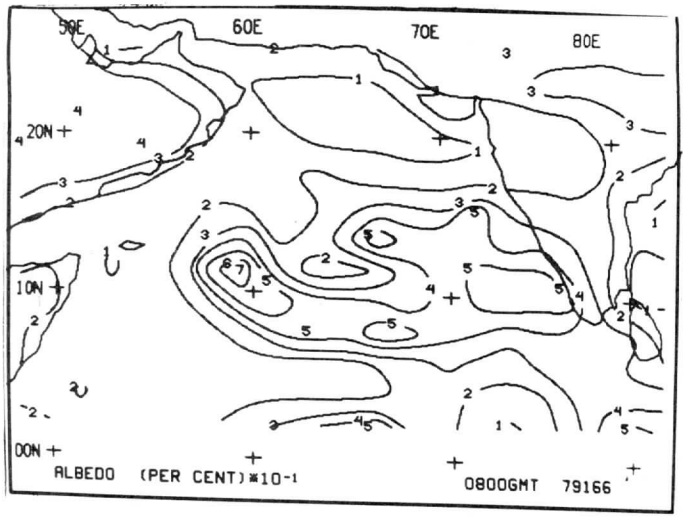
50E
60E
70E
80E
20N
10N
00N
ALBEDO (PER CENT)*10-1
0800GMT 79166

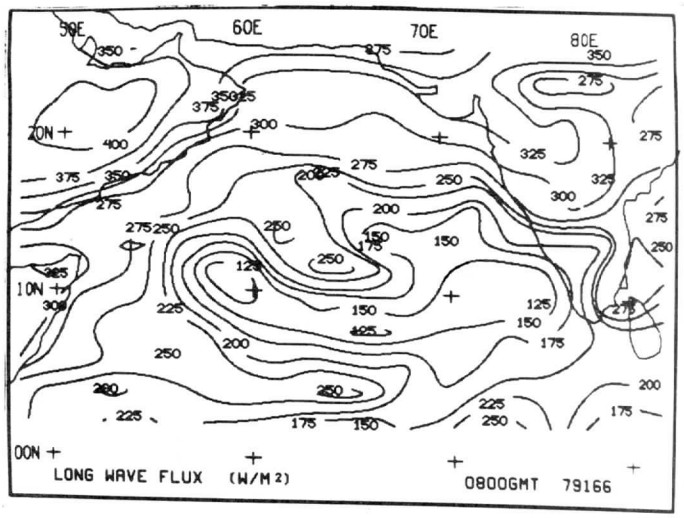
50E
60E
70E
80E
20N
10N
00N
LONG WAVE FLUX (W/M2)
0800GMT 79166

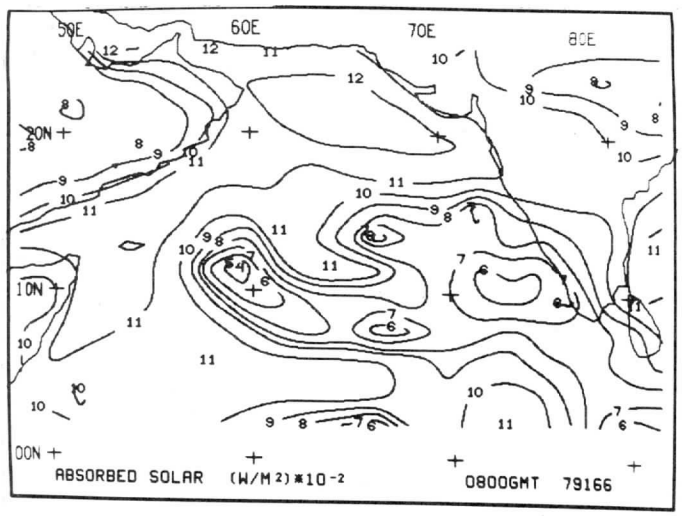
50E
60E
70E
80E
20N
10N
00N
ABSORBED SOLAR (W/M2)*10-2
0800GMT 79166

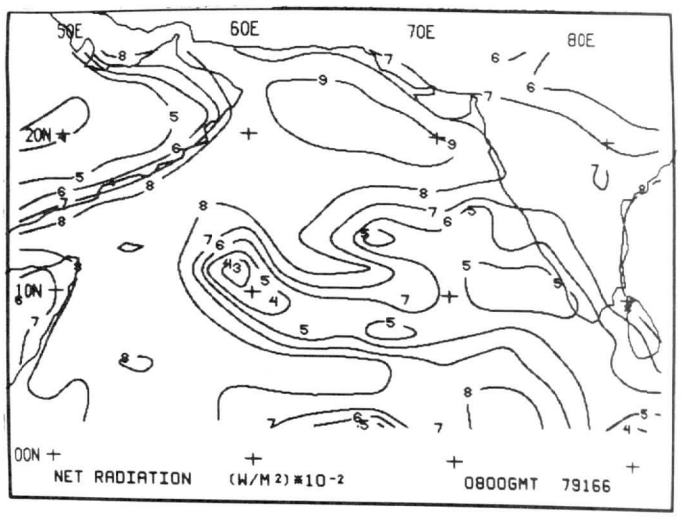
50E
60E
70E
80E
20N
10N
00N
NET RADIATION (W/M2)*10-2
0800GMT 79166

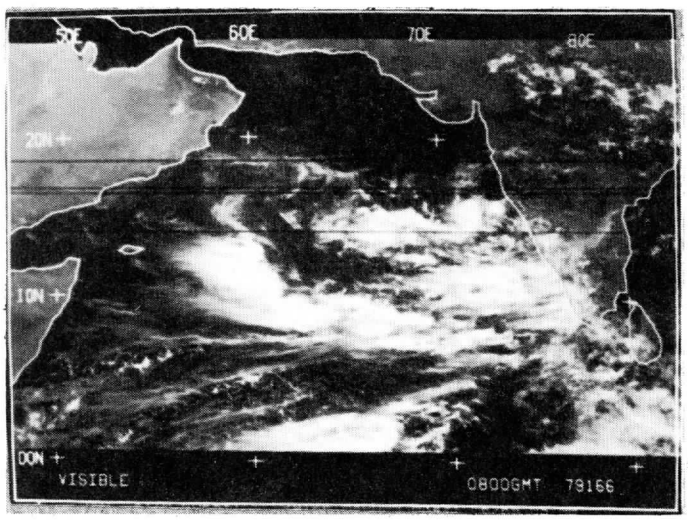
50E
60E
70E
80E
20N
10N
00N
VISIBLE
0800GMT 79166

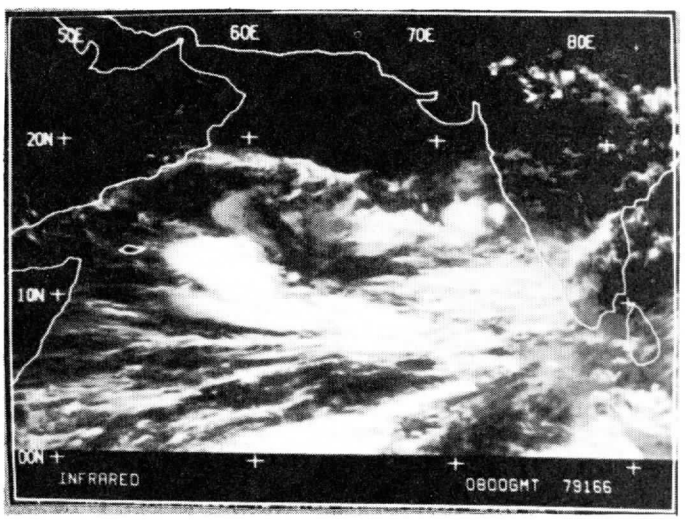
50E
60E
70E
80E
20N
10N
00N
INFRARED
0800GMT 79166

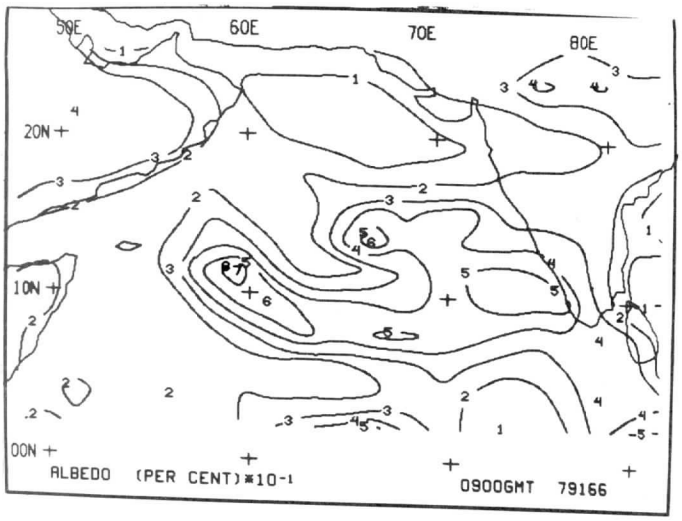
50E
60E
70E
80E
20N
10N
0ON
ALBEDO (PER CENT)*10-1
0900GMT 79166

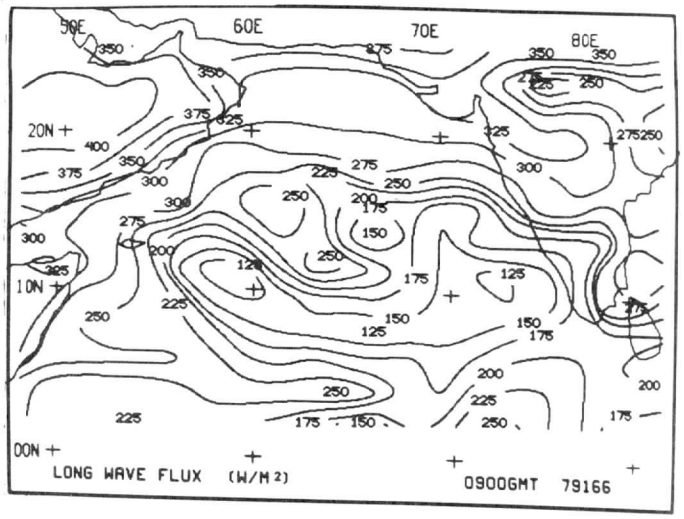
50E
60E
70E
80E
20N
10N
0ON
LONG WAVE FLUX (W/M2)
0900GMT 79166

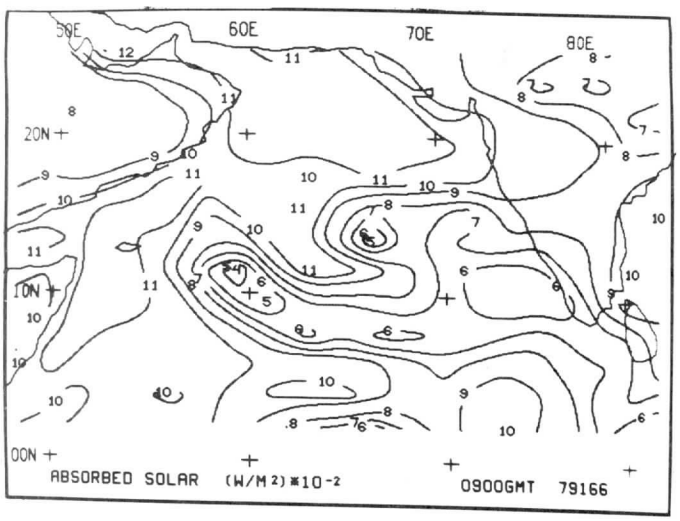
50E
60E
70E
80E
20N
10N
0ON
ABSORBED SOLAR (W/M2)*10-2
0900GMT 79166

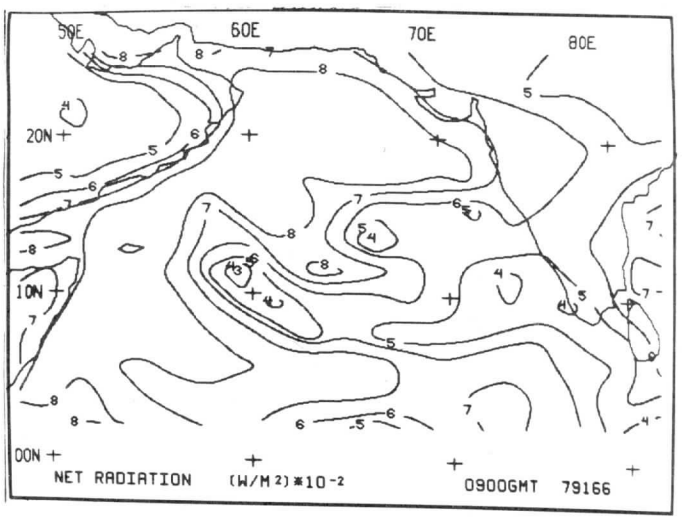
50E
60E
70E
80E
20N
10N
0ON
NET RADIATION (W/M2)*10-2
0900GMT 79166

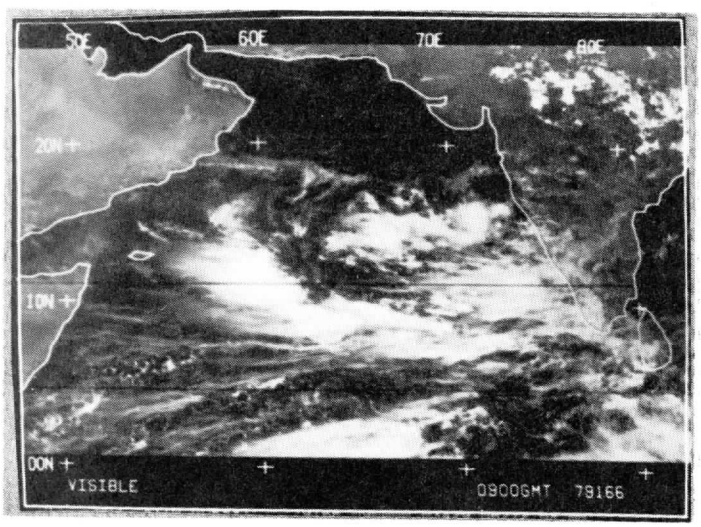
50E
60E
70E
80E
20N
10N
0ON
VISIBLE
0900GMT 79166

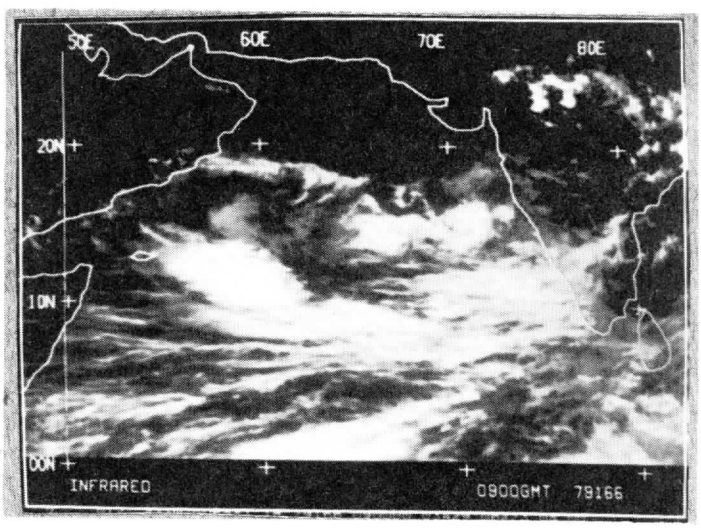
50E
60E
70E
80E
20N
10N
0ON
INFRARED
0900GMT 79166

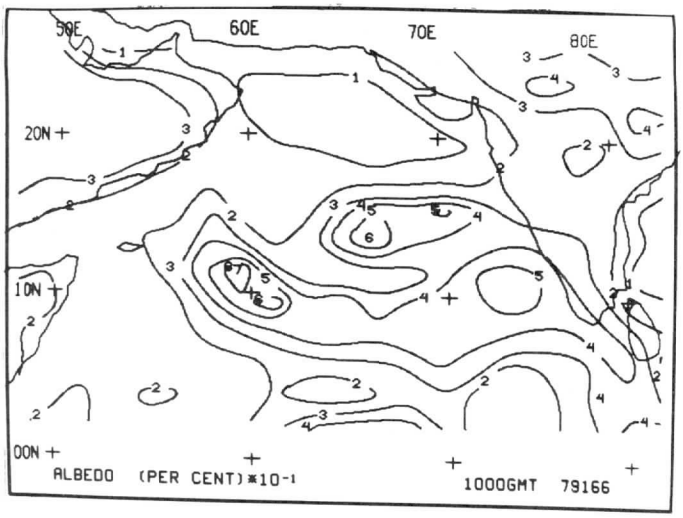
50E
60E
70E
80E
20N
10N
0ON
ALBEDO (PER CENT)*10-1
1000GMT 79166

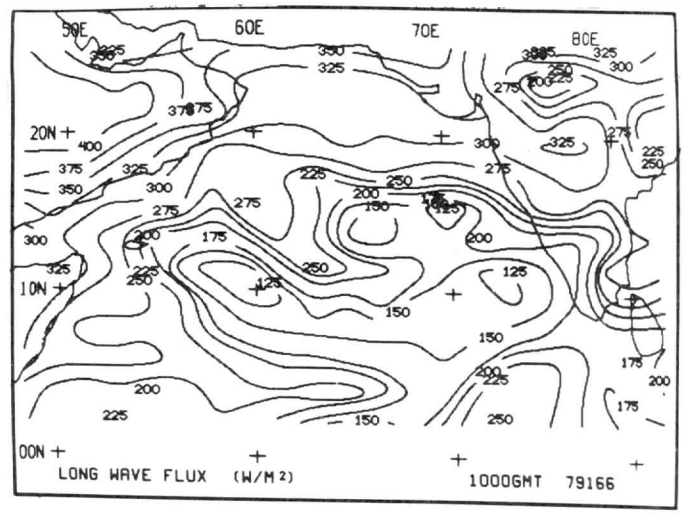
50E
60E
70E
80E
20N
10N
0ON
LONG WAVE FLUX (W/M2)
1000GMT 79166

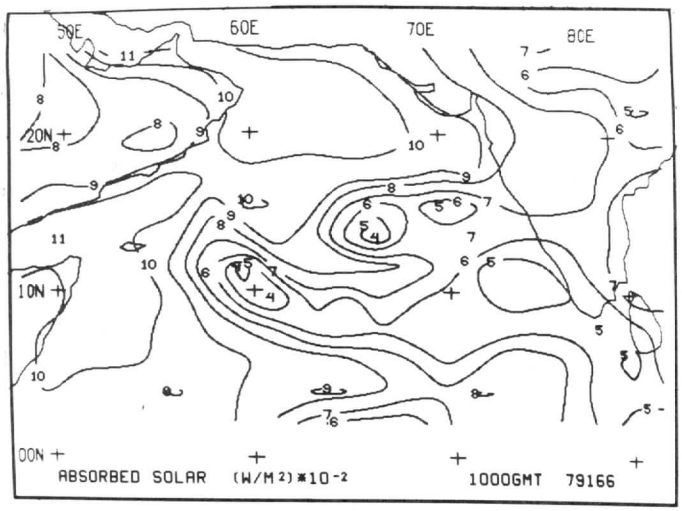
50E
60E
70E
80E
20N
10N
0ON
ABSORBED SOLAR (W/M2)*10-2
1000GMT 79166

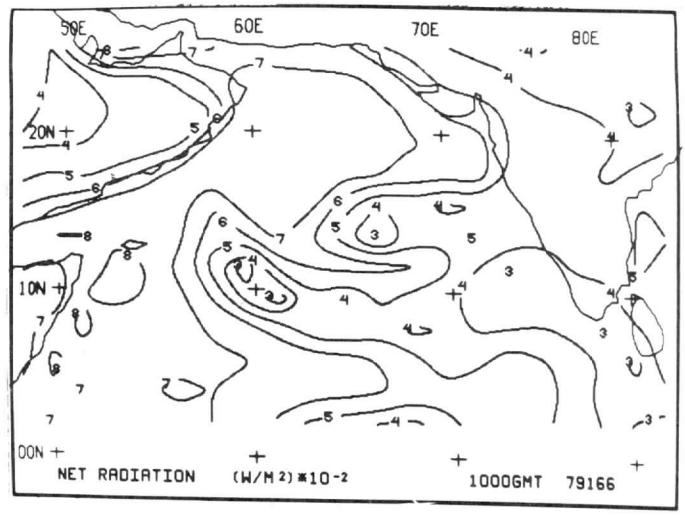
50E
60E
70E
80E
20N
10N
0ON
NET RADIATION (W/M2)*10-2
1000GMT 79166

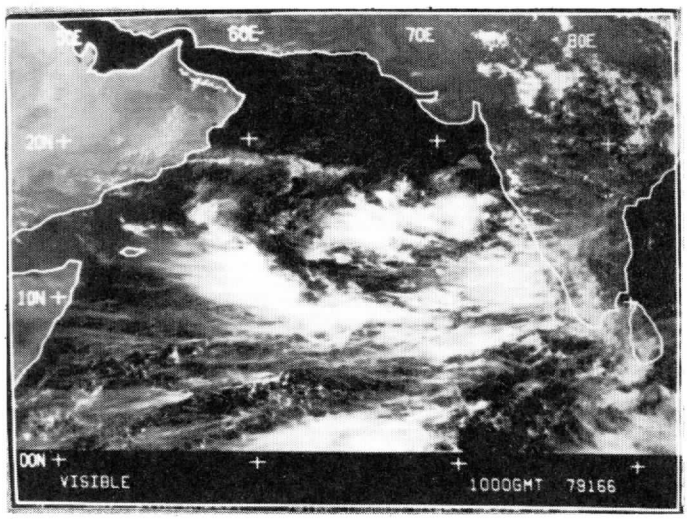
50E
60E
70E
80E
20N
10N
0ON
VISIBLE
1000GMT 79166

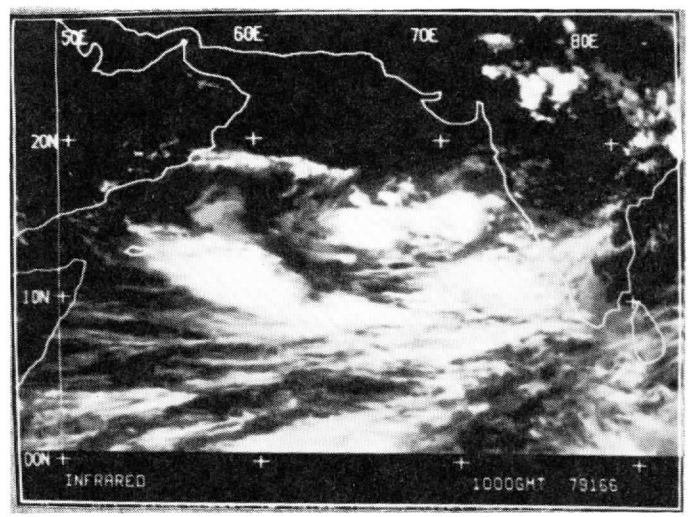
50E
60E
70E
80E
20N
10N
0ON
INFRARED
1000GMT 79166

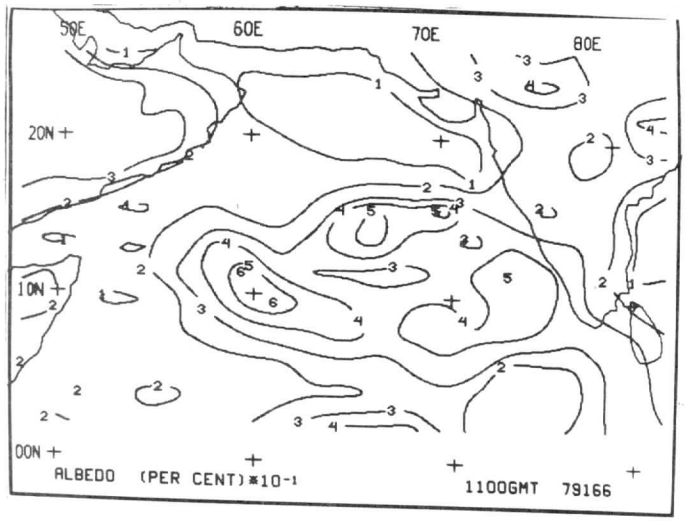
50E
60E
70E
80E
20N
10N
0ON
ALBEDO (PER CENT)*10-1
1100GMT 79166

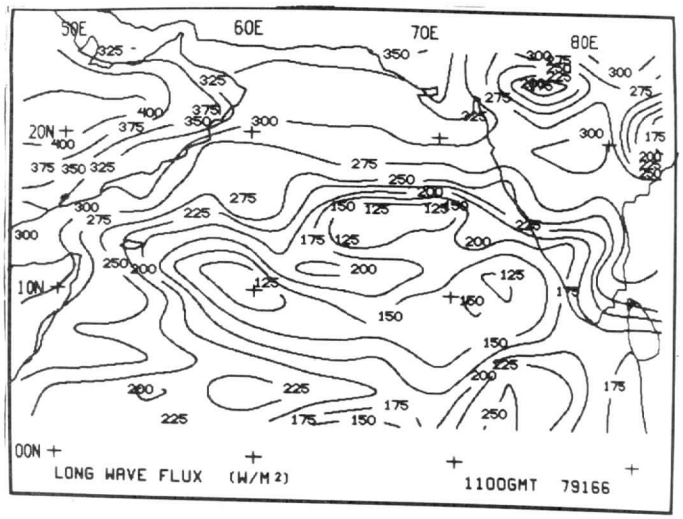
50E
60E
70E
80E
20N
10N
0ON
LONG WAVE FLUX (W/M2)
1100GMT 79166

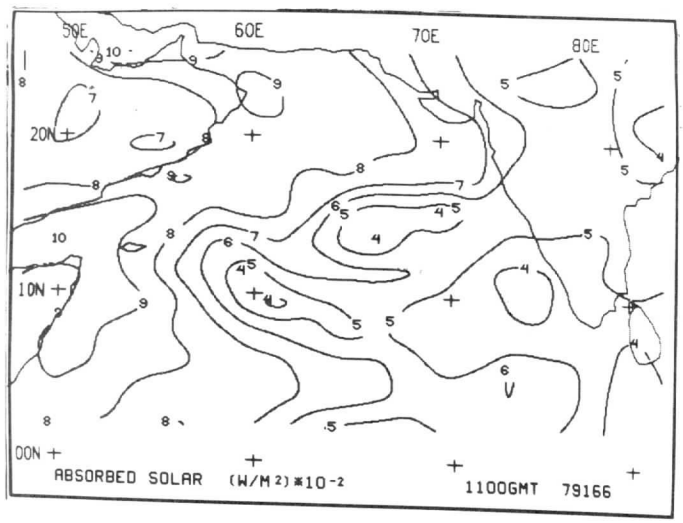
50E
60E
70E
80E
20N
10N
0ON
ABSORBED SOLAR (W/M2)*10-2
1100GMT 79166

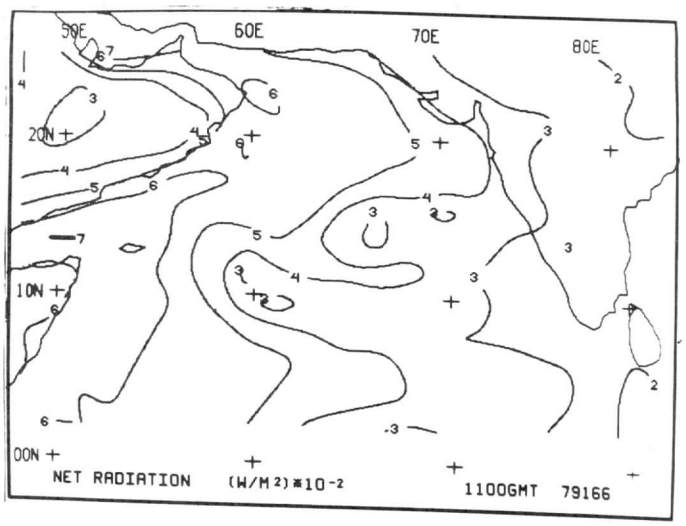
50E
60E
70E
80E
20N
10N
0ON
NET RADIATION (W/M2)*10-2
1100GMT 79166

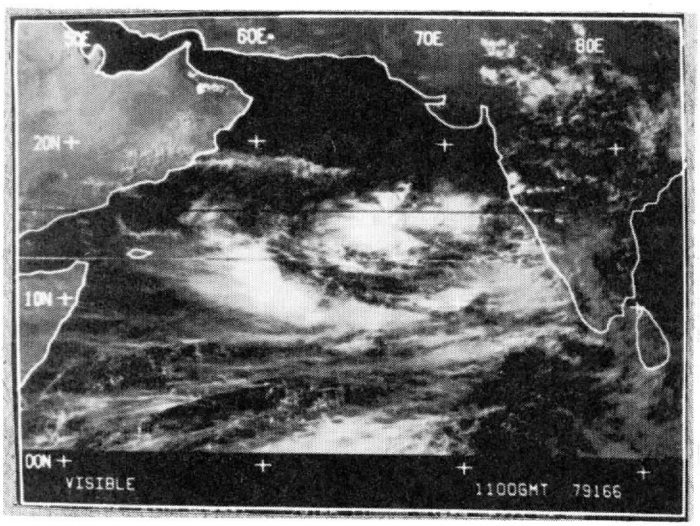
50E
60E
70E
80E
20N
10N
0ON
VISIBLE
1100GMT 79166

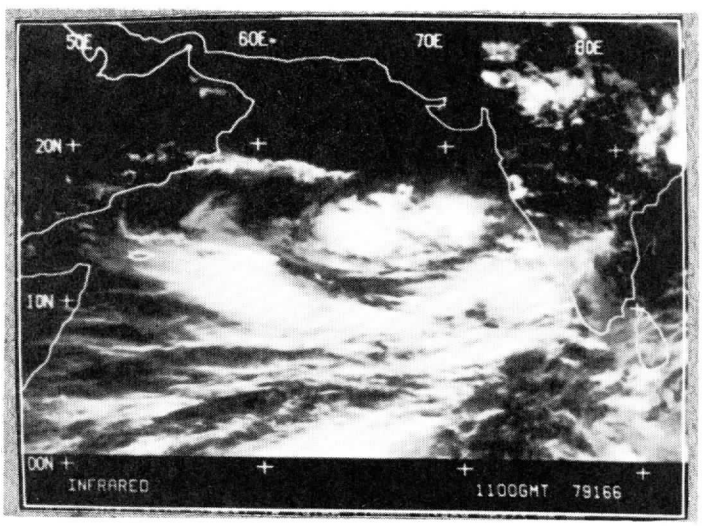
50E
60E
70E
80E
20N
10N
0ON
INFRARED
1100GMT 79166

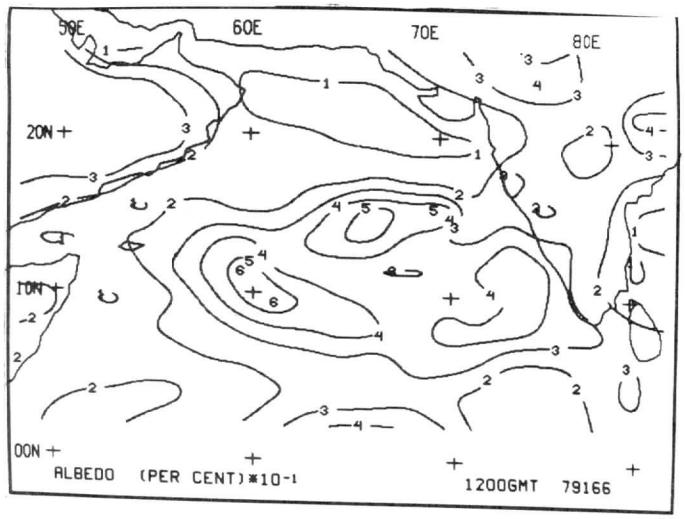
50E
60E
70E
80E
20N
10N
0ON
ALBEDO (PER CENT)*10-1
1200GMT 79166

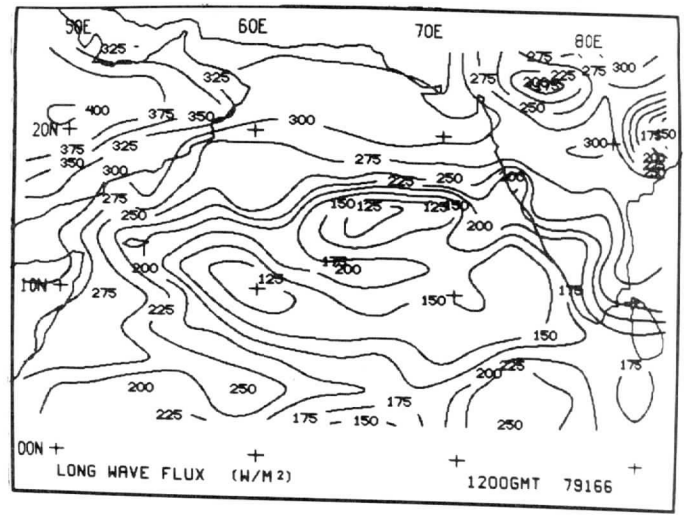
50E
60E
70E
80E
20N
10N
0ON
LONG WAVE FLUX (W/M2)
1200GMT 79166

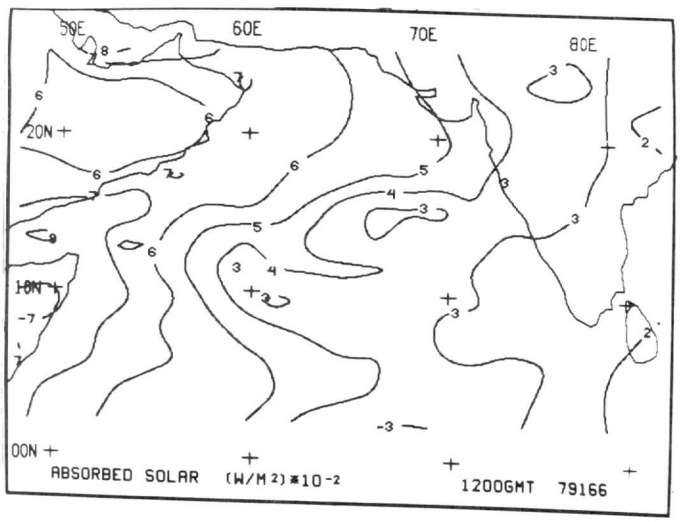
50E
60E
70E
80E
20N
10N
0ON
ABSORBED SOLAR (W/M2)*10-2
1200GMT 79166

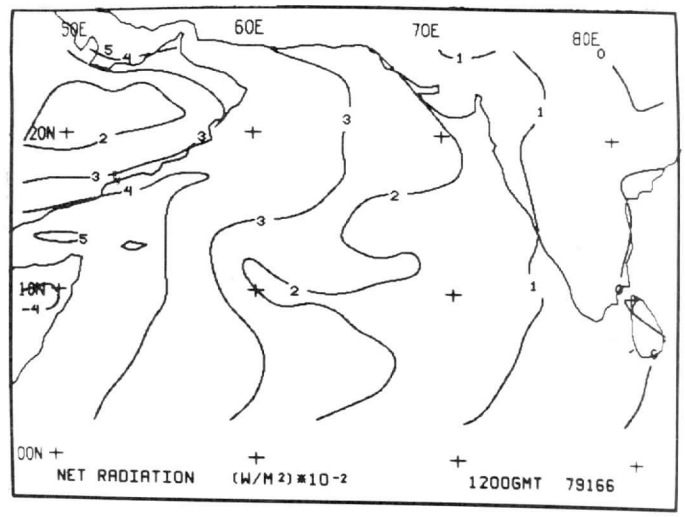
50E
60E
70E
80E
20N
10N
0ON
NET RADIATION (W/M2)*10-2
1200GMT 79166

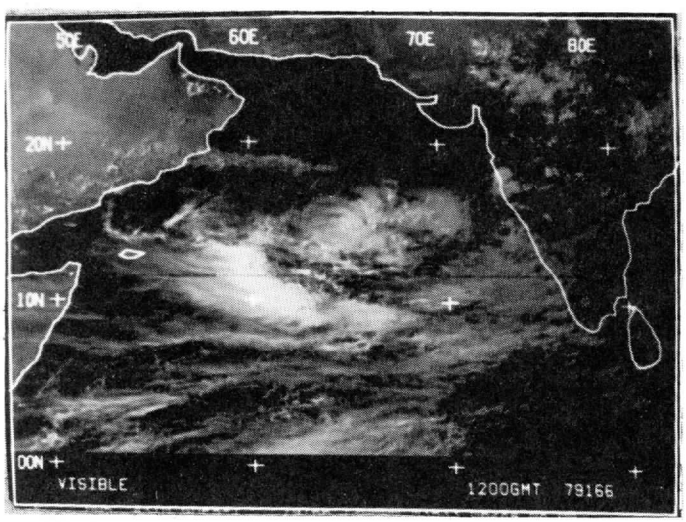
50E
60E
70E
80E
20N
10N
0ON
VISIBLE
1200GMT 79166

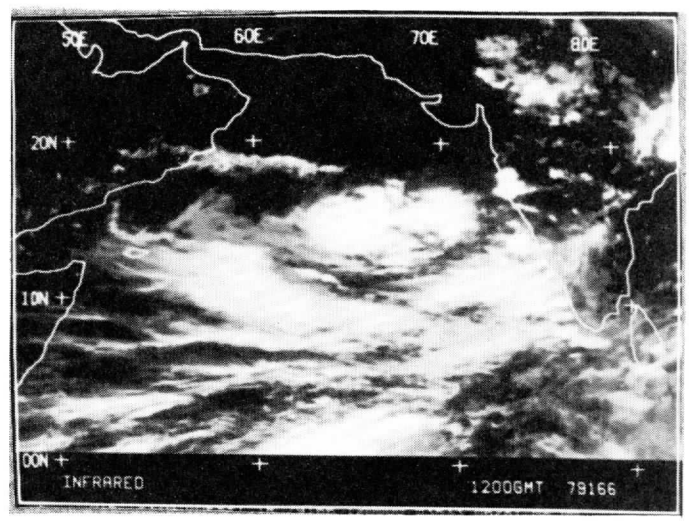
50E
60E
70E
80E
20N
10N
0ON
INFRARED
1200GMT 79166

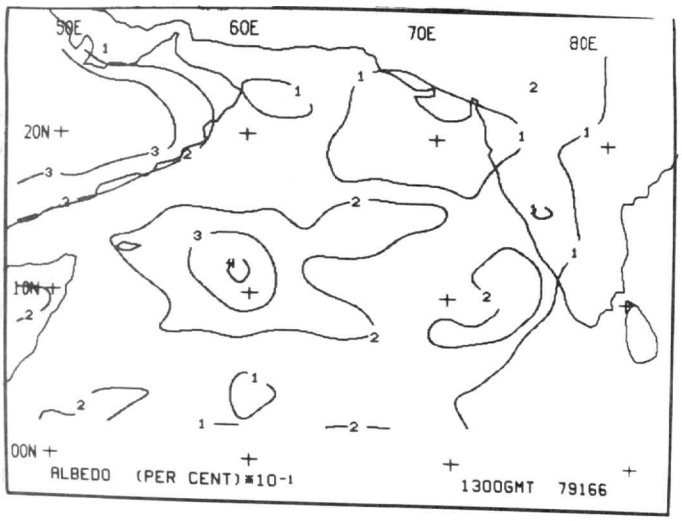
50E
60E
70E
80E
20N
10N
0ON
ALBEDO (PER CENT)*10-1
1300GMT 79166

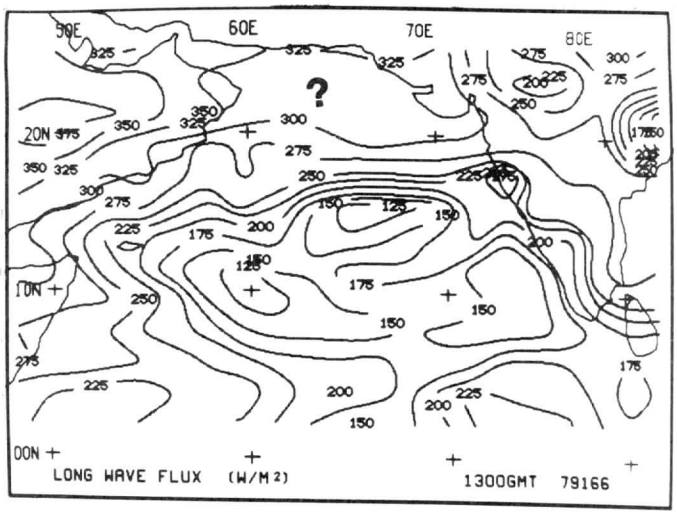
50E
60E
70E
80E
20N
10N
0ON
LONG WAVE FLUX (W/M2)
1300GMT 79166

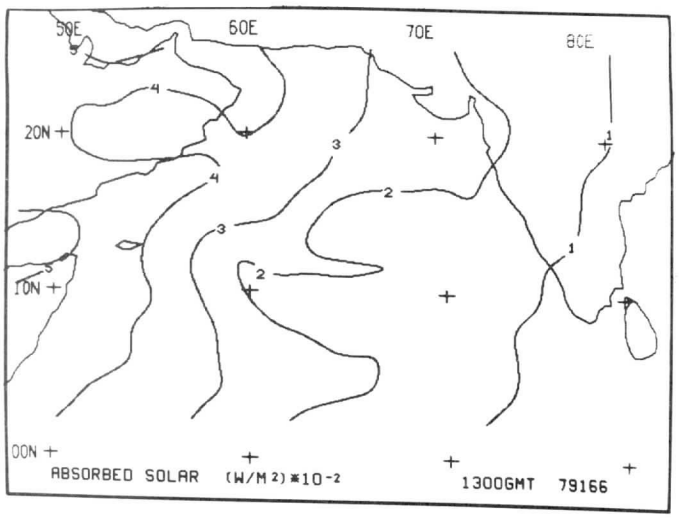
50E
60E
70E
80E
20N
10N
0ON
ABSORBED SOLAR (W/M2)*10-2
1300GMT 79166

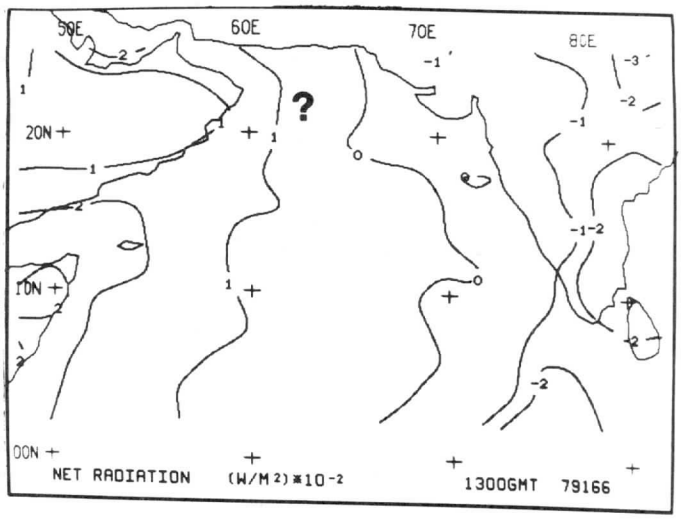
50E
60E
70E
80E
20N
10N
0ON
NET RADIATION (W/M2)*10-2
1300GMT 79166

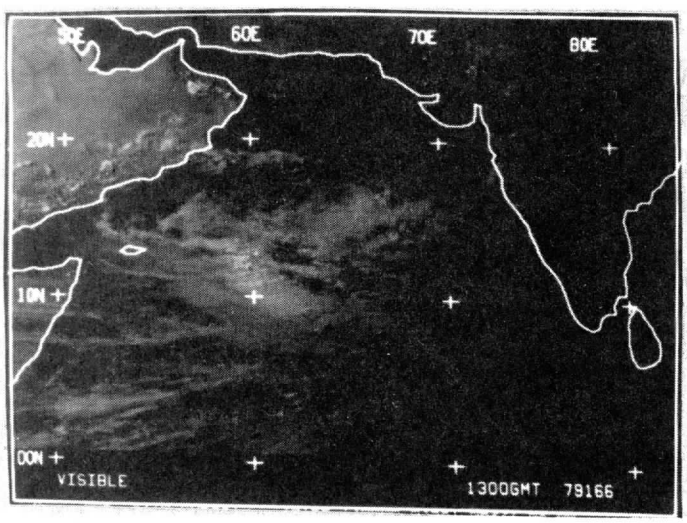
50E
60E
70E
80E
20N
10N
0ON
VISIBLE
1300GMT 79166

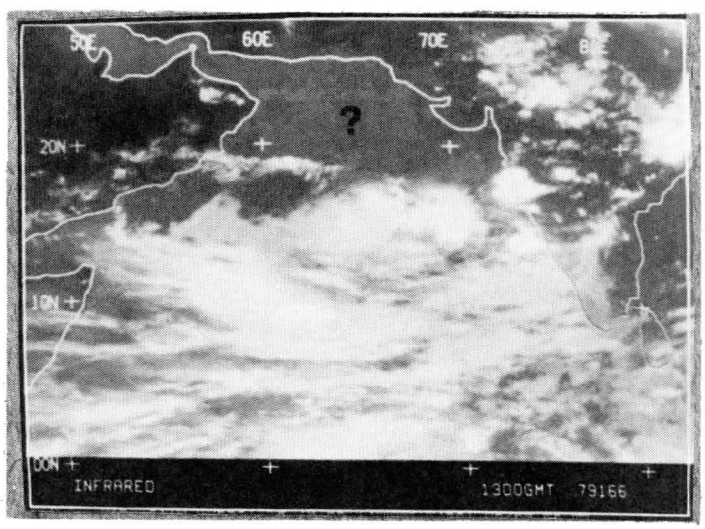
50E
60E
70E
20N
10N
0ON
INFRARED
1300GMT 79166

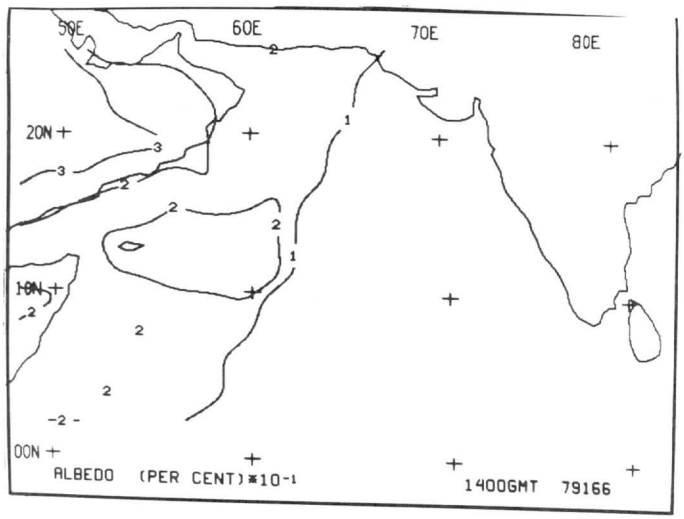
50E
60E
70E
80E
20N
10N
0ON
ALBEDO (PER CENT)*10-1
1400GMT 79166

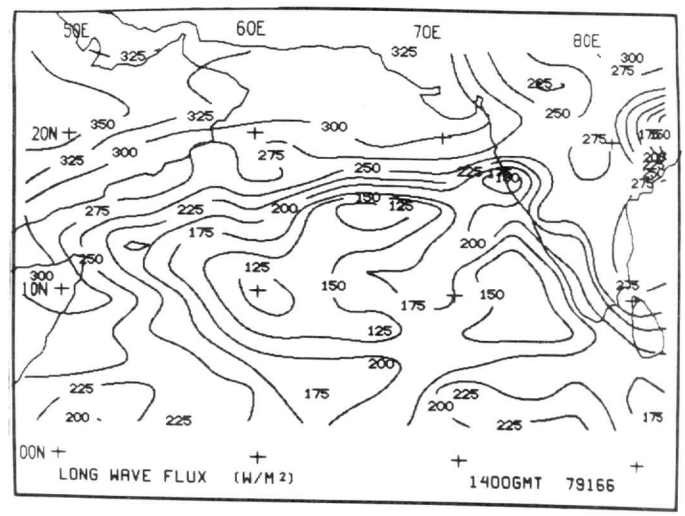
50E
60E
70E
80E
20N
10N
0ON
LONG WAVE FLUX (W/M2)
1400GMT 79166

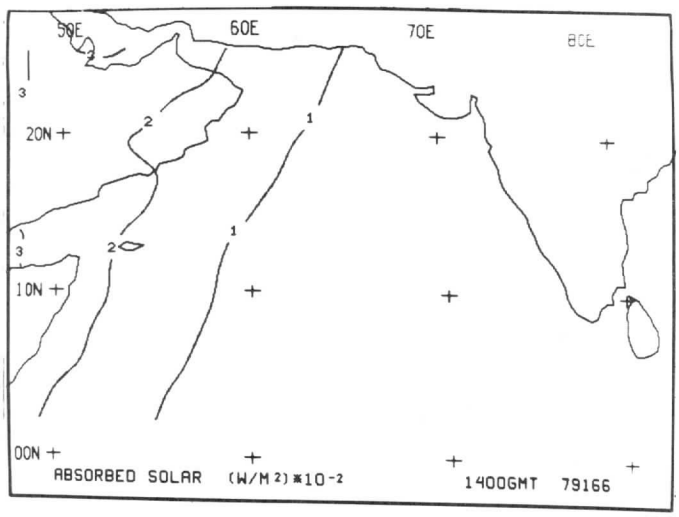
50E
60E
70E
80E
20N
10N
0ON
ABSORBED SOLAR (W/M2)*10-2
1400GMT 79166

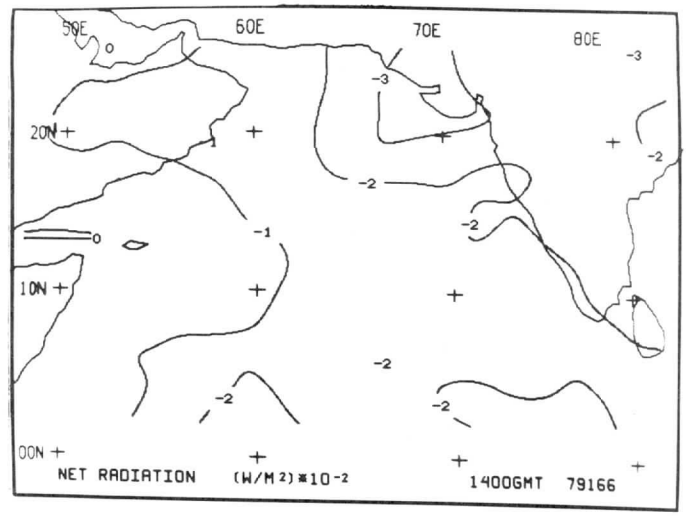
50E
60E
70E
80E
20N
10N
0ON
NET RADIATION (W/M2)*10-2
1400GMT 79166

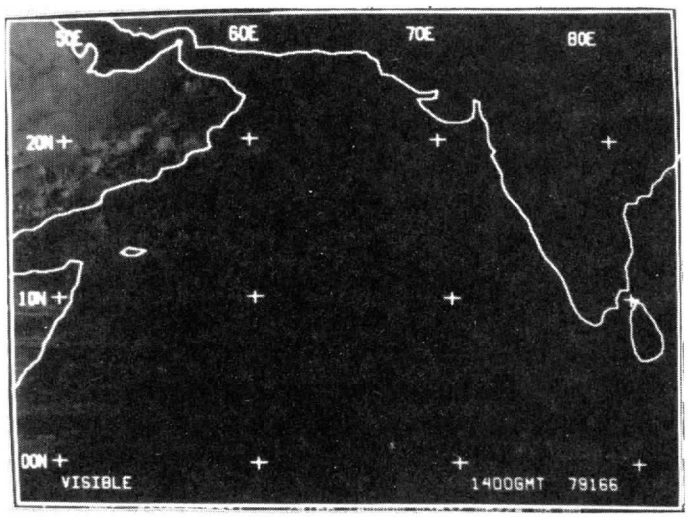
50E
60E
70E
80E
20N
10N
0ON
VISIBLE
1400GMT 79166

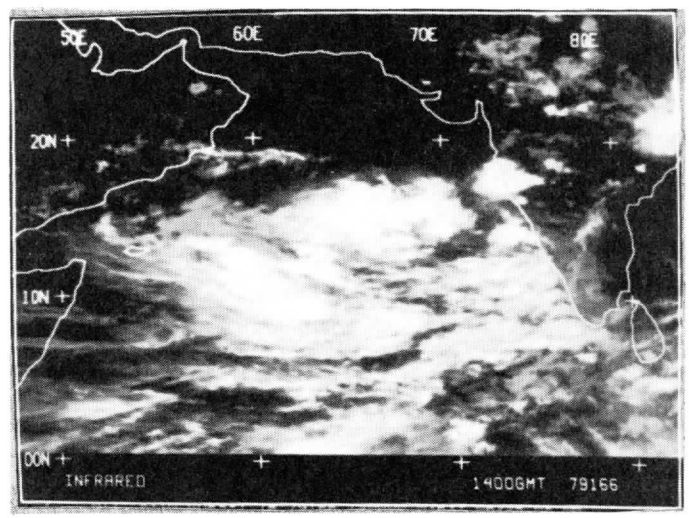
50E
60E
70E
80E
20N
10N
0ON
INFRARED
1400GMT 79166

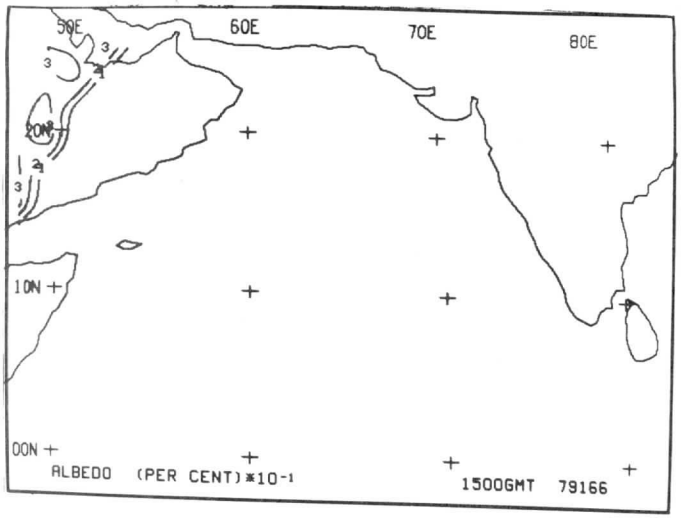
50E
60E
70E
80E
20N
10N
0ON
ALBEDO (PER CENT)*10-1
1500GMT 79166

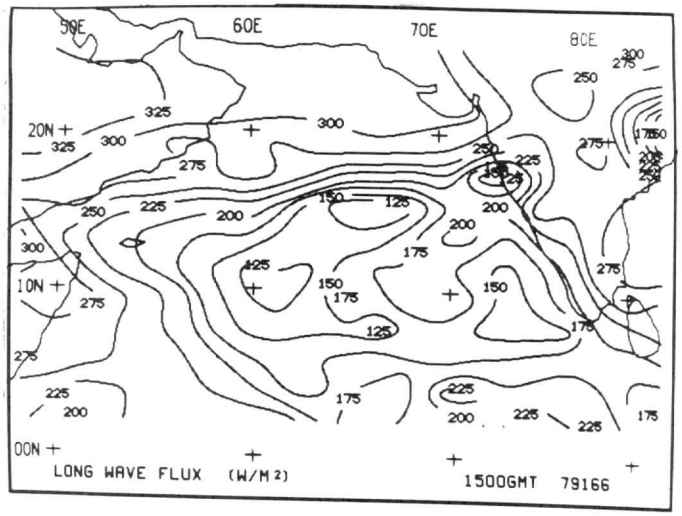
50E
60E
70E
80E
20N
10N
0ON
LONG WAVE FLUX (W/M2)
1500GMT 79166

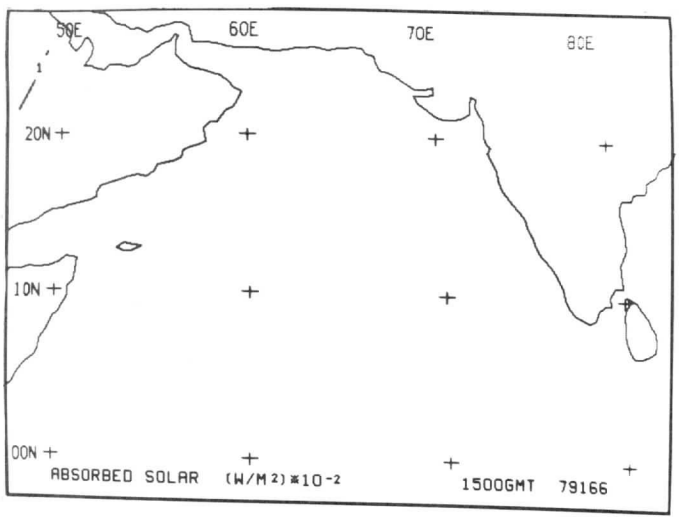
50E
60E
70E
80E
20N
10N
0ON
ABSORBED SOLAR (W/M2)*10-2
1500GMT 79166

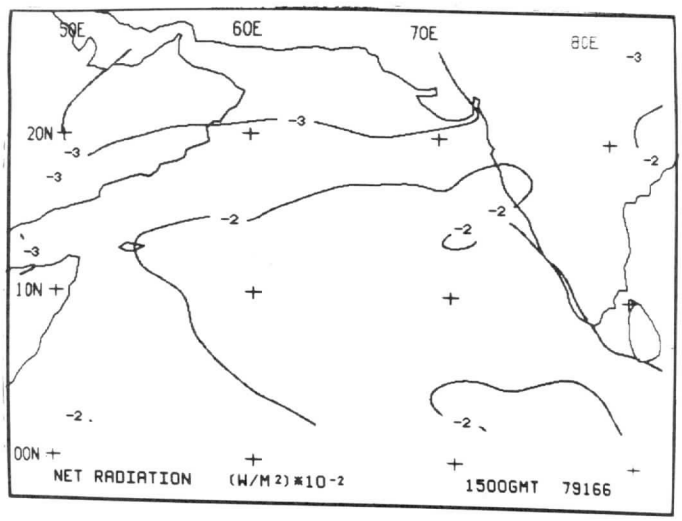
50E
60E
70E
80E
20N
10N
0ON
NET RADIATION (W/M2)*10-2
1500GMT 79166

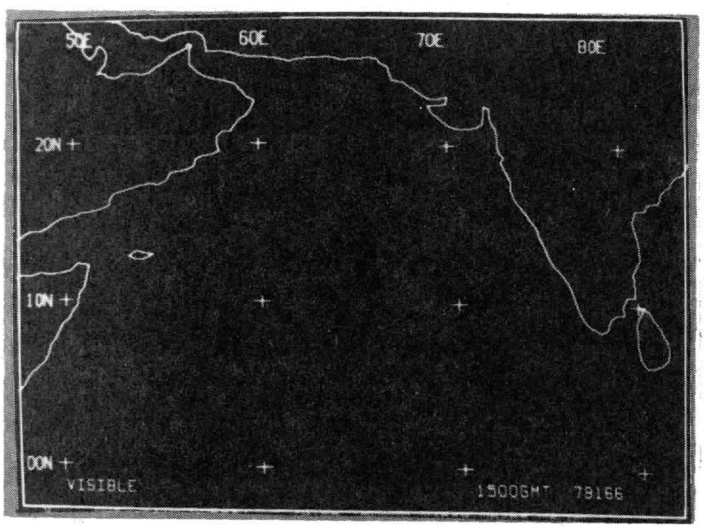
50E
60E
70E
80E
20N
10N
0ON
VISIBLE
1500GMT 79166

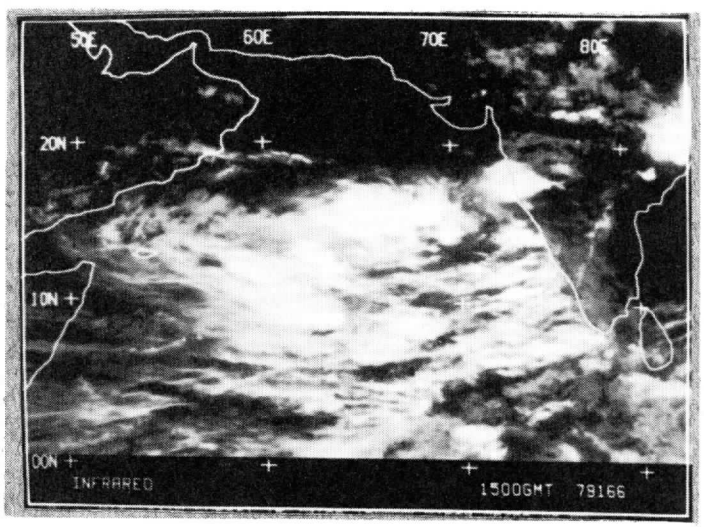
50E
60E
70E
80E
20N
10N
0ON
INFRARED
1500GMT 79166

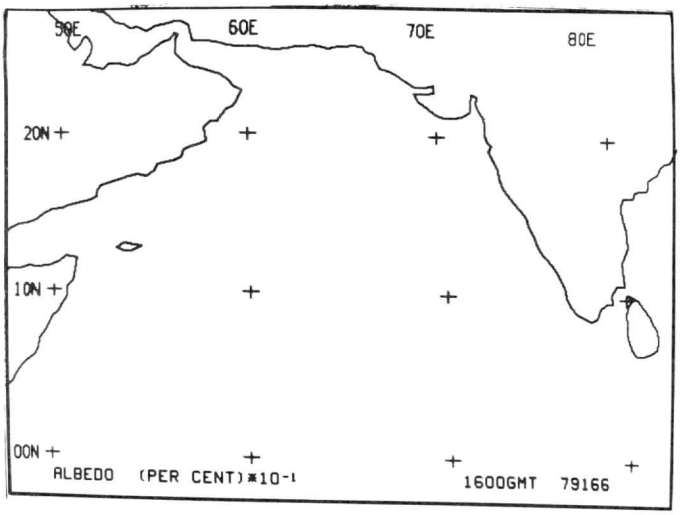
50E
60E
70E
80E
20N
10N
0ON
ALBEDO (PER CENT)*10-1
1600GMT 79166

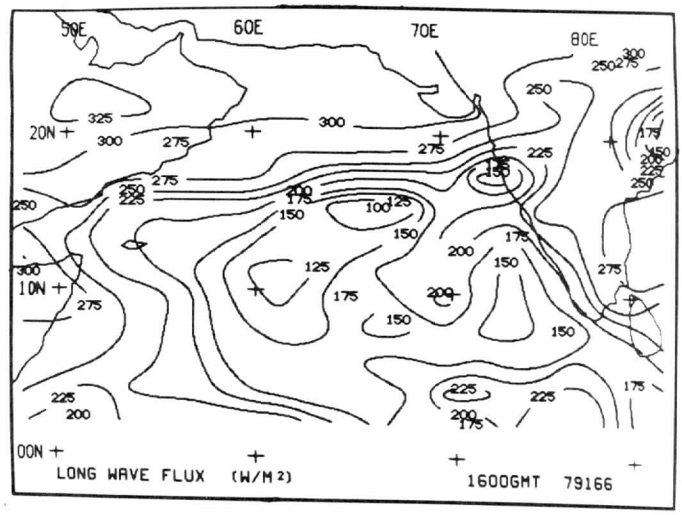
50E
60E
70E
80E
20N
10N
0ON
LONG WAVE FLUX (W/M2)
1600GMT 79166

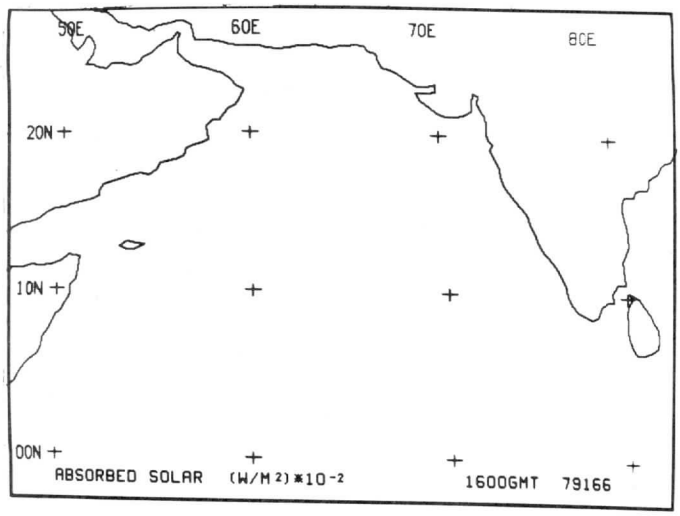
50E
60E
70E
80E
20N
10N
0ON
ABSORBED SOLAR (W/M2)*10-2
1600GMT 79166

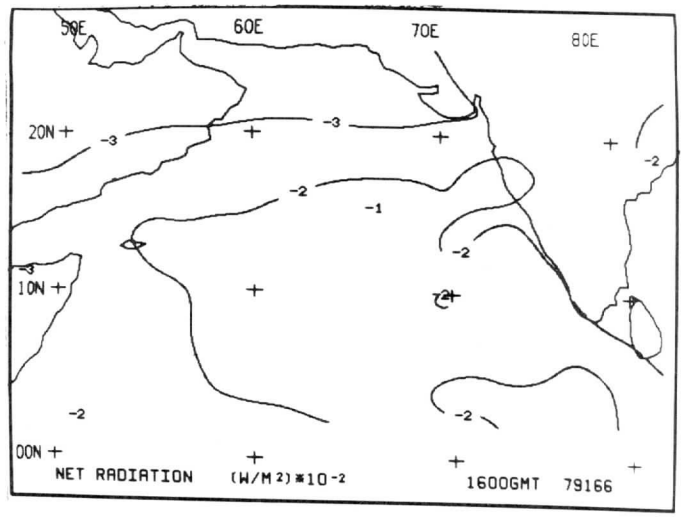
50E
60E
70E
80E
20N
10N
0ON
NET RADIATION (W/M2)*10-2
1600GMT 79166

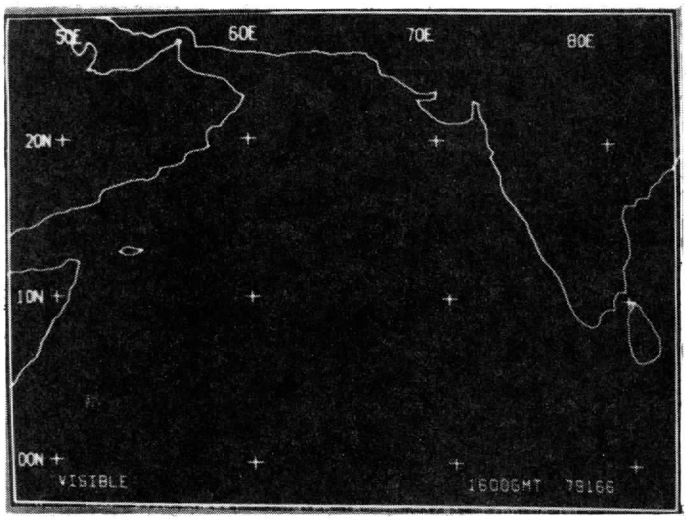
50E
60E
70E
80E
20N
10N
0ON
VISIBLE
1600GMT 79166

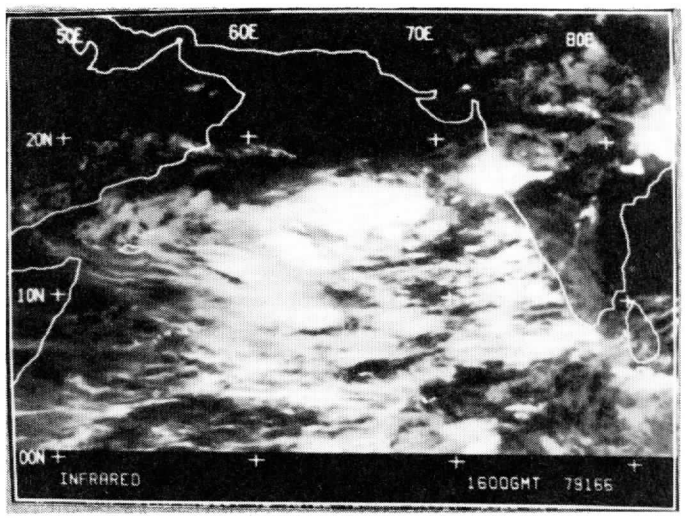
50E
60E
70E
80E
20N
10N
0ON
INFRARED
1600GMT 79166

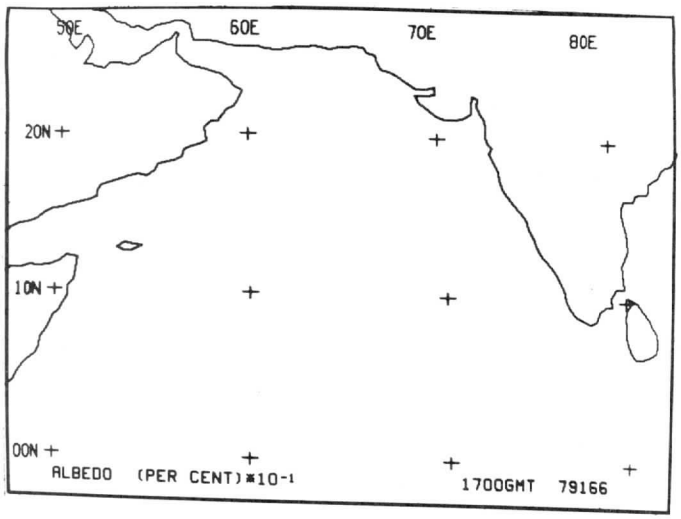
50E
60E
70E
80E
20N
10N
00N
ALBEDO (PER CENT)*10-1
1700GMT 79166

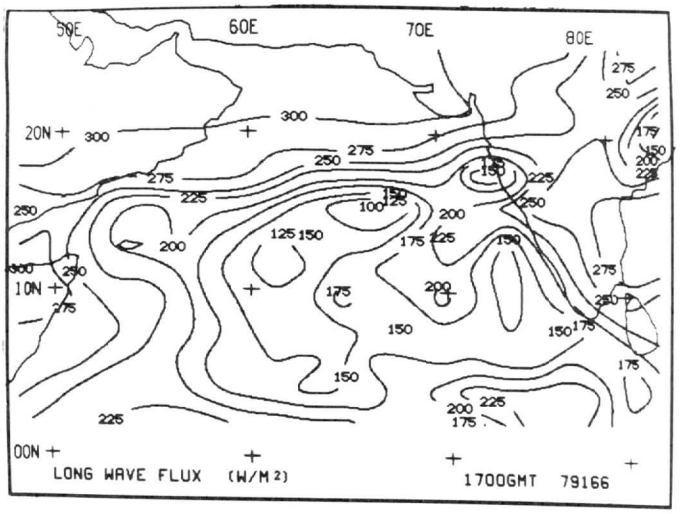
50E
60E
70E
80E
20N
10N
00N
LONG WAVE FLUX (W/M2)
1700GMT 79166

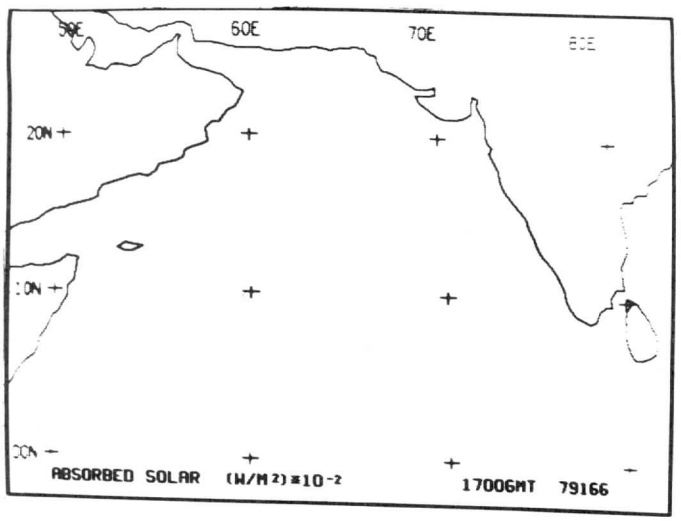
50E
60E
70E
80E
20N
10N
00N
ABSORBED SOLAR (W/M2)*10-2
1700GMT 79166

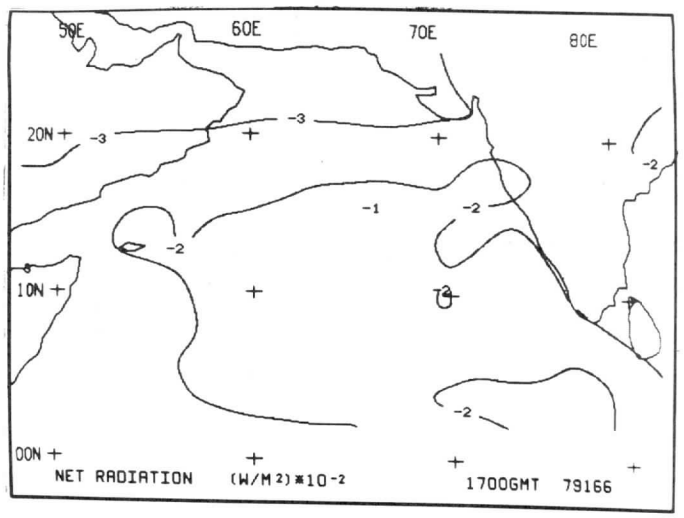
50E
60E
70E
80E
20N
10N
00N
NET RADIATION (W/M2)*10-2
1700GMT 79166

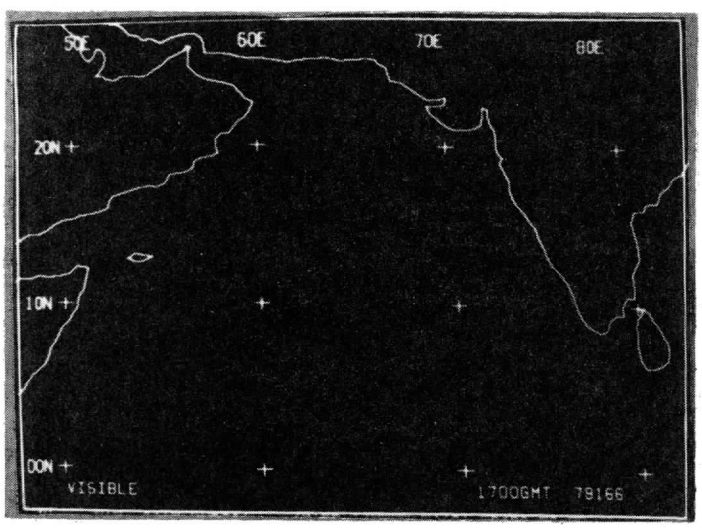
50E
60E
70E
80E
20N
10N
00N
VISIBLE
1700GMT 79166

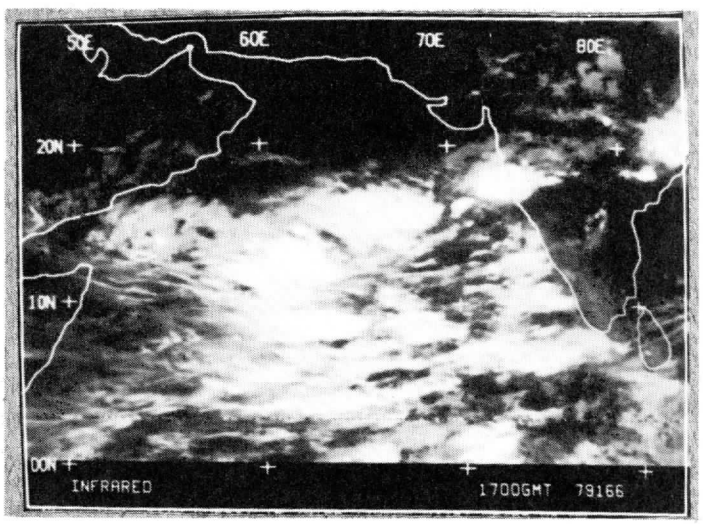
50E
60E
70E
80E
20N
10N
00N
INFRARED
1700GMT 79166

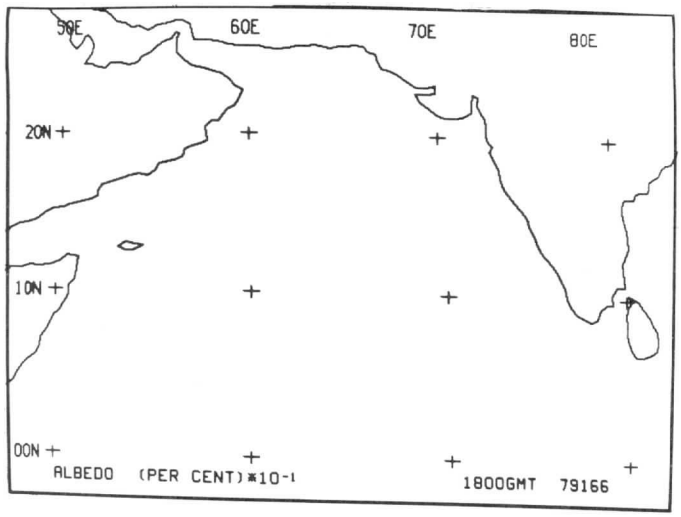
50E
60E
70E
80E
20N
10N
0ON
ALBEDO (PER CENT)*10-1
1800GMT 79166

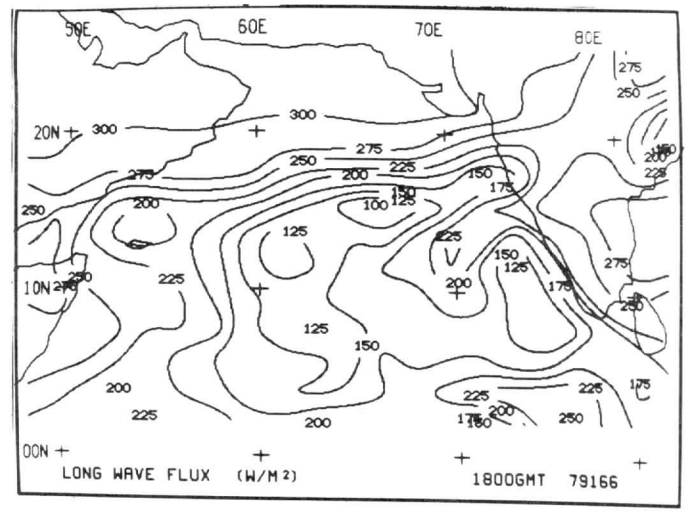
50E
60E
70E
80E
20N
10N
0ON
LONG WAVE FLUX (W/M2)
1800GMT 79166

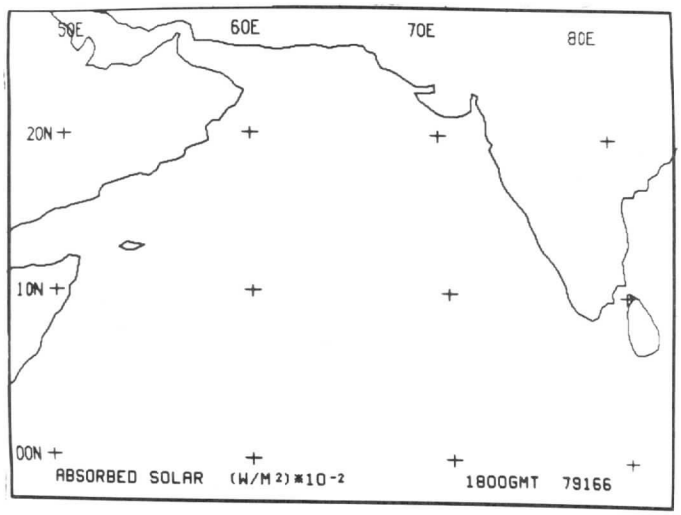
50E
60E
70E
80E
20N
10N
0ON
ABSORBED SOLAR (W/M2)*10-2
1800GMT 79166

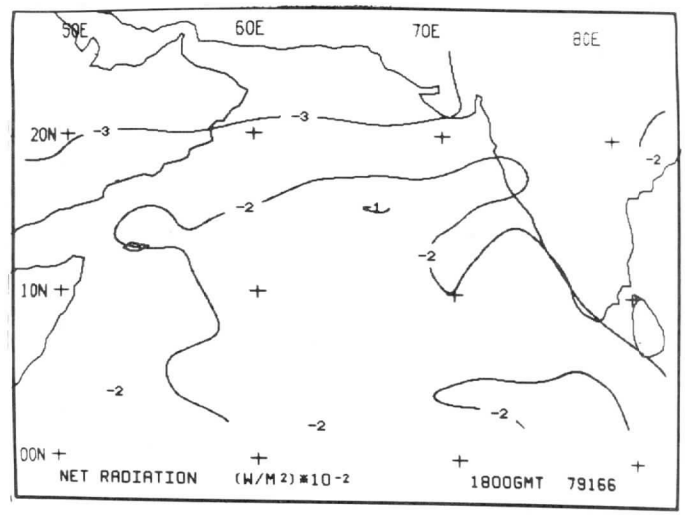
50E
60E
70E
80E
20N
10N
0ON
NET RADIATION (W/M2)*10-2
1800GMT 79166

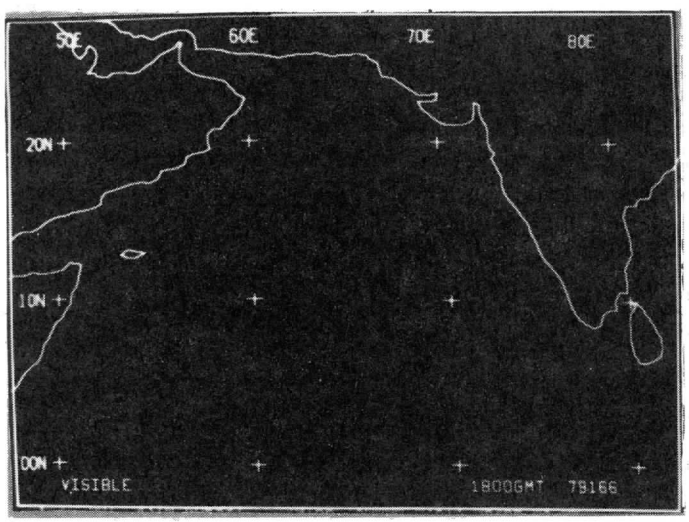
50E
60E
70E
80E
20N
10N
0ON
VISIBLE
1800GMT 79166

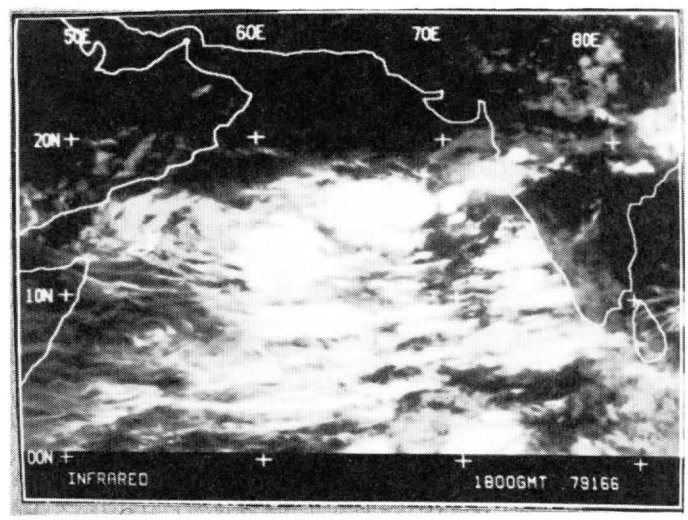
50E
60E
70E
80E
20N
10N
0ON
INFRARED
1800GMT 79166

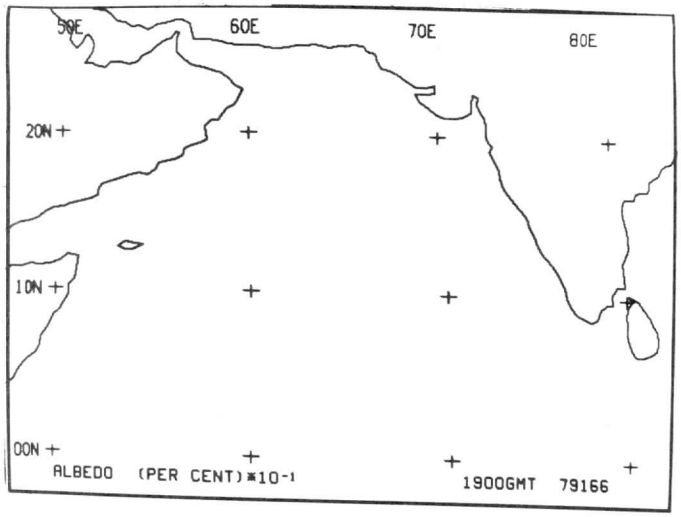
50E
60E
70E
80E
20N
10N
0ON
ALBEDO (PER CENT)*10-1
1900GMT 79166

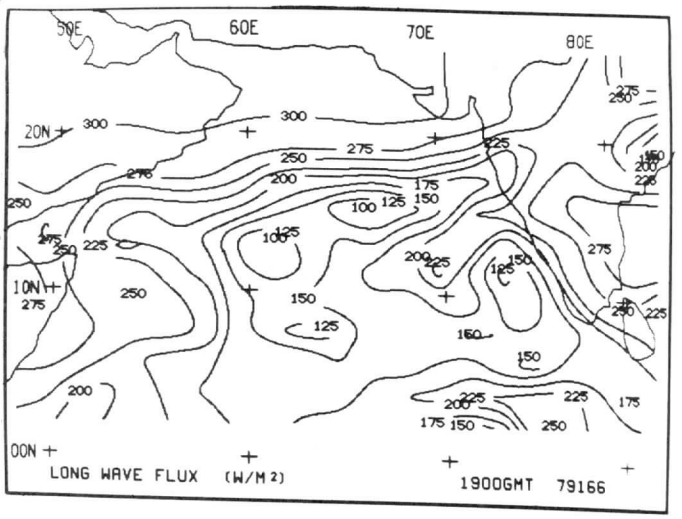
50E
60E
70E
80E
20N
10N
0ON
LONG WAVE FLUX (W/M2)
1900GMT 79166

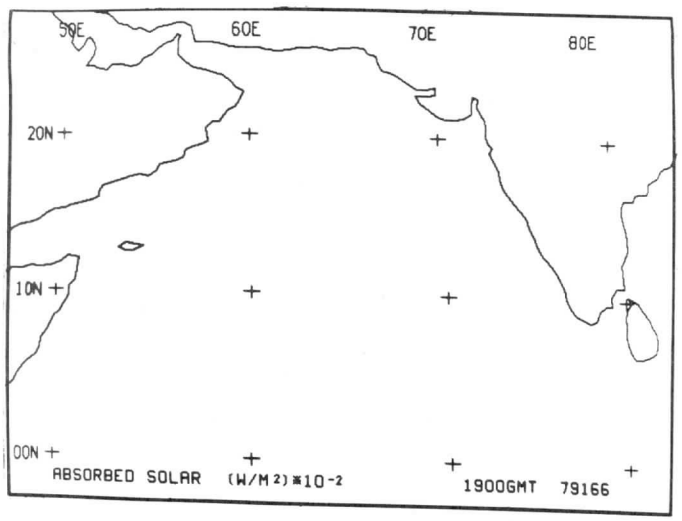
50E
60E
70E
80E
20N
10N
0ON
ABSORBED SOLAR (W/M2)*10-2
1900GMT 79166

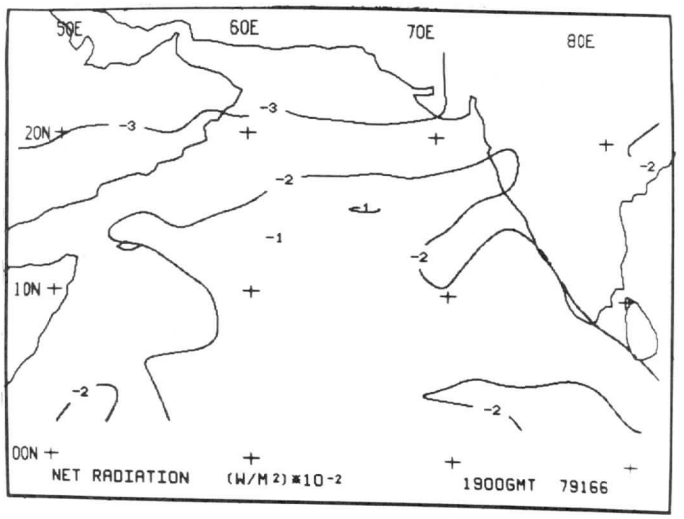
50E
60E
70E
80E
20N
10N
0ON
NET RADIATION (W/M2)*10-2
1900GMT 79166

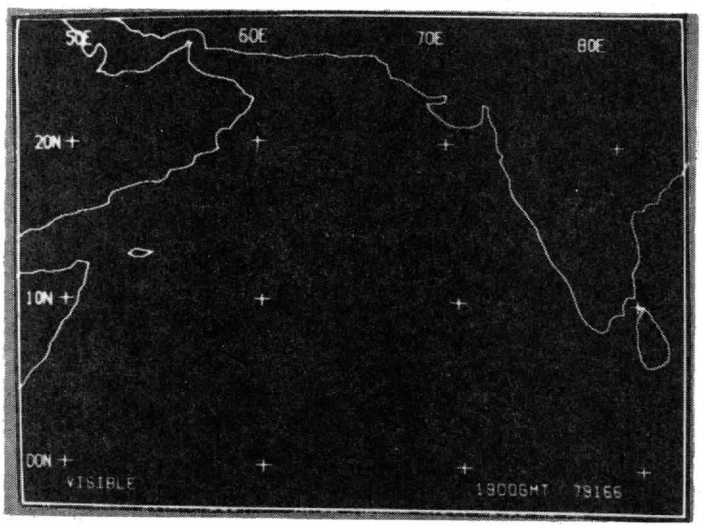
50E
60E
70E
80E
20N
10N
0ON
VISIBLE
1900GMT 79166

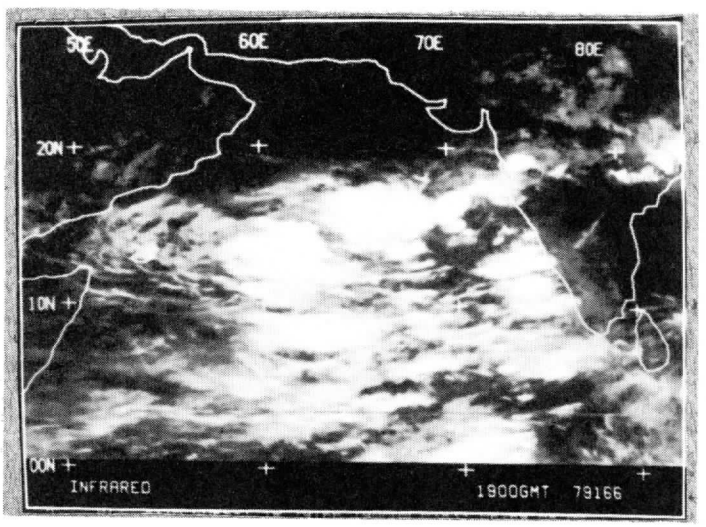
50E
60E
70E
80E
20N
10N
0ON
INFRARED
1900GMT 79166

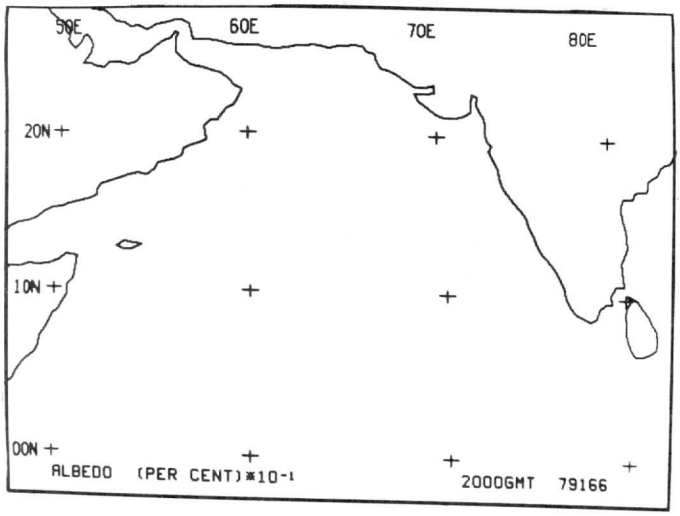
50E
60E
70E
80E
20N
10N
0ON
ALBEDO (PER CENT)*10-1
2000GMT 79166

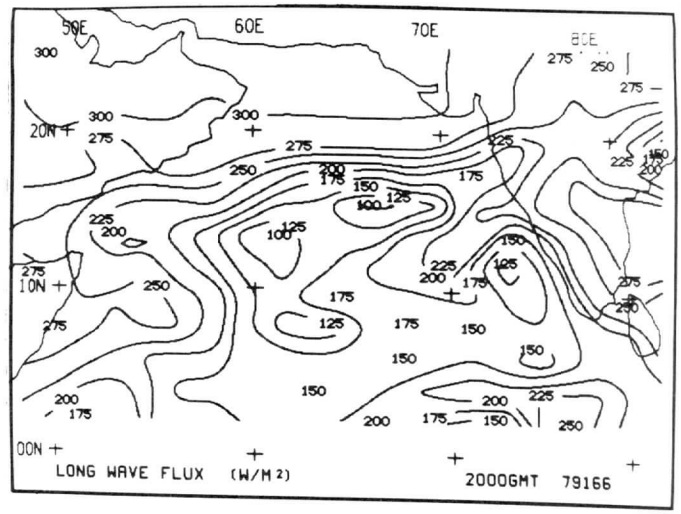
50E
60E
70E
80E
20N
10N
0ON
LONG WAVE FLUX (W/M2)
2000GMT 79166

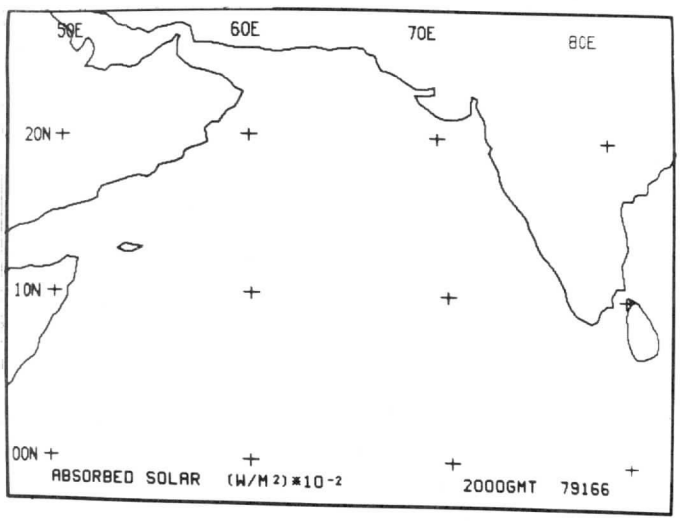
50E
60E
70E
80E
20N
10N
0ON
ABSORBED SOLAR (W/M2)*10-2
2000GMT 79166

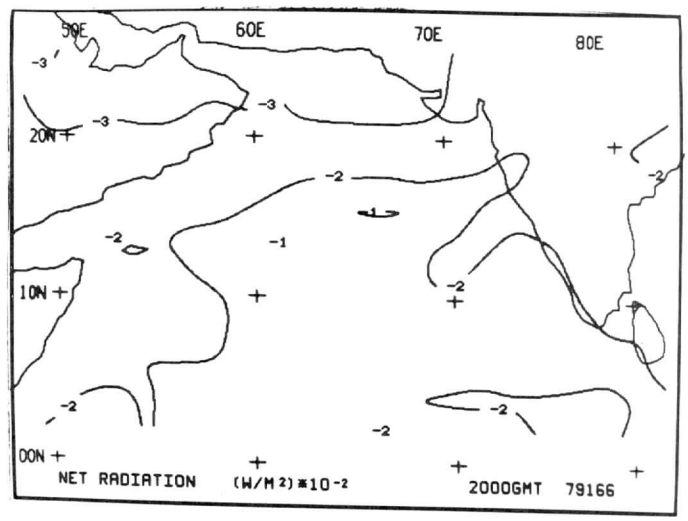
50E
60E
70E
80E
20N
10N
0ON
NET RADIATION (W/M2)*10-2
2000GMT 79166

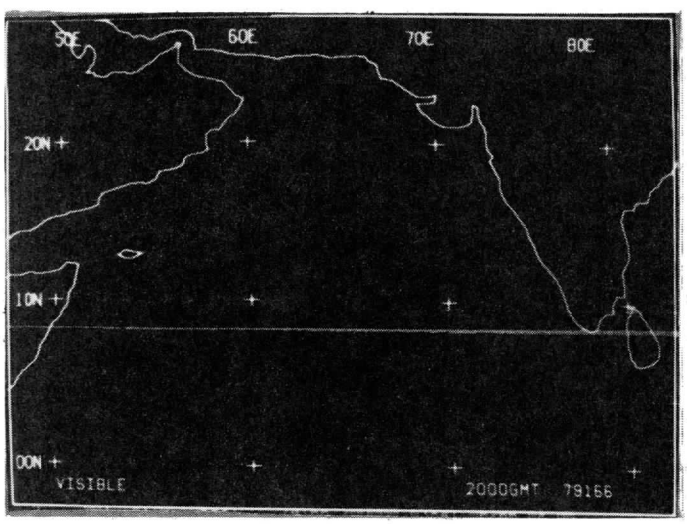
50E
60E
70E
80E
20N
10N
0ON
VISIBLE
2000GMT 79166

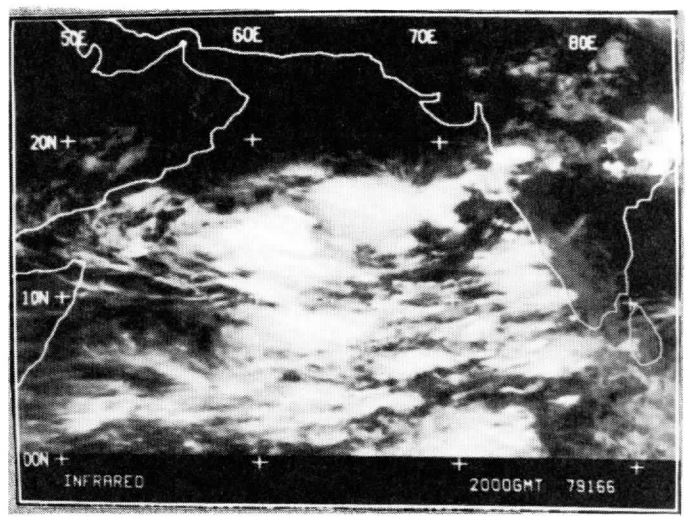
50E
60E
70E
80E
20N
10N
0ON
INFRARED
2000GMT 79166

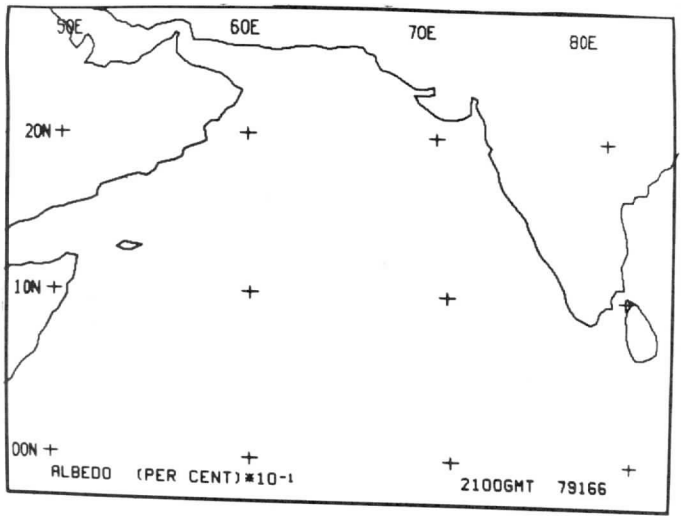
50E
60E
70E
80E
20N
10N
0ON
ALBEDO (PER CENT)*10-1
2100GMT 79166

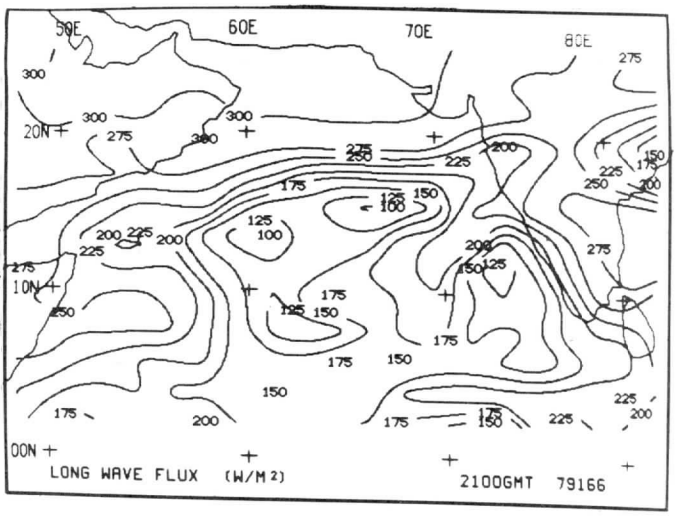
50E
60E
70E
80E
20N
10N
0ON
LONG WAVE FLUX (W/M2)
2100GMT 79166

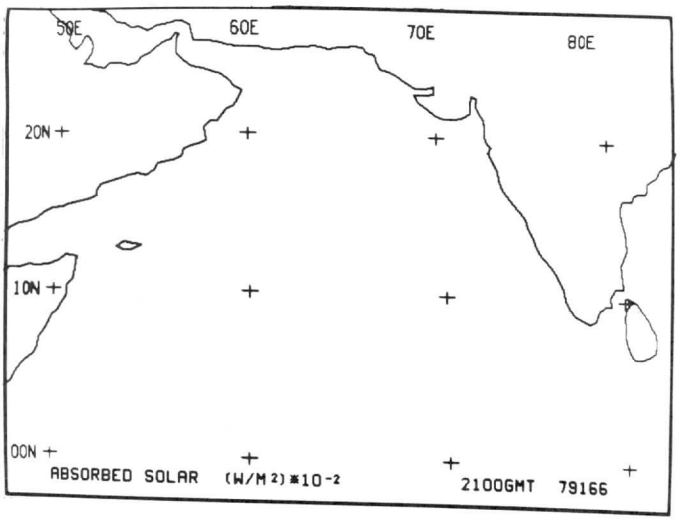
50E
60E
70E
80E
20N
10N
0ON
ABSORBED SOLAR (W/M2)*10-2
2100GMT 79166

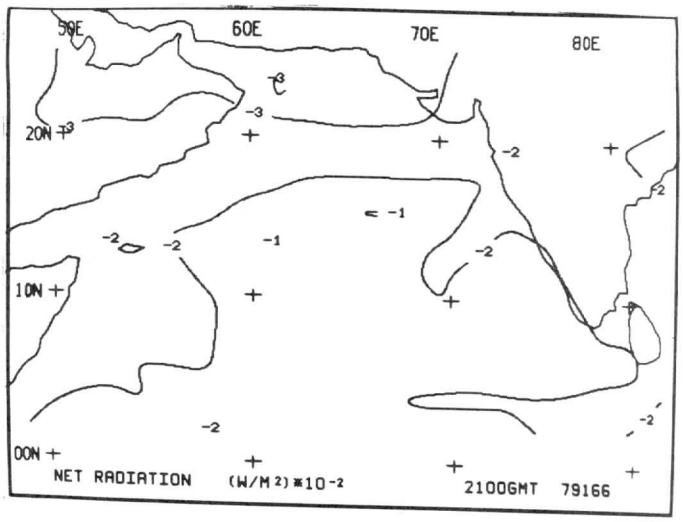
50E
60E
70E
80E
20N
10N
0ON
NET RADIATION (W/M2)*10-2
2100GMT 79166

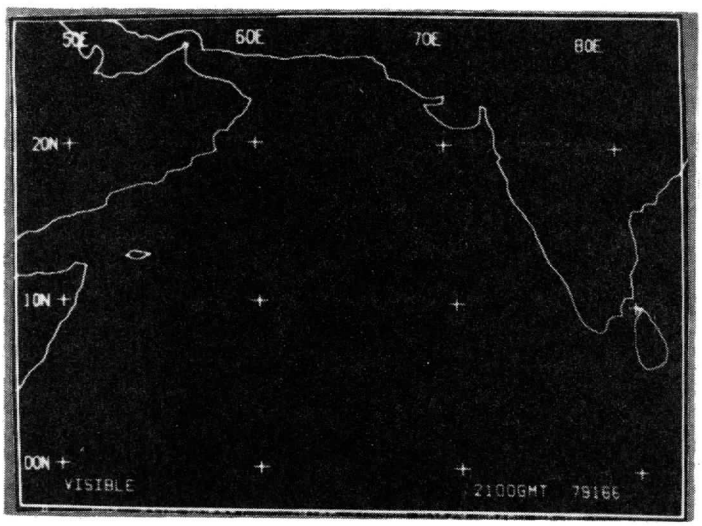
50E
60E
70E
80E
20N
10N
0ON
VISIBLE
2100GMT 79166

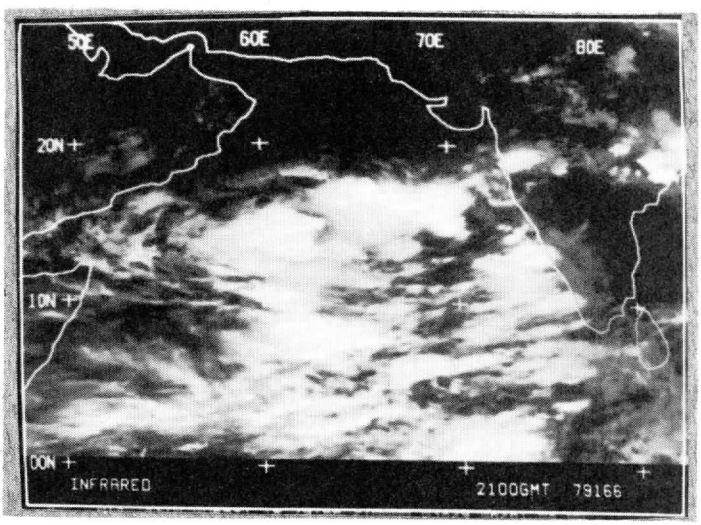
50E
60E
70E
80E
20N
10N
0ON
INFRARED
2100GMT 79166

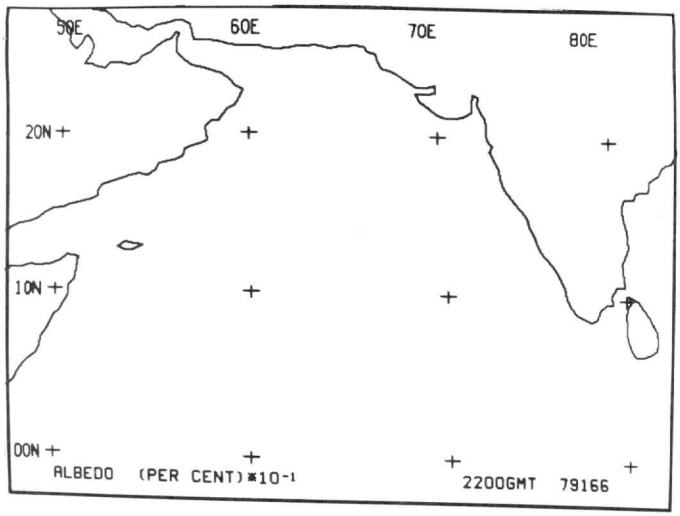
50E
60E
70E
80E
20N
10N
0ON
ALBEDO (PER CENT)*10-1
2200GMT 79166

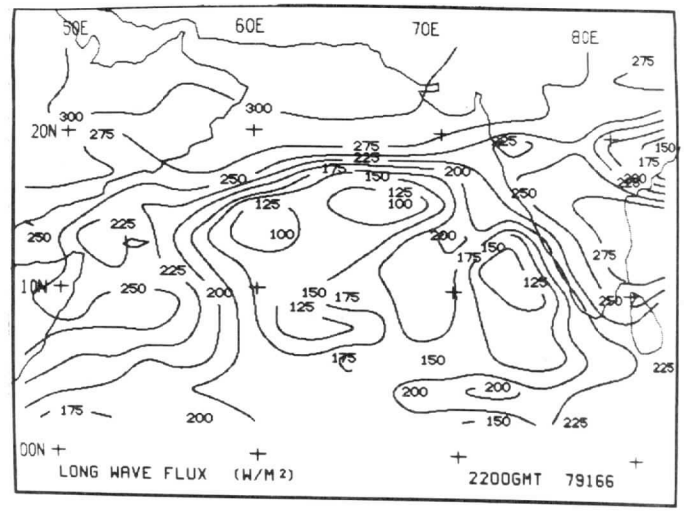
50E
60E
70E
80E
20N
10N
0ON
LONG WAVE FLUX (W/M2)
2200GMT 79166

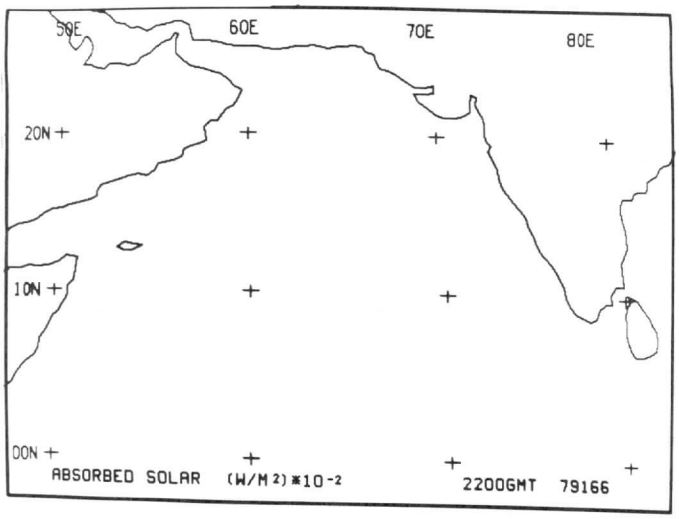
50E
60E
70E
80E
20N
10N
0ON
ABSORBED SOLAR (W/M2)*10-2
2200GMT 79166

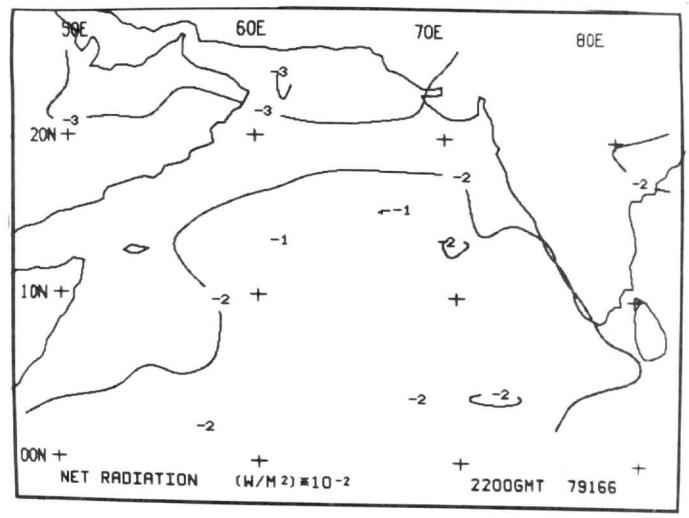
50E
60E
70E
80E
20N
10N
0ON
NET RADIATION (W/M2)*10-2
2200GMT 79166

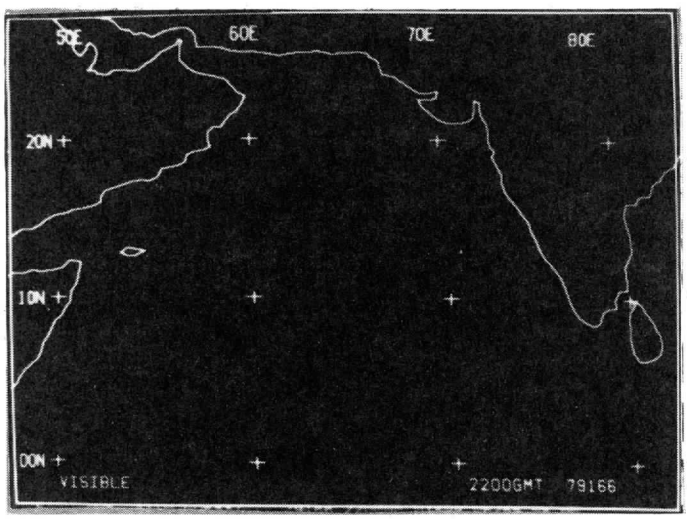
50E
60E
70E
80E
20N
10N
0ON
VISIBLE
2200GMT 79166

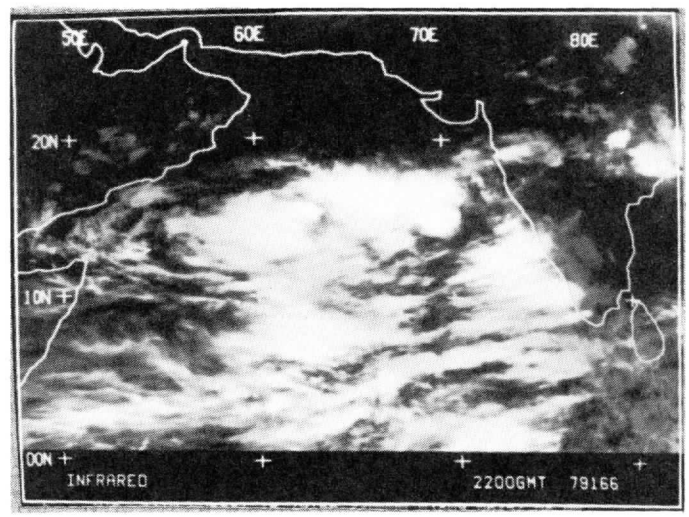
50E
60E
70E
80E
20N
10N
0ON
INFRARED
2200GMT 79166

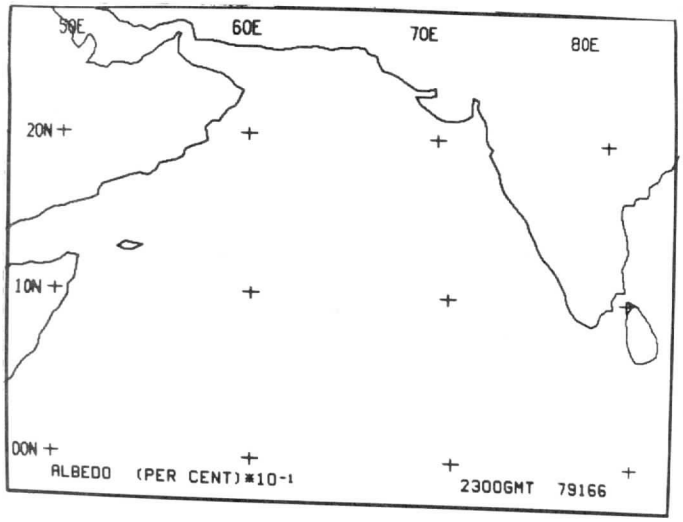
50E
60E
70E
80E
20N
10N
00N
ALBEDO (PER CENT)*10-1
2300GMT 79166

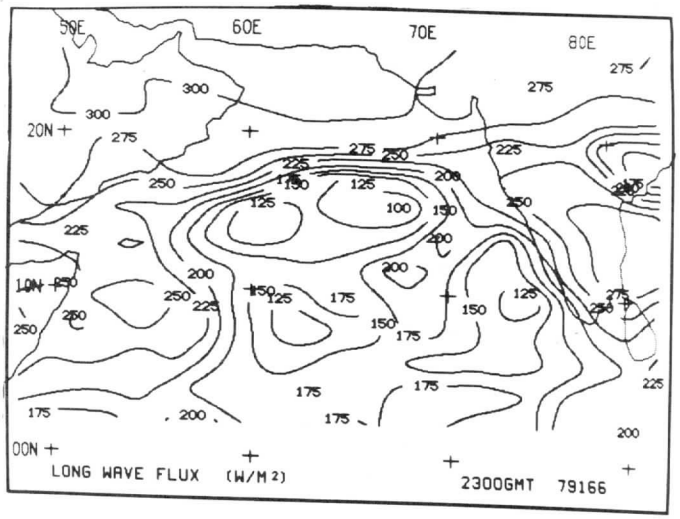
50E
60E
70E
80E
20N
10N
00N
LONG WAVE FLUX (W/M2)
2300GMT 79166

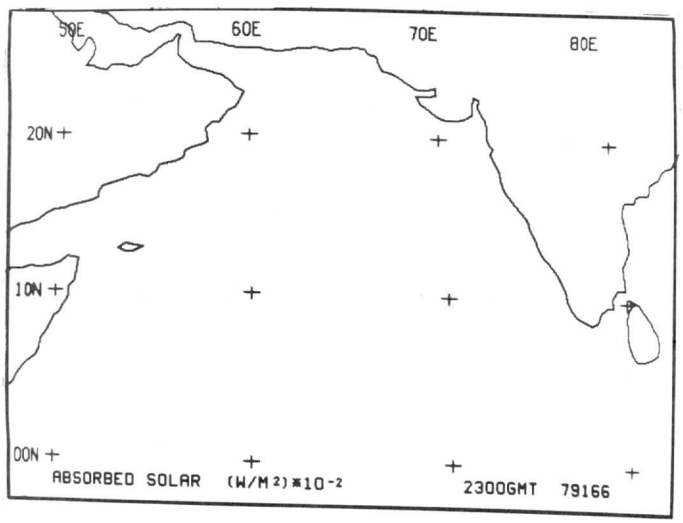
50E
60E
70E
80E
20N
10N
00N
ABSORBED SOLAR (W/M2)*10-2
2300GMT 79166

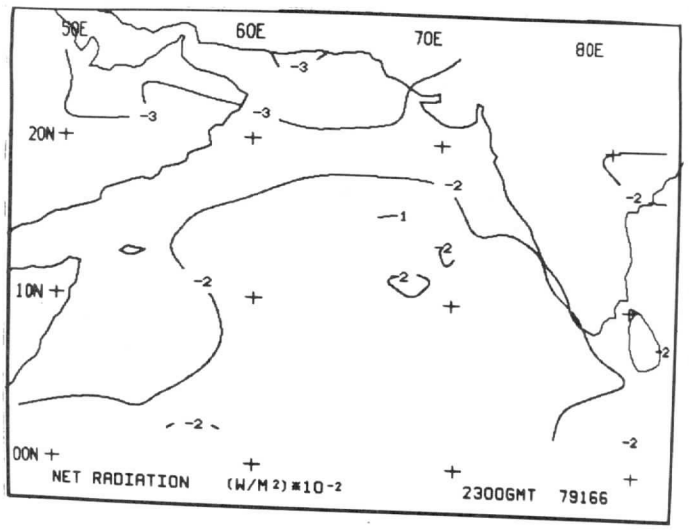
50E
60E
70E
80E
20N
10N
00N
NET RADIATION (W/M2)*10-2
2300GMT 79166

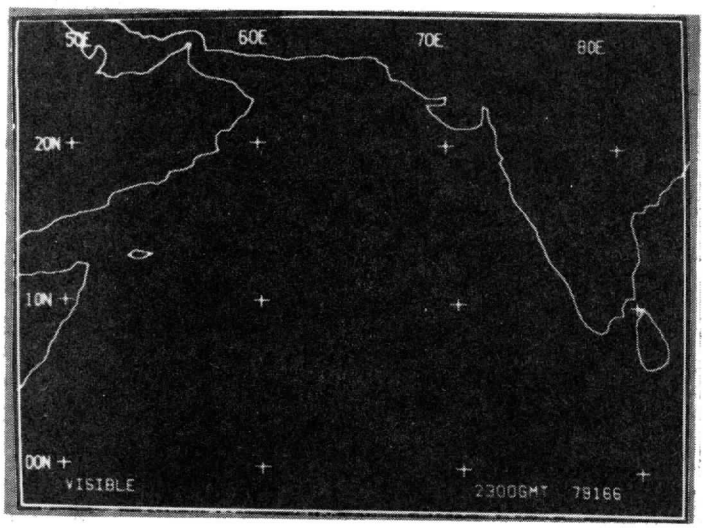
50E
60E
70E
80E
20N
10N
00N
VISIBLE
2300GMT 79166

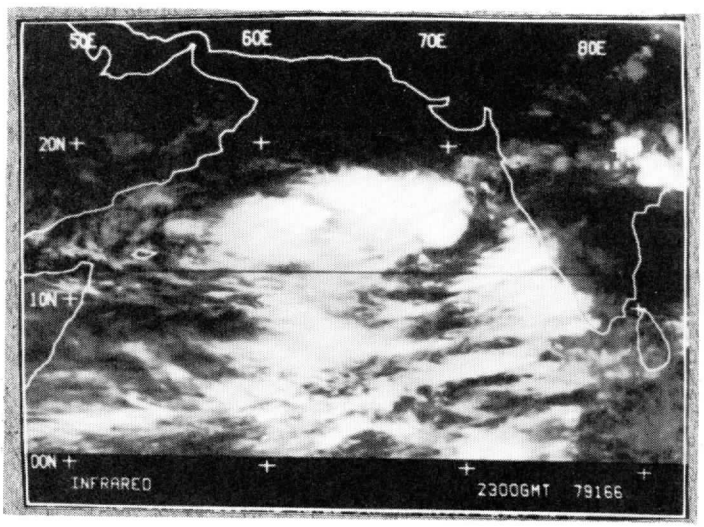
50E
60E
70E
80E
20N
10N
00N
INFRARED
2300GMT 79166

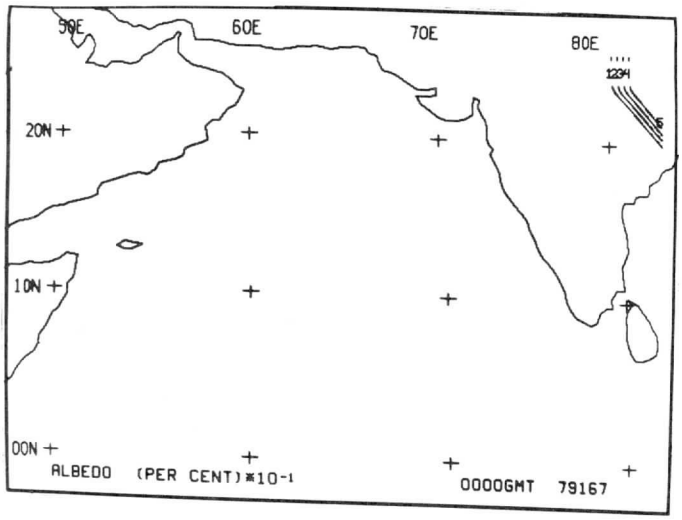
50E
60E
70E
80E
20N
10N
0ON
1234
ALBEDO (PER CENT)*10-1
0000GMT 79167

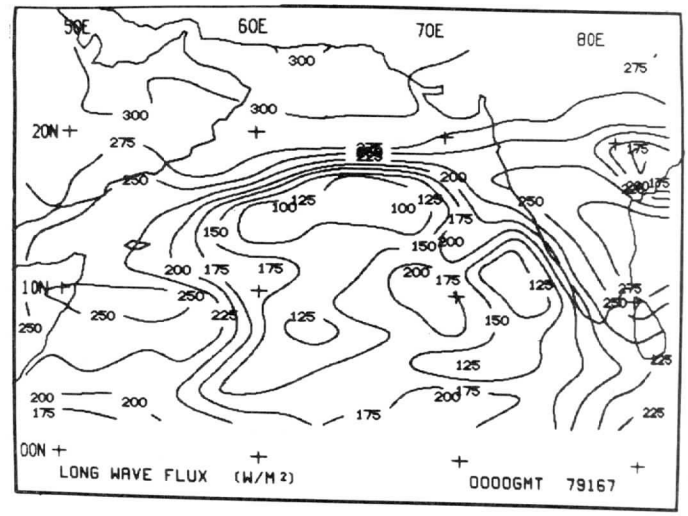
50E
60E
70E
80E
20N
10N
0ON
300
275
250
200
175
150
125
100
LONG WAVE FLUX (W/M2)
0000GMT 79167

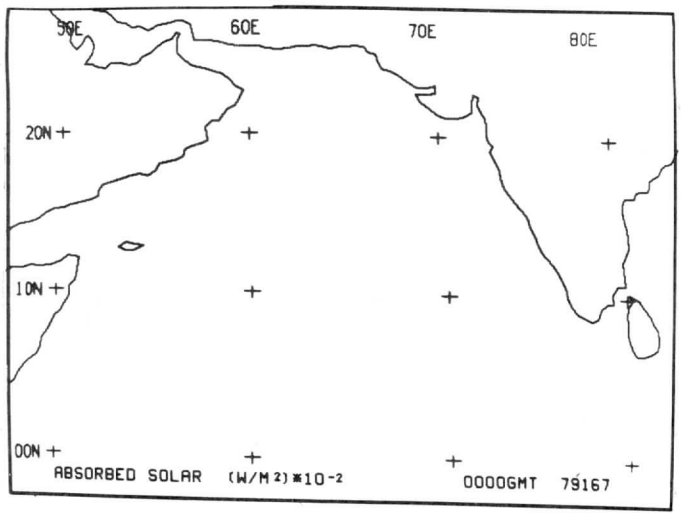
50E
60E
70E
80E
20N
10N
0ON
ABSORBED SOLAR (W/M2)*10-2
0000GMT 79167

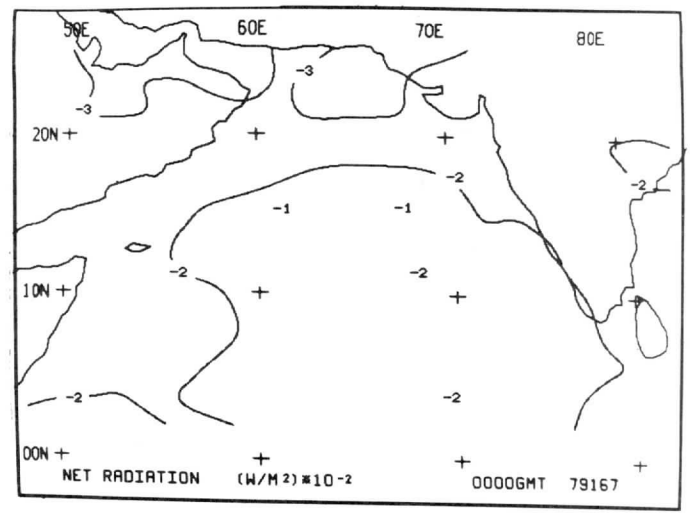
50E
60E
70E
80E
20N
10N
0ON
-3
-2
-1
NET RADIATION (W/M2)*10-2
0000GMT 79167

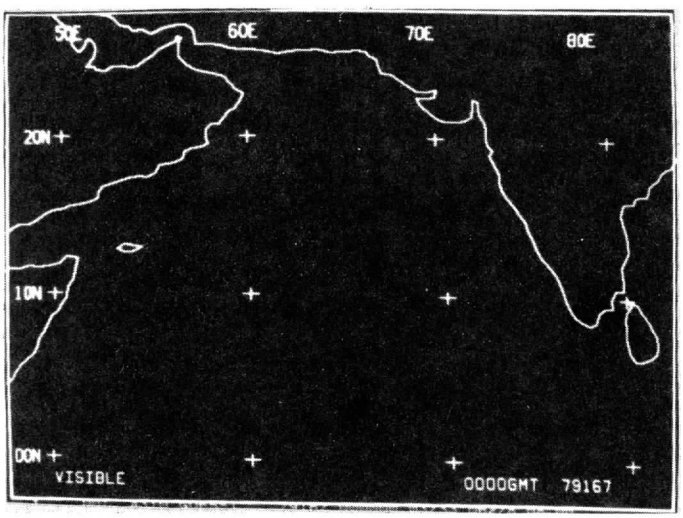
50E
60E
70E
80E
20N
10N
0ON
VISIBLE
0000GMT 79167

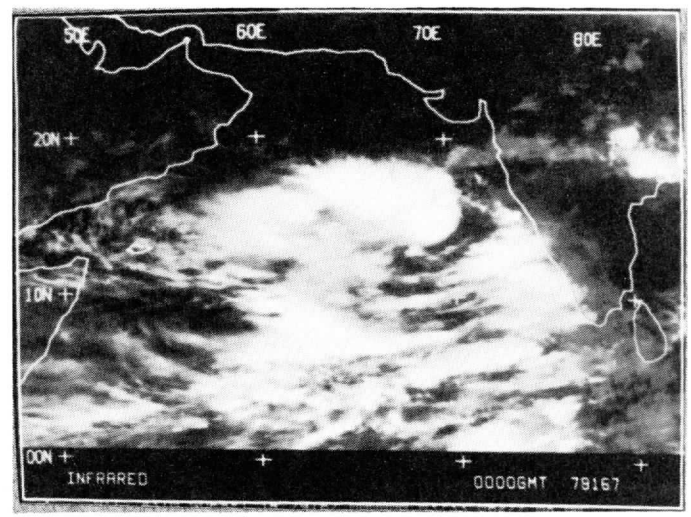
50E
60E
70E
80E
20N
10N
0ON
INFRARED
0000GMT 79167

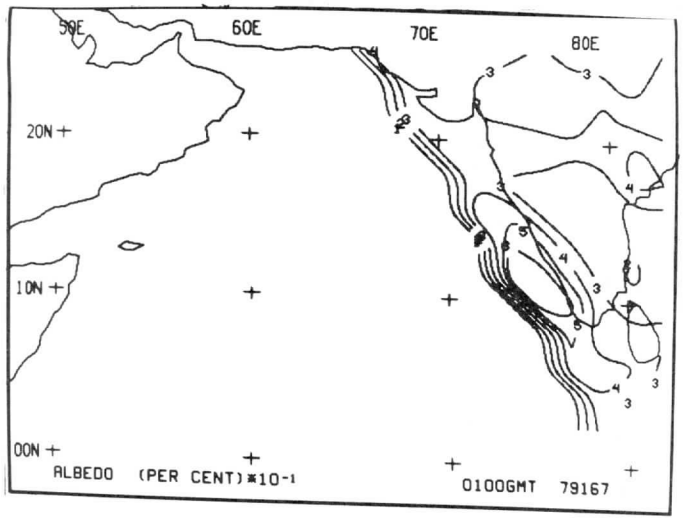
50E
60E
70E
80E
20N
10N
0ON
ALBEDO (PER CENT)*10-1
0100GMT 79167

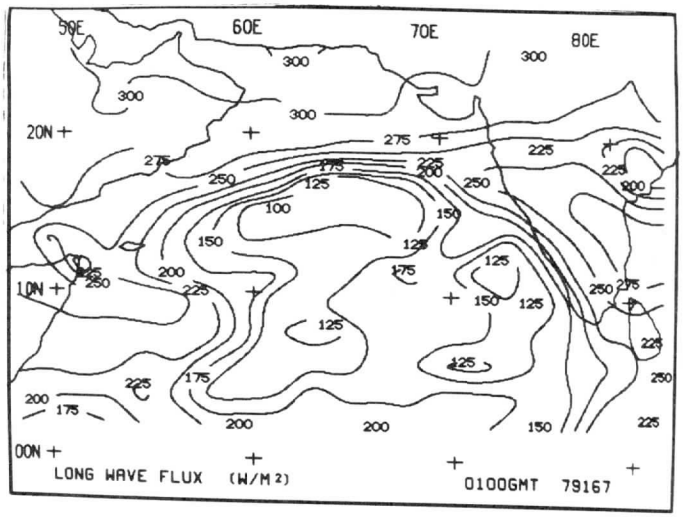
50E
60E
70E
80E
20N
10N
0ON
LONG WAVE FLUX (W/M2)
0100GMT 79167

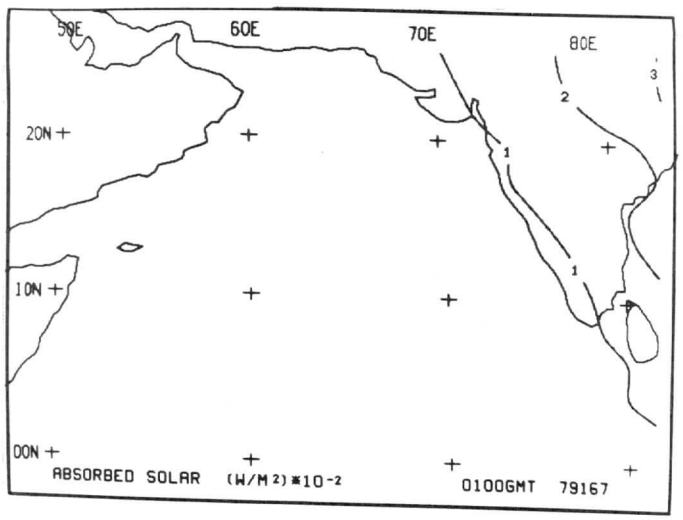
50E
60E
70E
80E
20N
10N
0ON
ABSORBED SOLAR (W/M2)*10-2
0100GMT 79167

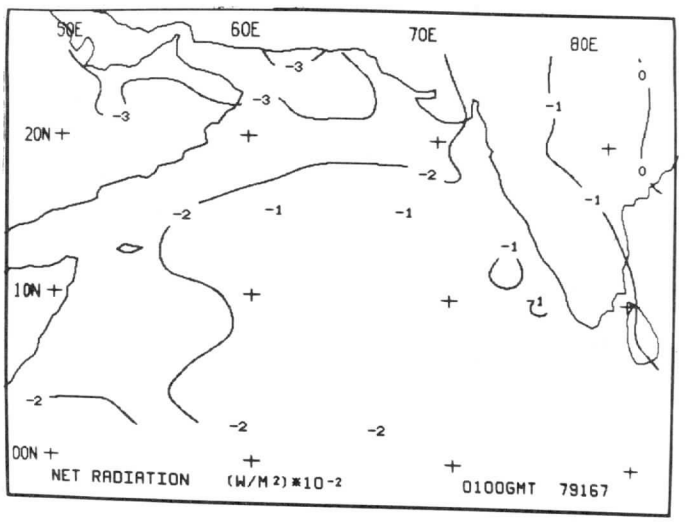
50E
60E
70E
80E
20N
10N
0ON
NET RADIATION (W/M2)*10-2
0100GMT 79167

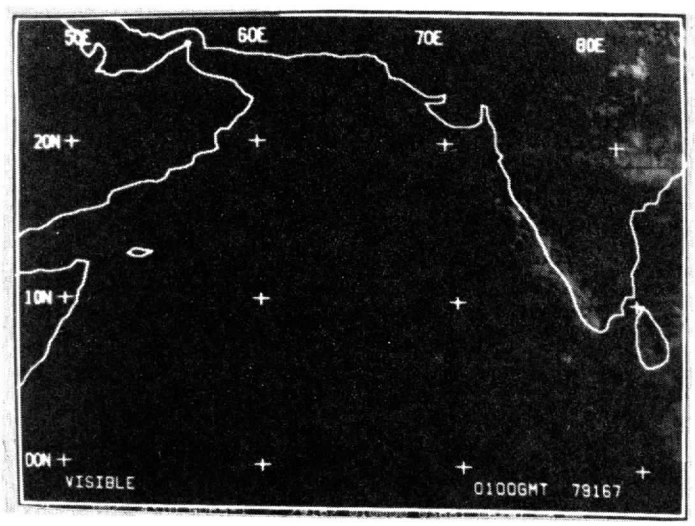
50E
60E
70E
80E
20N
10N
0ON
VISIBLE
0100GMT 79167

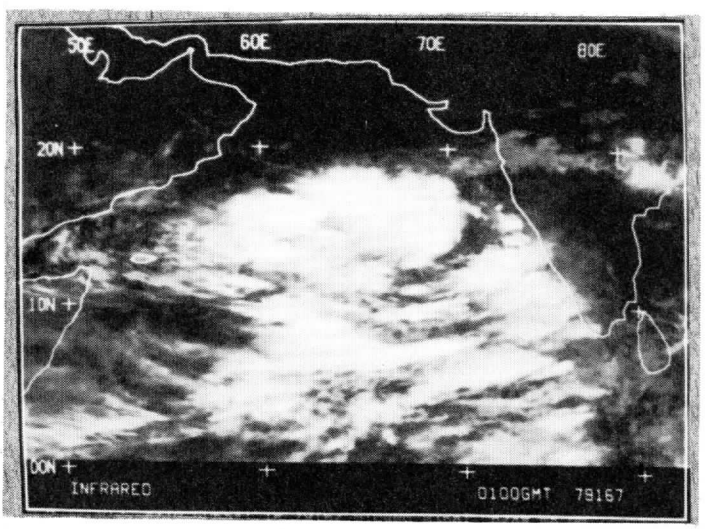
50E
60E
70E
80E
20N
10N
0ON
INFRARED
0100GMT 79167

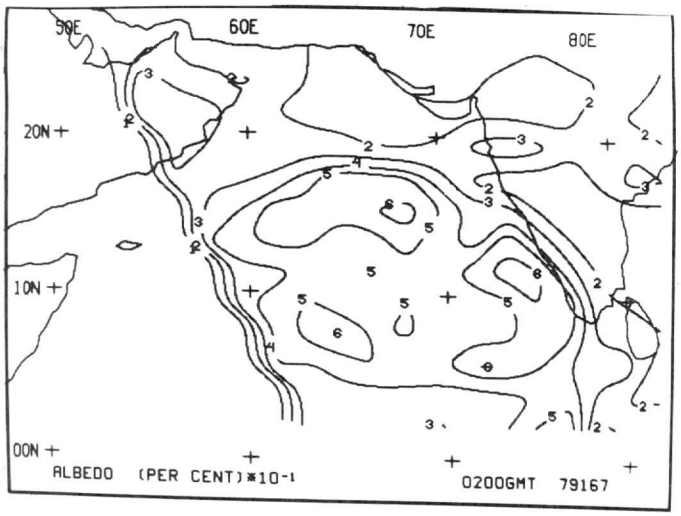
50E
60E
70E
80E
20N
10N
00N
ALBEDO (PER CENT)*10-1
0200GMT 79167

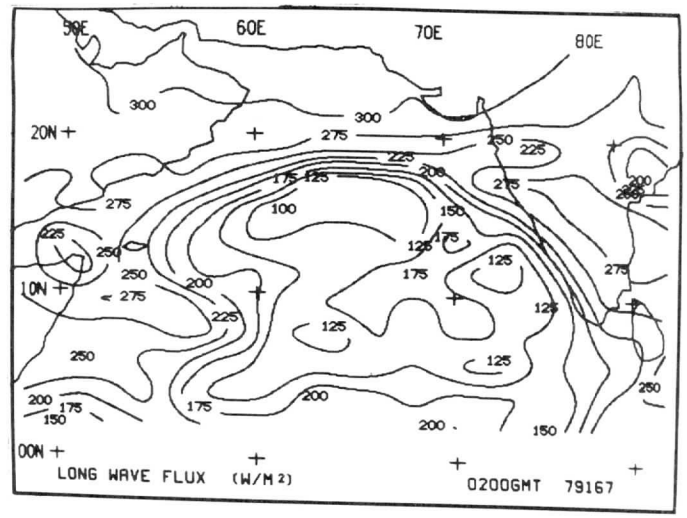
50E
60E
70E
80E
20N
10N
00N
LONG WAVE FLUX (W/M2)
0200GMT 79167

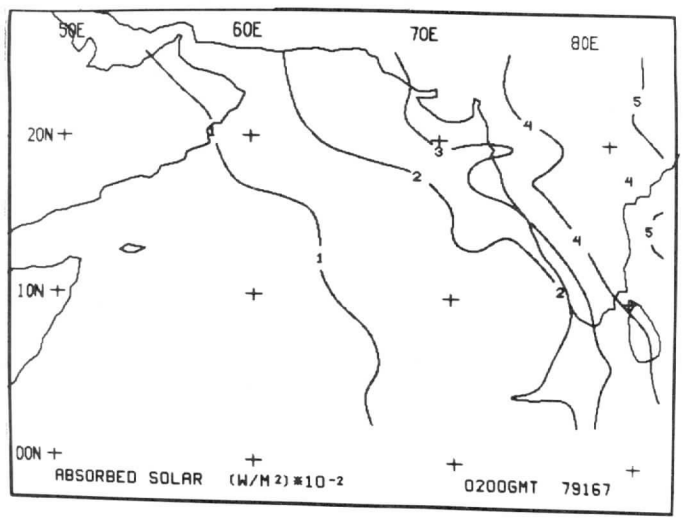
50E
60E
70E
80E
20N
10N
00N
ABSORBED SOLAR (W/M2)*10-2
0200GMT 79167

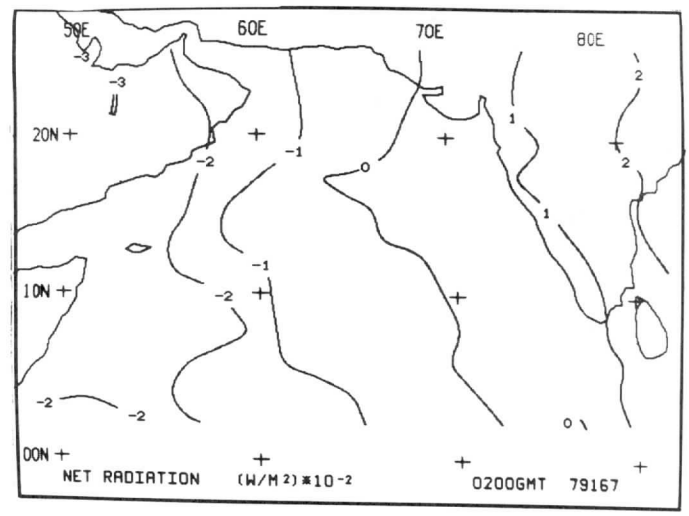
50E
60E
70E
80E
20N
10N
00N
NET RADIATION (W/M2)*10-2
0200GMT 79167

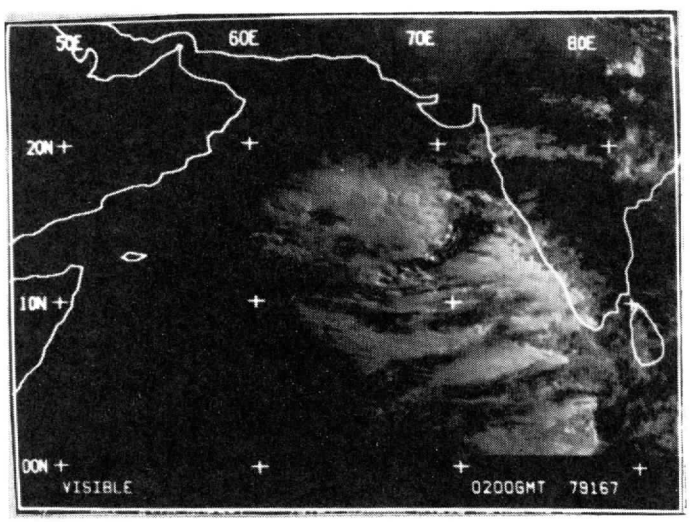
50E
60E
70E
80E
20N
10N
00N
VISIBLE
0200GMT 79167

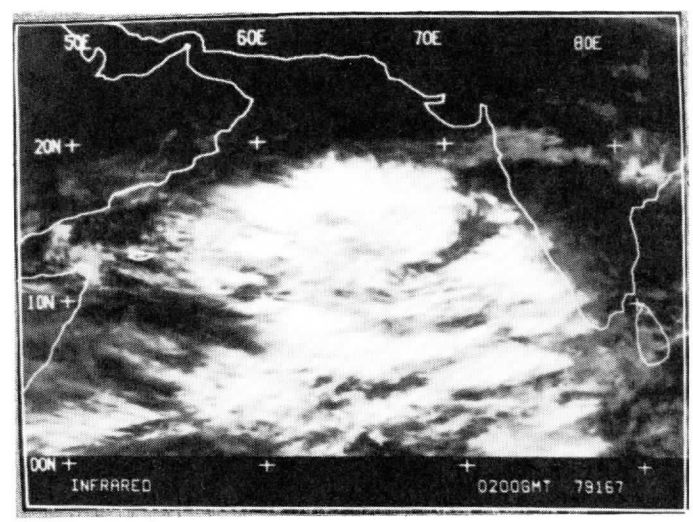
50E
60E
70E
80E
20N
10N
00N
INFRARED
0200GMT 79167

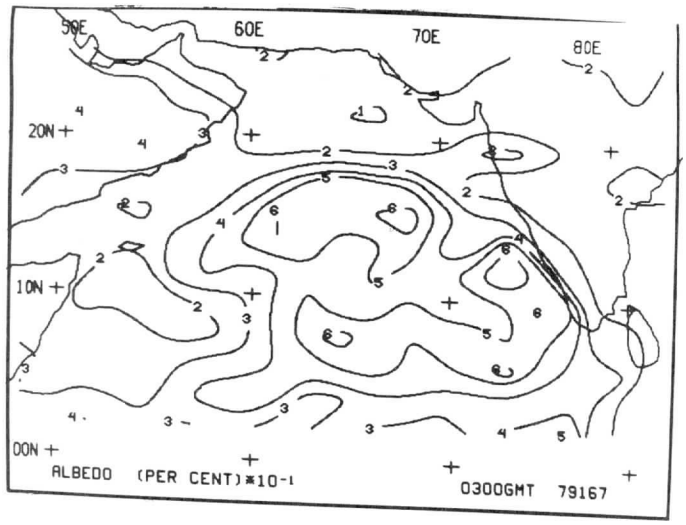
50E
60E
70E
80E
20N
10N
0ON
ALBEDO (PER CENT)*10-1
0300GMT 79167

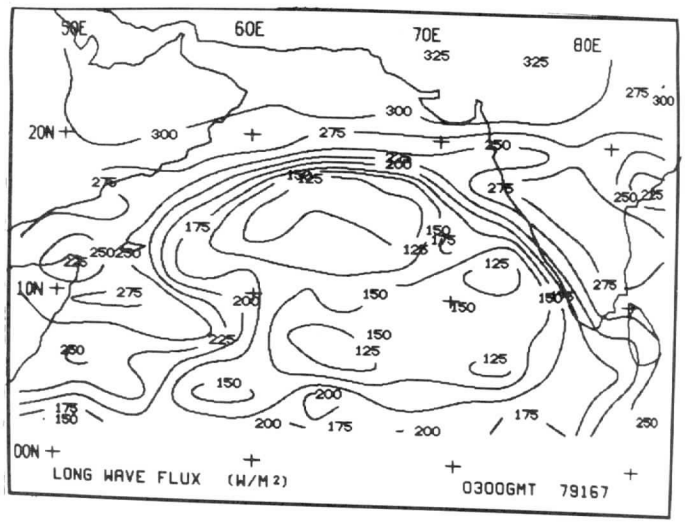
50E
60E
70E
80E
20N
10N
0ON
LONG WAVE FLUX (W/M2)
0300GMT 79167

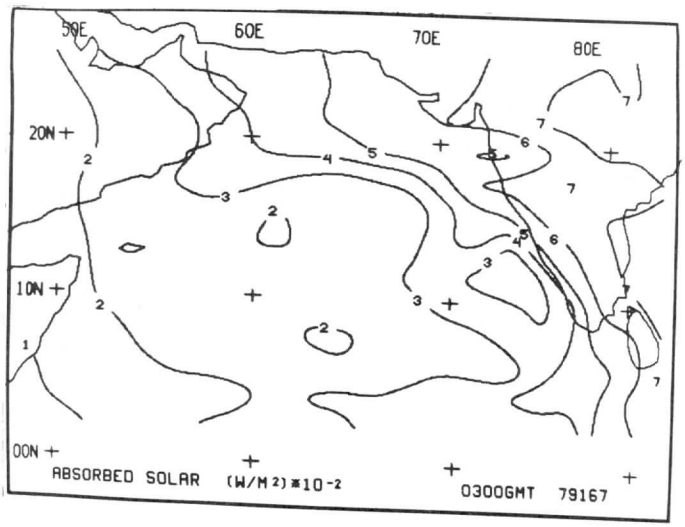
50E
60E
70E
80E
20N
10N
0ON
ABSORBED SOLAR (W/M2)*10-2
0300GMT 79167

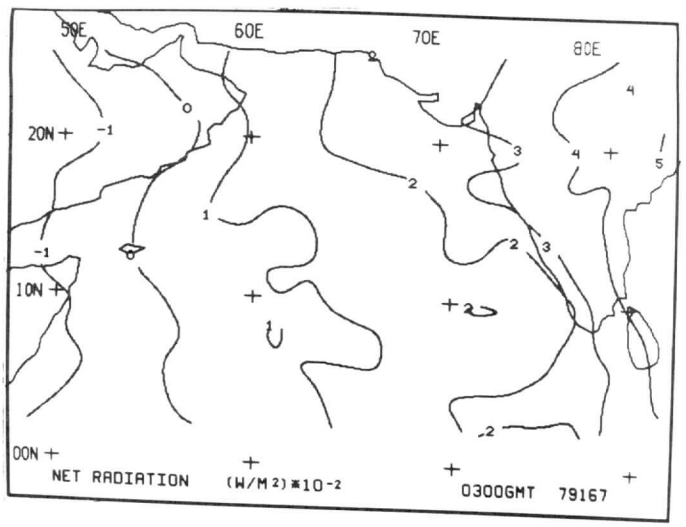
50E
60E
70E
80E
20N
10N
0ON
NET RADIATION (W/M2)*10-2
0300GMT 79167

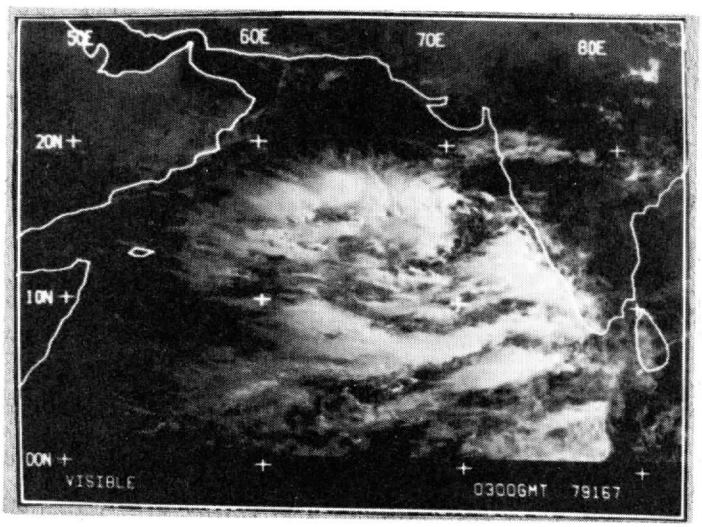
50E
60E
70E
80E
20N
10N
0ON
VISIBLE
0300GMT 79167

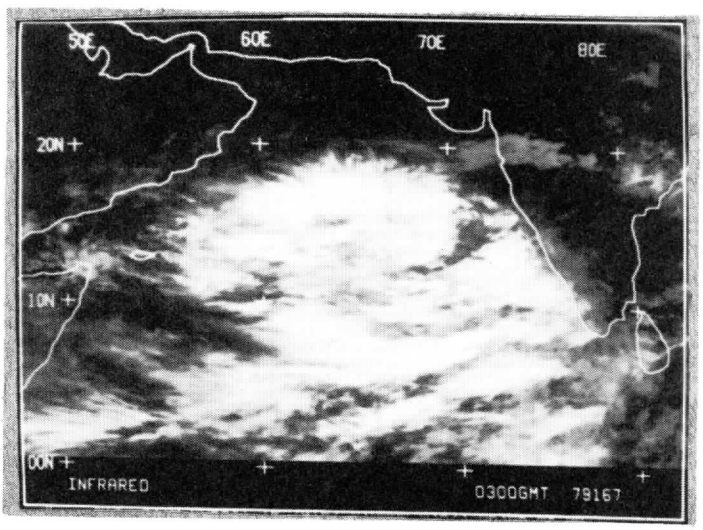
50E
60E
70E
80E
20N
10N
0ON
INFRARED
0300GMT 79167

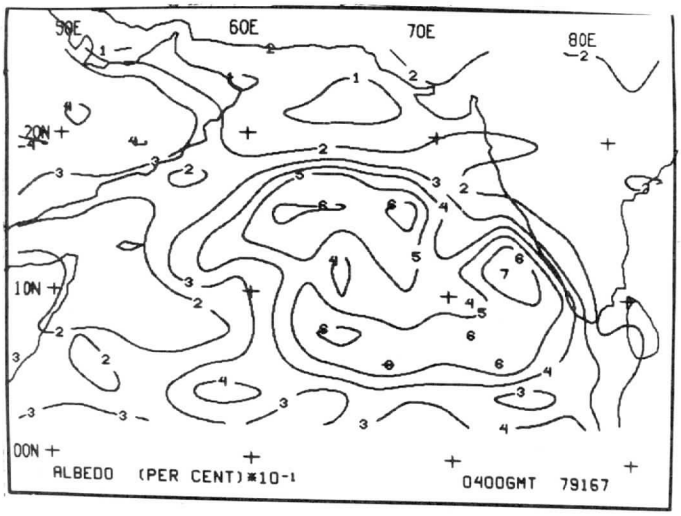
50E
60E
70E
80E
20N
10N
00N
ALBEDO (PER CENT)*10-1
0400GMT 79167

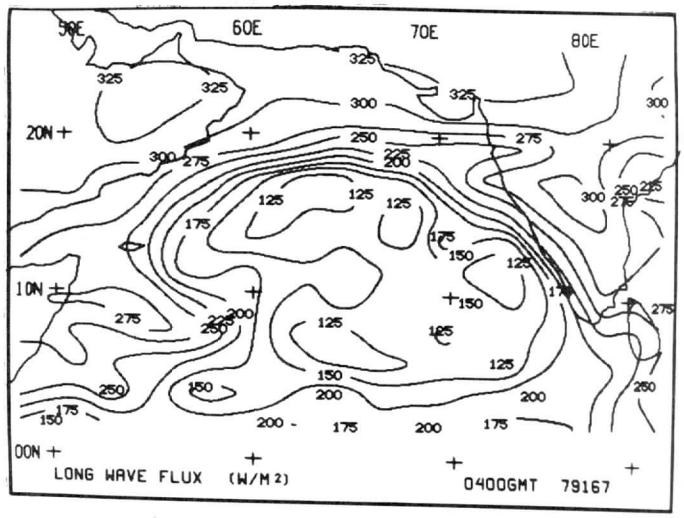
50E
60E
70E
80E
20N
10N
00N
LONG WAVE FLUX (W/M2)
0400GMT 79167

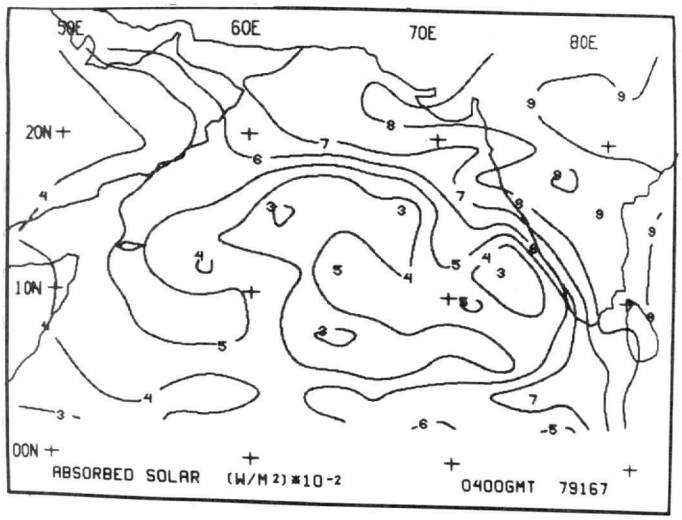
50E
60E
70E
80E
20N
10N
00N
ABSORBED SOLAR (W/M2)*10-2
0400GMT 79167

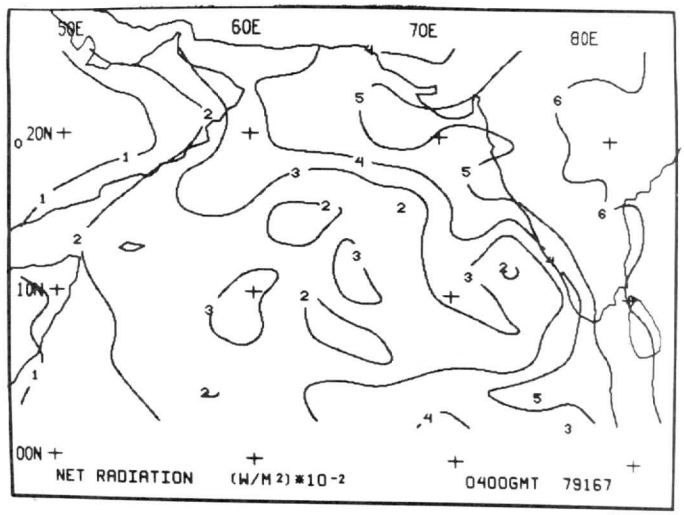
50E
60E
70E
80E
20N
10N
00N
NET RADIATION (W/M2)*10-2
0400GMT 79167

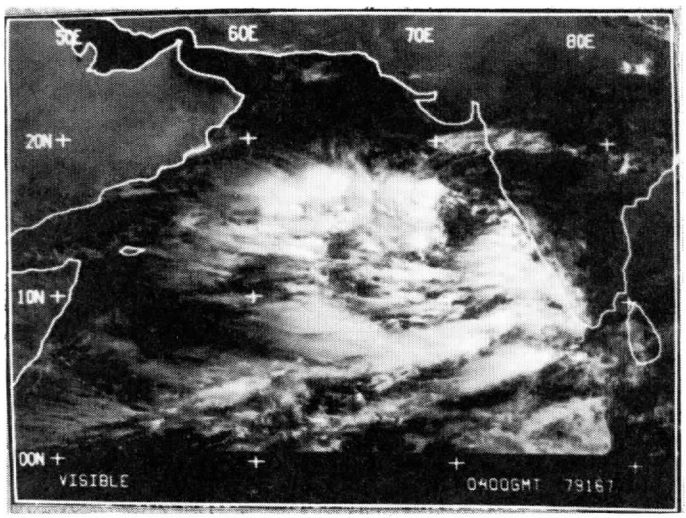
50E
60E
70E
80E
20N
10N
00N
VISIBLE
0400GMT 79167

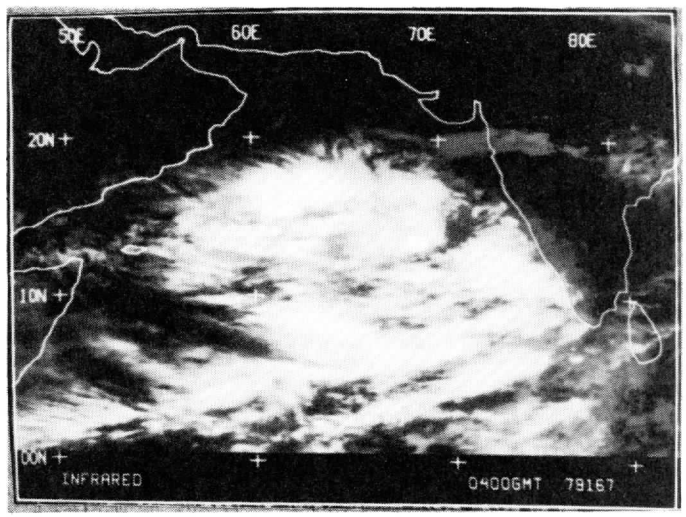
50E
60E
70E
80E
20N
10N
00N
INFRARED
0400GMT 79167

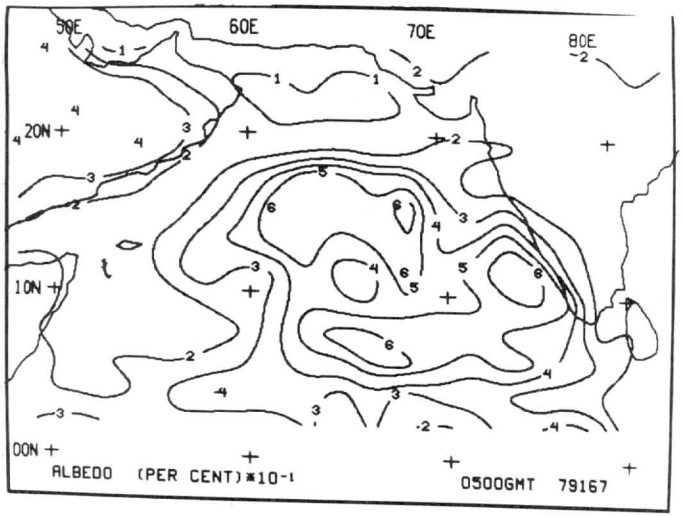
50E
60E
70E
80E
20N
10N
00N
ALBEDO (PER CENT)*10-1
0500GMT 79167

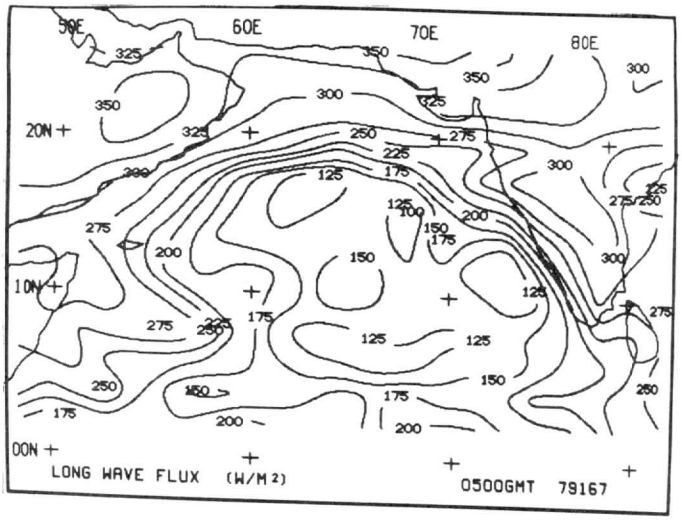
50E
60E
70E
80E
20N
10N
00N
LONG WAVE FLUX (W/M2)
0500GMT 79167

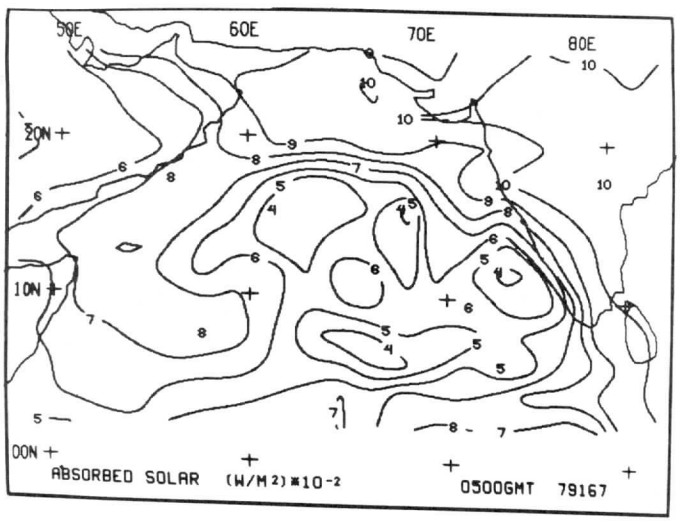
50E
60E
70E
80E
20N
10N
00N
ABSORBED SOLAR (W/M2)*10-2
0500GMT 79167

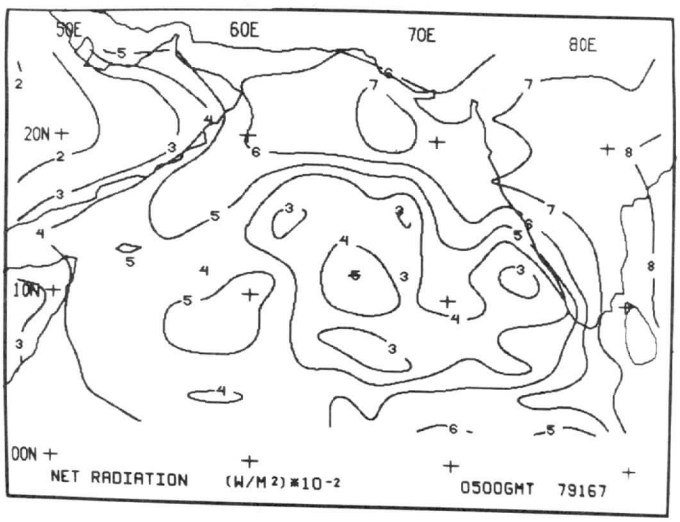
50E
60E
70E
80E
20N
10N
00N
NET RADIATION (W/M2)*10-2
0500GMT 79167

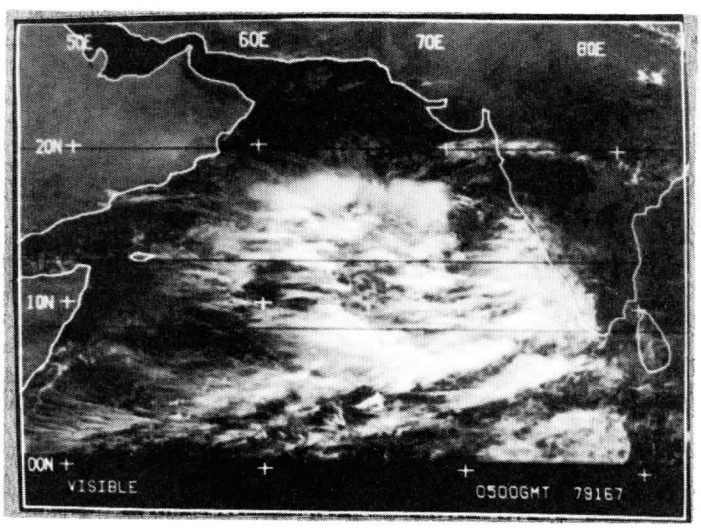
50E
60E
70E
80E
20N
10N
00N
VISIBLE
0500GMT 79167

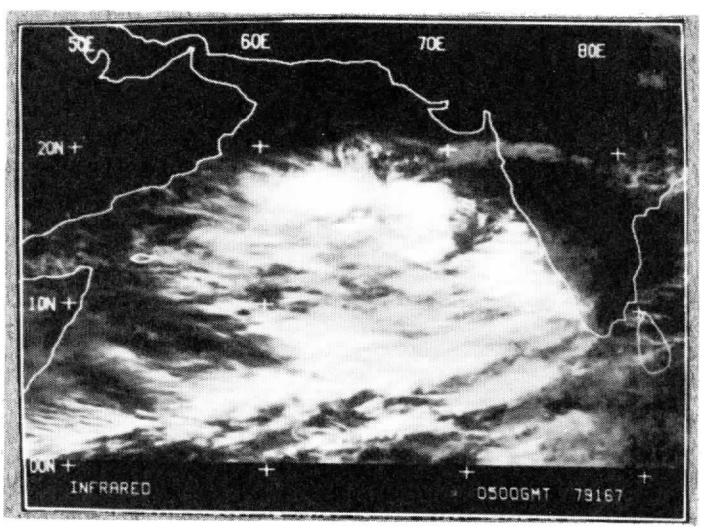
50E
60E
70E
80E
20N
10N
00N
INFRARED
0500GMT 79167

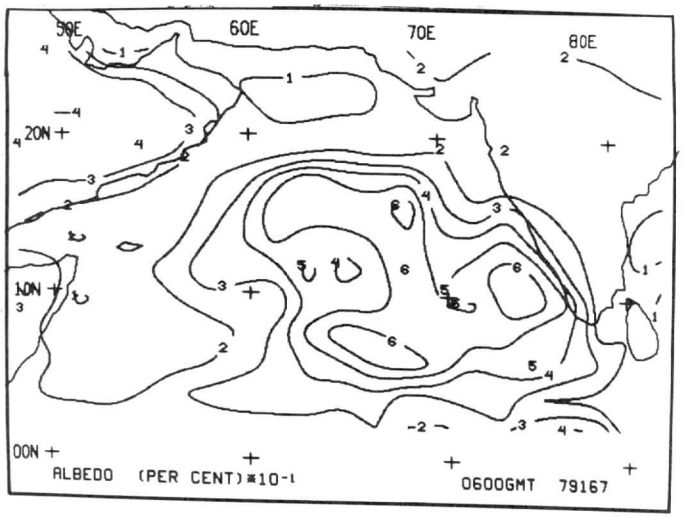
50E
60E
70E
80E
20N
10N
00N
ALBEDO (PER CENT)*10-1
0600GMT 79167

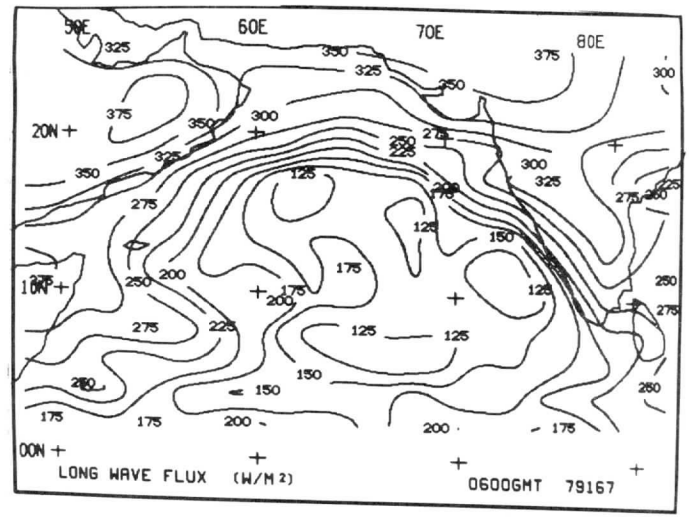
50E
60E
70E
80E
20N
10N
00N
LONG WAVE FLUX (W/M2)
0600GMT 79167

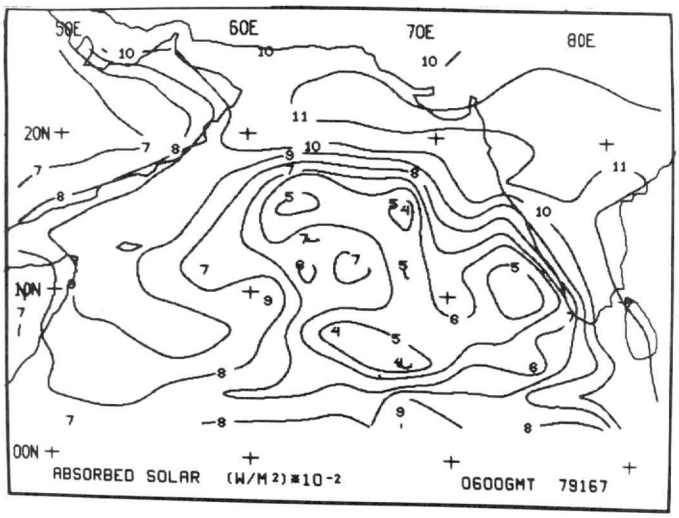
50E
60E
70E
80E
20N
10N
00N
ABSORBED SOLAR (W/M2)*10-2
0600GMT 79167

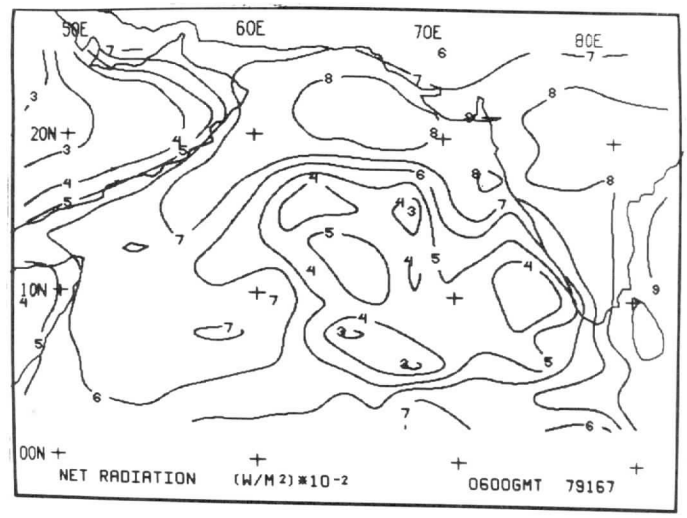
50E
60E
70E
80E
20N
10N
00N
NET RADIATION (W/M2)*10-2
0600GMT 79167

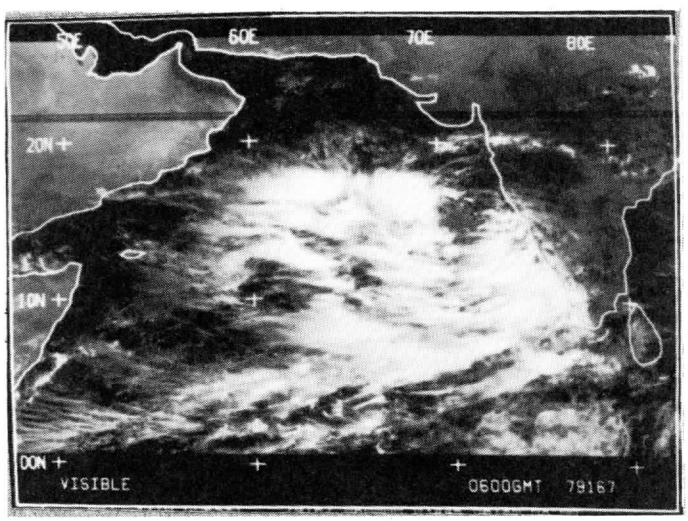
50E
60E
70E
80E
20N
10N
00N
VISIBLE
0600GMT 79167

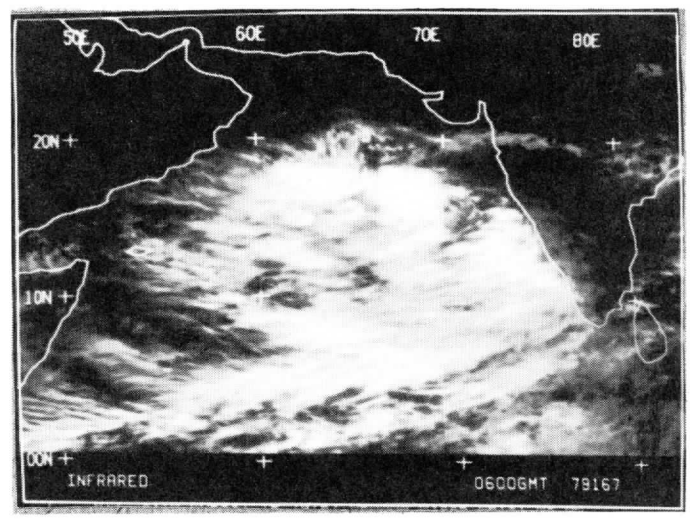
50E
60E
70E
80E
20N
10N
00N
INFRARED
0600GMT 79167

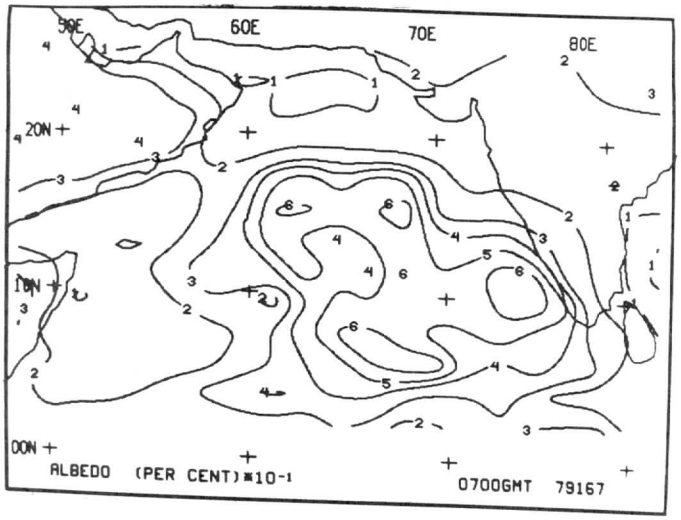
50E
60E
70E
80E
20N
10N
00N
ALBEDO (PER CENT)*10-1
0700GMT 79167

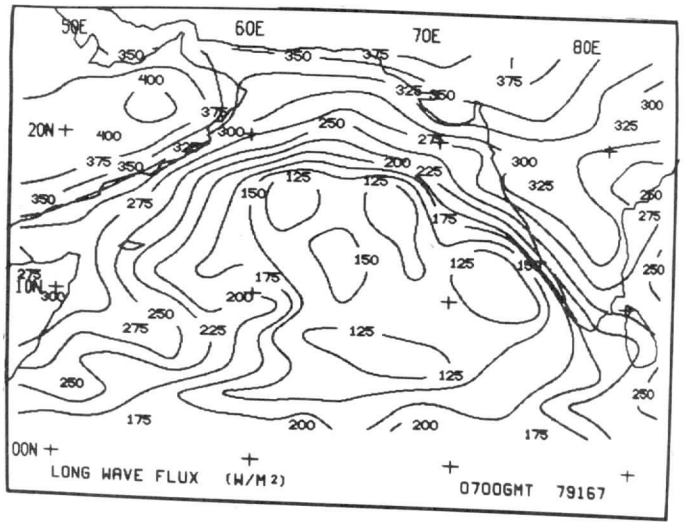
50E
60E
70E
80E
20N
10N
00N
LONG WAVE FLUX (W/M2)
0700GMT 79167

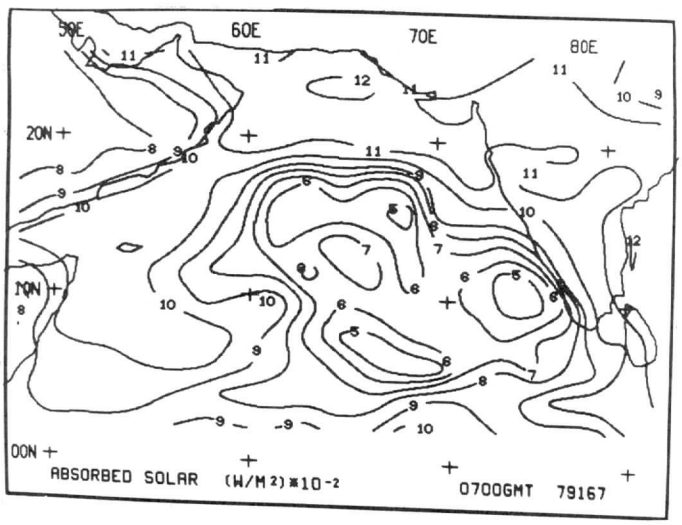
50E
60E
70E
80E
20N
10N
00N
ABSORBED SOLAR (W/M2)*10-2
0700GMT 79167

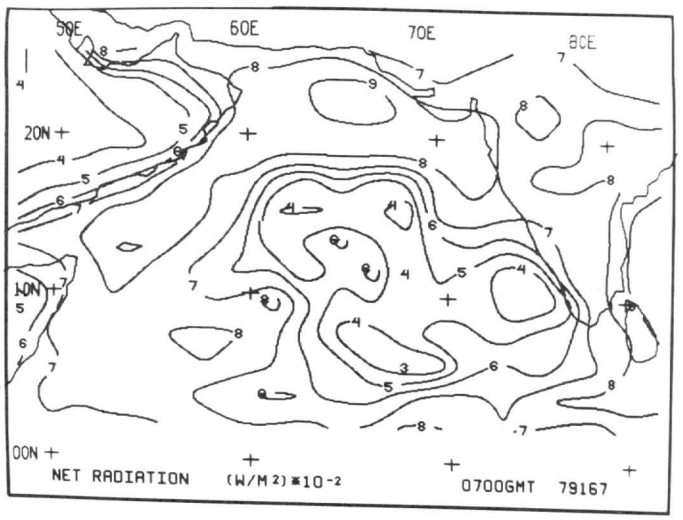
50E
60E
70E
80E
20N
10N
00N
NET RADIATION (W/M2)*10-2
0700GMT 79167

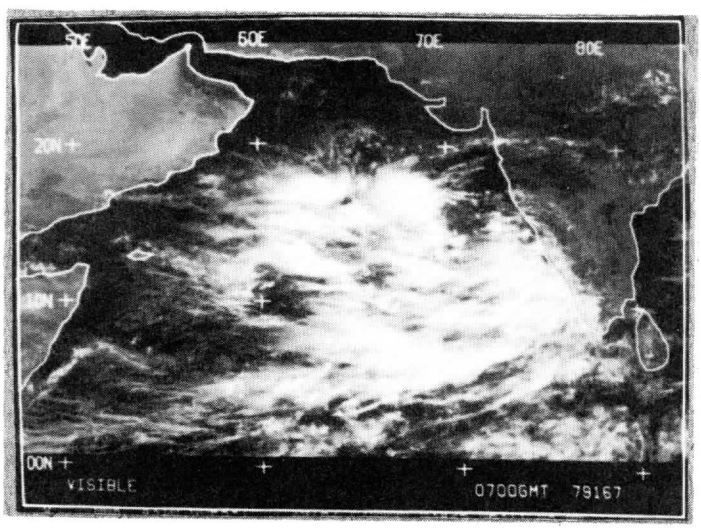
50E
60E
70E
80E
20N
10N
00N
VISIBLE
0700GMT 79167

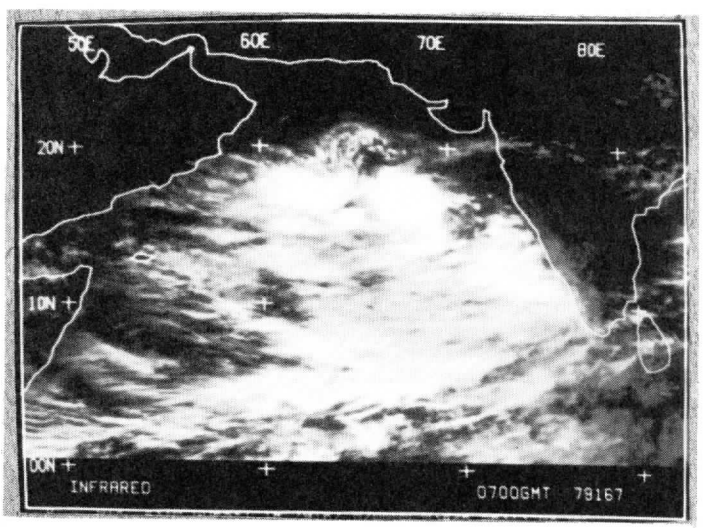
50E
60E
70E
80E
20N
10N
00N
INFRARED
0700GMT 79167

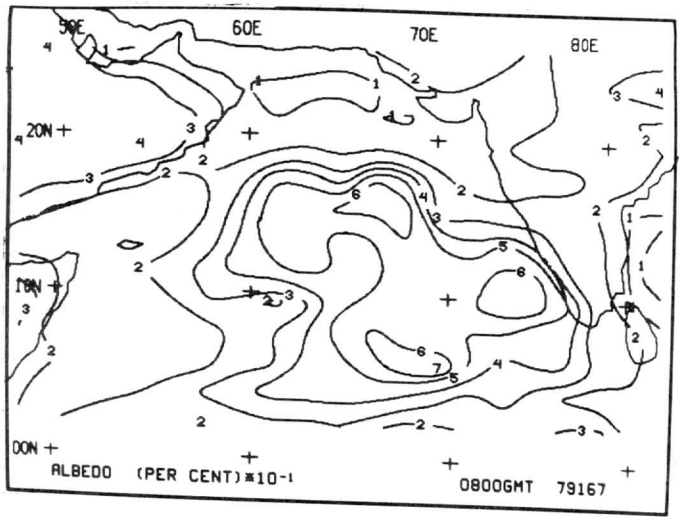
50E
60E
70E
80E
20N
10N
0ON
ALBEDO (PER CENT)*10-1
0800GMT 79167

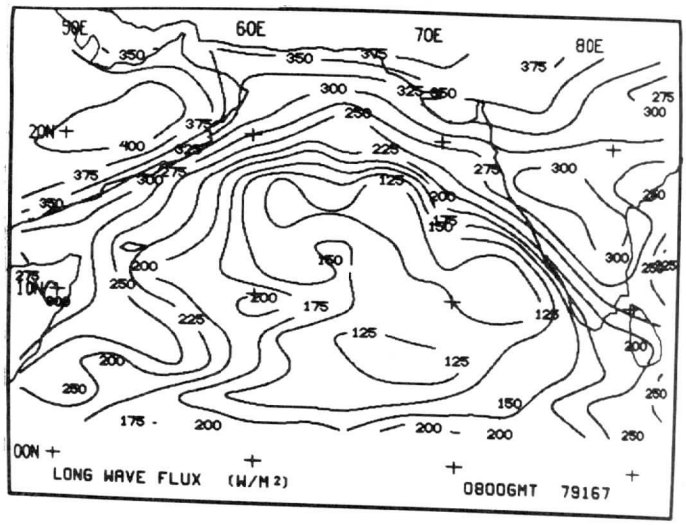
50E
60E
70E
80E
20N
10N
0ON
LONG WAVE FLUX (W/M2)
0800GMT 79167

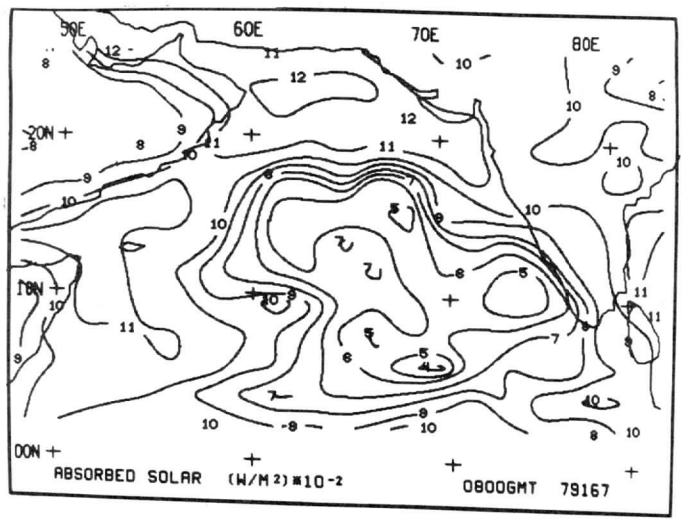
50E
60E
70E
80E
20N
10N
0ON
ABSORBED SOLAR (W/M2)*10-2
0800GMT 79167

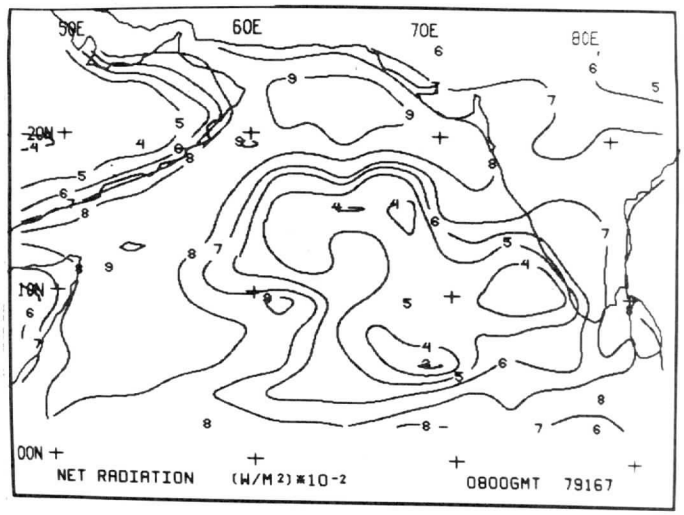
50E
60E
70E
80E
20N
10N
0ON
NET RADIATION (W/M2)*10-2
0800GMT 79167

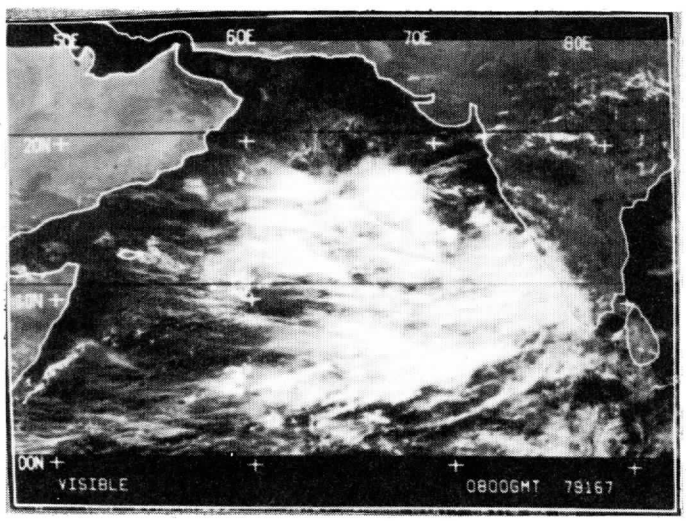
50E
60E
70E
80E
20N
10N
0ON
VISIBLE
0800GMT 79167

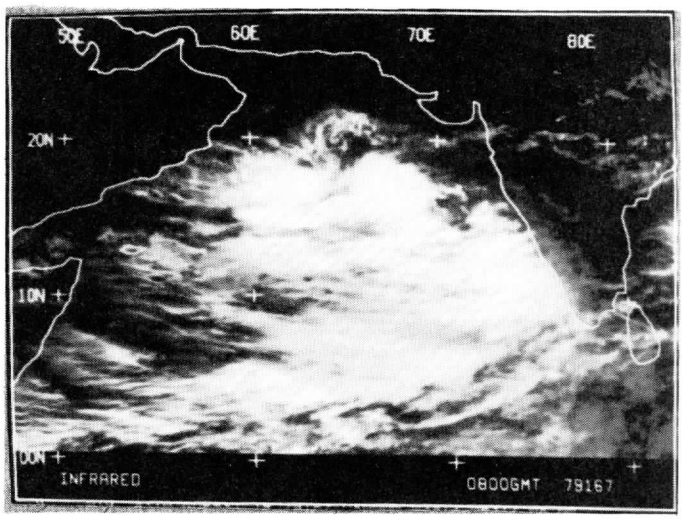
50E
60E
70E
80E
20N
10N
0ON
INFRARED
0800GMT 79167

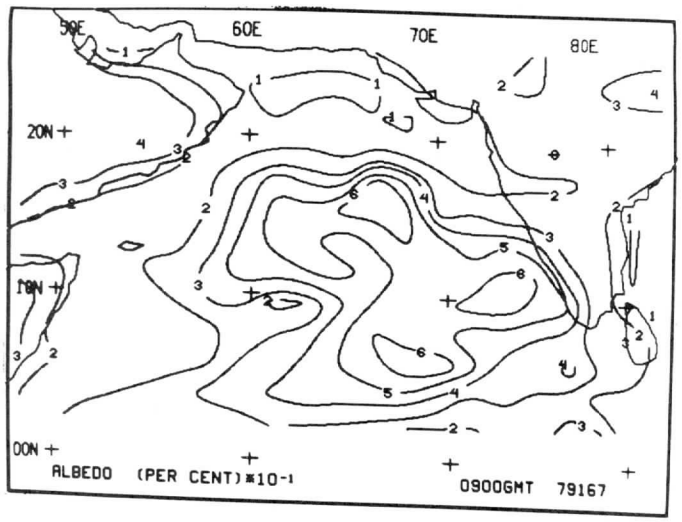
50E
60E
70E
80E
20N
10N
0ON
ALBEDO (PER CENT)*10-1
0900GMT 79167

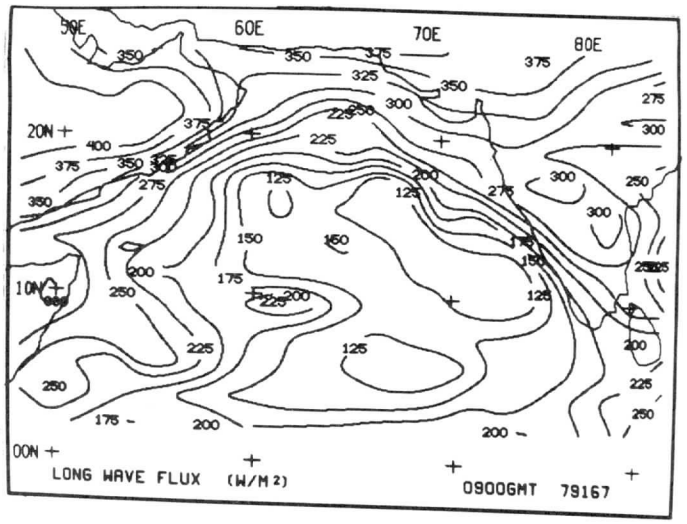
50E
60E
70E
80E
20N
10N
0ON
LONG WAVE FLUX (W/M2)
0900GMT 79167

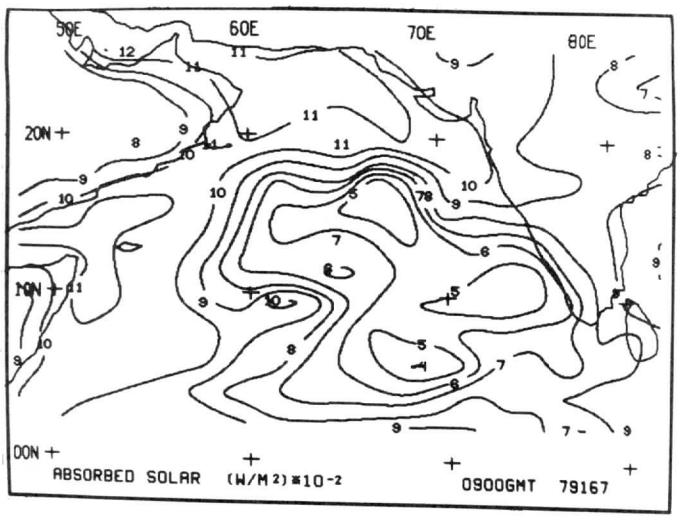
50E
60E
70E
80E
20N
10N
0ON
ABSORBED SOLAR (W/M2)*10-2
0900GMT 79167

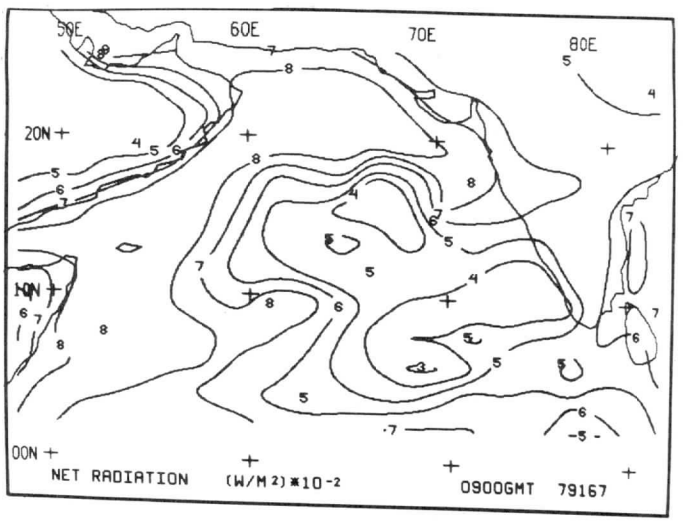
50E
60E
70E
80E
20N
10N
0ON
NET RADIATION (W/M2)*10-2
0900GMT 79167

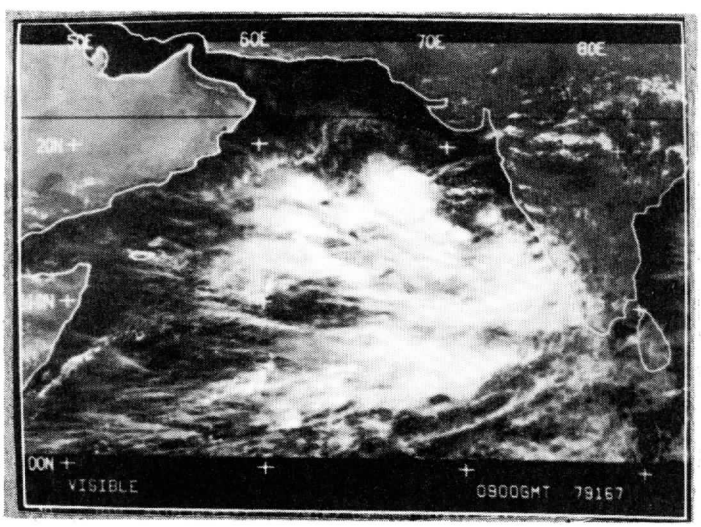
50E
60E
70E
80E
20N
10N
0ON
VISIBLE
0900GMT 79167

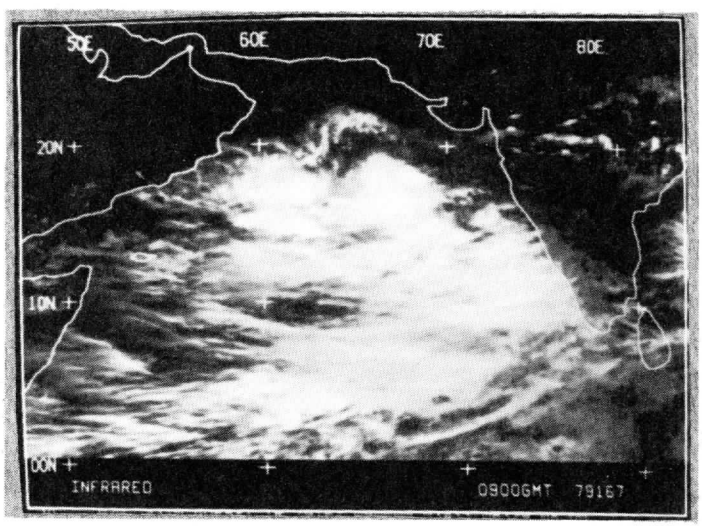
50E
60E
70E
80E
20N
10N
0ON
INFRARED
0900GMT 79167

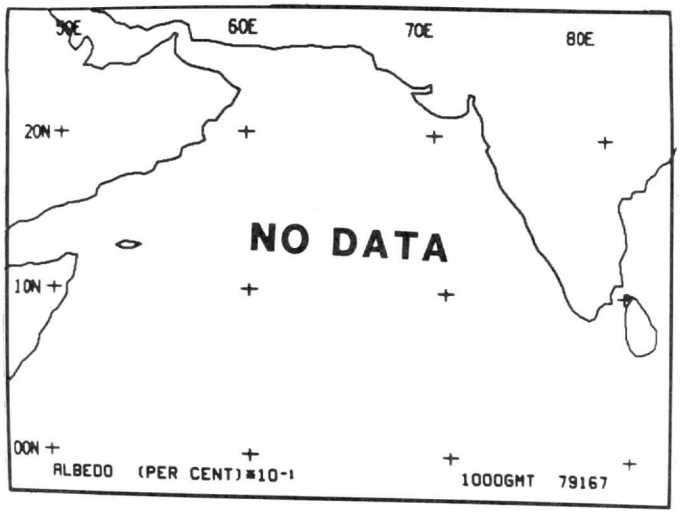
50E
60E
70E
80E
20N
10N
0ON
NO DATA
ALBEDO (PER CENT)*10-1
1000GMT 79167

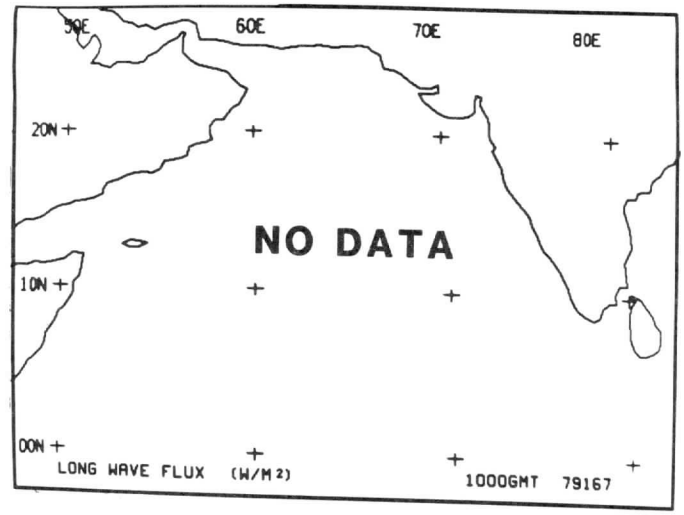
50E
60E
70E
80E
20N
10N
0ON
NO DATA
LONG WAVE FLUX (W/M2)
1000GMT 79167

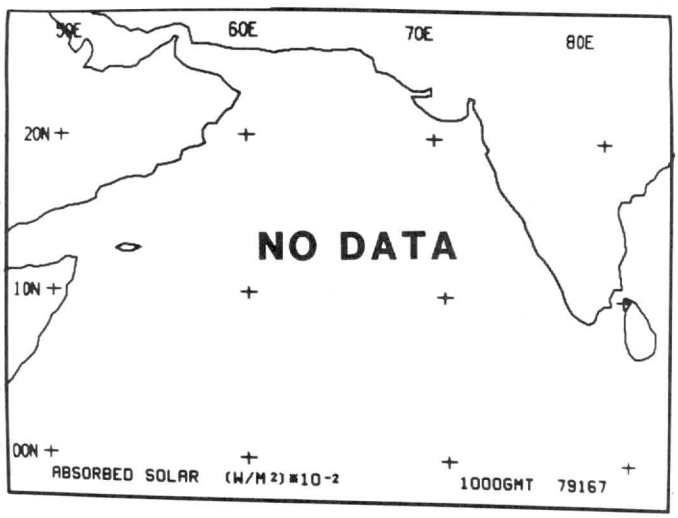
50E
60E
70E
80E
20N
10N
0ON
NO DATA
ABSORBED SOLAR (W/M2)*10-2
1000GMT 79167

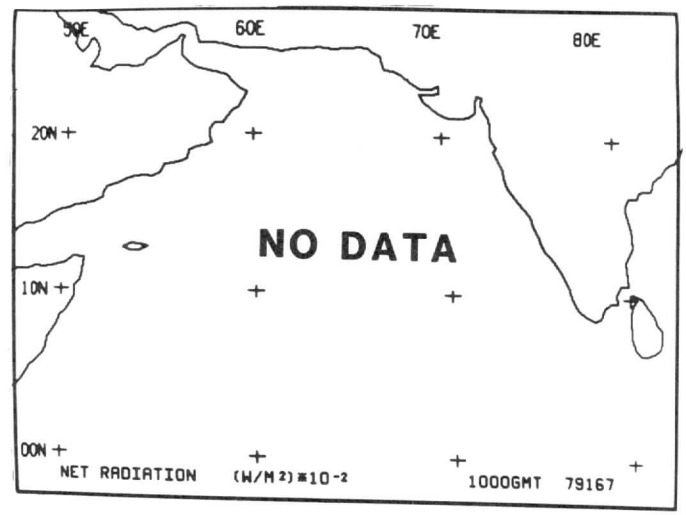
50E
60E
70E
80E
20N
10N
0ON
NO DATA
NET RADIATION (W/M2)*10-2
1000GMT 79167

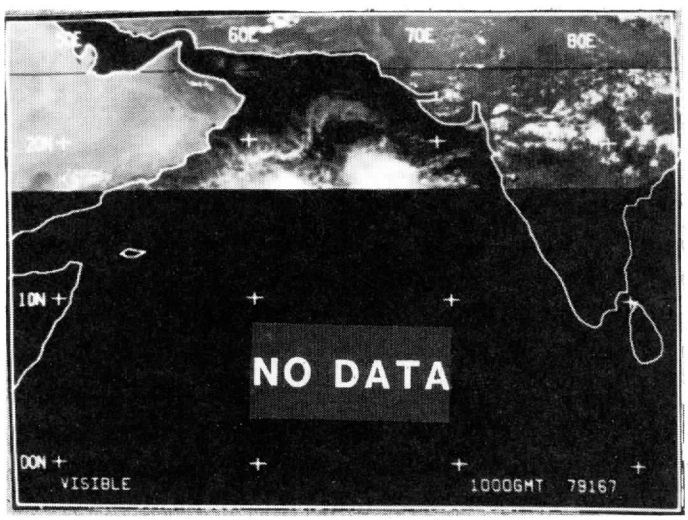
60E
70E
80E
20N
10N
0ON
NO DATA
VISIBLE
1000GMT 79167

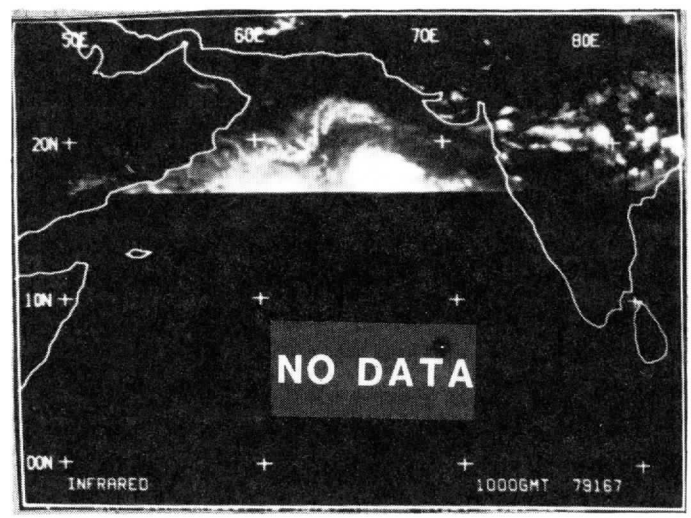
50E
60E
70E
80E
20N
10N
0ON
NO DATA
INFRARED
1000GMT 79167

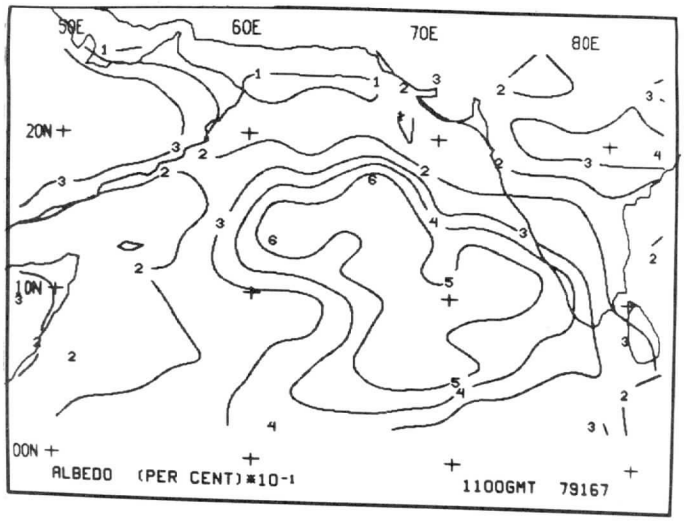
50E
60E
70E
80E
20N
10N
0ON
ALBEDO (PER CENT)*10-1
1100GMT 79167

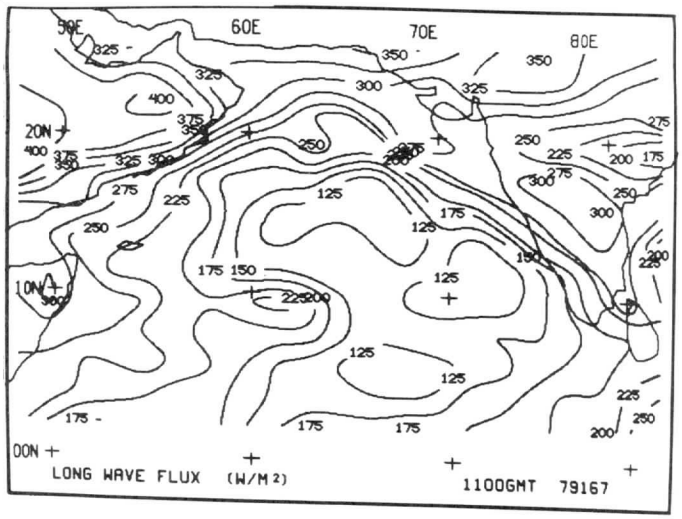
50E
60E
70E
80E
20N
10N
0ON
LONG WAVE FLUX (W/M2)
1100GMT 79167

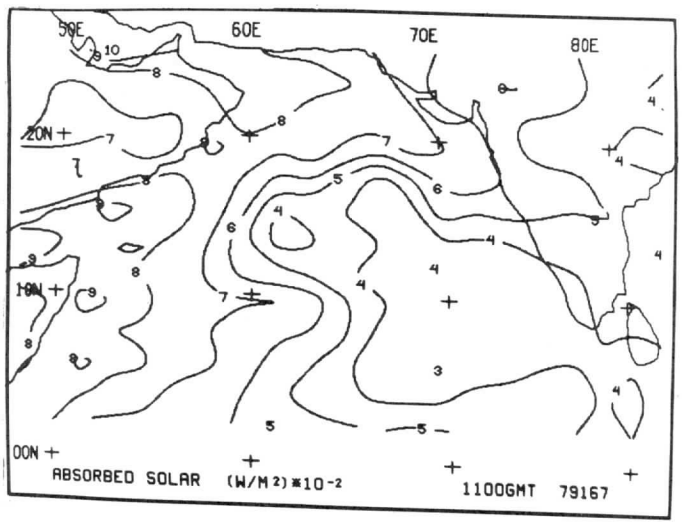
50E
60E
70E
80E
20N
10N
0ON
ABSORBED SOLAR (W/M2)*10-2
1100GMT 79167

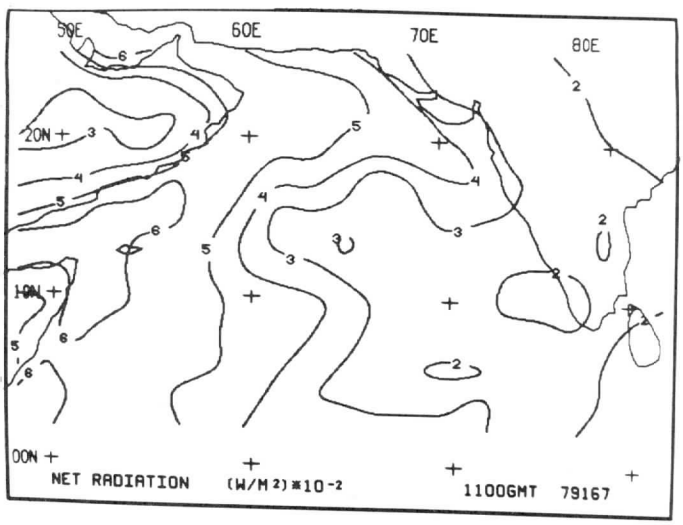
50E
60E
70E
80E
20N
10N
0ON
NET RADIATION (W/M2)*10-2
1100GMT 79167

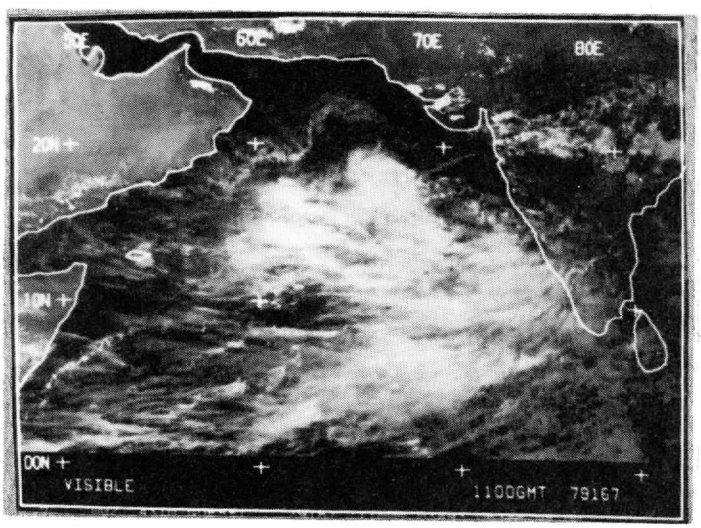
50E
60E
70E
80E
20N
10N
0ON
VISIBLE
1100GMT 79167

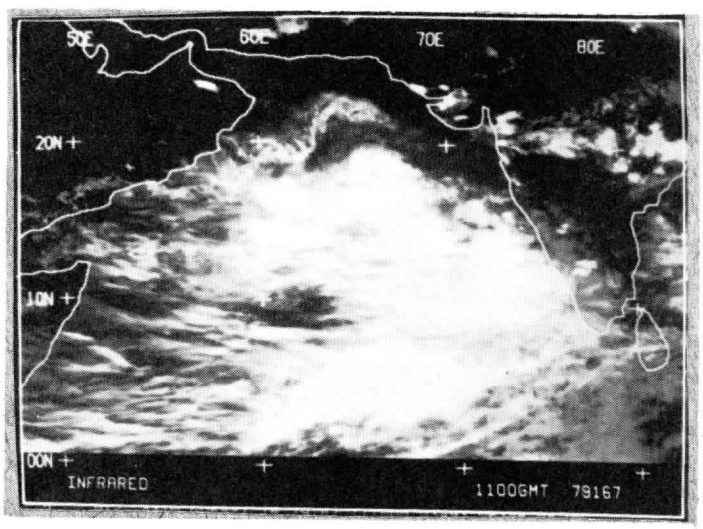
50E
60E
70E
80E
20N
10N
0ON
INFRARED
1100GMT 79167

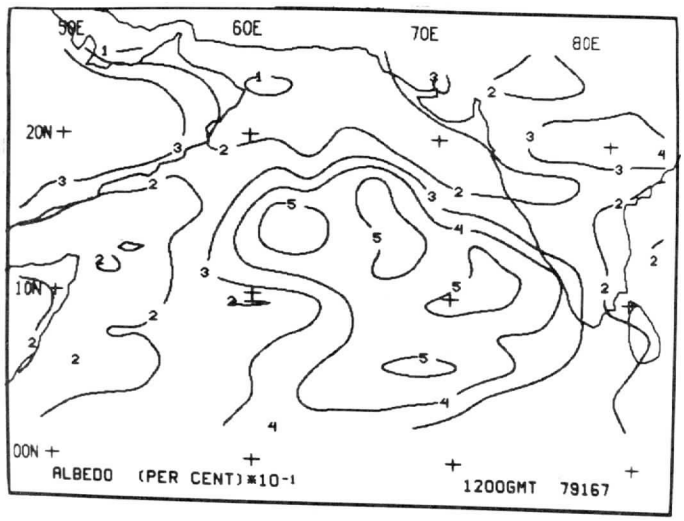
50E
60E
70E
80E
20N
10N
0ON
ALBEDO (PER CENT)*10-1
1200GMT 79167

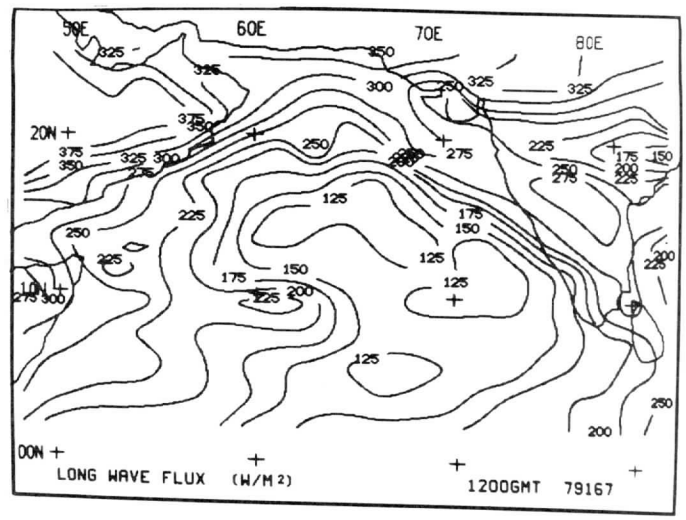
50E
60E
70E
80E
20N
10N
0ON
LONG WAVE FLUX (W/M2)
1200GMT 79167

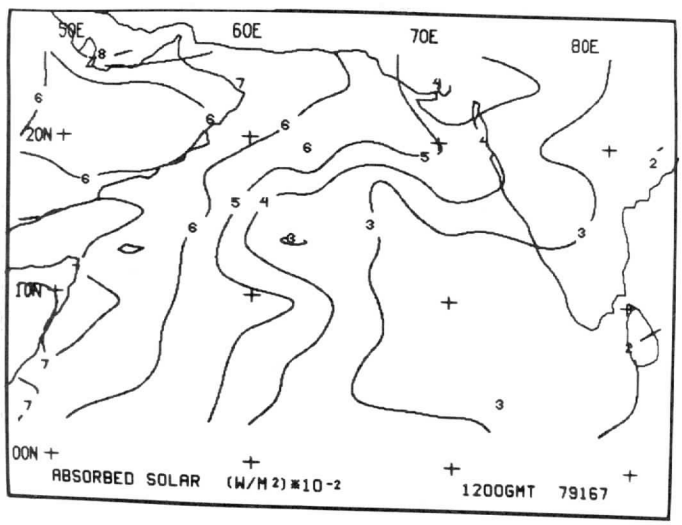
50E
60E
70E
80E
20N
10N
0ON
ABSORBED SOLAR (W/M2)*10-2
1200GMT 79167

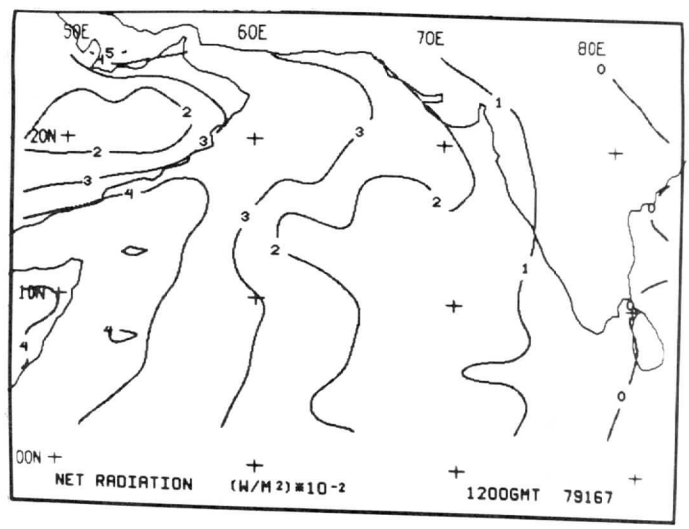
50E
60E
70E
80E
20N
10N
0ON
NET RADIATION (W/M2)*10-2
1200GMT 79167

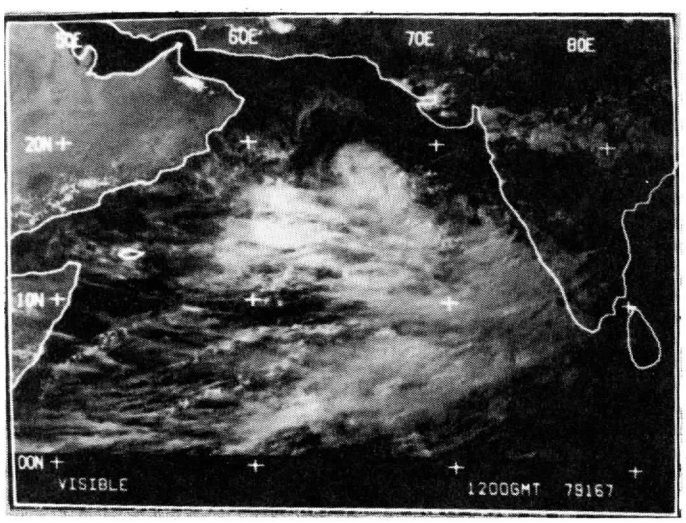
50E
60E
70E
80E
20N
10N
0ON
VISIBLE
1200GMT 79167

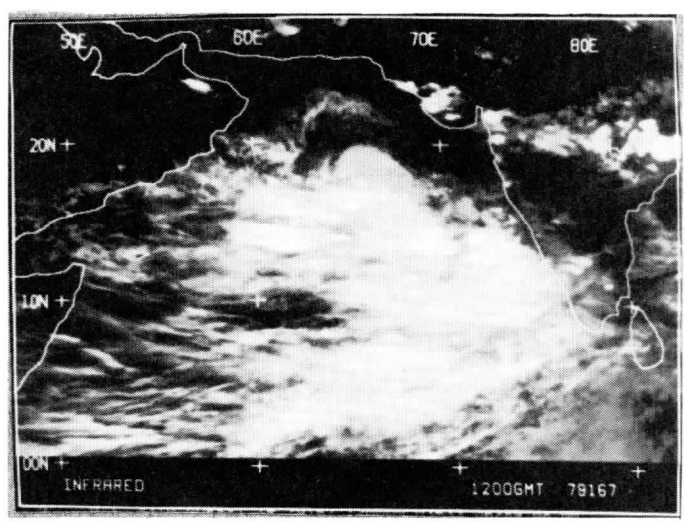
50E
60E
70E
80E
20N
10N
0ON
INFRARED
1200GMT 79167

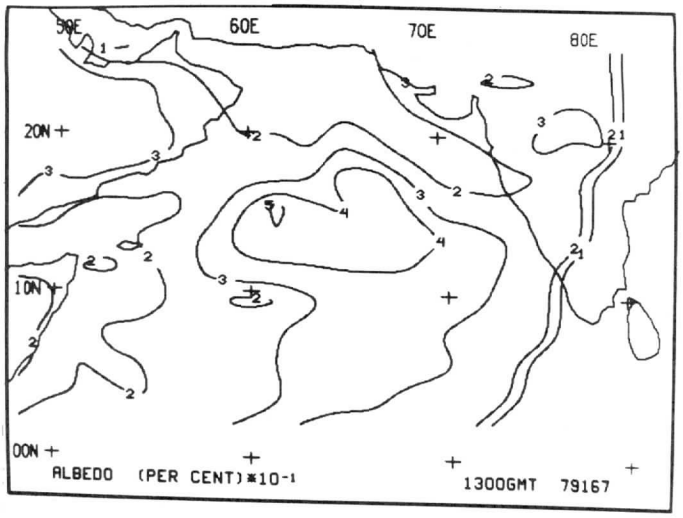
50E
60E
70E
80E
20N
10N
00N
ALBEDO (PER CENT)*10-1
1300GMT 79167

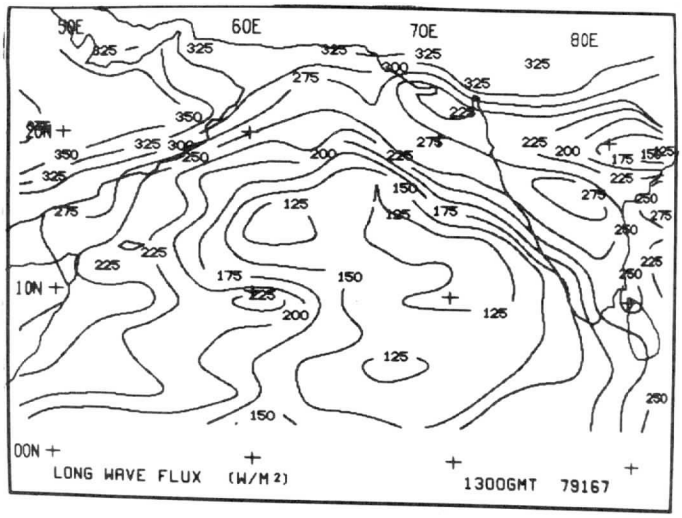
50E
60E
70E
80E
20N
10N
00N
LONG WAVE FLUX (W/M2)
1300GMT 79167

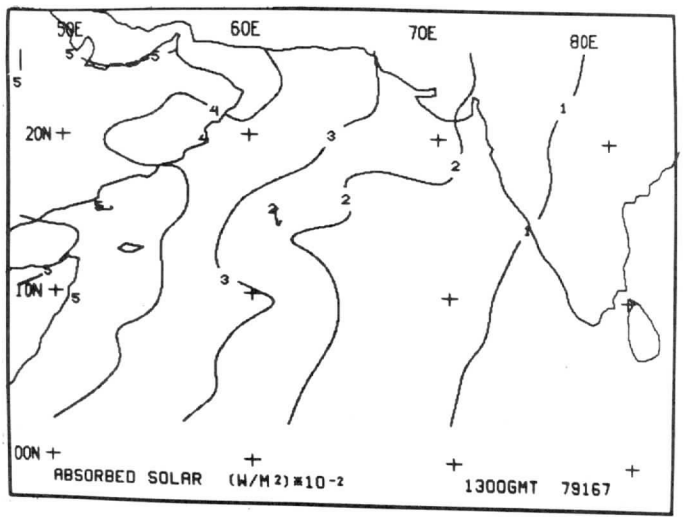
50E
60E
70E
80E
20N
10N
00N
ABSORBED SOLAR (W/M2)*10-2
1300GMT 79167

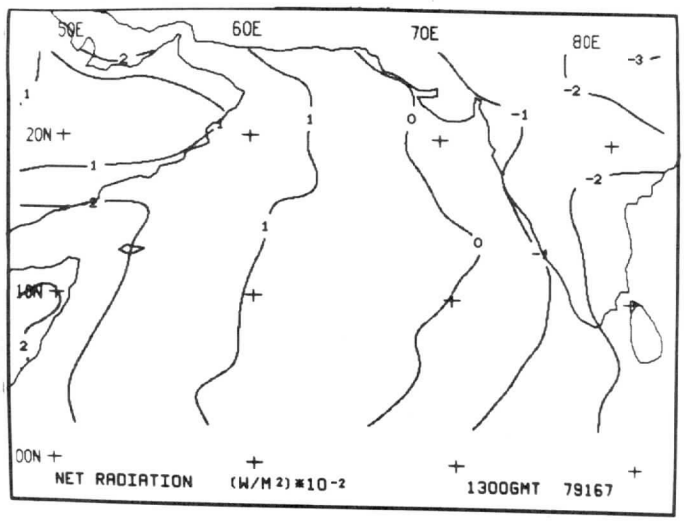
50E
60E
70E
80E
20N
10N
00N
NET RADIATION (W/M2)*10-2
1300GMT 79167

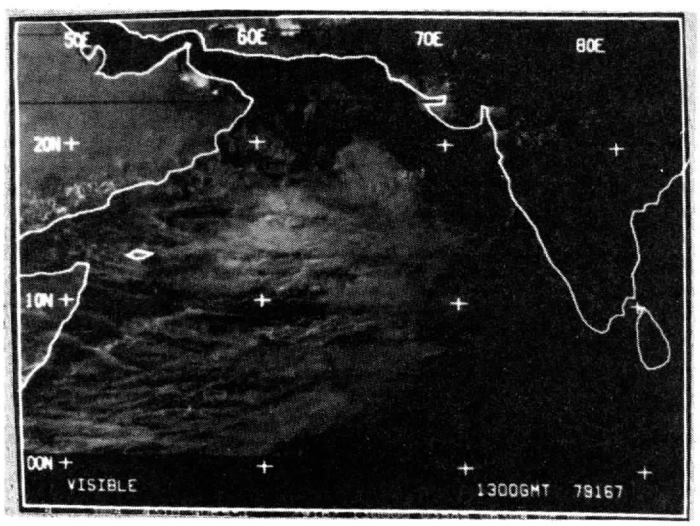
50E
60E
70E
80E
20N
10N
00N
VISIBLE
1300GMT 79167

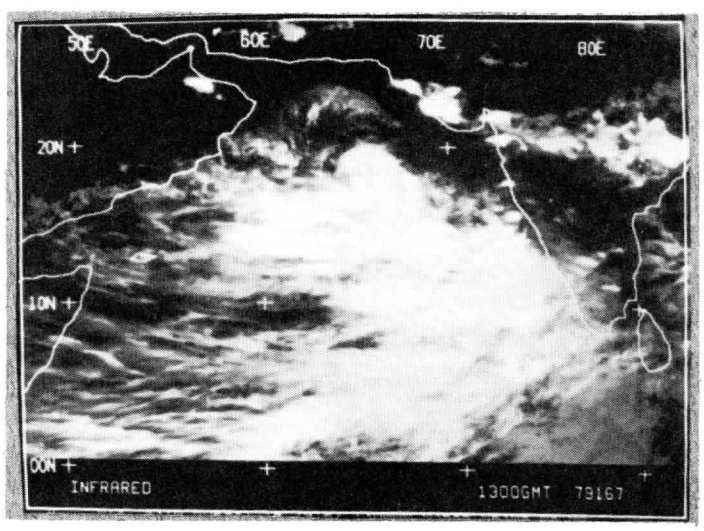
50E
60E
70E
80E
20N
10N
00N
INFRARED
1300GMT 79167

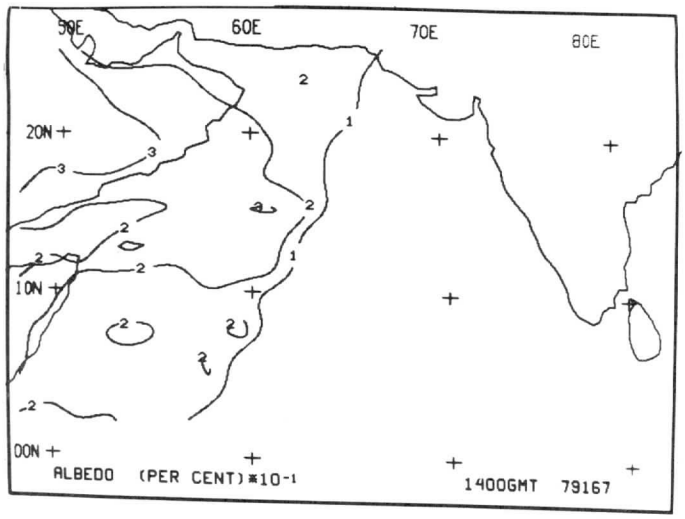
50E
60E
70E
80E
20N
10N
0ON
ALBEDO (PER CENT)*10-1
1400GMT 79167

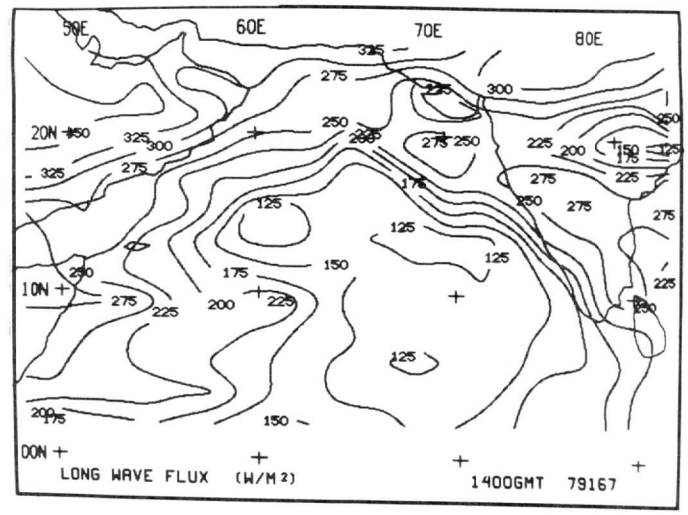
50E
60E
70E
80E
20N
10N
0ON
LONG WAVE FLUX (W/M2)
1400GMT 79167

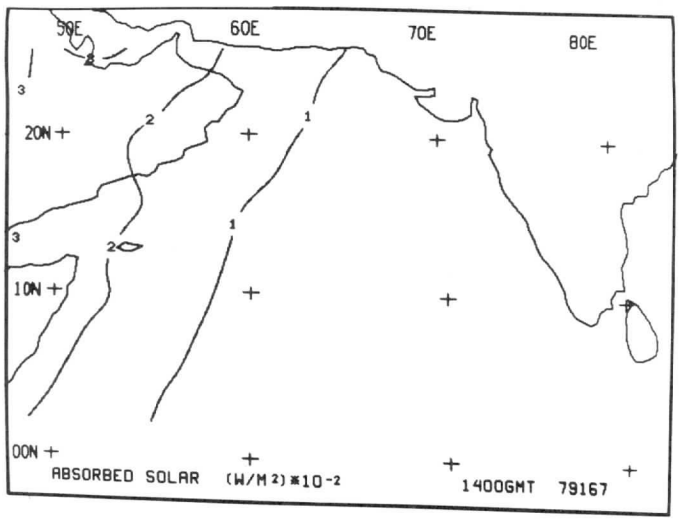
50E
60E
70E
80E
20N
10N
0ON
ABSORBED SOLAR (W/M2)*10-2
1400GMT 79167

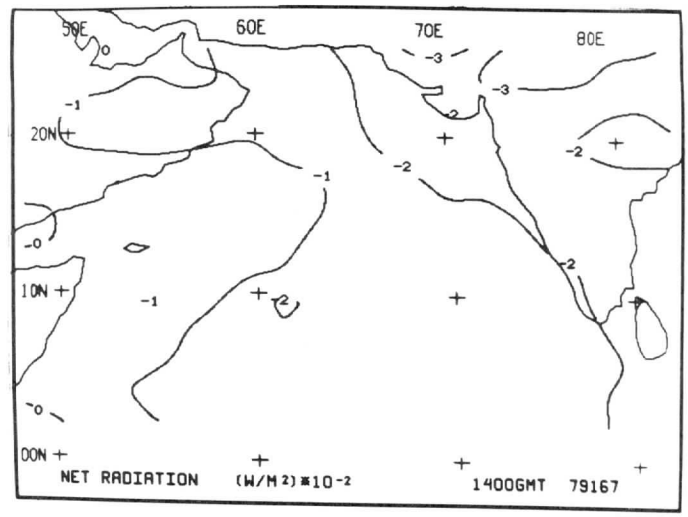
50E
60E
70E
80E
20N
10N
0ON
NET RADIATION (W/M2)*10-2
1400GMT 79167

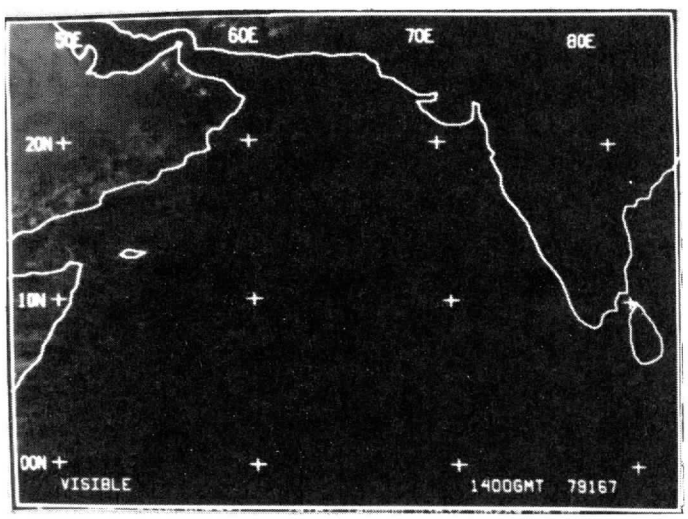
50E
60E
70E
80E
20N
10N
0ON
VISIBLE
1400GMT 79167

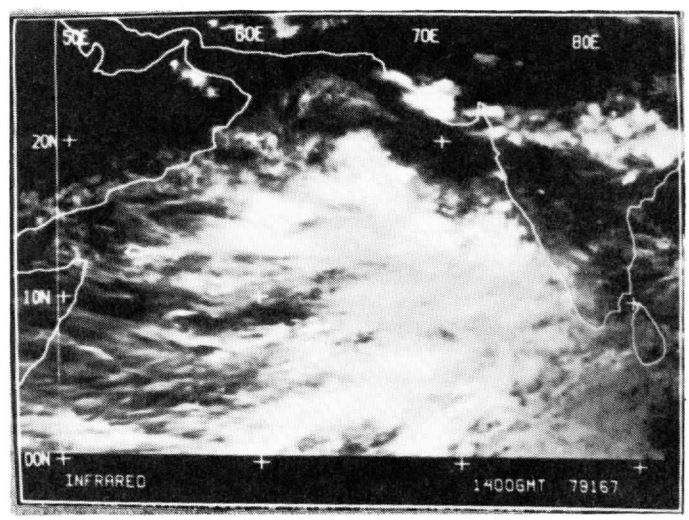
50E
60E
70E
80E
20N
10N
0ON
INFRARED
1400GMT 79167

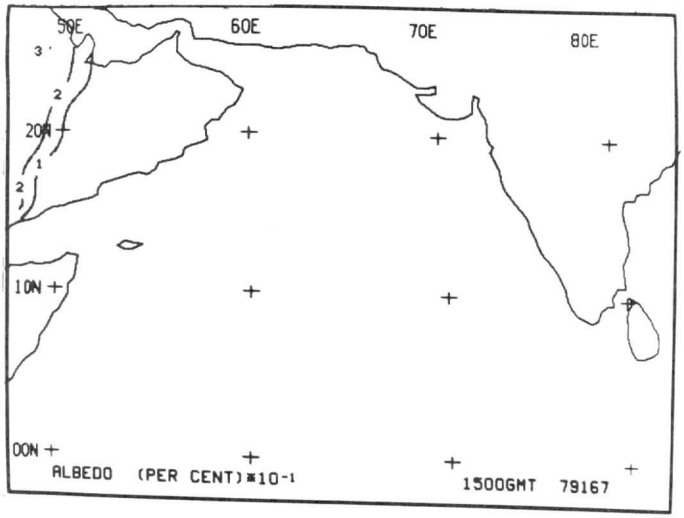
50E
60E
70E
80E
20N
10N
0ON
ALBEDO (PER CENT)*10-1
1500GMT 79167

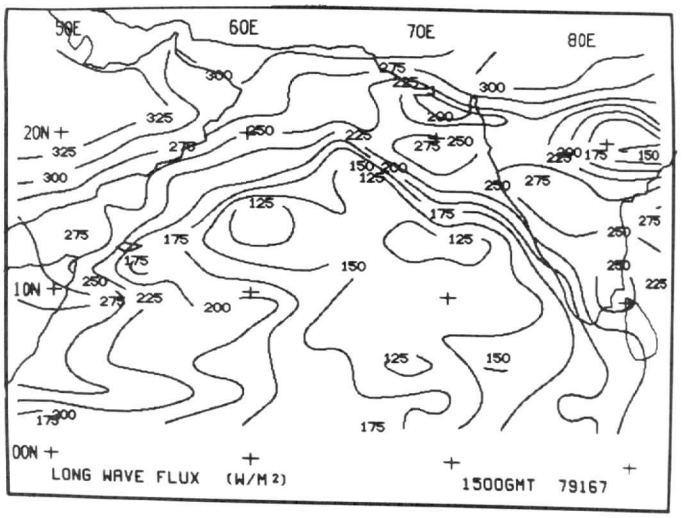
50E
60E
70E
80E
20N
10N
0ON
LONG WAVE FLUX (W/M2)
1500GMT 79167

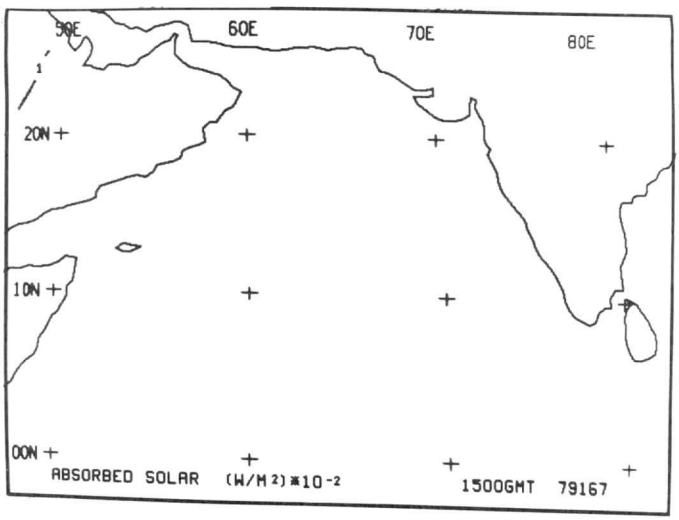
50E
60E
70E
80E
20N
10N
0ON
ABSORBED SOLAR (W/M2)*10-2
1500GMT 79167

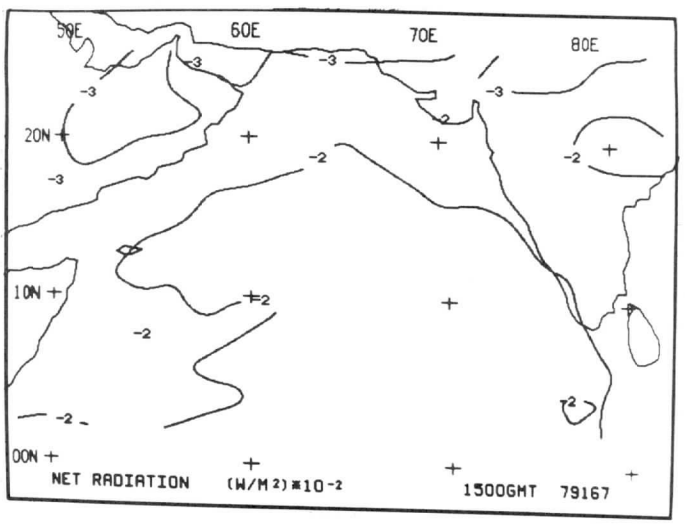
50E
60E
70E
80E
20N
10N
0ON
NET RADIATION (W/M2)*10-2
1500GMT 79167

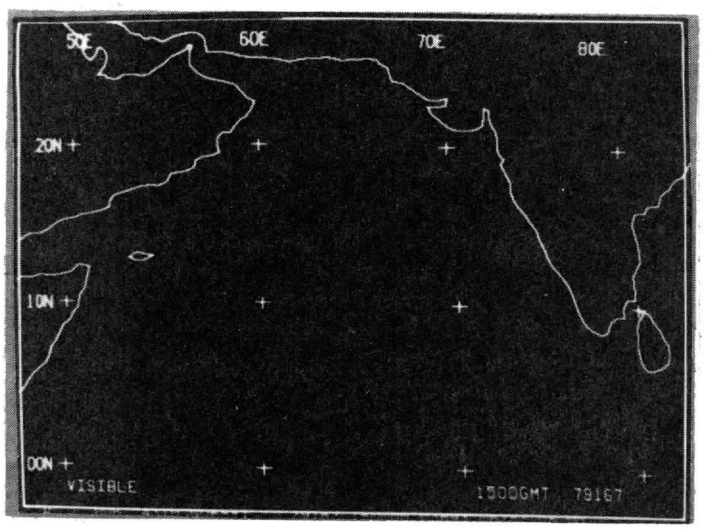
50E
60E
70E
80E
20N
10N
0ON
VISIBLE
1500GMT 79167

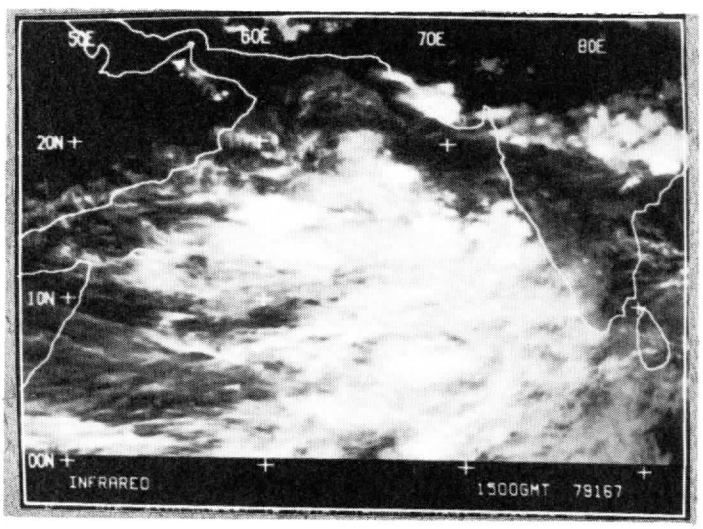
50E
60E
70E
80E
20N
10N
0ON
INFRARED
1500GMT 79167

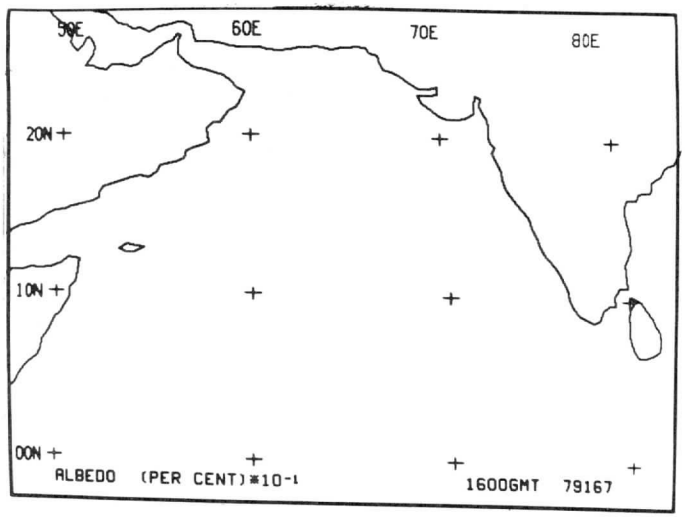
50E
60E
70E
80E
20N
10N
00N
ALBEDO (PER CENT)*10-1
1600GMT 79167

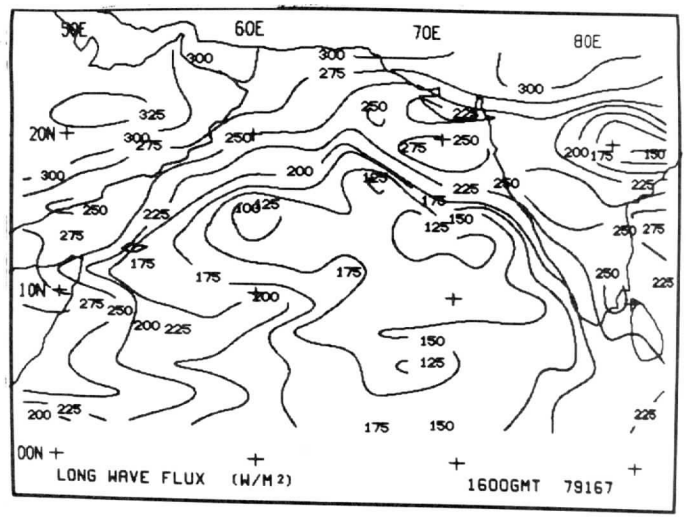
50E
60E
70E
80E
20N
10N
00N
LONG WAVE FLUX (W/M2)
1600GMT 79167

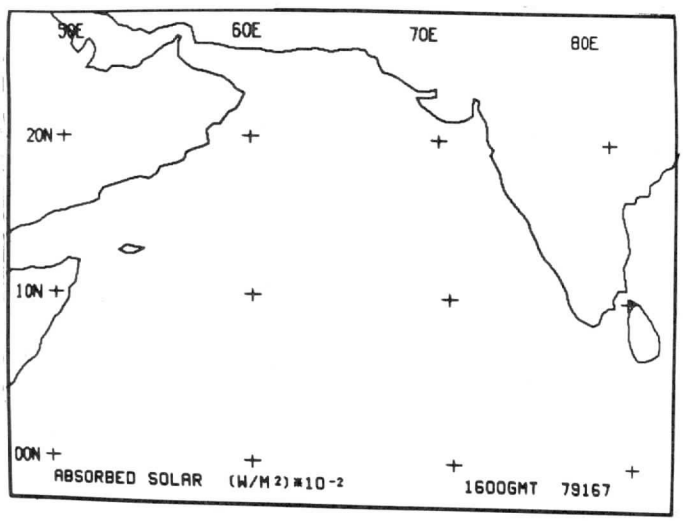
50E
60E
70E
80E
20N
10N
00N
ABSORBED SOLAR (W/M2)*10-2
1600GMT 79167

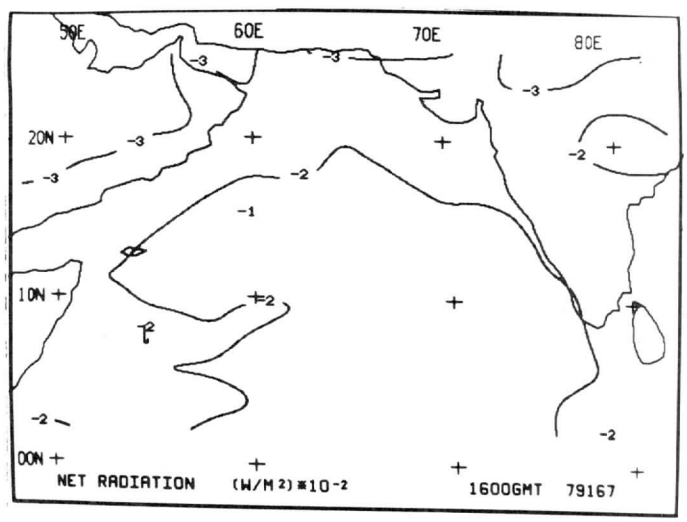
50E
60E
70E
80E
20N
10N
00N
NET RADIATION (W/M2)*10-2
1600GMT 79167

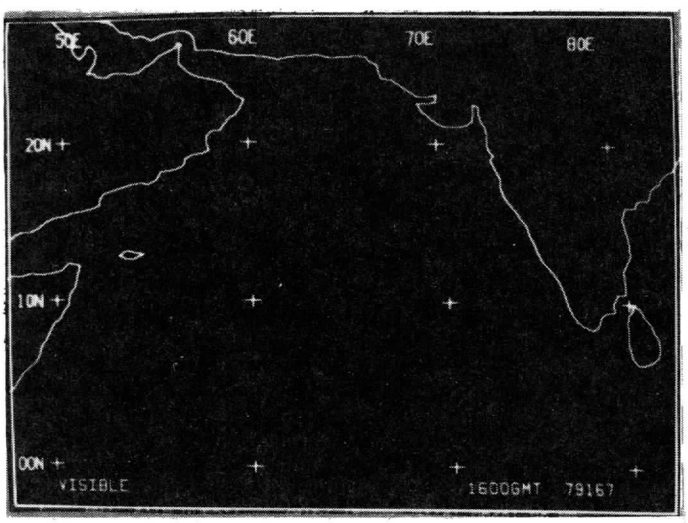
50E
60E
70E
80E
20N
10N
00N
VISIBLE
1600GMT 79167

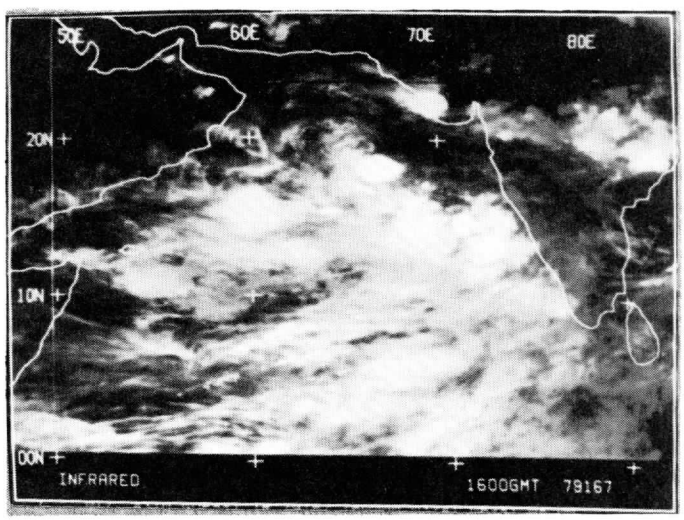
50E
60E
70E
80E
20N
10N
00N
INFRARED
1600GMT 79167

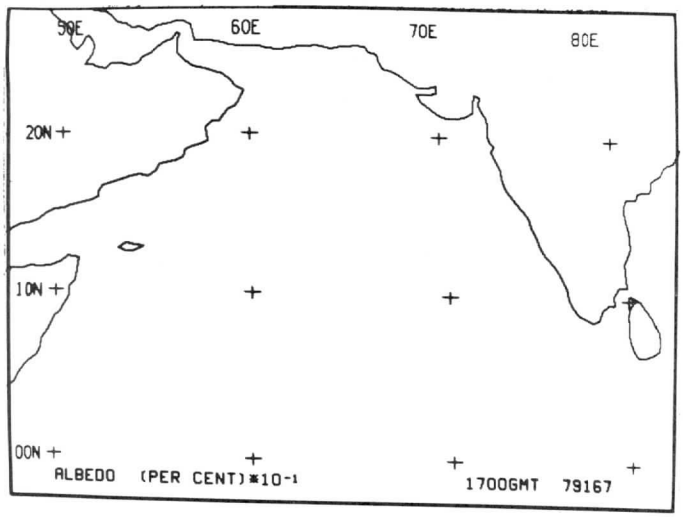
50E
60E
70E
80E
20N
10N
00N
ALBEDO (PER CENT)*10-1
1700GMT 79167

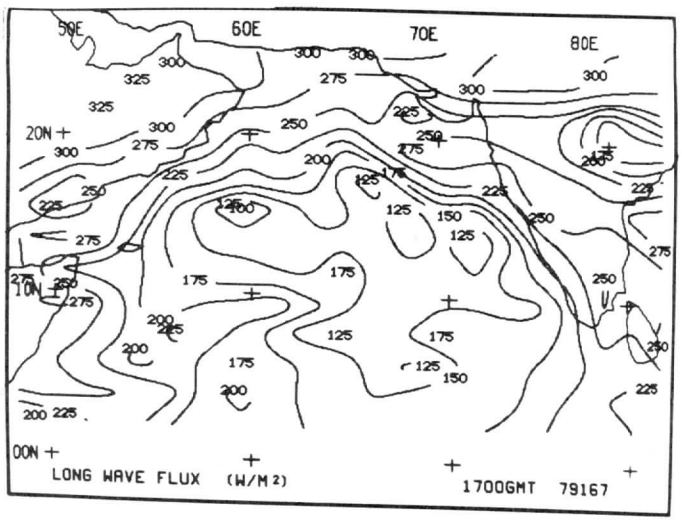
50E
60E
70E
80E
20N
10N
00N
LONG WAVE FLUX (W/M2)
1700GMT 79167

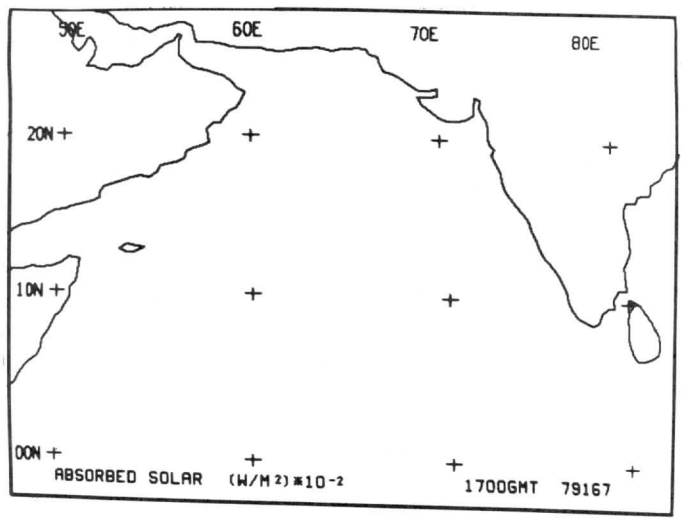
50E
60E
70E
80E
20N
10N
00N
ABSORBED SOLAR (W/M2)*10-2
1700GMT 79167

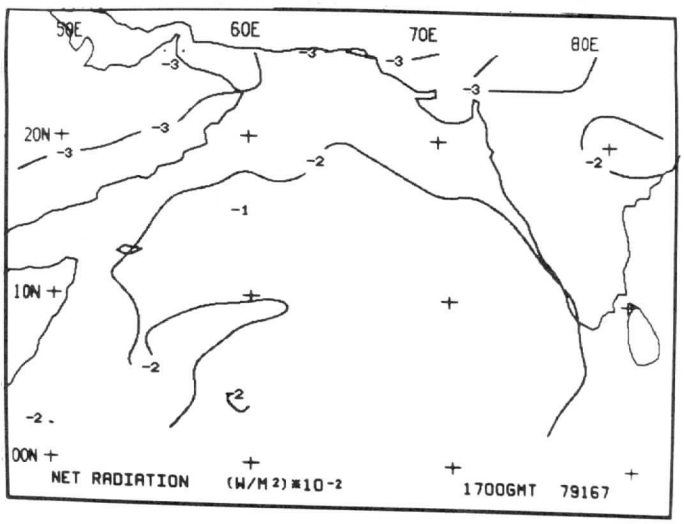
50E
60E
70E
80E
20N
10N
00N
NET RADIATION (W/M2)*10-2
1700GMT 79167

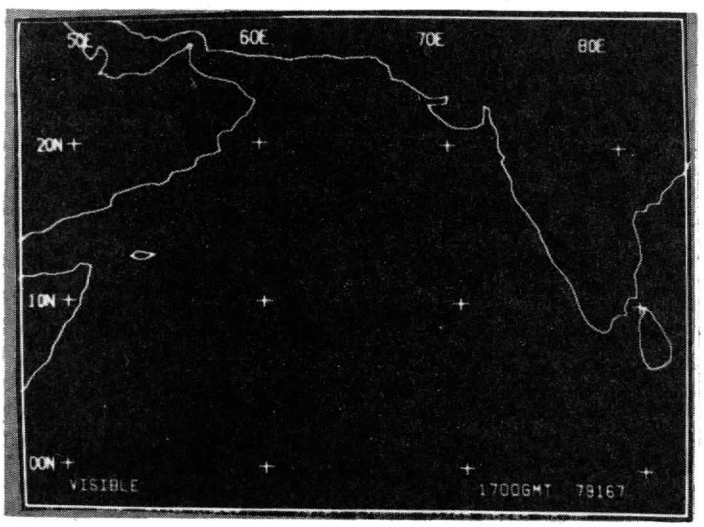
50E
60E
70E
80E
20N
10N
00N
VISIBLE
1700GMT 79167

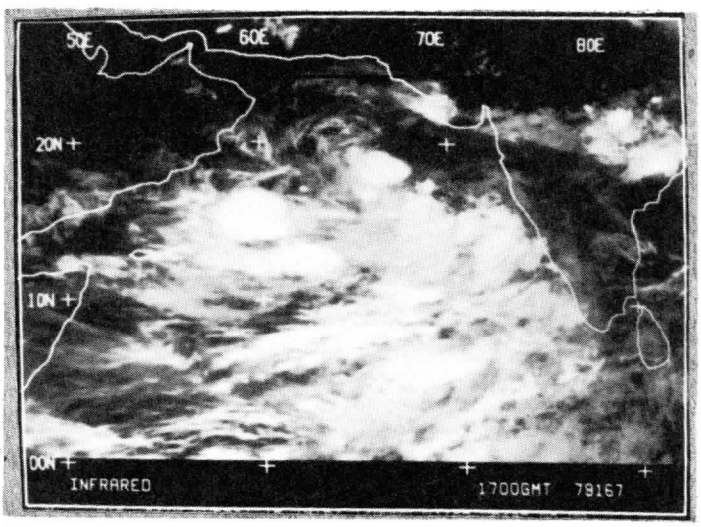
50E
60E
70E
80E
20N
10N
00N
INFRARED
1700GMT 79167

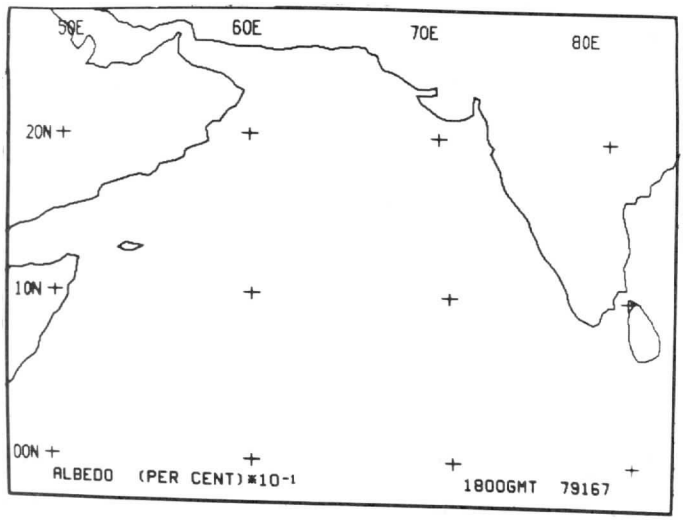
50E
60E
70E
80E
20N
10N
0ON
ALBEDO (PER CENT)*10-1
1800GMT 79167

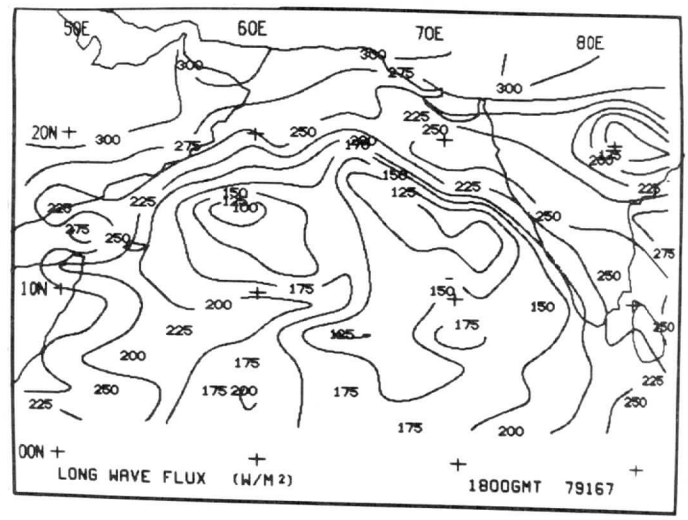
50E
60E
70E
80E
20N
10N
0ON
LONG WAVE FLUX (W/M2)
1800GMT 79167

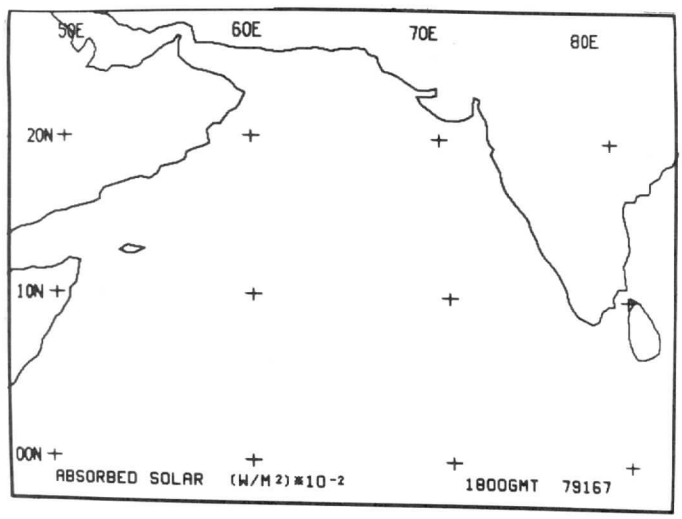
50E
60E
70E
80E
20N
10N
0ON
ABSORBED SOLAR (W/M2)*10-2
1800GMT 79167

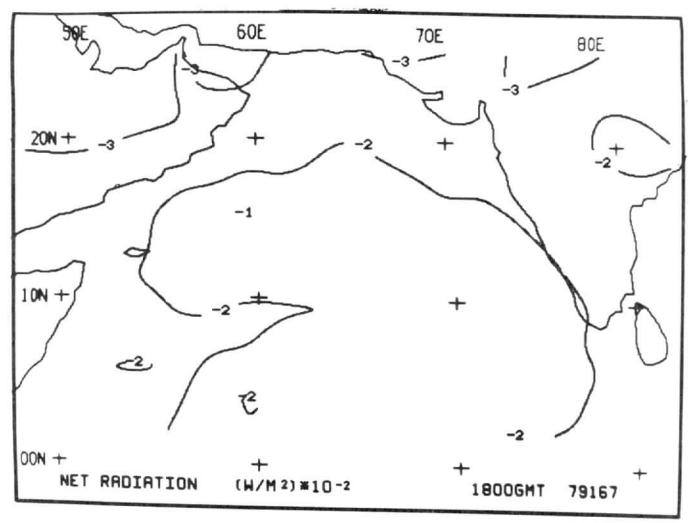
50E
60E
70E
80E
20N
10N
0ON
NET RADIATION (W/M2)*10-2
1800GMT 79167

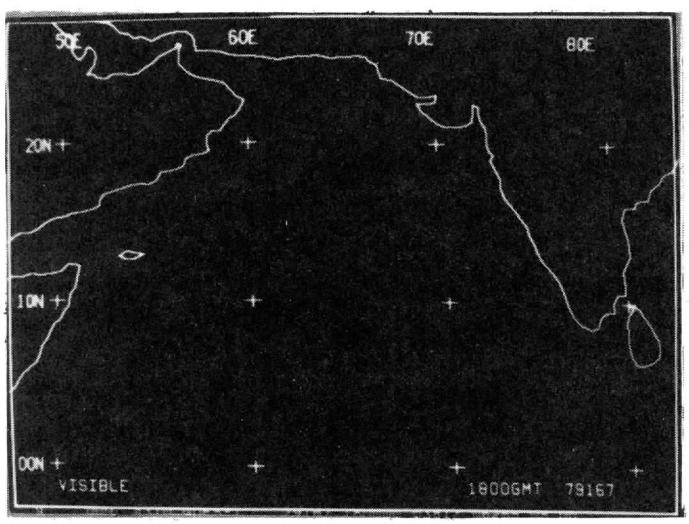
50E
60E
70E
80E
20N
10N
0ON
VISIBLE
1800GMT 79167

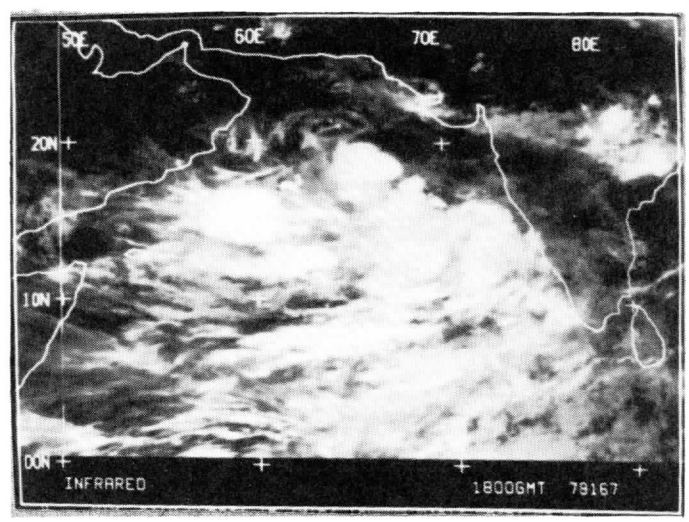
50E
60E
70E
80E
20N
10N
0ON
INFRARED
1800GMT 79167

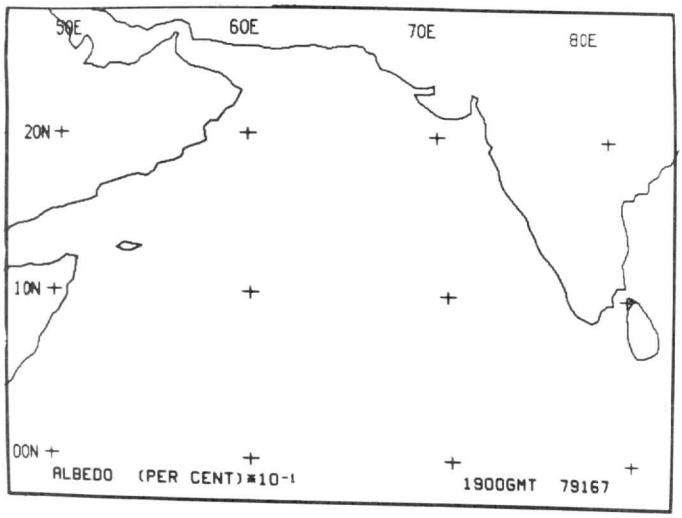
50E
60E
70E
80E
20N
10N
0ON
ALBEDO (PER CENT)*10-1
1900GMT 79167

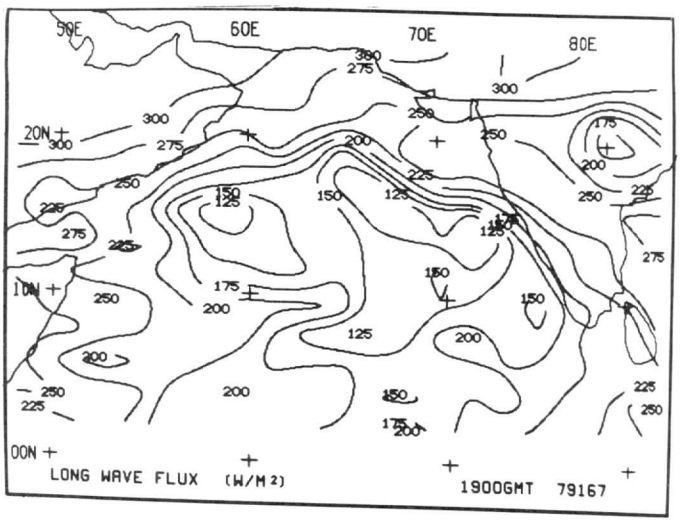
50E
60E
70E
80E
20N
10N
0ON
LONG WAVE FLUX (W/M2)
1900GMT 79167

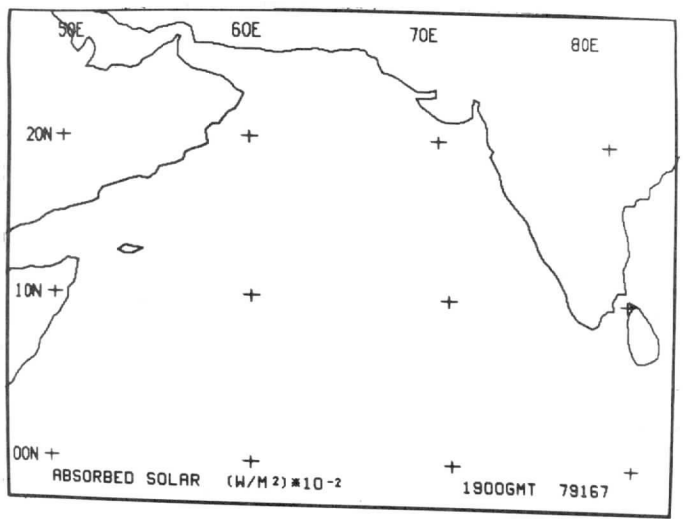
50E
60E
70E
80E
20N
10N
0ON
ABSORBED SOLAR (W/M2)*10-2
1900GMT 79167

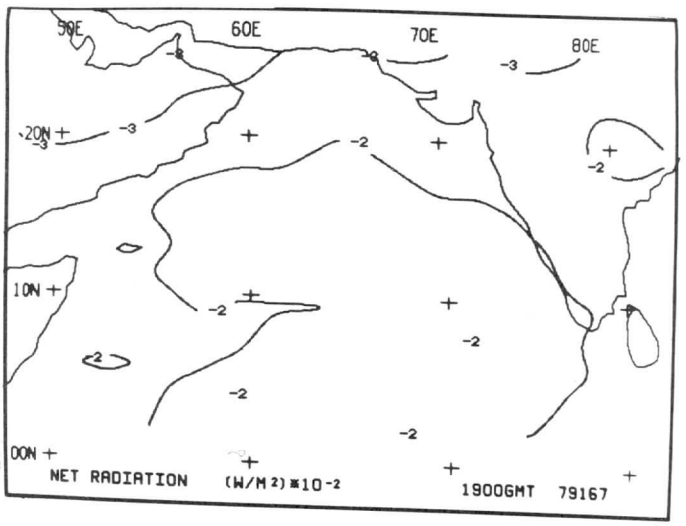
50E
60E
70E
80E
20N
10N
0ON
NET RADIATION (W/M2)*10-2
1900GMT 79167

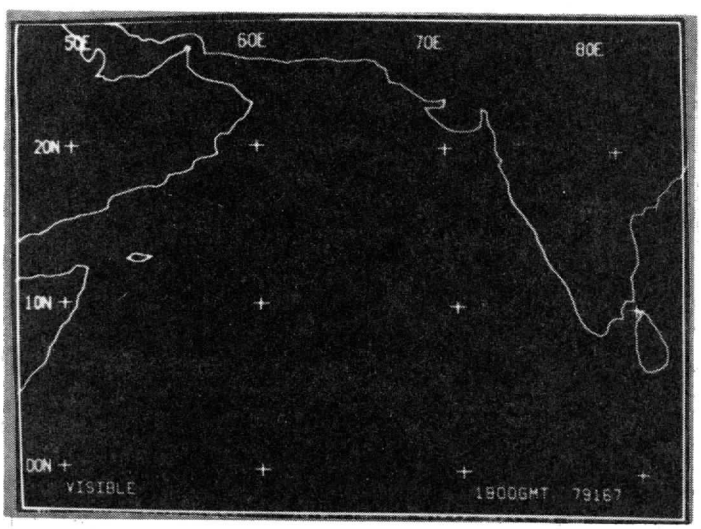
50E
60E
70E
80E
20N
10N
0ON
VISIBLE
1900GMT 79167

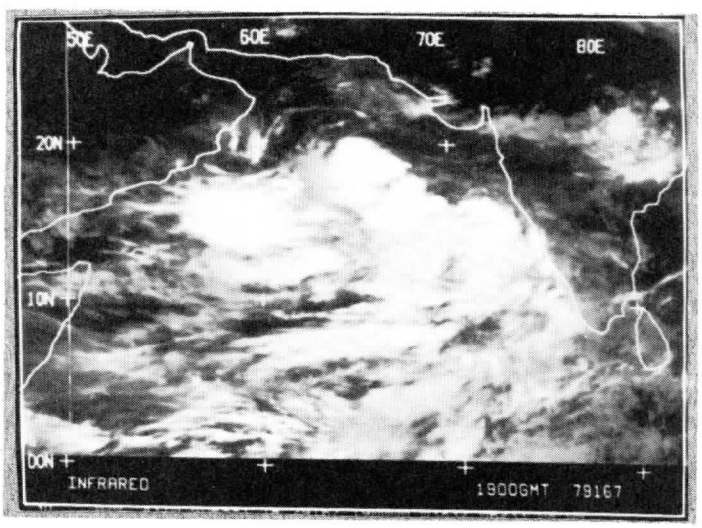
50E
60E
70E
80E
20N
10N
0ON
INFRARED
1900GMT 79167

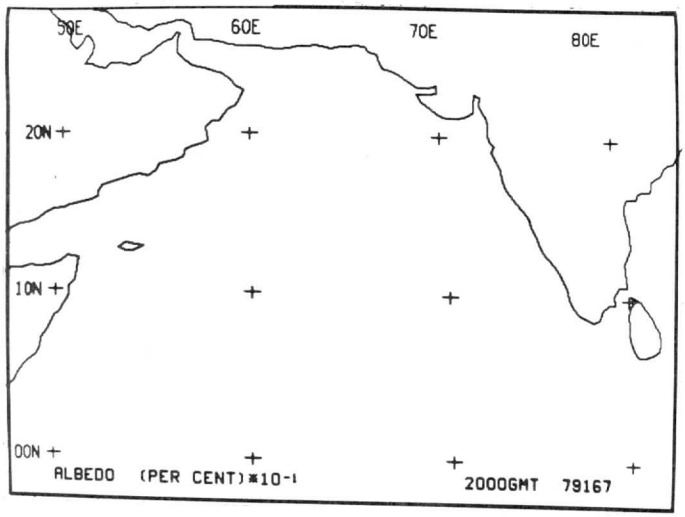
50E
60E
70E
80E
20N
10N
0ON
ALBEDO (PER CENT)*10-1
2000GMT 79167

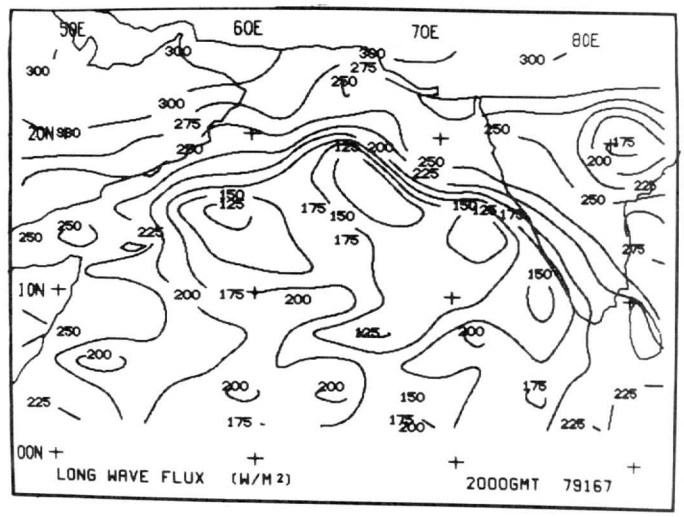
50E
60E
70E
80E
20N
10N
0ON
LONG WAVE FLUX (W/M2)
2000GMT 79167

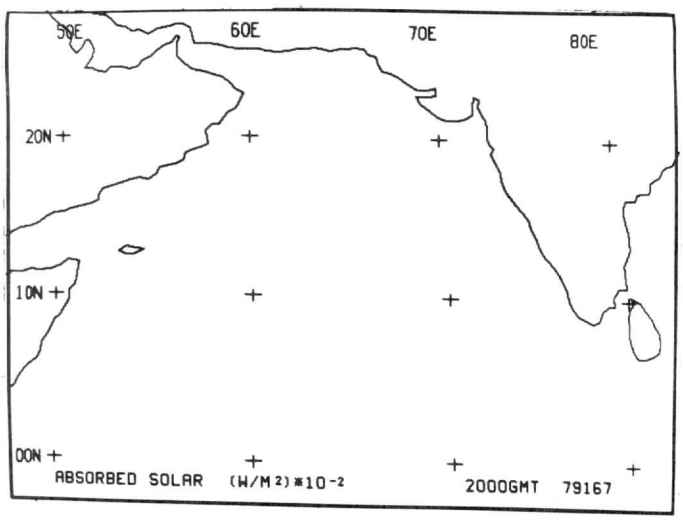
50E
60E
70E
80E
20N
10N
0ON
ABSORBED SOLAR (W/M2)*10-2
2000GMT 79167

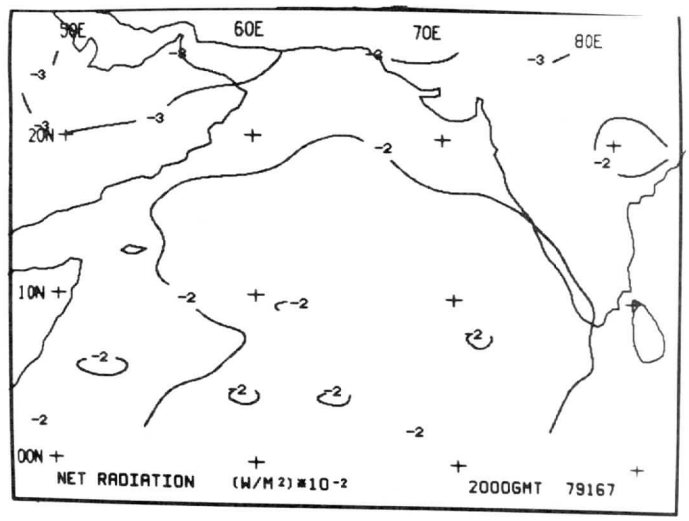
50E
60E
70E
80E
20N
10N
0ON
NET RADIATION (W/M2)*10-2
2000GMT 79167

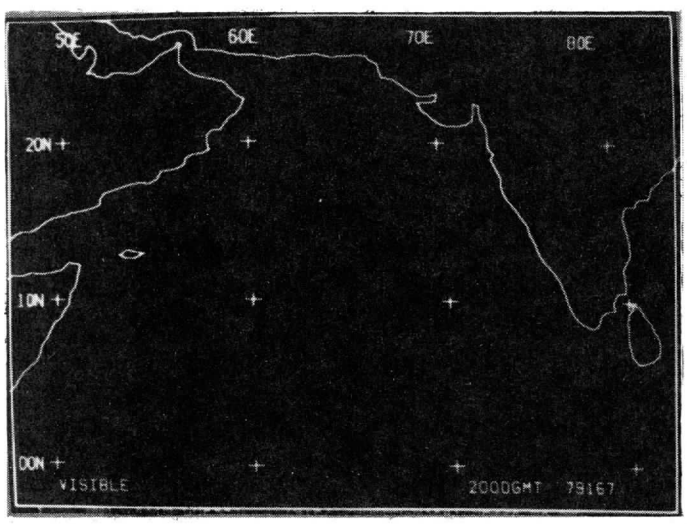
50E
60E
70E
80E
20N
10N
0ON
VISIBLE
2000GMT 79167

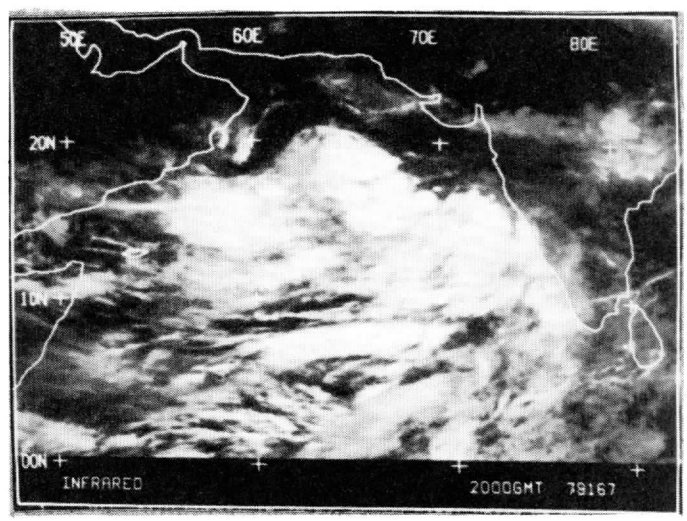
50E
60E
70E
80E
20N
10N
0ON
INFRARED
2000GMT 79167

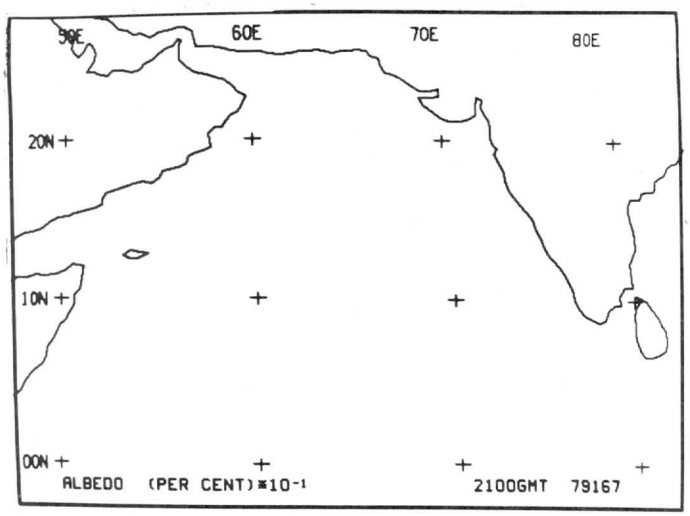
50E
60E
70E
80E
20N
10N
00N
ALBEDO (PER CENT)*10-1
2100GMT 79167

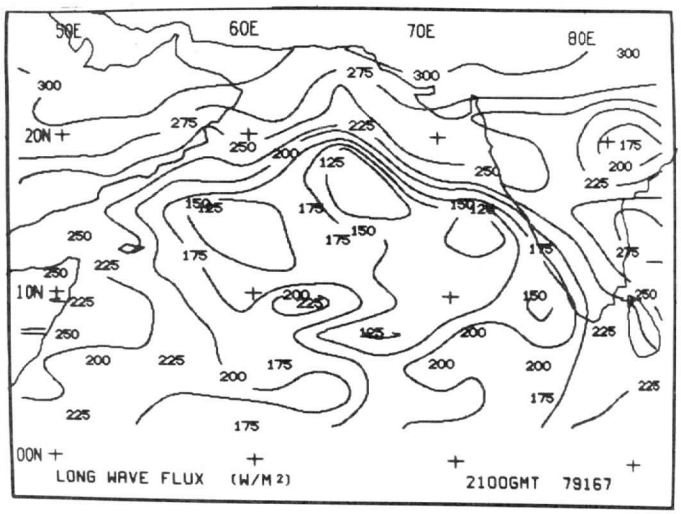
50E
60E
70E
80E
20N
10N
00N
LONG WAVE FLUX (W/M2)
2100GMT 79167

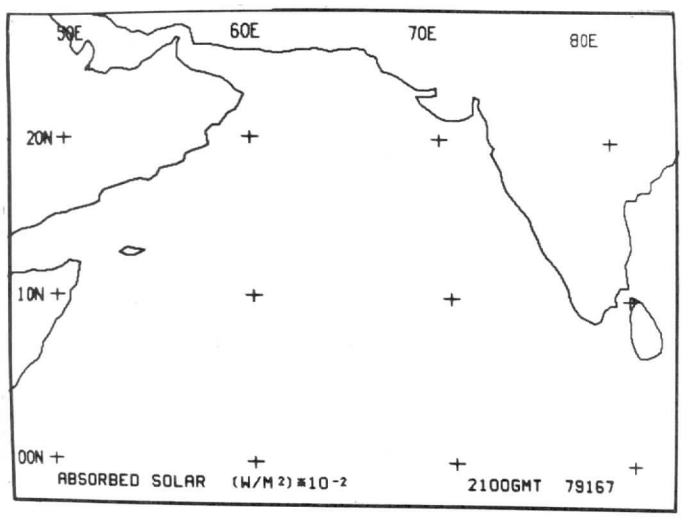
50E
60E
70E
80E
20N
10N
00N
ABSORBED SOLAR (W/M2)*10-2
2100GMT 79167

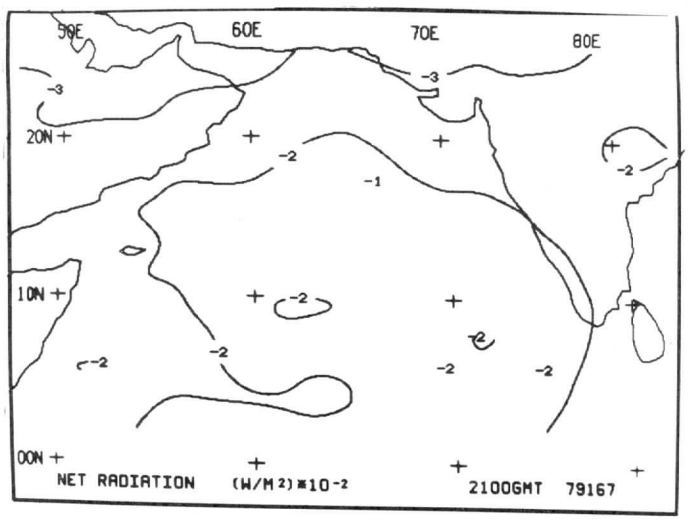
50E
60E
70E
80E
20N
10N
00N
NET RADIATION (W/M2)*10-2
2100GMT 79167

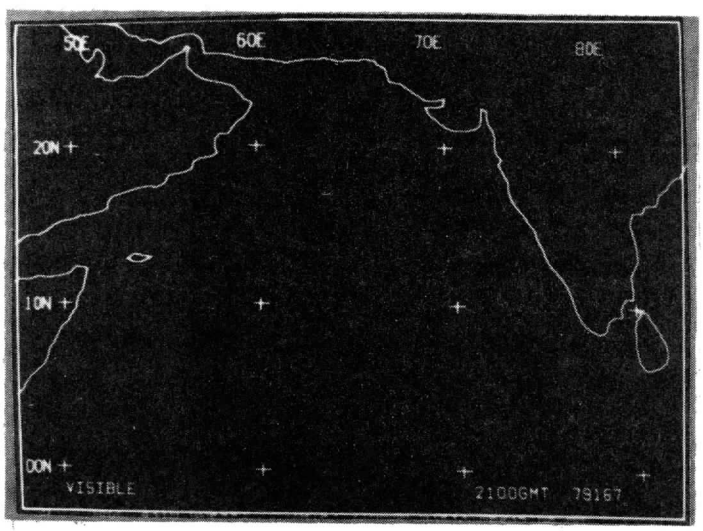
50E
60E
70E
80E
20N
10N
00N
VISIBLE
2100GMT 79167

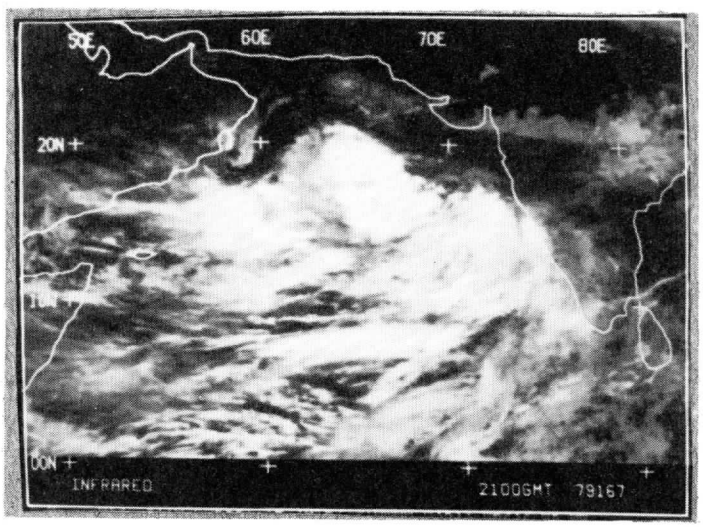
50E
60E
70E
80E
20N
00N
INFRARED
2100GMT 79167

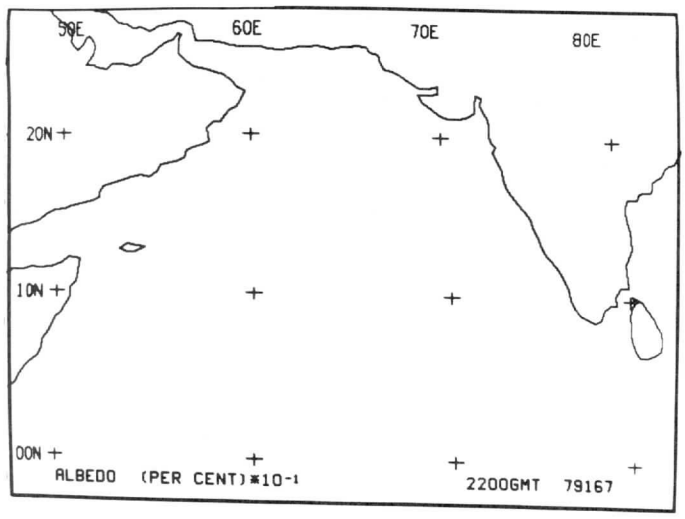
50E
60E
70E
80E
20N
10N
0ON
ALBEDO (PER CENT)*10-1
2200GMT 79167

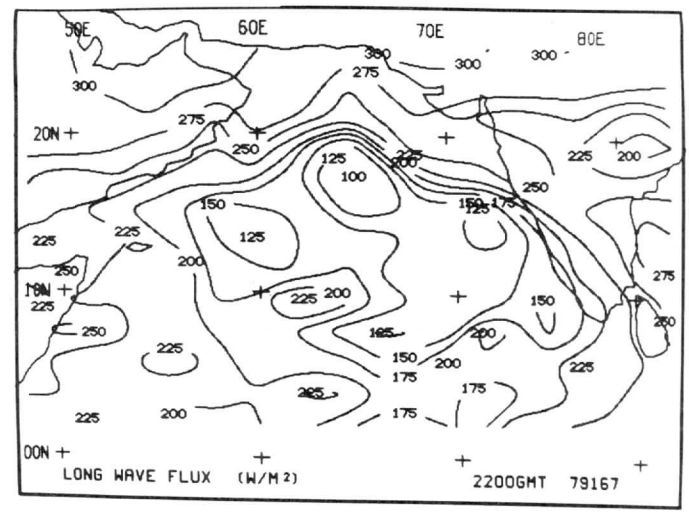
50E
60E
70E
80E
20N
10N
0ON
LONG WAVE FLUX (W/M2)
2200GMT 79167

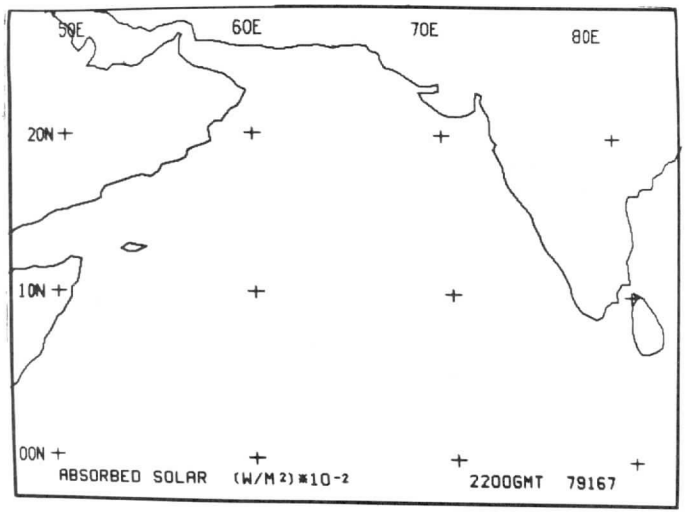
50E
60E
70E
80E
20N
10N
0ON
ABSORBED SOLAR (W/M2)*10-2
2200GMT 79167

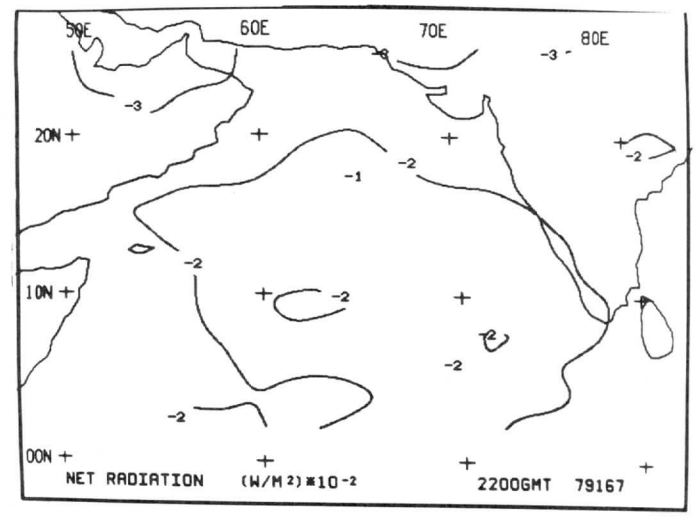
50E
60E
70E
80E
20N
10N
0ON
NET RADIATION (W/M2)*10-2
2200GMT 79167

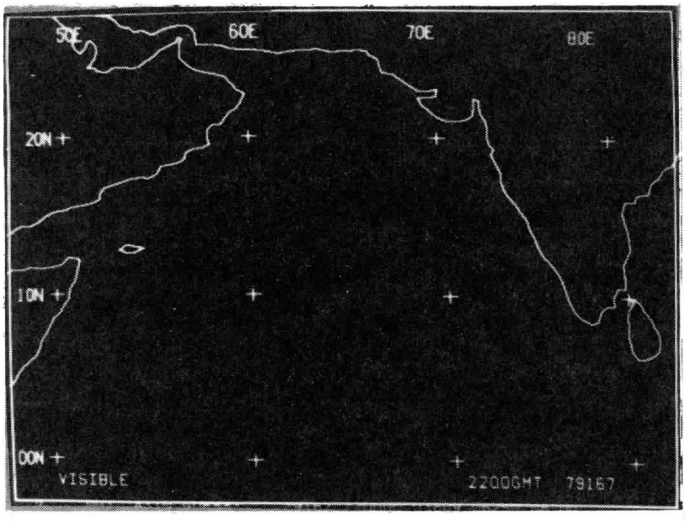
50E
60E
70E
80E
20N
10N
0ON
VISIBLE
2200GMT 79167

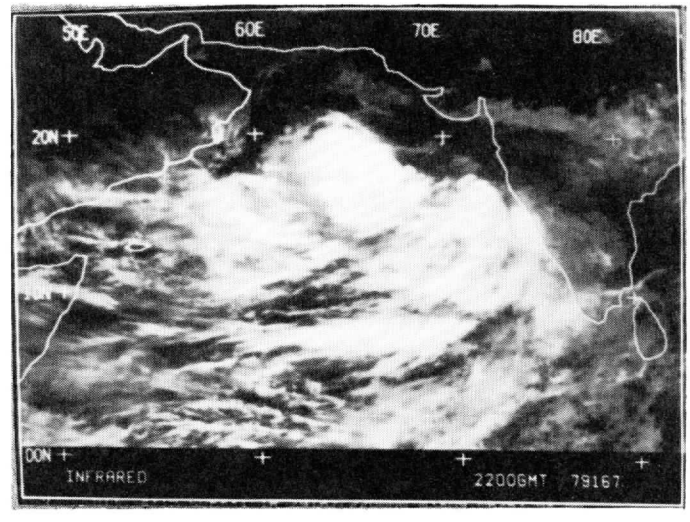
50E
60E
70E
80E
20N
0ON
INFRARED
2200GMT 79167

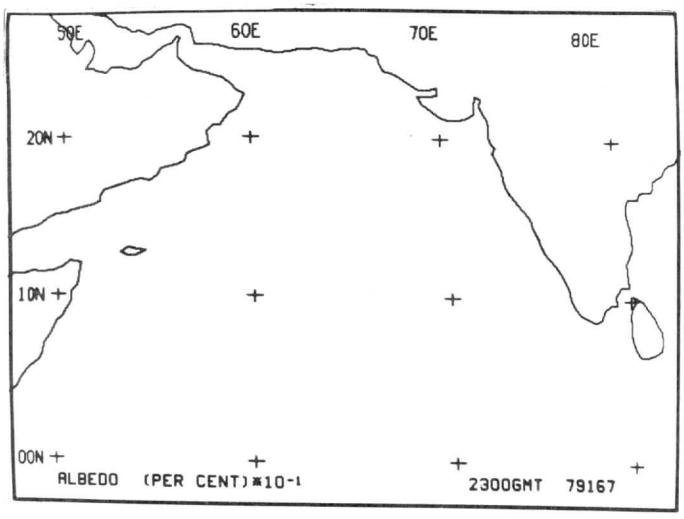
50E
60E
70E
80E
20N
10N
00N
ALBEDO (PER CENT)*10-1
2300GMT 79167

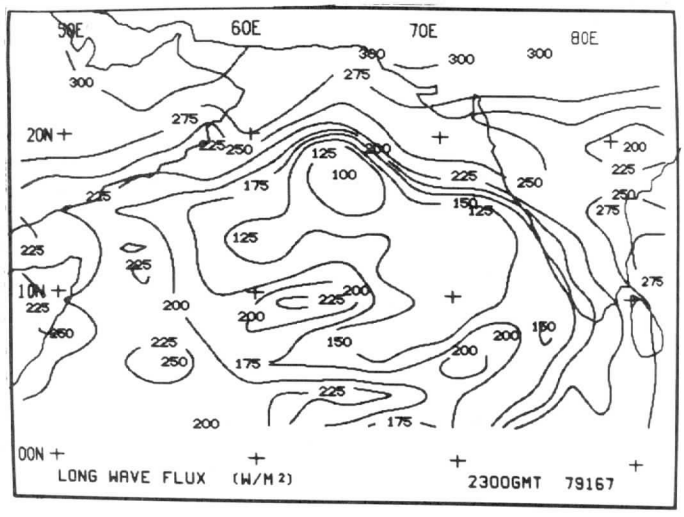
50E
60E
70E
80E
20N
10N
00N
LONG WAVE FLUX (W/M2)
2300GMT 79167

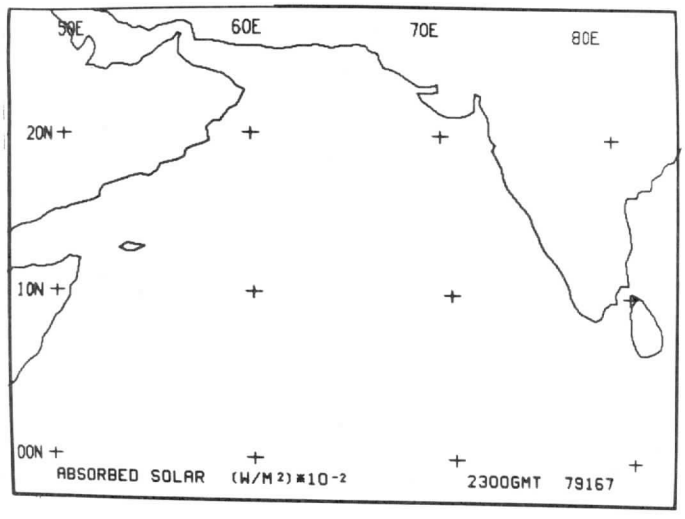
50E
60E
70E
80E
20N
10N
00N
ABSORBED SOLAR (W/M2)*10-2
2300GMT 79167

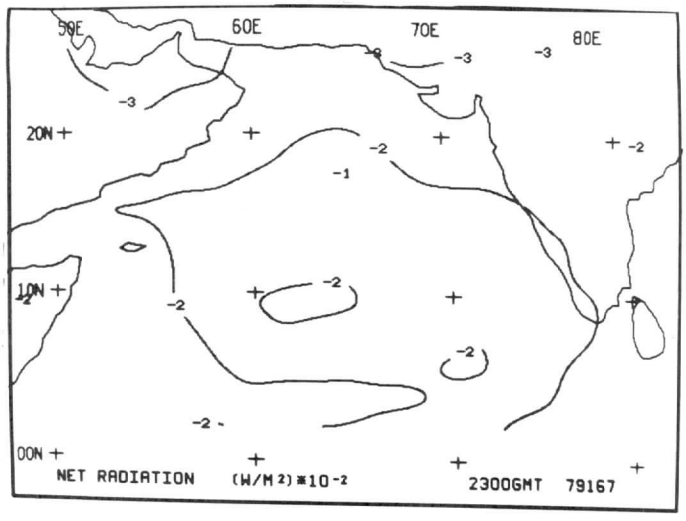
50E
60E
70E
80E
20N
10N
00N
NET RADIATION (W/M2)*10-2
2300GMT 79167

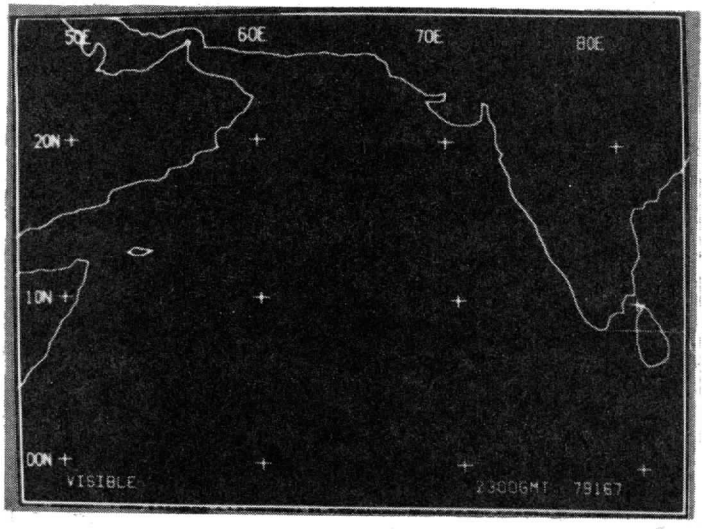
50E
60E
70E
80E
20N
10N
00N
VISIBLE
2300GMT 79167

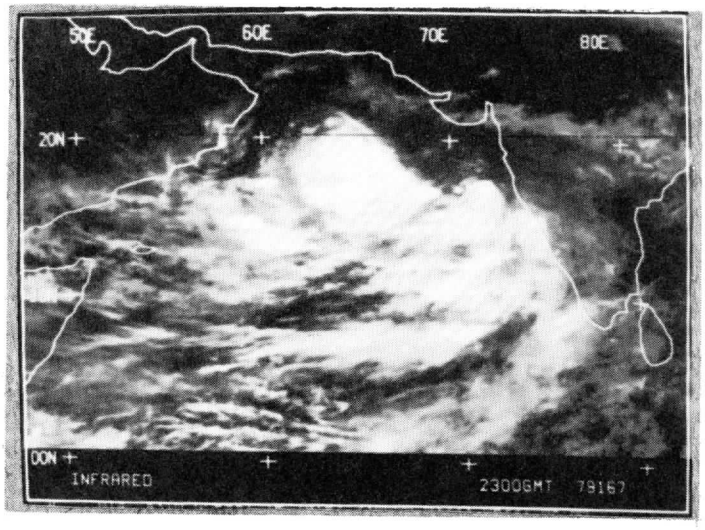
50E
60E
70E
80E
20N
00N
INFRARED
2300GMT 79167

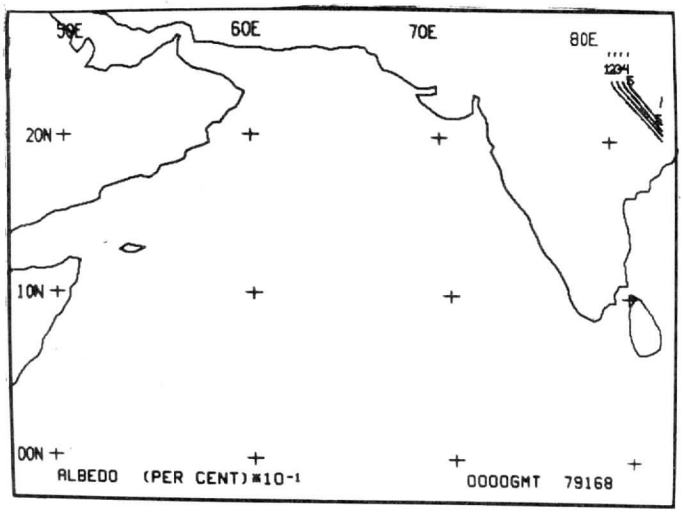
50E
60E
70E
80E
20N
10N
00N
ALBEDO (PER CENT)*10-1
0000GMT 79168

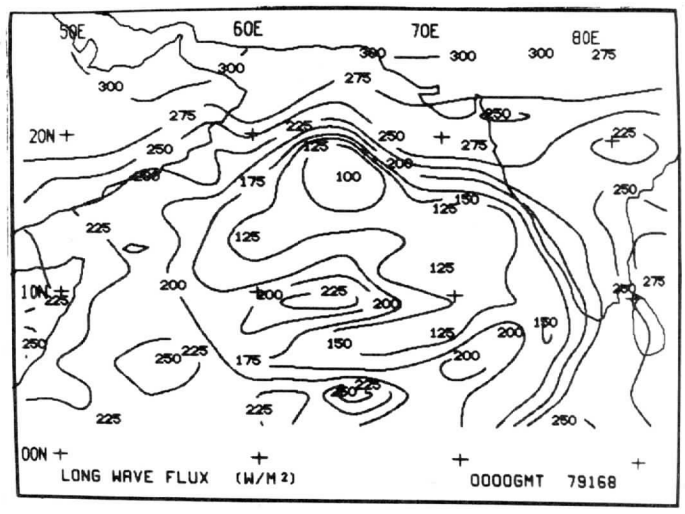
50E
60E
70E
80E
20N
10N
00N
LONG WAVE FLUX (W/M2)
0000GMT 79168

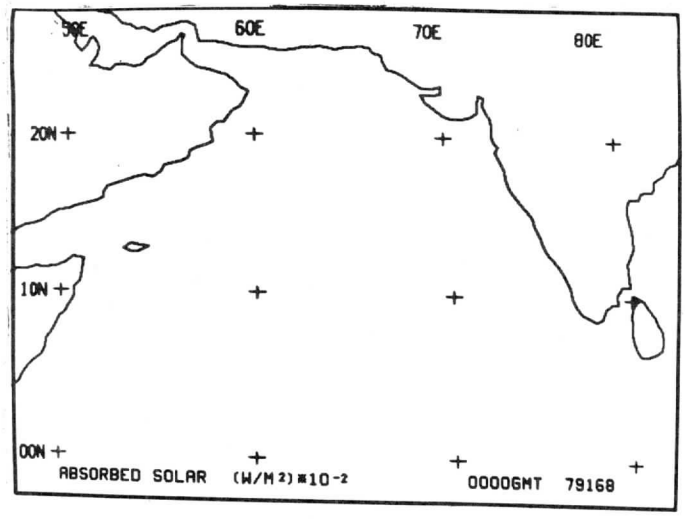
50E
60E
70E
80E
20N
10N
00N
ABSORBED SOLAR (W/M2)*10-2
0000GMT 79168

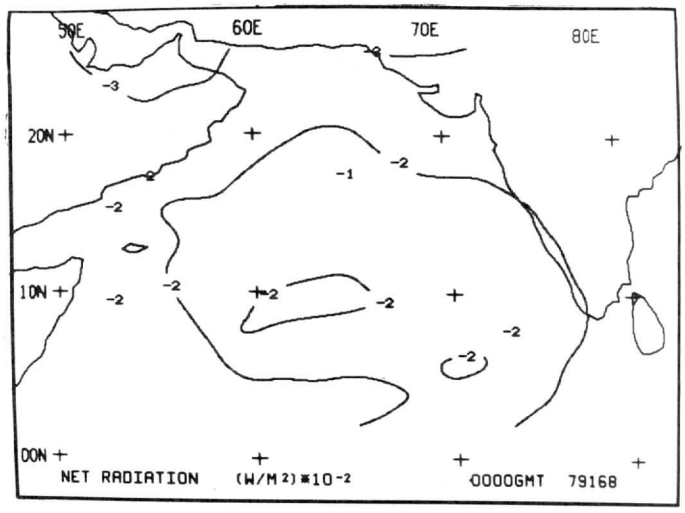
50E
60E
70E
80E
20N
10N
00N
NET RADIATION (W/M2)*10-2
0000GMT 79168

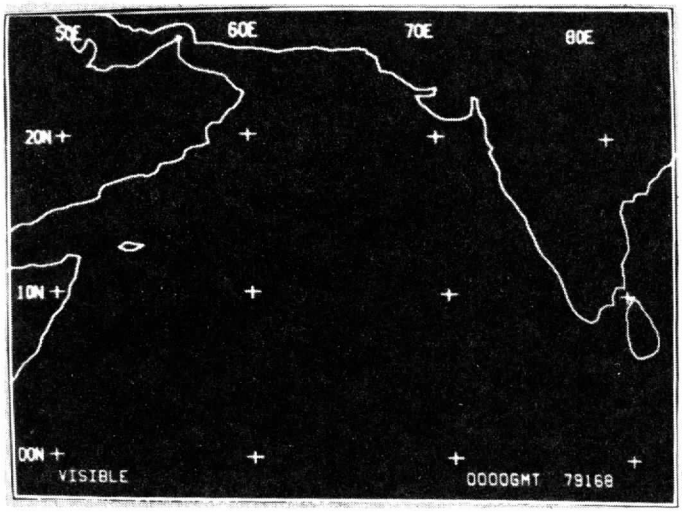
50E
60E
70E
80E
20N
10N
00N
VISIBLE
0000GMT 79168

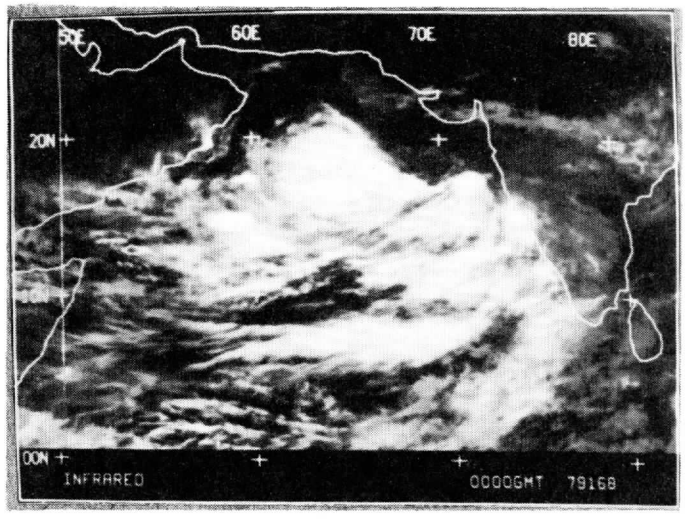
50E
60E
70E
80E
20N
00N
INFRARED
0000GMT 79168

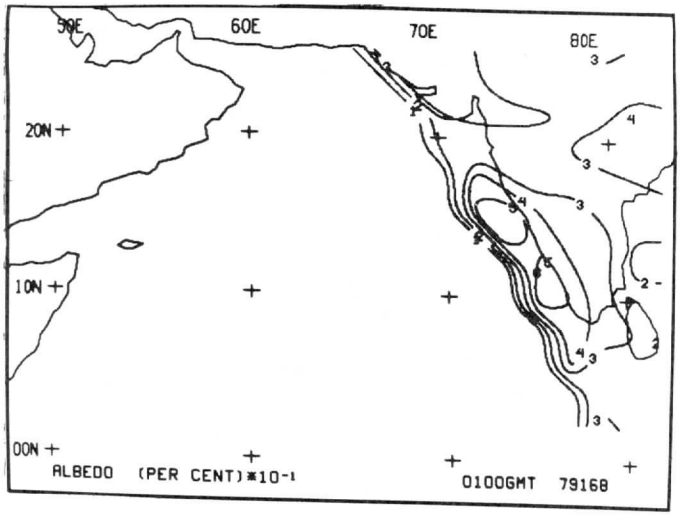
50E
60E
70E
80E
20N
10N
0ON
ALBEDO (PER CENT)*10-1
0100GMT 79168

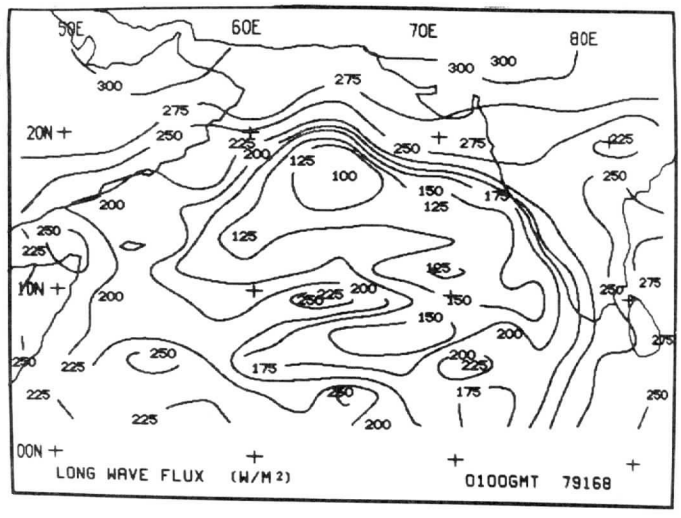
50E
60E
70E
80E
20N
10N
0ON
LONG WAVE FLUX (W/M2)
0100GMT 79168

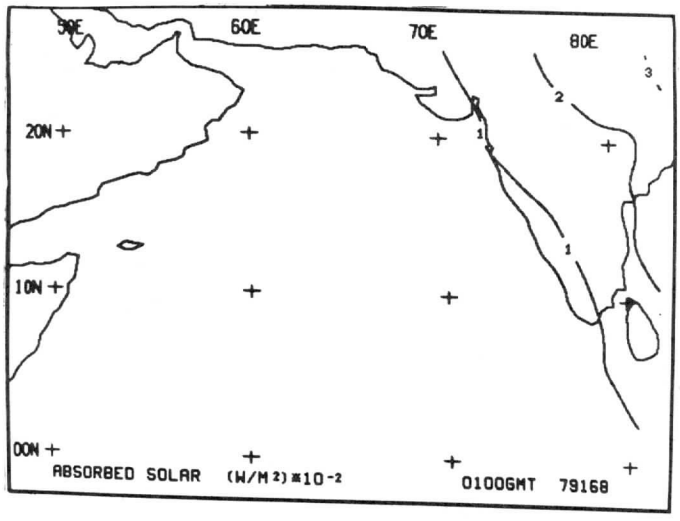
50E
60E
70E
80E
20N
10N
0ON
ABSORBED SOLAR (W/M2)*10-2
0100GMT 79168

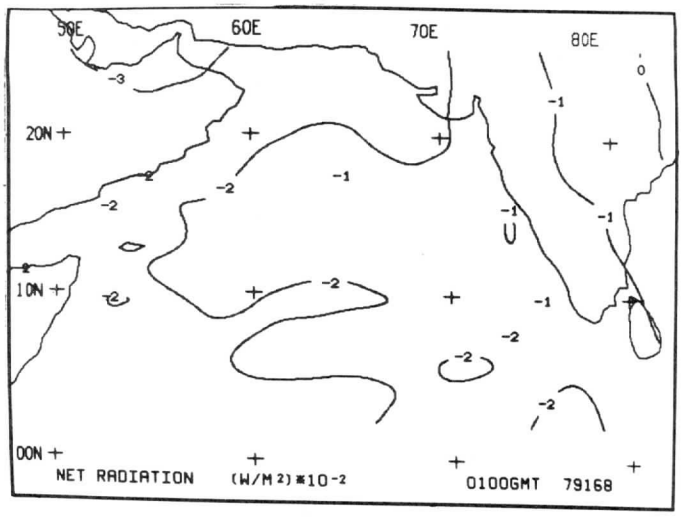
50E
60E
70E
80E
20N
10N
0ON
NET RADIATION (W/M2)*10-2
0100GMT 79168

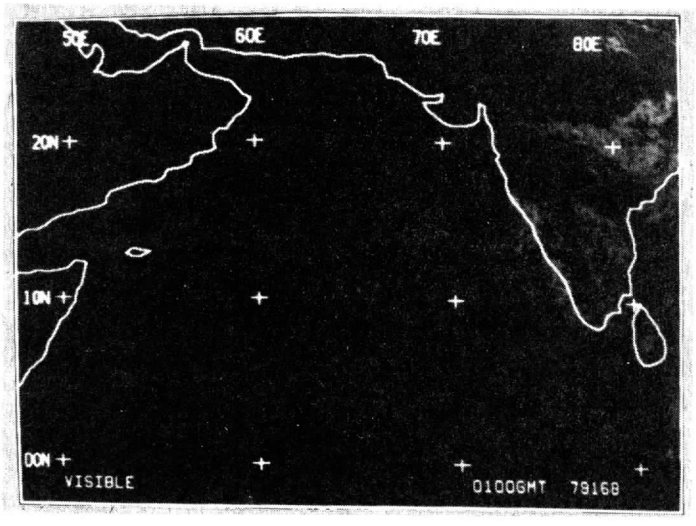
50E
60E
70E
80E
20N
10N
0ON
VISIBLE
0100GMT 79168

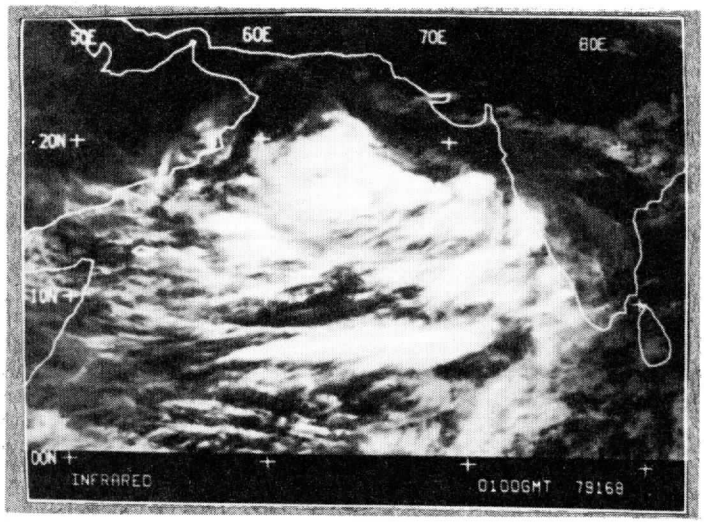
50E
60E
70E
80E
20N
10N
0ON
INFRARED
0100GMT 79168

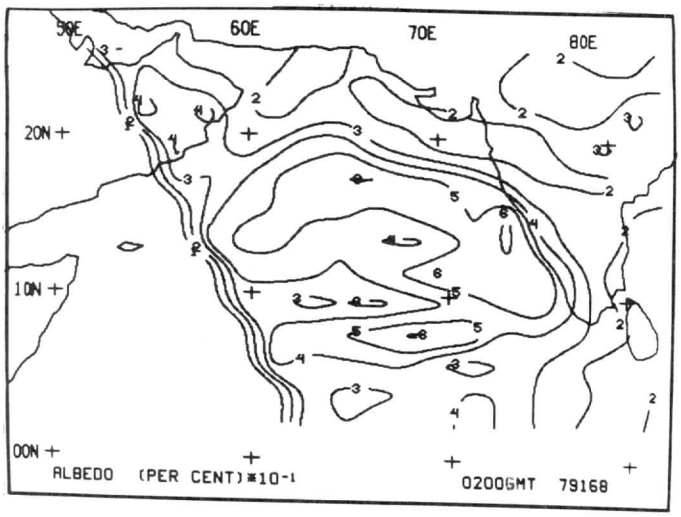
50E
60E
70E
80E
20N
10N
00N
ALBEDO (PER CENT)*10-1
0200GMT 79168

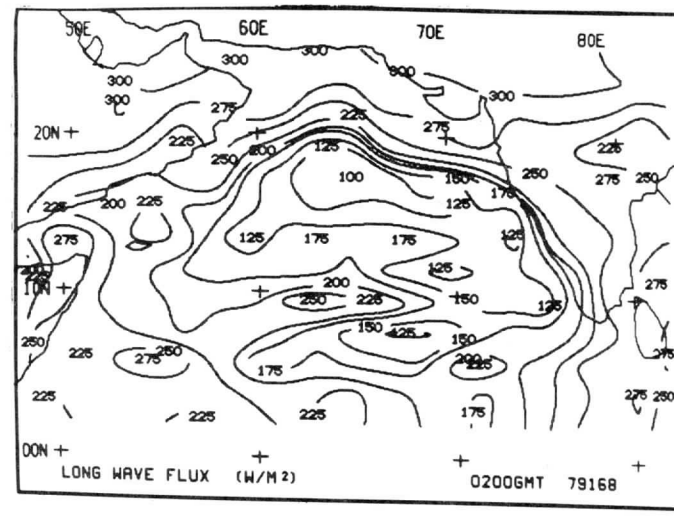
50E
60E
70E
80E
20N
10N
00N
LONG WAVE FLUX (W/M2)
0200GMT 79168

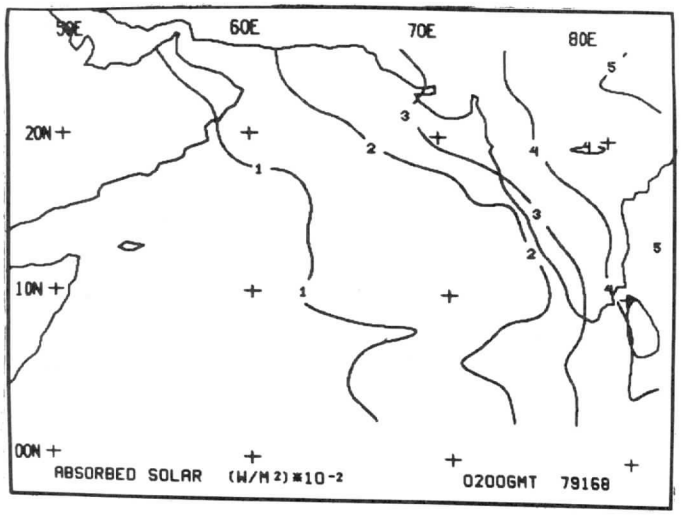
50E
60E
70E
80E
20N
10N
00N
ABSORBED SOLAR (W/M2)*10-2
0200GMT 79168

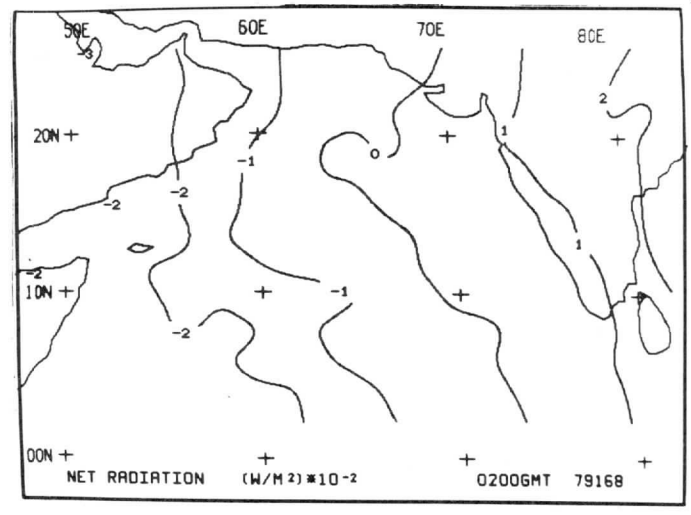
50E
60E
70E
80E
20N
10N
00N
NET RADIATION (W/M2)*10-2
0200GMT 79168

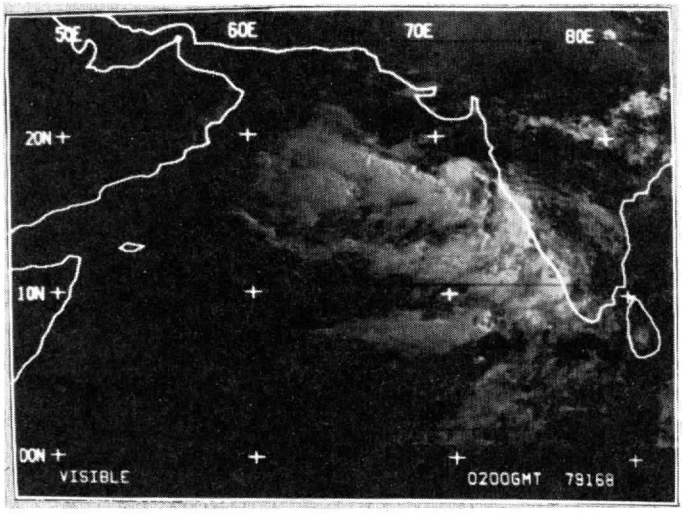
50E
60E
70E
80E
20N
10N
00N
VISIBLE
0200GMT 79168

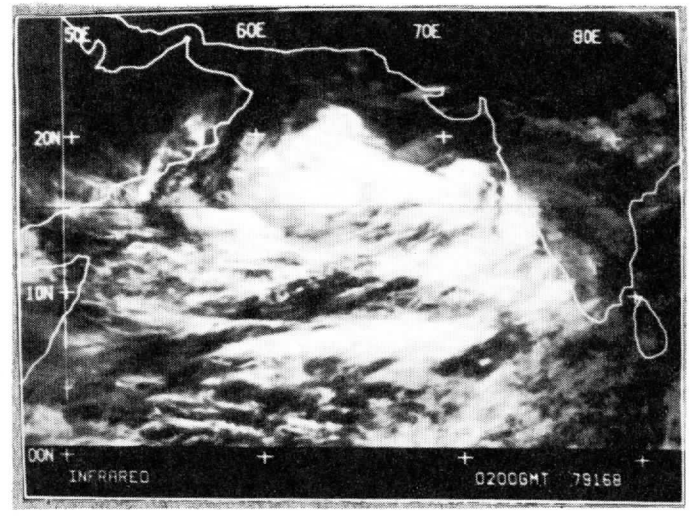
50E
60E
70E
80E
20N
10N
00N
INFRARED
0200GMT 79168

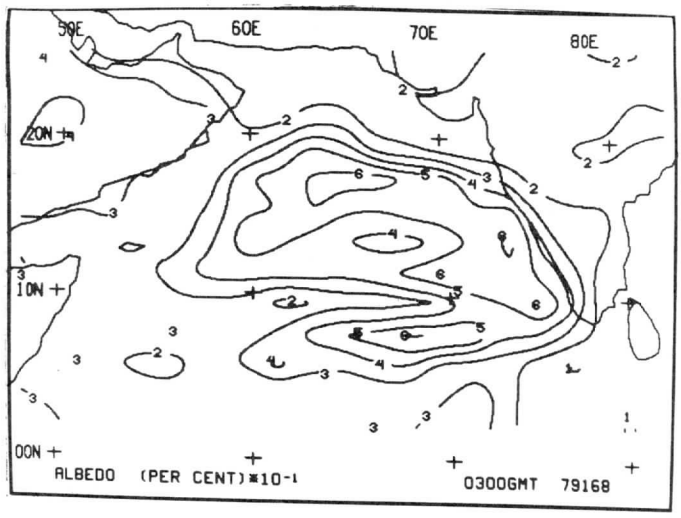
50E
60E
70E
80E
20N
10N
00N
ALBEDO (PER CENT)*10-1
0300GMT 79168

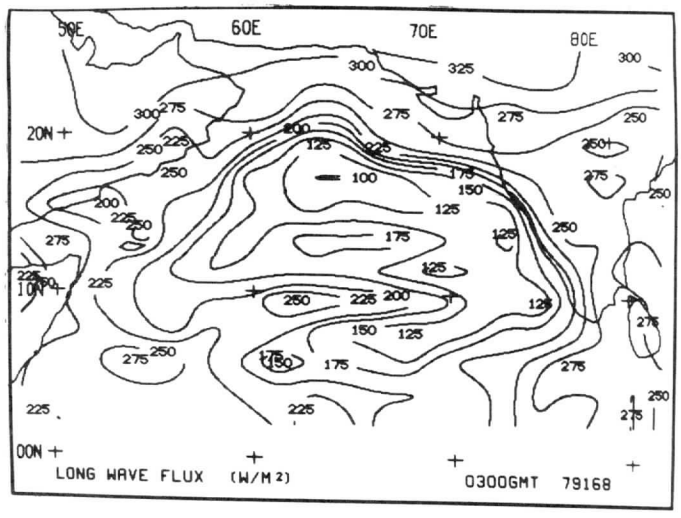
50E
60E
70E
80E
20N
10N
00N
LONG WAVE FLUX (W/M2)
0300GMT 79168

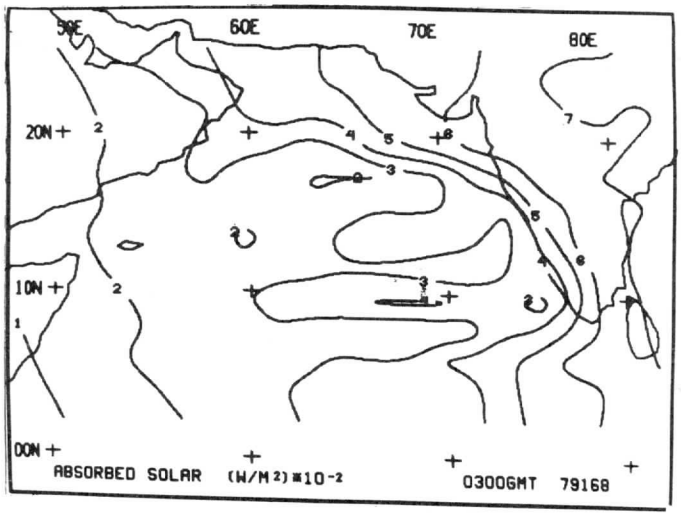
50E
60E
70E
80E
20N
10N
00N
ABSORBED SOLAR (W/M2)*10-2
0300GMT 79168

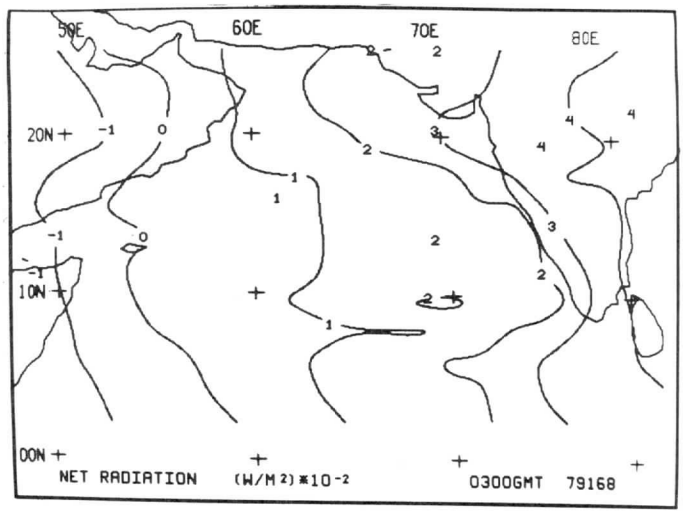
50E
60E
70E
80E
20N
10N
00N
NET RADIATION (W/M2)*10-2
0300GMT 79168

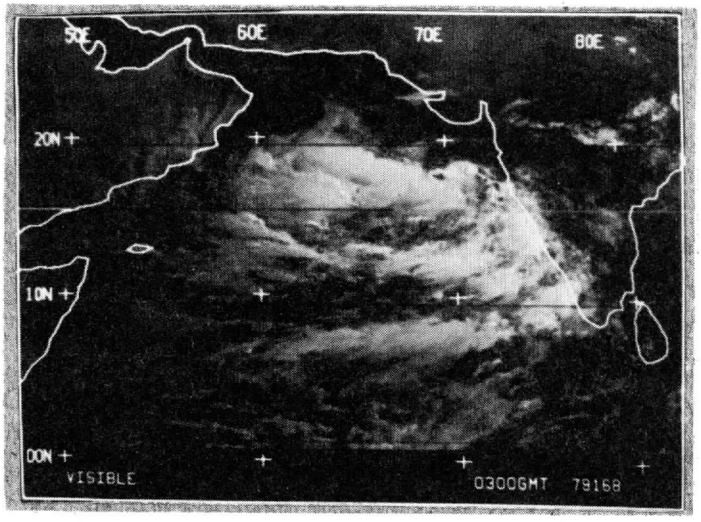
50E
60E
70E
80E
20N
10N
00N
VISIBLE
0300GMT 79168

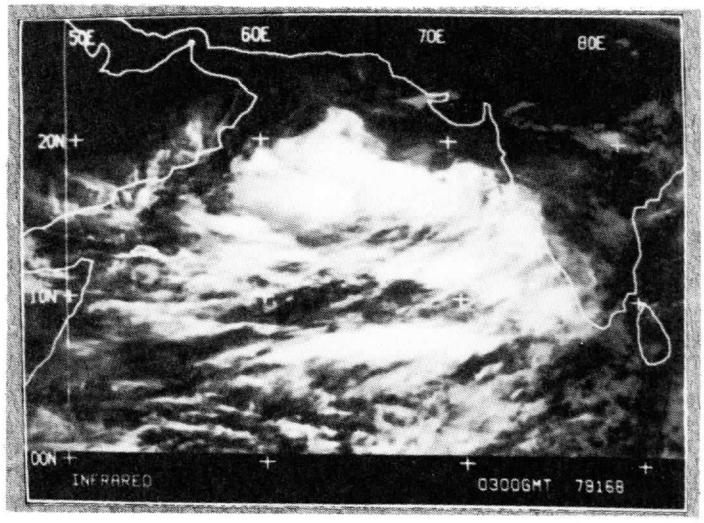
50E
60E
70E
80E
20N
10N
00N
INFRARED
0300GMT 79168

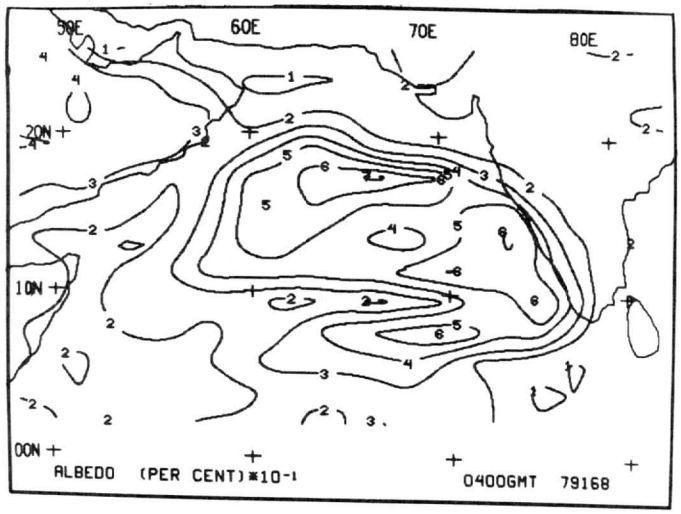
50E
60E
70E
80E
20N
10N
0ON
ALBEDO (PER CENT)*10-1
0400GMT 79168

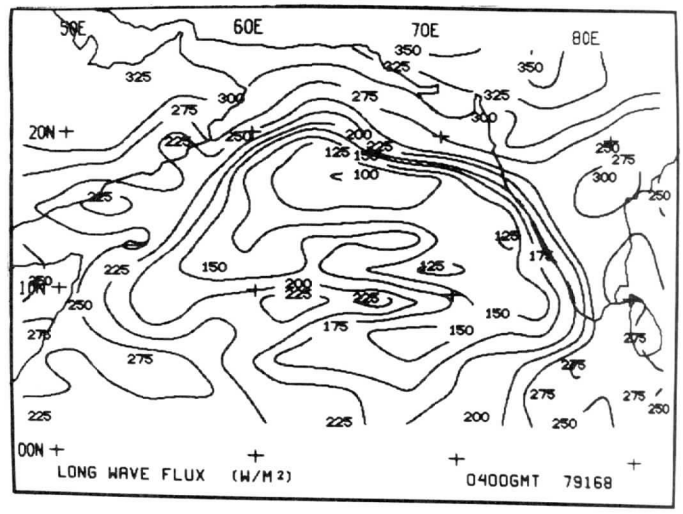
50E
60E
70E
80E
20N
10N
0ON
LONG WAVE FLUX (W/M2)
0400GMT 79168

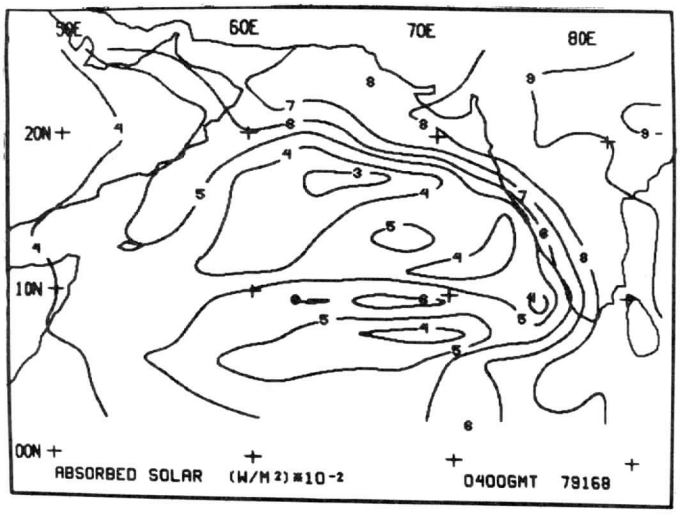
50E
60E
70E
80E
20N
10N
0ON
ABSORBED SOLAR (W/M2)*10-2
0400GMT 79168

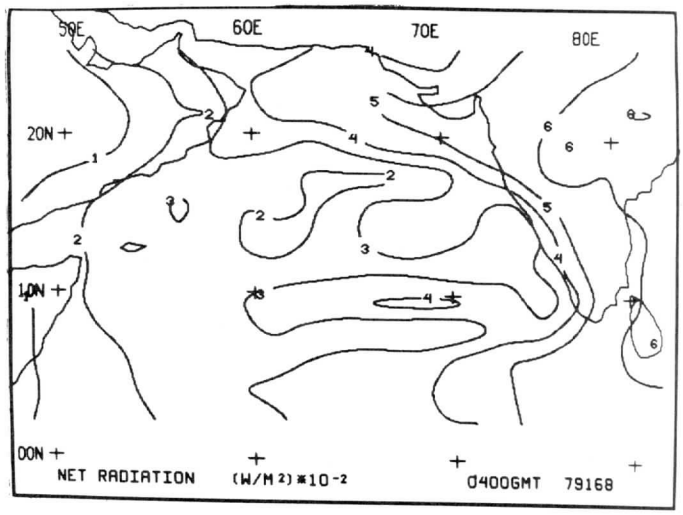
50E
60E
70E
80E
20N
10N
0ON
NET RADIATION (W/M2)*10-2
0400GMT 79168

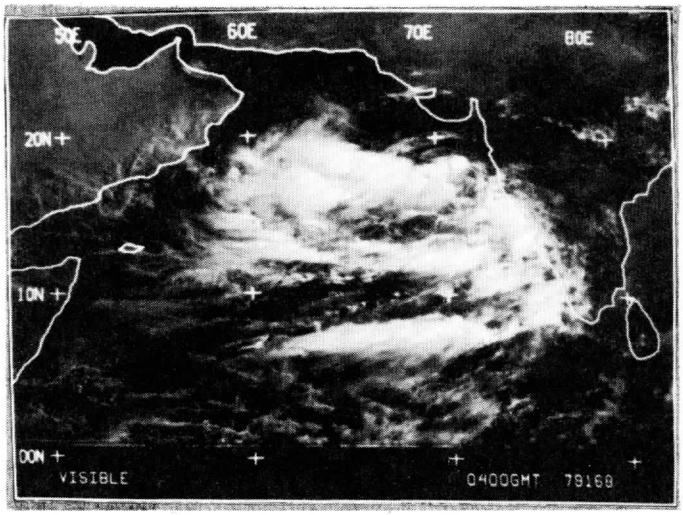
50E
60E
70E
80E
20N
10N
0ON
VISIBLE
0400GMT 79168

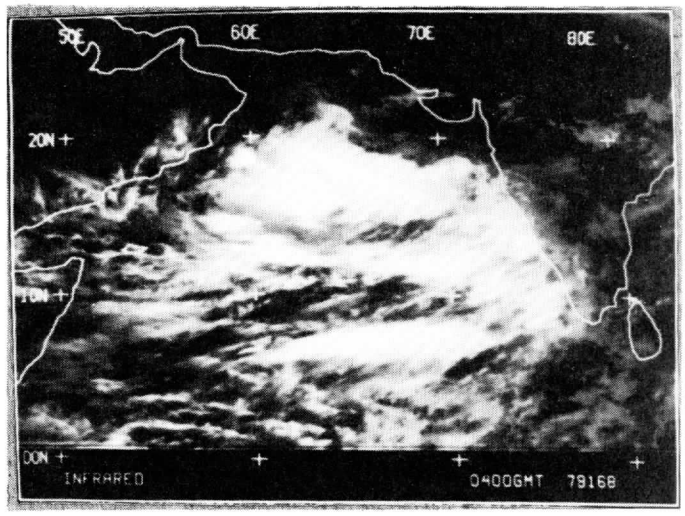
50E
60E
70E
80E
20N
10N
0ON
INFRARED
0400GMT 79168

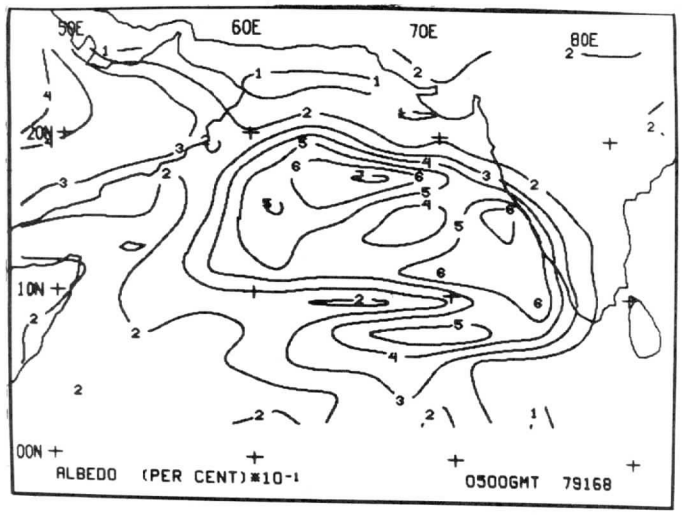
50E
60E
70E
80E
20N
10N
0ON
ALBEDO (PER CENT)*10-1
0500GMT 79168

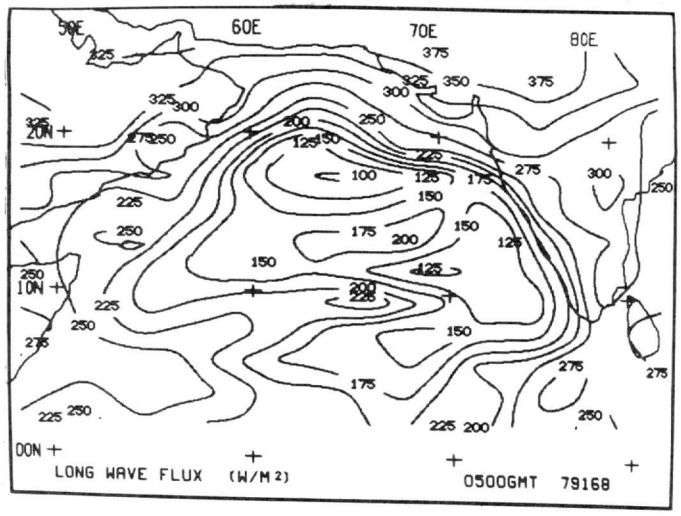
50E
60E
70E
80E
20N
10N
0ON
LONG WAVE FLUX (W/M2)
0500GMT 79168

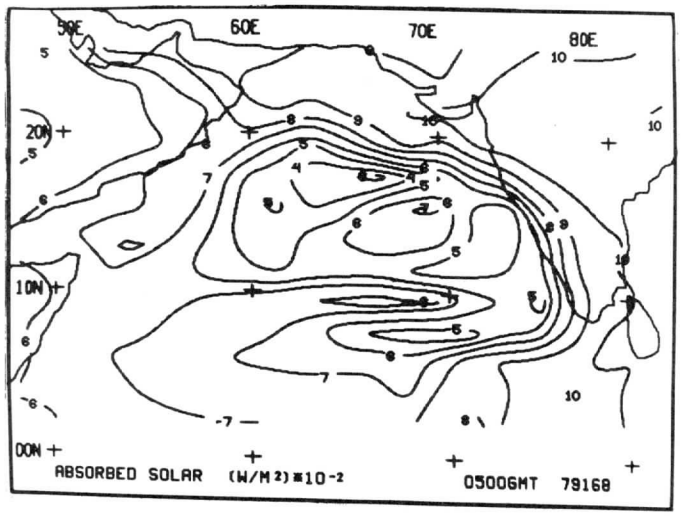
50E
60E
70E
80E
20N
10N
0ON
ABSORBED SOLAR (W/M2)*10-2
0500GMT 79168

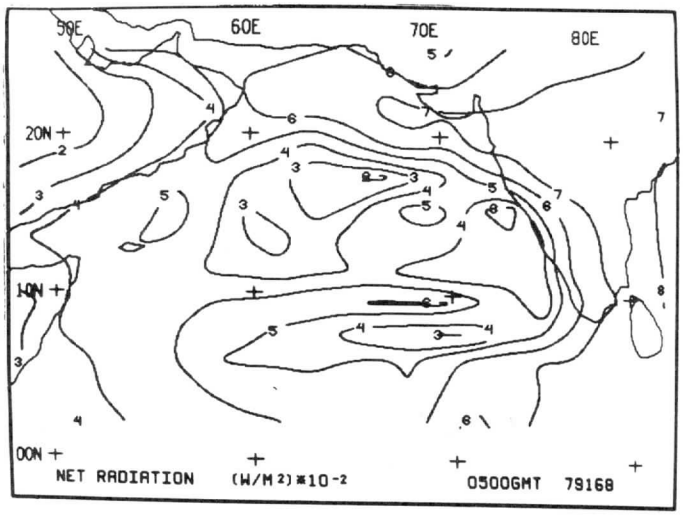
50E
60E
70E
80E
20N
10N
0ON
NET RADIATION (W/M2)*10-2
0500GMT 79168

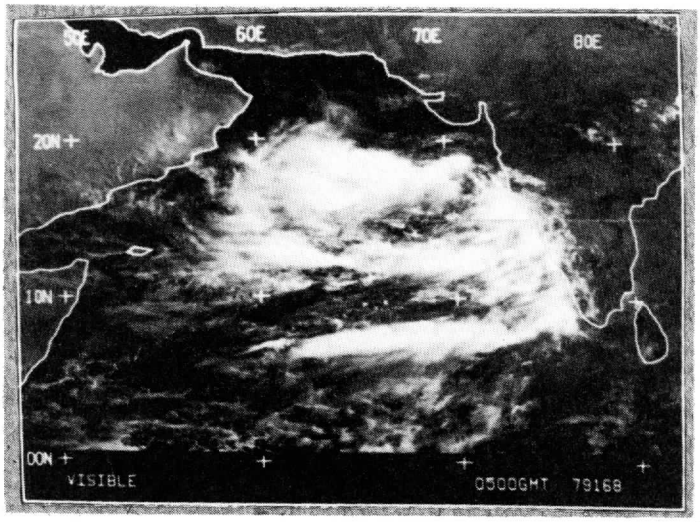
50E
60E
70E
80E
20N
10N
0ON
VISIBLE
0500GMT 79168

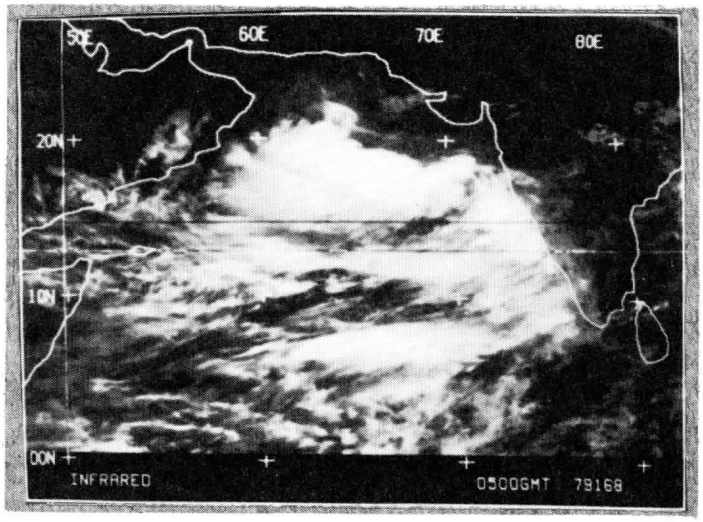
50E
60E
70E
80E
20N
10N
0ON
INFRARED
0500GMT 79168

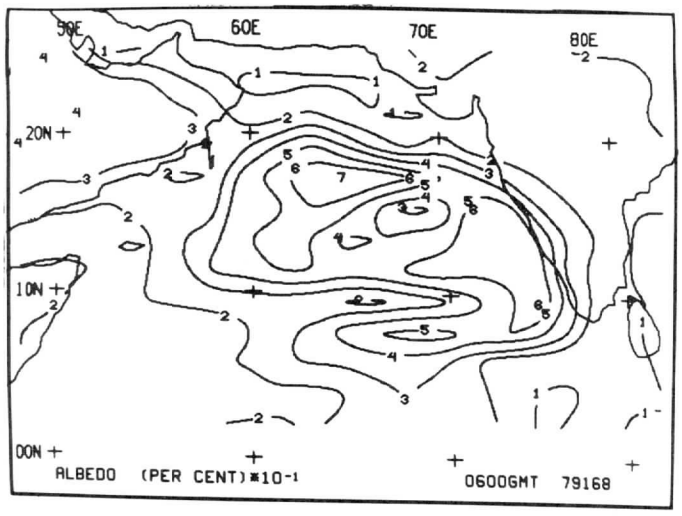
50E
60E
70E
80E
20N
10N
00N
ALBEDO (PER CENT)*10-1
0600GMT 79168

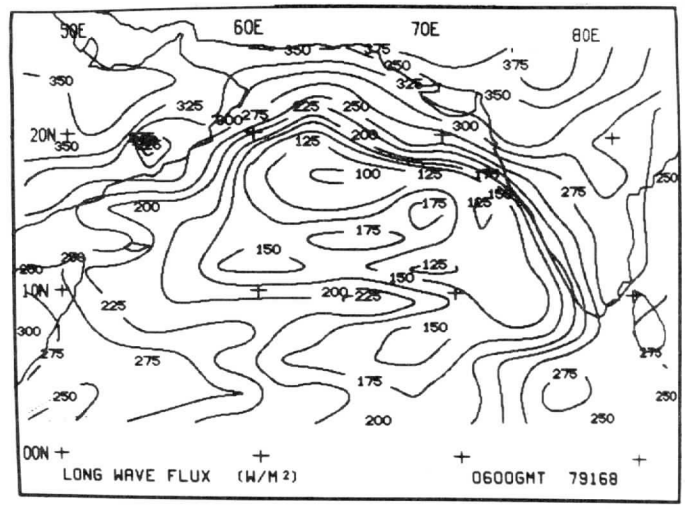
50E
60E
70E
80E
20N
10N
00N
LONG WAVE FLUX (W/M2)
0600GMT 79168

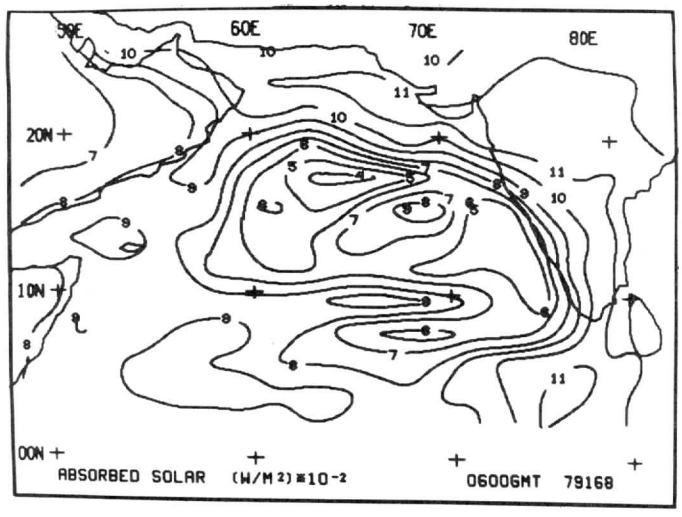
50E
60E
70E
80E
20N
10N
00N
ABSORBED SOLAR (W/M2)*10-2
0600GMT 79168

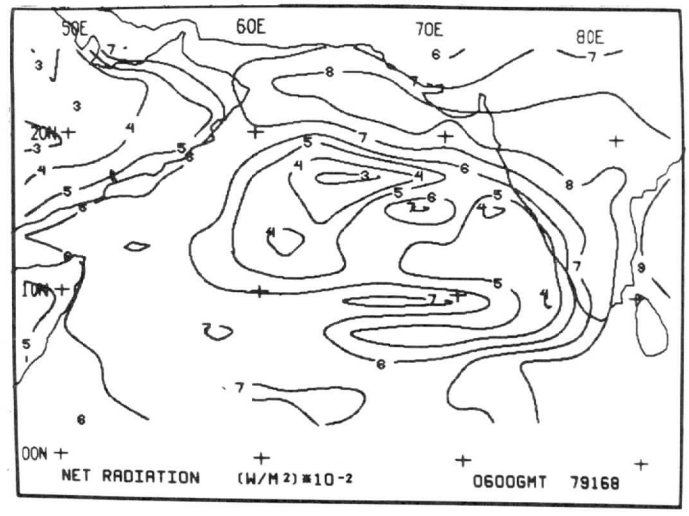
50E
60E
70E
80E
20N
10N
00N
NET RADIATION (W/M2)*10-2
0600GMT 79168

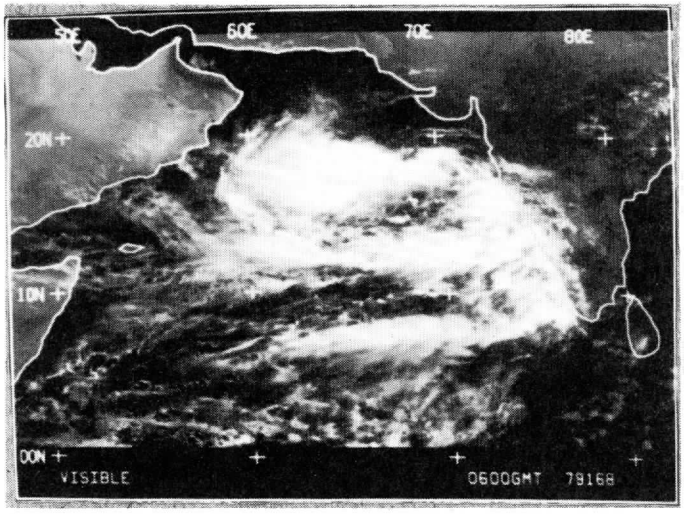
50E
60E
70E
80E
20N
10N
00N
VISIBLE
0600GMT 79168

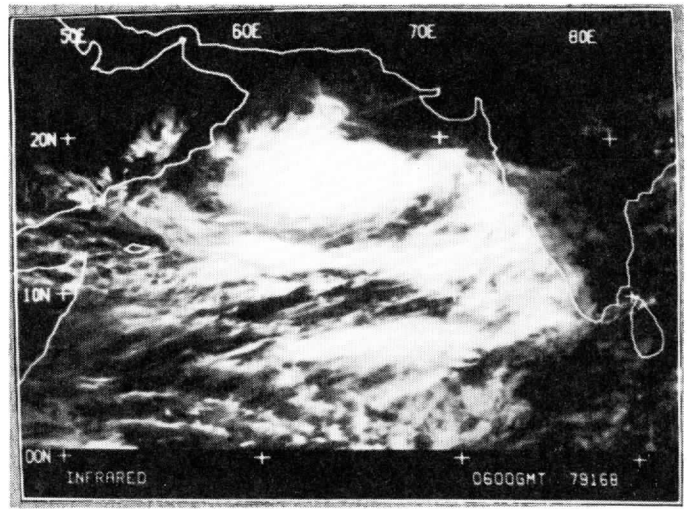
50E
60E
70E
80E
20N
10N
00N
INFRARED
0600GMT 79168

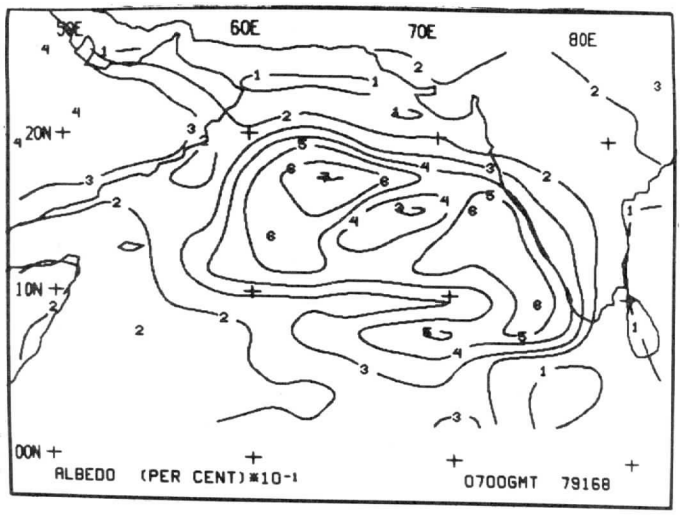
50E
60E
70E
80E
20N
10N
0ON
ALBEDO (PER CENT)*10-1
0700GMT 79168

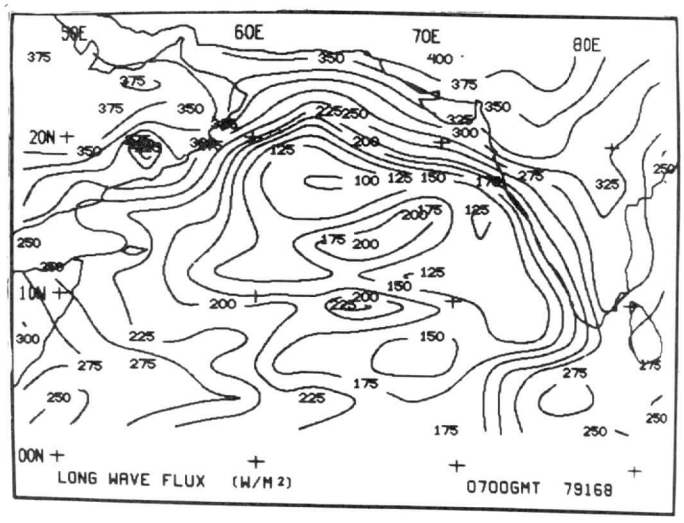
50E
60E
70E
80E
20N
10N
0ON
LONG WAVE FLUX (W/M2)
0700GMT 79168

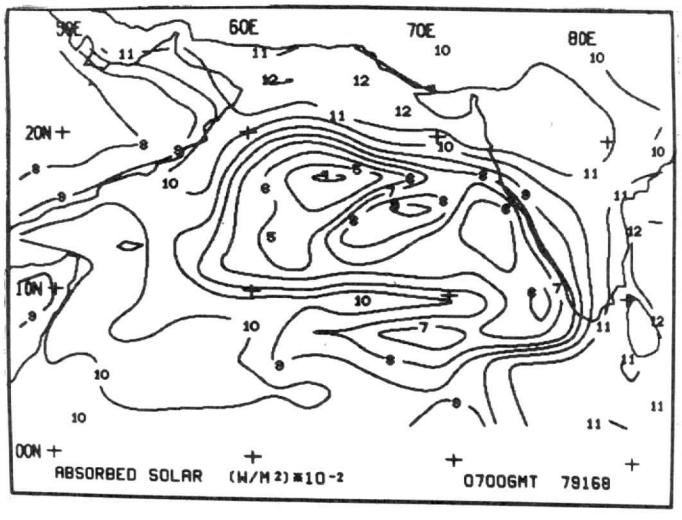
50E
60E
70E
80E
20N
10N
0ON
ABSORBED SOLAR (W/M2)*10-2
0700GMT 79168

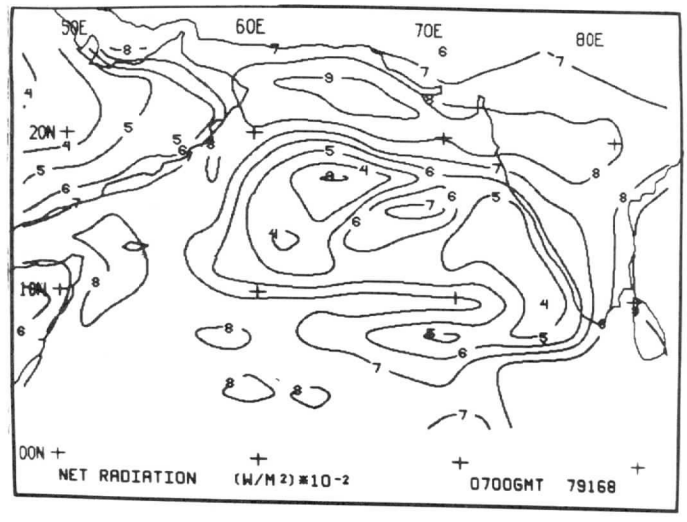
50E
60E
70E
80E
20N
10N
0ON
NET RADIATION (W/M2)*10-2
0700GMT 79168

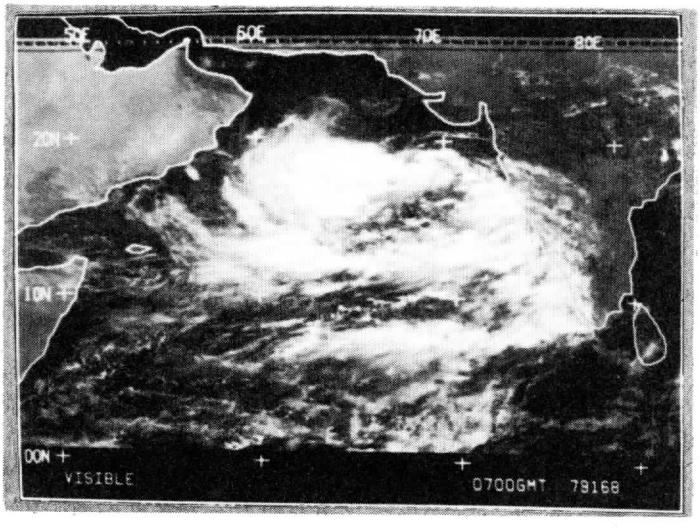
50E
60E
70E
80E
20N
10N
0ON
VISIBLE
0700GMT 79168

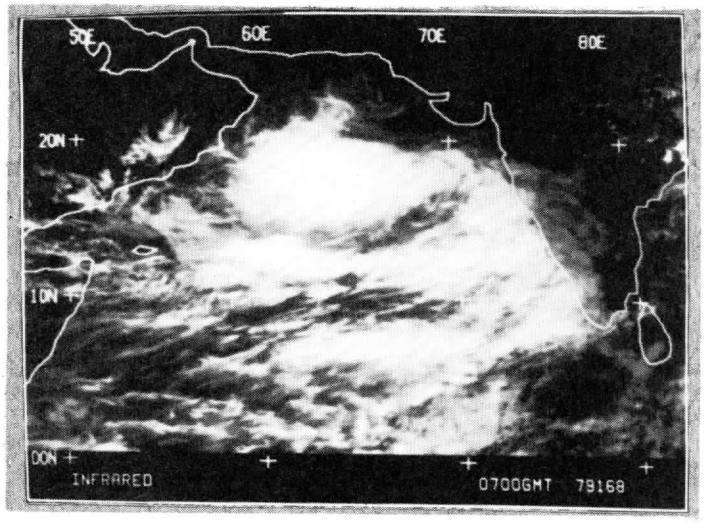
50E
60E
70E
80E
20N
10N
0ON
INFRARED
0700GMT 79168

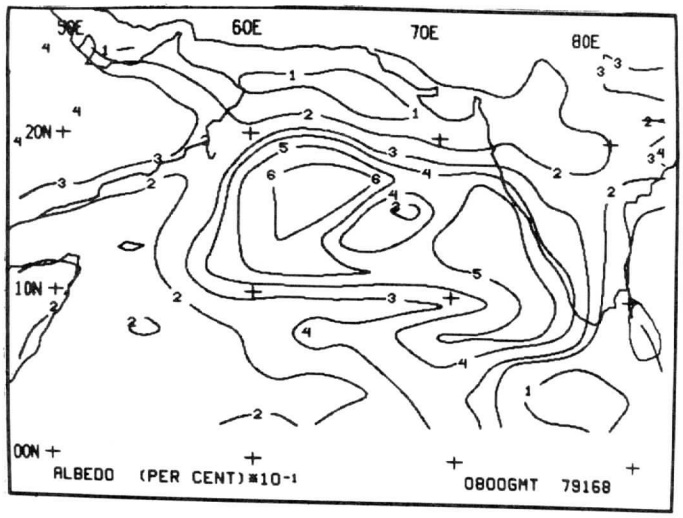
50E
60E
70E
80E
20N
10N
0ON
ALBEDO (PER CENT)*10-1
0800GMT 79168

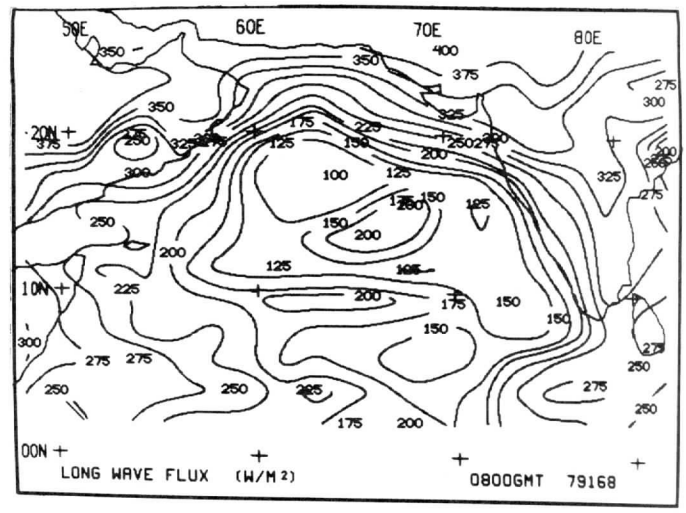
50E
60E
70E
80E
20N
10N
0ON
LONG WAVE FLUX (W/M2)
0800GMT 79168

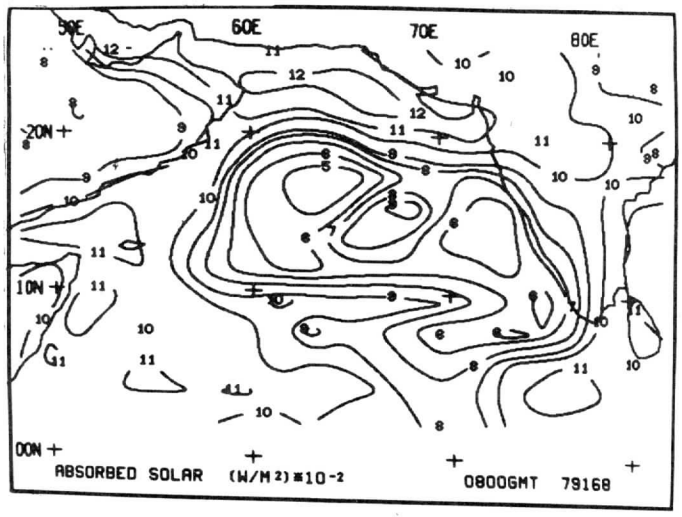
50E
60E
70E
80E
20N
10N
0ON
ABSORBED SOLAR (W/M2)*10-2
0800GMT 79168

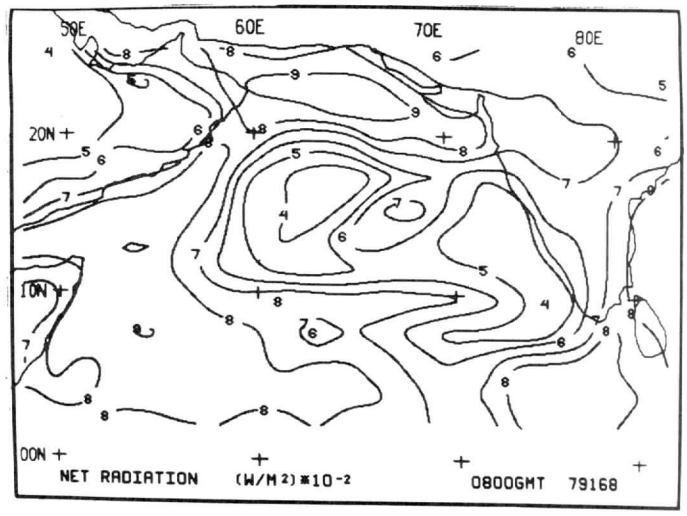
50E
60E
70E
80E
20N
10N
0ON
NET RADIATION (W/M2)*10-2
0800GMT 79168

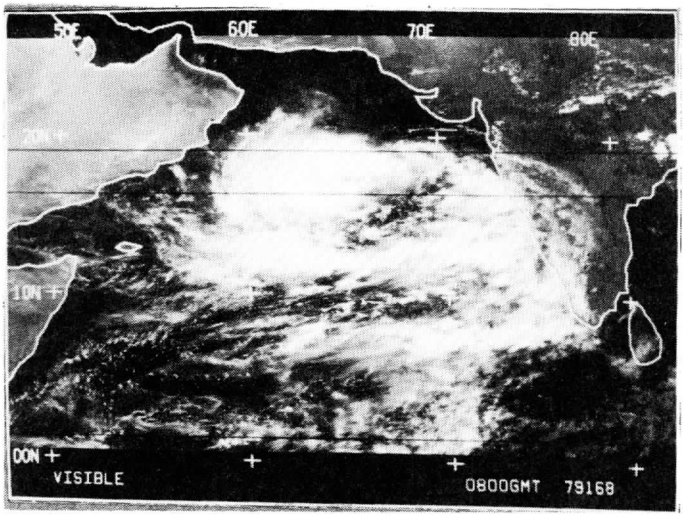
50E
60E
70E
80E
20N
10N
0ON
VISIBLE
0800GMT 79168

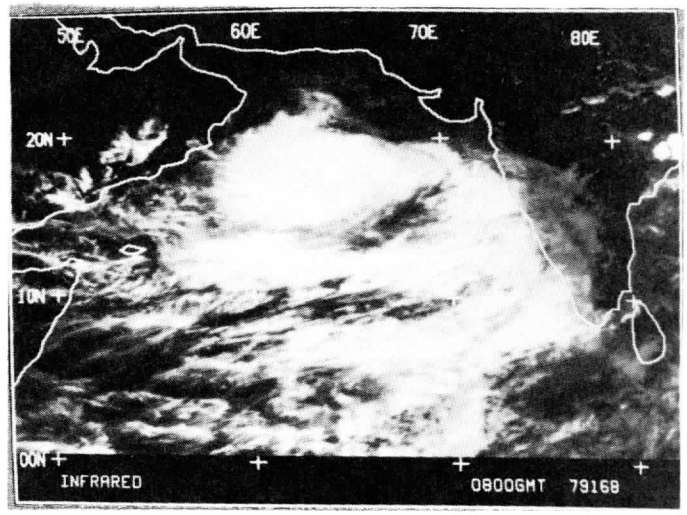
50E
60E
70E
80E
20N
10N
0ON
INFRARED
0800GMT 79168

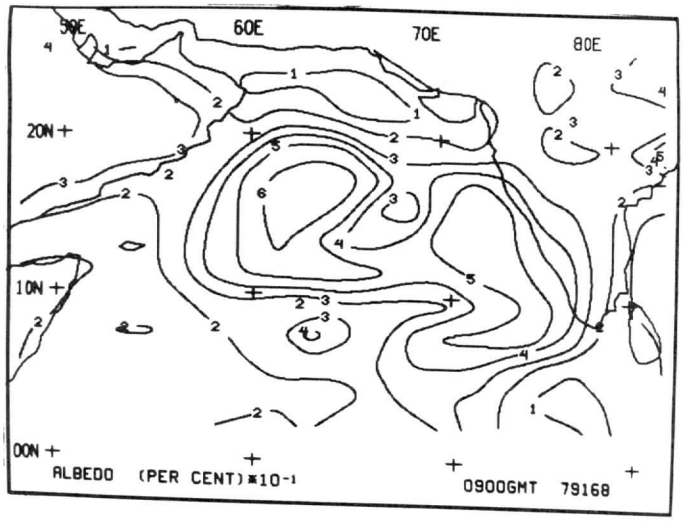
50E
60E
70E
80E
20N
10N
0ON
ALBEDO (PER CENT)×10-1
0900GMT 79168

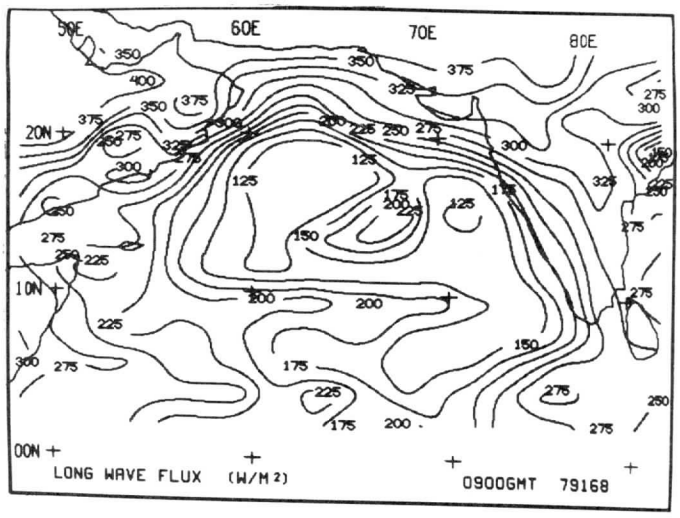
50E
60E
70E
80E
20N
10N
0ON
LONG WAVE FLUX (W/M2)
0900GMT 79168

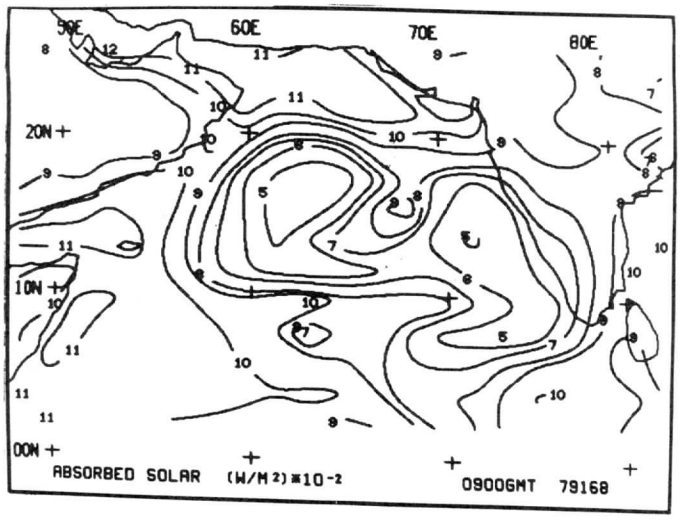
50E
60E
70E
80E
20N
10N
0ON
ABSORBED SOLAR (W/M2)×10-2
0900GMT 79168

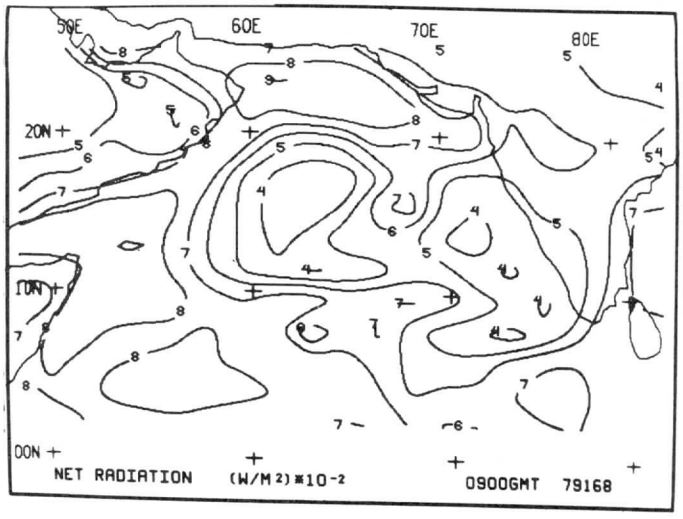
50E
60E
70E
80E
20N
10N
0ON
NET RADIATION (W/M2)×10-2
0900GMT 79168

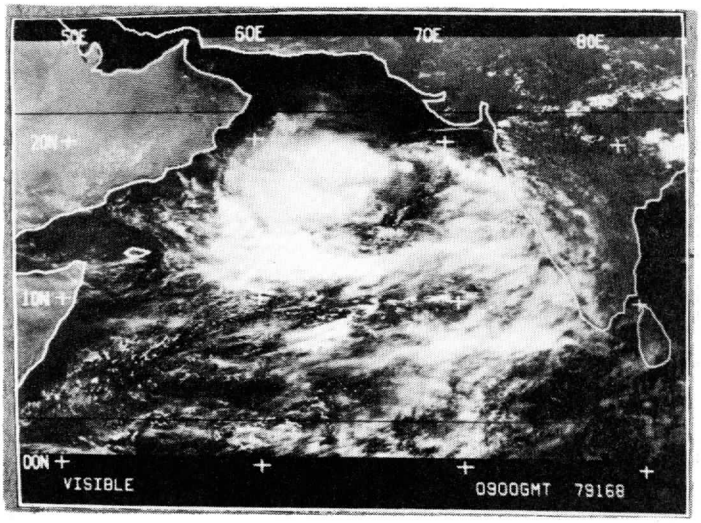
50E
60E
70E
80E
20N
10N
0ON
VISIBLE
0900GMT 79168

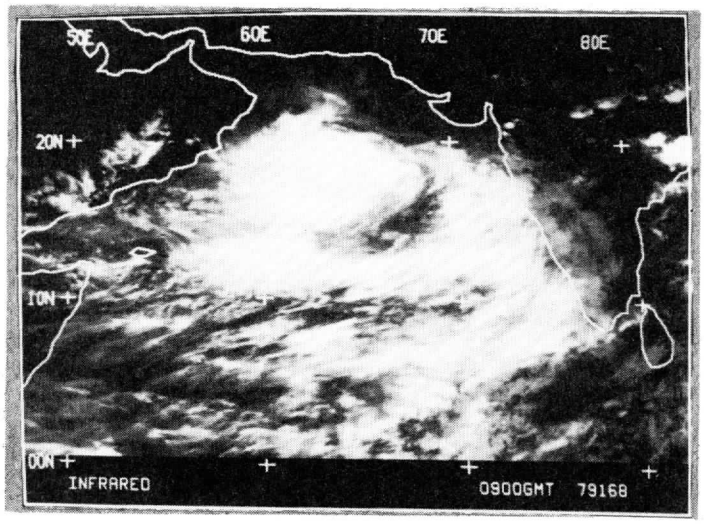
50E
60E
70E
80E
20N
10N
0ON
INFRARED
0900GMT 79168

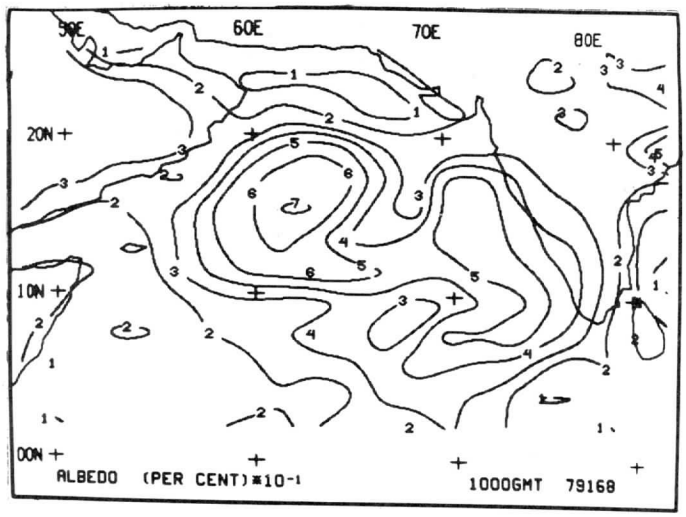
50E
60E
70E
80E
20N
10N
0ON
ALBEDO (PER CENT)*10-1
1000GMT 79168

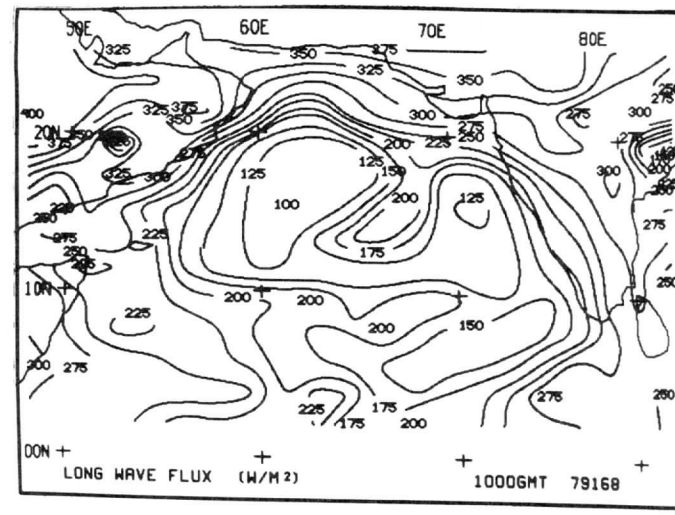
50E
60E
70E
80E
20N
10N
0ON
LONG WAVE FLUX (W/M2)
1000GMT 79168

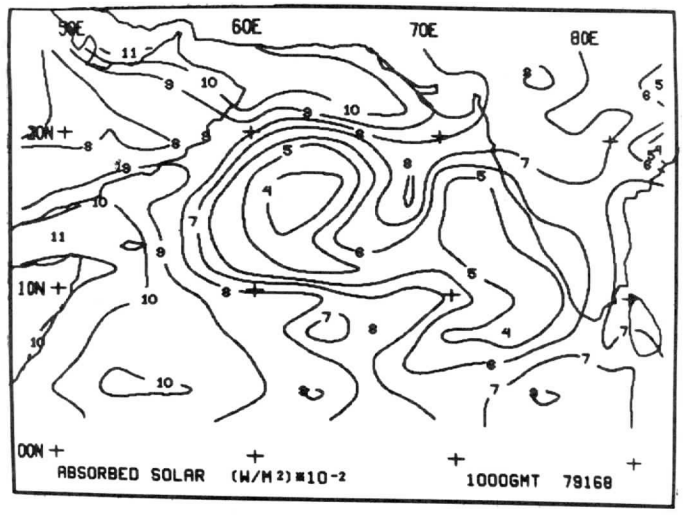
50E
60E
70E
80E
20N
10N
0ON
ABSORBED SOLAR (W/M2)*10-2
1000GMT 79168

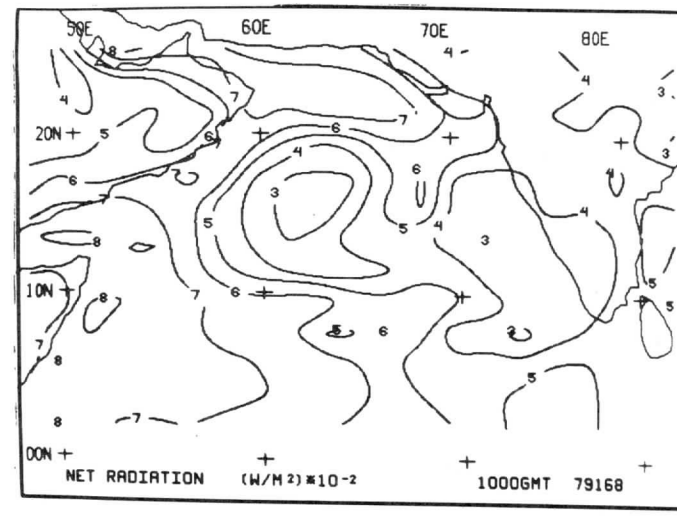
50E
60E
70E
80E
20N
10N
0ON
NET RADIATION (W/M2)*10-2
1000GMT 79168

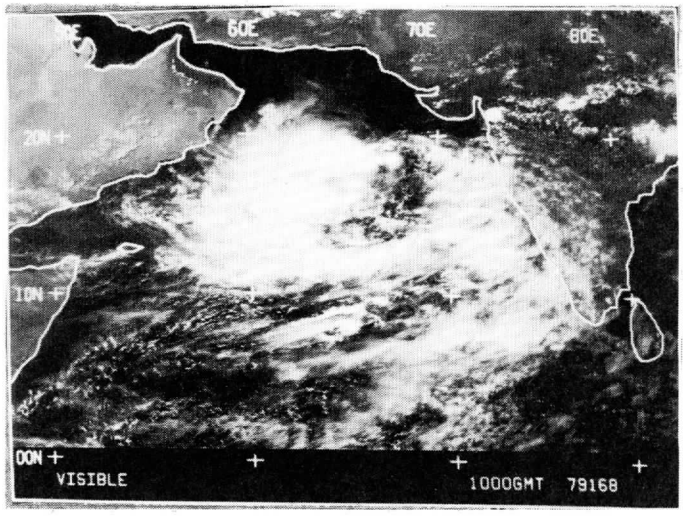
60E
70E
80E
20N
10N
0ON
VISIBLE
1000GMT 79168

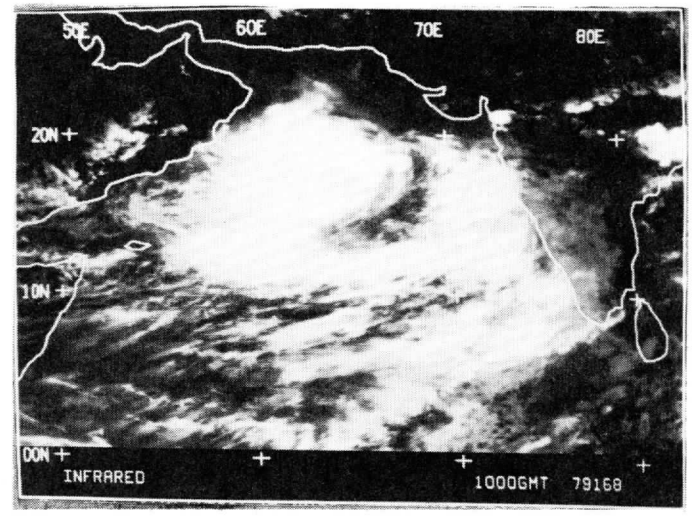
50E
60E
70E
80E
20N
10N
0ON
INFRARED
1000GMT 79168

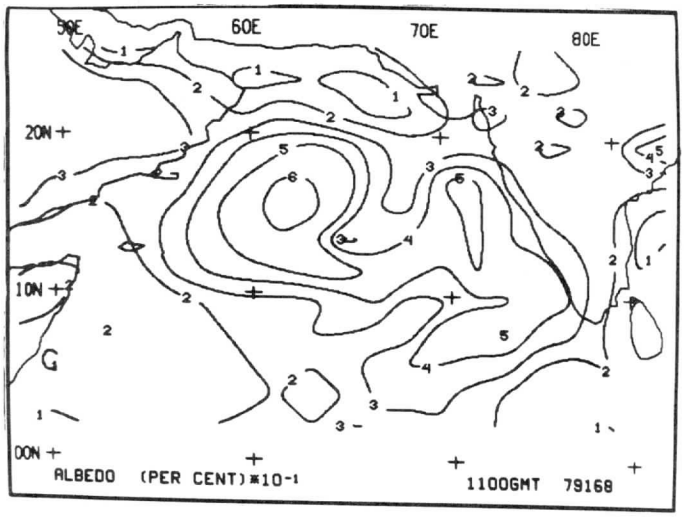
50E
60E
70E
80E
20N
10N
0ON
ALBEDO (PER CENT)*10-1
1100GMT 79168

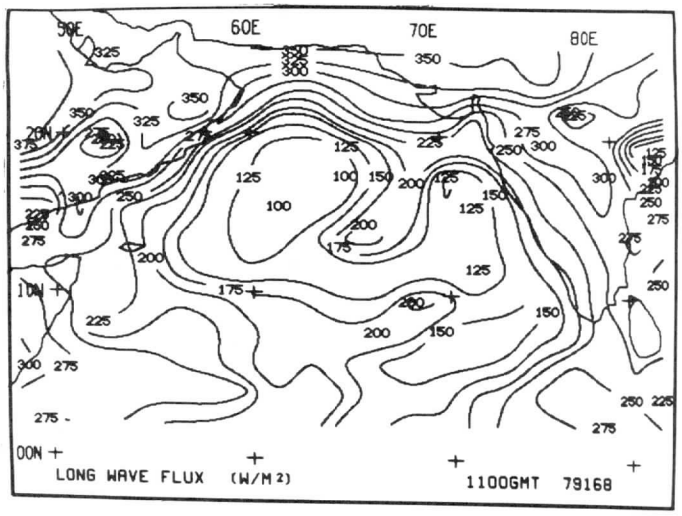
50E
60E
70E
80E
20N
10N
0ON
LONG WAVE FLUX (W/M2)
1100GMT 79168

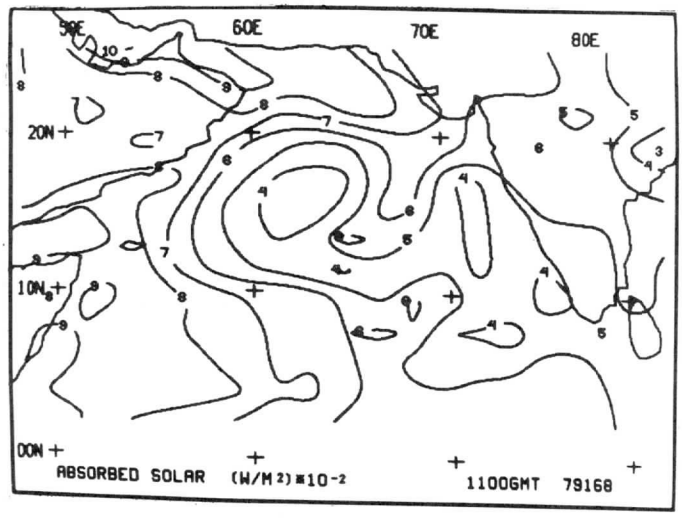
50E
60E
70E
80E
20N
10N
0ON
ABSORBED SOLAR (W/M2)*10-2
1100GMT 79168

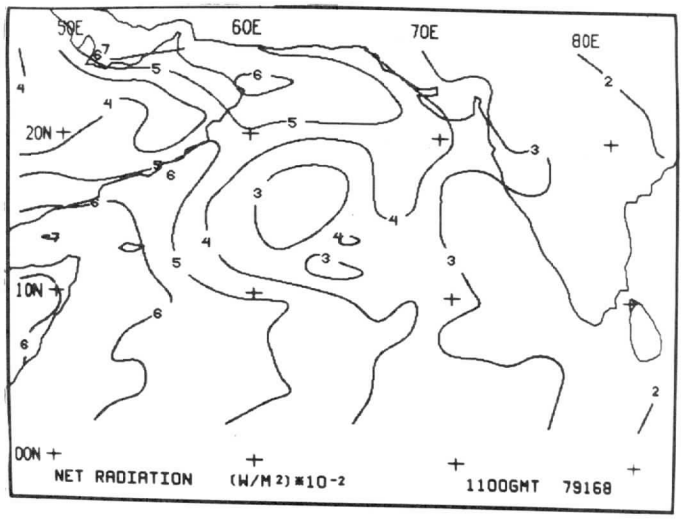
50E
60E
70E
80E
20N
10N
0ON
NET RADIATION (W/M2)*10-2
1100GMT 79168

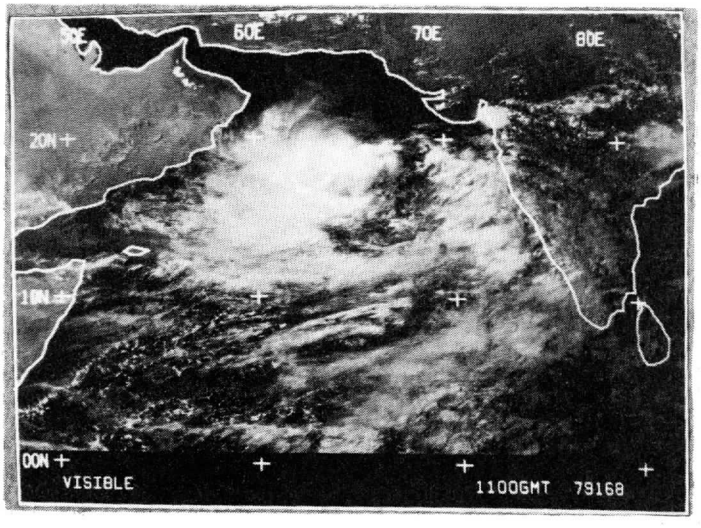
50E
60E
70E
80E
20N
10N
0ON
VISIBLE
1100GMT 79168

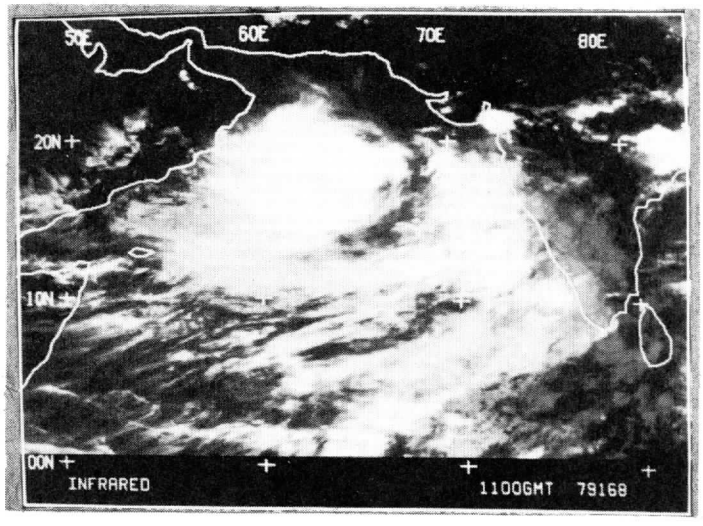
50E
60E
70E
80E
20N
10N
0ON
INFRARED
1100GMT 79168

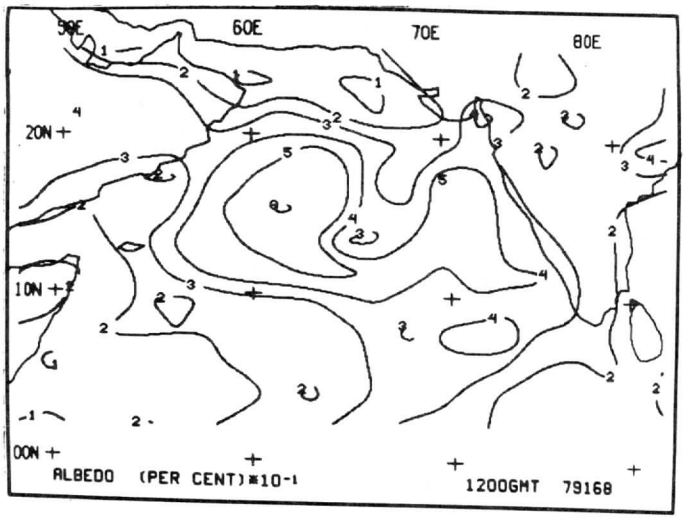
50E
60E
70E
80E
20N
10N
0ON
ALBEDO (PER CENT)*10-1
1200GMT 79168

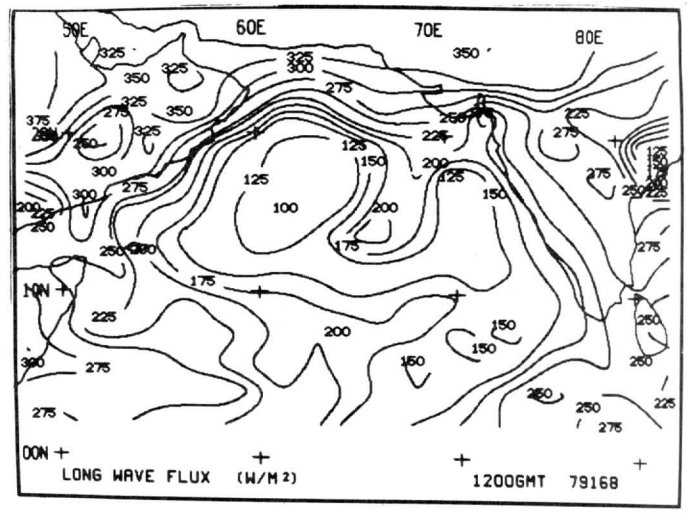
50E
60E
70E
80E
10N
0ON
LONG WAVE FLUX (W/M2)
1200GMT 79168

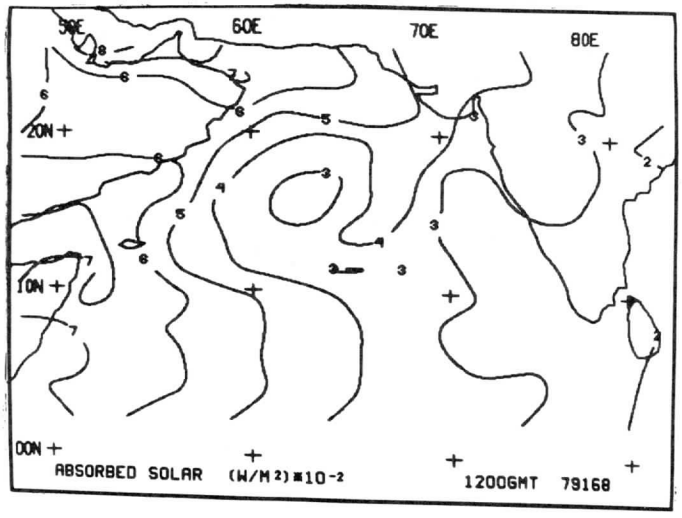
50E
60E
70E
80E
20N
10N
0ON
ABSORBED SOLAR (W/M2)*10-2
1200GMT 79168

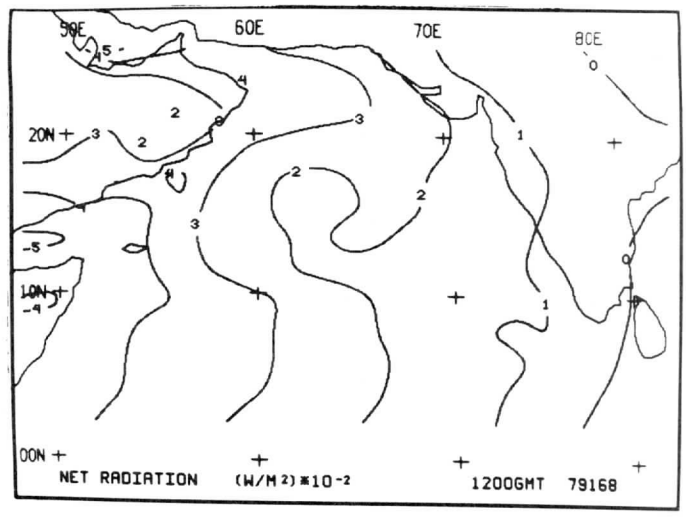
50E
60E
70E
80E
20N
10N
0ON
NET RADIATION (W/M2)*10-2
1200GMT 79168

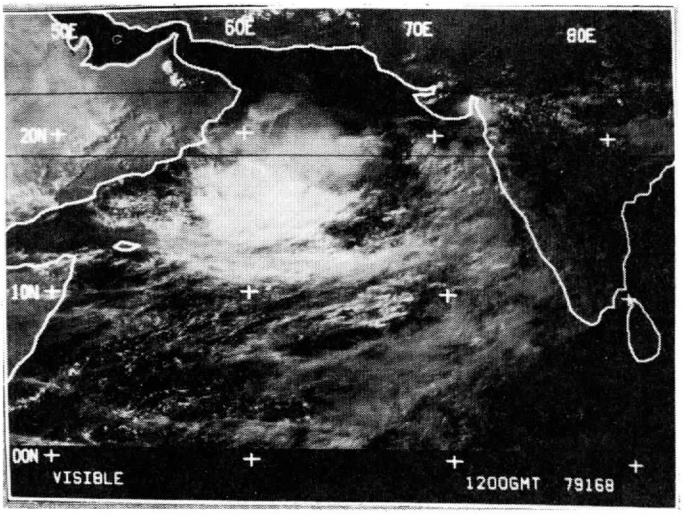
50E
60E
70E
80E
20N
10N
0ON
VISIBLE
1200GMT 79168

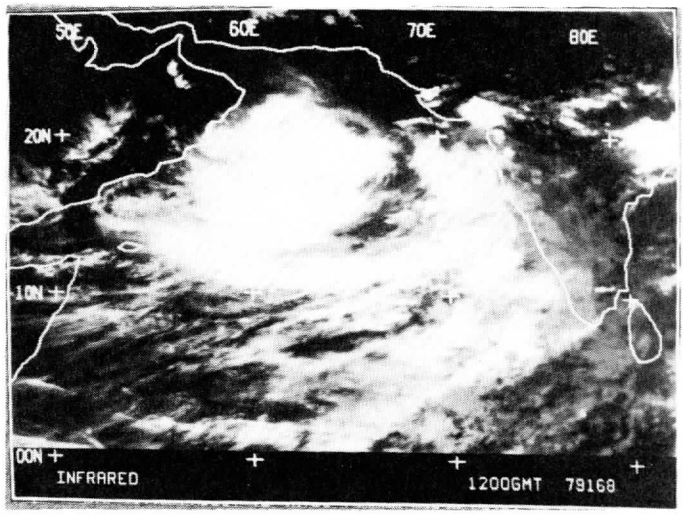
50E
60E
70E
80E
20N
10N
0ON
INFRARED
1200GMT 79168

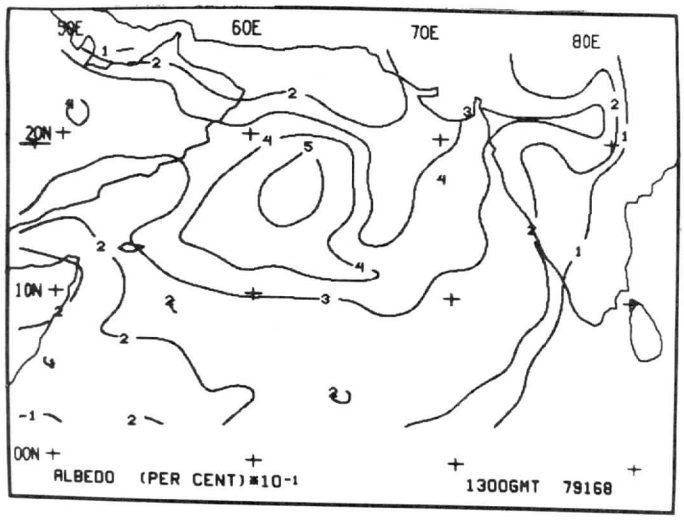
50E
60E
70E
80E
20N
10N
0ON
ALBEDO (PER CENT)*10-1
1300GMT 79168

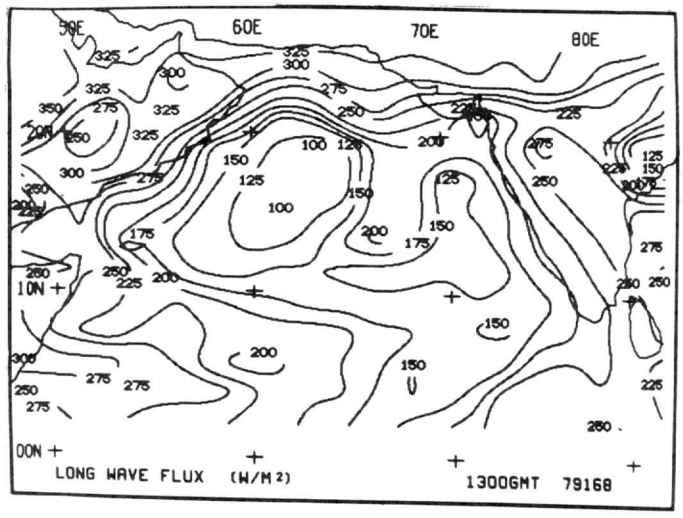
50E
60E
70E
80E
20N
10N
0ON
LONG WAVE FLUX (W/M2)
1300GMT 79168

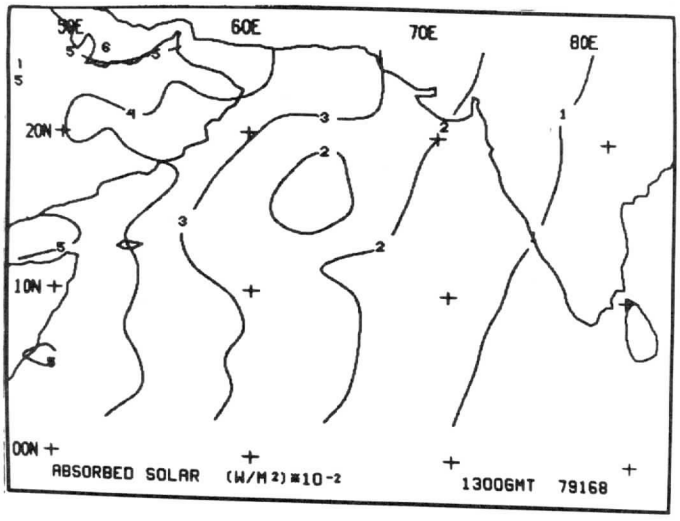
50E
60E
70E
80E
20N
10N
0ON
ABSORBED SOLAR (W/M2)*10-2
1300GMT 79168

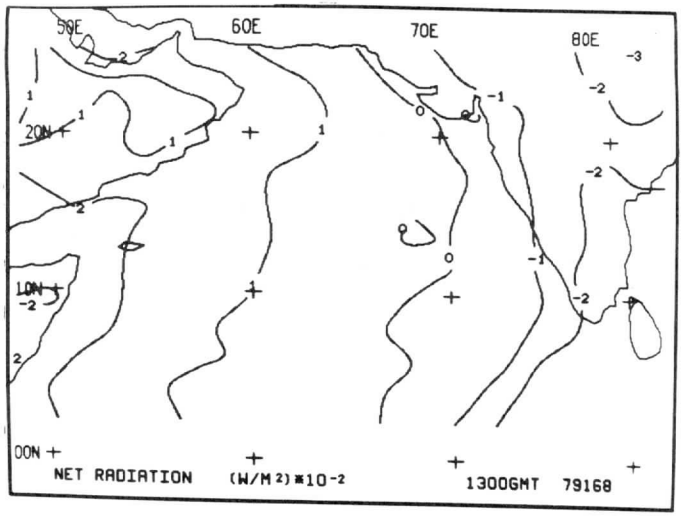
50E
60E
70E
80E
20N
10N
0ON
NET RADIATION (W/M2)*10-2
1300GMT 79168

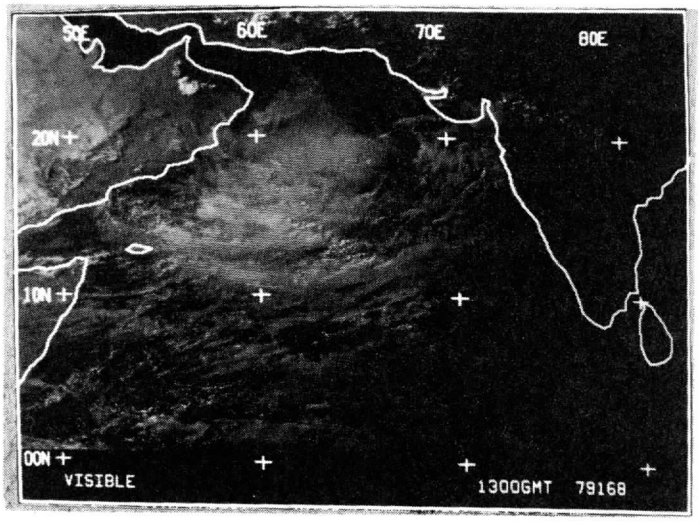
50E
60E
70E
80E
20N
10N
0ON
VISIBLE
1300GMT 79168

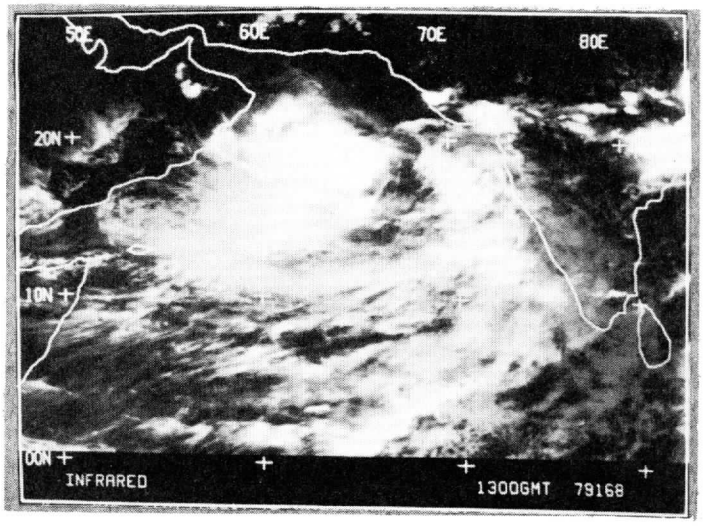
50E
60E
70E
80E
20N
10N
0ON
INFRARED
1300GMT 79168

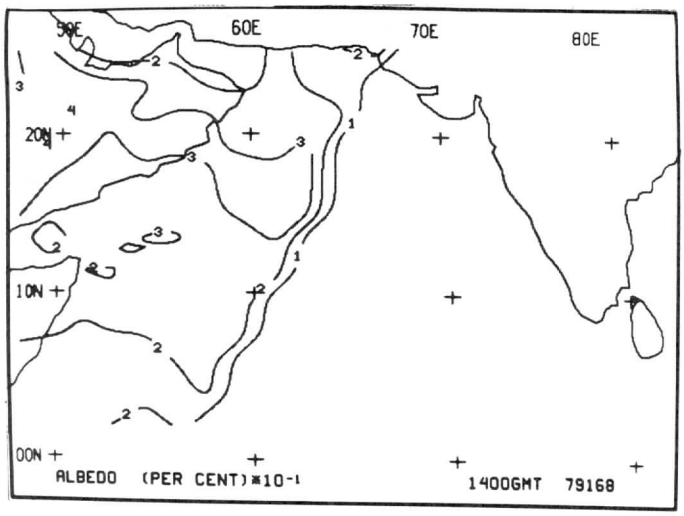
50E
60E
70E
80E
20N
10N
0ON
ALBEDO (PER CENT)*10-1
1400GMT 79168

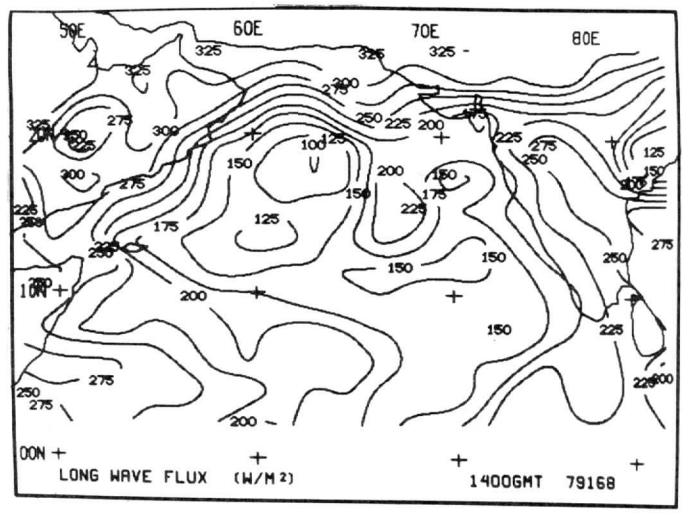
50E
60E
70E
80E
20N
10N
0ON
LONG WAVE FLUX (W/M2)
1400GMT 79168

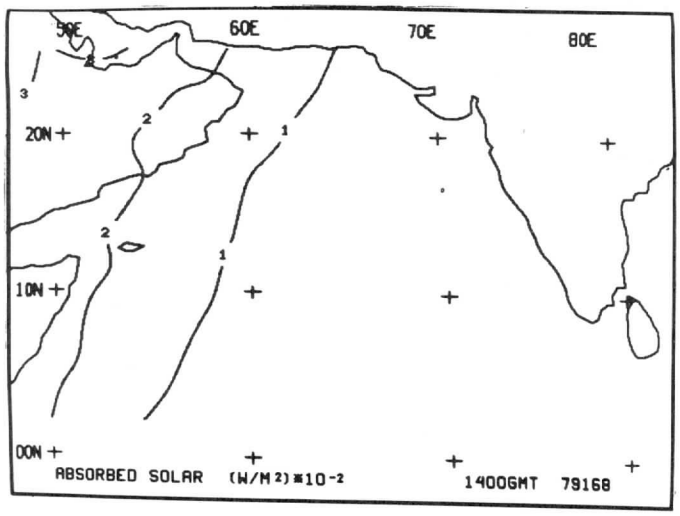
50E
60E
70E
80E
20N
10N
0ON
ABSORBED SOLAR (W/M2)*10-2
1400GMT 79168

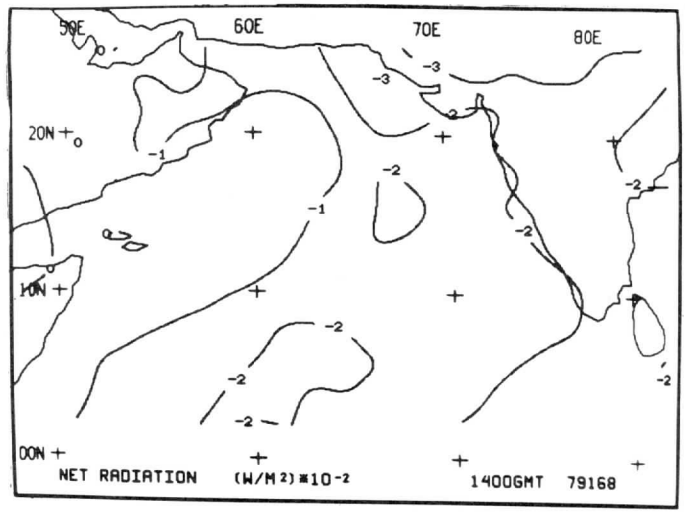
50E
60E
70E
80E
20N
10N
0ON
NET RADIATION (W/M2)*10-2
1400GMT 79168

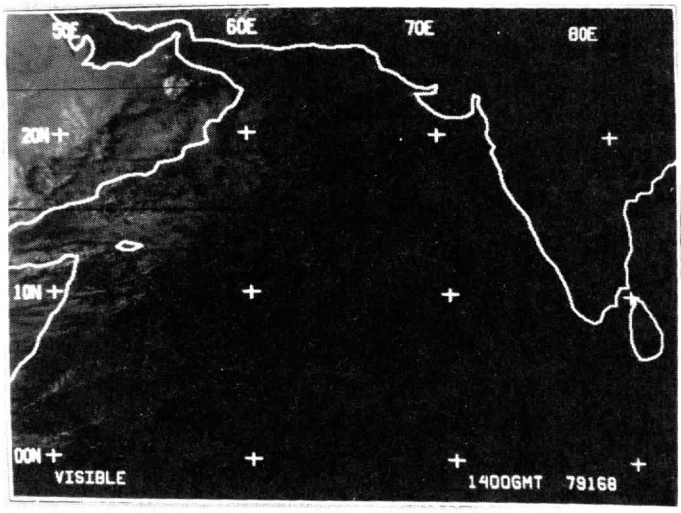
50E
60E
70E
80E
20N
10N
0ON
VISIBLE
1400GMT 79168

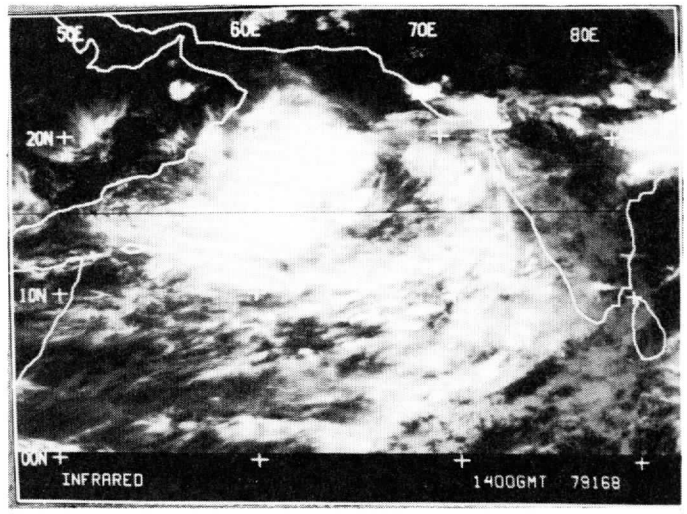
50E
60E
70E
80E
20N
10N
0ON
INFRARED
1400GMT 79168

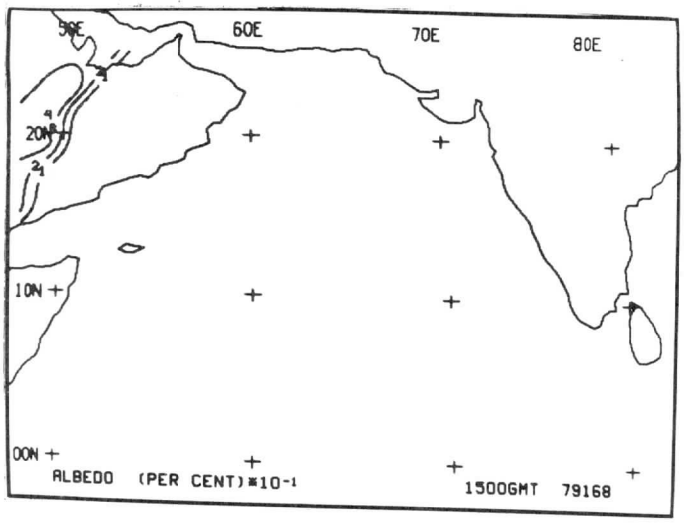
50E
60E
70E
80E
20N
10N
0ON
ALBEDO (PER CENT)*10-1
1500GMT 79168

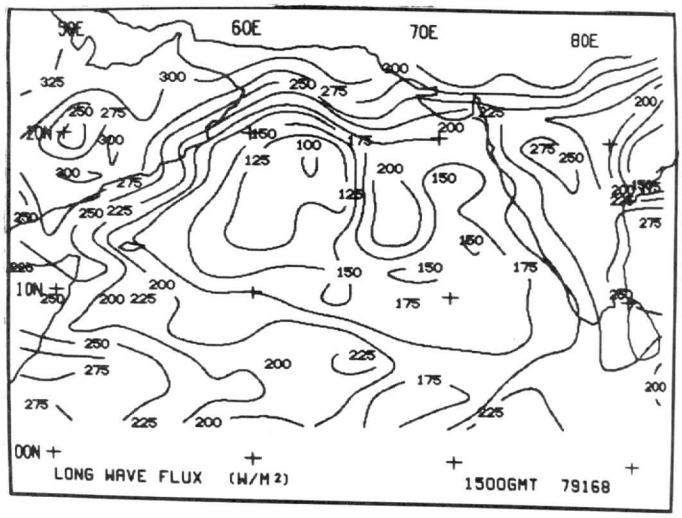
50E
60E
70E
80E
20N
10N
0ON
LONG WAVE FLUX (W/M2)
1500GMT 79168

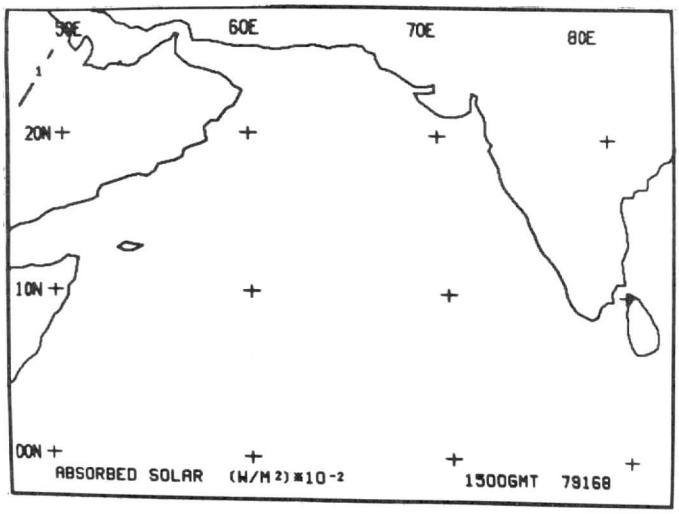
50E
60E
70E
80E
20N
10N
0ON
ABSORBED SOLAR (W/M2)*10-2
1500GMT 79168

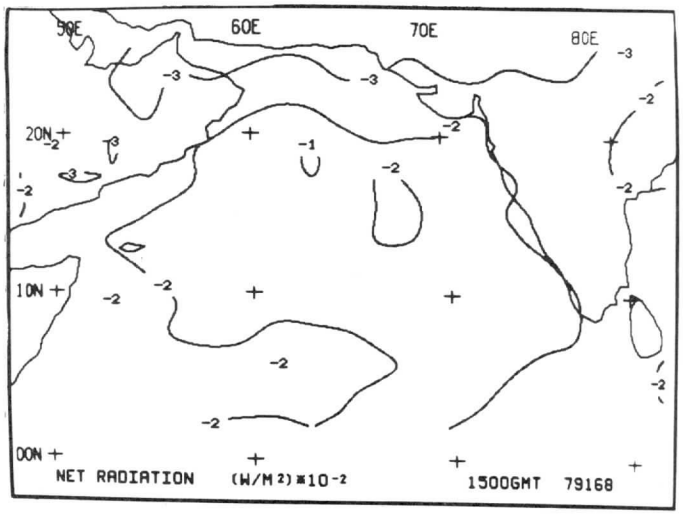
50E
60E
70E
80E
20N
10N
0ON
NET RADIATION (W/M2)*10-2
1500GMT 79168

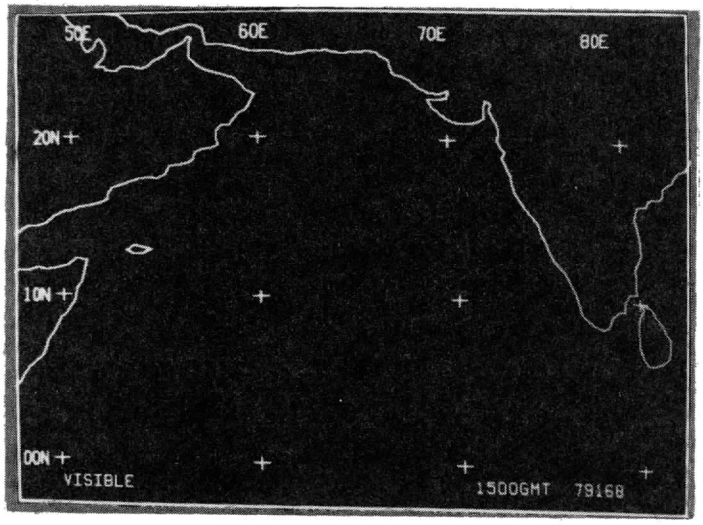
50E
60E
70E
80E
20N
10N
0ON
VISIBLE
1500GMT 79168

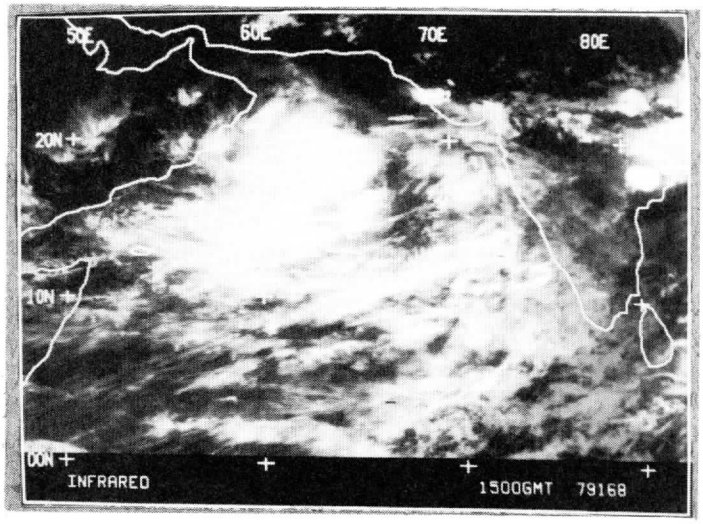
50E
60E
70E
80E
20N
10N
0ON
INFRARED
1500GMT 79168

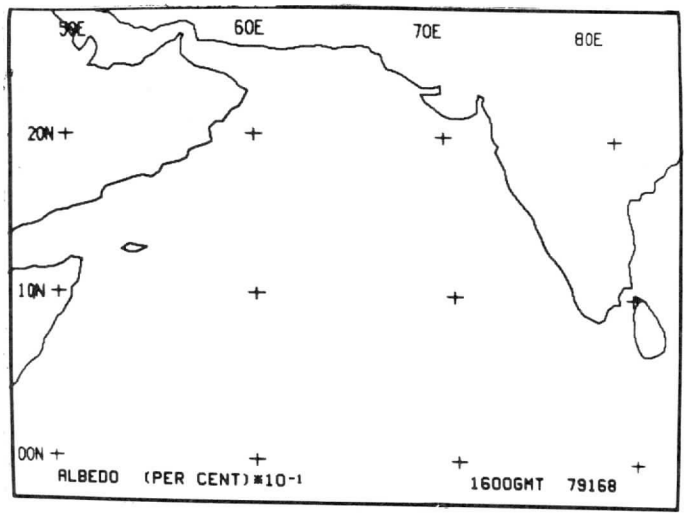
50E
60E
70E
80E
20N
10N
00N
ALBEDO (PER CENT)*10-1
1600GMT 79168

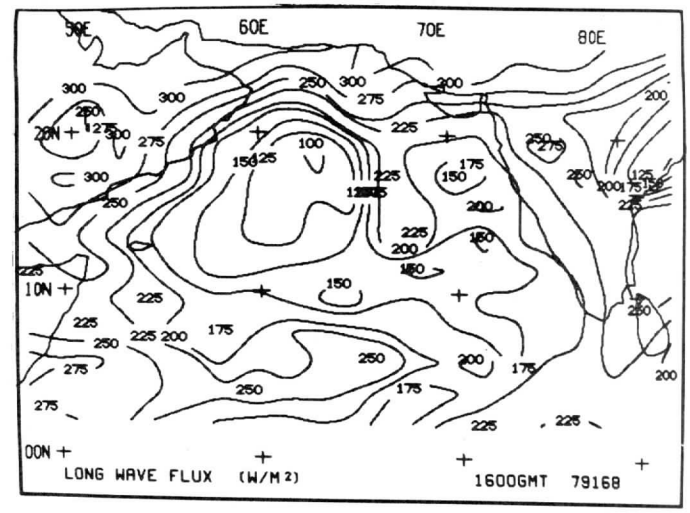
50E
60E
70E
80E
20N
10N
00N
LONG WAVE FLUX (W/M2)
1600GMT 79168

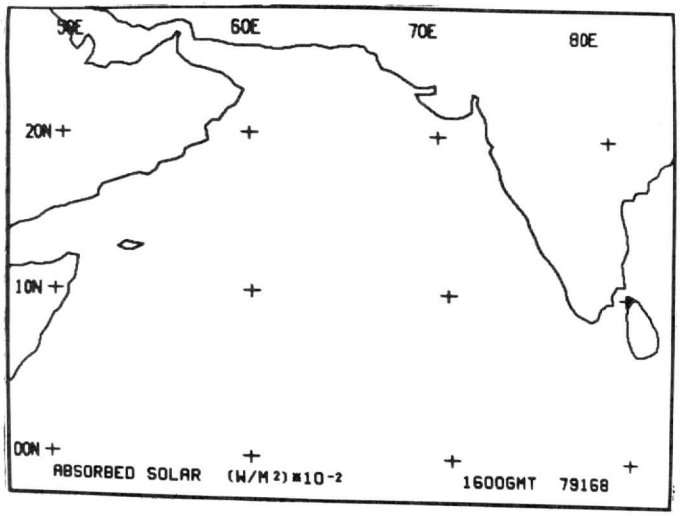
50E
60E
70E
80E
20N
10N
00N
ABSORBED SOLAR (W/M2)*10-2
1600GMT 79168

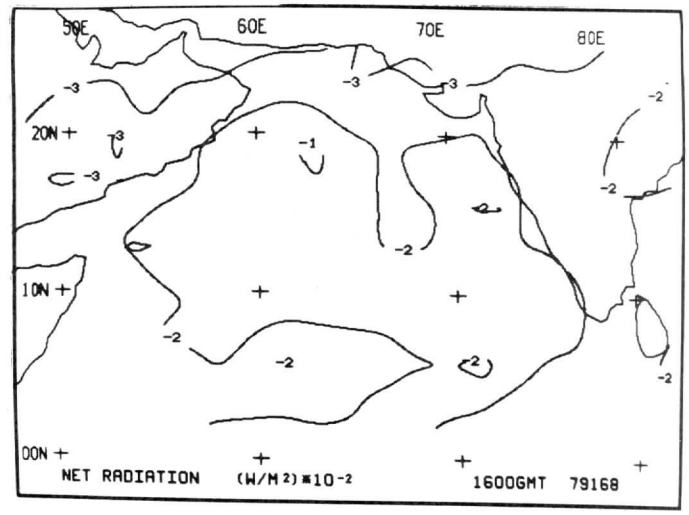
50E
60E
70E
80E
20N
10N
00N
NET RADIATION (W/M2)*10-2
1600GMT 79168

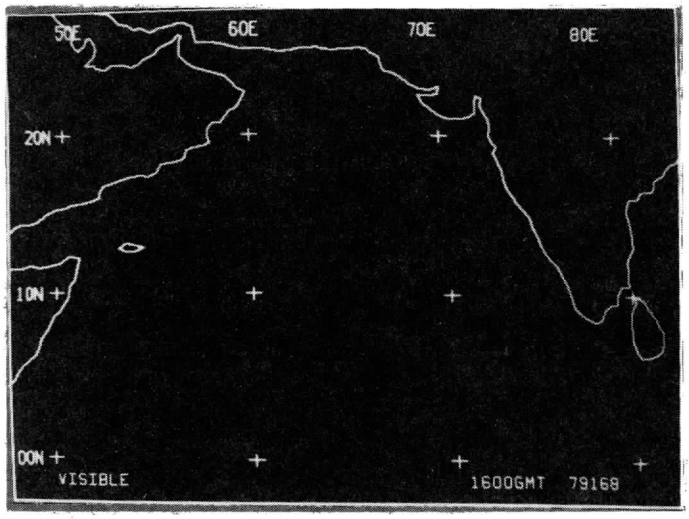
50E
60E
70E
80E
20N
10N
00N
VISIBLE
1600GMT 79168

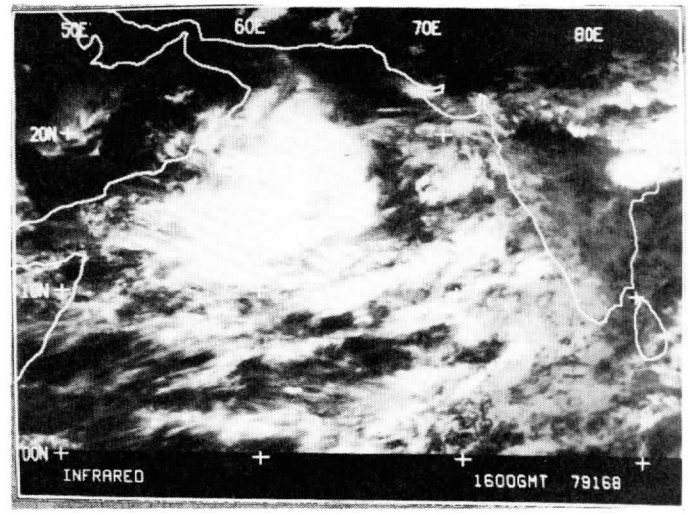
50E
60E
70E
80E
20N
10N
00N
INFRARED
1600GMT 79168

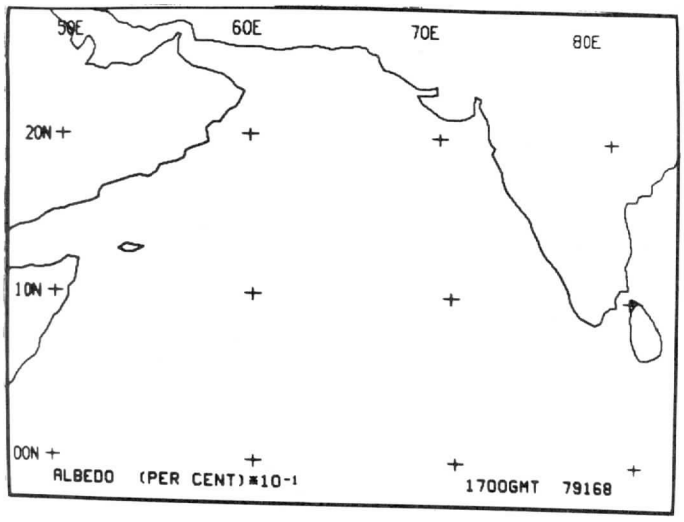
50E
60E
70E
80E
20N
10N
0ON
ALBEDO (PER CENT)*10-1
1700GMT 79168

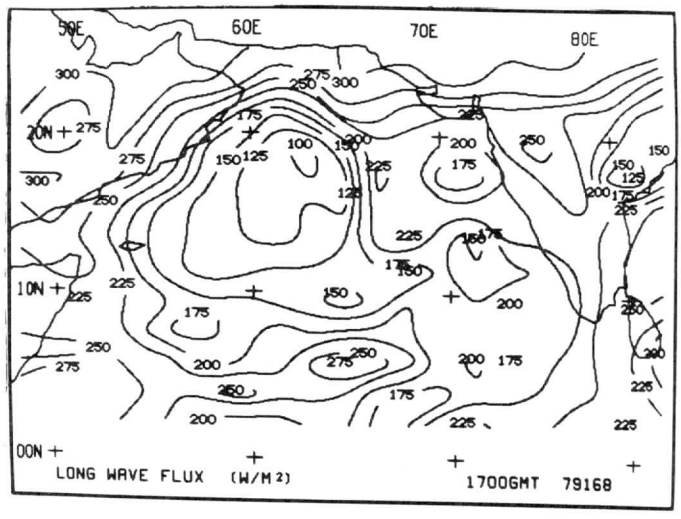
50E
60E
70E
80E
20N
10N
0ON
LONG WAVE FLUX (W/M2)
1700GMT 79168

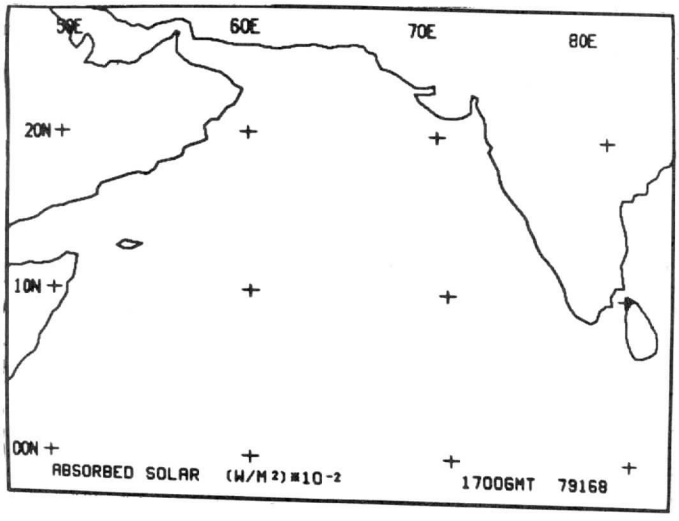
50E
60E
70E
80E
20N
10N
0ON
ABSORBED SOLAR (W/M2)*10-2
1700GMT 79168

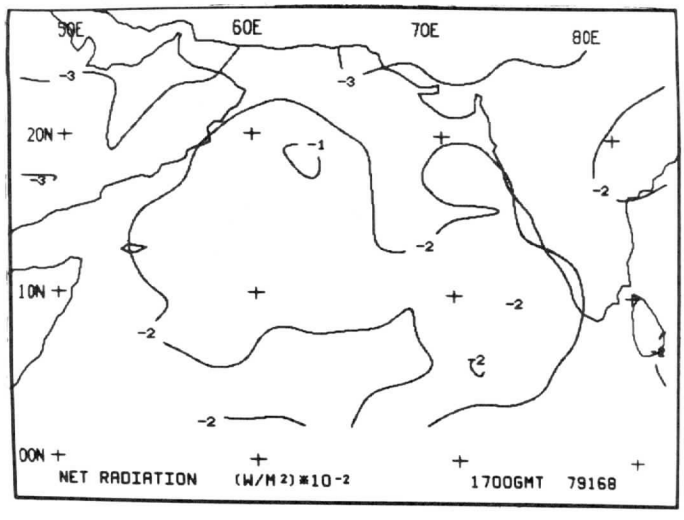
50E
60E
70E
80E
20N
10N
0ON
NET RADIATION (W/M2)*10-2
1700GMT 79168

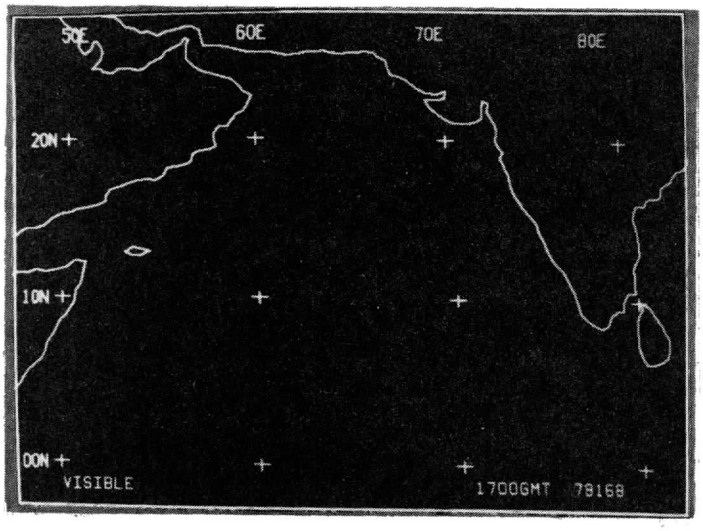
50E
60E
70E
80E
20N
10N
0ON
VISIBLE
1700GMT 79168

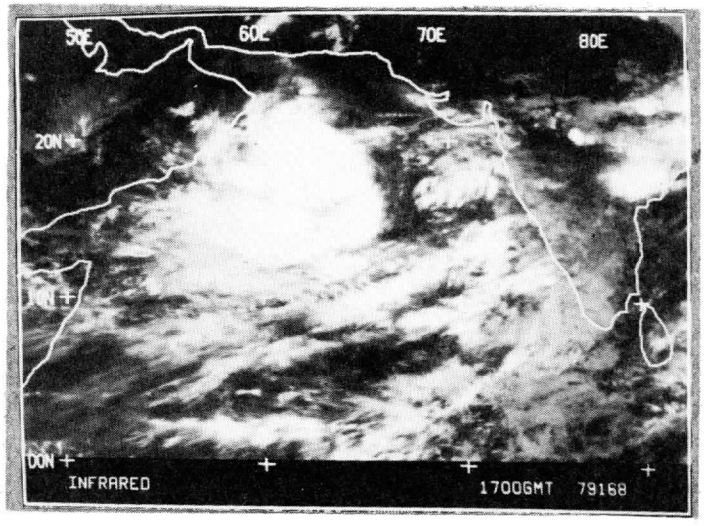
50E
60E
70E
80E
20N
10N
0ON
INFRARED
1700GMT 79168

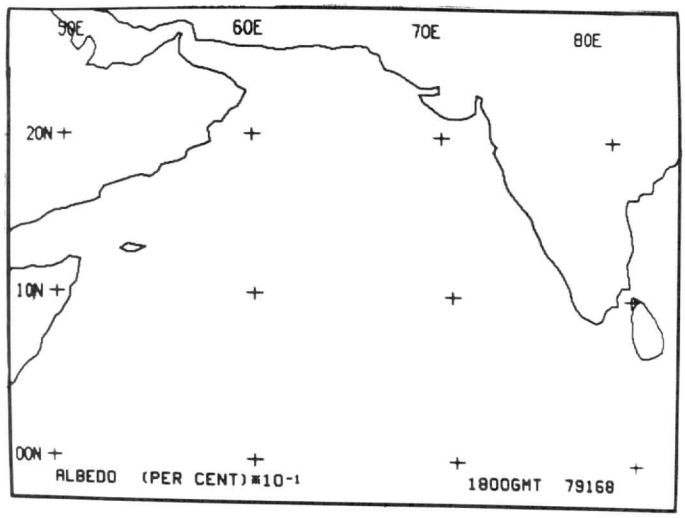
50E
60E
70E
80E
20N
10N
00N
ALBEDO (PER CENT)*10-1
1800GMT 79168

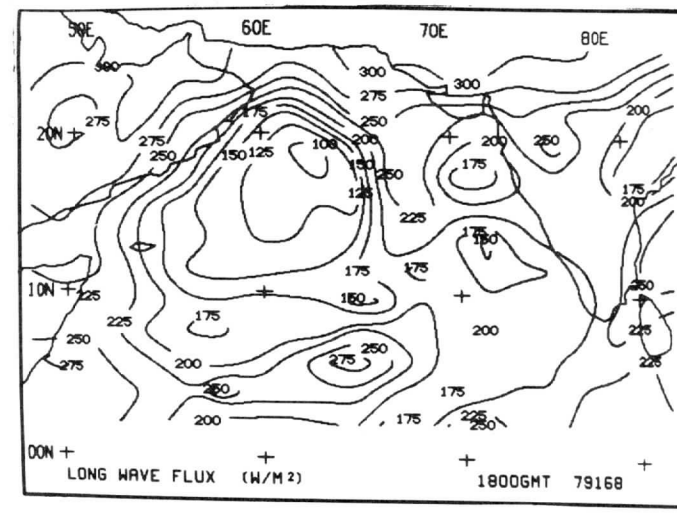
50E
60E
70E
80E
20N
10N
00N
LONG WAVE FLUX (W/M2)
1800GMT 79168

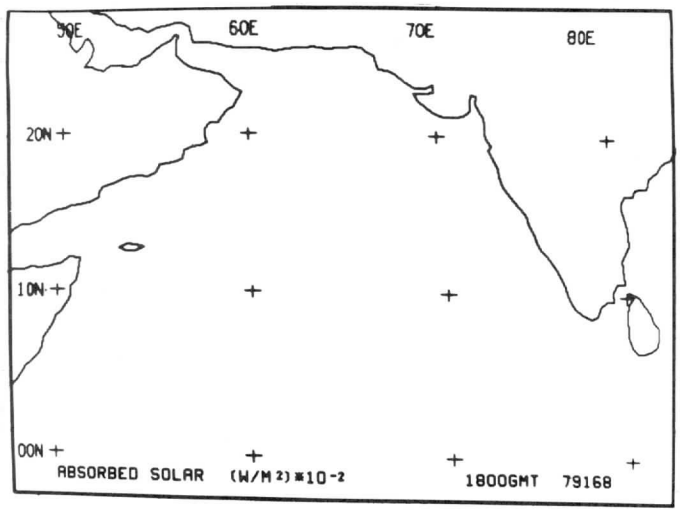
50E
60E
70E
80E
20N
10N
00N
ABSORBED SOLAR (W/M2)*10-2
1800GMT 79168

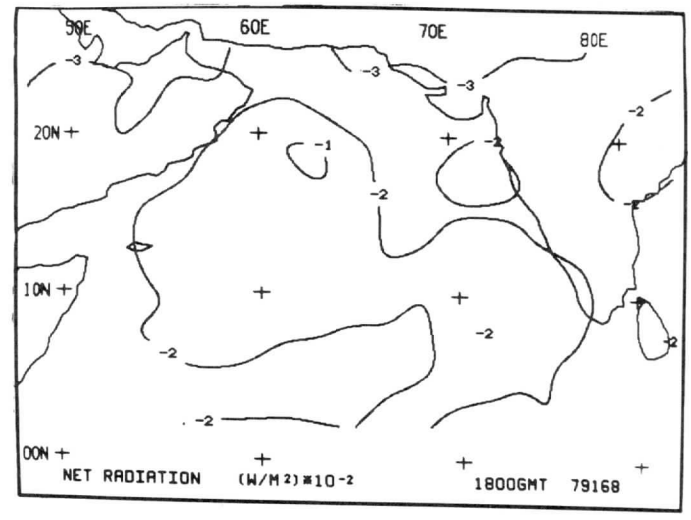
50E
60E
70E
80E
20N
10N
00N
NET RADIATION (W/M2)*10-2
1800GMT 79168

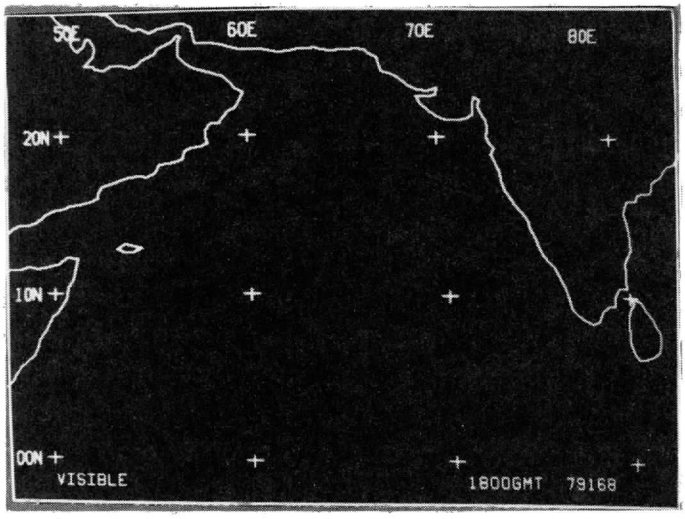
50E
60E
70E
80E
20N
10N
00N
VISIBLE
1800GMT 79168

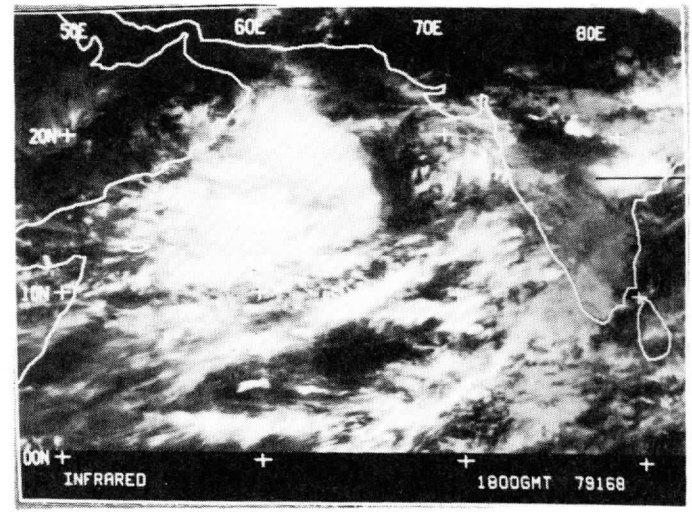
50E
60E
70E
80E
20N
10N
00N
INFRARED
1800GMT 79168

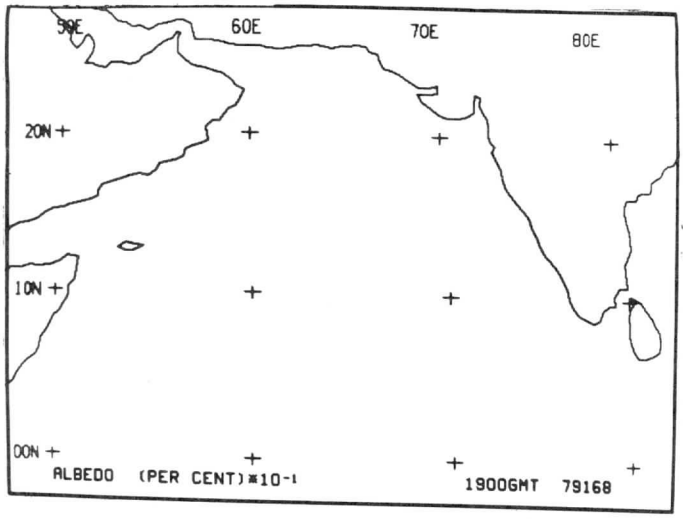
50E
60E
70E
80E
20N
10N
00N
ALBEDO (PER CENT)*10-1
1900GMT 79168

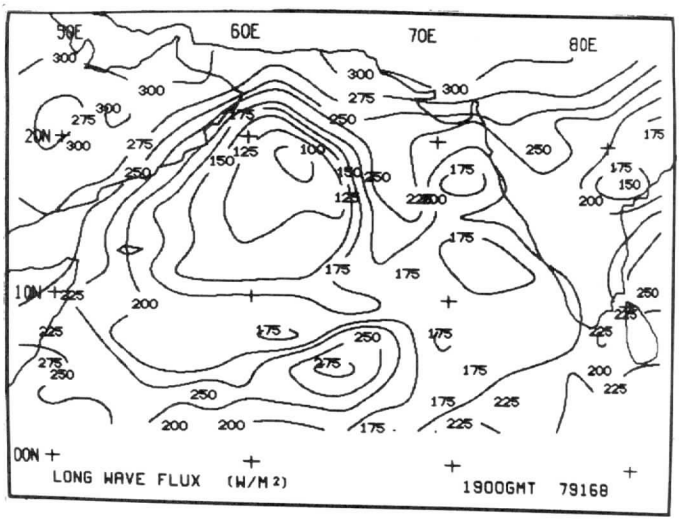
50E
60E
70E
80E
20N
10N
00N
LONG WAVE FLUX (W/M2)
1900GMT 79168

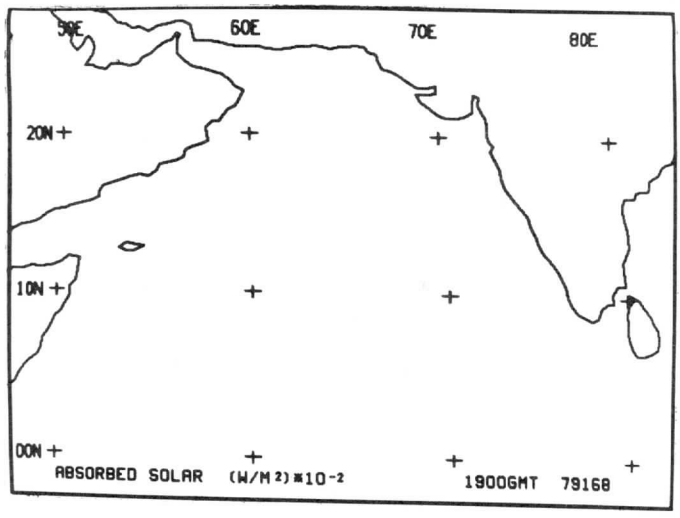
50E
60E
70E
80E
20N
10N
00N
ABSORBED SOLAR (W/M2)*10-2
1900GMT 79168

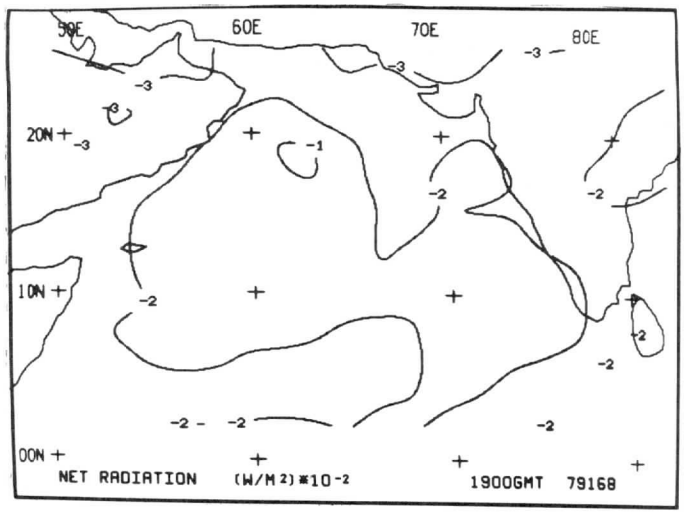
50E
60E
70E
80E
20N
10N
00N
NET RADIATION (W/M2)*10-2
1900GMT 79168

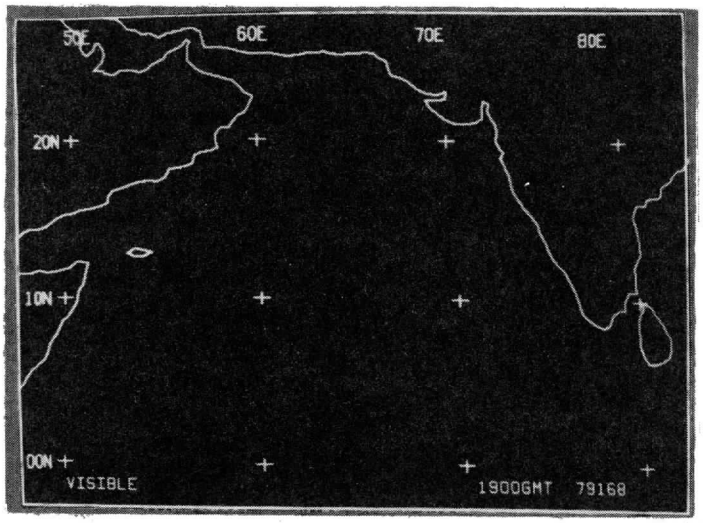
50E
60E
70E
80E
20N
10N
00N
VISIBLE
1900GMT 79168

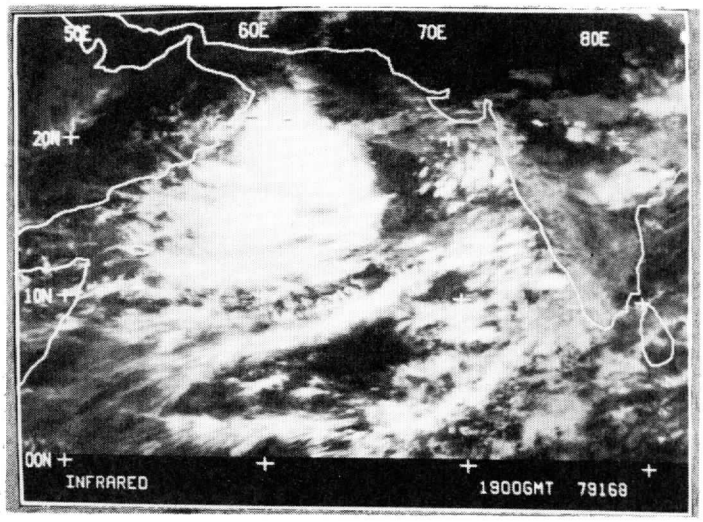
50E
60E
70E
80E
20N
10N
00N
INFRARED
1900GMT 79168

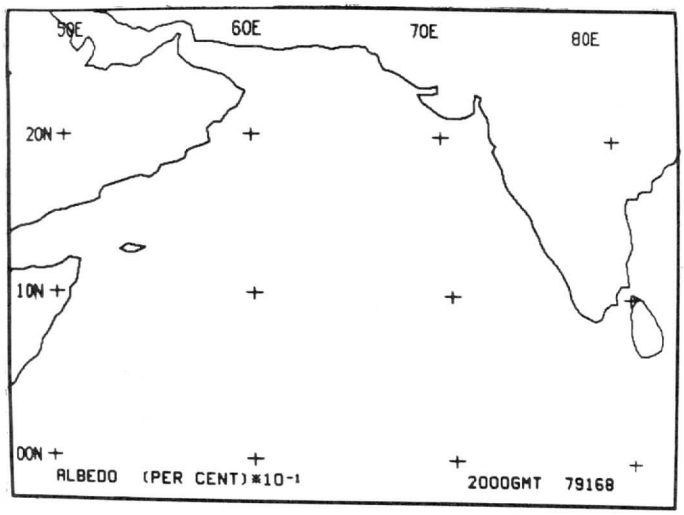
50E
60E
70E
80E
20N
10N
00N
ALBEDO (PER CENT)*10-1
2000GMT 79168

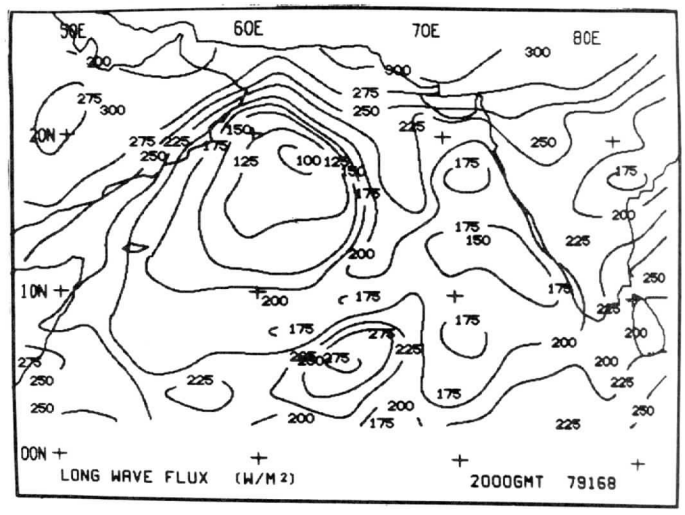
50E
60E
70E
80E
20N
10N
00N
LONG WAVE FLUX (W/M2)
2000GMT 79168

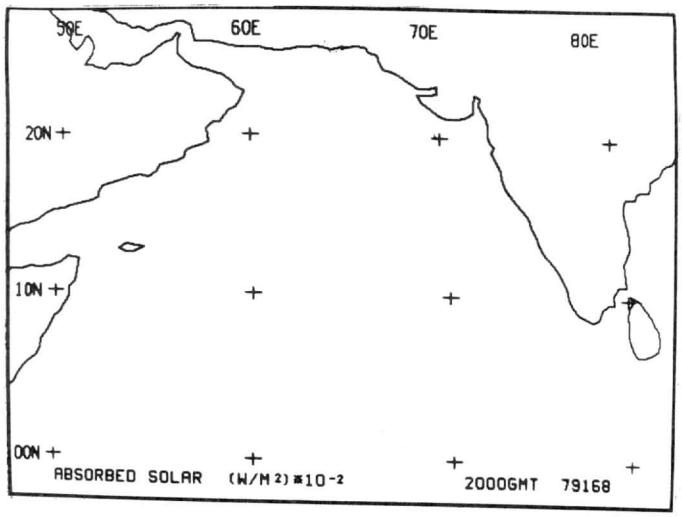
50E
60E
70E
80E
20N
10N
00N
ABSORBED SOLAR (W/M2)*10-2
2000GMT 79168

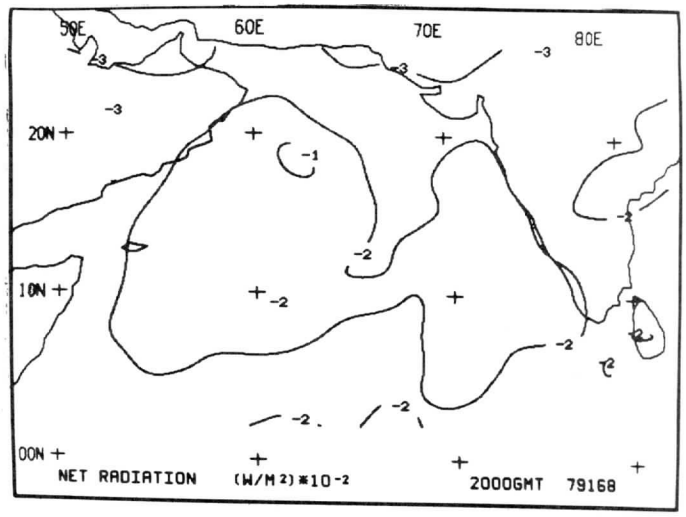
50E
60E
70E
80E
20N
10N
00N
NET RADIATION (W/M2)*10-2
2000GMT 79168

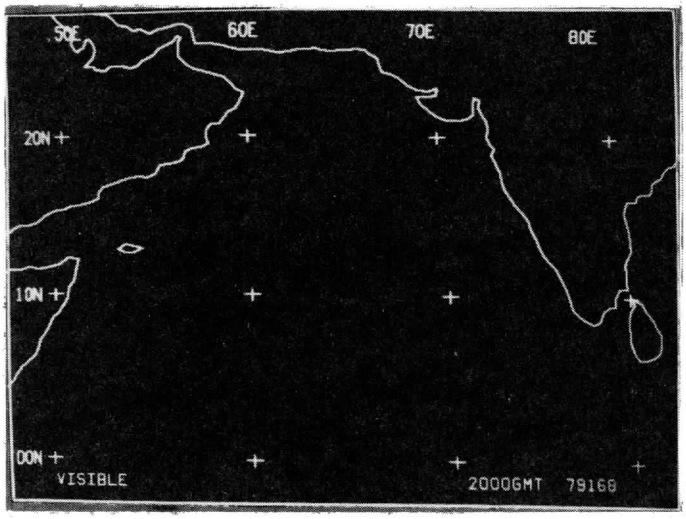
50E
60E
70E
80E
20N
10N
00N
VISIBLE
2000GMT 79168

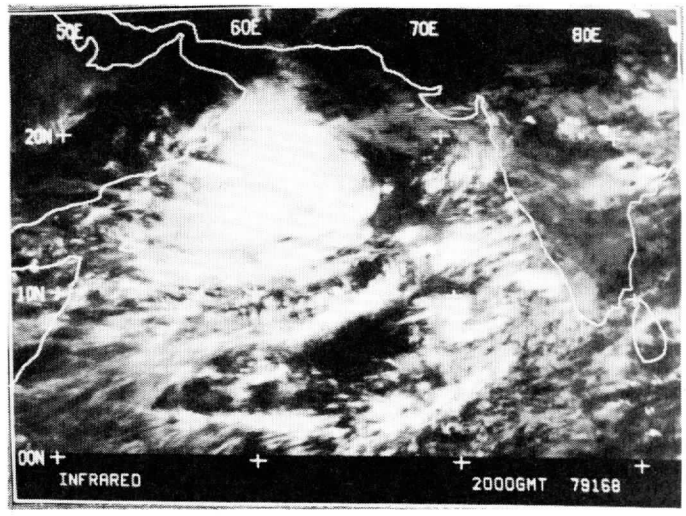
50E
60E
70E
80E
20N
10N
00N
INFRARED
2000GMT 79168

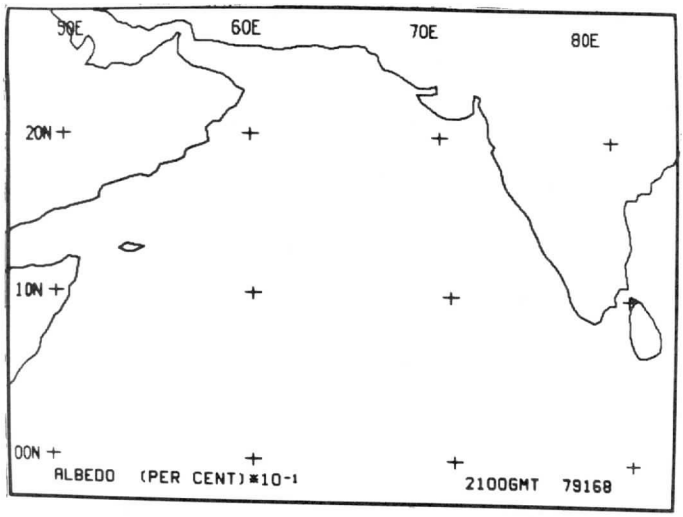
50E
60E
70E
80E
20N
10N
00N
ALBEDO (PER CENT)*10-1
2100GMT 79168

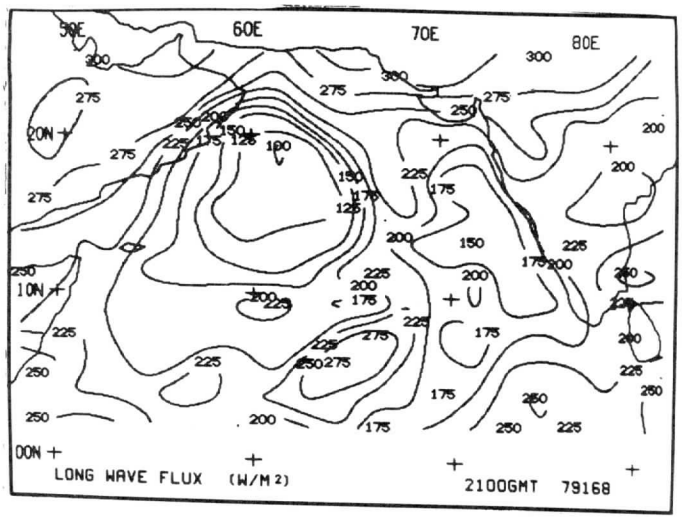
50E
60E
70E
80E
20N
10N
00N
LONG WAVE FLUX (W/M2)
2100GMT 79168

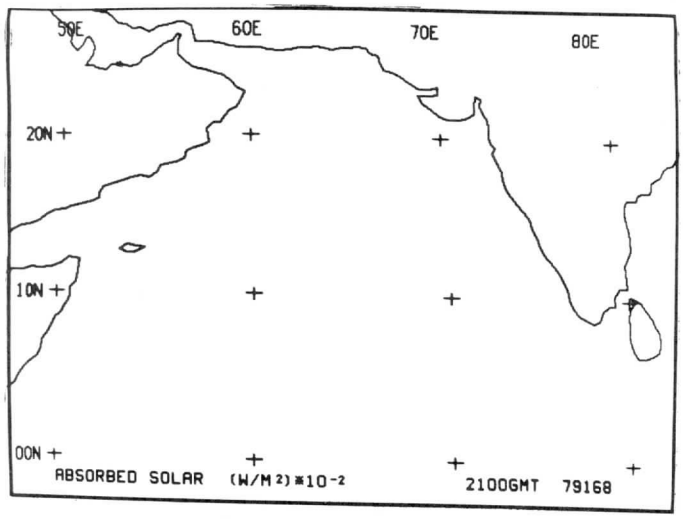
50E
60E
70E
80E
20N
10N
00N
ABSORBED SOLAR (W/M2)*10-2
2100GMT 79168

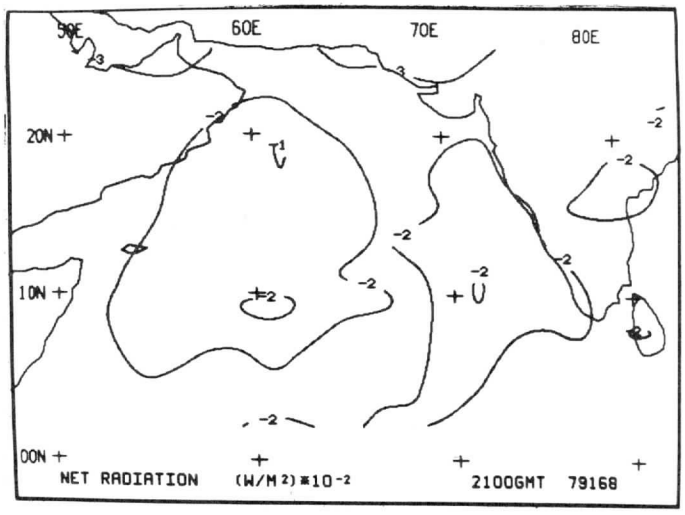
50E
60E
70E
80E
20N
10N
00N
NET RADIATION (W/M2)*10-2
2100GMT 79168

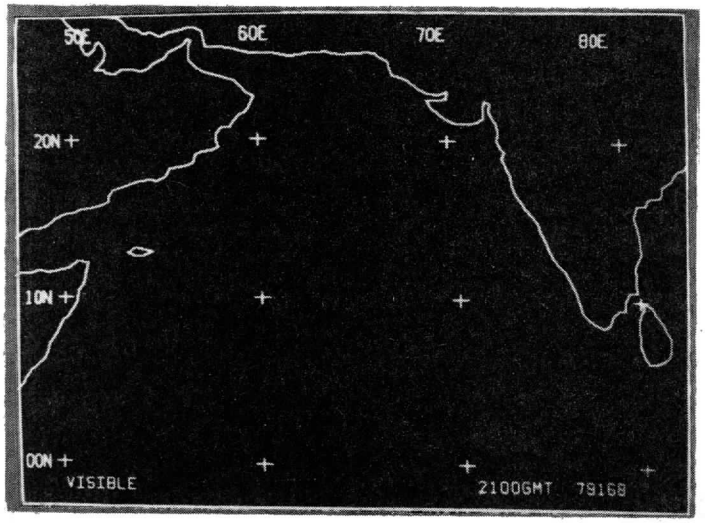
50E
60E
70E
80E
20N
10N
00N
VISIBLE
2100GMT 79168

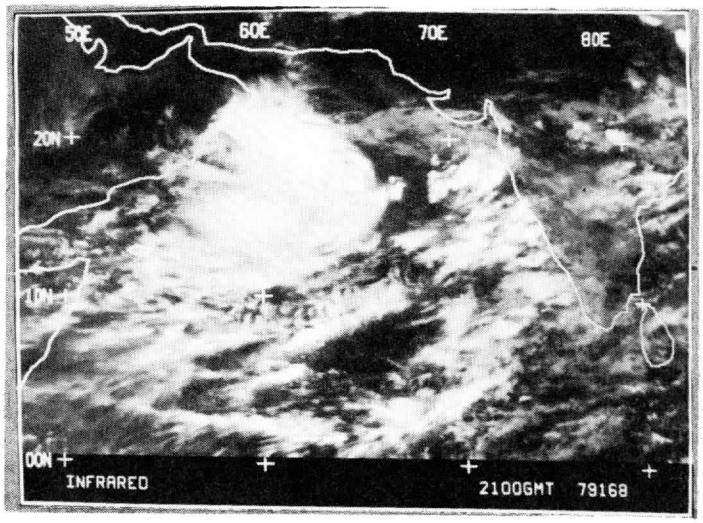
50E
60E
70E
80E
20N
10N
00N
INFRARED
2100GMT 79168

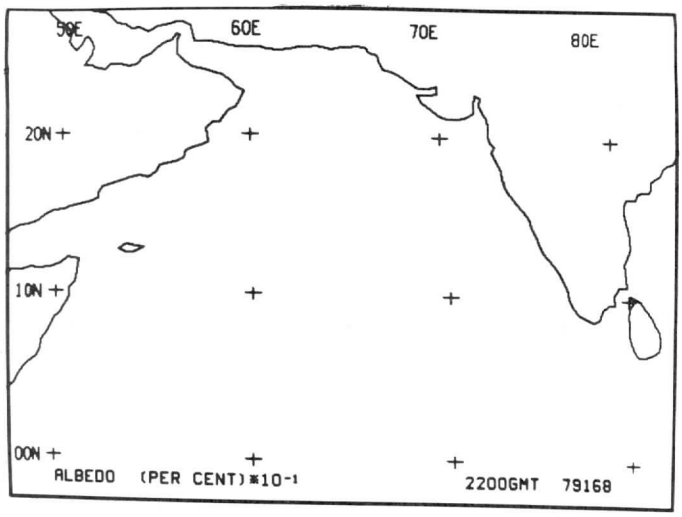
50E
60E
70E
80E
20N
10N
00N
ALBEDO (PER CENT)*10-1
2200GMT 79168

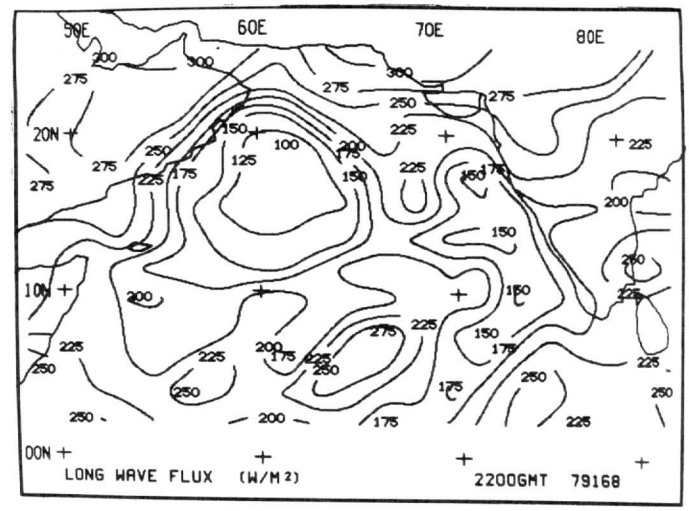
50E
60E
70E
80E
20N
10N
00N
LONG WAVE FLUX (W/M2)
2200GMT 79168

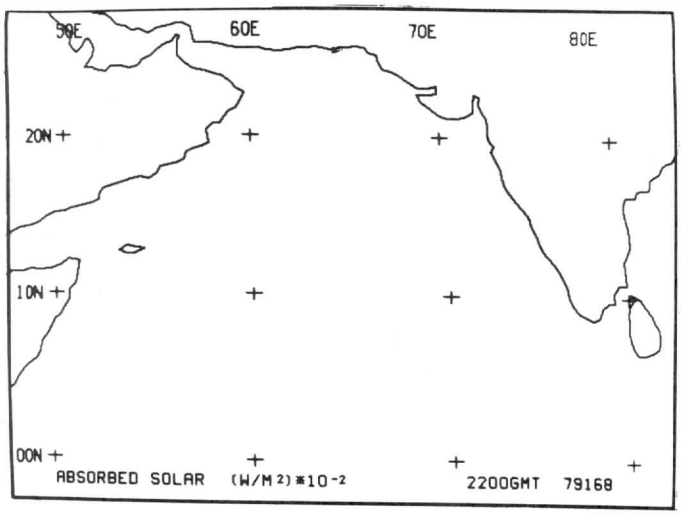
50E
60E
70E
80E
20N
10N
00N
ABSORBED SOLAR (W/M2)*10-2
2200GMT 79168

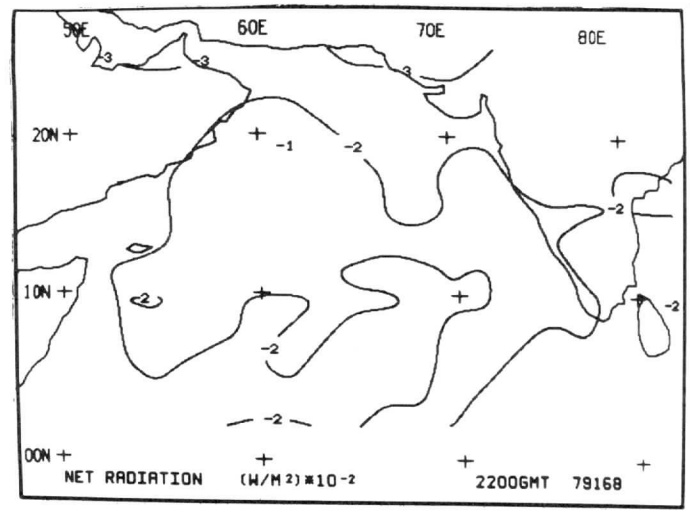
50E
60E
70E
80E
20N
10N
00N
NET RADIATION (W/M2)*10-2
2200GMT 79168

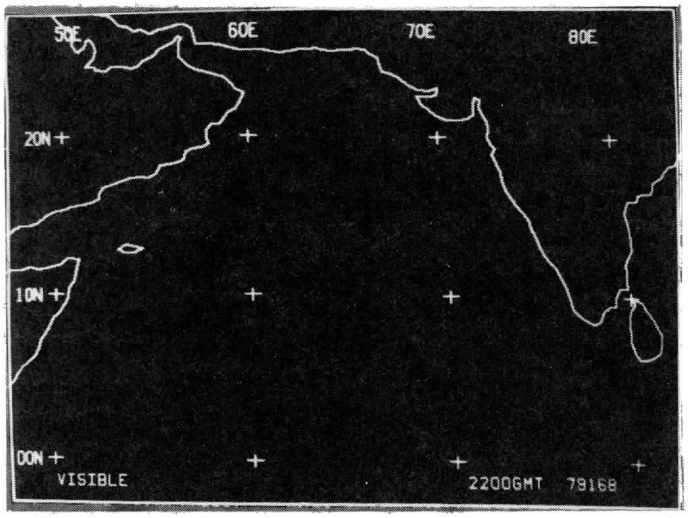
50E
60E
70E
80E
20N
10N
00N
VISIBLE
2200GMT 79168

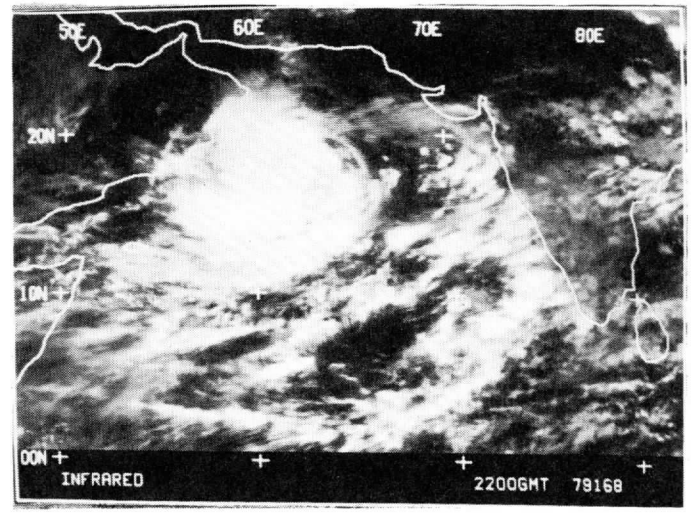
50E
60E
70E
80E
20N
10N
00N
INFRARED
2200GMT 79168

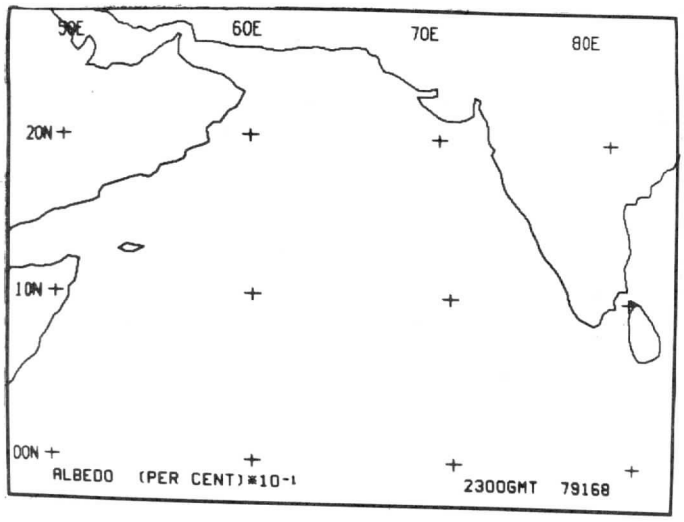
50E
60E
70E
80E
20N
10N
0ON
ALBEDO (PER CENT)*10-1
2300GMT 79168

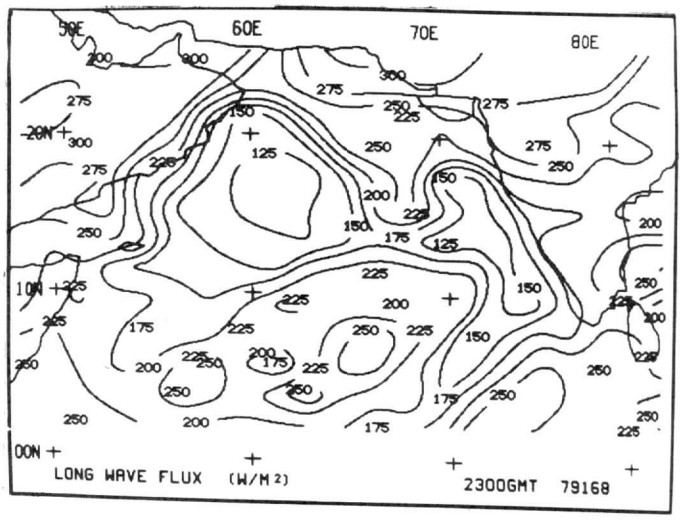
50E
60E
70E
80E
20N
10N
0ON
LONG WAVE FLUX (W/M2)
2300GMT 79168

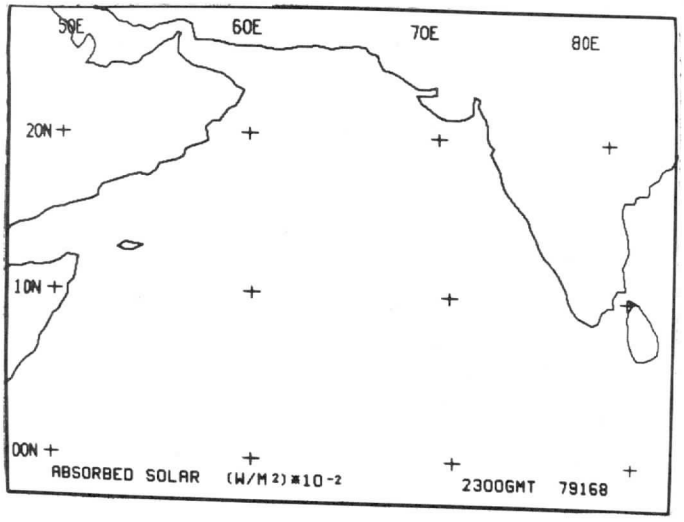
50E
60E
70E
80E
20N
10N
0ON
ABSORBED SOLAR (W/M2)*10-2
2300GMT 79168

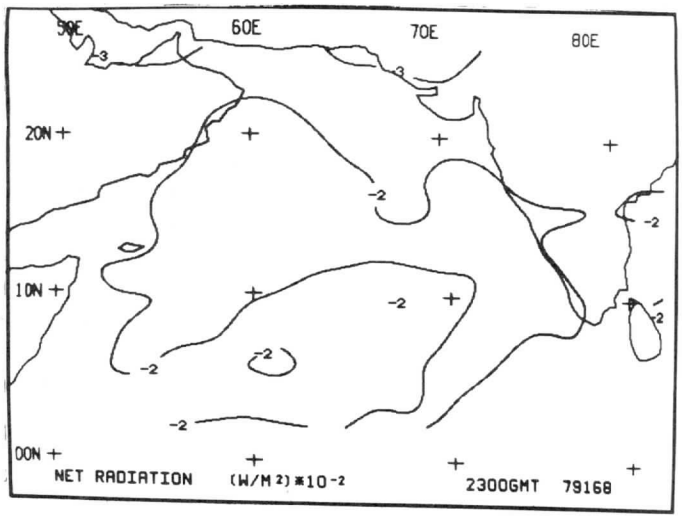
50E
60E
70E
80E
20N
10N
0ON
NET RADIATION (W/M2)*10-2
2300GMT 79168

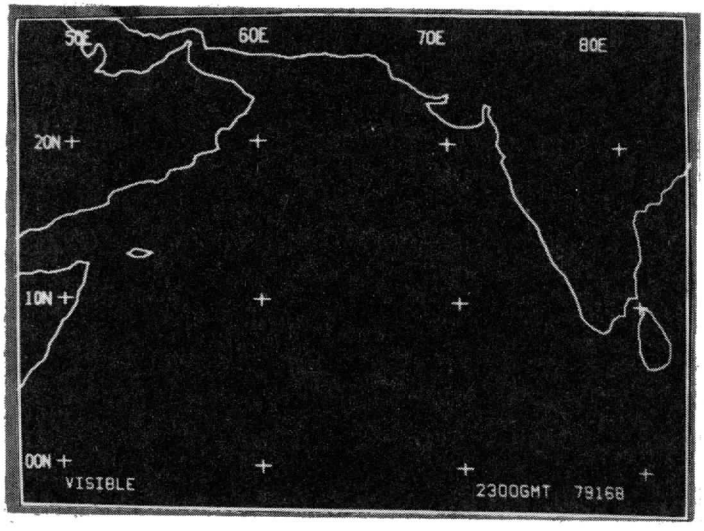
50E
60E
70E
80E
20N
10N
0ON
VISIBLE
2300GMT 79168

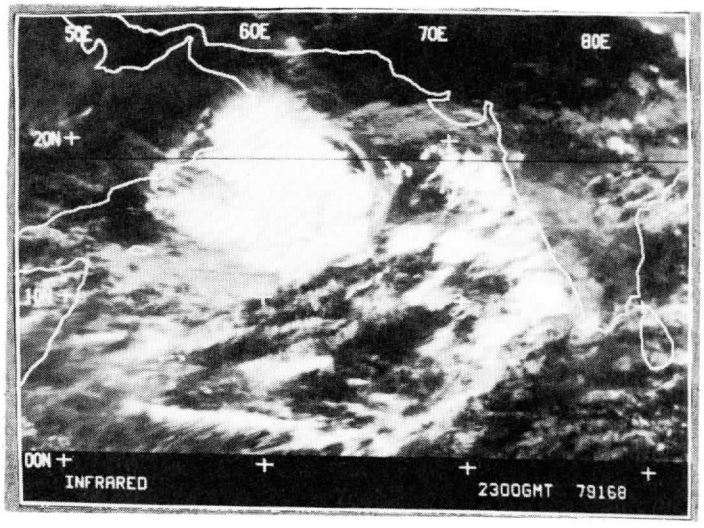
50E
60E
70E
80E
20N
10N
0ON
INFRARED
2300GMT 79168

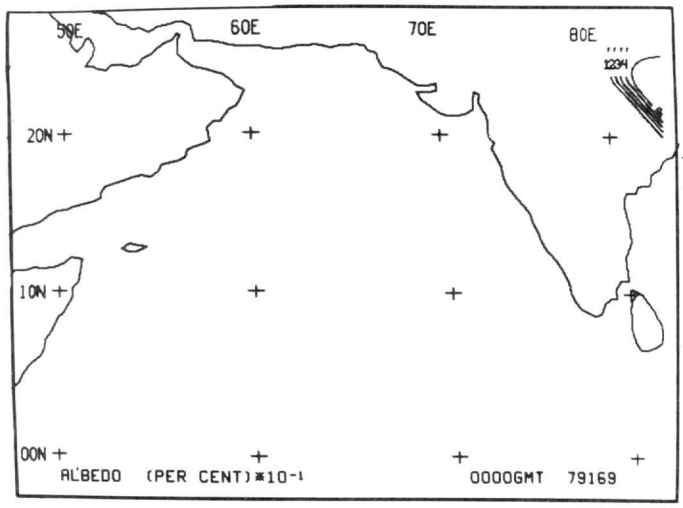
50E
60E
70E
80E
20N
10N
0ON
1234
ALBEDO (PER CENT)*10-1
0000GMT 79169

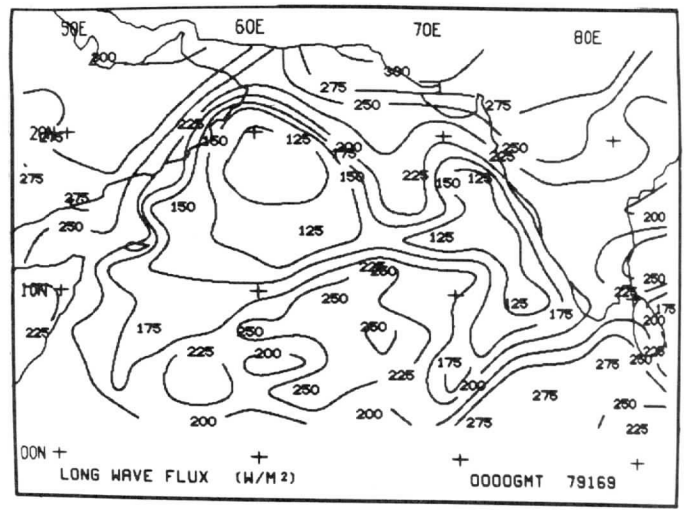
50E
60E
70E
80E
20N
10N
0ON
LONG WAVE FLUX (W/M2)
0000GMT 79169

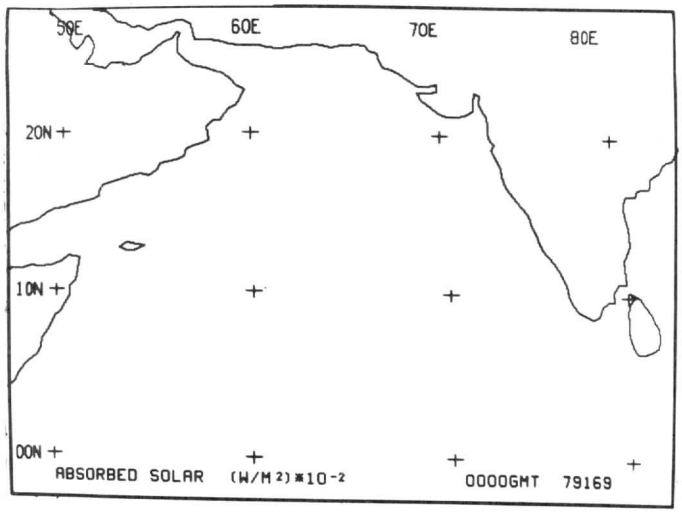
50E
60E
70E
80E
20N
10N
0ON
ABSORBED SOLAR (W/M2)*10-2
0000GMT 79169

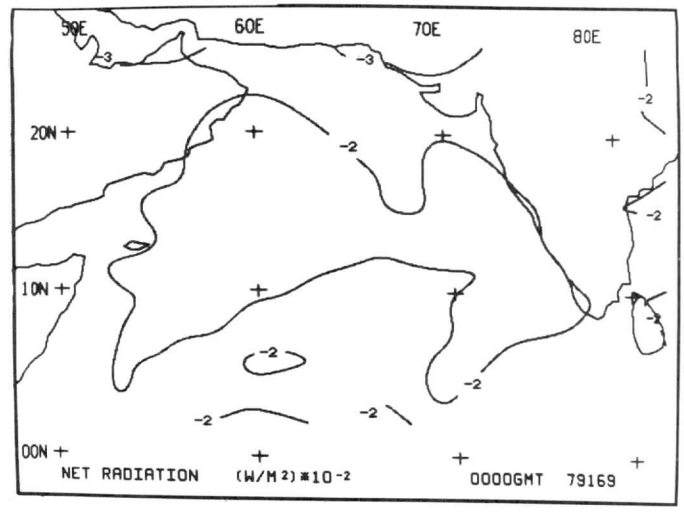
50E
60E
70E
80E
20N
10N
0ON
NET RADIATION (W/M2)*10-2
0000GMT 79169

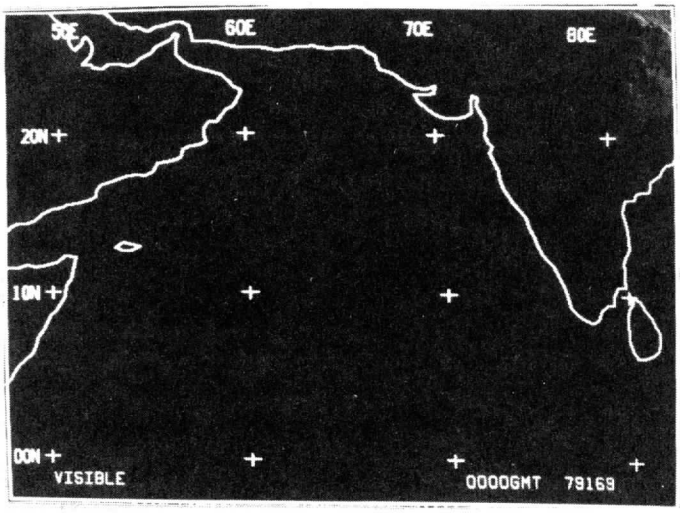
50E
60E
70E
80E
20N
10N
0ON
VISIBLE
0000GMT 79169

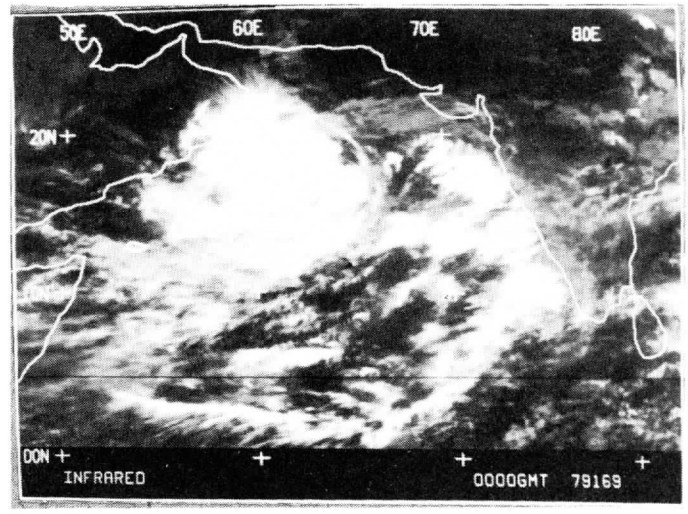
50E
60E
70E
80E
20N
0ON
INFRARED
0000GMT 79169

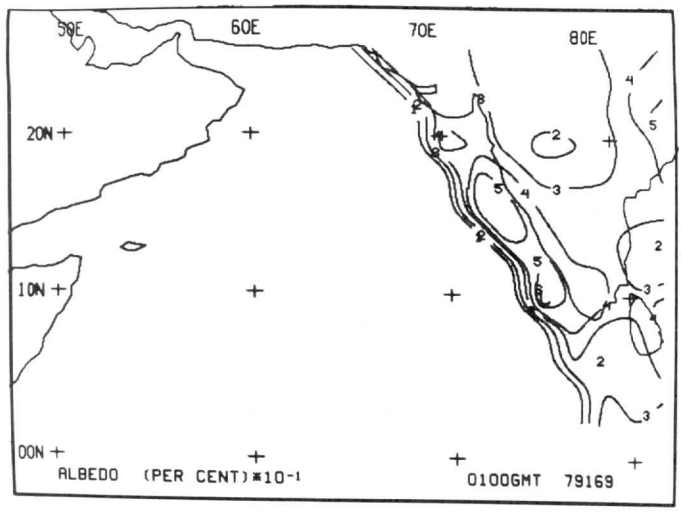
50E
60E
70E
80E
20N
10N
0ON
ALBEDO (PER CENT)*10-1
0100GMT 79169

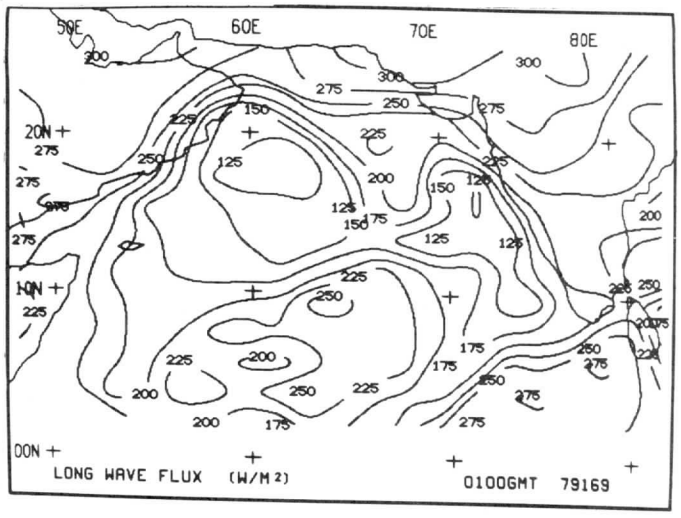
50E
60E
70E
80E
20N
10N
0ON
LONG WAVE FLUX (W/M2)
0100GMT 79169

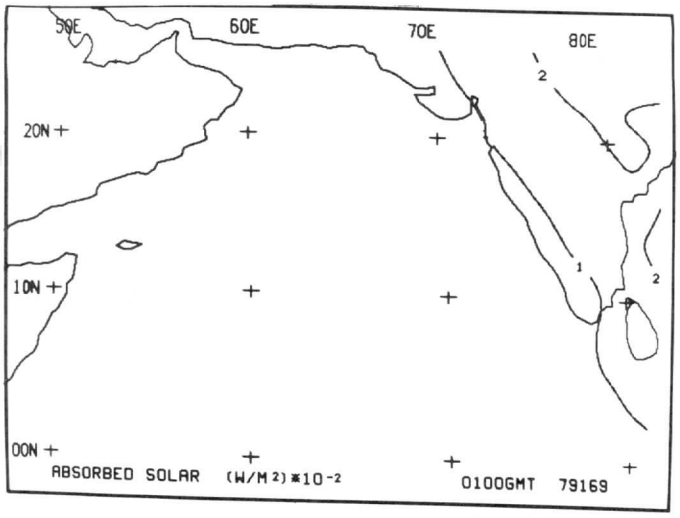
50E
60E
70E
80E
20N
10N
0ON
ABSORBED SOLAR (W/M2)*10-2
0100GMT 79169

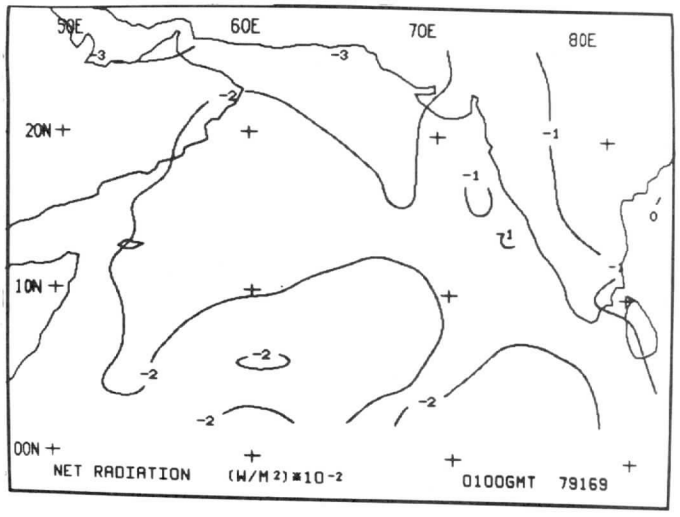
50E
60E
70E
80E
20N
10N
0ON
NET RADIATION (W/M2)*10-2
0100GMT 79169

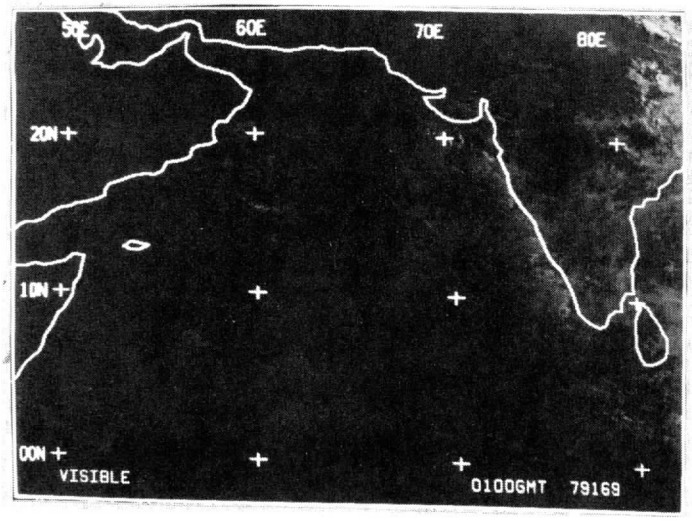
50E
60E
70E
80E
20N
10N
0ON
VISIBLE
0100GMT 79169

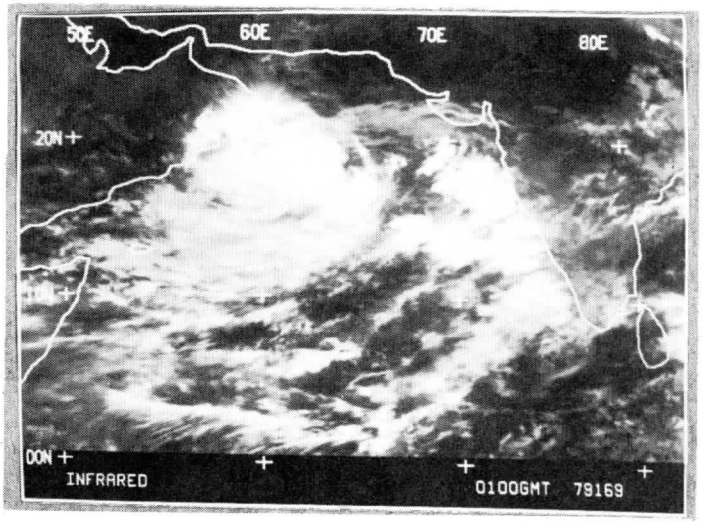
50E
60E
70E
80E
20N
0ON
INFRARED
0100GMT 79169

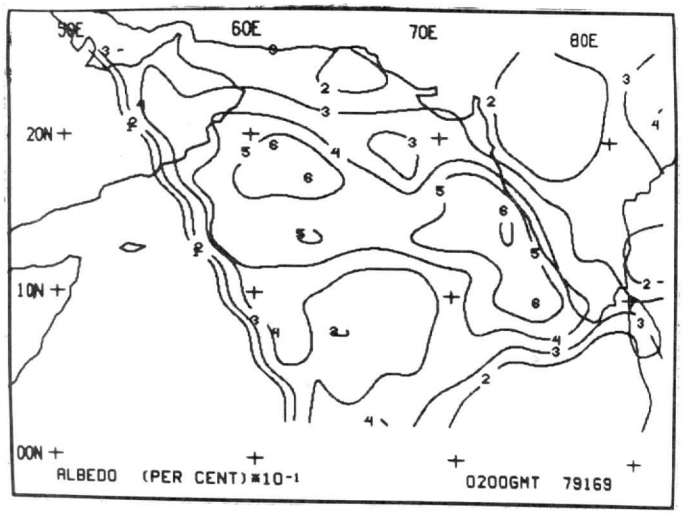
50E
60E
70E
80E
20N
10N
00N
ALBEDO (PER CENT)*10-1
0200GMT 79169

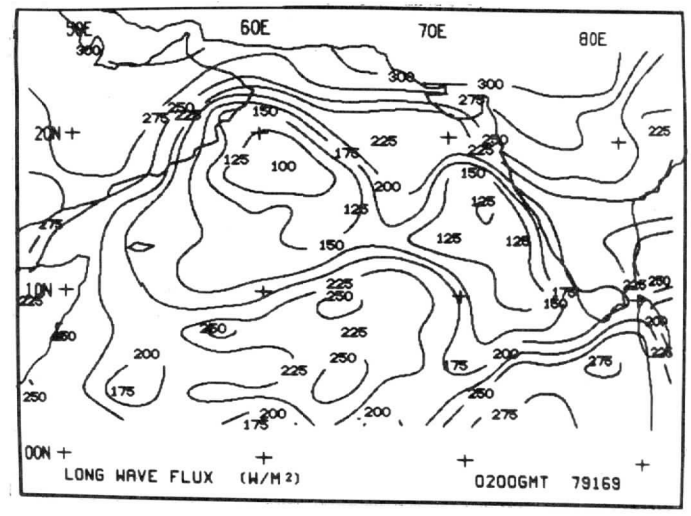
50E
60E
70E
80E
20N
10N
00N
LONG WAVE FLUX (W/M2)
0200GMT 79169

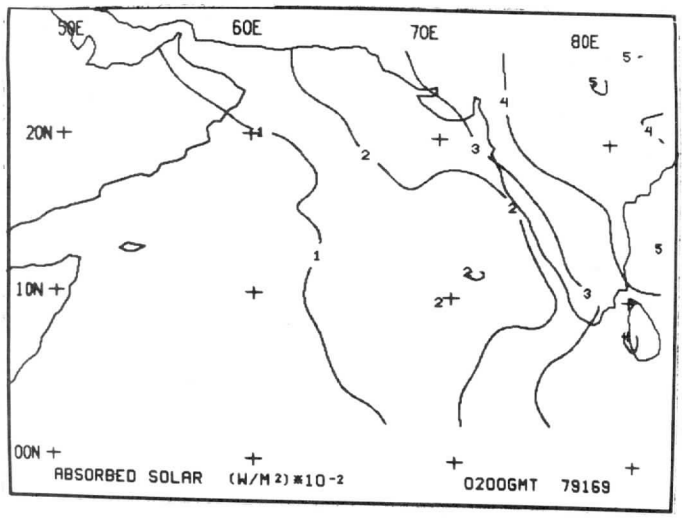
50E
60E
70E
80E
20N
10N
00N
ABSORBED SOLAR (W/M2)*10-2
0200GMT 79169

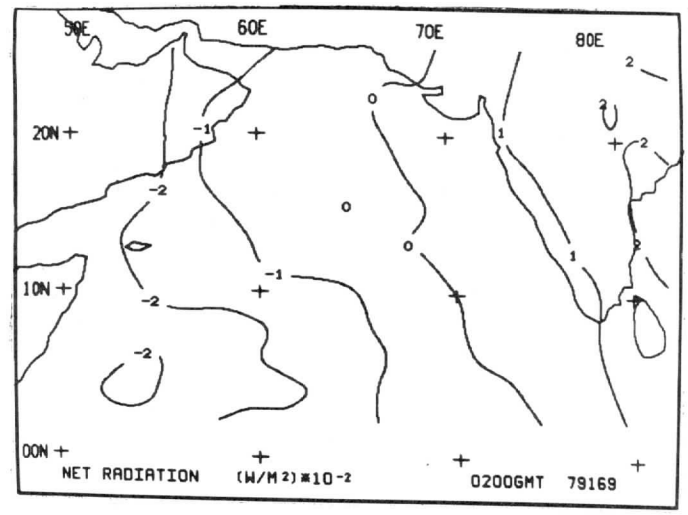
50E
60E
70E
80E
20N
10N
00N
NET RADIATION (W/M2)*10-2
0200GMT 79169

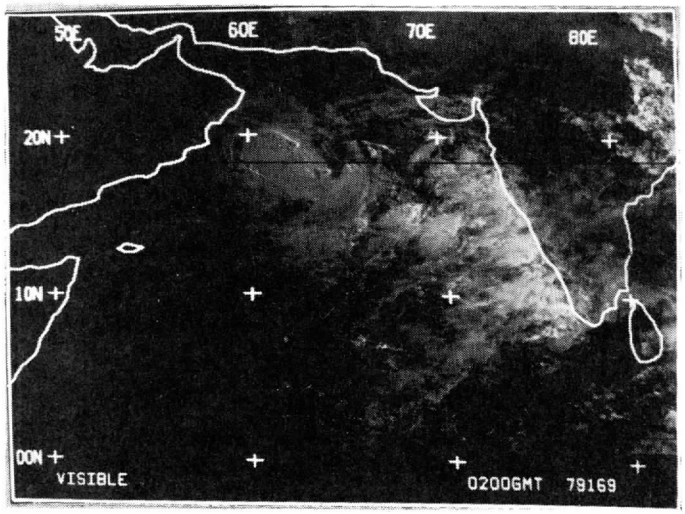
50E
60E
70E
80E
20N
10N
00N
VISIBLE
0200GMT 79169

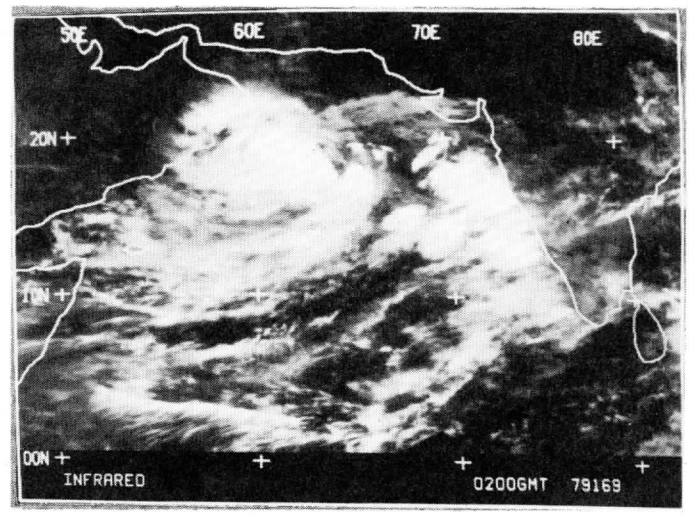
50E
60E
70E
80E
20N
10N
00N
INFRARED
0200GMT 79169

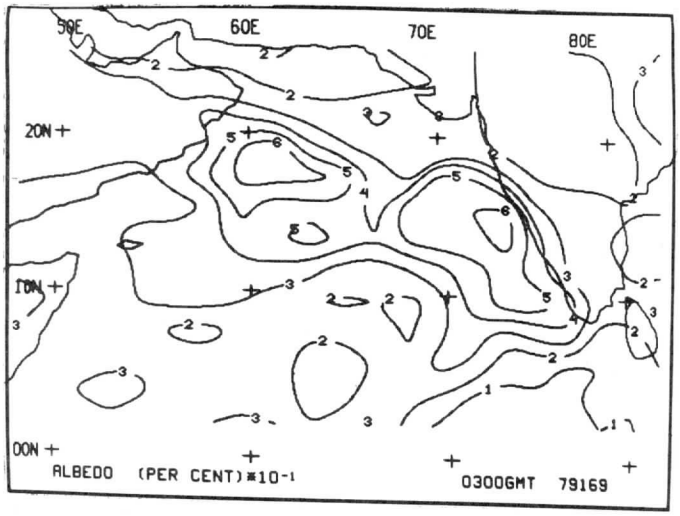
50E
60E
70E
80E
20N
10N
00N
ALBEDO (PER CENT)*10-1
0300GMT 79169

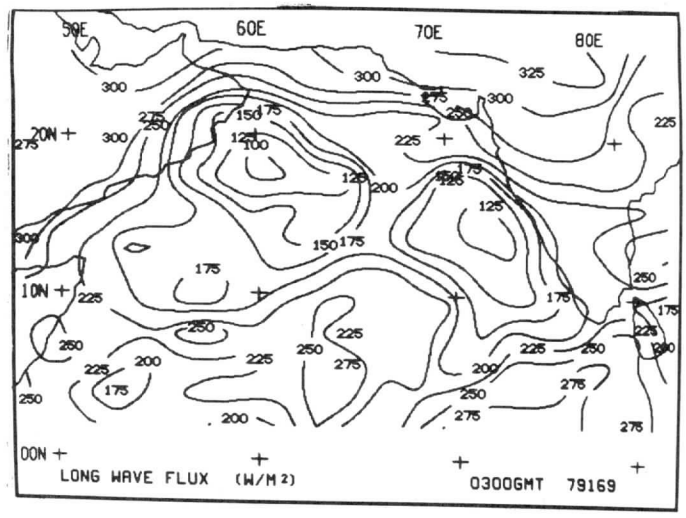
50E
60E
70E
80E
20N
10N
00N
LONG WAVE FLUX (W/M2)
0300GMT 79169

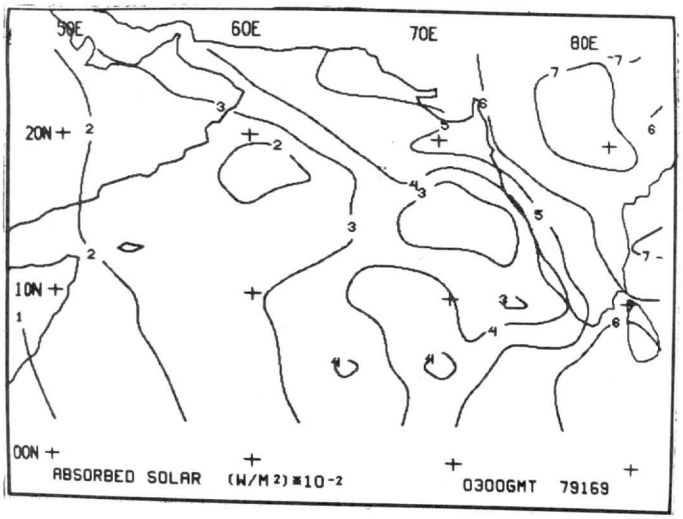
50E
60E
70E
80E
20N
10N
00N
ABSORBED SOLAR (W/M2)*10-2
0300GMT 79169

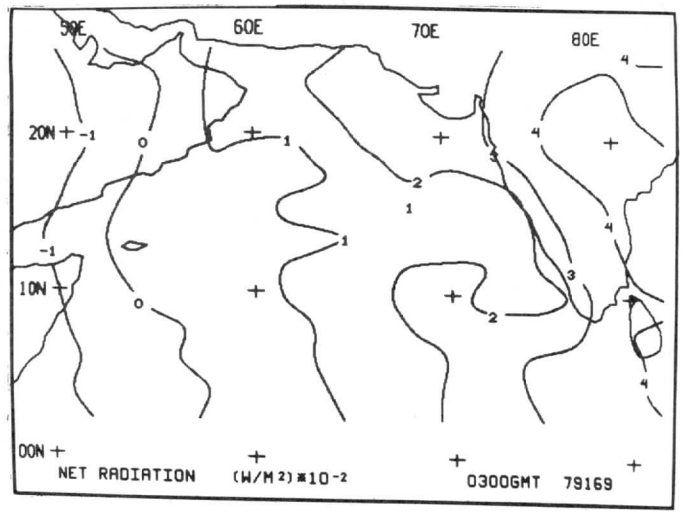
50E
60E
70E
80E
20N
10N
00N
NET RADIATION (W/M2)*10-2
0300GMT 79169

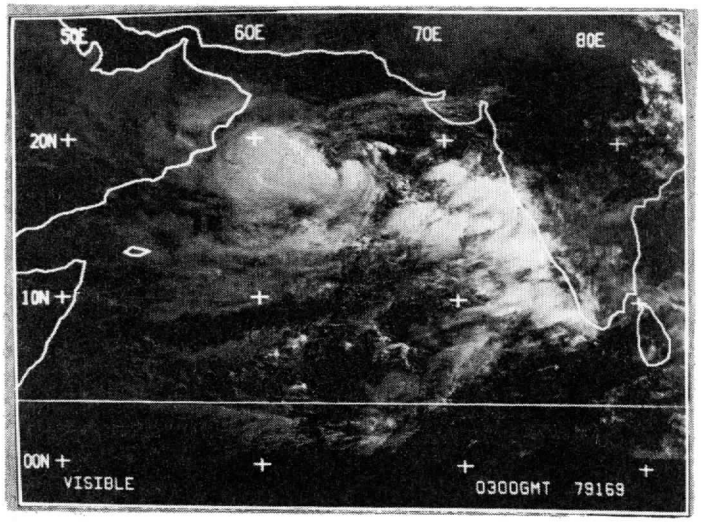
50E
60E
70E
80E
20N
10N
00N
VISIBLE
0300GMT 79169

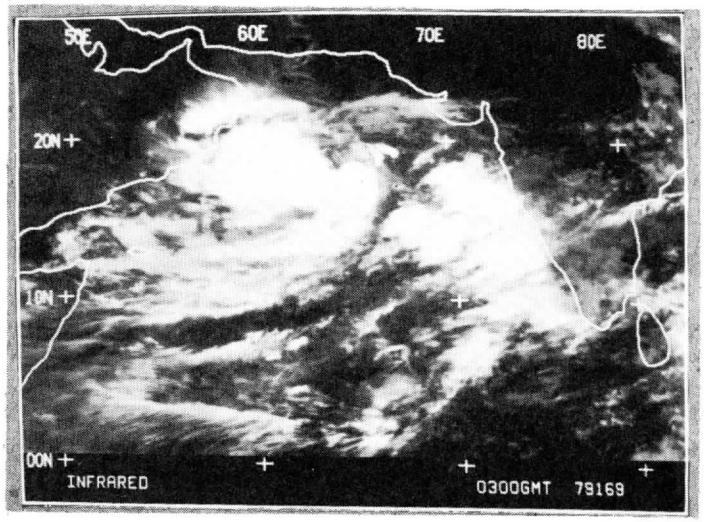
50E
60E
70E
80E
20N
10N
00N
INFRARED
0300GMT 79169

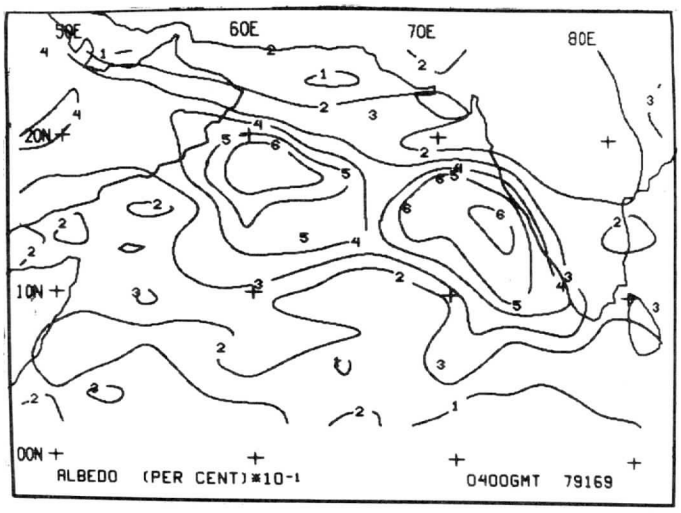
50E
60E
70E
80E
20N
10N
0ON
ALBEDO (PER CENT)*10-1
0400GMT 79169

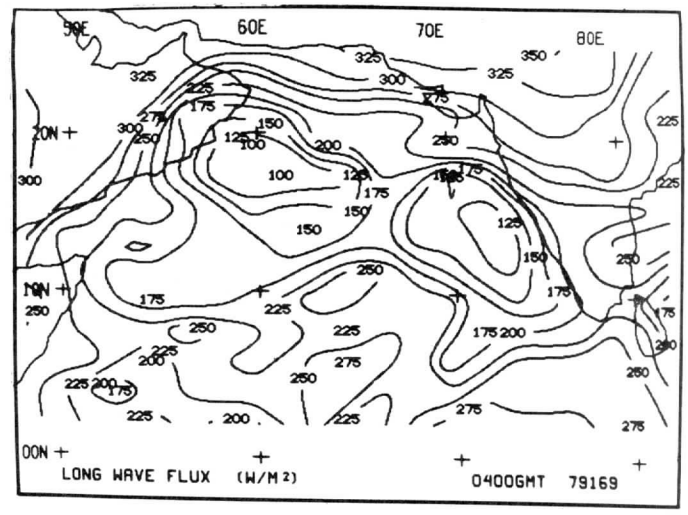
50E
60E
70E
80E
20N
10N
0ON
LONG WAVE FLUX (W/M2)
0400GMT 79169

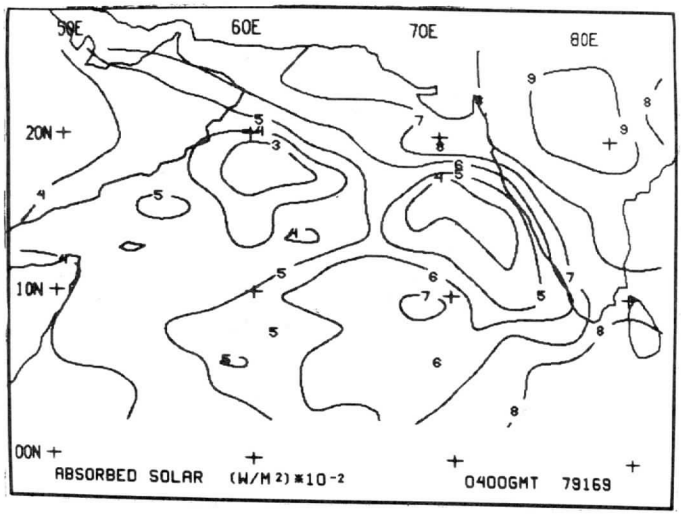
50E
60E
70E
80E
20N
10N
0ON
ABSORBED SOLAR (W/M2)*10-2
0400GMT 79169

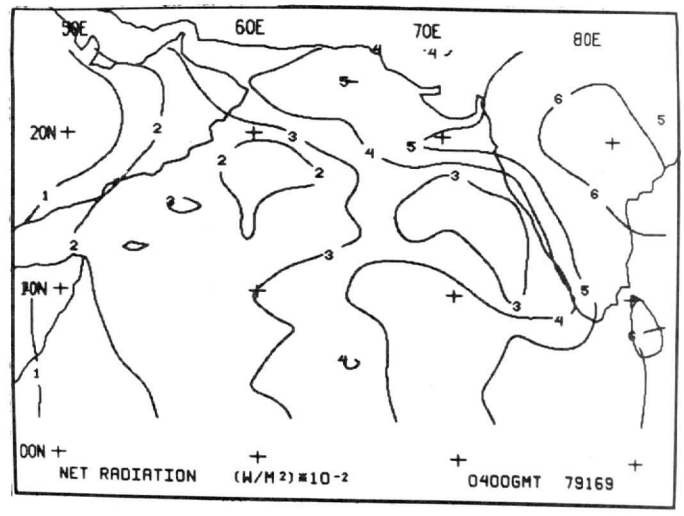
50E
60E
70E
80E
20N
10N
0ON
NET RADIATION (W/M2)*10-2
0400GMT 79169

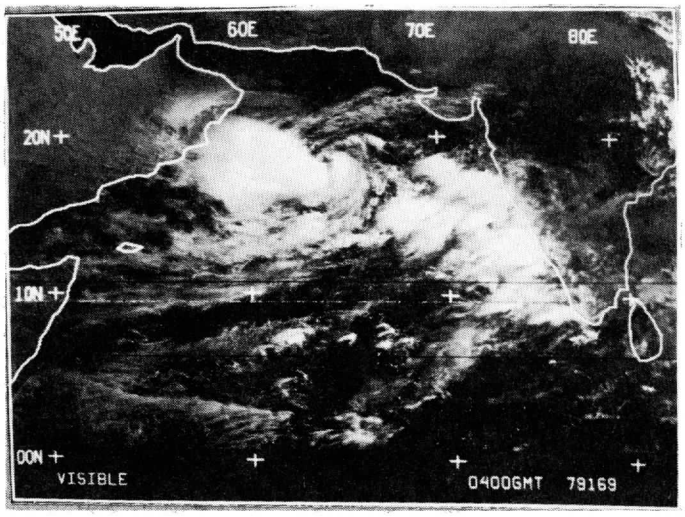
50E
60E
70E
80E
20N
10N
0ON
VISIBLE
0400GMT 79169

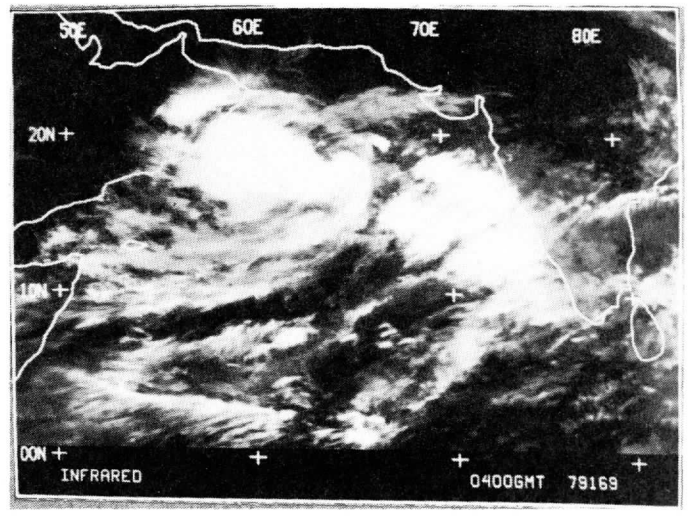
50E
60E
70E
80E
20N
10N
0ON
INFRARED
0400GMT 79169

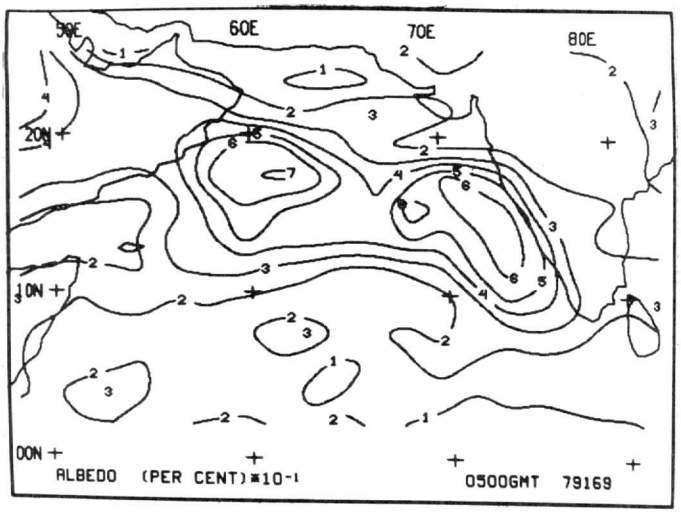
50E
60E
70E
80E
20N
10N
0ON
ALBEDO (PER CENT)*10-1
0500GMT 79169

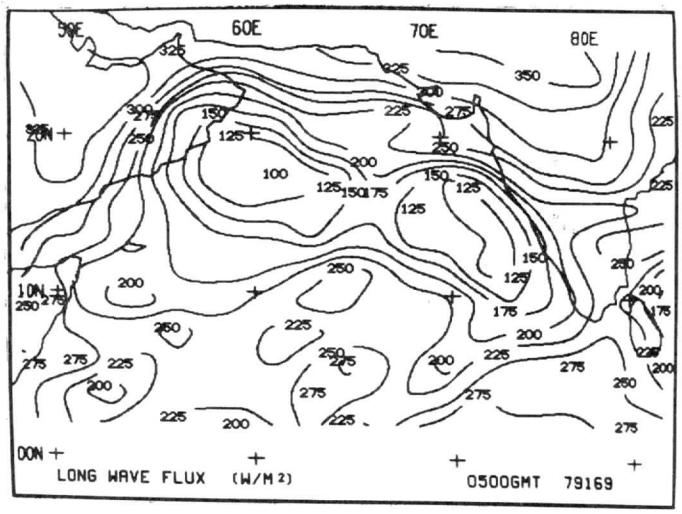
50E
60E
70E
80E
20N
10N
0ON
LONG WAVE FLUX (W/M2)
0500GMT 79169

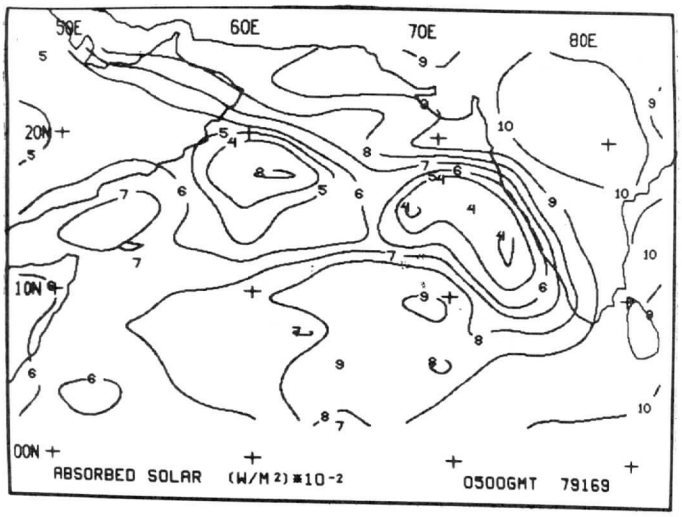
50E
60E
70E
80E
20N
10N
0ON
ABSORBED SOLAR (W/M2)*10-2
0500GMT 79169

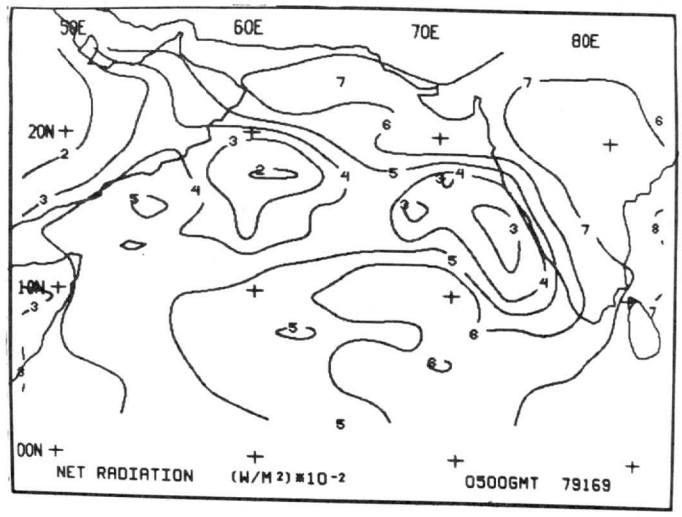
50E
60E
70E
80E
20N
10N
0ON
NET RADIATION (W/M2)*10-2
0500GMT 79169

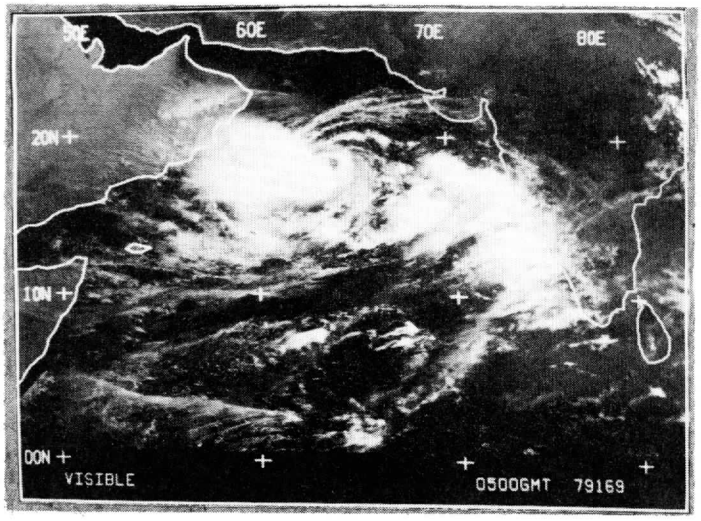
50E
60E
70E
80E
20N
10N
0ON
VISIBLE
0500GMT 79169

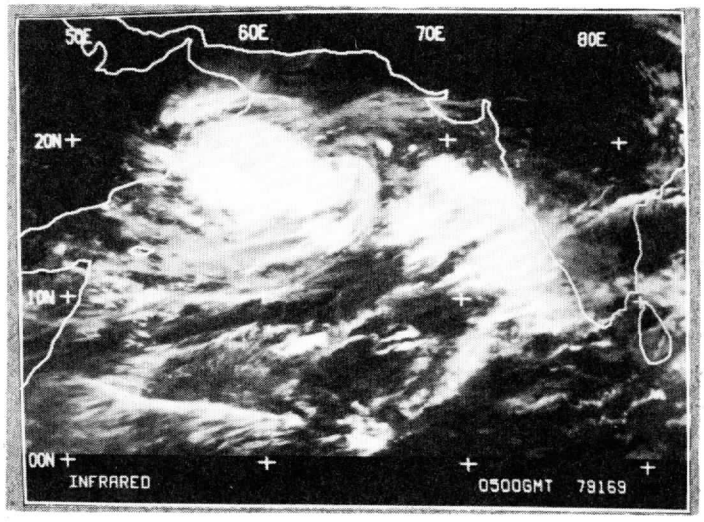
50E
60E
70E
80E
20N
10N
0ON
INFRARED
0500GMT 79169

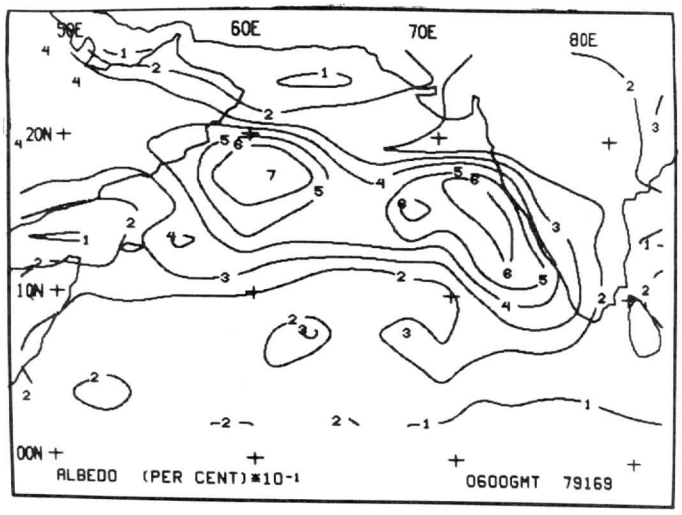
50E
60E
70E
80E
20N
10N
0ON
ALBEDO (PER CENT)*10-1
0600GMT 79169

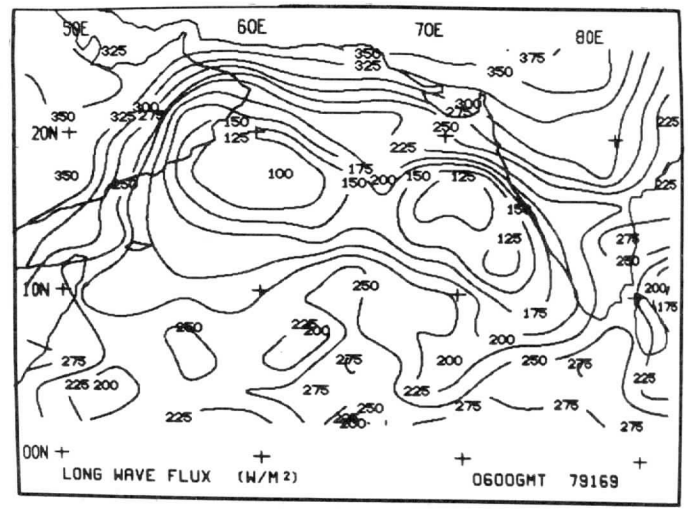
50E
60E
70E
80E
20N
10N
0ON
LONG WAVE FLUX (W/M2)
0600GMT 79169

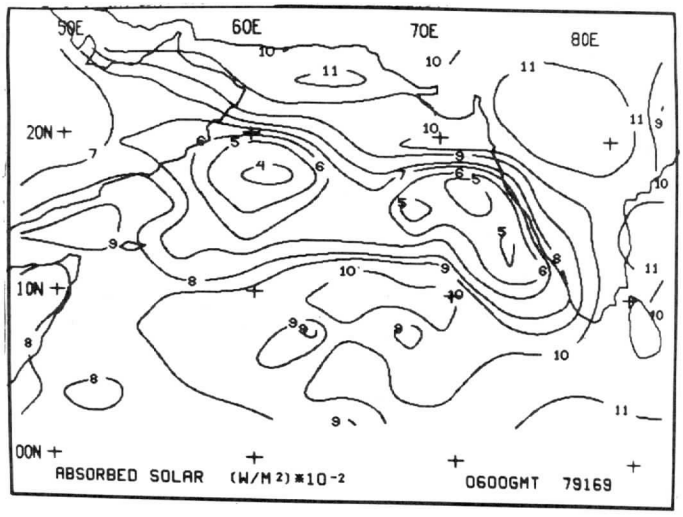
50E
60E
70E
80E
20N
10N
0ON
ABSORBED SOLAR (W/M2)*10-2
0600GMT 79169

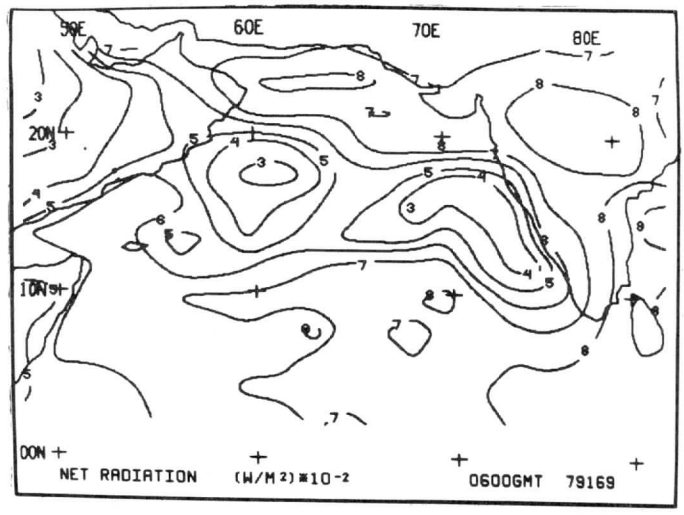
50E
60E
70E
80E
20N
10N
0ON
NET RADIATION (W/M2)*10-2
0600GMT 79169

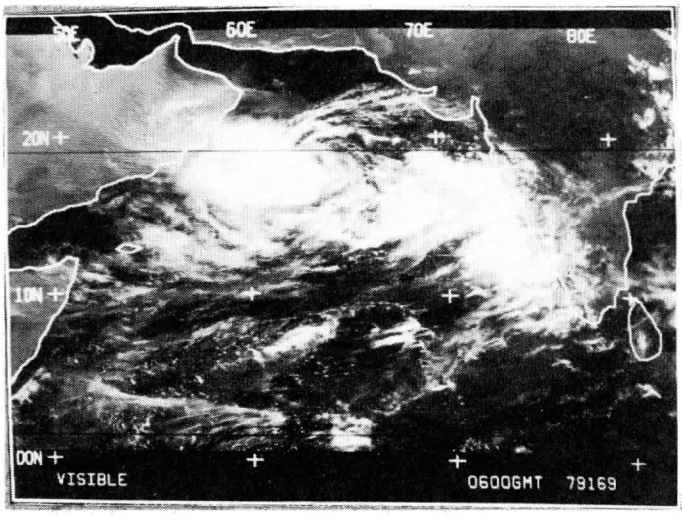
50E
60E
70E
80E
20N
10N
0ON
VISIBLE
0600GMT 79169

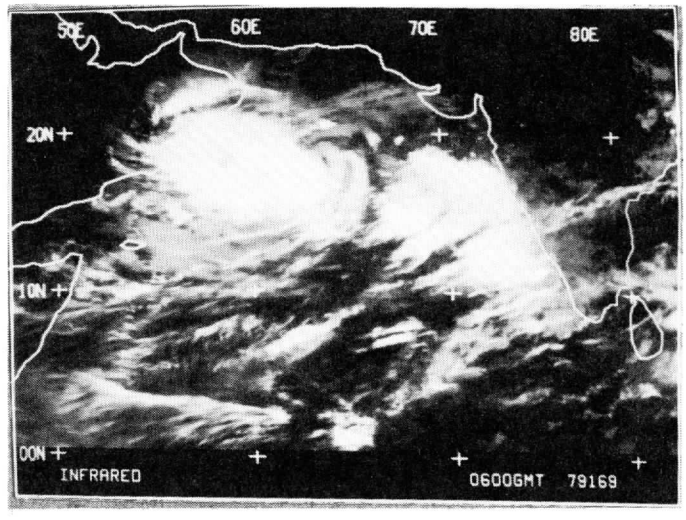
50E
60E
70E
80E
20N
10N
0ON
INFRARED
0600GMT 79169

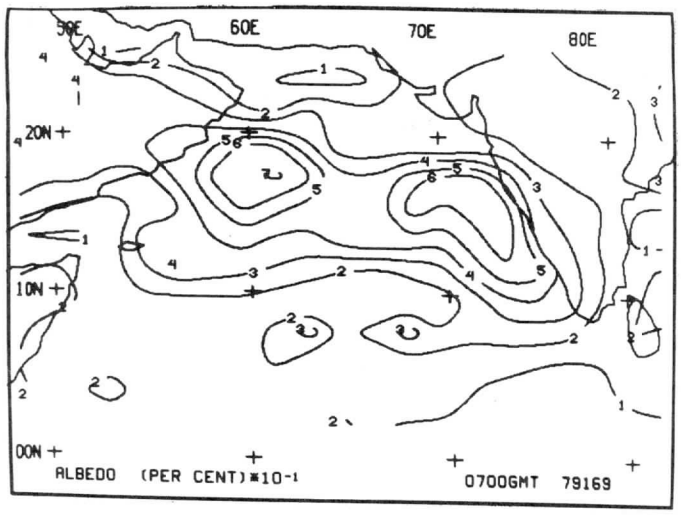
50E
60E
70E
80E
20N
10N
0ON
ALBEDO (PER CENT)*10-1
0700GMT 79169

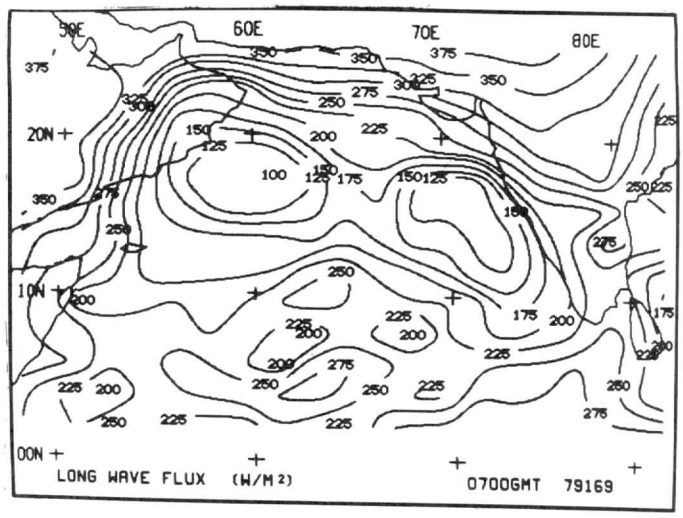
50E
60E
70E
80E
20N
10N
0ON
LONG WAVE FLUX (W/M2)
0700GMT 79169

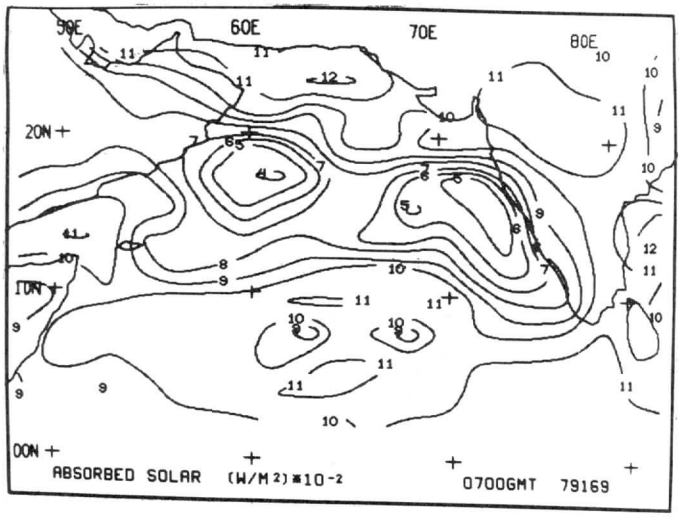
50E
60E
70E
80E
20N
10N
0ON
ABSORBED SOLAR (W/M2)*10-2
0700GMT 79169

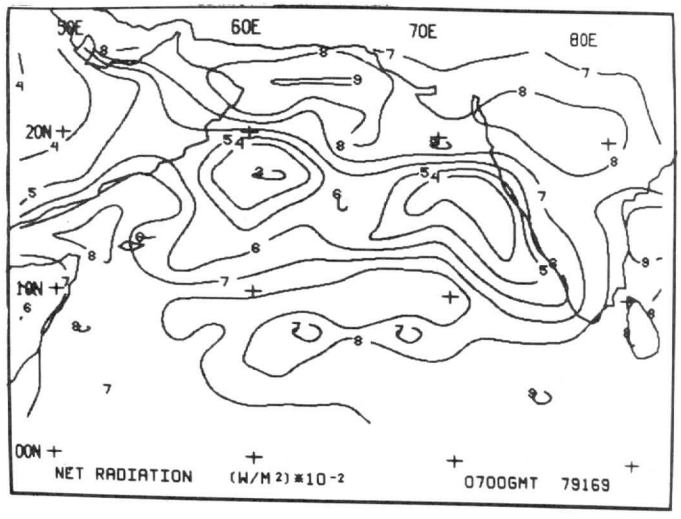
50E
60E
70E
80E
20N
10N
0ON
NET RADIATION (W/M2)*10-2
0700GMT 79169

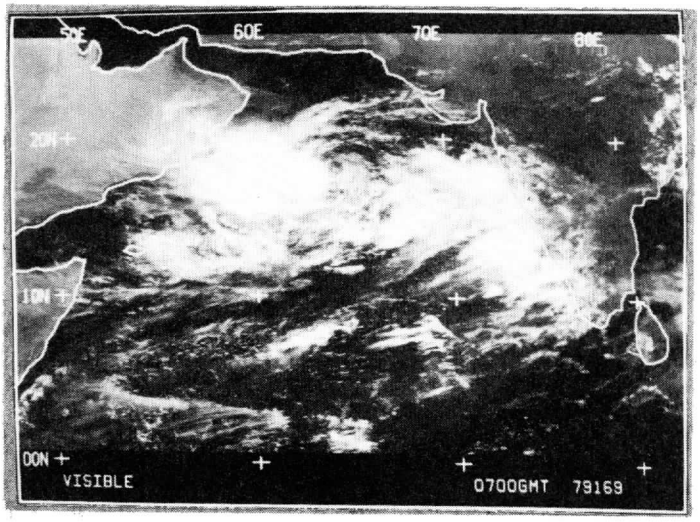
50E
60E
70E
80E
20N
10N
0ON
VISIBLE
0700GMT 79169

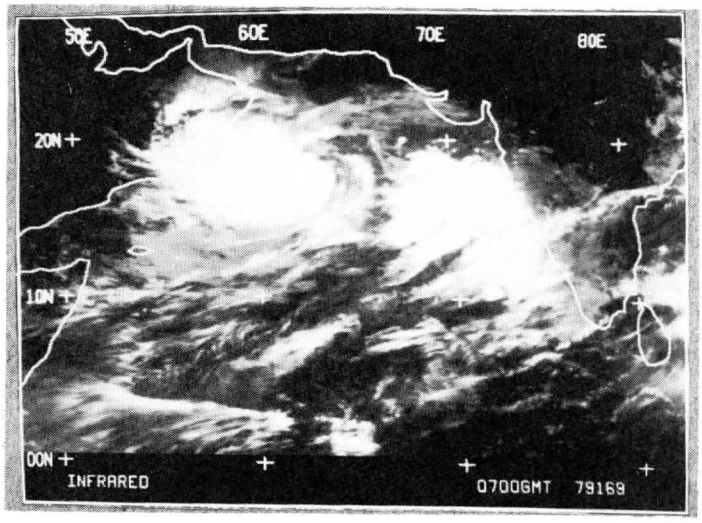
50E
60E
70E
80E
20N
10N
0ON
INFRARED
0700GMT 79169

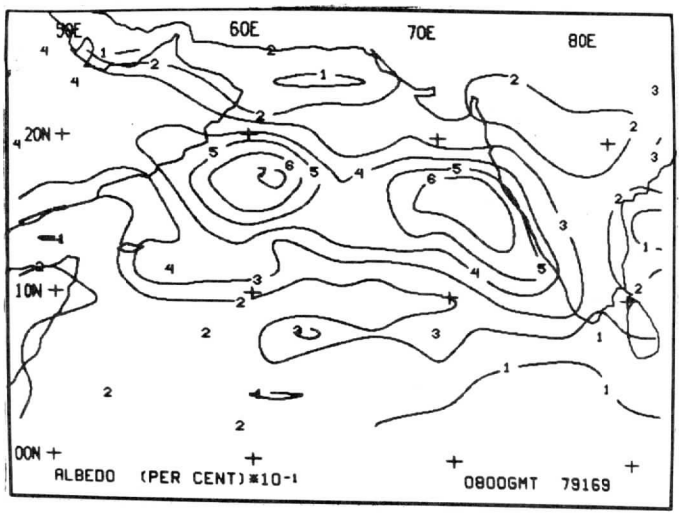
50E
60E
70E
80E
20N
10N
0ON
ALBEDO (PER CENT)*10-1
0800GMT 79169

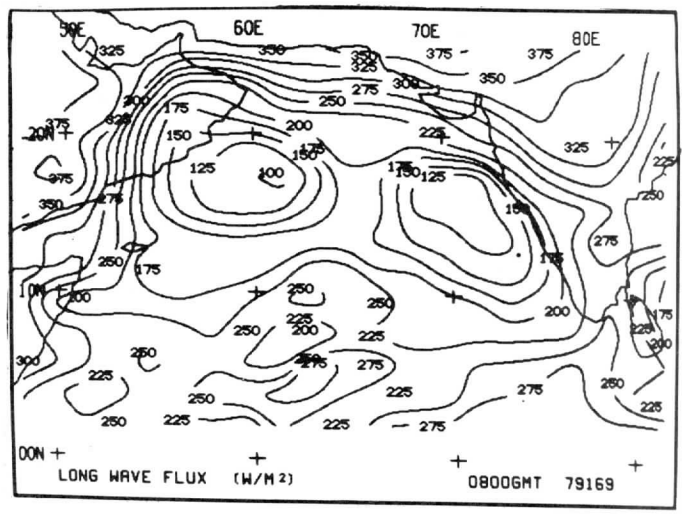
50E
60E
70E
80E
20N
10N
0ON
LONG WAVE FLUX (W/M2)
0800GMT 79169

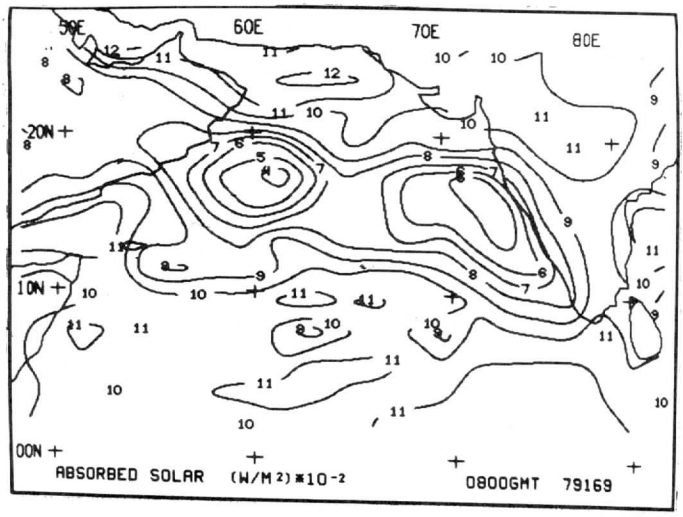
50E
60E
70E
80E
20N
10N
0ON
ABSORBED SOLAR (W/M2)*10-2
0800GMT 79169

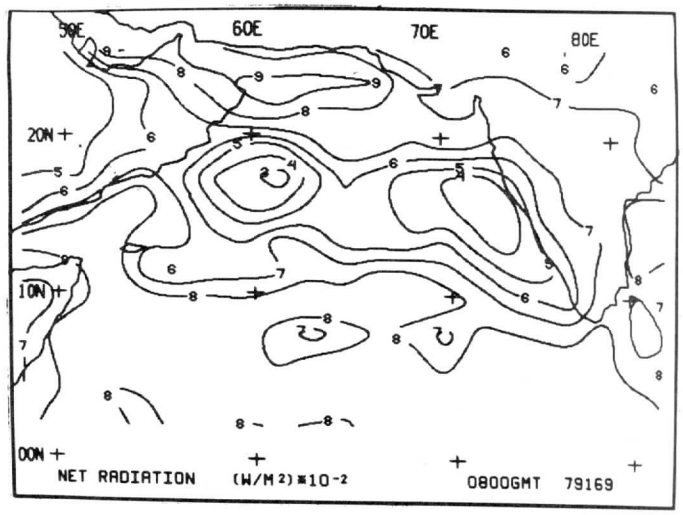
50E
60E
70E
80E
20N
10N
0ON
NET RADIATION (W/M2)*10-2
0800GMT 79169

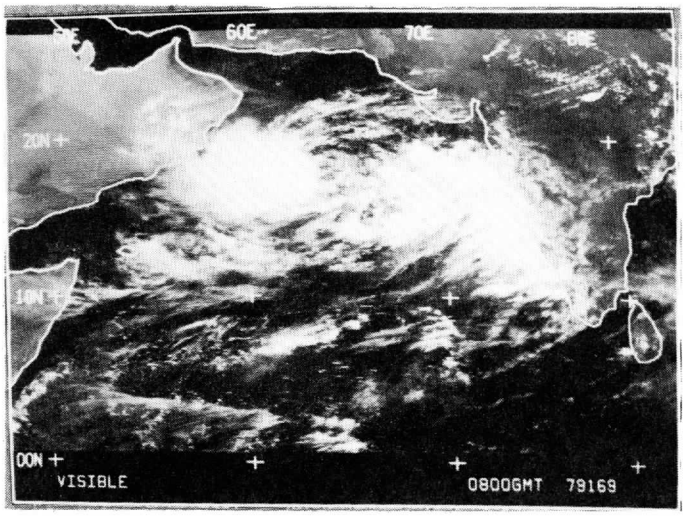
60E
70E
80E
20N
10N
0ON
VISIBLE
0800GMT 79169

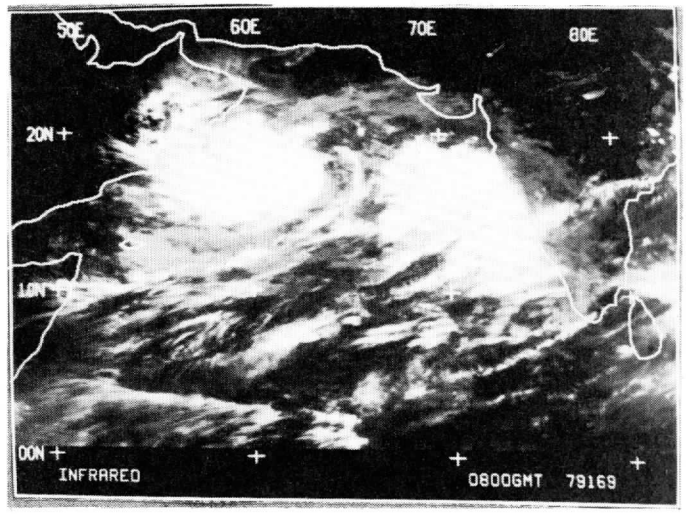
50E
60E
70E
80E
20N
10N
0ON
INFRARED
0800GMT 79169

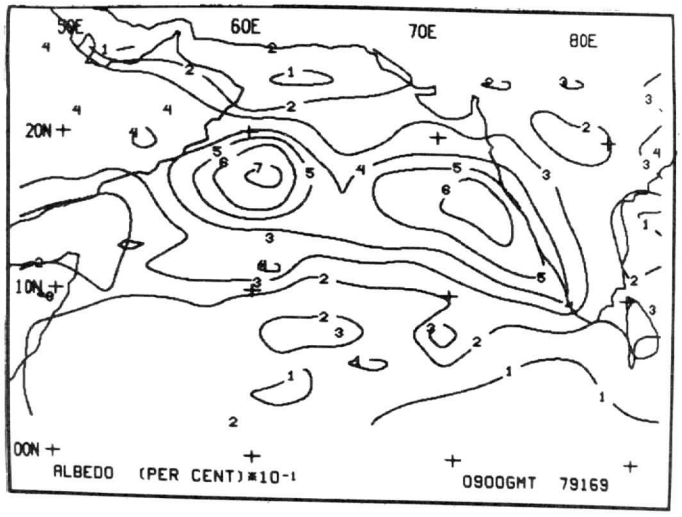
50E
60E
70E
80E
20N
10N
0ON
ALBEDO (PER CENT)*10-1
0900GMT 79169

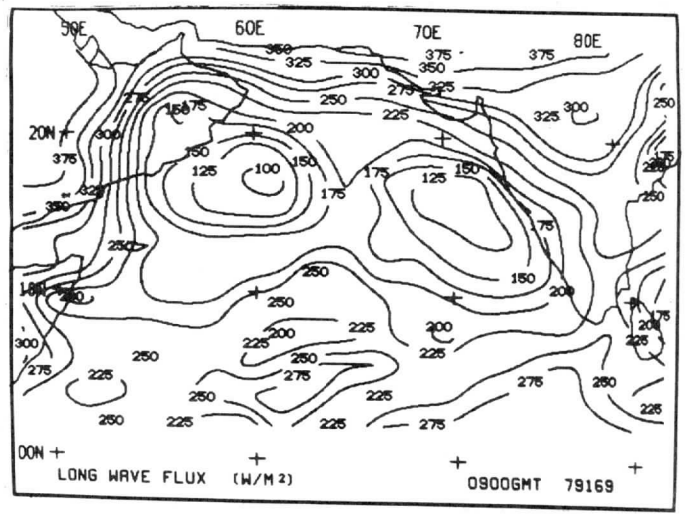
50E
60E
70E
80E
20N
10N
0ON
LONG WAVE FLUX (W/M2)
0900GMT 79169

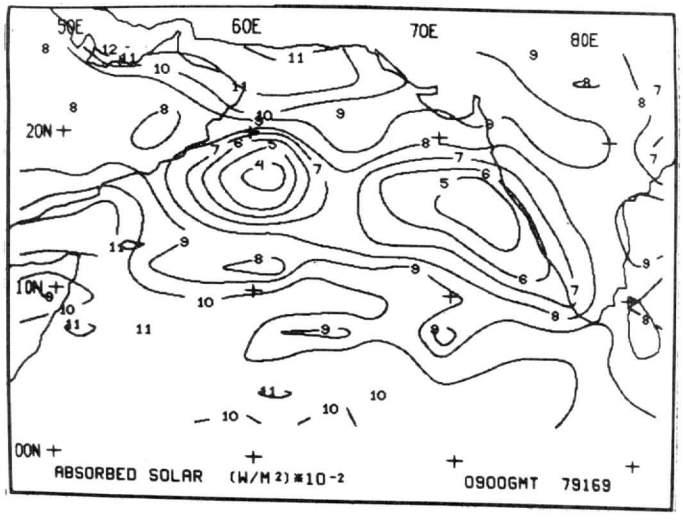
50E
60E
70E
80E
20N
10N
0ON
ABSORBED SOLAR (W/M2)*10-2
0900GMT 79169

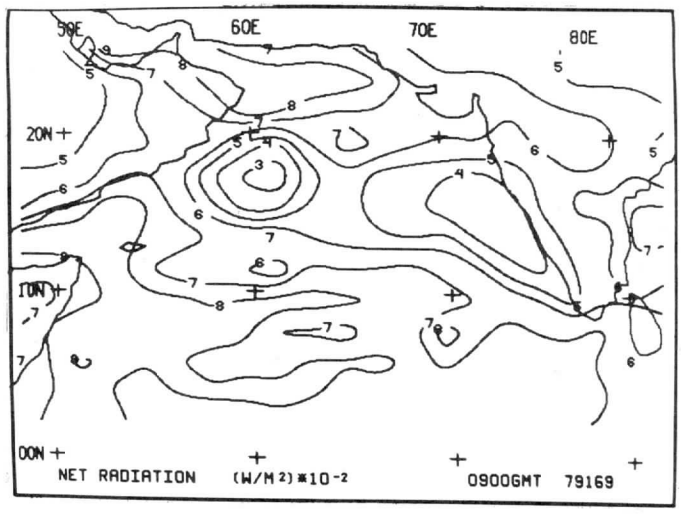
50E
60E
70E
80E
20N
10N
0ON
NET RADIATION (W/M2)*10-2
0900GMT 79169

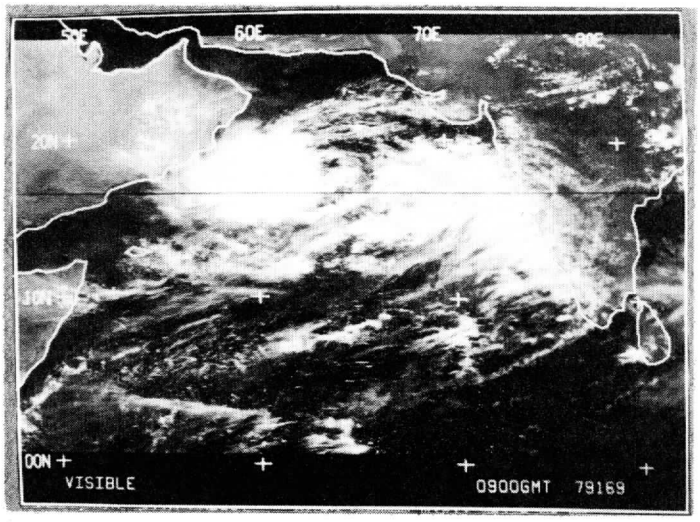
50E
60E
70E
80E
20N
10N
0ON
VISIBLE
0900GMT 79169

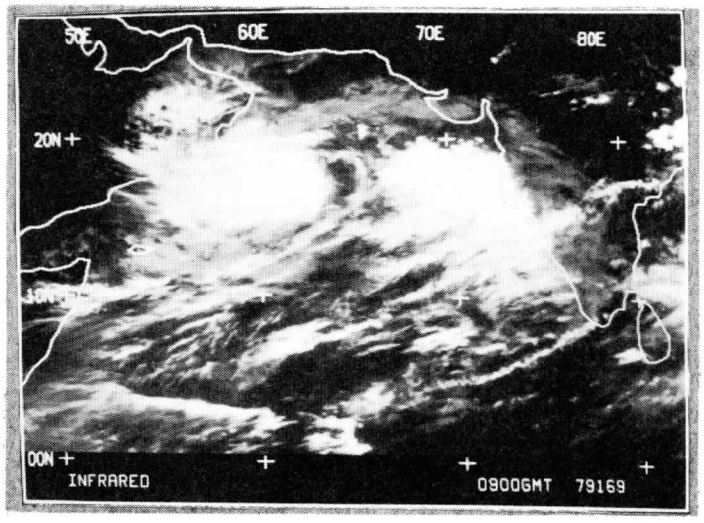
50E
60E
70E
80E
20N
10N
0ON
INFRARED
0900GMT 79169

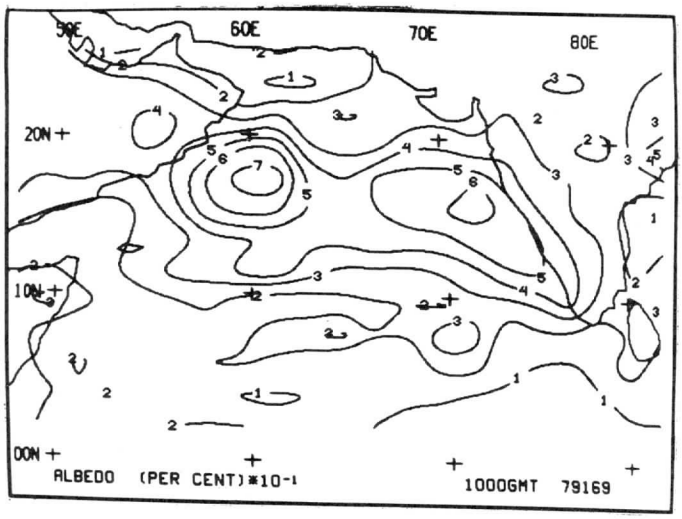
50E
60E
70E
80E
20N
10N
0ON
ALBEDO (PER CENT)*10-1
1000GMT 79169

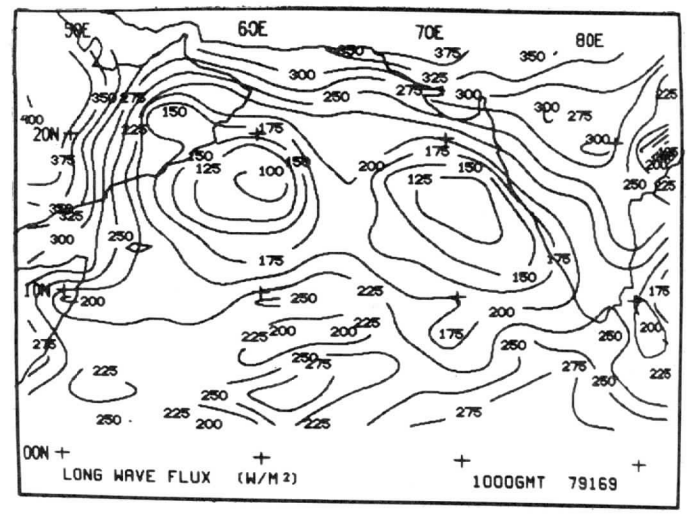
50E
60E
70E
80E
20N
10N
0ON
LONG WAVE FLUX (W/M2)
1000GMT 79169

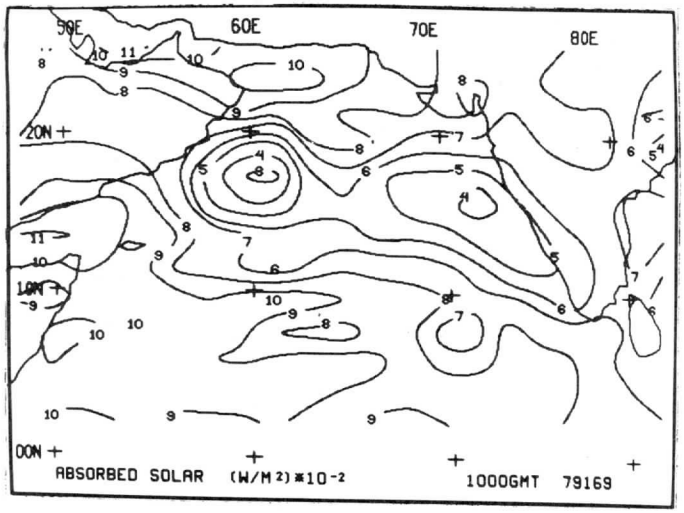
50E
60E
70E
80E
20N
10N
0ON
ABSORBED SOLAR (W/M2)*10-2
1000GMT 79169

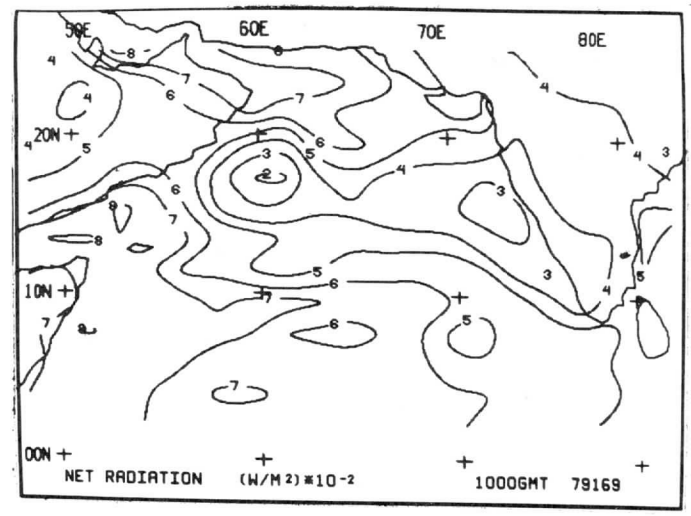
50E
60E
70E
80E
20N
10N
0ON
NET RADIATION (W/M2)*10-2
1000GMT 79169

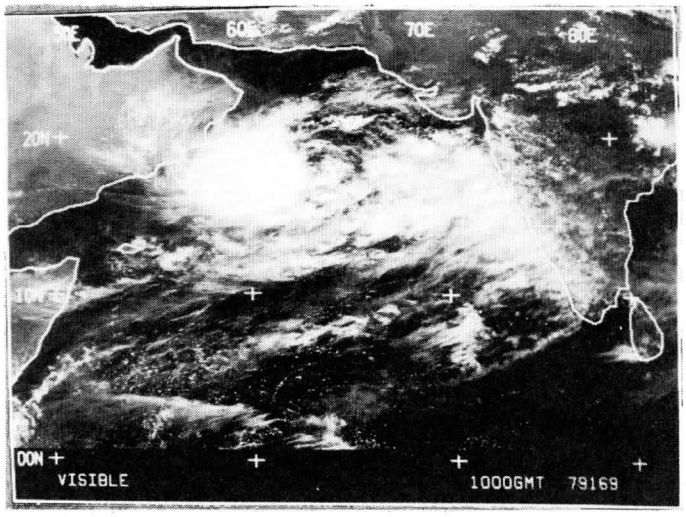
50E
60E
70E
80E
20N
10N
0ON
VISIBLE
1000GMT 79169

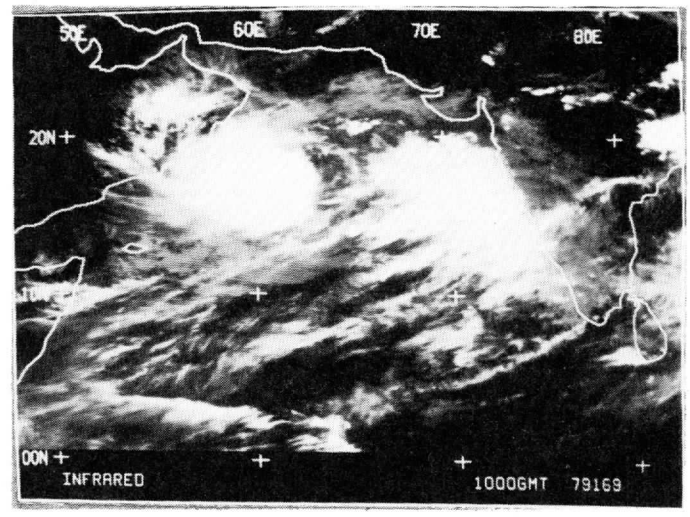
50E
60E
70E
80E
20N
10N
0ON
INFRARED
1000GMT 79169

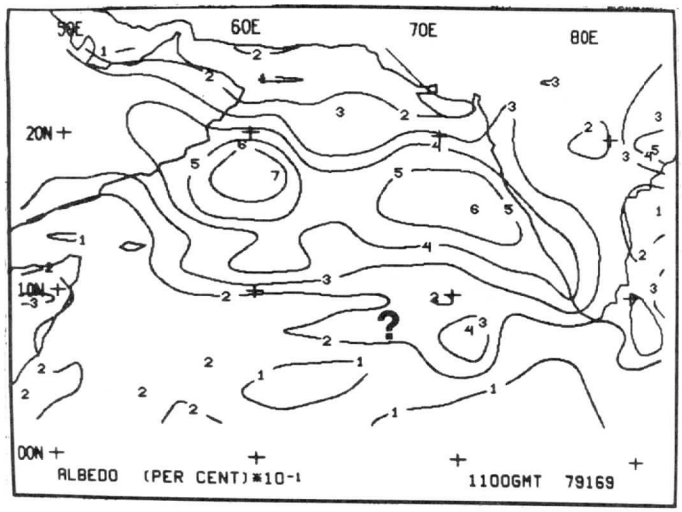
50E
60E
70E
80E
20N
10N
0ON
ALBEDO (PER CENT)*10-1
1100GMT 79169

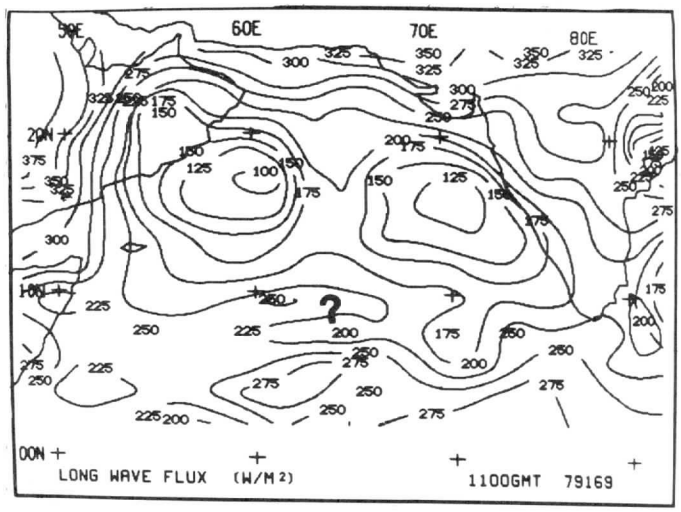
50E
60E
70E
80E
20N
10N
0ON
LONG WAVE FLUX (W/M2)
1100GMT 79169

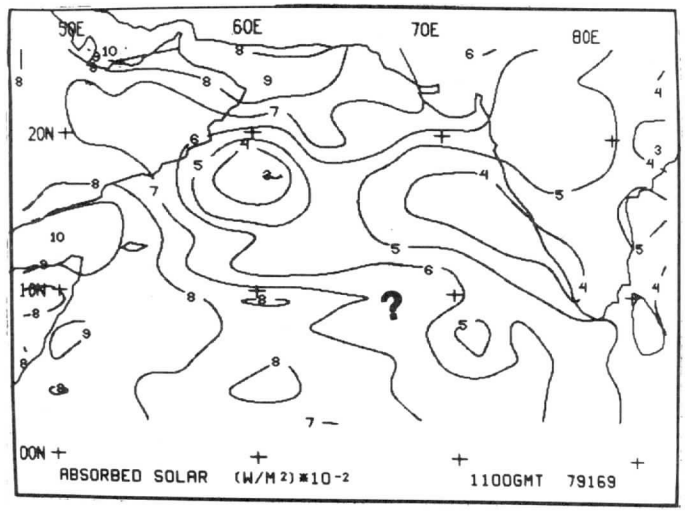
50E
60E
70E
80E
20N
10N
0ON
ABSORBED SOLAR (W/M2)*10-2
1100GMT 79169

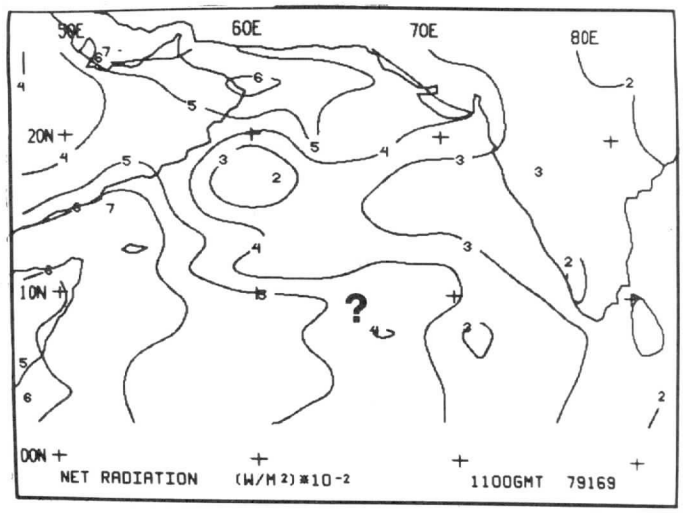
50E
60E
70E
80E
20N
10N
0ON
NET RADIATION (W/M2)*10-2
1100GMT 79169

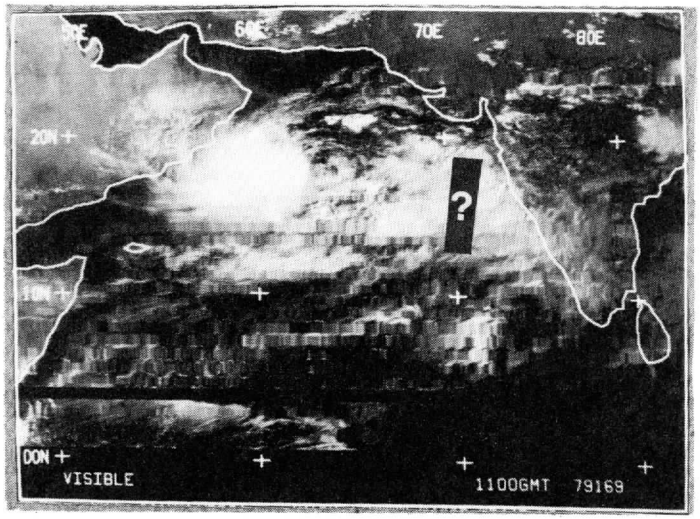
50E
60E
70E
80E
20N
10N
0ON
VISIBLE
1100GMT 79169

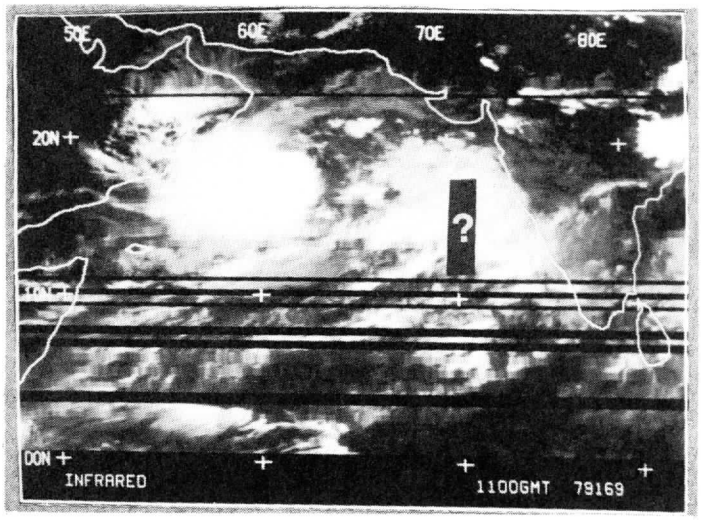
50E
60E
70E
80E
20N
0ON
INFRARED
1100GMT 79169

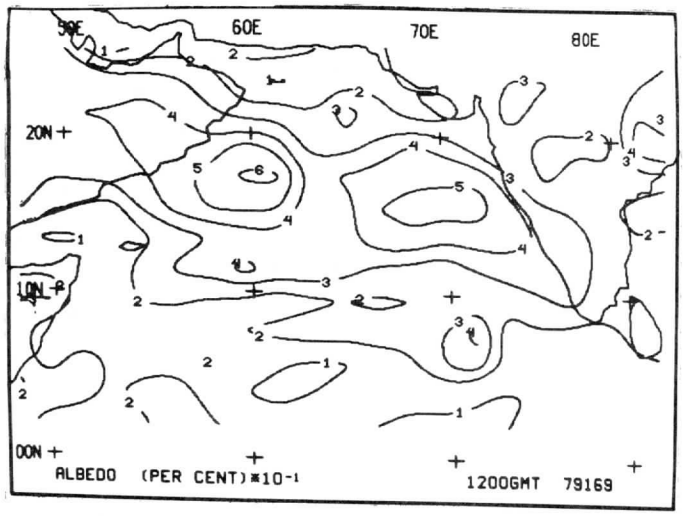
50E
60E
70E
80E
20N
10N
0ON
ALBEDO (PER CENT)*10-1
1200GMT 79169

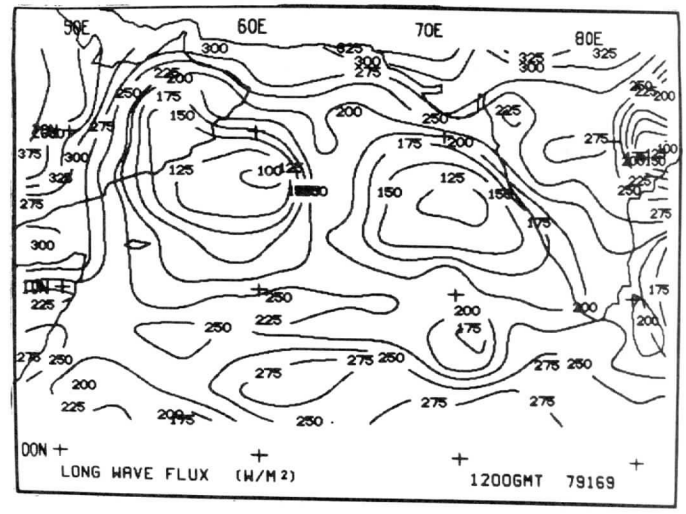
50E
60E
70E
80E
20N
10N
0ON
LONG WAVE FLUX (W/M2)
1200GMT 79169

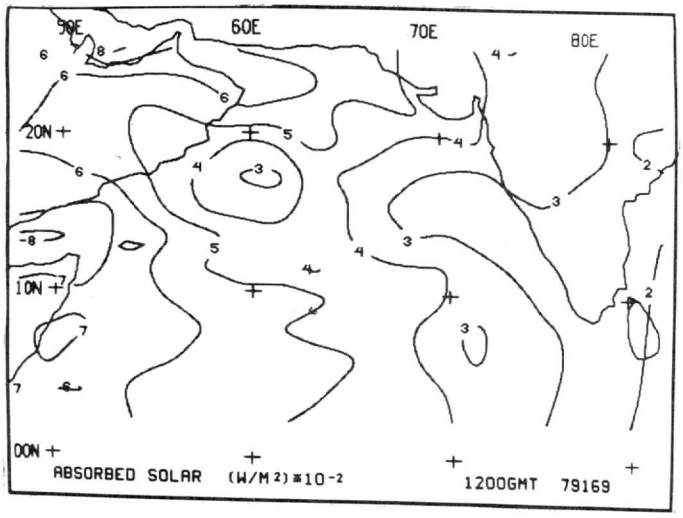
50E
60E
70E
80E
20N
10N
0ON
ABSORBED SOLAR (W/M2)*10-2
1200GMT 79169

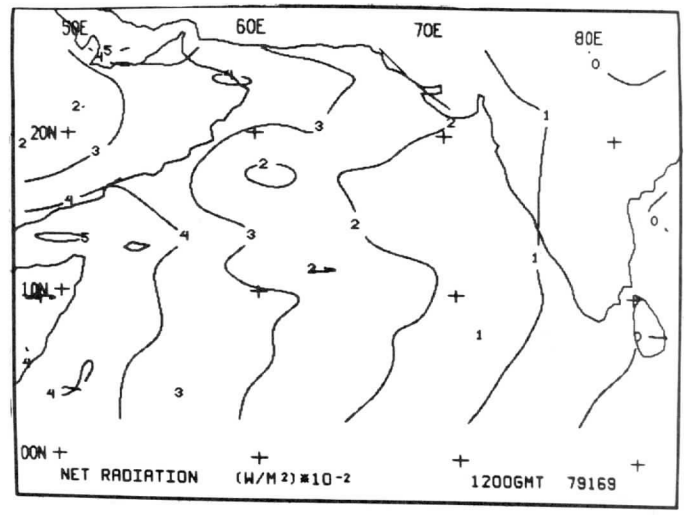
50E
60E
70E
80E
20N
10N
0ON
NET RADIATION (W/M2)*10-2
1200GMT 79169

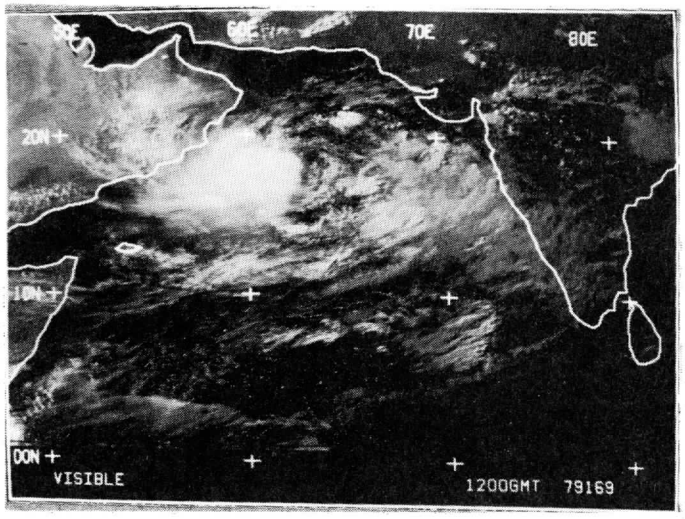
50E
60E
70E
80E
20N
10N
0ON
VISIBLE
1200GMT 79169

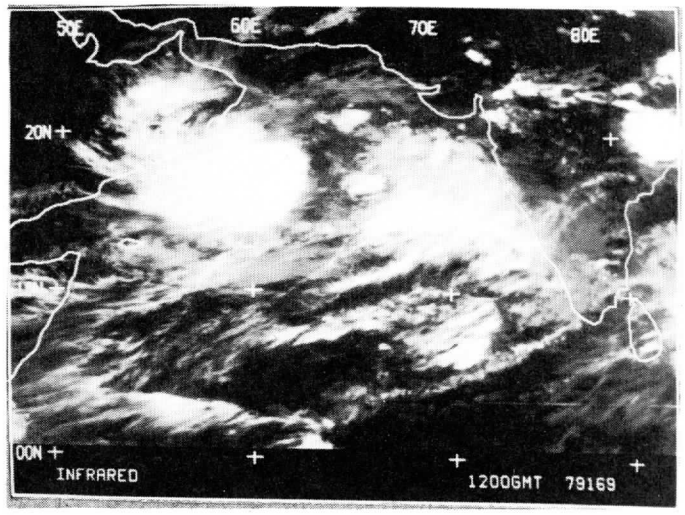
50E
60E
70E
80E
20N
0ON
INFRARED
1200GMT 79169

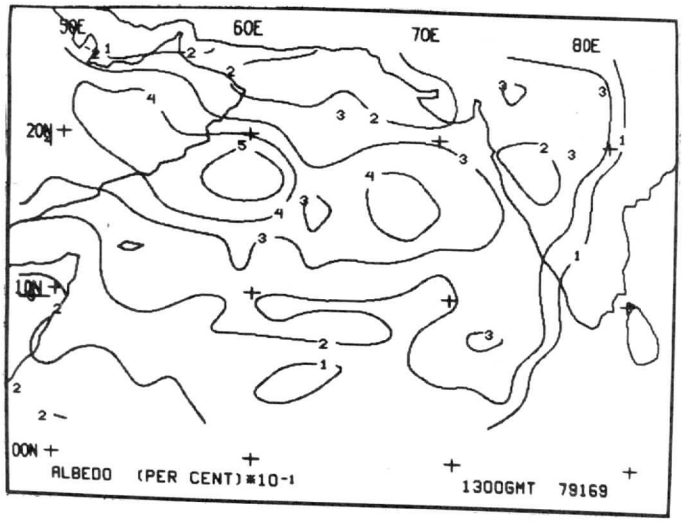
50E
60E
70E
80E
20N
10N
00N
ALBEDO (PER CENT)*10-1
1300GMT 79169

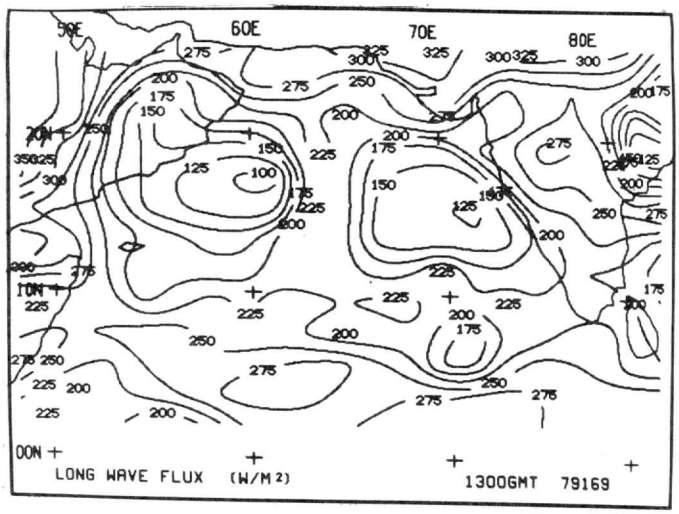
50E
60E
70E
80E
20N
10N
00N
LONG WAVE FLUX (W/M2)
1300GMT 79169

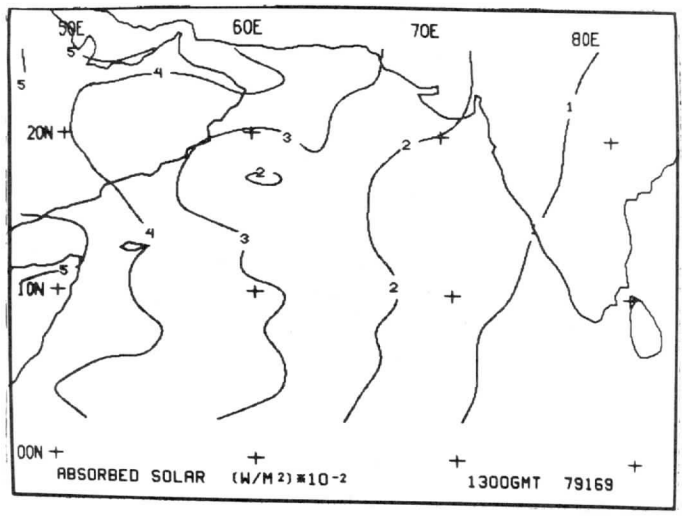
50E
60E
70E
80E
20N
10N
00N
ABSORBED SOLAR (W/M2)*10-2
1300GMT 79169

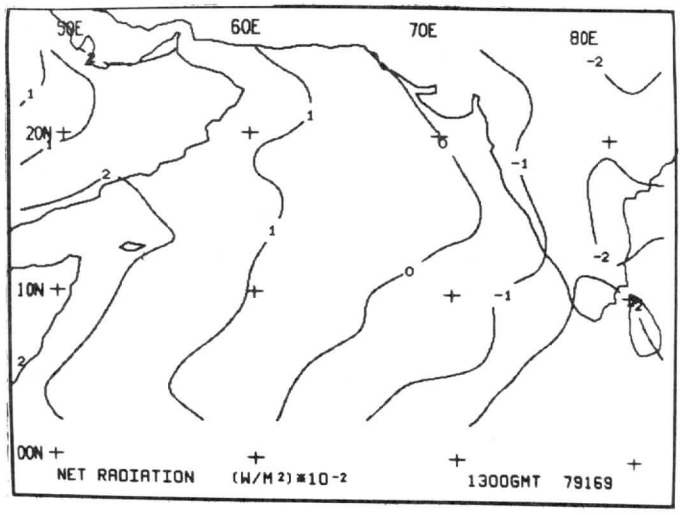
50E
60E
70E
80E
20N
10N
00N
NET RADIATION (W/M2)*10-2
1300GMT 79169

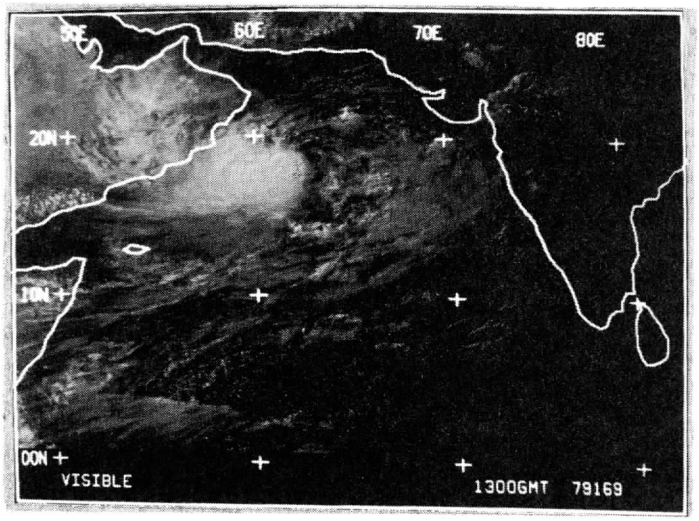
50E
60E
70E
80E
20N
10N
00N
VISIBLE
1300GMT 79169

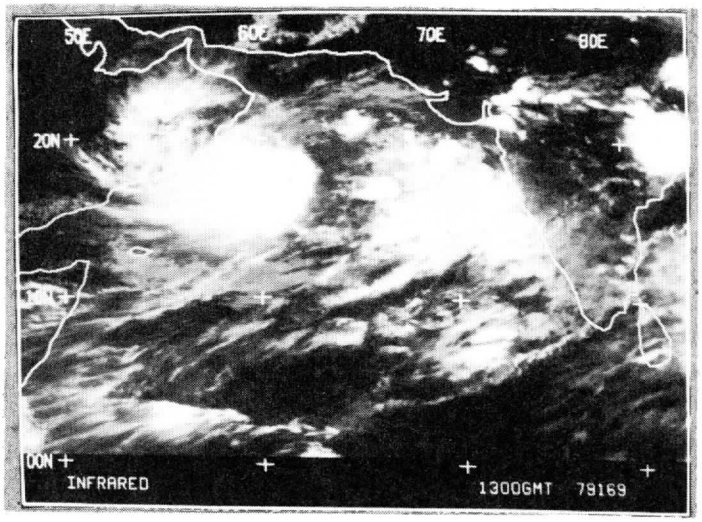
50E
60E
70E
80E
20N
10N
00N
INFRARED
1300GMT 79169

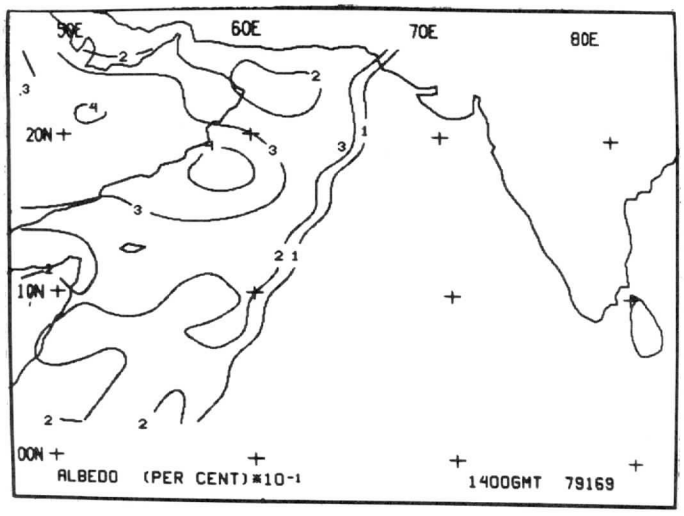
50E
60E
70E
80E
20N
10N
0ON
ALBEDO (PER CENT)*10-1
1400GMT 79169

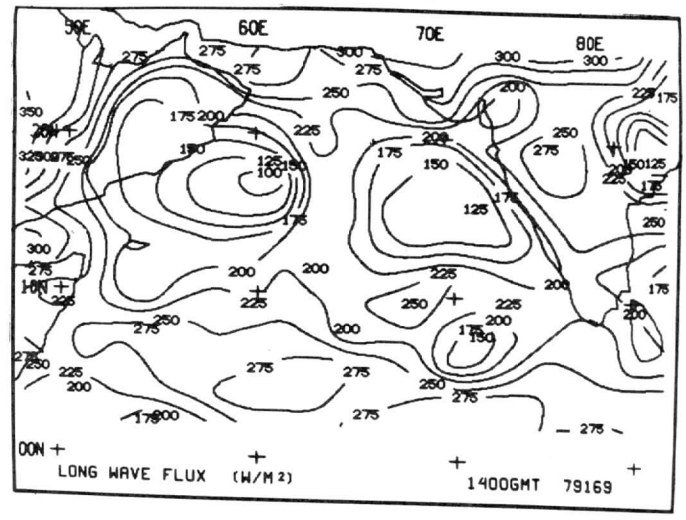
50E
60E
70E
80E
20N
10N
0ON
LONG WAVE FLUX (W/M2)
1400GMT 79169

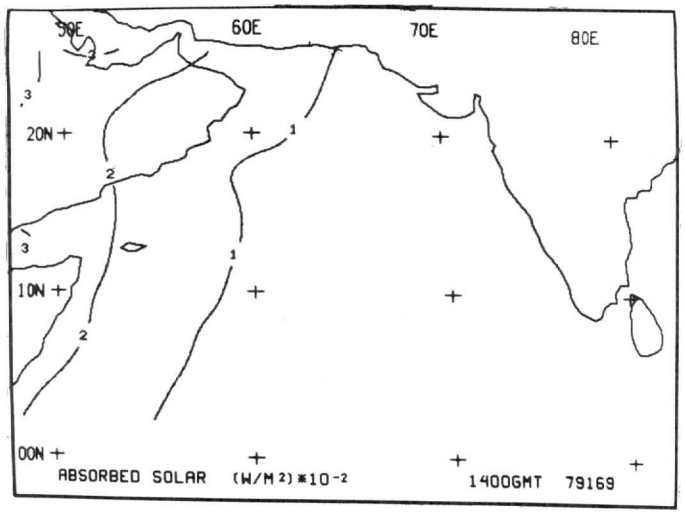
50E
60E
70E
80E
20N
10N
0ON
ABSORBED SOLAR (W/M2)*10-2
1400GMT 79169

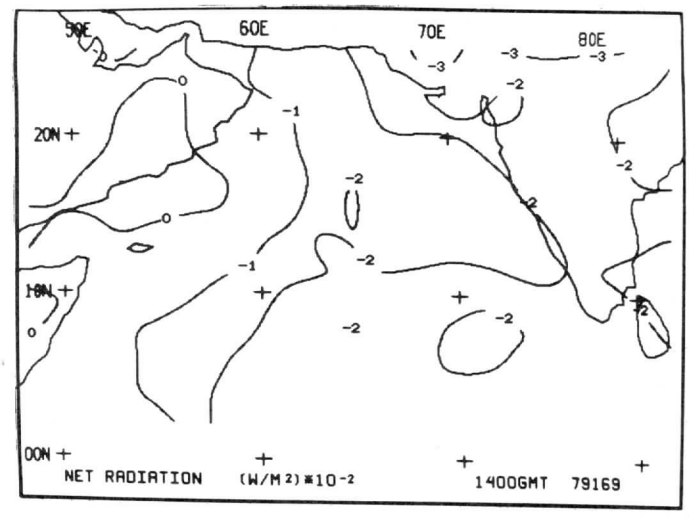
50E
60E
70E
80E
20N
10N
0ON
NET RADIATION (W/M2)*10-2
1400GMT 79169

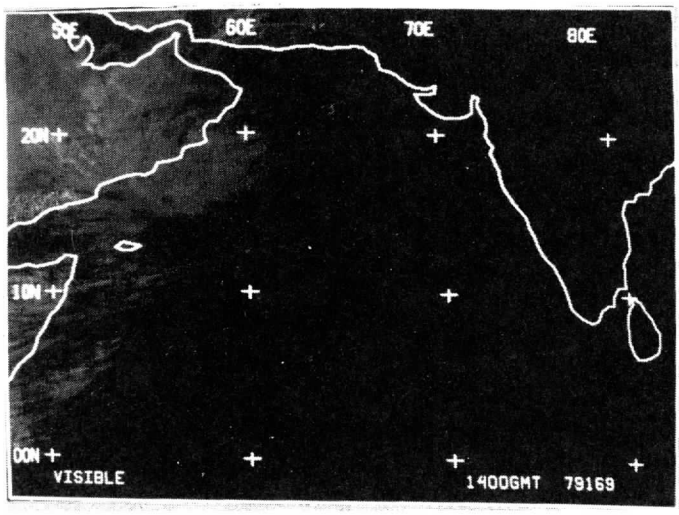
50E
60E
70E
80E
20N
10N
0ON
VISIBLE
1400GMT 79169

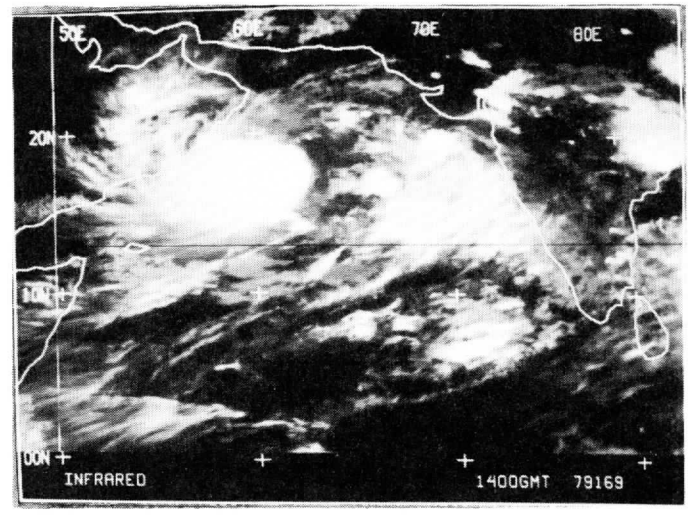
50E
60E
70E
80E
20N
0ON
INFRARED
1400GMT 79169

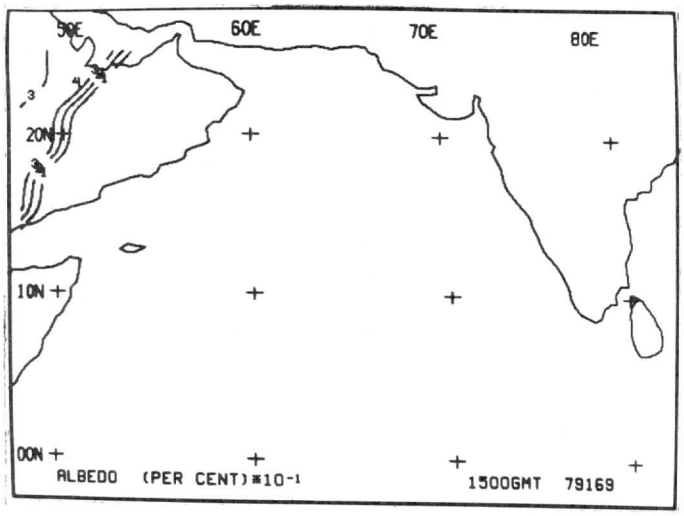
50E
60E
70E
80E
20N
10N
00N
ALBEDO (PER CENT)*10-1
1500GMT 79169

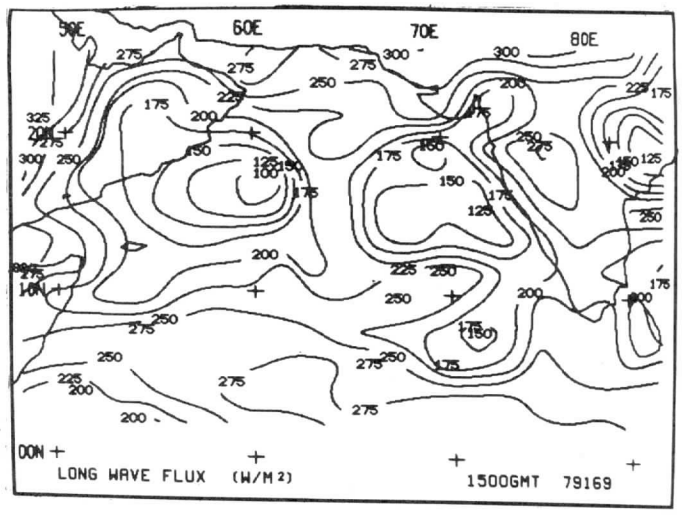
50E
60E
70E
80E
20N
10N
00N
LONG WAVE FLUX (W/M2)
1500GMT 79169

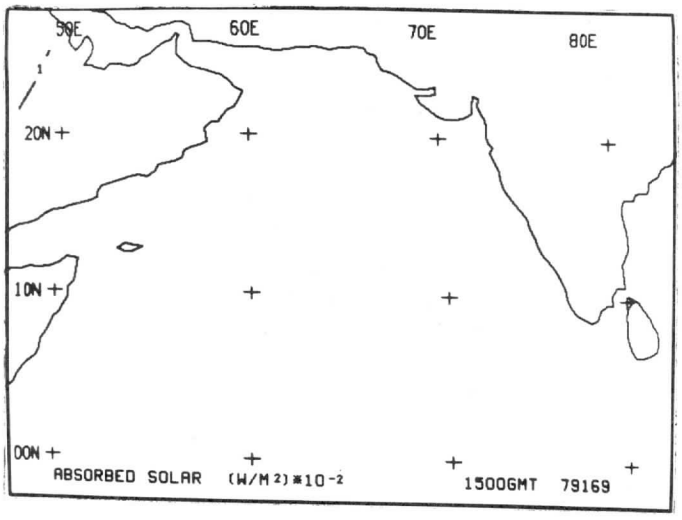
50E
60E
70E
80E
20N
10N
00N
ABSORBED SOLAR (W/M2)*10-2
1500GMT 79169

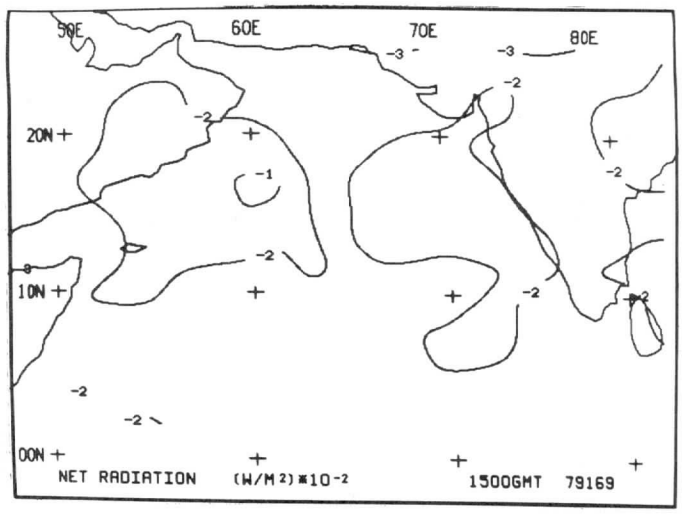
50E
60E
70E
80E
20N
10N
00N
NET RADIATION (W/M2)*10-2
1500GMT 79169

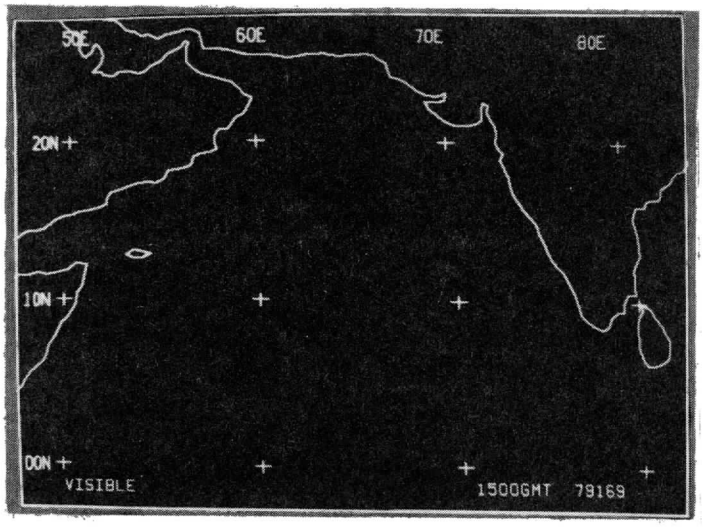
50E
60E
70E
80E
20N
10N
00N
VISIBLE
1500GMT 79169

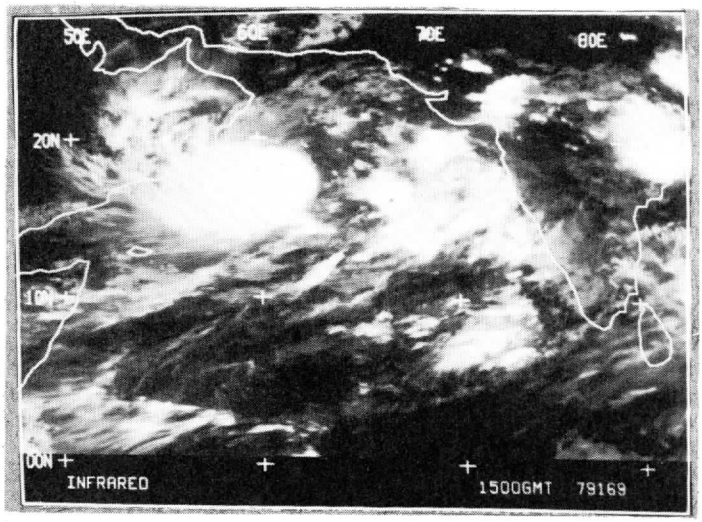
50E
60E
70E
80E
20N
10N
00N
INFRARED
1500GMT 79169

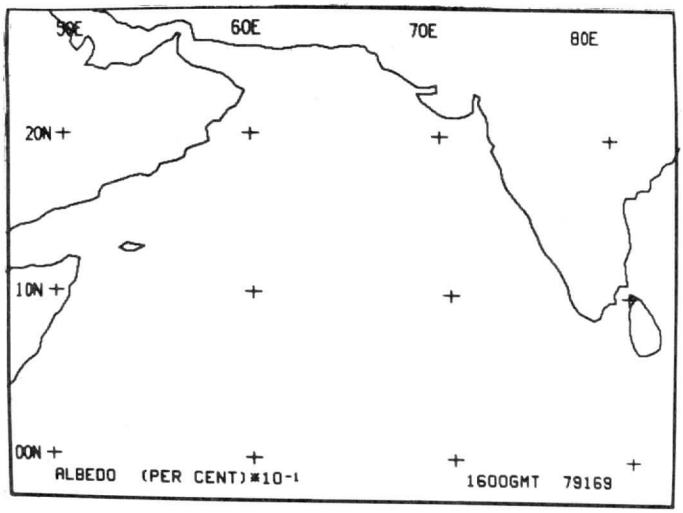
50E
60E
70E
80E
20N
10N
0ON
ALBEDO (PER CENT)*10-1
1600GMT 79169

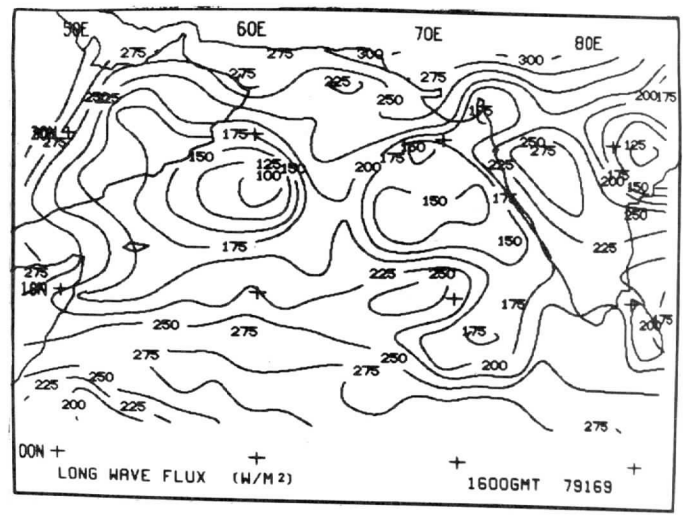
50E
60E
70E
80E
20N
10N
0ON
LONG WAVE FLUX (W/M2)
1600GMT 79169

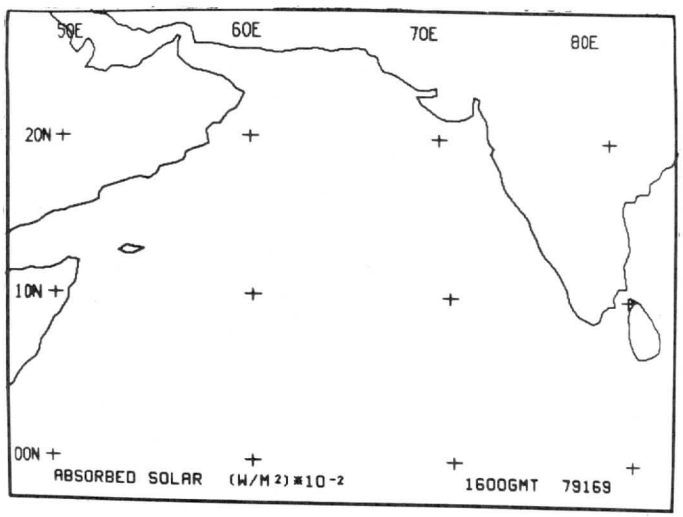
50E
60E
70E
80E
20N
10N
0ON
ABSORBED SOLAR (W/M2)*10-2
1600GMT 79169

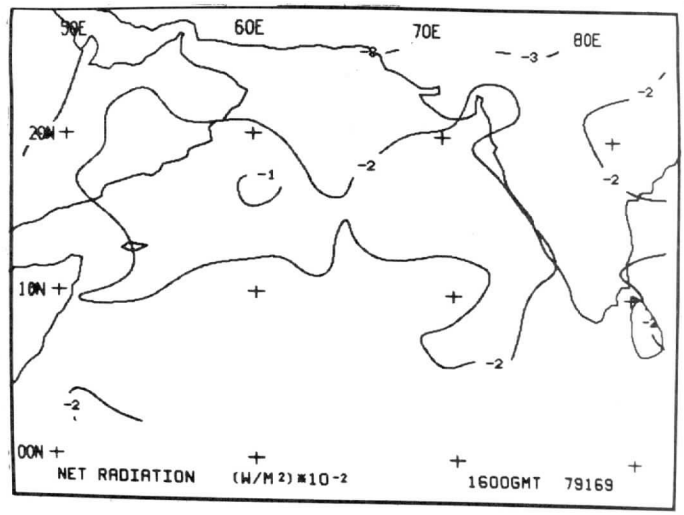
50E
60E
70E
80E
20N
10N
0ON
NET RADIATION (W/M2)*10-2
1600GMT 79169

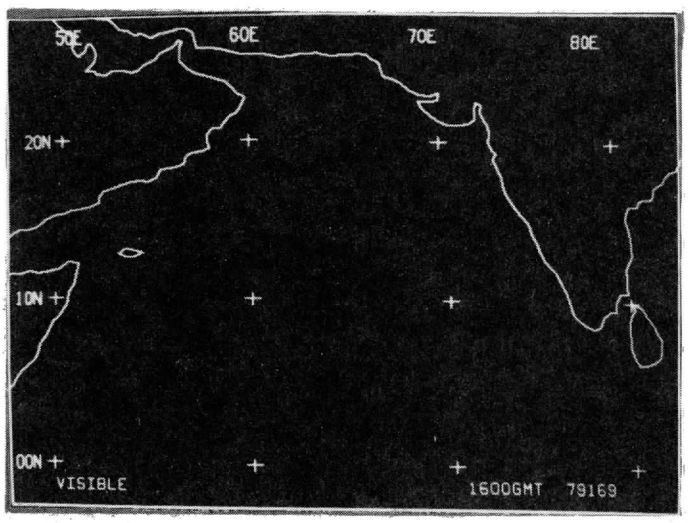
50E
60E
70E
80E
20N
10N
0ON
VISIBLE
1600GMT 79169

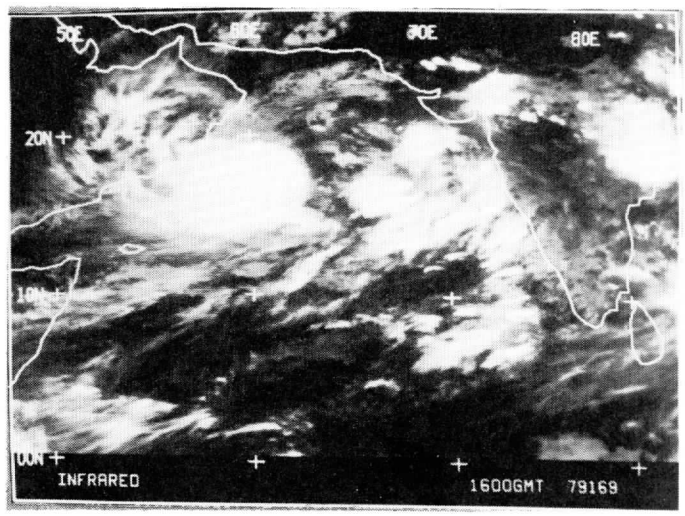
50E
80E
20N
10N
0ON
INFRARED
1600GMT 79169

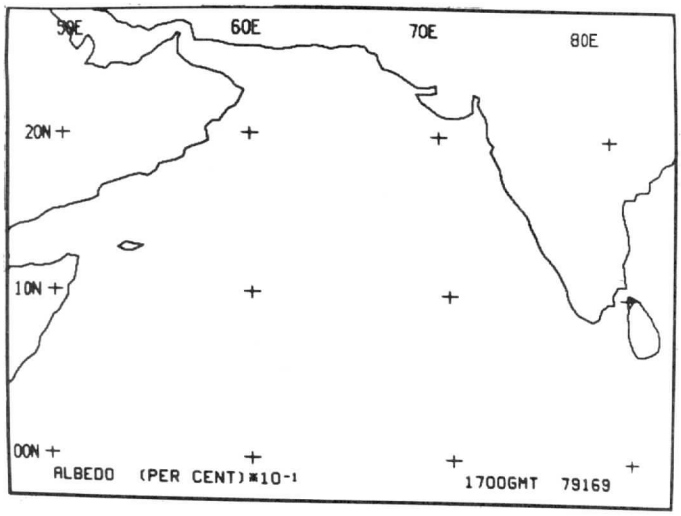
50E
60E
70E
80E
20N
10N
0ON
ALBEDO (PER CENT)*10-1
1700GMT 79169

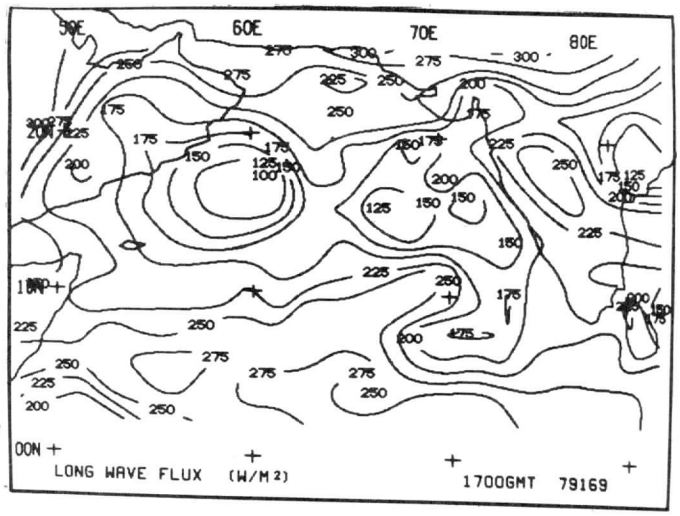
50E
60E
70E
80E
20N
10N
0ON
LONG WAVE FLUX (W/M2)
1700GMT 79169

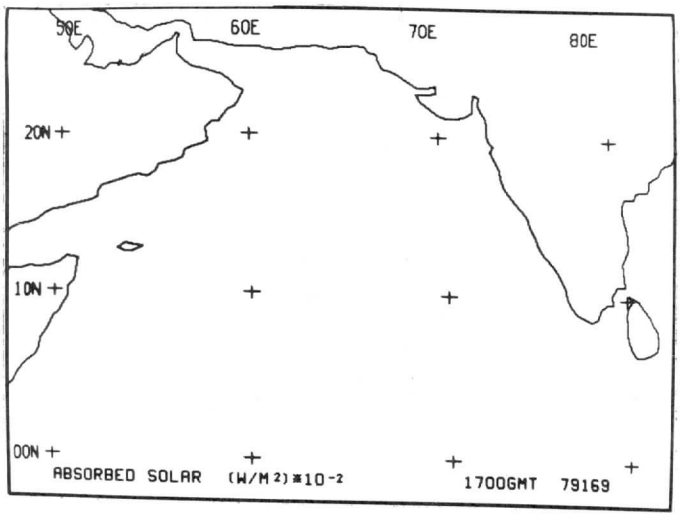
50E
60E
70E
80E
20N
10N
0ON
ABSORBED SOLAR (W/M2)*10-2
1700GMT 79169

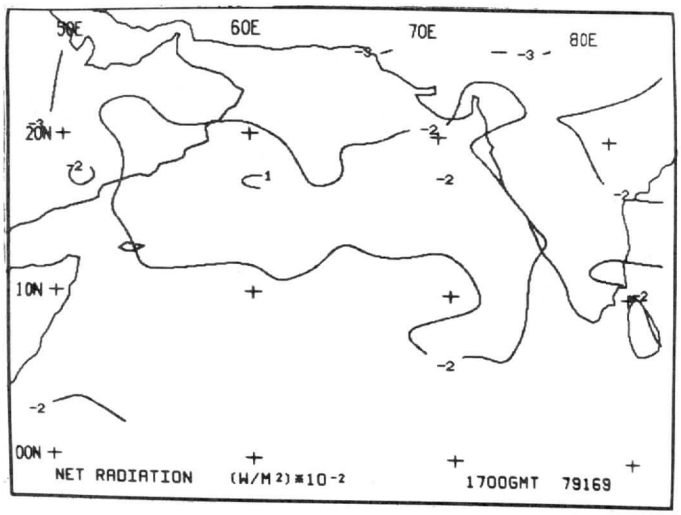
50E
60E
70E
80E
20N
10N
0ON
NET RADIATION (W/M2)*10-2
1700GMT 79169

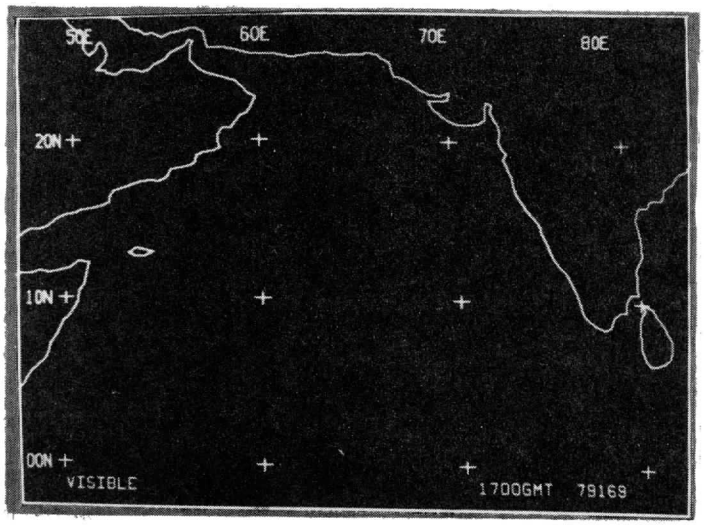
50E
60E
70E
80E
20N
10N
0ON
VISIBLE
1700GMT 79169

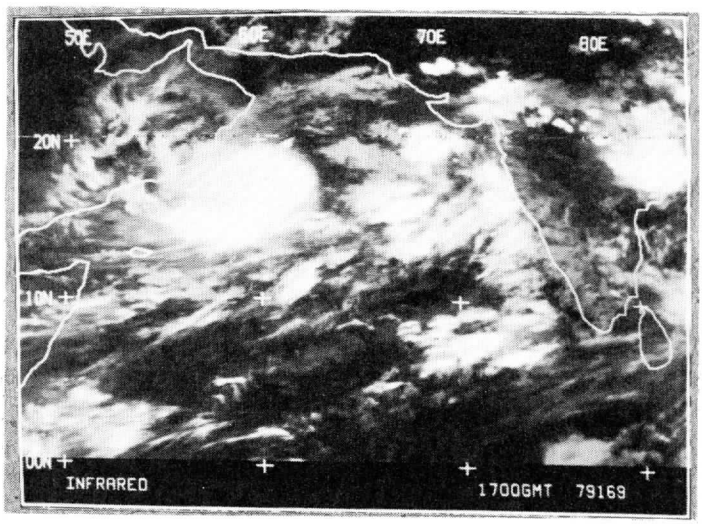
50E
70E
80E
20N
10N
0ON
INFRARED
1700GMT 79169

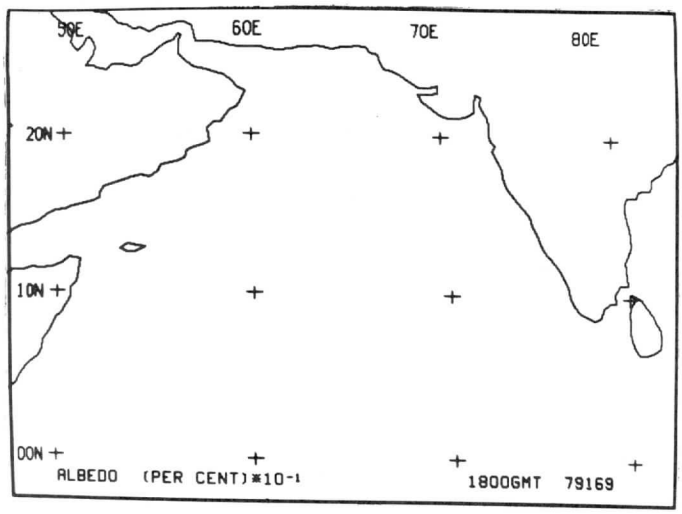
50E
60E
70E
80E
20N
10N
00N
ALBEDO (PER CENT)*10-1
1800GMT 79169

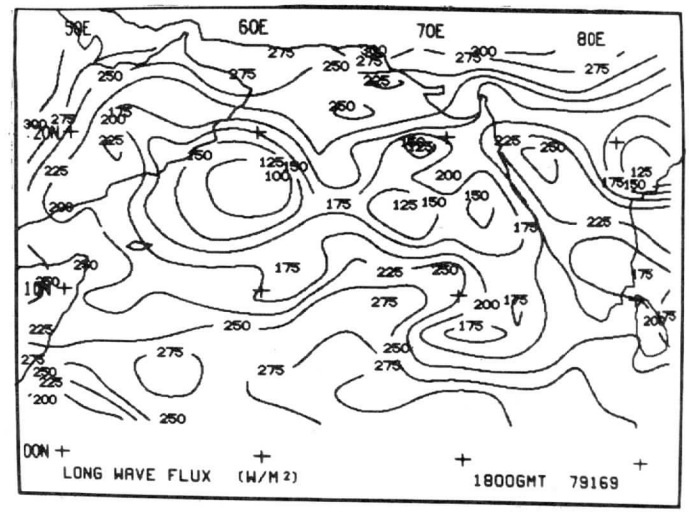
50E
60E
70E
80E
20N
10N
00N
LONG WAVE FLUX (W/M2)
1800GMT 79169

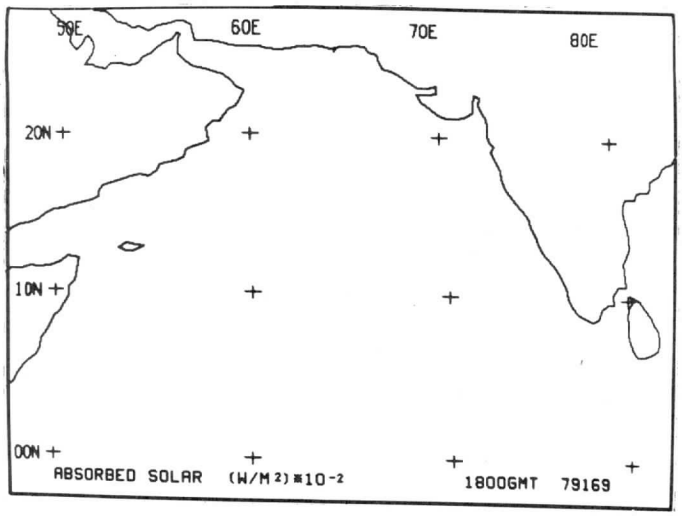
50E
60E
70E
80E
20N
10N
00N
ABSORBED SOLAR (W/M2)*10-2
1800GMT 79169

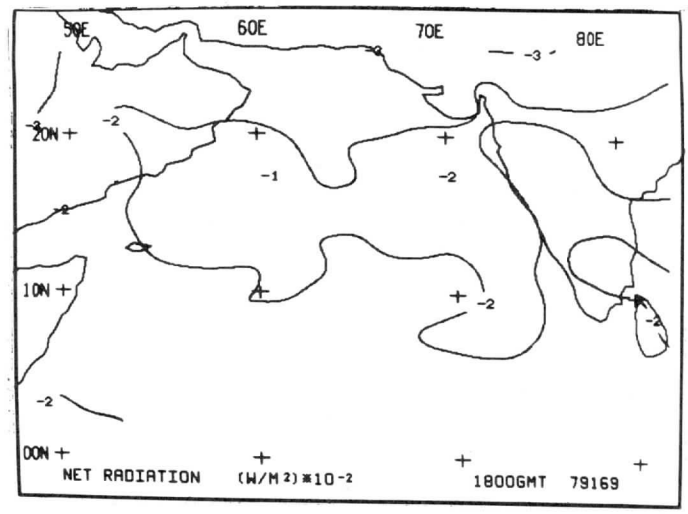
50E
60E
70E
80E
20N
10N
00N
NET RADIATION (W/M2)*10-2
1800GMT 79169

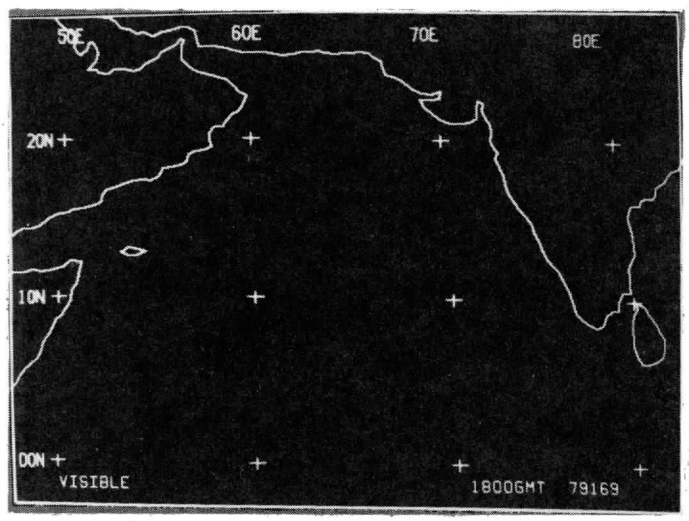
50E
60E
70E
80E
20N
10N
00N
VISIBLE
1800GMT 79169

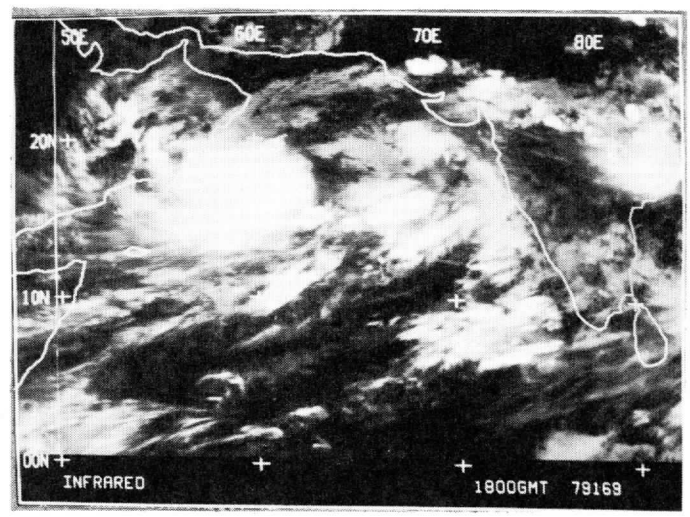
50E
60E
70E
80E
20N
10N
00N
INFRARED
1800GMT 79169

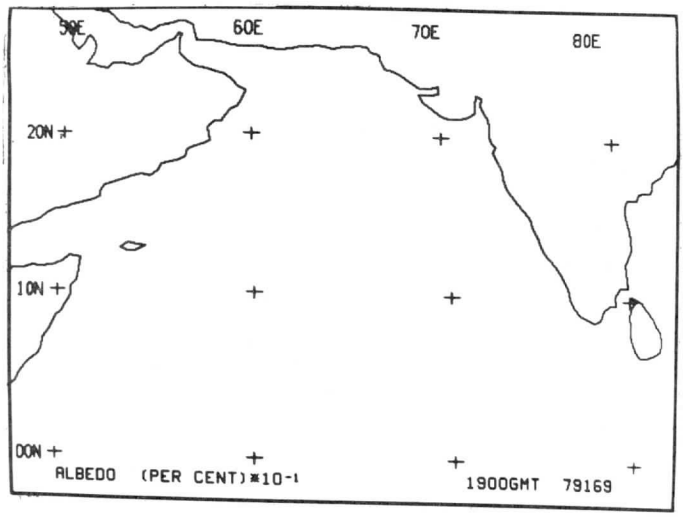
50E
60E
70E
80E
20N
10N
0ON
ALBEDO (PER CENT)*10-1
1900GMT 79169

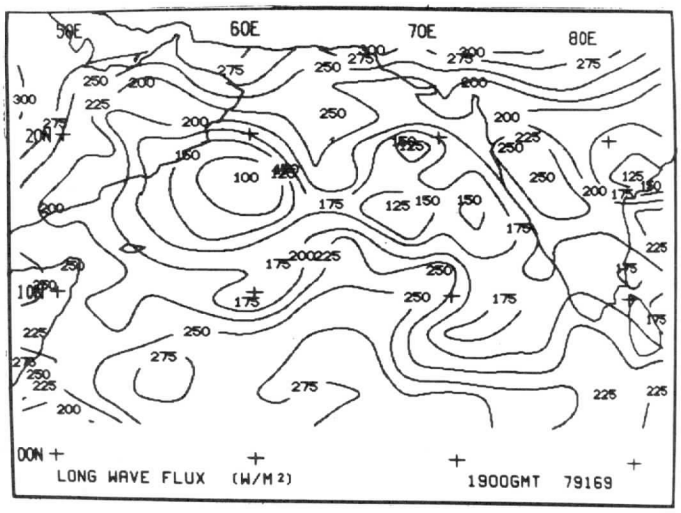
50E
60E
70E
80E
20N
10N
0ON
LONG WAVE FLUX (W/M2)
1900GMT 79169

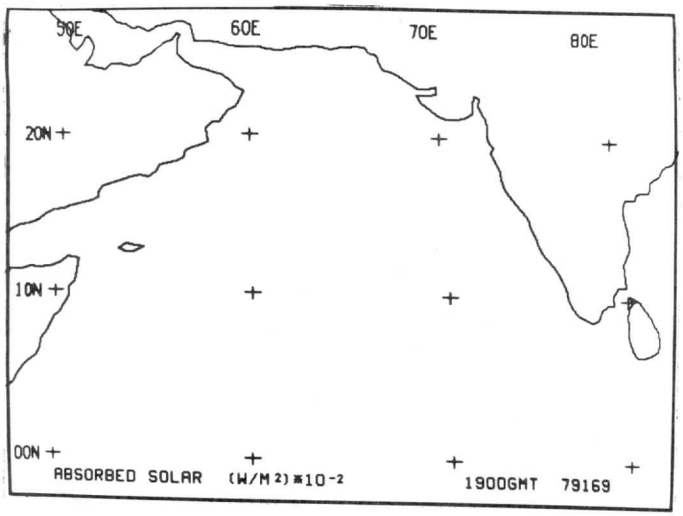
50E
60E
70E
80E
20N
10N
0ON
ABSORBED SOLAR (W/M2)*10-2
1900GMT 79169

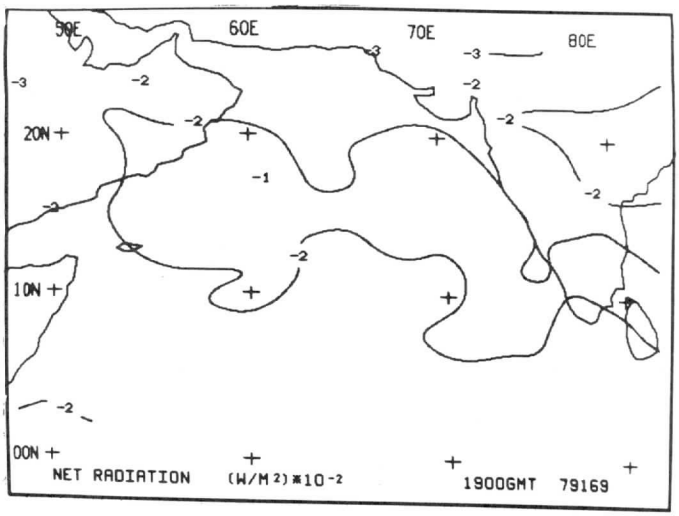
50E
60E
70E
80E
20N
10N
0ON
NET RADIATION (W/M2)*10-2
1900GMT 79169

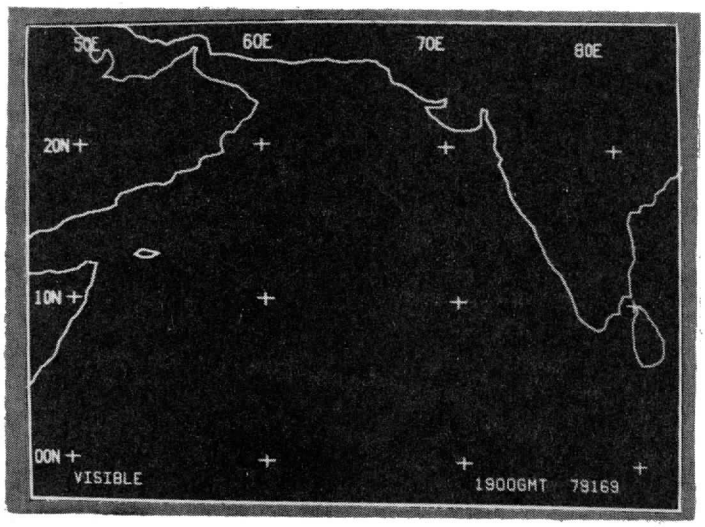
50E
60E
70E
80E
20N
10N
0ON
VISIBLE
1900GMT 79169

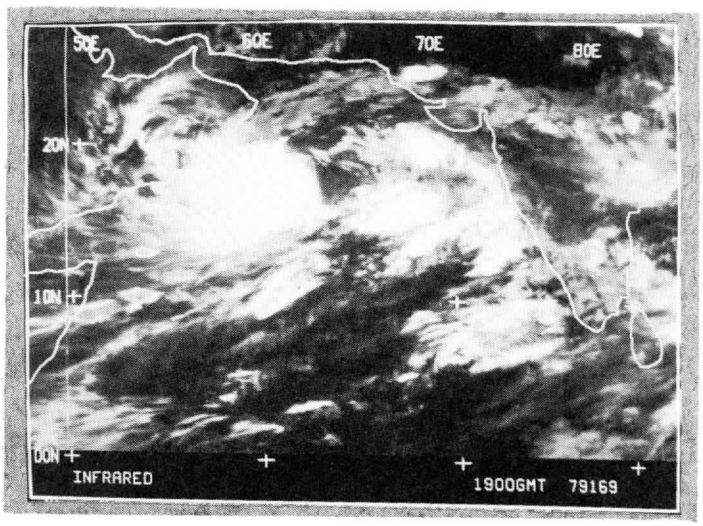
50E
60E
70E
80E
20N
10N
0ON
INFRARED
1900GMT 79169

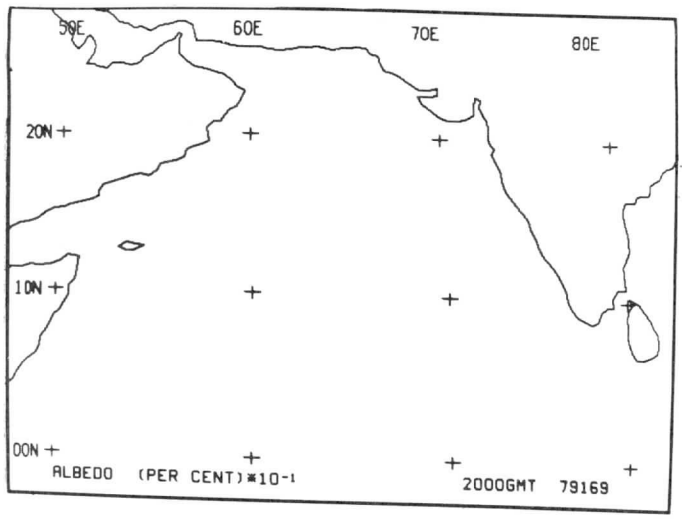
50E
60E
70E
80E
20N
10N
00N
ALBEDO (PER CENT)*10-1
2000GMT 79169

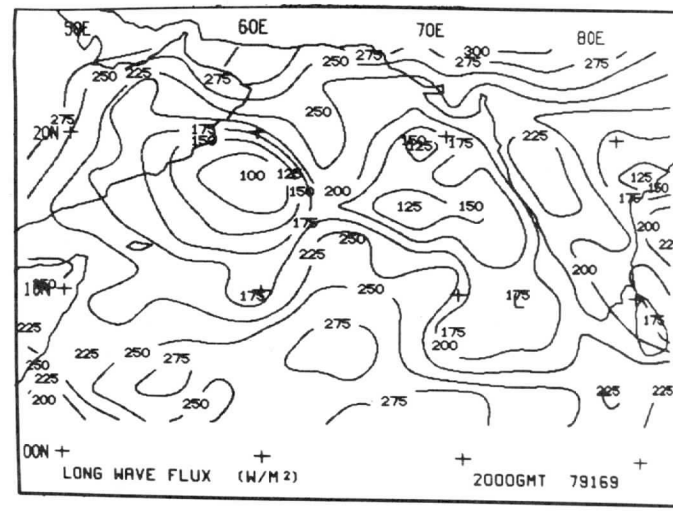
50E
60E
70E
80E
20N
10N
00N
LONG WAVE FLUX (W/M2)
2000GMT 79169

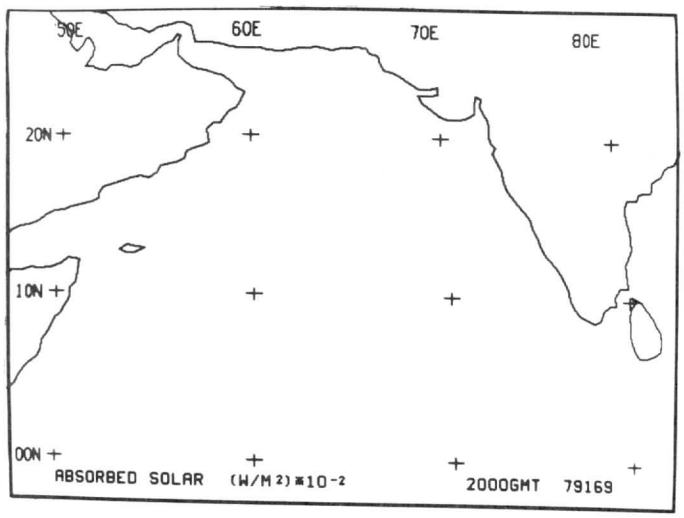
50E
60E
70E
80E
20N
10N
00N
ABSORBED SOLAR (W/M2)*10-2
2000GMT 79169

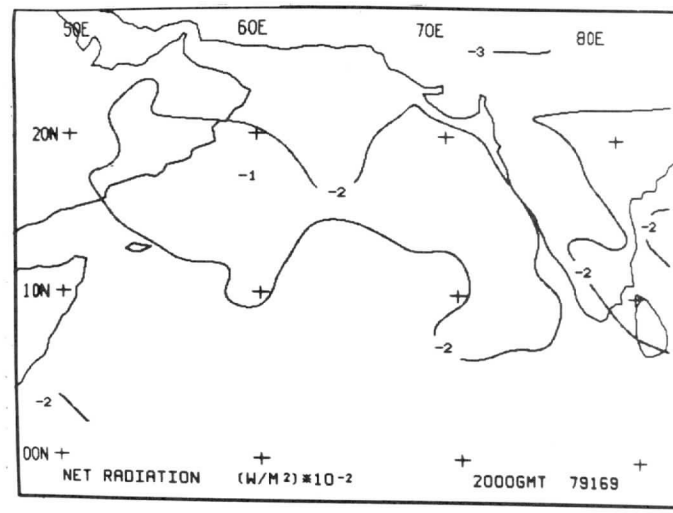
50E
60E
70E
80E
20N
10N
00N
NET RADIATION (W/M2)*10-2
2000GMT 79169

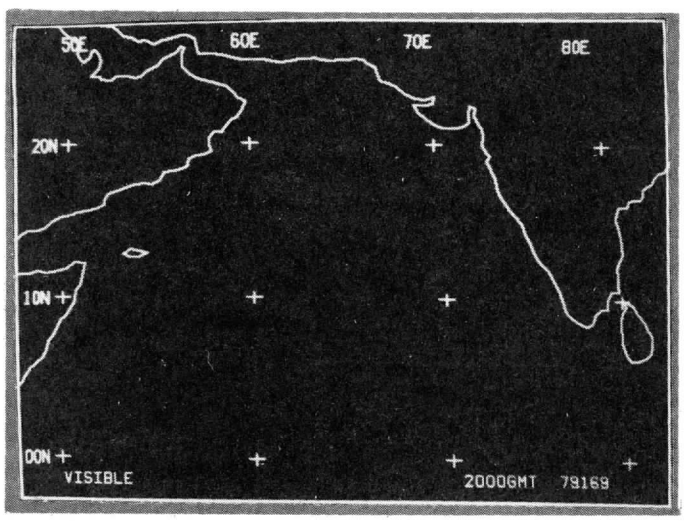
50E
60E
70E
80E
20N
10N
00N
VISIBLE
2000GMT 79169

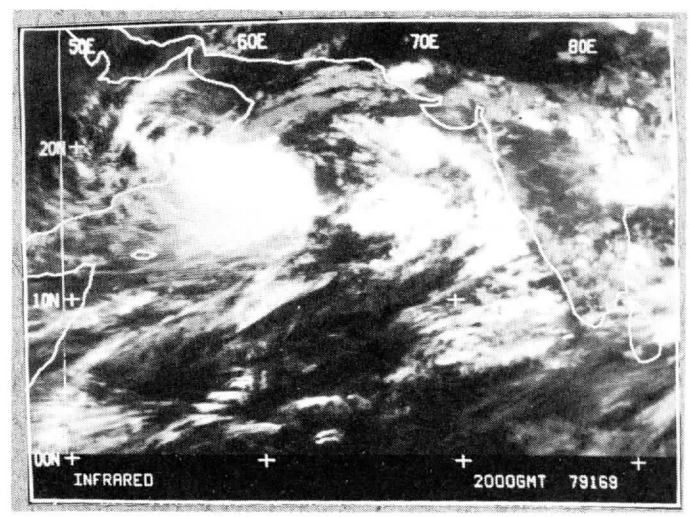
50E
60E
70E
80E
20N
10N
00N
INFRARED
2000GMT 79169

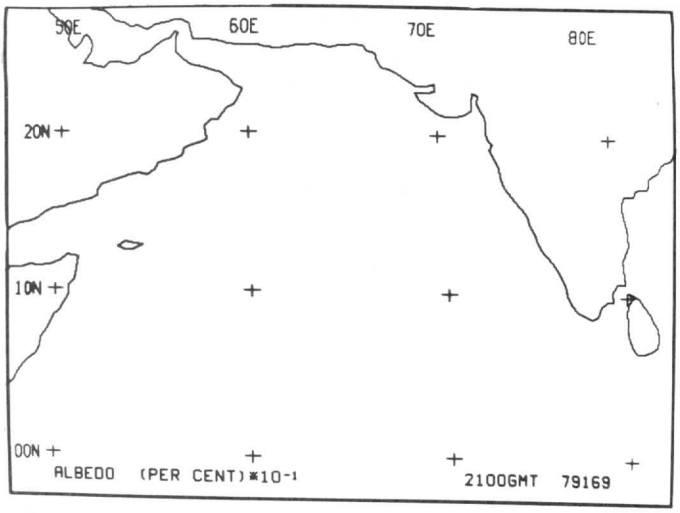
50E
60E
70E
80E
20N
10N
0ON
ALBEDO (PER CENT)*10-1
2100GMT 79169

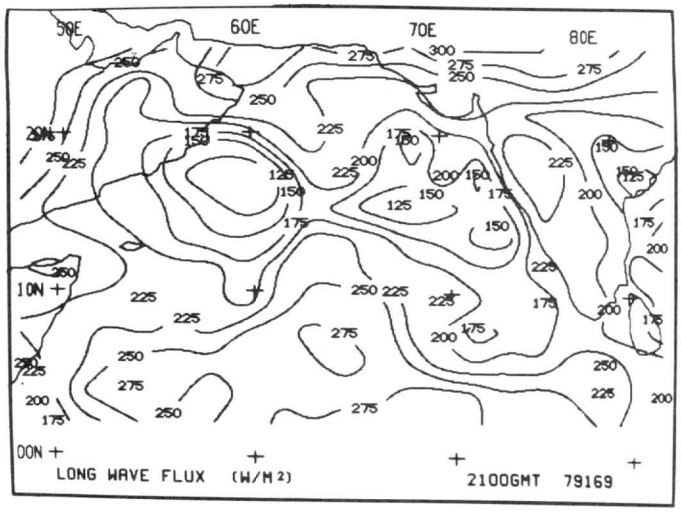
50E
60E
70E
80E
20N
10N
0ON
LONG WAVE FLUX (W/M2)
2100GMT 79169

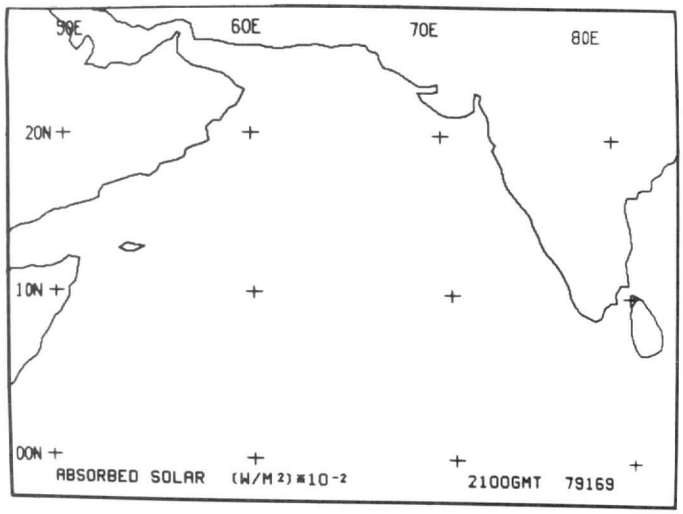
50E
60E
70E
80E
20N
10N
0ON
ABSORBED SOLAR (W/M2)*10-2
2100GMT 79169

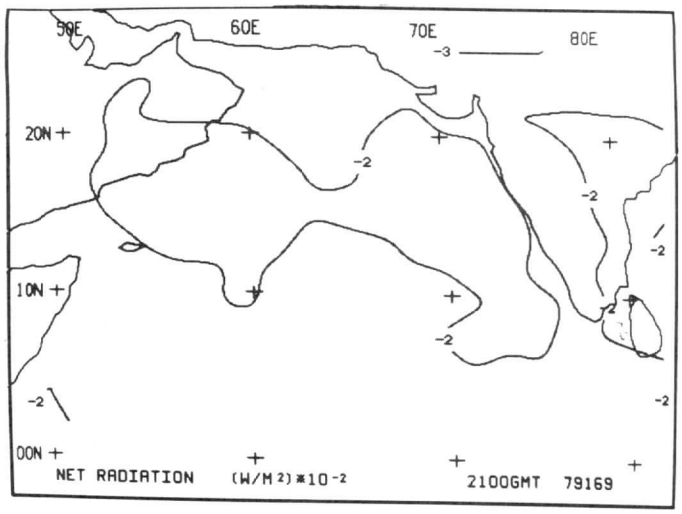
50E
60E
70E
80E
20N
10N
0ON
NET RADIATION (W/M2)*10-2
2100GMT 79169

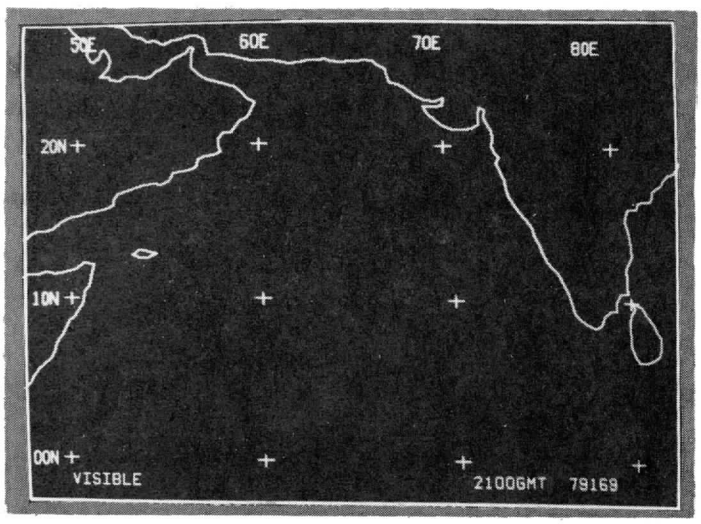
50E
60E
70E
80E
20N
10N
0ON
VISIBLE
2100GMT 79169

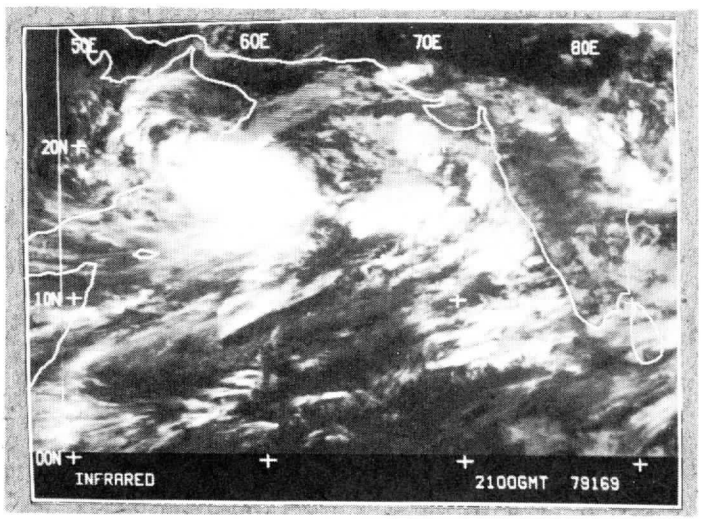
50E
60E
70E
80E
20N
10N
0ON
INFRARED
2100GMT 79169

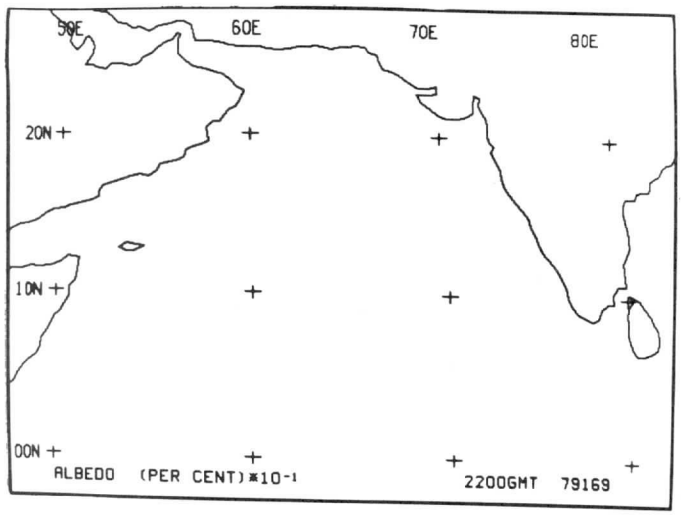
50E
60E
70E
80E
20N
10N
0ON
ALBEDO (PER CENT)*10-1
2200GMT 79169

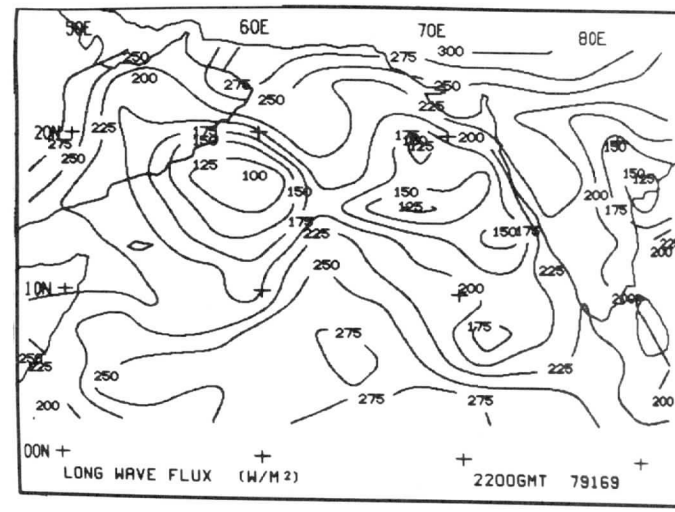
50E
60E
70E
80E
20N
10N
0ON
LONG WAVE FLUX (W/M2)
2200GMT 79169

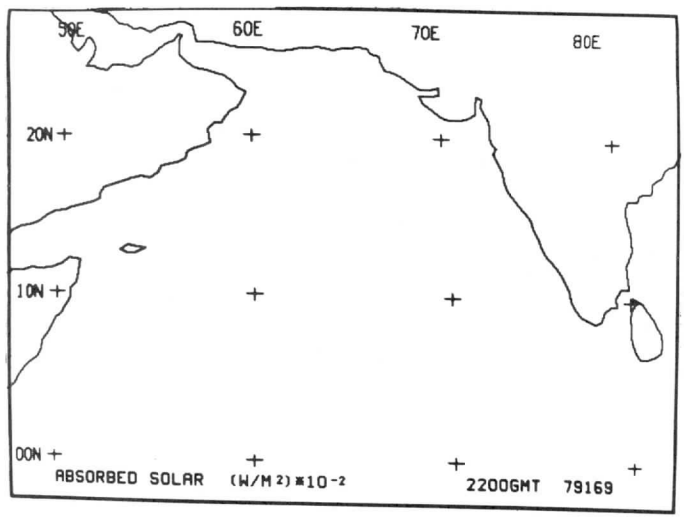
50E
60E
70E
80E
20N
10N
0ON
ABSORBED SOLAR (W/M2)*10-2
2200GMT 79169

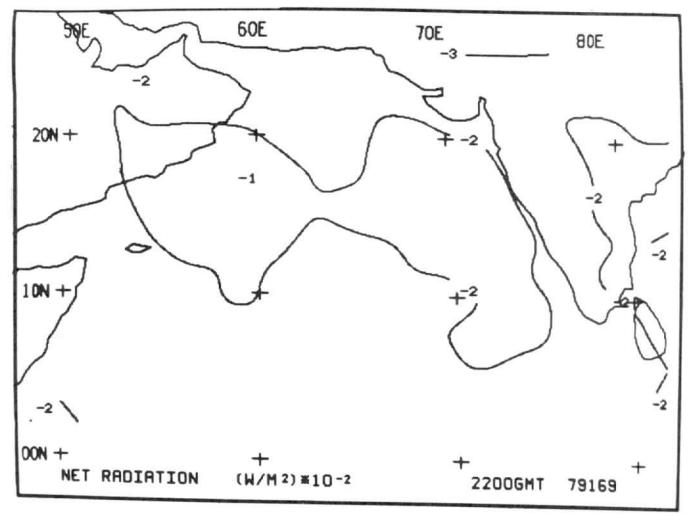
50E
60E
70E
80E
20N
10N
0ON
NET RADIATION (W/M2)*10-2
2200GMT 79169

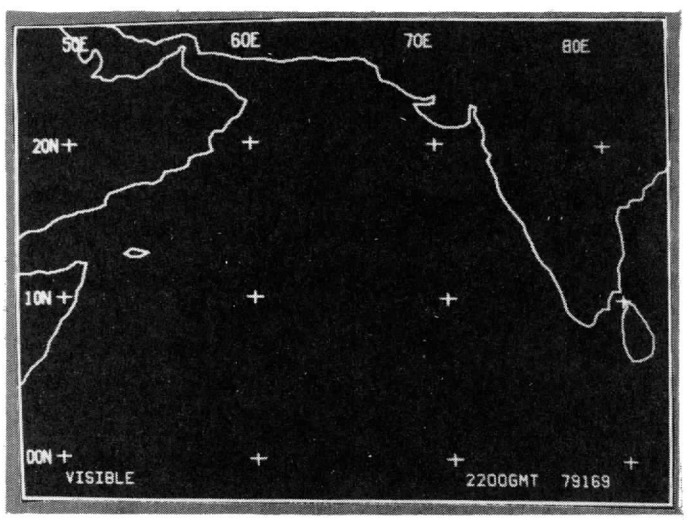
50E
60E
70E
80E
20N
10N
0ON
VISIBLE
2200GMT 79169

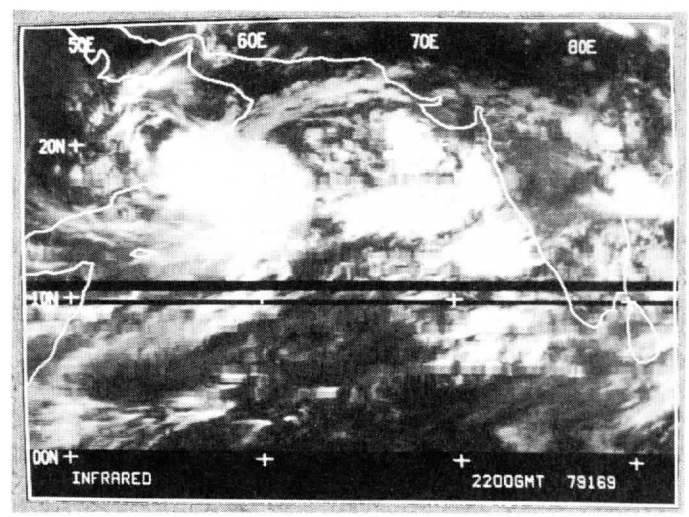
50E
60E
70E
80E
20N
10N
0ON
INFRARED
2200GMT 79169

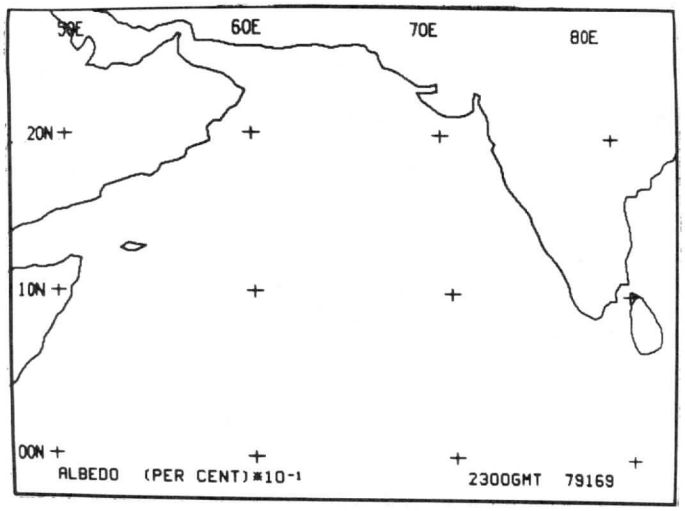
50E
60E
70E
80E
20N
10N
00N
ALBEDO (PER CENT)*10-1
2300GMT 79169

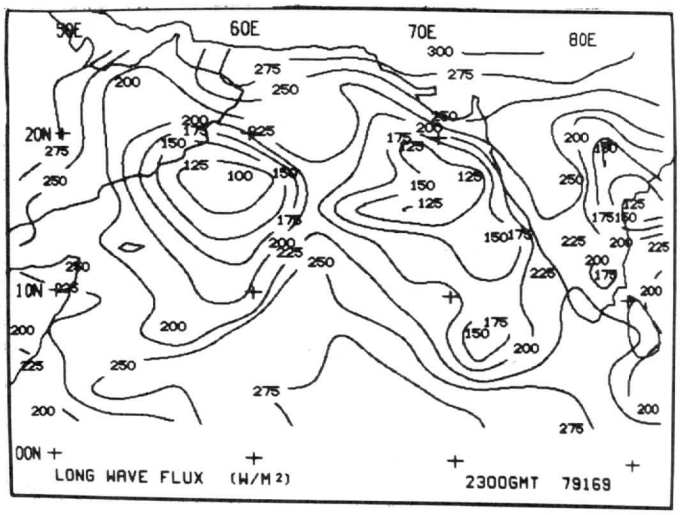
50E
60E
70E
80E
20N
10N
00N
LONG WAVE FLUX (W/M2)
2300GMT 79169

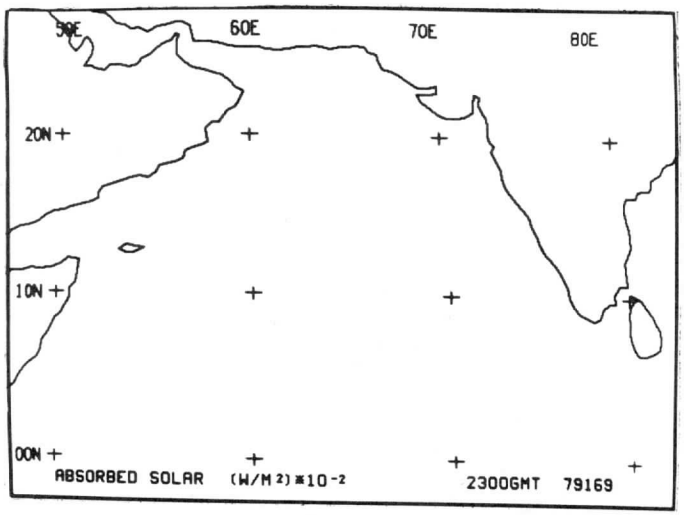
50E
60E
70E
80E
20N
10N
00N
ABSORBED SOLAR (W/M2)*10-2
2300GMT 79169

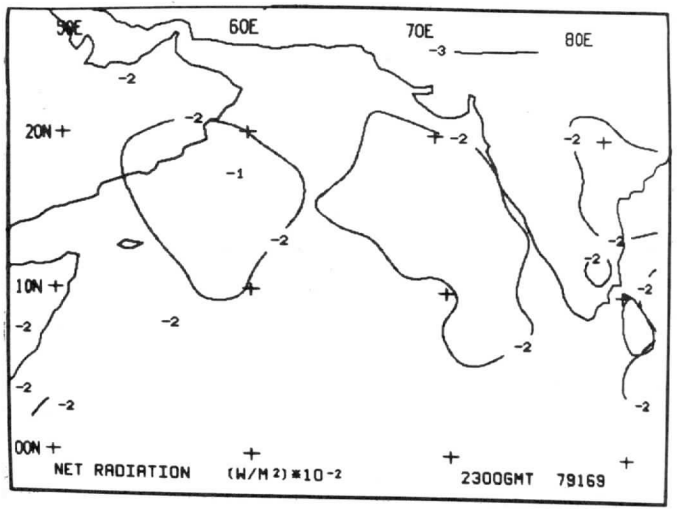
50E
60E
70E
80E
20N
10N
00N
NET RADIATION (W/M2)*10-2
2300GMT 79169

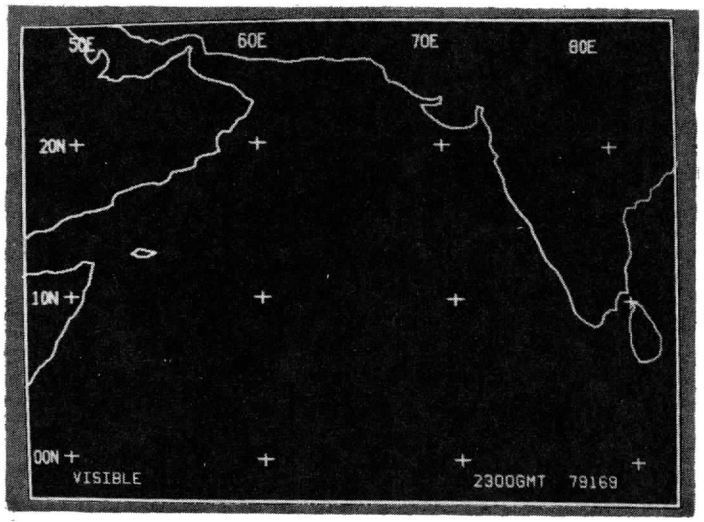
50E
60E
70E
80E
20N
10N
00N
VISIBLE
2300GMT 79169

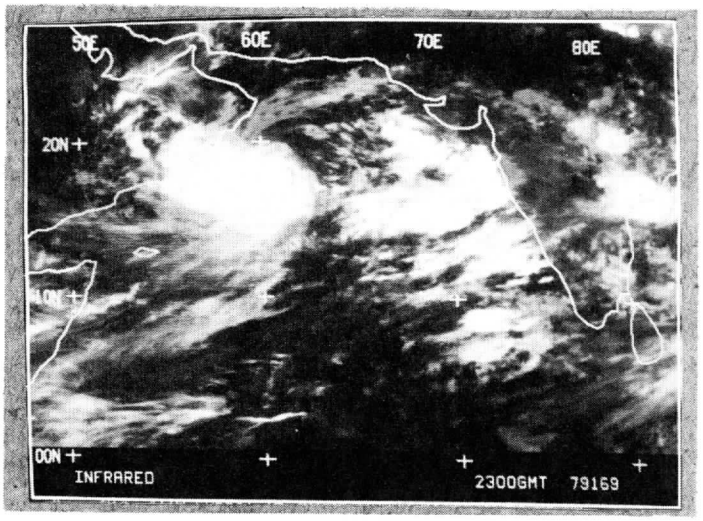
50E
60E
70E
80E
20N
00N
INFRARED
2300GMT 79169

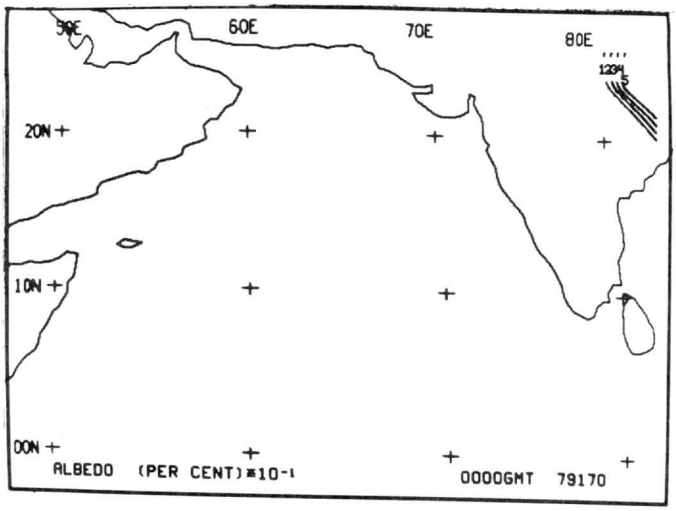
50E
60E
70E
80E
20N
10N
0ON
ALBEDO (PER CENT)*10-1
0000GMT 79170

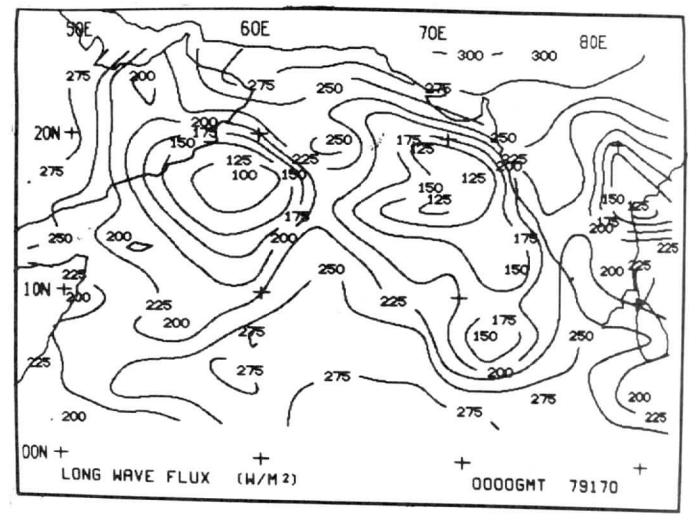
50E
60E
70E
80E
20N
10N
0ON
LONG WAVE FLUX (W/M2)
0000GMT 79170

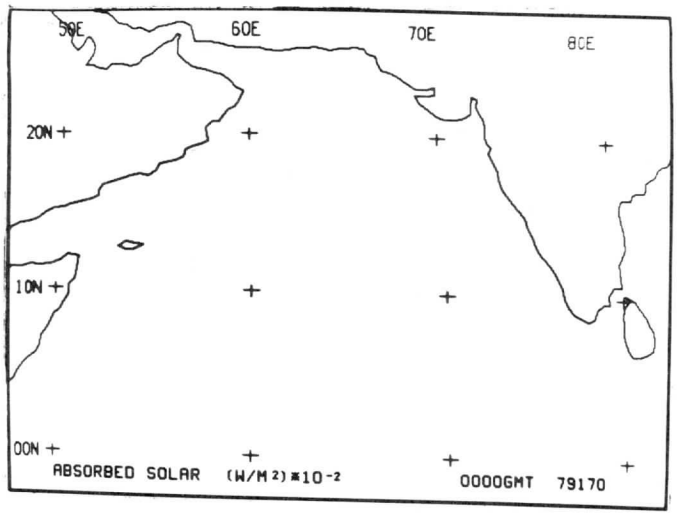
50E
60E
70E
80E
20N
10N
0ON
ABSORBED SOLAR (W/M2)*10-2
0000GMT 79170

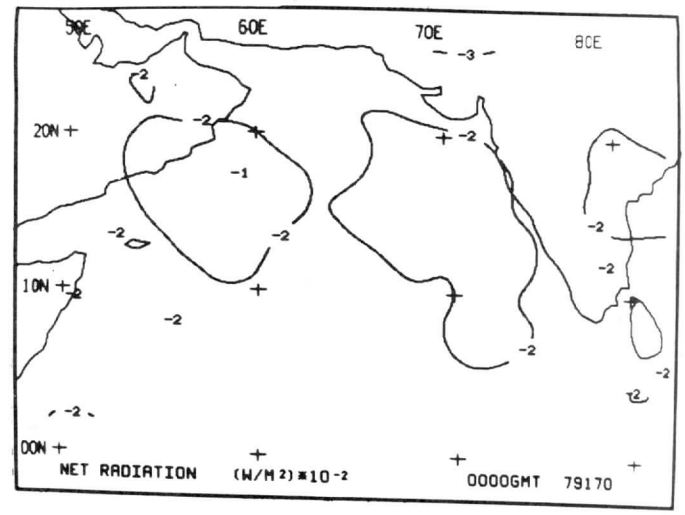
50E
60E
70E
80E
20N
10N
0ON
NET RADIATION (W/M2)*10-2
0000GMT 79170

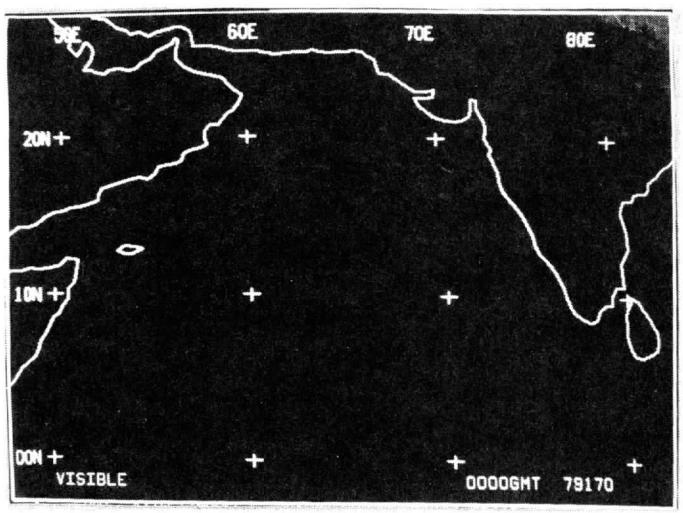
50E
60E
70E
80E
20N
10N
0ON
VISIBLE
0000GMT 79170

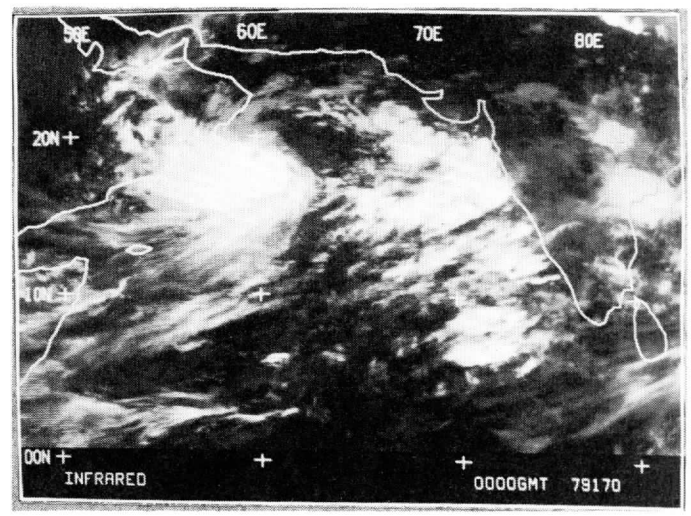
50E
60E
70E
80E
20N
10N
0ON
INFRARED
0000GMT 79170

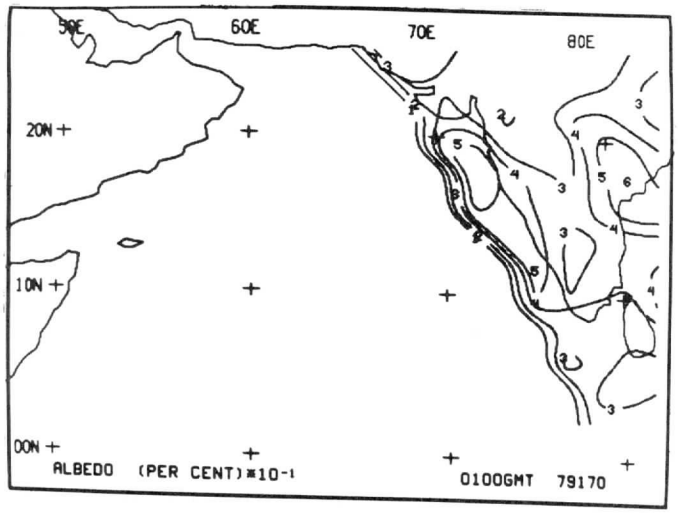
50E
60E
70E
80E
20N
10N
0ON
ALBEDO (PER CENT)×10-1
0100GMT 79170

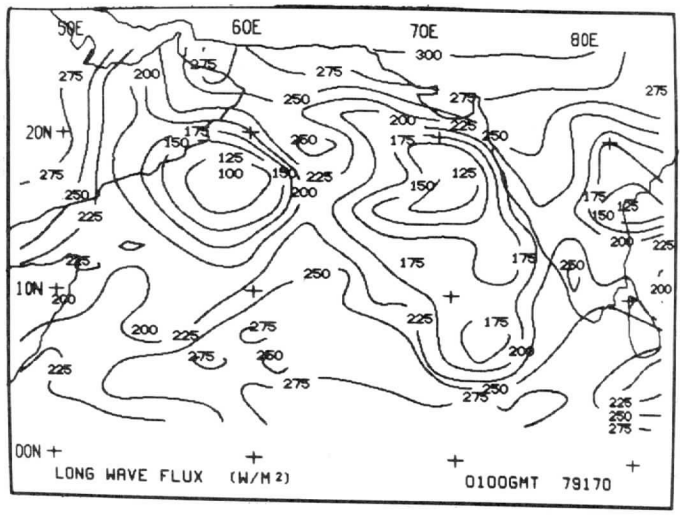
50E
60E
70E
80E
20N
10N
0ON
LONG WAVE FLUX (W/M2)
0100GMT 79170

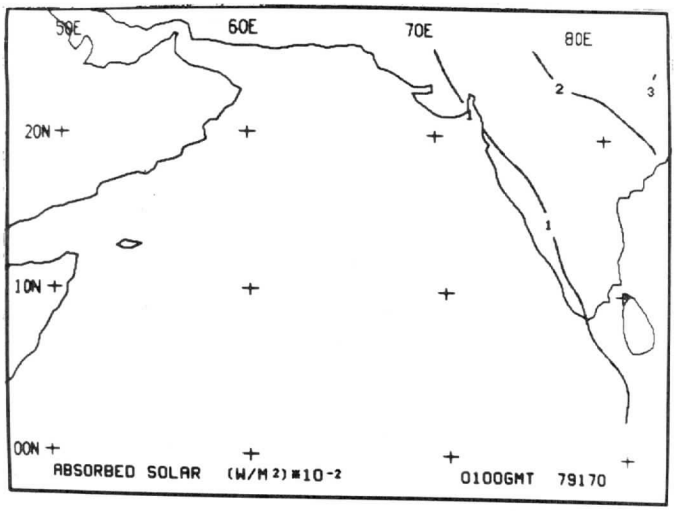
50E
60E
70E
80E
20N
10N
0ON
ABSORBED SOLAR (W/M2)×10-2
0100GMT 79170

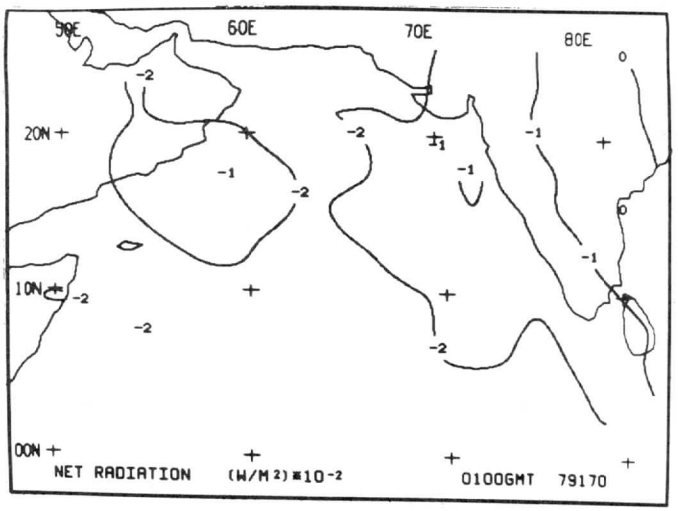
50E
60E
70E
80E
20N
10N
0ON
NET RADIATION (W/M2)×10-2
0100GMT 79170

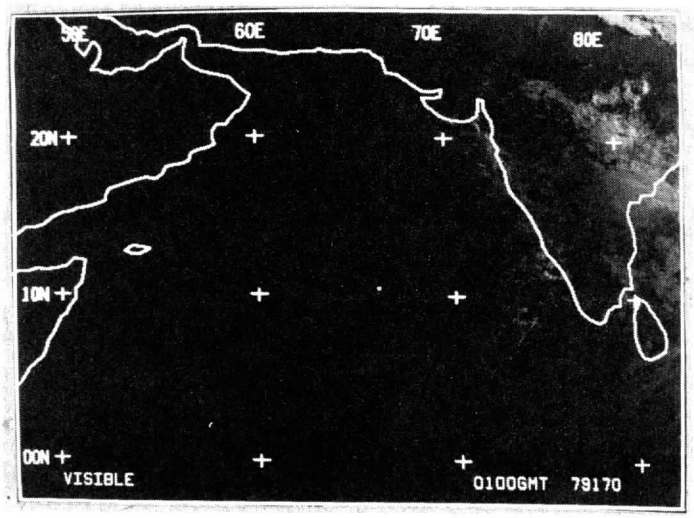
50E
60E
70E
80E
20N
10N
0ON
VISIBLE
0100GMT 79170

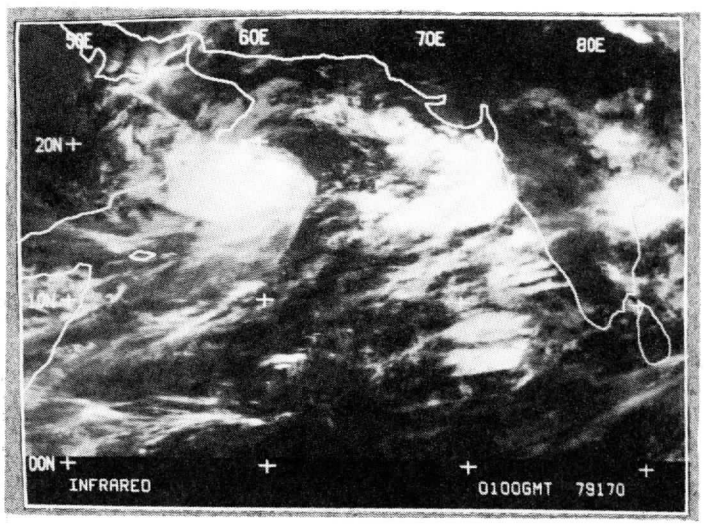
50E
60E
70E
80E
20N
10N
0ON
INFRARED
0100GMT 79170

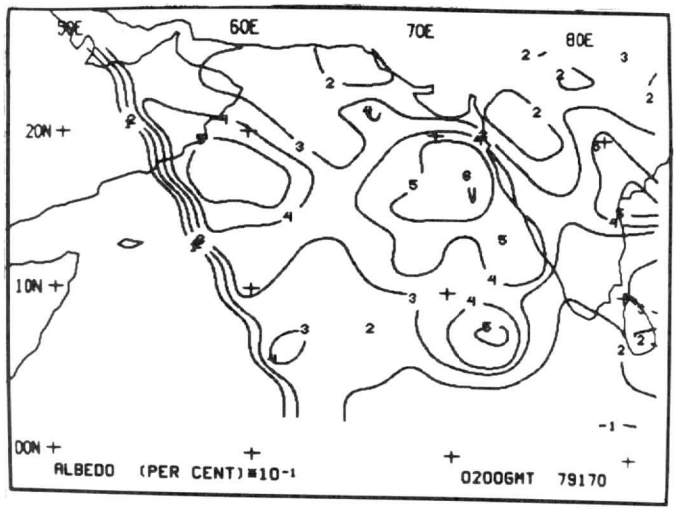
50E
60E
70E
80E
20N
10N
0ON
ALBEDO (PER CENT)*10-1
0200GMT 79170

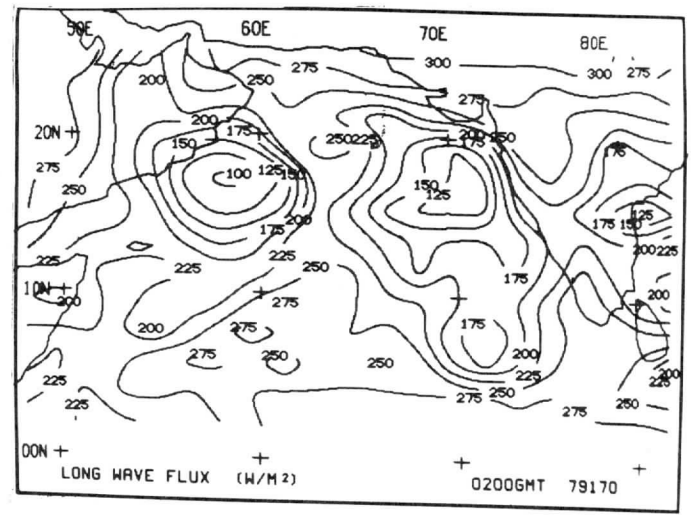
50E
60E
70E
80E
20N
10N
0ON
LONG WAVE FLUX (W/M2)
0200GMT 79170

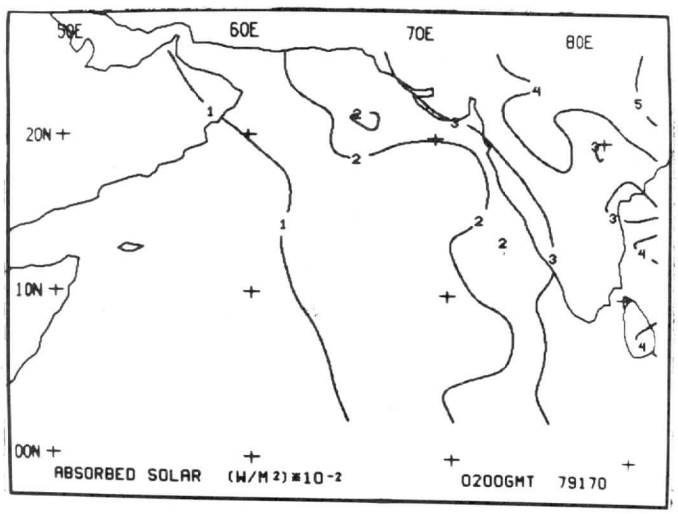
50E
60E
70E
80E
20N
10N
0ON
ABSORBED SOLAR (W/M2)*10-2
0200GMT 79170

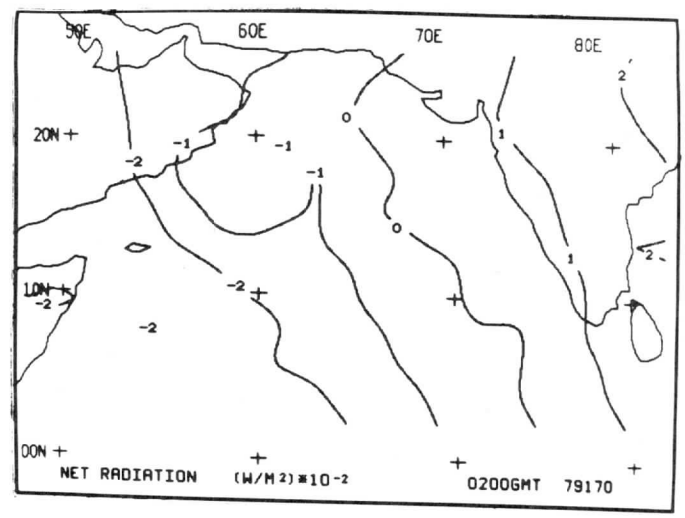
50E
60E
70E
80E
20N
10N
0ON
NET RADIATION (W/M2)*10-2
0200GMT 79170

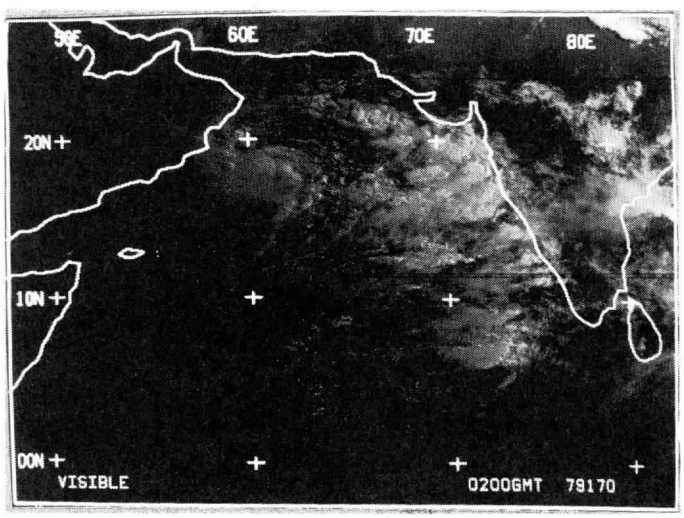
50E
60E
70E
80E
20N
10N
0ON
VISIBLE
0200GMT 79170

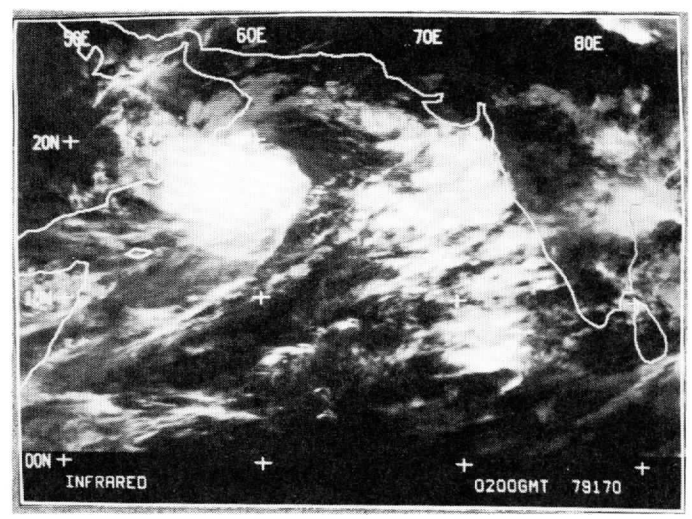
50E
60E
70E
80E
20N
0ON
INFRARED
0200GMT 79170

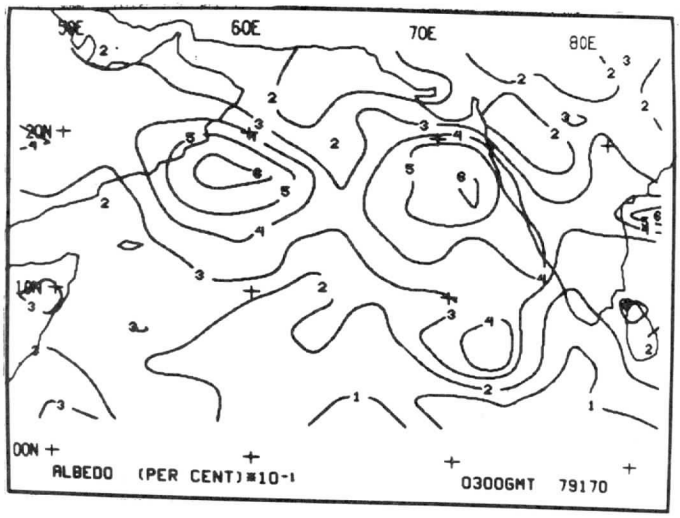
50E
60E
70E
80E
20N
10N
0ON
ALBEDO (PER CENT)*10-1
0300GMT 79170

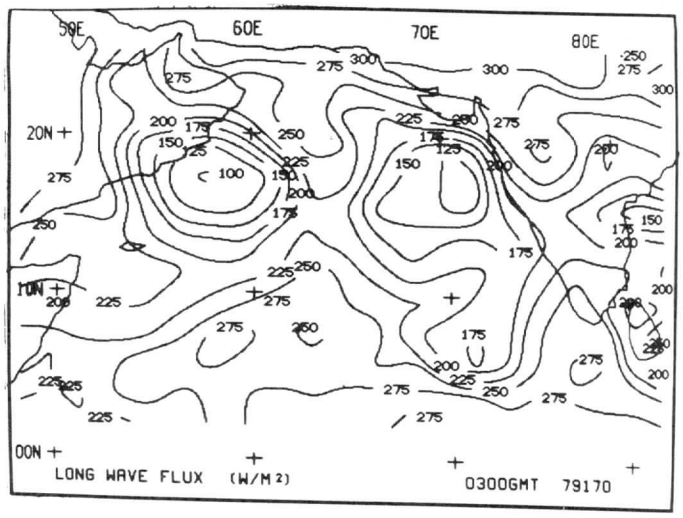
50E
60E
70E
80E
20N
10N
0ON
LONG WAVE FLUX (W/M2)
0300GMT 79170

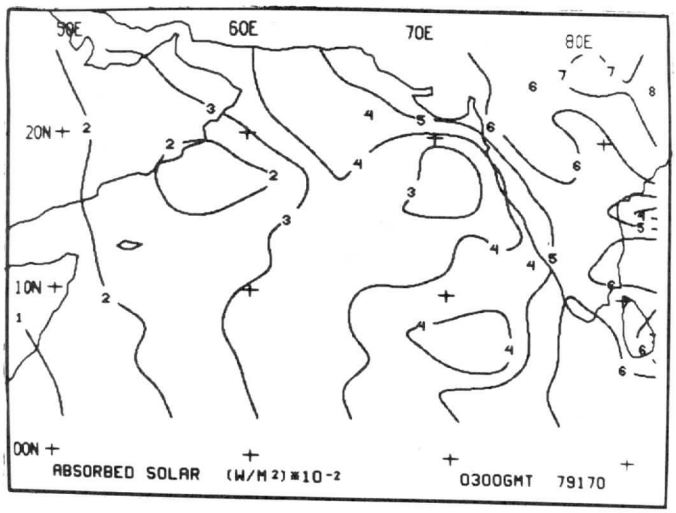
50E
60E
70E
80E
20N
10N
0ON
ABSORBED SOLAR (W/M2)*10-2
0300GMT 79170

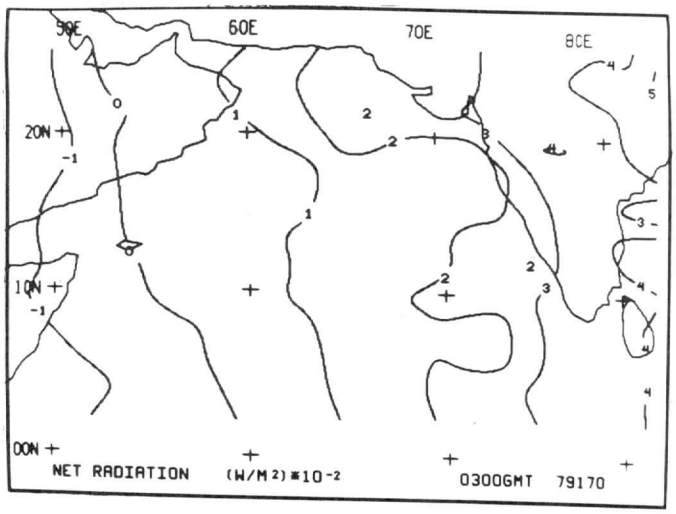
50E
60E
70E
80E
20N
10N
0ON
NET RADIATION (W/M2)*10-2
0300GMT 79170

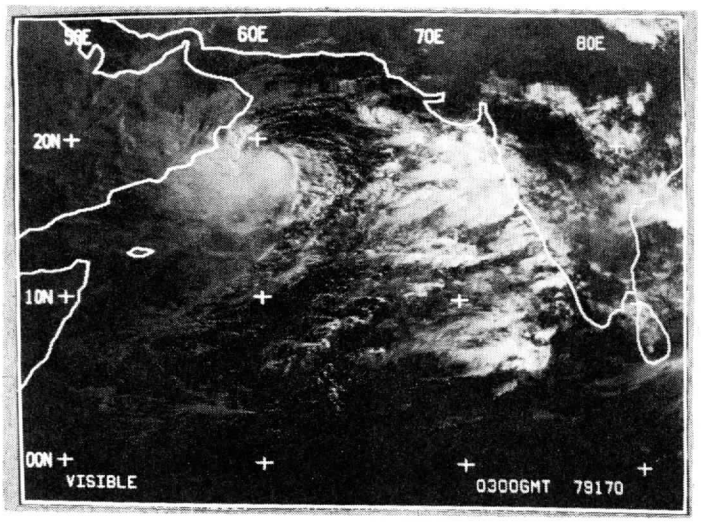
50E
60E
70E
80E
20N
10N
0ON
VISIBLE
0300GMT 79170

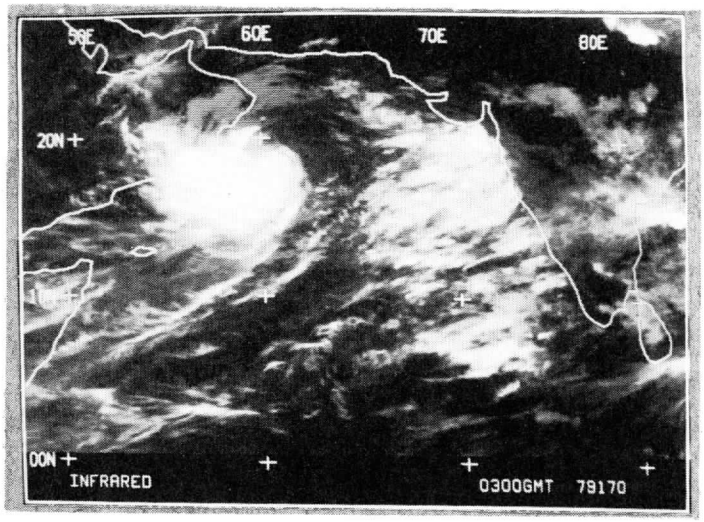
50E
60E
70E
80E
20N
0ON
INFRARED
0300GMT 79170

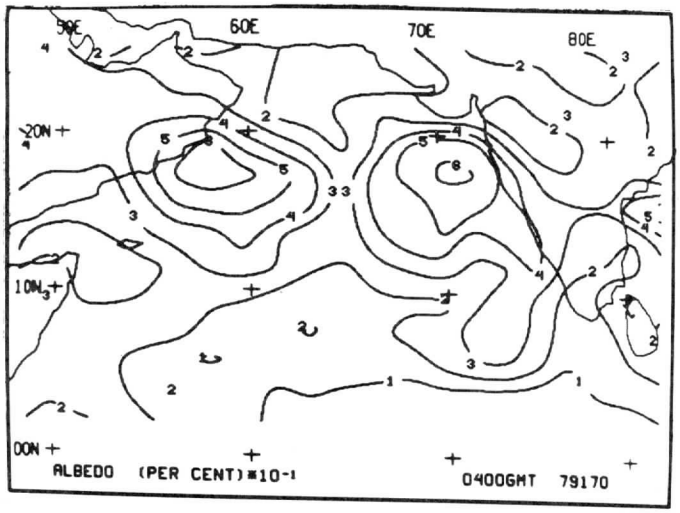
50E
60E
70E
80E
20N
10N
0ON
ALBEDO (PER CENT)×10-1
0400GMT 79170

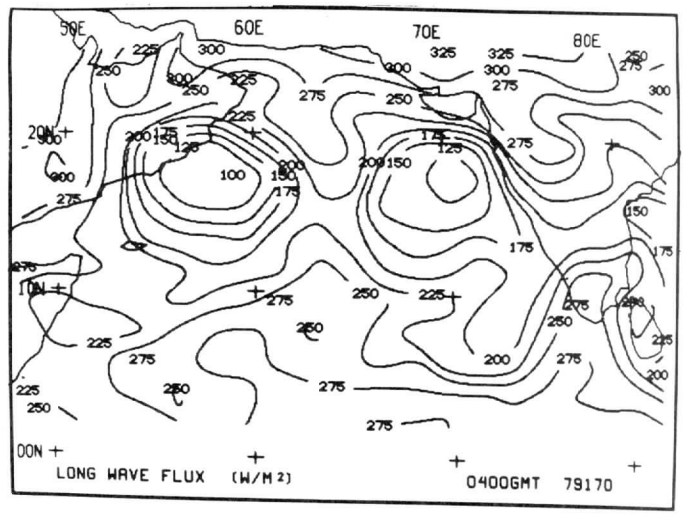
50E
60E
70E
80E
20N
10N
0ON
LONG WAVE FLUX (W/M2)
0400GMT 79170

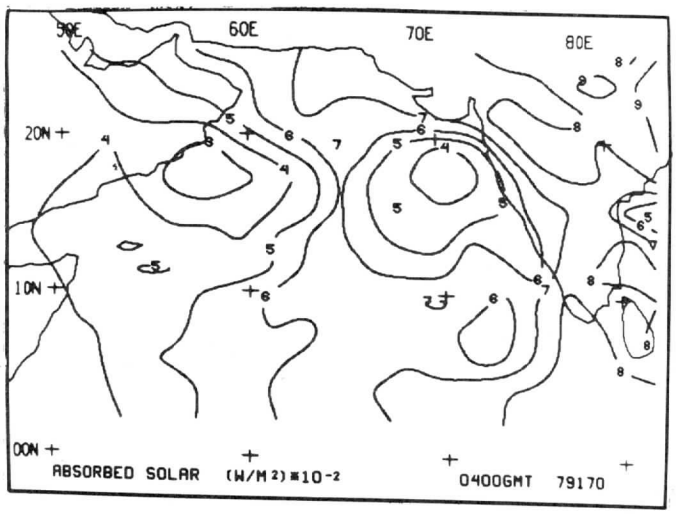
50E
60E
70E
80E
20N
10N
0ON
ABSORBED SOLAR (W/M2)×10-2
0400GMT 79170

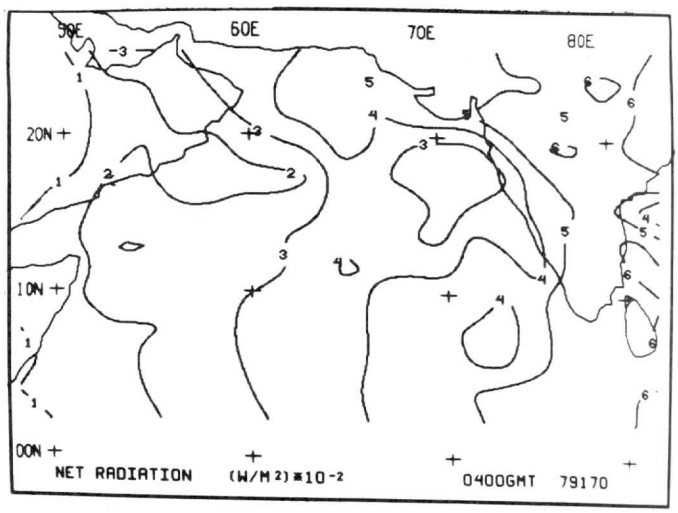
50E
60E
70E
80E
20N
10N
0ON
NET RADIATION (W/M2)×10-2
0400GMT 79170

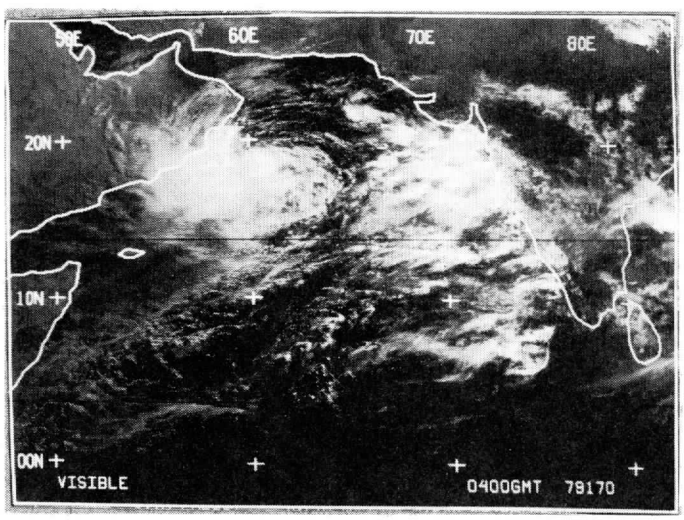
50E
60E
70E
80E
20N
10N
0ON
VISIBLE
0400GMT 79170

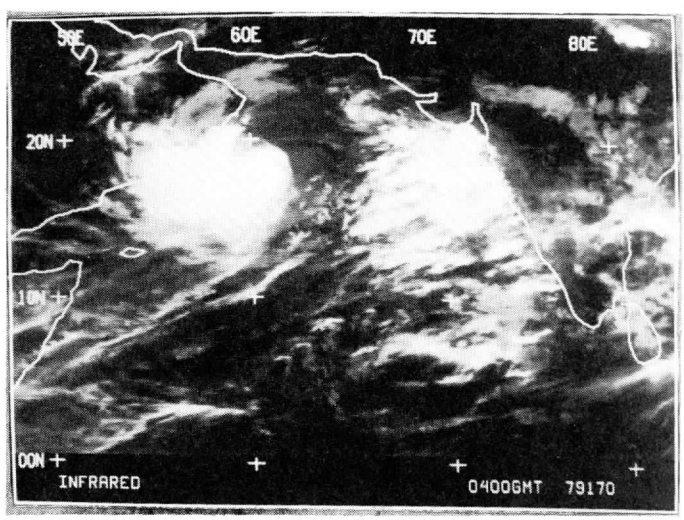
50E
60E
70E
80E
20N
10N
0ON
INFRARED
0400GMT 79170

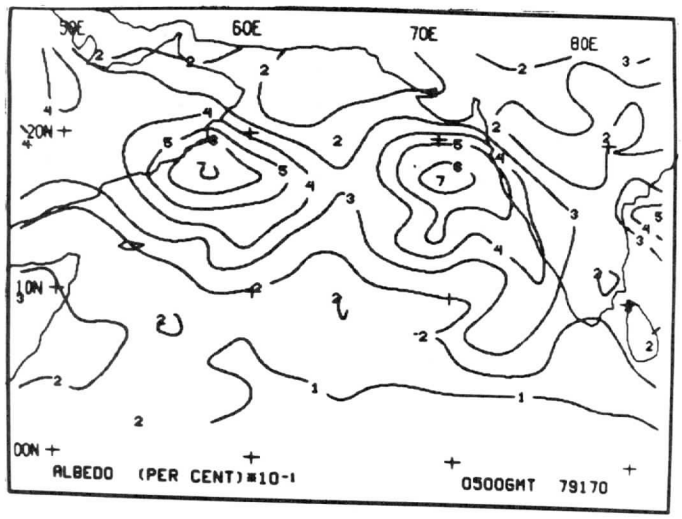
50E
60E
70E
80E
20N
10N
0ON
ALBEDO (PER CENT)*10-1
0500GMT 79170

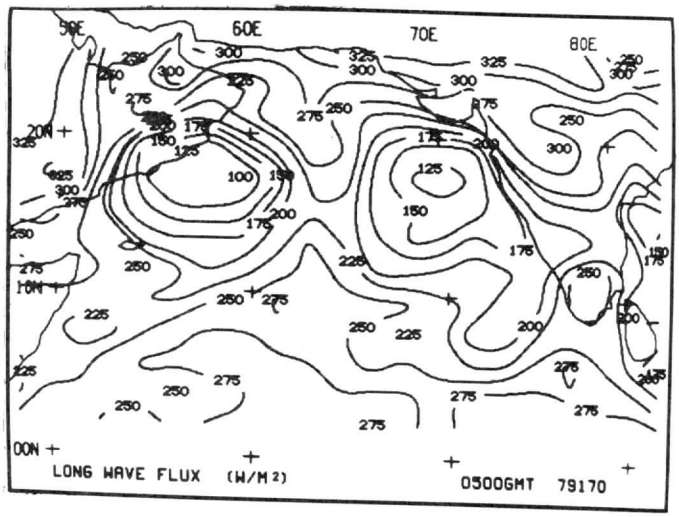
50E
60E
70E
80E
20N
10N
0ON
LONG WAVE FLUX (W/M2)
0500GMT 79170

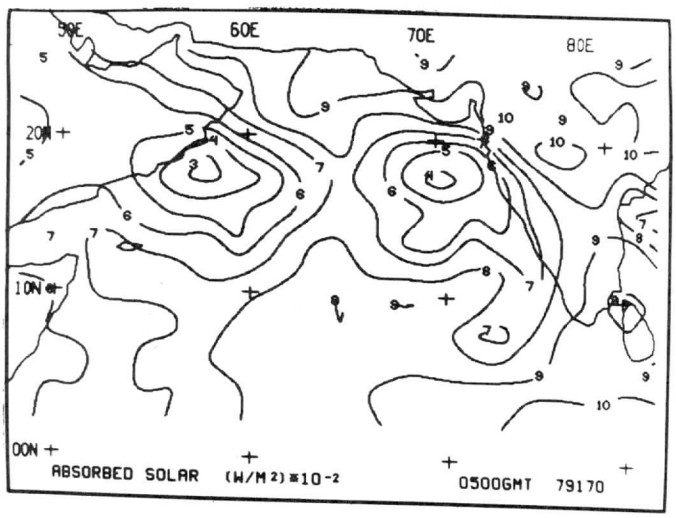
50E
60E
70E
80E
20N
10N
0ON
ABSORBED SOLAR (W/M2)*10-2
0500GMT 79170

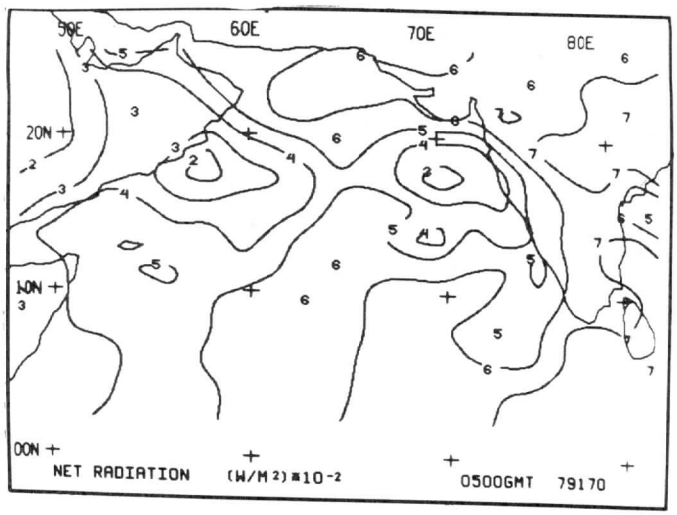
50E
60E
70E
80E
20N
10N
0ON
NET RADIATION (W/M2)*10-2
0500GMT 79170

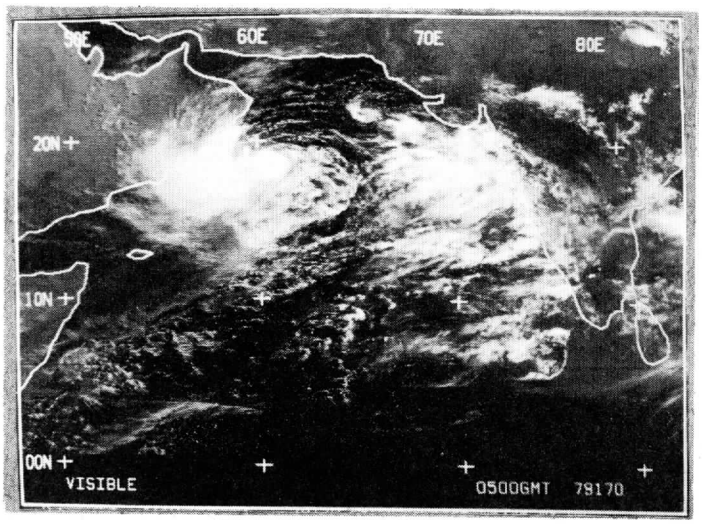
50E
60E
70E
80E
20N
10N
0ON
VISIBLE
0500GMT 79170

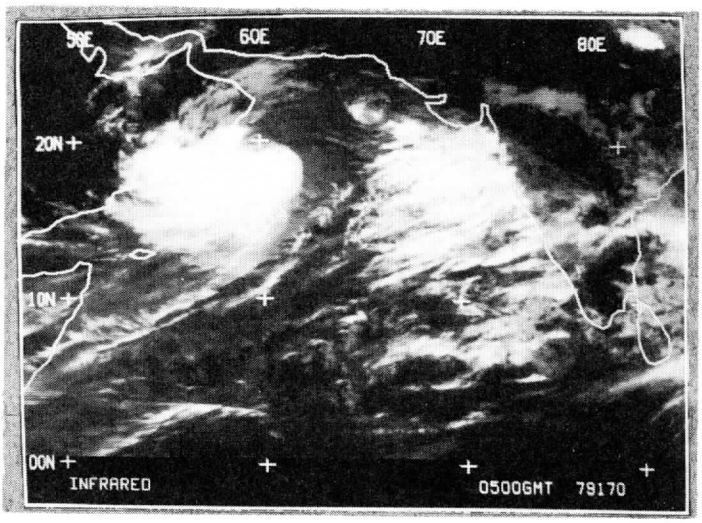
50E
60E
70E
80E
20N
10N
0ON
INFRARED
0500GMT 79170

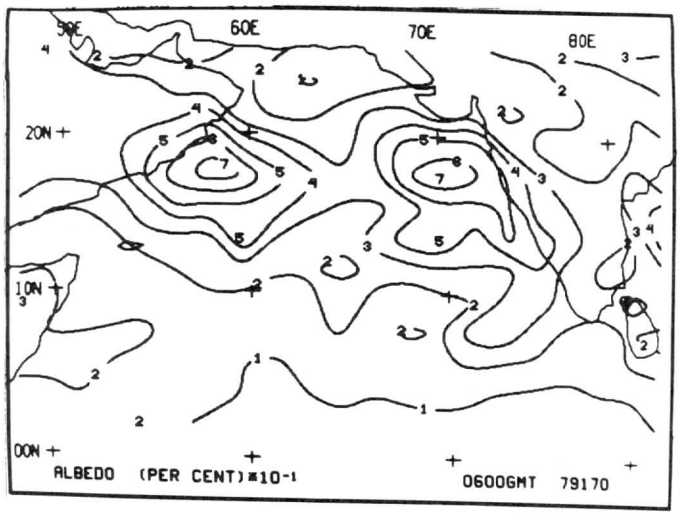
50E
60E
70E
80E
20N
10N
0ON
ALBEDO (PER CENT)*10-1
0600GMT 79170

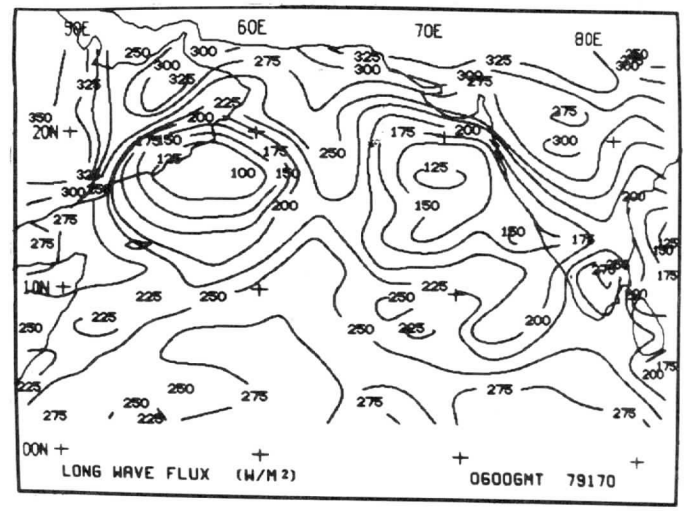
50E
60E
70E
80E
20N
10N
0ON
LONG WAVE FLUX (W/M2)
0600GMT 79170

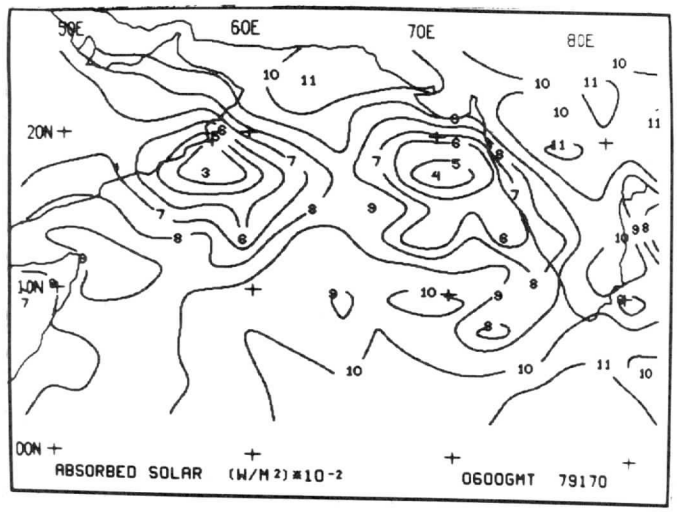
50E
60E
70E
80E
20N
10N
0ON
ABSORBED SOLAR (W/M2)*10-2
0600GMT 79170

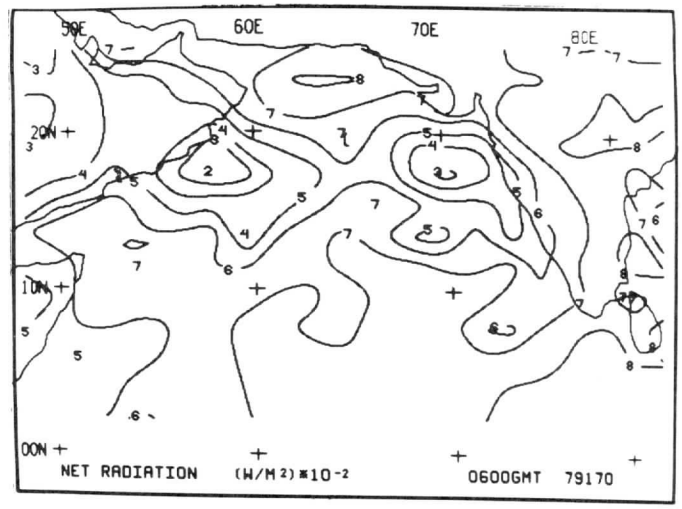
50E
60E
70E
80E
20N
10N
0ON
NET RADIATION (W/M2)*10-2
0600GMT 79170

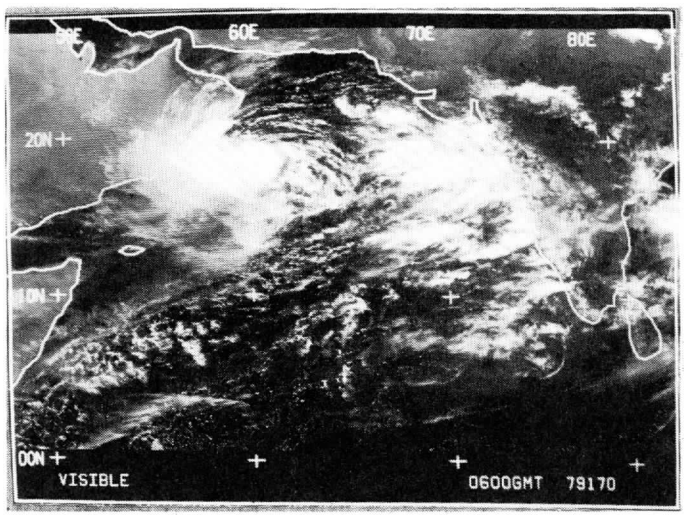
50E
60E
70E
80E
20N
10N
0ON
VISIBLE
0600GMT 79170

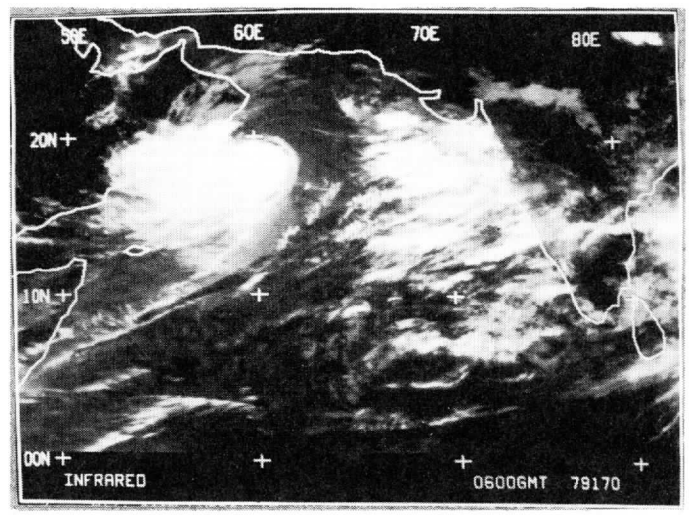
50E
60E
70E
80E
20N
10N
0ON
INFRARED
0600GMT 79170

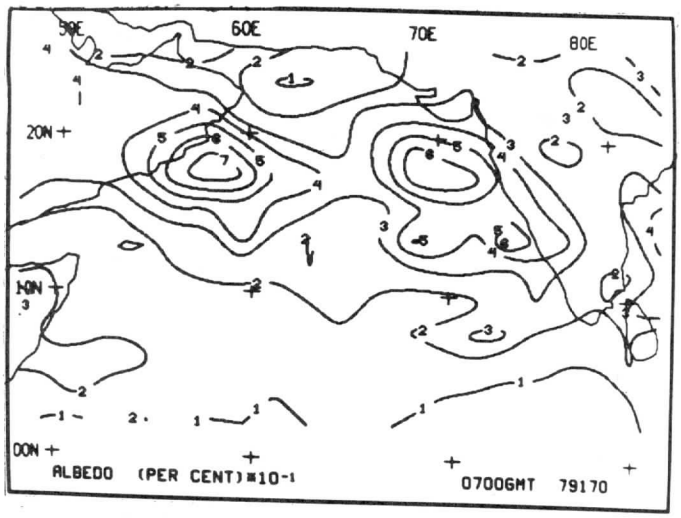
50E
60E
70E
80E
20N
10N
00N
ALBEDO (PER CENT)*10-1
0700GMT 79170

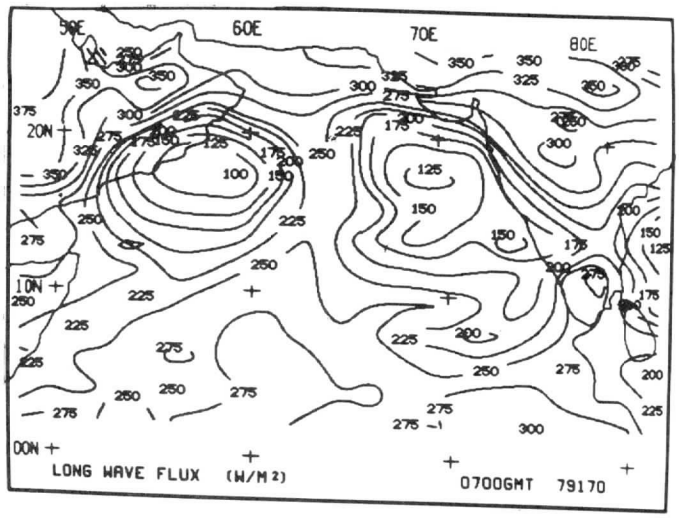
50E
60E
70E
80E
20N
10N
00N
LONG WAVE FLUX (W/M2)
0700GMT 79170

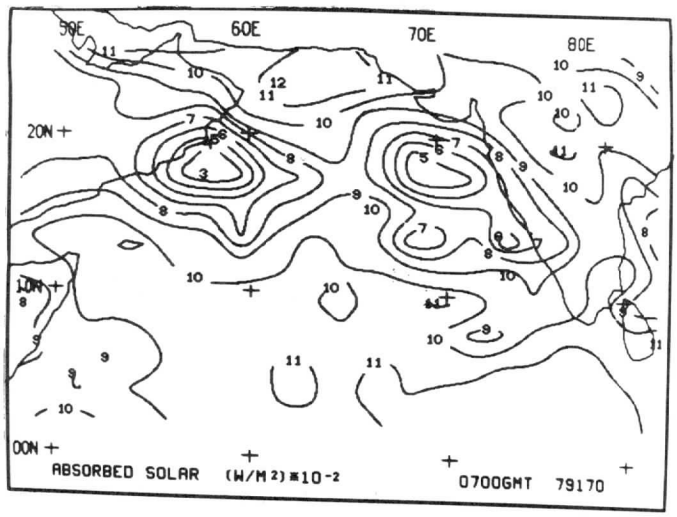
50E
60E
70E
80E
20N
10N
00N
ABSORBED SOLAR (W/M2)*10-2
0700GMT 79170

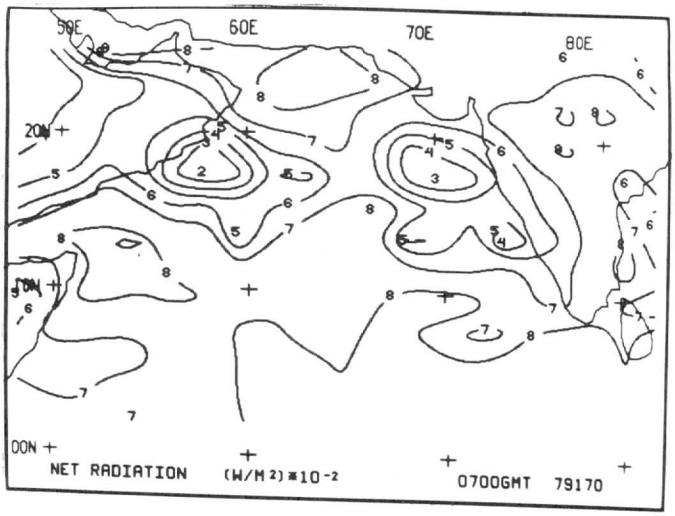
50E
60E
70E
80E
20N
10N
00N
NET RADIATION (W/M2)*10-2
0700GMT 79170

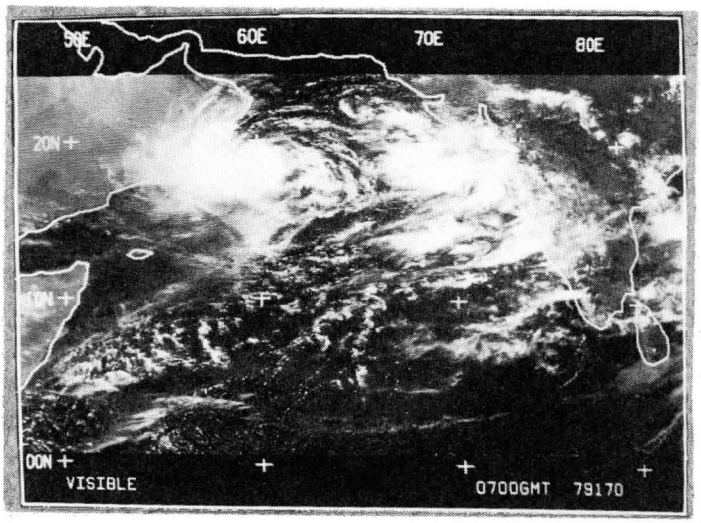
50E
60E
70E
80E
20N
10N
00N
VISIBLE
0700GMT 79170

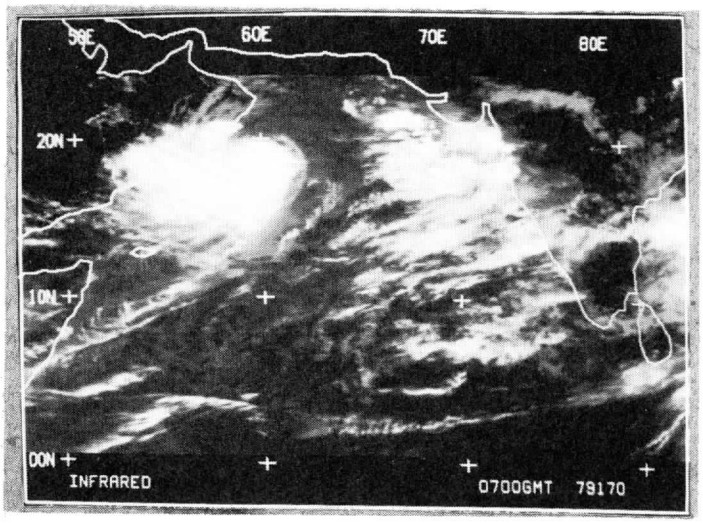
50E
60E
70E
80E
20N
10N
00N
INFRARED
0700GMT 79170

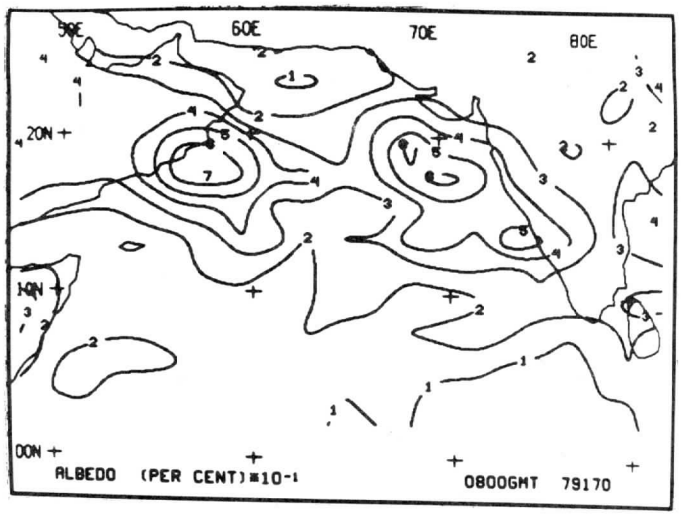
50E
60E
70E
80E
20N
10N
0ON
ALBEDO (PER CENT)*10-1
0800GMT 79170

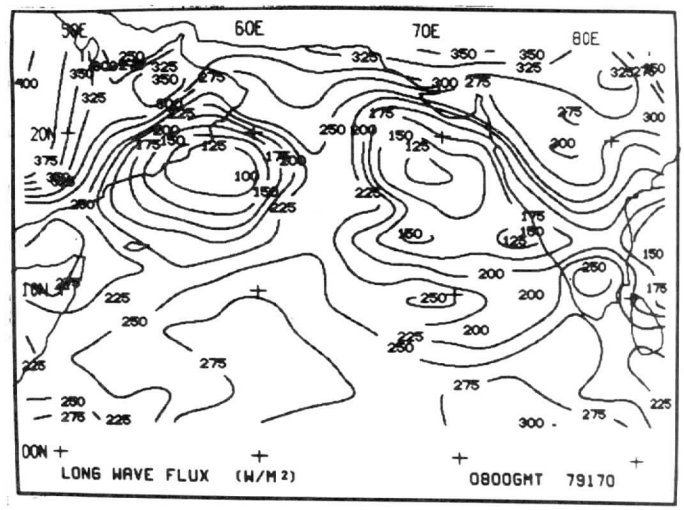
50E
60E
70E
80E
20N
10N
0ON
LONG WAVE FLUX (W/M2)
0800GMT 79170

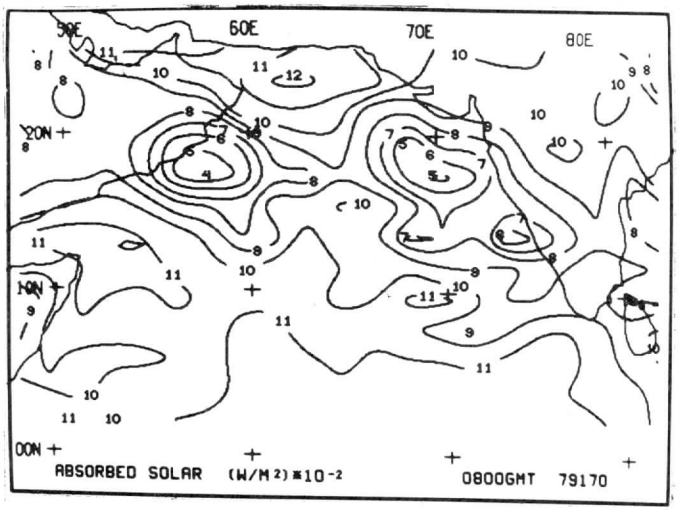
50E
60E
70E
80E
20N
10N
0ON
ABSORBED SOLAR (W/M2)*10-2
0800GMT 79170

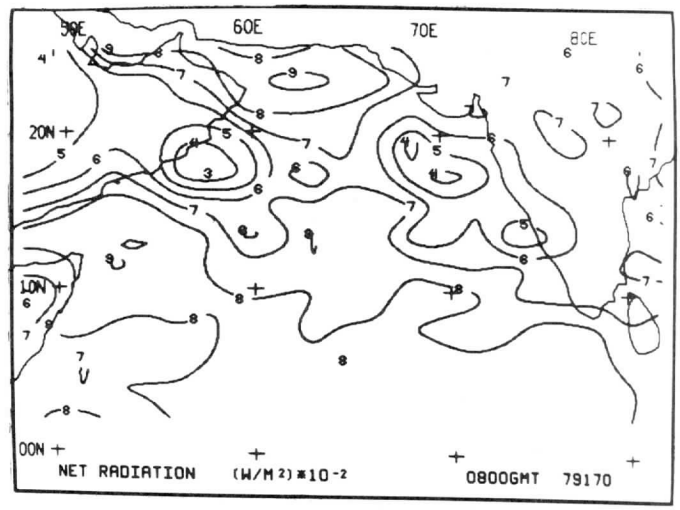
50E
60E
70E
80E
20N
10N
0ON
NET RADIATION (W/M2)*10-2
0800GMT 79170

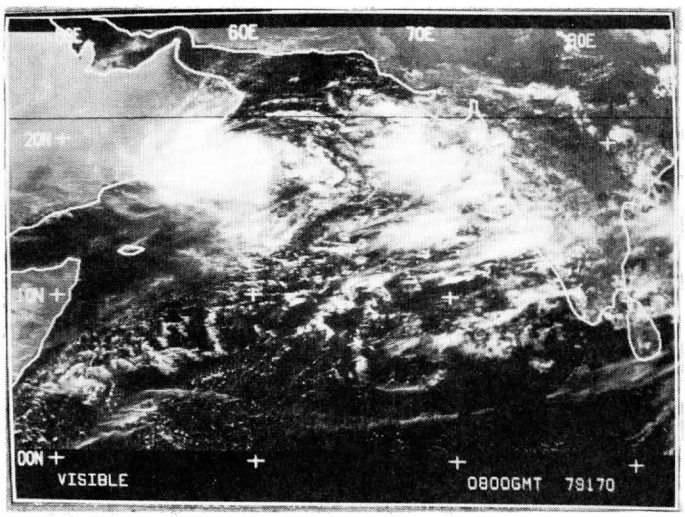
60E
70E
80E
20N
10N
0ON
VISIBLE
0800GMT 79170

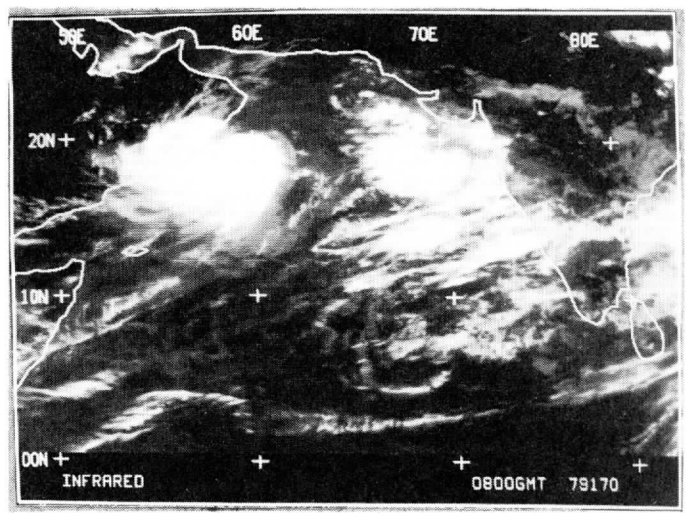
50E
60E
70E
80E
20N
10N
0ON
INFRARED
0800GMT 79170

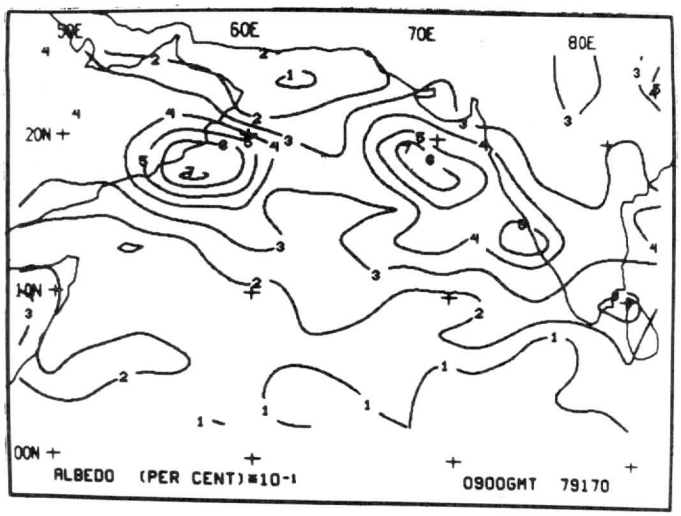
50E
60E
70E
80E
20N
10N
0ON
ALBEDO (PER CENT)×10-1
0900GMT 79170

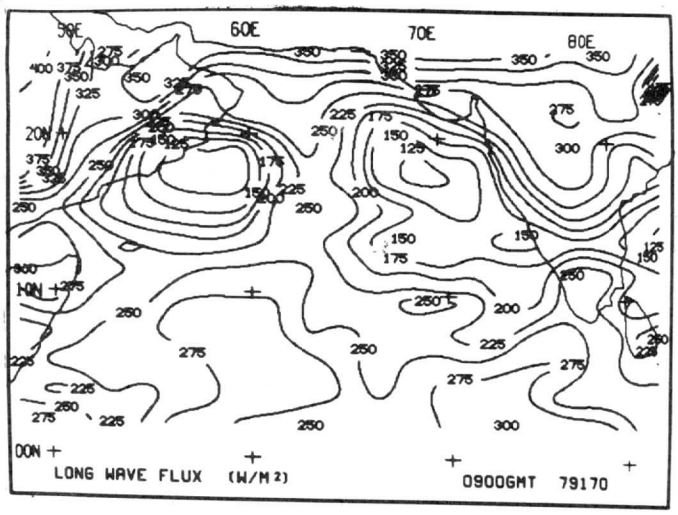
50E
60E
70E
80E
20N
10N
0ON
LONG WAVE FLUX (W/M2)
0900GMT 79170

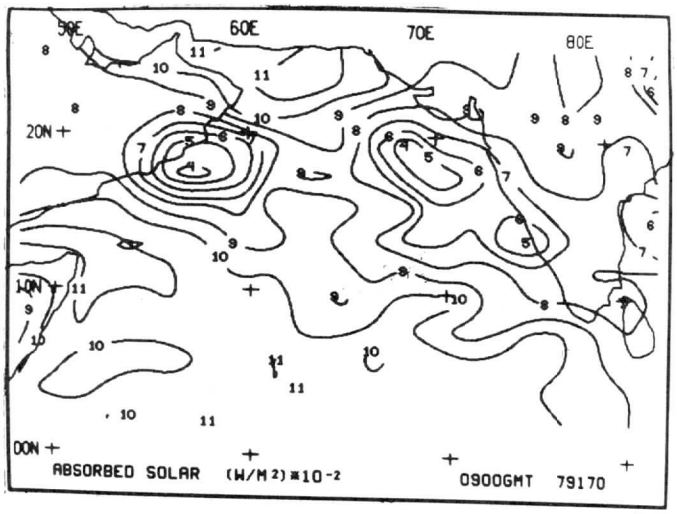
50E
60E
70E
80E
20N
10N
0ON
ABSORBED SOLAR (W/M2)×10-2
0900GMT 79170

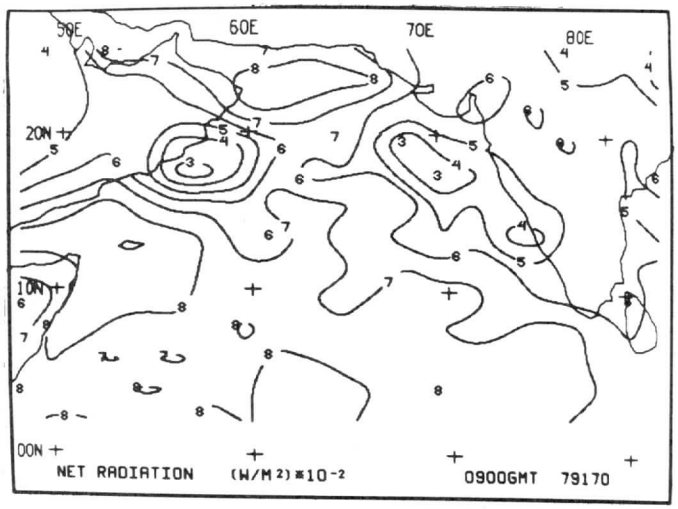
50E
60E
70E
80E
20N
10N
0ON
NET RADIATION (W/M2)×10-2
0900GMT 79170

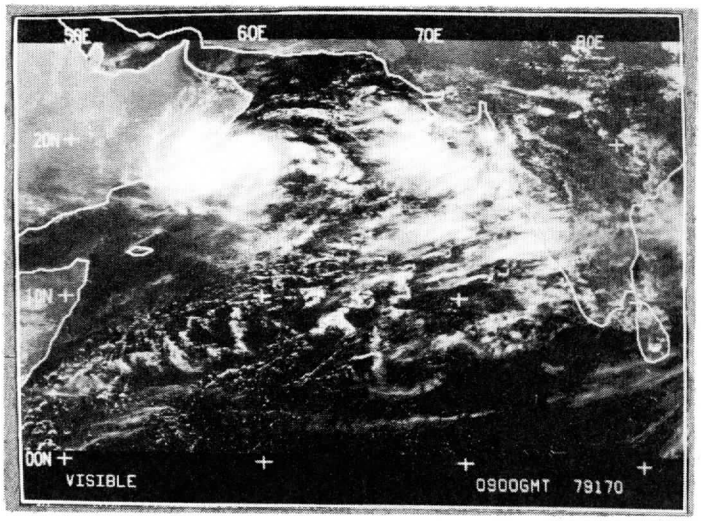
50E
60E
70E
80E
20N
10N
0ON
VISIBLE
0900GMT 79170

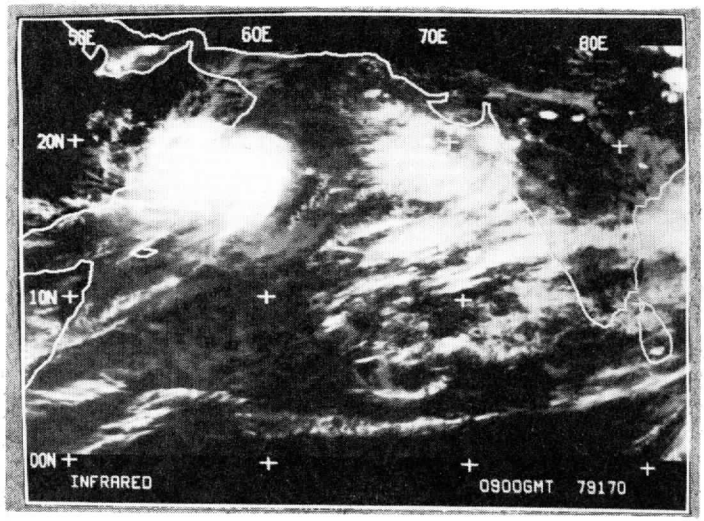
50E
60E
70E
80E
20N
10N
0ON
INFRARED
0900GMT 79170

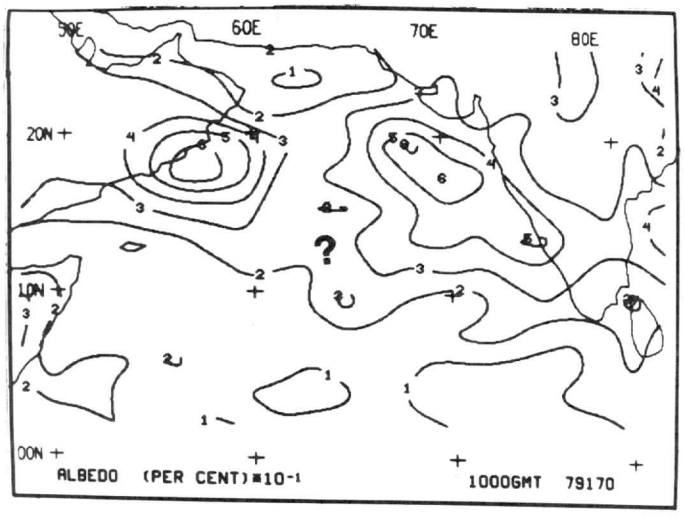
50E
60E
70E
80E
20N
10N
0ON
ALBEDO (PER CENT)*10-1
1000GMT 79170

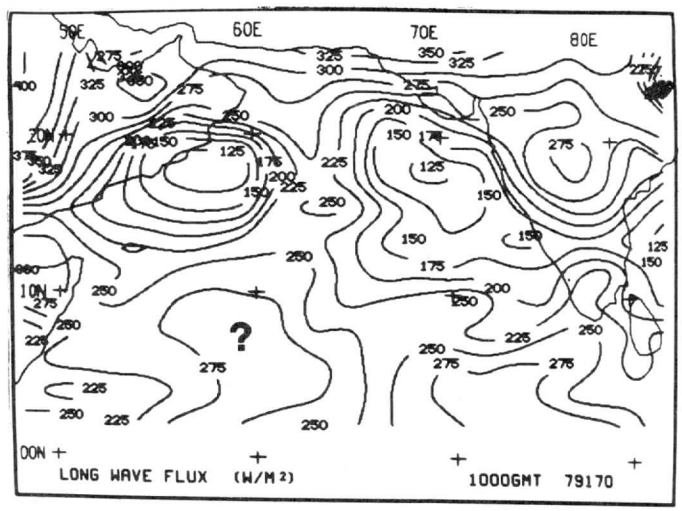
50E
60E
70E
80E
20N
10N
0ON
LONG WAVE FLUX (W/M2)
1000GMT 79170

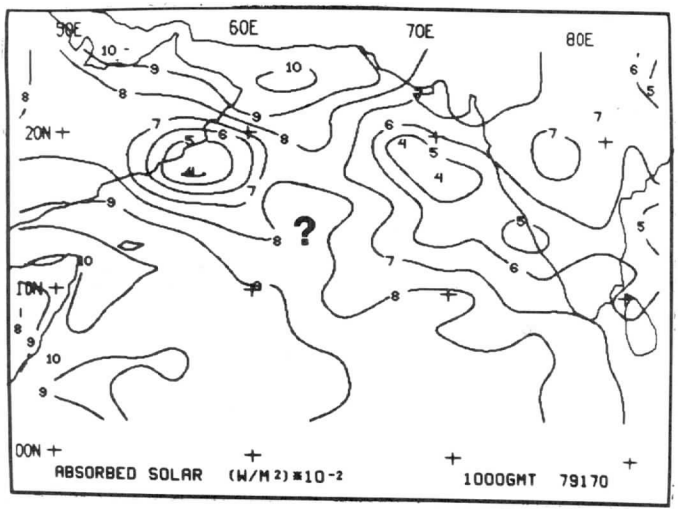
50E
60E
70E
80E
20N
10N
0ON
ABSORBED SOLAR (W/M2)*10-2
1000GMT 79170

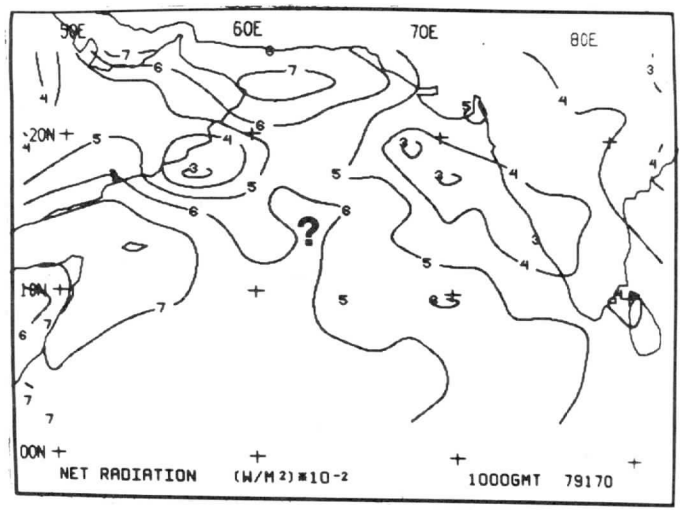
50E
60E
70E
80E
20N
10N
0ON
NET RADIATION (W/M2)*10-2
1000GMT 79170

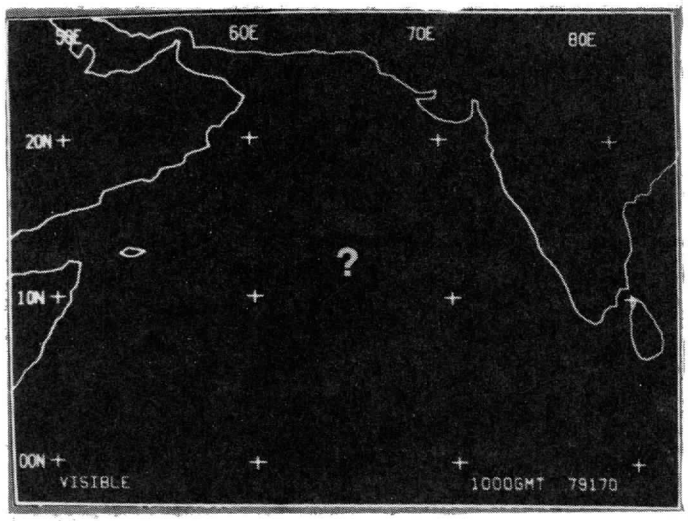
50E
60E
70E
80E
20N
10N
0ON
VISIBLE
1000GMT 79170

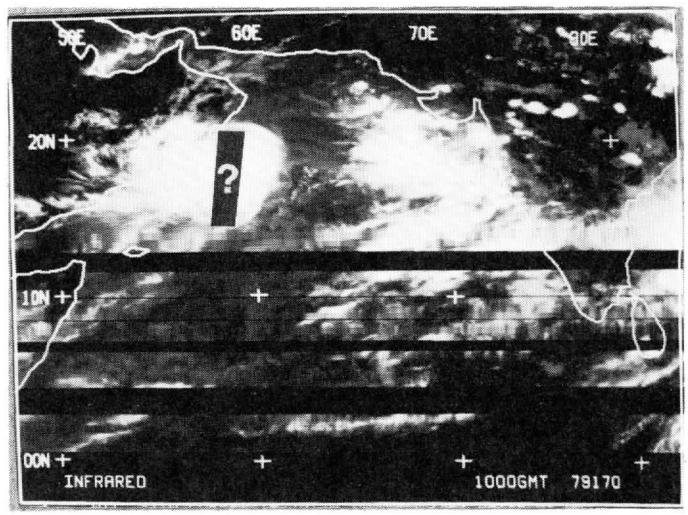
50E
60E
70E
80E
20N
10N
0ON
INFRARED
1000GMT 79170

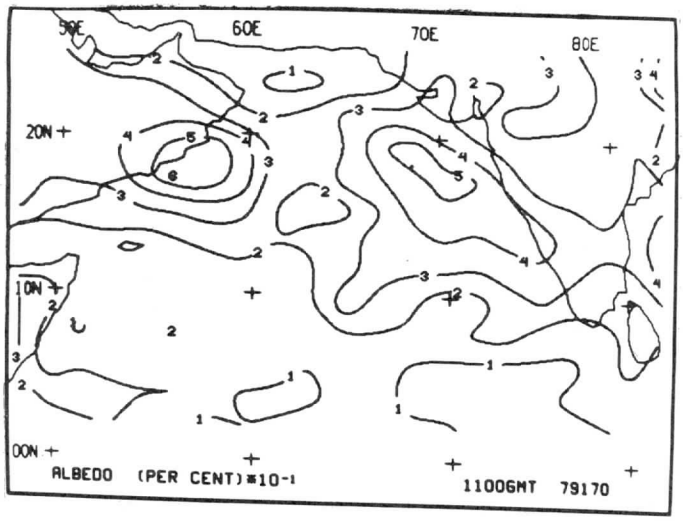
50E
60E
70E
80E
20N
10N
0ON
ALBEDO (PER CENT)*10-1
1100GMT 79170

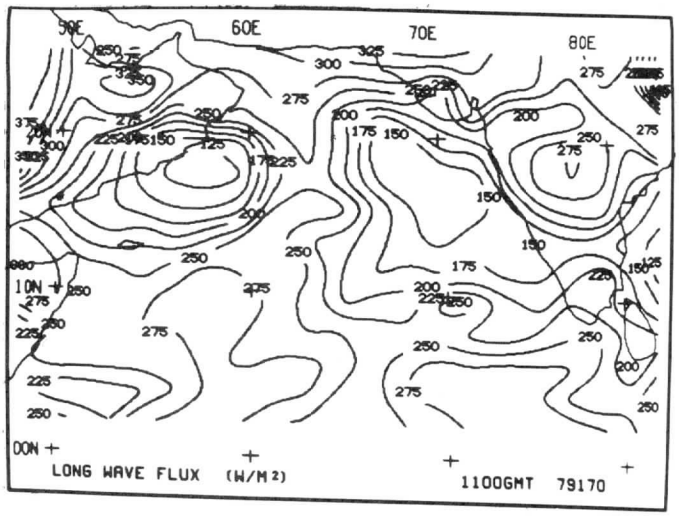
50E
60E
70E
80E
10N
0ON
LONG WAVE FLUX (W/M2)
1100GMT 79170

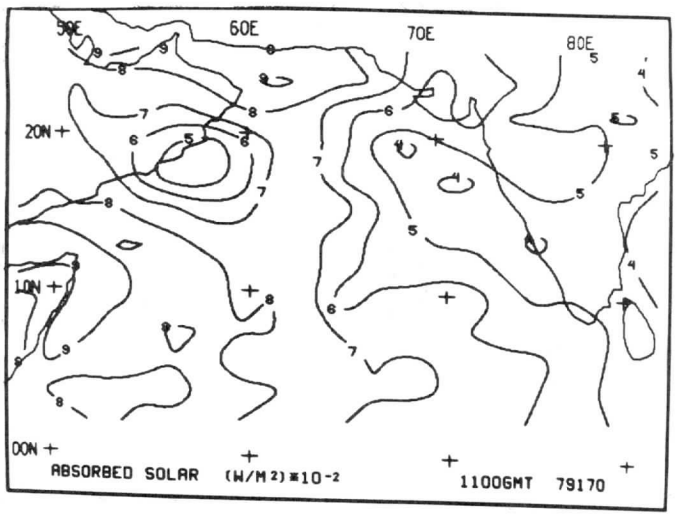
50E
60E
70E
80E
20N
10N
0ON
ABSORBED SOLAR (W/M2)*10-2
1100GMT 79170

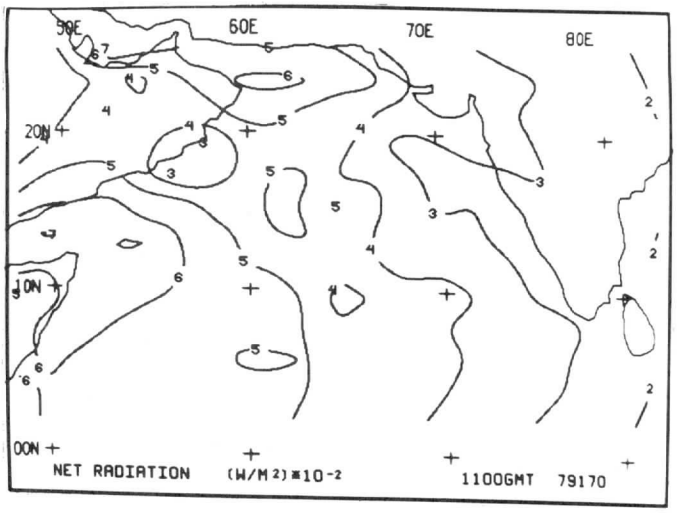
50E
60E
70E
80E
20N
10N
0ON
NET RADIATION (W/M2)*10-2
1100GMT 79170

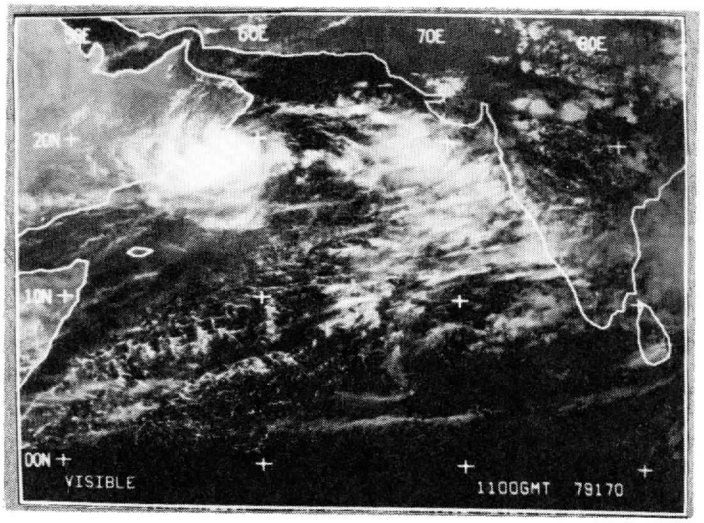
60E
70E
80E
20N
10N
0ON
VISIBLE
1100GMT 79170

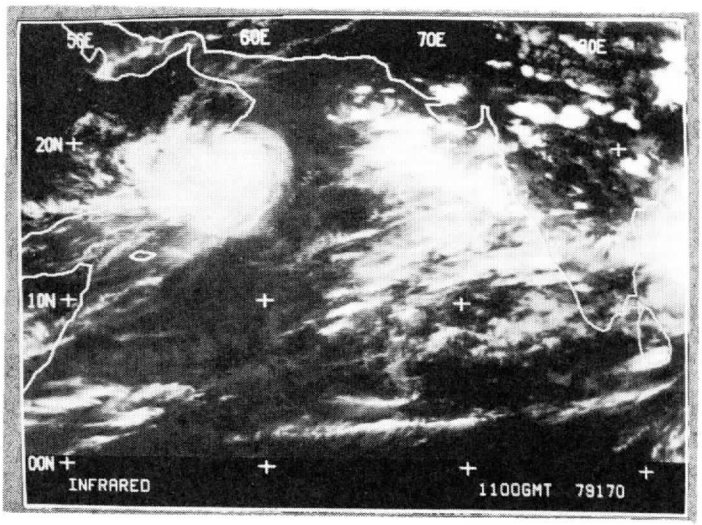
50E
60E
70E
80E
20N
10N
0ON
INFRARED
1100GMT 79170

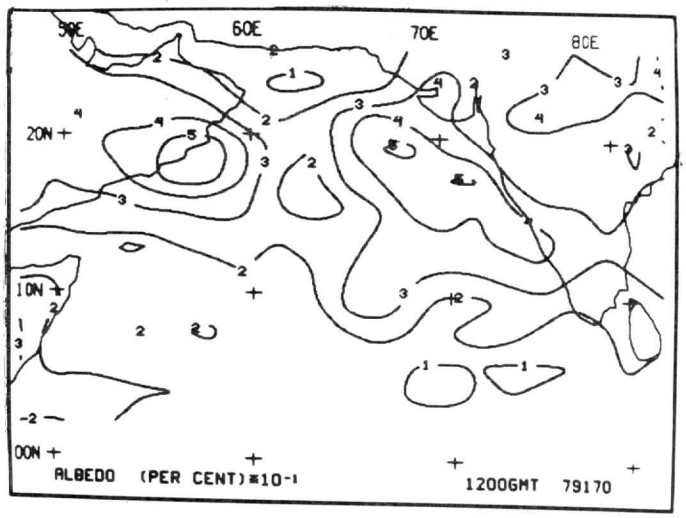
50E
60E
70E
80E
20N
10N
0ON
ALBEDO (PER CENT)*10-1
1200GMT 79170

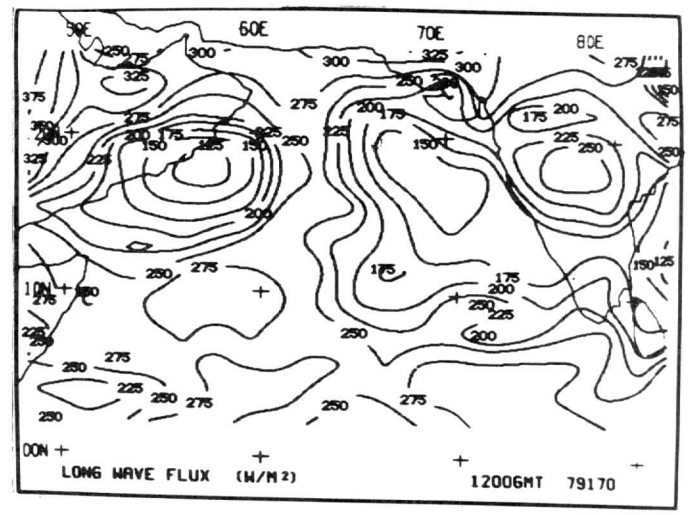
50E
60E
70E
80E
10N
0ON
LONG WAVE FLUX (W/M2)
1200GMT 79170

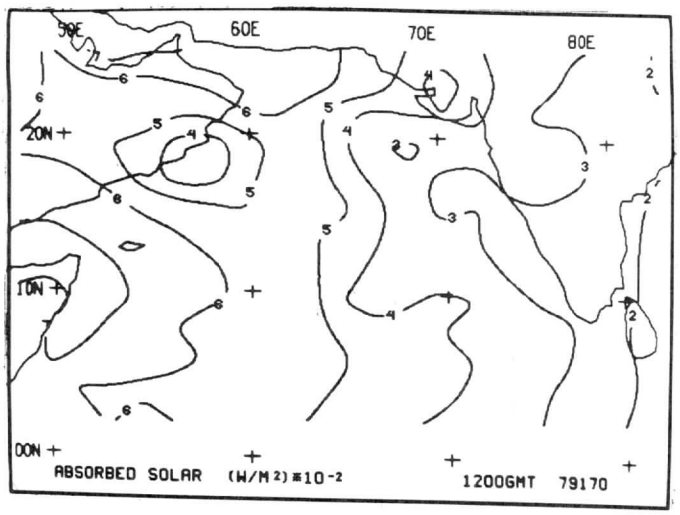
50E
60E
70E
80E
20N
10N
0ON
ABSORBED SOLAR (W/M2)*10-2
1200GMT 79170

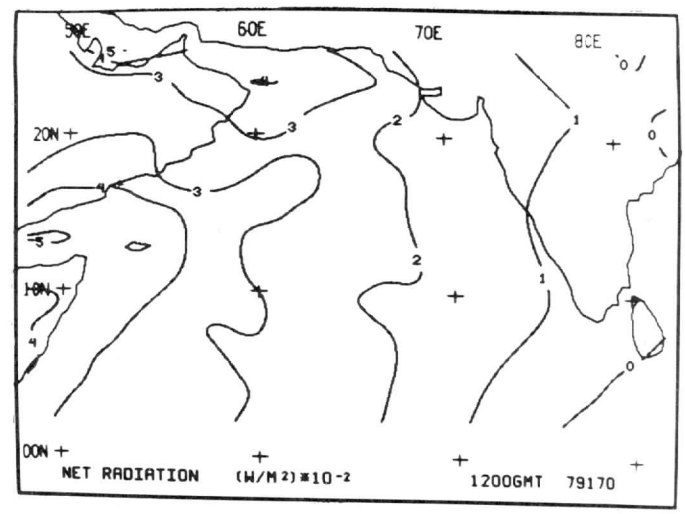
50E
60E
70E
80E
20N
10N
0ON
NET RADIATION (W/M2)*10-2
1200GMT 79170

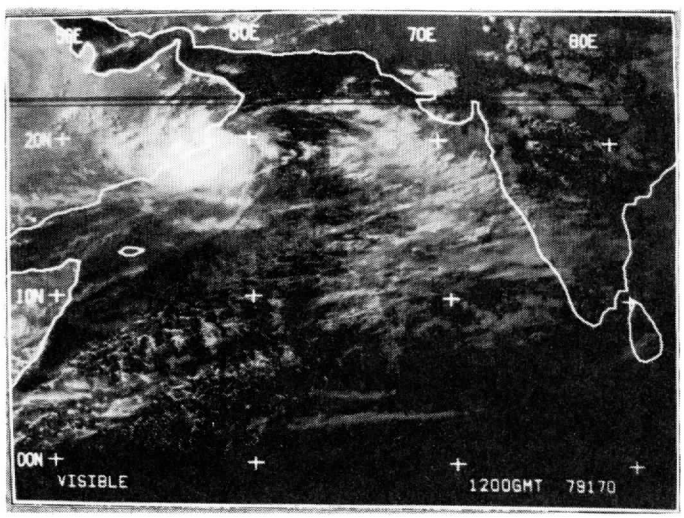
50E
60E
70E
80E
20N
10N
0ON
VISIBLE
1200GMT 79170

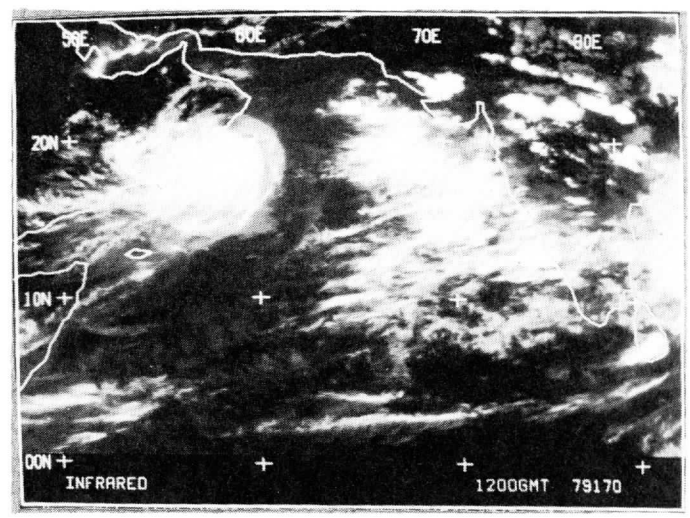
50E
60E
70E
80E
20N
10N
0ON
INFRARED
1200GMT 79170

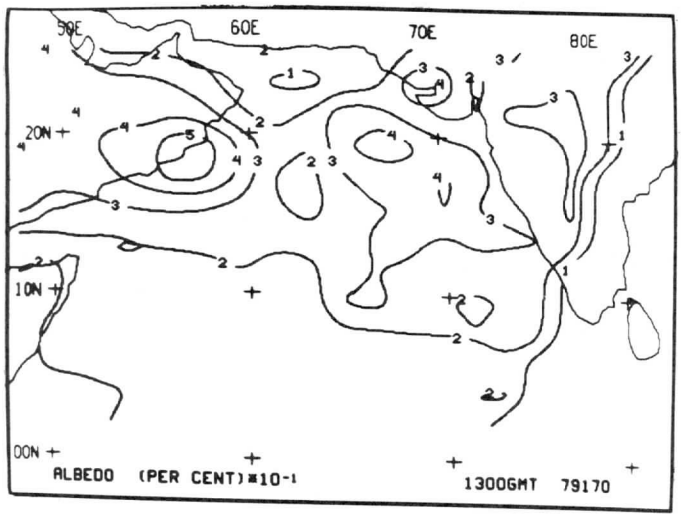
50E
60E
70E
80E
20N
10N
0ON
ALBEDO (PER CENT)*10-1
1300GMT 79170

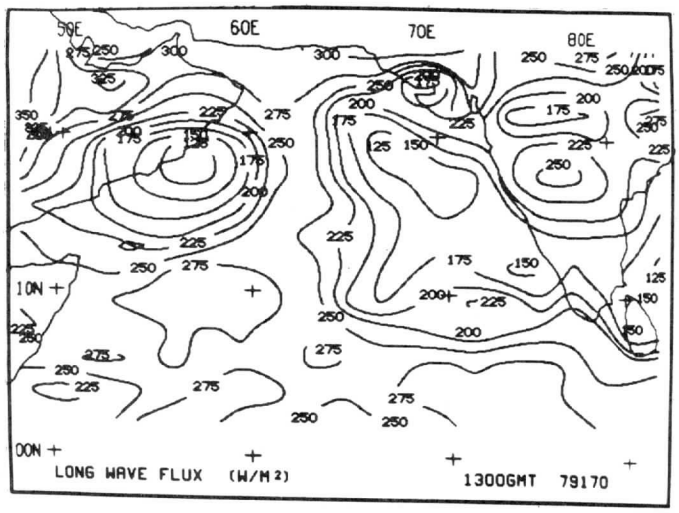
50E
60E
70E
80E
10N
0ON
LONG WAVE FLUX (W/M2)
1300GMT 79170

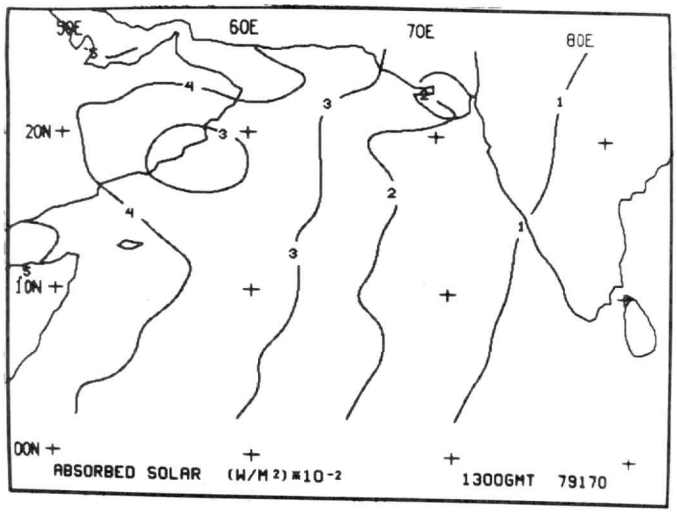
50E
60E
70E
80E
20N
10N
0ON
ABSORBED SOLAR (W/M2)*10-2
1300GMT 79170

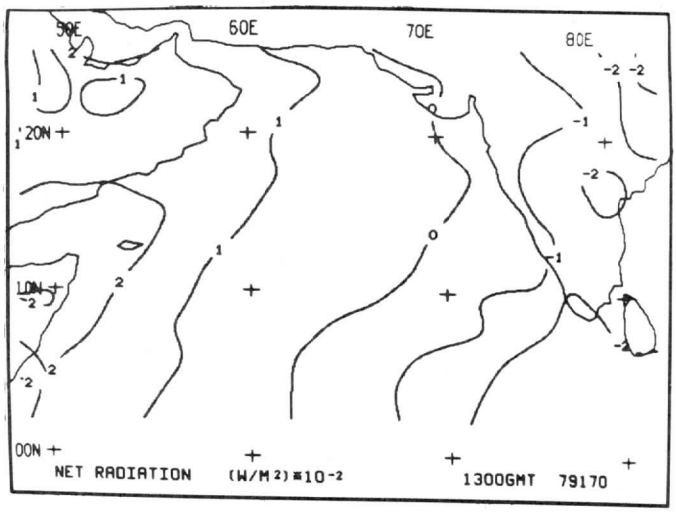
50E
60E
70E
80E
20N
10N
0ON
NET RADIATION (W/M2)*10-2
1300GMT 79170

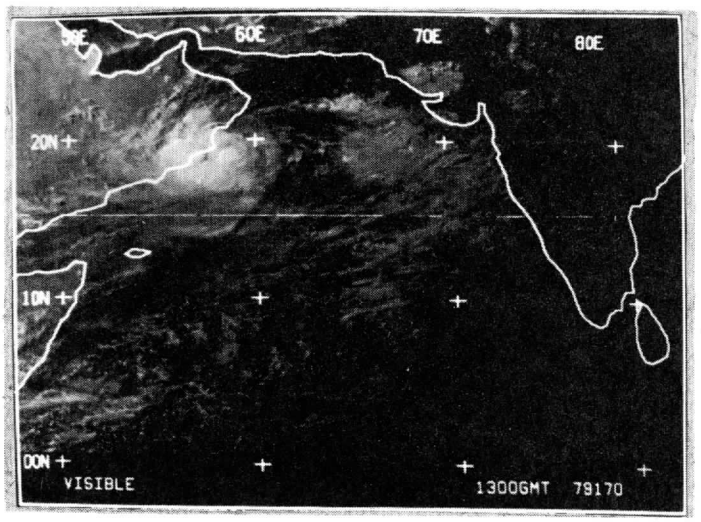
50E
60E
70E
80E
20N
10N
0ON
VISIBLE
1300GMT 79170

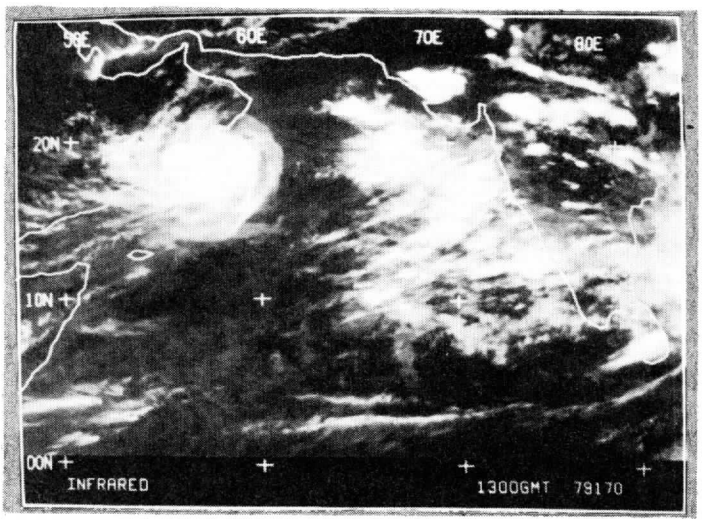
50E
60E
70E
80E
20N
10N
0ON
INFRARED
1300GMT 79170

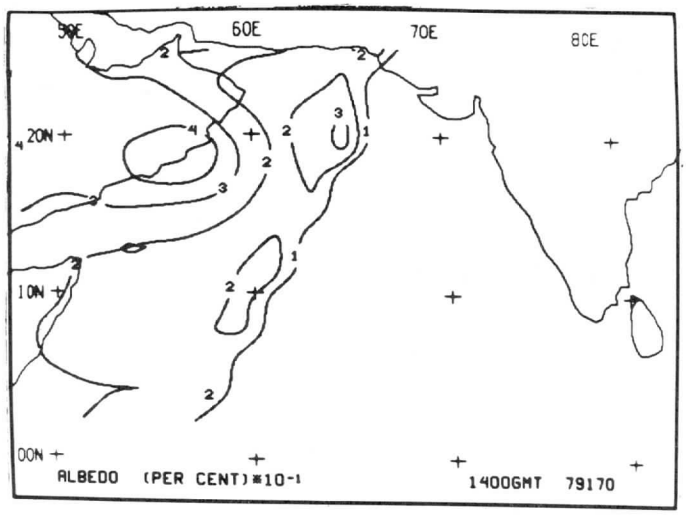
50E
60E
70E
80E
20N
10N
0ON
ALBEDO (PER CENT)*10-1
1400GMT 79170

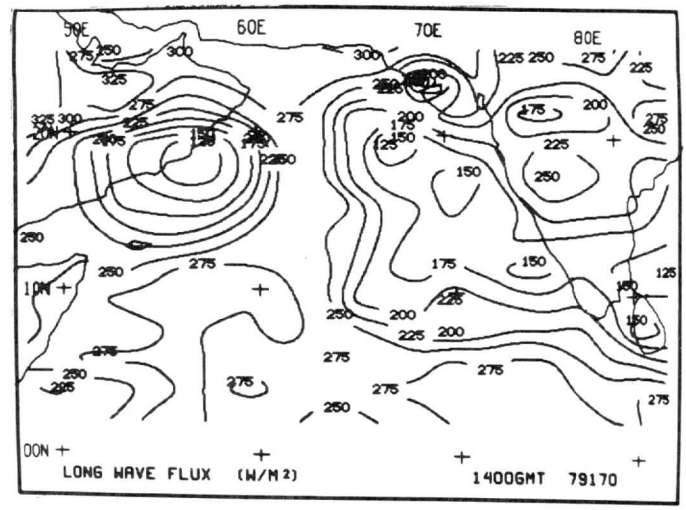
50E
60E
70E
80E
20N
10N
0ON
LONG WAVE FLUX (W/M2)
1400GMT 79170

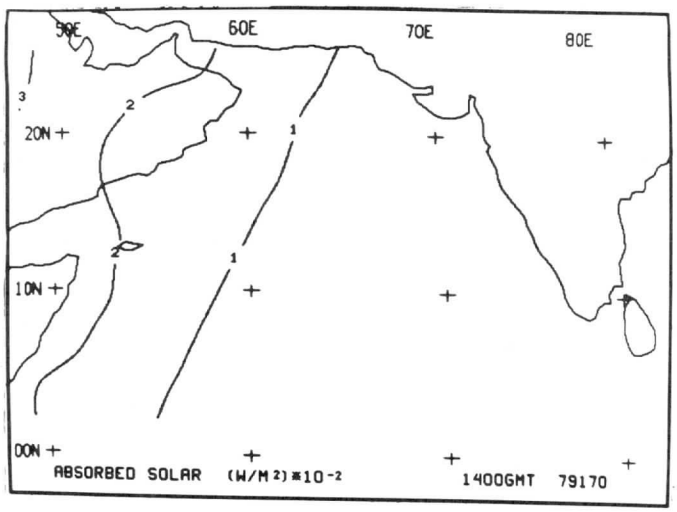
50E
60E
70E
80E
20N
10N
0ON
ABSORBED SOLAR (W/M2)*10-2
1400GMT 79170

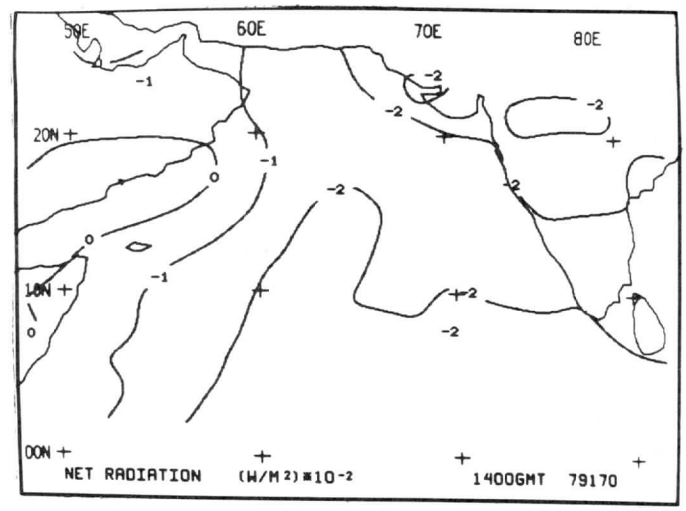
50E
60E
70E
80E
20N
10N
0ON
NET RADIATION (W/M2)*10-2
1400GMT 79170

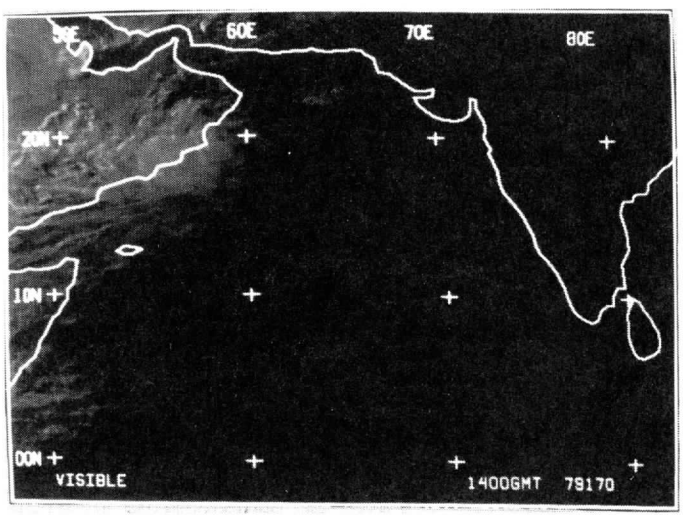
50E
60E
70E
80E
20N
10N
0ON
VISIBLE
1400GMT 79170

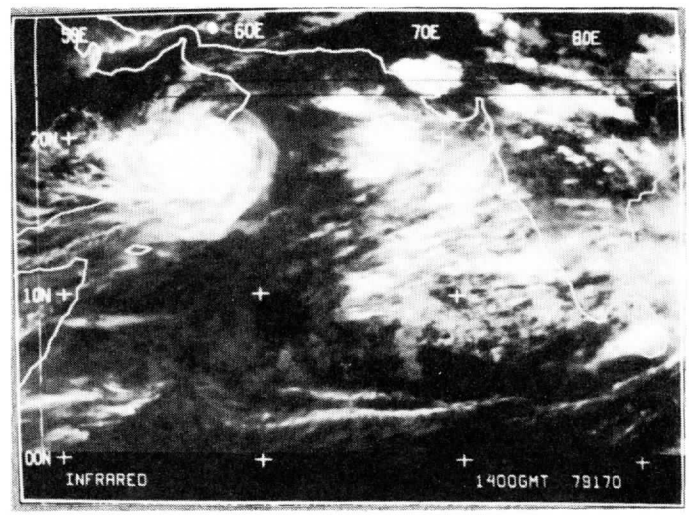
50E
60E
70E
80E
20N
10N
0ON
INFRARED
1400GMT 79170

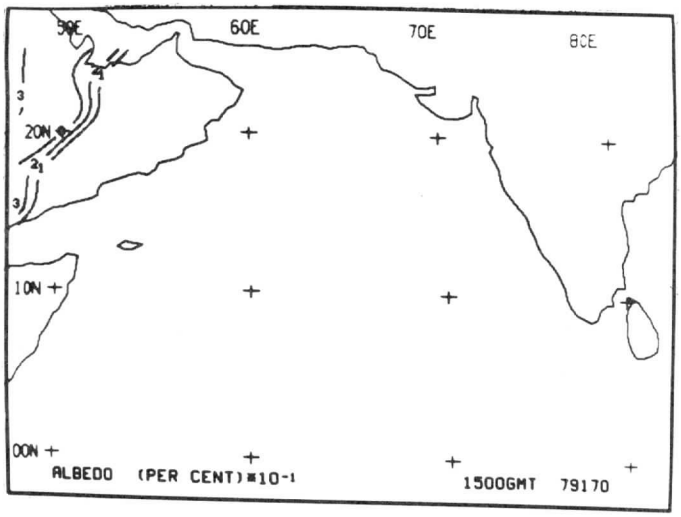
50E
60E
70E
80E
20N
10N
0ON
ALBEDO (PER CENT)×10-1
1500GMT 79170

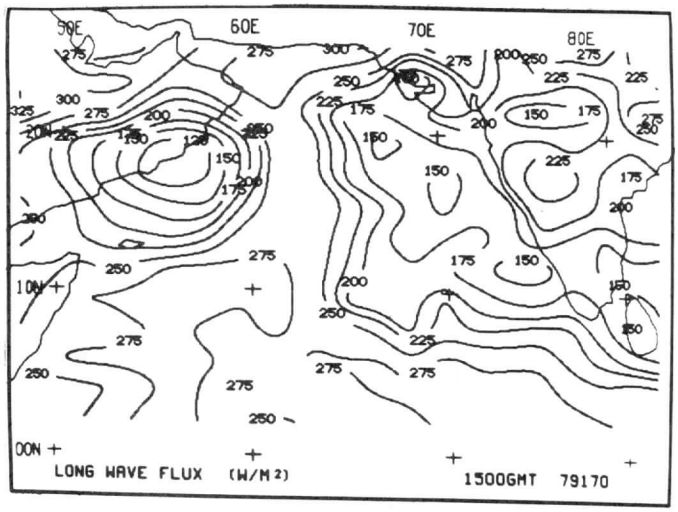
50E
60E
70E
80E
20N
10N
0ON
LONG WAVE FLUX (W/M2)
1500GMT 79170

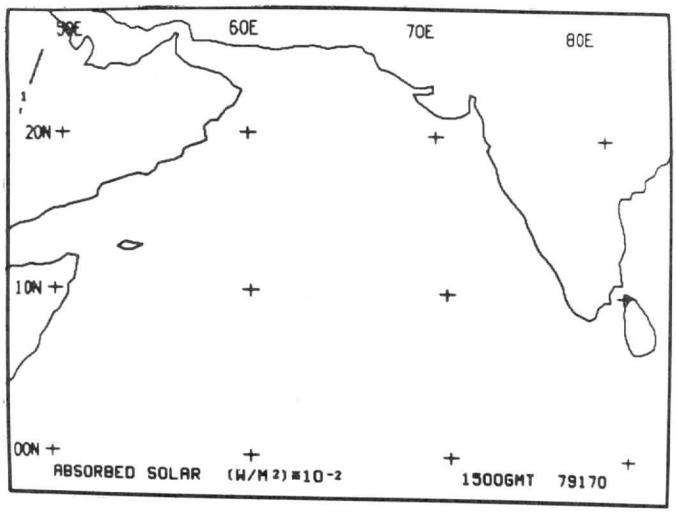
50E
60E
70E
80E
20N
10N
0ON
ABSORBED SOLAR (W/M2)×10-2
1500GMT 79170

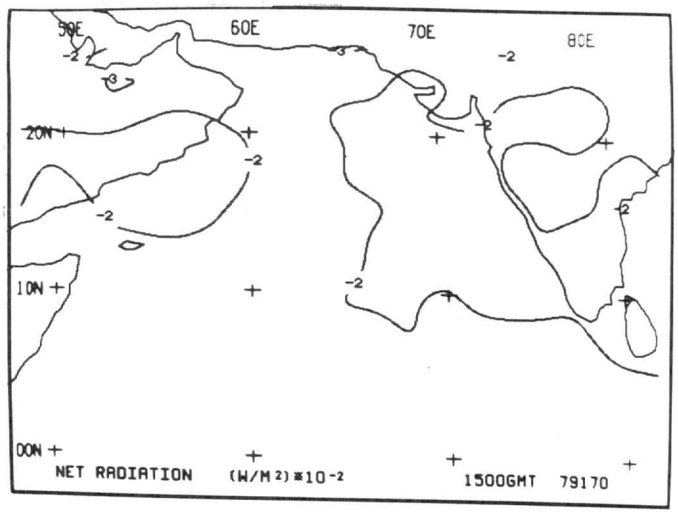
50E
60E
70E
80E
20N
10N
0ON
NET RADIATION (W/M2)×10-2
1500GMT 79170

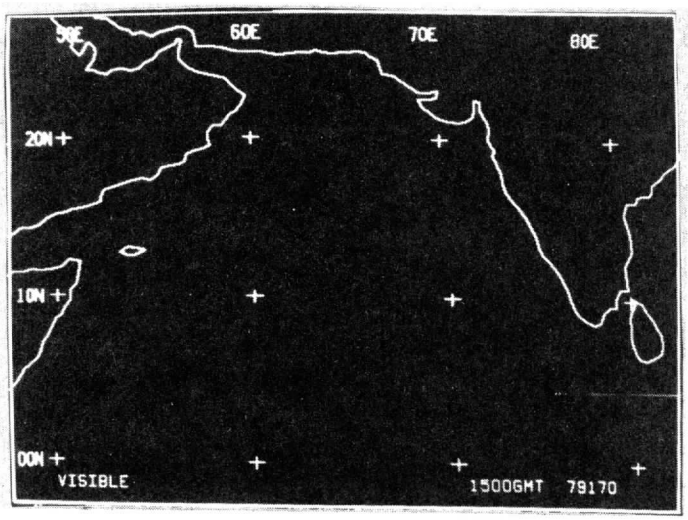
50E
60E
70E
80E
20N
10N
0ON
VISIBLE
1500GMT 79170

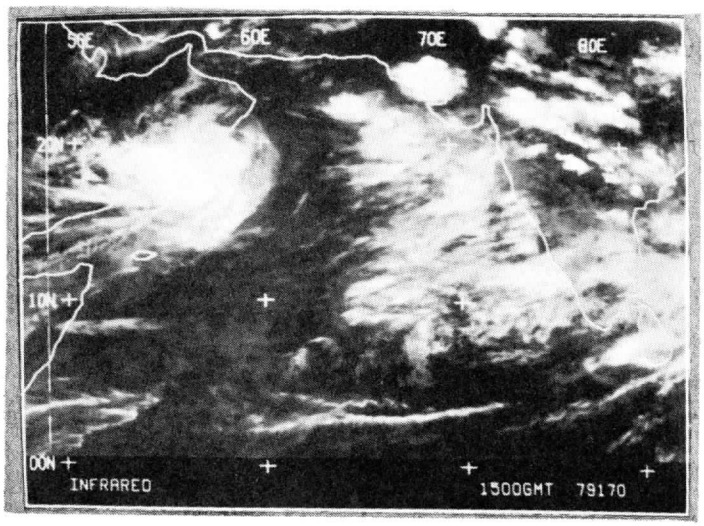
50E
60E
70E
80E
20N
10N
0ON
INFRARED
1500GMT 79170

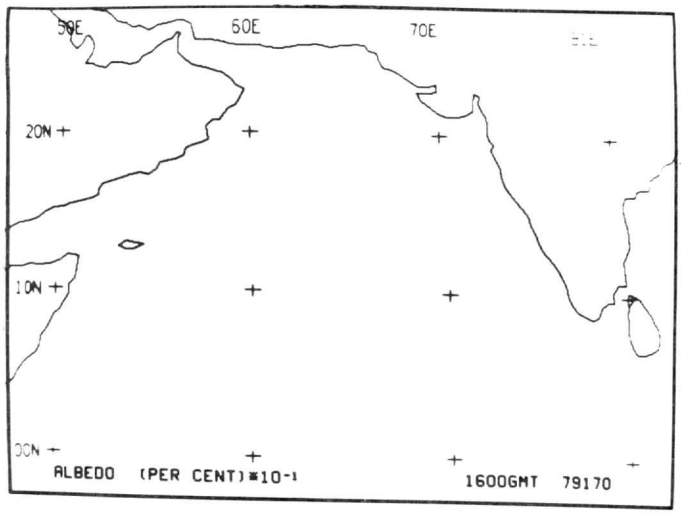
50E
60E
70E
20N
10N
00N
ALBEDO (PER CENT)*10-1
1600GMT 79170

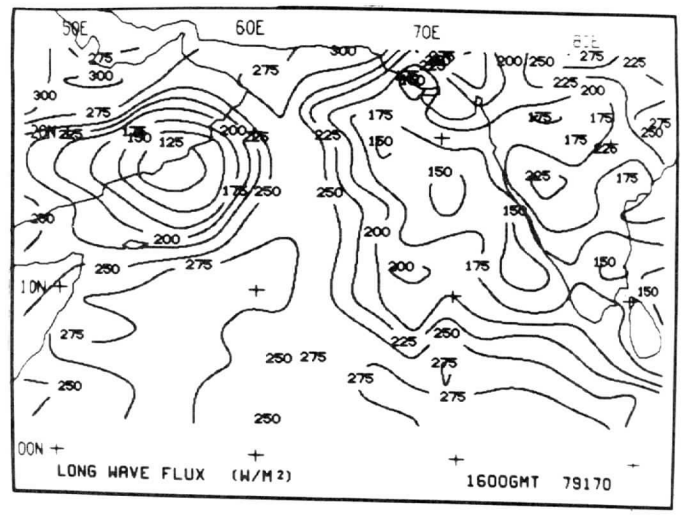
50E
60E
70E
80E
20N
10N
00N
LONG WAVE FLUX (W/M2)
1600GMT 79170

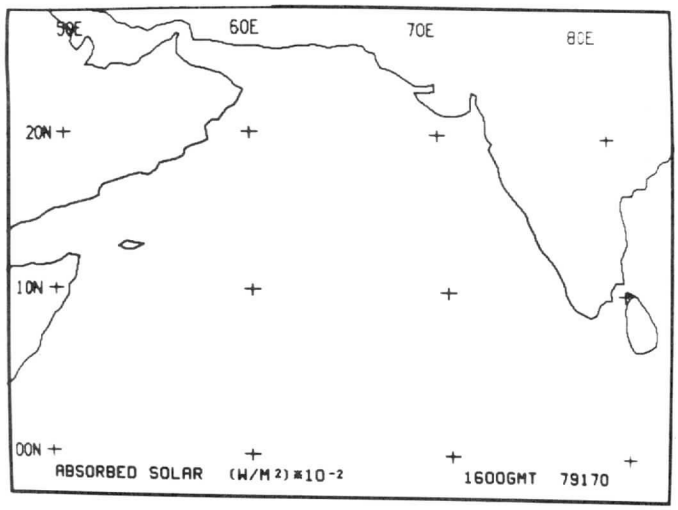
50E
60E
70E
80E
20N
10N
00N
ABSORBED SOLAR (W/M2)*10-2
1600GMT 79170

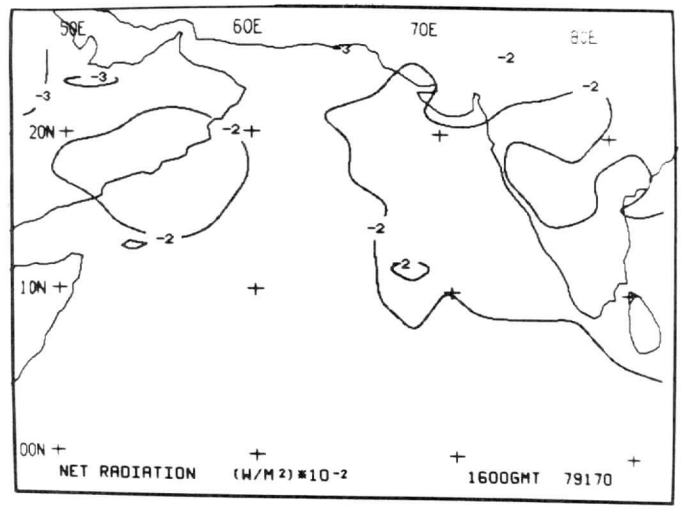
50E
60E
70E
80E
20N
10N
00N
NET RADIATION (W/M2)*10-2
1600GMT 79170

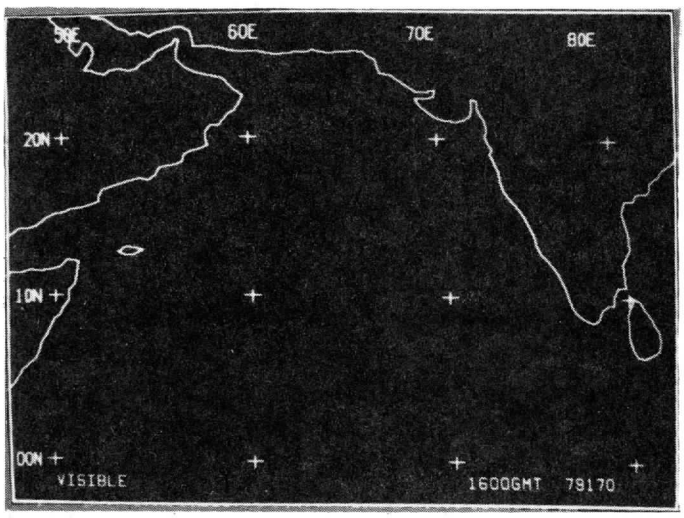
50E
60E
70E
80E
20N
10N
00N
VISIBLE
1600GMT 79170

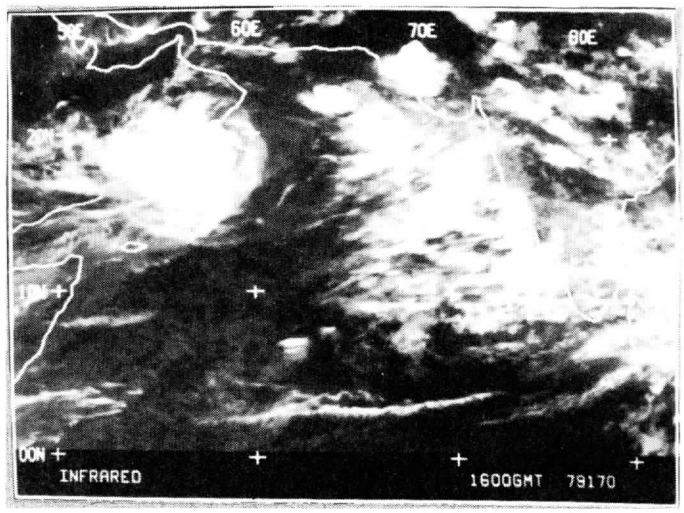
50E
60E
70E
80E
20N
10N
00N
INFRARED
1600GMT 79170

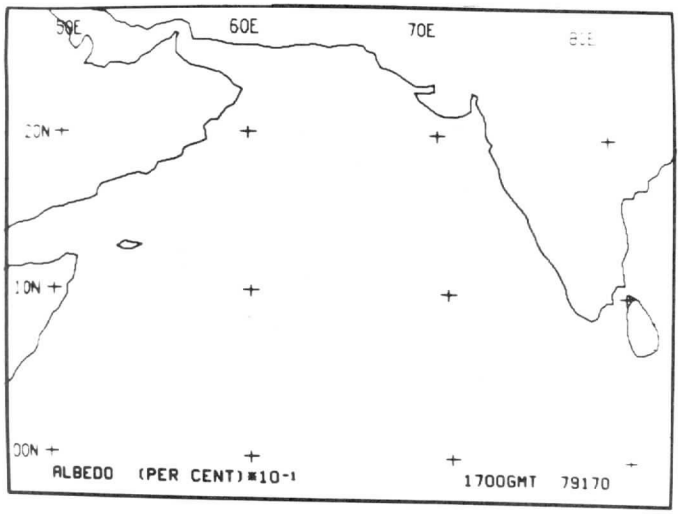
50E
60E
70E
20N
10N
0ON
ALBEDO (PER CENT)*10-1
1700GMT 79170

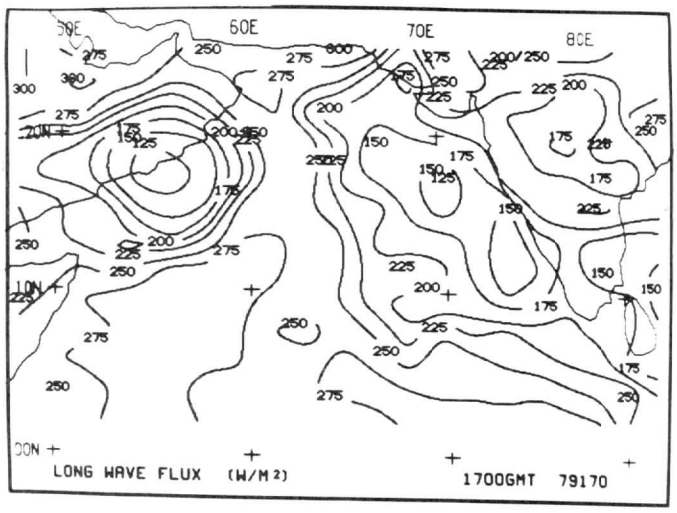
50E
60E
70E
80E
20N
10N
0ON
LONG WAVE FLUX (W/M2)
1700GMT 79170

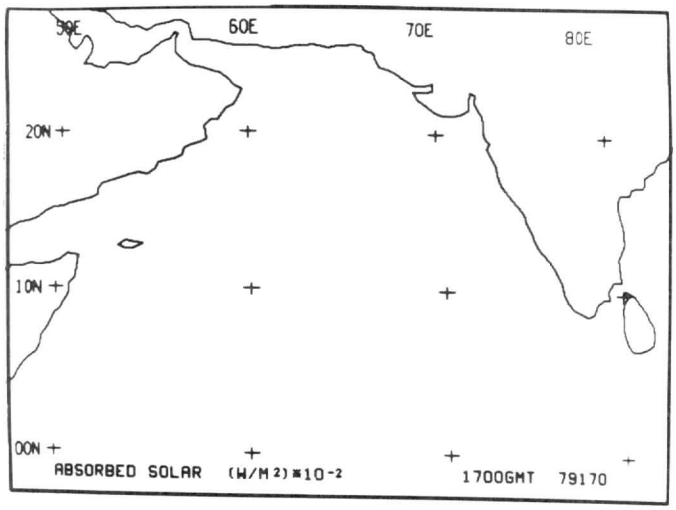
50E
60E
70E
80E
20N
10N
0ON
ABSORBED SOLAR (W/M2)*10-2
1700GMT 79170

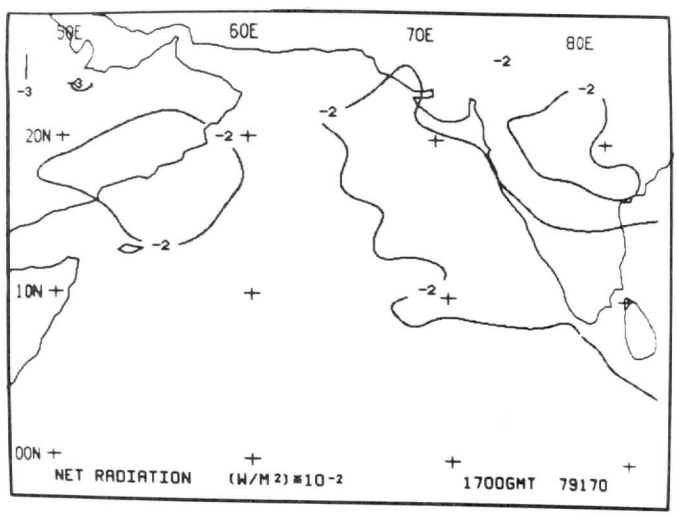
50E
60E
70E
80E
20N
10N
0ON
NET RADIATION (W/M2)*10-2
1700GMT 79170

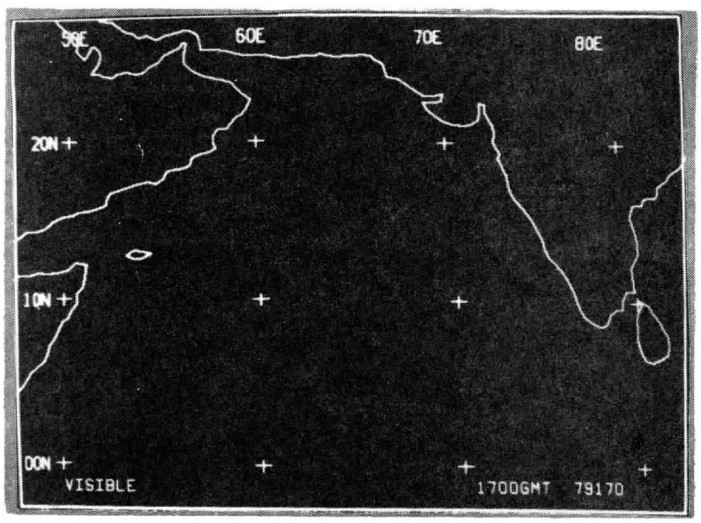
50E
60E
70E
80E
20N
10N
0ON
VISIBLE
1700GMT 79170

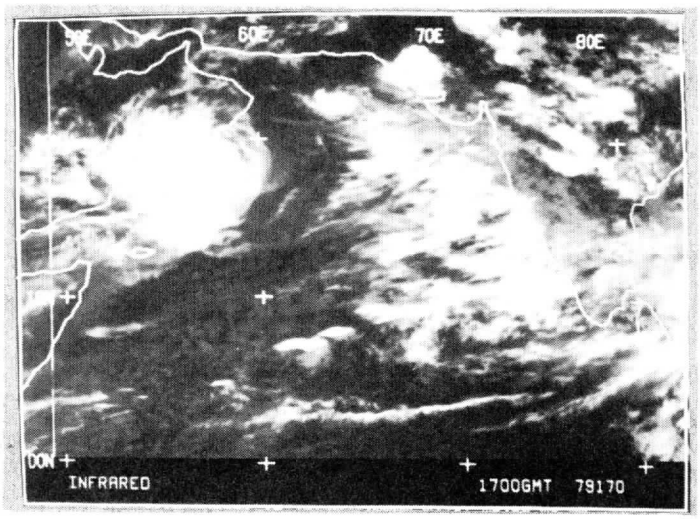
50E
60E
70E
80E
0ON
INFRARED
1700GMT 79170

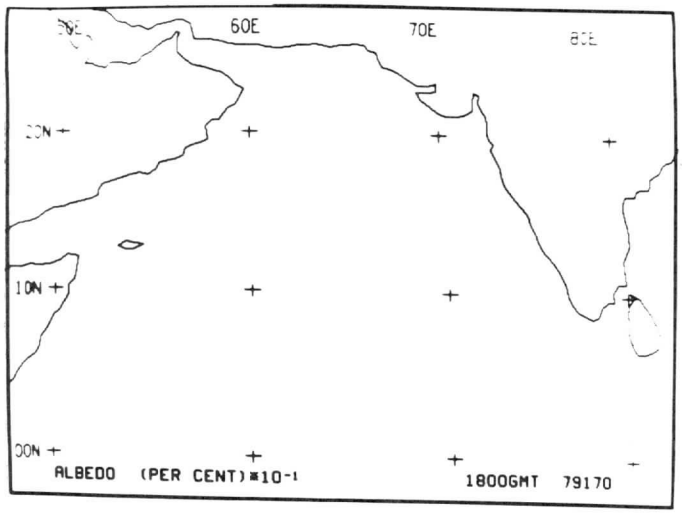
50E
60E
70E
80E
20N
10N
0ON
ALBEDO (PER CENT)*10-1
1800GMT 79170

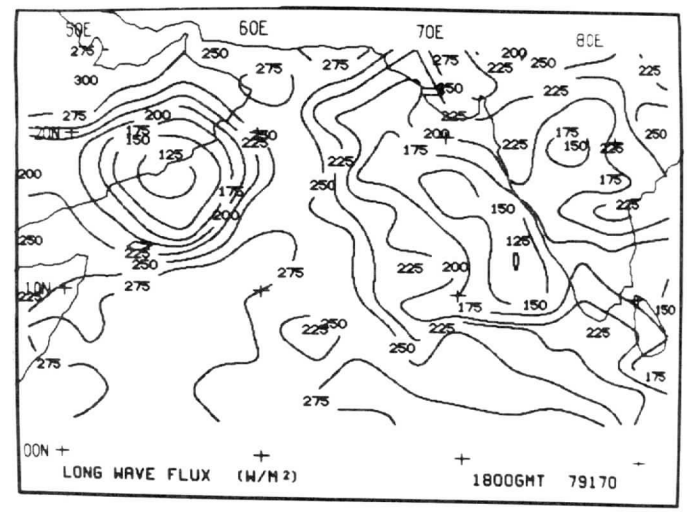
50E
60E
70E
80E
20N
10N
0ON
LONG WAVE FLUX (W/M2)
1800GMT 79170

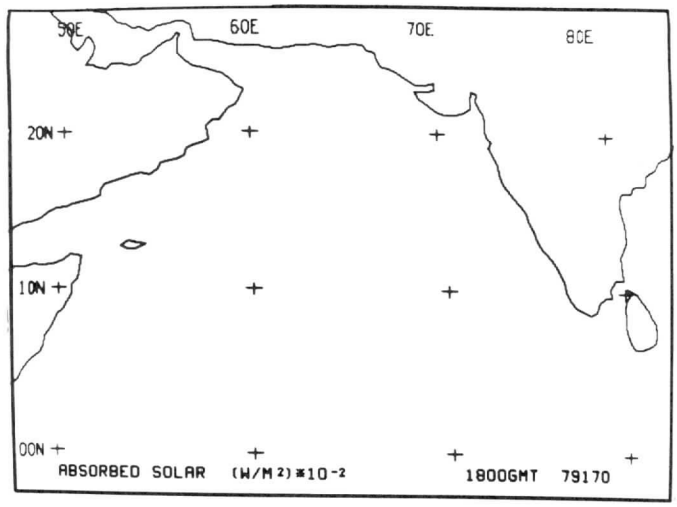
50E
60E
70E
80E
20N
10N
0ON
ABSORBED SOLAR (W/M2)*10-2
1800GMT 79170

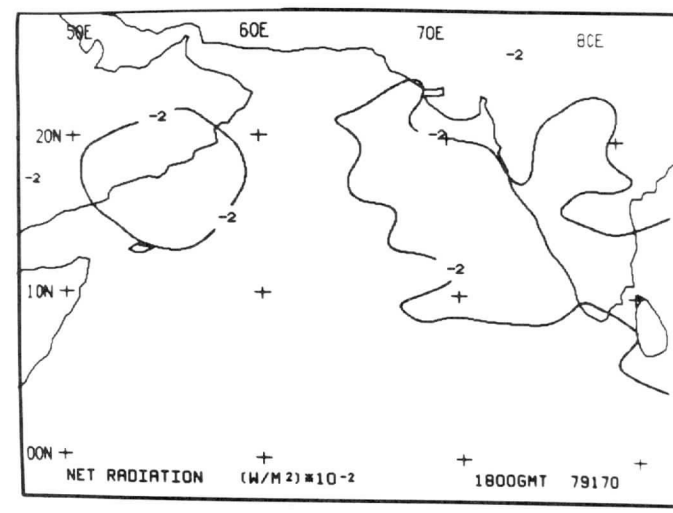
50E
60E
70E
80E
20N
10N
0ON
NET RADIATION (W/M2)*10-2
1800GMT 79170

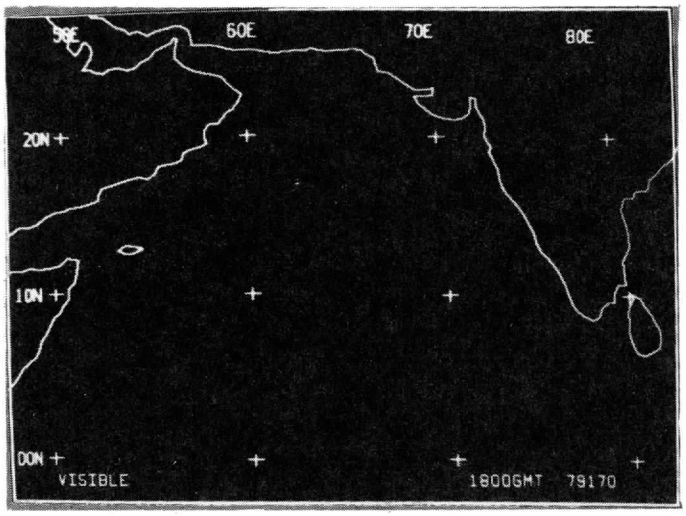
50E
60E
70E
80E
20N
10N
0ON
VISIBLE
1800GMT 79170

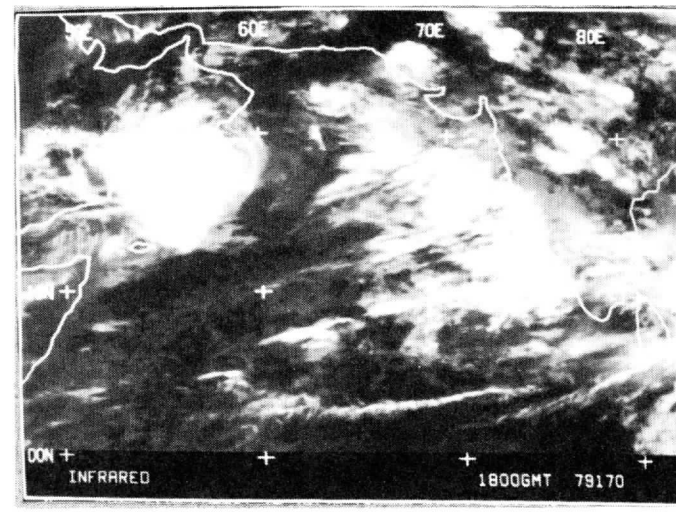
60E
70E
80E
0ON
INFRARED
1800GMT 79170

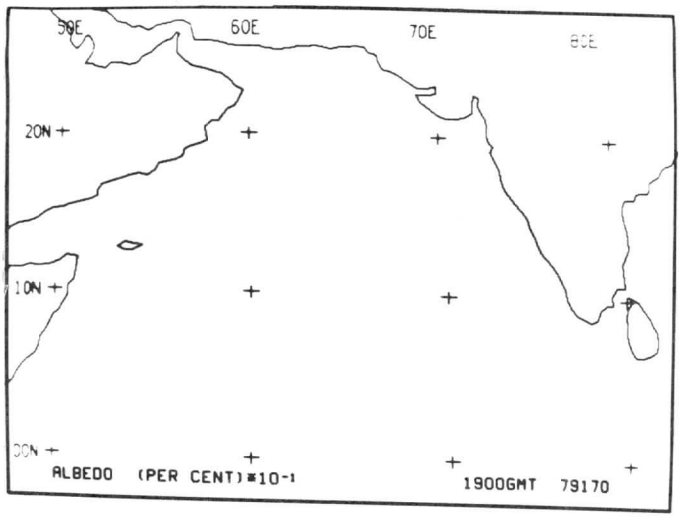
50E
60E
70E
80E
20N
10N
0ON
ALBEDO (PER CENT)*10-1
1900GMT 79170

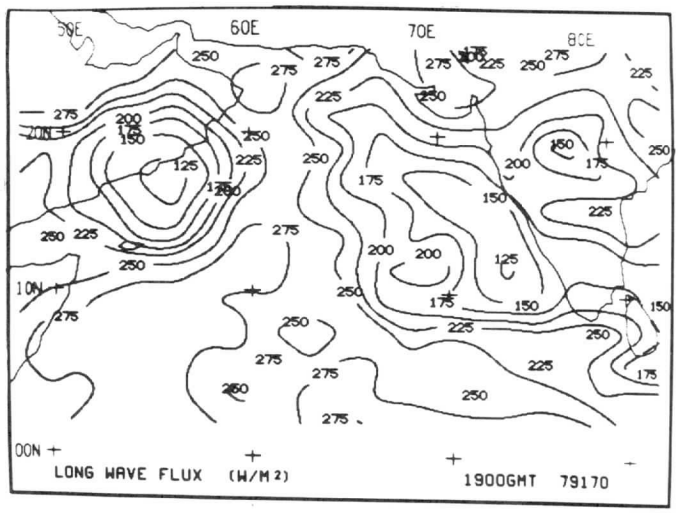
50E
60E
70E
80E
20N
10N
0ON
LONG WAVE FLUX (W/M2)
1900GMT 79170

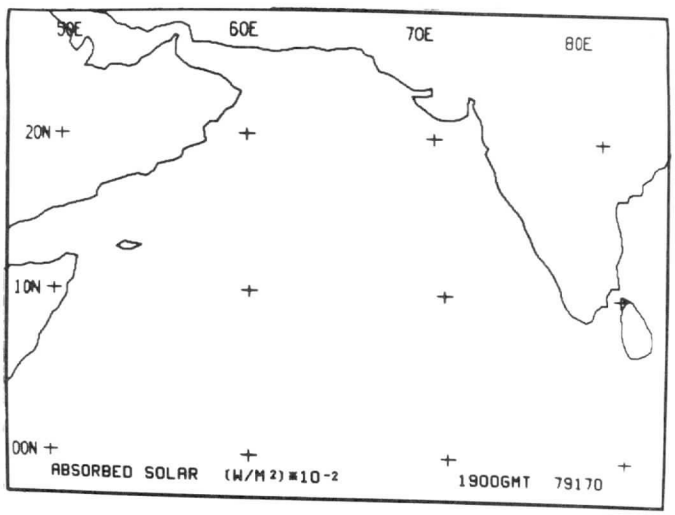
50E
60E
70E
80E
20N
10N
0ON
ABSORBED SOLAR (W/M2)*10-2
1900GMT 79170

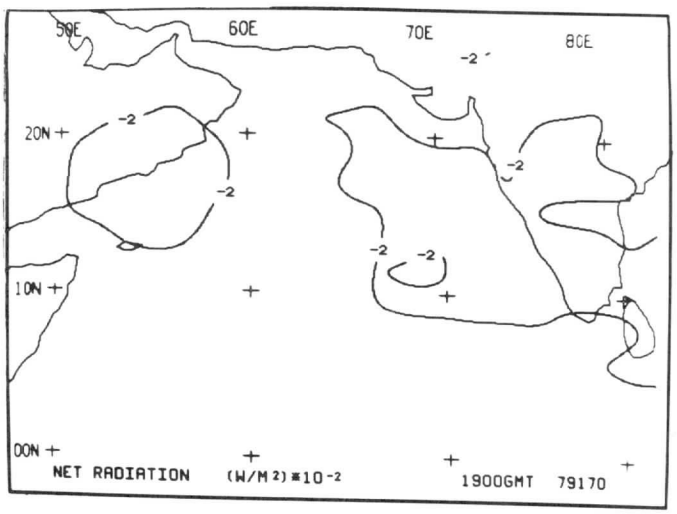
50E
60E
70E
80E
20N
10N
0ON
NET RADIATION (W/M2)*10-2
1900GMT 79170

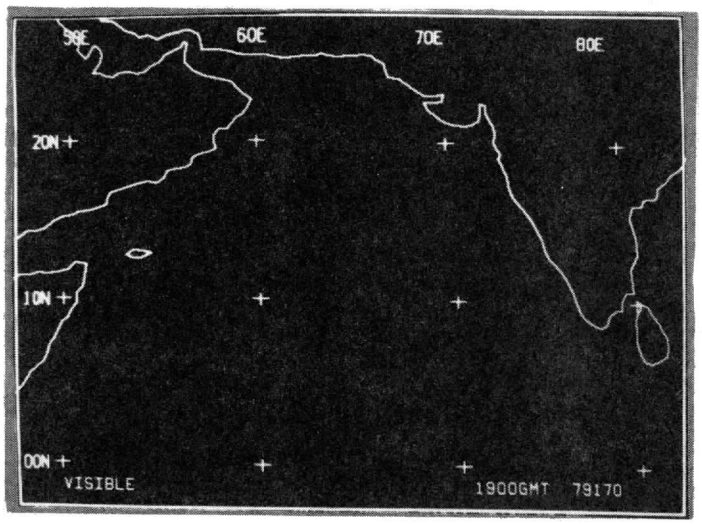
50E
60E
70E
80E
20N
10N
0ON
VISIBLE
1900GMT 79170

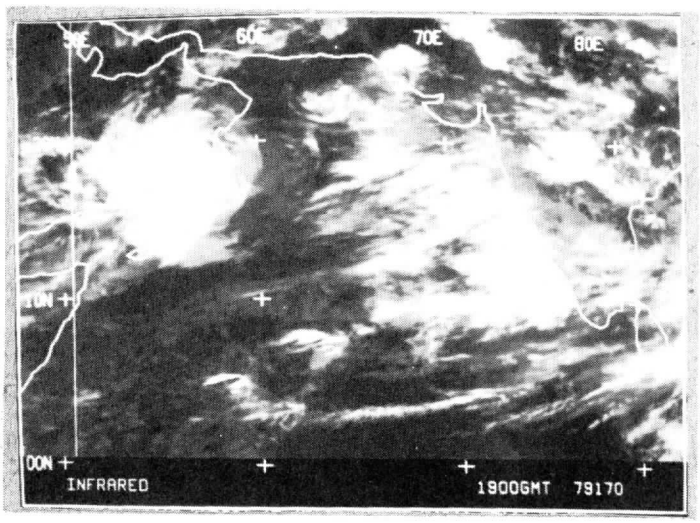
50E
60E
70E
80E
20N
10N
0ON
INFRARED
1900GMT 79170

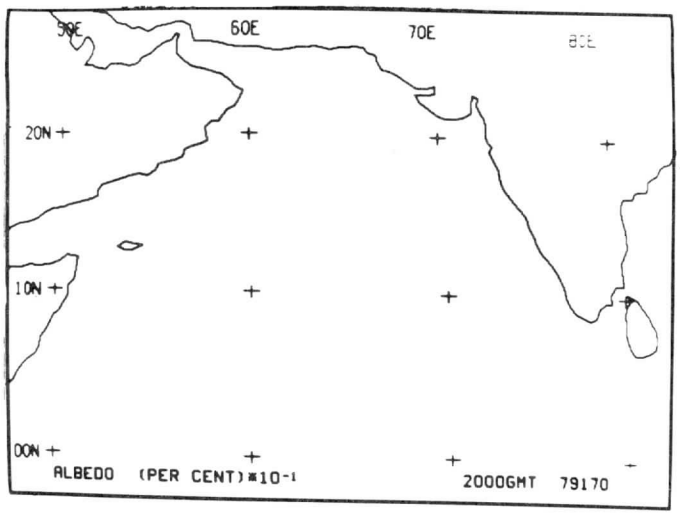
50E
60E
70E
80E
20N
10N
0ON
ALBEDO (PER CENT)*10-1
2000GMT 79170

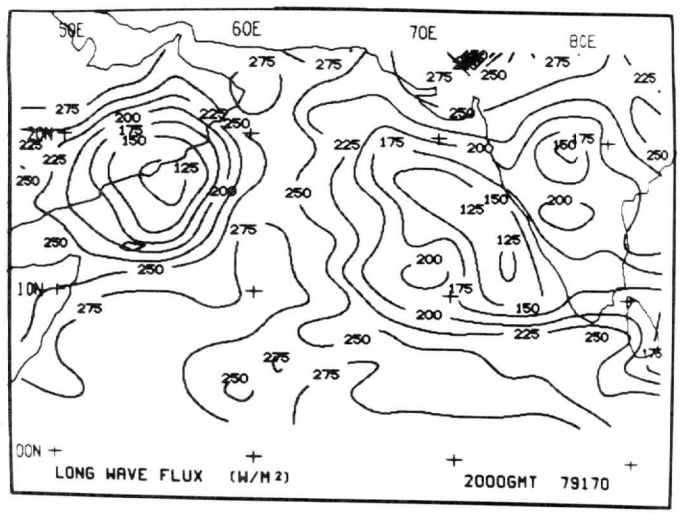
50E
60E
70E
80E
20N
10N
0ON
LONG WAVE FLUX (W/M2)
2000GMT 79170

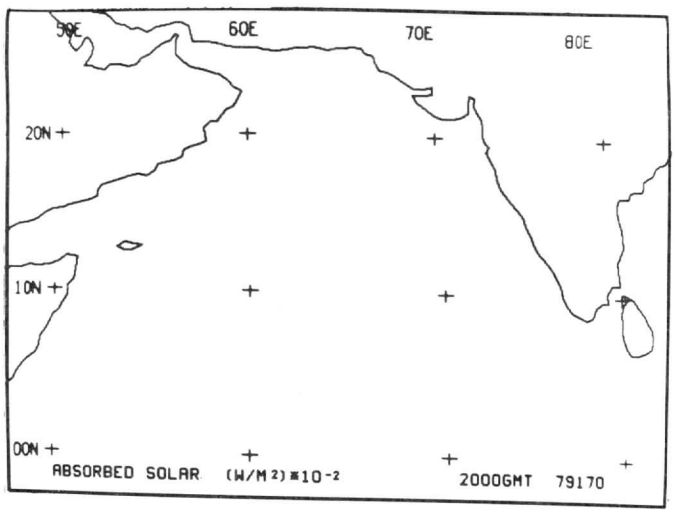
50E
60E
70E
80E
20N
10N
0ON
ABSORBED SOLAR (W/M2)*10-2
2000GMT 79170

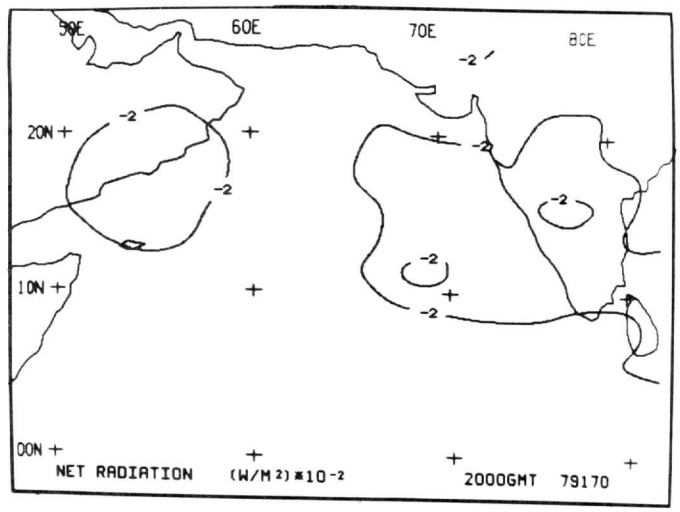
50E
60E
70E
80E
20N
10N
0ON
NET RADIATION (W/M2)*10-2
2000GMT 79170

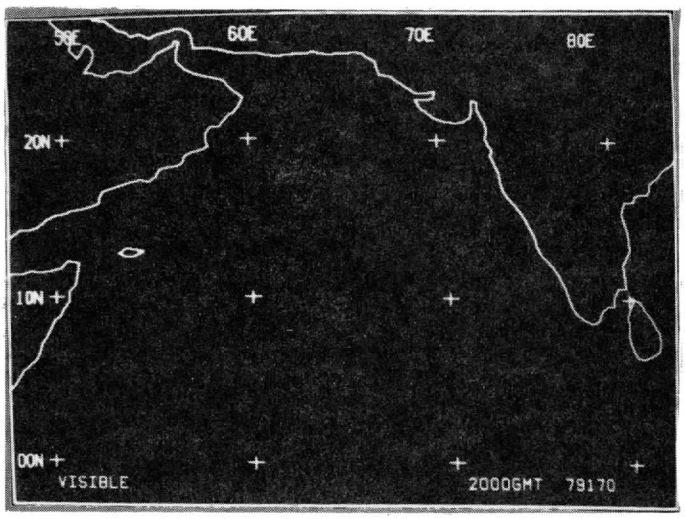
50E
60E
70E
80E
20N
10N
0ON
VISIBLE
2000GMT 79170

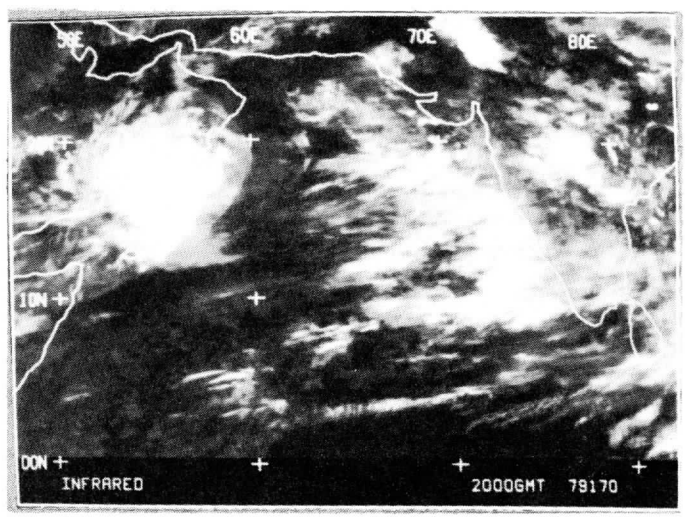
50E
60E
70E
80E
20N
10N
0ON
INFRARED
2000GMT 79170

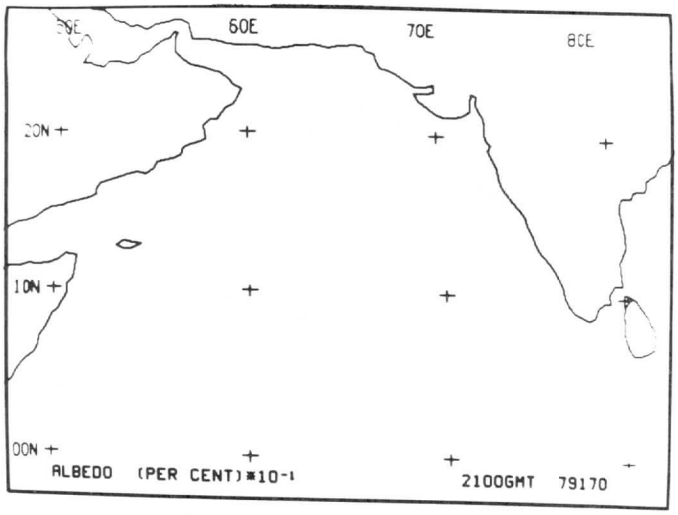
50E
60E
70E
80E
20N
10N
0ON
ALBEDO (PER CENT)*10-1
2100GMT 79170

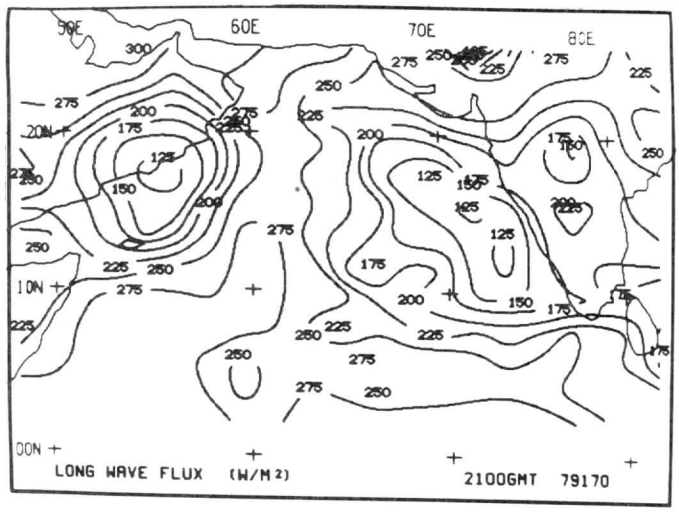
50E
60E
70E
80E
20N
10N
0ON
LONG WAVE FLUX (W/M2)
2100GMT 79170

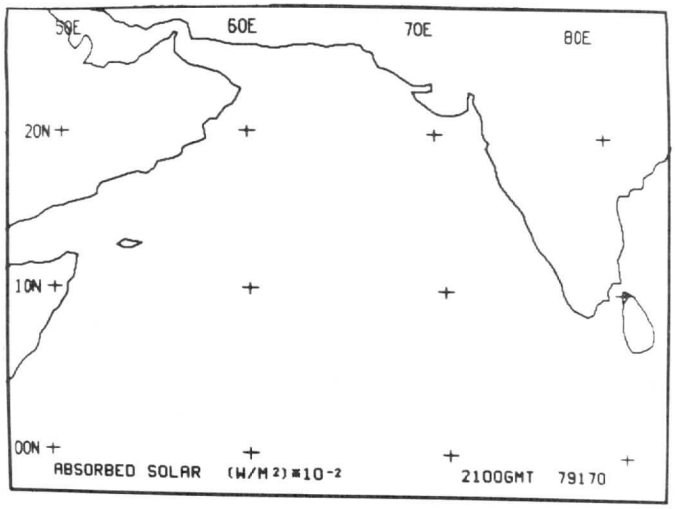
50E
60E
70E
80E
20N
10N
0ON
ABSORBED SOLAR (W/M2)*10-2
2100GMT 79170

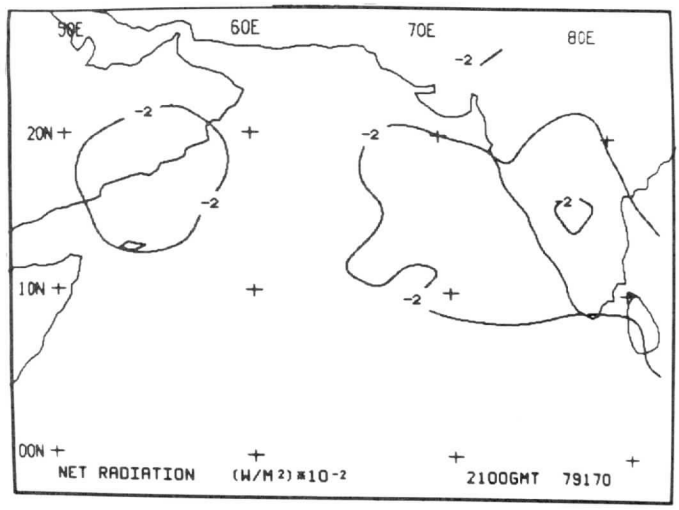
50E
60E
70E
80E
20N
10N
0ON
NET RADIATION (W/M2)*10-2
2100GMT 79170

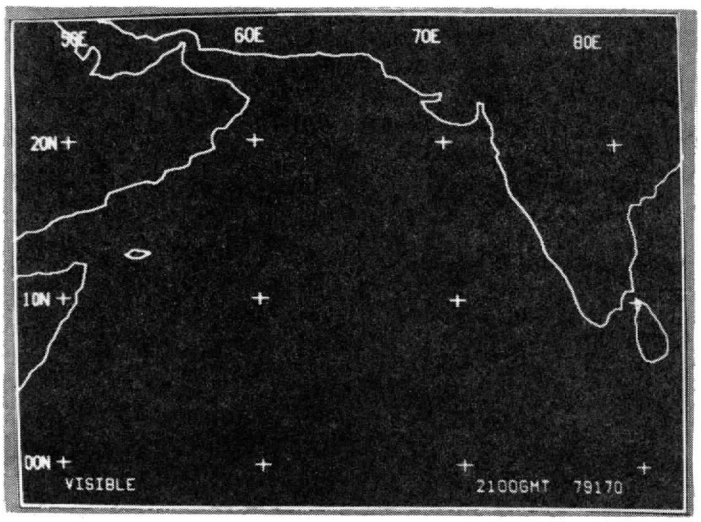
50E
60E
70E
80E
20N
10N
0ON
VISIBLE
2100GMT 79170

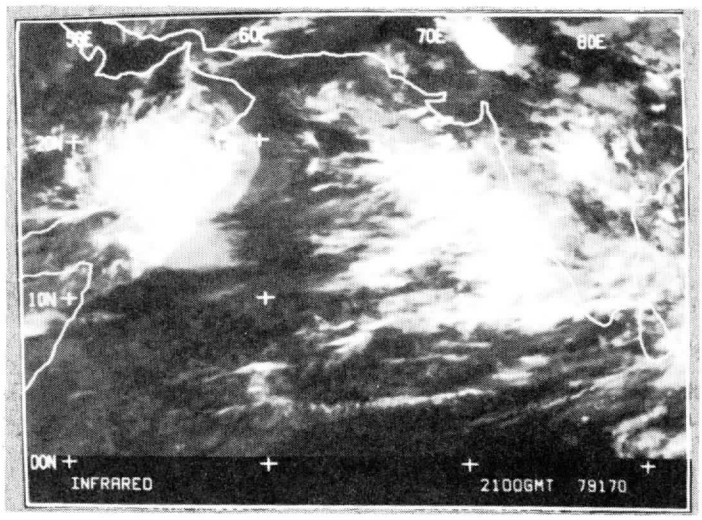
50E
60E
70E
80E
20N
10N
0ON
INFRARED
2100GMT 79170

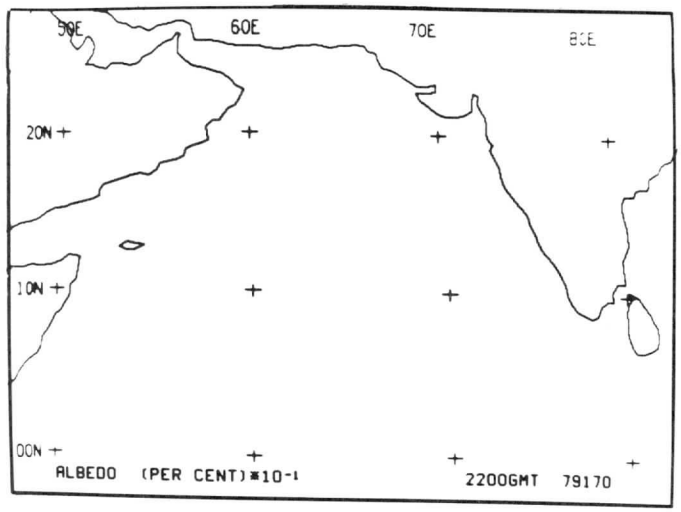
50E
60E
70E
80E
20N
10N
0ON
ALBEDO (PER CENT)*10-1
2200GMT 79170

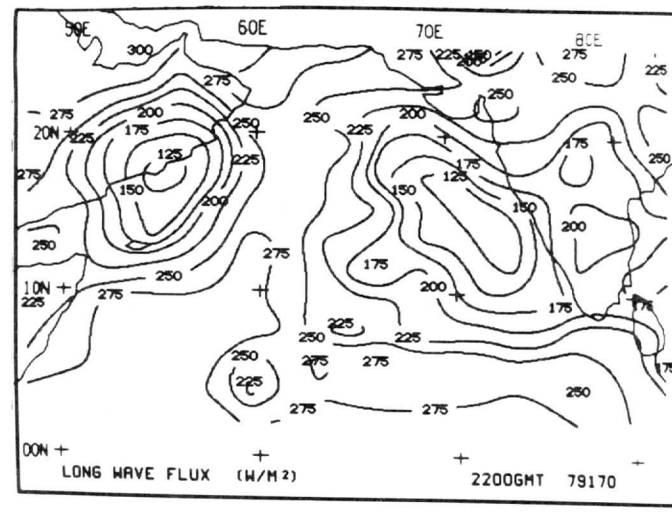
50E
60E
70E
80E
20N
10N
0ON
LONG WAVE FLUX (W/M2)
2200GMT 79170

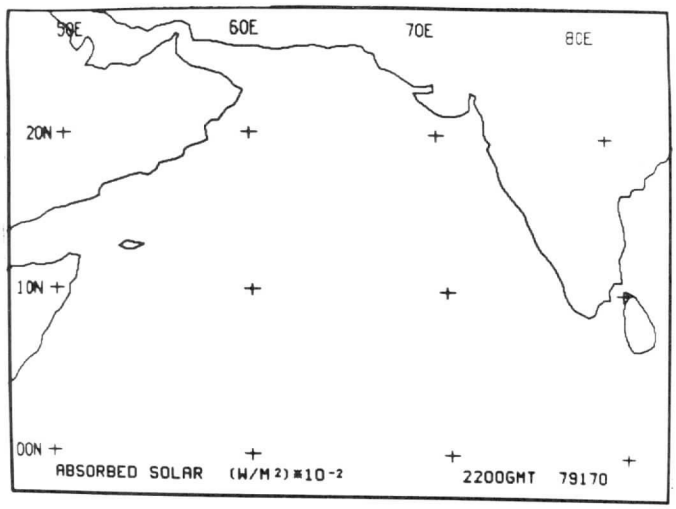
50E
60E
70E
80E
20N
10N
0ON
ABSORBED SOLAR (W/M2)*10-2
2200GMT 79170

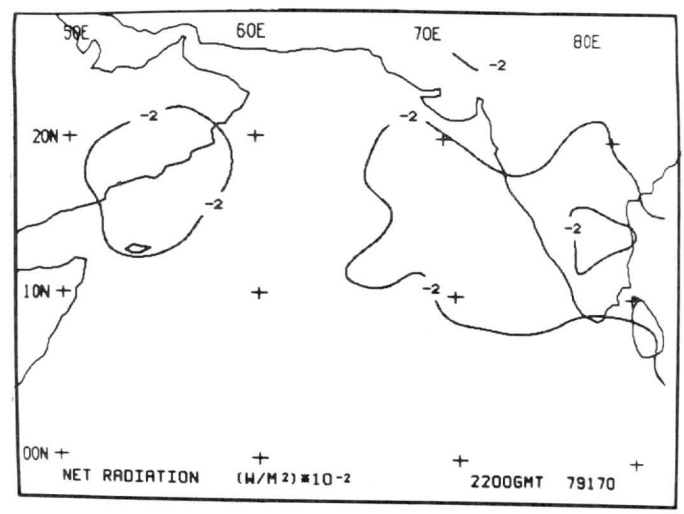
50E
60E
70E
80E
20N
10N
0ON
NET RADIATION (W/M2)*10-2
2200GMT 79170

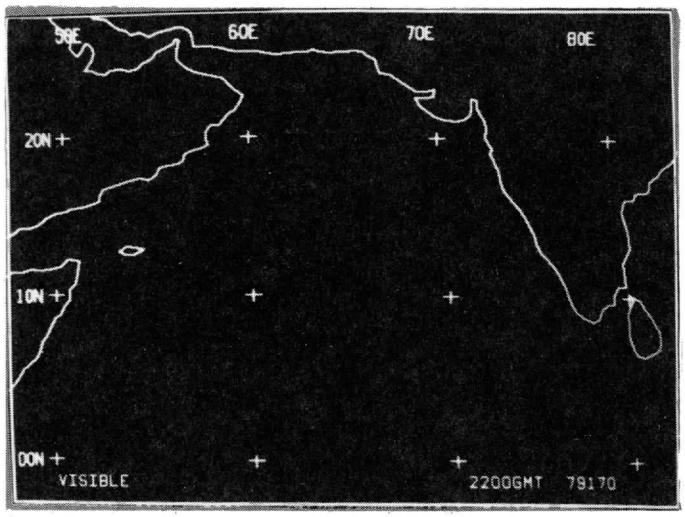
50E
60E
70E
80E
20N
10N
0ON
VISIBLE
2200GMT 79170

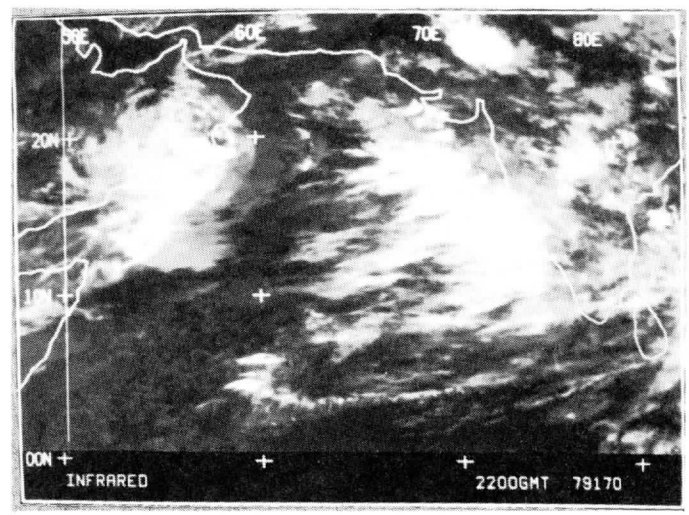
50E
60E
70E
80E
20N
10N
0ON
INFRARED
2200GMT 79170

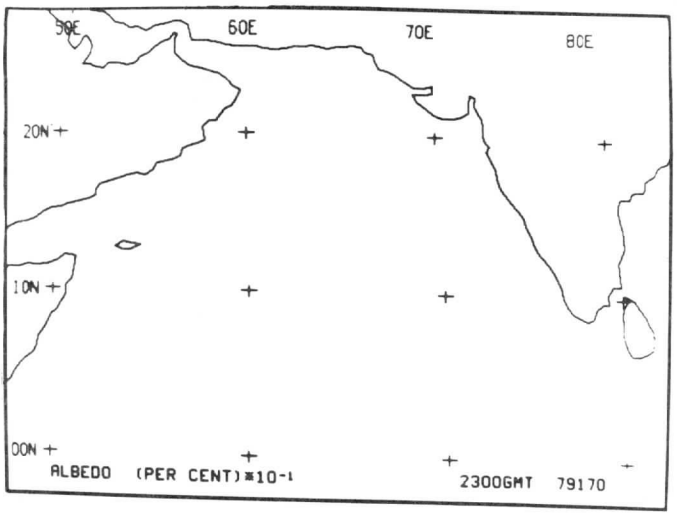
50E
60E
70E
80E
20N
10N
00N
ALBEDO (PER CENT)*10-1
2300GMT 79170

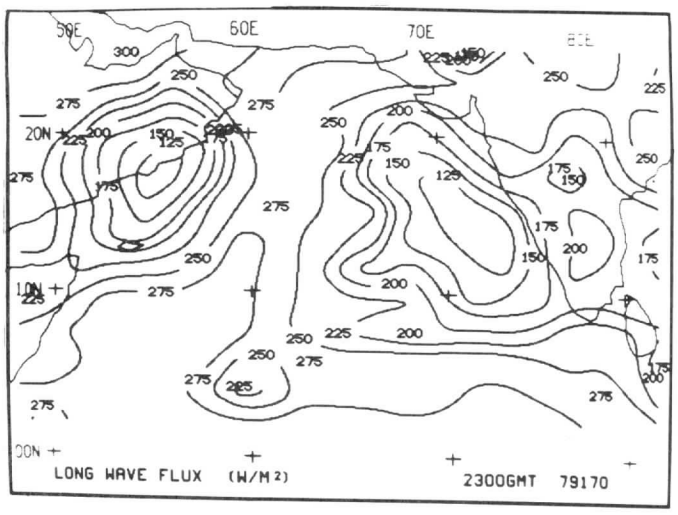
50E
60E
70E
80E
20N
10N
00N
LONG WAVE FLUX (W/M2)
2300GMT 79170

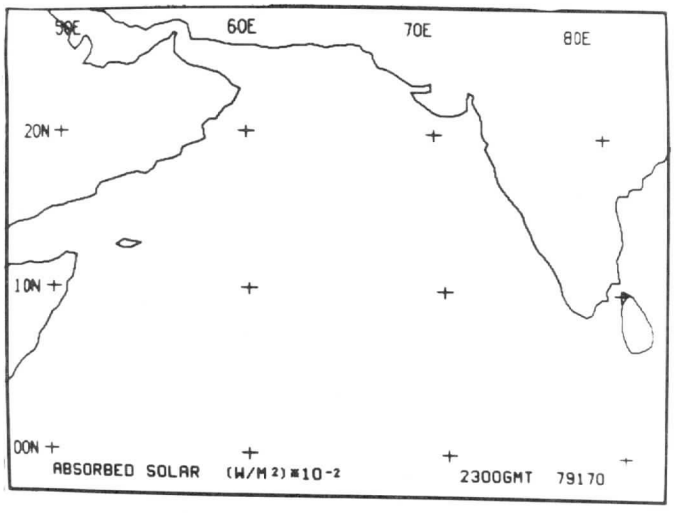
50E
60E
70E
80E
20N
10N
00N
ABSORBED SOLAR (W/M2)*10-2
2300GMT 79170

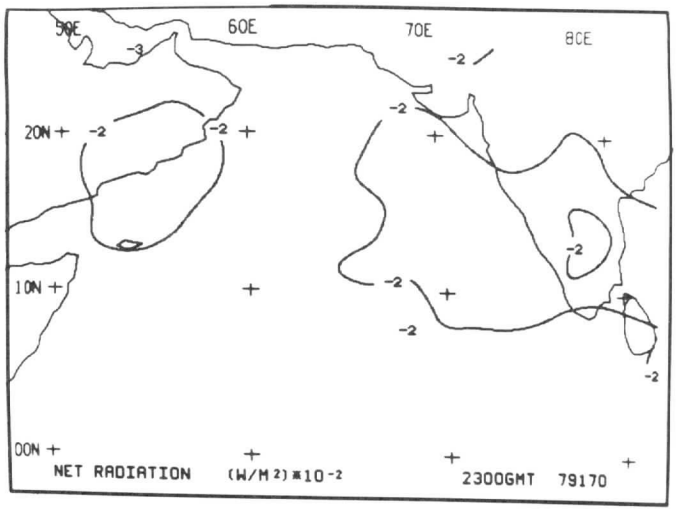
50E
60E
70E
80E
20N
10N
00N
NET RADIATION (W/M2)*10-2
2300GMT 79170

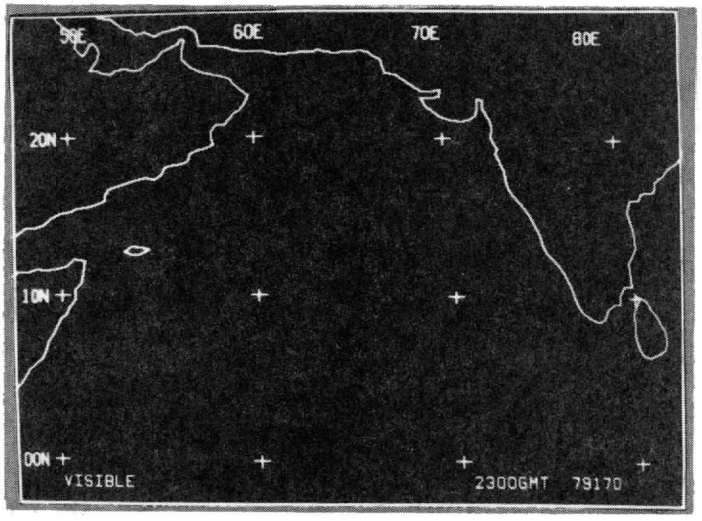
50E
60E
70E
80E
20N
10N
00N
VISIBLE
2300GMT 79170

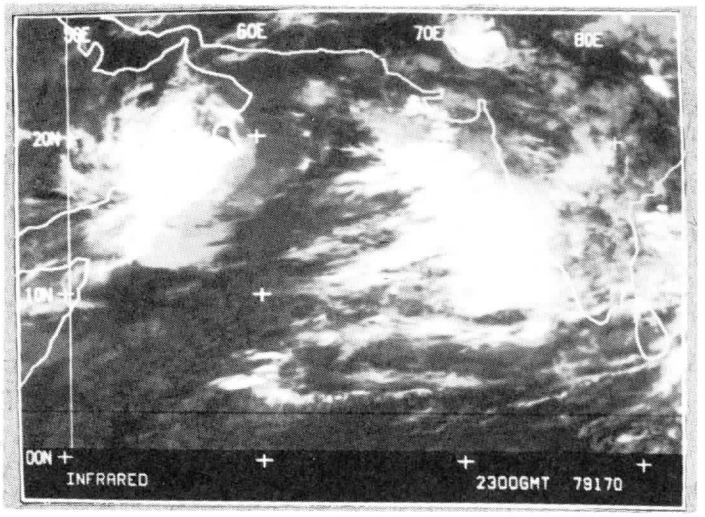
50E
60E
70E
80E
20N
10N
00N
INFRARED
2300GMT 79170

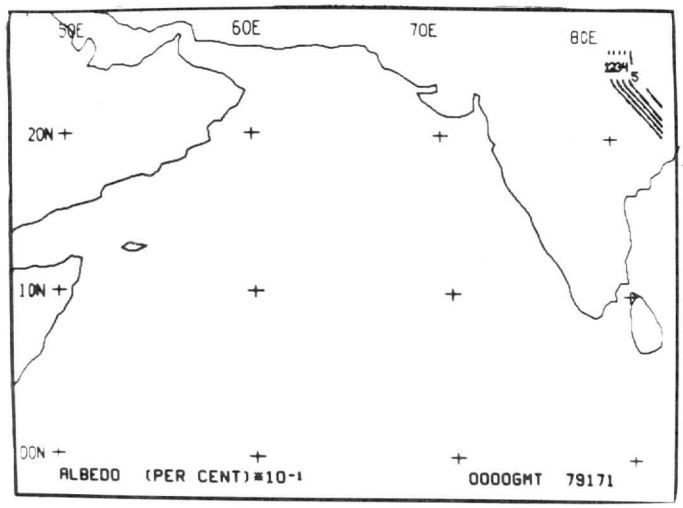
50E
60E
70E
80E
20N
10N
0ON
ALBEDO (PER CENT)*10-1
0000GMT 79171

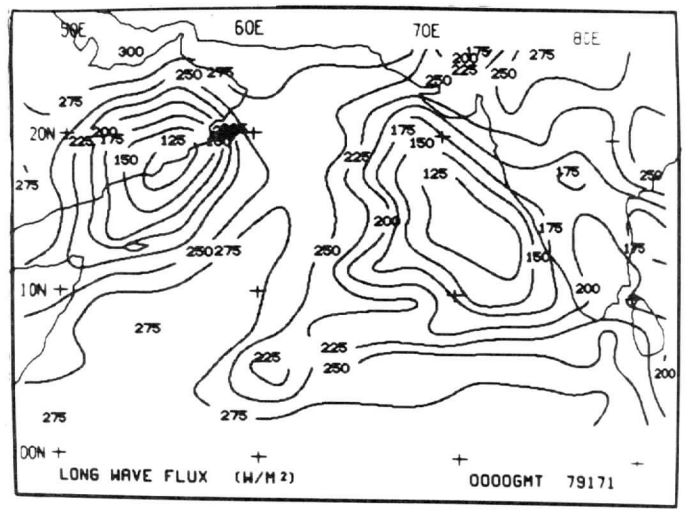
50E
60E
70E
80E
20N
10N
0ON
LONG WAVE FLUX (W/M2)
0000GMT 79171

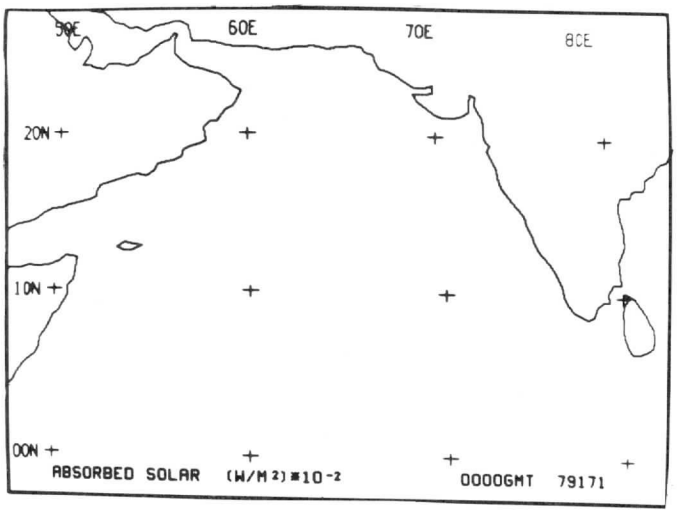
50E
60E
70E
80E
20N
10N
0ON
ABSORBED SOLAR (W/M2)*10-2
0000GMT 79171

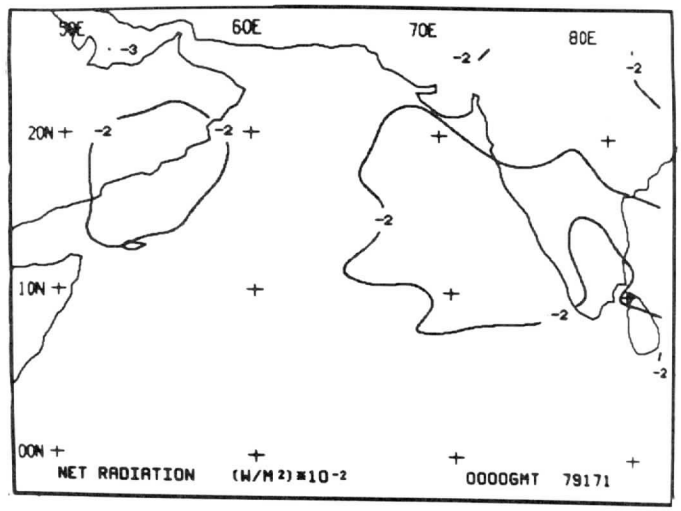
50E
60E
70E
80E
20N
10N
0ON
NET RADIATION (W/M2)*10-2
0000GMT 79171

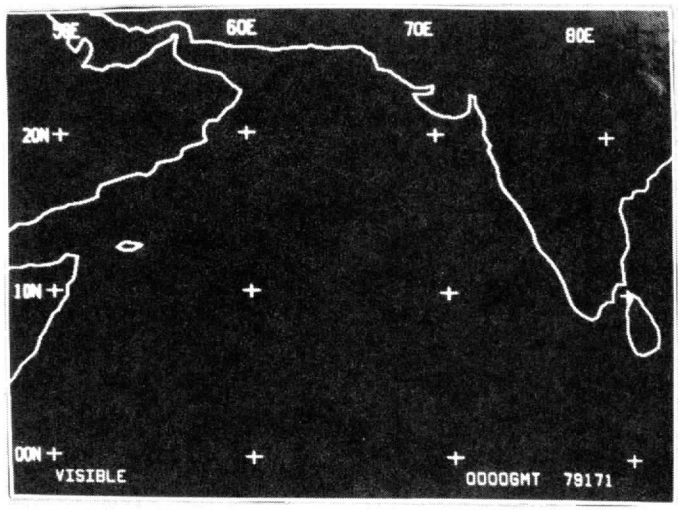
50E
60E
70E
80E
20N
10N
0ON
VISIBLE
0000GMT 79171

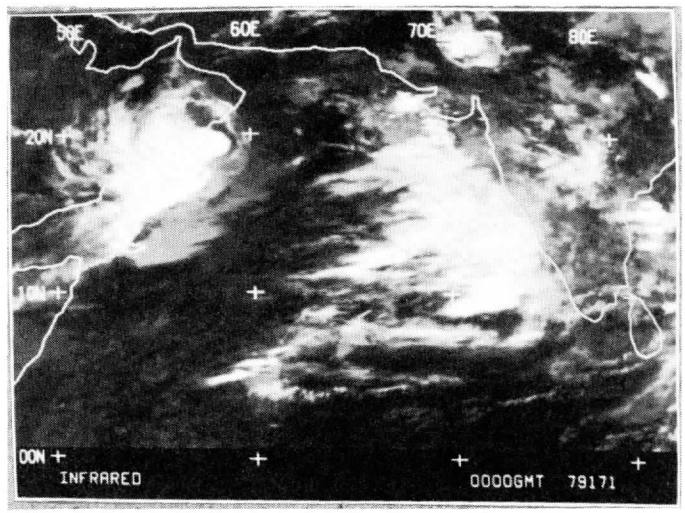
50E
60E
70E
80E
20N
10N
0ON
INFRARED
0000GMT 79171

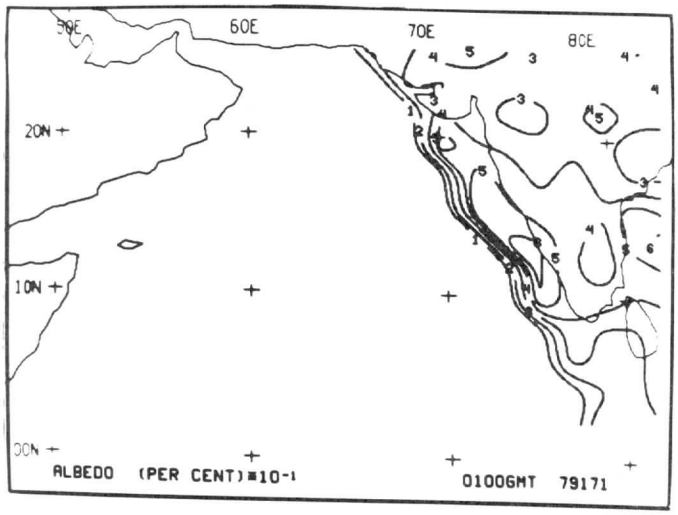
50E
60E
70E
80E
20N
10N
0ON
ALBEDO (PER CENT)*10-1
0100GMT 79171

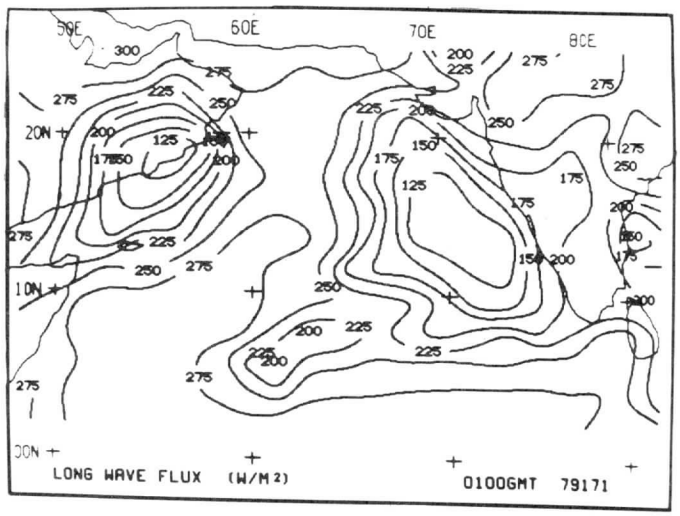
50E
60E
70E
80E
20N
10N
0ON
LONG WAVE FLUX (W/M2)
0100GMT 79171

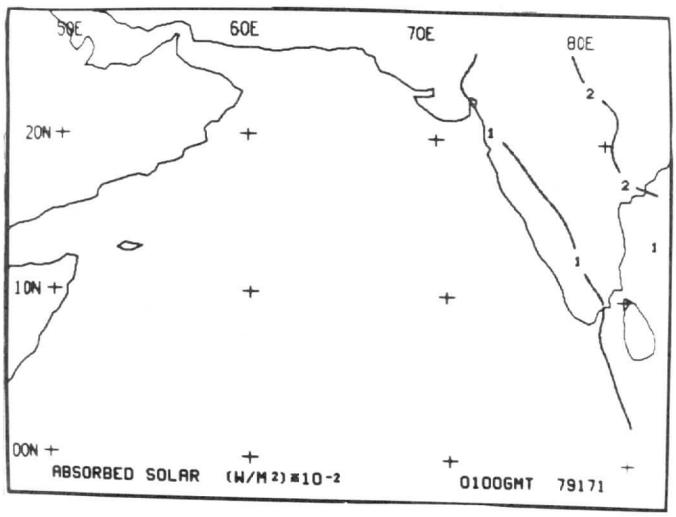
50E
60E
70E
80E
20N
10N
0ON
ABSORBED SOLAR (W/M2)*10-2
0100GMT 79171

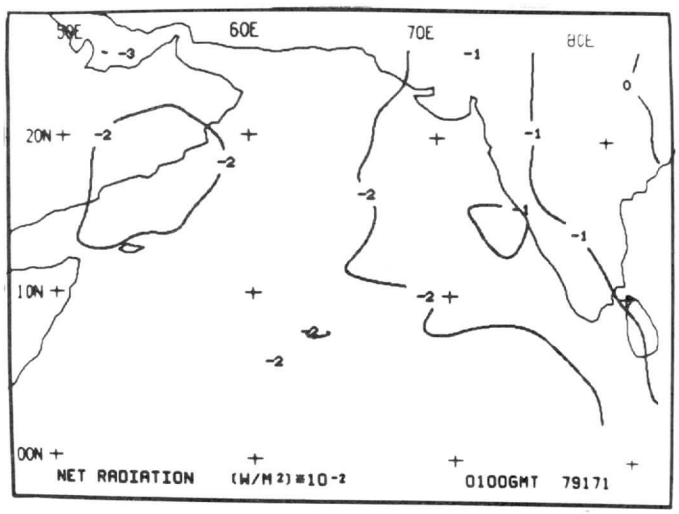
50E
60E
70E
80E
20N
10N
0ON
NET RADIATION (W/M2)*10-2
0100GMT 79171

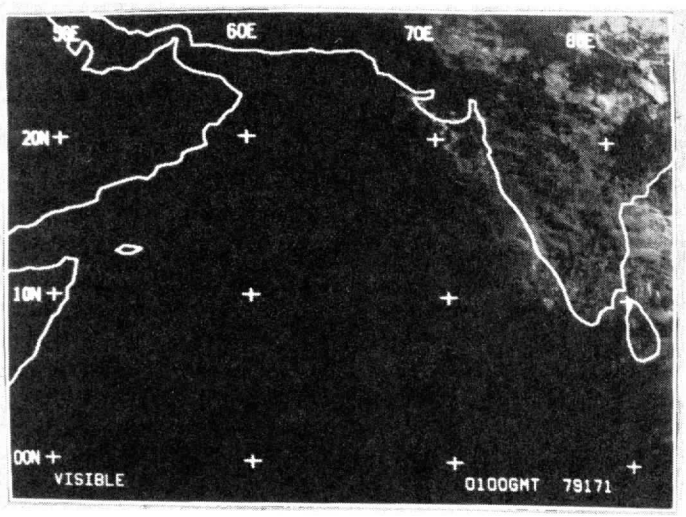
50E
60E
70E
80E
20N
10N
0ON
VISIBLE
0100GMT 79171

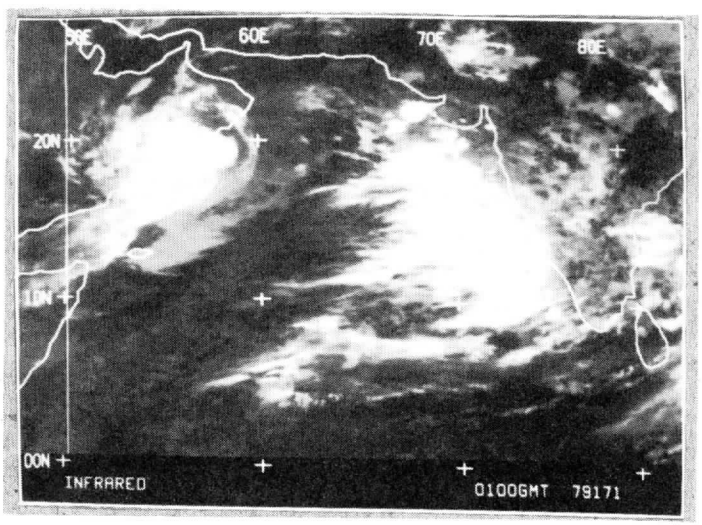
50E
60E
70E
80E
20N
10N
0ON
INFRARED
0100GMT 79171

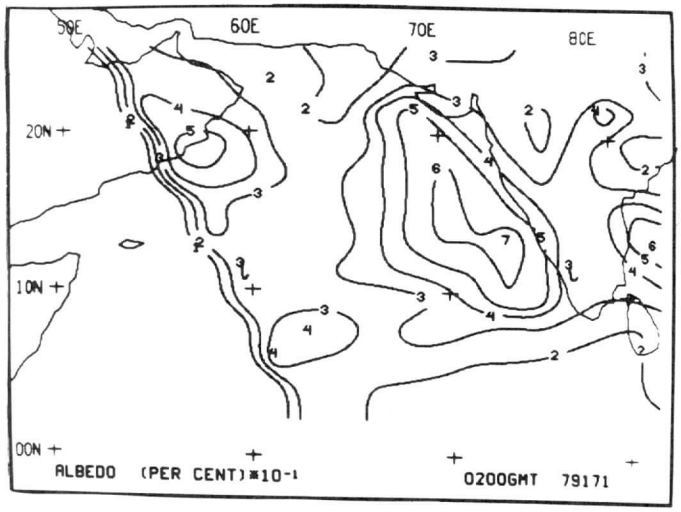
50E
60E
70E
80E
20N
10N
0ON
ALBEDO (PER CENT)*10-1
0200GMT 79171

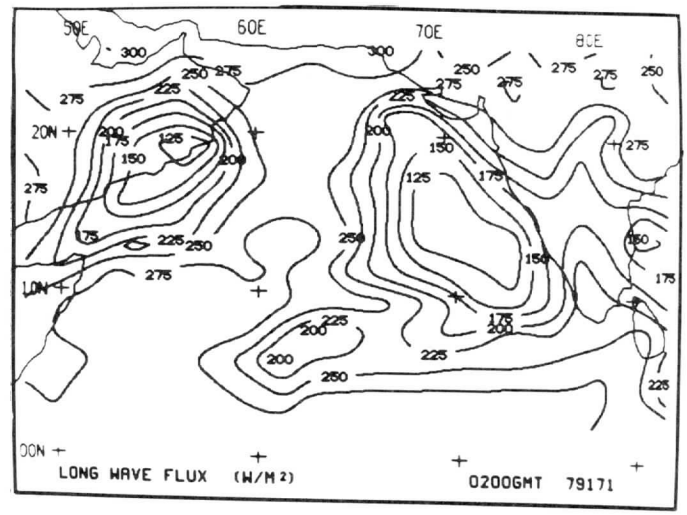
50E
60E
70E
80E
20N
10N
0ON
LONG WAVE FLUX (W/M2)
0200GMT 79171

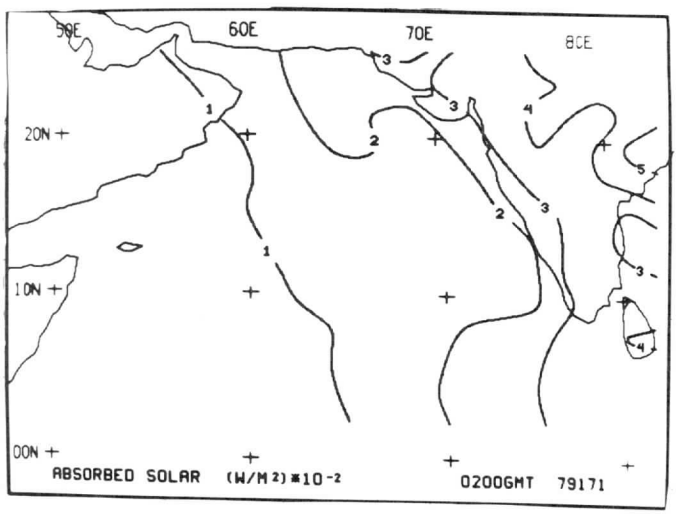
50E
60E
70E
80E
20N
10N
0ON
ABSORBED SOLAR (W/M2)*10-2
0200GMT 79171

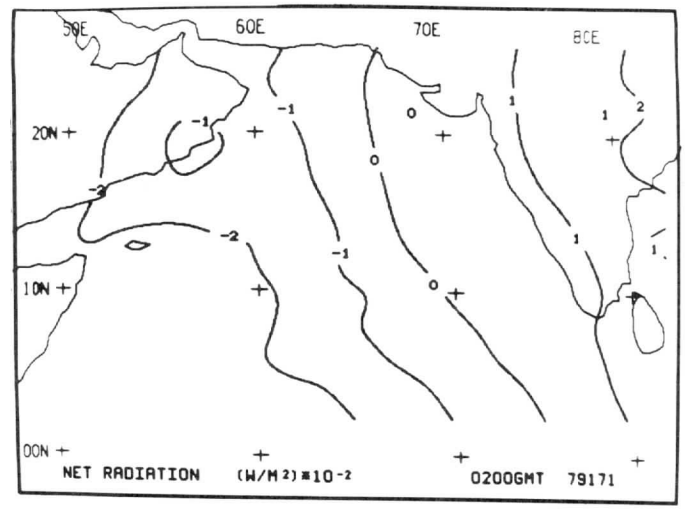
50E
60E
70E
80E
20N
10N
0ON
NET RADIATION (W/M2)*10-2
0200GMT 79171

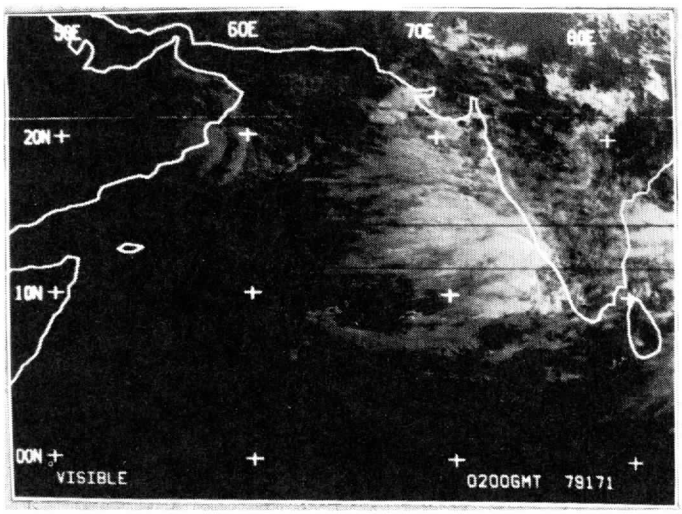
50E
60E
70E
80E
20N
10N
0ON
VISIBLE
0200GMT 79171

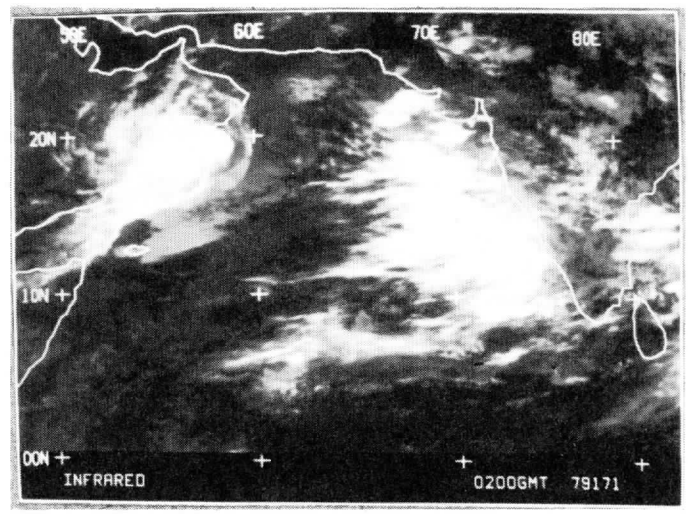
50E
60E
70E
80E
20N
10N
0ON
INFRARED
0200GMT 79171

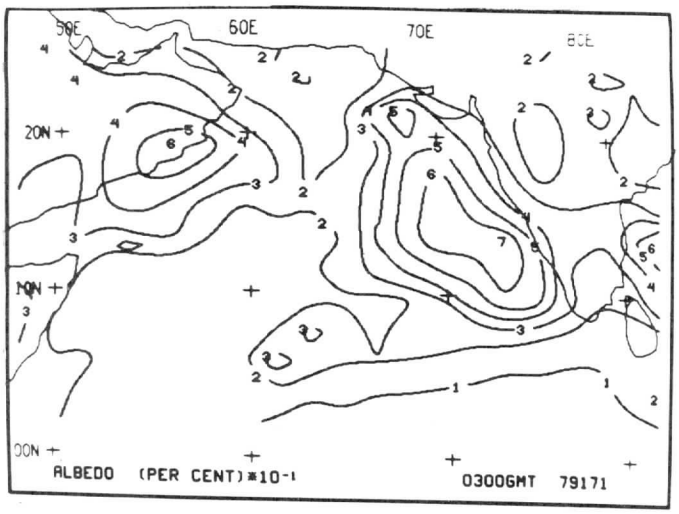
50E
60E
70E
80E
20N
10N
0ON
ALBEDO (PER CENT)*10-1
0300GMT 79171

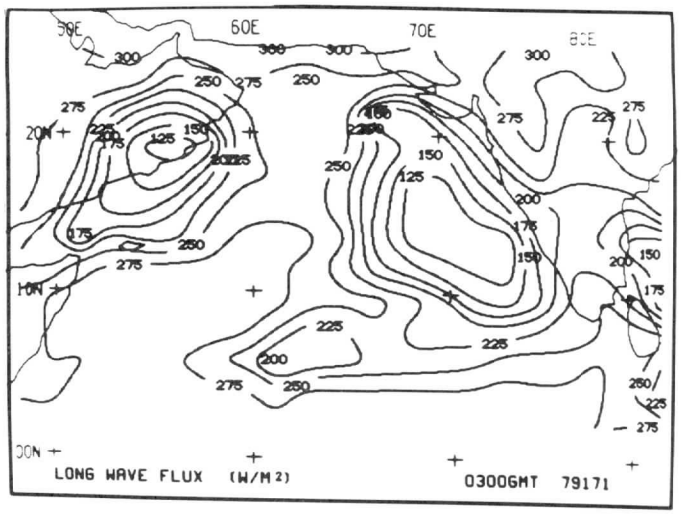
50E
60E
70E
80E
20N
10N
0ON
LONG WAVE FLUX (W/M2)
0300GMT 79171

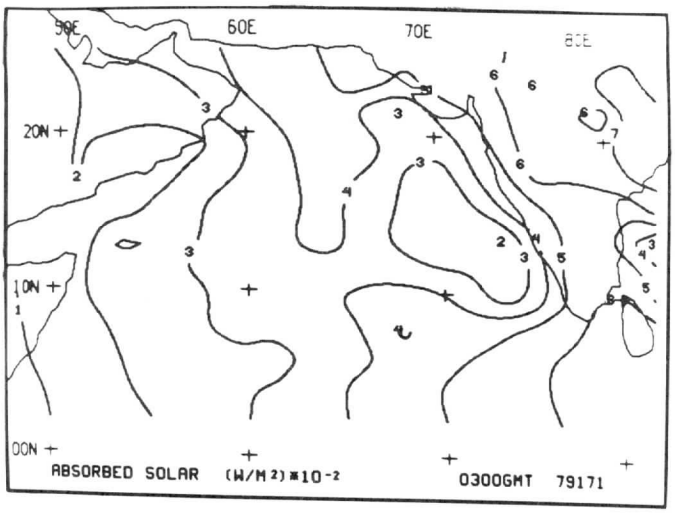
50E
60E
70E
80E
20N
10N
0ON
ABSORBED SOLAR (W/M2)*10-2
0300GMT 79171

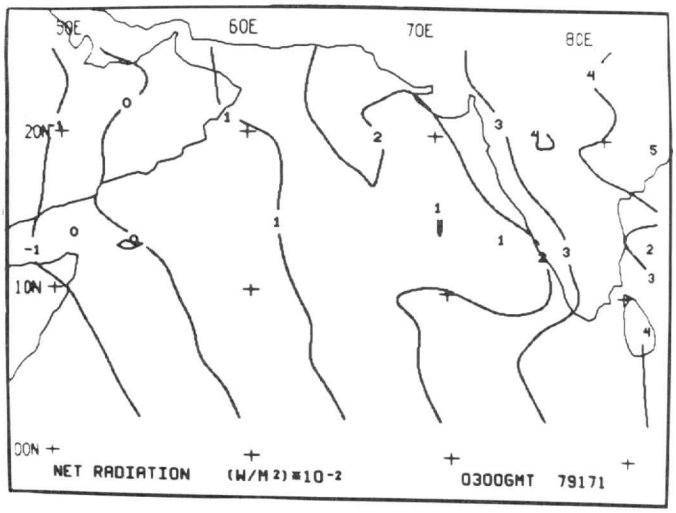
50E
60E
70E
80E
20N
10N
0ON
NET RADIATION (W/M2)*10-2
0300GMT 79171

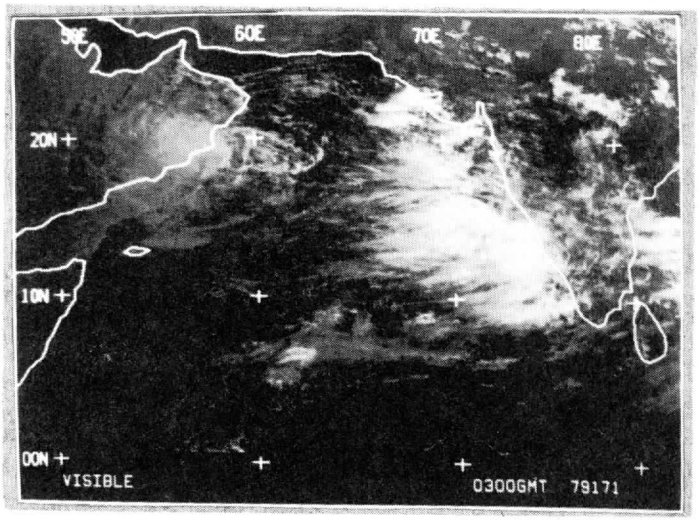
50E
60E
70E
80E
20N
10N
0ON
VISIBLE
0300GMT 79171

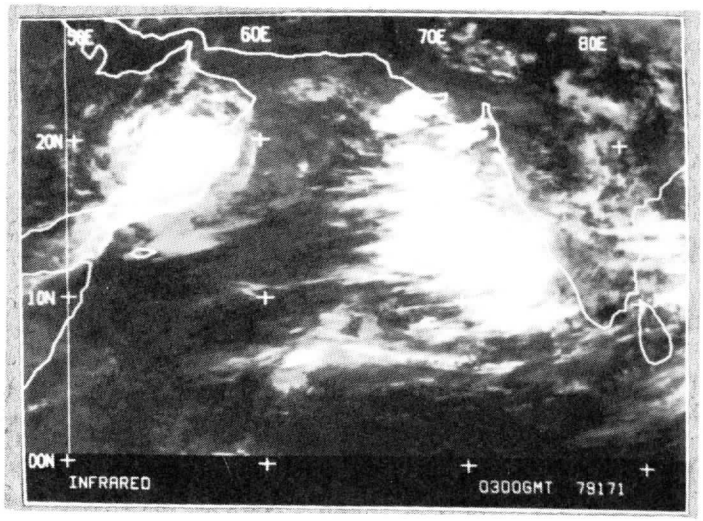
50E
60E
70E
80E
20N
10N
0ON
INFRARED
0300GMT 79171

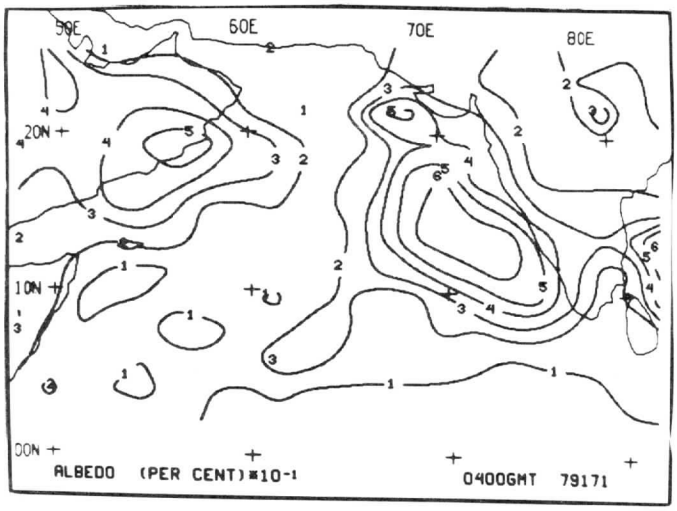
50E
60E
70E
80E
20N
10N
0ON
ALBEDO (PER CENT)*10-1
0400GMT 79171

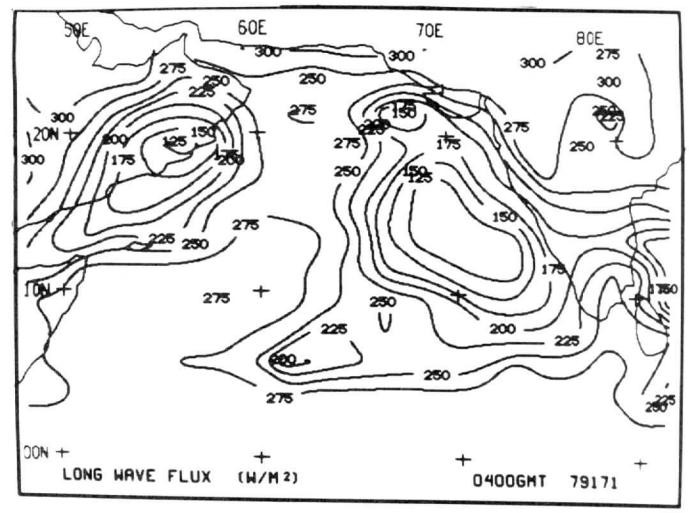
50E
60E
70E
80E
20N
10N
0ON
LONG WAVE FLUX (W/M2)
0400GMT 79171

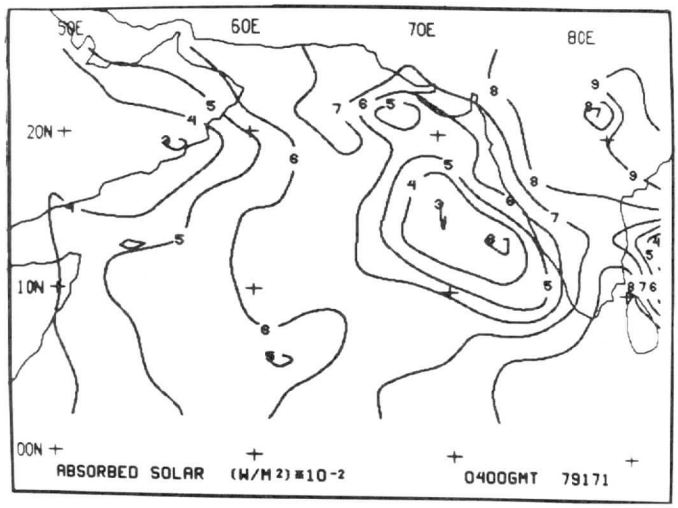
50E
60E
70E
80E
20N
10N
0ON
ABSORBED SOLAR (W/M2)*10-2
0400GMT 79171

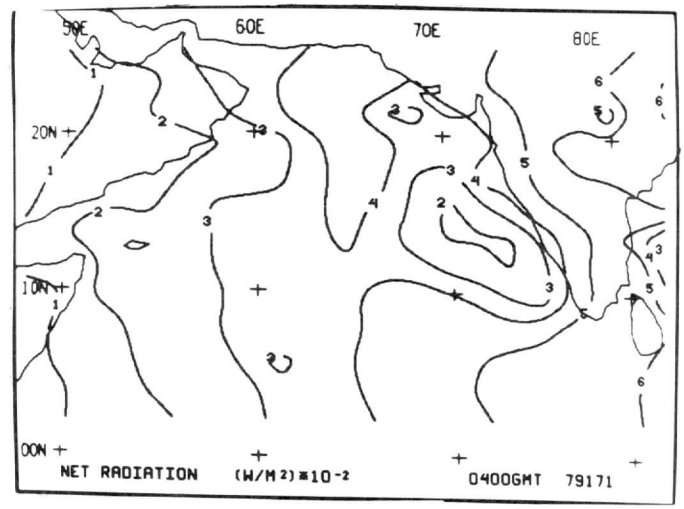
50E
60E
70E
80E
20N
10N
0ON
NET RADIATION (W/M2)*10-2
0400GMT 79171

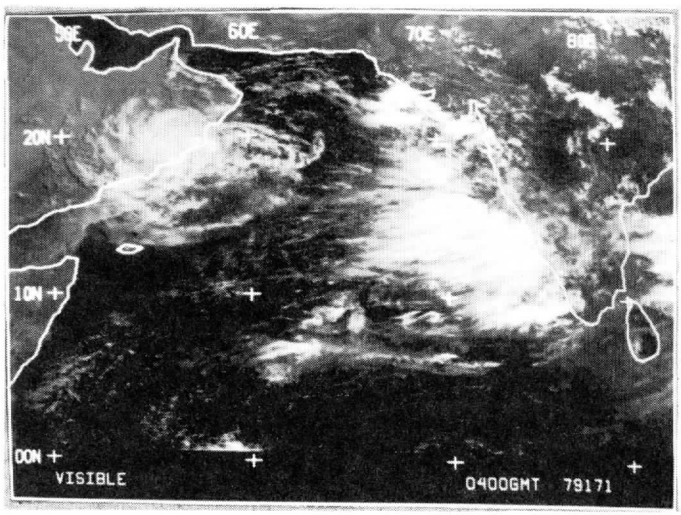
50E
60E
70E
80E
20N
10N
0ON
VISIBLE
0400GMT 79171

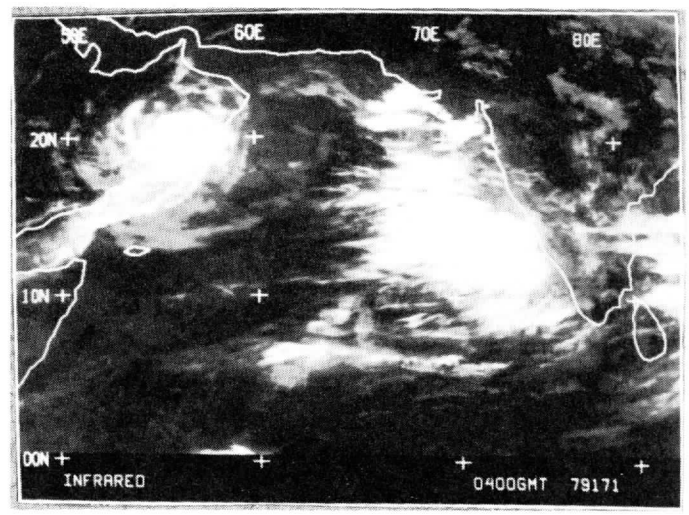
50E
60E
70E
80E
20N
10N
0ON
INFRARED
0400GMT 79171

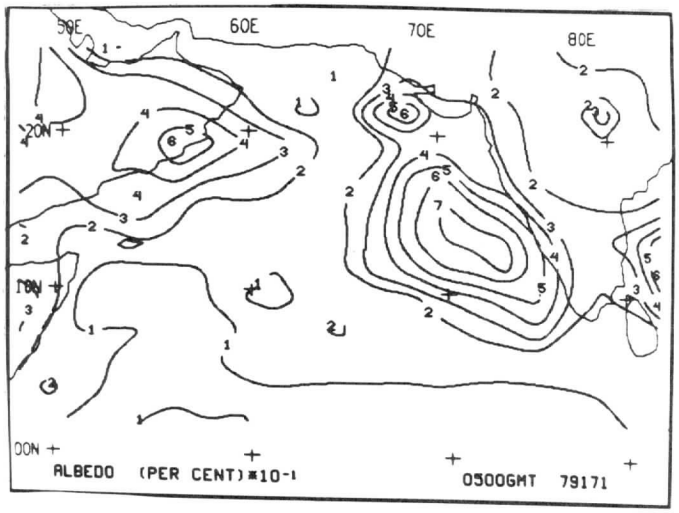
50E
60E
70E
80E
20N
10N
0ON
ALBEDO (PER CENT)×10-1
0500GMT 79171

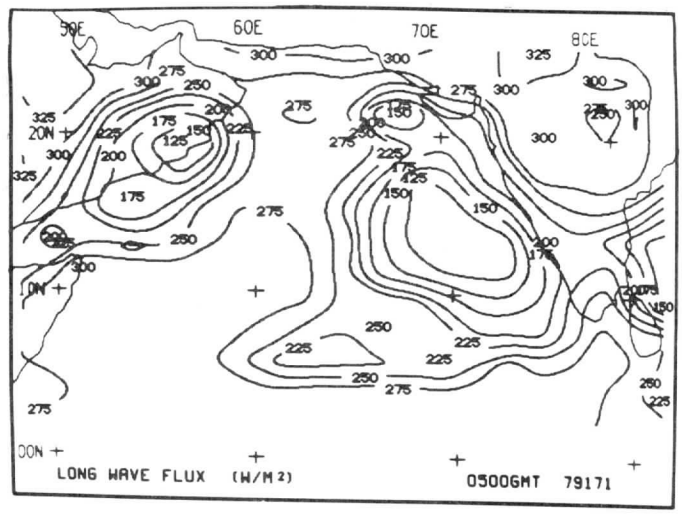
50E
60E
70E
80E
20N
10N
0ON
LONG WAVE FLUX (W/M2)
0500GMT 79171

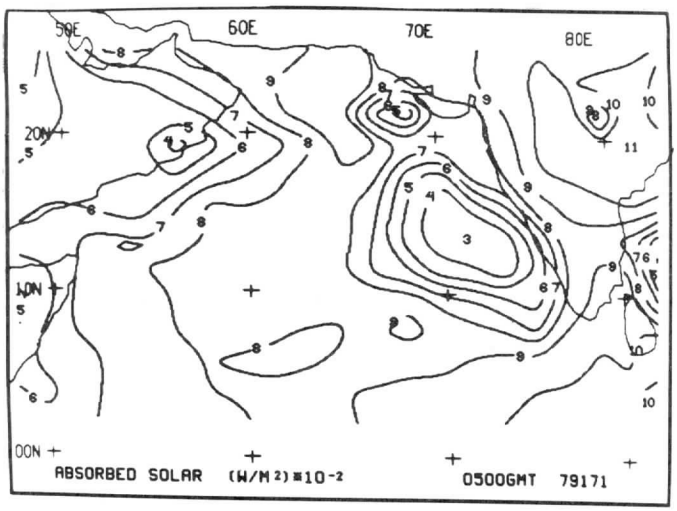
50E
60E
70E
80E
20N
10N
0ON
ABSORBED SOLAR (W/M2)×10-2
0500GMT 79171

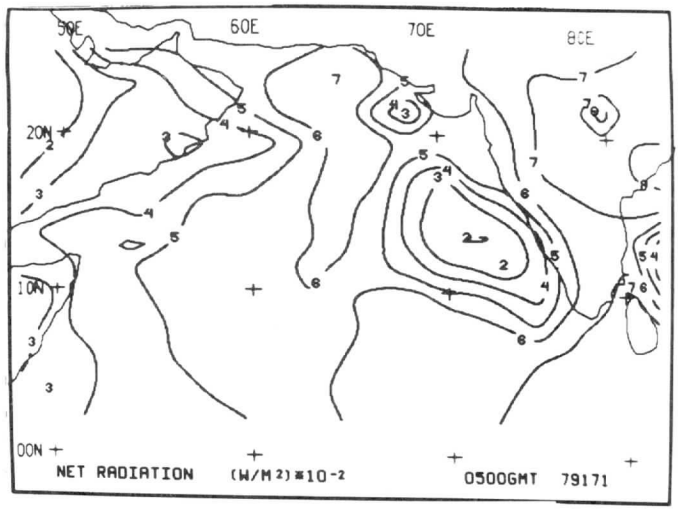
50E
60E
70E
80E
20N
10N
0ON
NET RADIATION (W/M2)×10-2
0500GMT 79171

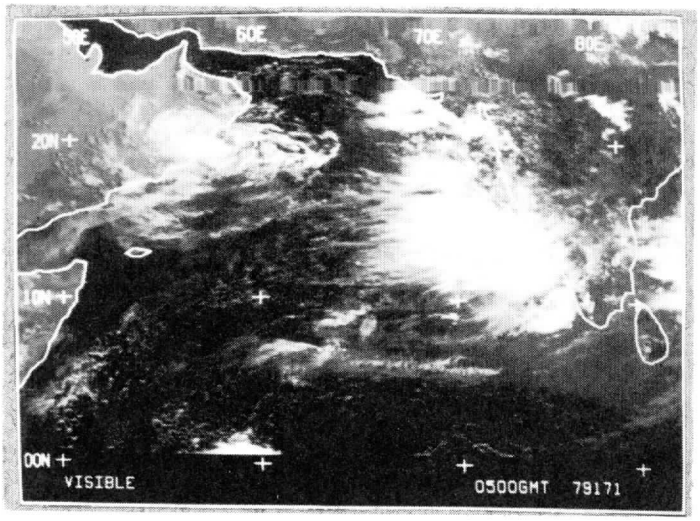
50E
60E
70E
80E
20N
10N
0ON
VISIBLE
0500GMT 79171

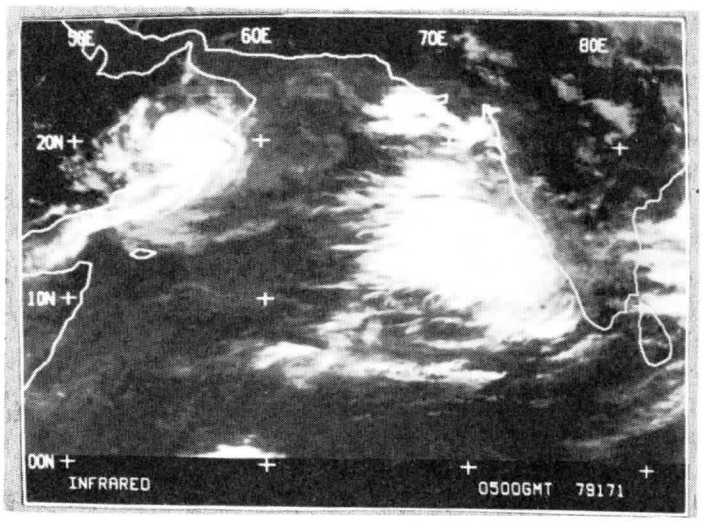
50E
60E
70E
80E
20N
10N
0ON
INFRARED
0500GMT 79171

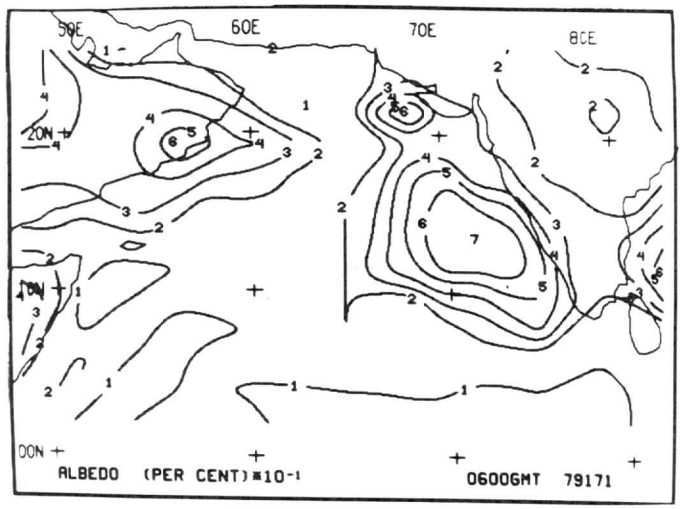
50E
60E
70E
80E
20N
10N
0ON
ALBEDO (PER CENT)*10-1
0600GMT 79171

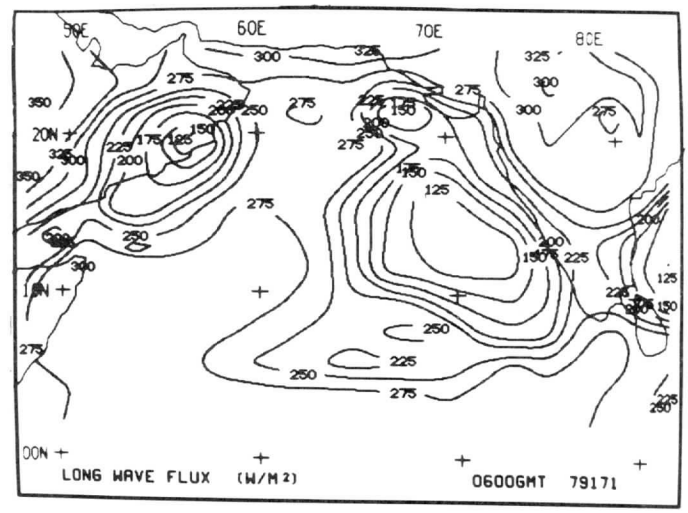
50E
60E
70E
80E
20N
10N
0ON
LONG WAVE FLUX (W/M2)
0600GMT 79171

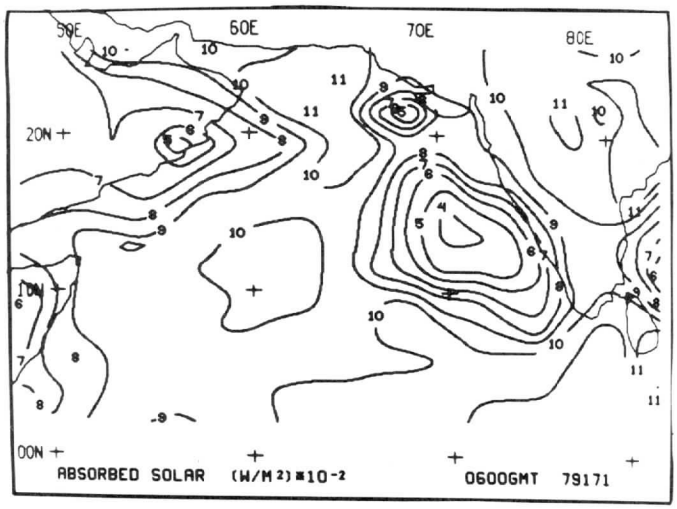
50E
60E
70E
80E
20N
10N
0ON
ABSORBED SOLAR (W/M2)*10-2
0600GMT 79171

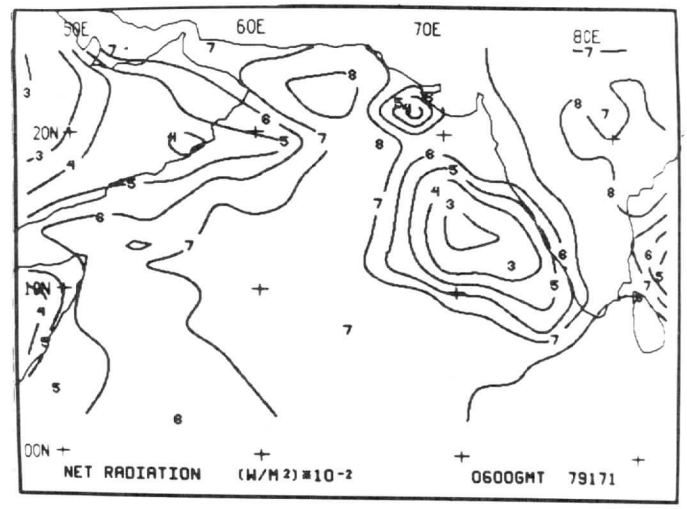
50E
60E
70E
80E
20N
10N
0ON
NET RADIATION (W/M2)*10-2
0600GMT 79171

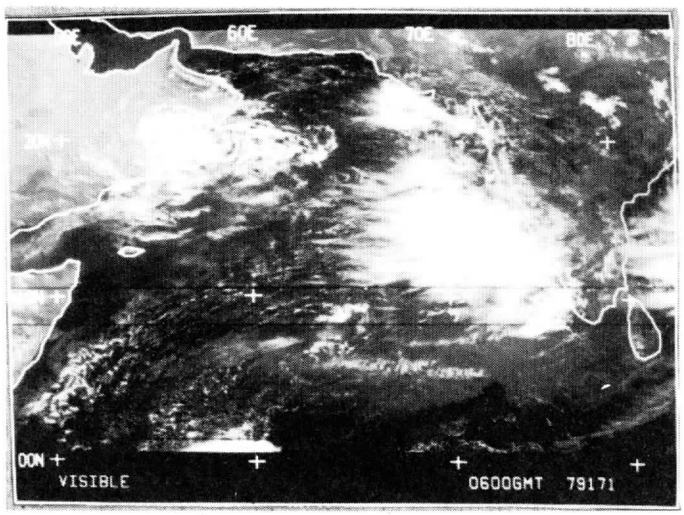
60E
70E
80E
0ON
VISIBLE
0600GMT 79171

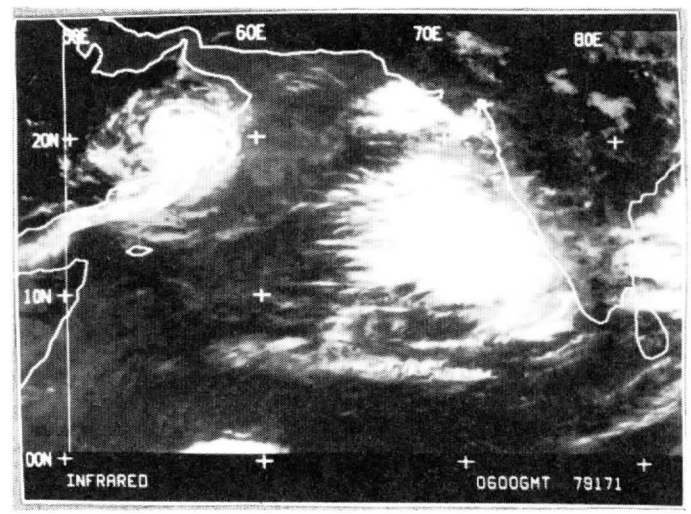
50E
60E
70E
80E
20N
10N
0ON
INFRARED
0600GMT 79171

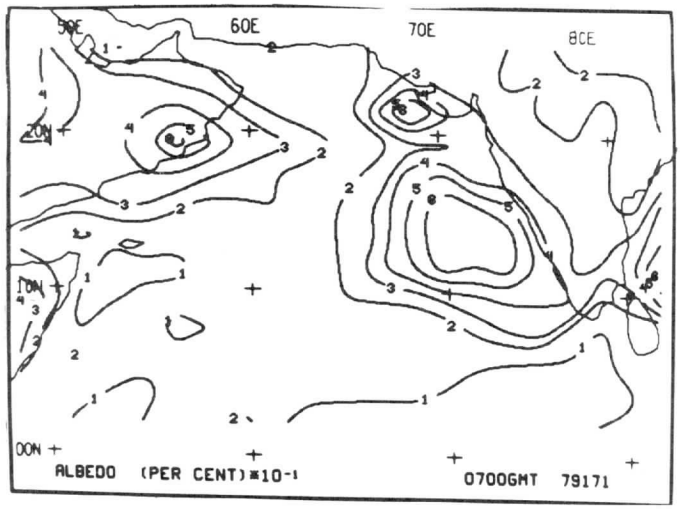
50E
60E
70E
80E
20N
10N
00N
ALBEDO (PER CENT)×10-1
0700GMT 79171

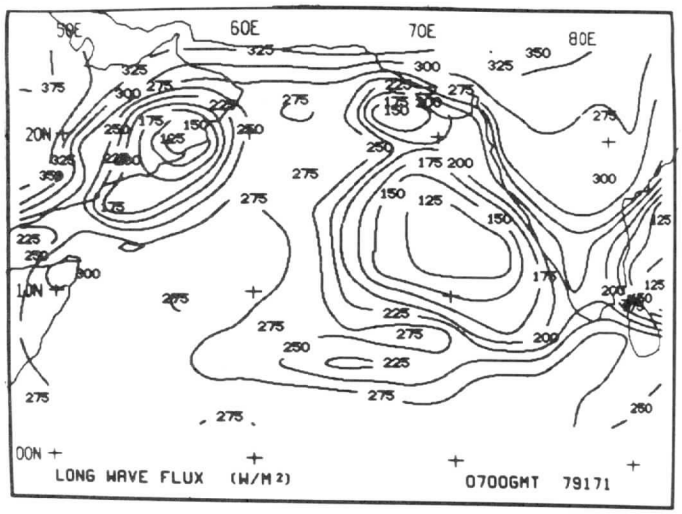
50E
60E
70E
80E
20N
10N
00N
LONG WAVE FLUX (W/M2)
0700GMT 79171

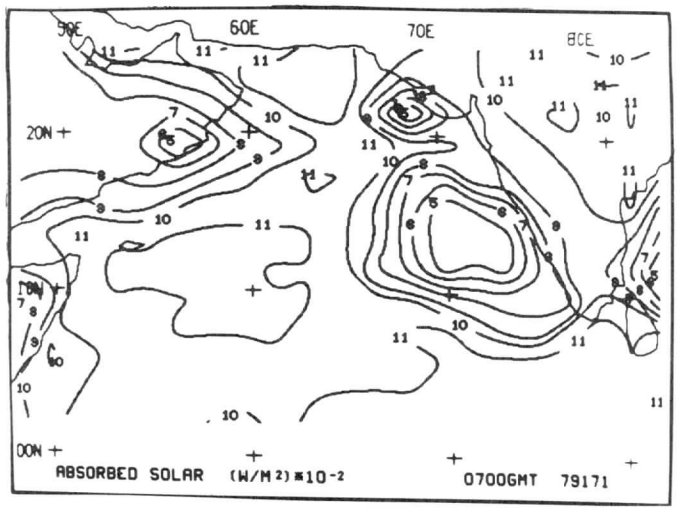
50E
60E
70E
80E
20N
10N
00N
ABSORBED SOLAR (W/M2)×10-2
0700GMT 79171

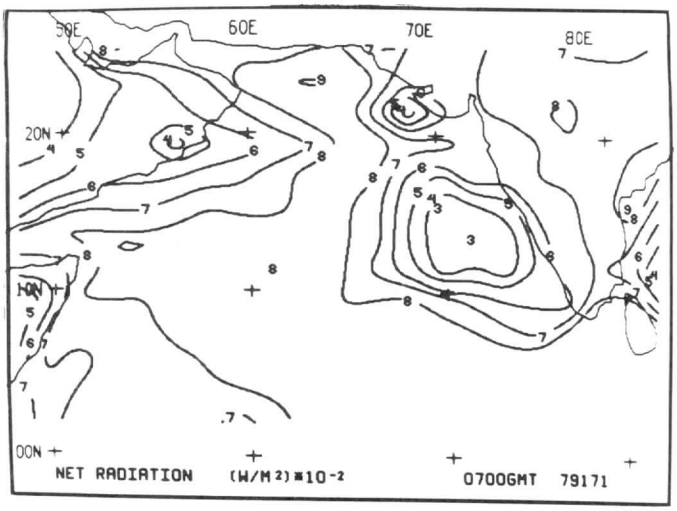
50E
60E
70E
80E
20N
10N
00N
NET RADIATION (W/M2)×10-2
0700GMT 79171

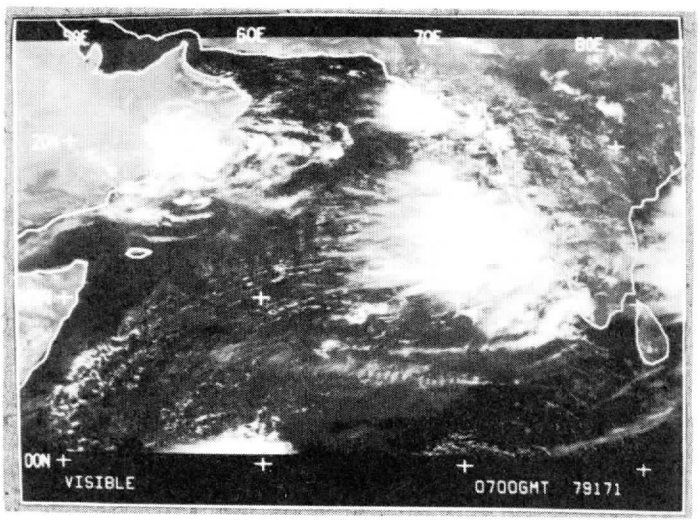
50E
60E
70E
80E
20N
10N
00N
VISIBLE
0700GMT 79171

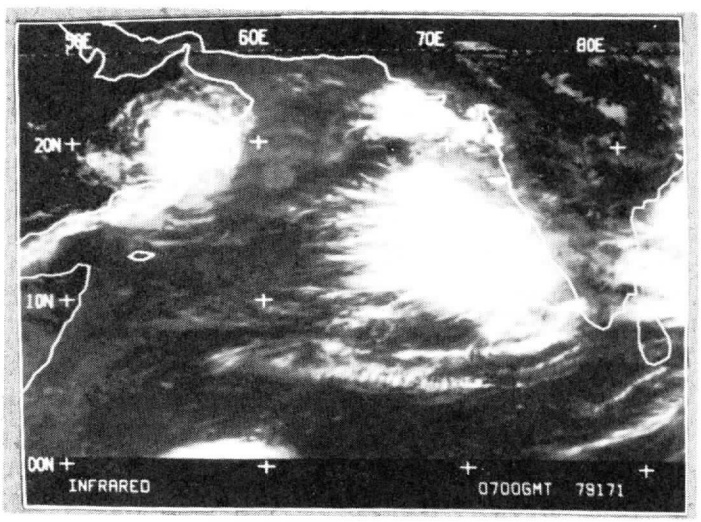
50E
60E
70E
80E
20N
10N
00N
INFRARED
0700GMT 79171

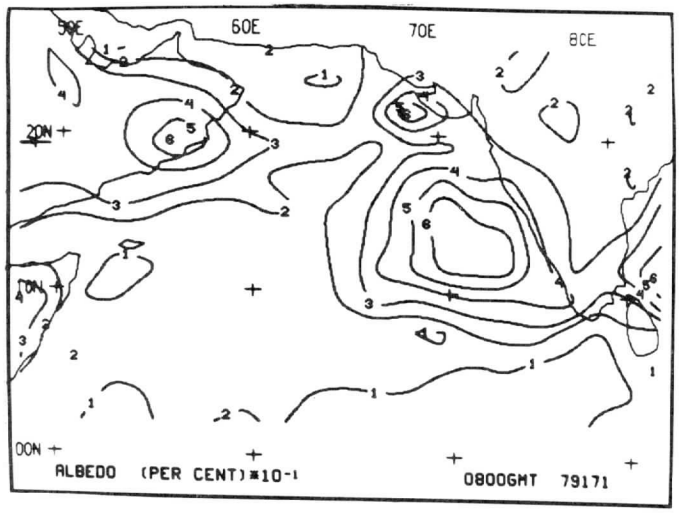
50E
60E
70E
80E
20N
10N
0ON
ALBEDO (PER CENT)*10-1
0800GMT 79171

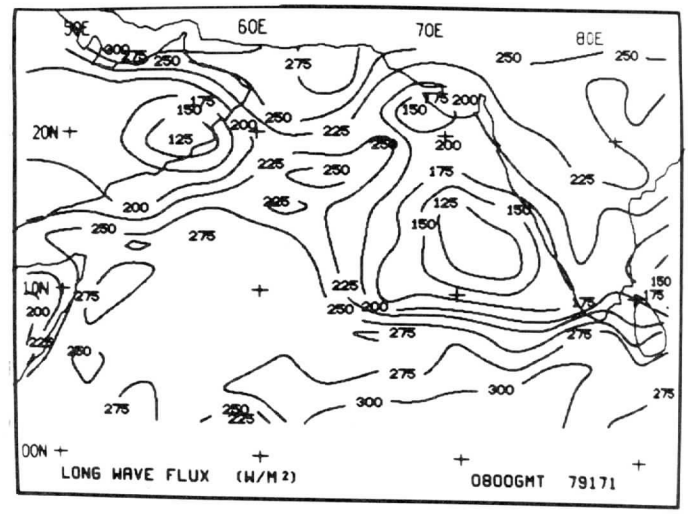
50E
60E
70E
80E
20N
10N
0ON
LONG WAVE FLUX (W/M2)
0800GMT 79171

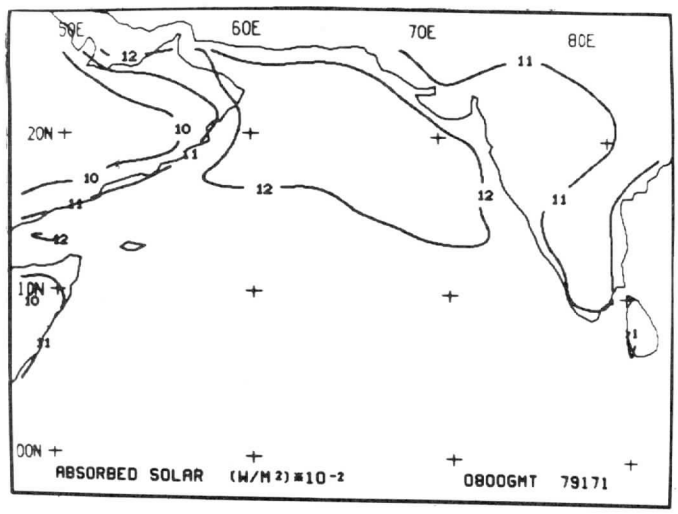
50E
60E
70E
80E
20N
10N
0ON
ABSORBED SOLAR (W/M2)*10-2
0800GMT 79171

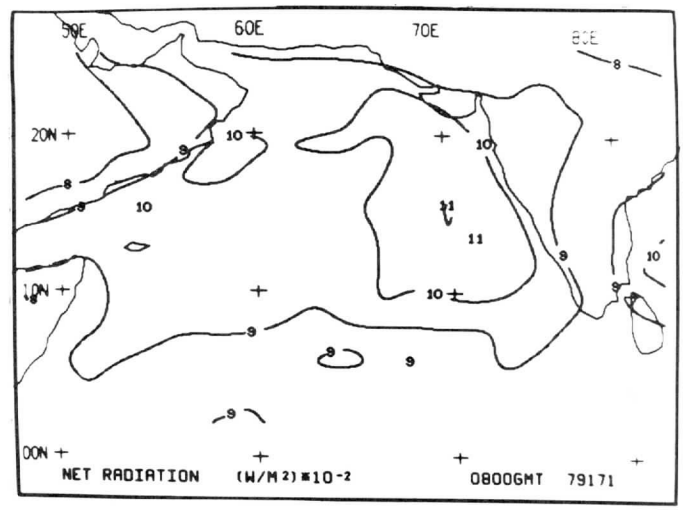
50E
60E
70E
80E
20N
10N
0ON
NET RADIATION (W/M2)*10-2
0800GMT 79171

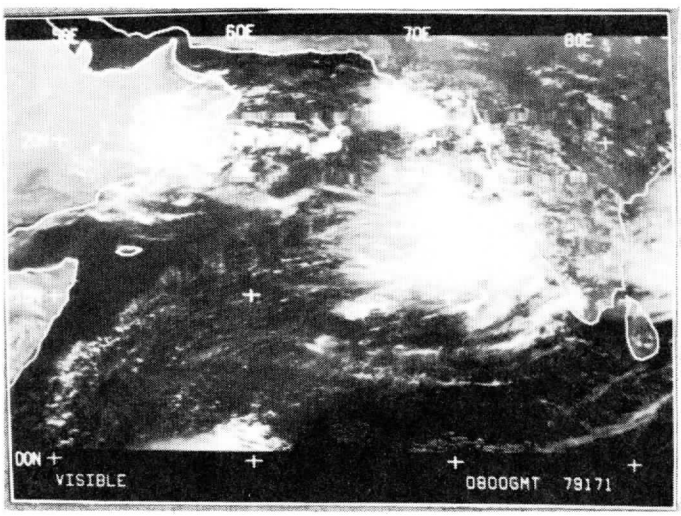
50E
60E
70E
80E
0ON
VISIBLE
0800GMT 79171

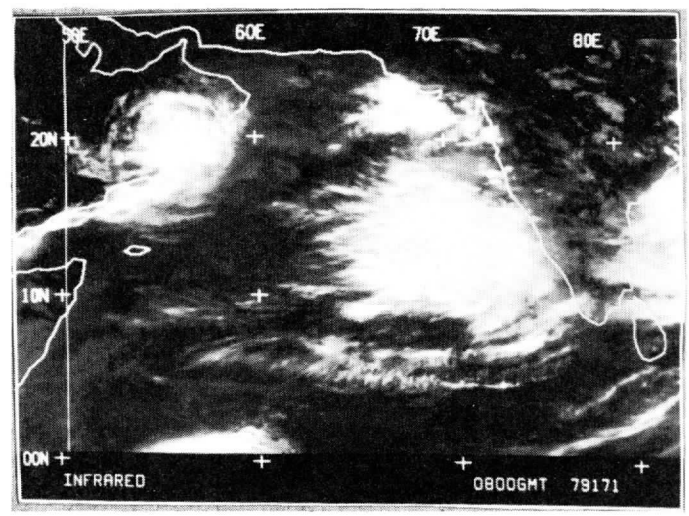
50E
60E
70E
80E
20N
10N
0ON
INFRARED
0800GMT 79171

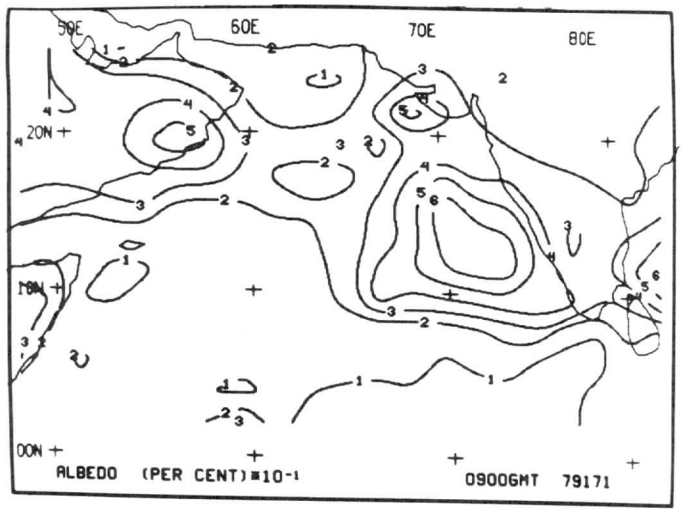
50E
60E
70E
80E
20N
10N
0ON
ALBEDO (PER CENT)*10-1
0900GMT 79171

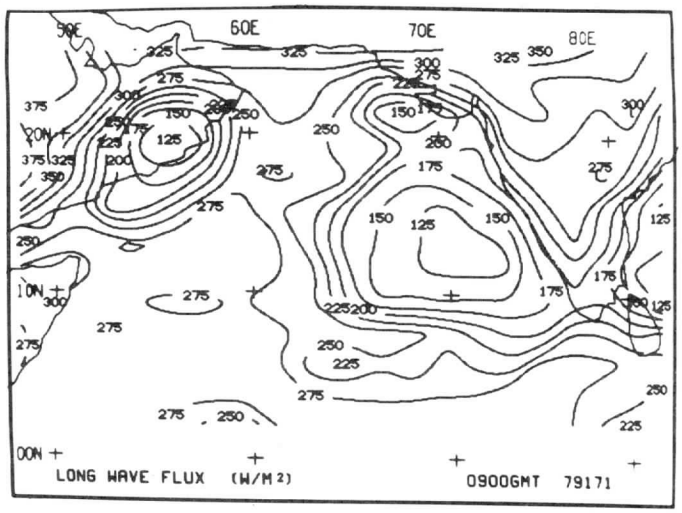
50E
60E
70E
80E
20N
10N
0ON
LONG WAVE FLUX (W/M2)
0900GMT 79171

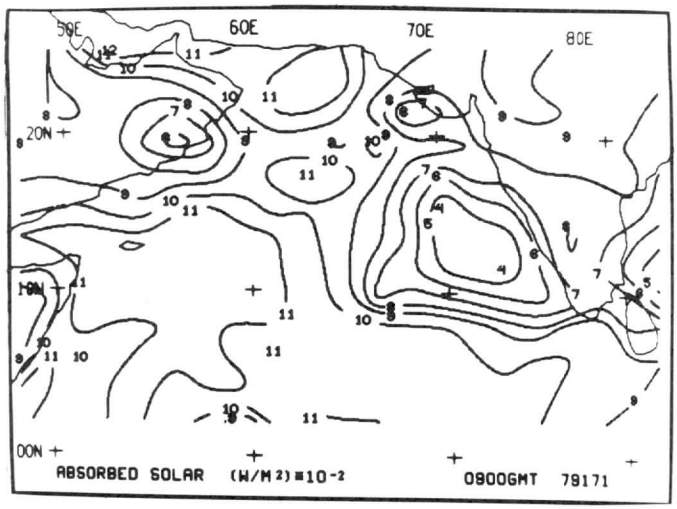
50E
60E
70E
80E
20N
10N
0ON
ABSORBED SOLAR (W/M2)*10-2
0900GMT 79171

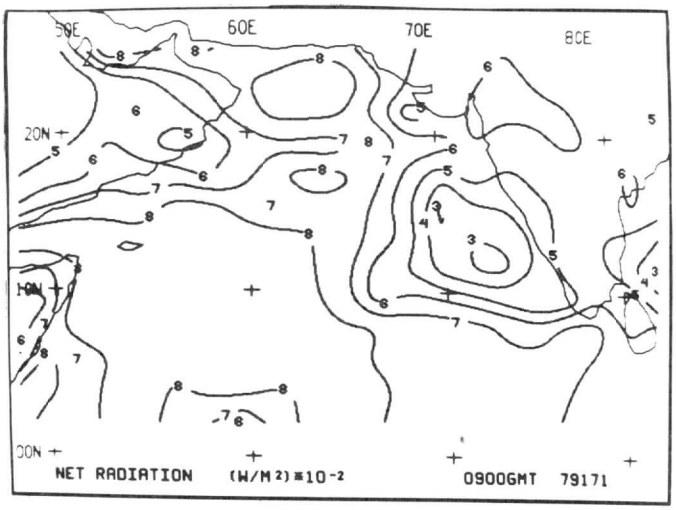
50E
60E
70E
80E
20N
10N
0ON
NET RADIATION (W/M2)*10-2
0900GMT 79171

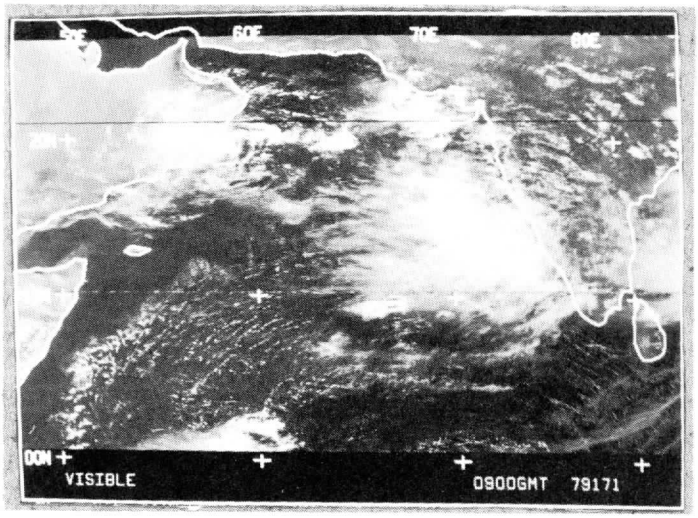
50E
60E
70E
80E
20N
10N
0ON
VISIBLE
0900GMT 79171

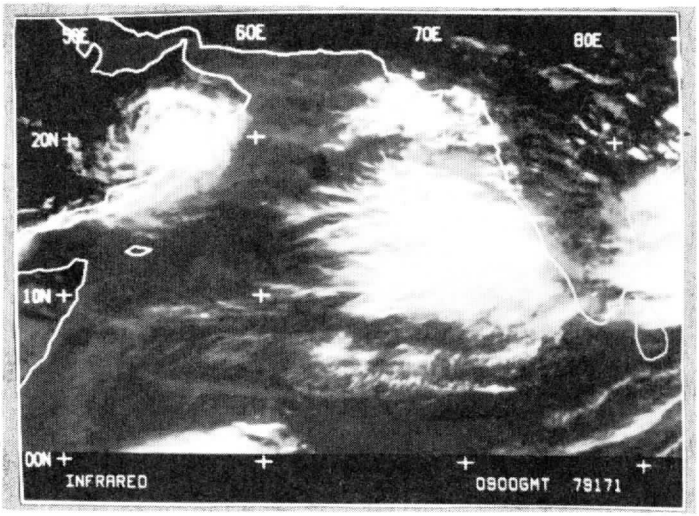
50E
60E
70E
80E
20N
10N
0ON
INFRARED
0900GMT 79171

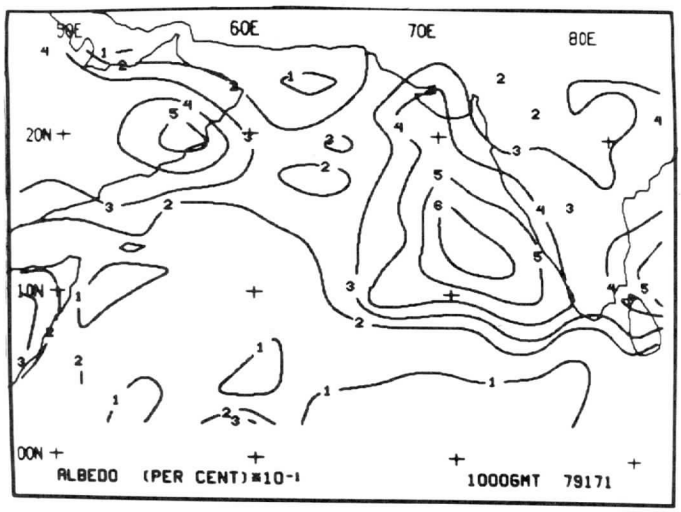
50E
60E
70E
80E
20N
10N
0ON
ALBEDO (PER CENT)*10-1
1000GMT 79171

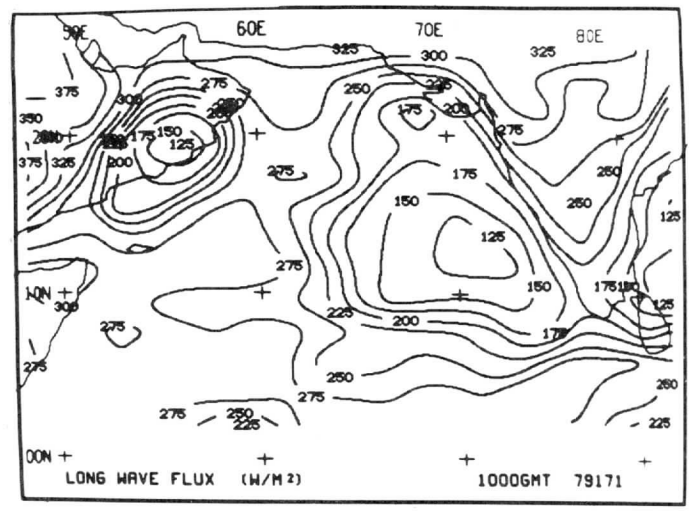
50E
60E
70E
80E
10N
0ON
LONG WAVE FLUX (W/M2)
1000GMT 79171

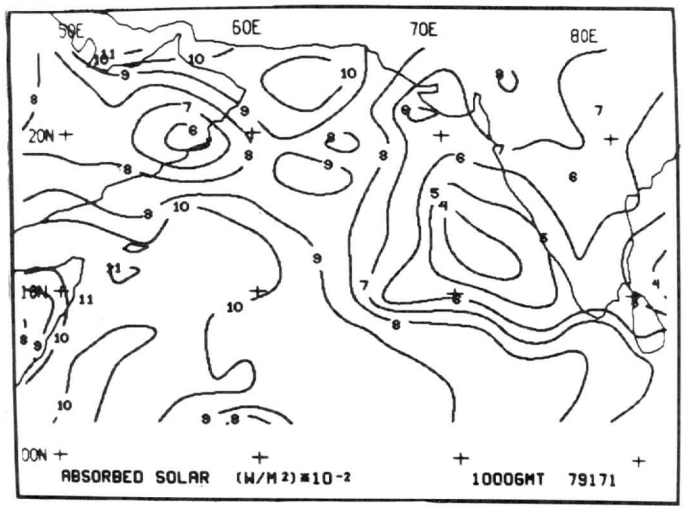
50E
60E
70E
80E
20N
10N
0ON
ABSORBED SOLAR (W/M2)*10-2
1000GMT 79171

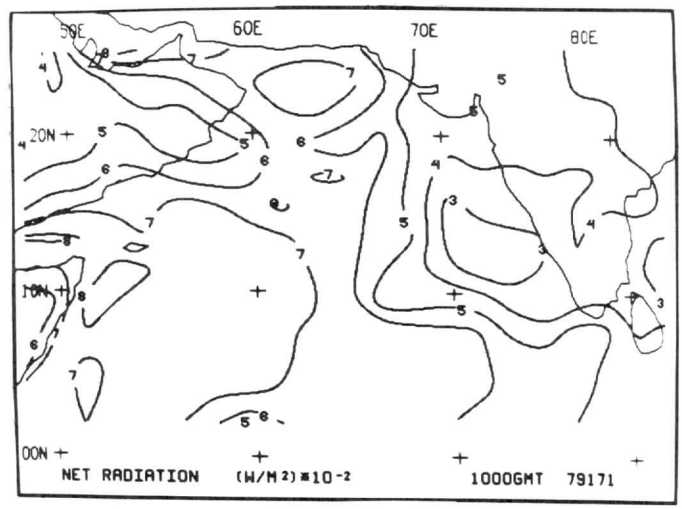
50E
60E
70E
80E
20N
10N
0ON
NET RADIATION (W/M2)*10-2
1000GMT 79171

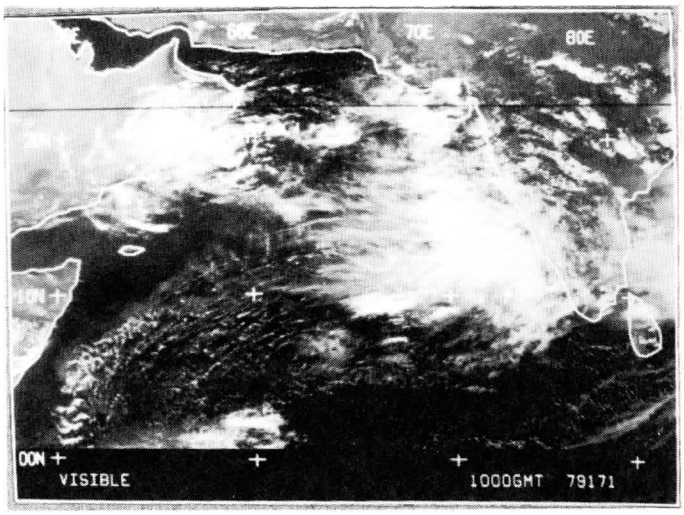
70E
80E
10N
0ON
VISIBLE
1000GMT 79171

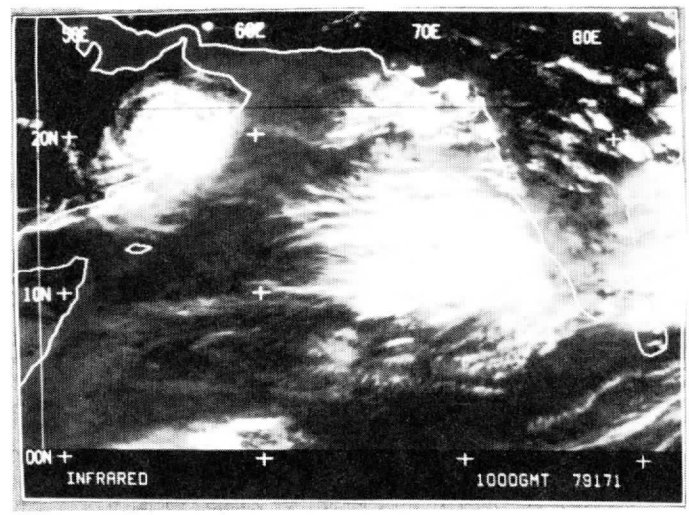
50E
60E
70E
80E
20N
10N
0ON
INFRARED
1000GMT 79171

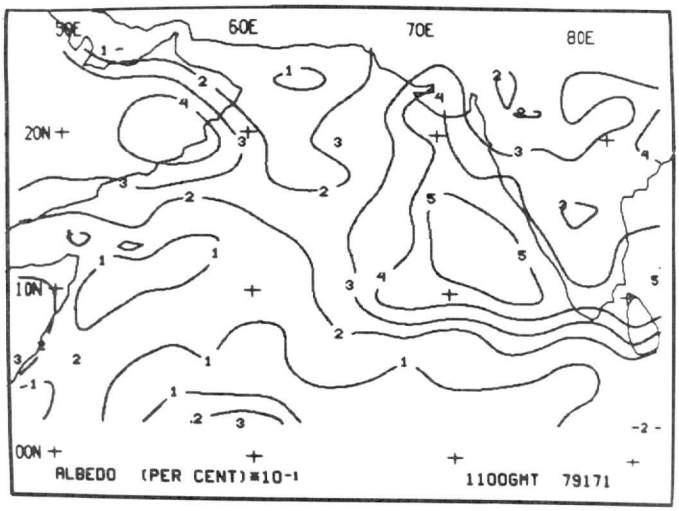
50E
60E
70E
80E
20N
10N
00N
ALBEDO (PER CENT)×10-1
1100GMT 79171

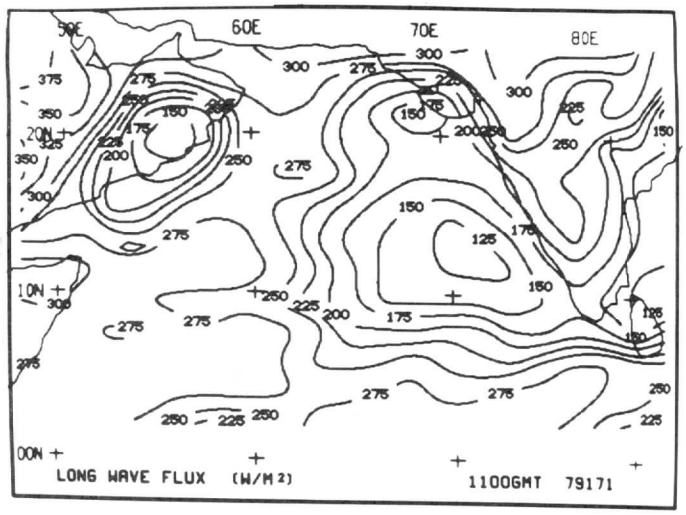
50E
60E
70E
80E
20N
10N
00N
LONG WAVE FLUX (W/M2)
1100GMT 79171

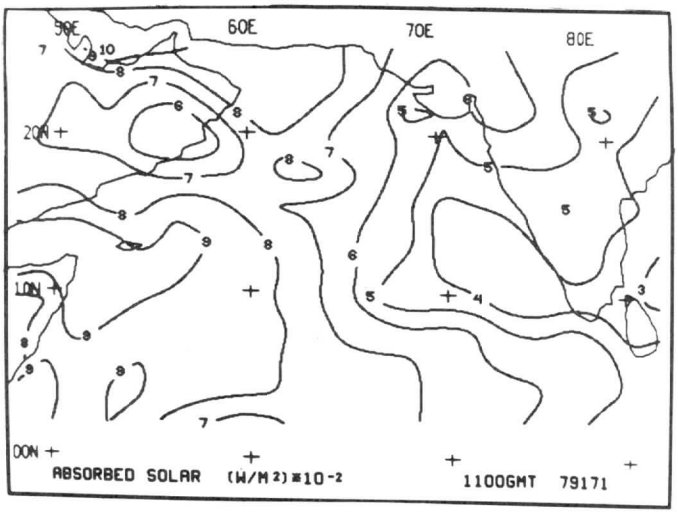
50E
60E
70E
80E
20N
10N
00N
ABSORBED SOLAR (W/M2)×10-2
1100GMT 79171

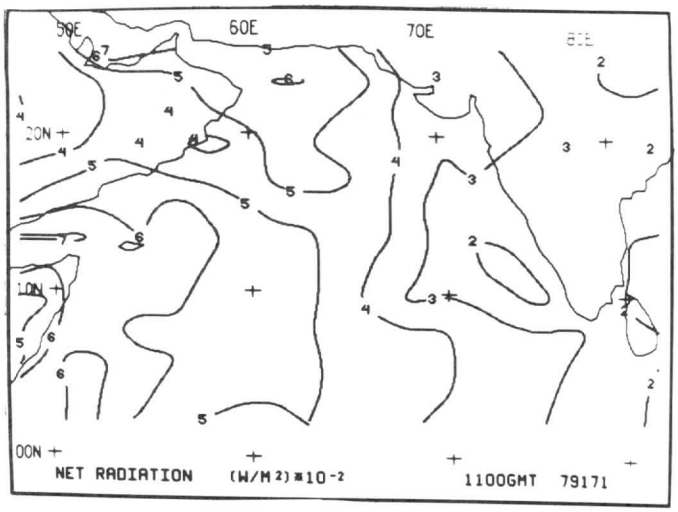
50E
60E
70E
80E
20N
10N
00N
NET RADIATION (W/M2)×10-2
1100GMT 79171

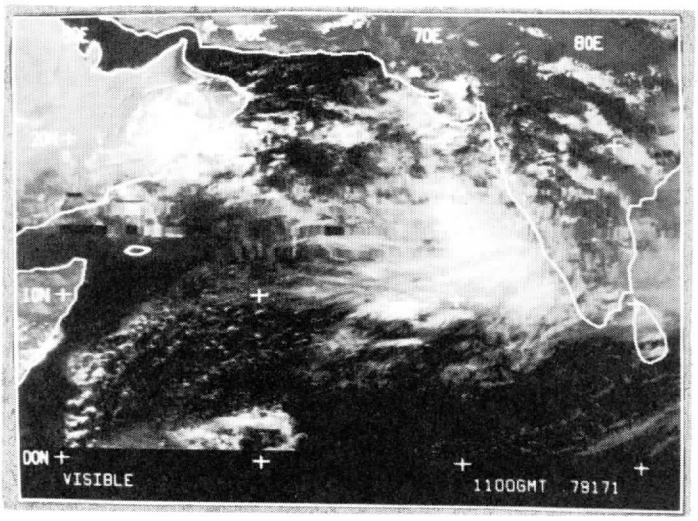
70E
80E
10N
00N
VISIBLE
1100GMT 79171

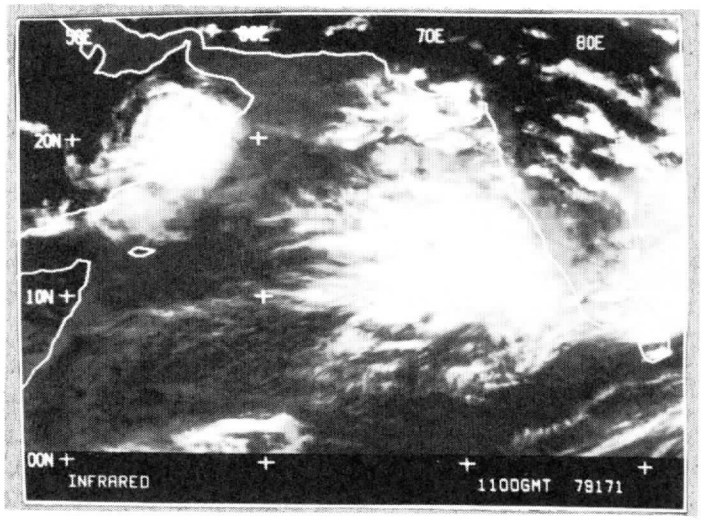
50E
70E
80E
20N
10N
00N
INFRARED
1100GMT 79171

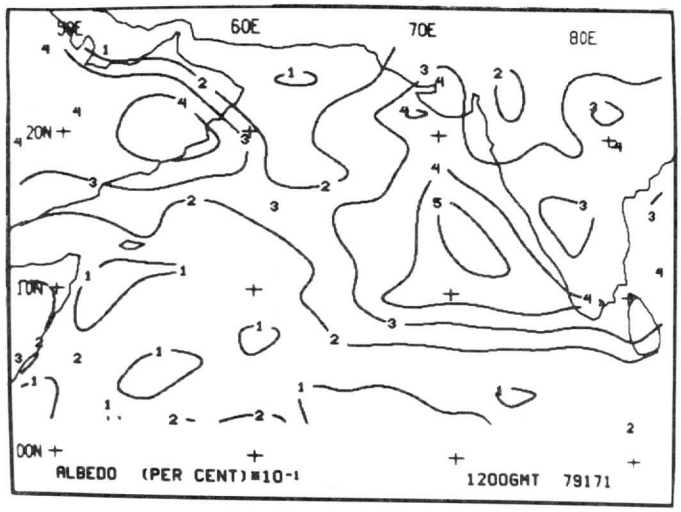
50E
60E
70E
80E
20N
10N
0ON
ALBEDO (PER CENT)*10-1
1200GMT 79171

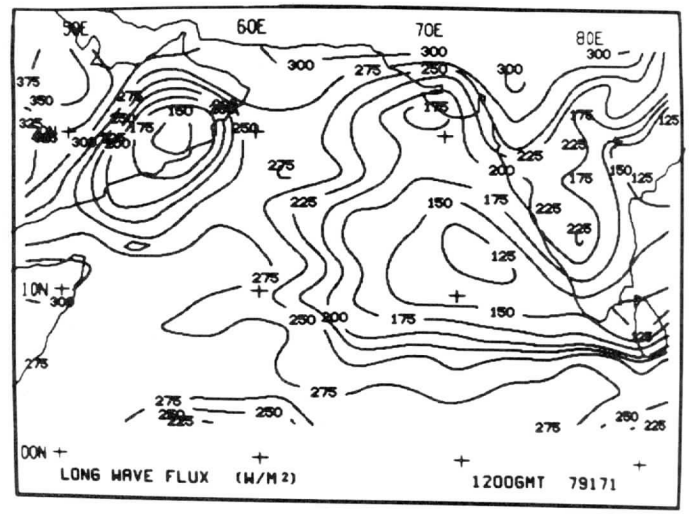
50E
60E
70E
80E
20N
10N
0ON
LONG WAVE FLUX (W/M2)
1200GMT 79171

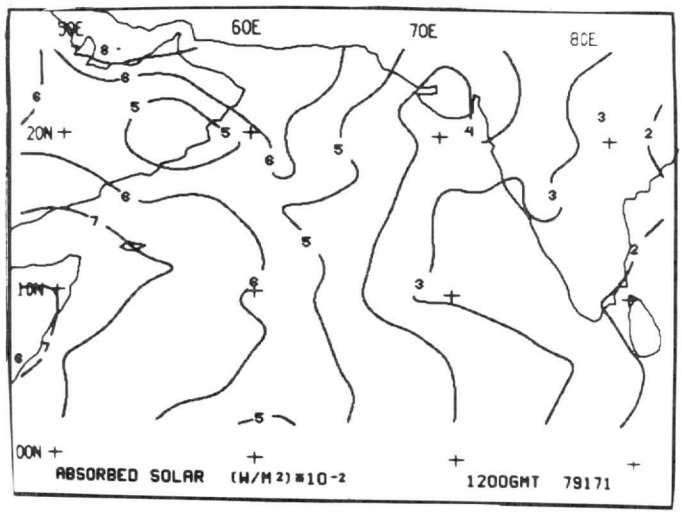
50E
60E
70E
80E
20N
10N
0ON
ABSORBED SOLAR (W/M2)*10-2
1200GMT 79171

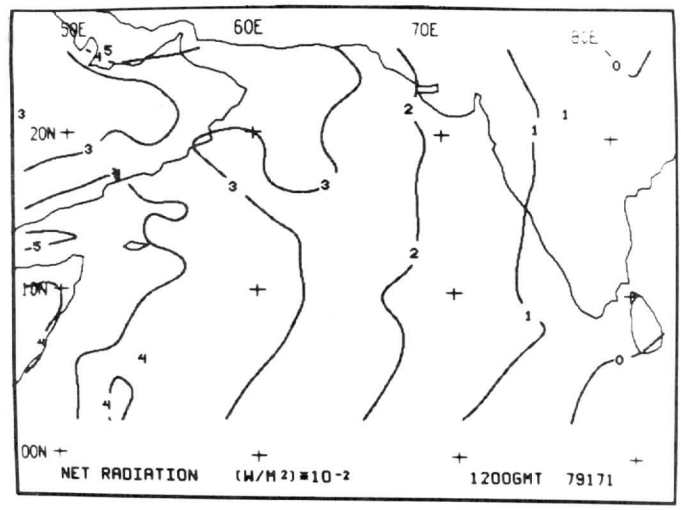
50E
60E
70E
80E
20N
10N
0ON
NET RADIATION (W/M2)*10-2
1200GMT 79171

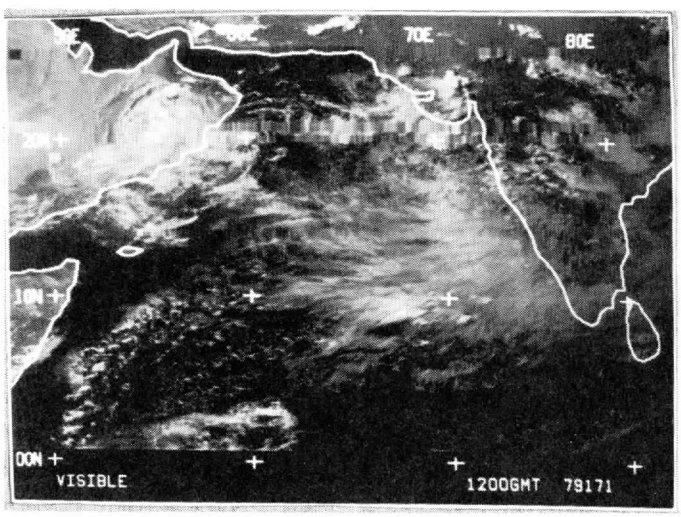
70E
80E
20N
10N
0ON
VISIBLE
1200GMT 79171

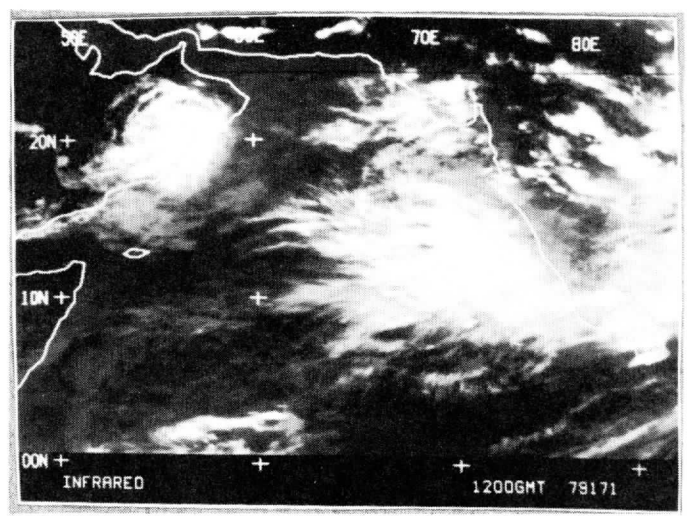
70E
80E
20N
10N
0ON
INFRARED
1200GMT 79171

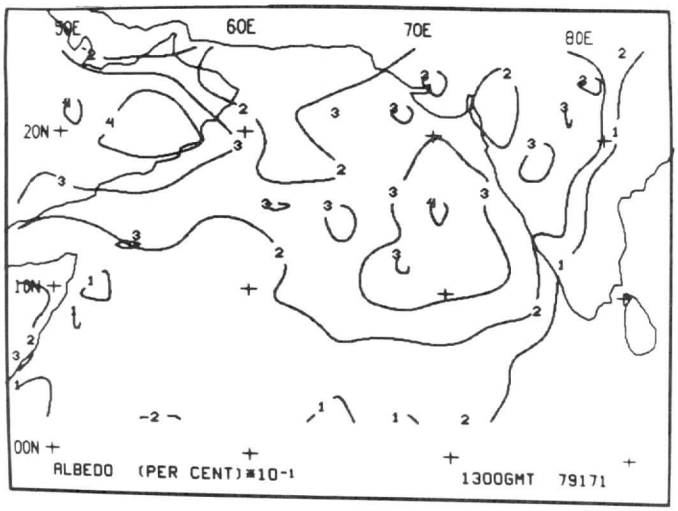
50E
60E
70E
80E
20N
10N
0ON
ALBEDO (PER CENT)*10-1
1300GMT 79171

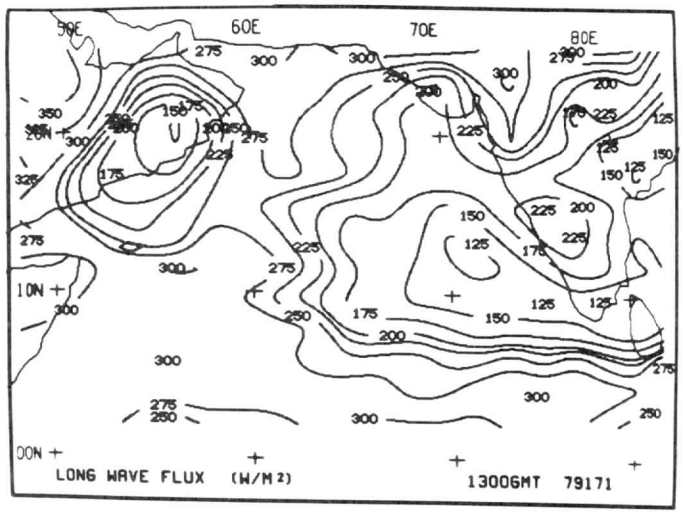
50E
60E
70E
80E
20N
10N
0ON
LONG WAVE FLUX (W/M2)
1300GMT 79171

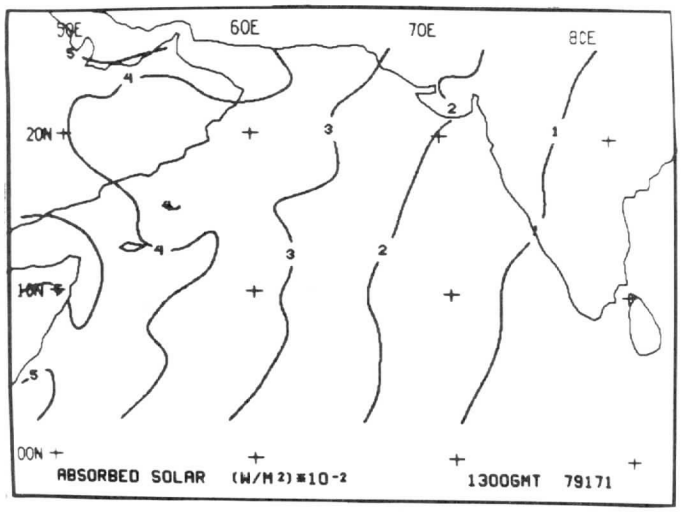
50E
60E
70E
80E
20N
10N
0ON
ABSORBED SOLAR (W/M2)*10-2
1300GMT 79171

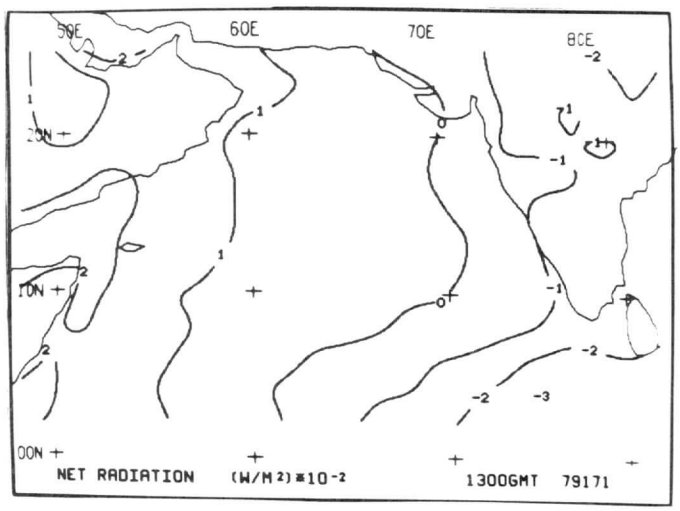
50E
60E
70E
80E
20N
10N
0ON
NET RADIATION (W/M2)*10-2
1300GMT 79171

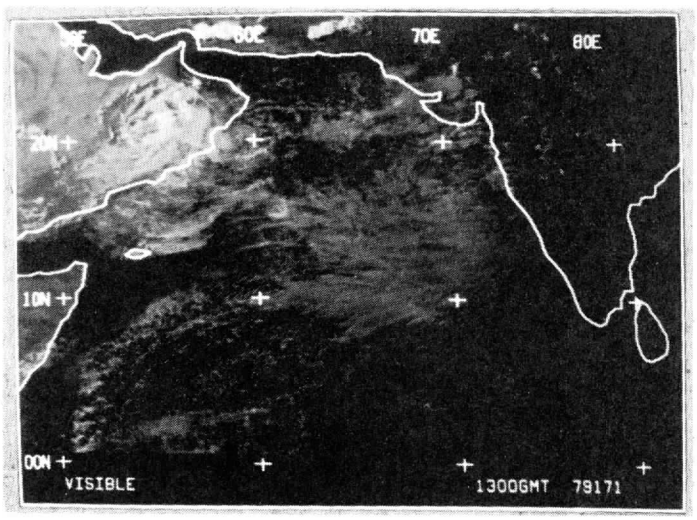
60E
70E
80E
20N
10N
0ON
VISIBLE
1300GMT 79171

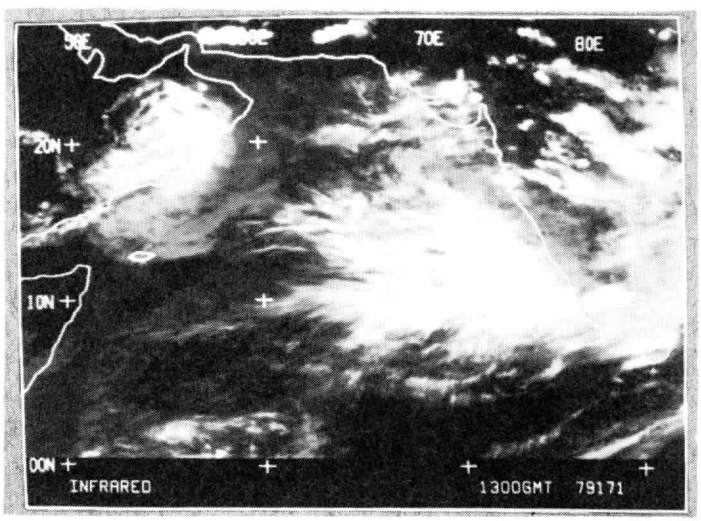
50E
70E
80E
20N
10N
0ON
INFRARED
1300GMT 79171

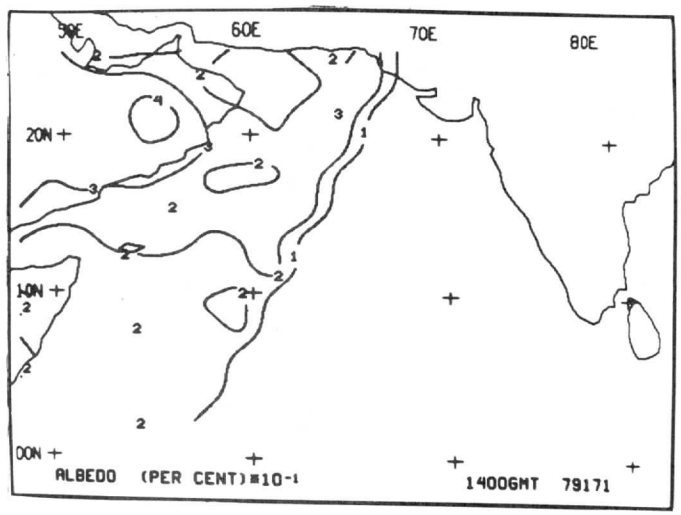
50E
60E
70E
80E
20N
10N
0ON
ALBEDO (PER CENT)*10-1
14006MT 79171

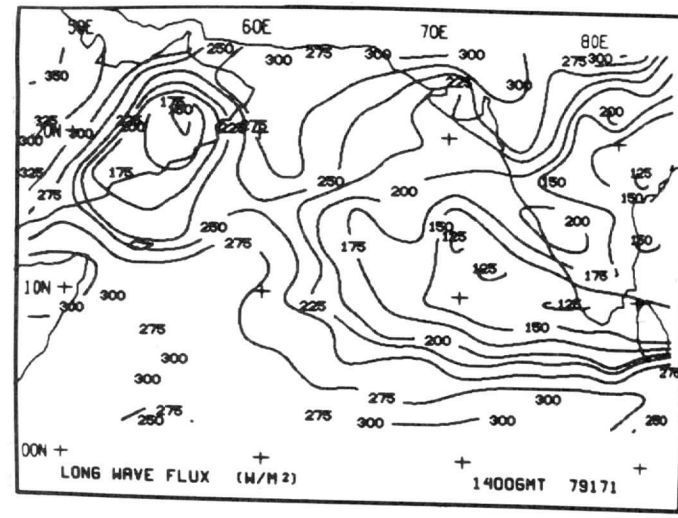
50E
60E
70E
80E
20N
10N
0ON
LONG WAVE FLUX (W/M2)
14006MT 79171

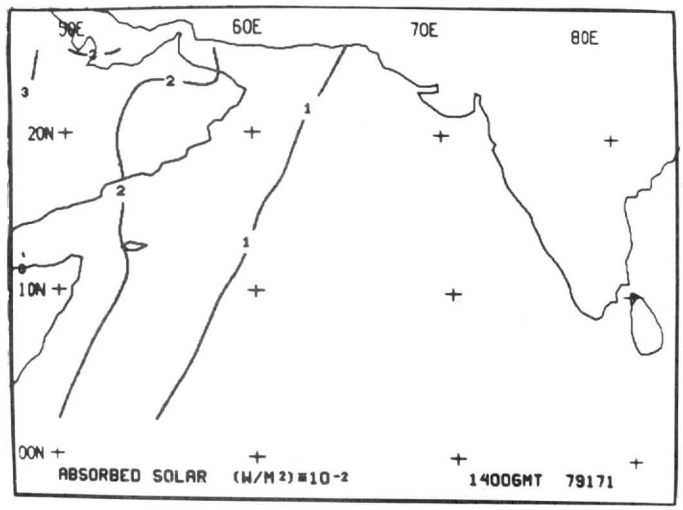
50E
60E
70E
80E
20N
10N
0ON
ABSORBED SOLAR (W/M2)*10-2
14006MT 79171

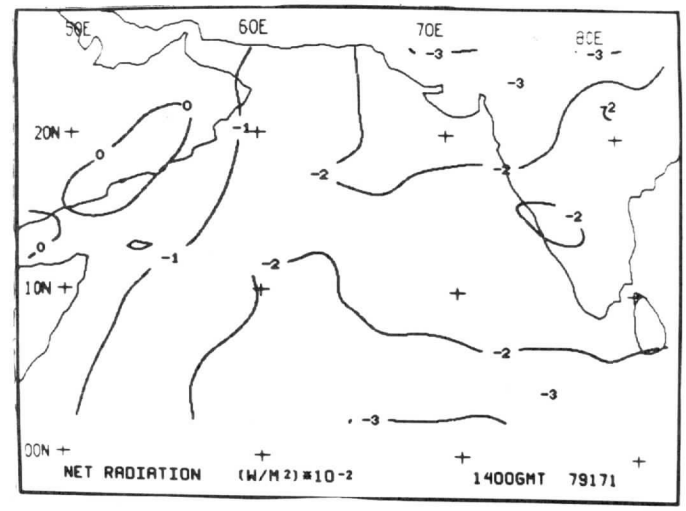
50E
60E
70E
80E
20N
10N
0ON
NET RADIATION (W/M2)*10-2
14006MT 79171

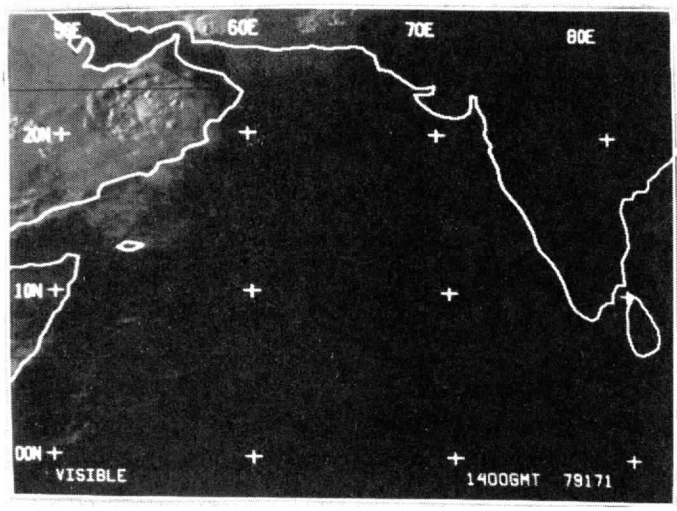
50E
60E
70E
80E
20N
10N
0ON
VISIBLE
14006MT 79171

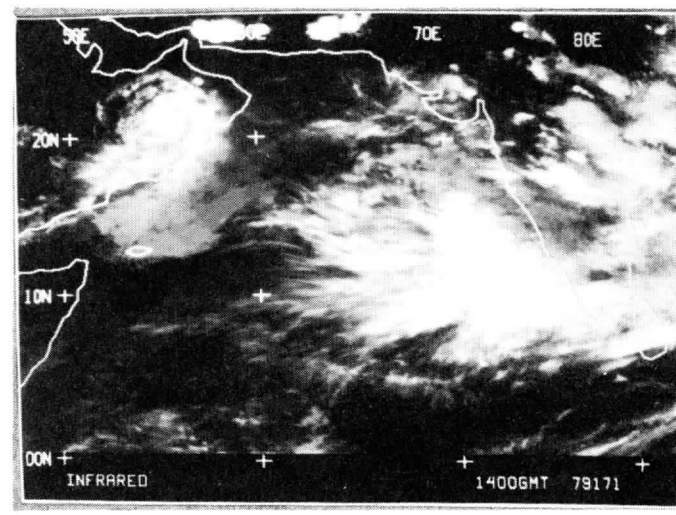
50E
70E
80E
20N
10N
0ON
INFRARED
14006MT 79171

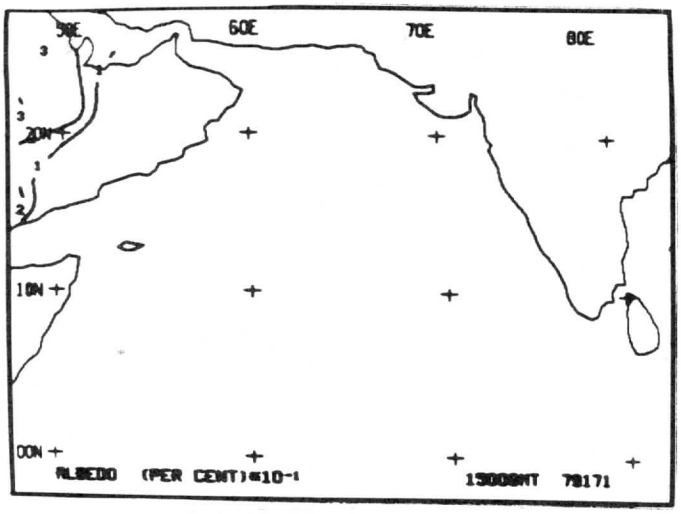
50E
60E
70E
80E
20N
10N
00N
ALBEDO (PER CENT)*10-1
1500GMT 79171

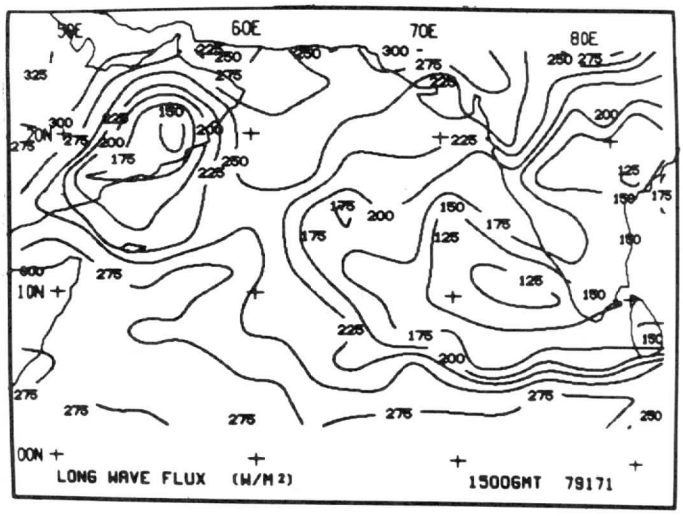
50E
60E
70E
80E
20N
10N
00N
LONG WAVE FLUX (W/M2)
1500GMT 79171

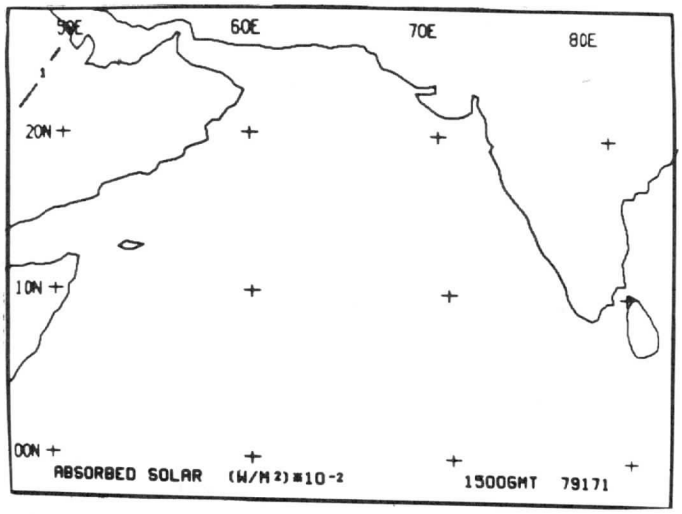
50E
60E
70E
80E
20N
10N
00N
ABSORBED SOLAR (W/M2)*10-2
1500GMT 79171

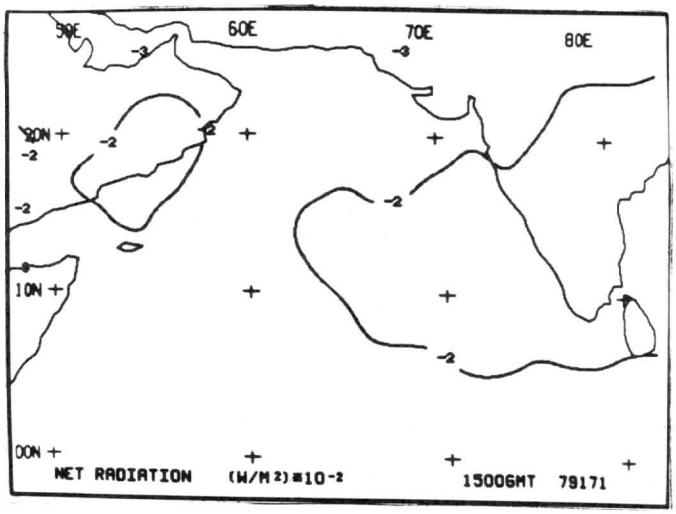
50E
60E
70E
80E
20N
10N
00N
NET RADIATION (W/M2)*10-2
1500GMT 79171

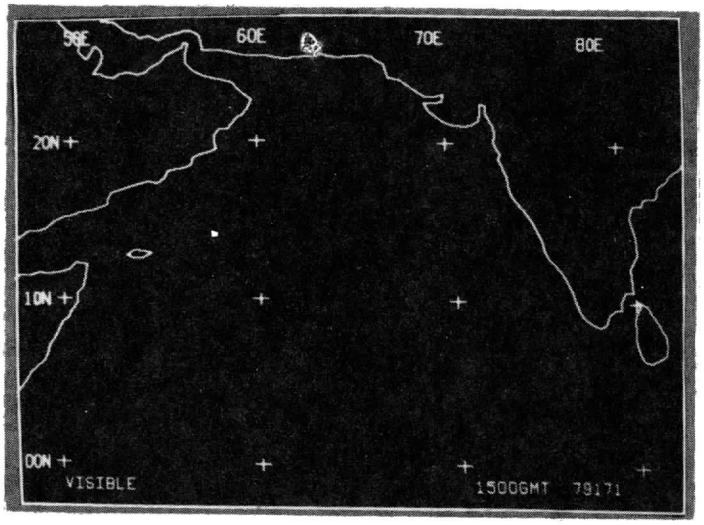
50E
60E
70E
80E
20N
10N
00N
VISIBLE
1500GMT 79171

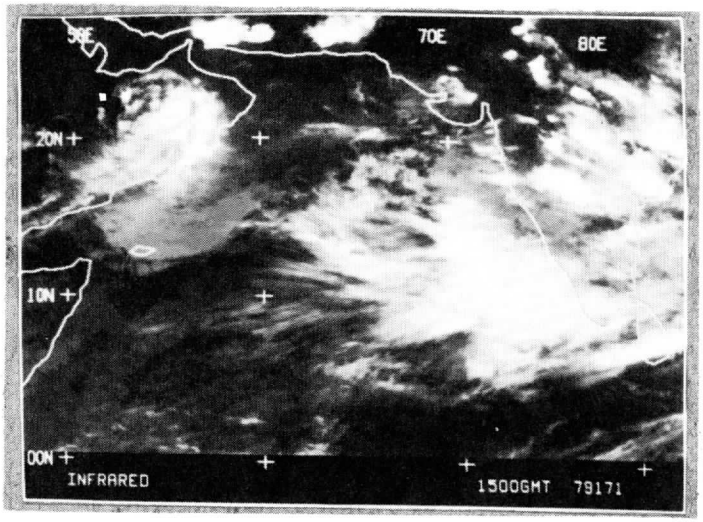
50E
70E
80E
20N
10N
00N
INFRARED
1500GMT 79171

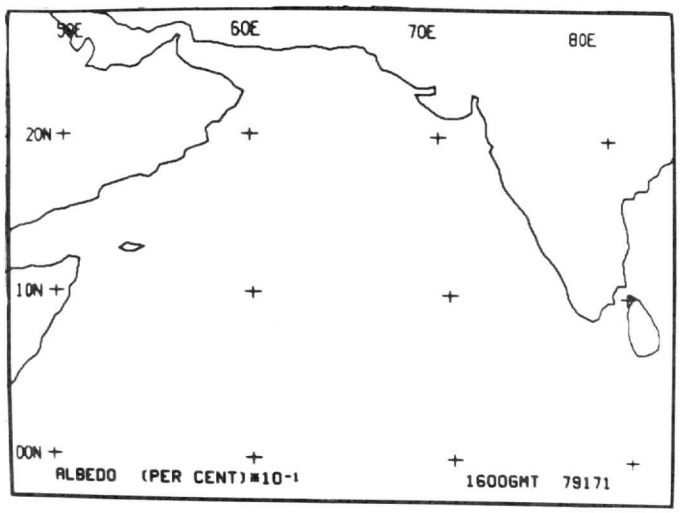
50E
60E
70E
80E
20N
10N
0ON
ALBEDO (PER CENT)*10-1
1600GMT 79171

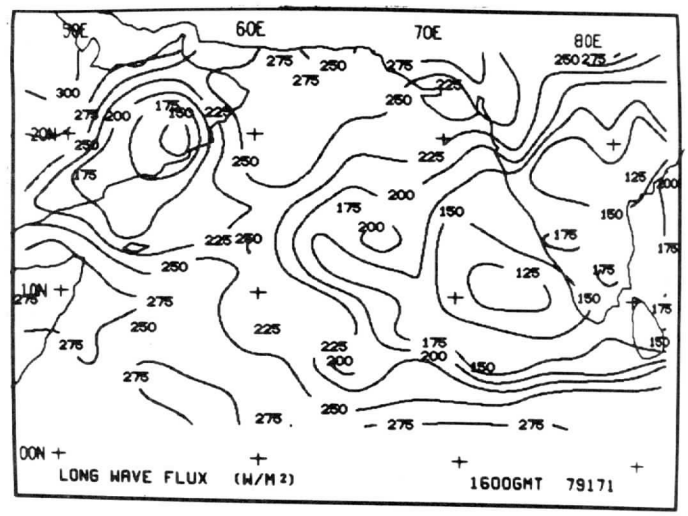
50E
60E
70E
80E
20N
10N
0ON
LONG WAVE FLUX (W/M2)
1600GMT 79171

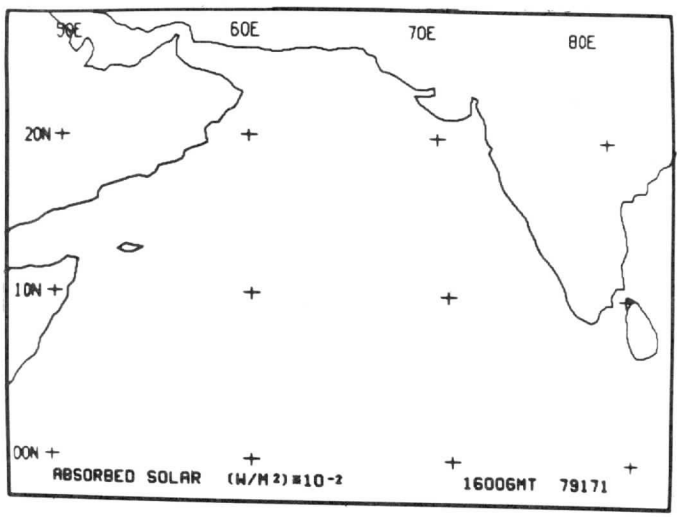
50E
60E
70E
80E
20N
10N
0ON
ABSORBED SOLAR (W/M2)*10-2
1600GMT 79171

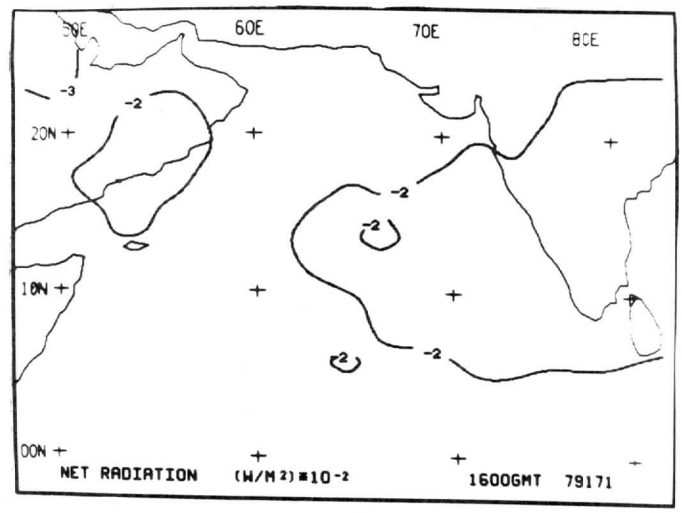
50E
60E
70E
80E
20N
10N
0ON
NET RADIATION (W/M2)*10-2
1600GMT 79171

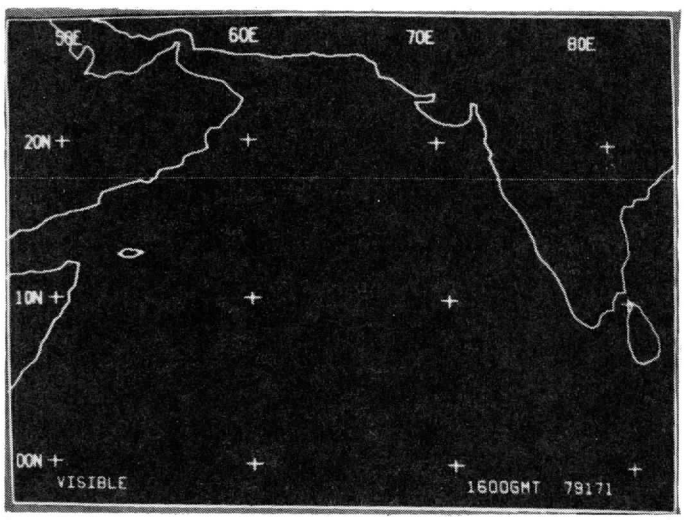
50E
60E
70E
80E
20N
10N
0ON
VISIBLE
1600GMT 79171

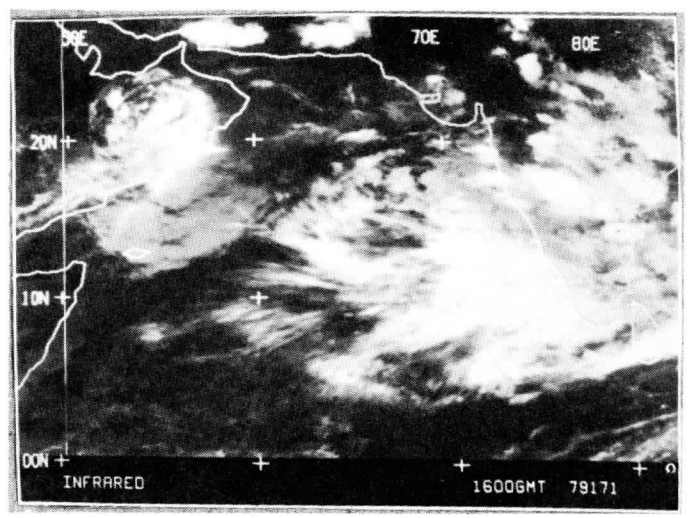
50E
70E
80E
20N
10N
0ON
INFRARED
1600GMT 79171

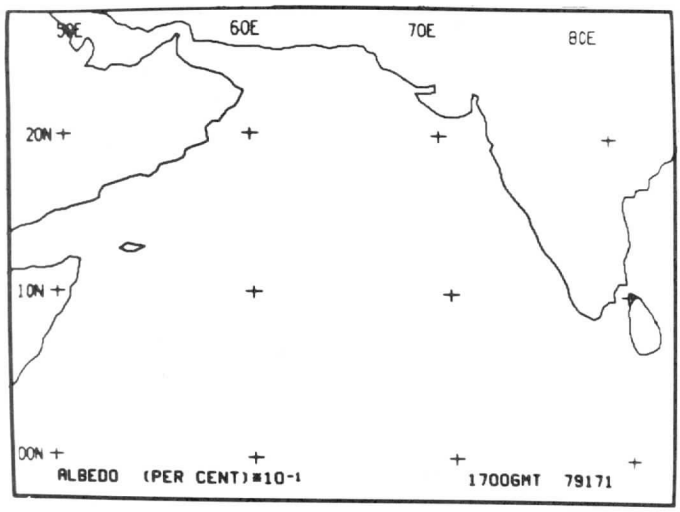
50E
60E
70E
80E
20N
10N
00N
ALBEDO (PER CENT)*10-1
1700GMT 79171

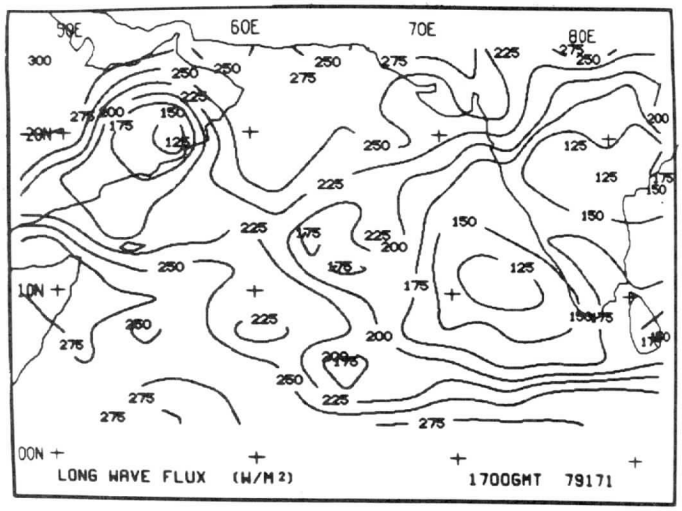
50E
60E
70E
80E
20N
10N
00N
LONG WAVE FLUX (W/M2)
1700GMT 79171

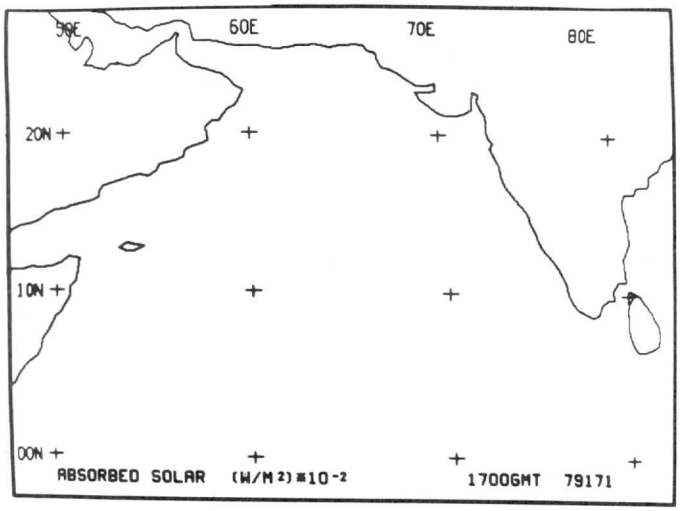
50E
60E
70E
80E
20N
10N
00N
ABSORBED SOLAR (W/M2)*10-2
1700GMT 79171

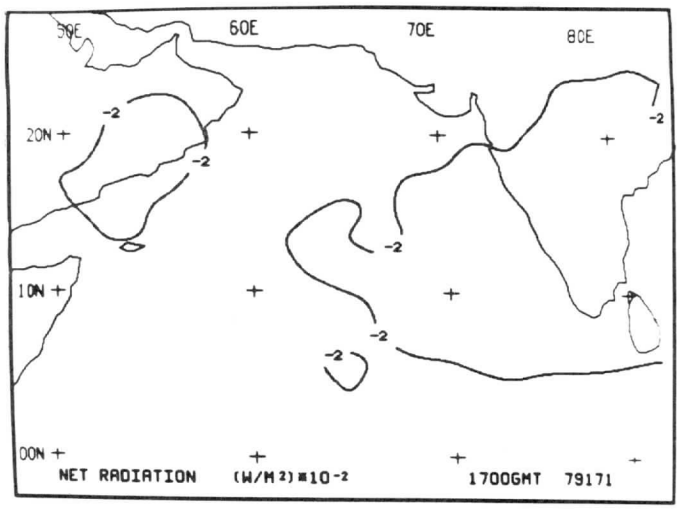
50E
60E
70E
80E
20N
10N
00N
NET RADIATION (W/M2)*10-2
1700GMT 79171

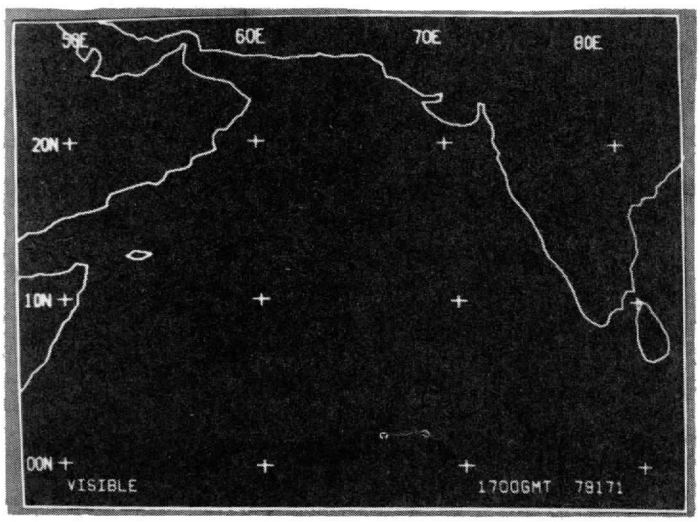
50E
60E
70E
80E
20N
10N
00N
VISIBLE
1700GMT 79171

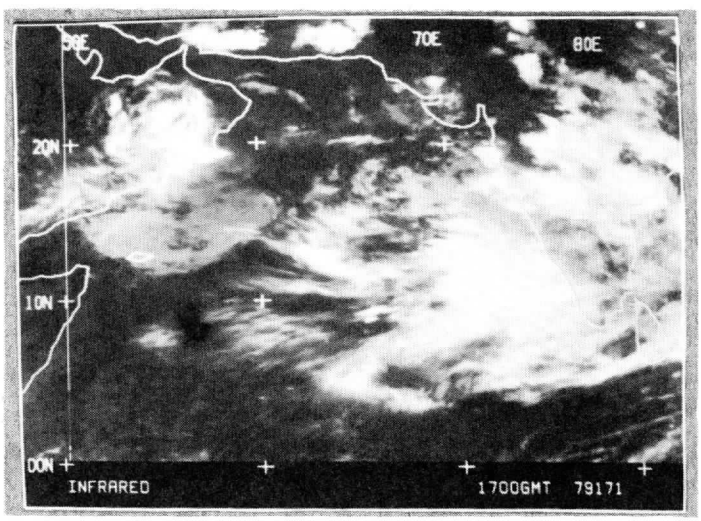
50E
70E
80E
20N
10N
00N
INFRARED
1700GMT 79171

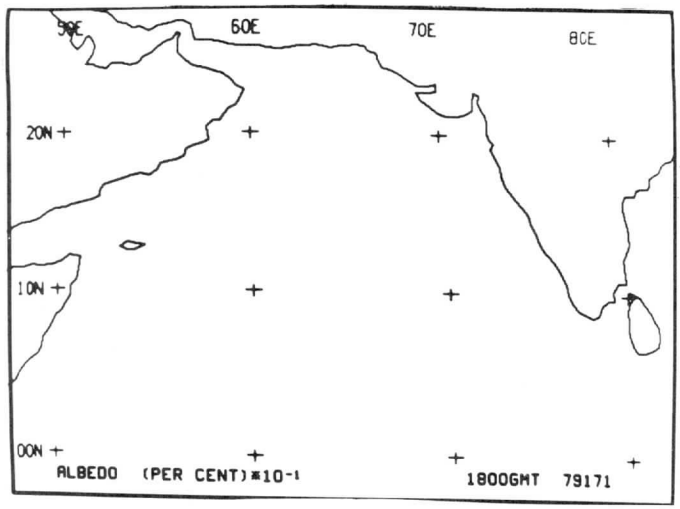
50E
60E
70E
80E
20N
10N
00N
ALBEDO (PER CENT)*10-1
1800GMT 79171

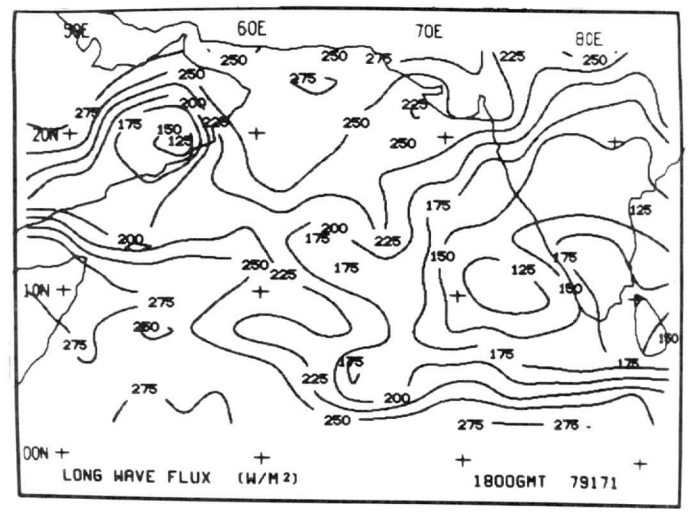
50E
60E
70E
80E
20N
10N
00N
LONG WAVE FLUX (W/M2)
1800GMT 79171

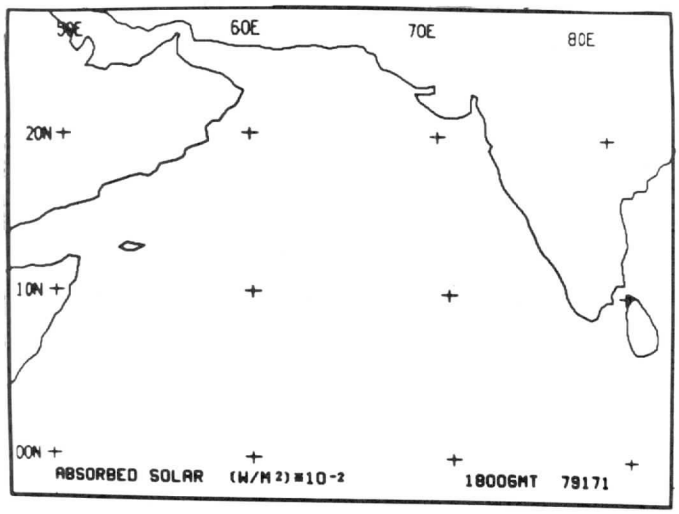
50E
60E
70E
80E
20N
10N
00N
ABSORBED SOLAR (W/M2)*10-2
1800GMT 79171

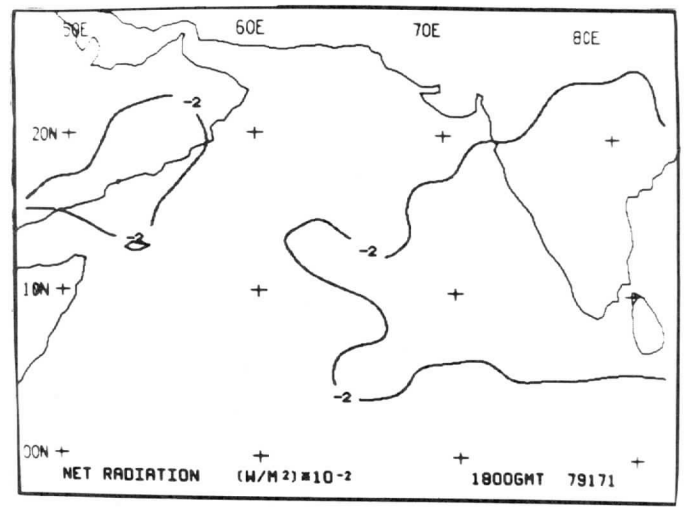
50E
60E
70E
80E
20N
10N
00N
NET RADIATION (W/M2)*10-2
1800GMT 79171

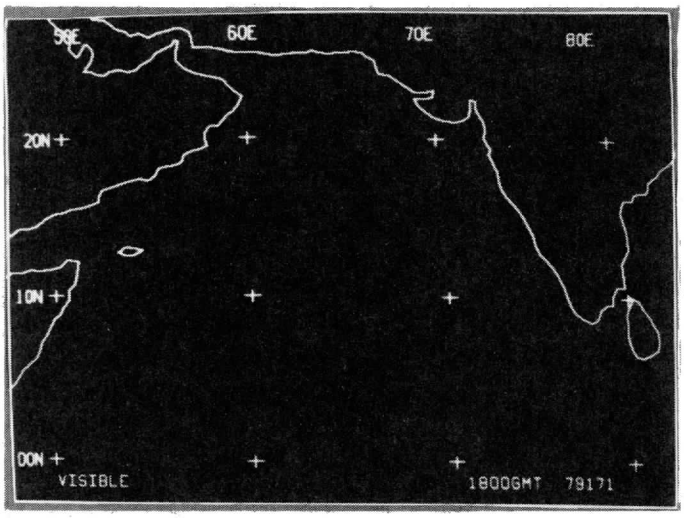
50E
60E
70E
80E
20N
10N
00N
VISIBLE
1800GMT 79171

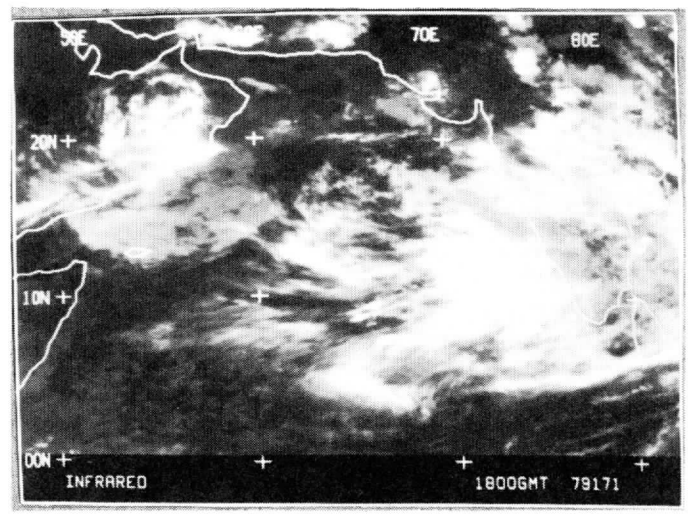
50E
70E
80E
20N
10N
00N
INFRARED
1800GMT 79171

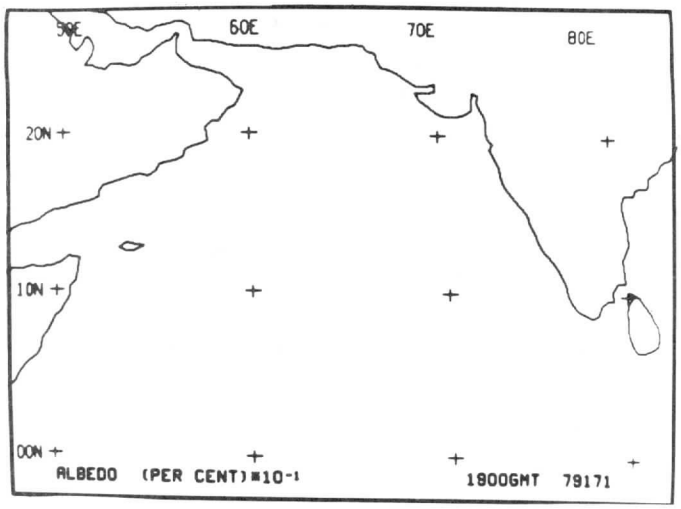
50E
60E
70E
80E
20N
10N
00N
ALBEDO (PER CENT)×10-1
1900GMT 79171

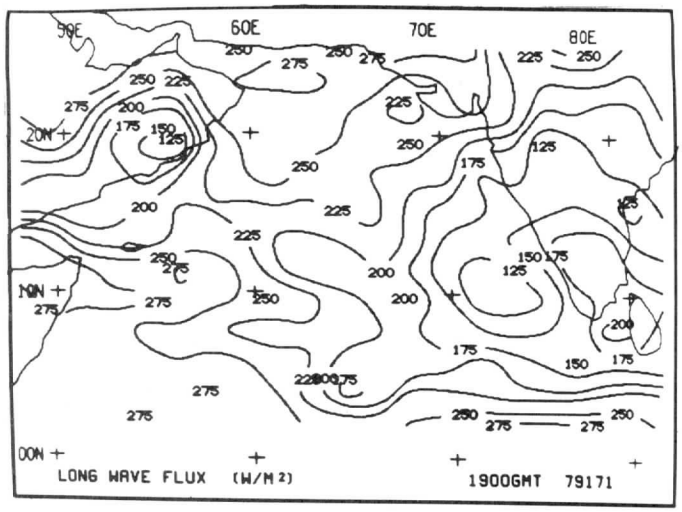
50E
60E
70E
80E
20N
10N
00N
LONG WAVE FLUX (W/M2)
1900GMT 79171

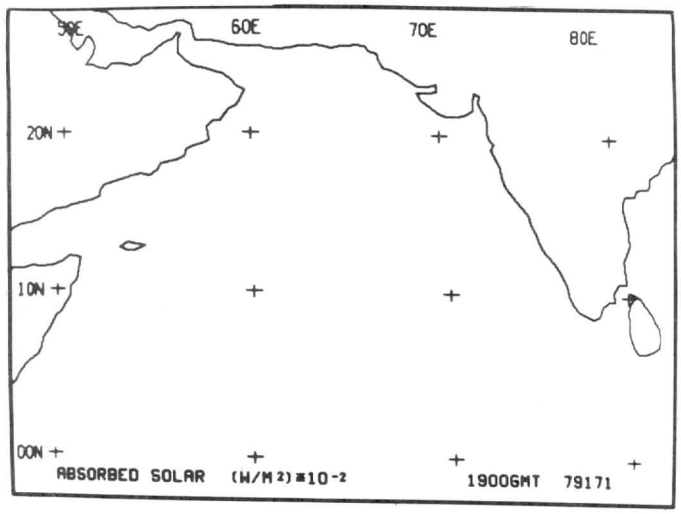
50E
60E
70E
80E
20N
10N
00N
ABSORBED SOLAR (W/M2)×10-2
1900GMT 79171

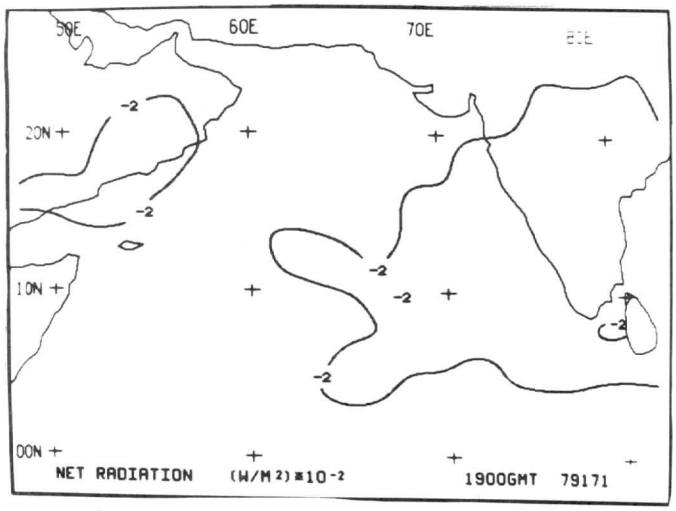
50E
60E
70E
80E
20N
10N
00N
NET RADIATION (W/M2)×10-2
1900GMT 79171

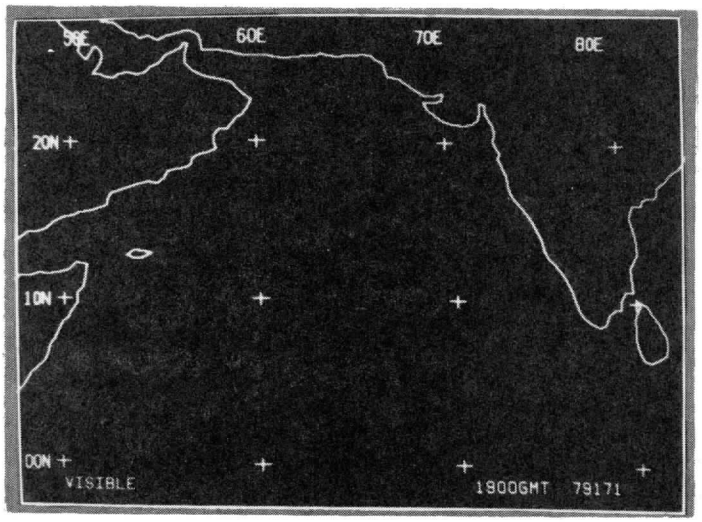
50E
60E
70E
80E
20N
10N
00N
VISIBLE
1900GMT 79171

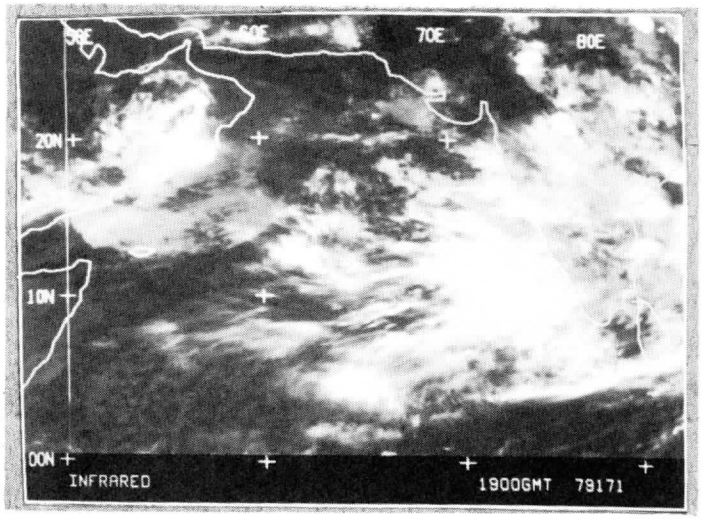
50E
60E
70E
80E
20N
10N
00N
INFRARED
1900GMT 79171

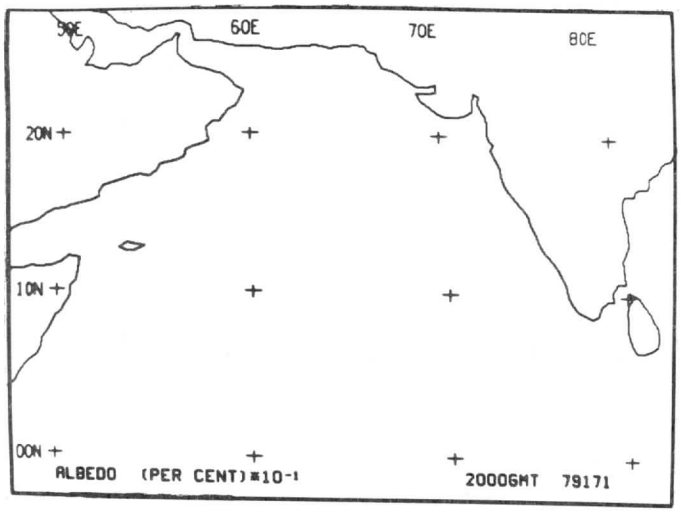
50E
60E
70E
80E
20N
10N
00N
ALBEDO (PER CENT)×10⁻¹
2000GMT 79171

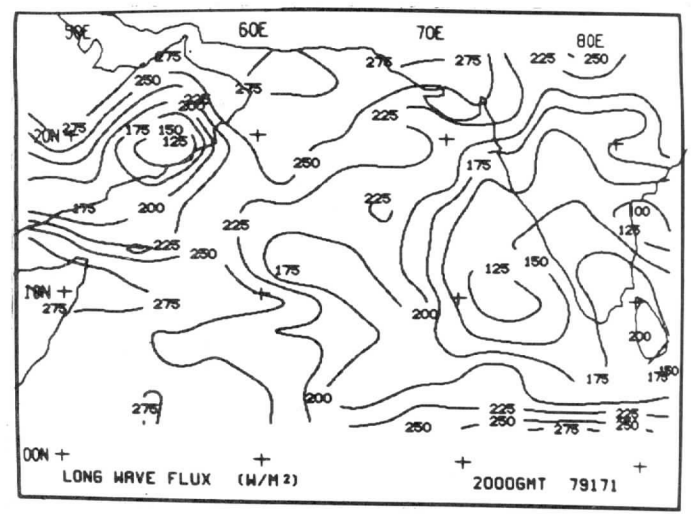
50E
60E
70E
80E
20N
10N
00N
LONG WAVE FLUX (W/M2)
2000GMT 79171

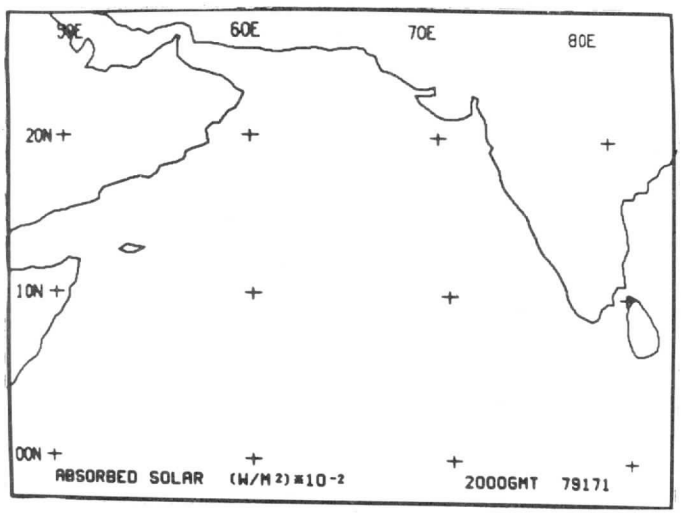
50E
60E
70E
80E
20N
10N
00N
ABSORBED SOLAR (W/M2)×10⁻²
2000GMT 79171

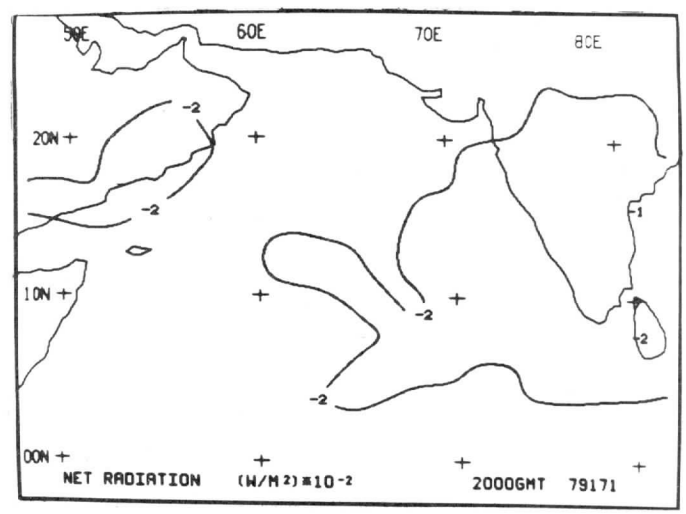
50E
60E
70E
80E
20N
10N
00N
NET RADIATION (W/M2)×10⁻²
2000GMT 79171

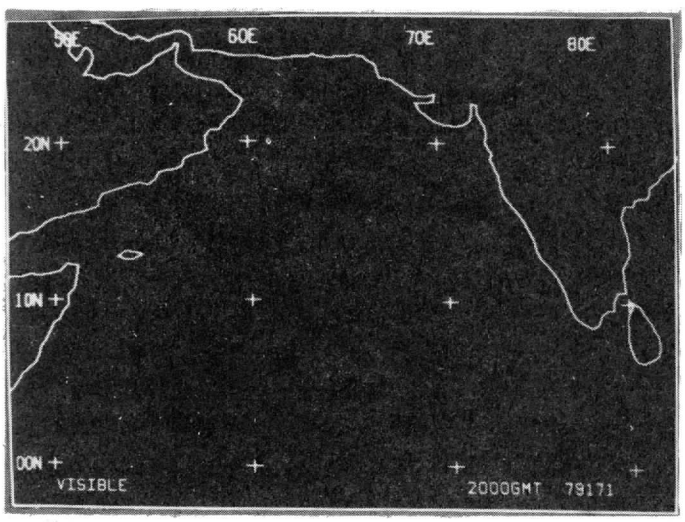
50E
60E
70E
80E
20N
10N
00N
VISIBLE
2000GMT 79171

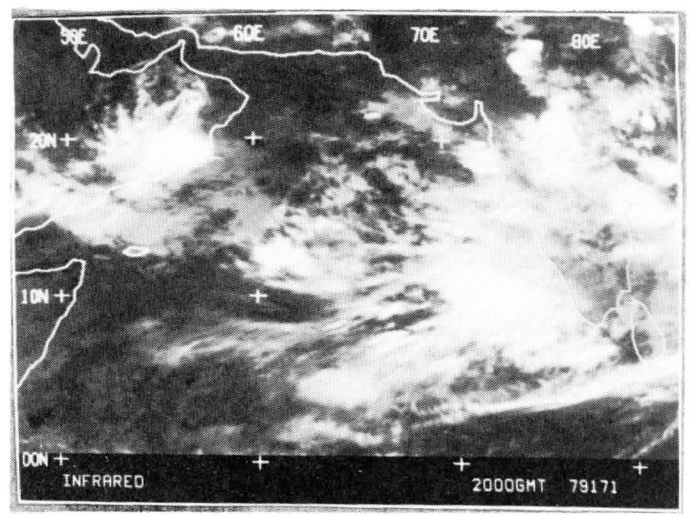
50E
60E
70E
80E
20N
10N
00N
INFRARED
2000GMT 79171

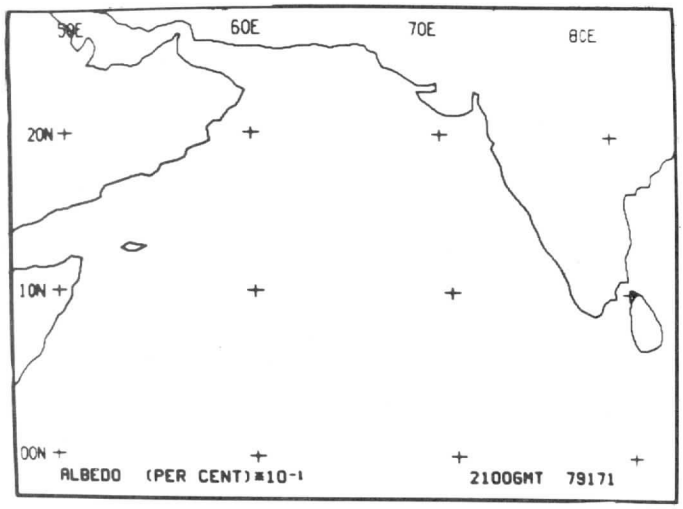
50E
60E
70E
80E
20N
10N
0ON
ALBEDO (PER CENT)×10⁻¹
2100GMT 79171

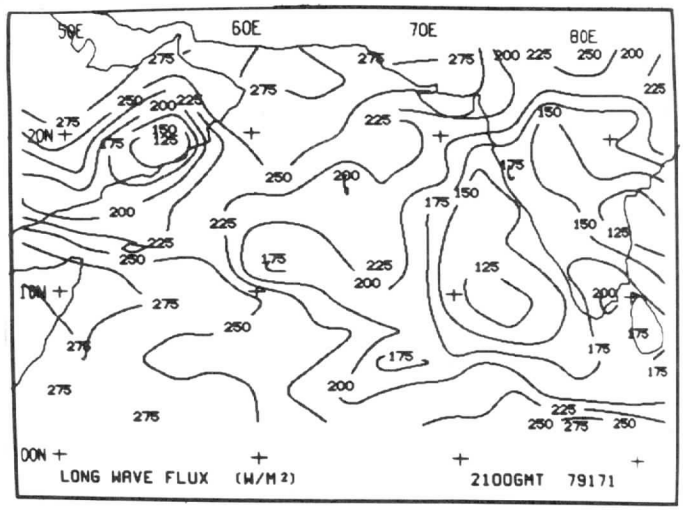
50E
60E
70E
80E
20N
10N
0ON
LONG WAVE FLUX (W/M2)
2100GMT 79171

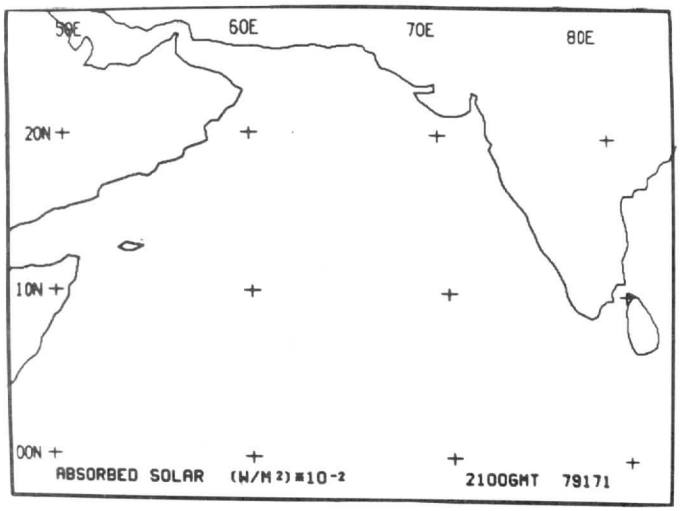
50E
60E
70E
80E
20N
10N
0ON
ABSORBED SOLAR (W/M2)×10-2
2100GMT 79171

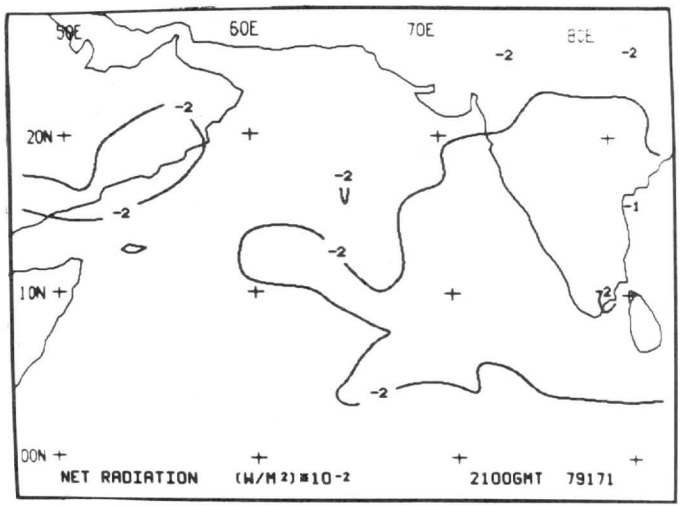
50E
60E
70E
80E
20N
10N
0ON
NET RADIATION (W/M2)×10-2
2100GMT 79171

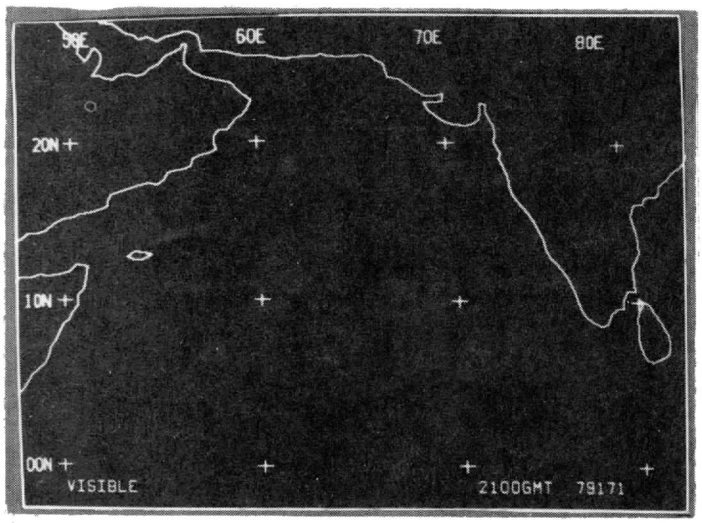
50E
60E
70E
80E
20N
10N
0ON
VISIBLE
2100GMT 79171

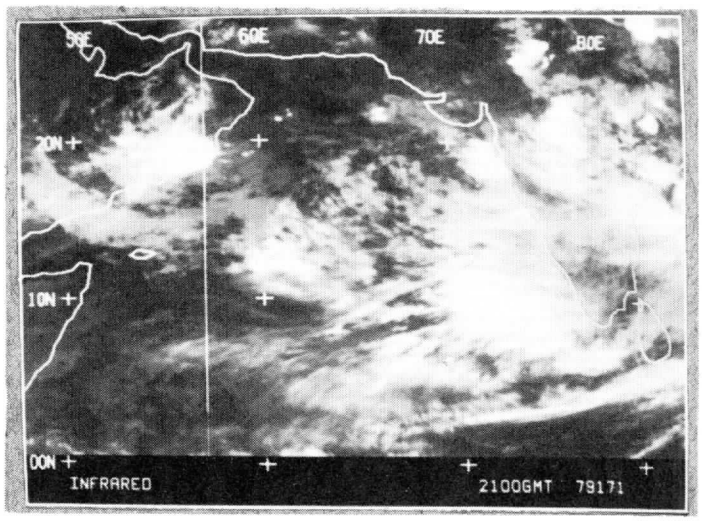
50E
60E
70E
80E
20N
10N
0ON
INFRARED
2100GMT 79171

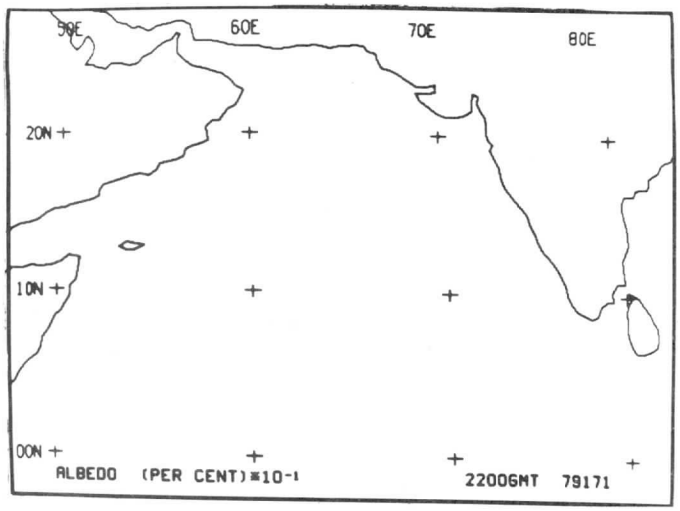
50E
60E
70E
80E
20N
10N
0ON
ALBEDO (PER CENT)×10-1
2200GMT 79171

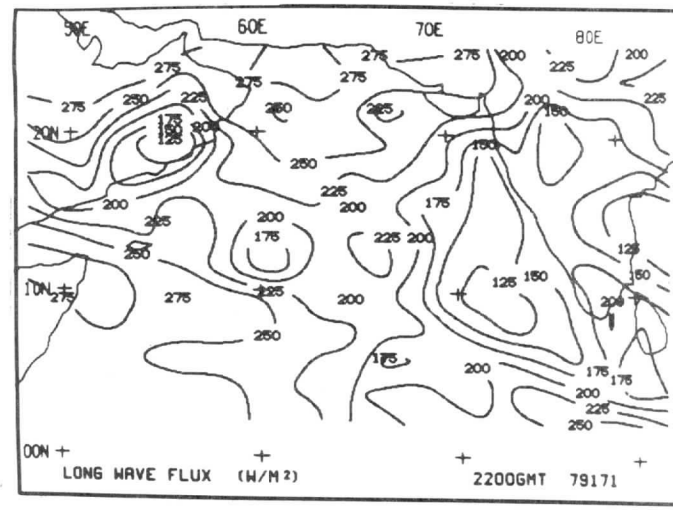
50E
60E
70E
80E
20N
10N
0ON
LONG WAVE FLUX (W/M2)
2200GMT 79171

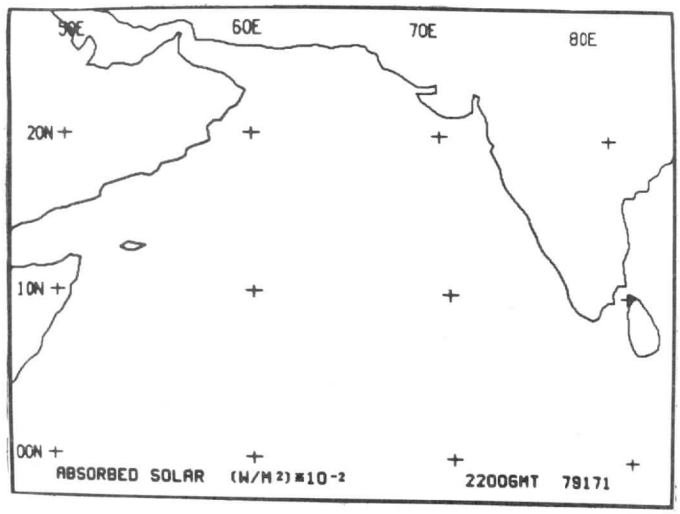
50E
60E
70E
80E
20N
10N
0ON
ABSORBED SOLAR (W/M2)×10-2
2200GMT 79171

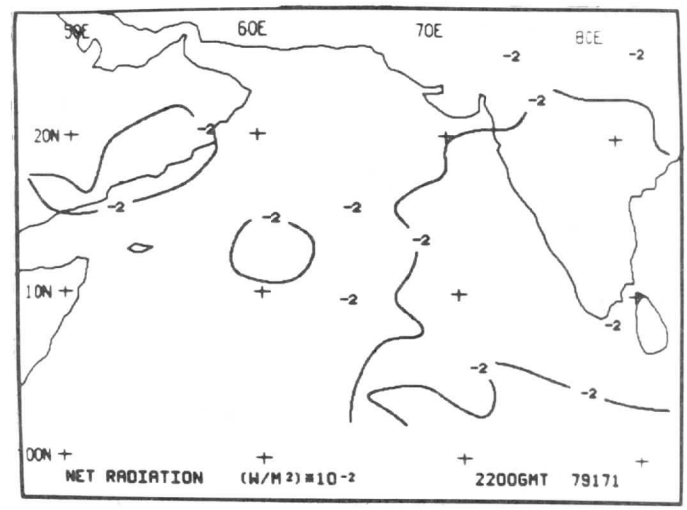
50E
60E
70E
80E
20N
10N
0ON
NET RADIATION (W/M2)×10-2
2200GMT 79171

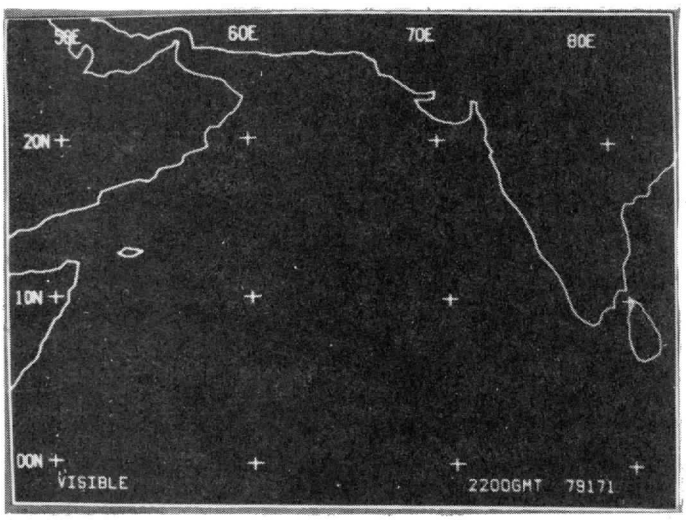
50E
60E
70E
80E
20N
10N
0ON
VISIBLE
2200GMT 79171

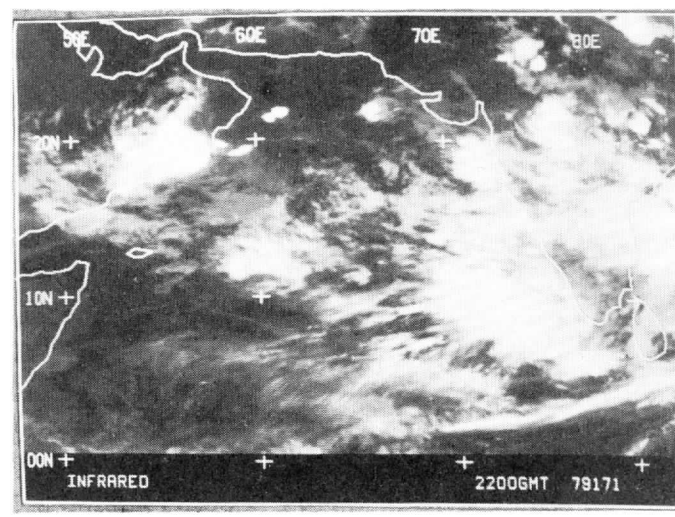
50E
60E
70E
80E
20N
10N
0ON
INFRARED
2200GMT 79171

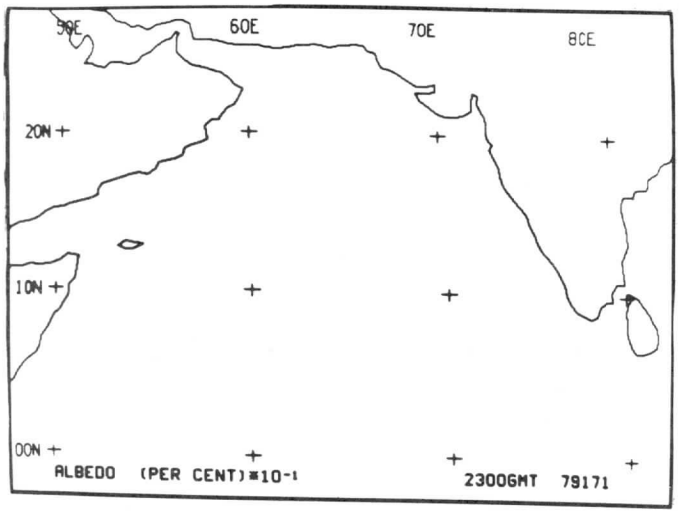
50E
60E
70E
80E
20N
10N
0ON
ALBEDO (PER CENT)×10-1
2300GMT 79171

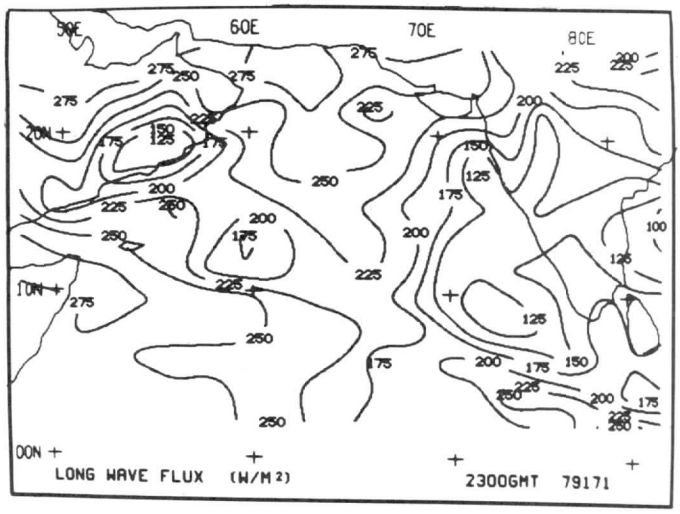
50E
60E
70E
80E
20N
10N
0ON
LONG WAVE FLUX (W/M2)
2300GMT 79171

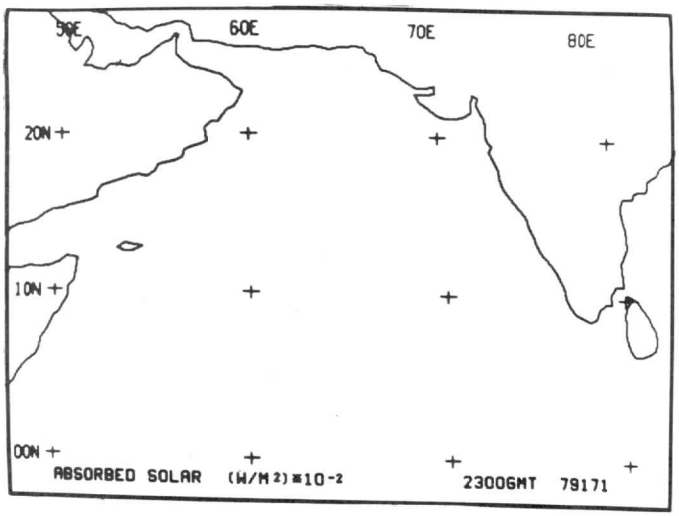
50E
60E
70E
80E
20N
10N
0ON
ABSORBED SOLAR (W/M2)×10-2
2300GMT 79171

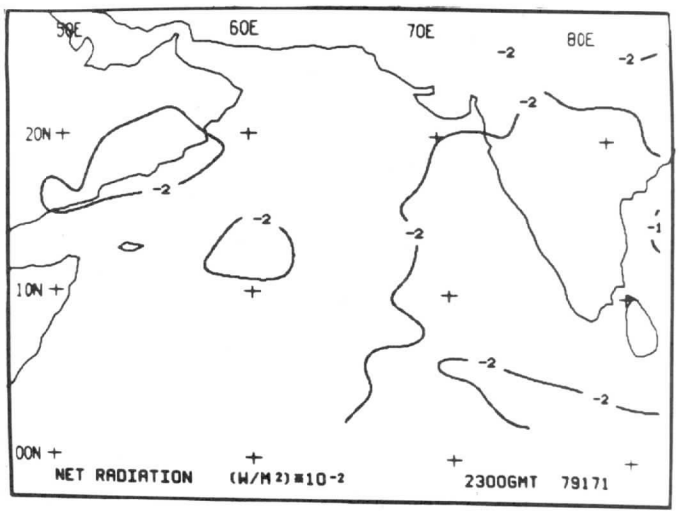
50E
60E
70E
80E
20N
10N
0ON
NET RADIATION (W/M2)×10-2
2300GMT 79171

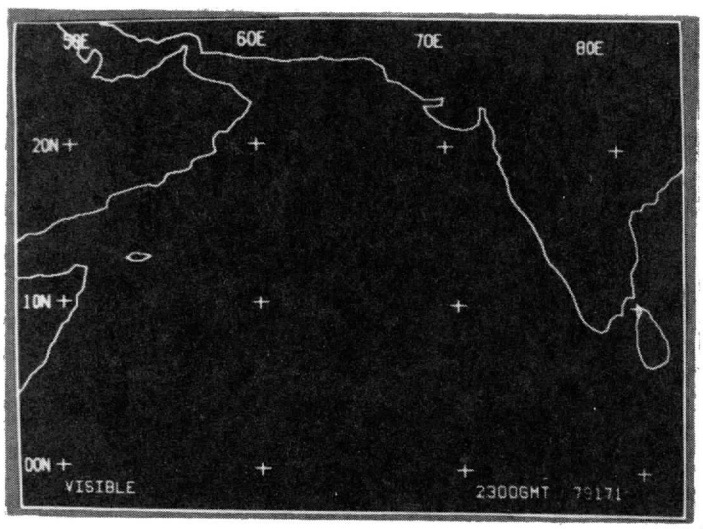
50E
60E
70E
80E
20N
10N
0ON
VISIBLE
2300GMT 79171

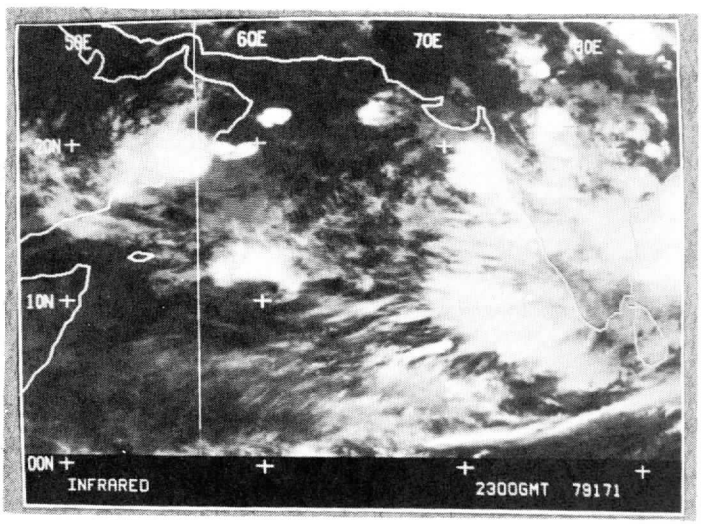
50E
60E
70E
80E
20N
10N
0ON
INFRARED
2300GMT 79171

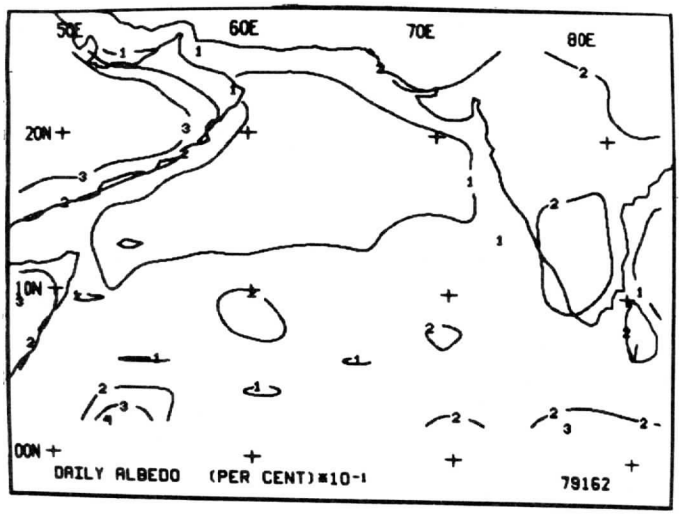
50E
60E
70E
80E
20N
10N
0ON
DAILY ALBEDO (PER CENT)×10-1
79162

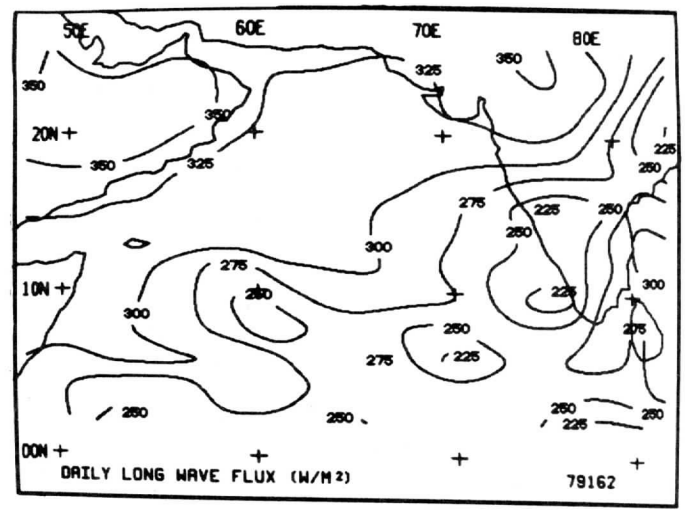
50E
60E
70E
80E
20N
10N
0ON
DAILY LONG WAVE FLUX (W/M2)
79162

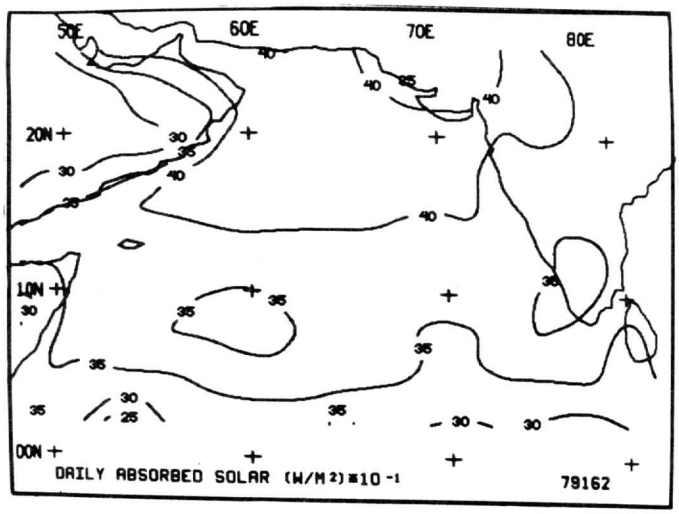
50E
60E
70E
80E
20N
10N
0ON
DAILY ABSORBED SOLAR (W/M2)×10-1
79162

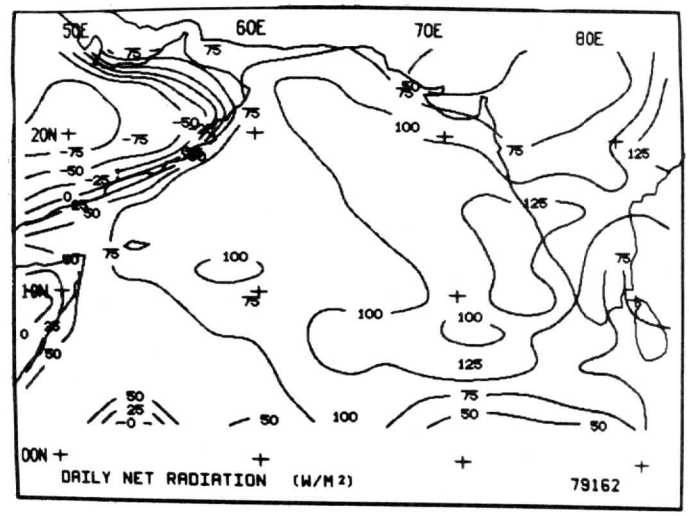
50E
60E
70E
80E
20N
10N
0ON
DAILY NET RADIATION (W/M2)
79162

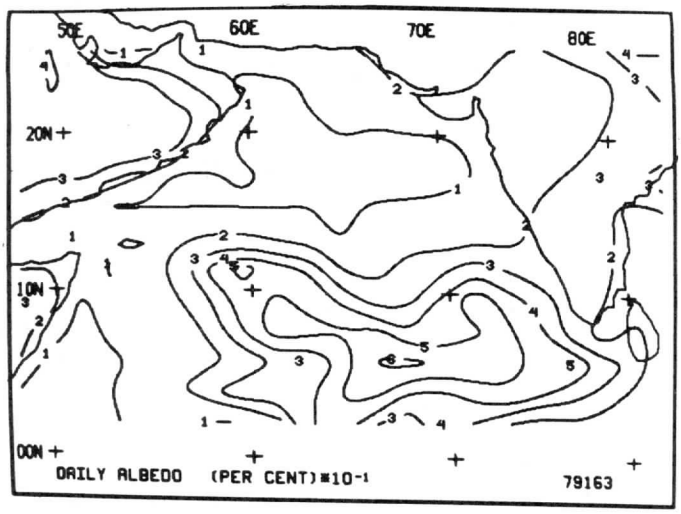
50E
60E
70E
80E
20N
10N
0ON
DAILY ALBEDO (PER CENT)*10-1
79163

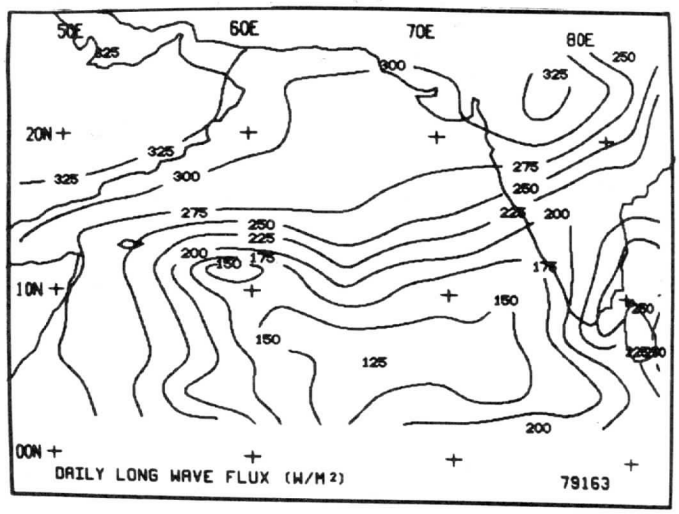
50E
60E
70E
80E
20N
10N
0ON
DAILY LONG WAVE FLUX (W/M2)
79163

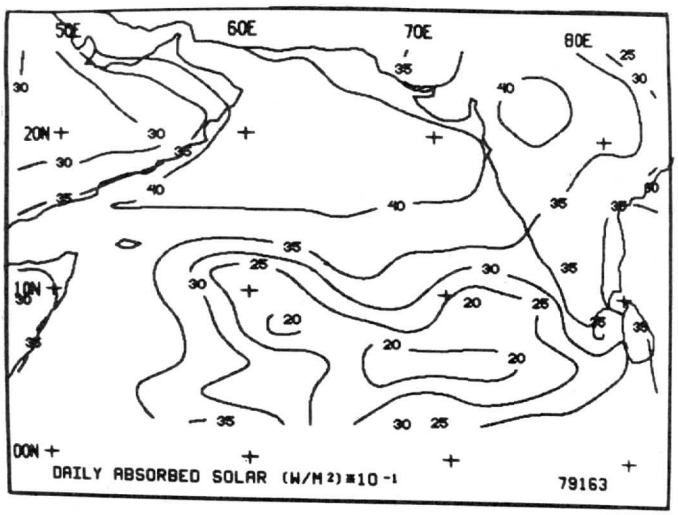
50E
60E
70E
80E
20N
10N
0ON
DAILY ABSORBED SOLAR (W/M2)*10-1
79163

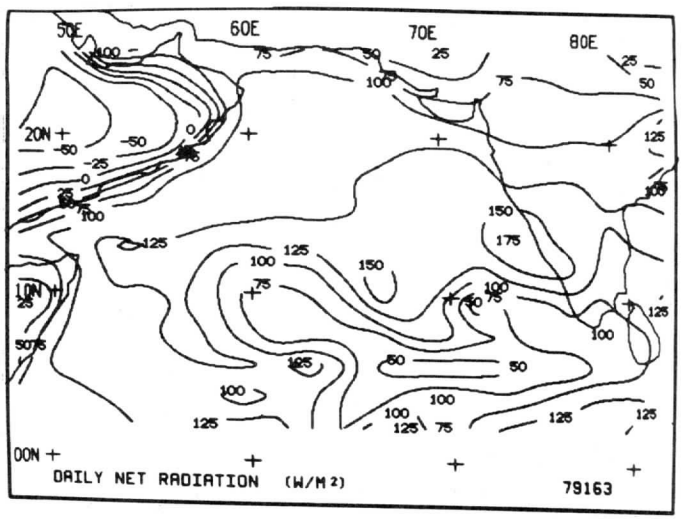
50E
60E
70E
80E
20N
10N
0ON
DAILY NET RADIATION (W/M2)
79163

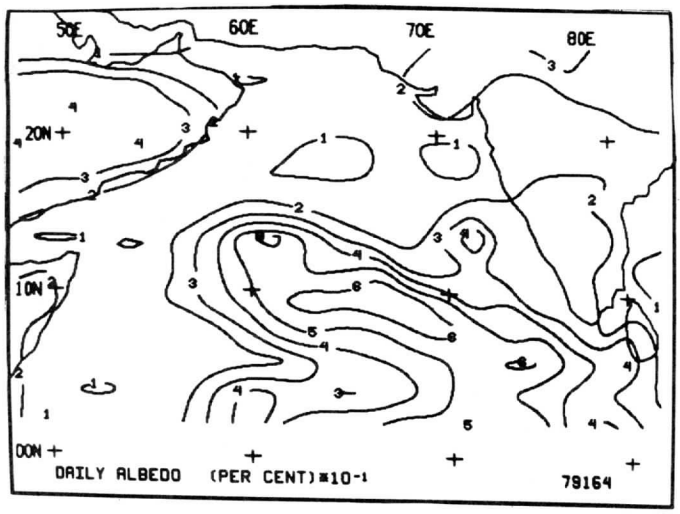
50E
60E
70E
80E
20N
10N
00N
DAILY ALBEDO (PER CENT)*10-1
79164

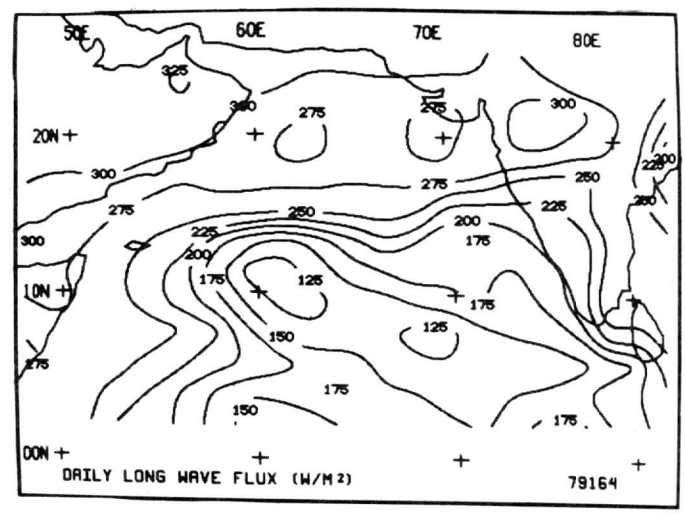
50E
60E
70E
80E
20N
10N
00N
DAILY LONG WAVE FLUX (W/M2)
79164

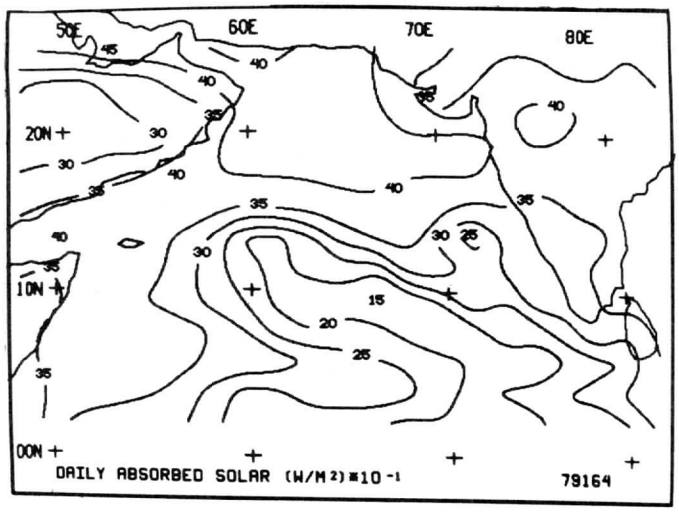
50E
60E
70E
80E
20N
10N
00N
DAILY ABSORBED SOLAR (W/M2)*10-1
79164

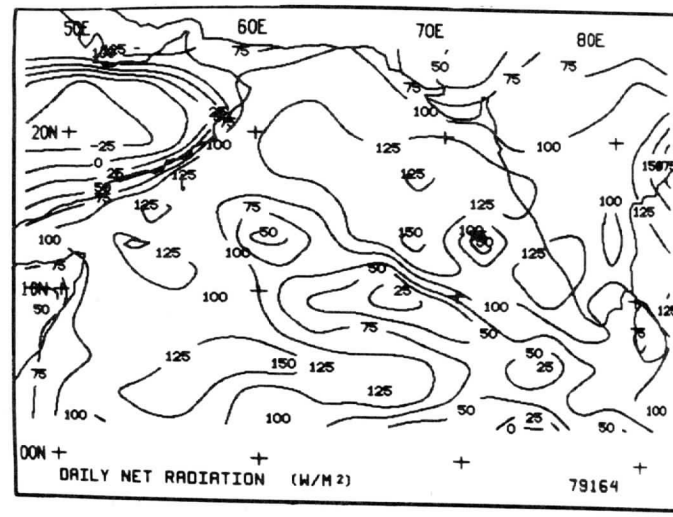
50E
60E
70E
80E
20N
10N
00N
DAILY NET RADIATION (W/M2)
79164

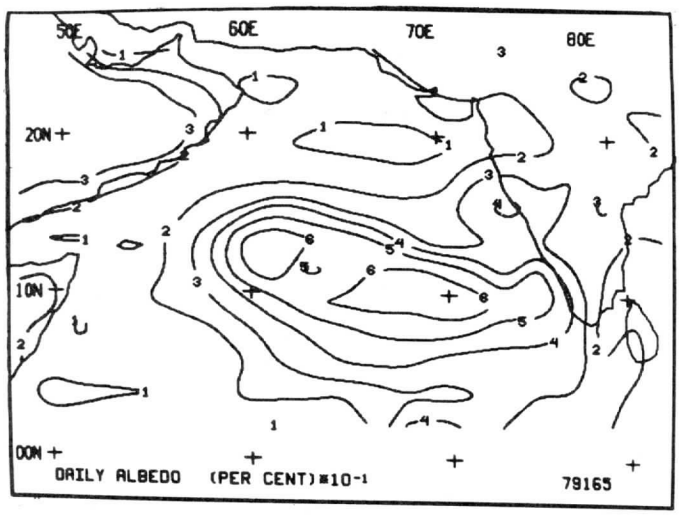
50E
60E
70E
80E
20N
10N
00N
DAILY ALBEDO (PER CENT)×10-1
79165

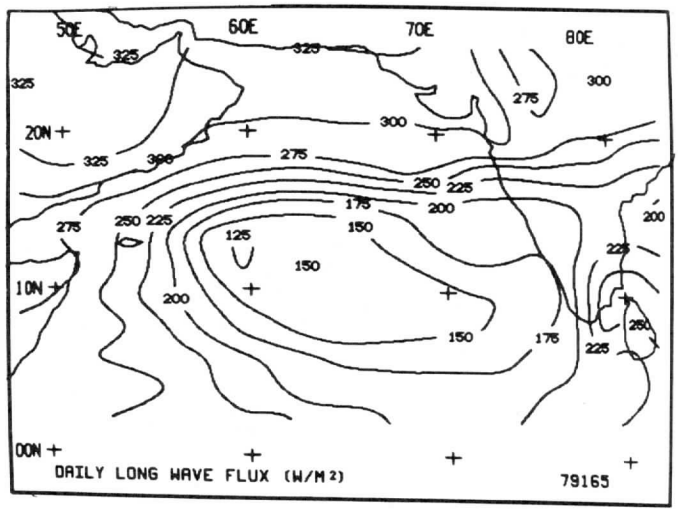
50E
60E
70E
80E
20N
10N
00N
DAILY LONG WAVE FLUX (W/M2)
79165

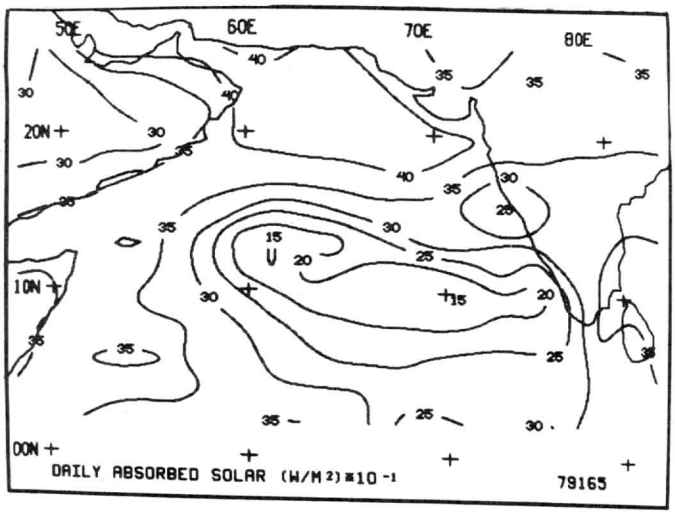
50E
60E
70E
80E
20N
10N
00N
DAILY ABSORBED SOLAR (W/M2)×10-1
79165

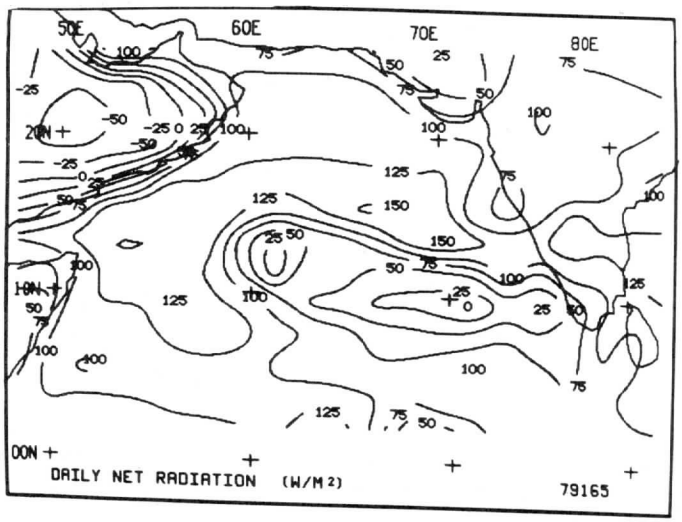
50E
60E
70E
80E
20N
10N
00N
DAILY NET RADIATION (W/M2)
79165

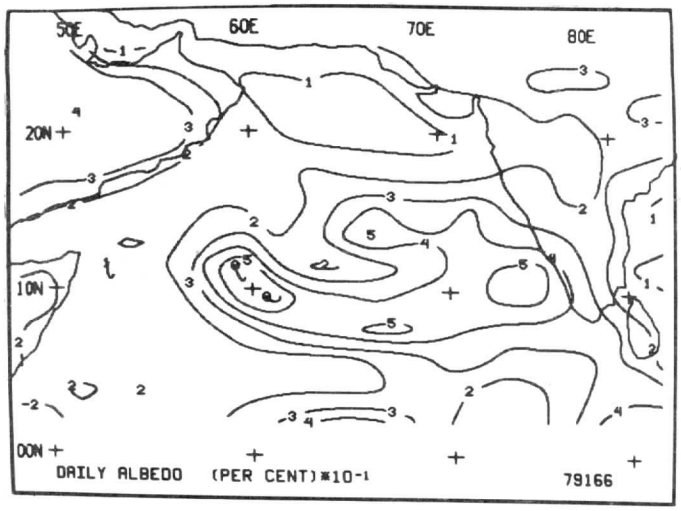
50E
60E
70E
80E
20N
10N
0ON
DAILY ALBEDO (PER CENT)*10-1
79166

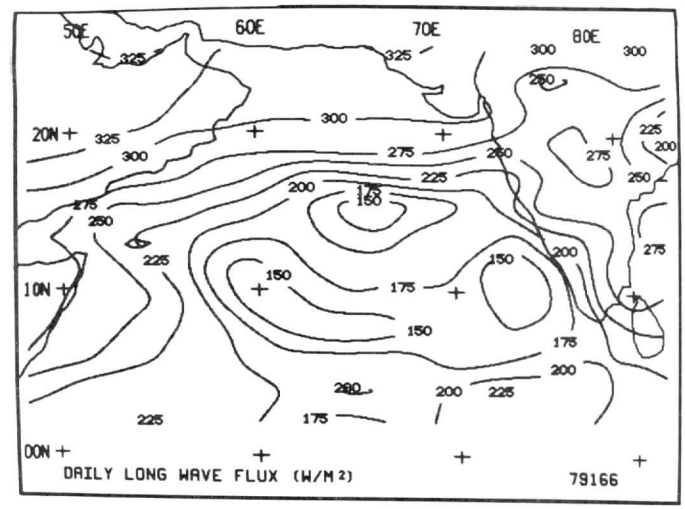
50E
60E
70E
80E
20N
10N
0ON
DAILY LONG WAVE FLUX (W/M2)
79166

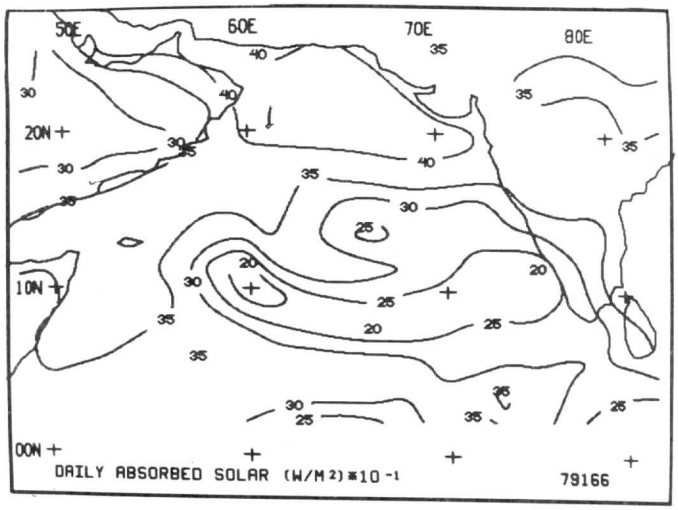
50E
60E
70E
80E
20N
10N
0ON
DAILY ABSORBED SOLAR (W/M2)*10-1
79166

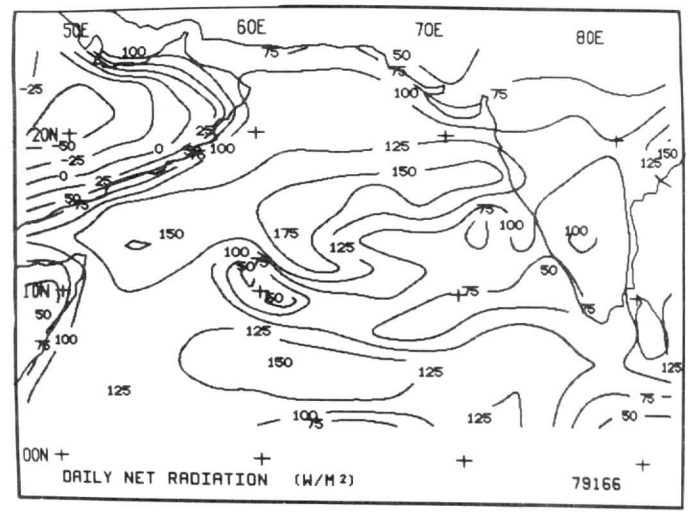
50E
60E
70E
80E
20N
10N
0ON
DAILY NET RADIATION (W/M2)
79166

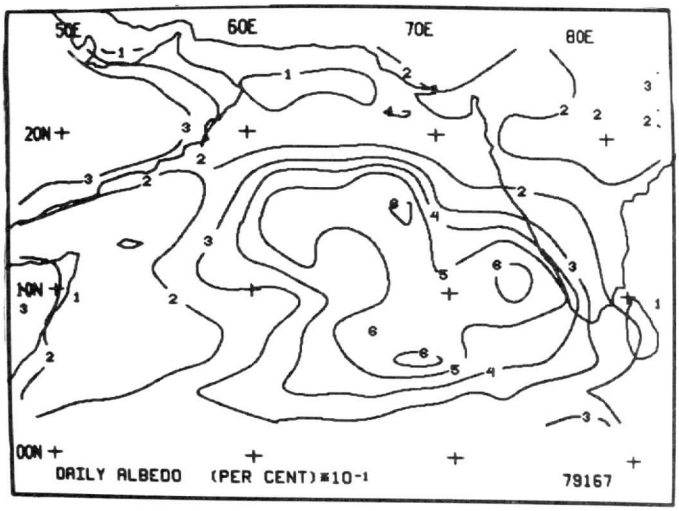
50E
60E
70E
80E
20N
10N
00N
DAILY ALBEDO (PER CENT)*10-1
79167

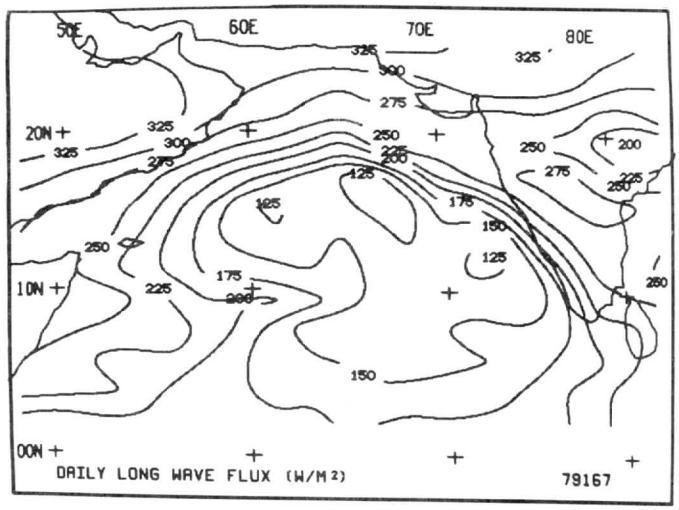
50E
60E
70E
80E
20N
10N
00N
DAILY LONG WAVE FLUX (W/M2)
79167

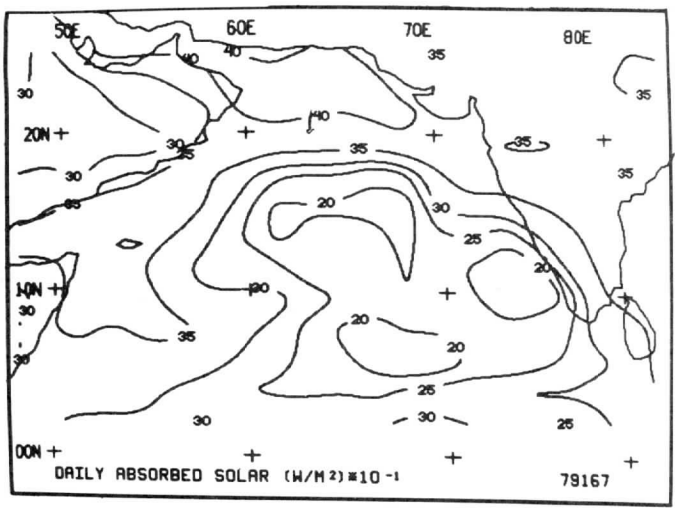
50E
60E
70E
80E
20N
10N
00N
DAILY ABSORBED SOLAR (W/M2)*10-1
79167

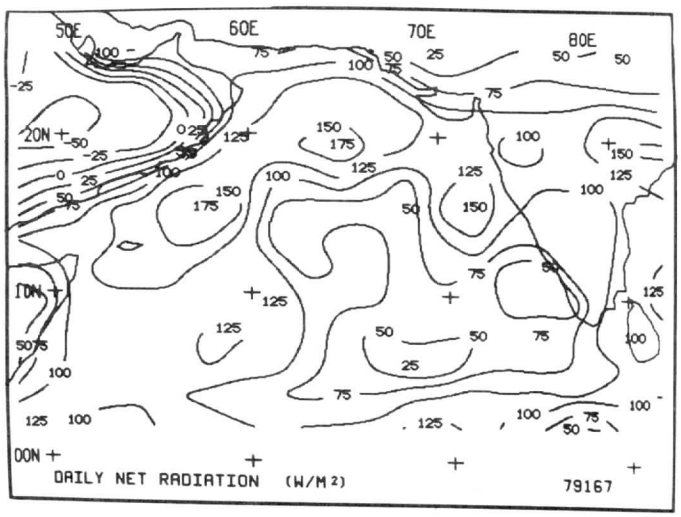
50E
60E
70E
80E
20N
10N
00N
DAILY NET RADIATION (W/M2)
79167

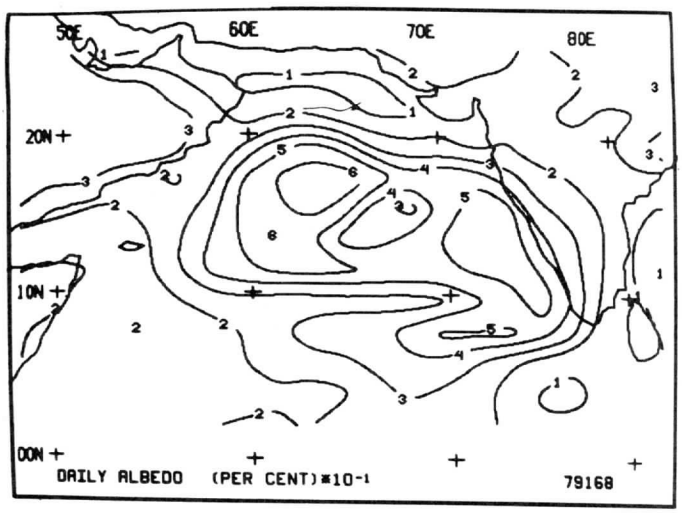
50E
60E
70E
80E
20N
10N
0ON
DAILY ALBEDO (PER CENT)*10-1
79168

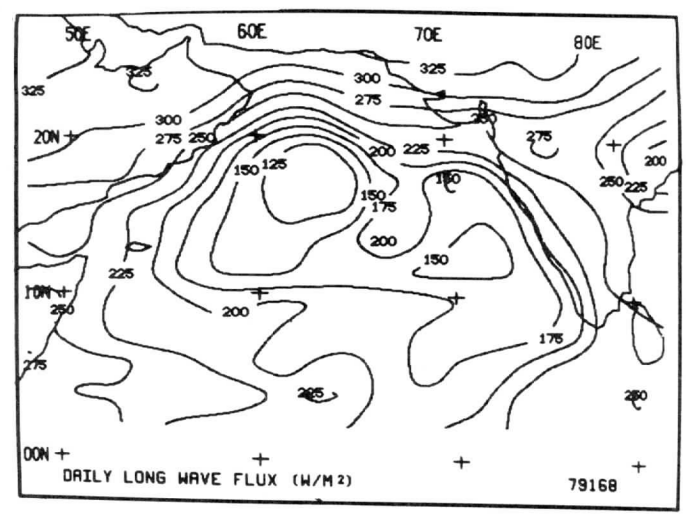
50E
60E
70E
80E
20N
10N
0ON
DAILY LONG WAVE FLUX (W/M2)
79168

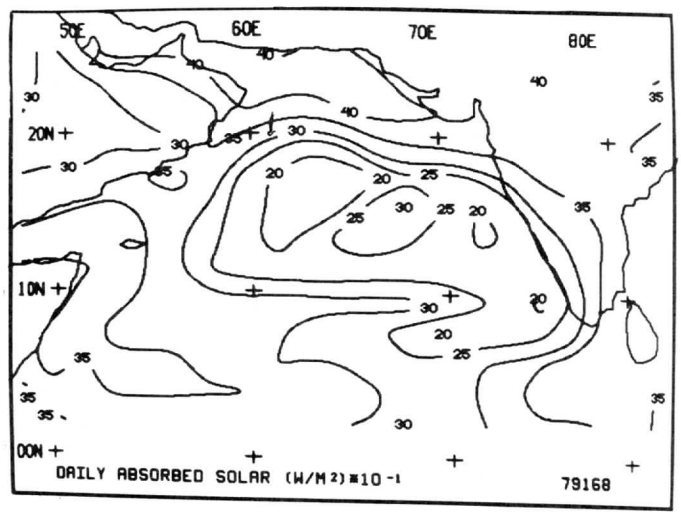
50E
60E
70E
80E
20N
10N
0ON
DAILY ABSORBED SOLAR (W/M2)*10-1
79168

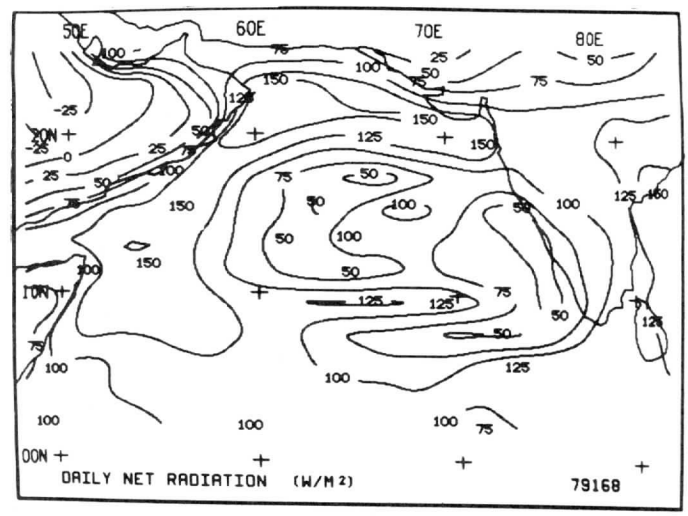
50E
60E
70E
80E
20N
10N
0ON
DAILY NET RADIATION (W/M2)
79168

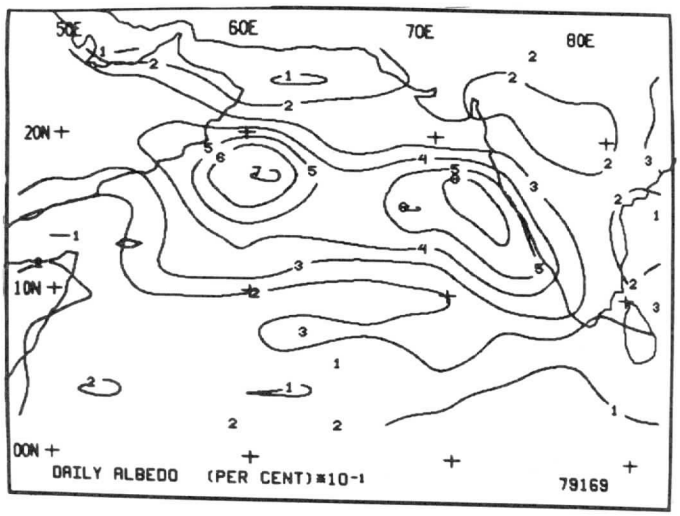
50E
60E
70E
80E
20N
10N
00N
DAILY ALBEDO (PER CENT)*10-1
79169

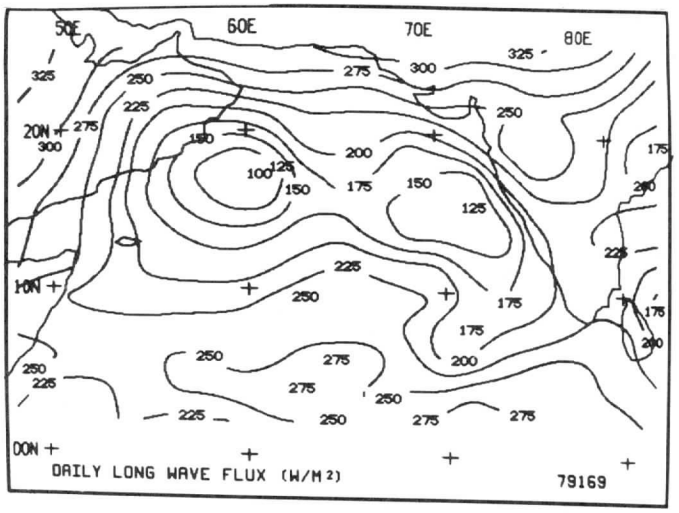
50E
60E
70E
80E
20N
10N
00N
DAILY LONG WAVE FLUX (W/M2)
79169

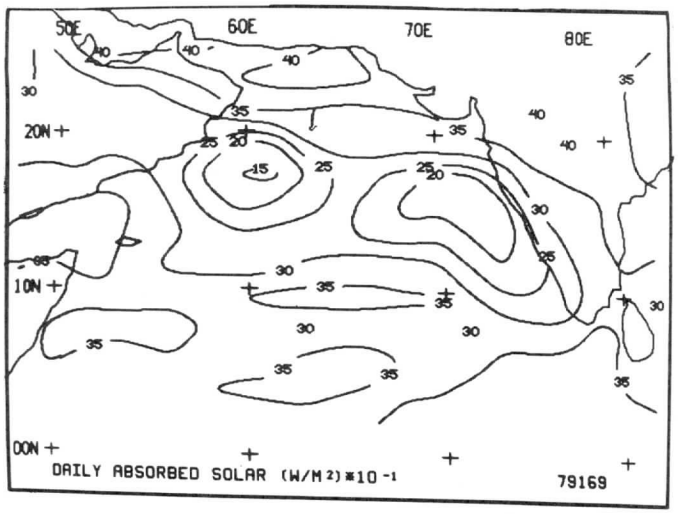
50E
60E
70E
80E
20N
10N
00N
DAILY ABSORBED SOLAR (W/M2)*10-1
79169

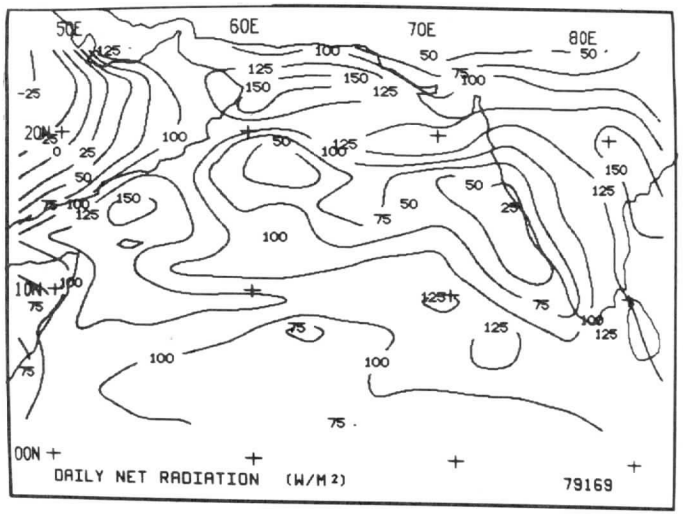
50E
60E
70E
80E
20N
10N
00N
DAILY NET RADIATION (W/M2)
79169

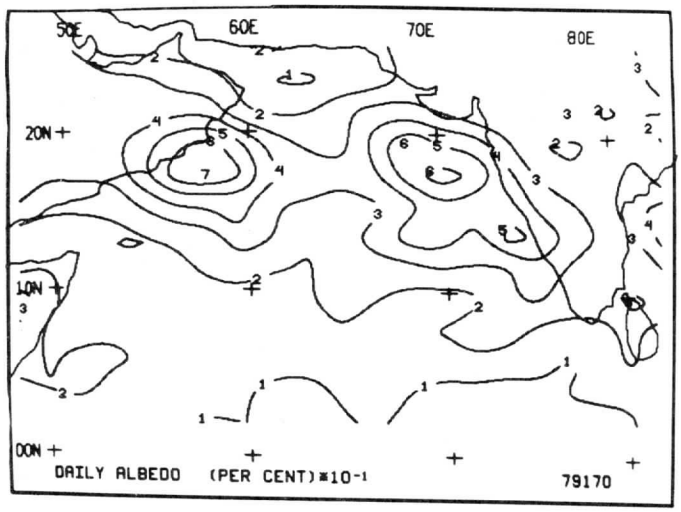
50E
60E
70E
80E
20N
10N
00N
DAILY ALBEDO (PER CENT)*10-1
79170

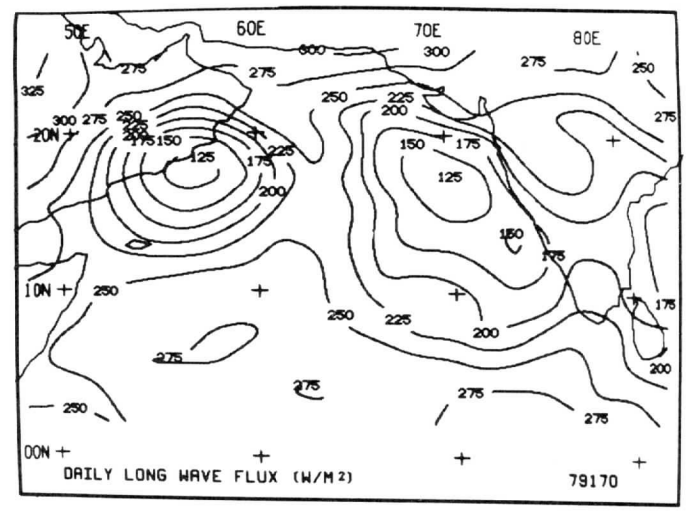
50E
60E
70E
80E
20N
10N
00N
DAILY LONG WAVE FLUX (W/M2)
79170

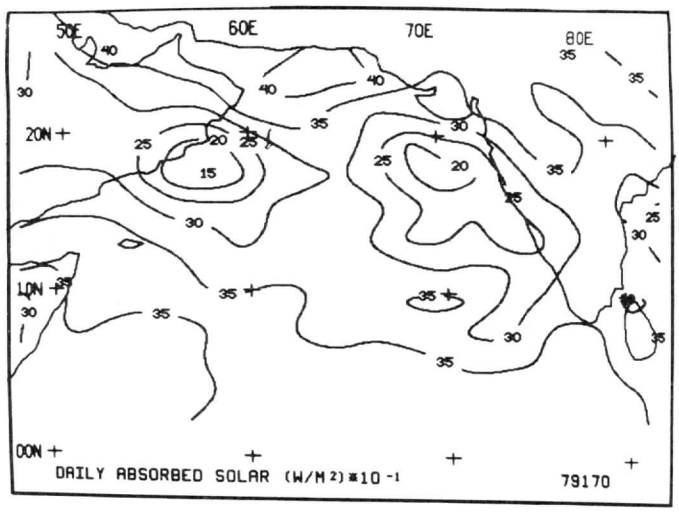
50E
60E
70E
80E
20N
10N
00N
DAILY ABSORBED SOLAR (W/M2)*10-1
79170

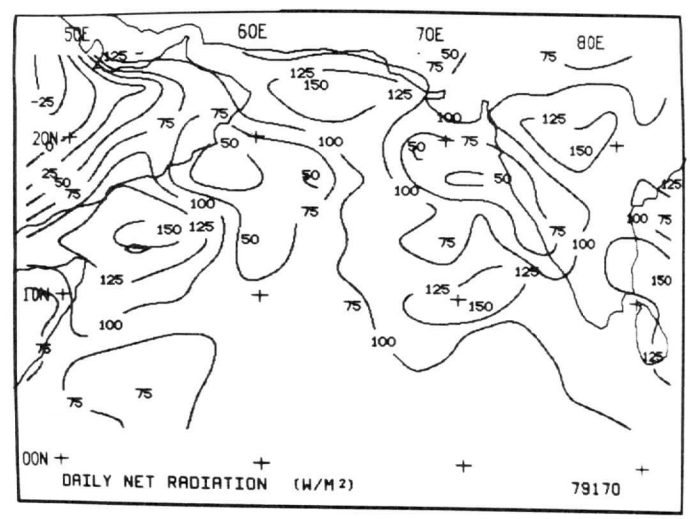
50E
60E
70E
80E
20N
10N
00N
DAILY NET RADIATION (W/M2)
79170

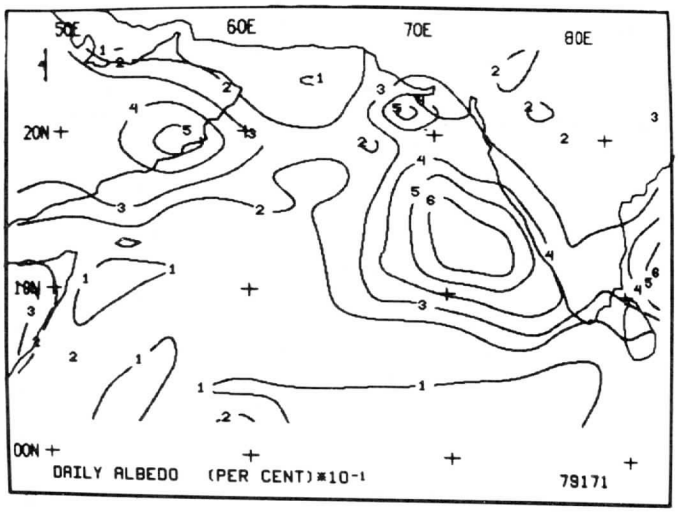
50E
60E
70E
80E
20N
10N
00N
DAILY ALBEDO (PER CENT)*10-1
79171

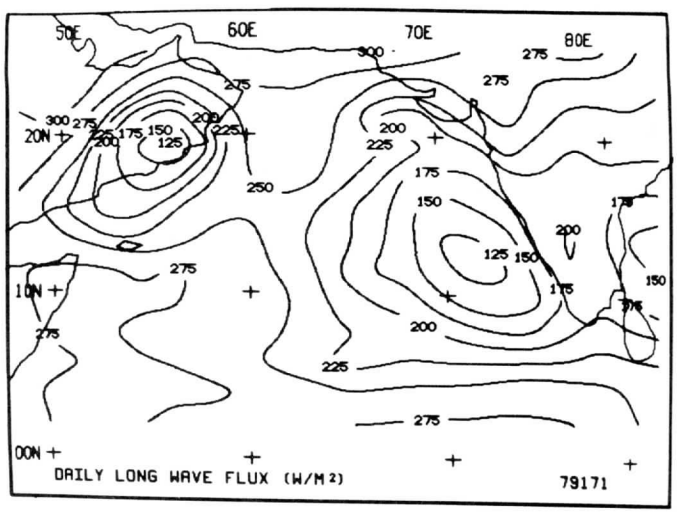
50E
60E
70E
80E
20N
10N
00N
DAILY LONG WAVE FLUX (W/M2)
79171

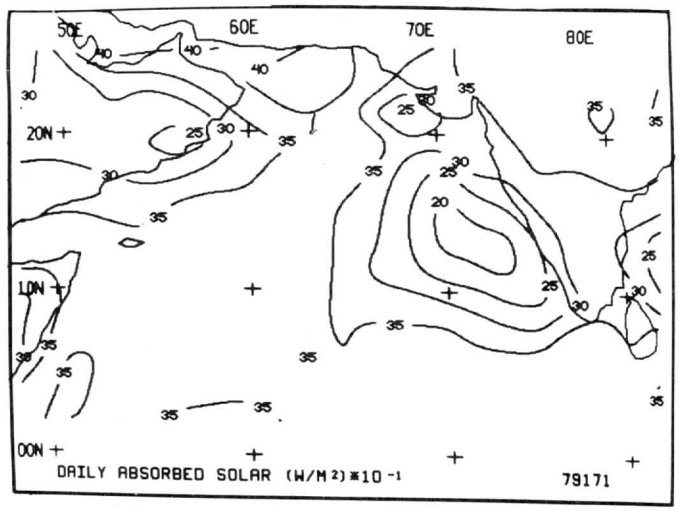
50E
60E
70E
80E
20N
10N
00N
DAILY ABSORBED SOLAR (W/M2)*10-1
79171

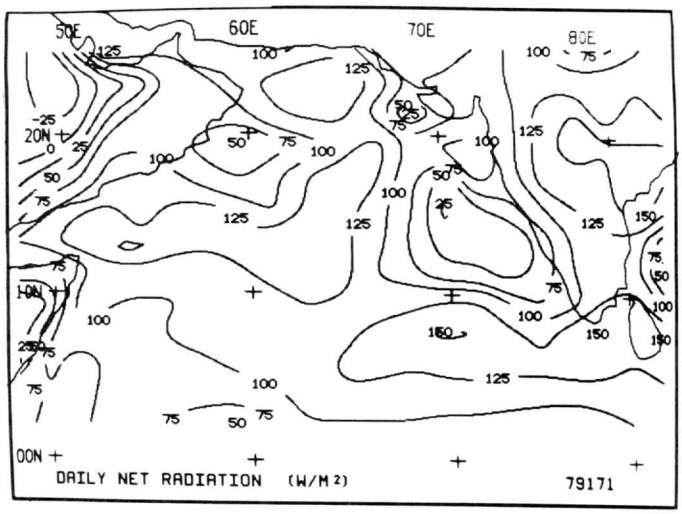
50E
60E
70E
80E
20N
10N
00N
DAILY NET RADIATION (W/M2)
79171

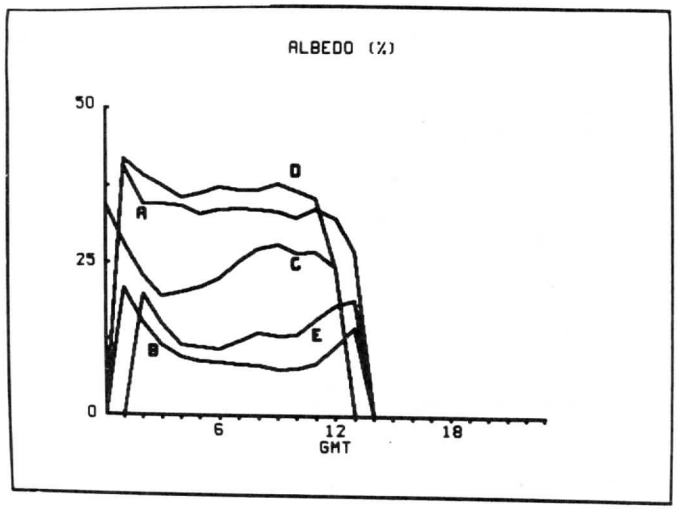

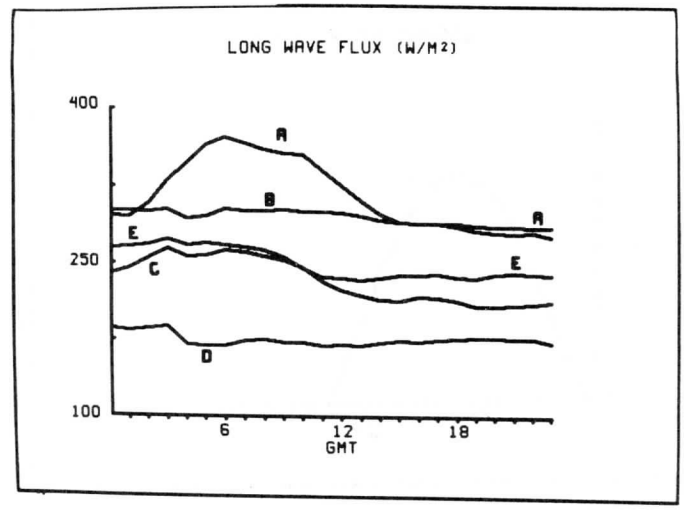

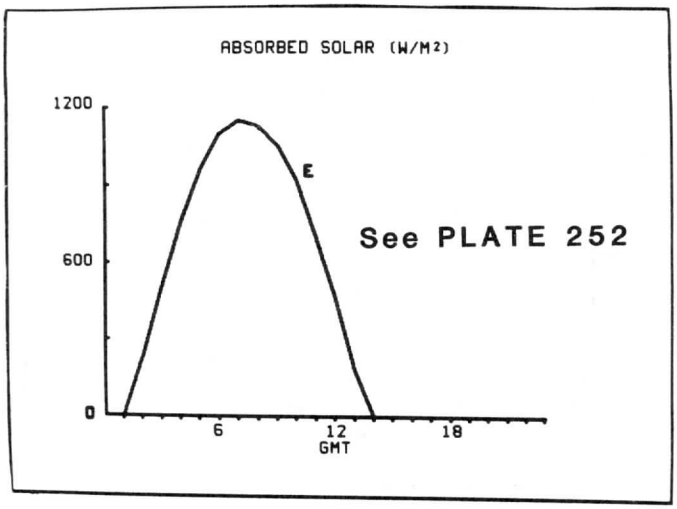

See PLATE 252

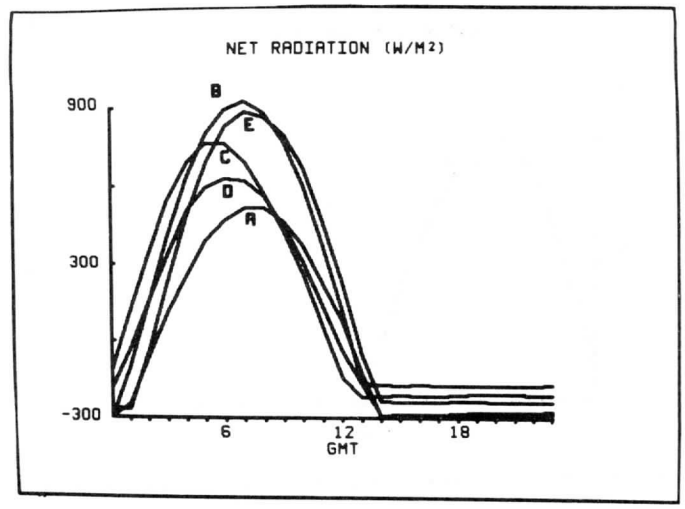

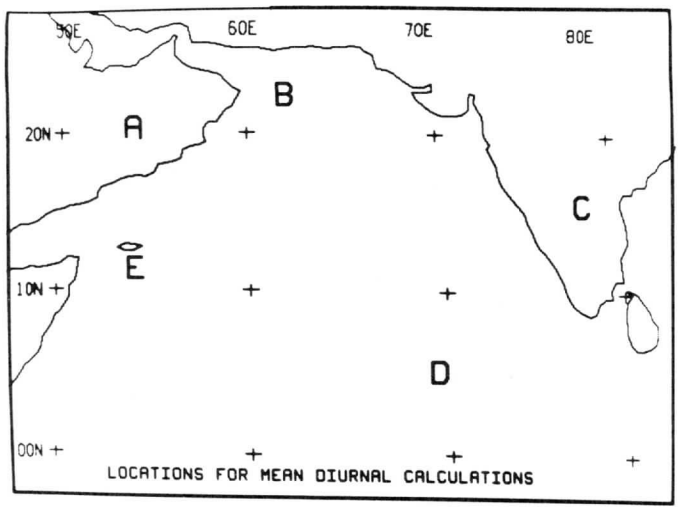

LOCATIONS FOR MEAN DIURNAL CALCULATIONS

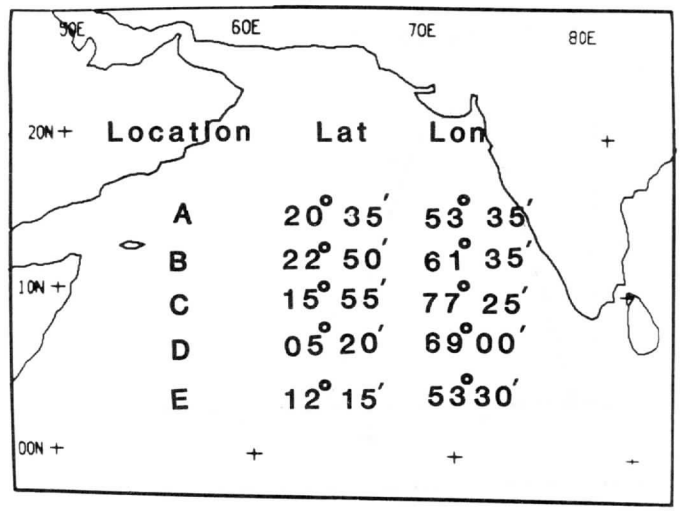

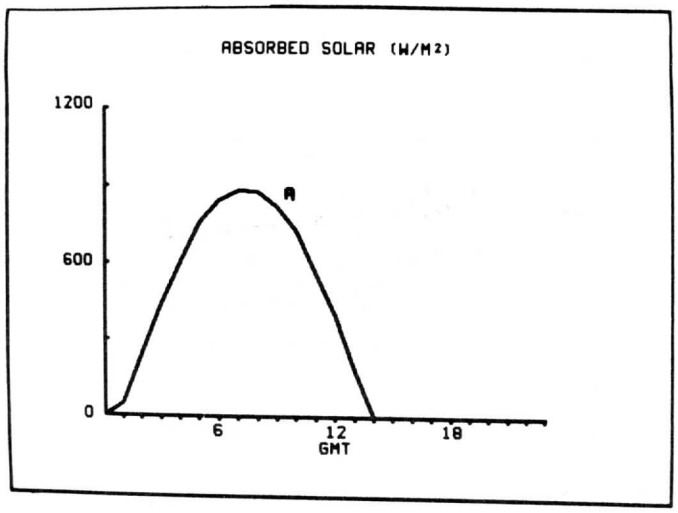
ABSORBED SOLAR (W/M2)
1200
600
0
A
6
12
18
GMT

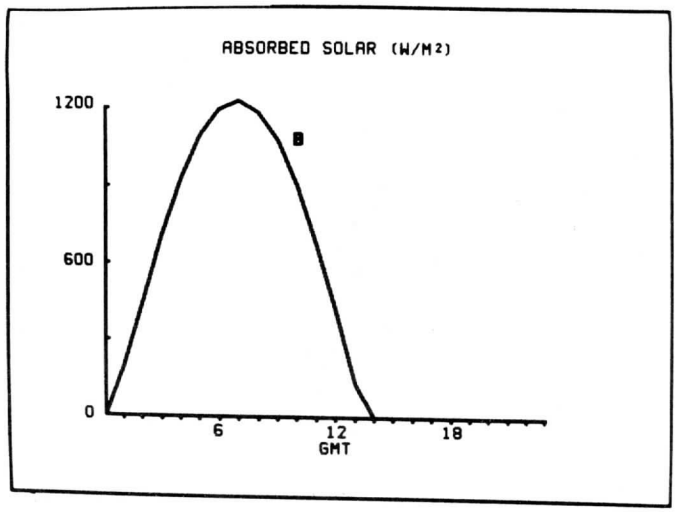
ABSORBED SOLAR (W/M2)
1200
600
0
B
6
12
18
GMT

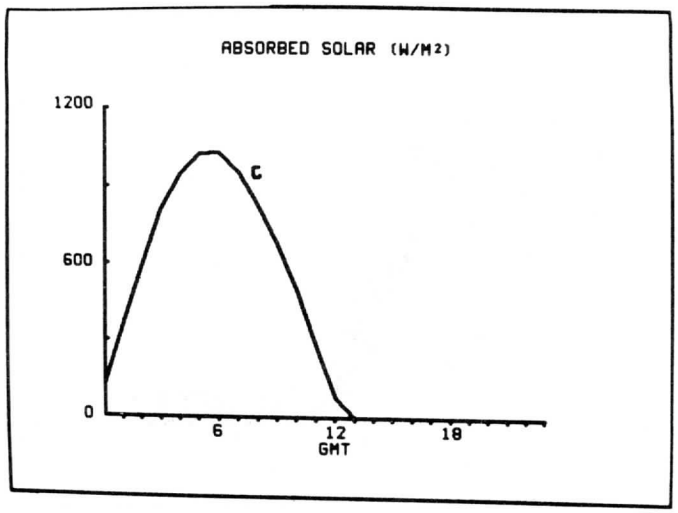
ABSORBED SOLAR (W/M2)
1200
600
0
C
6
12
18
GMT

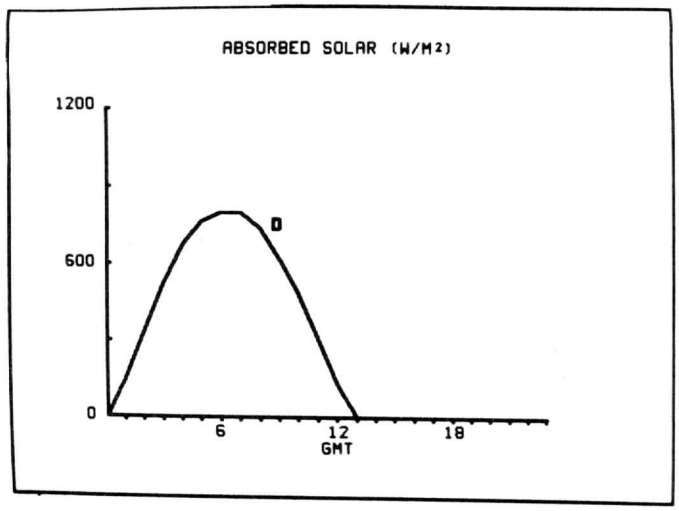
ABSORBED SOLAR (W/M2)
1200
600
0
D
6
12
18
GMT

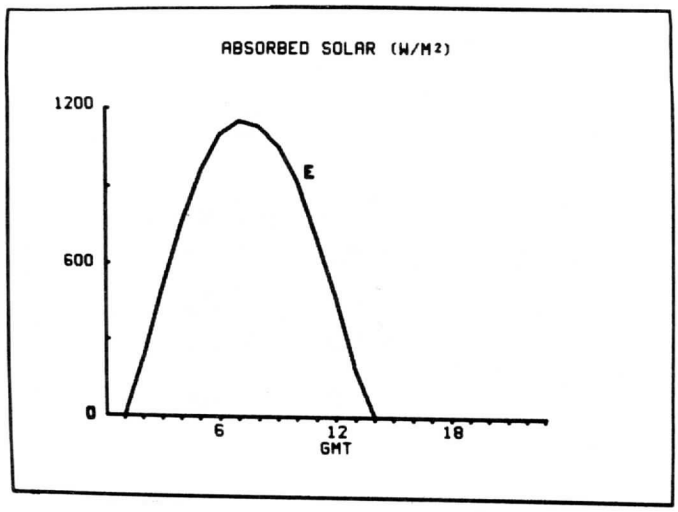
ABSORBED SOLAR (W/M2)
1200
600
0
E
6
12
18
GMT

APPENDIX B

THE REGIONAL CLOUD DISTRIBUTION DURING THE ONSET PHASE OF THE 1979 SUMMER MONSOON BASED ON GOES-I IMAGERY

by

Hassan Virji[1]
Space Science and Engineering Center
and
Leroy D. Herman
NOAA/NESDIS Development Laboratory
University of Wisconsin
1225 West Dayton Street
Madison, Wisconsin 53706

[1]Current affiliation: National Science Fouancation
Washington, DC

1984

Abstract

Regional cloud distribution parameters for the Arabian Sea region during the onset phase of the 1979 summer monsoon have been derived through analysis of bi-dimensional radiance histograms constructed from near local noon visible and infrared imagery from GOES-I. The technique and its limitations are discussed and the derived cloud distribution statistics corresponding to low, medium, high and cumulonimbus categories are presented.

1. Introduction

One objective of the 1979 Monsoon Experiment (MONEX) was to document the pattern of heating fields over main heat source and sink regions for various phases of the summer monsoon. A necessary ingredient for fulfilling this objective is the knowledge of cloud distribution over these regions. The cloud cover associated with the rapidly evolving onset vortex during the monsoon onset phase had a pronounced effect on the magnitude and spatial pattern of the earth and atmosphere radiation balance (Virji et al., 1982). Whereas few systematic conventional observations of cloud type, relative cover, top and bottom pressures were made over the Arabian Sea during the field phase of the summer MONEX, analysis of satellite imagery provides perhaps the best means for determining the regional cloud distribution parameters. This study examines the feasibility of such an approach.

Several investigators have considered the question of cloud classification from satellite imagery (Minnis and Harrison, 1983; Desbois et al., 1982; Smith et al., 1981; Fye, 1978; Reynolds and Vonder Haar, 1977). The usual technique for determination of cloud heights and amounts from satellite imagery involves objective analysis of multi-dimensional radiance histograms extracted from the imagery. The problem is to separate the many radiance classes of the histograms into cloud types, relative cloud cover, and to assign appropriate cloud top and base levels. A simplification generally made is that all observations producing a certain set of reflectance and brightness temperature values are assumed to result from a common cloud height, amount, and opacity. A schematic illustration of the resulting general empirical relationship between infrared and visual gray shades for various cloud and surface types is shown in Fig. 1.

Information on cloud types, depths, and amounts for various cloud modes are deduced from the radiance histograms using as empirical relations those formulated by Reynolds and Vonder Haar (1977) and Mosher (1976). The procedure used here to interpret the radiance histograms into information on cloud parameters has been summarized in Smith (1978). Realistic estimates of the relative accuracies to be expected from such analysis on a regional basis at a given time are 5% in cloud cover and 1 km in cloud top altitude.

During 1979, the GOES-I satellite was positioned at the equator and 58 E longitude. The infrared sensor (0.5-0.9 μm) on board malfunctioned after 21 June 1979, but concurrent radiance observations in the visibe and infrared channels are available for the onset phase of the 1979 summer monsoon and provide an opportunity to use the bi-dimensional histogram technique to deduce cloud distribution parameters during the evolution of the onset vortex over the Arabian Sea region. The purpose of this note is to report on cloud distribution during this period derived from the high resolution GOES-I imagery.

The analysis of bi-dimensional histograms from GOES-I satellite visible and infrared imagery for the onset phase of the 1979 summer monsoon is discussed in the next section. Estimates of the cloud distributions for the 1979 monsoon onset phase analyzed on a two degree grid are presented in Section 3.

2. Data and Analysis

The onset of the 1979 summer monsoon occurred during 11-20 June. For this period, hourly full resolution two channel Visible Infrared Spin-Scan Radiometer (VISSR) imagery for the region bounded by the equator to 28 N and 48 E to 84 E was displayed on the Man-computer Interactive Data Access System Data Access (McIDAS) facility at the University of Wisconsin-Madison. The GOES-I VISSR observations were calibrated using in-situ radiance measurements made by NASA

CV-990 instrumented aircraft in order to obtain representative measurements of reflectance from the satellite data (Smith et al., 1981). The reflectance (r_g) for the GOES-I spectral region 0.5-0.9 m was obtained from the calibration relation:

$$r_g = 0.0000164\ C_g - 0.00077$$

where C_g is the square of the digital brightness count (range 0-255) from the GOES-I visible channel divided by the cosine of the solar zenith angle and the earth-sun distance factor. The brightness temperature was determined from the standard calibration of the GOES-I infrared channel supplied by the National Environmental Satellite, Data, and Information Service (NESDIS). With the exception of poor quality infrared data between 0600-1500 GMT on 13 June 1979 all data at resolution 4 mi. from near local noon hour over the central Arabian Sea (approximately 1830 GMT) was used in the bi-dimensional radiance histogram analysis described below.

For each consecutive two degree square box within the study domain, a two-dimensional histogram of reflectivity and brightness temperature was computed. The four mile resolution data yielded a total of over 900 pixel values in each grid box along the northern edge of the domain and over 1000 pixel values in each grid box along the equator. The histogram values were coded in frequency class intervals of 10% units of reflectivity (visible grayshade) ranging between 0-100% and 10K degrees brightness temperature (infrared grayshade) over the total range 190-330 K. For typical 2 X 2 degree regions around selected grid points within the study domain shown in Fig. 2 (labeled A-F), the corresponding bi-dimensional histograms are displayed in Fig. 3. The clusters over different frequency classes in these examples corresponding to different cloud types conform with the schematic representation of Fig. 1.

The sea surface reflectivity under clear sky conditions (e.g., Fig. 2,

location A), is generally less than 10%, except in regions of specular reflection over the ocean. Land surface under similar conditions has higher reflectivity (greater than 15%) and generally higher brightness temperature (greater than 300 K). Exceptions could be land/sea areas under cloud shadows or where it has recently rained. Topography variations can cause further indeterminancy in the bi-dimensional radiance histogram frequencies. Most of the terrain within the study domain is under 3 km altitude, an exception being the northeastern corner where the permanent snow cover over the Himalayan mountain ranges would be in the high reflectivity and low surface temperature classes of the histogram

The large variability in the histogram frequencies depending upon the variety of surface and atmospheric conditions observed by the satellite is evident in the radiance histograms shown in Fig. 3. In particular, the radiance frequencies are spread over a broad spectrum of histogram classes at those grid locations where several cloud types are present (Fig. 3D). Several relative maxima can be identified in the cases corresponding to a mixture of different cloud types. A reduction of this spread into distinct clusters of observations, assumed to result from similar cloud height, amount, and opacity, can be achieved in several ways. For example gaussian distribution type least square fits have been used (Smith, 1978; Desbois et al., 1982). For the purposes of this preliminary analysis, the following somewhat simpler and faster approach was used.

An iterative search of the entries in the radiance histogram was used to identifies principal and other local maxima. On the first pass, all entries adjacent to and including the principal maxima were summed at the class location of the maxima. The adjacent class entries were then set to zero. In subsequent passes, maxima in descending order were similarly processed. Allowance was made for two or more adjacent classes being equal, in which case the order of adding

the entries into a maxima was decided by the relatively larger sum computed. Ten iterations were generally sufficient to reduce the entries into distinct classes accounting for over 99% of the total population of the histogram. Remaining entries (totaling less than 1%) were merged into the nearest cloud category.

An empirical calibration (table 1) of the bi-dimensional radiance histogram classes was used to assign cloud top and bottom pressure levels and thus appropriate vertical depths to the various cloud types. This calibration procedure, discussed by Mosher (1976) and Peslen, 1980, has been successfully used during the operational cloud tracking program of MONEX to assign pressure heights to the cloud wind data. The essential steps are as follows. First, optical thickness is computed from the observed visible brightness. The cloud depth is then calculated from the relation $T=\sigma pz$, where T is the optical thickness, z is the physical depth, σ is the scattering cross-section typical of the cloud type, and p is the number density of cloud particles. The plane-parallel doubling model of Hansen (1971) is assumed to be valid for the tropical standard atmosphere and the standard drop size distribution given in Deirmendjian (1969) is used. The minimum and maximum levels are set at 950 and 100 mb, and earth's surface temperature value for the calibration is fixed at 305 K. The resulting calibration is summarized in Table 1 where cloud top and bottom pressure levels are shown as a function of reflectivity and cloud top temperature.

The assumptions implicit in the conversion of the histogram categories into cloud depths limit the accuracy of the method. In particular, the use of the plane parallel model ignores the fact that clouds have different shapes. The leakage of radiation from the sides of finite clouds is not taken into consideration and the resulting indeterminacy in the cloud depth estimates can be significant (Suchman et al., 1981). Therefore, in this study the cloud types of

figure 1 are combined into four general categories corresponding to low, medium, high, and cumulonimbus clouds. This combination reduces some of the indeterminacy. The final product of the analysis for the selected cases from Fig. 3 is shown in Table 2. A careful comparison of the derived cloud populations over the region with ground based observations is not possible in view of sparse surface based observations. Few available ship and aircraft observations during this period seem to indicate that the above analysis produces a reasonable depiction of the cloud layers present. A comparison of this analysis with the nephanalysis of the Air Force Global Weather Central is currently in progress.

Note that when only two-dimensional radiance histograms based on visible and infrared imagery are used to compute cloud depths, semi-transparent clouds such as thin cirrus (emissivity $<<1$) can be misclassed due to infrared flux upwelling through the cloud, as is the case at location F (Fig. 2). In this case a small amount of thin cirrus cloud (around 5%) was present and misclassified as cumulus. Use of additional channels (e.g., water vapor channel, 5,7-7.1 m) can help reduce such indeterminacy (Desbois et al., 1982). However, for GOES-I data, we are restricted to availability of observations in only two channels.

An obvious problem in satellite determination of cloud parameters relates to the fact that overcast sky conditions at higher levels mask clouds at lower levels. Though several different cloud types can be recognized in the histogram, it is very difficult to delineate clouds which in reality are vertically stacked. A satisfactory resolution of this difficulty has not yet been achieved. The above deficiencies of the model should be kept in mind during the following discussion of the regional cloud distribution during the onset phase of the summer MONEX.

3. Cloud distribution

During the beginning of the onset of the 1979 summer monsoon, a major cloud cluster formed on 12 June at 8-12 N/75 E within a well defined 700 mb shear line (Sikka and Grossman, 1980). This shear line intensified and moved northward over the next two days. Concurrently, a significant increase in cloudiness occurred around 8-15 N/55-80 E leading to the formation of the onset vortex at 10 N/70 E. A tropical depression formed in the central Arabian Sea during 16-18 June which over the next four days drifted gradually northwestward toward Oman. Well defined cloud clusters developed within the vortex near 19 N/85 E toward the end of the onset phase.

The satellite derived cloud distributions are shown in Figures 4 and 5. for various cloud types at the beginning and end of the onset phase are shown in Figs. 4 and 5. The zonally averaged total cloud cover (Fig. 4) is seen to evolve northward over the Arabian Sea. While no significant change in the total cover occurred around the Horn of Africa (figure 5), the percent cover in the southwestern sector along the region of the low level jet axis underwent at least a two-fold increase during the onset phase. The cloud cover associated with the tropical depression which drifted to Oman by 20 June contributed to the 100% increase in the cover over this region of the Saudi Arabian peninsula. In contrast, in the region of the onset vortex, the total cover increased by at least two-fold. Concurrently, the total cloud cover over central India also increased two-fold, while southward over Sri Lanka, the total cover remained the same as at the beginning of the onset phase.

The breakdown of the total cover into various cloud types at the beginning and the end of the onset phase is also shown in Fig. 5. The northward transition of various cloud types as the onset phase progressed is clearly evident. In particular, a substantial increase in low level cloudiness occurs

in the western Arabian Sea in the region of the mean low level jet axis. Elsewhere, the signal in the low level cloudiness may have been obscured by increases in cloudiness at higher levels. The maxima in middle level cloudiness occur primarily along the boundaries of the regions of deep convection. The high level cloudiness represents the cirrus outflow from the cumulonimbus clouds and is maximized towards the end of the onset phase over the entire region consistent with the increase in the convective activity as the onset progressed northward. Perhaps the most interesting distribution is that of cumulonimbus clouds. At the beginning of the onset phase over the Arabian Sea (June 12), no two degree square region contains 100% coverage of the cumulonimbus-type. In contrast, at the end of the onset (June 20), 100% coverage occurs at a number of grid locations in the two convectively active regions of the onset vortex and the tropical depression.

The evolution of these convective regions is easily evident on a composite plot of the regions where significant cumulonimbus occurrence takes place (Fig. 6). Here, maximum values of cumulonimbus coverage taken from daily analyses at local noon have been replotted in sequence for each of the ten days of the onset phase. Besides the northward transition and increase in the cumulonimbus activity, two major regions of intense convection (Cb clusters) are evident from the beginning of the onset phase. The western Cb cluster was easily tracked on a sequence of images of the last five days of the onset as it developed into a tropical depression which drifted toward the coast of Oman. Considering the high-frequency pulsations in the cumulonimbus activity (more frequent than once a day), the depiction of cumulonimbus clusters in the eastern Arabian Sea are not reflective of continuous transitions, but generally represent descrete development of the intense convective activity progressively northward.

4. Further Remarks

The caliberated data from GOES-1 satellite during the 1979 monsoon onset period has been used to specify evolution of cloudiness distribution. The derived distribution has further been utilized together with thermodynamic state parameters to estimate tropospheric radiative heating distribution, a report on which is under preparation. The 2X2 degree cloudiness distribution parameters described for the period 11-20 June 1979 are available on computer compatible tapes at the Space Science and Engineering Center at the University of Wisconsin-Madison.

Acknowledgments

Drs. Fred Mosher and Paul Menzel's contribution in developing the caliberation (Table 1) was indispensable in this analyses. The work was funded by the National Science Foundation under Grant ATM 8205386.

5. References

Chou, M.-D., and A. Arking, 1980: Computation of infrared cooling rates in the water vapor bonds. J. Atmos. Sci., 37, 855-867.

Deirmendjian, D., 1969: Electromagnetic Scattering on Spherical Polydispersions. American Elsevier Publishing Company, Inc., New York, 290 pp.

Desbois, M., G. Seze, and G. Szejwach, 1982: Automatic classification of clouds on METEOSAT imagery: Application to high level clouds. J. Applied Meteor., 21, 401-412.

Fye, F. K., 1978: The AFGWC automated cloud analysis model. AFGWC Technical Memorandum 78-002, HQ AFGWC, Offutt Air Force Base, Nebraska, 97 pp.

Hansen, J. E., 1971: Multiple scattering of polarized light in planetary atmospheres, Part I. The doubling method. J. Atmos. Sci., 28, 120-125.

Minnis, P., and E. F. Harrison, 1983: Diurnal variability of regional cloud and surface radiative parameters derived from GOES data. J. Climate & Appl. Met., in press.

Mosher, F. R., 1976: Cloud height determination. Proceedings of the Symposium on Meteorological Observations from Space: Their Contribution to the First GARP Global Experiment, Proceedings of the 19th COSPAR Meeting, Philadelphia, Published by NCAR, Boulder, Colorado, pp. 201-204.

Peslen, C. A., 1980 Short-Interval SMS Wind Vector Determination for a Seven Local Storm Area. Mon. Wea. Rev.. 108, 1407-1418.

Reynolds, D. W., and T. H. Vonder Haar, 1977: A bispectral method for cloud parameter determination. Mon. Wea. Rev., 105, 446-457.

Sikka, D. R. and B. Grossman, 1980: Summer MONEX chronological Weather Summary. Published by the International Monex Management Center, New Dehli, India, 49 pp.

Smith, W. L., 1978: Status and plans for a cloud climatology programme. JOC Study Conference on the Parameterization of Extended Clouds and Radiation for Climate Models, September 27-October 9, 1978, Oxford, England. Published by the W.M.O.

Smith, W. L., L. D. Herman, A.J. Schreiner, H. W. Howell and W. P. Menzel, 1981: Radiation budget characteristics of the onset of the summer monsoon. Proc. of the International Conference on Early Results of FGGE and large-scale aspects of its monsoon experiments, Tallahassee, FL. Published by W. M. O., pp. 6-16 to 6-26.

Suchman, D., B. Auvine, R. Lord, D. Martin, F. Mosher and D. A. Santek, 1981: Improvements in the use of meteorological satellite data: Some techniques developed for GATE. Technical Report, Space Sci & Eng Ctr, University of Wisconsin-Madison, pp 1-24.

Virji, H., W. L. Smith, A. J. Schreiner, and L. D. Herman, 1982: Earth-atmosphere radiation balance from geostationary satellite data for the summer monsoon onset region. An Atlas, available from the Space Sci & Eng Ctr., University of Wisconsin-Madison, 254 pp.

Figure Captions

Fig. 1: A schematic illustration of the general emperical relationship between infrared and visual grayshades corresponding to various cloud and surface types (adapted from Fye, 1978)

Fig. 2: GOES-1 visible and infrared satellite photographs over the Arabian Sea for 1000 GMT, June 20, 1979. Locations A-F refer to the bi-dimensional histograms shown in Fig. 3.

Fig. 3: Histograms of temperature (degrees Kelvin) versus reflectivity (percent) corresponding to the locations A-F identified in Fig. 2.

Fig. 4: Zonally averaged total cloud cover along selected latitude bands in the Arabian Sea region during the onset phase of the monsoon.

Fig. 5: Breakdown of cloud cover into various types for June 12 and June 20, 1979.

Fig. 6: Evolution of principal cumulonimbus clusters during the monsoon onset. The center of maximum cumulonimbus cover is shown as a star or a circle. The coded numbers (xx-yy) correspond to the percent x 10 cover (xx), and date (yy) during June 1979.

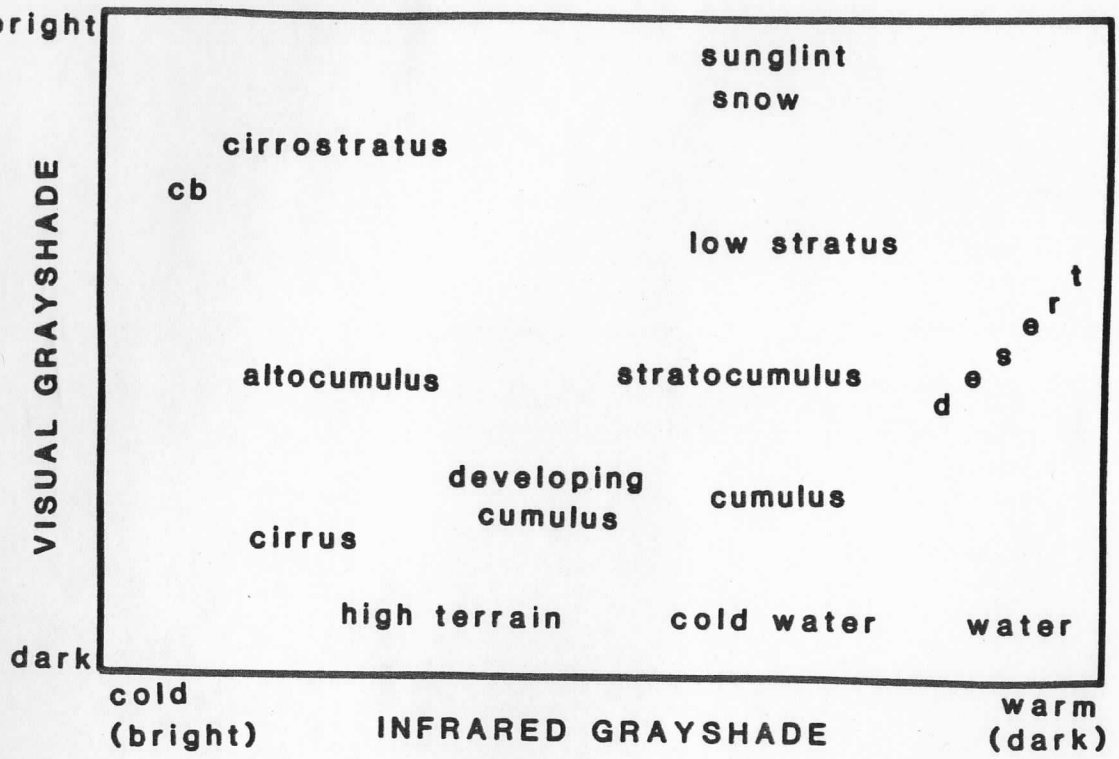
bright
dark
VISUAL GRAYSHADE
sunglint
snow
cirrostratus
cb
low stratus
desert
altocumulus
stratocumulus
developing cumulus
cumulus
cirrus
high terrain
cold water
water
cold (bright)
INFRARED GRAYSHADE
warm (dark)

FIG 1

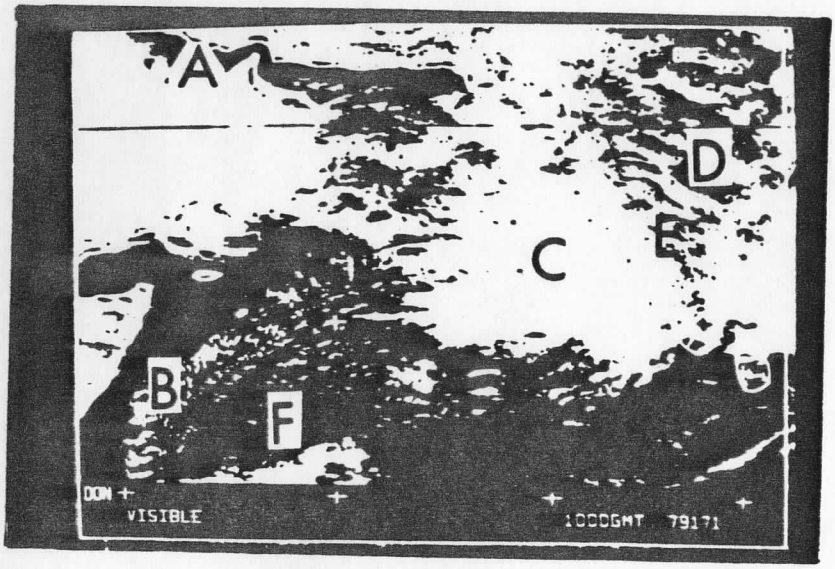
A
D
C
B
F
VISIBLE
1000GMT 79171

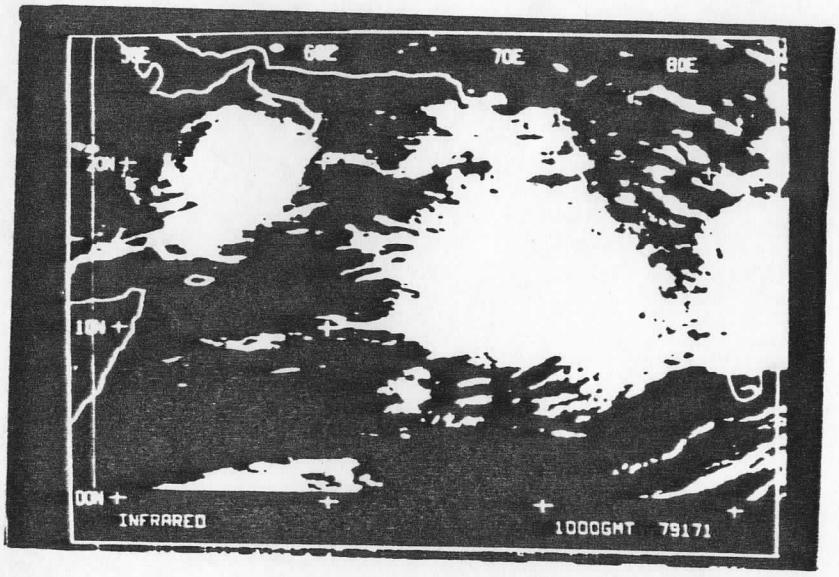
60E
70E
80E
INFRARED
1000GMT 79171

FIG 2

A LATITUDE = 26 LONGITUDE = 54

REFLECTIVITY	190	200	210	220	230	240	250	260	270	280	290	300	310	320	330
90 -100.0	0	0	0	0	0	0	0	0	0	0	0	0	0	0	0
80 - 89.9	0	0	0	0	0	0	0	0	0	0	0	0	0	0	0
70 - 79.9	0	0	0	0	0	0	0	0	0	0	0	0	0	0	0
60 - 69.9	0	0	0	0	0	0	0	0	0	0	0	0	0	0	0
50 - 59.9	0	0	0	0	0	0	0	0	0	0	0	0	1	0	0
40 - 49.9	0	0	0	0	0	0	0	0	0	0	0	0	2	0	0
30 - 39.9	0	0	0	0	0	0	0	0	0	0	0	1	5	0	0
20 - 29.9	0	0	0	0	0	0	0	0	0	0	0	4	31	0	0
10 - 19.9	0	0	0	0	0	0	0	0	0	0	0	10	3	0	0
0 - 9.9	0	0	0	0	0	0	0	0	0	0	0	861	0	0	0

TEMPERATURE

B LATITUDE = 4 LONGITUDE = 52

REFLECTIVITY	190	200	210	220	230	240	250	260	270	280	290	300	310	320	330
90 -100.0	0	0	0	0	0	0	0	0	0	0	0	0	0	0	0
80 - 89.9	0	0	0	0	0	0	0	0	0	0	1	0	0	0	0
70 - 79.9	0	0	0	0	0	0	0	0	0	0	10	0	0	0	0
60 - 69.9	0	0	0	0	0	0	0	0	0	0	17	0	0	0	0
50 - 59.9	0	0	0	0	0	0	0	0	0	1	35	0	0	0	0
40 - 49.9	0	0	0	0	0	0	0	0	0	0	49	0	0	0	0
30 - 39.9	0	0	0	0	0	0	0	0	0	0	72	0	0	0	0
20 - 29.9	0	0	0	0	0	0	0	0	0	0	132	0	0	0	0
10 - 19.9	0	0	0	0	0	0	0	0	0	0	289	0	0	0	0
0 - 9.9	0	0	0	0	0	0	0	0	0	0	559	3	0	0	0

TEMPERATURE

C LATITUDE = 14 LONGITUDE = 70

REFLECTIVITY	190	200	210	220	230	240	250	260	270	280	290	300	310	320	330
90 -100.0	3	22	31	0	0	0	0	0	0	0	0	0	0	0	0
80 - 89.9	4	170	221	36	0	0	0	0	0	0	0	0	0	0	0
70 - 79.9	0	55	239	84	2	0	0	0	0	0	0	0	0	0	0
60 - 69.9	0	1	38	59	3	0	0	0	0	0	0	0	0	0	0
50 - 59.9	0	0	13	37	10	0	0	0	0	0	0	0	0	0	0
40 - 49.9	0	0	1	0	0	0	0	0	0	0	0	0	0	0	0
30 - 39.9	0	0	0	0	0	2	0	0	0	0	0	0	0	0	0
20 - 29.9	0	0	0	0	0	1	0	0	0	0	0	0	0	0	0
10 - 19.9	0	0	0	0	0	0	0	0	0	0	0	0	0	0	0
0 - 9.9	0	0	0	0	0	0	0	0	0	0	0	0	0	0	0

TEMPERATURE

D LATITUDE = 20 LONGITUDE = 80

REFLECTIVITY	190	200	210	220	230	240	250	260	270	280	290	300	310	320	330
90 -100.0	0	4	5	1	2	1	0	0	0	0	0	0	0	0	0
80 - 89.9	7	39	16	4	2	1	0	0	1	0	0	0	0	0	0
70 - 79.9	6	30	14	11	6	0	0	1	2	2	2	0	0	0	0
60 - 69.9	0	14	10	8	7	7	3	0	0	0	1	0	0	0	0
50 - 59.9	0	1	8	2	3	4	5	1	1	2	4	0	0	0	0
40 - 49.9	0	0	2	0	3	3	4	4	2	4	5	1	0	0	0
30 - 39.9	0	0	0	4	4	5	7	8	7	10	15	2	0	0	0
20 - 29.9	0	0	0	0	1	6	10	10	10	14	43	17	0	0	0
10 - 19.9	0	0	0	0	0	0	1	1	11	19	140	250	2	0	0
0 - 9.9	0	0	0	0	0	0	0	0	0	2	3	1	0	0	0

TEMPERATURE

E LATITUDE = 14 LONGITUDE = 76

REFLECTIVITY	190	200	210	220	230	240	250	260	270	280	290	300	310	320	330
90 -100.0	0	0	0	0	0	0	0	0	0	0	0	0	0	0	0
80 - 89.9	0	0	0	0	0	0	1	5	3	0	0	0	0	0	0
70 - 79.9	0	0	0	0	0	0	8	15	4	2	0	0	0	0	0
60 - 69.9	0	0	0	0	0	0	9	105	49	8	0	0	0	0	0
50 - 59.9	0	0	0	0	0	0	14	116	97	28	0	0	0	0	0
40 - 49.9	0	0	0	0	0	0	19	38	59	22	0	0	0	0	0
30 - 39.9	0	0	0	0	0	0	17	35	79	45	5	0	0	0	0
20 - 29.9	0	0	0	0	0	0	2	7	41	69	33	0	0	0	0
10 - 19.9	0	0	0	0	0	0	0	0	4	20	16	0	0	0	0
0 - 9.9	0	0	0	0	0	0	0	0	0	0	0	0	0	0	0

TEMPERATURE

F LATITUDE = 4 LONGITUDE = 58

REFLECTIVITY	190	200	210	220	230	240	250	260	270	280	290	300	310	320	330
90 -100.0	0	0	0	0	0	0	0	0	0	0	0	0	0	0	0
80 - 89.9	0	0	0	0	0	0	0	0	0	0	0	0	0	0	0
70 - 79.9	0	0	0	0	0	0	0	0	0	0	1	0	0	0	0
60 - 69.9	0	0	0	0	0	0	0	0	0	0	7	0	0	0	0
50 - 59.9	0	0	0	0	0	0	0	0	0	1	2	0	0	0	0
40 - 49.9	0	0	0	0	0	0	0	0	0	2	16	0	0	0	0
30 - 39.9	0	0	0	0	0	0	0	0	0	3	25	0	0	0	0
20 - 29.9	0	0	0	0	0	0	0	0	0	7	42	0	0	0	0
10 - 19.9	0	0	0	0	0	0	0	0	0	6	145	0	0	0	0
0 - 9.9	0	0	0	0	0	0	0	0	0	2	881	28	0	0	0

TEMPERATURE

Fig 3.

TABLE 1

AN EMPIRICAL CALIBRATION OF BI-DIMENSIONAL RADIANCE HISTOGRAM CLASSES INTO CLOUD TOP AND BOTTOM PRESSURE LEVELS (AFTER MOSHER, 1976)

CLOUD TOP PRESSURE: (mb)	107	137	174	220	274	336	412	498	608	738	918
REFLECTIVITY (%)	CLOUD BOTTOM PRESSURE (mb)										
95	950	950	950	950	950	950	950	950	950	950	950
85	950	950	950	950	950	950	950	950	950	950	950
75	890	911	934	950	950	950	950	950	950	950	950
65	392	433	474	526	580	637	702	766	861	950	950
55	243	283	330	379	438	502	570	648	757	909	950
45	191	227	271	322	378	441	515	595	704	848	950
35	157	192	233	283	338	401	476	558	671	809	950
25	135	169	206	255	311	375	452	538	646	781	950
15	114	146	185	230	285	345	423	511	615	645	928
CLOUD TOP TEMPERATURE (deg. K)	195	205	215	225	235	245	255	265	275	285	295

TABLE 2

CLOUD DISTRIBUTION AT THE SELECTED LOCATIONS

SHOWN IN FIGS. 2 AND 3

CLOUD TYPE	% CLOUD COVER AT LOCATIONS					
	A	B	C	D	E	F
LOW (950-700 mb)	0	52	0	30	15	23
MIDDLE (699-400 mb)	0	0	0	12	85	0
HIGH (399-100 mb)	0	0	6	8	0	0
CUMULONIMBUS (950-100 mb)	0	0	94	19	0	0

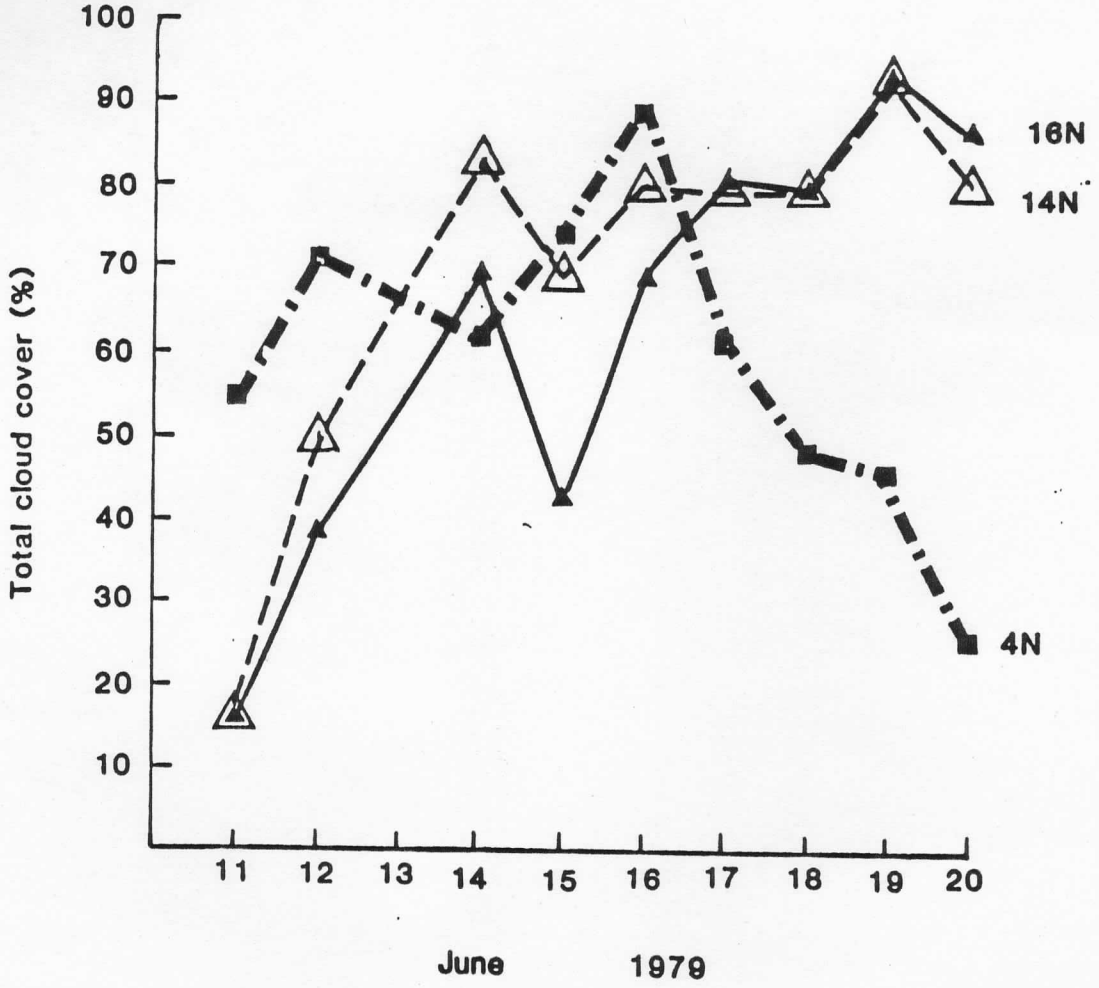
100
90
80
70
60
50
40
30
20
10
Total cloud cover (%)
16N
14N
4N
11
12
13
14
15
16
17
18
19
20
June
1979

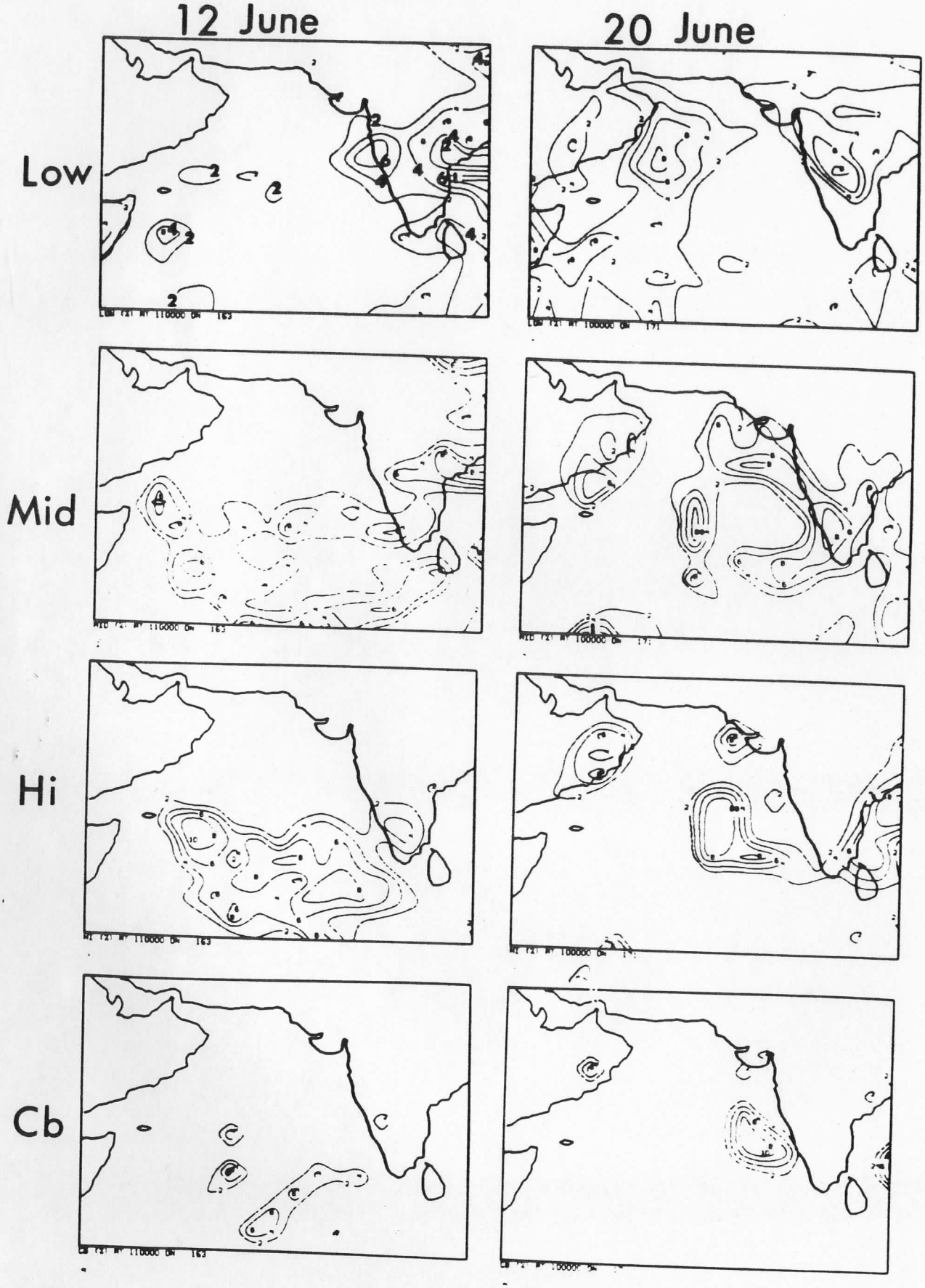

Fig 5

[% x 10]

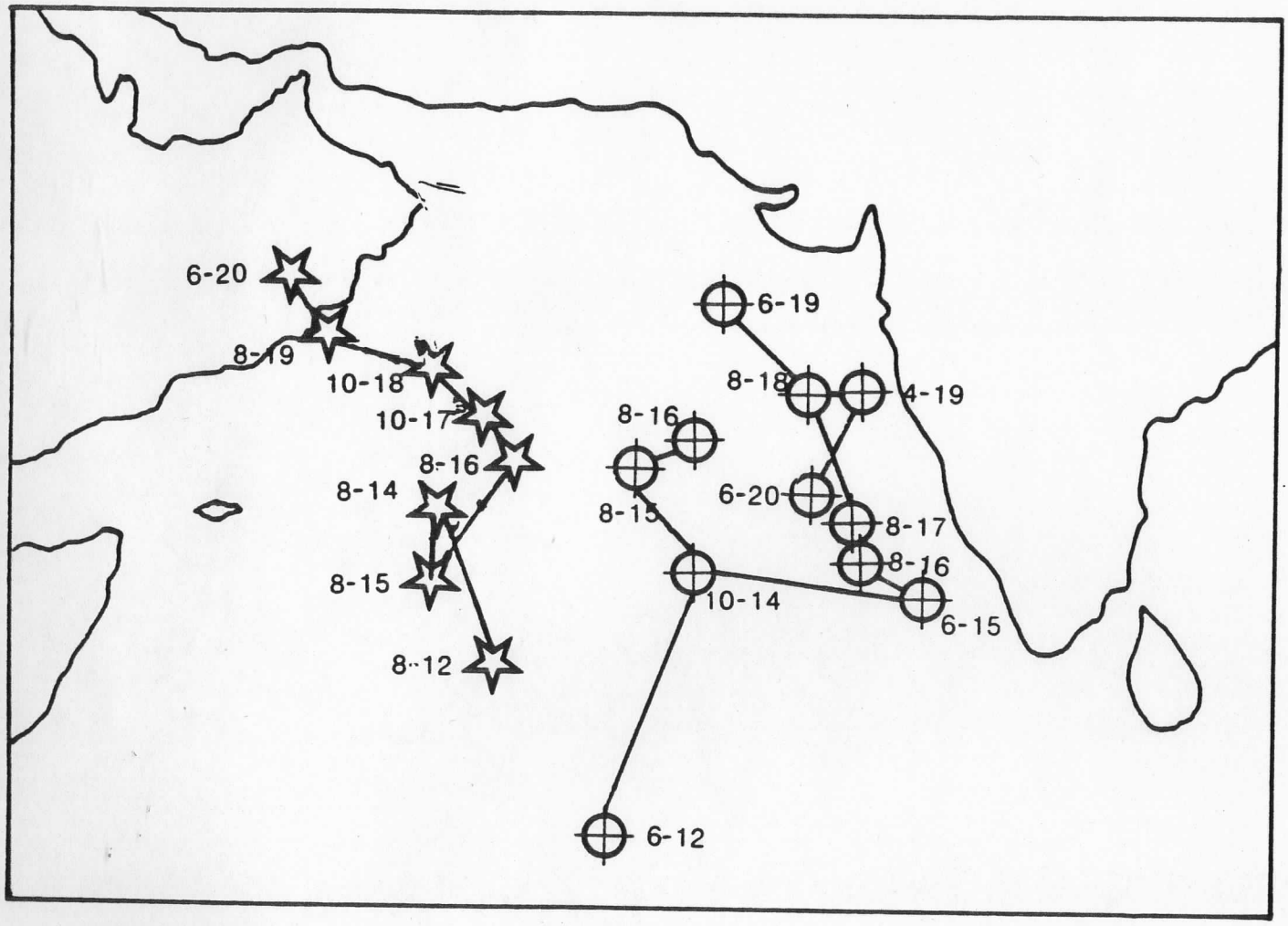
6-20
8-19
10-18
10-17
8-16
8-14
8-15
8-12
6-19
8-18
4-19
8-16
8-15
6-20
8-17
8-16
10-14
6-15
6-12

Fig 6

APPENDIX C

SATELLITE DERIVED EARTH AND ATMOSPHERE ENERGY BALANCE COMPONENTS DURING THE SUMMER MONEX

H. Virji[1], W.L. Smith[2], A.J. Schreiner[1], L. Herman[2], and P. Menzel[1]

[1]Space Science and Engineering Center and
and [2]Ness Development Laboratory,
University of Wisconsin-Madison, U.S.A.

The paucity of conventionally observed meteorological data over the monsoon region has been a major factor in the lack of understanding of the evolution of the earth and atmosphere energy balance over key monsoonal heat source-sink areas. The geostationary and polar orbiting satellite measurements obtained over the MONEX region during 1979 offer a unique opportunity to study the evolution of the energy budget over these areas. This report describes an ongoing research effort aimed at the determination of the large scale components of the earth and atmosphere energy balance using satellite measurements as the primary data.

All basic data is derived from full resolution GOES (Indian Ocean) VISSR imagery and TIROS-N sounder observations. Appropriate algorithms developed for use with the satellite measurements are used to derive high resolution fields of the components of radiation and heat budget for the onset, established, and break phases of the 1979 summer MONEX. The satellite derived estimates are carefully evaluated against available conventional surface based and dropsonde measurements in order to ensure reliable definition of the heating functions at the earth's surface and within the atmosphere.

The framework for the determination of the various energy balance components using satellite measurements is summarized in Table 1. The components considered as significant include: (a) at the top of the atmosphere, outgoing longwave flux, absorbed solar, and net radiation; (b) within the atmosphere, heating by shortwave and longwave radiative processes, dry convection, shallow and deep moist convection, sensible and latent heat fluxes from the earth's surface, and large-scale condensation; and (c) at the earth's surface, net radiation, fluxes of latent and sensible heat, and conductive heat fluxes into the surface.

Most of the effort to date has been devoted to (i) careful calibration of the GOES satellite VISSR measurements with in-situ MSR measurements obtained from CV-990 aircraft flights during the onset period of 1979 summer monsoon, (ii) determination at high temporal and spatial resolution of the components of the top radiation balance over the Arabian Sea and its littoral during the onset phase, and (iii) development of appropriate algorithms to retrieve profile soundings of temperature and moisture for the above region and to compute the atmospheric and surface heating components during the onset phase.

The results of the top radiation balance analysis from calibrated VISSR data are described in Smith et al., 1981. The following discussion is restricted to only a few examples of the energy budget

components derived for 1000 GMT on 20 June 1979. These illustrate that the satellite derived estimates provide a physically consistent description of the earth and atmosphere energy balance over the Arabian Sea and its littoral.

An analysis of the daily outgoing longwave flux at the top of the atmosphere for 20 June, 1979 during the onset period is shown in Fig. A. Satellite imagery for this day (not shown) indicates that the tropical storm associated with the developing onset vortex had moved onto coast of Oman and was dissipating, while the convective activity over the deepening onset vortex low was centered around 30 N, 70 E, just off the southwestern coast of India. The analysis of outgoing longwave flux clearly reflects the synoptic situation, with low values of less than 150 W m^{-2} over the areas of major cloudiness associated with the onset vortex. High values of outgoing longwave flux (values exceeding 300 W m^{-2}) exist over the Saudi Arabian desert.

While only one example of an energy balance component at the top is shown, all components listed in Table 1 have been computed at hourly intervals on a 2°x2° grid. An atlas of this unique data set for the onset phase is under preparation.

Examples of precipitable water (W) in the atmospheric column and vertically integrated total horizontal flux divergence of moist static energy, are shown in Figs. B, and C, D, E, respectively. Precipitable water and moist static energy have been calculated at mandatory levels from TIROS-N sounder data and horizontal divergence fields have been derived from GOES cloud winds obtained by Young et al., 1980.

The precipitable water content pattern (Fig. B) shows good correlation with the ambient low level flow pattern. A maximum of W is located along the axis of the low level Somali jet. Maxima of total horizontal flux divergence of moist static energy integrated through the atmospheric column occur over Saudi Arabia and the western coast of India (Fig. C). This heating component for a two layer atmosphere (surface-500 mb shown in Fig. D and 499-100 mb shown in Fig. E) clearly shows that the maxima over Saudi Arabia is confined to the lower tropospheric layer while that over western coast of India is located primarily in the upper tropospheric layer. In contrast, horizontal heat flux convergence is evident in the lower layer over the eastern Arabian Sea and in the upper layer over the Saudi Arabian desert. Considering the ambient tropospheric flow patterns in the lower and upper layers, a direct coupling between the heat fluxes from the developing heat low over Saudi Arabia and the intense monsoon onset vortex near the Indian coast is indicated. This result is in agreement with other studies of the interaction between the Saudi Arabian heat low and the monsoon onset-type vortex over eastern Arabian Sea which were based on sparse conventional surface-based data (see for example, Ramage, 1966). A detailed analysis of the evolution of this tropospheric link between the above key heat source regions for the summer MONEX period is being carried out using the satellite data.

Radiation heating is another important tropospheric energy balance component. Preliminary estimates of the tropospheric cooling rates due to IR irradiance for the 20 June 1979 conditions (clear over Saudi Arabia and India, partly cloudy over the Arabian Sea) for typical 2°x2° grid box are plotted in Fig. G. These cooling rates were calculated using the algorithms due to Chou and Arking (1980, 81) together with temperature, humidity profiles obtained from TIROS-N data and cloud distribution for the Arabian Sea case derived from an analysis of VISSR imagery. In the case shown in Fig. G, complete cloud cover over Arabian Sea between 800-900mb and 200-300mb layers was prescribed. The resulting profiles are comparable to those obtained from analyses of ship based observations obtained during the summer MONEX by the Soviet ship network.

Examples of surface radiative heating fields are shown in Figs. F and I. TIROS-N satellite derived water vapor profiles and VISSR based estimates of cloudiness and surface temperature have been utilized to determine the outgoing longwave flux component shown in Fig. F. As expected, the values of this radiative component are relatively uniform and lower over the Arabian Sea compared to the surrounding land area. Highest values of outgoing longwave flux occur over the Saudi Arabian desert and over northwestern India.

The net shortwave radiation at the surface is calculated using the algorithm developed by Gautier et al. (1980). This simple physical model in which Rayleigh scattering is taken into account, requires specification of water vapor absorption in cloudy and clear regions. TIROS-N sounder data were used for this purpose. In addition, the surface albedo estimates shown in Fig. H were derived from VISSR imagery for local noon conditions using minimum brightness normalization technique. Low surface albedo values of less than 3% are found over most of the Arabian Sea. A localized region of about 10% albedo in central Arabian Sea is due to sunglint effect which is not completely removed by the minimum brightness normalization method. High surface albedo values of 25-40% are found over the Saudi Arabian desert. These satellite derived estimates are in fair agreement with numerous surface based measurements.

An example of a calculation of the daily net shortwave radiation at the surface based upon the algorithm due to Gautier et al. (1980) using the surface albedo values of Fig. H and water vapor profiles from TIROS-N sounder data is shown in Fig. I. Low values (less than 90 wm^{-2}) occur under the cloudy zones in the onset vortex region. Over clear oceanic regions in northern Arabian Sea, the net shortwave radiation at the surface averages about 330 wm^{-2} which represents an attenuation of about 70 wm^{-2} (17%) by clear atmosphere from the absorbed solar radiation of about 400 wm^{-2} at the top of the atmosphere. This value of attenuation due to clear air column is reasonable in view of numerous ground based and aircraft measurements. High values of net shortwave heating of the surface also occur over the desert regions of Saudi Arabia, as would be expected.

While some of the analyses presented above ~~is~~ are preliminary and the techniques for determining various heating functions are undergoing

refinement, it is evident from the foregoing that the satellite derived estimates yield a physically consistent description of the large scale components of the earth and atmosphere energy balance over the Arabian Sea and its littoral.

Acknowledgment

This research was supported by the National Science Foundation, under Grant ATM-801-4892.

References

Chou, M-D., and A. Arking, 1980: Computation of infrared cooling rates in the water vapor bands. J. Atmos. Sci., 37, 855-867.

Chou, M-D., and A. Arking, 1981: An efficient method for computing the absorption of solar radiation by water vapor. J. Atmos. Sci. 38, 798-807.

Gautier, C., G. Diak, and S. Messe, 1980: A simple physical model to estimate incident solar radiation at the surface from GOES satellite data. J. Appl. Met., 19, 1005-1012.

Ramage, C.S., 1966: The summer atmospheric circulation over the Arabian Sea. J. Atmos. Sci., 23, 144-150.

Smith, W.L., L.D. Herman, A. Schreiner, H.B. Howell, and P. Menzel, 1981: Radiation budget characteristics of the onset of the summer monsoon. Proc. of the international conference on early results of FGGE and large-scale aspects of its monsoon experiments, Tallahassee, FL. (ed. J.A. Young), pp. 6-16 through 6-26.

Young, J.A., H. Virji, D. Wylie, and C. Lo, 1980: Summer monsoon windsets from geostationary satellite data (an atlas). Space Science and Engineering Center and the Dept. of Meteor., U of Wisconsin-Madison, 127 pp.

Table 1

SATELLITE DERIVED EARTH AND ATMOSPHERE ENERGY BALANCE COMPONENTS DURING THE SUMMER MONEX

	DATA	PARAMETERS	RESOLUTION AND PERIOD
1. EARTH-ATMOSPHERE (TOP) RADIATION BUDGET $F_{N,top} = F_{A,top} - F_{L,top}$ (via Smith et al, 1981)	MSR calibrated GOES I.O. VISSR imagery at 8km resolution at hourly intervals	a) Outgoing Longwave flux ($F_{L,top}$) b) Absorbed Solar radiation ($F_{A,top}$) c) Net Radiation ($F_{N,top}$)	Onset of 1979 summer monsoon (10-20 June) over the Arabian Sea and its littoral.
2. HEATING IN THE ATMOSPHERE $\int \frac{\partial Q}{\partial t} \frac{dp}{g} + \int (\nabla \cdot \nabla Q) \frac{dp}{g} + \int \omega \frac{\partial Q}{\partial p} \frac{dp}{g} = F_{SW} + F_{LW} + LP + LE_o + Q_o$ id $Q = CpT + gz + Lq$	TIROS-N sounder and GOES I.O. cloud winds ($\vec{V}$) at 2°x 2° spatial resolution, 1000 GMT (Young, et al, 1980) GOES I.O. VISSR/ derived relative cloud cover	a) $T, T_d, \Delta z$ (via Smith & Woolf, 1981) b) C_pT, gz, Lq, and Q c) for 2 or 3 layer atmosphere: (i) $\int (\nabla \cdot \vec{V}) Q \frac{dp}{g}$ (ii) $\int (\nabla Q \cdot \vec{V}) \frac{dp}{g}$ d) F_{SW}, F_{LW} (via Chou-Arking, 1980, 1981)	Mandatory levels, 2°x 2° 1000 GMT, same period as above.
3. HEATING AT THE EARTH SURFACE $F_{N,sfc} = (F_{N,SW} + F_{N,LW})_{sfc} + LE_o + Q_o + S_o$	GOES I.O. VISSR image at 8 km resolution at hourly intervals and TIROS-N temperature humidity soundings and T_{skin}	a) Albedo b) $F_{N,SW}$ (via Gautier et al., 1980) c) $F_{N,LW}$ (via TIROS-N T_{skin} and Chou-Arking) d) $F_{N,sfc}$	2°x 2° 2°x 2°, hourly (0500 - 1200 GMT) 2°x 2°, 1000 GMT

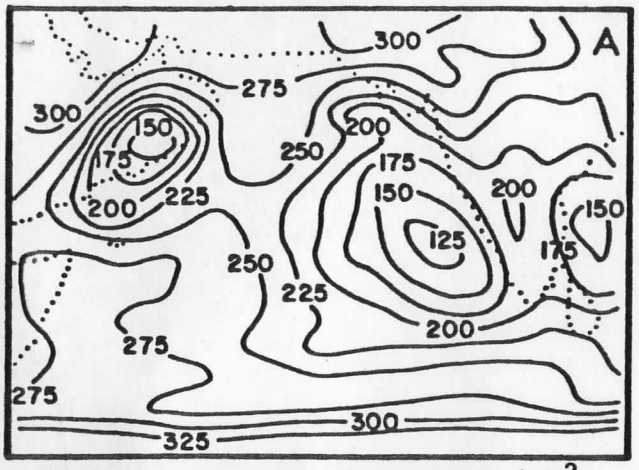

OUTGOING LONGWAVE FLUX (TOP) wm^{-2}

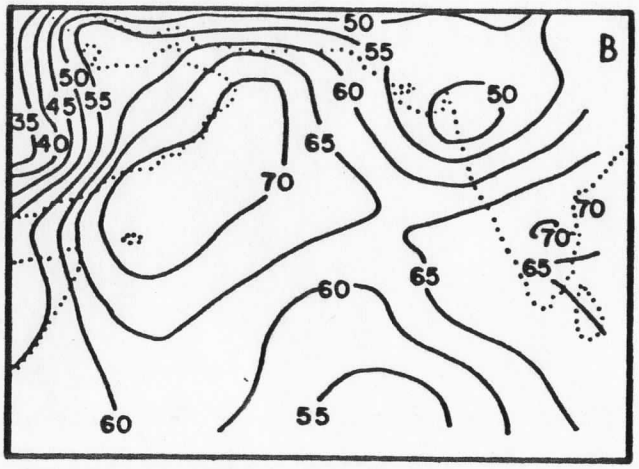

PRECIPITABLE WATER mm

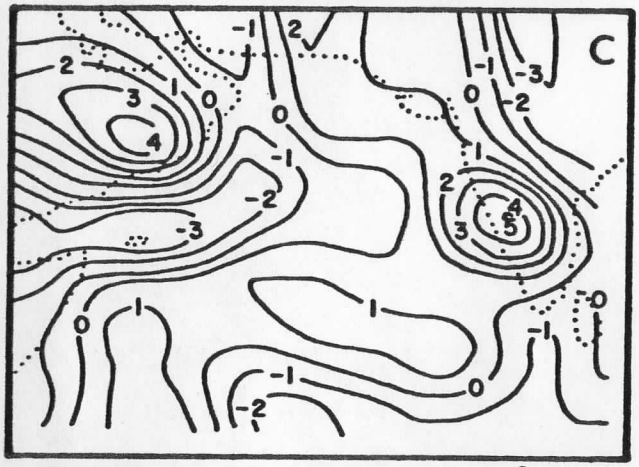

HORIZONTAL FLUX DIV. OF Q (sfc-100 mb)

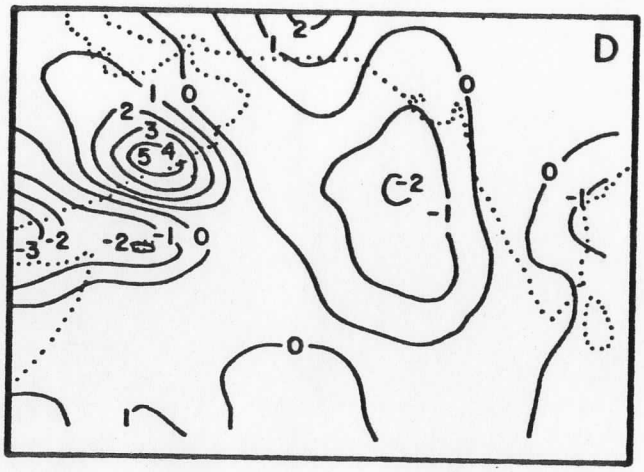

HORIZONTAL FLUX DIV. OF Q (sfc-500mb)

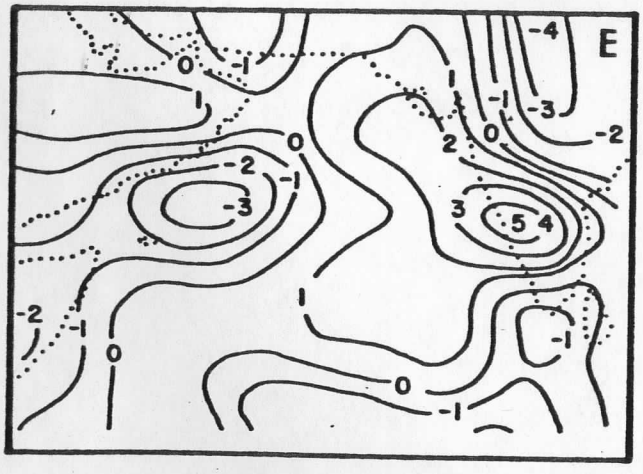

HORIZONTAL FLUX DIV. OF Q (499-100 mb)

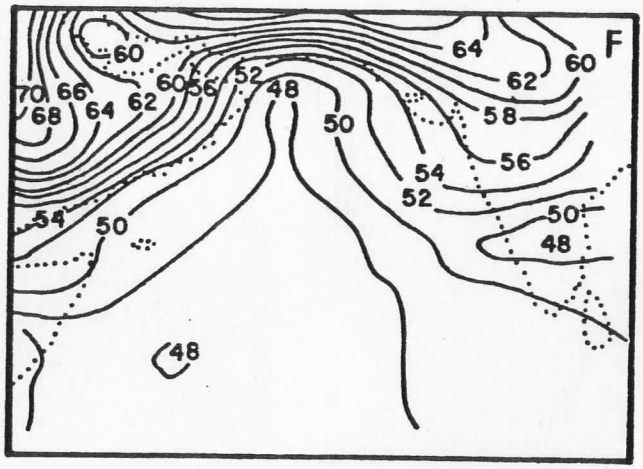

OUTGOING LONGWAVE FLUX (sfc) wm^{-2}

Figure A: Outgoing longwave flux (top) in wm^{-2}, Figure B: Precipitable water in mm
Figure C: Horizontal flux divergence of moist static energy in wm^{-2},
Figure D: same as in C except for sfc-500 mb, Figure E: same as in C except for 499-100 mb, Figure F: Outgoing longwave flux (sfc) wm^{-2}

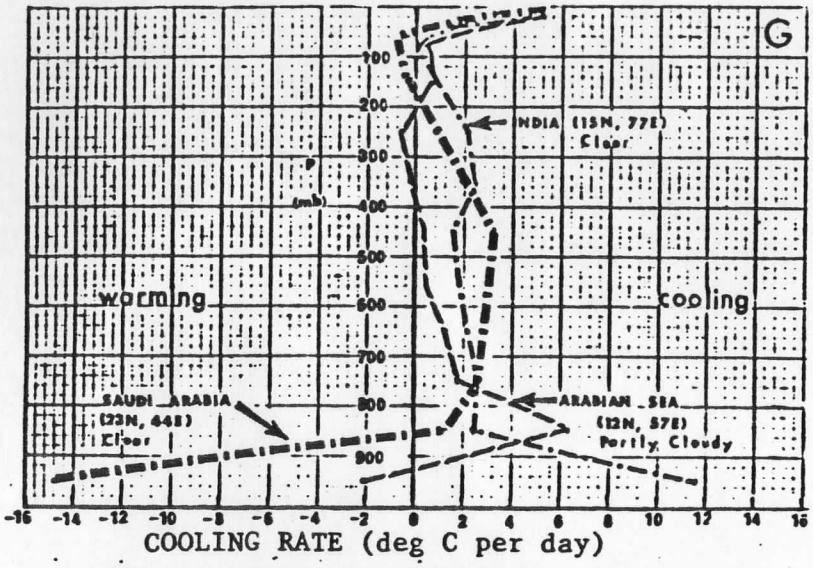

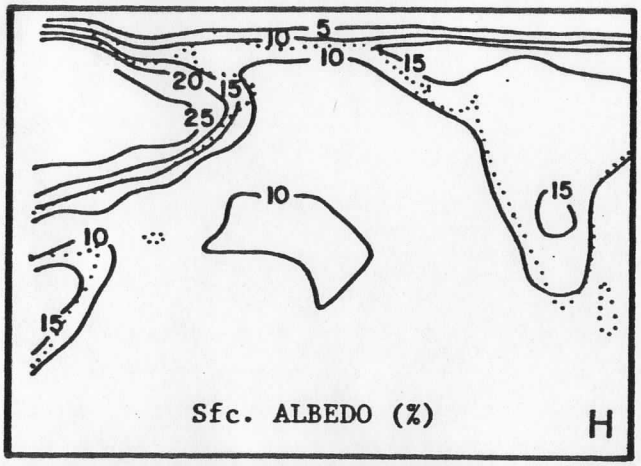

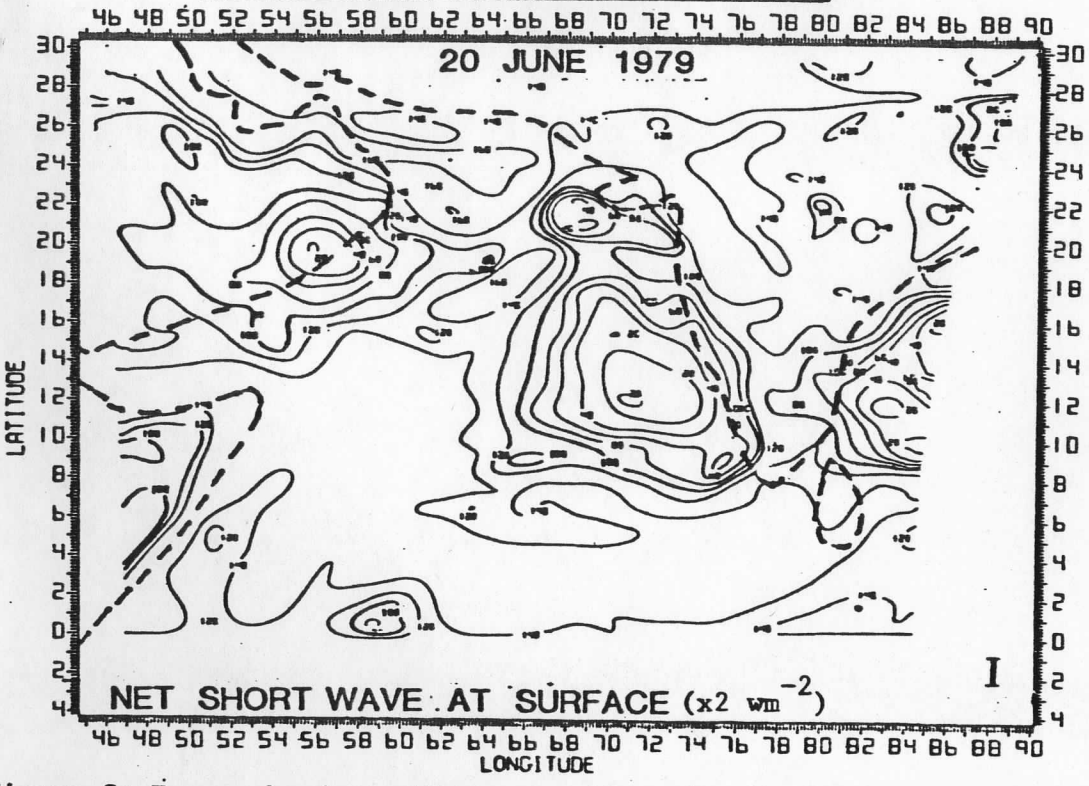

Figure G: Tropospheric cooling rate (deg C/day) over Saudi Arabia, Arabian Sea, and India on 20 June 1979 at 1000 GMT (see text for details)
Figure H: Surface Albedo (%), Figure I: Net SW at sfc (x2 wm^{-2})